FOUNDATION DESIGN

PRINCIPLES AND PRACTICES

Third Edition

Donald P. Coduto William A. Kitch
Man-chu Ronald Yeung

Foundation Design

Principles and Practices

Third Edition

Donald P. Coduto

William A. Kitch

Man-chu Ronald Yeung

Professors of Civil Engineering
California State Polytechnic University, Pomona

PEARSON

Boston Columbus Indianapolis New York San Francisco Hoboken
Amsterdam Cape Town Dubai London Madrid Milan Munich Paris Montreal Toronto
Delhi Mexico City São Paulo Sydney Hong Kong Seoul Singapore Taipei Tokyo

Vice President and Editorial Director, ECS: *Marcia J. Horton*
Executive Editor: *Holly Stark*
VP of Marketing: *Christy Lesko*
Director of Field Marketing: *Tim Galligan*
Product Marketing Manager: *Bram van Kempen*
Field Marketing Manager: *Demetrius Hall*
Marketing Assistant: *Jon Bryant*
Senior Managing Editor: *Scott Disanno*
Production Project Manager: *Greg Dulles*
Program Manager: *Erin Ault*
Global HE Director of Vendor Sourcing and Procurement: *Diane Hynes*
Operations Specialist: *Maura Zaldivar-Garcia*
Cover Designer: *Black Horse Designs*
Manager, Rights and Permissions: *Rachel Youdelman*
Full-Service Project Management: *Shylaja Gattupalli, Jouve India*
Composition: *Jouve India*
Printer/Binder: *Edwards Brothers*
Cover Printer: *Phoenix Color/Hagerstown*
Typeface: 10/12 *Times LT Std-Roman*

Pearson Education Ltd., *London*
Pearson Education Singapore, Pte. Ltd
Pearson Education Canada, Inc.
Pearson Education—Japan
Pearson Education Australia PTY, Limited
Pearson Education North Asia, Ltd., *Hong Kong*
Pearson Educación de Mexico, S.A. de C.V.
Pearson Education Malaysia, Pte.Ltd.
Pearson Education, Inc., *Upper Saddle River, New Jersey*

Library of Congress Cataloging-in-Publication Data

Coduto, Donald P.
Foundation design : principles and practices / Donald P. Coduto, William A. Kitch, Man-chu Ronald Yeung, Professors of Civil Engineering, California State Polytechnic University, Pomona. — Third edition.
pages cm
Includes bibliographical references and index.
ISBN 978-0-13-341189-8 (alk. paper)
ISBN 0-13-341189-3 (alk. paper)
1. Foundations. I. Kitch, William A. II. Yeung, Man-chu Ronald III. Title.
TA775.C63 2014
624.1'5—dc23 2014035178

10 9 8 7 6 5 4 3 2 1

PEARSON

www.pearsonhighered.com

ISBN 0-13-341189-3
ISBN 978-0-13-341189-8

Contents

Preface

Publication of this third edition of *Foundation Design: Principles and Practices* comes twenty years after the 1994 release of the first edition. The original book, along with the second edition published in 2001, enjoyed widespread use among students, researchers, and practicing engineers both in the United States and abroad.

Two new co-authors, William A. Kitch and Man-chu Ronald Yeung, have collaborated with the original author, Donald P. Coduto, to produce this third edition. All three are professors at California State Polytechnic University, Pomona, and previously collaborated on a new edition of *Geotechnical Engineering: Principles and Practices*, which is the companion volume to this book.

WHAT IS NEW IN THIS EDITION

This new edition reflects advancements in theory and practice over the past thirteen years, constructive suggestions we have received from readers, as well as our experiences using the book as a text in our undergraduate and graduate level foundation engineering courses. As part of this update, some chapters have been deleted, others have been added, and much of the book has been reorganized. Nearly every page has some revisions.

The most substantive and pervasive changes are the increased emphasis on limit state design and the inclusion of load and resistance factor design (LRFD) in both the structural and geotechnical aspects of the analysis and design process. These changes reflect the broader use of limit state design in engineering practices, such as the AASHTO code in North America and other codes around the world. Allowable stress design (ASD) methods have been retained, as this method is still widely used. Other noteworthy changes include:

- A new chapter on uncertainty and risk in foundation engineering.
- Design procedures that place greater emphasis on the distinction between serviceability limit states and ultimate limit states.
- Improved coverage of auger piles, including a new chapter on axial load design, which reflects advancements in this technology.

- A completely revised chapter on pile dynamics with more in depth material on Wave Equation Analysis and a new section on pulse load testing.
- Better integration with widely available software. For example, the chapter on laterally loaded piles is now based on the assumption that the reader has access to lateral load analysis software.
- A new chapter on serviceability limit states in piles.
- New chapters on foundations in rocks and intermediate geomaterials and ground improvement.
- Many new and updated example problems and homework problems.

A complete solutions manual as well as PowerPoint slides of the various illustrations and tables may be downloaded from the Instructor's Resource Center located at www.pearsonhighered.com/Coduto. This material is provided solely for the use of instructors in teaching their courses and assessing student learning. All requests for instructor access are verified against our customer database and/or through contacting the requestor's institution. Contact your local sales representative for additional assistance or support.

ACKNOWLEDGMENTS

In addition to insights gained from our review of the technical literature and from our own professional experience, we received substantial help from numerous professional friends and colleagues. Through many stimulating discussions, peer reviews of draft chapters, and in many other ways, they helped us improve the manuscript. Dr. Frank Raushe, PE; Daniel Zepeda, SE; Mike Kapuskar, GE; and Rick Drake, SE were especially generous in their assistance.

Our current and former students Gerald Aspiras, Brian Barnhart, Alejandro Irigoyen, Jiang Ly, Zachary Murray, Christopher Sandoval, and John Schober assisted with proofreading, problem solutions, and various insights from a student's perspective. Kevin Coduto assisted with file management and photo editing. Multiple drafts also were tested in the classroom at Cal Poly Pomona, and we appreciate our students' patience as we experimented with various methods of explaining different concepts, as well as their assistance in proofreading the text.

We appreciate the support from Holly Stark and Scott Disanno at Pearson, who made this project possible, as well as Pavithra Jayapaul and Shylaja Gattupalli at Jouve-India who provided excellent production support. Finally we thank our families for their patience as we devoted long hours to finishing this project.

Donald P. Coduto
William A. Kitch
Man-chu Ronald Yeung

Claremont, California

Notation and Units of Measurement

There is no universally accepted notation in foundation engineering. However, the notation used in this book, as described in the following table, is generally consistent with popular usage.

Symbol	Description	Typical Units		Defined in Chapter
		English	SI	
A	Base area of foundation	ft^2	m^2	Ch 3
A_0	Initial cross-sectional area	in^2	mm^2	Ch 4
A_1	Cross-sectional area of column	in^2	mm^2	Ch 10
A_2	Base area of frustum	in^2	mm^2	Ch 10
A_c	Cross-sectional area of concrete	in^2	mm^2	Ch 10
A_f	Cross-sectional area at failure	in^2	mm^2	Ch 4
A_g	Gross cross-sectional area	in^2	mm^2	Ch 10
A_p	Area of an individual plate	ft^2	m^2	Ch 18
A_r	Rod surface area	ft^2	m^2	Ch 18
A_s	Steel area	in^2	mm^2	Ch 10
A_{tg}	Area of pile group tip	ft^2	m^2	Ch 15
A_{tr}	Area of transverse reinforcing steel	in^2	mm^2	Ch 10
a	CPT net area ratio	Unitless	Unitless	Ch 4
a	Hoek-Brown constant given by Equation 25.5	Unitless	Unitless	Ch 25
a_{unl}	Pile acceleration at the unloading point	g	g	Ch 19
a_θ	Factor in N_q equation	Unitless	Unitless	Ch 7
B	Width of foundation	ft & in	mm	Ch 3
B_b	Diameter at base of foundation	ft	m	Ch 16
B_e	Equivalent footing width	ft	m	Ch 8
B_g	Width of pile group	ft	m	Ch 15
B_q	CPT pore pressure ratio	Unitless	Unitless	Ch 4

B_s	Diameter of shaft	ft	m	Ch 16
B'	Effective foundation width	ft-in	m	Ch 6
b	Unit length	ft	m	Ch 10
b_0	Length of critical shear surface	in	mm	Ch 10
b_c, b_q, b_γ	Bearing capacity base inclination factors	Unitless	Unitless	Ch 7
b_w	Length of critical shear surface	in	mm	Ch 10
C	Capacity of a structural element	Varies	Varies	Ch 2
C_1	Depth factor	Unitless	Unitless	Ch 8
C_2	Secondary creep factor	Unitless	Unitless	Ch 8
C_3	Shape factor	Unitless	Unitless	Ch 8
C_A	Aging factor	Unitless	Unitless	Ch 4
C_B	SPT borehole diameter correction	Unitless	Unitless	Ch 4
C_c	Compression index	Unitless	Unitless	Ch 3
C_{OCR}	Overconsolidation correction factor	Unitless	Unitless	Ch 4
C_P	Grain size correction factor	Unitless	Unitless	Ch 4
C_R	SPT rod length correction	Unitless	Unitless	Ch 4
C_r	Recompression index	Unitless	Unitless	Ch 3
C_S	SPT sampler correction	Unitless	Unitless	Ch 4
C_s	Side friction coefficient	Unitless	Unitless	Ch 15
C_t	Toe coefficient	Unitless	Unitless	Ch 15
COV	Coefficient of variation of a random variable	Unitless	Unitless	Ch 2
c	Concrete cover or spacing between bars	in	mm	Ch 10
c	Factor in Engineering News Formula	in	mm	Ch 19
c	Wave velocity in pile	ft/s	m/s	Ch 19
c	Column or wall width	in	mm	Ch 10
c'	Effective cohesion	lb/ft^2	kPa	Ch 3
c'_{adj}	Adjusted effective cohesion	lb/ft^2	kPa	Ch 7
c_n	Depth to the neutral axis in beam bending	in	mm	Ch 10
c_T	Total cohesion	lb/ft^2	kPa	Ch 3
D	Depth of foundation	ft & in	mm or m	Ch 3
D	Demand placed on a structural element	Varies	Varies	Ch 2
D	Dead load	Varies	Varies	Ch 5
D	Depth of socket embedment	ft	m	Ch 25
D	Disturbance factor	Unitless	Unitless	Ch 25
D_2	Distance from transducers to pile tip	ft	m	Ch 19
D_{50}	Grain size at which 50 percent is finer	–	mm	Ch 4
D_{min}	Minimum required embedment depth	ft	m	Ch 22
D_r	Relative density	percent	percent	Ch 3
D_w	Depth from ground surface to groundwater table	ft	m	Ch 7
d	Effective depth	in	mm	Ch 10

d	Vane diameter	in	mm	Ch 4
d	Depth factor in Equation 25.15	Unitless	Unitless	Ch 25
d_b	Reinforcing bar diameter	in	mm	Ch 10
d_c, d_q, d_γ	Bearing capacity depth factors	Unitless	Unitless	Ch 7
E	A probabilistic event	NA	NA	Ch 2
E	Portion of steel in center section	Unitless	Unitless	Ch 10
E	Modulus of elasticity	lb/in^2	MPa	Ch 2
E	Earthquake load	Varies	Varies	Ch 5
E_0	Modulus at ground surface	lb/ft^2	kPa	Ch 8
E_{25}	Secant modulus	lb/ft^2	kPa	Ch 20
E_a	Energy lost in appurtenances during pile driving	ft-lb	Joules	Ch 19
E_c	Modulus of elasticity for concrete	lb/in^2	MPa	Ch 14
E_D	DMT modulus	lb/ft^2	kPa	Ch 4
E_h	Kinetic energy of hammer during pile driving	ft-lb	Joules	Ch 19
E_i	Deformation modulus of intact rock	k/in^2	MPa	Ch 25
E_l	Viscous energy lost in soil during pile driving	ft-lb	Joules	Ch 19
E_m	SPT hammer efficiency	Unitless	Unitless	Ch 4
E_m	Rock mass deformation modulus	k/in^2	MPa	Ch 25
E_p	Energy lost in pile during driving	ft-lb	Joules	Ch 19
E_r	Rated energy of pile hammer	ft-lb	Joules	Ch 19
E_s	Equivalent modulus of elasticity	lb/ft^2	kPa	Ch 8
E_s	Work done on soil during pile driving	ft-lb	Joules	Ch 19
E_s	Modulus of elasticity for steel	lb/in^2	MPa	Ch 14
E_u	Undrained modulus of elasticity	lb/ft^2	kPa	Ch 4
EI	Expansion index	Unitless	Unitless	Ch 27
e	Eccentricity	ft	m	Ch 6
e	Void ratio	Unitless	Unitless	Ch 3
e	Base of natural logarithms	2.7183	2.7183	–
e_0	Initial void ratio	Unitless	Unitless	Ch 3
e_a	Efficiency factor for appurtenance losses in pile driving	Unitless	Unitless	Ch 19
e_B	Eccentricity in the B direction	ft	m	Ch 6
e_h	Efficiency of pile driving hammer	Unitless	Unitless	Ch 19
e_L	Eccentricity in the L direction	ft	m	Ch 6
e_{max}	Maximum void ratio	Unitless	Unitless	Ch 3
e_{min}	Minimum void ratio	Unitless	Unitless	Ch 3
F	Factor of safety	Unitless	Unitless	Ch 2
F	Force applied in pile driving or dynamic testing	k	kN	Ch 19

F_a	Body force due to acceleration in dynamic testing	k	kN	Ch 19
F_d	Dynamic force applied in dynamic testing	k	kN	Ch 19
F_r	CPT normalized friction ratio	Unitless	Unitless	Ch 4
F_{unl}	Force in pile at the unloading point	k	kN	Ch 19
F_v	Damping force applied in dynamic testing	k	kN	Ch 19
f	Mobilized unit side friction resistance	lb/ft^2	kPa	Ch 14
f_a	Allowable axial stress	lb/in^2	MPa	Ch 21
f_b	Allowable flexural stress	lb/in^2	MPa	Ch 21
f'_c	28-day compressive strength of concrete	lb/in^2	MPa	Ch 10
f_n	Nominal unit side friction capacity	lb/ft^2	kPa	Ch 13
f_{pc}	Effective prestress on gross section	lb/in^2	MPa	Ch 21
f_s	CPT cone side friction	T/ft^2	MPa or kg/cm^2	Ch 4
f_v	Allowable shear stress	lb/in^2	MPa	Ch 21
f_y	Yield strength of steel	lb/in^2	MPa	Ch 10
G	Shear modulus	Unitless	Unitless	Ch 4
G_s	Specific gravity of solids	Unitless	Unitless	Ch 3
GSI	Geological Strength Index	Unitless	Unitless	Ch 25
g_c, g_q, g_γ	Bearing capacity ground inclination factors	Unitless	Unitless	Ch 7
H	Thickness of soil stratum	ft	m	Ch 3
H	Earth pressure load	Varies	Varies	Ch 5
H	Initial height of specimen immediately before soaking	in	mm	Ch 27
h	Hammer stroke	in	m	Ch 19
h	Expansion of soil	in	mm	Ch 27
h_0	Initial height of sample	in	mm	Ch 27
I	Moment of inertia	in^4	mm^4	Ch 21
I_c	CPT normalized soil behavior type index	Unitless	Unitless	Ch 4
I_D	DMT material index	Unitless	Unitless	Ch 4
I_E, I_F, I_G	Stress influence factors	Unitless	Unitless	Ch 8
I_P	Plasticity index	Unitless	Unitless	Ch 3
I_r	Rigidity index	Unitless	Unitless	Ch 15
I_ε	Strain influence factor	Unitless	Unitless	Ch 8
$I_{\varepsilon c}$	Strain influence factor for continuous foundation	Unitless	Unitless	Ch 8
$I_{\varepsilon p}$	Peak strain influence factor	Unitless	Unitless	Ch 8
$I_{\varepsilon s}$	Strain influence factor for square foundation	Unitless	Unitless	Ch 8
I_σ	Stress influence factor	Unitless	Unitless	Ch 3
I_0, I_1	Stress influence factors	Unitless	Unitless	Ch 8
i_c, i_q, i_γ	Bearing capacity load inclination factors	Unitless	Unitless	Ch 7

J_S	Smith damping factor	Unitless	Unitless	Ch 19
J_p	Pile damping factor	Unitless	Unitless	Ch 19
j_s	Soil damping factor	Unitless	Unitless	Ch 19
K	Coefficient of lateral earth pressure	Unitless	Unitless	Ch 3
K	Bulk modulus	Unitless	Unitless	Ch 4
K_0	Coefficient of lateral earth pressure at rest	Unitless	Unitless	Ch 3
K_a	Coefficient of active earth pressure	Unitless	Unitless	Ch 3
K_D	DMT horizontal stress index	Unitless	Unitless	Ch 4
K_E	Factor in Fleming method	Unitless	Unitless	Ch 20
K_p	Coefficient of passive earth pressure	Unitless	Unitless	Ch 3
K_s	Side resistance flexibility factor	Unitless	Unitless	Ch 20
K_{sp}	Empirical coefficient in Equation 25.15	Unitless	Unitless	Ch 25
K_t	Toe resistance flexibility factor	Unitless	Unitless	Ch 20
K_t	Coefficient of lateral earth pressure at ground surface	Unitless	Unitless	Ch 15
K_{tr}	Splitting term for development length	in	mm	Ch 10
k	Factor in computing depth factors	Unitless	Unitless	Ch 7
k_s	Coefficient of subgrade reaction	$1b/in^3$	kN/m^3	Ch 11
k_s	LCPC side friction factor	Unitless	Unitless	Ch 15
k_t	LCPC toe bearing factor	Unitless	Unitless	Ch 15
L	Length of foundation	ft-in	mm	Ch 3
L	Live load	Varies	Varies	Ch 5
L_F	Factor in Fleming method	ft	m	Ch 20
L_g	Length of pile group	ft	m	Ch 15
LL	Liquid limit (see w_L)	Unitless	Unitless	Ch 3
L_r	Live roof load	Varies	Varies	Ch 5
L'	Effective foundation length	ft-in	m	Ch 6
l	Cantilever distance	in	mm	Ch 10
l_d	Development length	in	mm	Ch 10
l_{dh}	Development length for hook	in	mm	Ch 10
M	Constrained modulus	$1b/ft^2$	kPa	Ch 4
M	Moment load	ft-k	kN-m	Ch 5
M_n	Nominal moment load capacity	ft-k	kN-m	Ch 10
M_s	Flexibility factor	Unitless	Unitless	Ch 20
M_u	Factored moment load	ft-k	kN-m	Ch 5
M_{uc}	Factored moment on the section being analyzed	in-lb	kN-m	Ch 10
m	Safety margin	Unitless	Unitless	Ch 2
m	Factor in computing load inclination factors	Unitless	Unitless	Ch 7
m_b	Hoek-Brown constant given by Equation 25.3	Unitless	Unitless	Ch 25

m_i	m_b for intact rock	Unitless	Unitless	Ch 25
m_v	Coefficient of compressibility	ft^2/1b	1/kpa	Ch 4
N	SPT blow count recorded in field	Blows/ft	Blows/ 300 mm	Ch 4
N	Nominal load capacity	Varies	Varies	Ch 5
N	Number of piles in a group	Unitless	Unitless	Ch 15
N_B	Becker blow count	Blows/ft	Blows/ 300 mm	Ch 4
N_w	Stress wave number	Unitless	Unitless	Ch 19
N_c, N_q, N_γ	Bearing capacity factors	Unitless	Unitless	Ch 7
N_c^*, N_q^*, N_γ^*, N_σ	Bearing capacity factors	Unitless	Unitless	Ch 15
N_u	Breakout factor	Unitless	Unitless	Ch 16
N_{cr}^*	Bearing capacity factor for rock	Unitless	Unitless	Ch 25
$N_{1,60}$	SPT blow count corrected for field procedures and overburden stress	Blows/ft	Blows/ 300 mm	Ch 4
N_{60}	SPT blow count corrected for field procedures	Blows/ft	Blows/ 300 mm	Ch 4
n	Porosity	percent	percent	Ch 3
n	CPT stress exponent	Unitless	Unitless	Ch 4
OCR	Overconsolidation ratio	Unitless	Unitless	Ch 3
P	Normal load	k	kN	Ch 5
$P(E)$	Probability of event, E	NA	NA	Ch 2
P_a	Allowable downward load capacity	k	kN	Ch 9
P_a	Active earth pressure resultant force	lb	kN	Ch 3
P_a	Atmospheric pressure	1 ton/ft^2	100 kPa	Ch 4
$P_{a,up}$	Allowable upward load capacity	k	kN	Ch 13
P_{ag}	Allowable load capacity of pile group	k	kN	Ch 15
P_{up}	Upward load	k	kN	Ch 13
$P_{up,n}$	Nominal upward load capacity	k	kN	Ch 13
P_f	Probability of failure	Unitless	Unitless	Ch 2
P_f	Axial load at failure	lb	N	Ch 4
PI	Plasticity index (see I_P)	Unitless	Unitless	Ch 3
P_j	Final jacking force	k	kN	Ch 18
PL	Plastic limit (see w_P)	Unitless	Unitless	Ch 3
P_m	p multiplier	Unitless	Unitless	Ch 22
P_n	Nominal downward load capacity	k	kN	Ch 5
P_{nb}	Nominal column bearing capacity	k	kN	Ch 10
P_p	Passive earth pressure resultant force	lb	kN	Ch 3
P_s	Side friction resistance	k	kN	Ch 13

P_t	Toe bearing resistance	k	kN	Ch 13
P'_t	Net toe bearing resistance	k	kN	Ch 13
P_u	Factored normal load	k	kN	Ch 5
p	Lateral soil resistance per unit length of pile	lb	kN	Ch 22
p	Air pressure inside pneumatic caisson	lb/in^2	MPa	Ch 12
p_0, p_1	DMT pressure readings	lb/in^2	kPa	Ch 4
p_a	Atmospheric pressure	lb/in^2	kPa	Ch 16
p_u	Ultimate lateral soil resistance per unit length of pile	lb	kN	Ch 22
Q_c	Compressibility factor	Unitless	Unitless	Ch 4
Q_{tn}	CPT normalized cone tip resistance	Unitless	Unitless	Ch 4
q	Bearing pressure	lb/ft^2	kPa	Ch 6
q	Quake	in	mm	Ch 19
q'	Net bearing pressure	lb/ft^2	kPa	Ch 6
q'	Mobilized net unit toe bearing resistance	lb/ft^2	kPa	Ch 14
q_a	Allowable bearing capacity	lb/ft^2	kPa	Ch 7
q_A	Allowable bearing pressure	lb/ft^2	kPa	Ch 6
$q_{A,SLS}$	Allowable bearing pressure based on serviceability limit state	lb/ft^2	kPa	Ch 9
$q_{A,ULS}$	Allowable bearing pressure based on ultimate limit state	lb/ft^2	kPa	Ch 9
q_c	CPT cone resistance	T/ft^2	MPa or kg/cm^2	Ch 4
q_E	Effective cone resistance	T/ft^2	kg/cm^2 or MPa	Ch 15
q_{Eg}	Factor in Eslami and Fellenius method	T/ft^2	kg/cm^2 or MPa	Ch 15
q_{eq}	Equivalent bearing pressure	lb/ft^2	kPa	Ch 6
$q_{\max}$	Maximum bearing pressure	lb/ft^2	kPa	Ch 6
$q_{\min}$	Minimum bearing pressure	lb/ft^2	kPa	Ch 6
q_n	Nominal unit bearing capacity	lb/ft^2	kPa	Ch 7
q'_n	Nominal unit toe bearing capacity	lb/ft^2	kPa	Ch 13
q_t	Corrected SPT cone tip resistance	T/ft^2	MPa or kg/cm^2	Ch 4
q'_{tr}	Reduced net unit toe bearing resistance	lb/ft^2	kPa	Ch 15
q_u	Unconfined compressive strength	lb/ft^2	kPa	Ch 4
R	Reliability	Unitless	Unitless	Ch 2
R	Rain load	Varies	Varies	Ch 5
R	Total resistance of pile during driving	k	kN	Ch 19

R_d	Dynamic resistance of pile during driving	Unitless	Unitless	Ch 19
R_f	Friction ratio in CPT	Unitless	Unitless	Ch 4
RMR	Rock Mass Rating	Unitless	Unitless	Ch 25
RQD	Rock quality designation	Unitless	Unitless	Ch 25
R_s	Static resistance of pile during driving	Unitless	Unitless	Ch 19
R_u	Ultimate static resistance of pile during driving	k	kN	Ch 19
R_{ur}	Required ultimate static resistance of pile during driving	k	kN	Ch 19
r	Rigidity factor	Unitless	Unitless	Ch 8
S	Snow load	Varies	Varies	Ch 5
S	Slope of pile from the vertical	radians	radians	Ch 22
S	Elastic section modulus	in^3	mm^3	Ch 21
S	Degree of saturation	percent	percent	Ch 3
S	Column spacing	ft	m	Ch 5
S_{mi}	Joint spacing of the ith discontinuity set	ft	m	Ch 25
SR	Spacing ratio	Unitless	Unitless	Ch 25
S_t	Sensitivity	Unitless	Unitless	Ch 3
s	Shear strength	lb/ft^2	kPa	Ch 3
s	Center-to-center spacing of piles or reinforcing bars	in	mm	Ch 15
s	Pile set	in	mm	Ch 19
s	Hoek-Brown constant given by Equation 25.4	Unitless	Unitless	Ch 25
s_c, s_q, s_γ	Bearing capacity shape factors	Unitless	Unitless	Ch 7
s_u	Undrained shear strength	lb/ft^2	kPa	Ch 3
s_v	Vertical spacing of discontinuity	ft	m	Ch 25
T	Thickness of foundation	ft-in	mm	Ch 10
T_f	Torque at failure	in-lb	N-m	Ch 4
TMI	Thornthwaite moisture index	Unitless	Unitless	Ch 27
t	Time	yr	yr	Ch 7
t	Factor in rock bearing formula	Unitless	Unitless	Ch 25
t_d	Aperture of discontinuity	in	mm	Ch 25
t_p	Wave propagation time in pile driving	s	s	Ch 19
t_{unl}	Time at which pile velocity is zero	s	s	Ch 19
U	Generic factored load	Varies	Varies	Ch 5
u	Displacement of pile or pile segment	in	mm	Ch 19
u	Pore water pressure	lb/ft^2	kPa	Ch 3
u_0	Equilibrium pore water pressure	lb/ft^2	kPa	Ch 4
u_2	Pore water pressure behind CPT cone	lb/ft^2	kPa	Ch 4
u_D	Pore water pressure at bottom of foundation	lb/ft^2	kPa	Ch 6

u_e	Excess pore water pressure	lb/ft^2	kPa	Ch 3
V	Shear load	k	kN	Ch 5
V_a	Allowable shear load capacity	k	kN	Ch 7
V_c	Nominal shear capacity of concrete	lb	kN	Ch 10
V_n	Nominal shear load capacity	k	kN	Ch 7
V_{nc}	Nominal shear capacity on critical surface	lb	kN	Ch 10
V_s	Nominal shear capacity of reinforcing steel	lb	kN	Ch 10
V_u	Factored shear load	k	kN	Ch 5
V_{uc}	Factored shear load on critical surface	lb	kN	Ch 10
V_v	Volume of voids	m^2	ft^2	Ch 3
v	Pile hammer impact velocity	in/s	m/s	Ch 19
v	Velocity of pile or pile segment	ft/s	m/s	Ch 19
W	Wind load	Varies	Varies	Ch 5
W_f	Weight of foundation	lb	kN	Ch 6
W_r	Hammer ram weight	lb	kN	Ch 19
w	Moisture content	percent	percent	Ch 3
w_L	Liquid limit	Unitless	Unitless	Ch 3
w_P	Plastic limit	Unitless	Unitless	Ch 3
w_s	Shrinkage limit	Unitless	Unitless	Ch 3
Y_{50}	Lateral deflection required to achieve one-half of the ultimate soil resistance	in	mm	Ch 22
y	Lateral deflection	in	mm	Ch 22
y_t	Lateral deflection at top of foundation	in	mm	Ch 22
Z_M	DMT gage zero offset pressure	lb/in^2	kPa	Ch 4
z	Depth below ground surface	ft	m	Ch 3
z	Settlement	in	mm	Ch 20
z_f	Depth below bottom of foundation	ft	m	Ch 3
z_i	Depth of the midpoint of the socket	ft	m	Ch 25
z_w	Depth below the groundwater table	ft	m	Ch 3
α	Wetting coefficient	Unitless	Unitless	Ch 27
α	Adhesion factor	Unitless	Unitless	Ch 15
α	Slope of footing bottom	deg	deg	Ch 7
α_M	Constrained modulus coefficient for CPT	Unitless	Unitless	Ch 4
α_P	Load sharing ratio	Unitless	Unitless	Ch 24
α_E	Joint modification factor	Unitless	Unitless	Ch 25
β	Modulus to shear strength ratio	Unitless	Unitless	Ch 4
β	Normalized modulus	Unitless	Unitless	Ch 8
β	Side friction factor in β method	Unitless	Unitless	Ch 15
β_0, β_1	Correlation factors for modulus based on SPT	Unitless	Unitless	Ch 4
β_z	Footing shape and rigidity factor	Unitless	Unitless	Ch 25

γ	Unit weight	lb/ft^3	kN/m^3	Ch 3
γ	Load factor	Unitless	Unitless	Ch 5
γ'	Buoyant unit weight	lb/ft^3	kN/m^3	Ch 2
γ'	Effective unit weight	lb/ft^3	kN/m^3	Ch 7
γ_b	Buoyant unit weight	lb/ft^3	kN/m^3	Ch 3
γ_c	Unit weight of concrete	lb/ft^3	kN/m^3	Ch 6
γ_d	Dry unit weight	lb/ft^3	kN/m^3	Ch 3
γ_w	Unit weight of water	lb/ft^3	kN/m^3	Ch 3
$\Delta\sigma_z$	Change in vertical stress	lb/ft^2	kPa	Ch 3
δ	Total settlement	in	mm	Ch 3
δ_a	Allowable total settlement	in	mm	Ch 5
δ_c	Consolidation settlement	in	mm	Ch 3
δ_D	Differential settlement	in	mm	Ch 5
δ_{Da}	Allowable differential settlement	in	mm	Ch 5
δ_d	Distortion settlement	in	mm	Ch 3
δ_e	Settlement due to elastic compression	in	mm	Ch 20
δ_s	Secondary compression settlement	in	mm	Ch 3
δ_s	Settlement due to mobilization of side friction	in	mm	Ch 20
δ_t	Settlement due to mobilization of toe bearing	in	mm	Ch 20
δ_t	Vertical displacement required to mobilize the full side friction resistance, assumed to be 25 mm (1 in)	in	mm	Ch 25
δ_{toe}	Displacement at pile toe	in	mm	Ch 20
δ_w	Heave or settlement due to wetting	in	mm	Ch 27
δ_z	Displacement at a point on the pile	in	mm	Ch 20
ε	Normal strain	Unitless	Unitless	Ch 3
ε_{50}	Axial strain at which 50 percent of the soil strength is mobilized	Unitless	Unitless	Ch 22
ε_a	Axial strain	Unitless	Unitless	Ch 4
ε_c	Hydrocollapse strain	Unitless	Unitless	Ch 28
ε_f	Strain at failure	Unitless	Unitless	Ch 4
ε_r	Radial strain	Unitless	Unitless	Ch 4
ε_t	Tensile strain in reinforcement	Unitless	Unitless	Ch 10
ε_w	Potential swell strain	Unitless	Unitless	Ch 27
ε_z	Vertical strain	Unitless	Unitless	Ch 3
η	Factor in Shields chart	Unitless	Unitless	Ch 7
η	Group efficiency factor	Unitless	Unitless	Ch 15
θ_a	Allowable angular distortion	radians	radians	Ch 5
λ	Factor in Shields chart	Unitless	Unitless	Ch 7
λ	Lightweight concrete factor	Unitless	Unitless	Ch 10

λ	Vane shear correction factor	Unitless	Unitless	Ch 4
λ_i	Frequency of the ith discontinuity set	ft^{-1}	m^{-1}	Ch 25
μ	Average or mean of a random variable	Unitless	Unitless	Ch 2
μ	Coefficient of friction	Unitless	Unitless	Ch 7
ν	Poisson's ratio	Unitless	Unitless	Ch 4
ν_m	Poisson's ratio of rock mass	Unitless	Unitless	Ch 25
ρ	Mass density	lb_m/ft^3	kg/m^3	Ch 19
ρ	Steel ratio	Unitless	Unitless	Ch 10
ρ_{min}	Minimum steel ratio	Unitless	Unitless	Ch 10
σ	Total stress	lb/ft^2	kPa	Ch 3
σ	Normal pressure imparted on a surface	lb/ft^2	kPa	Ch 3
σ	Standard deviation	Unitless	Unitless	Ch 2
σ'	Effective stress	lb/ft^2	kPa	Ch 3
σ'_1	Major effective principal stress at failure	lb/ft^2	kPa	Ch 25
σ'_3	Minor effective principal stress at failure	lb/ft^2	kPa	Ch 25
σ'_c	Preconsolidation stress	lb/ft^2	kPa	Ch 3
σ_{ci}	Uniaxial compressive strength of the intact rock	k/in^2	MPa	Ch 25
σ'_h	Horizontal stress	lb/ft^2	kPa	Ch 25
σ'_m	Preconsolidation margin	lb/ft^2	kPa	Ch 3
σ_n	Fluid pressure exerted by the concrete in socket during placement	lb/ft^2	kPa	Ch 25
σ_p	Representative passive pressure	lb/ft^2	kPa	Ch 3
σ_s	Swell pressure	lb/ft^2	kPa	Ch 27
σ_t	Threshold collapse stress	lb/ft^2	kPa	Ch 28
σ_x	Horizontal total stress	lb/ft^2	kPa	Ch 3
σ'_x	Horizontal effective stress	lb/ft^2	kPa	Ch 3
σ_z	Vertical total stress	lb/ft^2	kPa	Ch 3
σ'_z	Vertical effective stress	lb/ft^2	kPa	Ch 3
σ'_{z0}	Initial vertical effective stress	lb/ft^2	kPa	Ch 3
σ_{zD}	Vertical total stress at depth D below the ground surface	lb/ft^2	kPa	Ch 7
σ'_{zD}	Vertical effective stress at depth D below the ground surface	lb/ft^2	kPa	Ch 7
σ'_{zf}	Final effective stress	lb/ft^2	kPa	Ch 3
σ'_{zp}	Initial vertical effective stress at depth of peak strain influence factor	lb/ft^2	kPa	Ch 8
$\Phi(x)$	Cumulative distribution function for the standard normal distribution	Unitless	Unitless	Ch 2
ϕ	Resistance factor	Unitless	Unitless	Ch 5
ϕ'	Effective friction angle	deg	deg	Ch 3
ϕ'_{adj}	Adjusted effective friction angle	deg	deg	Ch 7

ϕ_f	Soil-foundation interface friction angle	deg	deg	Ch 15
ϕ_{rc}	Socket wall interface friction angle, assumed to be 30 degrees	deg	deg	Ch 25
ϕ_T	Total friction angle	deg	deg	Ch 3
ψ	Factor in Shields chart	Unitless	Unitless	Ch 7
ψ_e	Coating factor for computing development length	Unitless	Unitless	Ch 10
ψ_s	Reinforcement size factor for computing development length	Unitless	Unitless	Ch 10
ψ_t	Location factor for computing development length	Unitless	Unitless	Ch 10
Ω	Probability or sample space	NA	NA	Ch 2
ω	Tilt of a structure	Unitless	Unitless	Ch 5

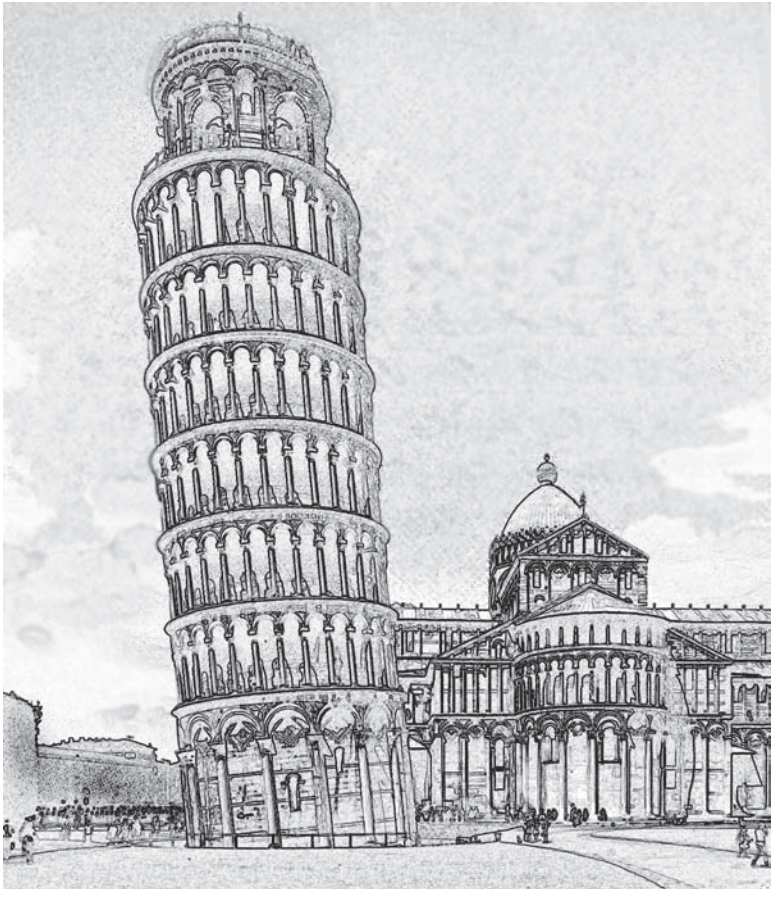

Part A

General Principles

1

Foundations

The foundations are properly called the basis of the fabrick, viz. that part of it under ground which sustains the whole edifice above; and therefore of all the errors that can be committed in building, those made in the foundation are most pernicious, because they at once occasion the ruin of the whole fabrick, nor can they be rectified without the utmost difficulty.

Venetian architect Andrea Palladio (1508–1580)
as translated by Isaac Ware, 1738

Builders have long recognized the importance of a solid foundation, and that the integrity of a structure can be no greater than that of its foundation. If a foundation fails, the overlying structure fails with it. These truths were especially evident in Palladio's renaissance Venice, where heavy masonry structures were being built on small islands in a lagoon underlain by very soft soils. In addition, as Palladio observed, defects in the foundation are very difficult to repair after the structure has been built. Thus, well-designed and well-constructed foundations continue to be an essential part of successful construction.

However, foundations can also be very expensive, so over-designed foundations are needlessly wasteful and inefficient. Our goal is to provide sturdy foundations that properly support the superstructure, while avoiding costly over-design. The methods of doing so form the subject of this book.

1.1 FOUNDATION CLASSIFICATION

Foundations are structural elements that transfer loads from the superstructure to the underlying soil or rock. A structure may be supported on a system of individual foundations, or on a single large foundation. Engineers classify foundations into two broad categories: *shallow foundations* and *deep foundations*, as shown in Figure 1.1.

Shallow foundations transmit the structural loads to the soils immediately beneath the foundation, and are discussed in Chapters 6 to 11. The most common type is a *spread footing*, which spreads the applied load over a sufficiently large area to maintain soil stresses within tolerable limits. Spread footings are easy and inexpensive to build, and are most often used to support small to medium size structures on sites with good soil conditions. Typically, each column has its own spread footing, although sometimes multiple closely-spaced columns are supported on a single footing. Thus, a building might have dozens of individual footings.

The second type of shallow foundation is a *mat foundation* (also called a *raft foundation*), which normally encompasses the entire footprint of the structure. Mats have the advantage of providing structural continuity and rigidity, as well as spreading the load over a larger area.

Conversely, deep foundations transmit much, or all, of the applied load to deeper soils, and are discussed in Chapters 12 to 24. *Piles* are long slender structural members that can be either prefabricated and driven into the ground, or cast in place. *Caissons* are large prefabricated boxes that are sunk into place and filled with concrete to form a foundation. The load-carrying capacity of soils generally increases with depth, and deep foundations engage a larger volume of soil, so they are most often used on larger and heavier structures, especially when the shallow soils are poor.

The terminology used to describe and classify foundations is sometimes inconsistent. Different terms are sometimes used to describe the same thing, and the same term is sometimes used to describe different things. Even the term "foundation" is sometimes used to describe the underlying soil or rock rather than a structural element. This book uses terminology that reflects common practice, and alternative terms are included in context.

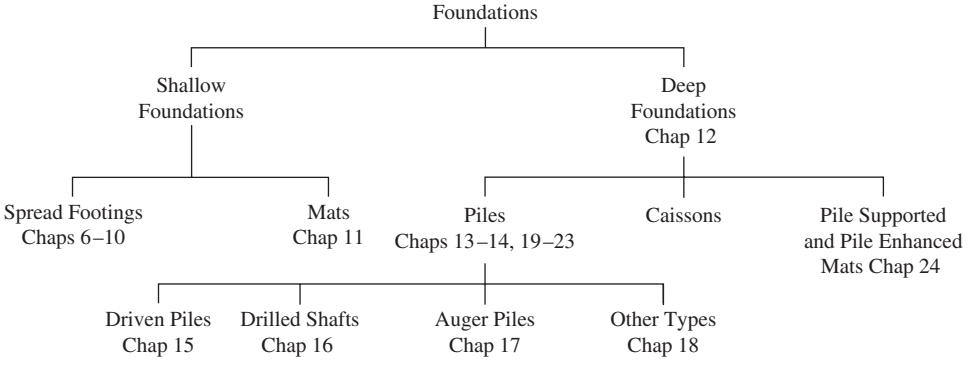

Figure 1.1 Classification of foundations.

1.2 THE EMERGENCE OF MODERN FOUNDATION ENGINEERING

The history of foundations extends for thousands of years, and impressive projects were built hundreds or even thousands of years ago. For example, 4,000 to 5,000 years ago the alpine lake dwellers in Europe used timber piles to support their houses. Also, in the year 55 BCE, Julius Caesar built a pile-supported bridge across the Rhine River to facilitate his conquest of Gaul. In Shanghai, the 40 m tall Longhua Pagoda was constructed on soft clay in 977 CE using a foundation of bricks laid on a wooden raft supported by closely-spaced wooden piles, a design very similar to today's pile-supported mat, and has stood firm for over 1,000 years while some newer buildings nearby have been badly damaged by excessive settlement (Kerisel, 1987).

Early foundation designs were based on precedent, intuition, and common sense. Through trial-and-error, builders developed rules for selecting, sizing, and constructing foundations. For example, even as late as the nineteenth century, the width of spread footings supporting masonry walls in New York City was set at 1.5 times the width of the wall when founded on compact gravel, and 3.0 times the width of the wall when founded on sand or stiff clay (Powell, 1884).

These empirical rules, combined with good judgment, usually produced acceptable results as long as they were applied to structures and soil conditions similar to those encountered in the past. However, the results were sometimes disastrous when builders extrapolated the rules to new conditions. This problem became especially troublesome when new building materials and methods of construction began to appear during the last quarter of the nineteenth century. The introduction of steel and reinforced concrete led to a gradual transition away from rigid masonry structures supported primarily on bearing walls to more flexible frame structures that used columns. These new materials also permitted structures to be taller and heavier than before. In addition, as good sites became increasingly scarce, builders were forced to consider sites with poorer soil conditions, which made foundation design and construction much more difficult. Thus, the old rules for foundation design no longer applied.

The introduction of these new building materials led to more rational design methods, the beginning of what we now call structural engineering, and this rational approach naturally extended to the foundations. Geotechnical engineering, which began in earnest during the 1920s, further added to our understanding of foundations and the mechanical processes of transferring loads into the ground. Thus, instead of simply developing new empirical rules, engineers began to investigate the behavior of foundations and develop more rational methods of design, establishing the discipline of foundation engineering. This transition began in the late nineteenth century, rapidly progressed through the twentieth century, and continues in the twenty-first century.

These advances in analysis and design were accompanied by tremendous improvements in construction methods and equipment. For example, modern pile driving hammers enable construction of huge high-capacity piles that far exceed the capabilities of timber piles driven by falling weights. These advances have enabled building at sites where foundation construction had previously been impossible or impractical.

It is now possible to build reliable, cost-effective, high-capacity foundations for a wide range of modern structures, even on very difficult sites. Advances in design and construction continue to be developed in the twenty-first century, so future engineers will probably have even greater capabilities. Nevertheless, precedent, empiricism, common sense, and engineering judgment are still important, and continue to have a role in modern foundation engineering.

The Eiffel Tower

The Eiffel Tower, Figure 1.2, is an excellent example of a new type of structure in which the old rules for foundations no longer applied. It was built for the Paris Universal Exposition of 1889 and was the tallest structure in the world. Alexandre Gustave Eiffel, the designer and builder, was very conscious of the need for adequate foundations, and clearly did not want to create another Leaning Tower of Pisa (Kerisel, 1987).

The Eiffel Tower is adjacent to the Seine River, and is underlain by difficult soil conditions, including uncompacted fill and soft alluvial soils. Piers for the nearby Pont de l'Alma (Alma bridge), which were founded in this alluvium, had already settled nearly 1 m. The tower could not tolerate such settlements.

Figure 1.2 Two legs of the Eiffel Tower are underlain by softer soils, and thus could have settled more than the other two. Fortunately, Eiffel carefully explored the soil's conditions, recognized this potential problem, and designed the foundations to accommodate these soil conditions. His foresight and diligence resulted in a well-designed foundation system that has not settled excessively (Courtesy by Shutterstock).

Eiffel began exploring the subsurface conditions using the crude drilling equipment of the time, but was not satisfied with the results. He wrote: "What conclusions could one reasonably base on the examination of a few cubic decimeters of excavated soil, more often than not diluted by water, and brought to the surface by the scoop?" (Kerisel, 1987). Therefore, he devised a new means of exploring the soils, which consisted of driving a 200 mm diameter pipe filled with compressed air. The air kept groundwater from entering the tube, and thus permitted recovery of higher quality samples.

Eiffel's studies revealed that the two legs of the tower closest to the Seine were underlain by deeper and softer alluvium, and were immediately adjacent to an old river channel that had filled with soft silt. The foundation design had to accommodate these soil conditions, or else the two legs on the softer soils would settle more than the other two, causing the tower to tilt toward the river.

Based on his study of the soil conditions, Eiffel placed the foundations for the two legs furthest from the river on the shallow but firm alluvial soils. The bottoms of these foundations were above the groundwater table, so their construction proceeded easily. However, he made the foundations for the other two legs much deeper so they too were founded on firm soils. This required excavating about 12 m below the ground surface (6 m below the groundwater table). As a result of Eiffel's diligence, the foundations have safely supported the tower for more than a century, and have not experienced excessive differential settlements.

Chicago

The advancement of foundation engineering in Chicago also illustrates many of the worldwide changes in practice that occurred during the late nineteenth and early twentieth centuries (Peck, 1999). Rapid population growth and other factors drove a sustained construction boom that, in many ways, made the city a laboratory for new design and construction methods. Chicago is particularly interesting from a geotechnical perspective, because the city is underlain by saturated clay to a depth of about 100 ft. This is a stark contrast to New York City, where competent bedrock is often easily within reach and provides adequate bearing for the large buildings in most of Manhattan.

During the early part of this period, virtually all buildings in Chicago were comparatively small and supported on spread footings. This foundation type continued to be used as the size and weight of buildings increased. A significant advance came in 1873 when Frederick Baumann, a Chicago architect, published the pamphlet *The Art of Preparing Foundations, with Particular Illustration of the "Method of Isolated Piers" as Followed in Chicago* (Baumann, 1873). He appears to be the first to explicitly recommend that the base area of a footing should be proportional to the applied load, and that the loads should act concentrically upon the footing. He also gave allowable bearing pressures for Chicago soils and specified tolerable limits for total and differential settlements.

As buildings became increasingly larger and heavier, foundation settlement became increasingly problematic. The auditorium building, constructed between 1887 and 1889 on spread footings, is one of the most noteworthy examples. Most of the building had a height of 10 stories, but part of it consisted of a 19-story tower, as shown in Figure 1.3.

Figure 1.3 The auditorium building in Chicago experienced 28 in of settlement, but is still in service more than a century after its completion. This structure helped usher in new foundation designs that are less susceptible to settlement.

Although designed according to the state of the art at the time, the tower portion ultimately settled 28 in, with significant differential settlements between the tower and the less heavily loaded areas.

It became clear that spread footings were not adequate for larger buildings, even when designed according to Baumann's guidelines. Driven piles were then used on some buildings, but a new method, the Chicago caisson,[1] was introduced in 1892 by William

[1] In this case, the term "caisson" is being used to describe a foundation that we would classify as a cast-in-place pile. This is quite different from our usage of the term, which describes a method that uses large prefabricated boxes that are sunk into place and filled with concrete.

Sooy-Smith, a former civil war general turned foundation engineer. This method consisted of hand-excavating a cylindrical hole about 1 m in diameter down to harder bearing stratum, then filling the hole with cast-in-place concrete. Local engineers developed methods of designing and building these caissons, which solved the excessive settlement problem and soon became the foundation of choice. Modern high-rise buildings in Chicago, such as the Willis Tower (formerly known as the Sears Tower), still use drilled shafts, which are modern machine-dug versions of the Chicago caisson.

San Francisco–Oakland Bay Bridge

The original San Francisco–Oakland Bay Bridge, constructed between 1933 and 1936, required innovative foundations because of the poor soils conditions and deep water (Husband, 1936). For example, the foundation for one of the piers on the west span extends through an unprecedented 21 m (70 ft) of water, then 43 m (140 ft) of soil (much of it soft clay) to bedrock. This was far too deep for pneumatic caissons, which were the standard method of the day, so legendary foundation engineer Daniel Moran (1864–1937) was retained to help develop new technologies for building these foundations.

Based on Moran's work, several of the piers on both spans were constructed using a new type of massive caisson constructed of concrete and steel in a nearby shipyard. Initially airtight, the caisson was floated to the site, then accurately positioned in place on the bay floor by slowly filling its chambers with water. The underlying soil was then progressively excavated through the chambers using clamshell buckets until reaching the required depth. The caisson was then filled with concrete. In contrast, portions of the bridge near the Oakland shore were in much shallower water and had much shorter spans, so the piers were supported on groups of driven timber piles.

The eastern span was subsequently replaced with a new bridge, which was completed in 2013. Advances in heavy marine driven pile technology over the intervening 80 years, much of which was developed for offshore drilling platforms, resulted in a completely different foundation system. The new bridge is supported on 1.8 to 2.5 m (6–8 ft) diameter steel pipe piles driven with an exceptionally large hydraulic pile hammer to depths of 60 to 100 m (200–330 ft) (Saba et al., 2004). A total of 160 piles were used on the entire project.

1.3 THE FOUNDATION ENGINEER

Foundation engineering does not fit completely within any of the traditional civil engineering subdisciplines. Instead, the foundation engineer must be multidisciplinary and possess a working knowledge in each of the following areas:

- **Structural engineering**—A foundation is a structural member that must be capable of transmitting the applied loads, so we must also understand the principles and practices of structural engineering. In addition, the foundation supports a structure, so we must understand the sources and nature of structural loads and the structure's tolerance of foundation movements.

- **Geotechnical engineering**—All foundations interact with the ground, so the design must reflect the engineering properties and behavior of the adjacent soil and rock. Thus, the foundation engineer must understand geotechnical engineering. Most foundation engineers also consider themselves to be geotechnical engineers.
- **Construction engineering**—Finally, foundations must be built. Although the actual construction is performed by contractors and construction engineers, it is very important for the design engineer to have a thorough understanding of construction methods and equipment to develop a design that can be economically built. This knowledge also provides essential background when solving problems that develop during construction.

This book focuses primarily on the design of foundations, and thus emphasizes the geotechnical and structural engineering aspects. Discussions of construction methods and equipment are generally limited to those aspects that are most important to design engineers. Other important aspects of foundation construction which are primarily of interest to contractors are beyond the scope of this book.

1.4 CODES, STANDARDS, AND TECHNICAL LITERATURE

Foundation design and construction is subject to the provisions of various codes, which define the methods for computing applied loads, the load-carrying capacity of various structural materials, performance requirements, detailing requirements, and other aspects. Some of these provisions are similar to those that apply to other structural members, while others are unique to foundations. Most codes have a separate chapter specifically addressing foundations.

Codes are legally binding, and thus must be followed. The two most commonly used codes in the United States are:

- The International Building Code (IBC), which governs the design of most buildings (ICC, 2012). This code replaced the American model building codes (the Uniform Building Code, the National Building Code, and the Standard Building Code) as well as many local codes. The IBC has legal authority only when adopted by a state, city, or other regulatory authority, and these authorities sometimes include modifications. For example, building construction in California is governed by the California Building Code, which is a modified version of the IBC. Although the IBC and its variants is by far the most commonly used building code in the United States, some parts of the country use different codes. For example, the City of Chicago has its own unique building code.
- AASHTO *LRFD Bridge Design Specifications* (AASHTO, 2012) governs the design of highway structures. The American Association of State Highway and Transportation Officials is a consortium of the various state departments of transportation (DOTs), and thus has substantial influence on state DOT construction projects, as well as those for local governments. These state and local agencies

sometimes modify the AASHTO specifications and add additional requirements. For example, the Washington State Department of Transportation specifies a particular type of concrete be used in all drilled shaft foundations.

Other widely-used codes include:

- Eurocode, which is used in the European Union, typically with country-specific modifications. Eurocode 7 addresses geotechnical design, including foundations.
- The National Building Code of Canada (NBC)
- The National Building Code of India

A number of standards also impact the design and construction of foundations. Unlike codes, standards do not have the force of law (except when explicitly referenced or adopted in a code). However, they have a very significant impact on practice. Applicable standards widely used in North America include:

- The AREMA Manual for Railway Engineering, published by the American Railway Engineering and Maintenance of Way Association. It governs the design of railroad structures in the United States and Canada.
- Various standards published by the American Petroleum Institute (API) which govern facilities used to produce petrochemical products. The most notable of these from a foundation engineering perspective are offshore drilling platforms (API, 2000).
- Minimum Design Loads for Buildings and Other Structures, ASCE/SEI Standard 7-10, published by the American Society of Civil Engineers.
- Building Code Requirements for Structural Concrete (ACI 318-11), published by the American Concrete Institute (ACI, 2011).
- Steel Construction Manual, published by the American Institute of Steel Construction (AISC, 2011).
- Various standards published by the American Society for Materials and Testing (ASTM). These standards typically address test procedures and construction material specifications.

Detailed discussions of the requirements for all of these codes and standards are beyond the scope of this book, and they are constantly changing. Selected provisions from the 2012 IBC and the 2012 AASHTO codes and the ASCE 7-10 and ACI 318-11 standards are included when appropriate and other codes are occasionally referenced. These references are included in brackets. For example, [IBC 1801.1] refers to Section 1801.1 of the IBC. However, this book is not a substitute for codes or standards, so engineers should always refer to the current edition of the applicable publications when designing foundations.

Building codes represent *minimum* design requirements. Simply meeting code requirements does not necessarily produce a satisfactory design, especially in foundation

engineering. Often, these requirements must be exceeded and, on occasion, it is appropriate to seek exceptions from certain requirements. In addition, many important aspects of foundation engineering are not even addressed in the codes or standards. Therefore, think of these publications as guides, and certainly not as a substitute for engineering knowledge, judgment, or common sense.

Finally, foundation engineering has a rich collection of technical literature. Most of this material can be found in professional journals and conference proceedings, as well as in books. This book includes generous references to the technical literature, and the authors encourage the readers to consult technical literature for additional information and insights.

SUMMARY

Major Points

1. Foundations are structural elements that transfer loads from the superstructure to the underlying soil or rock.
2. The central objective of foundation engineering is to design and build foundations that provide reliable support for the superstructure, while avoiding wasteful and expensive over-design.
3. Foundation engineering requires a synthesis of knowledge and skills from geotechnical engineering, structural engineering, and construction engineering.
4. Mankind has been building foundations for millennia, often with very impressive results. Modern foundation engineering began to appear in the late nineteenth century as methods based primarily on precedent and common sense began to be supplemented by rational designs based on the principles of structural mechanics and soil mechanics.
5. Advances in construction methods and equipment have facilitated a much broader range of construction technologies.
6. Foundations are classified into two broad categories: shallow and deep.
7. Foundation designs are subject to the provisions of applicable codes and standards.

Vocabulary

Caisson
Deep foundation
Foundation
Mat
Pile
Shallow foundation
Spread footing

2

Uncertainty and Risk in Foundation Design

In these matters, the only certainty is that nothing is certain.

Pliny the Elder (23 AD–79 AD)

Structural engineering has been defined as "The art of moulding materials we do not really understand into shapes we cannot really analyze, so as to withstand forces we cannot really assess, in such a way that the public does not really suspect" (Brown, 1967, pg. viii). We could apply the same definition, even more emphatically, to foundation engineering. In spite of the many advances in foundation engineering theory, there are still many gaps in our understanding. In a 1985 address at the Eleventh International Conference on Soil Mechanics, Ralph Peck noted that "Uncertainties have always been an inherent part of soil mechanics and its applications," (Peck, 1985). This statement was not likely to have surprised the engineers of 1985 and should not surprise those of the twenty-first century.

Foundation engineers have been dealing with uncertainty and risk since the dawn of geotechnical engineering early in the twentieth century. As Christian points out in his 2004 Terzaghi Lecture (Christian, 2004), there are four ways of dealing with uncertainty: ignoring it, being conservative, using the observational method, or quantifying it. Ignoring uncertainty is a recipe for disaster and no competent engineer would follow this path. Geotechnical engineers have traditionally used a combination of conservatism and the observational method (Peck, 1969) to manage uncertainty and risk. Quantification of geotechnical risk is only just beginning to enter into the standard of care of geotechnical engineering and only for large and difficult projects. In contrast structural engineers have been applying and improving risk mitigation techniques based on quantifying uncertainty

for many decades, and most structural design codes are now based, in part, on some level of quantification of risk and reliability. The differences in structural and geotechnical approaches to risk management reflect differences in the nature of these two disciplines. Since foundation engineering is a melding of these two disciplines, the foundation engineer must understand how each discipline manages risk in order to manage the risks in foundation engineering. This chapter is intended to provide a short introduction to probability theory and how it is applied to characterize the uncertainty of foundation design and help the engineer to design foundations with an acceptable level of risk.

2.1 SOURCES AND TYPES OF UNCERTAINTY

Traditionally, engineers have treated material properties such as the undrained shear strength of a soil, or the unconfined compressive strength of concrete as deterministic variables. That is, the material property has a specific value if it could just be determined accurately. However, any engineer who has looked at a boring log or data from a Standard Penetration Test is keenly aware that there is significant uncertainty in determining soil properties. Similarly, we always select a model for the behavior of engineering systems, whether rational or empirical, such as Terzaghi's bearing capacity theory for the behavior of shallow foundations on soils or Euler's buckling theory for the capacity of axially loaded columns. Our observations of real structures tell us that these models contain significant uncertainty.

In dealing with uncertainty, it is helpful to distinguish two broad sources or categories of uncertainty. The first are those uncertainties associated with the inherent randomness of nature and is called *aleatory* uncertainty. For example, the undrained shear strength in a certain soil stratum beneath a site varies both spatially (at different points) and temporally (at different times). If we obtain a finite number of soil samples and determine the shear strength of these samples using "perfectly correct" methods, we could then use this information to estimate a strength value to a particular point in this stratum. The difference between this strength and the actual strength at that point is the aleatory uncertainty. This uncertainty can be reduced by taking more samples, but can never be eliminated.

Figures 2.1 and 2.2 present examples of aleatory uncertainty. Figure 2.1 presents the variability of measured unconfined compressive strength of sandstone at a particular foundation site. Figure 2.2 presents the variability of unit weight of a soil compacted as the subgrade for a road. Each of these figures clearly shows a variability in the soil properties that is due to the randomness of the processes that created these materials. A key characteristic of aleatory uncertainty is that no amount of observation or testing can eliminate this uncertainty—its existence is part of the nature of these materials. In the case of these two soils, if we took more samples and performed more tests or used more accurate test methods, we might slightly improve our estimates of the underlying distributions shown in Figures 2.1 and 2.2, but we could not eliminate the inherent variability of these soil properties.

The second category includes uncertainties due to our imperfect knowledge of a system or process; this category is called *epistemic* uncertainty. One example of epistemic

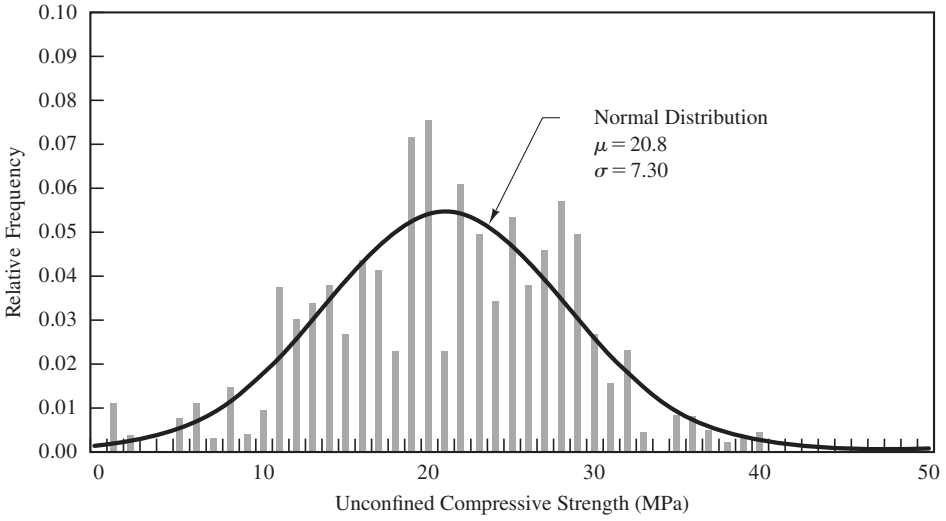

Figure 2.1 Histogram and the corresponding normal distribution of unconfined compressive strength of sandstone sampled at the Confederation Bridge site, Canada (data from Becker et al., 1998).

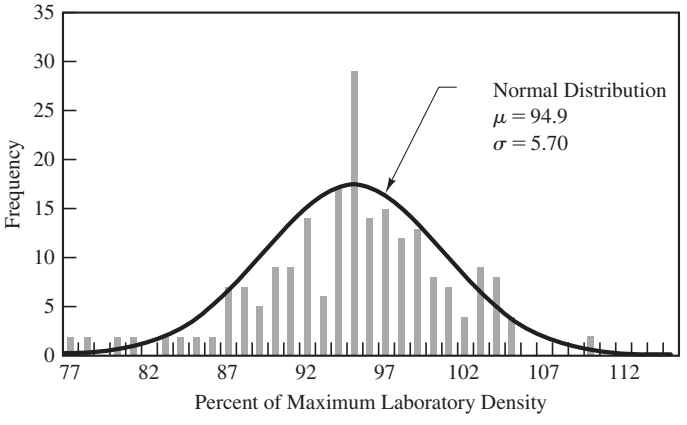

Figure 2.2 Histogram and the corresponding normal distribution of dry unit weight of a compacted soil at a road site in Los Alamos, New Mexico (data from Petit, 1967).

uncertainty is pile capacity determined by the dynamic test methods discussed in Chapter 19, which relate the number of hammer blows required to drive a pile a certain distance with the static capacity of the pile. The earliest models for pile-driving behavior, from the nineteenth and early twentieth century, were pile-driving formulas. As discussed in Section 19.1, these formulas proved to be wildly inaccurate. The development of wave equation analysis in the mid-twentieth century, computers in the late-twentieth century, and high-speed digital data

acquisition in the twenty-first century have improved our knowledge about the dynamics of pile driving and greatly reduced the uncertainty associated with predicting pile capacity from hammer blow counts, as discussed in Section 19.2. A key characteristic of epistemic uncertainty is that it can be reduced by gathering more or better information, or by improving our processes or models. Uncertainties in measured soil properties due to sample disturbance or testing errors are other examples of epistemic uncertainty. In these situations the uncertainty of the measured soil properties can be reduced by developing better sampling and testing techniques.

It is important to distinguish between aleatory and epistemic uncertainty because we must deal with them differently in the design process. Since aleatory uncertainties are naturally occurring and cannot be eliminated, it is critical that we identify them early in the design process and properly characterize them. However, once they are properly characterized, their uncertainty must be accepted in the design process. There is no point in expending additional money investigating aleatory uncertainties since gathering more information will not reduce them. Epistemic uncertainty, in contrast, can be reduced by gaining more knowledge, either through better theories, models, and test methods or by gathering more information. When faced with epistemic uncertainty in the design process, the expenditure of additional money to gather more information can reduce the uncertainty and its associated risk. This gives the designer the opportunity to evaluate the cost of the additional information against the benefit of having it.

2.2 PROBABILITY THEORY

Whether the source of uncertainty is aleatory or epistemic, we can characterize it using the mathematics of probability theory. This section presents a brief overview of probability theory for the limited purposes of this book. A more complete discussion of the subject is available in many textbooks on probability, such as Benjamin and Cornell (1970) or Ang and Tang (2007).

Basic Elements of Probability

Probability theory starts with the concept of *probability space* or *sample space* which is a set of all possible outcomes for an event and commonly denoted as Ω. For example, the sample space for the toss of a fair die is $\Omega = [1, 2, 3, 4, 5, 6]$. This is a *discrete sample space* in that the event can take on only a finite number of defined values. The sample space for the undrained shear of a given soil would be $\Omega = [0 - \infty]$. This is an example of a *continuous sample space* in that the undrained shear strength can take on any one of an infinite number of values between zero and infinity. An *event*, usually denoted as E, is a subset of the sample space, Ω, and a possible outcome of a process or system. For example, an event might be the roll of a die coming up as 3 or the value of an undrained shear strength test being 123.7 kPa. Variables that can take on multiple values within a sample space are called *random variables*. They can be either discrete or continuous depending upon the nature of the sample space.

The *probability function* is a procedure for determining the probability of events. Every event must have a probability between 0 and 1 inclusive. An impossible event has a probability of 0 and a certain event has a probability of 1. The probability of all possible events must be 1. For a discrete random variable the probability function is called the *probability mass function* (PMF) and denoted as $p(x)$. For the roll of a fair die, the PMF is

$$p(x) = \frac{1}{6} \tag{2.1}$$

That is, each of the possible outcomes (1, 2, 3, 4, 5, or 6) has the same probability of 1/6. The probability of an event E, denoted as $P(E)$, is the sum of $p(x)$ for all x contained in E or

$$P(E) = \sum_{x \in E} p(x) \tag{2.2}$$

Using Equation 2.2, the probability of all possible outcomes of the roll of a die is

$$P(x \in \Omega) = \frac{1}{6} + \frac{1}{6} + \frac{1}{6} + \frac{1}{6} + \frac{1}{6} + \frac{1}{6} = 1 \tag{2.3}$$

For continuous random variables, the probability function is called the *probability density function* (PDF) and denoted as $f_X(x)$. For continuous variables, the probability of an event E is written as

$$P(E) = \int_{x \in E} f_X(x)\, dx \tag{2.4}$$

And the probability of all possible outcomes is

$$P(x \in \Omega) = \int_{\Omega} f_X(x)\, dx = 1 \tag{2.5}$$

For a continuous random variable, there is no probability that the variable takes on a specific value since there are an infinite number of possible values. We can only compute the probability that the variable takes on a value within a specific range. For example, the probability that the undrained shear strength is between 20 and 50 kPa is computed as

$$P(20 \leq x \leq 50) = \int_{20}^{50} f_X(x)\, dx \tag{2.6}$$

The *cumulative distribution function* (CDF), denoted as $F_X(x)$, is the probability that the random variable, X, takes on a value less than x. For continuous random variables, the CDF is

$$F_X(x) = \int_{-\infty}^{x} f_X(x)\,dx \tag{2.7}$$

Figure 2.3 shows (a) the PDF and (b) the CDF for the undrained shear strength of a soil. The hatched area of Figure 2.3a is the probability that the shear strength is between the values a and b. The dashed lines in Figure 2.3b show the probability that the shear strength is less than a or less than b.

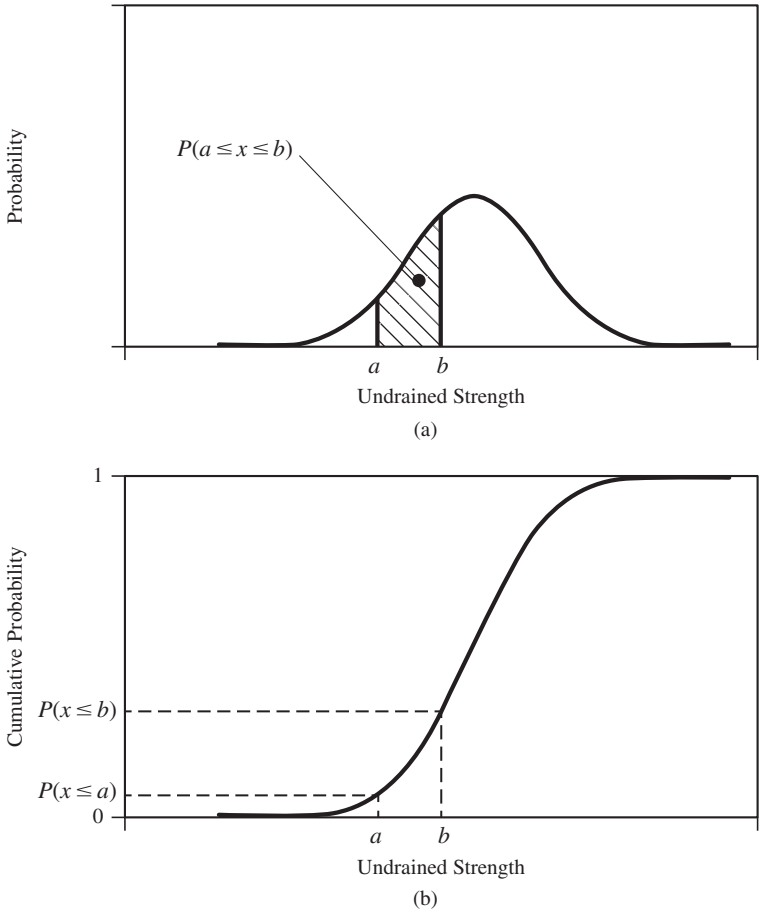

Figure 2.3 (a) Probability distribution function (PDF) and (b) cumulative distribution function (CDF) for undrained strength assuming a normally distributed random variable.

Mathematical Expectation

While a random variable can take on any value in the sample set, it is more likely to take on some values than others. In Figures 2.1 and 2.2, we see that more samples occur in the center of the distribution for each variable. If we take many, many samples, we will observe a central tendency or value that is most likely to occur. This value is called the expected value or *mean* or *average* of the random variable and denoted as μ. Mathematically, the mean is

$$\mu_X = \int_{-\infty}^{\infty} x f_X(x)\, dx \tag{2.8}$$

We should note that Equation 2.8 is also the equation for the center of mass of the PDF, so another interpretation of the mean of a random variable is the location of the centroid of the PDF for that variable.

Dispersion or Variability

Another important characteristic of a random variable is how much dispersion or variability there is around the mean value. We measure this dispersion by the *standard deviation* of the random variable, denoted as σ. The standard deviation is computed from the PDF as

$$\sigma_X = \sqrt{\int_{-\infty}^{\infty} (x - \mu_X)^2 f_X(x)\, dx} \tag{2.9}$$

The standard deviation will be in the units of the original variable. It is often valuable to have a normalized version of the standard deviation which can be used to compare the dispersion of two or more random variables that may be measured in different units. The normalized version of the standard deviation is called the *coefficient of variation* (COV) and defined as

$$\text{COV} = \frac{\sigma_X}{\mu_X} \tag{2.10}$$

which is simply the standard deviation normalized by the mean.

Figure 2.4 illustrates three different PDFs and their corresponding CDFs. All three distributions have different means, with $\mu_1 < \mu_2 < \mu_3$. Distributions 1 and 2 have the same standard deviation. However, $\text{COV}_1 > \text{COV}_2$ because $\mu_1 < \mu_2$. The standard deviation of distribution 3 is less than that of distributions 1 or 2.

Useful Probability Density Functions

There are a number of PDFs that are particularly useful in engineering. We will cover only the *normal distribution* and the *log-normal distribution* for illustration in this chapter.

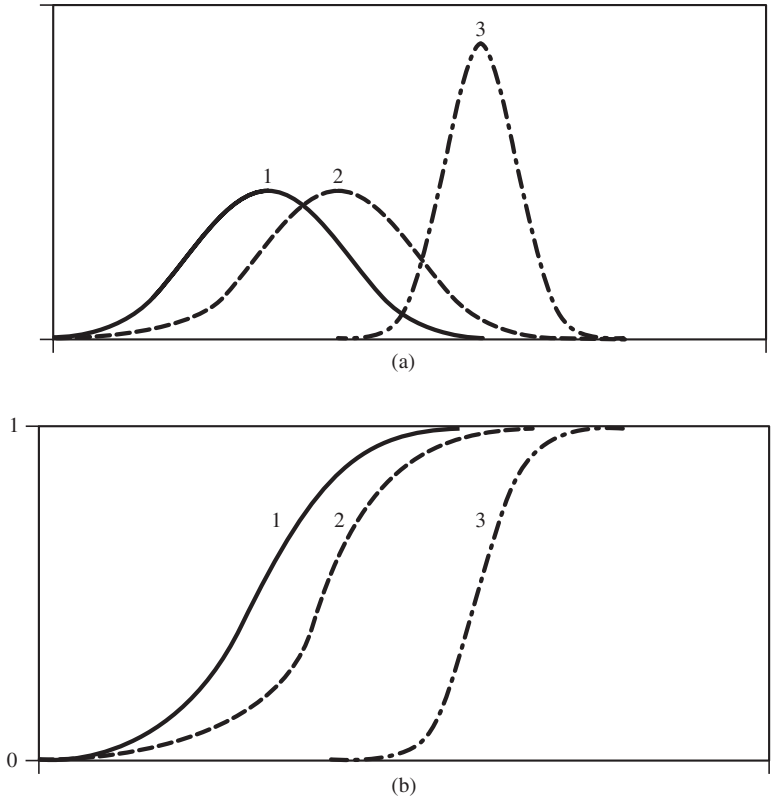

Figure 2.4 (a) Probability distribution function (PDF) and (b) cumulative distribution function (CDF) for three normally distributed random variables.

Normal or Gaussian Distribution

A common PDF is the normal, or Gaussian, distribution. Figure 2.3a illustrates what the PDF for undrained shear strength might look like if s_u was a normally distributed random variable. The equation for the normal PDF is

$$f_s(s_u) = \frac{1}{\sigma_s\sqrt{2\pi}} \exp\left[-\frac{1}{2}\left(\frac{s_u - \mu_s}{\sigma_s}\right)^2\right] \tag{2.11}$$

where

μ_s = mean of the random variable s_u
σ_s = standard deviation of the random variable s_u

Figure 2.3b illustrates the CDF for the normal distribution. The CDF is related to the PDF by Equation 2.7. Therefore, the CDF for the normal distribution is

$$F_s(s_u) = \int_{-\infty}^{s_u} \frac{1}{\sigma_s\sqrt{2\pi}} \exp\left[-\frac{1}{2}\left(\frac{s_u - \mu_s}{\sigma_s}\right)^2\right] ds_u \tag{2.12}$$

There is no closed form solution for Equation 2.12. It must be evaluated numerically or looked up in tables. Note that the CDF must have a value from 0 to 1 since a probability of 1 represents a certain event and that it must be monotonically increasing from $-\infty$ to ∞.

A normal distribution with a $\mu = 0$ and $\sigma = 1$ is called the *standard normal* distribution and has a PDF of

$$f_X(x) = \frac{1}{\sqrt{2\pi}} e^{-\left(\frac{1}{2}\right)x^2} \tag{2.13}$$

The CDF for the standard normal distribution is commonly designated as $\Phi(X)$ or

$$\Phi(x) = F_X(x) = \int_{-\infty}^{x} \frac{1}{\sqrt{2\pi}} e^{-\left(\frac{1}{2}\right)x^2} dx \tag{2.14}$$

Values of standard normal distribution CDF are presented in Table B.1 (see Appendix B). The standard normal distribution can be used to compute probabilities for any normally distributed variable using Equation 2.15.

$$P(X \leq a) = \Phi\left(\frac{a - \mu_X}{\sigma_X}\right) \tag{2.15}$$

where

X = normally distributed random variable with a mean of μ_x and standard deviation of σ_x

Using experimental data, we can estimate the probability density function of a random variable. For example, Figures 2.1 and 2.2 show, in addition to the histogram of measured values, the normal distribution estimated from those measured values. Note that the PDF estimated from the measured values does not exactly match the measured histogram. The difference between the measured values and the estimated PDF is due to sampling error, the discussion of which is beyond the scope of this text. What is important to understand is that there is uncertainty in our estimate of the mean and standard deviation of a variable.

Example 2.1

From the compaction data shown in Figure 2.1 we can estimate the mean and standard deviation of the underlying distribution. Assuming that relative compaction is normally distributed, the estimated mean is 94.9 percent and the estimated standard deviation is 5.7. Assuming these values represent the true mean and standard deviation of relative compaction, we can compute the probability that the soil compacted at a given location in the field is less than 90 percent relative compaction.

Solution

$$P(x \leq 90\%) = \Phi\left(\frac{90 - 94.9}{5.7}\right)$$
$$= \Phi(-0.860)$$

We note that Table B.1 shows values only for $x \geq 0.5$. However, since the normal distribution is symmetric, $\Phi(-x) = 1 - \Phi(x)$, so

$$P(x \leq 90\%) = 1 - \Phi(0.860)$$

From Table B.1,

$$\Phi(0.860) = \mathbf{0.8051}$$

And the probability of one soil sample having relative compaction less than 90 percent is $P(x \leq 90\%) = 1 - 0.8051 = \mathbf{19.49}\%$

Log-normal Distribution

There are two major shortcomings of the normal distribution. One of the shortcomings is that it is symmetric. A second shortcoming is that the normal distribution allows for negative values, particularly when the COV is large. In practice we often see distributions of random variables that are skewed or wish to fit a PDF to a quantity that cannot be negative. An example common in geotechnical is illustrated in Figure 2.5, which presents data for the tangent of the residual friction angle for a mudstone taken from a series of lab tests. Since the friction angle cannot take on a value less than zero, the distribution is generally skewed as shown in Figure 2.5. We can fit such data with a log-normal distribution, which is simply a normal distribution of the natural log of the original variable. That is, if X is

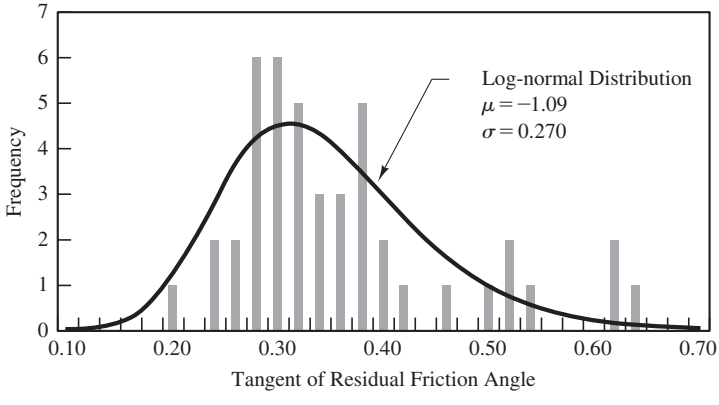

Figure 2.5 Histogram of tangent of residual friction angle of mudstone at the Confederation Bridge site, Canada (data from Becker et al., 1998).

log-normally distributed, then $Y = \ln X$ is normally distributed. It follows then that the probability that X is less than a can be computed using the standard normal CDF, Φ, in the following form

$$P(X < a) = \Phi\left(\frac{\ln a - \mu_{\ln X}}{\sigma_{\ln X}}\right) \tag{2.16}$$

Figure 2.5 shows the PDF of the log-normal distribution fit to the data presented.

Functions of Normally and Log-normally Distributed Random Variables

We can also write functions of random variables, and the result of a function of random variables will, itself, be a new random variable. An important characteristic of normally distributed random variables is that a linear function of the random variables will also be normally distributed. Specifically, if $Z = aX + bY$, where a and b are constants, and X and Y are normally distributed and independent (uncorrelated) random variables, then Z will also be normally distributed with the following parameters.

$$\mu_z = a\mu_X + b\mu_Y \tag{2.17}$$

$$\sigma_z = \sqrt{a^2\sigma_X^2 + b^2\sigma_Y^2} \tag{2.18}$$

As an example, let us consider the bearing capacity of a simple footing. It will be shown in Chapter 7 that the nominal bearing capacity, q_n, of a continuous footing founded on a saturated clay under undrained conditions is

$$q_n = 5.7s_u + \gamma D \tag{2.19}$$

where

s_u = undrained shear strength of the soil
γ = unit weight of the soil
D = depth of the footing

If we assume the depth of the footing, D, is known and both undrained shear strength, s_u, and the unit weight of the soil, γ, are normally distributed random variables with means of μ_s and μ_γ, and standard deviations of σ_s and σ_γ, then, the nominal bearing capacity is also a normally distributed random variable. If s_u and γ are statistically independent (not correlated), then the mean and standard deviation of the nominal bearing capacity, q_u, are

$$\mu_q = 5.7\mu_s + D\mu_\gamma \tag{2.20}$$

$$\sigma_q = \sqrt{5.7^2\sigma_s^2 + D^2\sigma_\gamma^2} \tag{2.21}$$

And the nominal bearing capacity, q_u, will also be normally distributed. It is always the case that a linear function of normally distributed variables is itself a normally distributed random variable. In a similar fashion, it can also be shown that the multiple of two or more log-normally distributed variables will also be log-normally distributed.

Example 2.2

Assume we are building a foundation on a saturated clay deposit with an average undrained shear strength of 2,000 lb/ft^2 and a COV of 0.2. The average unit weight for the soil is 102 lb/ft^3 with a COV of 0.05. What is the mean short-term nominal bearing capacity of a continuous footing founded at a depth of 5 ft? What is the probability that the nominal bearing capacity of a certain footing would be less than 75 percent of the mean nominal bearing capacity if the undrained shear strength and unit weight are normally distributed and independent?

Solution

Using Equation 2.17, we compute the mean nominal bearing capacity as

$$\begin{aligned}\mu_{q_n} &= 5.7(2{,}000) + 5(102)\\ &= 11{,}910 \text{ 1b/ft}^2\end{aligned}$$

To compute the standard deviation of nominal bearing capacity, we must first compute the standard deviations of the undrained shear strength and unit weight from their COVs using Equation 2.10:

$$\begin{aligned}\sigma_{s_u} &= 0.2(2{,}000)\\ &= 400 \text{ 1b/ft}^2\\ \sigma_\gamma &= 0.05(102)\\ &= 5.1 \text{ 1b/ft}^3\end{aligned}$$

Using Equation 2.18, we compute the standard deviation of the nominal bearing capacity as

$$\begin{aligned}\sigma_{q_n} &= \sqrt{5.7^2(400)^2 + 5^2(5.1)^2}\\ &= 2{,}280 \text{ 1b/ft}^2\end{aligned}$$

We can then compute the probability that the nominal bearing capacity is less that 75 percent of the mean value ($0.75 \times 11{,}910 = 8{,}933$) using Equation 2.15:

$$\begin{aligned}P(q \le 8{,}933) &= \Phi\left(\frac{8{,}933 - 11{,}910}{2{,}280}\right)\\ &= \Phi(-1.31)\\ &= 1 - \Phi(1.31)\end{aligned}$$

Using Table B.1,

$$\begin{aligned}P(q \le 8{,}933) &= 1 - 0.90490\\ &= \mathbf{0.0951 \text{ or } 9.51\%}\end{aligned}$$

2.3 FAILURE, RELIABILITY, AND RISK

The primary objective of the design engineer is to protect the health and safety of the public (IBC [101.2], AASHTO [2.5.1]). To accomplish this objective the engineer must design a structure such that the risk of a person occupying a building or traveling over a bridge is acceptably small. Even stating this objective implies that there is some risk in using a building or bridge. We all take many risks each day. But what exactly is risk?

According to dictionaries, risk is "possibility of loss or injury" (Merriam-Webster online), or "exposure to the chance of injury or loss" (Dictionary.com). These two definitions identify two key aspects, or components, of risk. The first is that there is uncertainty in risk, identified by the words "possibility" and "chance" in the definitions. The second component is a cost (loss or injury) that one may incur should we be subject to an undesirable event. Therefore, we see that risk is a combination of probability of some loss and the cost of that loss.

In terms of foundation engineering, the probability of loss is the probability that a structure will fail or simply the *probability of failure*, P_f. The *reliability, R,* is simply the complement of the probability of failure.

$$R = 1 - P_f \tag{2.22}$$

Since risk includes both the cost of failure and the probability of failure, we will define risk as the product of the probability of failure and cost of failure.

$$\text{Risk} = P_f\,(\text{Cost of Failure}) \tag{2.23}$$

Formulating the Probability of Failure: Safety Factor and Safety Margin

If we are to compute risk we must first be able to compute the probability of failure. This will require a mathematical formulation for P_f. There are two common ways of quantifying the acceptability of a structure as it relates to risk. One is the *factor of safety, F*, which is the ratio of the capacity of a structure to the demand placed on the structure.

$$F = \frac{\text{Capacity}}{\text{Demand}} \tag{2.24}$$

In this formulation, the structure has failed when F is less than or equal to one and the probability of failure is

$$P_f = P(F \leq 1) \tag{2.25}$$

An alternative to the factor of safety is the *safety margin, m*, which is the difference between capacity and demand.

$$m = \text{Capacity} - \text{Demand} \tag{2.26}$$

In this formulation, the structure has failed when m is less than or equal to zero and the probability of failure is

$$P_f = P(m \leq 0) \tag{2.27}$$

Either formulation of the probability of failure, Equation 2.25 or 2.27, can be used to compute the probability of failure so long as a PDF can be determined for the factor of safety, F, or the safety margin, m. As an example, we will compute the probability of failure of the footing in Example 2.2 for a certain loading.

Example 2.3

Compute the probability of failure of the footing in Example 2.2 assuming it is subject to an applied bearing stress, q, with a mean of 3,500 lb/ft^2 and standard deviation of 800 lb/ft^2.

Solution

Since the applied bearing stress, q, and the nominal bearing capacity, q_n, are both normally distributed, we will use the safety margin, m, to compute the probability of failure since it is a linear function of q and q_n and will, therefore, also be normally distributed.

$$m = q_n - q$$

Using Equation 2.17, we compute μ_m as

$$\mu_m = 11{,}910 - 3{,}500 = 8{,}410 \text{ lb/ft}^2$$

Using Equation 2.18, we compute σ_m as

$$\sigma_m = \sqrt{2{,}280^2 + 800^2} = 2{,}416 \text{ lb/ft}^2$$

Using Equation 2.15, we compute the probability that the safety margin is less than zero as

$$\begin{aligned} P(m \leq 0) &= \Phi\left(\frac{0 - 8{,}410}{2{,}416}\right) \\ &= \Phi(-3.48) = 1 - \Phi(3.48) \\ &= 2.5 \times 10^{-4} \end{aligned}$$

So $\boldsymbol{P_f = 2.5 \times 10^{-4}}$ **or the reliability of the foundation would be 99.975 percent.**

Acceptable Levels of Risk

We have shown a way to compute the probability of failure, at least for simple problems. If we can then estimate the loss should a failure occur, we can compute the risk of that failure. For example, if the failure of the footing in Example 2.3 caused the collapse of a

building which would cost the owner \$20 million from law suits and \$10 million to rebuild the building, then the risk to the owner, would be \$30 million times 2.5×10^{-4} or \$7,500. The question that remains is, "is this an acceptable risk?" The answer to this question is clearly subjective and depends upon the person or group taking the risk.

One method used to evaluate the acceptability of a certain level of risk is to examine the risks that society finds acceptable. This is often done with the use of an F-N diagram which is a plot of annual probability of an event as a function of the total deaths caused by the event. Figure 2.6 shows F-N data for both natural and man-made causes. In these F-N diagrams the cost of failure is measured in equivalent lives lost. Note that as the number of lives lost increases the probability of occurrence decreases. The probability axis is displayed as an annual probability. Therefore, the cumulative probability over the life of a civil engineering structure (40–100 years) will be higher than that shown. F-N diagrams are useful in that they are objective measures of the risks humans face daily. It is interesting to note, for example, that the probability of dying from an accident at a nuclear plant is about the same as the probability of dying from a meteorite strike, and both are 3 to 4 orders of magnitude less likely than any other of the hazards shown in Figure 2.6.

Data like those shown in Figure 2.6 show us what the current risks are from certain events, but they do not necessarily tell us that these historical risks are acceptable. Acceptability of risks must be interpreted through public reaction and governmental response to failures. A number of regulatory agencies or governmental bodies have used the F-N format and historic risk data to develop design guidelines for major projects. Figure 2.7 shows such guidelines developed by two governmental agencies (Hong Kong

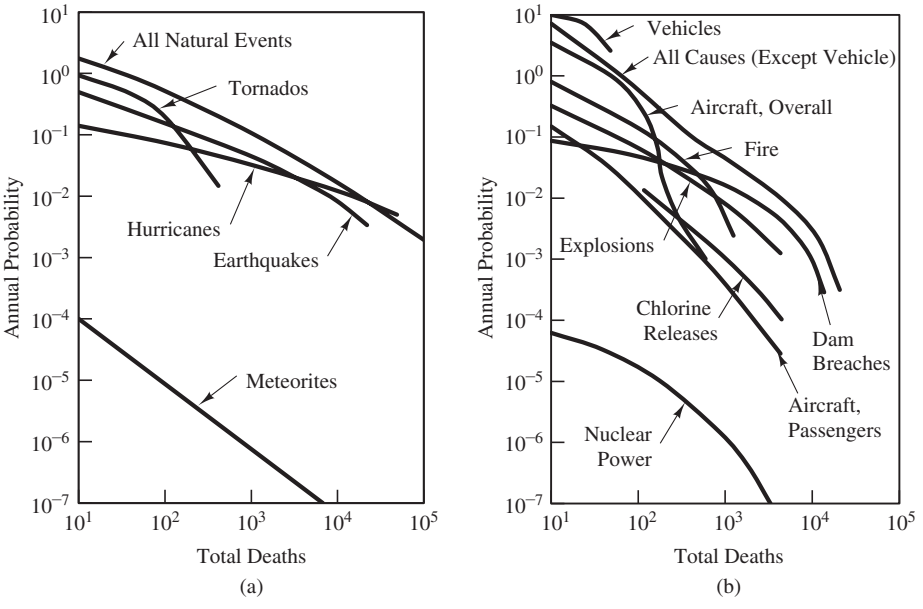

Figure 2.6 F-N diagrams for (a) natural events and (b) man-made causes (data from Proske, 2004).

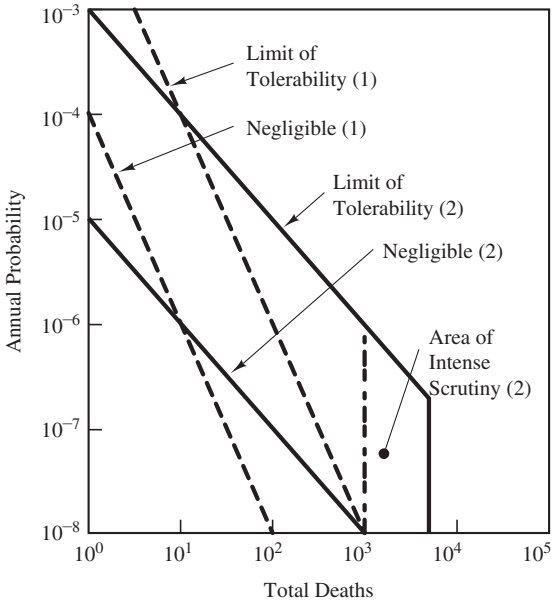

Figure 2.7 F-N diagrams used by (1) Denmark and (2) Hong Kong to evaluate the acceptability of project risk (data from Jan Duijm, 2009 and Govt. of Hong Kong, 1998).

and Denmark). The guidelines each have an upper bound above which the risk is unacceptable and a lower bound below which the risk is deemed acceptable. In the region between the bounds, designers must take action to mitigate the risk to make it "as low as reasonably practicable" (Govt. of Hong Kong, 1998). Typically such guidelines are used only for major projects, such as large earth dams, nuclear power plants, or major chemical plants, which have the potential to cause a large number of deaths if a failure occurs.

For foundations for typical structures not warranting special analysis, there seems to be a consensus that the appropriate probability of failure for design should be 10^{-3} to 10^{-4} or 0.1 to 0.01 percent (Ellingwood et al., 1980; Meyerhof, 1994; Phoon et al., 1995; Paikowsky, 2004). This guidance does not distinguish the cost of failure and, therefore, does not constitute a true risk evaluation. It should be assumed this range of failure probability is for typical structures. Structures with high consequences of failure should be designed for probabilities of failure at the low end of this range or even lower.

2.4 APPLYING RELIABILITY THEORY IN PRACTICE

Reliability-Based Design

Reliability-based design is a design method where the engineer determines the estimated probability of failure of a proposed design and uses that probability of failure, along with estimated failure costs, to determine the adequacy of the design. If we have statistical characterizations of applied loads, the material strengths, and the uncertainties in the analysis process, it is possible to compute the probability of failure of a given structural

or geotechnical design using structural reliability theory. Techniques for performing such computations have been developed over the past 20 to 30 years and are regularly used for expensive, complex, and high-risk facilities, such as off-shore platforms and nuclear power plants. However, such methods are complex and time consuming. It is not yet practical to use reliability-based design for routine projects and these methods are not covered in this text. Those interested in such methods are referred to one of the many texts on the subject, such as Madsen et al. (1985), Melchers (1999), or Baecher and Christian (2003).

Deterministic Safety Factor-Based Methods

The two most common design methods used in foundation design are *allowable stress design* (ASD) and *load and resistance factor design* (LRFD). Both these methods use factors of safety to ensure the appropriate reliability of foundation designs. However, they are both deterministic, that is, they do not explicitly include any random variables or probability computations in their application. In this section, we will describe how reliability is incorporated into these methods and some of their limitations. The application of these methods to design is covered in some detail in Chapter 5.

Allowable Stress Design

ASD uses a single factor of safety, F, to ensure the reliability of a design. This is done using the equation

$$D < \frac{C}{F} \tag{2.28}$$

where

C = capacity
D = demand

In Equation 2.28, we are using the terms demand and capacity in a general sense to denote any particular part of a foundation or a foundation system. The factor of safety is always greater than one. It must account for uncertainties in the demand (loads) placed on the system, the uncertainty of strength of materials used, and uncertainty in the analysis methods used to compute the capacity.

ASD methods have been used since the nineteenth century in engineering design. Traditionally, the required factor of safety was determined empirically, based on experience. The process of determining adequate factors of safety based on experience is time consuming and inexact. Initially, high factors of safety were used until a foundation system was used many times and experience gained. If performance was good, the factor of safety might be reduced. When failures occurred, the conditions were analyzed and the required factor of safety adjusted. Over many decades of experience, enough experience and knowledge was gained to determine a factor of safety that proved adequate.

The ASD system has proved to be a reasonable method to design reliable foundation systems for well over 50 years. As noted in Section 2.3, researchers have estimated that foundations designed with this system generally have a probability of failure of 10^{-4} to 10^{-3}. It is possible to calibrate the ASD factor of safety using probabilistic measurements as shown in Example 2.4.

Example 2.4

A certain pile has a mean capacity of 800 kN as computed with design method A. A statistical analysis of a number of piles designed with this method indicates that the COV for this method is 0.45. The downward demand placed on this pile has a mean value of 250 kN. Based on loads in similar applications, the COV of the demand is estimated to be 0.27. Compute the factor of safety, based on mean values, and the probability of failure of this pile assuming capacity and demand are independent and normally distributed.

Solution

Based on mean values the factor of safety is simply the mean capacity divided by the mean resistance.

$$F = \frac{\mu_C}{\mu_D} = \frac{800}{250} = 3.2$$

To compute the probability of failure, we will first compute the mean and standard deviation of the safety margin, then compute the probability that the safety margin is less than zero. First we compute the mean and standard deviation of the safety margin, $m = C - D$.

$$\begin{aligned}
\mu_m &= \mu_C - \mu_D = 800 - 250 = 550 \\
\sigma_D &= \mathrm{COV}_D(\mu_D) = 0.2(250) = 50 \\
\sigma_C &= \mathrm{COV}_C(\mu_C) = 0.35(800) = 280 \\
\sigma_m &= \sqrt{\sigma_C^2 + \sigma_D^2} = \sqrt{50^2 + 280^2} = 284
\end{aligned}$$

And the probability m is less than or equal to 0 is

$$\begin{aligned}
P(m \le 0) &= 1 - \Phi\left(\frac{550}{284}\right) = 1 - \Phi(1.93) \\
&= \mathbf{0.026}
\end{aligned}$$

Commentary

This probability of failure of 0.026 (2.6%) is quite high. If the foundation was dependent upon this single pile, it would not be acceptable. However, if this pile was part of a pile group, as is common, the failure of a single pile would not necessarily cause the failure of structure. In this case the reliability of the pile system would be much higher than the reliability of a single pile. Ultimately, it is the system reliability that is of concern to us. However, this topic is beyond the scope of this chapter.

Example 2.5

For the pile described in Example 2.4, compute the factor of safety required to achieve a target probability of failure of 0.01.

Solution

To determine the required factor of safety, we will determine what mean pile capacity is required to meet the target probability of failure assuming our pile demand is 250 kN and the COVs are as stated in Example 2.4. If we do this, we can write the following equation for the probability of failure.

$$P(m \leq 0) = 0.01 = 1 - \Phi\left(\frac{\mu_C - 250}{\sqrt{(0.35\mu_C)^2 + 50^2}}\right)$$

Using an iterative solution we determine $\mu_C = 1{,}378$ kN and the factor of safety is then

$$F_{req} = \frac{1{,}378}{250} = \mathbf{5.5}$$

While it is possible to determine the required factor of safety using the method shown in Example 2.5, that is not the way required factors of safety have been determined historically. This is mainly due to the lack of statistical data on geotechnical capacity. Additionally, the method relies on a single factor of safety, it is not very flexible. The single factor of safety, by necessity, is controlled by the weakest link in the system. Parts of the system will be over-designed when a single factor of safety is used. As the geotechnical data needed to evaluate the reliability of foundations has gradually become available, it has been applied in the LRFD format because of the advantages it has over the ASD format.

Load and Resistance Factor Design

Like the ASD method, the LRFD method is a deterministic design method. There are two key distinctions between the methods that are important from a reliability standpoint. The first is that LRFD uses multiple partial factors of safety rather than a single global factor of safety. LRFD has the form

$$\sum \gamma_i D_i < \phi C \tag{2.29}$$

where

D_i = a certain demand (dead load, live load, wind load, etc.)
γ_i = load factor or partial safety factor for the demand
ϕ = resistance factor or partial safety factor for the capacity

In the case where the demand consists of a dead load and live load component, there would be three partial safety factors in Equation 2.29, γ_{dead}, γ_{live}, and ϕ. The load factors, γ, are used to account for the uncertainty in the different demands (both magnitude and location) and the resistance factor, ϕ, is used to account for the uncertainty in the geotechnical material properties and the analysis process used to determine the capacity.

The second important distinction is that the load and resistance factors in LRFD are selected based on a probabilistic analysis rather than on past experience. The processes of calibrating LRFD for a certain foundation system starts with determining the target reliability (or probability of failure) and collecting sufficient statistical data to characterize the uncertainty of the loads and the uncertainty of the material properties and analysis methods. Once we have this information we can use an optimization process to compute the required load and resistance factors to achieve the target reliability. The process is similar, in concept, to Example 2.5, but much more complicated because we now have three (or more) different partial safety factors that must be optimized simultaneously. The great advantage of using the LRFD method rather than the ASD method in doing this calibration is that it will generate designs where the probability of failure is consistent across different load combinations and different failure mechanisms.

SUMMARY

Major Points

1. All of the inputs to foundation design, loads, material properties, and analysis methods are uncertain to some degree.
2. Two types of uncertainty are aleatory uncertainty, due to natural randomness of things, and epistemic uncertainty, due to our lack of knowledge about things.
3. Using the tools of probability theory we can characterize the uncertainty of our design inputs and estimate the probability of failure of foundation systems.
4. The reliability of a system is the complement of the probability of failure.
5. Risk is the probability of failure times the consequence or cost of failure.
6. Acceptable risks are generally determined based on society's reaction to and tolerance of the consequences of failure. The F-N diagram is a useful way to present this information.
7. The historic probability of failure of foundation systems is estimated to be between 10^{-3} to 10^{-4}, which corresponds to a reliability of 0.999 to 0.9999.
8. ASD uses a single factor of safety to determine acceptable designs and the required factor of safety has generally been determined empirically through observed performance of structures without probabilistic analysis.
9. LRFD uses multiple partial factors of safety (load and resistance factors) to determine the acceptability of designs, and the required partial factors of safety have been determined using probabilistic methods in order to achieve a target reliability.

Vocabulary

Aleatory uncertainty
Allowable stress design (ASD)
Coefficient of variation (COV)
Cumulative distribution function (CDF)
Epistemic uncertainty
Load and resistance factor design (LRFD)
Log-normal distribution
Mean
Normal distribution
Probability density function (PDF)
Probability of failure
Random variable
Reliability
Reliability-based design
Risk
Safety margin
Standard deviation

QUESTIONS AND PRACTICE PROBLEMS

Section 2.1: Types of Uncertainty

2.1 Classify the uncertainty associated with the following items as either aleatory or epistemic and explain your reason for your classification: average wind speed over a 30-day period, location of a certain applied load, change in strength of a soil caused by sampling method, capacity determined by a certain analysis method, magnitude of live load caused by vehicles traveling on a bridge, soil shear strength as measured by a certain method.

2.2 Figure 2.1 shows the PDF for a normal distribution determined from the unconfined compression tests shown in the histogram. Does the mean and standard deviation of this PDF represent aleatory or epistemic uncertainty? Explain.

2.3 List three sources of epistemic uncertainty associated with determining the soil strength at a given site and describe how you might reduce these uncertainties.

2.4 Using a random number generator create a sample of four relative densities using the PDF presented in Figure 2.2. Repeat the exercise to create three different sample sets. Compute the mean and standard deviation of your sample. Compute the mean and standard deviation of each sample set. Compare the means and standard deviations of your samples with each other and with the mean and standard deviation of the original distribution. Discuss the differences among the sample sets and the original distribution, including the type of uncertainties you are dealing with. How many samples do you think are needed to reliably determine the mean and standard deviation of the relative density of this particular soil?

Section 2.2: Probability Theory

2.5 A certain column will carry a dead load estimated to be 400 k with a COV of 0.1 and a live load of 200 k with a COV of 0.25. What is the mean and standard deviation of the total column load? Assuming the load is normally distributed, what is the probability that this load will exceed 750 k?

2.6 A simply supported beam has a length of 3 m and carries a distributed load with a mean of 5 kN/m and a COV of 0.2. Assuming the load is normally distributed, what are the mean and standard deviation of the maximum moment in the beam? What is the probability the maximum moment will exceed 7 kN-m?

2.7 Using the data shown in Figure 2.5, determine the probability that the tangent of the friction angle for the mudstone at the Confederation Bridge site is less than 0.25.

Section 2.3: Failure, Reliability, and Risk

2.8 The capacity for a certain foundation system is estimated to be 620 kN with a COV of 0.3. The demand on the foundation is estimated to be 150 kN with a COV of 0.15. Compute the mean factor of safety of this foundation and its probability of failure assuming both capacity and demand are normally distributed.

2.9 We wish to design a shallow foundation with a probability of failure of 10^{-3}. The footing supports a column carrying a dead load with a mean of 30 k and COV of 0.05 and a live load with a mean of 10 k and COV of 0.15. Based on the uncertainty of soil properties and our analysis method, we estimate the COV of the foundation capacity to be 0.2. For what mean capacity does the foundation need to be designed? Assume both loads and capacity are normally distributed.

2.10 Assume the foundation in Problem 2.9 was to support a high-voltage transmission line near the Danish city of Århus. If the transmission line fails, it will potentially kill 50 people. If the computed probability of failure is for a design life of 100 years, is risk associated with the failure of design acceptable based on the Danish guidance in Figure 2.7? Explain.

Section 2.4: Applying Reliability Theory in Practice

2.11 For the footing in Example 2.2, compute the factor of safety required for a probability of failure of 5×10^{-4} assuming the COV of the demand is 0.15

2.12 If the ASD design method has worked satisfactorily for over 50 years, what's the value in changing to the LRFD method?

3

Soil Mechanics

Measure it with a micrometer,
mark it with chalk,
cut it with an axe.

An admonition to maintain a consistent degree of precision throughout the analysis, design, and construction phases of a project.

Engineers classify earth materials into two broad categories: *rock* and *soil*. Although both materials play an important role in foundation engineering, most foundations are supported by soil. In addition, foundations on rock are often designed much more conservatively because of the rock's greater strength, whereas economics precludes overconservatism when building foundations on soil. Therefore, it is especially important for the foundation engineer to be familiar with soil mechanics.

Users of this book should already have acquired at least a fundamental understanding of the principles of soil mechanics. This chapter reviews these principles, emphasizing those that are most important in foundation analyses and design. *Geotechnical Engineering: Principles and Practices* (Coduto et al., 2011), the companion volume to this book, explores all of these topics in much more detail. Relevant principles of rock mechanics are included in later chapters within the context of specific applications and in Chapter 25.

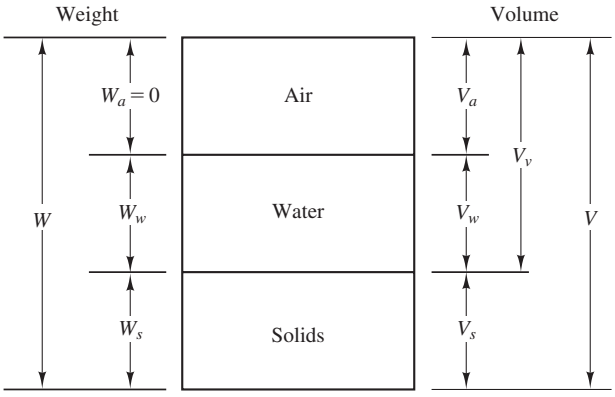

Figure 3.1 A phase diagram describes the relative proportions of solids, water, and air in a soil. The weight of the air, W_a, is negligible.

TABLE 3.1 DEFINITIONS AND TYPICAL VALUES OF COMMON SOIL WEIGHT-VOLUME PARAMETERS

			Typical Range	
Parameter	Symbol	Definition	SI	English
Unit weight	γ	$\frac{W}{V}$	14–20 kN/m^3	90–130 lb/ft^3
Dry unit weight	γ_d	$\frac{W_s}{V}$	9–19 kN/m^3	60–125 lb/ft^3
Unit weight of water	γ_w	$\frac{W_w}{V_w}$	9.8 kN/m^3	62.4 lb/ft^3
Buoyant unit weight	γ_b	$\gamma_{sat} - \gamma_w$	4–10 kN/m^3	28–68 lb/ft^3
Degree of saturation	S	$\frac{V_w}{V_v} \times 100\%$	2–100%	2–100%
Moisture content	w	$\frac{W_w}{W_s} \times 100\%$	3–70%	3–70%
Void ratio	e	$\frac{V_v}{V_s}$	0.1–1.5	0.1–1.5
Porosity	n	$\frac{V_v}{V} \times 100\%$	9–60%	9–60%
Specific gravity of solids	G_s	$\frac{W_s}{V_s\gamma_w}$	2.6–2.8	2.6–2.8

γ_{sat} is the unit weight, γ, when $S = 100\%$.

3.1 REVIEW AND NOMENCLATURE

Weight-Volume Relationships

Soil is a *particulate material* that can contain all three phases of matter (solid, liquid, and gas) simultaneously. The weights and volumes of these three phases can be depicted by a *phase diagram*, as shown in Figure 3.1, from which standard parameters can be defined. Table 3.1 contains the definitions of weight-volume parameters commonly used in foundation engineering, along with typical numerical values. These values are not absolute limits, and unusual soils may have properties outside these ranges. In addition, Table 3.2 presents typical values of unit weights for various soils.

Relative Density

The *relative density*, D_r, is a convenient way to express the void ratio of sands and gravels. It is based on the void ratio of the soil, e, the *minimum index void ratio*, $e_{\min}$, and the *maximum index void ratio*, $e_{\max}$:

$$D_r = \frac{e_{\max} - e}{e_{\max} - e_{\min}} \times 100\% \tag{3.1}$$

TABLE 3.2 TYPICAL UNIT WEIGHTS

Soil Type and Unified Soil Classification	Typical Unit Weight, γ			
	Above Groundwater Table		Below Groundwater Table	
	(kN/m^3)	(lb/ft^3)	(kN/m^3)	(lb/ft^3)
GP — Poorly-graded gravel	17.5–20.5	110–130	19.5–22.0	125–140
GW — Well-graded gravel	17.5–22.0	110–140	19.5–23.5	125–150
GM — Silty gravel	16.0–20.5	100–130	19.5–22.0	125–140
GC — Clayey gravel	16.0–20.5	100–130	19.5–22.0	125–140
SP — Poorly-graded sand	15.0–19.5	95–125	19.0–21.0	120–135
SW — Well-graded sand	15.0–21.0	95–135	19.0–23.0	120–145
SM — Silty sand	12.5–21.0	80–135	17.5–22.0	110–140
SC — Clayey sand	13.5–20.5	85–130	17.5–21.0	110–135
ML — Low plasticity silt	11.5–17.5	75–110	12.5–20.5	80–130
MH — High plasticity silt	11.5–17.5	75–110	11.5–20.5	75–130
CL — Low plasticity clay	12.5–17.5	80–110	11.5–20.5	75–130
CH — High plasticity clay	12.5–17.5	80–110	11.0–19.5	70–125

TABLE 3.3 CONSISTENCY OF COARSE-GRAINED SOILS AT VARIOUS RELATIVE DENSITIES (data from Lambe and Whitman, 1969)

Relative Density, D_r(%)	Classification
0–15	Very loose
15–35	Loose
35–65	Medium dense[a]
65–85	Dense
85–100	Very dense

[a]Lambe and Whitman used the term "medium," but "medium dense" is better because "medium" usually refers to the particle size distribution.

The values of $e_{\min}$ and $e_{\max}$ are determined by conducting standard laboratory tests [ASTM D4253 and D4254]. The in situ e could be computed from the unit weight of the soil, but accurate measurements of the unit weight of clean sands and gravels are difficult to obtain. Therefore, engineers often obtain D_r from correlations based on in situ tests, as described in Chapter 4. A relationship between consistency of sands and gravels and relative density is shown in Table 3.3.

The relative density applies only to sands and gravels with less than 15 percent fines. It can be an excellent indicator of the engineering properties of such soils, and it is therefore an important part of many analysis methods. However, other considerations, such as stress history, mineralogical content, particle size distribution, and fabric (the configuration of the particles) also affect the engineering properties.

3.2 SOIL CLASSIFICATION

Standardized systems of classifying soils are very important, and many such systems have been developed. A proper classification reveals much useful information to a foundation engineer.

Unified Soil Classification System

The most common soil classification system for foundation engineering problems is the *Unified Soil Classification System* (USCS) [ASTM D2487]. The USCS uses the *particle size distribution curve* and the *Atterberg Limits* of a soil to arrive at its *group symbol* and *group name*. The particle sizes are defined in Table 3.4, and the Atterberg limits commonly used are the *liquid limit* (w_L or LL) and the *plastic limit* (w_P or PL). The *plasticity index,* I_p or PI, is the difference between the liquid limit and the plastic limit:

$$I_p = w_L - w_P \tag{3.2}$$

Figure 3.2 presents an abbreviated outline of the USCS group symbols.

Cohesive Versus Cohesionless Soils

Soils also can be divided into two broad categories: cohesionless and cohesive. In cohesionless soils, such as clean sands, the individual particles interact primarily through sliding friction and interlocking. In contrast, cohesive soils, such as clays, also are subject to other interparticle forces that appear to make the particles stick together. Because cohesive soils, consisting of clays and clayey silts, behave very differently than cohesionless soils, consisting of nonplastic silts, sands, and gravels, most analysis and design methods in geotechnical engineering, including those for foundation design presented in this book, apply only to either cohesive soils or cohesionless soils.

The distinction between cohesive and cohesionless is not exactly the same as fine grained and coarse grained per the USCS. Some soils that are coarse grained per the USCS, such as clayey sands (USCS group symbol SC) behave as cohesive soils because of their substantial fines content, especially if the fines are clayey. Therefore, unless a particular analysis or design method prescribes a way to determine the material type or types to which the method is applicable, one may categorize soils per USCS into cohesive and cohesionless soils as follows:

- Cohesive soils: CL, CH, plastic ML, MH, SC, GC
- Cohesionless soils: GW, GP, GM, SW, SP, SM, and nonplastic ML

It is important to note that many real soils do not fall neatly into either category and that unsaturated soils also have their own behavior. Note also that the term "clays" is sometimes used to mean cohesive soils, and the term "sands" is used to represent all cohesionless soils.

TABLE 3.4 ASTM PARTICLE SIZE CLASSIFICATION (per ASTM D2487)

Sieve Size		Particle Diameter			
Passes	Retained on	(in)	(mm)	Soil Classification	
	12 in	>12	>350	Boulder	Rock
12 in	3 in	3–12	75.0–350	Cobble	Fragments
3 in	3/4 in	0.75–3	19.0–75.0	Coarse gravel	
3/4 in	#4	0.19–0.75	4.75–19.0	Fine gravel	
#4	#10	0.079–0.19	2.00–4.75	Coarse sand	Soil
#10	#40	0.016–0.079	0.425–2.00	Medium sand	
#40	#200	0.0029–0.016	0.075–0.425	Fine sand	
#200		<0.0029	<0.075	Fines (silt + clay)	

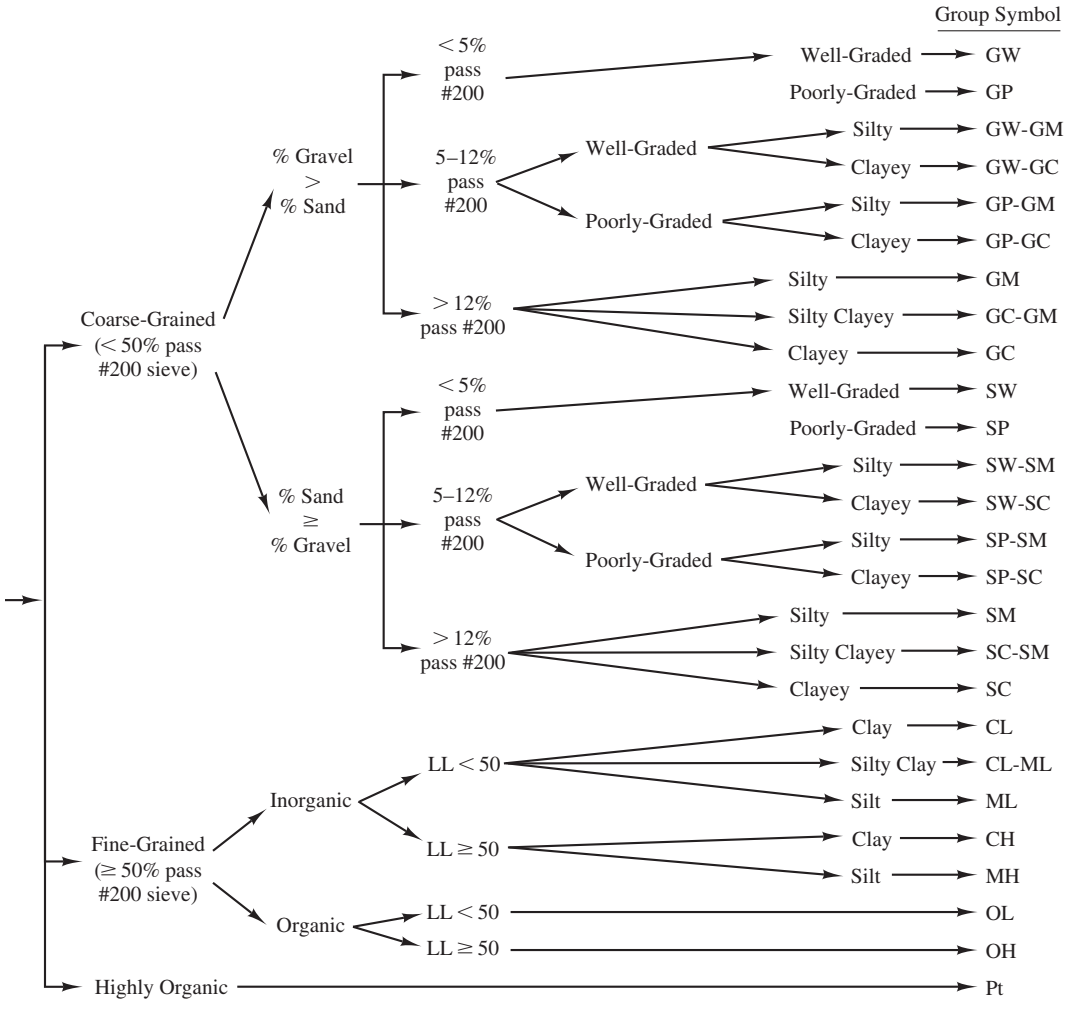

Figure 3.2 Abbreviated outline of the Soil Classification System (adapted from ASTM D2487 and used with permission of ASTM).

Other Geomaterials

The distinction between rock and soil is not always as clear as one might expect. Some soils are very hard while some rocks are very soft. In some cases, a material that a geologist would classify as "rock" is actually weaker than another material classified as a "soil". Materials in this "in-between" zone are sometimes called *intermediate geomaterials* (IGMs). Chapter 25 discusses foundation design methods for IGMs and rocks.

3.3 STRESS

Many foundation engineering analyses require knowledge of the stresses in the soil. These stresses have two kinds of sources:

- *Geostatic stresses* are the result of the force of gravity acting directly on the soil mass.
- *Induced stresses* are caused by external loads, such as foundations.

Both normal and shear stresses may be present in a soil. These are represented by the variables σ and τ, respectively. We will identify the direction of normal stresses using subscripts σ_x and σ_y for the two perpendicular horizontal stresses (which, for foundation design purposes are usually assumed to be equal in magnitude) and σ_z is the downward vertical stress.

Geostatic Stresses

The most important geostatic stress is the vertical compressive stress because it is directly caused by gravity. Geotechnical engineers compute this stress more often than any other. The geostatic vertical total stress, σ_z, is:

$$\sigma_z = \sum \gamma H \tag{3.3}$$

where

σ_z = geostatic vertical total stress
γ = unit weight of soil stratum
H = thickness of soil stratum

We carry this summation from the ground surface down to the point at which the stress is to be computed. Part of the vertical total stress is carried by the solid particles, and the rest is carried by the pore water. The part carried by the solids is called the *effective stress*, σ'. The effective stress is a very important parameter because it controls most soil behavior. It is computed as follows:

$$\sigma' = \sigma - u \tag{3.4}$$

In the case of vertical stress:

$$\sigma_z' = \sigma_z - u \tag{3.5}$$

where

σ_z' = vertical effective stress
σ_z = vertical total stress
u = pore water pressure

Combining Equations 3.3 and 3.5 gives:

$$\sigma_z' = \sum \gamma H - u \tag{3.6}$$

Horizontal Stress

The geostatic horizontal stress also is important for many engineering analyses. It may be expressed either as total horizontal stress, σ_x, or effective horizontal stress, σ_x'. The ratio of the horizontal to vertical effective stresses is defined as the *coefficient of lateral earth pressure*, K:

$$K = \frac{\sigma_x'}{\sigma_z'} \tag{3.7}$$

The value of K in undisturbed ground is known as the *coefficient of lateral earth pressure at rest*, K_0, and can vary between about 0.2 and 6. Typical values are between 0.35 and 0.7 for normally consolidated soils and between 0.5 and 3 for overconsolidated soils. The most accurate way to determine K_0 is by measuring σ_x in situ using methods such as the pressuremeter, dilatometer, or stepped blade, and combining it with computed values of σ_z and u. A less satisfactory method is to measure K_0 in the laboratory using a triaxial compression machine or other equipment. Unfortunately, this method suffers from problems because of sample disturbance, stress history, and other factors.

The most common method of assessing K_0 is by using empirical correlations with other soil properties. Several such correlations have been developed, including the following by Mayne and Kulhawy (1982), which is based on laboratory tests on 170 soils that ranged from clay to gravel. This formula is applicable only when the ground surface is level:

$$K_0 = (1 - \sin \phi')\text{OCR}^{\sin \phi'} \tag{3.8}$$

where

K_0 = coefficient of lateral earth pressure at rest
ϕ' = effective friction angle
OCR = overconsolidation ratio

Section 3.6 discusses lateral earth pressures in more detail. Chapter 4 discusses methods of obtaining K from empirical correlations with other in situ tests, such as the cone penetration test.

Example 3.1

The soil profile beneath a certain site consists of 5.0 m of silty sand underlain by 13.0 m of clay. The groundwater table is at a depth of 2.8 m below the ground surface. The sand has a unit weight of 19.0 kN/m^3 above the groundwater table and 20.0 kN/m^3 below. The clay has

a unit weight of 15.7 kN/m^3, an effective friction angle of 35°, and an overconsolidation ratio of 2. Compute σ_x, σ_x', σ_z, and σ_z' at a depth of 11.0 m.

Solution

$$\sigma_z = \sum \gamma H$$
$$= (19.0 \text{ kN/m}^3)(2.8 \text{ m}) + (20.0 \text{ kN/m}^3)(2.2 \text{ m}) + (15.7 \text{ kN/m}^3)(6.0 \text{ m})$$
$$= \mathbf{191 \text{ kPa}}$$
$$u = \gamma_w z_w = (9.8 \text{ kN/m}^3)(8.2 \text{ m}) = \mathbf{80 \text{ kPa}}$$
$$\sigma_z' = \sigma_z - u$$
$$= 191 \text{ kPa} - 80 \text{ kPa} = \mathbf{111 \text{ kPa}}$$
$$K_0 = (1 - \sin \phi')\text{OCR}^{\sin \phi'}$$
$$= (1 - \sin 35°)2^{\sin 35°} = 0.635$$
$$\sigma_x' = K\sigma_z'$$
$$= (0.635)(111 \text{ kPa}) = \mathbf{70 \text{ kPa}}$$
$$\sigma_x = \sigma_x' + u$$
$$= 70 \text{ kPa} + 80 \text{ kPa} = \mathbf{150 \text{ kPa}}$$

Induced Stresses

Induced stresses are stress changes at depth that are caused by external loads placed on or near the surface, such as loads from structural foundations. These stresses are a very important part of foundation engineering, and most of the related geotechnical analyses focus on the soil's response to these stresses.

The most common loading condition for geotechnical analyses is the *area load*, which is a load distributed evenly across a horizontal area. Examples include spread footing foundations, tanks, wheel loads, stacked inventory in a warehouse, and small fills. We define the contact pressure between this load and the ground as the *bearing pressure*, q:

$$q = \frac{P}{A} \tag{3.9}$$

where

q = bearing pressure
P = applied vertical load
A = area upon which the load acts

In the case of spread footing foundations, P must include both the column load and the weight of the foundation, so Equation 3.9 will be reformulated in Chapter 6 specifically for use in spread footing design.

For area loads, we normally compute the induced stress in relation to the bearing pressure using the equation:

$$\Delta\sigma_z = I_\sigma q \tag{3.10}$$

where

$\Delta\sigma_z$ = induced vertical stress
I_σ = influence factor for vertical stress
q = bearing pressure

The stress influence factor represents a decimal fraction of the vertical applied bearing stress present at a point under the ground. The influence factor will take on different forms depending on the nature of the applied surface stress and the model used to compute the induced stress.

Boussinesq's Method

Boussinesq (1885) developed the classic solution for induced stresses in an infinite, homogeneous, isotropic, elastic half-space due to an external point load applied at and normal to the infinite surface of the half space. The term *infinite elastic half-space* means that the linear elastic material extends infinitely in all directions beneath a plane (which in our case is the ground surface). Newmark (1935) then integrated the Boussinesq equation to produce a solution for I_σ at a depth z_f beneath the corner of a rectangular loaded area of width B and length L, as shown in Figure 3.3. This solution produces the following two equations:

If $B^2 + L^2 + z_f^2 < \dfrac{B^2L^2}{z_f^2}$:

$$I_\sigma = \frac{1}{4\pi}\left[\left(\frac{2BLz_f\sqrt{B^2 + L^2 + z_f^2}}{z_f^2(B^2 + L^2 + z_f^2) + B^2L^2}\right)\left(\frac{B^2 + L^2 + 2z_f^2}{B^2 + L^2 + z_f^2}\right) + \pi - \sin^{-1}\frac{2BLz_f\sqrt{B^2 + L^2 + z_f^2}}{z_f^2(B^2 + L^2 + z_f^2) + B^2L^2}\right] \tag{3.11}$$

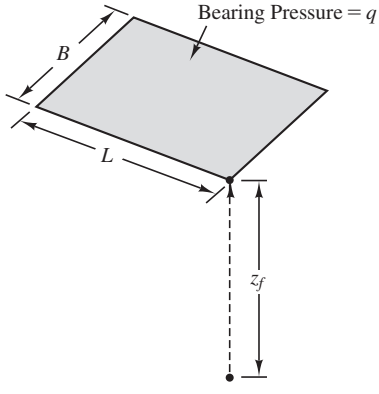

Figure 3.3 Newmark's solution for induced vertical stress beneath the corner of a rectangular loaded area.

Otherwise:

$$I_\sigma = \frac{1}{4\pi}\left[\left(\frac{2BLz_f\sqrt{B^2 + L^2 + z_f^2}}{z_f^2(B^2 + L^2 + z_f^2) + B^2L^2}\right)\left(\frac{B^2 + L^2 + 2z_f^2}{B^2 + L^2 + z_f^2}\right)\right.$$
$$\left. + \sin^{-1}\frac{2BLz_f\sqrt{B^2 + L^2 + z_f^2}}{z_f^2(B^2 + L^2 + z_f^2) + B^2L^2}\right] \tag{3.12}$$

where

I_σ = stress influence factor at a point beneath the corner of a rectangular loaded area
B = width of the foundation
L = length of the foundation
z_f = vertical distance from the loaded area at the surface (always > 0)

Notes:

1. The $\sin^{-1}$ term must be expressed in radians.
2. Newmark's solution is often presented as a single equation with a $\tan^{-1}$ term, but that equation is incorrect when $B^2 + L^2 + z_f^2 < B^2L^2/z_f^2$.
3. It is customary to use B as the shorter dimension and L as the longer dimension, as shown in Figure 3.3.

Example 3.2

A vertical load of 260 kN is applied to a 1.2 m × 1.2 m area at the ground surface that is level. Compute the induced vertical stress, $\Delta\sigma_z$, at a point 1.5 m below the corner of this square loaded area.

Solution

$$q = \frac{P}{A} = \frac{260\text{ kN}}{(1.2\text{ m})^2} = 181\text{ kPa}$$

$$B^2 + L^2 + z_f^2 = 1.2^2 + 1.2^2 + 1.5^2 = 5.130$$

$$B^2L^2/z_f^2 = (1.2)^2(1.2)^2/(1.5)^2 = 0.9216$$

$B^2 + L^2 + z_f^2 > \dfrac{B^2L^2}{z_f^2}$ therefore, use Equation 3.12:

$$I_\sigma = \frac{1}{4\pi}\left[\left(\frac{2BLz_f\sqrt{B^2 + L^2 + z_f^2}}{z_f^2(B^2 + L^2 + z_f^2) + B^2L^2}\right)\left(\frac{B^2 + L^2 + 2z_f^2}{B^2 + L^2 + z_f^2}\right)\right.$$
$$\left. + \sin^{-1}\frac{2BLz_f\sqrt{B^2 + L^2 + z_f^2}}{z_f^2(B^2 + L^2 + z_f^2) + B^2L^2}\right]$$

$$I_\sigma = \frac{1}{4\pi}\left[\left(\frac{2(1.2)(1.2)(1.5)\sqrt{5.130}}{(1.5)^2(5.130) + (1.2)^2(1.2)^2}\right)\left(\frac{(1.2)^2 + (1.2)^2 + 2(1.5)^2}{5.130}\right)\right.$$

$$\left. + \sin^{-1}\frac{2(1.2)(1.2)(1.5)\sqrt{5.130}}{(1.5)^2(5.130) + (1.2)^2(1.2)^2}\right]$$

$$= 0.146$$

$$\Delta\sigma_z = I_\sigma q$$

$$= (0.146)(181)$$

$$= \mathbf{26.4\ kPa}$$

Using superposition, Newmark's solution of Boussinesq's method also can be used to compute $\Delta\sigma_z$ at other locations, both beneath and beyond the footing. This technique is shown in Figure 3.4, and illustrated in Example 3.3.

Example 3.3

Compute the induced vertical stress, $\Delta\sigma_z$, at a point 1.5 m below the center of the loaded area described in Example 3.2.

Solution

Since Newmark's solution of Boussinesq's equation considers only stresses beneath the corner of a rectangular loaded area, we must divide the loaded area in question into four equal quadrants. These quadrants meet at the center of the loaded area, beneath which is where we wish to compute $\Delta\sigma_z$. Since each quadrant imparts one-quarter of the total load on one-quarter of the total area, the bearing pressure is the same as computed in Example 3.2. However, the remaining computations must be redone using $B = L = 1.2\text{ m}/2 = 0.6\text{ m}$.

$$B^2 + L^2 + z_f^2 = 0.6^2 + 0.6^2 + 1.5^2 = 2.970$$

$$B^2L^2/z_f^2 = (0.6)^2(0.6)^2/(1.5)^2 = 0.0576$$

$B^2 + L^2 + z_f^2 < \dfrac{B^2L^2}{z_f^2}$ therefore, use Equation 3.12:

$$I_\sigma = \frac{1}{4\pi}\left[\left(\frac{2BLz_f\sqrt{B^2 + L^2 + z_f^2}}{z_f^2(B^2 + L^2 + z_f^2) + B^2L^2}\right)\left(\frac{B^2 + L^2 + 2z_f^2}{B^2 + L^2 + z_f^2}\right)\right.$$

$$\left. + \sin^{-1}\frac{2BLz_f\sqrt{B^2 + L^2 + z_f^2}}{z_f^2(B^2 + L^2 + z_f^2) + B^2L^2}\right]$$

$$I_\sigma = \frac{1}{4\pi}\left[\left(\frac{2(0.6)(0.6)(1.5)\sqrt{2.970}}{(1.5)^2(2.970) + (0.6)^2(0.6)^2}\right)\left(\frac{(0.6)^2 + (0.6)^2 + 2(1.5)^2}{2.970}\right)\right.$$
$$\left. + \sin^{-1}\frac{2(0.6)(0.6)(1.5)\sqrt{2.970}}{(1.5)^2(2.970) + (0.6)^2(0.6)^2}\right]$$
$$= 0.0602$$

Since there are four identical "sub-loaded areas," we must multiply the computed stress by four.

$$\Delta\sigma_z = 4I_\sigma q$$
$$= (4)(0.0602)(181)$$
$$= \mathbf{43.6\ kPa}$$

Chart Solutions

Another way to estimate induced stresses is to use nondimensional charts. Figures 3.5 through 3.8 are some of many such charts that have been developed. The curves in Figures 3.5 through 3.7, which connect points of equal induced stress, are sometimes called pressure bulbs or stress bulbs.

These charts are easy to use, but do not have the flexibility or computational accuracy of a properly implemented numerical solution. Other charts also have been developed for more complex loading conditions (see U.S. Navy, 1982; Poulos and Davis, 1974). However, readily available computer-based numerical solutions (e.g., Rocscience Inc., 2014 and Geo-Slope Intl., 2014) have replaced the more complex chart solutions. In spite of the availability of numerical solutions, the charts provide a visual sense of how the stresses are distributed. For example, Figure 3.5 contains the solution for a circular loaded area. Similarly, Figures 3.6 and 3.7 contain the solutions for a square loaded area and a semi-infinite strip load (such as a long embankment). Figures 3.6 and 3.7 clearly show that the stresses induced by a strip load exceed those induced by a square loaded area of the same width. Notice also that stresses induced by a strip load extend to a much

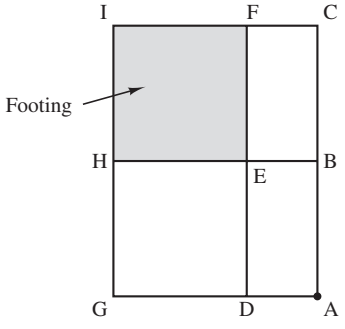

Figure 3.4 Using Newmark's solution and superposition to find the induced vertical stress at any point beneath a rectangular loaded area.

To Compute Stress at Point A Due to Load from Footing EFIH:
$(\Delta\sigma_v')_A = (\Delta\sigma_v')_{ACIG} - (\Delta\sigma_v')_{ACFD} - (\Delta\sigma_v')_{ABHG} + (\Delta\sigma_v')_{ABED}$

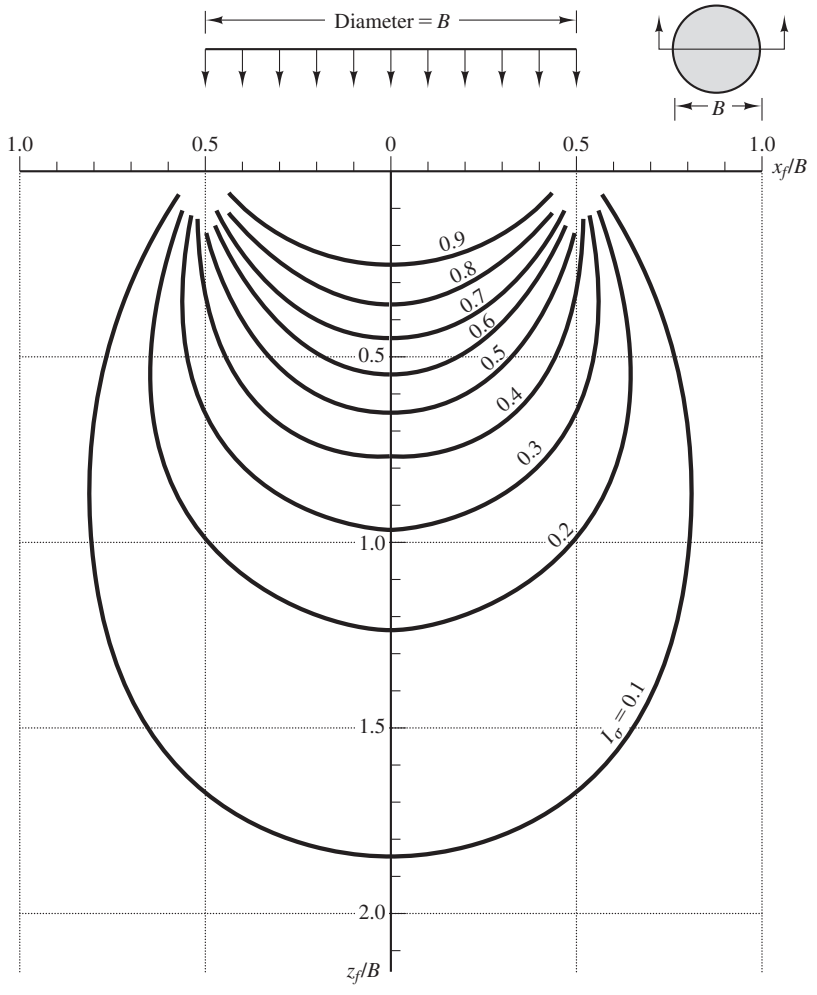

Figure 3.5 Influence factors for induced vertical stress under a circular loaded area, per Boussinesq.

greater depth than those induced by a square loaded area. Finally, Figure 3.8 presents influence factors for loads under the corner of a rectangular loaded area.

Approximate Methods

Sometimes it is useful to have simple approximate methods of computing induced stresses beneath loaded areas. The widespread availability of computers has diminished the need for these methods, but they still are useful when a quick answer is needed, or when a computer is not available.

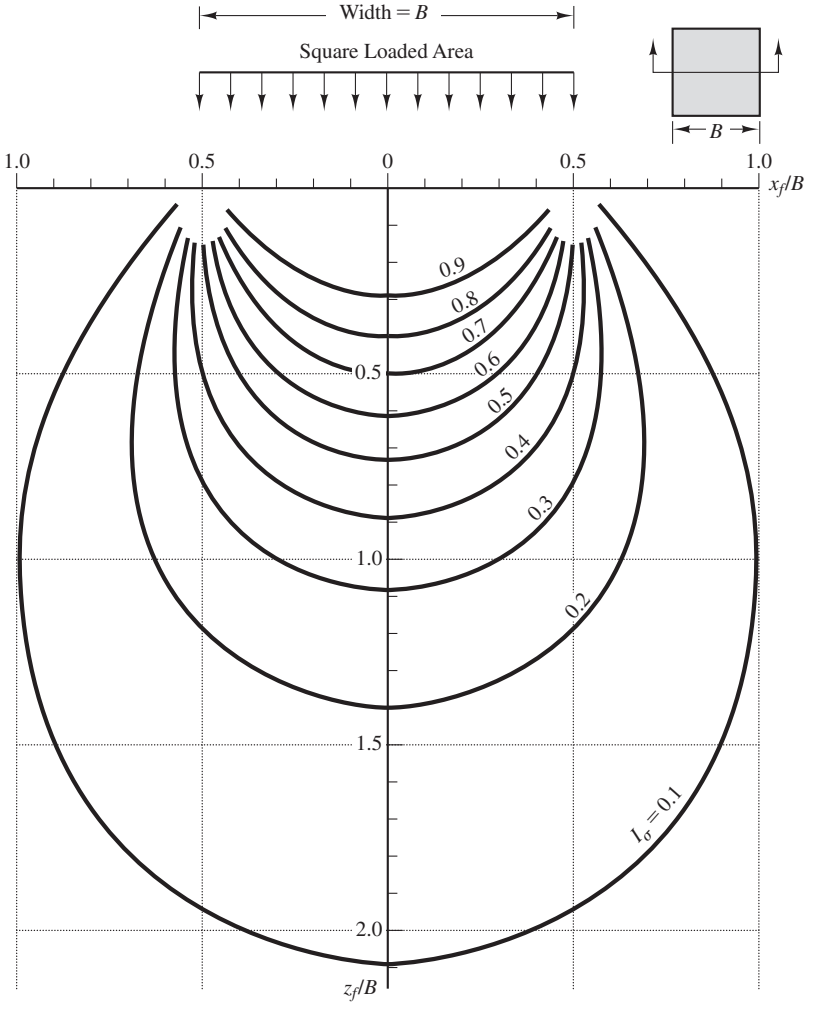

Figure 3.6 Influence factors for induced vertical stress under a square loaded area, per Boussinesq.

The following approximate formulas compute the induced vertical stress, σ_z, beneath the center of an area load. They produce answers that are within 5 percent of the Boussinesq values, which is more than sufficient for virtually all practical problems.

For circular loaded areas (Poulos and Davis, 1974),

$$I_\sigma = 1 - \left(\frac{1}{1 + \left(\frac{B}{2z_f} \right)^2} \right)^{1.5} \tag{3.13}$$

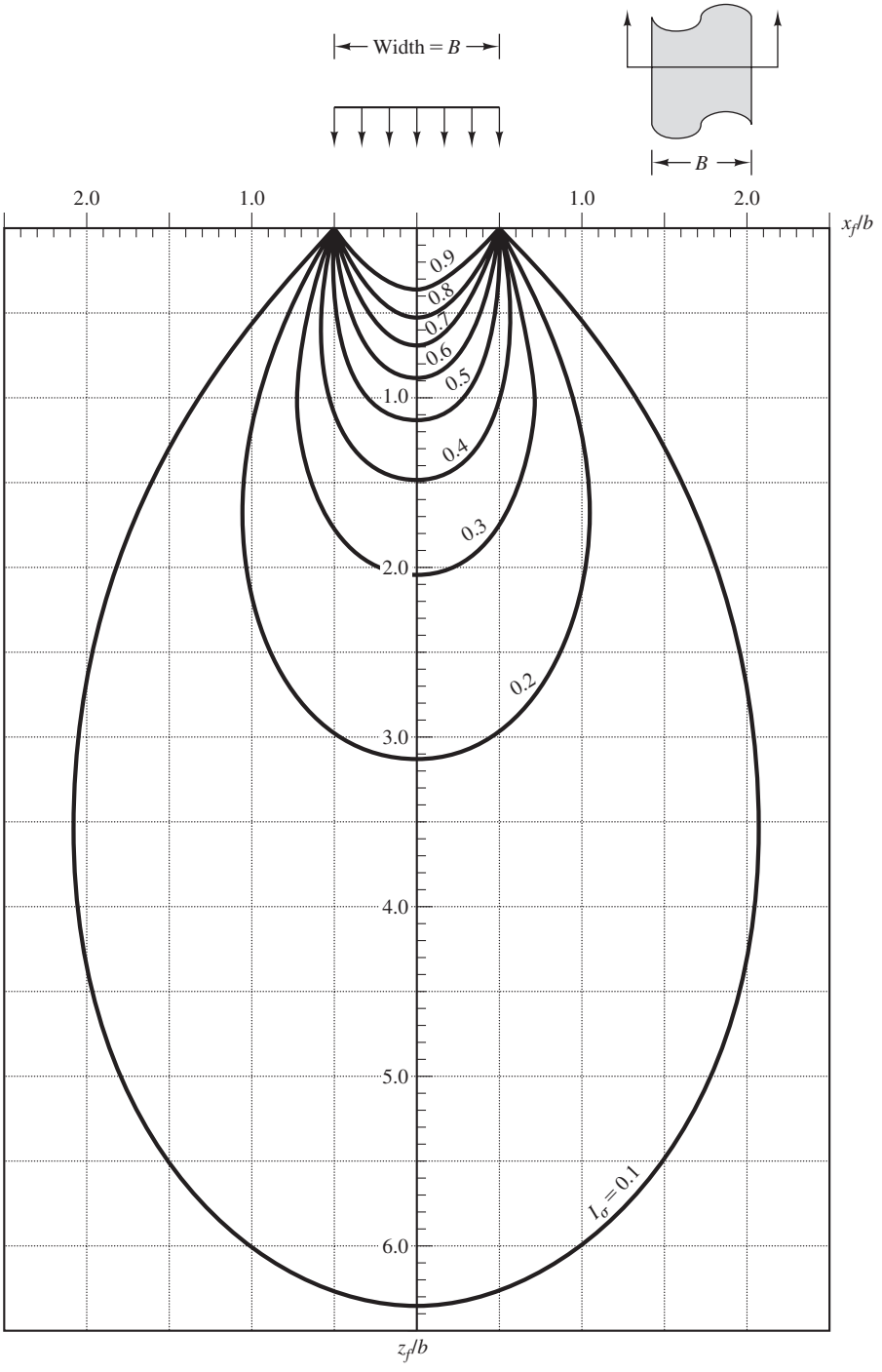

Figure 3.7 Influence factors for induced vertical stress under a semi-infinite strip load, per Boussinesq.

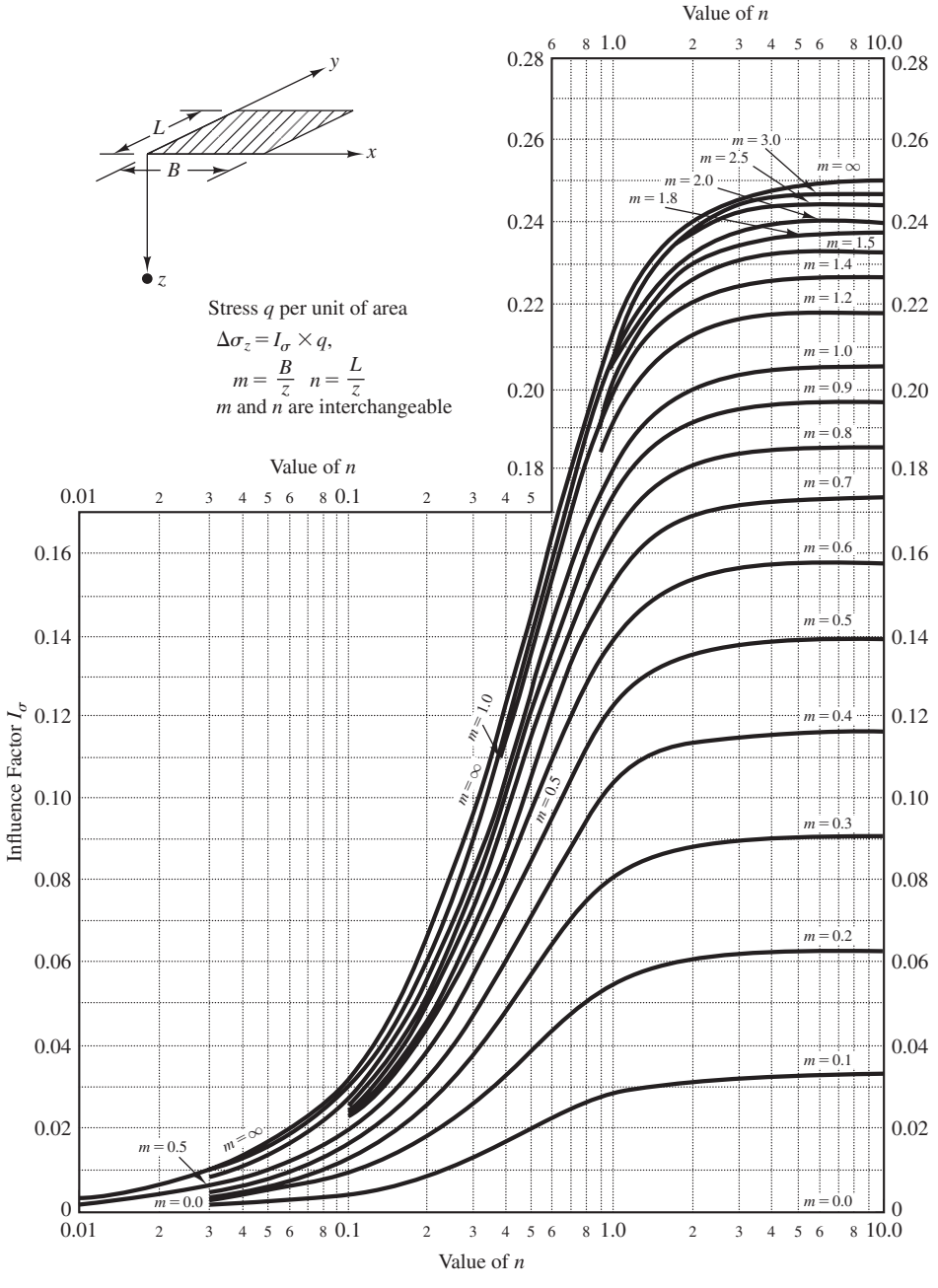

Figure 3.8 Influence factors for induced vertical stress beneath the corner of a rectangular loaded area (U.S. Navy, 1982).

For square loaded areas,

$$I_\sigma = 1 - \left(\frac{1}{1 + \left(\frac{B}{2z_f} \right)^2} \right)^{1.76} \tag{3.14}$$

For continuous loaded areas (also known as strip loads) of width B and infinite length,

$$I_\sigma = 1 - \left(\frac{1}{1 + \left(\frac{B}{2z_f} \right)^{1.38}} \right)^{2.60} \tag{3.15}$$

For rectangular loaded areas of width B and length L,

$$I_\sigma = 1 - \left(\frac{1}{1 + \left(\frac{B}{2z_f} \right)^{1.38+0.62B/L}} \right)^{2.60-0.84B/L} \tag{3.16}$$

where

I_σ = influence factor for vertical stress beneath the center of a loaded area
z_f = depth from bottom of loaded area to point
B = width or diameter of loaded area
L = length of loaded area

A commonly used approximate method, called the 1:2 method, is to draw surfaces inclined downward at a slope of 1 horizontal to 2 vertical from the edge of the loaded area, as shown in Figure 3.9. To compute the $\Delta\sigma_z$ at a depth z_f below the loaded area, simply draw a horizontal plane at this depth, compute the area of this plane inside the

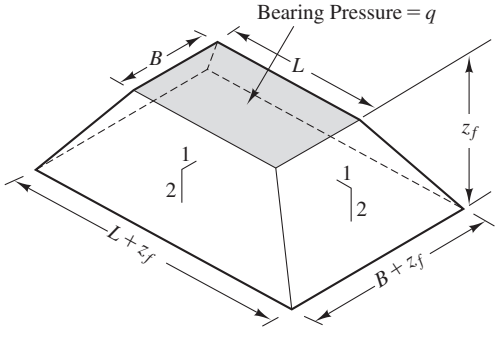

Figure 3.9 Use of 1:2 method to compute the average $\Delta\sigma_z$ at a specified depth below a loaded area.

inclined surfaces, and divide the total applied load by this area. The $\Delta\sigma_z$ computed by this method is an estimate of the average across this area, and is most often used for approximate settlement computations. When applied to a rectangular loaded area, the 1:2 method produces the following formula for the influence factor for vertical stress, at a depth z_f:

$$I_\sigma = \frac{BL}{(B + z_f)(L + z_f)} \tag{3.17}$$

The primary advantage of this method is that Equation 3.17 can easily be derived from memory by simply applying the principles of geometry.

Numerical Analyses

If the shape of the loaded area is too complex, it becomes necessary to use a numerical analysis to compute the induced stresses. The term *numerical analysis* (or *numerical method*) refers to a class of problem-solving methods that use a series of simplified equations assembled in a way that approximately models the actual system. For example, we could divide a loaded area into a large number of sub-areas, then replace the total load by point loads acting at the centers of the sub-areas and compute the induced stresses using the Boussinesq formulas and superposition. Many engineering disciplines use these methods to develop solutions to problems that otherwise would be very difficult or impossible to solve. The finite element method and the finite difference method are examples of numerical methods.

3.4 COMPRESSIBILITY AND SETTLEMENT

The stresses induced by foundation loads (discussed in Section 3.3) generate strain in the soil which leads to deformation. The vertical deformation of a foundation under loading is called *settlement*. *Compressibility* is a soil property that describes the relationship between stress and strain in soils. The greater the compressibility of a soil, the more strain it will experience under a given stress. The term *compression* represents the change in height of a soil layer due to a change in stress, and the settlement is equal to the sum of the compression values of the soil layers under a foundation. The higher the compressibility of a soil, the greater the settlement for a given applied foundation stress.

Physical Processes

Since settlement is a displacement of a point caused by a change in stress, we can compute the magnitude of settlement if we know (a) the magnitude of the change in stress and (b) the stress-strain properties of the soil. For many materials, such as steel and concrete, this is a relatively simple problem solved by measuring the stress-strain properties of the material associated with linear elasticity (e.g., Young's modulus and Poisson's ratio), determining the applied stresses and then computing the strains and displacements using the

3D Hooke's law. However, soils, because of their particulate and multiphase makeup, have a much more complicated stress-strain behavior that reflects multiple physical processes and elasto-plastic behavior, some of which are time-dependent. We can think of settlement in soils as being the result of three physical processes:

- **Distortion settlement**, δ_d, is the settlement that results from lateral movements of the soil in response to changes in σ'_z. Distortion settlement occurs without significant volume change or particle rearrangement, and is similar to the Poisson's effect where an object loaded in the vertical direction expands laterally. Distortion settlements primarily occur when the load is confined to a small area, such as a structural foundation.
- **Consolidation settlement** (also known as *primary consolidation settlement*), δ_c, occurs over time when a soil is subjected to an increase in σ'_z and the individual particles respond by rearranging into a tighter packing. The volume of the solid particles themselves remains virtually unchanged, so the change in the total volume (and the resulting strain) is due solely to a decrease in the volume of the voids, V_v. The pore water is, for practical purposes, incompressible, so if the soil is saturated ($S = 100\%$), this reduction in V_v can occur only if some of the pore water is squeezed out of the soil. In some cases, this flow process occurs as quickly as the load is applied, but in other situations, it occurs much more slowly. The rate of consolidation will depend on the hydraulic properties of the soil, the degree of saturation of the soil, and other factors. All soils experience some settlement due to consolidation when they are subjected to an increase in σ'_z, and this is usually the most important source of settlement.
- **Secondary compression settlement**, δ_s, is a form of creep that also occurs over time. It is differentiated from primary consolidation in that it occurs at a constant σ'_z. The physics of secondary compression are not well understood, but secondary compression is always time dependent and can be significant in highly plastic clays or organic soils, but it is negligible in sands and gravels.

The settlement below a foundation, δ, is the sum of these three components:

$$\delta = \delta_d + \delta_c + \delta_s \tag{3.18}$$

Because soil settlement can have both time dependent and non-time dependent components, it is often categorized in terms of *short-term settlement* (or *immediate settlement*), which occurs as quickly as the load is applied, and *long-term settlement* (or *delayed settlement*), which occurs over a longer period. Many engineers associate consolidation settlement solely with the long-term settlement of cohesive soils. However, this is not strictly true as pointed out by Salgado (2008). Consolidation settlement is related to volume change due to change in effective stress regardless of the soil type or time required for the volume change. Table 3.5 illustrates the relationships among soil type, sources of settlement, and their time dependence. In general, settlement of cohesive soils will generally be dominated by long-term settlement (consolidation settlement), where settlement of cohesionless soils will generally be dominated by short-term settlement (both distortion and consolidation settlement).

TABLE 3.5 TIME-RATES AND MAGNITUDES OF SOIL SETTLEMENT PROCESSES (adapted from Salgado, 2008)

	Soil Types			
	Clays and Silts		Sands and Gravels	
Time Frame	Process	Magnitude	Process	Magnitude
Short-term	Distortion	Negligible to small	Distortion	Negligible to small
			Consolidation	Small to moderate
Long-term	Consolidation	Moderate to large	Secondary compression	Negligible to small
	Secondary compression	Small to large		

Settlement caused by unusual soils will be discussed in Chapters 27 and 28. Chapter 27 discusses settlement or heave caused by wetting or drying of expansive soils, and Chapter 28 discusses settlement due to the hydrocollapse of collapsible soils when they become wetted. Other less common sources of settlement, such as those from underground mines, sinkholes, or tunnels, also can be important in foundation engineering, but they are beyond the scope of our discussion.

Fundamentals of Computing Settlement

Regardless of whether the engineer is computing long-term settlement or short-term settlement or whether the settlement is dominated by distortion, consolidation, or secondary compression, the vertical settlement of a footing is the integration of vertical strain under the footing, or mathematically:

$$\delta = \int_{z_0}^{z_\infty} \varepsilon_z dz \tag{3.19}$$

where

z_0 = depth at the base of the foundation where the stress is applied
z_∞ = depth where the induced stress is negligible

To solve Equation 3.19, we must have a relationship between stress and strain in soil. In general, we can ignore distortion strain when computing foundation settlement. Therefore, we use one-dimensional strain conditions in our analyses, also called one-dimensional compression.

Stress-Strain Models for Soils

Methods of describing the stress-strain behavior of soil are sometimes unclear and often misunderstood. Early work on deformation of soils by Terzaghi (1925) reported the modulus as a linear function of stress and strain as is traditional for many materials, such as steel

and concrete. Casagrande's early work on soil deformation (1932) also plotted deformation as a linear function of effective stress. However, somewhere in the mid-1930s, researchers switched to plotting soil deformation versus the natural log of effective stress (Janbu, 1998). Also, the use of change in void ratio, Δe, was used to represent deformation rather than strain as is commonly used. This method relating stress and strain is called the e-log-p method. Technically, this should be titled the e-log-σ' but we use p to represent effective stress because it is both simpler to type and traditional. The e-log-p method is still in use today, though a number of researchers and practitioners have advocated returning to the simpler linear plots of stress versus strain (e.g., Janbu, 1998 and Wesley, 2012), which we will call the modulus based method in this text. Both the e-log-p and modulus based method have their place in foundation engineering.

Modulus Based Method

In this method, the relationship between the one-dimensional compression of soil and the change in stress is written as:

$$\varepsilon_z = \frac{\Delta\sigma_z}{M} \tag{3.20}$$

Where M is the constrained modulus.

We use M instead of the more general Young's modulus E because of the assumption of one-dimensional compression under which the soils can deform only in the vertical direction. From elastic theory, E and M are related by Poisson's ratio as shown in Equation 3.21, which can be used to compute the constrained modulus from Young's modulus if we have an estimate of the Poisson's ratio:

$$M = E\frac{(1-\nu)}{(1+\nu)(1-2\nu)} \tag{3.21}$$

It is important to point out that soils are not elastic and the modulus is dependent upon many factors including the stress level. We generally use a secant formulation for the modulus as shown in Figure 3.10. This allows direct computation of the strain for a given stress using Equation 3.20. If we used a tangent formulation for the modulus, as shown

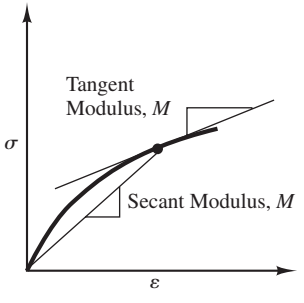

Figure 3.10 Stress-strain curve for one-dimensional compression showing the secant formulation versus the tangent formulation of constrained modulus, M, for a given point on the stress-strain curve.

in Figure 3.10, then it would be necessary to determine the entire stress-strain curve and integrate Equation 3.20 as a function of stress to determine the strain. The secant modulus formulation is much simpler; the difficulty is determining the appropriate secant modulus.

e-Log-*p* Method

In this method, the stress-strain model is semi-logarithmic as shown in Figure 3.11. The term p is a shorthand for effective stress, σ', and dates back to typewriter days, when it was easy to type p but difficult to typeset σ'. This model is sometimes shown as void ratio, e, versus log σ', Figure 3.11a, and sometimes as strain, ε, versus log σ', Figure 3.11b. The two are equivalent since the strain and void ratio are related by the initial void ratio, e_0, by Equation 3.22:

$$\varepsilon = \frac{\Delta e}{1 + e_0} \tag{3.22}$$

In the e-log-p method, the stress-strain curve is represented by two straight lines, as shown in Figure 3.11a. The preconsolidation stress, σ'_c, is the greatest effective stress the soil has experienced in its geologic history. At stresses less than the preconsolidation stress, the soil is relatively stiff and its strain-stress behavior follows the recompression curve. At stresses greater than the preconsolidation stress, the soil is more compressible and its strain-stress behavior follows the virgin curve. Soils whose existing effective stress in the field, σ'_{z0}, is less than the preconsolidation stress, σ'_c, are said to be *overconsolidated*. Soils whose existing effective stress in the field is equal to the preconsolidation stress are said to be *normally consolidated*. We measure the degree of overconsolidation using the *overconsolidation ratio* (OCR), defined in Equation 3.23, or the *overconsolidation margin*, σ'_m, defined in Equation 3.24:

$$\text{OCR} = \frac{\sigma'_c}{\sigma'_{z0}} \tag{3.23}$$

$$\sigma'_m = \sigma'_c - \sigma'_{z0} \tag{3.24}$$

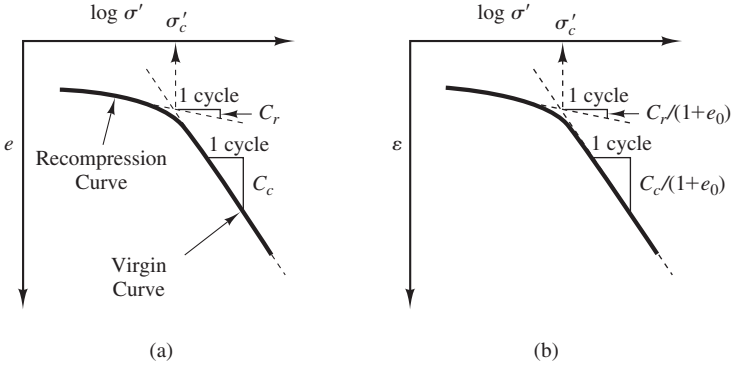

Figure 3.11 Semi-logarithmic or e-log-p formulation of the soil stress-strain curve: (a) e versus log σ'; and (b) ε versus log σ'.

Using this model the vertical strain is computed using Equations 3.25 through 3.27.

For normally consolidated soils where $\sigma_c' \approx \sigma_{z0}'$, all of the loading occurs on the virgin curve and the vertical strain is computed as:

$$\varepsilon_z = \frac{C_c}{1 + e_0} \log\left(\frac{\sigma_{zf}'}{\sigma_{z0}'}\right) \tag{3.25}$$

For overconsolidated soils where $\sigma_{zf}' \leq \sigma_c'$, all of the loading occurs on the recompression curve and the vertical strain is computed as:

$$\varepsilon_z = \frac{C_r}{1 + e_0} \log\left(\frac{\sigma_{zf}'}{\sigma_{z0}'}\right) \tag{3.26}$$

For overconsolidated soils where $\sigma_{zf}' > \sigma_c'$, part of the loading occurs along the recompression curve and part along the virgin curve. In this case the vertical strain is computed as:

$$\varepsilon_z = \frac{C_r}{1 + e_0} \log\left(\frac{\sigma_c'}{\sigma_{z0}'}\right) + \frac{C_c}{1 + e_0} \log\left(\frac{\sigma_{zf}'}{\sigma_c'}\right) \tag{3.27}$$

where

C_c = compression index
C_r = recompression index
e_0 = initial void ratio
σ_{z0}' = initial vertical effective stress
σ_c' = preconsolidation stress
σ_{zf}' = final vertical effective stress

The foundation engineer must make a decision about which type of stress-strain model to use when computing settlement. This will depend upon both the compressibility characteristics of the soils and the magnitude of the footing-induced stresses. Figure 3.12 presents the one-dimensional stress-strain behavior of a sample of a lightly overconsolidated clay (data from Wesley, 2010, Figure 8.10). The stress-strain curve is plotted in both arithmetic and *e*-log-*p* forms. Using the semi-log form of the stress-strain curve for this soil (Figure 3.12a), the preconsolidation stress, σ_c', is readily apparent and the compression index, C_c, and recompression index, C_r, can be accurately established. In contrast, the arithmetic form of the stress-strain curve, Figure 3.12b, is highly non-linear. Typically for normally consolidated or lightly overconsolidated soft clays, the *e*-log-*p* form of the stress-strain curve is a good model and works well for settlement computations.

This is not the case for highly overconsolidated stiff clays, sand and gravels, or IGMs. For these soils, the *e*-log-*p* form of the stress-strain curve can be very misleading. Figure 3.13 shows the stress-strain curve for a residual tropical red clay soil (data from Wesley, 2010, Figure 8.12). As seen in Figure 3.13a, there is no apparent break in the semi-log form of the curve that indicates a preconsolidation pressure. In fact,

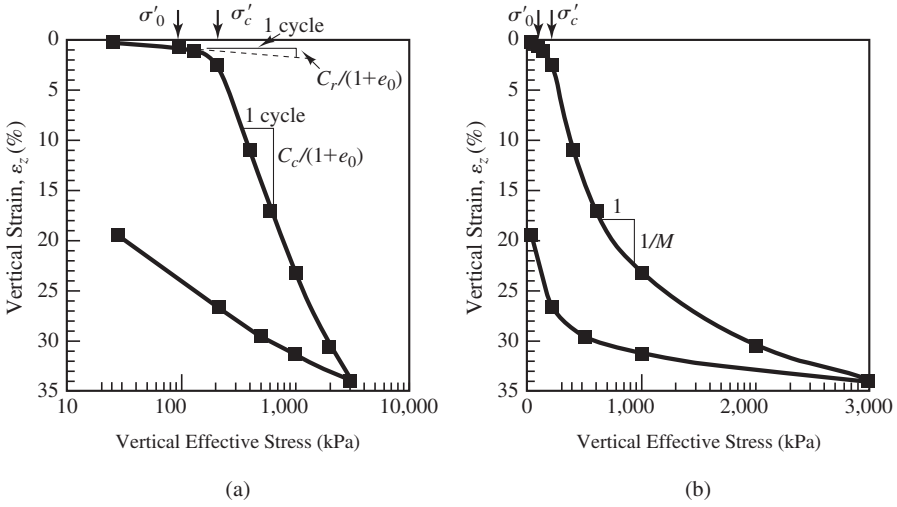

Figure 3.12 Stress-strain curve for a lightly overconsolidated soft clay plotted in: (a) the semi-logarithmic (e-log-p); and (b) arithmetic (linear) forms (data from Wesley, 2010, Figure 8.10).

the arithmetic form of the stress-strain curve shown in Figure 3.13b clearly shows that the soil is continually getting stiffer as the stress increases and that there is no transition between a stiff overconsolidated region and a softer normally consolidated region. Figure 3.13c expands the lower portion of the stress-strain curve in the region typical of induced stresses we would expect to see from typical foundations. While the curve in this region has a concave shape, it could satisfactorily be modeled with a constant modulus.

In general, the semi-log form of the stress-strain curve is appropriate for normally consolidated or lightly overconsolidated soft- to medium-saturated clays, and the stress-strain properties are best expressed using Equations 3.25 through 3.27. In most other cases, including sands and highly overconsolidated clays, the linear or arithmetic form is more appropriate, as expressed by Equation 3.20. However, rather than relying on descriptions of soil types, the best way to determine the appropriate stress-strain model is to plot stress-strain data in both arithmetic and e-log-p forms, determining the stress range over which the soil will be loaded in the field, and selecting the best model.

Computing Foundation Settlement

Once we have determined the appropriate form of the stress-strain curve, we must determine the compressibility parameters (M, C_c, C_r, etc.). Chapter 4 will discuss how to determine these parameters from field or laboratory tests. Once this is done, we compute the change in vertical stress under the foundation using the techniques presented in Section 3.3. Then the settlement is computed by solving the integral in Equation 3.19 using distribution of induced stress computed and the appropriate stress-strain model. From a practical standpoint, we generally divide the soil into a series of horizontal layers, assume the stress change and soil properties for each are constant, and replace the integral in Equation 3.19 with a summation.

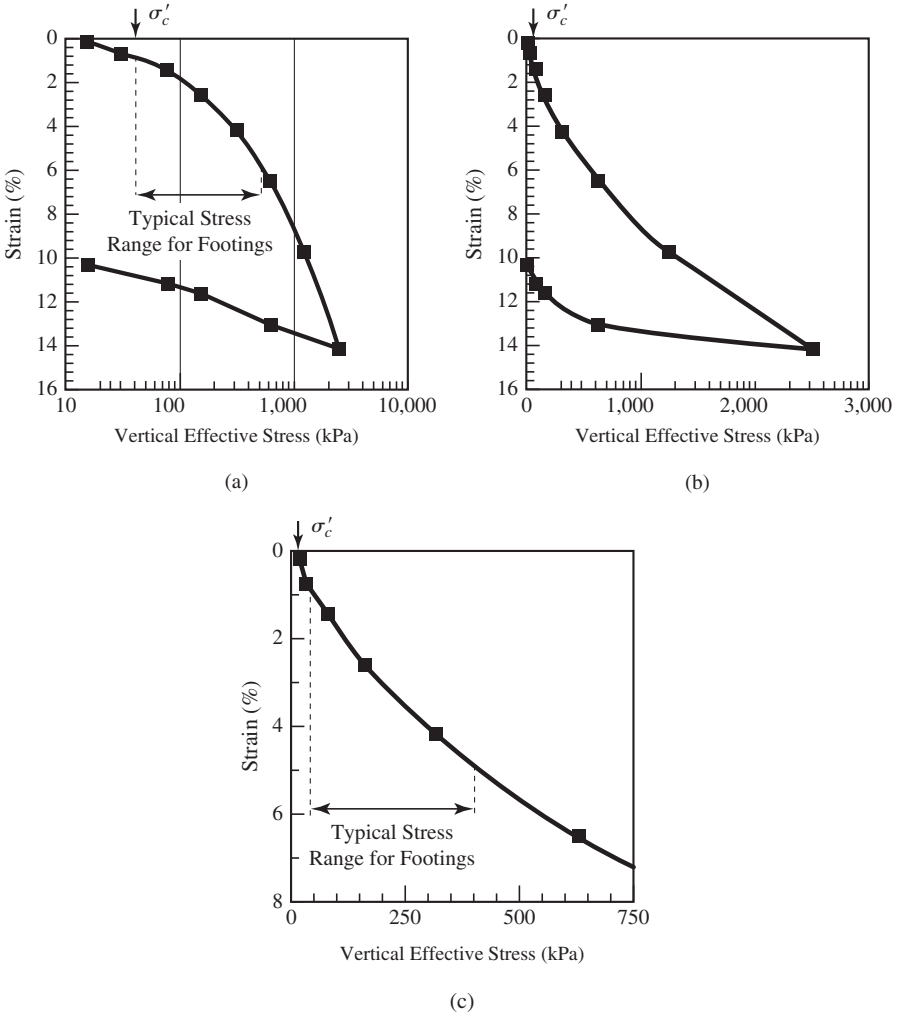

Figure 3.13 Stress-strain curve for a residual clay plotted in: (a) semi-logarithmic *e*-log-*p*; (b) arithmetic forms; and (c) expansion of low end of arithmetic form (data from Wesley, 2010, Figure 8.12).

Modulus Based Method

For cases where the soil can be modeled using an arithmetic stress-strain curve, we compute the settlement, δ, using the constrained modulus, M. In this case the settlement is computed combining Equations 3.19 and 3.20 to get Equation 3.28:

$$\delta = \sum_{i=1}^{n} \frac{\Delta\sigma_i'}{M_i} H_i \tag{3.28}$$

where

$\Delta\sigma_i' =$ change in effective stress of the i^{th} layer
$M_i =$ constrained modulus of the i^{th} layer
$H_i =$ thickness of the i^{th} layer

The soil mechanics literature often uses the term *coefficient of volume compressibility*, m_v, to describe the linear relationship between stress and strain in one-dimensional compression. In this book, we will use the term constrained modulus, M, because it is a well-defined term in elasticity and commonly understood by many disciplines.

Example 3.4

A 10 m × 30 m mat foundation is to be built on the surface of a 20 m thick layer of unsaturated silty sand. The silty sand is underlain by a stiff bedrock material. The water table is at a great depth. The silty sand is relative uniform and in situ testing indicates it has a constrained modulus of 19 MPa. The building applies a uniform stress of 50 kPa at the base of the mat. Compute the settlement under the center of the mat.

Solution

Since we are told the soil is relatively uniform and given a constrained modulus, it is appropriate to use the modulus based method. We will consider only the consolidation of the silty sand since it is underlain by much stiffer bedrock. Since the water table is at a great depth, we will assume the pore pressure is zero and the effective stress is equal to the total stress.

The solution process is to divide the compressible soil into layers, determine the change in vertical stress for each layer, then compute the strain and compression of each layer. Finally, we will sum the compressions of the individual layers to determine the total settlement.

We choose to divide the silty sand into 10 layers each 2 m thick. This is a small enough number of layers to allow a simple hand solution but large enough to provide reasonably accurate results. We use Equation 3.16 to compute the change in stress at the center of each layer and Equation 3.20 to compute the strain of each layer. Finally, we sum the compression of each layer to determine the total settlement using Equation 3.28. The results of these calculations are shown in the following table.

Layer No.	Depth to Layer Midpoint (m)	Layer Thickness (cm)	$\Delta\sigma'$ (kPa)	M (kPa)	ε_v	Layer Compression (cm)
1	1	200	49.9	19,000	0.26	0.53
2	3	200	46.8	19,000	0.25	0.49
3	5	200	40.0	19,000	0.21	0.42
4	7	200	32.9	19,000	0.17	0.35
5	9	200	26.8	19,000	0.14	0.28
6	11	200	22.1	19,000	0.12	0.23

(*continued*)

Layer No.	Depth to Layer Midpoint (m)	Layer Thickness (cm)	$\Delta\sigma'$ (kPa)	M (kPa)	ε_v	Layer Compression (cm)
7	13	200	18.5	19,000	0.10	0.19
8	15	200	15.6	19,000	0.08	0.16
9	17	200	13.4	19,000	0.07	0.14
10	19	200	11.6	19,000	0.06	0.12
						$\delta = 2.29$

Comments

The total computed settlement of 2.3 cm is under the center of the mat. If the mat was perfectly flexible, the settlement at the edges would be significantly less. However, the mat is in fact quite rigid. This effect is discussed in Chapter 8. In any case, 2.3 cm is a relatively large settlement and may not be tolerable. Chapter 5 discusses acceptable settlement limits. There are many details left out of this analysis, in particular the stiffness of the mat foundation. More details on the design of mat foundations are presented in Chapter 11.

e-log-*p* Method

For this case we must determine whether the soil is normally consolidated or overconsolidated. In the case where the soil is normally consolidated, the settlement, δ, is computed by combining Equations 3.19 and 3.25 as:

$$\delta = \sum_{i=1}^{n} H_i \left(\frac{C_c}{1 + e_0} \right)_i \log \left(\frac{(\sigma'_{zf})_i}{(\sigma'_{z0})_i} \right) \tag{3.29}$$

Overconsolidated Case I is when $\sigma'_{zf} \leq \sigma'_c$ and the settlement, δ, is computed by combining Equations 3.19 and 3.26 as:

$$\delta = \sum_{i=1}^{n} H_i \left(\frac{C_r}{1 + e_0} \right)_i \log \left(\frac{(\sigma'_{zf})_i}{(\sigma'_{z0})_i} \right) \tag{3.30}$$

Overconsolidated Case II is when $\sigma'_{zf} > \sigma'_c$ and the settlement, δ, is computed by combining Equations 3.19 and 3.27 as:

$$\delta = \sum_{i=1}^{n} H_i \left[\left(\frac{C_r}{1 + e_0} \right)_i \log \left(\frac{(\sigma'_c)_i}{(\sigma'_{z0})_i} \right) + \left(\frac{C_c}{1 + e_0} \right)_i \log \left(\frac{(\sigma'_{zf})_i}{(\sigma'_c)_i} \right) \right] \tag{3.31}$$

Example 3.5

A 5 ft square footing carries a sustained load of 20 k. It is constructed on the surface of a 40 ft thick saturated lightly overconsolidated clay soil. Based on laboratory tests, the clay can

be adequately modeled using the *e*-log-*p* method. The laboratory tests provide the following compressibility information for the clay:

$$\gamma = 120 \text{ lb/ft}^3$$

$$\frac{C_c}{1 + e_0} = 0.08$$

$$\frac{C_r}{1 + e_0} = 0.003$$

$$\sigma'_m = 600 \text{ lb/ft}^2$$

The groundwater table is located at the ground surface. Compute the settlement of the footing.

Solution

From examining Figure 3.6, we see that at a depth of $2B$ the induced stress from a square loaded area is approximately 10 percent of the applied load. Therefore, it should be sufficiently accurate to compute the compressibility to only a depth of 10 ft, even though the compressible layer is much thicker. We will divide the clay into 5 layers, each 2 ft thick.

The compression of the first layer is computed in the following fashion.

Compute the initial effective vertical stress considering the groundwater table at the ground surface

$$\sigma'_{z0} = 1 \text{ ft}(120 \text{ lb/ft}^2) - 1 \text{ ft}(62.4 \text{ lb/ft}^2)$$

Using Equation 3.14 to compute the induced stress:

$$\Delta\sigma_z = \frac{20{,}000 \text{ lb}}{(5 \text{ ft})^2}\left[1 - \left(\frac{1}{1 + \left(\frac{5}{2(1)}\right)^2}\right)^{1.76}\right] = 800 \text{ lb/ft}^2(0.9694) = 775 \text{ lb/ft}^2$$

$$\sigma'_{zf} = \sigma'_{z0} + \Delta\sigma'_z = 58 \text{ lb/ft}^2 + 775 \text{ lb/ft}^2 = 833 \text{ lb/ft}^2$$

$$\sigma'_c = \sigma'_{z0} + \sigma'_m = 58 \text{ lb/ft}^2 + 600 \text{ lb/ft}^2 = 658 \text{ lb/ft}^2$$

Since $\sigma'_{zf} > \sigma'_c$, this is case OC-II and the layer compression is computed using Equation 3.31:

$$\delta = 24 \text{ in}\left[(0.003)\log\left(\frac{658}{58}\right) + (0.08)\log\left(\frac{833}{658}\right)\right] = 0.27 \text{ in}$$

This process is repeated for the remaining layers noting that when $\sigma'_{zf} < \sigma'_c$, Equation 3.30 is used to compute δ. The following table shows the results of these calculations.

Layer No.	Depth to Layer Midpoint (ft)	Layer Thickness (ft)	Computed at Layer Midpoint σ'_{z0} (lb/ft^2)	$\Delta\sigma_{z0}$ (lb/ft^2)	σ'_{zf} (lb/ft^2)	σ'_c (lb/ft^2)	Case	$\frac{C_c}{1+e_0}$	$\frac{C_r}{1+e_0}$	δ (in)
1	1	2	58	776	833	658	OC-II	0.08	0.003	0.27
2	3	2	173	484	657	773	OC-I	0.08	0.003	0.04
3	5	2	288	260	548	888	OC-I	0.08	0.003	0.02
4	7	2	403	152	556	1,003	OC-I	0.08	0.003	0.01
5	9	2	518	98	616	1,118	OC-I	0.08	0.003	0.01

$\delta = 0.35$

Comments

This total settlement of 0.35 inches is most likely acceptable for most structures. Some details of computing settlement of spread footings have been omitted in this example. Chapter 8 provides detailed guidance on computing settlements of spread footings.

Other Factors Affecting Settlement

Equations 3.28 through 3.31 explicitly account for only one-dimensional compression under the center of a foundation placed on an isotropic, homogeneous soil. There are several other factors that will affect settlement including:

1. Foundation shape
2. Poisson effect, that is, effect of horizontal stresses and strains
3. Effect of shear stresses
4. Depth of foundation below the ground surface
5. Point below the foundation being considered, that is, center versus edge
6. Foundation rigidity
7. Foundation roughness
8. Soil homogeneity
9. Non-linear soil properties
10. Drainage conditions, that is, undrained versus drained

In some cases, these factors can be accounted for using theoretical and analytical methods. In other cases, empirical methods can be used. More information on computing settlements for the various foundation systems is covered in later chapters.

3.5 SHEAR STRENGTH

Structural foundations also induce significant shear stresses into the ground. If these shear stresses exceed the shear strength of the soil or rock, failure occurs. Therefore, we must be able to assess these shear stresses and strengths and design foundations such that the shear stresses are sufficiently smaller than the shear strength.

Drained and Undrained Conditions

Excess pore water pressures generated from loading a soil will impact the effective stress, and thus the shear strength of the soil, so the generation and dissipation of these excess pore water pressures are important considerations in shear strength evaluations. Geotechnical engineers often evaluate this problem by considering two limiting conditions: the drained condition and the undrained condition. Before describing these conditions, we will discuss the volume change tendencies in a soil during loading that lead directly to excess pore water pressure generation.

Volume Change During Loading

When soils are loaded (or unloaded) there is always volume change. In theory, these volume changes can be separated into two distinct parts: (1) contraction (compression) or dilation (expansion) due to changes in the hydrostatic (all-around) mean normal stress, and (2) contraction or dilation due to changes in the deviator stress.

Volume Change Due to Mean Normal Stress

When a soil is subjected to an increase or decrease of the hydrostatic mean normal stress, the soil skeleton formed by the soil particles will compress or expand, respectively. In the Mohr circle model, the mean normal stress corresponds to the distance between the center of the circle and the origin. As the circle moves farther to the right, the mean normal stress increases and the soil compresses. As the circle moves to the left, the mean normal stress decreases and the soil expands. Because the stress state is hydrostatic, no shear stresses are induced in the soil.

Volume Change Due to Deviator Stress

When a soil is subjected to an increase in the deviator stress, shear stresses are induced in the soil. These induced shear stresses will cause the soil particles to rearrange and can lead to volume change. In the Mohr circle model, this corresponds to an increase in the diameter of the circle without changing the location of the center of the circle. The magnitude and sign of the volumetric change due to a deviator stress increase depends on both the density of the soil and the magnitude of the mean normal stress. A loose soil subjected to a high mean normal stress will contract during shear. This results in a decrease of the voids

volume. Conversely, a dense soil subjected to a low mean normal stress will dilate during shear. This results in an increase in the voids volume. An intermediate condition also is possible, where the void ratio and mean normal stress are such that little or no changes in volume occur during shear. Furthermore, if a soil is medium dense and sheared, it may contract initially then dilate.

If the soil is saturated, these volume change tendencies will drive some of the pore water into or out of the voids. Understanding this process, and its consequences, is a key part of understanding shear strength and soil behavior.

The Drained Condition

We define the drained condition as a limiting condition under which there is no excess pore water pressure in the soil. The important consequence of the drained condition is that the pore water pressure is equal to the hydrostatic pore water pressure and is thus easily computed. Therefore, effective stress and strength also are easily computed.

The drained condition can develop in one of two ways:

1. If the soil is saturated, its hydraulic conductivity is sufficiently high, and the rate of loading (and therefore the rate of voids volume change) is sufficiently low, then the necessary volume of water can easily flow into or out of the voids. Any excess pore water pressures generated during loading will be quickly dissipated. Most loads are applied fairly slowly. For example, the dead load from a building is generated as the building is constructed, a process that typically occurs over weeks or months. If the soil is cohesionless, the hydraulic conductivity is usually sufficiently high that the pore water has enough time to move as needed. Thus, cohesionless soils under static loading are usually under the drained condition, and the shear strength may be evaluated using the hydrostatic pore water pressure.
2. If a long time has elapsed after the end of loading, any excess pore water pressure generated during loading will have dissipated. In this case, the drained condition will be reached in the soil in the long term regardless of what type of soil it is.

The Undrained Condition

A completely different situation occurs in a saturated soil that has a low hydraulic conductivity or when the loading is very rapid. In this case, the rate of loading, and thus the rate of voids volume change, is faster than the rate of drainage, so there is not enough time for the necessary volume of pore water to flow into or out of the voids. The limiting condition, in which virtually no pore water movement takes place and excess pore water pressures are generated, is called the undrained condition.

Under the undrained condition, since water cannot flow into or out of the soil, the soil will respond by developing excess pore water pressures to compensate for the tendency of the soil to either contract or dilate. The magnitude of the excess pore water pressure will depend on both the changes in the mean normal stress and changes in the

deviator stress. If the soil contracts during shear, then the excess pore water pressure will be positive because the soil wants to push water out of the pores to contract. Conversely, if the soil dilates during shear, then the excess pore water pressure will be negative because the soil wants to draw water into the pores to expand. In either case, this phenomenon can have a significant impact on the effective stress and thus on the shear strength.

The hydraulic conductivity of cohesive soils is several orders of magnitude smaller than that of cohesionless soils, so even typical rates of loading, such as those from placement of a fill or construction of a building, are very high relative to the rate of drainage. Thus, saturated cohesive soils are most often assumed to be under the undrained condition during the loading or construction period in the short term and their shear strength must be analyzed accordingly. Therefore, the geotechnical engineer must directly or indirectly account for the excess pore water pressures generated during loading. However, a long time after the end of construction, all the excess pore water pressures will have dissipated and the condition in cohesive soils reaches the drained condition. Therefore, for cohesive soils, the condition for shear strength evaluation changes from the undrained condition in the short term to the drained condition in the long term.

An especially interesting situation occurs when cohesionless soils, which are normally drained, are subjected to very rapid loading, such as from machine vibrations or from an earthquake. In this case, the rate of loading may be very high relative to the rate of drainage, thus producing the undrained condition. Similarly, if the rate of loading is extremely low, the drainage condition during loading for cohesive soils, which normally is undrained, can be assumed to be drained.

Intermediate Drainage Conditions

The actual drainage conditions in the field are often such that some, but not all, of the necessary pore water movement occurs. Thus, the real drainage condition may be somewhere between drained and undrained conditions. Although a geotechnical engineer could attempt to evaluate these intermediate drainage conditions, this is rarely done in practice. Instead, we nearly always conduct strength evaluations assuming either the drained or undrained condition exists in the field.

Mohr–Coulomb Failure Criterion

In geotechnical practice, the shear strength of a soil is usually determined using the *Mohr–Coulomb failure criterion*. This failure criterion can be written in terms of effective stress parameters or total stress parameters and used in effective stress analyses or total stress analyses, respectively.

Effective Stress Analyses

The shear strength of a soil is developed only by the solids of the soil; the water and air, representing the other two phases of the soil, have no shear strength. Therefore, the shear strength is fundamentally controlled by the effective stress, σ', because the effective stress

is the portion of the total stress, σ, carried by the solid particles. In terms of effective stress parameters, the Mohr–Coulomb failure criteria can be written as:

$$s = c' + \sigma' \tan \phi' = c' + (\sigma - u) \tan \phi' \tag{3.32}$$

where

s = shear strength
c' = effective cohesion
σ = total normal stress acting on the shear surface
σ' = effective normal stress acting on the shear surface
ϕ' = effective friction angle
u = pore water pressure

This is called the effective stress Mohr–Coulomb failure criterion. Once c' and ϕ' are determined, we can evaluate the shear strength in the field using Equation 3.32. We compute the effective stresses in the field, assuming the drained or undrained condition. For the drained case, we can calculate the effective stresses using the hydrostatic or steady state pore water pressures which represent the worst conditions anticipated during the life of the project.

Total Stress Analyses

Analyses based on effective stresses are possible only if we can predict the effective stresses in the field. This is a simple matter under the drained condition when only hydrostatic or steady state pore water pressures are present, but can become very complex under the undrained condition when there are excess pore water pressures. For example, when a fill is placed over a saturated cohesive soil, excess pore water pressures develop in the soil due to the increase in mean normal stress. In addition, some soils also develop additional excess pore water pressures due to increased deviator stress, as described earlier. Often these excess pore water pressures are difficult to predict, especially those due to shearing.

Because of these difficulties, geotechnical engineers sometimes evaluate problems based on total stresses instead of effective stresses. This approach involves reducing the laboratory data in terms of total stresses and expressing it using the total stress parameters c_T and ϕ_T. Equation 3.32 then needs to be rewritten in terms of total stresses as:

$$s = c_T + \sigma \tan \phi_T \tag{3.33}$$

where

s = shear strength
c_T = total cohesion
σ = total stress acting on the shear surface
ϕ_T = total friction angle

This is called the total stress Mohr–Coulomb failure criterion.

The total stress analysis method assumes the excess pore water pressures developed in the laboratory test are the same as those in the field, and thus are implicitly incorporated into c_T and ϕ_T. This assumption introduces some error into the analysis, but it becomes an unfortunate necessity when we cannot predict the magnitudes of excess pore water pressures in the field. It also demands the laboratory tests be conducted in a way that simulates the field conditions as closely as possible.

The shear strength of a soil really depends on effective stresses, so total stress analyses are less desirable than effective stress analyses, and the results need to be viewed with more skepticism. However, there are many times when we must use total stress analyses because we have no other practical alternative.

Shear Strength of Saturated Cohesionless Soils

The rate of drainage in cohesionless soils is very high because of their high hydraulic conductivities. In other words, any excess pore water pressures that may develop in these soils dissipate very rapidly because water flows through them very quickly and easily. In addition, most of the load acting on foundations usually consists of dead and live loads, which are applied over a period of days or weeks. This is much slower than the rate of drainage in cohesionless soils. Therefore, when designing foundations on cohesionless soils, we can nearly always assume the drained condition applies. Therefore, the pore water pressure equals the hydrostatic pore water pressure, and we can compute the vertical effective stress using Equation 3.5.

The effective cohesion, c', and effective friction angle, ϕ', can be obtained from laboratory tests (as discussed later in this chapter) or from in situ tests (as discussed in Chapter 4). For clean or silty sands and gravels (USCS group symbols SM, SP, SW, GM, GP, and GW), it is normally best to use $c' = 0$. Some cohesion may be present in clayey sands and gravels (group symbols SC and GC), but it should be used only with great caution, because it may not be present in the field. Figure 3.14 presents typical values of ϕ', and may be used to check the lab or field test results.

Finally, knowing the values of c', ϕ', and σ', we can compute the shear strength using Equation 3.32.

Shear Strength of Saturated Cohesive Soils

The hydraulic conductivity of cohesive soils is about one million times smaller than that of cohesionless soils, so the rate of drainage in these soils is very low—much lower than the rate of loading. Therefore, undrained conditions are typically present in such soils. This means significant excess pore water pressures may be present during and immediately after loading. Eventually, these excess pore water pressures dissipate, as shown by the plot of pore water pressure with time for the undrained case in Figure 3.15.

The hydraulic conductivity of silts is greater than that of clays, but it still is much smaller than that of sands. Once again, the undrained condition is usually assumed to apply, although less time is required for the excess pore water pressures to dissipate.

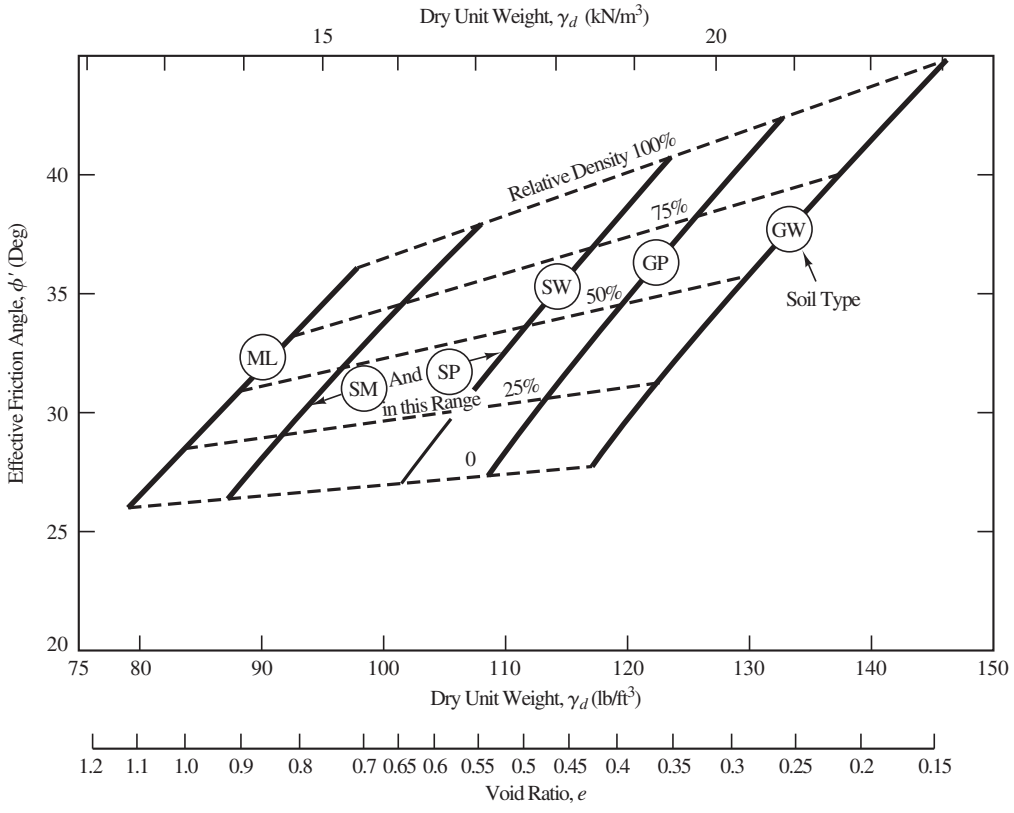

Figure 3.14 Typical ϕ' values for sands, gravels, and silts without plastic fines (adapted from U.S. Navy, 1982a).

To understand the impact of these excess pore water pressures, compare the two sets of plots in Figure 3.15, along with the Equations 3.5 and 3.32. In both cases, the vertical total stress, σ_z, and the shear stress, τ, increase as the load P is applied. Under the drained condition, the vertical effective stress, σ_z', and the shear strength, s, both rise concurrently with σ_z, so both τ and s reach their peak values at the end of loading.

However, under the undrained condition, the temporary presence of excess pore water pressures (the spike in the u plot) causes a lag in the increase in shear strength. Although τ reaches its peak at the end of loading, s is still low, thus producing a temporary drop in the factor of safety, F. Then, as the excess pore water pressures dissipate, both s and F slowly climb.

The most likely time for failure is immediately after construction (i.e., when F is at a minimum). Therefore, foundations are normally designed to have a certain minimum factor of safety at this critical moment. To accomplish this goal, we need to consider the excess pore water pressures, either explicitly or implicitly.

In principle, we should be able to determine the magnitude of the excess pore water pressure, u_e, and use Equations 3.5 and 3.32 to compute the shear strength immediately

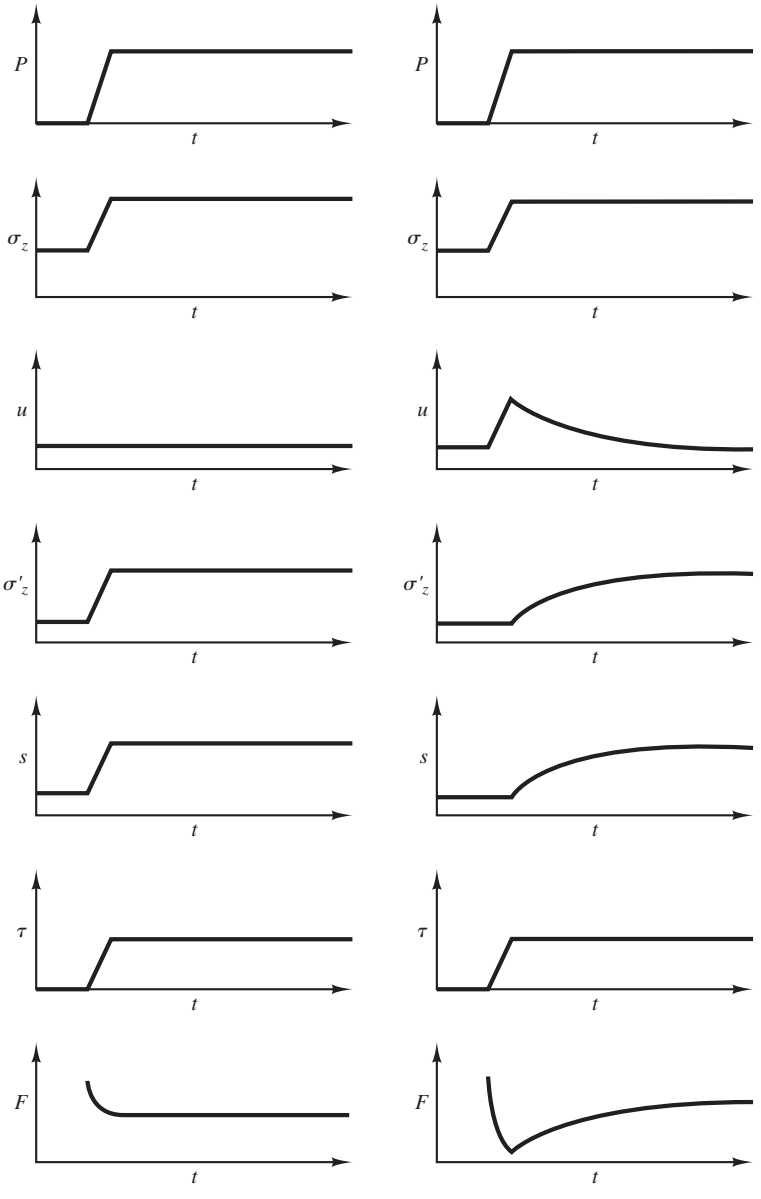

(a) The drained condition

(b) The undrained condition short-term
The drained condition long-term

Figure 3.15 Changes in normal and shear stresses, pore water pressure, shear strength and factor of safety with time at a point in a saturated soil subjected to a load P under drained versus undrained conditions.

after construction. This method is called an effective stress analysis. We then could use this shear strength as the basis for a foundation design that provides the minimum acceptable factor of safety. Unfortunately, the magnitude of u_e is difficult to determine, especially in overconsolidated soils, so this method is not economically viable for most foundation projects.

Because of this problem, engineers normally resort to performing a total stress analysis and compute the shear strength using Equation 3.33. This equation is based on c_T and ϕ_T, which are determined by evaluating the laboratory test data in terms of total stress instead of effective stress. Presumably, the consequences of the excess pore water pressures are implicit within these values. We then assume the excess pore water pressures in the field are the same as those in the lab, and apply Equation 3.33 to the field conditions without needing to know the magnitude of the excess pore water pressures.

If the soil is truly saturated and truly undrained, then $\phi_T = 0$ (even though $\phi' > 0$) because newly applied loads are carried entirely by the pore water and do not change ϕ' or s. This is very convenient because the second term in Equation 3.33 drops out and we no longer need to compute σ. We call this a "$\phi = 0$ analysis," and the shear strength is called the *undrained shear strength*, s_u, where $s_u = c_T$. Usually we assign an appropriate s_u value for each saturated undrained stratum based on laboratory or field test results, as discussed in Chapter 4. We should note, however, that the value of s_u is not unique because it depends on how the soil is loaded to failure. Due to the differences in the details of the loading process, such as the loading rate and the eventual failure mode, different laboratory and in situ tests may give different s_u values. For example, the vane shear test gives s_u values that need to be corrected by an empirical factor, as described in Chapter 4.

Many geotechnical analysis methods use this s_u value directly. Other analysis methods require the shear strength to be defined using c and ϕ. When using the later type with saturated undrained analysis, we set $c = s_u$ and $\phi = 0$.

In reality, s_u is probably not constant throughout a particular soil stratum, even if the soil appears to be homogenous. In general, s_u increases with depth because the lower portions of the stratum have been consolidated to correspondingly greater loads, and thus have a higher shear strength. The shallow portions also have higher strengths if they had once dried out (desiccated) and formed a crust. Finally, the natural non-uniformities in a soil stratum produce variations in s_u. We can accommodate these variations by simply taking an average value, or by dividing the stratum into smaller layers.

As mentioned above, it is common to find that s_u increases with depth, with the ratio of s_u to σ_z' or σ_c' a constant. Indeed, many researchers have developed empirical correlations for the s_u/σ_z' or s_u/σ_c' ratio. Note that these two ratios are the same for normally consolidated soils. For example, Terzaghi et al. (1996) gives an average s_u/σ_c' ratio that can be used in stability analyses of embankments and footings as:

$$s_u/\sigma_c' = 0.22 \tag{3.34}$$

For lightly overconsolidated cohesive soils, Jamiolkowski et al. (1985) gives:

$$s_u/\sigma_c' = 0.23 \pm 0.04 \tag{3.35}$$

The s_u or s_u/σ'_z ratio also may be determined from in situ test data as described in Chapter 4.

Sensitivity

Some cohesive soils exhibit a significant decrease in strength when disturbed. This phenomenon is call *sensitivity*, S_t, and is measured as the ratio of the undrained strength of a disturbed sample to that of a remolded sample:

$$S_t = \frac{s_{u,\text{ disturbed}}}{s_{u,\text{ remolded}}} \tag{3.36}$$

Soils with a sensitivity value of 4 or less are considered insensitive.

Shear Strength of Saturated Intermediate Soils

Thus far we have divided soils into two distinct categories of cohesive and cohesionless soils. Cohesionless soils do not develop excess pore water pressures during static loading, and thus may be evaluated using effective stress analysis and hydrostatic pore water pressures. Conversely, cohesive soils do develop excess pore water pressures, and thus require more careful analysis. They also may have problems with sensitivity and creep. Although many "real-world" soils neatly fit into one of these two categories, others behave in ways that are intermediate between these two extremes. Their field behavior is typically somewhere between being drained and undrained (i.e., they develop some excess pore water pressures, but not as much as would occur in a cohesive soil).

Although there are no clear-cut boundaries, these intermediate soils typically include those with unified classification SC, GC, SC-SM, or GC-GM, as well as some SM, GM, and ML soils. Proper shear strength evaluations for engineering analyses require much more engineering judgment, which is guided by a thorough understanding of soil strength principles. When in doubt, it is usually conservative to evaluate these soils using the techniques described for cohesive soils.

Shear Strength of Unsaturated Soils

Thus far we have only considered soils that are saturated ($S = 100\%$). The strength of unsaturated soils ($S < 100\%$) is generally greater, but more difficult to evaluate. Nevertheless, many engineering projects encounter these soils, so geotechnical engineers need to have methods of evaluating them. This has been a topic of ongoing research (Fredlund et al., 2012), and standards of practice are not yet as well established as those for saturated soils.

Some of the additional strength in unsaturated soils is caused by negative pore water pressures. These negative pore water pressures increase the effective stress, and thus increase the shear strength. However, this additional strength is very tenuous and is easily lost if the soil becomes wetted.

Geotechnical engineers usually base designs on the assumption that unsaturated soils could become wetted in the future. This wetting could come from a rising groundwater table, irrigation, poor surface drainage, broken pipelines, or other causes. Therefore, we usually saturate (or at least "soak") soil samples in the laboratory before performing strength tests. This is intended to remove the apparent cohesion and thus simulate what are usually the "worst case" field conditions. We then determine the highest likely elevation for the groundwater table, which may be significantly higher than its present location, and compute positive pore water pressures accordingly. Finally, we assume $u = 0$ in soils above the groundwater table.

3.6 LATERAL EARTH PRESSURES

The geostatic horizontal stress is introduced in Section 3.3, along with the at-rest lateral earth pressure coefficient K_0. This section discusses the active and passive lateral earth pressures that may develop between a foundation such as a footing in the ground and the surrounding soil. It also presents the Rankine's theory of lateral earth pressures.

This section only considers lateral earth pressures in soils that are homogeneous and isotropic (ϕ and γ have the same values everywhere, and each has the same value in all directions at every point) as well as cohesionless ($c = 0$).

Lateral earth pressure theories may be used with either effective stress analyses (c', ϕ') or total stress analyses (c_T, ϕ_T). However, effective stress analyses are appropriate for cohesionless soils, and are the only type we will consider in this chapter.

Rankine's Theory for Cohesionless Soils

Assumptions

Rankine approached the lateral earth pressure problem with the following assumptions:

1. The soil is homogeneous, isotropic, and cohesionless as defined above.
2. The shear surface is a plane. In reality, it is slightly concave upward, but this is a reasonable assumption (especially for the active case) and it simplifies the analysis.
3. The ground surface is planar (although it does not necessarily need to be level).
4. The vertical surface on which the lateral earth pressure acts is infinitely long in the horizontal direction. This is called a *plane strain condition* because all the strains occur in a plane normal to the infinitely long axis.
5. There is sufficient lateral displacement to develop the active or passive condition.
6. The resultant of the normal and shear forces that acts in a direction parallel to the ground surface.
7. The vertical surface on which the lateral earth pressure acts is frictionless.

We will only examine the special case in which the ground surface is horizontal.

Active Condition

To explain the active condition, consider the footing shown in Figure 3.16. Further consider the soil element 1 shown behind the left side of the footing. Suppose Mohr circle A in Figure 3.17 represents the state of stress in element 1 in Figure 3.16 in the at-rest condition. In this case, σ_z' and σ_x' are the major and minor principal stresses, respectively, and the inclined lines are the Mohr—Coulomb failure envelopes. Because the Mohr circle does not touch the failure envelope, the shear stress, τ, is less than the shear strength, s. This is typically true because in the at-rest condition, the soil has not failed and is in equilibrium.

Now, consider the active condition in the soil in which the footing is permitted to move to the right away from the soil on the right a short distance. Note that in this case, because of assumption 6 above, there are no shear forces acting on the vertical surface of the foundation, that is, this surface is a principal plane. Therefore, σ_z' and σ_x' will remain the major and minor principal stresses, respectively, with σ_x' decreasing as the foundation moves away from the soil. This causes the Mohr circle to expand to the left until the circle touches the failure envelope and the soil fails in shear, Figure 3.17 circle B. This shear failure will occur along the failure surfaces shown in on the left side of the footing in Figure 3.16. The inclination of these failure surfaces can be shown to be $45° + \phi'/2$ with the horizontal, as shown in Figure 3.16. At this state, the horizontal stress is at its

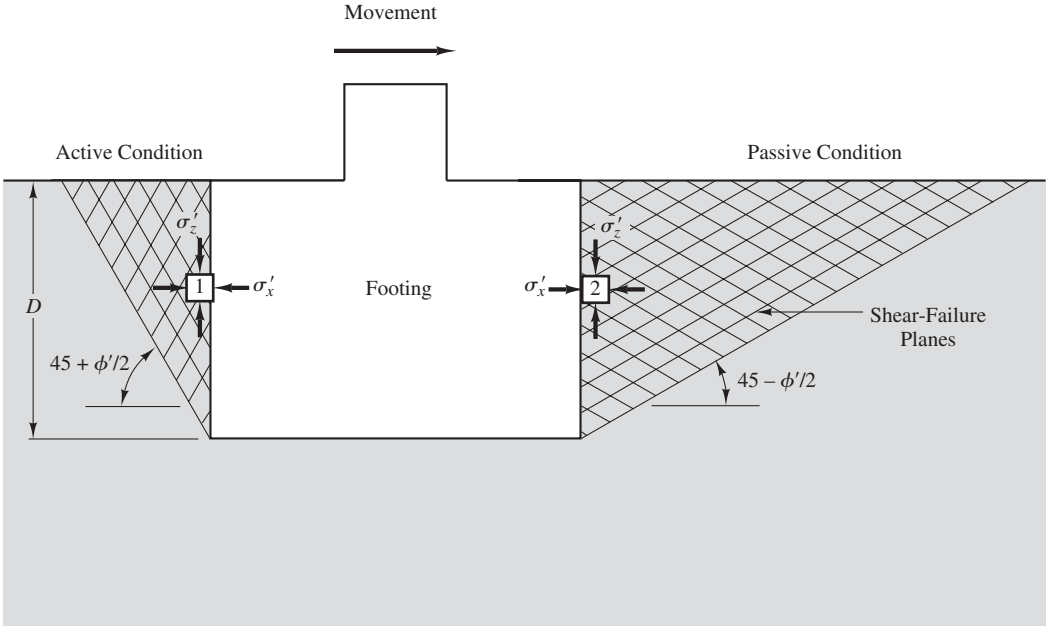

Figure 3.16 Development of active and passive earth pressures on sides of a footing as it is pushed to one side.

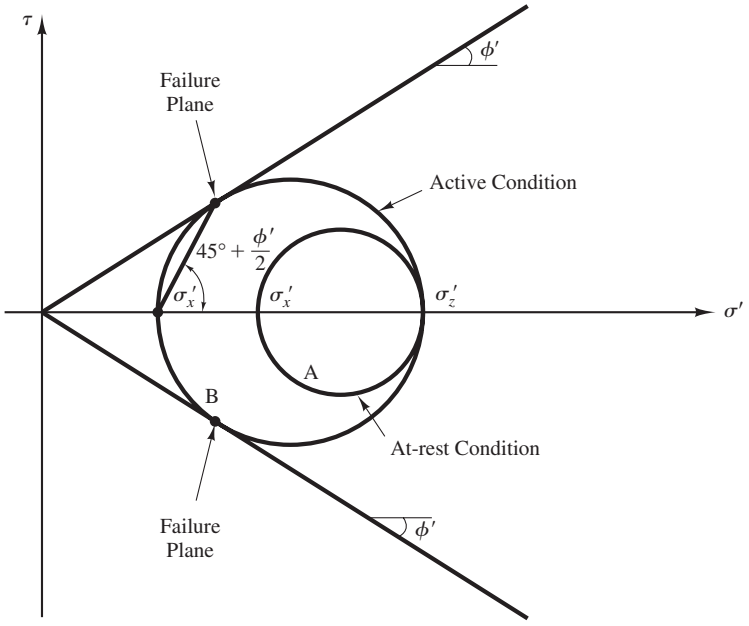

Figure 3.17 Changes in the stress state in a soil as it transitions from the at-rest condition to the active condition.

minimum, the soil is in the *active condition*, and the coefficient of active earth pressure K_a is given by:

$$K_a = \tan^2(45° - \phi'/2) \tag{3.37}$$

A plot of the active pressure with depth would show that the theoretical pressure distribution is triangular. Therefore the total active resultant force, P_a, is given by:

$$P_a = \frac{\gamma D^2 K_a}{2} \tag{3.38}$$

where

P_a = Total resultant force between foundation and soil under the active condition per unit length of foundation
K_a = coefficient of active earth pressure
D = embedment of foundation shown in Figure 3.16

Passive Condition

The *passive condition* is the opposite of the active condition. In this case, the footing moves *into* the soil on the right, as shown in Figure 3.16, and the Mohr circle changes, as shown in Figure 3.18. Notice how the vertical stress remains constant whereas the horizontal stress changes in response to the induced horizontal strains.

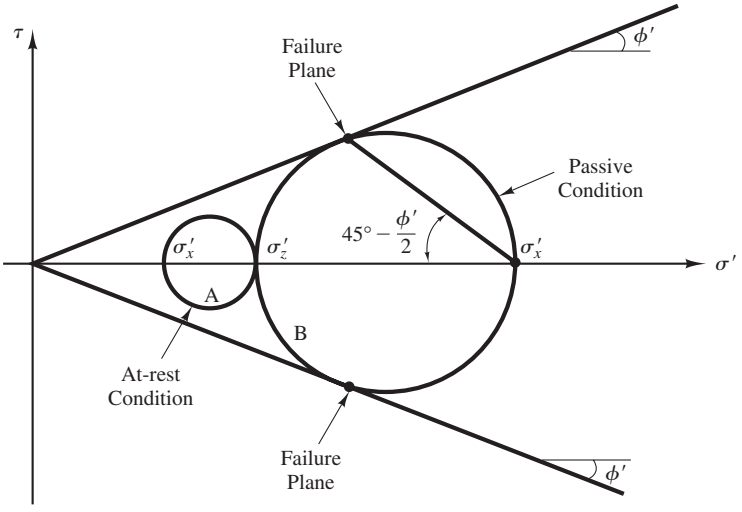

Figure 3.18 Changes in the stress state in a soil as it transitions from the at-rest condition to the passive condition.

In a homogeneous soil, the failure surfaces in the passive case are inclined at an angle of $45° - \phi'/2$ from the horizontal, as shown in Figure 3.16. At this state, the soil is in the *passive condition*, and the coefficient of passive earth pressure K_p is given by:

$$K_p = \tan^2(45° + \phi'/2) \tag{3.39}$$

A plot of the passive pressure with depth would show that the theoretical pressure distribution is triangular. Therefore the total passive resultant force is given by:

$$P_p = \frac{\gamma D^2 K_p}{2} \tag{3.40}$$

where

P_p = Total resultant force between foundation and soil under the passive condition per unit length of foundation
K_p = coefficient of passive earth pressure
D = embedment of foundation shown in Figure 3.16

Displacements Required to Mobilize Active and Passive Pressure

There must be strain in the soil in order for it to move from the at-rest state to either the active or the passive state. By examining Figure 3.17, it can be seen that there is relatively little stress change and soil goes from the at-rest condition (circle A) to the active condition. Therefore, there is relatively little strain and, correspondingly, relatively little displacement required to reach the active state. In contrast, by examining Figure 3.18 it can be seen that

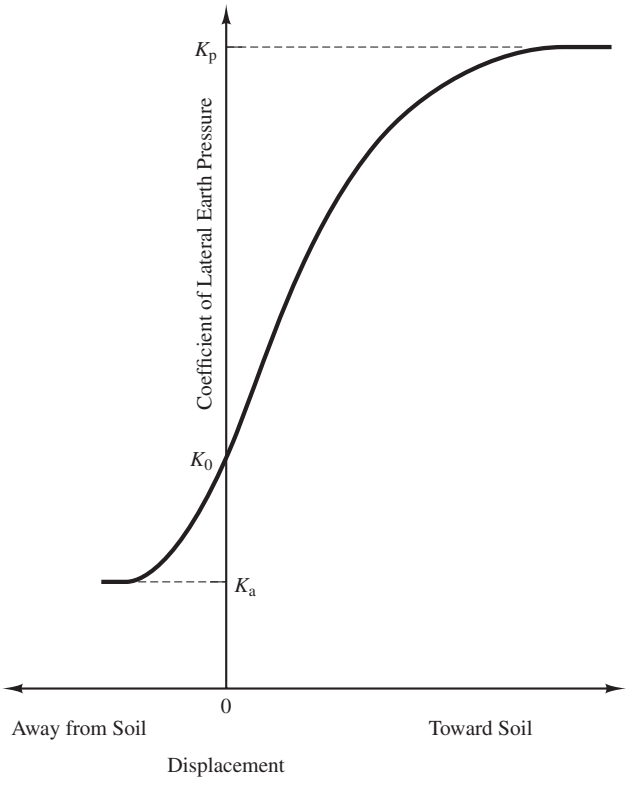

Figure 3.19 Relative displacement required to reach active and passive earth pressure.

there is a great deal more stress change between the at-rest state (circle A) and the passive state (circle B). Therefore, much more strain and displacement are required to reach the passive state. Figure 3.19 illustrates this difference between the displacement required to mobilize passive earth pressure compared to active earth pressure.

SUMMARY

Major Points

1. Soil is a particulate material, which means it is an assemblage of individual particles. Its engineering properties are largely dependent on the interactions between these particles.
2. Soil can potentially include all three phases of matter (solid, liquid, and gas) simultaneously. It is helpful to measure the relative proportions of these three phases, and we express these proportions using standard weight-volume parameters.

3. The relative density is a special parameter often used to describe the void ratio of sands and gravels.
4. The particle sizes in soil vary over several orders of magnitude, from sub-microscopic clay particles to gravel, cobbles, and boulders.
5. Clays are a special kind of soil because of their extremely small particle sizes and because of the special interactions between these particles and between the solids and the pore water.
6. Plasticity describes the relationship between moisture content and consistency in clays and silts. These relationships are quantified using the Atterberg limits.
7. Various soil classification systems are used in civil engineering. The most common system is the Unified Soil Classification System (USCS), which uses a standard system of group symbols and group names. In this book most methods are for either cohesive or cohesionless soils, which can be mapped to USCS classifications. Methods for IGMs and rocks are presented in Chapter 25.
8. Soils have both normal and shear stresses. They have two sources: geostatic stresses are those due to the force of gravity acting on the soil mass, while induced stresses are due to applied external loads, such as foundations.
9. Settlement in soils can be the result of various processes. It can be estimated from an analysis of the stress-strain behavior of soils. The stress strain relationship can be model using either the modulus method or the e-log-p method.
10. Soils in the field can be either normally consolidated or overconsolidated, depending on the difference between the current vertical effective stress and the preconsolidation stress, which is the greatest past value of this stress.
11. The degree of overconsolidation may be expressed using the overconsolidation margin or the overconsolidation ratio.
12. Shear strength in soil depends on the drainage condition and can be undrained or drained.
13. Shear strength analyses may be based on effective stresses or total stresses. Effective stress analyses are more accurate models of soil behavior, but are difficult to perform when excess pore water pressures are present.
14. The drained condition is present when the rate of loading is low relative to the rate of drainage. This is nearly always the case in cohesionless soils. The undrained condition occurs when the reverse is true, which occurs in cohesive soils. However, in the long-term, the drained condition can be considered for both cohesionless and cohesive soil.
15. Lateral earth pressure can exist between foundations in the ground and the surrounding soils. The active condition occurs in the soil if the foundation moves away from the soil, and the passive condition occurs if the foundation moves into the soil. The Rankine's theory can be used to compute active and passive lateral earth pressures. Much more displacement is required to mobilize the passive earth pressure compared to that displacement required to mobilize the active earth pressure.

Vocabulary

Atterberg limits
Boulder
Clay
Cobble
Coefficient of lateral earth pressure
Cohesion
Compression index
Consolidation
Consolidation settlement
Consolidation test
Constrained modulus
Degree of saturation
Distortion settlement
Drained condition
Dry unit weight
Effective stress
Effective stress analysis
Excess pore water pressure
Fines
Friction angle
Geostatic stress
Gravel
Group name
Group symbol
Horizontal stress
Induced stress
Intermediate geomaterials (IGMs)
Liquid limit
Mohr circle
Mohr–Coulomb failure criterion
Moisture content
Normally consolidated
Overconsolidated
Overconsolidation margin
Overconsolidation ratio
Particulate material
Phase diagram
Plastic limit
Plasticity
Poisson's ratio
Pore water pressure
Porosity
Rebound curve
Recompression curve
Recompression index
Relative density
Sand
Secondary compression settlement
Settlement
Silt
Specific gravity
Stress
Total stress
Total stress analysis
Undrained condition
Undrained shear strength
Unified Soil Classification System
Unit weight
Virgin curve
Void ratio
Weight-volume relationship
Young's modulus

QUESTIONS AND PRACTICE PROBLEMS

Section 3.1 Review and Nomenclature

3.1 Explain the difference between moisture content and degree of saturation.

3.2 A certain saturated sand ($S = 100\%$) has a moisture content of 25.1 percent and a specific gravity of solids of 2.68. It also has a maximum index void ratio of 0.84 and a minimum index void ratio of 0.33. Compute its relative density and classify its consistency.

3.3 Consider a soil that is being placed as a fill and compacted using a sheepsfoot roller (a piece of construction equipment). Will the action of the roller change the void ratio of the soil? Explain.

3.4 A sample of soil has a volume of 0.45 ft^3 and a weight of 53.3 lb. After being dried in an oven, it has a weight of 45.1 lb. It has a specific gravity of solids of 2.70. Compute its moisture content and degree of saturation before it was placed in the oven.

Section 3.3 Stress

3.5 A site is underlain by a soil that has a unit weight of 18.7 kN/m^3 above the groundwater table and 19.9 kN/m^3 below. The groundwater table is located at a depth of 3.5 m below the ground surface. Compute the total vertical stress, pore water pressure, and effective vertical stress at the following depths below the ground surface:

a. 2.2 m

b. 4.0 m

c. 6.0 m

3.6 The sub-surface profile at a certain site is shown in Figure 3.20. Compute u, σ_x, σ_z, σ'_x, and σ'_z at Point A.

3.7 A vertical load of 300 kN is applied to a 1.5 m $\times$ 1.5 m area at the ground surface that is level.

a. Compute the induced vertical stress, $\Delta\sigma_z$, at a point 2.0 m below the corner of this square loaded area.

b. Compute the induced vertical stress, $\Delta\sigma_z$, at a point 2.0 m below the center of this square loaded area.

3.8 A vertical load of 20 k is applied to a 6.0 ft $\times$ 4.0 ft area at the ground surface that is level.

a. Compute the induced vertical stress, $\Delta\sigma_z$, at a point 6.0 ft below the corner of this rectangular loaded area.

b. Compute the induced vertical stress, $\Delta\sigma_z$, at a point 6.0 ft below the center of this rectangular loaded area.

Section 3.4 Compressibility and Settlement

3.9 A 3 m $\times$ 3 m footing is to be built on the surface of a 15 m thick layer of unsaturated sand. The sand is underlain by a very dense gravel layer. The water table is at a great depth. The sand is relatively uniform and in situ testing indicates it has a constrained modulus of 10 MPa. The footing load is 200 kN. Compute the settlement under the center of the footing.

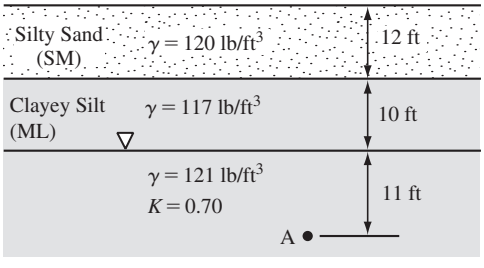

Figure 3.20 Soil profile for Problem 3.6.

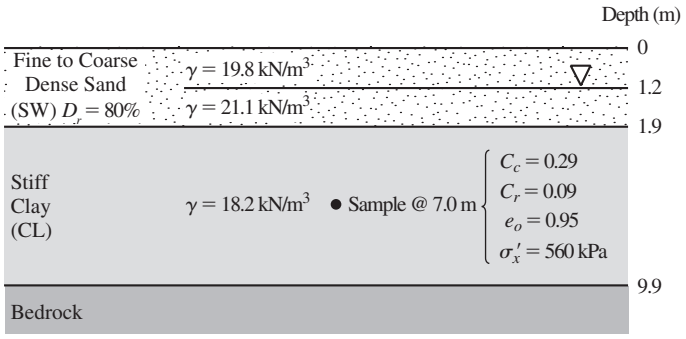

Figure 3.21 Soil profile for Problem 3.11.

3.10 A 3 ft square footing carries a sustained load of 10 k. It is placed on the surface of a 30 ft thick saturated overconsolidated clay underlain by dense sand. Based on laboratory tests, the clay can be adequately modeled using the *e*-log-*p* method. The laboratory tests provide the following compressibility information for the clay:

$$\gamma = 123 \text{ lb/ft}^3$$

$$\frac{C_c}{1 + e_0} = 0.06$$

$$\frac{C_r}{1 + e_0} = 0.002$$

$$\sigma'_m = 900 \text{ lb/ft}^2$$

The groundwater table is located at the ground surface. Compute the settlement of the footing.

3.11 A 2m thick fill is to be placed on the soil shown in Figure 3.21. Once it is compacted, this fill will have a unit weight of 19.5 kN/m^3. Compute the ultimate consolidation settlement.

Section 3.5 Shear Strength

3.12 Estimate the effective friction angle of the following soils:

- **a.** Silty sand with a dry unit weight of 110 lb/ft^3.
- **b.** Poorly-graded gravel with a relative density of 70 percent.
- **c.** Very dense well-graded sand.

3.13 Explain the difference between the drained condition and the undrained condition.

3.14 A soil has $c' = 5$ kPa and $\phi' = 32°$. The effective stress at a point in the soil is 125 kPa. Compute the shear strength normal to this stress at this point.

Section 3.6 Lateral Earth Pressures

3.15 A footing with an embedment of 2 m is embedded in a sand with a unit weight of 125 lb/ft^3 and a ϕ' of 36°. If the footing is subjected to a horizontal load that causes it to move horizontally, compute the total active and passive resultant forces acting on the footing.

Comprehensive

3.16 The soil profile at a certain site is as follows:

Depth (ft)	γ (lb/ft^3)	c' (lb/ft^2)	ϕ' (degree)	s_u (lb/ft^2)
0–12	119			1,000
12–20	126	200	20	
20–32	129	0	32	

The groundwater table is at a depth of 15 ft.

Develop plots of pore water pressure, total vertical stress, effective total stress, and shear strength on a horizontal plane versus depth. All four of these plots should be superimposed on the same diagram with the parameters on the horizontal axis (increasing to the right) and depth on the vertical axis (increasing downward).

Hint: Because the cohesion and friction angle suddenly change at the strata boundaries, the shear strength also may change suddenly at these depths.

3.17 Repeat problem 3.16 using the following data:

Depth (m)	γ (kN/m^3)	c' (kPa)	ϕ' (degree)	s_u (kPa)
0–5	18.5			50
5–12	20.0	8.4	21	
12–20	20.5	0	35	

The groundwater table is at a depth of 7 m.

3.18 A 9 ft thick fill is to be placed on the soil shown in Figure 3.22. Once it is compacted, this fill will have a unit weight of 122 lb/ft^3. Compute the ultimate settlement caused by consolidation of the underlying clay.

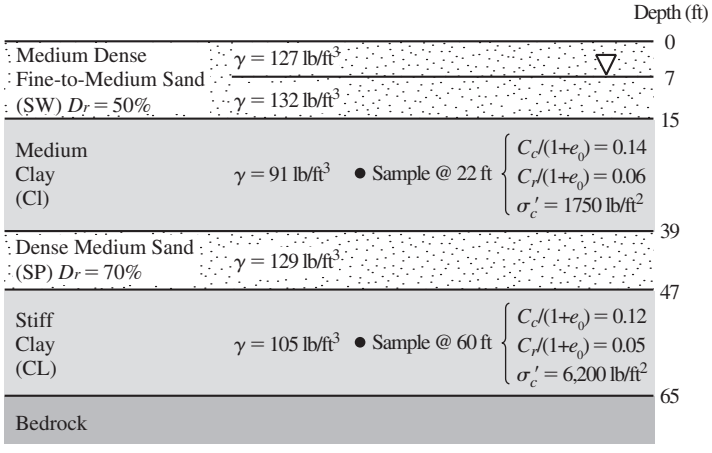

Figure 3.22 Soil profile for Problem 3.18.

4

Subsurface Investigation and Characterization

Before digging [for a foundation] you must make holes in several places to locate the different soil layers and ensure that a firm soil is thick and not underlain by clay, sandy soil, or a soil that will compress under the load. Another way of determining if the ground is suitable is to beat a large wooden joist six or eight feet long into the ground. If the soil resists and the sound is dry and light, then the earth is firm; if the sound is heavy without any resistance, we can conclude the foundation will be worthless.

Pierre Bullet from *L'Architecture Pratique,* 1691 (Translated and paraphrased by the second author of this text)

One of the fundamental differences between the practices of structural engineering and geotechnical engineering is the way each determines the engineering properties of the materials with which they work. For practical design problems, structural engineers normally find the necessary material properties by referring to handbooks. For example, if one wishes to use A36 steel, its engineering properties (strength, modulus of elasticity, etc.) are well known and can be found from a variety of sources. It is not necessary to measure the strength of A36 steel each time we use it in a design (although routine strength tests may be performed later as a quality control function). Conversely, the geotechnical engineer works with soil and rock, both of which are natural materials with variable and often unknown engineering properties. Natural geomaterials are naturally variable, and at any given site, they may exhibit their variability in the form of different soil strata in the

subsurface. Even within a stratum that may look uniform visually, there is usually at least some variability in the properties of the soil in the stratum. This natural spatial variability of geomaterials means we must perform a site investigation and characterization program to identify and test the materials at each new site before conducting any analysis.

Modern soil investigation and characterization techniques have progressed far beyond Bullet's method of beating the earth with wooden rafters. A variety of techniques are available, as discussed in this chapter, yet this continues to be the single largest source of uncertainties in foundation engineering. Our ability to perform analyses far exceeds our ability to determine the appropriate values of the soil properties to input into these analyses. Therefore, it is very important for the foundation engineer to be familiar with the available techniques, know when to use them, and understand the degree of precision (or lack of precision!) associated with them.

For purposes of this discussion, we will divide these techniques into three categories:

- **Site investigation** includes methods of defining the soil profile and other relevant data and recovering soil samples.
- **Laboratory testing** includes testing the soil samples in order to determine relevant engineering properties.
- **In situ testing** includes methods of testing the soils in-place, thus avoiding the difficulties associated with recovering samples.

As discussed in Chapter 2, the reliability of a geotechnical design depends heavily on the reliability of input values of soil properties in the analyses, which in turn depends on the level of site investigation and characterization carried out. For example, the allowable stress design (ASD) method (to be introduced in Chapter 5) implicitly assumes that the site investigation and characterization has been performed to some appropriate standard based on past experience, to go with the acceptable value of the factor of safety used by the method. Similarly, the resistance factors in the load and resistance factor design (LRFD) method (also to be introduced in Chapter 5) are developed assuming certain levels of site investigation and characterization. Indeed, some LRFD methods allow the use of different values of the same resistance factor for different levels of site investigation and characterization performed.

Many organizations have produced manuals and specifications to provide guidance on how to plan and execute a site investigation and characterization program. One example is the Federal Highway Administration Subsurface Investigation Reference Manual by Mayne et al. (2002). Generally speaking, a geotechnical engineer should perform site investigation and characterization in accordance with specifications and guidance provided by the client and relevant standards. For example, AASHTO (2012) contains provisions that govern site investigation and characterization. These published manuals and specifications certainly are useful resources, and when used along with local experience and engineering judgment, they can lead to an effective site investigation and characterization program.

4.1 SITE INVESTIGATION

The objectives of the site investigation phase include:

- Determining the locations and thicknesses of the soil strata
- Determining the location of the groundwater table as well as any other groundwater-related characteristics
- Recovering soil samples
- Defining special problems and concerns

Typically, we accomplish these goals using a combination of literature searches and onsite exploration techniques.

Background Literature Search

Before conducting any new exploration at a project site, gather whatever information that is already available, both on the proposed structure and the subsurface conditions at the site. Important information about the structure would include:

- Its location and dimensions
- The type of construction, column loads, column spacing, and allowable settlements
- Its intended use
- The finish floor elevation
- The number and depth of any basements
- The depth and extent of any proposed grading
- Local building code requirements

The literature search also should include an effort to obtain at least a preliminary idea of the subsurface conditions. It would be very difficult to plan an exploration program with no such knowledge. Fortunately, many methods and resources are often available to gain a preliminary understanding of the local soil conditions. These may include one or more of the following:

- Determining the geologic history of the site, including assessments of anticipated rock and soil types, the proximity of faults, and other geologic features
- Gathering copies of boring logs and laboratory test results from previous investigations on this or other nearby sites
- Reviewing soil maps developed for agricultural purposes
- Reviewing old and new aerial photographs and topographic maps (may reveal previous development or grading at the site)
- Reviewing water well logs (helps establish historic groundwater levels)

- Locating underground improvements, such as utility lines, both onsite and immediately offsite, along with locating foundations of adjacent structures, especially those that might be impacted by the proposed construction

At some sites, this type of information may be plentiful, whereas at others, it may be scarce or nonexistent.

Field Reconnaissance

Along with the background literature search, the foundation engineer should visit the site and perform a field reconnaissance. Often such visits will reveal obvious concerns that may not be evident from the literature search or the logs of the exploratory borings.

The field reconnaissance would include obtaining answers to such questions as the following:

- Is there any evidence of previous development on the site?
- Is there any evidence of previous grading on the site?
- Is there any evidence of landslides or other stability problems?
- Are nearby structures performing satisfactorily?
- What are the surface drainage conditions?
- What types of soil and/or rock are exposed at the ground surface?
- Will access problems limit the types of subsurface exploration techniques that can be used?
- Might the proposed construction affect existing improvements? (E.g., a fragile old building adjacent to the site might be damaged by vibrations from pile driving.)
- Do any offsite conditions affect the proposed development? (E.g., potential flooding, mudflows, rockfalls, etc.)

Subsurface Exploration and Sampling

The heart of the site investigation phase consists of exploring the subsurface conditions and sampling the soils. These efforts provide most of the basis for developing a design soil profile. A variety of techniques are available to accomplish these goals.

Exploratory Borings

The most common method of exploring the subsurface conditions is to drill a series of vertical holes in the ground. These are known as *borings* or *exploratory borings* and are typically 75 to 600 mm (3–24 in) in diameter and 3 to 30 m (10–100 ft) deep. They can be drilled with hand augers or with portable power equipment, but they are most commonly drilled using a truck-mounted rig, as shown in Figure 4.1.

A wide variety of drilling equipment and techniques are available to accommodate the various subsurface conditions that might be encountered. Sometimes it is possible to drill an open hole using a *flight auger* or a *bucket auger*, as shown in Figure 4.2.

Figure 4.1 A truck-mounted drill rig.

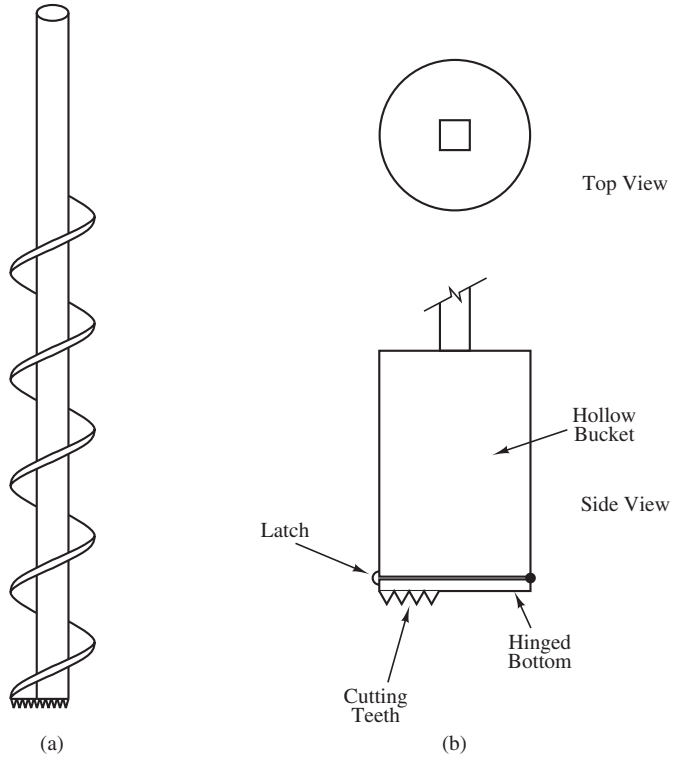

Figure 4.2 (a) Flight auger; and (b) Bucket auger.

However, if the soil is subject to *caving* (i.e., the sides of the boring falling in) or *squeezing* (the soil moving inward, reducing the diameter of the boring), then it will be necessary to provide some type of lateral support during drilling. Caving is likely to be encountered in clean sands, especially below the groundwater table, while squeezing is likely in soft saturated clays.

One method of dealing with caving or squeezing soils is to use *casing*, as shown in Figure 4.3a. This method involves temporarily lining some or all of the boring with a steel pipe. Alternatively, we could use a *hollow-stem auger*, as shown in Figure 4.3b. The driller screws each of these augers into the ground and obtains soil samples by lowering sampling tools through a hollow core. When the boring is completed, the augers are removed. Finally, we could use a *rotary wash boring*, as shown in Figure 4.3c. These borings are filled with a bentonite slurry (a combination of bentonite clay and water) or a polymer slurry to provide hydrostatic pressure on the sides of the boring and thus prevent caving.

Drilling through rock, especially hard rock, requires different methods and equipment. Engineers often use *coring*, which recovers intact cylindrical specimens of the rock.

There are no absolute rules to determine the required number, spacing, and depth of exploratory borings. Such decisions are based on the findings from the field reconnaissance, along with engineering judgment and knowledge of customary standards of practice. This is a subjective process that involves many factors, including:

- How large is the site?
- What kinds of soil and rock conditions are expected?
- Is the soil profile erratic, or is it consistent across the site?
- What is to be built on the site (small building, large building, bridge, etc.)?
- How critical is the proposed project (i.e., what would be the consequences of a failure?)?
- How large and heavy are the proposed structures?
- Are all areas of the site accessible to drill rigs?

Although we will not know the final answers to some of these questions until the site characterization program is completed, we should have at least a preliminary idea based on the literature search and field reconnaissance.

In terms of the number of borings, the International Building Code (ICC, 2012) suggests a minimum of two borings for built-over areas up to 465 m^2 (5,000 ft^2), and at least one additional boring for each additional 233 m^2 (2,500 ft^2) of built-over areas up to 1,860 m^2 (20,000 ft^2). For built-over areas larger than 1,860 m^2 (20,000 ft^2), ICC (2012) suggests at least eight borings plus at least one additional boring for each additional 465 m^2 (5,000 ft^2). In addition, Table 4.1 presents rough guidelines for determining the normal spacing of exploratory borings. However, it is important to recognize that there is no single "correct" solution for the required number and depth of borings, and these guidelines must be tempered with appropriate engineering judgment. For bridge structures AASTHO [10.4.2] recommends a minimum of one boring per substructure which is

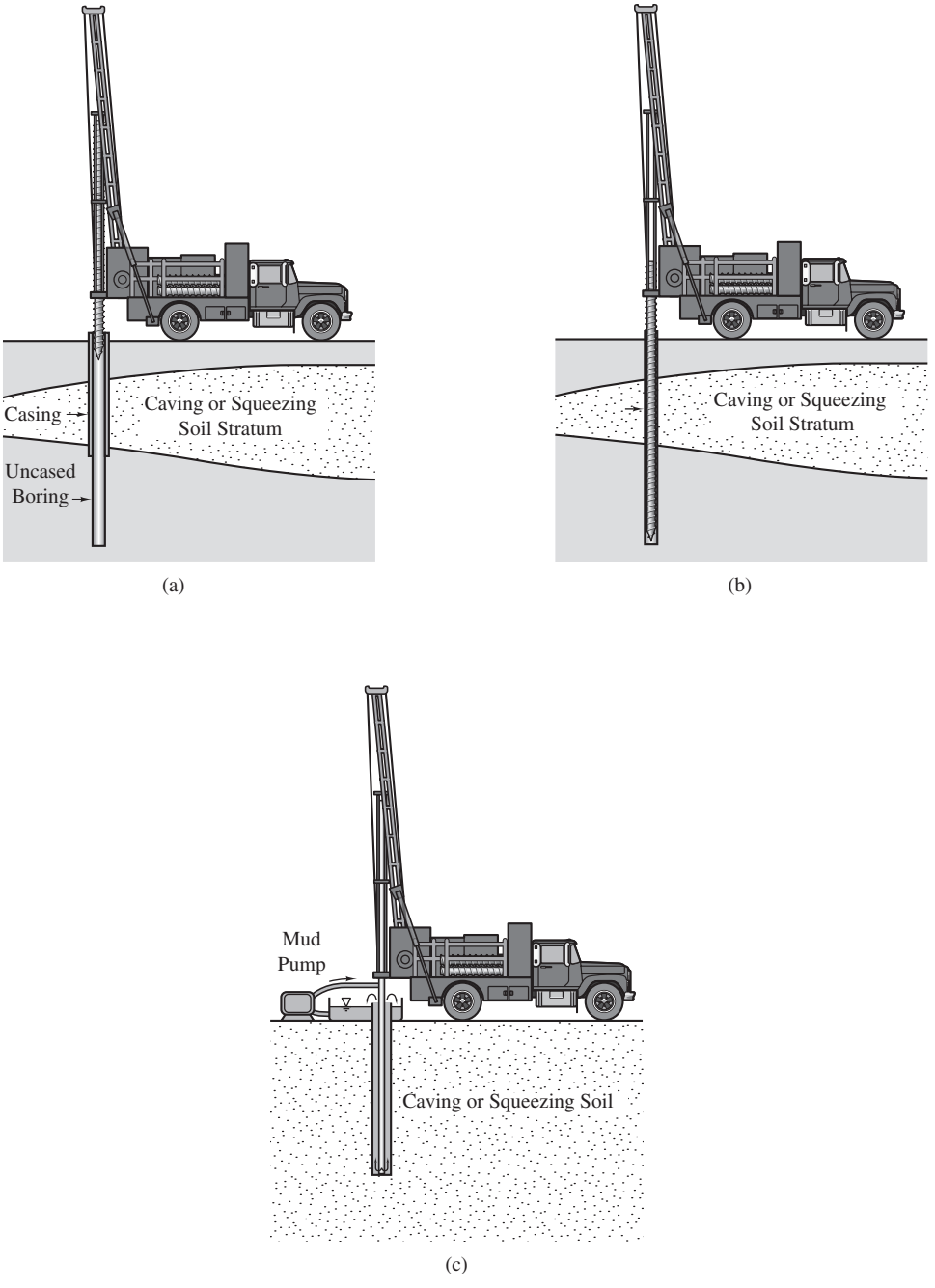

Figure 4.3 Methods of dealing with caving or squeezing soils: (a) casing; (b) hollow-stem auger; and (c) rotary wash boring.

TABLE 4.1 ROUGH GUIDELINES FOR SPACING EXPLORATORY BORINGS FOR PROPOSED MEDIUM TO HEAVY WEIGHT BUILDINGS, TANKS, AND OTHER SIMILAR STRUCTURES

	Structure Footprint Area for Each Exploratory Boring	
Subsurface Conditions	(m^2)	(ft^2)
Poor quality and/or erratic	100–300	1,000–3,000
Average	200–400	2,000–4,000
High quality and uniform	300–1,000	3,000–10,000

less than 30 m (100 ft) wide and a minimum of two borings for each substructure which is wider than 30 m (100 ft).

Borings generally should extend at least to a depth such that the change in vertical effective stress due to the new construction is less than 10 percent of the initial vertical effective stress. For buildings on spread footing or mat foundations, this criterion is met by following the guidelines in Table 4.2. If fill is present, the borings must extend through it and into the natural ground below, and if soft soils are present, the borings should extend through them and into firmer soils below. For heavy structures, at least some of the borings should be carried down to bedrock, if possible, but certainly well below the depth of any proposed pile foundations.

On large projects, the drilling program might be divided into two phases: a preliminary phase to determine the general soil profile and a final phase based on the results of the preliminary borings.

The conditions encountered in an exploratory boring are normally presented in the form of a *boring log*, as shown in Figure 4.4. These logs also indicate the sample locations and might include some of the laboratory test results.

TABLE 4.2 GUIDELINES FOR DEPTHS OF EXPLORATORY BORINGS FOR BUILDINGS ON SHALLOW FOUNDATIONS (Adapted from Sowers, 1979.)

	Minimum Depth of Borings (S = number of stories; D = anticipated depth of foundation)	
Subsurface Conditions	(m)	(ft)
Poor	$6\,S^{0.7} + D$	$20\,S^{0.7} + D$
Average	$5\,S^{0.7} + D$	$15\,S^{0.7} + D$
Good	$3\,S^{0.7} + D$	$10\,S^{0.7} + D$

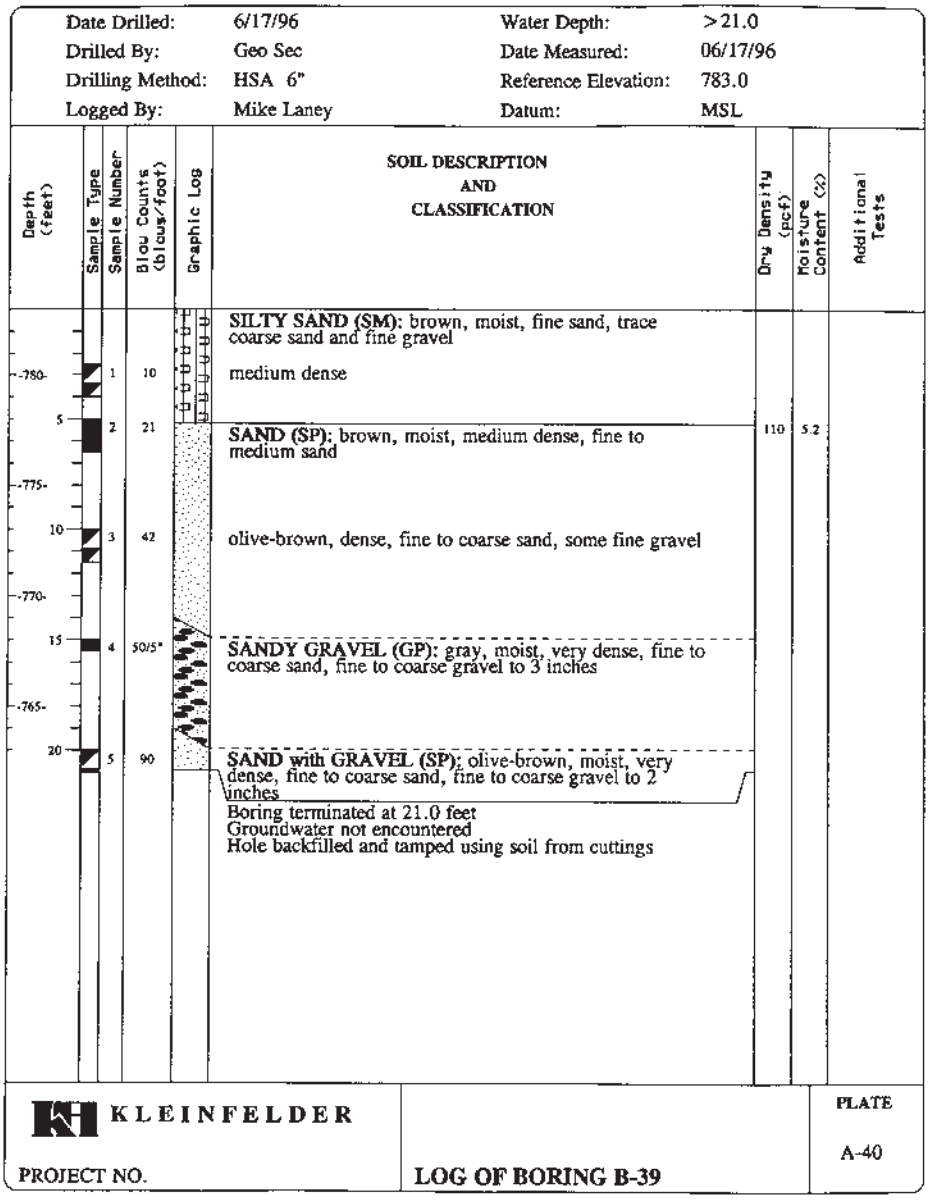

Figure 4.4 A boring log. Samples 2 and 4 were obtained using a heavy-wall sampler, and the corresponding blowcounts are the number of hammer blows required to drive the sampler. Samples 1, 3, and 5 are standard penetration tests, and the corresponding blowcounts are the N_{60} values, as discussed later in this chapter. If the groundwater table had been encountered, it would have been shown on the log (Courtesy of Kleinfelder, Inc.).

Soil Sampling

One of the primary purposes of drilling the exploratory borings is to obtain representative soil samples. We use these samples to determine the soil profile and to perform laboratory tests.

There are two categories of samples: disturbed and undisturbed. A *disturbed sample* (sometimes called a *bulk* sample) is one in which there is no attempt to retain the in-place structure of the soil. The driller might obtain such a sample by removing the cuttings off the bottom of a flight auger and placing them in a bag. Disturbed samples are suitable for many purposes, such as classification and Proctor compaction tests.

A truly *undisturbed sample* is one in which the soil is recovered completely intact and its in-place structure and stresses are not modified in any way. Such samples are desirable for laboratory tests that depend on the structure of the soil, such as consolidation tests and shear strength tests. Unfortunately, the following problems make it almost impossible to obtain a truly undisturbed soil sample:

- Shearing and compressing the soil during the process of inserting the sampling tool
- Relieving the sample of its in situ stresses
- Possible drying and desiccation
- Vibrating the sample during recovery and transport

Some soils are more susceptible to disturbance than others. For example, techniques are available to obtain good quality samples of medium clays, while clean sands are almost impossible to sample without extensive disturbance. However, even the best techniques produce samples that are best described as "relatively undisturbed."

A variety of sampling tools is available. Some of these tools are shown in Figure 4.5. Those with thin walls produce the least disturbance, but they may not have the rigidity needed to penetrate hard soils.

Groundwater Monitoring

The position and movements of the groundwater table are very important factors in foundation design. Therefore, subsurface investigations must include an assessment of groundwater conditions. This is often done by installing an *observation well* in the completed boring to monitor groundwater conditions. Such wells typically consist of a slotted or perforated PVC pipe, as shown in Figure 4.6. Once the groundwater level has stabilized, we can locate it by lowering a probe into the observation well.

We usually compare observation well data with historic groundwater records, or at least consider the season of the year and the recent precipitation patterns to determine the design groundwater level. This design level should represent the worst (i.e., highest) groundwater level that is likely to occur during the design life of the project. This level is often shallower than that observed in the observation wells.

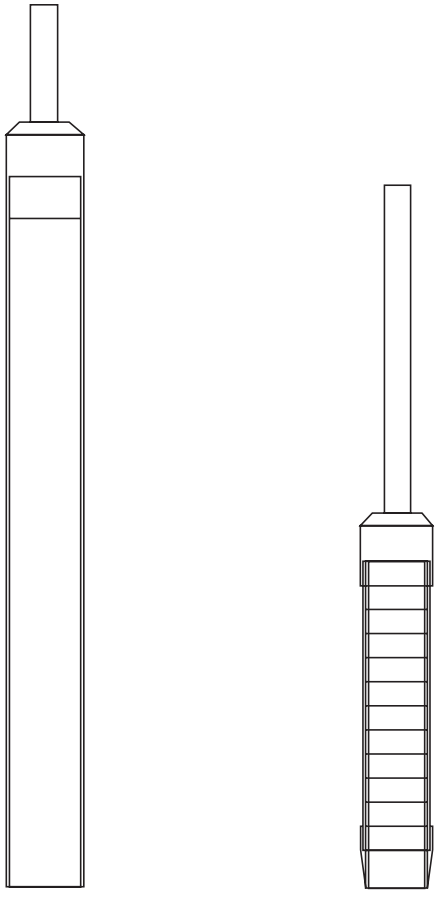

Figure 4.5 Common soil sampling tools: (a) Shelby tube samples have thin walls to reduce sample disturbance; and (b) Ring-lined barrel samplers have thicker walls to withstand harder driving. Both are typically 60 to 100 mm (2.5–4 in) in diameter.

Exploratory Trenches

Sometimes it is only necessary to explore the upper 3 m (10 ft) of the soil. This might be the case for lightweight structures on sites where the soil conditions are good, or on sites with old shallow fills of questionable quality. Additional shallow investigations might also be necessary to supplement a program of exploratory borings. In such cases, it can be very helpful to dig *exploratory trenches* (also known as *test pits*) using a backhoe as shown in Figure 4.7. Exploratory trenches provide more information than a boring of comparable depth (because more of the soil is exposed) and are often less expensive. Disturbed samples can easily be recovered with a shovel, and undisturbed samples can be obtained using hand-held sampling equipment.

Two special precautions are in order when using exploratory trenches: First, these trenches must be adequately shored before anyone enters them (see OSHA Excavation

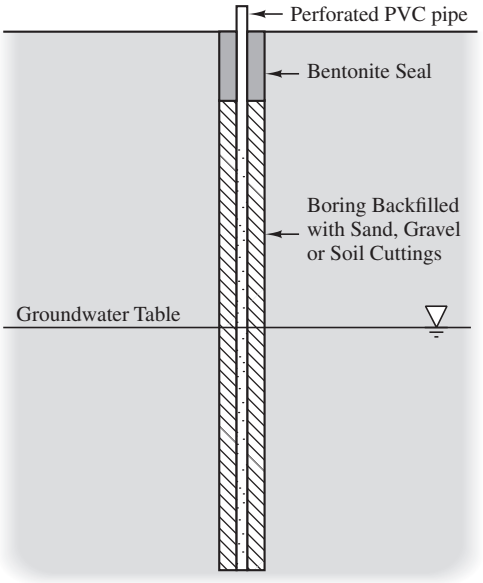

Figure 4.6 A typical observation well.

Figure 4.7 This exploratory trench was dug by the backhoe in the background, and has been stabilized using aluminum-hydraulic shoring. An engineering geologist is logging the soil conditions in one wall of the trench.

Regulations). Many individuals, including one of the first author's former colleagues, have been killed by neglecting to enforce this basic safety measure. Second, these trenches must be properly backfilled to avoid creating an artificial soft zone that might affect future construction.

4.2 LABORATORY TESTING

Soil samples obtained from the field are normally brought to a soil mechanics laboratory for further classification and testing. This method is sometimes called *ex-situ testing*. The purpose of the testing program is to determine the appropriate engineering properties of the soil as follows:

- **Classification, weight-volume, and index tests**—Several routine tests are usually performed on many of the samples to ascertain the general characteristics of the soil profile. These include:
  - Moisture content
  - Unit weight (density)
  - Atterberg limits (plastic limit and liquid limit)
  - Particle size distribution (sieve and hydrometer analyses)

  These tests are inexpensive and can provide a large quantity of valuable information.
- **Consolidation tests**—Foundation designs also require an assessment of soil compressibility, which provides the necessary data for settlement analyses. In cohesive soils, this data is most often obtained by conducting laboratory consolidation or oedometer tests, as discussed later in this chapter.
- **Shear strength tests**—Virtually all foundation designs require an assessment of shear strength. Common shear strength tests include the direct shear test, the unconfined compression test, and the triaxial compression test, as discussed later in this chapter. Shear strength also may be determined from in situ tests, also discussed later in this chapter.
- **Compaction tests**—Sometimes it is necessary to place compacted fills at a site, and place the foundations on these fills. In such cases, we perform Proctor compaction tests to assess the compaction characteristics of the soil.
- **Corrosivity tests**—When corrosion or sulfate attack is a concern, as discussed in Chapter 5, we need to perform special tests such as resistivity tests and sulfate content tests, and then use the results to design appropriate protective measures.

Consolidation (Oedometer) Tests

To predict the magnitude of consolidation settlement, δ_c, in a soil, we need to know its stress-strain properties. This normally requires obtaining soil samples in the field, bringing them to the laboratory, subjecting them to a series of loads, and measuring the corresponding settlements. We do this by conducting a *consolidation test* (also known as an *oedometer*

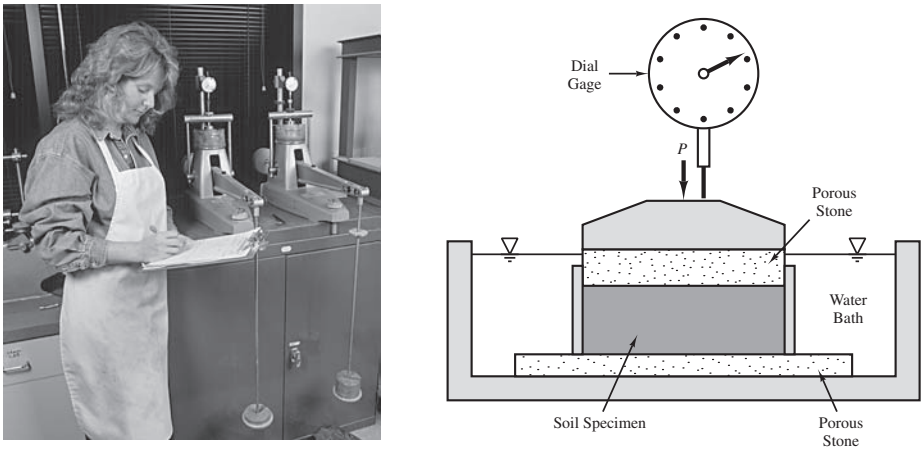

Figure 4.8 (a) Performing consolidation test in the laboratory. The two consolidometers use weights in the foreground to load the specimens. (b) Cross section of a consolidometer cell which holds the specimen.

test), which is performed in a *consolidometer* (or *oedometer*) as shown in Figure 4.8. It can be seen that the soil specimen tested in the consolidometer is constrained laterally, simulating one-dimensional (1-D) consolidation in the vertical direction. In this case, the vertical stress is related to the vertical strain by the constrained modulus M.

The methods of computing settlement using consolidation test data are already discussed in Section 3.4; here we elaborate more on how to perform the test and interpret the data.

Because we are mostly interested in the engineering properties of natural soils as they exist in the field, consolidation tests are usually performed on high quality "undisturbed" samples. It is fairly simple to obtain these samples in soft to medium clays, but quite difficult in clean sands. It also is important for samples that were saturated in the field to remain so during storage and testing, because irreversible changes can occur if they are allowed to dry.

Sometimes engineers need to evaluate the consolidation characteristics of proposed compacted fills, and do so, by performing consolidation tests on samples that have been remolded and compacted in the laboratory. These tests are usually less critical because well-compacted fills have a low compressibility.

Test Procedure and Results

The test procedure consists of applying a series of normal loads to the sample, allowing it to consolidate completely under each load, and measuring the corresponding vertical deformations. The stress-strain data from a consolidation test can be plotted in many different ways. They can be plotted in the conventional way as stress versus strain with linear scales for the two axes, giving a conventional stress-strain curve. Figure 4.9a is an example

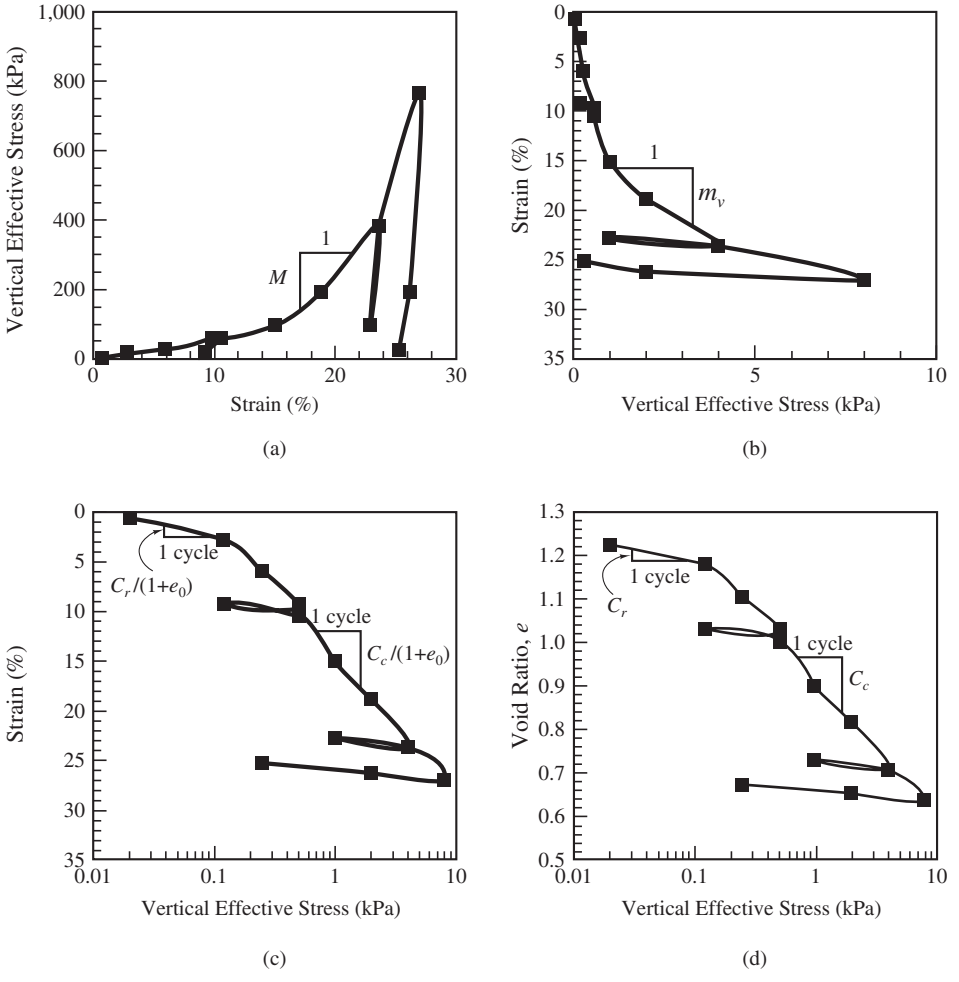

Figure 4.9 Results of a consolidation test on a soft marine silt. (a) Data plotted as stress versus strain. (b) Data plotted as strain versus stress. (c) Data plotted as strain versus log-stress. (d) Data plotted as void ratio versus log-stress.

of such a stress-strain curve based on data from a consolidation test on a marine silt (Landslide Technology, 2005). It can be seen from this curve that the stress-strain behavior is nonlinear. We can obtain the 1-D constrained tangent modulus M as the slope of the curve, which may vary with stress or strain:

$$M = \frac{d\sigma_z'}{d\varepsilon_z} \tag{4.1}$$

where

σ_z' = vertical effective stress
ε_z = vertical strain

Now, if we switch the axes in Figure 4.9a, the curve will be a plot of strain versus stress as shown in Figure 4.9b. The slope of this curve is defined as the coefficient of compressibility, m_v, which is the reciprocal of M:

$$m_v = \frac{d\varepsilon_z}{d\sigma_z'} = \frac{1}{M} \tag{4.2}$$

We can further convert the plot of strain versus stress into a semi-log strain-stress curve by plotting ε versus $\log \sigma_z'$, as shown in Figure 4.9c. Finally, by converting ε to void ratio e, we arrive at the e-log-p curve that is often used to present consolidation test data, as shown in Figure 4.9d.

An illustration of a typical e-log-p curve is shown in Figure 4.10. This curve can be considered a hybrid stress-strain curve that depicts the stress-strain behavior of a soil under 1-D consolidation. It shows consolidation both in terms of ε_z and change in e. Typically, the e-log-p curve consists of multiple linear segments which are approximately linear. The segment, indicated by Curve AB, is called the *recompression curve*. The middle segment, indicated by Curve BC, is called the *virgin curve*. On reaching Point C, the sample is progressively unloaded, thus producing the third segment called the *rebound curve*, CD.

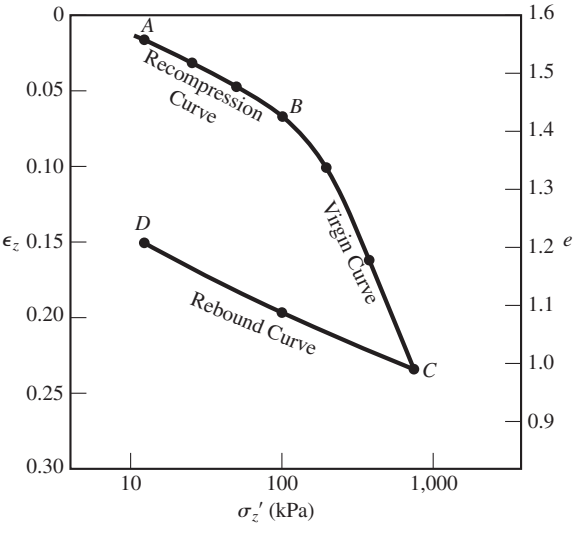

Figure 4.10 Illustration of typical results of a laboratory consolidation test. The initial void ratio, e_0, is 1.60.

Figure 4.11 illustrates the idealized bilinear e-log-p. The slope of the virgin curve is called the *compression index*, C_c:

$$C_c = -\frac{de}{d \log \sigma_z'} \tag{4.3}$$

Since the virgin curve is approximated as a straight line (on a semilogarithmic plot), we can obtain a numerical value for C_c by selecting any two points, a and b, on this line, as shown in Figure 4.11, and rewriting Equation 4.3 as:

$$C_c = -\frac{e_a - e_b}{(\log \sigma_z')_b - (\log \sigma_z')_a} \tag{4.4}$$

Equation 4.4 is used when the test results have been plotted in terms of void ratio ($e - \sigma_z'$). Alternatively, if the data is plotted only in the vertical strain form ($\varepsilon_z - \sigma_z'$), then:

$$\frac{C_c}{1 + e_0} = \frac{(\varepsilon_z)_b - (\varepsilon_z)_a}{(\log \sigma_z')_b - (\log \sigma_z')_a} \tag{4.5}$$

where

e_0 = initial void ratio (i.e., at beginning of test)

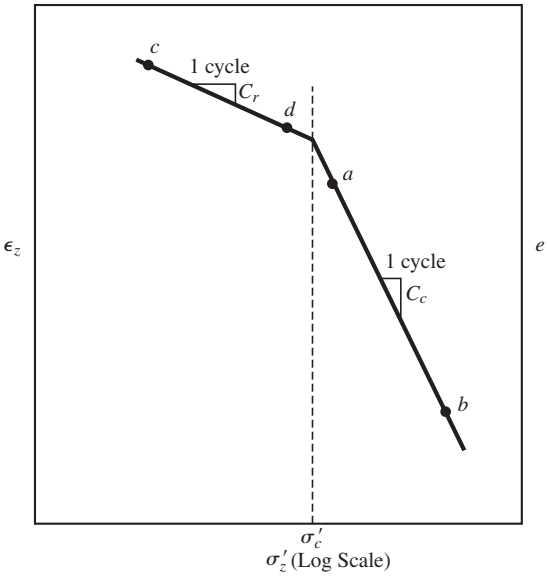

Figure 4.11 Illustration of an idealized bilinear e-log-p curve. The slopes of the two parts of the curve on a semilogarithmic e versus σ_z' plot are C_c and C_r. The break in slope occurs at the preconsolidation stress, σ_c'.

When using Equations 4.4 and 4.5, it is convenient to select points a and b such that $\log (\sigma_z')_b = 10 \log (\sigma_z')_a$. This makes the denominator of both equations equal to 1, which simplifies the computation. This choice also demonstrates that C_c could be defined as the reduction in void ratio per tenfold increase (one log-cycle) in effective stress.

In theory, the recompression and rebound curves have nearly equal slopes, but the rebound curve is more reliable because it is less sensitive to sample disturbance effects. This slope, which we call the *recompression index*, C_r, is defined in the same way as C_c and can be found using Equation 4.6 or 4.7 with points c and d on the recompression curve:

Using void ratio data:

$$C_r = -\frac{e_d - e_c}{(\log \sigma_z')_d - (\log \sigma_z')_c} \tag{4.6}$$

Using strain data:

$$\frac{C_r}{1 + e_0} = \frac{(\varepsilon_z)_d - (\varepsilon_z)_c}{(\log \sigma_z')_d - (\log \sigma_z')_c} \tag{4.7}$$

Another important parameter from the consolidation test results is the stress that corresponds to the break-in-slope in Figure 4.11. This is called the *preconsolidation stress*, σ_c', and represents the greatest vertical effective stress the soil has ever experienced. The value of σ_c' obtained from the consolidation test represents only the conditions at the point where the sample was obtained. If the sample had been taken at a different elevation, the preconsolidation stress would change accordingly.

Lastly, it can be shown that M, m_v, and C_c or C_r are inter-related as follows:

$$M = \frac{1}{m_v} = \frac{2.3\,(1 + e_0)\,\sigma_z'}{(C_c \text{ or } C_r)} \tag{4.8}$$

Note that C_c should be used if σ_z' of the soil puts it on the virgin curve and that C_r should be used if σ_z' of the soil puts it on the recompression or rebound curve.

In summary, the 1-D consolidation settlement can be estimated using either the constrained modulus M or compression indices C_c and C_r, as discussed in Section 3.4. Chapter 8 discusses these methods of settlement calculation in more detail.

Laboratory Shear Strength Tests

The shear strength parameters, c' and ϕ' (or c_T and ϕ_T), may be determined by performing laboratory or in situ tests. This section discusses some of the more common laboratory tests.

Several different laboratory tests are commonly used to measure the shear strength of soils. Each has its advantages and disadvantages, and no one test is suitable for all

circumstances. When selecting a test method, we must consider many factors, including the following:

- Soil type
- Initial moisture content and need, if any, to saturate the sample
- Required drainage conditions (drained or undrained)

Direct Shear Test

The French engineer Alexandre Collin may have been the first to measure the shear strength of a soil (Head, 1982). His tests, conducted in 1846, were similar to the modern direct shear test. The test as we now know it [ASTM D3080] was perfected by several individuals during the first half of the twentieth century.

The apparatus, shown in Figure 4.12, typically accepts a 60 to 75 mm (2.5–3.0 in) diameter cylindrical specimen and subjects it to a certain effective stress. The shear stress is then slowly increased until the soil fails along the surface shown in the figure. The test is normally repeated on new specimens of the same soil until three sets of effective stress and shear strength measurements are obtained. A plot of this data produces values of the cohesion, c, and friction angle, ϕ.

The direct shear test has the advantage of being simple and inexpensive and it is an appropriate method when we need the drained strength of cohesionless soils. It also can be used to obtain the drained strength of cohesive soils, but produces less reliable results because we have no way of controlling the drainage conditions other than varying the speed of the test. The direct shear test also has the disadvantages of forcing the shear to occur along a specific plane instead of allowing the soil to fail along the weakest zone, and it produces nonuniform strains in the sample, which can produce erroneous results in strain-softening soils.

Unconfined Compression Test

The unconfined compression test [ASTM D2166], shown in Figure 4.13, uses a tall, cylindrical specimen of cohesive soil subjected to an axial load. This load is applied quickly (i.e., only a couple of minutes to failure) to maintain the undrained condition.

At the beginning of the test, this load and the stresses in the soil are both equal to zero. As the load increases, the stresses in the soil increase, as shown by the Mohr circles in Figure 4.14, until the soil fails. The soil appears to fail in compression, and the test results are often expressed in terms of the compressive strength; it actually fails in shear on diagonal planes, as shown in Figure 4.13b. The cross-sectional area of the specimen increases as the test progresses, and the area at failure, A_f, is given by:

$$A_f = \frac{A_0}{1 - \varepsilon_f} \tag{4.9}$$

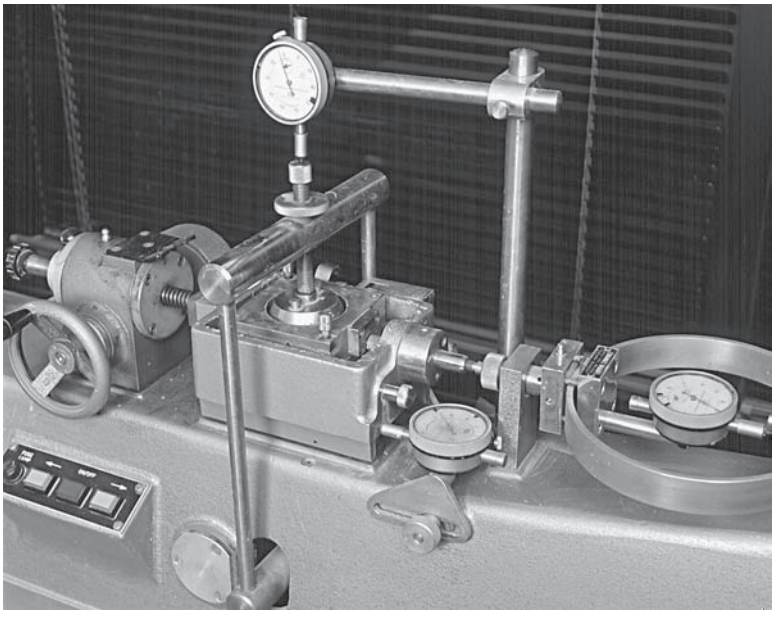

(a)

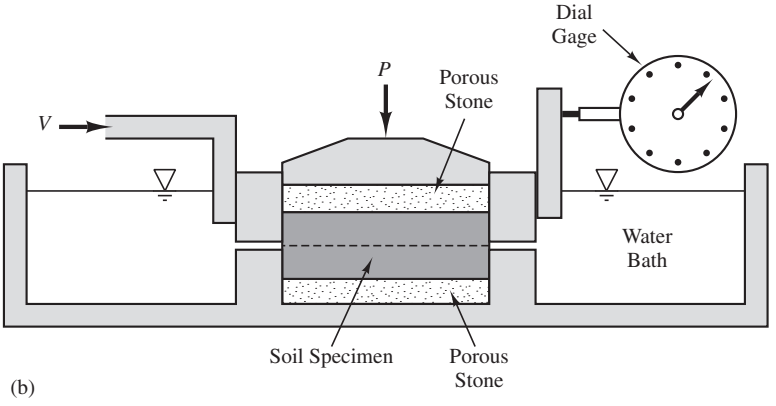

(b)

Figure 4.12 (a) A direct shear machine. The sample is inside the specimen holder, directly below the upper dial gage. (b) Cross section through the specimen holder showing the soil specimen and shearing action.

where

A_f = cross-sectional area at failure
A_0 = initial cross-sectional area
ε_f = axial strain at failure

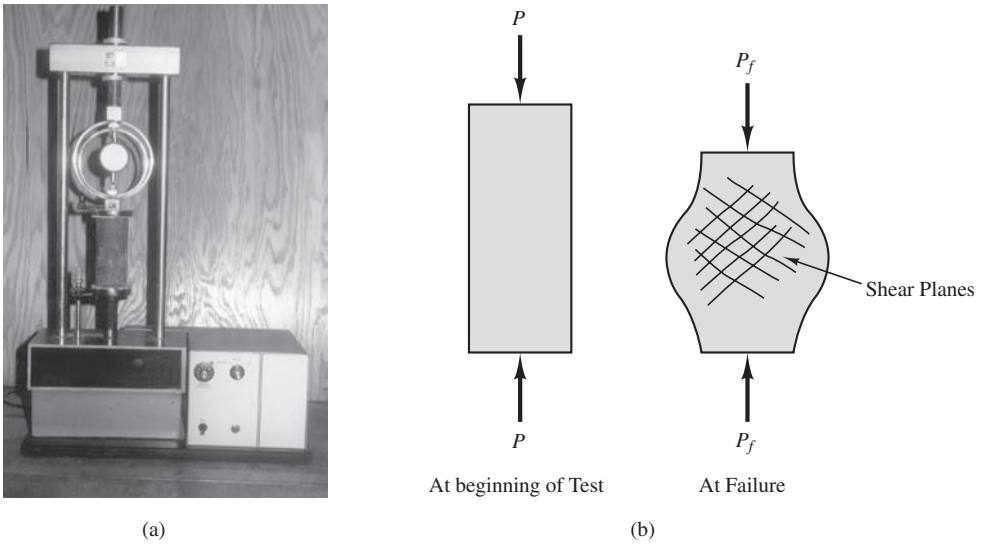

Figure 4.13 (a) An unconfined compression test machine. (b) Force analysis of an unconfined compression test.

Therefore, the undrained shear strength, s_u, is given by:

$$s_u = \frac{P_f}{2A_f} \tag{4.10}$$

where

s_u = undrained shear strength
P_f = axial load at failure

This test is inexpensive and in common use. It does not force failure to occur along a predetermined surface, and thus it reflects the presence of weak zones or planes. It usually provides conservative (low) results because the horizontal stress is zero rather than

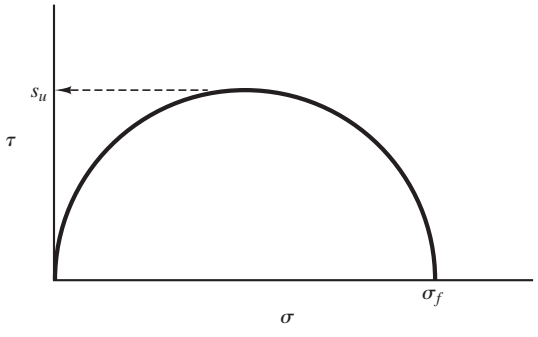

Figure 4.14 Mohr circle at failure in an unconfined compression test.

what it was in the field and because of sample disturbance. Tests of fissured clays are often misleading unless a large specimen is used because the fissures in small specimen are rarely representative of those in the field.

Triaxial Compression Test

The triaxial compression test [ASTM D2850] may be thought of as an extension of the unconfined compression test. The cylindrical soil specimen is now located inside a pressurized chamber that supplies the desired lateral stress, as shown in Figures 4.15 and 4.16. Although the apparatus required to perform this test is much more complex, it also allows more flexibility and greater control over the test. It can measure either the drained or undrained strength of nearly any type of soil. In addition, unsaturated soils can be effectively saturated before testing.

The three most common types of triaxial compression tests are as follows:

- **The *unconsolidated-undrained (UU) test* (also known as a quick or Q test):** Horizontal and vertical stresses, usually equal to the vertical stress that was present in the field, are applied to the sample. No consolidation is permitted, and the soil is sheared under undrained conditions. The result is expressed as an s_u value.

Figure 4.15 A triaxial test system (courtesy of Geocomp Corp.).

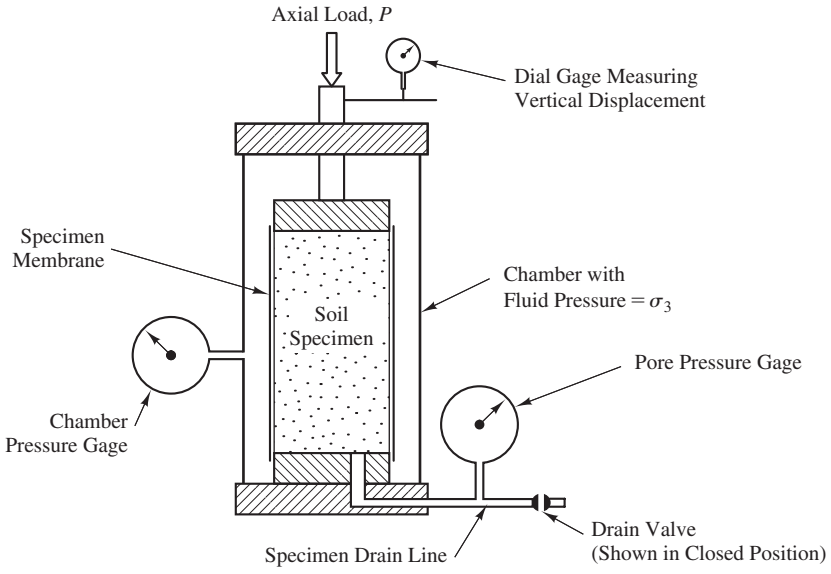

Figure 4.16 Schematic of a triaxial cell.

- **The *consolidated-drained (CD) test* (also known as a slow or S test):** Horizontal and vertical stresses, usually equal to or greater than the vertical stress that was present in the field, are applied and the soil is allowed to consolidate. Then, it is sheared under drained conditions. Typically, three of these tests are performed at different confining stresses to find the values of the drained strength parameters c' and ϕ'.
- **The *consolidated-undrained test* (also known as a rapid or R test):** The initial stresses are applied as with the CD test and the soil is allowed to consolidate. However, the shearing occurs under undrained conditions. The results could be interpreted to give the s_u as a function of the effective consolidation stress, and it is also possible to obtain the drained strength parameters c' and ϕ' by measuring pore water pressures during the test and computing the effective stresses.

4.3 IN SITU TESTING

Laboratory tests on "undisturbed" soil samples are no better than the quality of the sample. Depending on the type of test, the effects of sample disturbance can be significant, especially in cohesionless soils. Fortunately, we can often circumvent these problems by using *in situ* (in-place) testing methods. These entail bringing the test equipment to the field and testing the soils in-place. In addition to bypassing sample disturbance problems, in situ tests have the following advantage:

- They are usually less expensive, so a greater number of tests can be performed, thus characterizing the soil in more detail.

The test results are available immediately. However, they also have disadvantages, including:

- Often no sample is obtained, thus making soil classification more difficult.
- The engineer has less control over confining stresses and drainage.

In most cases, we must use empirical correlations and calibrations to convert in situ test results to appropriate engineering properties for design. Many such methods have been published, and some of them are included in this book. Most of these correlations were developed for clays of low to moderate plasticity or for quartz sands, and thus may not be appropriate for special soils such as very soft clays, organic soils, sensitive clays, fissured clays, cemented soils, calcareous sands, micaceous sands, collapsible soils, and frozen soils.

Some in situ test methods have been in common use for several decades, while others are relative newcomers. Many of these tests will probably continue to become more common in engineering practice.

Standard Penetration Test (SPT)

One of the most common in situ tests is the standard penetration test, or SPT. This test was originally developed in the late 1920s and has been used most extensively in North and South America, the United Kingdom, and Asia. Because of this long record of experience, the test is well established in engineering practice. Unfortunately, it is also plagued by many problems that affect its accuracy and reproducibility and is slowly being replaced by other test methods, especially on larger and more critical projects.

Test Procedure

The test procedure was not standardized until 1958 when ASTM standard D1586 first appeared. It is essentially as follows:

1. Drill a 60 to 200 mm (2.5–8 in) diameter exploratory boring to the depth of the first test.
2. Insert the SPT sampler (also known as a *split-spoon sampler*) into the boring. The shape and dimensions of this sampler are shown in Figure 4.17. It is connected via steel rods to a 63.5 kg (140 lb) hammer, as shown in Figure 4.18.
3. Using either a rope and cathead arrangement or an automatic tripping mechanism, raise the hammer to a distance of 760 mm (30 in) and allow it to fall. This energy drives the sampler into the bottom of the boring. Repeat this process until the sampler has penetrated a distance of 450 mm (18 in), recording the number of hammer blows required for each 150 mm (6 in) interval. Stop the test if more than fifty blows are required for any of the intervals, or if more than one hundred total blows are required. Either of these events is known as *refusal* and is so noted on the boring log.
4. Compute the N value by summing the blow counts for the last 300 mm (12 in) of penetration. The blow count for the first 150 mm (6 in) is retained for reference

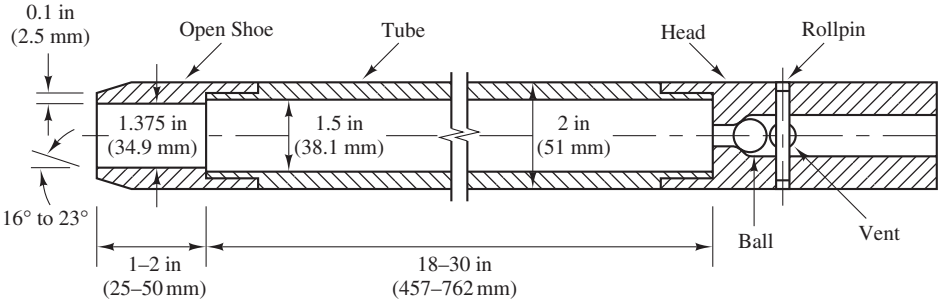

Figure 4.17 The SPT sampler (adapted from ASTM D1586; copyright ASTM, used with permission).

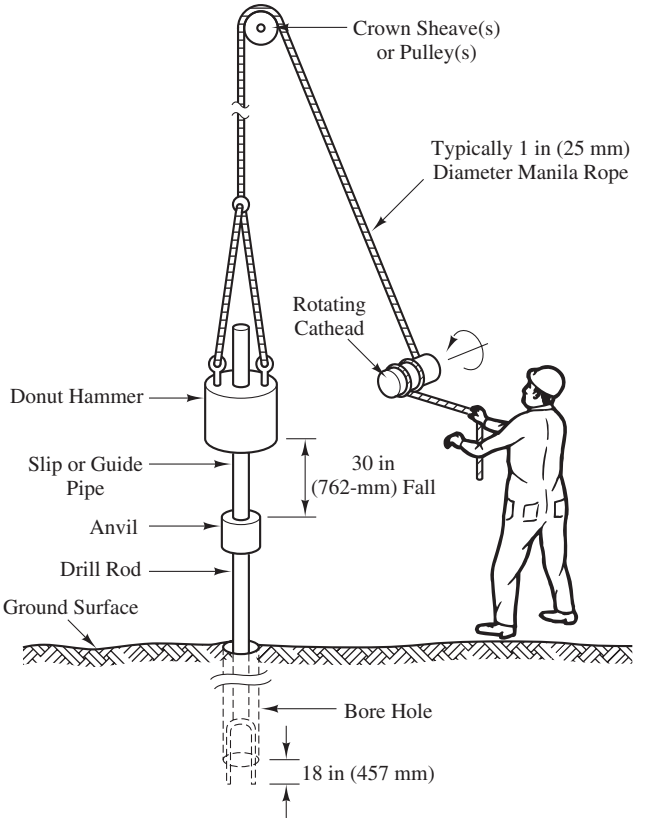

Figure 4.18 The SPT sampler in place in the boring with hammer, rope, and cathead (adapted from Kovacs et al., 1981).

purposes, but not used to compute N because the bottom of the boring is likely to be disturbed by the drilling process and may be covered with loose soil that fell from the sides of the boring. Note that the N value is the same regardless of whether the engineer is using English or SI units.

5. Remove the SPT sampler; remove and save the soil sample.
6. Drill the boring to the depth of the next test and repeat Steps 2 through 6 as required.

Thus, N values may be obtained at intervals no closer than 450 mm (18 in), and typically the test is conducted at depth intervals of 1.5 to 3.0 m (5–10 ft).

Unfortunately, the procedure used in the field varies, partially due to changes in the standard, but primarily as a result of variations in the test procedure and poor workmanship. The test results are sensitive to these variations, so the N value is not as repeatable as we would like. Fortunately, automatic hammers are becoming more popular. They are much more consistent than hand-operated hammers, and thus improve the reliability of the test.

Although much has been said about the disadvantages of the SPT, it does have at least three important advantages over other in situ test methods: First, it obtains a sample of the soil being tested. While SPT samples are highly disturbed, they do permit direct soil classification. Most of the other methods do not include sample recovery, so soil classification must be based on conventional sampling from nearby borings and on correlations between the test results and soil type. Second, it is very fast and inexpensive because it is performed in borings that would have been drilled anyway. Finally, nearly all drill rigs used for soil exploration are equipped to perform this test, whereas other in situ tests require specialized equipment that may not be readily available.

Corrections to the Test Data

We can improve the raw SPT data by applying certain correction factors. The variations in testing procedures may be at least partially compensated by converting the measured N to N_{60} as follows (Skempton, 1986):

$$N_{60} = \frac{E_m C_B C_S C_R N}{0.60} \tag{4.11}$$

where

N_{60} = SPT N value corrected for field procedures
E_m = hammer efficiency (from Table 4.3)
C_B = borehole diameter correction (from Table 4.4)
C_S = sampler correction (from Table 4.4)
C_R = rod length correction (from Table 4.4)
N = measured SPT N value

TABLE 4.3 SPT HAMMER EFFICIENCIES (Adapted from Clayton, 1990.)

Country	Hammer Type (per Figure 4.19)	Hammer Release Mechanism	Hammer Efficiency, E_m
Argentina	Donut	Cathead	0.45
Brazil	Pin Weight	Hand dropped	0.72
China	Automatic	Trip	0.60
	Donut	Hand dropped	0.55
	Donut	Cathead	0.50
Colombia	Donut	Cathead	0.50
Japan	Donut	Tombi trigger	0.78–0.85
	Donut	Cathead 2 turns + special release	0.65–0.67
UK	Automatic	Trip	0.73
USA	Safety	2 turns on cathead	0.55–0.60
	Donut	2 turns on cathead	0.45
Venezuela	Donut	Cathead	0.43

Many different hammer designs are in common use, none of which is 100 percent efficient. Some common hammer designs are shown in Figure 4.19, and typical hammer efficiencies are listed in Table 4.3. Many of the SPT-based design correlations were developed using hammers that had an efficiency of about 60 percent, so Equation 4.11 corrects the results from other hammers to that which would have been obtained if a 60 percent efficient hammer was used.

TABLE 4.4 BOREHOLE, SAMPLER, AND ROD CORRECTION FACTORS (Adapted from Skempton, 1986.)

Factor	Equipment Variables	Value
Borehole diameter factor, C_B	65–115 mm (2.5–4.5 in)	1.00
	150 mm (6 in)	1.05
	200 mm (8 in)	1.15
Sampling method factor, C_S	Standard sampler	1.00
	Sampler without liner (not recommended)	1.20
Rod length factor, C_R	3–4 m (10–13 ft)	0.75
	4–6 m (13–20 ft)	0.85
	6–10 m (20–30 ft)	0.95
	>10 m (>30 ft)	1.00

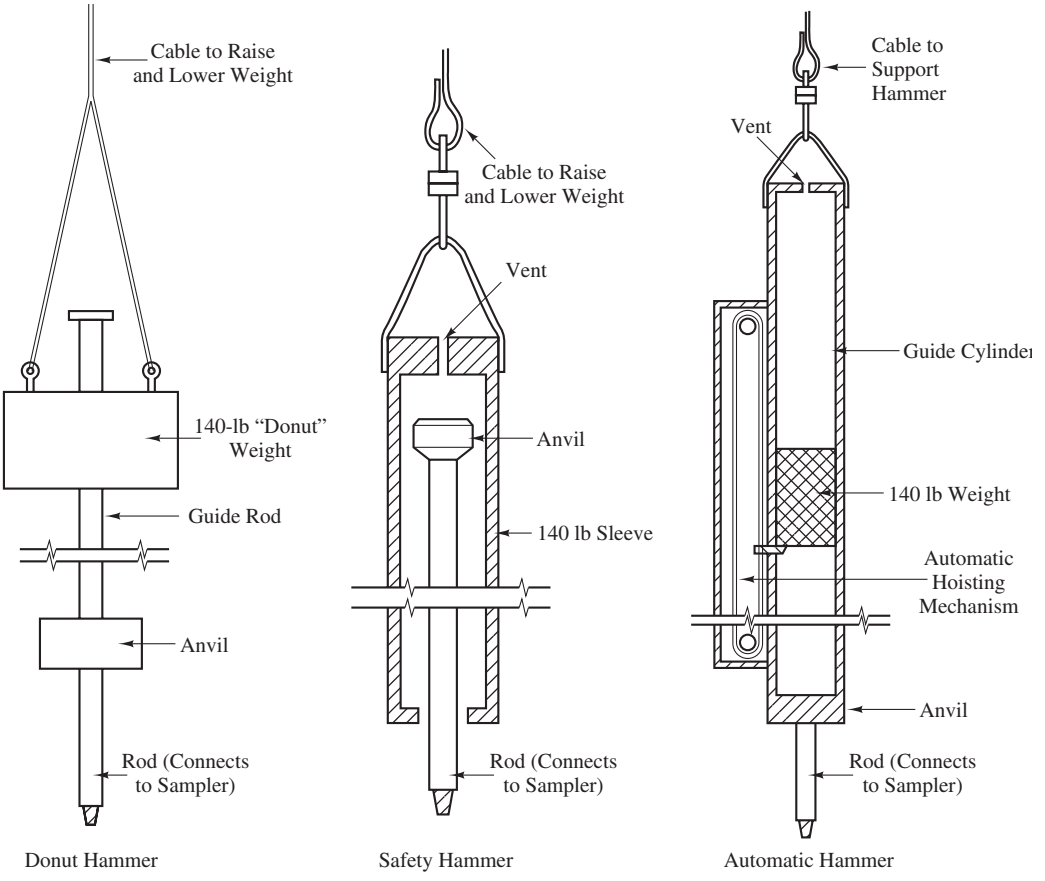

Figure 4.19 Types of SPT hammers.

The SPT data also may be adjusted using an *overburden correction* that compensates for the effects of effective stress. Deep tests in a uniform soil deposit will have higher N values than shallow tests in the same soil, so the overburden correction adjusts the measured N values to what they would have been if the vertical effective stress, σ_z', was 100 kPa (2,000 lb/ft^2). The corrected value, $N_{1,60}$, is (Liao and Whitman, 1985):

$$N_{1,60} = N_{60}\sqrt{\frac{100\ \text{kPa}}{\sigma_z'}} \qquad \text{(4.12 SI)}$$

$$N_{1,60} = N_{60}\sqrt{\frac{2{,}000\ \text{lb/ft}^2}{\sigma_z'}} \qquad \text{(4.12 English)}$$

where

$N_{1,60}$ = SPT N-value corrected for field procedures and overburden stress
σ'_z = vertical effective stress at the test location (kPa or lb/ft^2)
N_{60} = SPT N-value corrected for field procedures

Although Liao and Whitman did not place any limits on this correction, it is probably best to limit corrected $N_{1,60}$ such that $N_{1,60} \leq 2N_{60}$. This limit avoids excessively high $N_{1,60}$ values at shallow depths.

The use of correction factors is often a confusing issue. Corrections for field procedures are always appropriate, but the overburden correction may or may not be appropriate depending on the procedures used by those who developed the analysis method under consideration. In this book, the overburden correction should be applied only when the analysis procedure calls for an $N_{1,60}$ value.

Uses of SPT Data

The SPT N value, as well as many other test results, is only an *index* of soil behavior. It does not directly measure any of the conventional engineering properties of soil and is useful only when appropriate correlations are available. Many such correlations exist, all of which were obtained empirically.

Unfortunately, most of these correlations are very approximate, especially those based on fairly old data that were obtained when test procedures and equipment were different from those now used. In addition, because of the many uncertainties in the SPT results, all of these correlations have a wide margin of error.

Be especially cautious when using correlations between SPT results and engineering properties of clays because these functions are especially crude. In general, the SPT should be used only in cohesionless soils.

Cone Penetration Test (CPT)

The *cone penetration test* or CPT is another common in situ test (Schmertmann, 1978; De Ruiter, 1981; Meigh, 1987; Robertson and Campanella, 1989; Briaud and Miran, 1991; Robertson, 2009; Robertson and Cabal, 2012). The CPT has been used extensively in Europe for over half a century, and now is also widely used in North America and elsewhere. All cone penetrometers have a cone-shaped tip with a 60 degrees apex angle. They come in different sizes, with the two most common sizes having projected areas of 10 cm^2 and 15 cm^2. A mini-cone and a large cone with projected areas of 2 cm^2 and 40 cm^2, respectively, are also available. Figure 4.20a shows the different sized cones currently used in geotechnical practice.

Nearly all CPTs in use today are *electronic cones* [ASTM D5778]. Every electronic cone has two major parts, a cone-shaped tip and a cylindrical sleeve. The cone is mounted on a set of steel rods and a hydraulic ram then pushes this assembly into the ground while instruments measure the resistance to penetration. The *cone resistance*, q_c, is the total force acting on the cone divided by its projected area; the *sleeve friction*, f_s, is the total

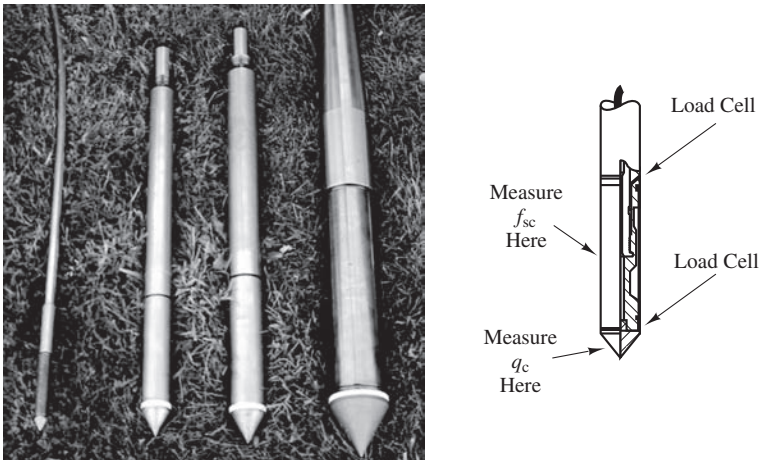

(a) (b)

Figure 4.20 Types of CPT cones: (a) different sizes of cones currently used; and (b) cutaway of a typical cone illustrating the measurement locations (Greg Drilling).

frictional force acting on the friction sleeve divided by the sleeve surface area. It is common to express the side friction in terms of the *friction ratio*, R_f:

$$R_f = \frac{f_s}{q_c} \times 100\% \tag{4.13}$$

Electronic cones include built-in strain gages and measures q_c and f_s at very small intervals, practically giving a continuous sounding with depth. Figure 4.20b shows a cutaway of an electronic cone showing where measurements are made. The CPT defines the soil profile with much greater resolution than does the SPT. CPT rigs are often mounted in large three-axle trucks such as the one in Figure 4.21. These are typically capable of producing maximum thrusts of 100 to 200 kN (10–20 tons). Smaller, trailer-mounted or truck-mounted rigs also are available.

The CPT has been the subject of extensive research and development (Robertson and Campanella, 1983; Robertson, 2009) and thus is becoming increasingly useful to the practicing engineer. Some of this research effort has led to the development of cones equipped with pore pressure transducers in order to measure the excess pore water pressures that develop while conducting the test. These are known as *piezocones*, and the enhanced procedure is known as a CPT with pore pressure measurements or CPTu. These devices are especially useful in saturated clays. Another enhancement to the CPT is to add geophones to the penetrometer to allow the measurement of shear wave velocities in a seismic CPT or SCPT. At present, it is possible to perform a seismic CPT with pore pressure measurements or SCPTu. A typical plot of CPTu results is shown in Figure 4.22.

Figure 4.21 A truck-mounted CPT rig. A hydraulic ram, located inside the truck, pushes the cone into the ground using the weight of the truck as a reaction.

Uses of CPT Data

The CPT is an especially useful way to evaluate soil profiles. Since it retrieves data continuously with depth (with electronic cones), the CPT is able to detect fine changes in the stratigraphy. Therefore, engineers often use the CPT in the first phase of subsurface investigation, saving boring and sampling for the second phase. The CPT is much less prone to error due to differences in equipment and technique, and thus is more repeatable and reliable than the SPT. For some projects, it may be sufficient to use only the CPT.

The CPT also can be used to assess the engineering properties of the soil through the use of empirical correlations. Those correlations intended for use in cohesionless soils are generally more accurate and most commonly used. They are often less accurate in cohesive soils because of the presence of excess pore water pressures and other factors. Correlations are also available to directly relate CPT results with foundation behavior. These are especially useful in the design of deep foundations as discussed in Chapter 13.

Corrected CPT Parameters

Because of the geometry of the cone penetrometer, the pore pressure just behind the cone, u_2, will affect the q_c measured and q_c must be corrected by the following equation:

$$q_t = q_c + u_2(1 - a) \tag{4.14}$$

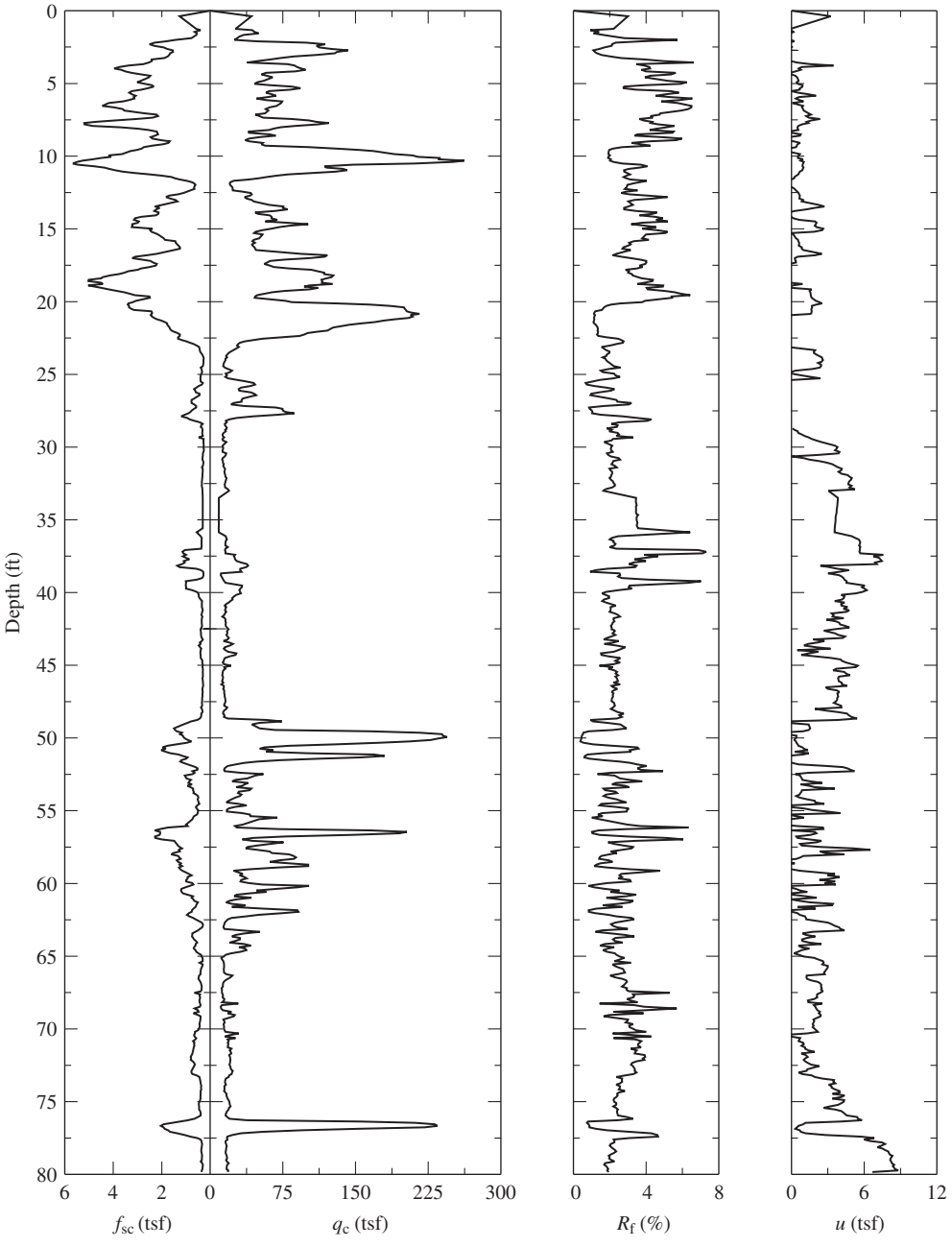

Figure 4.22 Sample CPT test results. These results were obtained from a piezocone, and thus also included a plot of pore water pressure, u, versus depth. All stresses and pressures are expressed in tons per square foot (tsf). For practical purposes, $1\,\text{tsf} = 1\,\text{kg/cm}^2$ (Data from Alta Geo Cone Penetrometer Testing Services, Sandy, Utah).

where

q_t = corrected cone resistance
a = net area ratio

The value of a is measured in the laboratory and is typically between 0.70 and 0.85 (Robertson and Cabal, 2012). For sands, q_t can be taken to be the same as q_c because q_c is usually much larger than u_2.

The sleeve friction f_s must be corrected for pore pressure effects as well if the end areas of the sleeve are different; however, most cones have equal end-area sleeves, in which case this correction is not necessary. Therefore, we will assume in this book that it is not necessary to correct f_s. In practice, if such a sleeve friction correction was needed, it would be included in the CPT data presented to the engineer.

Normalized CPT Parameters

The corrected CPT parameters may be normalized to obtain dimensionless parameters as follows (Robertson and Wride, 1998; Zhang et al., 2002; Robertson, 2009; Robertson and Cabal, 2012):

$$Q_{tn} = \left(\frac{q_t - \sigma_{z0}}{p_a}\right)\left(\frac{p_a}{\sigma'_{z0}}\right)^n \tag{4.15}$$

$$F_r = \left(\frac{f_s}{q_t - \sigma_{z0}}\right) \times 100\% \tag{4.16}$$

$$B_q = \frac{u_2 - u_0}{q_t - \sigma_{z0}} = \frac{\Delta u}{q_t - \sigma_{z0}} \tag{4.17}$$

where

Q_{tn} = normalized cone resistance
F_r = normalized friction ratio
B_q = Pore pressure ratio
σ_{z0} = vertical total stress before cone penetration
σ'_{z0} = vertical effective stress before cone penetration
u_0 = equilibrium water pressure
Δu = excess penetration pore pressure
P_a = atmospheric pressure (100 kPa or 1 tsf)
n = stress exponent

Note that n depends on the soil type and stress history and that the value of n can be taken to be 1.0 for clay-like soils, and can be obtained for a general soil using an iterative procedure described in the next section.

Correlation with Soil Behavior Type

The CPT does not recover any soil samples during penetration. However, there are well-accepted methods for evaluating soil behavior type (SBT) from the test data. Soil behavior type is slightly different from standard soil classification, such as that from the Unified Soil Classification System, but it could be argued that SBT is actually more useful than USCS. Robertson (2010) presents an updated normalized SBT (SBTn) chart as shown in Figure 4.23. In this chart, the SBTn depends on normalized CPT parameters Q_{tn} and F_r. If $n = 1$, Q_{tn} and F_r can readily be determined using Equations 4.15 and 4.16. If $n \neq 1$, an iterative procedure is used to first compute n as follows (Robertson and Cabal, 2012):

1. Use a trial n value (use an initial value of 1) and compute Q_{tn} and F_r.
2. Compute the SBTn index I_c using the following equation:

$$I_c = \left[(3.47 - \log Q_{tn})^2 + (\log F_r + 1.22)^2 \right]^{0.5} \tag{4.18}$$

3. Compute n using the following equation:

$$n = 0.381(I_c) + 0.05\left(\frac{\sigma'_{z0}}{p_a}\right) - 0.15 \leq 1.0 \tag{4.19}$$

4. Compare the computed n value in Step 3 to the trial n value in Step 1. If the absolute change in n (Δn) is larger than 0.01, repeat Steps 1 through 4. This iteration continues until $\Delta n \leq 0.01$, in which case the final n value will be used to calculate the final Q_{tn}.

The SBTn correlations can be programmed into a computer, and often are printed along with the test results. Studies have shown that Figure 4.23 typically has a high degree of accuracy in predicting the SBT when verified with real soil samples (Robertson and Cabal, 2012).

While the CPT probe does not retrieve samples, CPT rigs can be used to obtain small soil samples by replacing the cone with a special sampling tool. This sampling method requires pushing a new sounding, typically very close to the CPT sounding, and sampling strata of interest as identified by the CPT.

Correlation with SPT *N*-Value

Since the SPT and CPT are two of the most common in situ tests, it often is useful to convert results from one to the other. The ratio q_c/N_{60} as a function of the mean grain size, D_{50}, is shown in Figure 4.24. Note that N_{60} does not include an overburden correction.

Be cautious about converting CPT data to equivalent N values, and then using SPT-based analysis methods. This technique compounds the uncertainties because it uses two correlations—one to convert to N, and then another to compute the desired quantity.

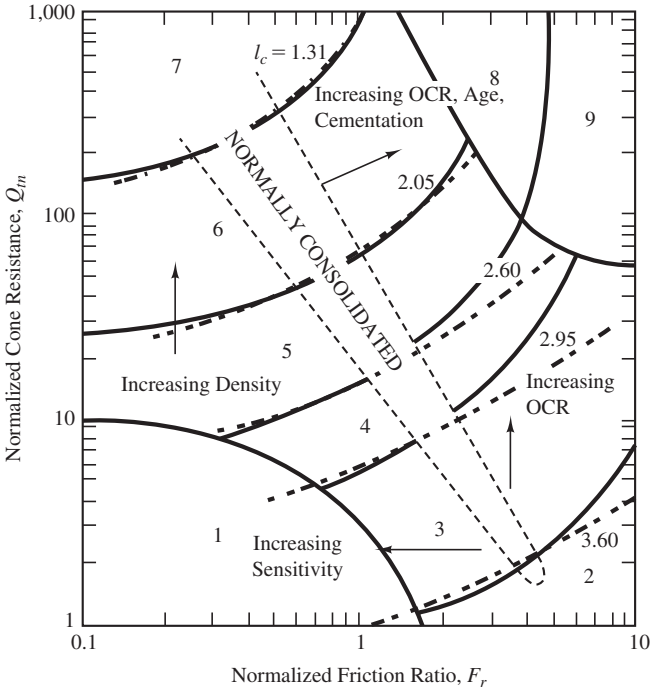

Zone	*Soil Behavior Type*	I_c
1	*Sensitive, fine grained*	N/A
2	*Organic soils—clay*	>3.6
3	*Clays—silty clay to clay*	2.95–3.6
4	*Silt mixtures—clayey silt to silty clay*	2.60–2.95
5	*Sand mixtures—silty sand to sandy silt*	2.05–2.6
6	*Sand—clean sand to silty sand*	1.31–2.05
7	*Gravelly sand to dense sand*	<1.31
8	*Very stiff sand to clayey sand**	N/A
9	*Very stiff, fine grained**	N/A

** Heavily overconsolidated or cemented*

Figure 4.23 Normalized CPT Soil Behavior Type (SBTn) chart (Robertson, 2010).

Example 4.1

Using the CPT log in Figure 4.22, determine the SBTn for the soil stratum located between depths of 28 and 48 ft, and compute the equivalent SPT *N*-value. Assume the groundwater table is below 48 ft and the unit weight of the soil above 48 ft is 120 lb/ft^3.

Solution

By inspection this stratum has $q_c = 15$ tsf, $R_f = 2.0\%$, and $u_2 = 4$ tsf. Assume $a = 0.8$ and $n = 1$.

$$q_t = q_c + u_2(1 - a) = 15 + 4(1 - 0.8) = 15.8 \text{ tsf}$$

$$\sigma_{z0} = \sigma'_{z0} = \frac{28 + 48}{2}(120) = 4{,}560 \text{ lb/ft}^2 = 2.28 \text{ tsf}$$

$$Q_{tn} = \left(\frac{q_t - \sigma_{z0}}{p_a}\right)\left(\frac{p_a}{\sigma'_{z0}}\right)^n = \left(\frac{15.8 - 2.28}{1}\right)\left(\frac{1}{2.28}\right)^1 = 5.9$$

$$F_r = \left(\frac{f_s}{q_t - \sigma_{z0}}\right) \times 100\% = \left(\frac{(15)(0.02)}{15.8 - 2.28}\right) \times 100\% = 2.2\%$$

According to the SBTn chart in Figure 4.23, this soil belongs to Zone 3 and is probably a normally consolidated silty clay to clay.

No grain-size data is available. However, based on the SBTn and Table 3.4, the mean grain size, D_{50}, is probably about 0.002 mm. According to Figure 4.24, $q_c/N_{60} = 1$. Therefore, $\boldsymbol{N_{60} = 15.}$

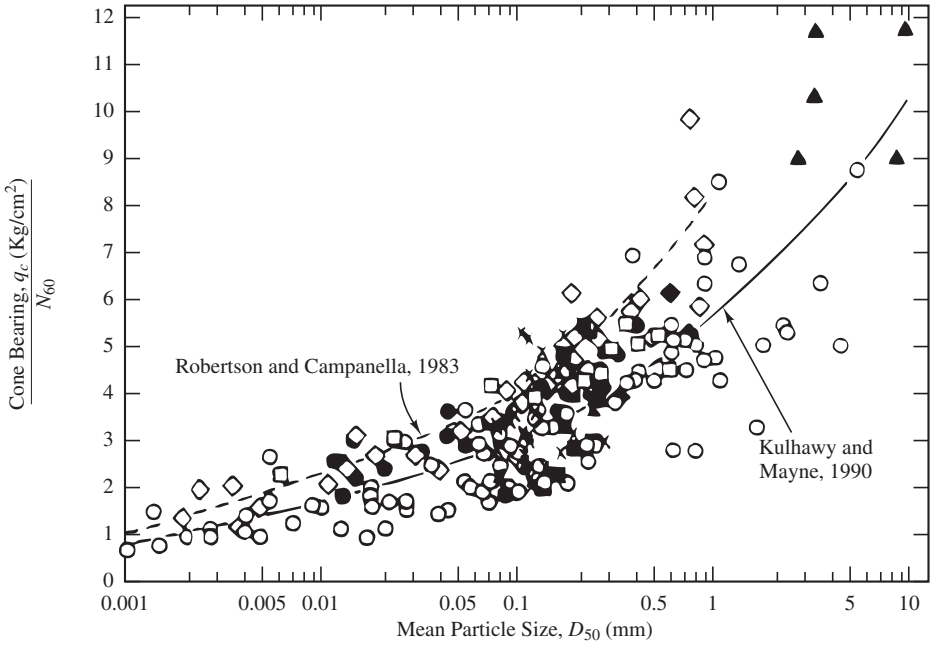

Figure 4.24 Correlation between q_c/N_{60} and the mean grain size, D_{50} (adapted from Kulhawy and Mayne, 1990). Copyright © 1990, Electric Power Research Institute, reprinted with permission.

Dilatometer Test

The dilatometer (Marchetti, 1980; Schmertmann, 1986b, 1988a, and 1988b; Marchetti et al., 2001), which is one of the newer in situ test devices, was developed during the late 1970s in Italy by Silvano Marchetti. It is also known as a *flat dilatometer* or a *Marchetti dilatometer* and consists of a 95 mm wide, 15 mm thick metal blade with a thin, flat, expandable, 60 mm diameter circular steel membrane on one side, as shown in Figure 4.25. The primary benefit of the dilatometer test (DMT) is that it measures the lateral stress condition and compressibility of the soil.

The DMT and CPT are complementary tests (Schmertmann, 1988b). The cone is a good way to evaluate soil strength, whereas the dilatometer assesses compressibility and in situ stresses. These three kinds of information form the basis for most foundation engineering analyses. In addition, the dilatometer blade is most easily pressed into the ground

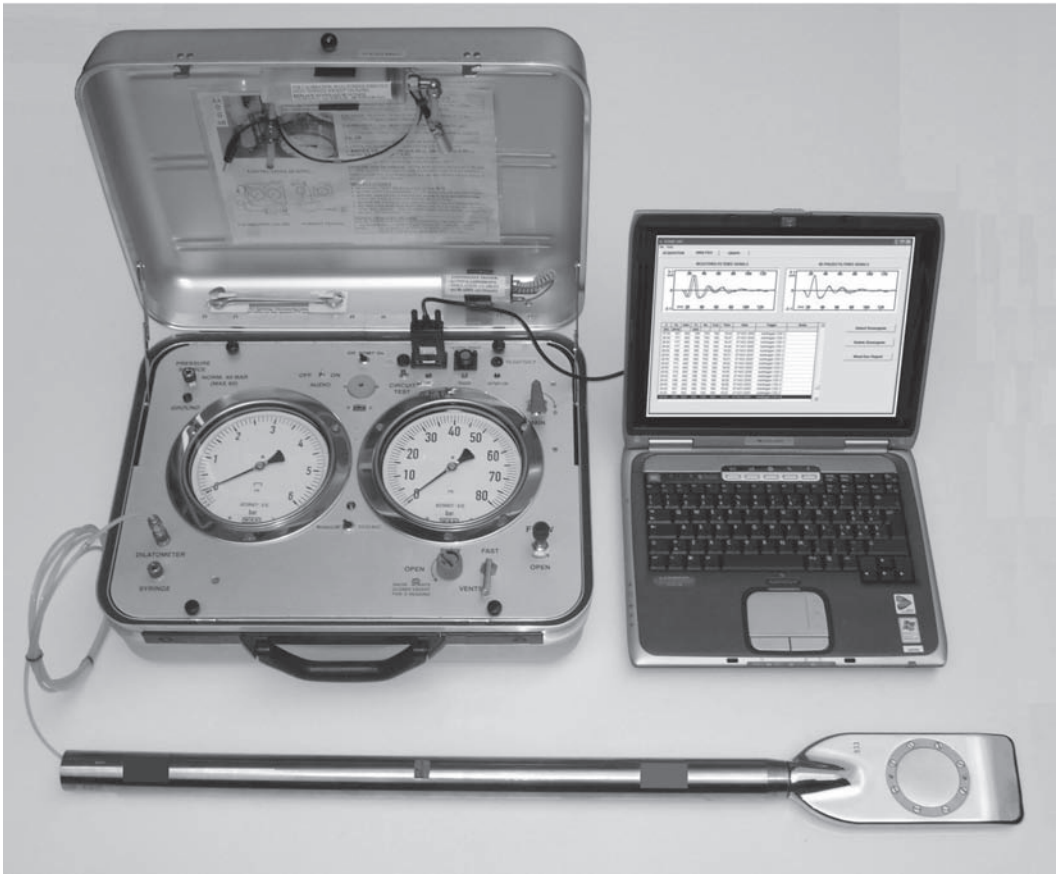

Figure 4.25 The Marchetti dilatometer along with its control unit. In addition to the DMT blade, this dilatometer contains accelerometers that can be used to measure shear wave in soil. The computer on the right is used to record shear waves generated from the ground surface. (Courtesy or Dr. Marchetti).

using a conventional CPT rig, so it is possible to conduct both CPT and DMT tests while mobilizing only a minimum of equipment.

The dilatometer test is a relative newcomer but has become a common engineering tool, especially in Europe. Engineers have had extensive experience with it, and the analysis and design methods based on DMT results are well developed. Furthermore, its relatively low cost, versatility, and compatibility with the CPT suggest that it will be more and more widely used in the United States in the future. It has very good repeatability, and can be used in soft to moderately stiff soils (i.e., those with $N \leq 40$), and provides more direct measurements of stress-strain properties. The DMT [ASTM D6635] is briefly described as follows (Schmertmann, 1986a; Marchetti et al., 2001):

1. Press the dilatometer into the soil to the desired depth using a CPT rig or some other suitable device.
2. Apply nitrogen gas pressure to the membrane to press it outward. Using a pressure gage, record the pressure required to cause the membrane to just lift off its seat and begin to move laterally into the soil (the *A* pressure) and the pressure required to move the membrane 1.10 mm laterally into the soil (the *B* pressure). The equipment is set up to sound an audio signal or buzzer to alert the tester when these membrane movements are reached.
3. Depressurize the membrane and record the pressure acting on the membrane when it returns to its original position, that is when it just lifted off its seat. This is the *C* pressure, which can be converted to the equilibrium pore pressure in the soil.
4. Advance the dilatometer 150 to 300 mm deeper into the ground and repeat the test. Continue until reaching the desired depth.

Each of these test sequences typically requires 1 to 2 minutes to complete, so a typical *sounding* (a complete series of DMT tests between the ground surface and the desired depth) may require about 2 hours. In contrast, a comparable CPT sounding might be completed in about 30 minutes.

The *A*, *B*, and *C* pressures are first corrected for membrane stiffness, pressure gage zero offset and other factors using some equipment calibration readings to obtain the corrected first reading p_0, corrected second reading p_1, and the equilibrium pore pressure u_0 (Marchetti et al., 2001):

$$p_0 = 1.05(A - Z_M + \Delta A) - 0.05(B - Z_M - \Delta B) \tag{4.20}$$

$$p_1 = B - Z_M - \Delta B \tag{4.21}$$

$$u_0 = p_2 = C - Z_M + \Delta A \tag{4.22}$$

where

ΔA and ΔB = corrections obtained from membrane calibration

Z_M = gage zero offset (Z_M is the gage pressure when the gage is vented to the atmosphere; use $Z_M = 0$ if the same gage is used to measure ΔA and ΔB)

The corrected readings are then used to compute the *intermediate DMT parameters*, the material index I_D, horizontal stress index K_D, and the dilatometer modulus E_D:

$$I_D = \left(\frac{p_1 - p_0}{p_0 - u_0}\right) \tag{4.23}$$

$$K_D = \frac{p_0 - u_0}{\sigma'_{z0}} \tag{4.24}$$

$$E_D = 34.7(p_1 - p_0) \tag{4.25}$$

where

σ'_{z0} = vertical effective stress before blade penetration

Researchers have developed correlations between these intermediate DMT parameters and certain engineering properties of the soil (Schmertmann, 1988b; Kulhawy and Mayne, 1990; Marchetti et al., 2001), including:

- Soil type
- Coefficient of at-rest lateral earth pressure, K_0
- Overconsolidation ratio, OCR
- Undrained shear strength, s_u
- Friction angle, ϕ'
- Constrained modulus, M

Correlation with Soil Type

Marchetti (1980) correlates soil type with I_D as follows:

Clays: $0.1 < I_D < 0.6$
Silts: $0.6 < I_D < 1.8$
Sands: $1.8 < I_D < 10$

This correlation generally gives reasonable descriptions of "normal" soils. It sometimes incorrectly identifies a clay as a silt or vice versa and would identify a sand-clay mixture as a silt.

Vane Shear Test (VST)

The Swedish engineer John Olsson developed the vane shear test (VST) in the 1920s to test the sensitive Scandinavian marine clays in situ. The VST has grown in popularity, especially since the Second World War, and is now used around the world.

This test [ASTM D2573] consists of inserting a metal vane into the soil, as shown in Figure 4.26, and rotating it until the soil fails in shear. The undrained shear strength may be determined from the torque at failure, the vane dimensions, and other factors. The vane can be advanced to greater depths by simply pushing it deeper (especially in softer

soils) or the test can be performed below the bottom of a boring and repeated as the boring is advanced. However, because the vane must be thin to minimize soil disturbance, it is only strong enough to be used in soft to medium cohesive soils. The test is performed rapidly (about 1 minute to failure) and therefore measures only the undrained strength.

The shear surface has a cylindrical shape, and the data analysis neglects any shear resistance along the top and bottom of this cylinder. Usually the vane height-to-diameter ratio is 2, which, when combined with the applied torque, produces the following theoretical formula:

$$s_u = \frac{6T_f}{7\pi d^3} \tag{4.26}$$

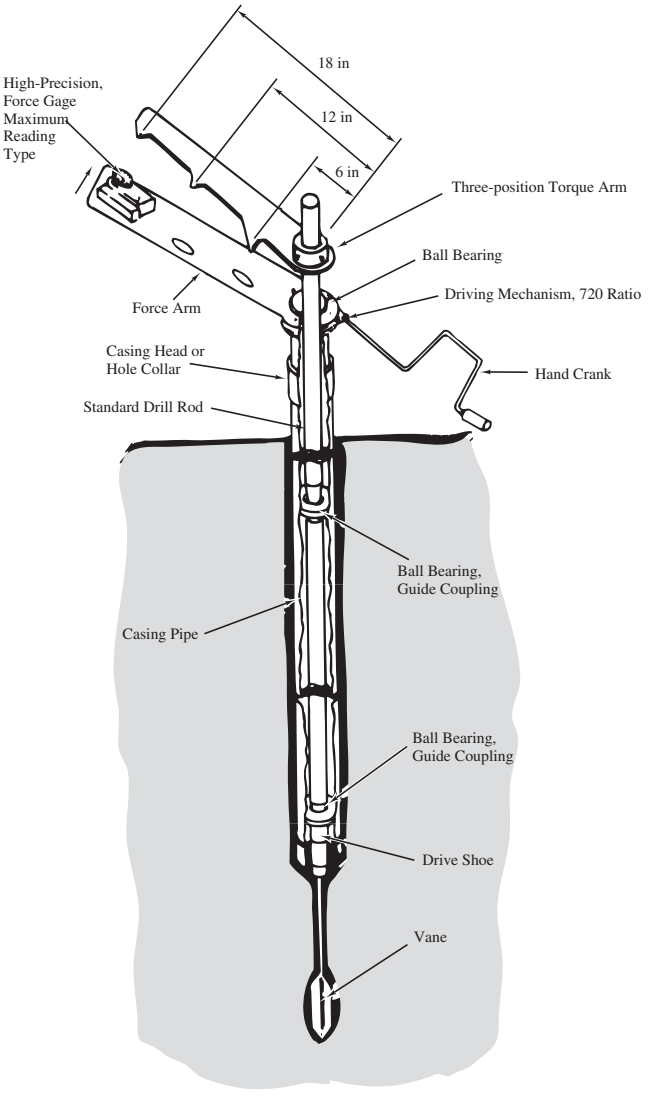

Figure 4.26 The vane shear test (U.S. Navy, 1982a).

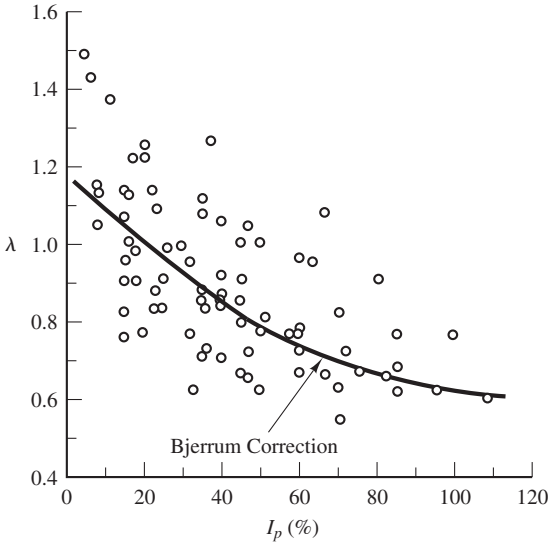

Figure 4.27 Vane shear correction factor, λ (data from Terzaghi et al, 1996).

where

s_u = undrained shear strength
T_f = torque at failure
d = diameter of vane

However, several researchers have analyzed failures of embankments, footings, and excavations using vane shear tests (knowing that the factor of safety was 1.0) and found that Equation 4.26 often overestimates s_u. Therefore, an empirical correction factor, λ, as shown in Figure 4.27, is applied to the test results:

$$s_u = \frac{6\lambda T_f}{7\pi d^3} \tag{4.27}$$

An additional correction factor of 0.85 should be applied to test results from organic soils other than peat (Terzaghi et al, 1996).

Pressuremeter Test (PMT)

In 1954, a young French engineering student named Louis Ménard began to develop a new type of in situ test: the pressuremeter test. Although Kögler had done some limited work on a similar test some twenty years earlier, it was Ménard who made it a practical reality.

The pressuremeter is a cylindrical balloon that is inserted into the ground and inflated, as shown in Figures 4.28 and 4.29. Measurements of volume and pressure can

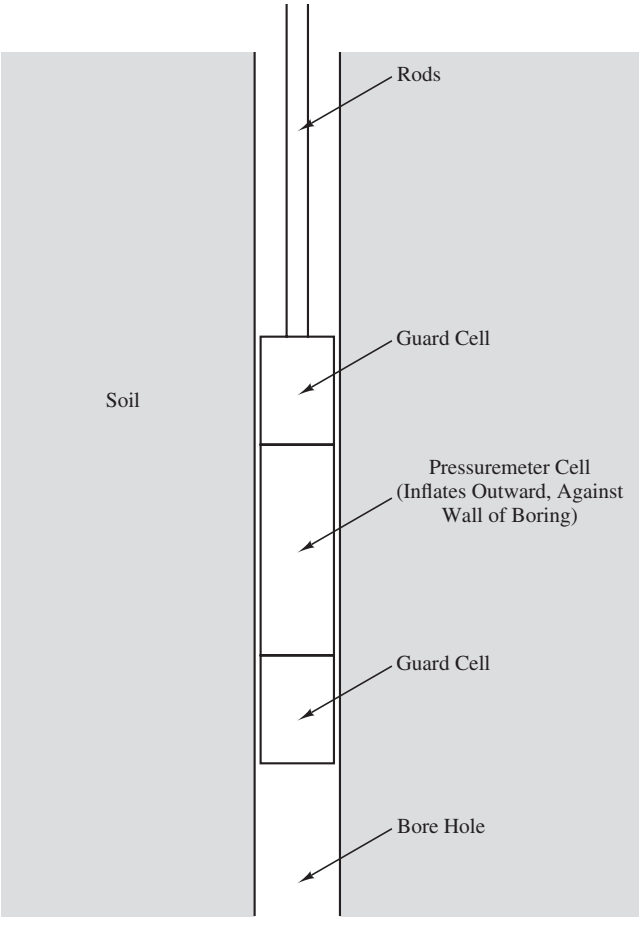

Figure 4.28 Schematic of the pressuremeter test.

be used to evaluate the in situ stress, compressibility, and strength of the adjacent soil and thus the behavior of a foundation (Baguelin et al., 1978; Briaud, 1992).

The PMT may be performed in a carefully drilled boring or the test equipment can be combined with a small auger to create a self-boring pressuremeter. The latter design provides less soil disturbance and more intimate contact between the pressuremeter and the soil.

The PMT produces much more direct measurements of soil compressibility and lateral stresses than the SPT and CPT. Thus, in theory, it should form a better basis for settlement analyses, and possibly for pile capacity analyses. However, the PMT is a difficult test to perform and is limited by the availability of the equipment and personnel trained to use it.

Although the PMT is widely used in France and Germany, it is used only occasionally in other parts of the world. However, it may become more popular in the future.

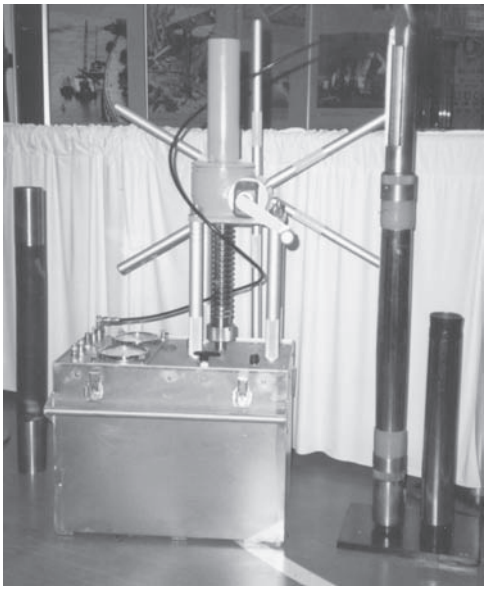

Figure 4.29 A complete pressuremeter set, including three different cell assemblies and the control unit.

Becker Penetration Test

Soils that contain a large percentage of gravel and those that contain cobbles or boulders create problems for most in situ test methods. Often, the in situ test device is not able to penetrate through such soils (it meets *refusal*) or the results are not representative because the particles are about the same size as the test device. Frequently, even conventional drilling equipment cannot penetrate through these soils.

One method of penetrating through these very large-grained soils is to use a *Becker hammer drill*. This device, developed in Canada, uses a small diesel pile-driving hammer and percussion action to drive a 135 to 230 mm (5.5–9.0 in) diameter double-wall steel casing into the ground. The cuttings are sent to the top by blowing air through the casing. This technique has been used successfully on very dense and coarse soils.

The Becker hammer drill also can be used to assess the penetration resistance of these soils using the *Becker penetration test*, which is monitoring the hammer blowcount. The number of blows required to advance the casing 300 mm (1 ft) is the Becker blowcount, N_B. Several correlations are available to convert it to an equivalent SPT N-value (Harder and Seed, 1986). One of these correlation methods also considers the bounce chamber pressure in the diesel hammer.

Comparison of In Situ Test Methods

Each of the in situ test methods has its strengths and weaknesses. Table 4.5 compares some of the important attributes of the tests described in this chapter.

TABLE 4.5 ASSESSMENT OF IN SITU TEST METHODS (Based on Mitchell, 1978a; used with permission of ASCE.)

	Test Methods				
Characteristics	Standard Penetration Test	Cone Penetration Test	Pressuremeter Test	Dilatometer Test	Becker Penetration Test
Simplicity and Durability of Apparatus	Simple; rugged	Complex; rugged	Complex; delicate	Complex; moderately rugged	Simple, rugged
Ease of Testing	Easy	Easy	Complex	Easy	Easy
Continuous Profile or Point Values	Point	Continuous	Point	Point	Continuous
Basis for Interpretation	Empirical	Empirical; theory	Empirical; theory	Empirical; theory	Empirical
Suitable Soils	All except gravels	All except gravels	All	All except gravels	Sands through boulders
Equipment Availability and Use in Practice	Universally available: used routinely	Generally available; used routinely	Difficult to locate; used on special projects	Difficult to locate; used on special projects	Difficult to locate; used on special projects
Potential for Future Development	Limited	Great	Great	Great	Uncertain

4.4 DETERMINATION OF SOIL PROPERTIES FOR FOUNDATION DESIGN

This section presents ways to determine common soil properties required for foundation design. These soil properties can be estimated from empirical formulas, measured by laboratory tests directly, or correlated with in situ test results. For some properties, typical values are given.

General Soil Properties

Unit Weight

The in situ unit weight is typically determined in the laboratory using undisturbed samples. Typical unit weights of different soils are given in Table 3.2.

Overconsolidation Ratio

Correlation with SPT Data

The overconsolidation ratio OCR can be difficult to ascertain in sands. Empirical correlations that relate OCR to the SPT N_{60} can be used to estimate the OCR of a sand. For OCR in sands, silty sands, and sandy silts, Mayne (2007) gives the following empirical correlation:

$$\text{OCR} = \frac{\sigma_c'}{\sigma_{z0}'} = \frac{0.47 p_a N_{60}^m}{\sigma_{z0}'} \tag{4.28}$$

where

p_a = atmospheric pressure (100 kPa or 1 tsf)
m = 0.6 for clean quartzitic sands or 0.8 for silty sands to sandy silts

Another empirical formula, intended for gravels, is attributed to Kulhawy and Chen (2007):

$$\text{OCR} = \frac{\sigma'_c}{\sigma'_{z0}} = \frac{0.15 p_a N_{60}}{\sigma'_{z0}} \tag{4.29}$$

Both Equations 4.28 and 4.29 certainly provide very rough estimates of the OCR, but at least they provide some basis for estimating the OCR of sands.

Correlation with CPT Data

A simple way to estimate the OCR of cohesive soils is through this empirical correlation due to Kulhawy and Mayne (1990) using CPT data:

$$\text{OCR} = kQ_{t1} = k\left(\frac{q_t - \sigma_{z0}}{\sigma'_{z0}}\right) \tag{4.30}$$

where

k = 0.2 to 0.5 (use an average of 0.3)

It is valid for $Q_{t1} < 20$, and higher values of k should be used for aged, heavily overconsolidated clays.

Correlation with DMT Data

According to Marchetti (1980), the OCR of uncemented clays can be estimated through this empirical correlation with DMT Data:

$$\text{OCR} = (0.5\, K_D)^{1.56} \tag{4.31}$$

Note that for normally consolidated clays with OCR = 1, K_D = 2 and that this correlation does not apply to "cemented-structured-aged" clays.

It is more difficult to correlate DMT data with the OCR of sands, and only very rough estimates can be obtained using both M from DMT data and q_c from the CPT (see Marchetti et al., 2001).

Coefficient of Lateral Earth Pressure at Rest

Mayne and Kulhawy (1982) give an empirical correlation (Equation 3.8) that relates K_0 to OCR and ϕ'.

Correlation with CPT Data

Kulhawy and Mayne (1990) present an equation that gives a very rough estimate of the K_0 value from CPT data:

$$K_0 = 0.1Q_{t1} = 0.1\left(\frac{q_t - \sigma_{z0}}{\sigma'_{z0}}\right) \tag{4.32}$$

Because of the considerable scatter in the data used to develop Equation 4.32, this correlation gives a very rough estimate of the value of K_0.

Correlation with DMT Data

Marchetti (1980) presents an equation that gives an estimate of the K_0 value for uncemented clays using DMT Data:

$$K_0 = \left(\frac{K_D}{1.5}\right)^{0.47} - 0.6 \tag{4.33}$$

For sands, Baldi et al. (1986) provide a correlation that relates K_0 to K_D and q_c from the CPT:

$$K_0 = 0.376 + 0.095K_D - K\left(\frac{q_c}{\sigma'_{z0}}\right) \tag{4.34}$$

where

$K =$ 0.005 for "seasoned" sands and 0.002 for "freshly deposited" sands (Marchetti et al., 2001)

Relative Density of Cohesionless Soils

Correlation with SPT Data

The relative density is a useful parameter that describes the consistency of cohesionless soils, as discussed in Chapter 3. It may be determined from SPT data using the following empirical correlation (Kulhawy and Mayne, 1990):

$$D_r = \sqrt{\frac{N_{1,60}}{C_P C_A C_{\text{OCR}}}} \times 100\% \tag{4.35}$$

$$C_P = 60 + 25 \log D_{50} \tag{4.36}$$

$$C_A = 1.2 + 0.05 \log\left(\frac{t}{100}\right) \tag{4.37}$$

$$C_{\text{OCR}} = \text{OCR}^{0.18} \tag{4.38}$$

where

D_r = relative density (in decimal form)
$N_{1,60}$ = SPT N-value corrected for field procedures and overburden stress
C_P = grain-size correction factor
C_A = aging correction factor
C_{OCR} = overconsolidation correction factor
D_{50} = grain size at which 50 percent of the soil is finer (mm)
t = age of soil (time since deposition) (years)
OCR = overconsolidation ratio

Rarely will we have test data to support all of the parameters in Equations 4.35 to 4.38, so it often is necessary to estimate some of them. If a particle size distribution curve is not available, D_{50} may be estimated from a visual examination of the soil with reference to Table 3.4. Geologists can sometimes estimate the age of sand deposits, but Equation 4.37 is not very sensitive to the chosen value, so a "wild guess" is probably sufficient. A value of $t = 1{,}000$ years is probably sufficient for most analyses. The overconsolidation ratio is rarely known in sands, but values of about 1 in loose sands ($N_{60} < 10$) to about 4 in dense sands ($N_{60} > 50$) should be sufficient for Equation 4.38.

Correlation with CPT Data

The following is an approximate relationship between CPT results and the relative density of sands (adapted from Kulhawy and Mayne, 1990):

$$D_r = \sqrt{\left(\frac{q_c}{315 Q_c OCR^{0.18}}\right)\sqrt{\frac{100kPa}{\sigma'_{z0}}}} \times 100\% \qquad \text{(4.39 SI)}$$

$$D_r = \sqrt{\left(\frac{q_c}{315 Q_c OCR^{0.18}}\right)\sqrt{\frac{2{,}000lb/ft^2}{\sigma'_{z0}}}} \times 100\% \qquad \text{(4.39 English)}$$

where

q_c = cone resistance (ton/ft^2 or kg/cm^2)
Q_c = compressibility factor
= 0.91 for highly compressible sands
= 1.00 for moderately compressible sands
= 1.09 for slightly compressible sands
For purposes of using this formula, a sand with a high fines content or a high mica content is "highly compressible," whereas a pure quartz sand is "slightly compressible."
OCR = overconsolidation ratio
σ'_{z0} = vertical effective stress (lb/ft^2 or kPa)

Strength Properties

The undrained and drained strengths of soils are required to analyze different design scenarios.

Undrained Shear Strength of Cohesive Soils

The undrained shear strength of cohesive soils can be estimated using empirical correlations, for example, Equations 3.34 and 3.35. It also can be measured by laboratory UU and CU triaxial tests or in situ tests including the VST, CPT, and DMT.

Correlation with VST Data

Using VST data, Equations 4.26 or 4.27 can be used to estimate the undrained shear strength of a cohesive soil.

Correlation with CPT Data

For cohesive soils, the undrained shear strength, s_u, can be correlated with CPT data (Robertson and Cabal, 2012):

$$s_u = \frac{q_t - \sigma_{z0}}{N_{kt}} \tag{4.40}$$

where N_{kt} varies from 10 to 20, with an average of 15. N_{kt} tends to decrease with increasing soil sensitivity and increase with increasing plasticity.

The CPT results also have been correlated with shear strength ratio for cohesive soils. Robertson and Cabal (2012) give:

$$s_u/\sigma'_{z0} = Q_{t1}/N_{kt} \tag{4.41}$$

where

$Q_{t1} = Q_{tn}$ with $n = 1.0$ (clay-like soils)
$N_{kt} =$ 10 to 20 with an average of 15 (also used in Equation 4.40)

Correlation with DMT Data

For cohesive soils, the undrained shear strength, s_u, can be correlated with DMT data (Marchetti, 1980):

$$s_u = 0.22\sigma'_{z0}(0.5\mathrm{K}_D)^{1.25} \tag{4.42}$$

Experience has shown that this correlation is quite dependable and adequate for everyday practice.

Drained Strength of Cohesionless Soils

Correlation with SPT Data

DeMello (1971) suggested a correlation between SPT results and the effective friction angle of uncemented sands, ϕ', as shown in Figure 4.30. This correlation should be used only for depths greater than about 2 m (7 ft).

Example 4.2

A 6 in diameter exploratory boring has been drilled through a fine sand to a depth of 19 ft. An SPT N-value of 23 was obtained at this depth using a USA safety hammer with a standard sampler. The boring then continued to greater depths, eventually encountering the groundwater table at a depth of 35 ft. The unit weight of the sand is unknown. Compute $N_{1,60}$, ϕ', and D_r at the test location, and use this data to classify the consistency of the sand.

Solution

Per Table 3.2, SP soils above the groundwater table typically have a unit weight of 95 to 125 lb/ft^3. The measured N-value of 23 suggests a moderately dense sand, so use $\gamma = 115$ lb/ft^3. Therefore, at the sample depth:

$$\sigma_z' = \sum \gamma H - u = (115 \text{ lb/ft}^3)(19 \text{ ft}) - 0 = 2{,}185 \text{ lb/ft}^2$$

$$N_{60} = \frac{E_m C_B C_S C_R N}{0.60} = \frac{(0.57)(1.05)(1.00)(0.85)(23)}{0.60} = 19.5$$

$$N_{1,60} = N_{60}\sqrt{\frac{2{,}000 \text{ lb/ft}^2}{\sigma_z'}} = 19.5\sqrt{\frac{2{,}000 \text{ lb/ft}^2}{2{,}185 \text{ lb/ft}^2}} = \mathbf{18.7}$$

Per Figure 4.30: $\phi' = \mathbf{40°}$

D_{50} was not given. However, the soil is classified as a fine sand, and Table 3.4 indicates such soils have grain sizes of 0.075 to 0.425 mm. Therefore, use $D_{50} = 0.2$ mm.

$$C_P = 60 + 25 \log D_{50} = 60 + 25 \log (0.2) = 42.5$$

t was not given, so use $t = 1{,}000$ years.

$$C_A = 1.2 + 0.05 \log\left(\frac{t}{100}\right) = 1.2 + 0.05 \log\left(\frac{1{,}000}{100}\right) = 1.25$$

OCR was not given, so use OCR $= 2.5$.

$$C_{OCR} = OCR^{0.18} = 2.5^{0.18} = 1.18$$

$$D_r = \sqrt{\frac{N_{1,60}}{C_P C_A C_{OCR}}} \times 100\% = \sqrt{\frac{18.7}{(42.5)(1.25)(1.18)}} \times 100\% = \mathbf{55}\%$$

Per Table 3.3, the soil is **Medium Dense**.

Correlation with CPT Data

The CPT results also have been correlated with shear strength parameters, especially in sands. Figure 4.31 presents Robertson and Campanella's 1983 correlation for uncemented, normally consolidated quartz sands. For overconsolidated sands, subtract 1 to 2° from the effective friction angle obtained from this figure.

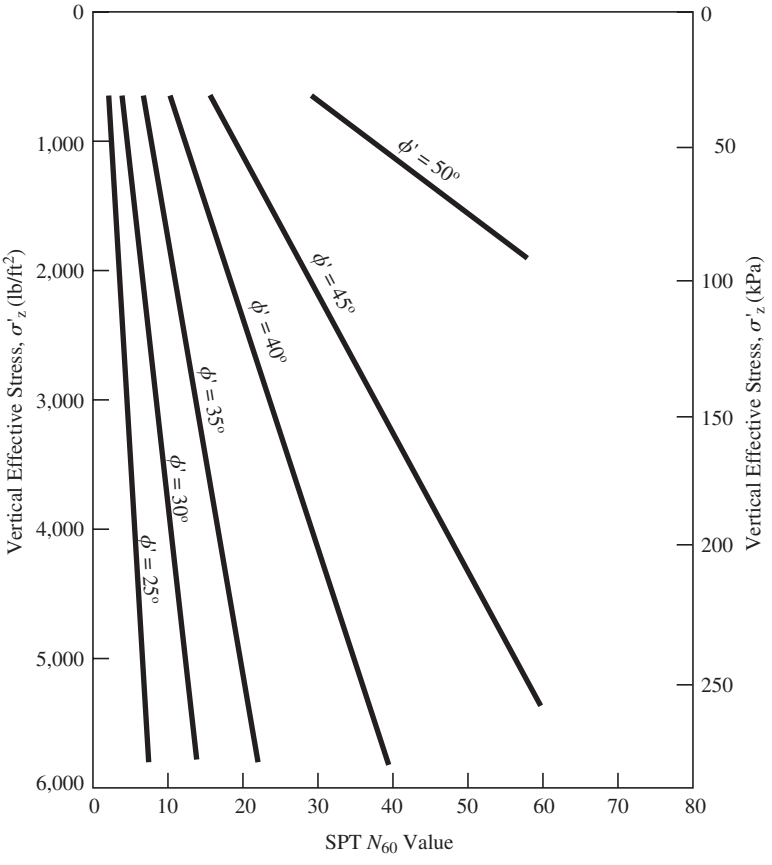

Figure 4.30 Empirical correlation between N_{60} and ϕ for uncemented sands (adapted from DeMello, 1971).

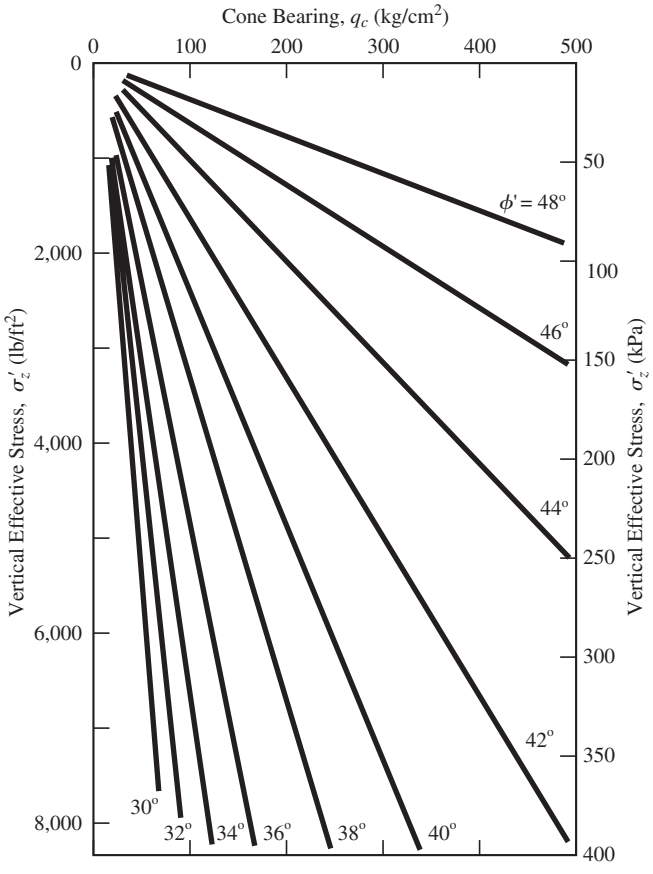

Figure 4.31 Relationship between CPT results, overburden stress, and effective friction angle for uncemented, normally consolidated quartz sands (adapted from Robertson and Campanella, 1983).

Correlation with DMT Data

Marchetti (1997) derived a formula that gives the lower bound friction angle of sands:

$$\phi' = 28° + 14.6° \log K_D - 2.1° \log^2 K_D \tag{4.43}$$

Note that Equation 4.43 gives a lower bound value of ϕ'; the most likely value would be 2 to 4° above this value.

Another way to obtain an estimate of ϕ' of sands is to first compute K_0 from DMT and CPT data using Equation 4.34 and then obtain ϕ' from the chart derived from the theory of Durgunoglu and Mitchell (1975), as shown in Figure 4.32.

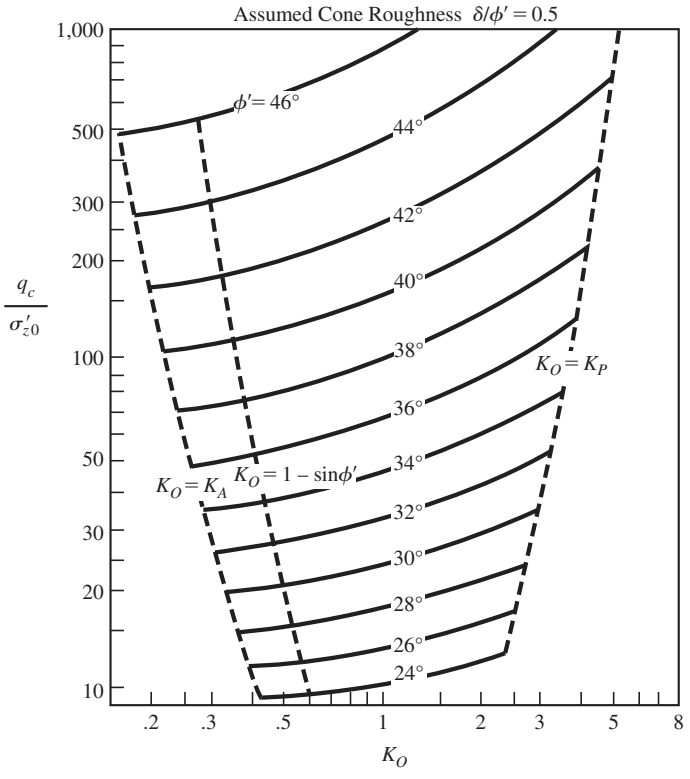

Figure 4.32 Graphical equivalent of the theory of Durgunoglu and Mitchell (1975) (data from Marchetti, 1985).

Stress-Strain Properties

In order to compute settlement of a foundation, we need to know both Poisson's ratio, ν, and Young's modulus, E, of the soil. The modulus can be determined by either field measurements or laboratory measurements. Field determination of modulus can be done by either directly measuring modulus from a device such as the dilatometer or pressuremeter, or through indirect correlations to measurements from an in situ test such as the SPT, CPT, or VST. Determining Poisson's ratio for soils is significantly more difficult. Part of the problem is that Poisson's ratio is a function of stress level and changes during loading.

Poisson's Ratio

For the case of undrained loading of a saturated soil, the Poisson's ratio ν can be taken to be 0.5, the value corresponding to the case of no volume change. In practice, the value of Poisson's ratio is usually estimated based on soil type and loading conditions. Table 4.6

TABLE 4.6 TYPICAL VALUES OF POISSON'S RATIO FOR SOILS AND ROCKS (Adapted from Kulhawy et al., 1983.)

Soil or Rock Type	Drainage Conditions	Poisson's Ratio, ν
Saturated clay	undrained	0.50
Partially saturated clay	undrained	0.30–0.40
Dense sand	drained	0.30–0.40
Loose sand	drained	0.10–0.30
Sandstone	-	0.25–0.30
Granite	-	0.23–0.27

presents typical values of Poisson's ratio for soil and rock. The Poisson's ratio for sands is dependent on relative density. For computational convenience Trautmann and Kulhawy (1987) recommend using Equation 4.44 to estimate Poisson's ratio. While this equation is a function of the friction angle rather than relative density it provides a reasonable estimate.

$$\nu = 0.1 + 0.3\frac{\phi' - 25^\circ}{45^\circ - 25^\circ} \tag{4.44}$$

where

ϕ' = the drained friction angle in degrees

If triaxial tests are performed with measurements of both the volumetric and axial strains, the Poisson's ratio can be computed as

$$\nu = \frac{\Delta\varepsilon_r}{\Delta\varepsilon_a} \tag{4.45}$$

where

ε_r = radial strain
ε_a = axial strain

In both the laboratory and the field, it is now possible to measure the bulk and shear moduli, K and G, respectively, using seismic measurements. If these measurements are made, we can compute the Poisson's ratio using elastic theory as

$$\nu = \frac{3K - 2G}{6K + 2G} \tag{4.46}$$

The shortcoming of this method is that the seismic waves used to measure K and G are made at very low stress levels and aren't necessarily representative of working stress levels for foundations.

Undrained elastic modulus of cohesive soils

For undrained loading of saturated clays, it is possible to estimate the undrained elastic modulus, E, from the undrained shear strength, s_u, and the overconsolidation ratio, OCR. A number of different investigators have developed such correlations. The data are usually presented in the form

$$E = \beta s_u \tag{4.47}$$

where β is a dimensionless parameter which is a function of both OCR and plasticity of the soil.

Figure 4.33 provides typical ranges of β for clays. It was compiled by Duncan and Buchignani (1976) from a number of sources. The undrained shear strength may be measured in laboratory from unconfined compression or unconsolidated undrained triaxial tests on undisturbed samples or from in situ vane shear tests.

Drained modulus of cohesive soils

In the laboratory, we can use data from the 1-D consolidation test to determine the drained modulus of a cohesive soil. Because of the boundary conditions in this test the modulus computed is the constrained modulus, M, rather than the Young's modulus. M can be computed using Equation 3.20. From elastic theory, the Young's modulus, E, and the constrained modulus, M, are related by Equation 3.21, which can be used to compute the Young's modulus from the constrained modulus and Poisson's ratio.

Drained Modulus of Cohesionless Soils

For cohesionless soils we are nearly always concerned only about the drained modulus. For these soils it is best to determine the modulus from in situ tests because of the difficulty in

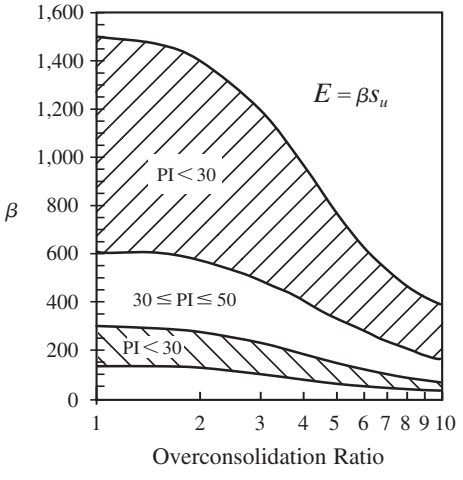

Figure 4.33 Chart for estimating the undrained modulus of clays based on overconsolidation ratio, plasticity, and undrained shear strength (data from Duncan and Buchingnai, 1976).

retrieving undisturbed samples for laboratory testing. The most common in situ tests available for determining modulus are the SPT, CPT, and the flat plate DMT. Of these three methods, the DMT is preferred because it directly measures stress and deformation from which a modulus is computed. Both the SPT and CPT are strength tests. Determining modulus from these tests is based on empirical correlations between these strength measures and compressibility.

Correlation with SPT Data

Several direct correlations between the drained Young's modulus, E, and N_{60} have been developed, often producing widely disparate results (Anagnostopoulos, 1990; Kulhawy and Mayne, 1990). This scatter is probably caused in part by the lack of precision in the SPT, and in part by the influence of other factors besides N_{60}. Nevertheless, the following relationship should produce approximate, if somewhat conservative, values of E:

$$E = \beta_0\sqrt{OCR} + \beta_1 N_{60} \tag{4.48}$$

where

β_0, β_1 = correlation factors from Table 4.7
OCR = overconsolidation ratio
N_{60} = SPT N-value corrected for field procedures

Drained modulus of cohesive and cohesionless soils

There are correlations that work for both cohesive and cohesionless soils and that relate the drained modulus and in situ test data.

Correlation with DMT Data

As described in Section 4.3, the DMT involves pushing a thin blade into the soil and then expanding a small circular loading button into the soil and measuring the stress required to move the button 1 mm into the soil. From the stress and deflection measurements it is

TABLE 4.7 β FACTORS FOR EQUATION 4.48

	β_0		β_1	
Soil Type	(kPa)	(lb/ft^2)	(kPa)	(lb/ft^2)
Clean sands (SW and SP)	5,000	100,000	1,200	24,000
Silty sands and clayey sands (SM and SC)	2,500	50,000	600	12,000

possible to directly compute the DMT modulus, E_D. Due to the boundary conditions of the loading in the DMT it can be shown that the relationship between the DMT modulus and Young's modulus, E, is (Marchetti, 1980):

$$E_D = \frac{E}{(1 - \nu^2)} \tag{4.49}$$

It is also possible to estimate the drained constrained modulus from DMT data. Marchetti et al. (2001) presents the drained constrained modulus, M, as:

$$M = R_M E_D \tag{4.50}$$

where R_M is a coefficient related to the material index, I_D, and the horizontal stress index, K_D, measured during DMT testing. See Section 4.3 for descriptions of I_D and K_D. Marchetti et al. (2001) relate the correction factor R_M to I_D and K_D as follows:

For $I_D \leq 0.6$:

$$R_M = 0.14 + 2.36 \log K_D \tag{4.51}$$

For $I_D \geq 3$:

$$R_M = 0.5 + 2 \log K_D \tag{4.52}$$

For $0.6 < I_D < 3$:

$$R_M = R_{M,0} + (2.5 - R_{M,0}) \log K_D \tag{4.53}$$

where

$$R_{M,0} = 0.14 + 0.15 (I_D - 0.6) \tag{4.54}$$

For $K_D > 10$:

$$R_M = 0.32 + 2.18 \log K_D \tag{4.55}$$

For $R_M < 0.85$, use:

$$R_M = 0.85 \tag{4.56}$$

Correlation with CPT Data

The drained constrained modulus M can be estimated from CPT data using the following empirical equation (Robertson and Cabal, 2012):

$$M = \alpha_M (q_t - \sigma_{z0}) \tag{4.57}$$

where

α_M = constrained modulus coefficient

Robertson and Cabal (2012) related the coefficient α_M to Q_{t1} and I_c as follows:

When $I_c > 2.2$ (fine-grained soils) use:

$$\alpha_M = Q_{t1} \text{ when } Q_{t1} < 14 \tag{4.58}$$

$$\alpha_M = 14 \text{ when } Q_{t1} > 14 \tag{4.59}$$

When $I_c < 2.2$ (coarse-grained soils) use:

$$\alpha_M = 0.0188\left[10^{(0.55I_c+1.68)}\right] \tag{4.60}$$

Schmertmann developed the first empirical correlations between soil modulus and the CPT cone resistance, q_c (Schmertmann, 1970; and Schmertmann et al., 1978). Schmertmann developed this correlation to compute the settlement of rigid footings on sand. As such the modulus is the *equivalent Young's modulus for vertical static compression*, E_s. Because of the lateral strain associated with footing settlement, Schmertmann's modulus, E_s, is larger than the Young's modulus, but smaller than the constrained modulus. However, given the accuracy of the correlations, little additional error is introduced by assuming Schmertmann's modulus, E_s, is equal to the constrained modulus, M. Since Schmermann's original work, other data have been made available to improve correlations. Table 4.8 presents a range of recommended design values of E_s/q_c. It is usually best to treat all soils as being young and normally consolidated unless there is compelling evidence to the contrary. When interpreting the CPT data for computing modulus, do not apply an overburden correction to q_c.

Compression Index (*e*-log-*p* Model)

Values of C_c and C_r are given for different classifications of compressibility in Table 4.9. Table 4.10 gives typical ranges of overconsolidation margins for soils having different degrees of overconsolidation.

TABLE 4.8 ESTIMATING EQUIVALENT SOIL MODULUS, E_S, VALUES FROM CPT RESULTS
[Adapted from Schmertmann et al. (1978), Robertson and Campanella (1989), and other sources.]

Soil Type	USCS Group Symbol	E_S/q_c
Young, normally consolidated clean silica sands (age < 100 years)	SW or SP	2.5–3.5
Aged, normally consolidated clean silica sands (age > 3,000 years)	SW or SP	3.5–6.0
Overconsolidated clean silica sands	SW or SP	6.0–10.0
Normally consolidated silty or clayey sands	SM or SC	1.5
Overconsolidated silty or clayey sands	SM or SC	3

TABLE 4.9 CLASSIFICATION OF SOIL COMPRESSIBILITY

$\frac{C_c}{1+e_0}$ or $\frac{C_r}{1+e_0}$	Classification
0–0.05	Very slightly compressible
0.05–0.10	Slightly compressible
0.10–0.20	Moderately compressible
0.20–0.35	Highly compressible
>0.35	Very highly compressible

TABLE 4.10 TYPICAL RANGES OF OVERCONSOLIDATION MARGINS

Overconsolidation Margin, σ'_m		
(kPa)	(lb/ft^2)	Classification
0	0	Normally consolidated
0–100	0–2,000	Slightly overconsolidated
100–400	2,000–8,000	Moderately overconsolidated
>400	$>8{,}000$	Heavily overconsolidated

4.4 SYNTHESIS OF FIELD AND LABORATORY DATA

Investigation and testing programs often generate large amounts of information that can be difficult to sort through and synthesize. Real soil profiles are nearly always very complex, so the borings will not correlate and the test results will often vary significantly. Therefore, we must develop a simplified soil profile before proceeding with the analysis. In many cases, this simplified profile is best defined in terms of a 1-D function of soil type and engineering properties versus depth: an idealized boring log. However, when the soil profile varies significantly across the site, one or more vertical cross sections may be in order. The development of these simplified profiles requires a great deal of engineering judgment along with interpolation and extrapolation of the data. It is important to have a feel for the approximate magnitude of the many uncertainties in this process and reflect them in an appropriate degree of conservatism. This judgment comes primarily with experience combined with a thorough understanding of the field and laboratory methodologies.

Uncertainty in Measured Properties

Chapter 2 and the introduction to this chapter discussed the natural variability of geomaterials. This variability coupled with testing and other errors lead to uncertainties in the measured soil properties. For example, the drilling and sampling process introduces a bias in the

samples obtained in that soil samples are invariably weakened by sample disturbance. As a result, almost all laboratory-measured soil strength parameters have a negative bias because of sample disturbance nearly always reduces the strength. On the other hand, in the case of rocks or IGMs, the small sample may miss significant defects and therefore give a positive strength bias. This bias should be taken into account in arriving at design properties.

The variability of a property can be quantified by the coefficient of variation, COV. Estimates of the means and ranges of COV of different laboratory-measured parameters are given in Table 4.11. Similar estimates for different field-measured parameters are provided in Table 4.12.

Selection of Characteristic Values of Soil Properties

The characteristic value of a soil property is the value of the property to be used in a certain design methodology. In general, the characteristic value should be selected in accordance

TABLE 4.11 ESTIMATES OF THE VARIABILITY OF SOIL PROPERTIES MEASURED IN LABORATORY TESTS

Property	Soil Type	COV Range (%)	Mean COV(%)	Reference
D_r	Sand	11–36	9	2
γ	Fine-grained	3–20	9	2
γ_d		2–13	7	
s_u	Clay, silt	6–56	33	2
ϕ	Clay, silt	10–56	21	2
	Sand	5–11	9	
tan ϕ	Clay, silt	6–46	21	2
	Sand	5–14	9	
LL	Fine-grained	7–39	18	2
PL		6–34	16	
PI		9–57	29	
C_c, C_r	Sandy clay	–	26	2
	Clay	–	30	
σ'_c	–	–	19	1
c_v	–	33–68	–	4
OCR	–	10–35	–	3

References:
1 – Harr (1987)
2 – Phoon et al. (1995)
3 – Lacasse and Nadim (1996)
4 – Duncan (2000)

TABLE 4.12 ESTIMATES OF THE COEFFICIENT OF VARIATION OF FIELD MEASUREMENTS OF SOIL PROPERTIES (Data from Phoon et al. (1995))

Test	Parameter	Soil Type	COV Range (%)	Mean COV (%)
CPT	q_c	Sand	10–81	38
	q_c	Silty clay	5–40	27
Vane Shear	s_u	Clay	4–44	24
SPT	N	Sand	19–62	54
DMT	A parameter	Sand to clayey sand	20–53	33
		Clay	12–32	20
	B parameter	Sand to clayey sand	13–59	37
		Clay	12–38	20
	E_D	Sand to clayey sand	9–92	50
		Sand, silt	7–67	36
	I_D	Sand to clayey sand	16–130	53
		Sand, silt	8–48	30
	K_D	Sand to clayey sand	20–99	44
		Sand, silt	17–67	38

with the specifications or guidance provided by the design method. For example, AASHTO (2012) specifies that average property values should be used for some properties used in the LRFD method. However, in cases where insufficient or poor strength data are available to determine the average value, the engineer may decide to use a more conservative characteristic value such as one standard deviation below the average strength value. It cannot be overemphasized that one should always use past experience and engineering judgment in selecting the characteristic values to be used in a design.

4.5 ECONOMICS

The site investigation and soil testing phase of foundation engineering is the single largest source of uncertainties. No matter how extensive it is, there is always some doubt whether the borings accurately portray the subsurface conditions, whether the samples are representative, and whether the tests are correctly measuring the soil properties. Engineers attempt to compensate for these uncertainties by applying factors of safety in our analyses. Unfortunately, this solution also increases construction costs.

In an effort to reduce the necessary level of conservatism in the foundation design, the engineer may choose a more extensive investigation and testing program to better define the soils. The additional costs of such efforts will, to a point, result in decreased

construction costs, as shown in Figure 4.34. For example, in some LRFD methods, higher resistance factors are allowed if a more thorough site investigation is performed. However, at some point, this becomes a matter of diminishing returns, and eventually the incremental cost of additional investigation and testing does not produce an equal or larger reduction in construction costs. The minimum on this curve represents the optimal level of effort.

An example of this type of economic consideration is a decision regarding the value of conducting full-scale pile load tests (see Chapter 12). On large projects, the potential savings in construction costs will often justify one or more tests, whereas on small projects, a conservative design developed without the benefit of load tests may result in a lower total cost.

We also must decide whether to conduct a large number of moderately precise tests (such as the SPT) or a smaller number of more precise but expensive tests (such as the PMT). Handy (1980) suggested the most cost-effective test is the one with a variability consistent with the variability of the soil profile. Thus, a few precise tests might be appropriate in a uniform soil deposit, but more data points, even if they are less precise, are more valuable in an erratic deposit.

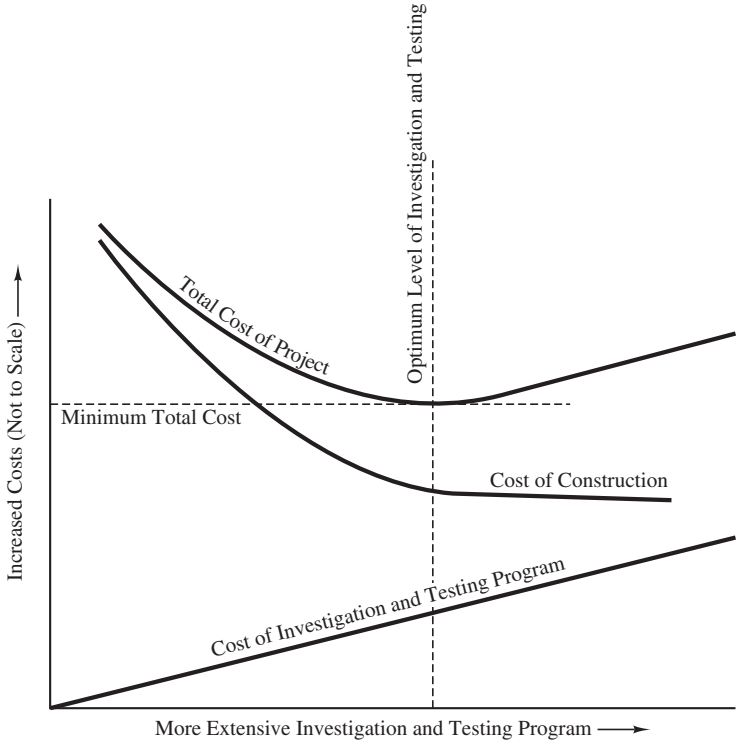

Figure 4.34 Cost effectiveness of more extensive investigations and testing programs.

SUMMARY

Major Points

1. Soil and rock are natural materials. Therefore, their engineering properties vary from site to site and must be determined individually for each project. This process is known as site investigation and characterization.
2. The site investigation and characterization program should follow relevant standards. Many design methods assume a certain level of site investigation and characterization and a certain way of selecting characteristic values for design, to go along with the safety factor(s) recommended.
3. The first step in a site investigation and characterization program typically consists of conducting a background literature search and a field reconnaissance.
4. Site exploration efforts usually include drilling exploratory borings and/or digging exploratory trenches, as well as obtaining soil and rock samples from these borings or trenches.
5. We bring these soil and rock samples to a laboratory to conduct standard laboratory tests. These tests help classify the soil, determine its strength, and assess its compressibility. Other tests might also be conducted.
6. In situ tests are those conducted in the ground. These techniques are especially useful in soils that are difficult to sample, such as clean sands. In situ methods include the standard penetration test (SPT), the cone penetration test (CPT), the vane shear test (VST), the pressuremeter test (PMT), the dilatometer test (DMT), and the Becker penetration test. In situ test data can be correlated with many different soil parameters.
7. An investigation and testing program will typically generate large amounts of data, even though only a small portion of the soil is actually tested. The engineer must synthesize this data into a simplified form to be used in analyses and design.
8. Investigation and testing always involves uncertainties and risks. These can be reduced, but not eliminated, by drilling more borings, retrieving more samples, and conducting more tests. However, there are economic limits to such endeavors, so we must determine what amount of work is most cost effective.

Vocabulary

Becker penetration test	Coefficient of variation	Field reconnaissance
Blow count	Cone penetration test	Flight auger
Boring log	Coring	Hammer
Bucket auger	Dilatometer test	Hollow-stem auger
Casing	Disturbed sample	In situ test
Caving	Exploratory boring	Observation well
Characteristic value	Exploratory trench	Overburden correction

Pressuremeter test	Site investigation	Undisturbed sample
Rotary wash boring	Squeezing	Vane shear test
Shelby tube sampler	Standard penetration test	

QUESTIONS AND PRACTICE PROBLEMS

4.1 Describe a scenario that would require a very extensive site investigation and laboratory testing program (i.e., one in which a large number of borings and many laboratory and/or in situ tests would be necessary).

4.2 How would you go about determining the location of the groundwater table in the design soil profile? Recall that this is not necessarily the same as the groundwater table that was present when the borings were made.

4.3 A five-story office building is to be built on a site underlain by moderately uniform soils. Bedrock is at a depth of over 200 m. This building will be 50 m wide and 85 m long, and the foundations will be founded at a depth of 1 m below the ground surface. Determine the required number and depth of the exploratory borings.

4.4 A two-story reinforced concrete building is to be built on a vacant parcel of land. This building will be 100 ft wide and 200 ft long. Based on information from other borings on adjacent properties, you are reasonably certain that the soils below a depth of 5 to 8 ft (1.5–2.5 m) are strong and relatively incompressible. However, the upper soils are questionable because several uncompacted fills have been found in the neighborhood. Not only are these uncompacted fills loose, they have often contained various debris such as wood, rocks, and miscellaneous trash. However, none of these deleterious materials is present at the ground surface at this site.

Plan a site investigation program for this project and present your plan in the form of written instructions to your field crew. This plan should include specific instructions regarding what to do, where to do it, and any special instructions. You should presume that the field crew is experienced in soil investigation work, but is completely unfamiliar with this site.

4.5 Discuss the advantages of the CPT over the standard penetration test.

4.6 A standard penetration test was performed in a 150 mm diameter boring at a depth of 9.5 m below the ground surface. The driller used a UK-style automatic trip hammer and a standard SPT sampler. The actual blow count, N, was 19. The soil is a normally consolidated fine sand with a unit weight of 18.0 kN/m^3 and $D_{50} = 0.4$ mm. The groundwater table is at a depth of 15 m. Determine the following:

a. N_{60}
b. $N_{1,60}$
c. D_r
d. Consistency (based on Table 3.3)
e. ϕ'

4.7 Using the CPT data in Figure 4.22, a unit weight of 115 lb/ft^3, and an overconsolidation ratio of 3, determine the following for the soil between depths of 21 and 23 ft. Use a groundwater depth of 15 ft below the ground surface.

a. Soil behavior type

b. D_r (assume the soil has some fines, but no mica)

c. Consistency (based on Table 3.3)

d. ϕ'

e. N_{60} (use an estimated D_{50} of 0.60 mm)

4.8 Classify the soil stratum between depths of 66 and 80 ft in Figure 4.22. What is the significance of the spike in the plots at a depth of 77 ft?

4.9 The following standard penetration test results were obtained in a uniform silty sand:

Depth (m)	1	2	3	5
N_{60}	12	13	18	15

The groundwater table is at a depth of 2.5 m. Assume a reasonable value for γ, then determine ϕ' for each test. Finally, determine a single design ϕ' value for this stratum.

4.10 A series of vane shear tests have been performed on a soft clay stratum. The results of these tests are as follows:

Depth (m)	5.0	5.5	7.5	9.0
T_f (N-m)	9.0	10.7	12.0	14.7

The vane was 60 mm in diameter and 120 mm long. The soil has a liquid limit of 100 and a plastic limit of 30. Compute the undrained shear strength for each test, then develop a plot of undrained shear strength versus depth. This plot should have depth on the vertical axis, with zero at the top of the plot.

4.11 A DMT was performed in a normally consolidated clay at a depth of 10 m, giving a K_D of 2.1. The clay has a unit weight of 118 lb/ft^3, and the groundwater table is at the ground surface. Estimate the undrained shear strength of the clay at a depth of 10 m.

5

Performance Requirements

If a builder builds a house for a man and does not make its construction firm, and the house which he has built collapses and causes the death of the owner of the house, that builder shall be put to death.

From *The Code of Hammurabi*, Babylon, circa 2000 BC

The goal of the engineer is to design structures that do not fail. While this statement is obvious, applying it to designs requires that we define failure, a task which is not so clear. For help, we look to the prominent twentieth century geotechnical engineer who defined failure as "an unacceptable difference between expected and observed performance," Leonards (1982). While Leonards' definition might also seem obvious, it explicitly requires the engineer to determine the expected performance or *performance requirements* of a structure—a task that is deceivingly complex. This chapter will examine the performance of structural foundations and provide guidance for their design.

To demonstrate the complexity of determining performance requirements consider two scenarios. The first concerns two structures, a retail structure and a hospital, both of which are constructed in a seismically active area and both are designed considering the maximum likely earthquake for the area. Several years after the structures are built, the design earthquake occurs. Neither building collapses during the earthquake and no lives are lost. However, both buildings suffer significant structural damage and must be demolished. Did both buildings fail during the earthquake? Certainly, both owners will see the performance as a failure. However, as engineers, we could credibly argue that the hospital failed while the retail store did not. We can make this claim because of the design objectives built into the *International Building Code (2013 Edition)* and similar modern building codes, which categorize structures based on their risk to human life and put these two structures in different categories with different performance requirements [IBC 1604.5].

The retail structure would be considered as a Category II structure with "substantial hazard to human life in the event of failure" [IBC Table 1604.5]. The design requirements for this structure are to not collapse during the design earthquake and allow occupants to safely exit the building, but it is not expected to survive the design earthquake. In comparison, the hospital is a Category IV structure designated as "essential" [IBC Table 1604.5] because of the role it would play in responding to the earthquake and saving lives. The design requirements for Category IV structures are that they not only survive the design earthquake, but are able to perform their designed function immediately after the earthquake. Based on these definitions, the retail building performed properly and the hospital failed, even those both suffered the same level of damage—one met expectations and the other did not.

The second scenario concerns two structures, an industrial warehouse and an expensive home, both built on compressible soils. Both structures undergo some settlement and several years after construction, both exhibit interior cracks up to 3 mm wide. In this case there is no threat to human life from the performance of either structure. However, the performance of the house can arguably be considered a failure and will likely generate expensive lawsuits, while the cracks in the warehouse are certainly acceptable and might not even be noticed.

5.1 TYPES OF FAILURE AND LIMIT STATES

The above two scenarios demonstrate some important characteristics of performance requirements. The first is that acceptable performance is a comparison between actual and expected behavior (as stated by Leonards) not an absolute level of performance. In both scenarios, the actual performance of the two structures was the same, but the acceptability of that performance was different in each case. A related observation is that the status of acceptable versus unacceptable depends upon the point of view of the observer.

A second important observation is that not all failures have the same impact for building owners or occupants. Therefore, we categorize failures by defining two broad limit states. The *ultimate limit state (ULS)* encompasses failure modes that involve fracture of structural materials or of the soil, and thus result in serious structural damage or collapse. Such failures can cause substantial property damage, as well as possible serious injuries or loss of life. Clearly, engineers and owners should expend significant resources to avoid such failures. In contrast, the *serviceability limit state (SLS)* encompasses failures that adversely affect the functionality of the structure, but do not threaten the basic structural integrity and do not pose a significant risk of serious injury or loss of life. The excessive settlement in the earlier illustration is an example of a serviceability problem. Exceeding the serviceability limit state causes a decrease in functionality or value of a structure beyond that expected. However, this is not to say the failure to meet serviceability limits is not costly—it may be very costly indeed, but the cost of such failures is orders of magnitude less than the costs associated with exceeding ultimate limit states.

A final, though less obvious, observation is that building codes provide significant guidance in defining performance requirements for ultimate limit states but little guidance

for serviceability limit states. Chapter 16 of the IBC (Structural Design) is 56 pages long and devotes less than one page to serviceability limits [IBC 1604.3]. There is, for example, no guidance in the IBC for acceptable cracking in walls. There are reasons for this apparent discrepancy. First, the purpose of the IBC and other building codes is to protect the public health and safety [IBC 1.1.2]. As such, the economic losses of owners are not of significant importance to the maintainers of building codes. Second, the nature of serviceability limits is highly dependent upon the use and economic value of a particular structure in a particular location at a particular time. It is only through good communication between the owner and the engineer that the serviceability requirements for a specific structure can be determined. This is not something that can be effectively specified in a general code.

5.2 ULTIMATE LIMIT STATES

As discussed above, this limit state is concerned with preventing catastrophic failure of structures. One of the primary goals of building codes is to assure adequate safety against exceeding ultimate limit states. There are two different approaches to evaluating ultimate limit states, *allowable stress design (ASD)* and *ultimate strength design (USD)*.

Allowable Stress Design

The allowable stress design method is the older of the two methods. ASD is distinguished by three key characteristics. First, it compares expected working loads on a structure with the nominal capacity of the structural elements. For this reason, ASD is also called the *working stress design method*. Second, it uses a single factor of safety to determine the adequacy of a design. The fundamental design equation for ASD is:

$$\text{Design Load} < \frac{\text{Nominal Capacity}}{\text{Factor of Safety}} \tag{5.1}$$

Finally, acceptable factors of safety in the ASD method are based on empirical and informal evaluations of satisfactory and unsatisfactory behavior of structures. Many decades of experience have formed the basis for customary factors of safety in the ASD method, and these values are considered to be satisfactory for design. However, they are primarily the result of experience and engineering judgment rather than formal reliability studies.

The roots of ASD date back at least to the nineteenth century, perhaps earlier, and this is the oldest ULS methodology. However, it sometimes generates designs that are more conservative than necessary. One of the reasons for these conservative results is that the various sources of uncertainty are all lumped into a single parameter, the factor of safety. Additionally, since this method focuses on working stresses, it does not do a very good job of modeling behavior or structures in extreme events such as earthquakes, hurricanes, tornados, or tsunamis—which are the rare events that often result in exceeding

ultimate limit states. Therefore, certain systems within a structure are often overdesigned in the ASD method.

Ultimate Strength Design or Load and Resistance Factor Design

The ultimate strength design method uses a different approach. Rather than comparing expected working stresses to yield strength, this method compares the highest reasonably likely loads to the ultimate strength. Rather than using a single factor of safety as ASD, USD uses multiple partial factors of safety, and thus provides a better framework for evaluating the various sources of uncertainty. Some of these partial factors of safety are applied to the loads through the use of *load factors*, γ, most of which are greater than one, to the nominal loads to obtain the *factored load*, U, in the following fashion:

$$U = \gamma_1 D + \gamma_2 L + \gamma_3 E + \cdots \tag{5.2}$$

where

U = factored load
γ = load factor
D = dead load
L = liveload
E = earthquake load

Different load factors are applied for each type of load. In this fashion the uncertainty of each type of load can be modeled individually. For example, live loads are generally more uncertain than dead load, so the load factor for live loads is greater than that for dead loads. Using this method, the factored load, U, represents the highest likely load a structural element might reasonably experience during the life of the structure.

In addition, partial factors of safety are applied to the capacity side of the equation. These are called *resistance factors* or *strength reduction factors*, ϕ, and are applied to the nominal load capacity of a given structural element. In this method, the design must satisfy the following criterion:

$$U < \phi N \tag{5.3}$$

where

ϕ = resistance factor
N = nominal load capacity

Because the ultimate strength design method uses separate load and resistance factors, it is commonly called the *load and resistance factor design (LRFD)* method in North America, and that is the term we will use to refer to this method throughout this text.

Another important characteristic of the LRFD method is that the load and resistance factors are based on reliability analysis in addition to the past experience and empiricism

used in the ASD method. By using multiple partial factors of safety (i.e., load factors and resistance factors) and calibrating them using reliability analysis, LRFD is able to develop designs which provide a more consistent reliability over the different failure modes. This characteristic, along with the use of ultimate loads and resistances, makes LRFD designs more economical while providing the same or higher reliability than the older ASD method.

Geotechnical Ultimate Limit States

Geotechnical ultimate limit states are those that address the ability of the soil or rock to accept the loads imparted by the foundation without failing. The strength of soil is governed by its capacity to sustain shear stresses, so we satisfy geotechnical strength requirements by comparing shear stresses with shear strengths and designing accordingly.

For example, in the case of spread footing foundations, one of the important geotechnical ultimate limit states is the *bearing capacity* of the soil. If this load-bearing capacity of the soil is exceeded, the resulting shear failure is called a *bearing capacity failure*, as shown in Figure 5.1. Later in this book we will examine such failures in detail, and learn how to design foundations that have a sufficient factor of safety against such failures.

Geotechnical ultimate limit state analyses are most commonly performed using allowable stress design (ASD) methods. However, with the adoption of the American Association of State Highway and Transportation Officials (AASHTO) code for bridge design, LRFD methods are now being implemented for many highway structure designs.

Structural Ultimate Limit States

Structural strength limit states address the foundation's structural integrity and its ability to safely carry the applied loads. Typical structural ultimate limit states that must be checked during design include compressive failure of axially loaded members and flexural or shear failure in beams. For example, pile foundations made from A572 Grade 50 steel are normally designed for a maximum allowable compressive stress of 345 MPa (50,000 lb/in^2). Thus, the thickness of the steel must be chosen such that the stresses induced by the design

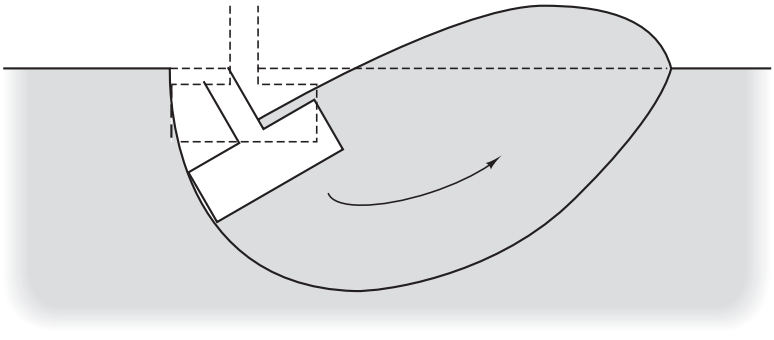

Figure 5.1 A bearing capacity failure beneath a spread footing foundation. The soil has failed in shear, causing the foundation to collapse.

loads do not exceed this allowable value. Foundations that are loaded beyond their structural capacity will, in principle, fail catastrophically.

Structural strength analyses are conducted using either ASD or LRFD methods, depending on the type of foundation, the structural materials, and the governing code. In some cases either method may be used, while in other cases the codes specify one or the other.

Types and Sources of Loads

The foundation design process cannot begin until the *design loads* have been determined. It is important to understand that design loads for evaluating ultimate limit states are not the actual loads that a structure will experience at any given moment in time. They are the loads that the engineer has determined are prudent and realistic for design purposes. The designer must consider that different loads have different characteristics, depending upon their source or method of application. For example, many loads are externally applied to a structure (e.g., weight of automobiles on a bridge or people in a structure), while others are internally applied (e.g., thermal expansion or self-weight of structural elements). Many loads are permanent (e.g., post-tensioning loads or self-weight loads); others are transient (e.g., wind or earthquake loads). The engineer must consider these characteristic when determining the design loads. The key load characteristics to be considered are magnitude, duration, uncertainty, and mode of action. To aid the engineer in characterizing loads, building codes have developed standard classifications for loads based on their source. The classifications vary on the type of structure being designed.

For building structures ASCE 7: *Minimum Design Loads for Buildings and Other Structures* uses the following load categories:

- ***Dead loads*** (D) are those caused by the weight of the structure, including permanently installed equipment.
- ***Weight of ice*** (D_i) are those due to the accumulation of ice on a structure.
- ***Live loads*** (L) are those caused by the intended use and occupancy. These include loads from people, furniture, inventory, maintenance activities, moveable partitions, moveable equipment, vehicles, and other similar sources.
- ***Roof live loads*** (L_r) are live loads applied to the roof of a structure.
- ***Snow loads*** (S) and ***rain loads*** (R) are a special type of live load caused by the accumulation of snow or rain. Sometimes rain loads due to ponding (the static accumulation of water on the roof) are considered separately.
- ***Earth pressure loads*** (H) are caused by the weight and lateral pressures from soil or rock, such as those acting on a retaining wall.
- ***Fluid loads*** (F) are those caused by fluids with well-defined pressures and maximum heights, such as water in a storage tank.
- ***Flood loads*** (F_a) are those caused by both static and dynamic action of water during flood events.
- ***Earthquake loads*** (E) are the result of accelerations from earthquakes.

- ***Wind loads*** (*W*) are imparted by wind onto the structure.
- ***Self-straining loads*** (*T*) are those caused by temperature changes, shrinkage, moisture changes, creep, differential settlement, and other similar processes.

The *AASHTO LRFD Bridge Design Specifications* uses a different set of load categories specific to bridges. This code groups loads into two large categories, permanent and transient.

- **Permanent loads**
  - ***Creep effects*** (*CR*) are those due to slow time dependent movements in materials.
  - ***Downdrag loads*** (*DD*) are forces applied to foundations when adjacent soils consolidate and pull the foundation down.
  - ***Structural dead loads*** (*DC*) are those due to structural components and nonstructural attachments.
  - ***Wearing surface dead loads*** (*DW*) are those due to the pavement surface and utilities.
  - ***Horizontal earth pressures*** (*EH*) are those due to lateral force of earth.
  - ***Locked in loads*** (*DC*) are those due to effects from construction process including jacking apart of cantilevers in segmental construction.
  - ***Earth surcharge loads*** (*EC*) are those due to embankment or other loadings at the ground surface.
  - ***Vertical earth pressure*** (*EV*) are those due to dead load of earth fill.
  - ***Post-tensioning loads*** (*PS*) are secondary forces due to post-tensioning.
  - ***Shrinkage loads*** (*SH*) are those due to shrinkage of concrete after placement.

- **Transient loads**
  - ***Braking loads*** (*BR*) are those due to vehicular braking.
  - ***Centrifugal loads*** (*CE*) are those due to turning vehicles.
  - ***Vehicle collision loads*** (*CT*) are those due to impacts of vehicles.
  - ***Vessel collision loads*** (*PS*) are those due to impacts of waterborne vessels.
  - ***Earthquake loads*** (*EQ*) are those due to accelerations from earthquakes.
  - ***Friction loads*** (*FR*) are those due to friction of vehicle wheels.
  - ***Ice loads*** (*IC*) are those due to accumulation of ice on the bridge structure.
  - ***Vehicle dynamic loads*** (*IM*) are those due to dynamic vertical motion of vehicles.
  - ***Live surcharge loads*** (*LS*) are those due to transient surcharge loads.
  - ***Pedestrian live loads*** (*PL*) are those due to weight of pedestrians.
  - ***Settlement loads*** (*SE*) are force effects due to settlement.
  - ***Temperature gradient loads*** (*TG*) are force effects due to expansion or contraction caused by differential temperatures across the structure.
  - ***Uniform temperature loads*** (*TU*) are those due to expansion or contraction due to uniform temperature changes.

- ***Water and stream loads*** (*WA*) are those due to both static and dynamic action of water on the structure.
- ***Wind loads on live loads*** (*WL*) are those due to wind action on the vehicles moving on the structure.
- ***Wind loads on structure*** (*PS*) are those due to wind action directly on the structure.

Structural engineers compute the dead loads by simply summing the weights of the structural members. These weights can be accurately predicted and remain essentially constant throughout the life of the structure, so the design dead load values should be very close to the actual dead loads. Incorrect design dead loads are usually due to miscommunication between the structural engineer and others. For example, remodeling may result in new walls, or HVAC (heating, ventilation, and air conditioning) equipment may be heavier than anticipated. Dead loads also can differ if the as-built dimensions are significantly different from those shown on the design drawings. Notice that the AASHTO bridge design guidance divides the dead loads into structural dead loads and pavement dead loads, whereas the ASCE building design guidance had only one category for dead loads. This is due to the different nature of the operation of bridges versus buildings. It is common for weight of bridge pavements to change over time as the road surface is overlaid or milled where the structural elements do not change over time. Therefore, AASHTO separates these two loads.

Some design loads must be computed from the principles of mechanics. For example, fluid loads in a tank are based on fluid statics. The remaining design loads are usually dictated by codes. For example, the International Building Code specifies a floor live load of 2 kPa (40 lb/ft^2) for design of classrooms [IBC Table 1607.1] (which is the same as the live load used for prisons cells!). Most of these code-based design loads are conservative, which is appropriate. This means the real service loads acting on a foundation are probably less than the design loads used for analyzing ultimate limit states.

Load Combinations

The various loads potentially affecting a structure do not all necessarily occur at the same moment in time. It is highly unlikely, for example, to have the design dead load, live load, earthquake load, and wind load all occur simultaneously. To account for the different loading possibilities, engineers have developed different load combinations that represent likely loading events for typical structures. To determine the design load for a given structure, engineers must check all the reasonable load combinations and select the most critical load combination for design; the load combination giving the highest total load.

During the development of building codes, each code specified its own load combinations, which led to much confusion for engineers. In the last two decades significant consolidation and unification of codes has occurred. Today, for the foundation engineer working in North America, there are two main codes which govern load combinations. For buildings, ASCE 7-10: *Minimum Design Loads for Buildings and Other Structures* (ASCE, 2010) has unified the design loads and has been adopted by the American Concrete Institute (ACI), the American Institute of Steel Construction (AISC), and in a slightly modified form, the *International Building Code* (ICC, 2012).

The second code of interest to North American foundation engineers is the *AASHTO LRFD Bridge Design Specifications* (AASHTO, 2012). This code is appropriate for designing highway bridges and associated transportation structures such as retaining walls. There are other codes that are applicable to other structures. For example, the *Manual for Railway Engineering*, maintained by the American Railway Engineering and Maintenance-of-Way Association (AREMA), is appropriate for the design of railway structures. However, this book will use primarily the ASCE, ACI, and AISC codes for buildings, and the AASHTO code for highway structures.

As described above, ASCE 7 (2010) and AASHTO (2012) define substantially different load categories due to the different nature of buildings versus bridges. Likewise, each code defines different load combinations. Another key difference between these two codes is that ASCE 7 provides load combinations for both ASD and LRFD methods, while AASTHO provides only LRFD load combinations. For examples in the chapter, we will present only the ASCE 7 load combinations.

It is critical that the foundation engineer uses the appropriate code for the appropriate structure. In later chapters, we will discuss design methods for different foundation systems. Different codes will specify different design methods each with its associated design loads. It is critical that the code used for design and analysis match the code used to determine the loads. Do not mix codes!

Load Combinations for ASD

ASCE 7 defines the ASD design load as the greatest of the following eight load combinations [ASCE 2.4.1]:

$$D + F + H \tag{5.4}$$

$$D + F + L + H \tag{5.5}$$

$$D + F + H + (L_r \text{ or } S \text{ or } R) \tag{5.6}$$

$$D + F + 0.75L + H + 0.75(L_r \text{ or } S \text{ or } R) \tag{5.7}$$

$$D + F + H + (0.6W \text{ or } 0.7E) \tag{5.8}$$

$$D + F + 0.75L + H + 0.75(0.6W) + 0.75(L_r \text{ or } S \text{ or } R) \tag{5.9}$$

$$D + F + 0.75L + H + 0.75(0.7E) + 0.75S \tag{5.10}$$

$$0.6D + H + 0.6W \tag{5.11}$$

$$0.6(D + F) + H + 0.7E \tag{5.12}$$

The above equations assume the earth pressure loads, H, act in the same direction as primary loading of the structure. If earth pressure loads resist the primary load and are permanent, then the load factor for H changes to 0.6. If the earth pressures loads resist but are not permanent, they are not included in load combination [ASCE 2.4.1].

The greatest design load computed using Equations 5.4 through 5.12 is called the *unfactored design load* or simply the *unfactored load*. This is to distinguish this design load from that determined using the LRFD method. Although some of the ASD load combinations use multipliers on some of the loads, these are not load factors in the sense defined by the LRFD method. Once the most critical (greatest) load combination is determined, the engineer must then ensure that the foundation elements satisfy Equation 5.1.

Load Combinations for LRFD

The design load determined in the LRFD method is called the *factored design load* or simply the *factored load*, U. According to ASCE 7 [ASCE 2.3.2] the factored load is the greatest of:

$$1.4(D + F) + 1.6H \tag{5.13}$$

$$1.2(D + F) + 1.6L + 1.6H + 0.5(L_r \text{ or } S \text{ or } R) \tag{5.14}$$

$$1.2(D + F) + 1.6H + 1.6(L_r \text{ or } S \text{ or } R) + (L \text{ or } 0.5W) \tag{5.15}$$

$$1.2(D + F) + W + L + 1.6H + 0.5(L_r \text{ or } S \text{ or } R) \tag{5.16}$$

$$1.2(D + F) + E + L + 1.6H + 0.2S \tag{5.17}$$

$$0.9D + W + 1.6H \tag{5.18}$$

$$0.9(D + F) + E + 1.6H \tag{5.19}$$

The load factor of 1.6 for earth pressure loads, H, assumes these loads add to the primary loading of the structure. If earth pressure loads resist the primary load and are permanent, then the load factor for H changes to 0.9. If the earth pressures loads resist but are not permanent, they are not included in computing the factored load. In certain special cases, the live load factors may be reduced [ASCE 3.2.3].

As discussed earlier, the AASHTO bridge design code uses substantially more load categories than the ASCE code for buildings. The AASHTO code uses a total of 13 load combinations to determine the factored load, U [AASHTO 3.4.1]. Additionally, these load combinations contain a number of variants, leading to well over 30 load combinations for typical bridge designs. It is critical that the designer be consistent in code usage. As discussed in Section 2.4, the load and resistance factors in LRFD codes are calibrated together to achieve the target reliability. Mixing resistance factors from one code with load factors from another code will invalidate this calibration and may produce unsafe designs.

Once the most critical load combination is determined, the engineer must then ensure that the foundation elements satisfy Equation 5.3.

Foundation Loads or Demands

The design loads determined using the load combinations presented above (unfactored loads in the case ASD methods and factored loads in the case of LRFD methods) are the external loads and internal loads (due to thermal expansion or structural deformation)

applied to the structure. To design a foundation, the engineer must analyze the structure's reaction to the applied loads and determine the demand or loads applied to the foundation itself. The structural design loads generate four different demands or loads on foundations as illustrated in Figure 5.2:

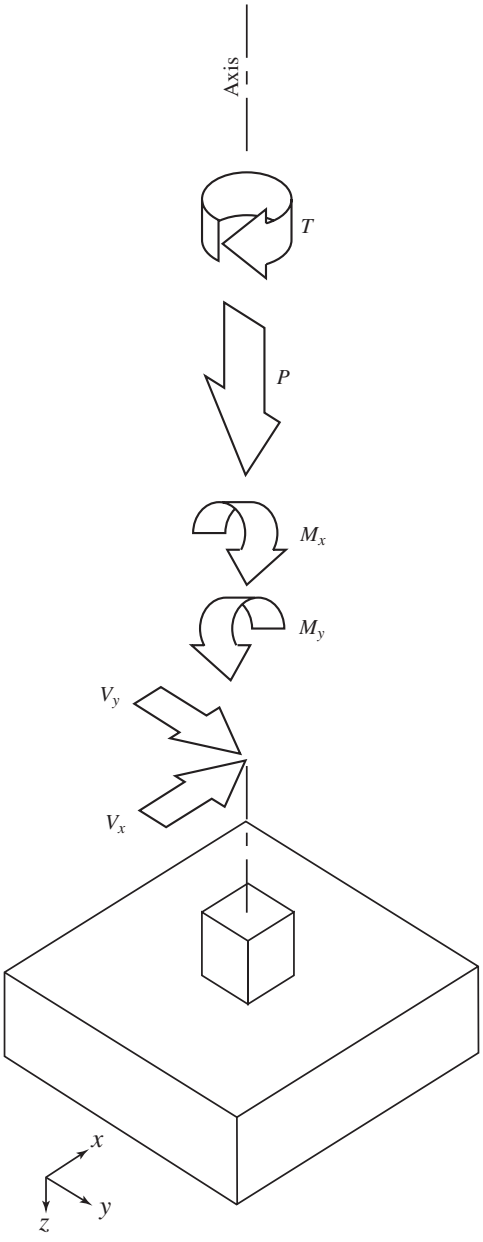

Figure 5.2 Types of structural loads acting on a foundation.

- ***Normal load***, designated by the variable P for unfactored load or P_u for factored load.
- ***Shear load***, designated by the variable V for unfactored load or V_u for factored load.
- ***Moment***, designated by the variable M for unfactored load or M_u for factored demand.
- ***Torsion***, designated by the variable T for unfactored load or T_u for factored load.

Unfactored loads are used in the ASD method and factored loads are used in the LRFD method.

Normal loads are those that act parallel to the foundation axis. Usually this axis is vertical, so the normal load becomes the vertical component of the applied load. It may act either downward in compression, P, or upward in tension, P_{up}.

Shear loads act perpendicular to the foundation axis. They may be expressed as two perpendicular components, V_x and V_y. Moments also may be expressed using two perpendicular components, M_x and M_y. Sometimes torsion, T, is also important, such as with cantilever highway signs. However, in most foundation designs the torsion is small and may be ignored.

Most foundations, especially those that support buildings or bridges, are designed primarily to support downward normal loads, so this type of loading receives the most attention in this book. However, other types of loads also can be important, and in some cases can control the design. For example, the design of foundations for electrical transmission towers is often controlled by upward normal loads induced by overturning moments on the tower.

In the ASD method, Equations 5.4 through 5.12 are be used to compute all foundation loads (normal, shear, and moment) from a given set of loadings. In the ASD formulation, the symbols P, V, and M are used to designate the resulting demand. The component loads use subscript relating to the load type. For example, when evaluating the normal load, Equation 5.8 produces $P = P_D + 0.6P_W$ or $P = P_D + 0.7P_E$, whichever is greater. When combining these loads, be sure to consider their direction. For example, when evaluating the normal load, some components may induce compression, while others induce tension. Equation 5.4 governs only when some of the loads act in opposite directions. For example, if a certain column is subjected to a 500 kN compressive dead load and a 100 kN tensile live load, the design load would be 500 kN per Equation 5.4.

When using the LRFD method, Equations 5.13 through 5.19 are used and the resulting loads are called factored loads and the symbols P_u, V_u, and M_u are used to designate the resulting demand. For example, when evaluating normal load, Equation 5.18 produces $P_u = 0.9P_D + P_W + 1.6P_H$.

Example 5.1

Compute the foundation design loads for the simple cantilevered structure shown in Figure 5.3. Use the ASD method as presented in ASCE 7.

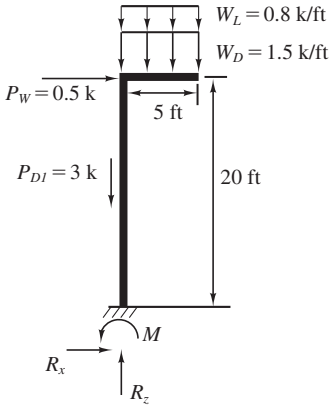

Figure 5.3 Figure for Example 5.1.

Solution

The foundation design loads will be the reactions at the base of the column, R_x, R_z, and M, computed using the load combinations in Equations 5.4 through 5.12. Using equilibrium we can determine the following equations for the reactions at the base of the column.

$$R_z = 5W_D + P_{D1} + 5W_L$$

$$R_x = P_w \qquad \text{(Ex-5.1.1)}$$

$$M = 2.5(5W_D) + 2.5(5W_L) - 20P_W \qquad \text{(Ex-5.1.2)}$$

The design compressive load, P, will be equal to the maximum value of R_z computed using Equations 5.4 through 5.12.

$P = (5W_D + P_{D1}) = 5 \times 1.5 + 3 = 10.5$ k

$P = (5W_D + P_{D1}) + 5W_L = (5 \times 1.5 + 3) + 5(0.8) = 14.5$ k $\Leftarrow$ **Controls**

$P = (5W_D + P_{D1}) = 5 \times 1.5 + 3 = 10.5$ k

$P = (5W_D + P_{D1}) + 0.75(5W_L) = (5 \times 1.5 + 3) + 0.75(5 \times 0.8) = 13.5$ k

$P = (5W_D + P_{D1}) = (5 \times 1.5 + 3) = 10.50$ k

$P = (5W_D + P_{D1}) + 0.75(5W_L) = (5 \times 1.5 + 3) + 0.75(5 \times 0.8) = 13.5$ k

$P = (5W_D + P_{D1}) + 0.75(5W_L) = (5 \times 1.5 + 3) + 0.75(5 \times 0.8) = 13.5$ k

$P = 0.6(5W_D + P_{D1}) = 0.6(5 \times 1.5 + 3) = 6.3$ k

$P = 0.6(5W_D + P_{D1}) = 0.6(5 \times 1.5 + 3) = 6.3$ k

The unfactored design compressive load for the foundation is controlled by Equation 5.5 and $P = 14.5$ k.

The design shear load for this example, V, will be equal to the wind load, P_W, as shown in Equation Ex-5.1.1. In this case only Equations 5.8, 5.9, and 5.11 apply.

$$V = 0.6P_W = 0.6(0.5) = 0.30 \text{ k}$$

$$V = 0.75(0.6P_W) = 0.75(0.6 \times 0.5) = 0.23 \text{ k}$$

$$V = 0.6P_W = 0.6(0.5) = 0.30 \text{ k}$$

Equations 5.8 and 5.11 control and the unfactored design shear load, V, is 0.3 k.

The design moment for this example, M, is defined by Equation Ex-5.1.2. Note that there is no moment applied to the structure, but there is a design moment for the foundation. If we check Equations 5.4 through 5.12, we will find that Equation 5.5 governs.

$$\begin{aligned} M &= 2.5(5w_D) + 2.5(5w_L) \\ &= 2.5(5 \times 1.5) + 2.5(5 \times 0.8) = 28.75 \text{ k-ft} \end{aligned}$$

So the design foundation loads according to ASD method are:

$$\boldsymbol{P = 14.5 \text{ k}}$$

$$\boldsymbol{V = 0.3 \text{ k}}$$

$$\boldsymbol{M = 28.75 \text{ k-ft}}$$

We will now compute the design loads using LRFD method in Example 5.2.

Example 5.2

Compute the factored design foundation loads for the structure shown in Figure 5.3 using LRFD methods as presented in ASCE 7.

Solution

The equilibrium conditions for this example are the same as Example 5.1 and Equations 5.20 through 5.22 still define the design, compressive load, shear load, and moment. However, in this example we must use Equations 5.13 through 5.19 to compute the design loads and these loads will now be factored design loads.

The factored design compressive load will be governed by the reactions computed in Example 5.1 and Equations 5.13 through 5.19 and will be the greatest of:

$$P_u = 1.4(5W_D + P_{D1}) = 1.4(5 \times 1.5 + 3) = 14.7 \text{ k}$$

$$P_u = 1.2(5W_D + P_{D1}) + 1.6(5W_l) = 1.2(5 \times 1.5 + 3) + 1.6(5 \times 0.8) = 19.0 \text{ k}$$

$$P_u = 1.2(5W_D + P_{D1}) + \max(5W_L \text{ or } 0.8P_W)$$

$$= 1.2(5 \times 1.5 + 3) + (5 \times 0.8) = 16.6 \text{ k}$$

$$P_u = 1.2(5W_D + P_{D1}) + 5W_L = 1.2(5 \times 1.5 + 3) + (5 \times 0.8) = 16.6 \text{ k}$$

$$P_u = 1.2(5W_D + P_{D1}) + 5W_L = 1.2(5 \times 1.5 + 3) + (5 \times 0.8) = 16.6 \text{ k}$$

$$P_u = 0.9(5W_D + P_{D1}) = 0.9(5 \times 1.5 + 3) = 9.45 \text{ k}$$

$$P_u = 0.9(5W_D + P_{D1}) = 0.9(5 \times 1.5 + 3) = 9.45 \text{ k}$$

Equation 5.14 controls and the factored design compressive load, P_u, is 19.0 k.

The design shear load for this example, V, will be equal to the wind load, P_W, as shown in Example 5.1. In this case only Equations 5.15, 5.16, and 5.18 apply for computing the factored shear load.

$$V_u = (0.5P_W) = 0.5 \times 0.5 = 0.25 \text{ k}$$

$$V_u = P_W = 0.5 \text{ k}$$

$$V_u = P_W = 0.5 \text{ k}$$

Equations 5.16 and 5.18 control and the factored design shear load, V_u, is 0.5 k.

The design moment for this example, M, has dead, live, and wind components as shown in Example 5.1. If we check Equations 5.13 through 5.19, we will find that Equation 5.14 governs.

$$M_u = 1.2(2.5(5W_D)) + 1.6(2.5(5W_L))$$

$$= 1.2(2.5(5 \times 1.5)) + 1.6(2.5(5 \times 0.8)) = 38.5 \text{ k-ft}$$

So the design foundation loads according to ASD method are:

$$\boldsymbol{P_u = 19.0 \text{ k}}$$

$$\boldsymbol{V_u = 0.5 \text{ k}}$$

$$\boldsymbol{M_u = 38.5 \text{ k-ft}}$$

5.3 SERVICEABILITY LIMIT STATES

As discussed in Section 5.1, in addition to meeting the ultimate limit state requirements, structures must also meet their functional requirements or *serviceability limit states*. There are many different serviceability limit states, but they can generally be categorized into two groups, those associated with deformations and those associated with durability.

Deformation-Related Serviceability Limits

Deformation-related serviceability limits address structural movements that do not threaten or approach collapse, but may still interfere with the use the structure. Common deformation-related serviceability limits for foundations include:

- **Settlement**—Nearly all foundations experience some downward movement as a result of the applied loads. This movement is called *settlement*. Keeping settlements within tolerable limits is usually the most important foundation serviceability requirement.
- **Heave**—Sometimes foundations move upward instead of downward. We call this upward movement *heave*. The most common source of heave is the swelling of expansive soils.
- **Tilt**—When settlement or heave occurs only on one side of the structure, it may begin to *tilt*. The Leaning Tower of Pisa is an extreme example of tilt.
- **Lateral movement**—Foundations subjected to lateral loads (shear or moment) deform horizontally. This *lateral movement* also must remain within acceptable limits to avoid structural distress.
- **Vibration**—Some foundations, such as those supporting certain kinds of heavy machinery, are subjected to strong vibrations. Such foundations need to accommodate these vibrations without experiencing resonance or other problems.

Failure to satisfy these requirements does not generally result in catastrophic failure or loss of lives, but it can cause increased maintenance costs, aesthetic problems, diminished usefulness of the structure, and other similar effects.

Settlement

The vertical downward load is usually the greatest load acting on foundations, and the resulting vertical downward movement is usually the largest and most important serviceability limit states to be considered. We call this vertical downward movement as *settlement*. Sometimes settlement also occurs as a result of other causes unrelated to the presence of the foundation, such as consolidation due to the placement of a fill.

Although foundations with zero settlement would be ideal, this is not an attainable goal. Stress and strain always go together, so the imposition of loads from the foundation always causes some settlement in the underlying soils. Therefore, the question that faces the foundation engineer is not *if* the foundation will settle, but rather defining the *amount* of settlement that would be tolerable and designing the foundation to accommodate this requirement. This design process is analogous to that for beams where the deflection must not exceed some maximum tolerable value.

Structural Response to Settlement

Structures can settle in many different ways, as shown in Figure 5.4. Sometimes the settlement is uniform, so the entire structure moves down as a unit, as shown in Figure 5.4a. In

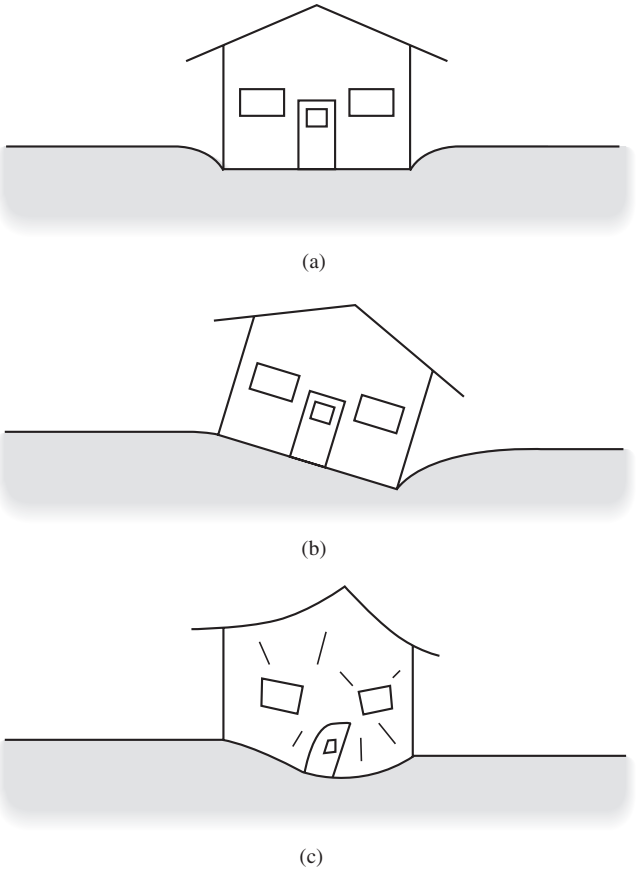

Figure 5.4 Modes of settlement: (a) uniform; (b) tilting with no distortion; (c) distortion.

this case, there is no damage to the structure itself, but there may be problems with its interface with the adjacent ground or with other structures. Another possibility is settlement that varies linearly across the structure as shown in Figure 5.4b. This causes the structure to tilt. Finally, Figure 5.4c shows a structure with irregular settlements. This mode distorts the structure and typically is the greatest source of problems.

The response of structures to foundation settlement is very complex, and a complete analysis would require consideration of many factors. Such analyses would be very time consuming, and are thus not practical for the vast majority of structures. Therefore, we simplify the problem by describing settlement using only two parameters: total settlement and differential settlement (Skempton and MacDonald, 1956; Polshin and Tokar, 1957; Burland and Wroth, 1974; Grant et al., 1974; Wahls, 1981; Wahls, 1994; Frank, 1994).

Total Settlement

The *total settlement*, δ, is the change in foundation elevation from the original unloaded position to the final loaded position, as shown in Figure 5.5.

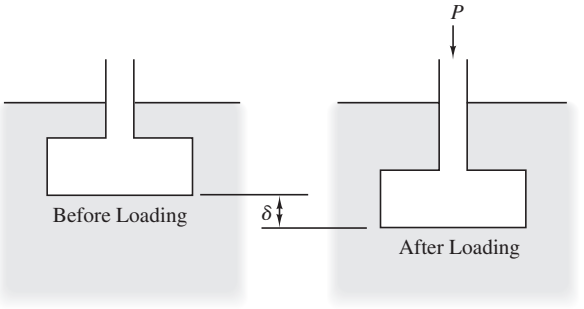

Figure 5.5 Total settlement in a spread footing foundation.

Structures that experience excessive total settlements might have some of the following problems:

- **Connections with existing structures**—Sometimes buildings must join existing structures. In such cases, the floors in the new building must be at the same elevation as those in the existing building. However, if the new building settles excessively, the floors will no longer match, causing serious serviceability problems.
- **Utility lines**—Buildings, tanks, and many other kinds of structures are connected to various utilities, many of which are located underground. If the structure settles excessively, the utility connections can be sheared or distorted. This is especially troublesome with gravity flow lines, such as sewers.
- **Surface drainage**—The ground floor of buildings must be at a slightly higher elevation than the surrounding ground so rainwater does not enter. However, settlement might destroy these drainage patterns and cause rainwater to enter the structure.
- **Access**—Vehicles and pedestrians may need to access the structure, and excessive settlement might impede them.
- **Aesthetics**—Excessive settlement may cause aesthetic problems long before there is any threat to structural integrity or serviceability.

Some structures have sustained amazingly large total settlements, yet remain in service. For example, many buildings have had little or no ill effects even after settling as much as 250 mm (10 in). Others have experienced some distress, but continue to be used following even greater settlements. Some of the most dramatic examples are located in Mexico City, where some buildings have settled more than 2 m (7 ft) and are still in use. Some bridges, tanks, and other structures also might tolerate very large settlements. However, these are extreme examples. Normally engineers have much stricter performance requirements.

Table 5.1 presents typical design values for the allowable total settlement, δ_a. These values already include a factor of safety, and thus may be compared directly to the predicted settlement. The design meets total settlement requirements if the following condition is met:

$$\delta \leq \delta_a \tag{5.20}$$

TABLE 5.1 TYPICAL ALLOWABLE TOTAL SETTLEMENTS FOR FOUNDATION DESIGN

	Typical Allowable Total Settlement, δ_a	
Type of Structure	(mm)	(in)
Office buildings	12–50 (25 is the most common value)	0.5–5.0 (1.0 is the most common value)
Heavy industrial buildings	25–75	1.0–3.0
Bridges	50	2.0

where

δ = total settlement of foundation
δ_a = allowable total settlement

Methods of computing δ are covered later in this book.

When using Table 5.1, keep the following caveats in mind:

1. Customary engineering practice in this regard varies significantly between regions, which is part of the reason for the wide ranges of values in this table. For example, an office building in one city may need to be designed for a total settlement of 12 mm (0.5 in), while the same building in another state might be designed using 25 mm (1.0 in). It is important to be aware of local practices, since engineers are normally expected to conform to them. However, it also is important to recognize that local practices in some areas are overly conservative and produce foundations that are more expensive than necessary.
2. Foundations with large total settlements also tend to have large differential settlements. Therefore, limits on allowable differential settlement often indirectly place limits on total settlement that are stricter than those listed in Table 5.1. Chapter 8 discusses this aspect in more detail.

If the predicted settlement, δ, is greater than δ_a, we could consider any or all of the following measures:

- **Adjust the foundation design**—Adjustments in the foundation design often will solve problems with excessive settlement. For example, the settlement of spread footing foundations can be reduced by increasing their width.
- **Use a more elaborate foundation**—For example, we might use piles instead of spread footings, thus reducing the settlement.

- **Improve the properties of the soil**—For example, removing compressible soils near the surface and replacing them with engineered fill. This and other available techniques are discussed in Chapter 26.
- **Redesign the structure so it is more tolerant of settlements**—For example, flexible joints could be installed on pipes as shown in Figure 5.6.

Differential Settlement

Engineers normally design the foundations for a structure such that all of them have the same computed total settlement. Thus, in theory, the structure will settle uniformly. Unfortunately, the actual performance of the foundations will usually not be exactly as predicted, with some of them settling more than expected and others less. This discrepancy between predicted behavior and actual behavior has many causes, including the following:

- **The soil profile may not be uniform across the site**—This is nearly always true, no matter how uniform it might appear to be.
- **The ratio between the actual load and the design load may be different for each column**—Thus, the column with the lower ratio will settle less than that with the higher ratio.
- **The ratio of dead load to live load may be different for each column**—Settlement computations are usually based on dead-plus-live a portion of the load, and the foundations are sized accordingly. However, in many structures, much of the live load will

Figure 5.6 This flexible, extendible pipe coupler has ball joints at each end and can telescope to allow lengthening or shortening. These couplers can be installed where utility lines enter structures, thus accommodating differential settlement, lateral movement, extension, and compression. For example, a 203 mm (8 in) diameter connector can accommodate differential settlements of up to 510 mm (20 in) (Courtesy of Romac Industries, Inc.).

rarely, if ever, occur, so foundations that have a large ratio of design live load to design dead load will probably settle less than those carrying predominantly dead loads.

- **The as-built foundation dimensions may differ from the plan dimensions**—This will cause the actual settlements to be correspondingly different.

The *differential settlement*, δ_D, is the difference in total settlement between two foundations or between two points on a single foundation. Differential settlements are generally more troublesome than total settlements because they distort the structure, as shown in Figure 5.4c. This causes cracking in walls and other members, jamming in doors and windows, poor aesthetics, and other problems. If allowed to progress to an extreme, differential settlements could threaten the integrity of the structure. Figures 5.7 and 5.8 show examples of structures that have suffered excessive differential settlement.

Therefore, we define a maximum *allowable differential settlement*, δ_{Da}, and design the foundations so that:

$$\delta_D \leq \delta_{Da} \tag{5.21}$$

In buildings, δ_{Da} depends on the potential for jamming in doors and windows, excessive cracking in walls and other structural elements, aesthetic concerns, and other similar issues. The physical processes that cause these serviceability problems are very complex, and depend on many factors, including the type and size of the structure, the

Figure 5.7 This wood-frame house was built on an improperly compacted fill, and thus experienced excessive differential settlements. The resulting distortions produce drywall cracks up to 6 in (15 mm) wide, as shown in this photograph, along with additional cracks in the exterior walls and floor slab.

Figure 5.8 This old brick building has experienced excessive differential settlement, as evidenced by the diagonal cracks in the exterior wall.

properties of the building materials and the subsurface soils, and the rate and uniformity of the settlement (Wahls, 1994). These processes are much too complex to model using rational structural analyses, so engineers depend on empirical methods to develop design values of δ_{Da} These methods are based on measurements of the actual differential settlements in real buildings and assessments of their performance.

Comprehensive studies of differential settlements in buildings include Skempton and MacDonald (1956), Polshin and Tokar (1957), and Grant et al. (1974). Skempton and MacDonald's work is based on the observed performance of ninety-eight buildings of various types, forty of which had evidence of damage due to excessive settlements. Polshin and Tokar reported the results of 25 years of observing the performance of structures in the Soviet Union and reflected Soviet building codes. The study by Grant et al. encompassed data from ninety-five buildings, fifty-six of which had damage.

Table 5.2 presents a synthesis of these studies, expressed in terms of the allowable angular distortion, θ_a. These values already include a factor of safety of at least 1.5, which is why they are called "allowable." We use them to compute δ_{Da} as follows:

$$\delta_{Da} = \theta_a S \tag{5.22}$$

where

δ_{Da} = allowable differential settlement
θ_a = allowable angular distortion (from Table 5.2)
S = column spacing (horizontal distance between columns)

TABLE 5.2 ALLOWABLE ANGULAR DISTORTION, θ_a (compiled from Wahls, 1994; AASHTO, 2012; and other sources)

Type of Structure	θ_a
Steel tanks	1/25
Bridges with simply-supported spans	1/125
Bridges with continuous spans	1/250
Buildings which are very tolerant of differential settlements, such as industrial buildings with corrugated steel siding and no sensitive interior finishes	1/250
Typical commercial and residential buildings	1/500
Overhead traveling crane rails	1/500
Buildings which are especially intolerant of differential settlement, such as those with sensitive wall or floor finishes	1/1,000
Machinery[a]	1/1,500
Buildings with unreinforced masonry load-bearing walls	
Length/height ≤ 3	1/2,500
Length/height ≥ 5	1/1,250

[a] Large machines, such as turbines or large punch presses, often have their own foundation, separate from that of the building that houses them. It often is appropriate to discuss allowable differential settlement issues with the machine manufacturer.

Empirical data also suggests that typical buildings have architectural damage at $\theta \approx 1/300$ and structural damage at $\theta \approx 1/150$ (Stephenson, 1995). However, both these values and those in Table 5.2 especially depend on the type of exterior cladding, because cracks in the cladding can allow water to enter the structure and damage the interior. For example, corrugated metal siding tolerates much more differential settlement than stucco. In addition, it may be wise to use lower δ_a and δ_{Da} values for warehouses, tanks, and other structures in which the live load represents a large portion of the total load and does not occur until after the structure is complete.

Be sure to consider local practice and precedent when developing design values of δ_{Da}. Engineers in some areas routinely design structures to accommodate relatively large settlements when owners are willing to accept some long-term maintenance costs (i.e., repairing minor cracking, rebuilding entranceways, etc.) in exchange for reduced construction costs. However, in other areas, even small settlements induce lawsuits, so foundations are designed to meet stricter standards.

Methods for computing δ_D are discussed later in this book within the chapters related to the type of foundation being considered.

Example 5.3

A steel-frame office building has a column spacing of 20 ft. It is to be supported on spread footings founded on a clayey soil. What are the allowable total and differential settlements?

Solution

Per Table 5.1, use $\delta_a = 1.0$ in.
Per Table 5.2, $\theta_a = 1/500$.

$$\begin{aligned}\delta_{Da} &= \theta_a S \\ &= (1/500)(20 \text{ ft}) \\ \delta_{Da} &= 0.04 \text{ ft} = \mathbf{0.5 \text{ in}}\end{aligned}$$

Rate of Settlement

It also is important to consider the rate of settlement and how it compares with the rate of construction. Foundations in sands settle about as rapidly as the loads are applied, whereas those in saturated clays move much more slowly.

In some structures, much of the load is applied to the foundation before the settlement's sensitive elements are in place. For example, settlements of bridge piers that occur before the deck is placed are far less important than those that occur after. Buildings may not be sensitive to differential settlements until after sensitive finishes, doors, and other architectural items are in place, yet if the foundation is in sand, most of the settlement may have already occurred by then.

However, other structures generate a large portion of their loads after they are completed. For example, the greatest load on a water storage tank is its contents.

Heave

Sometimes foundations move upward instead of downward. This kind of movement is called *heave*. It may be due to applied upward loads, but more often it is the result of external forces, especially those from expansive soils. The design criteria for heave are the same as those for settlement. However, if some foundations are heaving while others are settling, then the differential is the sum of the two.

Tilt

Excessive tilt is often a concern in tall, rigid structures, such as chimneys, silos, and water towers. To preserve aesthetics, the tilt, ω, from the vertical should be no more than 1/500 (7 min of arc). Greater tilts would be noticeable, especially in taller structures and those that are near other structures. In some cases, stricter limits on tilt are appropriate, especially for exceptionally tall structures. For comparison, the Leaning Tower of Pisa has a tilt of about 1/10.

Lateral Movement

Foundations subjected to lateral loads have corresponding lateral movements. These movements also have tolerable limits. For bridge foundations, Paikowsky et al. (2004) recommended maximum lateral movements of 7 to 50 mm (0.25–2.0 in). Buildings and

similar structures can generally tolerate up to 7 to 20 mm (0.25–0.75 in) of lateral movement before distress occurs. Specific lateral serviceability limits are project specific and must be determined by the structural engineer.

Vibration

Foundations that support large machinery are sometimes subjected to substantial vibratory loads. Such foundations must be designed to accommodate these vibratory loads without introducing problems, such as resonance. Designing for vibration is beyond the scope of this book. Readers interested in this topic are referred to Richart et al. (1970).

Design Loads for Serviceability Analyses

Serviceability limit states must be evaluated when the structure is functioning under its normal operating conditions or *service conditions*. Therefore, the loads used to analyze serviceability limit states will be very different from those used to analyze ultimate limit states. In ultimate limit state analysis we use high estimates of potential loads, but in serviceability limit state analysis we use typically expected loads. Serviceability loads must also be matched to the serviceability limit being analyzed. For example, the loads used to determine foundation deformation caused by vibrating machinery would be totally different from those used to determine long-term foundation settlement. Additionally, the magnitude of a certain serviceability limit will be a function of the use and expected performance of each structure. This is apparent in the allowable settlement and angular distortion limits listed in Tables 5.1 and 5.2. These characteristics of serviceability limits make the design loads particularly difficult to establish.

Another characteristic of serviceability design loads is that building codes provide only limited guidance. There are several reasons for this. The primary reason is that the purpose of most building codes is to protect public safety and property, not to ensure the economic viability of structures. A second reason for limited code guidance is that, by their very nature, serviceability limit states are dependent upon the expected functions of a particular structure. The guidance in ASCE 7 is typical. This document contains 388 pages, but devotes only a single page appendix to serviceability loads. The opening paragraph of this appendix states [ASCE 7, Appendix C]:

> This Appendix is not a mandatory part of the standard, but provides guidance for design for serviceability in order to maintain the function of a building and the comfort of its occupants during normal usage. Serviceability limits … shall be chosen with due regard to the intended function of the structure.

In general, codes do not provide load combinations or load factors that must be used in determining design serviceability loads for foundations. The ASD or LRFD methods apply only to ultimate limit states. The design service loads must be determined through good communications among the structural engineer, geotechnical engineer, and structure owner; and through good engineering judgment. The AASTHO bridge design manual (AASHTO,

2012) is an exception in this respect. It provides specific guidance for determining serviceability loads for bridge structures.

Settlement and differential settlement are typically the most important serviceability limit states in foundation engineering, and often control the design, so it is important to establish a reasonable design load. For settlement analyses, the engineer should use serviceability loads that consider all of the loads that are likely to persist over a long duration [ASCE 7, C.2]. This is sometimes called the *sustained load*, and includes all the dead load and some portion of the live load. The percentage of the live loads that should be used for settlement analyses will depend on the type and use of the structure. For example, ASCE 7 [Table 4.1] specifies design live loads for categories such as offices, corridors, and library stack rooms (where books are shelved). It is highly unlikely that live loads specified for offices and corridors will persist throughout an entire building for a duration long enough to cause settlement, and only a small portion of this load should be used when computing settlement. However, the live load for library stack rooms is significantly more likely to exist throughout a library and to persist for long durations. In this case it may be appropriate to use all or nearly all of this live load in a settlement analysis. Similarly, live loads for storage tanks and silos are likely to be persistent and should be considered in settlement computations. Short duration loads, such as wind loads and earthquake loads, are generally not considered in settlement analyses. In any case it is not appropriate to factor either the live or dead loads in settlement analyses, because the engineer is attempting to estimate the actual working load, not an extreme event.

It is common for engineers to use the total unfactored dead and live load ($D + L$) to compute settlement. Based on the previous discussion, this is almost always a conservative approach and will often lead to overestimated settlements. For routine design of light facilities, the overestimate may be relatively small and this can be an acceptable approach. However, for large structures, overly conservative settlement estimates can force a change to a more expensive foundation system. For large or high value structures, the engineer should develop project-specific service design loads. This may require special analyses of dead and live loads for the structure or inspections and evaluation of the performance of similar facilities. Establishing accurate serviceability loads requires effective communication between the geotechnical and structural engineer.

Durability-Related Serviceability Limits

Soil can be a very hostile environment to engineering materials. Whether they are made of concrete, steel, or wood, structural foundations may be susceptible to chemical and/or biological attack that can adversely affect their integrity. *Durability-related serviceability limits* are intended to ensure that foundations can resist the various physical, chemical, and biological processes that cause deterioration, so that the foundation will continue to provide adequate performance over the life of the structure. Durability limit states are often related to corrosion or other time dependent weakening of foundations. These limit states are highly dependent upon the environment in which the foundations exist. For example, durability of foundations for waterfront structures, such as docks and piers, can

be particularly important because of the corrosive nature of the salt water environment where these foundations are placed.

Corrosion of Steel

Under certain conditions, steel can be the object of extensive corrosion. This can be easily monitored when the steel is above ground, and routine maintenance, such as painting, will usually keep corrosion under control. However, it is impossible to inspect underground steel visually, so it is appropriate to be concerned about its potential for corrosion and long-term integrity.

Owners of underground steel pipelines are especially conscious of corrosion problems. They often engage in extensive corrosion surveys and include appropriate preventive measures in their designs. These procedures are well established and effective, but should they also be used for steel foundations such as H-piles or steel pipe piles?

For corrosion assessment, steel foundations can be divided into two categories: those in marine environments and those in land environments. Both are shown in Figure 5.9.

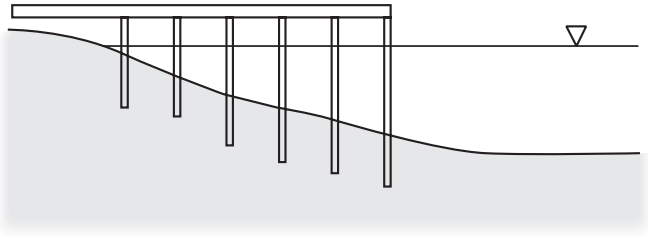

(a)

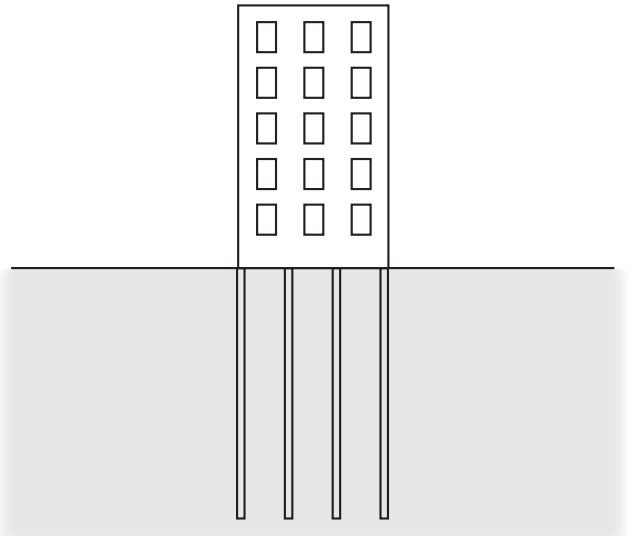

(b)

Figure 5.9 (a) Marine environments include piers, docks, drilling platforms, and other similar structures where a portion of the foundation is exposed to open water. (b) Land environments include buildings and other structures that are built directly on the ground and the entire foundation is buried.

Steel foundations in marine environments have a significant potential for corrosion, especially those exposed to salt water. Studies of waterfront structures have found that steel is lost at a rate of 0.075 to 0.175 mm/yr (Whitaker, 1976). This corrosion occurs most rapidly in the tidal and splash zones (Dismuke et al., 1981) and can also be very extensive immediately above the sea floor; then it becomes almost negligible at depths more than about 0.5 m (2 ft) below the sea floor. Such structures may also be prone to abrasion from moving sand, ships, floating debris, and other sources. It is common to protect such foundations with coatings or jackets, at least through the water and splash zones.

However, the situation in land environments is quite different. Based on extensive studies, Romanoff (1962, 1970) observed that no structural failures have been attributed to the corrosion of steel piles in land environments. One likely reason for this excellent performance record is that piles, unlike pipelines, can tolerate extensive corrosion, even to the point of occasionally penetrating through the pile, and remain serviceable.

Romanoff also observed that piles founded in natural soils (as opposed to fills) experienced little or no corrosion, even when the soil could be identified as potentially corrosive. The explanation for this behavior seems to be that natural soils contain very little free oxygen, an essential ingredient for the corrosion process.

However, fills do contain sufficient free oxygen and, under certain circumstances, can be very corrosive environments. Therefore, concern over corrosion of steel piles in land environments can normally be confined to sites where the pile penetrates through fill. Some fills have very little potential for corrosion, whereas others could corrode steel at rates of up to 0.08 mm/yr (Tomlinson, 1987), which means that a typical H-pile section could lose half of its thickness in about 50 years.

Schiff (1982) indicated that corrosion would be most likely in the following soil conditions:

- High moisture content
- Poorly aerated
- Fine grained
- Black or gray color
- Low electrical resistivity
- Low or negative redox potential
- Organic material present
- High chemical content
- Highly acidic
- Sulfides present
- Anaerobic microorganisms present

Areas where the elevation of the groundwater table fluctuates, such as tidal zones, are especially difficult because this scenario continually introduces both water and oxygen to the pile. Contaminated soils, such as sanitary landfills and shorelines near old sewer outfalls, are also more likely to have problems.

One of the most likely places for corrosion on land piles is immediately below a concrete pile cap. Local electrical currents can develop because of the change in materials, with the concrete acting as a cathode and the soil as an anode. Unfortunately, this is also the most critical part of the pile because the stresses are greatest there.

If the foundation engineer suspects that corrosion may be a problem, it is appropriate to retain the services of a corrosion engineer. Detailed assessments of corrosion and the development of preventive designs are beyond the expertise of most foundation engineers.

The corrosion engineer will typically conduct various tests to quantify the corrosion potential of the soil and consider the design life of the foundation to determine whether any preventive measures are necessary. Such measures could include the following:

- Use a different construction material (i.e., concrete, wood).
- Increase the thickness of steel sections by an amount equal to the anticipated deterioration.
- Cover the steel with a protective coating (such as coal tar epoxy) to protect it from the soil. This method is commonly used with underground tanks and pipes, and has also been successfully used with pile foundations. However, consider the possibility that some of the coating may be removed by abrasion when the pile is driven into the ground, especially when sands or gravels are present. Coatings can also be an effective means of combatting corrosion near pile caps, as discussed earlier. In this case, the coating is applied to the portion of the steel that will be encased in the concrete, thus providing the electrical insulation needed to stop or significantly slow the corrosion process.
- Provide a *cathodic protection system*. Such systems consist of applying a DC electrical potential between the foundation (the cathode) and a buried sacrificial metal (the anode). This system causes the corrosion to be concentrated at the anode and protects the cathode (see Figure 5.10). Rectifiers connected to a continuous power source provide the electricity. These systems consume only nominal amounts of electricity. In some cases, it is possible to install a self-energizing system that generates its own current.

Reinforced steel in concrete foundations is also susceptible to corrosion in adverse environments. The primary defense against corrosion of reinforcing steel is the concrete cover of the reinforcing bars. ACI 318 (ACI, 2011) requires a minimum cover of 70 mm (3 in) specifically to address corrosion potential. Additional cover can be used to increase the durability of reinforcement. In extremely aggressive environments, epoxy-coated rebar is an option.

Sulfate Attack on Concrete

Buried concrete is usually very resistant to corrosion and will remain intact for many years. However, serious degradation can occur in concrete subjected to soils or groundwater that contains high concentrations of sulfates (SO_4). These sulfates can react with the cement to form calcium sulfoaluminate (ettringite) crystals. As these crystals grow and expand, the

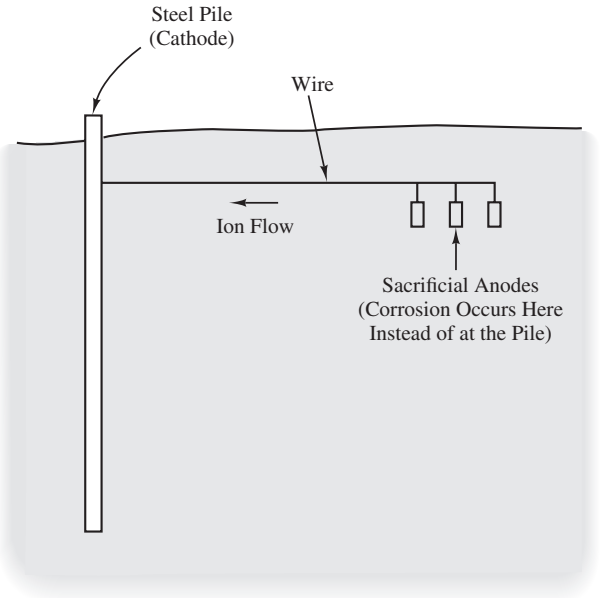

Figure 5.10 Use of a cathodic protection system to protect steel foundations from corrosion.

concrete cracks and disintegrates. In some cases, serious degradation has occurred within 5 to 30 years of construction. Although we do not yet fully understand this process (Mehta, 1983), engineers have developed methods of avoiding these problems.

We can evaluate a soil's potential for sulfate attack by measuring the concentration of sulfates in the soil and/or in the groundwater and comparing them with soils that have had problems with sulfate attack. Soils with some or all of the following properties are most likely to have high sulfate contents:

- Wet
- Fine-grained
- Black or gray color
- High organic content
- Highly acidic or highly alkaline

Some fertilizers contain a high concentration of sulfates that may cause problems when building in areas that were formerly used for agricultural purposes. The same is true for some industrial wastes. It is often wise to consult with corrosion experts in such cases. Seawater also has a high concentration: about 2,300 ppm.

If the laboratory tests indicate that the soil or groundwater has a high sulfate content, design the buried concrete to resist attack by using one or more of the following methods:

- **Reduce the water:cement ratio**—This reduces the permeability of the concrete, thus retarding the chemical reactions. This is one of the most effective methods of resisting sulfate attack. Suggested maximum ratios are presented in Table 5.3.

TABLE 5.3 USE OF SULFATE-RESISTING CEMENTS AND LOW WATER:CEMENT RATIOS TO AVOID SULFATE ATTACK OF CONCRETE (adapted from Kosmatka and Panarese, 1988; and PCA, 1991)

Water-Soluble Sulfates in Soil (% by weight)	Sulfates in Water (ppm)	Sulfate Attack Hazard	Cement Type	Maximum Water: Cement Ratio
0.00–0.10	0–150	Negligible	–	–
0.10–0.20	150–1,500	Moderate	II	0.50
0.20–2.00	1,500–10,000	Severe	V	0.45
>2.00	>10,000	Very severe	V plus pozzolan	0.45

- **Increase the cement content**—This also reduces the permeability. Therefore, concrete that will be exposed to problematic soils should have a cement content of at least 335 kg/m^3 (6 sacks/yd^3 or 564 lb/yd^3).
- **Use sulfate-resisting cement**—Type II low-alkali and type V Portland cements are specially formulated for use in moderate and severe sulfate conditions, respectively. Pozzolan additives to a type V cement also help. Type II is easily obtained, but type V may not be readily available in some areas. Table 5.3 gives specific guidelines.
- **Coat the concrete with an asphalt emulsion**—This is an attractive alternative for retaining walls or buried concrete pipes, but not for foundations.

Decay of Timber

The most common use of wood in foundations is timber piles. The lifespan of these piles varies depending on their environment. Even untreated timber piles can have a very long life if they are continually submerged below the groundwater table. This was illustrated when a campanile in Venice fell in 1902. The submerged timber piles, which had been driven in 900 AD, were found to be in good condition and were used to support the replacement structure (Chellis, 1962). However, when located above the groundwater table, timber can be subjected to deterioration from several sources (Chellis, 1961), including:

- **Decay** caused by the growth of fungi. This process requires moisture, oxygen, and favorable temperatures. These conditions are often most prevalent in the uppermost 2 m (6 ft) of the soil. If the wood is continually very dry, then decay will be limited due to the lack of moisture.
- **Insect attack**, including termites, beetles, and marine borers.
- **Fire**, especially in marine structures.

The worst scenario is one in which the piles are subjected to repeated cycles of wetting and drying. Such conditions are likely to be found near the groundwater table

because it usually rises and sinks with the seasons and near the water surface in marine applications where splashing and tides will cause cyclic wetting and drying.

To reduce problems of decay, insect attack, and fungi growth, timber piles are usually treated before they are installed. The most common treatment consists of placing them in a pressurized tank filled with creosote or some other preserving chemical. This *pressure treatment* forces some of the creosote into the wood and forms a thick coating on the outside, leaving a product that is almost identical to many telephone poles. When the piles are fully embedded into soil, creosote-treated piles normally have a life at least as long as the design life of the structure.

Timber piles also will lose part of their strength if they are subjected to prolonged high temperatures. Therefore, they should not be used under hot structures such as blast furnaces.

5.4 CONSTRUCTABILITY REQUIREMENTS

The third category of performance requirements is *constructability*. The foundation must be designed such that a contractor can build it without having to use extraordinary methods or equipment. There are many potential designs that might be quite satisfactory from a design perspective, but difficult or impossible to build.

For example, in order to construct driven piles, the pile driver lifts the pile into the air, and then drives it into the ground, as shown in Figure 5.11. Therefore, piles can be

Figure 5.11 Pile foundations are installed using a pile driver, such as this one. The pile is lifted into the vertical section, which is called the leads, then driven into the ground with the pile hammer. Thus, the pile driver must be slightly taller than the pile to be installed.

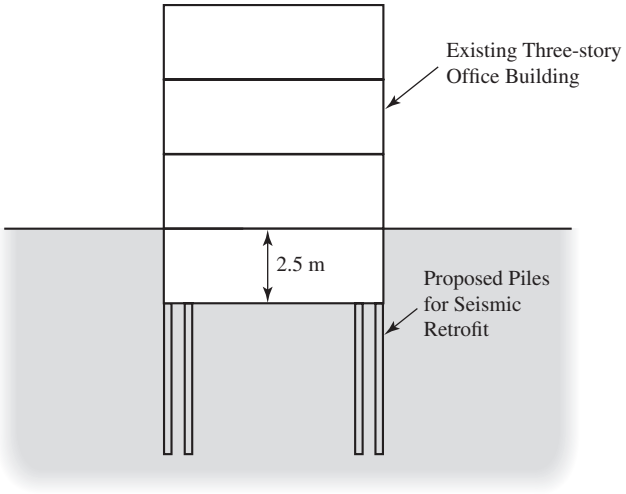

Figure 5.12 As part of a seismic retrofit project, a design engineer has called for installing 450 mm diameter, 9 m long prestressed concrete pile foundation to be installed beneath the basement of an existing building. This pile foundation design is unbuildable because the required pile-driving equipment would not fit in the basement, and because there is not enough room to set the pile upright.

installed only at locations that have sufficient headroom. Fortunately, the vast majority of construction sites have plenty of headroom.

Nevertheless, a design engineer who is not familiar with this construction procedure might ask for piles to be installed at a location with minimal headroom. For example, the pile design shown in Figure 5.12 is unbuildable because it is impossible to fit the required installation equipment into such a small space.

Karl Terzaghi expressed this concept very succinctly when he said:

Do not design on paper what you have to wish into the ground.

This is why it is important for design engineers to have at least a rudimentary understanding of construction practices.

5.5 ECONOMIC REQUIREMENTS

Foundation designs are usually more conservative than those in the superstructure. This approach is justified for the following reasons:

- Foundation designs rely on our assessments of the soil and rock conditions. These assessments always include considerable uncertainty.
- Foundations are not built with the same degree of precision as the superstructure. For example, spread footings are typically excavated with a backhoe and the sides of the excavation becomes the "formwork" for the concrete, compared to concrete members in the superstructure that are carefully formed with plywood or other materials.

- The structural materials may be damaged when they are installed. For example, cracks and splits may develop in a timber pile during hard driving.
- There is some uncertainty in the nature and distribution of the load transfer between foundations and the ground, so the stresses at any point in a foundation are not always known with as much certainty as might be the case in much of the superstructure.
- The consequences of a catastrophic failure are much greater.
- The additional weight brought on by the conservative design is of little consequence because the foundation is the lowest structural member and therefore does not affect the dead load on any other member. Additional weight in the foundation is actually beneficial in that it increases its uplift resistance.

However, gross over conservatism is not warranted. An overly conservative design can be very expensive to build, especially with large structures where the foundation is a greater portion of the total project cost. This also is a type of "failure": the failure to produce an economical design.

The nineteenth-century engineer Arthur Wellington once said that an engineer's job is that of "doing well with one dollar which any bungler can do with two." We must strive to produce designs that are both safe and cost-effective. Achieving the optimum balance between reliability (safety) and cost is part of good engineering.

Designs that minimize the required quantity of construction materials do not necessarily minimize the cost. In some cases, designs that use more materials may be easier to build, and thus have a lower overall cost. For example, spread footing foundations are usually made of low-strength concrete, even though it makes them thicker. In this case, the savings in materials and inspection costs are greater than the cost of buying more concrete.

SUMMARY

Major Points

1. The foundation engineer must determine the necessary performance requirements before designing a foundation.
2. There are two major classes of limit states:
   - Ultimate limit states: related to catastrophic failure. Foundations must consider both structural and geotechnical ultimate limit states.
   - Serviceability limit states: related to loss of functionality or value before catastrophic failure.
3. Loads are classified according to their source. These include dead loads, live loads, wind loads, earthquake loads, and several others.
4. There are two approaches to evaluating ultimate limit states. It is important to know which method is being used because the design computations must be performed accordingly.

- Allowable stress design (ASD) compares the demand generated by conservative estimates of loads, with working stress or yield capacity of structures. It uses a single factor of safety to ensure satisfactory performance.
- Load and resistance factor design (LRFD) compares demands generated by plausible events with the ultimate capacity of structures. It uses multiple load and resistance factors to ensure reliability of a structure.

5. Foundations must support various types of structural loads. These can include normal, shear, moment, and/or torsion loads. The magnitude and direction of these loads may vary during the life of the structure.
6. Serviceability requirements can be grouped into deformation-related limits (settlement, heave, tilt, lateral movement, vibration) and durability-related limits (corrosion and deterioration).
7. Serviceability loads are not generally specified by building codes. The engineer must carefully consider the type and use of a structure in order to consider the appropriate loads to use in a serviceability analysis.
8. Settlement is often the most important serviceability requirement. The response of structures to settlements is complex, so we simplify the problem by considering two types of settlement: total settlement and differential settlement. We assign maximum allowable values for each, and then design the foundations to satisfy these requirements.
9. Foundations must be buildable, so design engineers need to have at least a rudimentary understanding of construction methods and equipment.
10. Foundation designs must be economical. Although conservatism is appropriate, excessively conservative designs can be too needlessly expensive to build.

Vocabulary

Allowable angular distortion
Allowable differential settlement
Allowable stress design
Allowable total settlement
Braking load
Cathodic protection
Centrifugal load
Column spacing
Constructability requirement
Dead load
Design load
Differential settlement
Durability
Earth pressure load
Earthquake load
Economic requirement
Factored loads
Failure
Fluid load
Geotechnical ultimate limit state
Heave
Impact load
Lateral movement
Live load
Load factor
Load and resistance factor design
Moment
Normal load
Performance requirement
Resistance factor
Self-straining load
Serviceability limit state
Settlement
Shear load
Snow load
Stream flow loads

Strength requirement
Structural ultimate limit state
Sulfate attack
Tilt
Torsion
Total settlement
Ultimate strength design
Unfactored loads
Vibration
Wind load

QUESTIONS AND PRACTICE PROBLEMS

Section 5.1: Types of Failure and Limit States

5.1 The second paragraph of this chapter argues that a retail building that is damaged during an earthquake and must be demolished may not constitute a failure. Do you agree with this assessment? Defend your position.

Section 5.2: Ultimate Limit States

5.2 Why would the AASHTO separate structural dead loads from wearing surface dead loads and use different load factors for each, whereas ASCE 7 has only one category for dead loads?

5.3 A proposed column has the following design loads:

Axial load: $P_D = 200$ k, $P_L = 170$ k, $P_E = 50$ k, $P_W = 60$ k (all compression)

Shear load: $P_D = 0$, $P_L = 0$, $P_E = 40$ k, $P_W = 48$ k

Compute the design axial and shear loads for foundation design using ASD.

5.4 Repeat Problem 5.3 using LRFD with the ACI load factors.

5.5 A proposed column has the following design loads:

Axial load: $P_D = 1{,}100$ kN, $P_L = 750$kN, $P_E = 200$ kN, $P_W = 250$ kN (all compression)

Shear load: $P_D = 0$, $P_L = 0$, $P_E = 175$ k, $P_W = 220$ k

Compute the design axial and shear loads for foundation design using ASD.

5.6 Repeat Problem 5.5 using LRFD with the ACI load factors.

5.7 A certain foundation will experience a bearing capacity failure when it is subjected to a downward load of 2,200 kN. Using ASD with a factor of safety of 3, determine the maximum allowable load that will satisfy geotechnical ULS requirements.

5.8 A bridge foundation has a nominal load capacity of 1,700 kN. If the resistance factor for this foundation is 0.65, what is the ultimate factored load this foundation can carry using the LRFD method?

5.9 A steel pile foundation with a cross-sectional area of 15.5 in^2 and $f_y = 50$ k/in^2 is to carry axial compressive dead and live loads of 300 and 200 k, respectively. Using LRFD with the ASCE

load factors and a resistance factor of 0.90, determine whether this pile satisfies structural strength requirements for axial compression.

5.10 A timber pile 400 mm in diameter is subjected to the following axial compressive loads: dead = 600 kN, live = 250 kN, earthquake = 200 kN. If the allowable compressive stress in the pile using ASD methods is 8.28 MPa, is this pile adequate?

Section 5.3: Serviceability Limit States

5.11 A seven-story steel-frame office building will have columns spaced 7 m on-center and will have typical interior and exterior finishes. Determine the allowable total and differential settlements for this building.

5.12 A two-story reinforced concrete art museum is to be built using an unusual architectural design. It will include many tile murals and other sensitive wall finishes. The column spacing will vary between 5 and 8 m. Determine the allowable total and differential settlements for this building.

5.13 A 40 ft $\times$ 60 ft one-story agricultural storage building will have corrugated steel siding and no interior finish or interior columns. However, it will have two 20 ft wide roll-up doors. Determine the allowable total and differential settlement for this building.

5.14 A sandy soil has 0.03 percent sulfates. Evaluate the potential for sulfate attack of concrete exposed to this soil and recommend preventive design measures, if needed.

5.15 A certain clayey soil contains 0.30 percent sulfates. Would you anticipate a problem with concrete foundations in this soil? Are any preventive measures necessary? Explain.

5.16 A series of 50 ft long steel piles are to be driven into a natural sandy soil. The groundwater table is at a depth of 35 ft below the ground surface. Would you anticipate a problem with corrosion? What additional data could you gather to make a more informed decision?

5.17 A one-story steel warehouse building is to be built of structural steel. The roof is to be supported by steel trusses that will span the entire 70 ft width of the building and supported on columns adjacent to the exterior walls. These trusses will be placed 24 ft on-center. No interior columns will be present. The walls will be made of corrugated steel. There will not be any roll–up doors. Compute the allowable total and differential settlements.

5.18 The grandstands for a minor league baseball stadium are to be built of structural steel. The structural engineer plans to use a very wide column spacing (25 m) to provide the best spectator visibility. Compute the allowable total and differential settlements.

5.19 The owner of a 100-story building purchased a plumb bob with a very long string. He selected a day with no wind, and then gently lowered the plumb bob from his penthouse office window. When it reached the sidewalk, it was 1.0 m from the side of the building. Is this building tilting excessively? Explain.

5.20 A two-story department store identical to the one in Figure 5.13 is to be built. This structure will have reinforced masonry exterior walls. The ground floor will be slab-on-grade. The

Figure 5.13 Proposed department store for Problem 5.20.

reinforced concrete upper floor and roof will be supported on a steel-frame with columns 50 ft on-center. Determine the allowable total and differential settlements for this structure.

5.21 You are designing a pedestrian bridge to cross a busy urban street. The bridge connects an open plaza on one side of the street with a group of office buildings on the other. The estimated dead loads for the bridge deck are 350 lb/ft^2 and the code-specified live loads are 90 lb/ft^2. What serviceability load would you use to check the deflection of the bridge deck? What serviceability loads would you use to check the settlement of the bridge? Justify your answers.

This page intentionally left blank

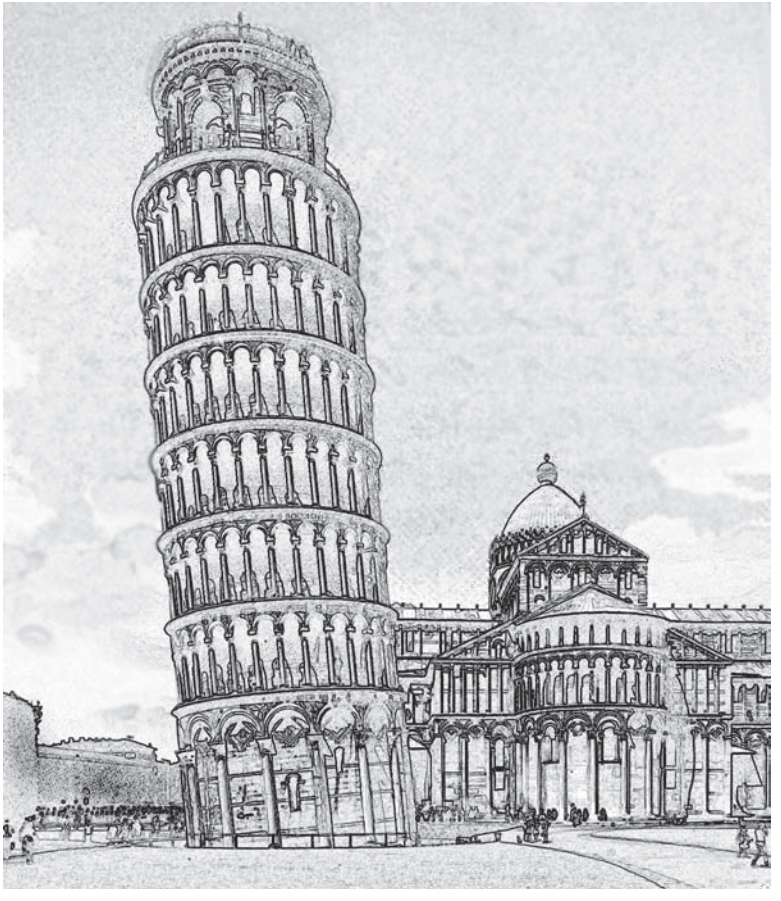

Part B

Shallow Foundation Analysis and Design

This page intentionally left blank

6

Shallow Foundations

The most important thing is to keep the most important thing the most important thing.

Anonymous

Shallow foundations, as defined in Chapter 1, include *spread footing foundations* and *mat foundations*. This chapter introduces both types of foundations. Chapters 7 to 10 discuss the various geotechnical and structural design aspects of spread footings, and Chapter 11 discusses mats.

6.1 SPREAD FOOTINGS

A spread footing (also known as a *footer* or simply a *footing*) is an enlargement at the bottom of a column or bearing wall that spreads the applied structural loads over a sufficiently large soil area. Typically, each column and each bearing wall has its own spread footing, so a typical structure may include dozens of individual footings.

Footing Types

Spread footings are by far the most common type of foundation, primarily because of their low cost and ease of construction. They are most often used in small- to medium-size structures on sites with moderate to good soil conditions, and can even be used on some large structures when they are located at sites underlain by exceptionally good soil or shallow bedrock.

Spread footings may be built in different shapes and sizes to accommodate individual needs, as shown in Figure 6.1. These include the following:

- *Square spread footings* (or simply *square footings*) have plan dimensions of $B \times B$. The depth from the ground surface to the bottom of the footing, or the depth of embedment, is D and the thickness is T. Square footings usually support a single centrally-located column.

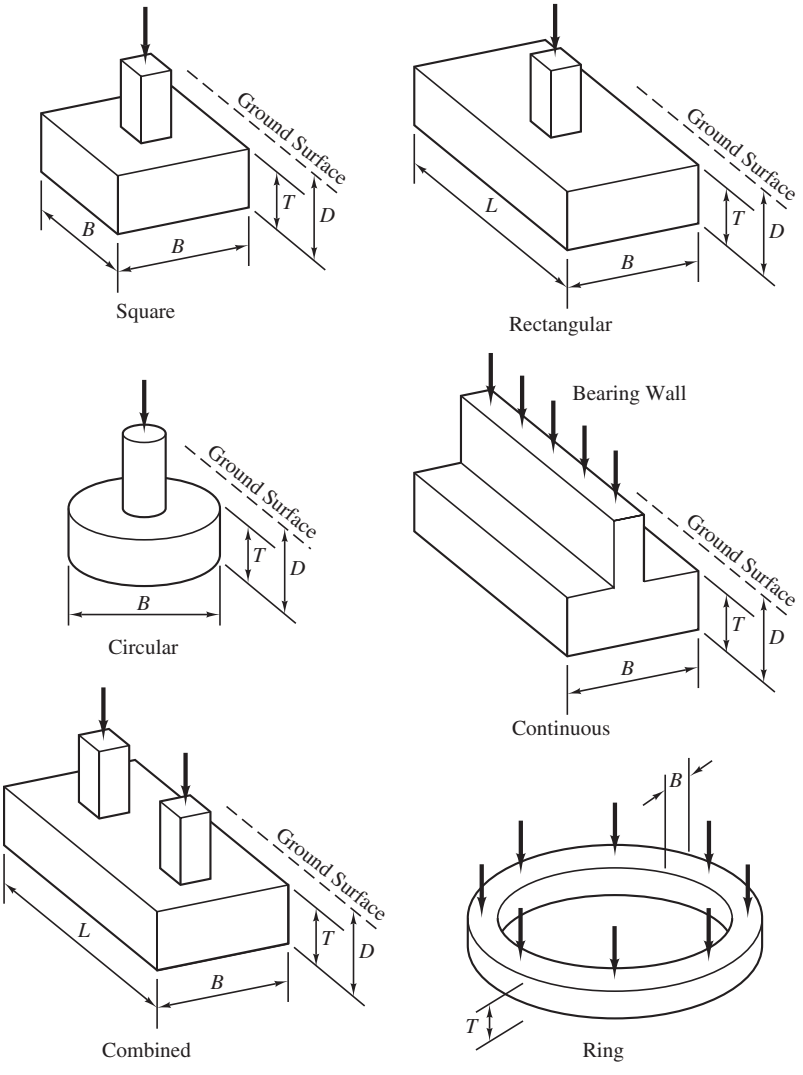

Figure 6.1 Spread footing shapes and dimensions.

- *Rectangular spread footings* have plan dimensions of $B \times L$, where L is the longest dimension. These are useful when obstructions prevent construction of a square footing with a sufficiently large base area or when large moment loads are present in one direction only.
- *Circular spread footings* are round in plan view. Smaller circular footings are constructed by drilling with an auger. These are frequently used as foundations for light standards, flagpoles, and power transmission lines. If these foundations extend to a large depth (i.e., D/B greater than about 3), they may behave more like a deep foundation (see Chapter 12). From a geotechnical perspective, circular tanks also act as circular footings.
- *Continuous spread footings* (also known as *wall footings* or *strip footings*) are used to support bearing walls.
- *Combined footings* are those that support more than one column. These are useful when columns are located too close together for each to have its own footing.
- *Ring spread footings* are continuous footings that have been wrapped into a circle. This type of footing is commonly used to support the walls of above-ground circular storage tanks. However, the contents of these tanks are spread evenly across the total base area, and this weight is probably greater than that of the tank itself. Therefore, the geotechnical analyses of tanks usually treat them as circular foundations with diameters equal to the diameter of the tank.

Sometimes it is necessary to build spread footings very close to a property line, another structure, or some other place where no construction may occur beyond one or more of the exterior walls. This circumstance is shown in Figure 6.2. Because such a footing cannot be centered beneath the column, the load is eccentric. This can cause the footing to rotate and thus produce undesirable moments and displacements in the column.

One solution to this problem is to use a *strap footing* (also known as a *cantilever footing*), which consists of an eccentrically loaded footing under the exterior column connected to the first interior column using a *grade beam*. This arrangement, which is similar to a combined footing, provides the necessary resisting moment in the exterior footing to counter the eccentric load. Sometimes we use grade beams to connect all of the spread footings in a structure to provide a more rigid foundation system.

Materials

Before the mid-nineteenth-century, almost all spread footings were made of masonry, as shown in Figure 6.3. *Dimension-stone footings* were built of stones cut and dressed to specific sizes and fit together with minimal gaps, while *rubble-stone footings* were built from random size material joined with mortar (Peck et al., 1974). These footings had very little tensile strength, so builders had to use large height-to-width ratios to keep the flexural stresses tolerably small and thus avoid tensile failures.

Although masonry footings were satisfactory for small structures, they became large and heavy when used in heavier structures, often encroaching into the basement as shown in Figure 6.4. For example, the masonry footings beneath the nine-story Home

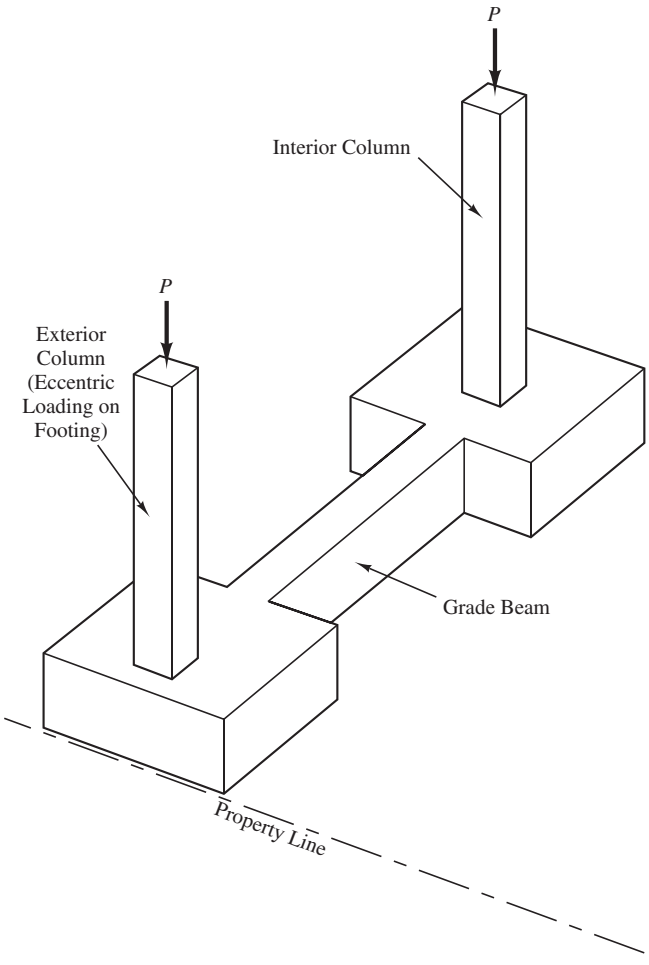

Figure 6.2 Use of a strap footing with a grade beam to support exterior columns when construction cannot extend beyond the property line.

Insurance Building in Chicago (built in 1885) had a combined weight equal to that of one of the stories (Peck, 1948). As larger structures became more common, it was necessary to develop footings that were shorter and lighter, yet still had the same base dimensions. This change required structural materials that could sustain flexural stresses.

The *steel grillage footings* used in the ten-story Montauk Block Building in Chicago in 1882, may have been the first spread footings designed to resist flexure. They included several layers of railroad tracks, as shown in Figure 6.5. The flexural strength of the steel permitted construction of a short and lightweight footing. Steel grillage footings, modified to use I-beams instead of railroad tracks, soon became the dominant design. They prevailed until the advent of reinforced concrete in the early twentieth century.

Figure 6.6 shows a typical reinforced concrete footing. These are very strong, economical, durable, and easy to build. Reinforced concrete footings are much thinner than the old masonry footings, so they do not require large excavations and do not intrude into basements. Thus, nearly all spread footings are now made of reinforced concrete.

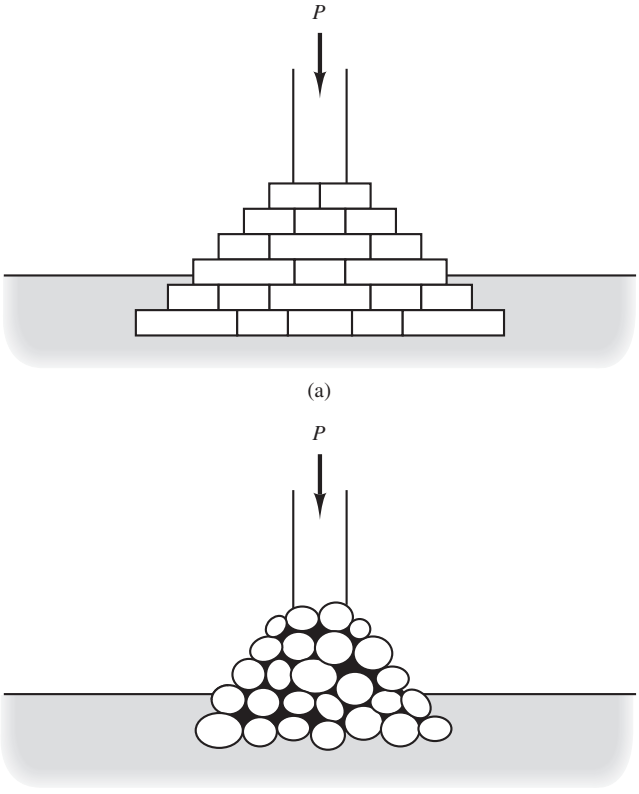

Figure 6.3 (a) Dimension-stone footing; and (b) Rubble-stone footing.

Figure 6.4 Dimensional stone foundation for Chicago Auditorium building built between 1887–89. Note both height and width of the foundation and the amount of space they occupy. (Library of Congress, Prints & Photographs Division, HABS, Reproduction number HABS ILL, 16-CHIG, 39-8.)

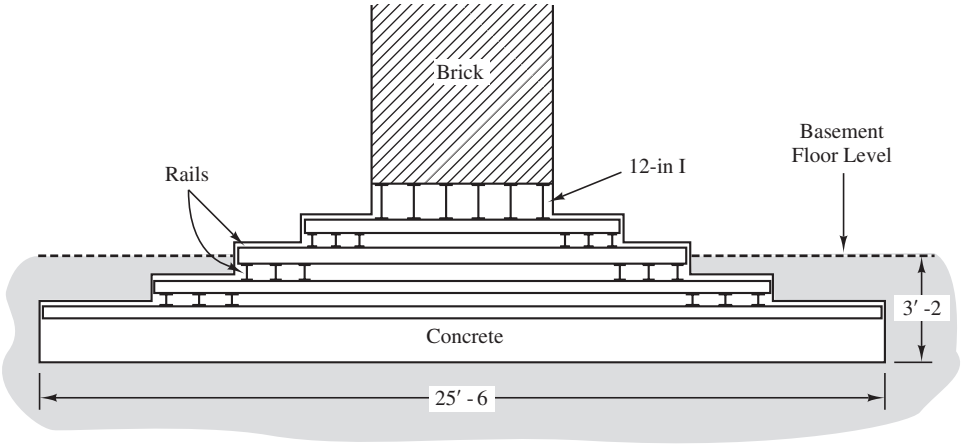

Figure 6.5 Steel grillage footing made from railroad tracks, Montauk Block Building, Chicago, 1882. The concrete that surrounded the steel was for corrosion protection only (Peck, 1948).

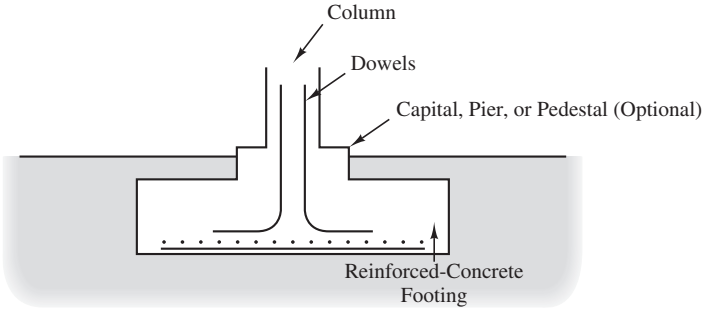

Figure 6.6 Reinforced-concrete spread footing.

Figure 6.7 A backhoe making an excavation for a spread footing.

Construction Methods

Contractors usually use a *backhoe* to excavate spread footings, as shown in Figure 6.7. Typically, some hand work is also necessary to produce a clean excavation. Once the excavation is open, it is important to check the exposed soils to verify that they are comparable to those used in the design. Inspectors often check the firmness of these soils using a 9 mm (3/8 in) diameter steel probe. If the soil conditions are not as anticipated, especially if they are too soft, it may be necessary to revise the design accordingly.

Most soils have sufficient strength to stand vertically until it is time to place the concrete. This method of placing the concrete directly against the soil is known as pouring a *neat footing*, as shown in Figure 6.8a. Sometimes shallow wood forms are placed above the excavation, as shown in Figure 6.8b, so the top of the footing is at the proper

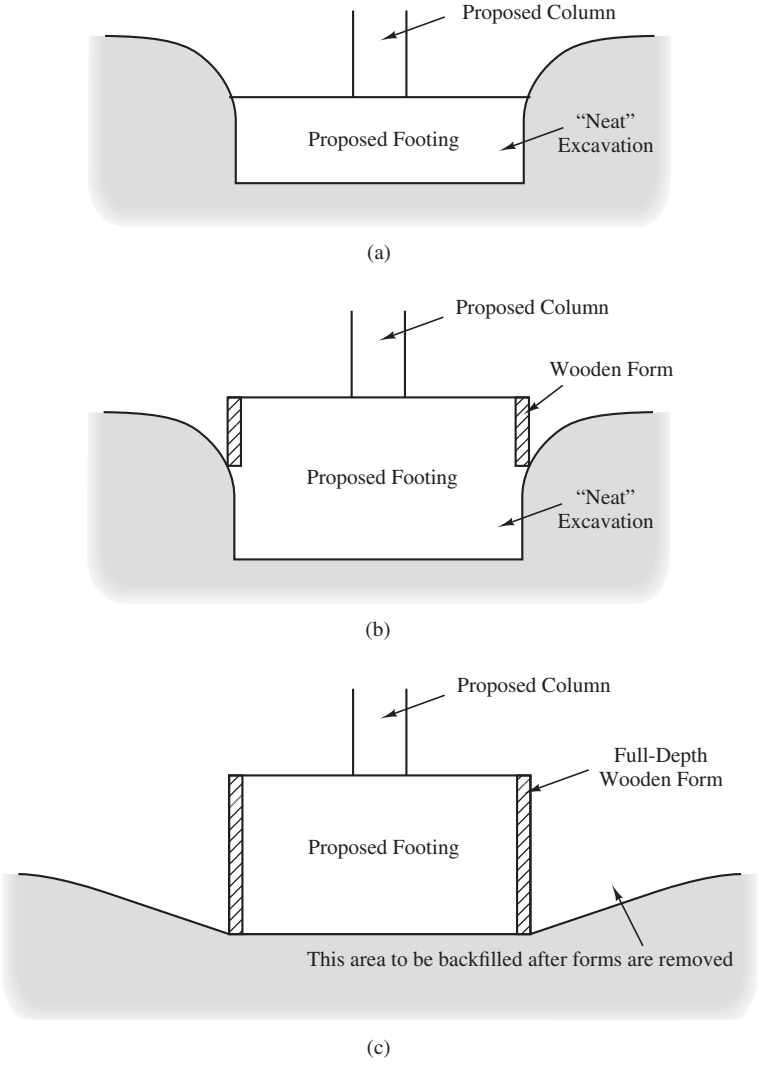

Figure 6.8 Methods of placing concrete in footings: (a) Neat excavation; (b) Neat excavation with wooden forms at the top; and (c) Formed footing with full-depth wooden forms.

Figure 6.9 A completed spread footing. The four bolts extending out of the footing will be connected to the base plate of a steel column.

elevation. If the soil will not stand vertically, such as with clean sands or gravels, it is necessary to make a larger excavation and build a full-depth wooden form, as shown in Figure 6.8c. This is known as a *formed footing*.

Once the excavation has been made and cleaned, and the forms (if needed) are in place, the contractor places the reinforcing steel. If the footing will support a wood or steel structure, threaded *anchor bolts* and/or steel brackets are embedded into the concrete. For concrete or masonry structures, short steel rebars, called *dowels* are placed such that they extend above the completed footing, thus providing for a lap splice with the column or wall steel. Chapter 10 discusses these connections in more detail. Finally, the concrete is placed and, once it has cured, the forms are removed. Figure 6.9 shows a completed spread footing in the field.

6.2 MATS

The second type of shallow foundation is a *mat foundation*. A mat is essentially a very large spread footing that usually encompasses the entire footprint of the structure, as shown in Figure 6.10. Mats also are known as *raft foundations*. They are always made of reinforced concrete. Conditions that may justify using mats rather than spread footings are discussed in Chapter 11.

Many buildings are supported on mat foundations, as are silos, chimneys, and other types of tower structures. Mats are also used to support storage tanks and large machines. The 75-story Texas Commerce Tower in Houston is one of the largest mat-supported structures in the world. Its mat is 3 m (9 ft 9 in) thick and is bottomed 19.2 m (63 ft) below the street level.

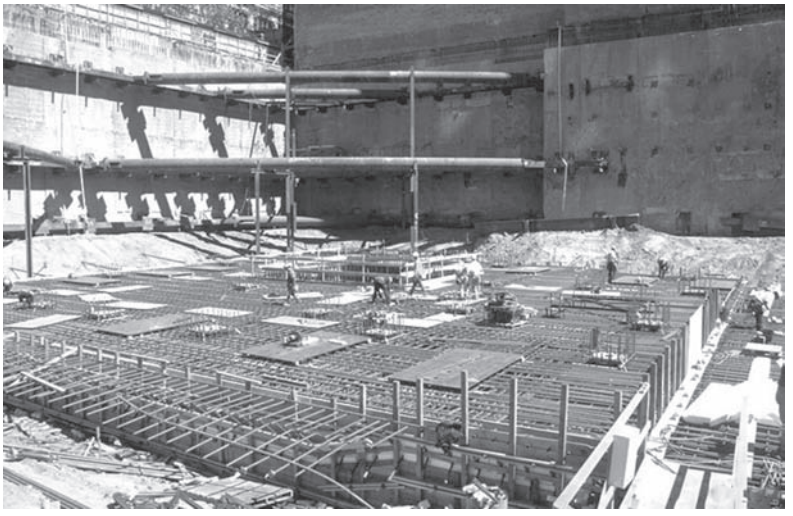

Figure 6.10 The central portion of a mat foundation for a hotel under construction in San Francisco in 1999. Note the heavy reinforcement for the foundation. When completed the mat extended to the edges of the excavation shown and varied from 1.2 to 2.5 m (4–8 ft) thick (courtesy of Ross Boulanger).

6.3 BEARING PRESSURE

The most fundamental parameter that defines the interface between a shallow foundation and the soil that supports it is the *bearing pressure*. This is the contact force per unit area between the bottom of the foundation and the underlying soil. Engineers recognized the importance of bearing pressure during the nineteenth century, thus forming the basis for later developments in bearing capacity and settlement theories.

Distribution of Bearing Pressure

Although the integral of the bearing pressure across the base area of a shallow foundation must be equal to the force acting between the foundation and the soil, this pressure is not necessarily distributed evenly. Analytical studies and field measurements (Schultze, 1961; Dempsey and Li, 1989; and others) indicate that the actual distribution depends on several factors, including the following:

- Eccentricity, if any, of the applied load
- Magnitude of the applied moment, if any
- Structural rigidity of the foundation
- Stress-strain properties of the soil
- Roughness of the bottom of the foundation

Figure 6.11 shows the distribution of bearing pressure along the base of flexible and rigid shallow foundations subjected to concentric vertical loads. Perfectly flexible foundations bend as necessary to maintain a uniform bearing pressure, as shown in Figures 6.11a and 6.11b, whereas perfectly rigid foundations settle uniformly but have variations in the bearing pressure, as shown in Figures 6.11c and 6.11d.

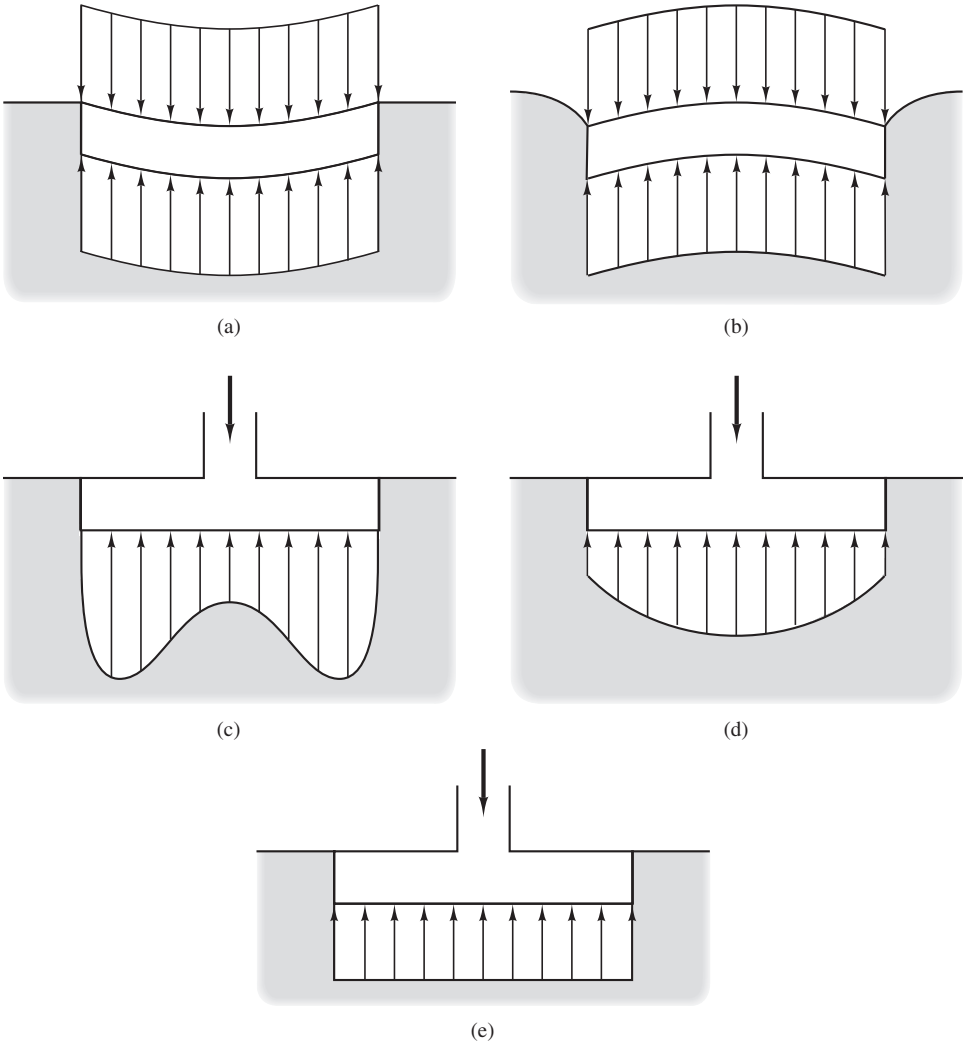

Figure 6.11 Distribution of bearing pressure along the base of footings subjected to concentric vertical loads: (a) flexible footing on clay; (b) flexible footing on sand; (c) rigid footing on clay; (d) rigid footing on sand; and (e) simplified distribution (after Taylor, 1948).

Real spread footings are close to being perfectly rigid, so the bearing pressure distribution is not uniform. However, bearing capacity and settlement analyses based on such a distribution would be very complex, so it is customary to assume that the pressure beneath concentric vertical loads is uniform across the base of the footing, as shown in Figure 6.11e. The error introduced by this simplification is not significant.

Mat foundations have a much smaller thickness-to-width ratio, and thus are more flexible than spread footings. In addition, we evaluate the flexural stresses in mats more carefully and develop more detailed reinforcing steel layouts. Therefore, we conduct more detailed analyses to determine the distribution of bearing pressure on mats. Chapter 11 discusses these analyses.

When analyzing shallow foundations, it is customary and reasonable to neglect any sliding friction along the sides of the footing and assume that the entire load is transmitted to the bottom. This is an important analytical difference between shallow and deep foundations, and will be explored in more detail in Chapter 12.

Computation of Bearing Pressure

The *bearing pressure* (or *gross bearing pressure*) along the bottom of a shallow foundation is:

$$q = \frac{P + W_f}{A} - u_D \tag{6.1}$$

where

q = bearing pressure
P = vertical column load
W_f = weight of foundation, including the weight of soil above the foundation, if any
A = base area of foundation (B^2 for square foundations or BL for rectangular foundations
u_D = pore water pressure at bottom of foundation (i.e., at a depth D below the ground surface).

Virtually all shallow foundations are made of reinforced concrete, so W_f is computed using a unit weight for concrete, γ_c, of 23.6 kN/m^3 (150 lb/ft^3). For simplicity, the overlying soil also can be assumed to have the same unit weight, which is slightly conservative.

The pore water pressure term accounts for uplift pressures (buoyancy forces) that are present if a portion of the foundation is below the groundwater table. If the groundwater table is at a depth greater than D, then set $u_D = 0$.

For continuous footings, we express the applied load and the weight of the footing in terms of force per unit length, such as 2,000 kN/m. We identify this unit length as b, as shown in Figure 6.12, which is usually 1 m or 1 ft. Thus, for simplicity, the load is still

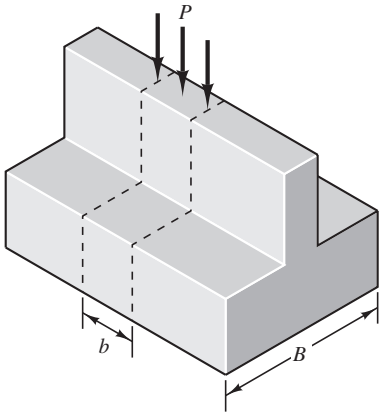

Figure 6.12 Definitions for load on continuous footings.

expressed using the variable P, and the weight using W_f, with the understanding that the load or weight is now given as a force per unit length. The bearing pressure for continuous footings is then:

$$q = \frac{P + W_f}{B} - u_D \tag{6.2}$$

We will use Equation 6.1 to compute the bearing stress for a square footing in Example 6.1.

Example 6.1

The 5 ft square footing shown in Figure 6.13 supports a column load of 100 k. Compute the bearing pressure.

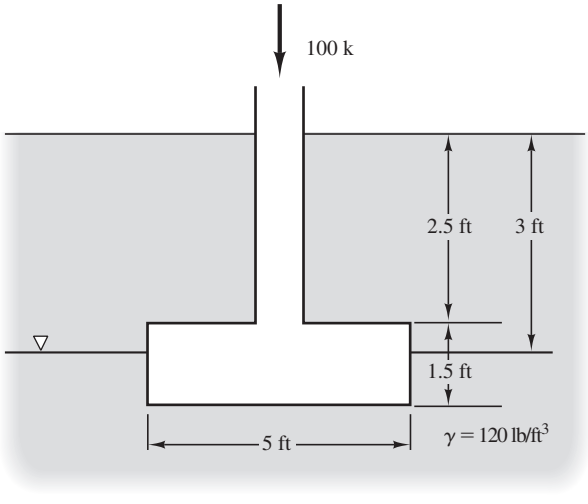

Figure 6.13 Spread footing for Example 6.1.

Solution

Use 150 lb/ft^3 for the unit weight of concrete, and compute W_f as if the concrete extends from the ground surface to a depth D (this is conservative when the footing is covered with soil because soil has a lower unit weight, but the error introduced is small).

$$W_f = (5\text{ ft})(5\text{ ft})(4\text{ ft})(150\text{ lb/ft}^3) = 15{,}000\text{ lb}$$

$$A = (5\text{ ft})(5\text{ ft}) = 25\text{ ft}^2$$

$$u_D = \gamma_w z_w = (62.4\text{ lb/ft}^3)(4\text{ ft} - 3\text{ ft}) = 62\text{ lb/ft}^2$$

$$q = \frac{P + W_f}{A} - u_D$$

$$= \frac{100{,}000\text{ lb} + 15{,}000\text{ lb}}{25\text{ ft}^2} - 62\text{ lb/ft}^2$$

$$= \mathbf{4{,}538\text{ lb/ft}^2}$$

Example 6.2

A 0.70 m wide continuous footing supports a wall load of 110 kN/m. The bottom of this footing is at a depth of 0.50 m below the adjacent ground surface and the soil has a unit weight of 17.5 kN/m^3. The groundwater table is at a depth of 10 m below the ground surface. Compute the bearing pressure.

Solution

Use 23.6 kN/m^3 for the unit weight of concrete.

Noting that both P and W_f are now forces per unit length and that their appropriate unit should be kN/m,

$$W_f = (0.70\text{ m})(0.50\text{ m})(23.6\text{ kN/m}^3) = 8\text{ kN/m}$$

$$u_D = 0$$

$$q = \frac{P + W_f}{B} - u_D = \frac{110\text{ kN/m} + 8\text{ kN/m}}{0.70\text{ m}} - 0 = \mathbf{169\text{ kPa}}$$

Net Bearing Pressure

An alternative way to define bearing pressure is the *net bearing pressure*, q', which is the difference between the gross bearing pressure, q, and the initial vertical effective stress, σ'_{z0}, at depth D. In other words, q' is a measure of the increase in vertical effective stress at depth D.

Use of the net bearing pressure simplifies some computations, especially those associated with settlement of spread footings, but it makes others more complex. Some

engineers prefer this method, while others prefer to use the gross bearing pressure. Therefore, it is important to understand which definition is being used. Either method will produce the same design, so long as it is used consistently and correctly. In this book we will use only the gross bearing pressure.

Foundations with Eccentric or Moment Loads

Most foundations are built so the vertical load acts through the centroid, thus producing a fairly uniform distribution of bearing pressure. However, sometimes it becomes necessary to accommodate loads that act through other points, as shown in Figure 6.14a. These are called *eccentric loads*, and they produce a non-uniform bearing pressure distribution. Assuming a linear distribution of the bearing pressure, the eccentricity, e, of the bearing pressure is given by:

$$e = \frac{Pe_L}{P + W_f} \tag{6.3}$$

where

e = eccentricity of bearing pressure distribution
P = applied vertical load (or the same per unit length for continuous footings)
e_L = eccentricity of applied vertical load
W_f = weight of footing (or the same per unit length for continuous footings)

Another similar condition occurs when moment loads are applied to foundations, as shown in Figure 6.14b. These loads also produce non-uniform bearing pressures. In this case, the eccentricity of the bearing pressure is:

$$e = \frac{M}{P + W_f} \tag{6.4}$$

where

M = applied moment load (or the same per unit length for continuous footings)

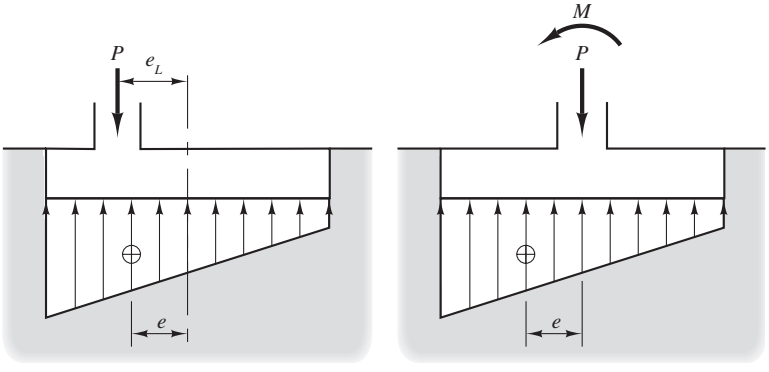

Figure 6.14 (a) Eccentric; and (b) Moment loads on spread footings.

In both cases, we assume the bearing pressure distribution beneath spread footings is linear, as shown in Figure 6.14. This is a simplification of the truth, but sufficiently accurate for practical design purposes. Note that this assumption may not be reasonable for mat foundations, and we perform more detailed analyses for mats, as discussed in Chapter 11.

One-Way Eccentric or Moment Loading

If the eccentric or moment loads occur only in the *B* direction, then the bearing pressure distribution is as shown in Figure 6.15.

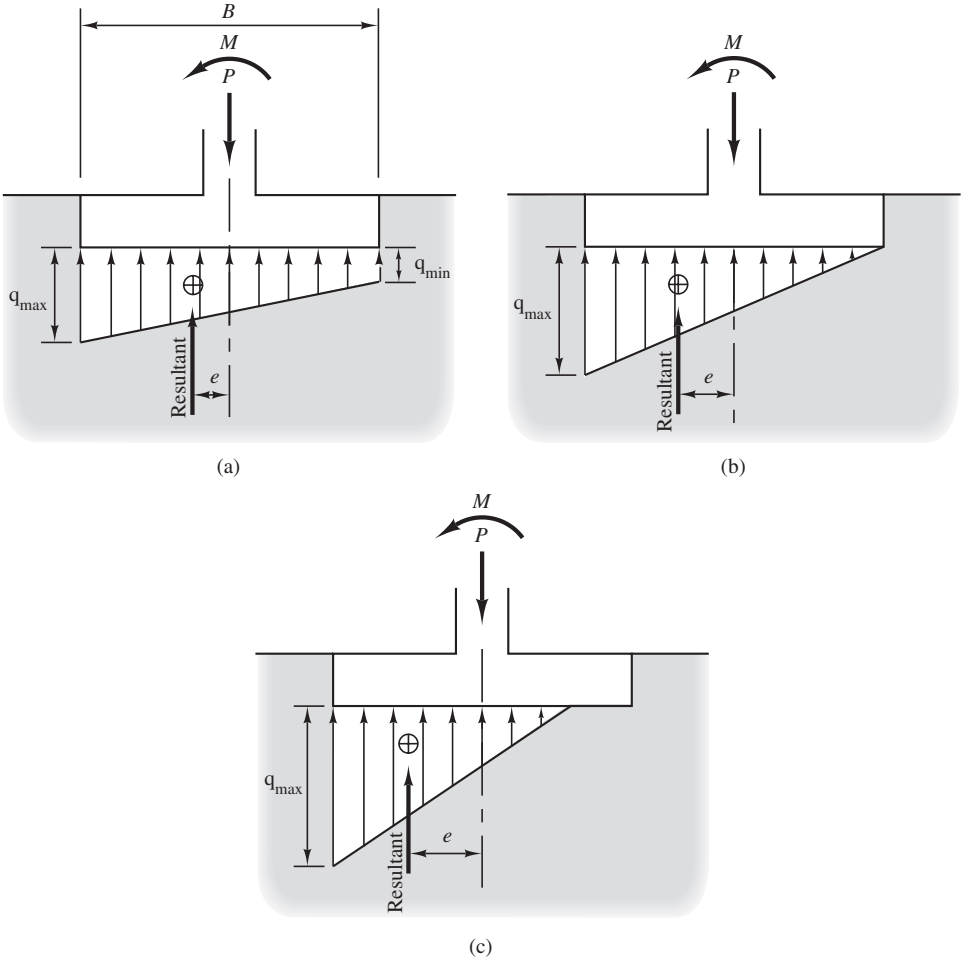

Figure 6.15 Distribution of bearing pressure beneath footings with various eccentricities: (a) $e < B/6$; (b) $e = B/6$; and (c) $e > B/6$.

If $e \leq B/6$ the bearing pressure distribution is trapezoidal, as shown in Figure 6.15a, and the minimum and maximum bearing pressures on square or rectangular foundations are:

$$q_{\min} = \left(\frac{P + W_f}{A} - u_D\right)\left(1 - \frac{6e}{B}\right) \tag{6.5}$$

$$q_{\max} = \left(\frac{P + W_f}{A} - u_D\right)\left(1 + \frac{6e}{B}\right) \tag{6.6}$$

where

$q_{\min}$ = minimum bearing pressure
$q_{\max}$ = maximum bearing pressure
P = column load
A = base area of foundation
u_D = pore water pressure along base of foundation
e = eccentricity of bearing pressure distribution
B = width of foundation

If the eccentric or moment load is only in the L direction, substitute L for B in Equations 6.5 and 6.6. For continuous footings, express P and W_f as forces per unit length and substitute B for A.

If $e = B/6$ (i.e., the resultant force acts at the third-point of the foundation), then $q_{\min} = 0$ and the bearing pressure distribution is triangular as shown in Figure 6.15b. Therefore, so long as $e \leq B/6$, there will be some contact pressure along the entire base area.

However, if $e > B/6$, the resultant of the bearing pressure acts outside the third-point and the pressure distribution is as shown in Figure 6.15c. Theoretically, there is tension on one side of the footing, but since soil cannot take tension, this side of the footing will lose all contact pressure with the ground. In addition, the high bearing pressure at the opposite side may cause a large settlement there. The actual behavior is likely an excessive tilting of the footing, which is not desirable. Therefore, we avoid this situation and design footings with eccentric or moment loads such that the following criterion is satisfied:

$$e \leq \frac{B}{6} \tag{6.7}$$

This criterion maintains compressive stresses along the entire base area.

For rectangular foundations with the moment or eccentric load in the long direction, substitute L for B in Equation 6.7.

Example 6.3

A 5 ft wide continuous footing is subjected to a concentric vertical load of 12 k/ft and a moment load of 8 ft-k/ft acting laterally across the footing, as shown in Figure 6.16. The groundwater table is at a great depth. Determine whether the resultant force on the base of the footing acts within the middle third and compute the maximum and minimum bearing pressures.

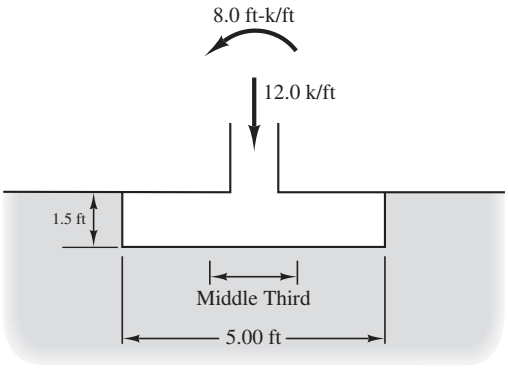

Figure 6.16 Proposed footing for Example 6.3.

Solution

$$W_f = (5.0 \text{ ft})(1.5 \text{ ft})(150 \text{ lb/ft}^3) = 1125 \text{ lb/ft}$$

$$e = \frac{M}{P + W_f} = \frac{8{,}000 \text{ ft-lb/ft}}{12{,}000 \text{ lb/ft} + 1{,}125 \text{ lb/ft}} = 0.610 \text{ ft}$$

$$\frac{B}{6} = \frac{5 \text{ ft}}{6} = 0.833 \text{ ft}$$

***e* < *B*/6; therefore the resultant is in the middle third.**

$$q_{\min} = \left(\frac{P + W_f}{B} - u_D\right)\left(1 - \frac{6e}{B}\right)$$

$$q_{\min} = \left(\frac{12{,}000 + 1125}{5.0} - 0\right)\left(1 - \frac{(6)(0.610)}{5.0}\right)$$

$$q_{\min} = \mathbf{703 \text{ lb/ft}^2}$$

$$q_{\max} = \left(\frac{P + W_f}{B} - u_D\right)\left(1 + \frac{6e}{B}\right)$$

$$q_{\max} = \left(\frac{12{,}000 + 1125}{5.0} - 0\right)\left(1 + \frac{(6)(0.610)}{5.0}\right)$$

$$q_{\max} = \mathbf{4546 \text{ lb/ft}^2}$$

When designing combined footings, try to arrange the footing dimensions and column locations so the resultant of the applied loads acts through the centroid of the footing. This produces a more uniform bearing pressure distribution. Some combined footing designs accomplish this by using a trapezoidal shaped footing (as seen in plan view) with the more lightly loaded column on the narrow side of the trapezoid. When this is not possible, be sure all of the potential loading conditions produce eccentricities no greater than *B*/6.

Two-Way Eccentric or Moment Loading

If the resultant load acting on the base is eccentric in both the B and L directions, it must fall within the diamond-shaped kern shown in Figure 6.17 for the contact pressure to be compressive along the entire base of the foundation. It falls within this kern only if the following condition is met:

$$\frac{6e_B}{B} + \frac{6e_L}{L} \leq 1.0 \tag{6.8}$$

where

e_B = eccentricity in the B direction
e_L = eccentricity in the L direction

If Equation 6.8 is satisfied, the magnitudes of q at the four corners of a square or rectangular shallow foundation are:

$$q = \left(\frac{P + W_f}{A} - u_D\right)\left(1 \pm \frac{6e_B}{B} \pm \frac{6e_L}{L}\right) \tag{6.9}$$

Example 6.4 will illustrate how to check that the resultant load lies within the kern and adjust the footing width as needed.

Example 6.4

A 3 m square footing supports a vertical column load of 200 kN and two moment loads with axes parallel to the sides of the footing, each having a magnitude of 124 kN-m. The embedment of the footing is 1 m, and the groundwater table is at a great depth. Determine whether eccentric loading requirements will be met. If these requirements are not met, determine the minimum footing width, B, needed to satisfy these requirements.

Solution

1. Check one-way eccentricity

$$P = 200 \text{ kN}$$

$$M = 124 \text{ kN-m}$$

$$W_f = (3 \text{ m})(3 \text{ m})(1 \text{ m})(23.6 \text{ kN/m}^3) = 212 \text{ kN}$$

$$e = \frac{M}{P + W_f} = \frac{124}{200 + 212} = 0.3 \text{ m}$$

$$\frac{B}{6} = \frac{3 \text{ m}}{6} = \mathbf{0.5 \text{ m}}$$

Therefore, $e \leq \dfrac{B}{6}$ OK for one-way eccentricity

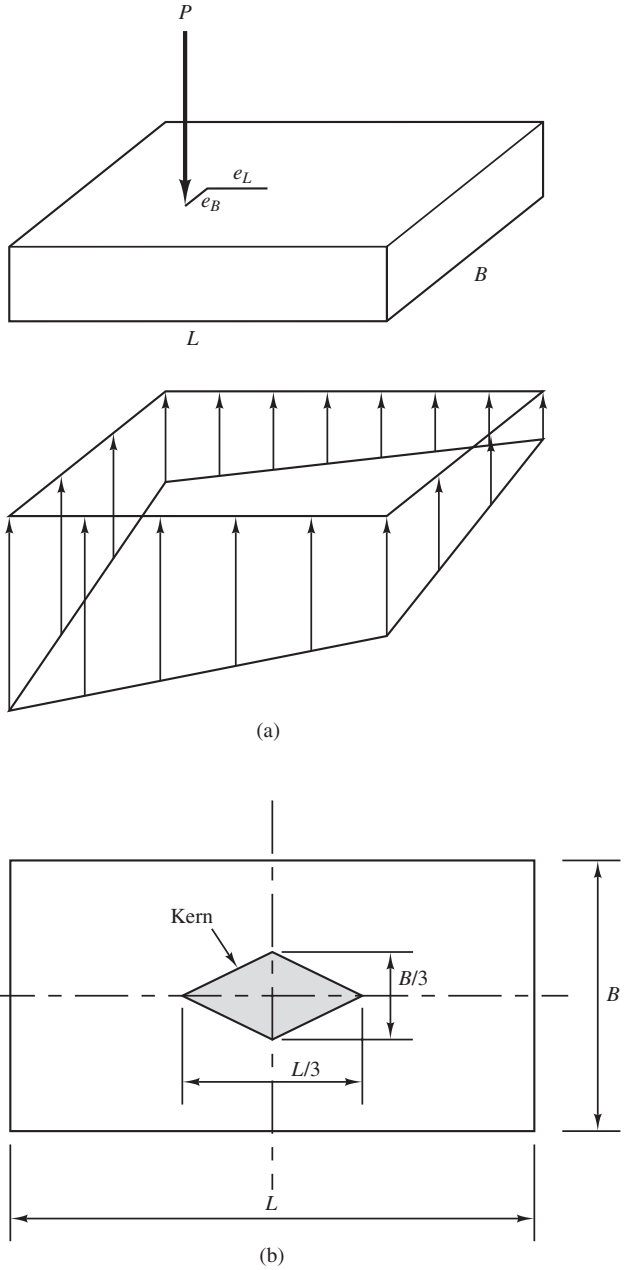

Figure 6.17 (a) Pressure distribution beneath spread footing with vertical load that is eccentric in both the B and L directions; and (b) To maintain $q \geq 0$ along with the entire base of the footing, the resultant force must be located within this diamond-shaped kern.

2. Check two-way eccentricity

$$\frac{6e_B}{B} + \frac{6e_L}{L} = \frac{6(0.3\text{ m})}{3\text{ m}} + \frac{6(0.3\text{ m})}{3\text{ m}} = 1.2 > 1 \text{ Not acceptable}$$

3. Conclusion
Although the footing is satisfactory for one-way eccentricity, it does not meet the criterion for two-way eccentricity because the resultant is outside the kern. This means a corner of the footing may lift up, causing excessive tilting. Therefore, it is necessary to increase B.

4. Revised Design
Assuming that the weight of the foundation does not change,

$$\frac{6e_B}{B} + \frac{6e_L}{L} = \frac{6(0.3\text{ m})}{B} + \frac{6(0.3\text{ m})}{L} = 1$$

Minimum B = minimum L = 3.6 m

Therefore, a 3.6 m × 3.6 m square footing would be required to keep the resultant within the kern. However, this is only one of many design criteria for spread footings. Other criteria, as discussed in Chapters 7 to 10, also need to be checked.

Equivalent Uniformly Loaded Footing

When we have a footing with an eccentric or moment loading, as shown in Figure 6.14, it is convenient, for computational purpose, to determine the dimensions of an *equivalent uniformly loaded footing*. The equivalent footing is a footing that carries the same applied load as the original footing but has different dimensions such that the resulting bearing pressure is uniform (Meyerhof, 1963; Brinch Hansen, 1970). This is accomplished by decreasing the footing width, B, to an equivalent width, B', and the length, L, to an equivalent length, L', as shown in Figure 6.18. The equivalent dimensions B' and L' are selected such that the net resultant load acts through the centroid of the equivalent footing.

For a footing with true dimensions $B \times L$, we can determine the equivalent dimensions B' and L' using the following process. First determine the eccentricities e_B and e_L from the applied load and moments using Equations 6.3 and 6.4. Next, check to ensure that the resultant footing load acts within the kern shown in Figure 6.18. If not, increase B and L such that this criterion is satisfied. Then compute the dimensions B' and L' using Equations 6.10 and 6.11:

$$B' = B - 2e_B \tag{6.10}$$

$$L' = L - 2e_L \tag{6.11}$$

The equivalent bearing pressure for this footing, q_{eq}, will be greater than the average bearing of the true footing and computed as:

$$q_{eq} = \frac{P + W_f}{B'L'} \tag{6.12}$$

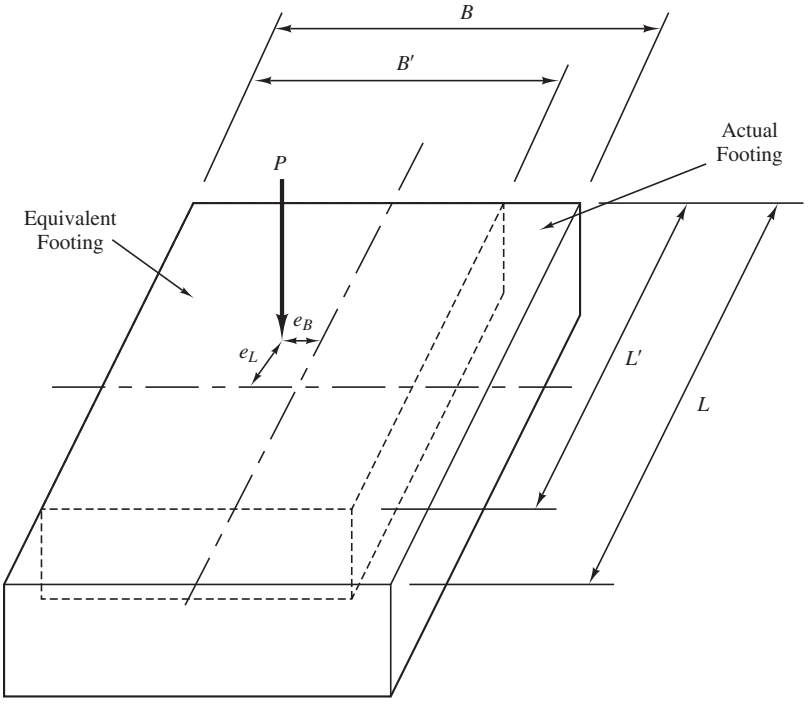

Figure 6.18 Equivalent uniformly loaded footing for a footing with eccentric applied loads or moments. The dimensions B' and L' are selected such that there is no eccentricity on the equivalent footing.

Example 6.5 will demonstrate how to determine the equivalent footing size and compute the equivalent bearing pressure.

Example 6.5

A 5 × 7 ft footing is founded at a depth of 2 ft and supports a vertical load of 80 k and a moment load of 30 ft-k in the B direction and 50 ft-k in the L direction. Determine the dimensions of the equivalent uniformly loaded footing and compute the equivalent bearing pressure.

Solution

First we must compute the eccentricities using Equation 6.4.

$$W_f = (5 \times 7 \times 2)(0.15) = 10.5 \text{ k}$$

$$e_B = \frac{30}{80 + 10.5} = 0.33$$

$$e_L = \frac{50}{80 + 10.5} = 0.55$$

Check to see that resultant acts within the kern using Equation 6.8.

$$\frac{6(0.33)}{5} + \frac{6(0.55)}{7} = 0.87 < 1.0 \qquad \therefore \text{OK}$$

Now compute equivalent dimensions B' and L' using Equations 6.10 and 6.11.

$$B' = 5 - 2(0.33) = 4.34 \text{ ft}$$
$$L' = 7 - 2(0.55) = 5.9 \text{ ft}$$

The equivalent bearing pressure is

$$q_{eq} = \frac{80 + 10.5}{4.34 \times 5.90} = 3.53 \text{ k/ft}^2$$

Discussion

Note that the average bearing pressure on the true footing is

$$q_{ave} = \frac{80 + 10.5}{5 \times 7} = 2.58 \text{ k/ft}^2$$
$$q_{\max} = \frac{80 + 10.5}{5 \times 7}\left(1 + \frac{6(0.33)}{5} + \frac{6(0.55)}{7}\right) = 4.83 \text{ k/ft}^2$$

Note that the equivalent uniform bearing pressure is an intermediate value between the average and maximum bearing pressure on the true footing. This intermediate value is a useful way to compute bearing capacity and settlement of an eccentrically loaded footing and will be used in Chapter 9 for the design of footings.

6.4 PRESUMPTIVE ALLOWABLE BEARING PRESSURES

An allowable bearing pressure is a pressure that, if exceeded, may present an unsafe condition as related to either ultimate or serviceability limit states. In Chapter 9, we will synthesize the footing design process and discuss allowable bearing pressure in detail. It is useful at this point to introduce the concept of *presumptive allowable bearing pressures* (also known as *prescriptive bearing pressures*).

Presumptive allowable bearing pressures are allowable bearing pressures obtained directly from the soil classification without any further analysis. These presumptive bearing pressures appear in building codes, as shown in Table 6.1. They are easy to implement, and do not require borings, laboratory testing, or extensive analyses. The engineer simply obtains the q_A value from the table and selects a footing width such that $q \leq q_A$.

Example 6.6

A footing supporting a column load of 140 kN is to be founded on a silty sand deposit at a depth of 0.7 m. The water table is at a great depth. Determine the width of a square footing that will support this column load.

Solution

First we compute the weight of the footing.

$$W_f = B^2 D\gamma_c = B^2 0.7(23.6) = 16.5B^2$$

Note that the weight of the footing is a function of the footing width. The bearing pressure is

$$q = \frac{P + W_f}{B^2} = \frac{140 + 16.5B^2}{B^2}$$

Solving for B gives

$$B = \sqrt{\frac{140}{q - 16.5}}$$

From Table 6.1 q_A for silty sand is 100 kPa. Substituting $q_A = 100$ for q gives

$$B = \sqrt{\frac{140}{100 - 16.5}} = \mathbf{1.3\ m}$$

TABLE 6.1 PRESUMPTIVE ALLOWABLE BEARING PRESSURES PER INTERNATIONAL BUILDING CODE (ICC, 2012)

Soil or Rock Classification	Allowable Bearing Stress, q_A kPa (lb/ft^2)
Crystalline bedrock	600
	(12,000)
Sedimentary and foliated rock	200
	(4,000)
Sandy gravel or gravel (GW and GP)	150
	(3,000)
Sand, silty sand, clayey sand, silty gravel, or clayey gravel (SW, SP, SM, SC, GM and GC)	100
	(2,000)
Clay, sandy clay, silty clay, or clayey silt	70
	(1,500)

SUMMARY

Major Points

1. Shallow foundations are those that transmit structural loads to the near-surface soils. There are two kinds: spread footing foundations and mat foundations.
2. Although other materials have been used in the past, today virtually all shallow foundations are made of reinforced concrete.
3. Spread footings are most often used in small- to medium-size structures on sites with moderate to good soil conditions. The bearing pressure is the contact pressure between the bottom of a spread footing and the underlying soils.
4. The actual distribution of bearing pressure is a complicated function depending upon the soil properties, footing stiffness, and eccentricity of the loading. We generally assume the bearing pressure is either uniform or distributed in a triangular fashion across the base of the footing.
5. If the loads applied to a footing are eccentric, or if moment loads are applied, the resulting bearing pressure distribution also will be eccentric. In such cases, the footing needs to be designed so the resultant of the bearing pressure is within the middle third of the footing (for one-way eccentricity) or in a diamond-shaped kern (for two-way eccentricity). This requirement ensures the entire base of the footing has compressive bearing pressures, and thus avoids problems with uplift.
6. Eccentrically loaded footings can be converted into an equivalent uniformly loaded footing. This method is used to simplify the design of eccentrically loaded footings.
7. Presumptive allowable bearing pressures are code specified pressures based on soil classification and not on analysis. They can be used to size footings for light structures founded on competent soils.

Vocabulary

Anchor bolts
Backhoe
Bearing pressure
Cantilever footing
Circular spread footing
Combined spread footing
Continuous spread footing
Dimension-stone footings
Dowels
Eccentric load
Embedment
Equivalent footing pressure
Equivalent footing width
Equivalent uniformly loaded footing
Footer
Footing
Formed footing
Grade beam
Gross bearing pressure
Kern
Mat foundation
Moment load
Neat footing
Net bearing pressure
Presumptive allowable bearing pressures
Raft foundation
Rectangular footing
Reinforced concrete footing
Ring footing
Rubble-stone footings
Shallow foundation
Spread footing
Square footing
Steel grillage footing
Strap footing

QUESTIONS AND PRACTICE PROBLEMS

Section 6.1 Spread Footings

6.1 What is the difference between a square footing and a continuous footing, and when would each type be used?

6.2 Describe a structure for which a ring footing would be appropriate.

6.3 Describe why a rectangular footing might be a good choice for a footing supporting a column with a moment load in one direction.

Section 6.3 Bearing Pressure

6.4 A 400 kN vertical downward column load acts at the centroid of a 1.5 m square footing. The bottom of this footing is 0.4 m below the ground surface and the top is flush with the ground surface. The groundwater table is at a depth of 3 m below the ground surface. Compute the bearing pressure.

6.5 A bearing wall carries a dead load of 5.0 k/ft and a live load of 3.0 k/ft. It is supported on a 3 ft wide, 2 ft deep continuous footing. The top of this footing is flush with the ground surface and the groundwater table is at a depth of 35 ft below the ground surface. Compute the bearing pressure for ultimate limit state design using the ASD method.

6.6 Repeat Problem 6.5 using the LRFD method with ASCE 7 load combinations.

6.7 A 5 ft square, 2 ft deep spread footing is subjected to a concentric vertical load of 60 k and an overturning moment of 30 ft-k. The overturning moment acts parallel to one of the sides of the footing, and the top of the footing is flush with the ground surface and the groundwater table is at a depth of 20 ft below the ground surface. Determine whether the resultant force acts within the middle third of the footing, compute the minimum and maximum bearing pressures and show the distribution of bearing pressure in a sketch. Determine the size of the equivalent uniformly loaded footing and compute the equivalent bearing pressure.

6.8 Consider the footing and loads in Problem 6.7, except that the overturning moment now acts at a 45° angle from the side of the footing (i.e., it acts diagonally across the top of the footing). Determine whether the resultant force acts within the kern. If it does, then compute the bearing pressure at each corner of the footing and show the pressure distribution in a sketch similar to Figure 6.17. Determine the size of the equivalent uniformly loaded footing and compute the equivalent bearing pressure.

6.9 The two columns in Figure 6.19 are to be supported on a combined footing. The vertical dead loads on Columns A and B are 500 and 1400 kN, respectively. Using the ASD method for ultimate limit state design, determine the required dimension B_2 so the resultant of the column loads acts through the centroid of the footing and express your answer as a multiple of 100 mm.

6.10 In addition to the dead loads described in Problem 6.9, Columns A and B in Figure 6.19 also can carry vertical live loads of up to 800 and 1200 k, respectively. The live loads vary with time, and thus may be present some days and absent other days. In addition, the live load on

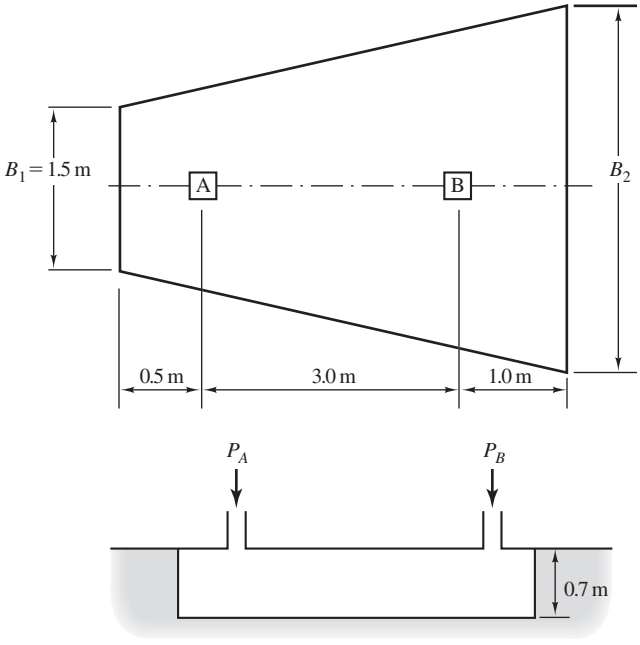

Figure 6.19 Proposed combined footing for Problems 6.9 and 6.10.

each column is independent of that on the other column (i.e., one could be carrying the full live load while the other has zero live load). Using the ASD method for ultimate limit state design and the dimensions obtained in Problem 6.9, and the worst possible combination of live loads, determine if the bearing pressure distribution always meets the eccentricity requirements described in this chapter. The groundwater table is at a depth of 10 m.

6.11 Repeat Problem 6.9 using the LRFD method with ASCE 7 load combinations.

6.12 Repeat Problem 6.10 using the LRFD method with ASCE 7 load combinations.

6.13 Derive Equations 6.5 and 6.6. Would these equations also apply to circular spread footings? Why or why not?

Section 6.4 Presumptive Allowable Bearing Pressure

6.14 A 1.5 m square footing is founded on a clay soil at a depth of 0.5 m. The ground water is at the ground surface. The footing is loaded at its centroid and carries a design load of 170 kN. Does this footing meet the presumptive allowable bearing pressure of the International Building Code? If not, design the footing such that it does meet these requirements.

6.15 A footing is carrying a design column load of 22 k and a moment of 5 k-ft in one direction. The footing will be founded on sand at a depth of 2 ft. The water table is 3 ft below the ground surface. Design the footing width for a square footing that will carry the design loads and meet the presumptive allowable bearing pressure per the International Building Code.

7

Spread Footings—Geotechnical Ultimate Limit States

When we are satisfied with the spot fixed on for the site of the city . . . the foundations should be carried down to a solid bottom, if such can be found, and should be built thereon of such thickness as may be necessary for the proper support of that part of the wall which stands above the natural level of the ground. They should be of the soundest workmanship and materials, and of greater thickness than the walls above. If solid ground can be come to, the foundations should go down to it and into it, according to the magnitude of the work, and the substruction to be built up as solid as possible. Above the ground of the foundation, the wall should be one-half thicker than the column it is to receive so that the lower parts which carry the greatest weight, may be stronger than the upper part . . . Nor must the mouldings of the bases of the columns project beyond the solid. Thus, also, should be regulated the thickness of all walls above ground.

Marcus Vitruvius, Roman Architect and Engineer
1st century BC as
translated by Morgan (1914)

Spread footings must satisfy a number of performance requirements, as discussed in Chapter 5. Performance requirements that relate to strength and stability are called strength requirements, and the limit states associated with these strength requirements are the

ultimate limit states. There are two geotechnical ultimate limit states that must be considered in spread footing design.

The first geotechnical ultimate limit state occurs when the soil beneath the footing fails in shear as a result of applied downward and/or moment loads. This kind of failure is called a *bearing capacity failure*. The second geotechnical ultimate limit state occurs when the footing slides horizontally as a result of applied shear loads.

This chapter explores these two geotechnical ultimate limit states and shows how to design spread footings against these failures using both the allowable stress design (ASD) and load and resistance factor design (LRFD) methods. Sections 7.1 to 7.9 deal with bearing capacity failures, and Section 7.10 covers sliding failures. Structural ultimate limit states are discussed in Chapter 10.

7.1 BEARING CAPACITY

Spread footings transmit the applied structural loads to the near-surface soils. In the process of doing so, they induce both compressive and shear stresses in these soils. The magnitudes of these stresses depend largely on the bearing pressure and the size of the footing. If the bearing pressure is large enough these shear stresses may exceed the shear strength of the soils, resulting in a bearing capacity failure. Researchers have identified three types of bearing capacity failures: *general shear failure*, *local shear failure*, and *punching shear failure*, as shown in Figure 7.1. A typical load-displacement curve for each mode of failure is shown in Figure 7.2.

General shear failure is the most common mode for spread footings. It occurs in soils that are relatively incompressible and reasonably strong, and in saturated, normally consolidated clays that are loaded rapidly enough that the undrained condition prevails. The failure surface is well defined, and failure occurs quite suddenly, as illustrated by the load-displacement curve. A clearly formed bulge appears on the ground surface adjacent to the spread footing. Although bulges may appear on both sides of the footing, ultimate failure occurs on one side only, and it is often accompanied by rotation of the footing.

The opposite extreme is punching shear failure. This mode of failure occurs in very loose sands, in a thin crust of strong soil underlain by a very weak soil, or in weak clays loaded under slow, drained conditions. The high compressibility of such soil profiles causes large settlements and poorly defined vertical shear surfaces. Little or no bulging occurs at the ground surface and failure develops gradually, as illustrated by the ever-increasing load depicted in the load-settlement curve.

The local shear failure is an intermediate case. The shear surfaces are well defined under the spread footing, and then become vague near the ground surface. A small bulge may occur, but considerable settlement, perhaps on the order of half the footing width, is necessary before a clear shear surface forms near the ground. Even then, a sudden failure does not occur, as happens in the general shear case. The footing just continues to sink ever deeper into the ground.

Vesić (1973) investigated these three modes of failure by conducting load tests on model circular foundations in a sand. These tests included both shallow and deep

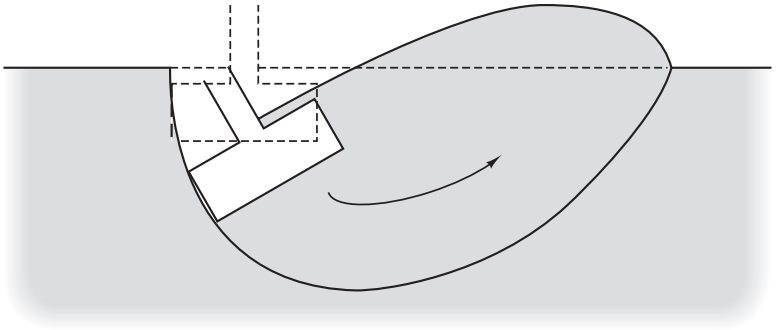

(a)

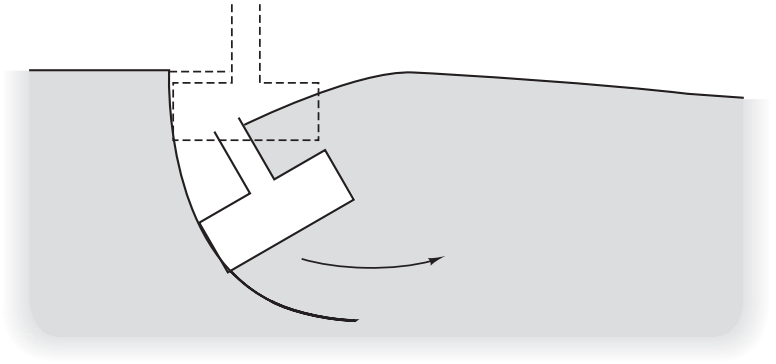

(b)

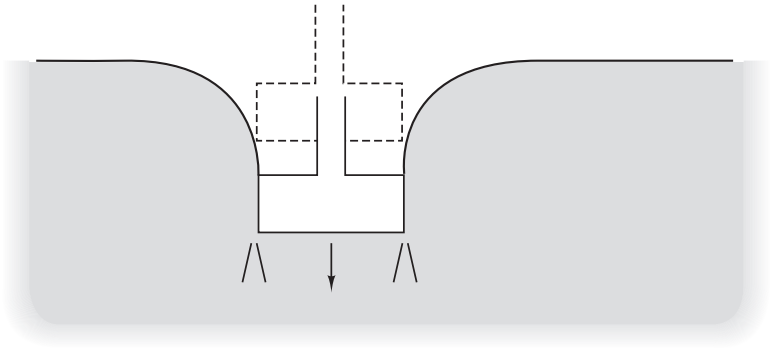

(c)

Figure 7.1 Modes of bearing capacity failure: (a) general shear failure; (b) local shear failure; and (c) punching shear failure.

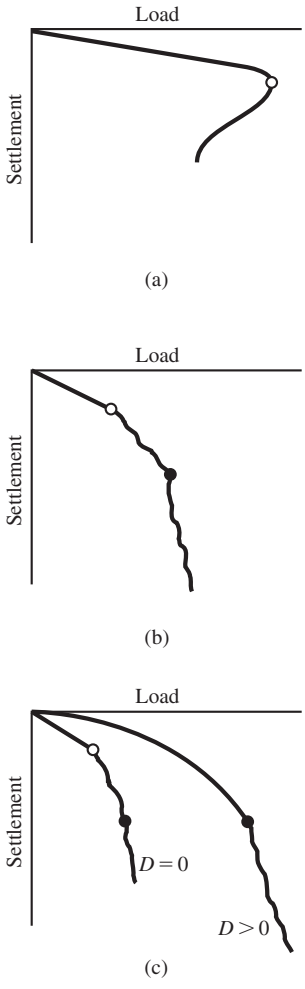

Figure 7.2 Typical load-displacement curves for different modes of bearing capacity failure: (a) general shear failure; (b) local shear failure; and (c) punching shear failure. The circles indicate various interpretations of failure (adapted from Vesić, 1963.)

foundations. The results, shown in Figure 7.3, indicate shallow foundations (D/B less than about 2) can fail in any of the three modes, depending on the relative density. However, deep foundations (D/B greater than about 4) are always governed by punching shear. Although these test results apply only to circular foundations in Vesić's sand and cannot necessarily be generalized to other soils, it does give a general relationship between the mode of failure, relative density, and the D/B ratio.

Complete quantitative criteria have yet to be developed to determine which of these three modes of failure will govern in any given circumstance, but the following guidelines are helpful:

- Spread footings in undrained cohesive soils are governed by the general shear case.
- Spread footings in dense cohesionless soils are governed by the general shear case. In this context, a dense sand is one with a relative density, D_r, greater than about 67%.

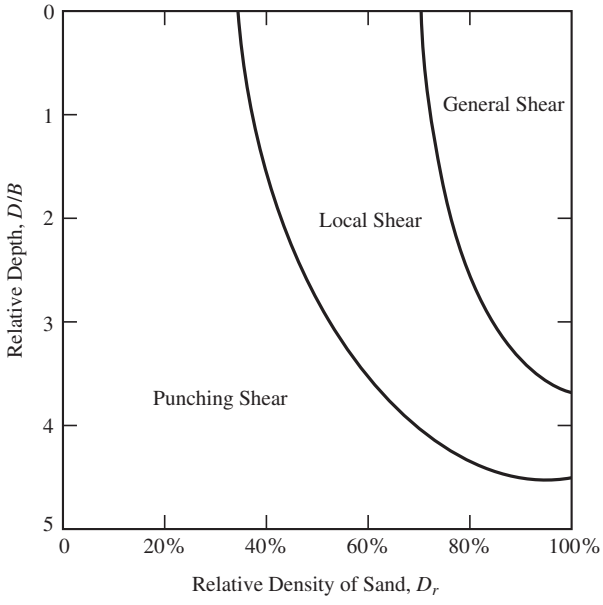

Figure 7.3 Modes of failure of model circular foundations in Chattahoochee Sand (adapted from Vesić, 1963 and 1973).

- Spread footings on loose to medium dense cohesionless soils ($30\% < D_r < 67\%$) are probably governed by local shear.
- Spread footings on very loose cohesionless soils ($D_r < 30\%$) are probably governed by punching shear.

For nearly all practical spread footing design problems, it is only necessary to check the general shear case, and then conduct settlement analyses to verify that the spread footings will not settle excessively. These settlement analyses implicitly protect against local and punching shear failures.

7.2 BEARING CAPACITY ANALYSES IN SOIL—GENERAL SHEAR CASE

Methods of Analyzing Bearing Capacity

To analyze spread footings for bearing capacity failures and design them in a way to avoid such failures, we must understand the relationship between bearing capacity, load, footing dimensions, and soil properties. Various researchers have studied these relationships using a variety of techniques, including:

- Assessments of the performance of real foundations, including full-scale load tests
- Load tests on model footings
- Bearing capacity theories
- Detailed numerical analyses, such as those using the finite element method (FEM)

Full-scale load tests, which consist of constructing real spread footings and loading them to failure, are the most precise way to evaluate bearing capacity. However, such tests are expensive, and thus are rarely, if ever, performed as a part of routine design. A few such tests have been performed for research purposes.

Model footing tests have been used to research bearing capacity, mostly because the cost of these tests is far below that of full-scale tests. Unfortunately, model tests have their limitations, especially when conducted in sands, because of uncertainties in applying the proper scaling factors. However, the advent of centrifuge model tests has partially overcome this problem.

The dominant way to assess bearing capacity of spread footings is to use bearing capacity theories. In a typical bearing capacity theory, the shape of the failure surface is defined in advance, as shown in Figure 7.1, and then equilibrium is considered to evaluate the stresses and strengths along this surface. These theories have their roots in Prandtl's studies of the punching resistance of metals (Prandtl, 1920). He considered the ability of very thick masses of metal (i.e., not sheet metal) to resist concentrated loads. Because of the various assumptions involved, the bearing capacity theories yield solutions that are usually corrected by applying empirical factors developed from model tests. While there are other approaches to analyze bearing capacity, we will consider only analyses based on bearing capacity theories because these analyses are used on the overwhelming majority of projects in practice.

Simple Bearing Capacity Formula

A simple bearing capacity theory can be developed by considering the continuous footing shown in Figure 7.4. Let us assume this footing experiences a bearing capacity failure, and that this failure occurs along a circular shear surface as shown. We will further assume the soil is undrained cohesive with a shear strength s_u. Finally, we will neglect the shear strength of the soil between the ground surface and a depth D, which is conservative. Thus, the soil in this zone is considered to be only a surcharge load that produces a vertical total stress of $\sigma_{zD} = \gamma D$ at a depth D.

The objective of this derivation is to obtain a formula for the nominal unit bearing capacity, q_n, which is the bearing pressure required to cause a bearing capacity failure. Considering equilibrium of a section of length b and taking moments about an axis through Point A perpendicular to the section, we obtain the following:

$$\sum M_A = (q_n Bb)(B/2) - (s_u \pi Bb)(B) - \sigma_{zD} Bb(B/2) = 0 \tag{7.1}$$

$$q_n = 2\pi s_u + \sigma_{zD} \tag{7.2}$$

It is convenient to define a new parameter, called a *bearing capacity factor*, N_c, and rewrite Equation 7.2 as:

$$q_n = N_c s_u + \sigma_{zD} \tag{7.3}$$

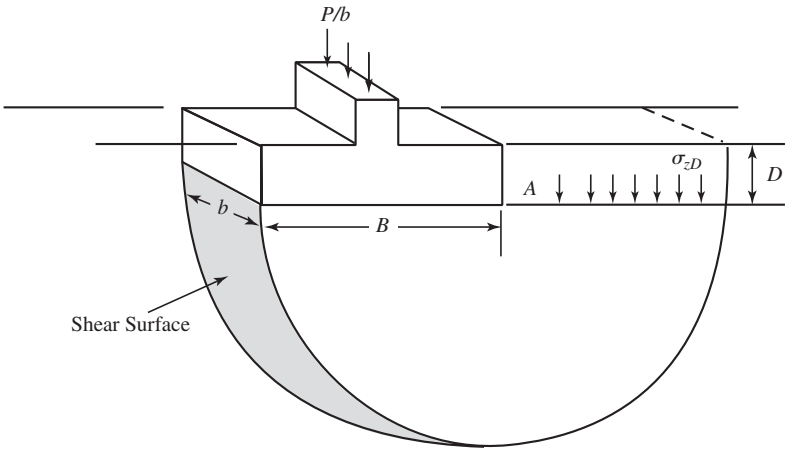

Figure 7.4 Bearing capacity analysis along a circular failure surface.

Equation 7.3 is known as a *bearing capacity formula*, and could be used to evaluate the bearing capacity of a proposed spread footing. According to this derivation, $N_c = 2\pi = 6.28$.

This simplified formula has only limited applicability in practice because it considers only continuous footings and undrained soil conditions ($\phi = 0$), and it assumes the footing rotates as the bearing capacity failure occurs. However, this simple derivation illustrates the general methodology required to develop more comprehensive and more accurate bearing capacity formulas.

Terzaghi's Bearing Capacity Formulas

Various bearing capacity theories were advanced in the first half of the twentieth century, but the first one to achieve widespread acceptance was that of Terzaghi (1943). His method includes the following assumptions:

- The depth of the footing is less than or equal to its width ($D \leq B$).
- The bottom of the footing is sufficiently rough that no sliding occurs between the footing and the soil.
- The soil beneath the footing is a homogeneous semi-infinite mass (i.e., the soil extends for a great distance below the footing and the soil properties are uniform throughout).
- The shear strength of the soil is described by the formula $s = c' + \sigma' \tan \phi'$.
- The general shear mode of failure governs.
- No consolidation of the soil occurs (i.e., settlement of the footing is due only to the shearing and lateral movement of the soil).
- The footing is very rigid in comparison to the soil.

- The soil between the ground surface and a depth D has no shear strength, and serves only as a surcharge load.
- The applied load is compressive and applied vertically through the centroid of the footing and no applied moment loads are present.

Terzaghi considered three zones in the soil, as shown in Figure 7.5. Immediately beneath the footing is a *wedge zone* that remains intact and moves downward with the footing. Next, a *radial shear zone* extends from each side of the wedge, where he took the shape of the shear planes to be logarithmic spirals. Finally, the outer portion is the *passive zone or linear shear zone* in which the soil shears along planar surfaces.

Since Terzaghi neglected the shear strength of soils between the ground surface and a depth D, the shear surface stops at this depth and the overlying soil has been replaced with the surcharge pressure σ'_{zD}. This approach is conservative, and is part of the reason for limiting the method to relatively shallow footings ($D \leq B$).

Terzaghi developed his theory for continuous footings (i.e., those with a very large L/B ratio). This is the simplest case because it is a two-dimensional problem. He then extended it to square and round footings by adding empirical coefficients obtained from model tests and produced the following bearing capacity formulas:

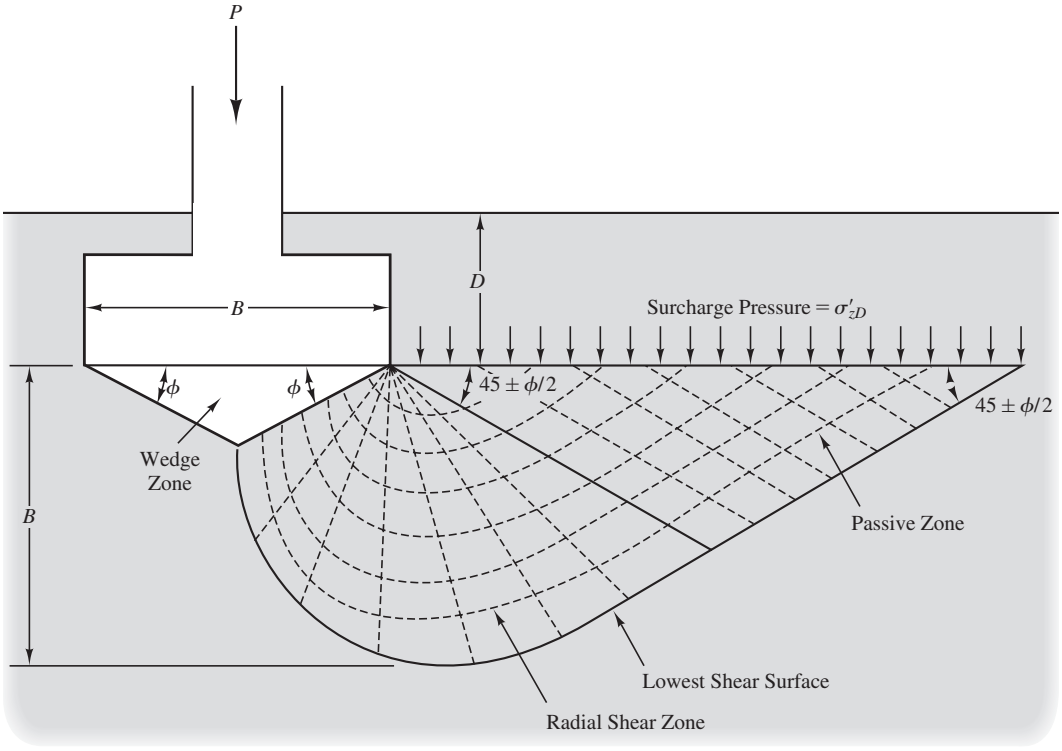

Figure 7.5 Geometry of failure surface for Terzaghi's bearing capacity formulas.

For square footings:

$$q_n = 1.3c'N_c + \sigma'_{zD}N_q + 0.4\gamma' BN_\gamma \tag{7.4}$$

For continuous footings:

$$q_n = c'N_c + \sigma'_{zD}N_q + 0.5\gamma' BN_\gamma \tag{7.5}$$

For circular footings:

$$q_n = 1.3c'N_c + \sigma'_{zD}N_q + 0.3\gamma' BN_\gamma \tag{7.6}$$

where

q_n = nominal unit bearing capacity
c' = effective cohesion of soil beneath footing
ϕ' = effective friction angle of soil beneath footing
σ'_{zD} = vertical effective stress at depth D below the ground surface ($\sigma'_{zD} = \gamma D$ if depth to groundwater table is greater than D)
γ' = effective unit weight of the soil ($\gamma' = \gamma$ if groundwater table is very deep; see discussion later in this chapter for shallow groundwater conditions)
D = depth of footing below ground surface
B = width (or diameter) of footing
N_c, N_q, N_γ = Terzaghi's bearing capacity factors $= f(\phi')$ (See Table 7.1, Figure 7.6, and Equations 7.7 through 7.12.)

TABLE 7.1 BEARING CAPACITY FACTORS

ϕ' (deg)	Terzaghi (for use in Equations 7.4 through 7.6)			Vesić (for use in Equation 7.13)		
	N_c	N_q	N_γ	N_c	N_q	N_γ
0	5.7	1.0	0.0	5.1	1.0	0.0
1	6.0	1.1	0.1	5.4	1.1	0.1
2	6.3	1.2	0.1	5.6	1.2	0.2
3	6.6	1.3	0.2	5.9	1.3	0.2
4	7.0	1.5	0.3	6.2	1.4	0.3
5	7.3	1.6	0.4	6.5	1.6	0.4
6	7.7	1.8	0.5	6.8	1.7	0.6
7	8.2	2.0	0.6	7.2	1.9	0.7
8	8.6	2.2	0.7	7.5	2.1	0.9

(*continued*)

TABLE 7.1 (Continued)

ϕ' (deg)	Terzaghi (for use in Equations 7.4 through 7.6)			Vesić (for use in Equation 7.13)		
	N_c	N_q	N_γ	N_c	N_q	N_γ
9	9.1	2.4	0.9	7.9	2.3	1.0
10	9.6	2.7	1.0	8.3	2.5	1.2
11	10.2	3.0	1.2	8.8	2.7	1.4
12	10.8	3.3	1.4	9.3	3.0	1.7
13	11.4	3.6	1.6	9.8	3.3	2.0
14	12.1	4.0	1.9	10.4	3.6	2.3
15	12.9	4.4	2.2	11.0	3.9	2.6
16	13.7	4.9	2.5	11.6	4.3	3.1
17	14.6	5.5	2.9	12.3	4.8	3.5
18	15.5	6.0	3.3	13.1	5.3	4.1
19	16.6	6.7	3.8	13.9	5.8	4.7
20	17.7	7.4	4.4	14.8	6.4	5.4
21	18.9	8.3	5.1	15.8	7.1	6.2
22	20.3	9.2	5.9	16.9	7.8	7.1
23	21.7	10.2	6.8	18.0	8.7	8.2
24	23.4	11.4	7.9	19.3	9.6	9.4
25	25.1	12.7	9.2	20.7	10.7	10.9
26	27.1	14.2	10.7	22.3	11.9	12.5
27	29.2	15.9	12.5	23.9	13.2	14.5
28	31.6	17.8	14.6	25.8	14.7	16.7
29	34.2	20.0	17.1	27.9	16.4	19.3
30	37.2	22.5	20.1	30.1	18.4	22.4
31	40.4	25.3	23.7	32.7	20.6	26.0
32	44.0	28.5	28.0	35.5	23.2	30.2
33	48.1	32.2	33.3	38.6	26.1	35.2
34	52.6	36.5	39.6	42.2	29.4	41.1
35	57.8	41.4	47.3	46.1	33.3	48.0
36	63.5	47.2	56.7	50.6	37.8	56.3
37	70.1	53.8	68.1	55.6	42.9	66.2
38	77.5	61.5	82.3	61.4	48.9	78.0
39	86.0	70.6	99.8	67.9	56.0	92.2
40	95.7	81.3	121.5	75.3	64.2	109.4
41	106.8	93.8	148.5	83.9	73.9	130.2

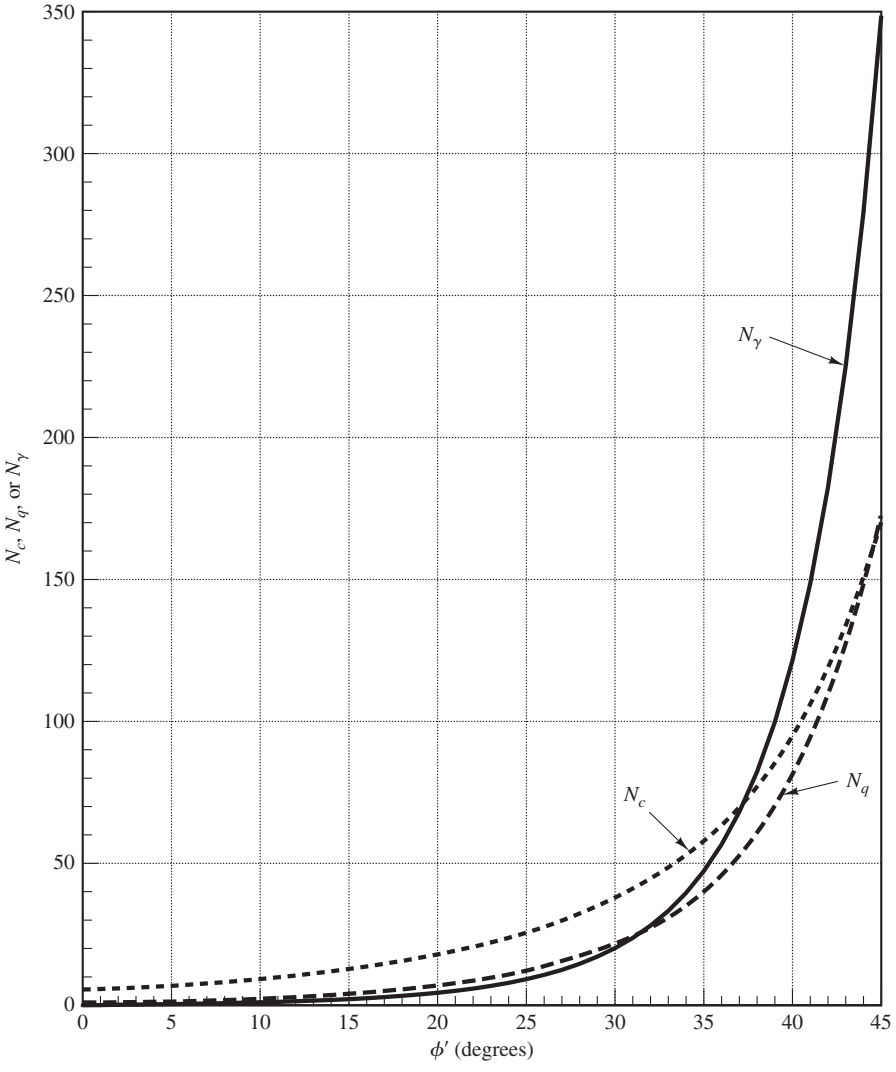

Figure 7.6 Terzaghi's bearing capacity factors.

Because of the shape and size of the failure surface, the values of c' and ϕ' only need to represent the soil between the bottom of the footing and a depth B below the bottom. The soils between the ground surface and a depth D are treated simply as overburden.

Terzaghi's formulas are presented in terms of effective stresses. However, they also may be used in total stress analyses by substituting c_T, ϕ_T, and σ_{zD} for c', ϕ', and σ'_{zD}, respectively. If saturated undrained conditions exist, we may conduct a total stress analysis with the shear strength defined as $c_T = s_u$ and $\phi_T = 0$. In this case, $N_c = 5.7$, $N_q = 1.0$, and $N\gamma = 0.0$.

Terzaghi's bearing capacity factors are:

$$N_q = \frac{a_\theta^2}{2\cos^2(45 + \phi'/2)} \tag{7.7}$$

$$a_\theta = e^{\pi(0.75-\phi'/360)\tan\phi'} \tag{7.8}$$

$$N_c = 5.7 \qquad (\text{for } \phi' = 0) \tag{7.9}$$

$$N_c = \frac{N_q - 1}{\tan\phi'} \qquad (\text{for } \phi' > 0) \tag{7.10}$$

$$N_\gamma = \frac{\tan\phi'}{2}\left(\frac{K_{p\gamma}}{\cos^2\phi'} - 1\right) \tag{7.11}$$

These bearing capacity factors are also presented in tabular form in Table 7.1. Notice that Terzaghi's N_c of 5.7 is smaller than the value of 6.28 derived from the simple bearing capacity analysis. This difference is the result of using a circular failure surface in the simple method and a more complex geometry in Terzaghi's method.

Terzaghi used a tedious graphical method to obtain values for $K_{p\gamma}$, then used these values to compute N_γ. He also computed values of the other bearing capacity factors and presented the results in plots of N_c, N_q, and N_γ as functions of ϕ'. These plots and tables such as Figure 7.6 and Table 7.1 still offer a convenient way to evaluate these parameters. However, the advent of computers and hand-held calculators has also generated the need for the following simplified formula for N_γ:

$$N_\gamma \approx \frac{2(N_q + 1)\tan\phi'}{1 + 0.4\sin(4\phi')} \tag{7.12}$$

The first author developed Equation 7.12 by fitting a curve to match Terzaghi's. It produces N_γ values within about 10 percent of Terzaghi's values. Alternatively, Kumbhojkar (1993) provides a more precise, but more complex, formula for N_γ.

Example 7.1

A square footing is to be constructed, as shown in Figure 7.7. The groundwater table is at a depth of 50 ft below the ground surface. Compute the nominal unit bearing capacity and the column load required to produce a bearing capacity failure.

Solution

For the purpose of evaluating bearing capacity, ignore the slab-on-grade floor.

For $\phi' = 30°$, $N_c = 37.2$, $N_q = 22.5$, and $N_\gamma = 20.1$ (from Table 7.1).

$$\sigma'_{zD} = \gamma D - u = (121 \text{ lb/ft}^3)(2 \text{ ft}) - 0 = 242 \text{ lb/ft}^2$$

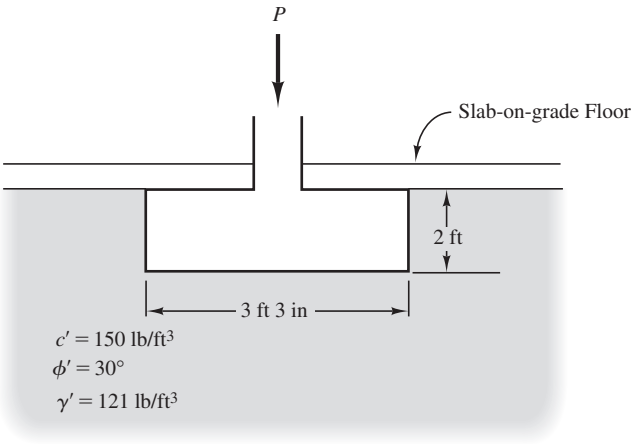

Figure 7.7 Proposed footing for Example 7.1.

$$q_n = 1.3c'N_c + \sigma'_{zD}N_q + 0.4\gamma' BN_\gamma$$

$$= (1.3)(150 \text{ lb/ft}^2)(37.2) + (242 \text{ lb/ft}^2)(22.5) + (0.4)(121 \text{ lb/ft}^3)(3.25 \text{ ft})(20.1)$$

$$= 7{,}254 + 5{,}445 + 3{,}162$$

$$= \mathbf{15{,}900 \text{ lb/ft}^2}$$

$$W_f = (3.25 \text{ ft})^2(2 \text{ ft})(150 \text{ lb/ft}^3) = 3{,}169 \text{ lb}$$

Setting $q = q_n$, using Equation 6.1, and solving for P gives:

$$q = \frac{P + W_f}{A} - u_D$$

$$15{,}900 \text{ lb/ft}^2 = \frac{P + 3{,}169 \text{ lb}}{(3.25 \text{ ft})^2} - 0$$

$$P = 165{,}000 \text{ lb}$$

$$P = \mathbf{165 \text{ k}}$$

According to this analysis, a column load of 165 k would cause a bearing capacity failure of this footing. Nearly half of this capacity comes from the first term in the bearing capacity formula and is therefore dependent on the cohesion of the soil. Since the cohesive strength is rather tenuous, it is prudent to use conservative values of c' in bearing capacity analyses. In contrast, the frictional strength is more reliable and does not need to be interpreted as conservatively.

Example 7.2

The proposed continuous footing shown in Figure 7.8 will support the exterior wall of a new industrial building. The underlying soil is an undrained clay, and the groundwater table is

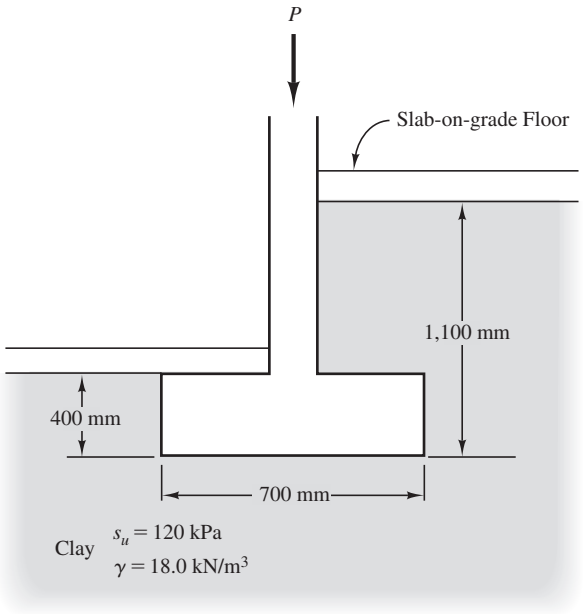

Figure 7.8 Proposed footing for Example 7.2.

below the bottom of the footing. Compute the nominal unit bearing capacity, and compute the wall load required to cause a bearing capacity failure.

Solution

This analysis uses the undrained shear strength, s_u. Therefore, we will use Terzaghi's bearing capacity formula with $c_T = s_u = 120$ kPa and $\phi_T = 0$.

For $\phi_T = 0$, $N_c = 5.7$, $N_q = 1$, and $N_\gamma = 0$ (values for $\phi' = 0$ from Table 7.1).

The depth of embedment, D, is measured from the lowest ground surface, so $D = 0.4$ m.

$$\sigma'_{zD} = \gamma D = (18.0)(0.4) = 7.2 \text{ kPa}$$

$$q_n = s_u N_c + \sigma'_{zD} N_q + 0.5\gamma' B N_\gamma$$

$$= (120)(5.7) + (7.2)(1) + 0.5\gamma' B(0)$$

$$= \mathbf{691 \text{ kPa}}$$

The zone above the bottom of the footing is partly concrete and partly soil. The weight of this zone is small compared to the wall load, so compute it using 21 kN/m^3 as the estimated weighted average for γ:

$$W_f = (0.7 \text{ m})\left(\frac{0.4 \text{ m} + 1.1 \text{ m}}{2}\right)(21 \text{ kN/m}^3) = 11 \text{ kN/m}^3$$

Using Equation 6.2:

$$q_n = q = \frac{P + W_f}{B} - u_D$$

$$691 \text{ kPa} = \frac{P + 11 \text{ kN/m}}{0.7 \text{ m}} - 0$$

$$P = \mathbf{473 \text{ kN/m}}$$

Terzaghi's method is still often used, primarily because it is simple and familiar. However, it does not consider special cases, such as rectangular footings, inclined loads, or footings with large depth-to-width ratios.

Vesić's Bearing Capacity Formulas

The topic of bearing capacity has spawned extensive research and numerous methods of analysis. Skempton (1951), Meyerhof (1953), Brinch Hansen (1961b), DeBeer and Ladanyi (1961), Meyerhof (1963), Brinch Hansen (1970), and many others have contributed. The bearing capacity formula developed by Vesić (1973, 1975) is based on theoretical and experimental findings from these and other sources and is an excellent alternative to Terzaghi's formulas. It produces more accurate bearing capacity values, and it applies to a much broader range of loading and geometry conditions. The primary disadvantage is its added complexity.

Vesić retained Terzaghi's basic format and added the following additional factors:

s_c, s_q, s_γ = shape factors
d_c, d_q, d_γ = depth factors
i_c, i_q, i_γ = load inclination factors
b_c, b_q, b_γ = base inclination factors
g_c, g_q, g_γ = ground inclination factors

He incorporated these factors into the bearing capacity formula as follows:

$$q_n = c'N_c s_c d_c i_c b_c g_c + \sigma'_{zD} N_q s_q d_q i_q b_q g_q + 0.5\gamma' B N_\gamma s_\gamma d_\gamma i_\gamma b_\gamma g_\gamma \tag{7.13}$$

Once again, this formula is written in terms of the effective stress parameters c' and ϕ', but also may be used in a total stress analysis by substituting c_T and ϕ_T for c' and ϕ', respectively. For undrained total stress analyses, use $c_T = s_u$ and $\phi_T = 0$.

Terzaghi's formulas consider only vertical loads acting on a footing with a horizontal base with a level ground surface, whereas Vesić's factors allow any or all of these conditions to vary. The notation for these factors is shown in Figure 7.9.

Shape Factors

Vesić considered a broader range of footing shapes and defined them in his s factors:

$$s_c = 1 + \left(\frac{B}{L}\right)\left(\frac{N_q}{N_c}\right) \tag{7.14}$$

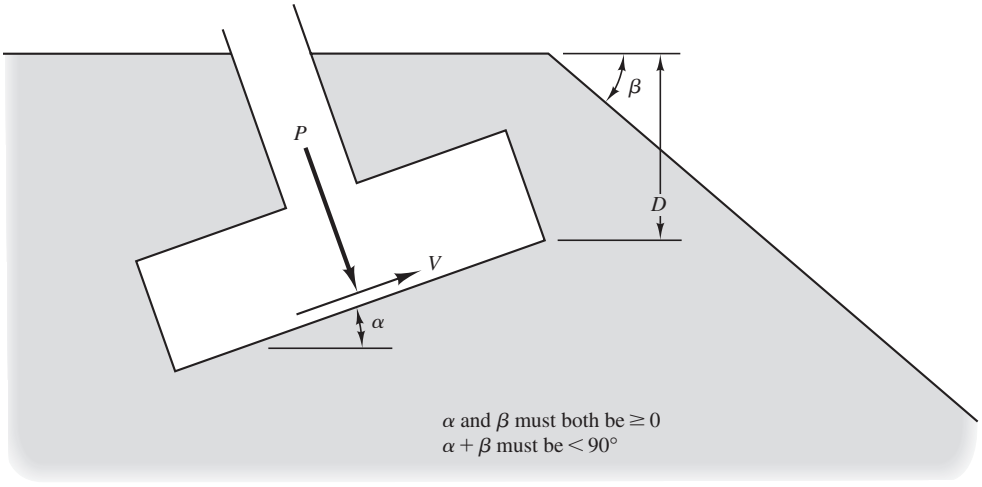

Figure 7.9 Notation for Vesić's load inclination, base inclination, and ground inclination factors. All angles are expressed in degrees.

$$s_q = 1 + \left(\frac{B}{L}\right)\tan\phi' \tag{7.15}$$

$$s_\gamma = 1 - 0.4\left(\frac{B}{L}\right) \tag{7.16}$$

For continuous footings, B/L is small, so s_c, s_q, and s_γ are close to 1. This means the shape factors may be ignored when analyzing continuous footings.

Depth Factors

Unlike Terzaghi, Vesić has no limitations on the depth of the footing. However, other methods should be used for pile foundations, for reasons discussed in Section 15.1. The depth of the footing is considered in the following depth factors:

$$d_c = 1 + 0.4k \tag{7.17}$$

$$d_q = 1 + 2k\tan\phi'(1 - \sin\phi')^2 \tag{7.18}$$

$$d_\gamma = 1 \tag{7.19}$$

For relatively shallow footings ($D/B \leq 1$), use $k = D/B$. For deeper footings ($D/B > 1$), use $k = \tan^{-1}(D/B)$ with the $\tan^{-1}$ term expressed in radians. Note that this produces a discontinuous function at $D/B = 1$.

Load Inclination Factors

The load inclination factors are for loads that do not act perpendicular to the base of the footing, but still act through its centroid (eccentric loads are discussed in Chapter 9). The variable P refers to the component of the load that acts perpendicular to the bottom of the footing, and V refers to the component that acts parallel to the bottom.

The load inclination factors are:

$$i_c = 1 - \frac{mV}{Ac'N_c} \geq 0 \tag{7.20}$$

$$i_q = \left[1 - \frac{V}{P + \dfrac{Ac'}{\tan\phi'}}\right]^m \geq 0 \tag{7.21}$$

$$i_\gamma = \left[1 - \frac{V}{P + \dfrac{Ac'}{\tan\phi'}}\right]^{m+1} \geq 0 \tag{7.22}$$

For loads inclined in the B direction:

$$m = \frac{2 + B/L}{1 + B/L} \tag{7.23}$$

For loads inclined in the L direction:

$$m = \frac{2 + L/\mathrm{B}}{1 + L/\mathrm{B}} \tag{7.24}$$

where

V = applied shear load
P = applied normal load
A = base area of footing
c' = effective cohesion (use $c = s_u$ for undrained analyses)
ϕ' = effective friction angle (use $\phi' = \phi_T = 0$ for undrained analyses)
B = footing width
L = footing length

If the load acts perpendicular to the base of the footing, the i factors equal 1 and may be neglected. The i_q and i factors also equal 1 when $\phi' = \phi_T = 0$.

See the discussion in Section 7.10 for additional information on design of spread footings subjected to applied shear loads.

Base Inclination Factors

The vast majority of footings are built with horizontal bases. However, if the applied load is inclined at a large angle from the vertical, it may be better to incline the base of the footing to the same angle so the applied load acts perpendicular to the base. However, keep in mind that such footings may be difficult to construct.

The base inclination factors are:

$$b_c = 1 - \frac{\alpha}{147^\circ} \tag{7.25}$$

$$b_q = b_\gamma = \left(1 - \frac{\alpha \tan \phi'}{57^\circ}\right)^2 \tag{7.26}$$

If the base of the footing is level, which is the usual case, all of the b factors become equal to 1 and may be ignored.

Ground Inclination Factors

Footings located near the top of a slope have a lower bearing capacity than those on level ground. To account for this, Vesić defined the ground inclination factors:

$$g_c = 1 - \frac{\beta}{147^\circ} \tag{7.27}$$

$$g_q = g_\gamma = (1 - \tan \beta)^2 \tag{7.28}$$

If the ground surface is level ($\beta = 0$), the g factors become equal to 1 and may be ignored.

Another method of estimating the bearing capacity of footings located on sandy slopes is presented in Section 7.8. Other considerations when placing footings on or near slopes are discussed in Chapter 9.

Bearing Capacity Factors

Vesić used the following formulas to compute the bearing capacity factors N_q and N_c:

$$N_q = e^{\pi \tan \phi'} \tan^2(45 + \phi'/2) \tag{7.29}$$

$$N_c = \frac{N_q - 1}{\tan \phi'} \qquad (\text{for } \phi' > 0) \tag{7.30}$$

$$N_c = 5.14 \qquad (\text{for } \phi' = 0) \tag{7.31}$$

Most other authorities also accept Equations 7.29 to 7.31, or others that produce very similar results. However, there is much more disagreement regarding the proper value of N_γ. Relatively small changes in the geometry of the failure surface below the footing can create significant differences in N_γ, especially in soils with high friction angles. Vesić recommended the following formula:

$$N_\gamma = 2(N_q + 1)\tan\phi' \tag{7.32}$$

Vesić's bearing capacity factors also are presented in tabular form in Table 7.1. The application of Vesić's formula is illustrated in Example 7.3 later in this chapter.

7.3 GROUNDWATER EFFECTS

The presence of shallow groundwater affects shear strength in two ways: the reduction of apparent cohesion, and the increase in pore water pressure. Both of these affect bearing capacity, and thus need to be considered.

Apparent Cohesion

Sometimes soil samples obtained from the exploratory borings are not saturated, especially if the site is in an arid or semi-arid area. These soils have additional shear strength due to the presence of apparent cohesion, as discussed in Section 3.5. However, this additional strength will disappear if the moisture content increases. Water may come from landscape irrigation, rainwater infiltration, leaking pipes, rising groundwater, or other sources. Therefore, we do not rely on the strength due to apparent cohesion.

In order to remove the apparent cohesion effects and simulate the "worst case" condition, geotechnical engineers usually wet the samples in the lab prior to testing. This may be done by simply soaking the sample, or, in the case of the triaxial test, by backpressure saturation. However, even with these precautions, the cohesion measured in the laboratory test may still include some apparent cohesion. Therefore, we often perform bearing capacity computations using a cohesion value less than that measured in the laboratory.

Pore Water Pressure

If there is enough water in the soil to develop a groundwater table, and this groundwater table is within the potential shear zone, then pore water pressures will be present, the effective stress and shear strength along the failure surface will be smaller, and the nominal unit bearing capacity will be reduced (Meyerhof, 1955). We must consider this effect when conducting bearing capacity computations.

When exploring the subsurface conditions, we determine the current location of the groundwater table and worst-case (highest) location that might reasonably be expected during the life of the proposed structure. We then determine which of the following three cases describes the worst-case field conditions as shown in Figure 7.10.

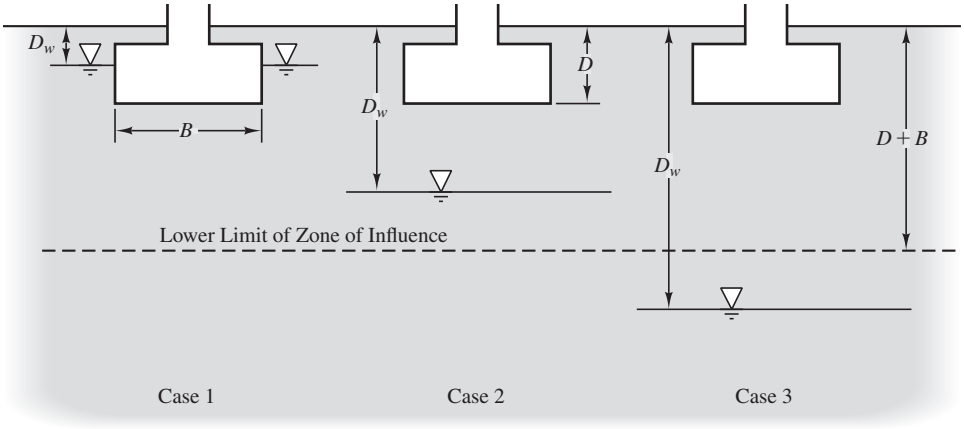

Figure 7.10 Three groundwater cases for bearing capacity analyses.

Case 1: $D_w \leq D$
Case 2: $D < D_w < D + B$
Case 3: $D + B \leq D_w$

We account for the decreased effective stresses along the failure surface by adjusting the effective unit weight, γ', in the third term of Equations 7.4 to 7.6 and 7.13 (Vesić, 1973). The effective unit weight is the value that, when multiplied by the appropriate soil thickness, will give the vertical effective stress. It is the weighted average of the buoyant unit weight, γ_b, and the unit weight, γ, and depends on the position of the groundwater table. We compute γ' as follows:

For Case 1 ($D_w \leq D$):

$$\gamma' = \gamma_b = \gamma - \gamma_w \tag{7.33}$$

For Case 2 ($D < D_w < D + B$):

$$\gamma' = \gamma - \gamma_w\left(1 - \left(\frac{D_w - D}{B}\right)\right) \tag{7.34}$$

For Case 3 ($D + B \leq D_w$; no groundwater correction is necessary):

$$\gamma' = \gamma \tag{7.35}$$

In Case 1, the second term in the bearing capacity formulas also is affected, but the appropriate correction is implicit in the computation of σ'_{zD}.

If a total stress analysis is being performed, do not apply any groundwater correction because the groundwater effects are supposedly implicit within the values of c_T and ϕ_T. In this case, simply use $\gamma' = \gamma$ in the bearing capacity equations, regardless of the groundwater table position.

Example 7.3

A 3 m square footing is to be built as shown in Figure 7.11. Compute the nominal unit bearing capacity.

Solution

Determine groundwater case:

$D_w = 1.5$ m; $D = 1.0$ m; $B = 3$ m $\quad D < D_w < D + B \quad \therefore$ Case 2 applies

Using Equation 7.34:

$$\gamma' = \gamma - \gamma_w\left(1 - \left(\frac{D_w - D}{B}\right)\right) = 18.5 - 9.8\left(1 - \left(\frac{1.5 - 1.0}{3.0}\right)\right) = 10.3 \text{ kN/m}^3$$

Use Vesić's method with γ' in the third term. Since $c' = 0$, there is no need to compute any of the other factors in the first term of the bearing capacity equation.

For $\phi' = 30°$, $N_q = 18.4$, and $N_\gamma = 22.4$ (from Table 7.1).

$$\begin{aligned}\sigma'_{zD} &= \gamma D - u \\ &= (18.5 \text{ kN/m}^3)(1.0 \text{ m}) - 0 \\ &= 18.5 \text{ kPa}\end{aligned}$$

$$s_q = 1 + \left(\frac{B}{L}\right)\tan\phi' = 1 + \left(\frac{3}{3}\right)\tan 30° = 1.58$$

$$k = \frac{D}{B} = \frac{1}{3} = 0.33$$

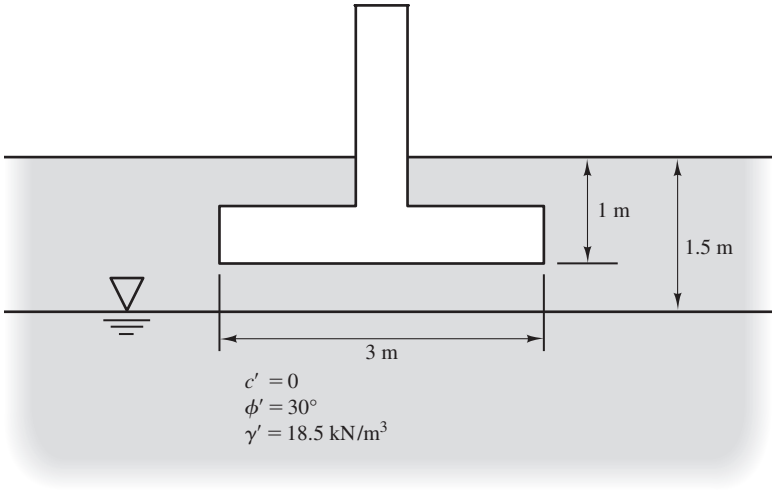

Figure 7.11 Proposed footing for Example 7.3.

$$d_q = 1 + 2k \tan \phi'(1 - \sin \phi')^2$$
$$= 1 + 2(0.33)\tan 30°(1 - \sin 30°)^2$$
$$= 1.10$$
$$s_\gamma = 1 - 0.4\left(\frac{3}{3}\right) = 0.6$$

The various i, b, and g factors in Vesić's equation are all equal to 1, and thus may be ignored.

$$q_n = c'N_c s_c d_c i_c b_c g_c + \sigma'_{zD} N_q s_q d_q i_q b_q g_q + 0.5\gamma' B N_\gamma s_\gamma d_\gamma i_\gamma b_\gamma g_\gamma$$
$$= 0 + 18.5(18.4)(1.58)(1.10) + 0.5(10.3)(3)(22.4)(0.6)(1)$$
$$= \mathbf{799\ kPa}$$

7.4 SELECTION OF SOIL STRENGTH PARAMETERS

Proper selection of the soil strength parameters, c' and ϕ', can be the most difficult part of performing bearing capacity analyses. Field and laboratory test data are often incomplete and ambiguous, and thus difficult to interpret. In addition, the computed nominal unit bearing capacity, q_n, is very sensitive to changes in the shear strength. For example, if a bearing capacity analysis on a sandy soil is based on $\phi' = 40°$, but the true friction angle is only 35° (a 13 percent drop), the nominal unit bearing capacity will be 50 to 60 percent less than expected. Thus, it is very important not to overestimate the soil strength parameters. This is why most engineers intentionally use a conservative interpretation of field and laboratory test data when assessing soil strength parameters.

Degree of Saturation and Location of Groundwater Table

As discussed in Section 7.3, soils that are presently dry could become wetted sometime during the life of the structure. It is prudent to design for the worst-case conditions, so we nearly always use the saturated strength when performing bearing capacity analyses, even if the soil is not currently saturated in the field. This produces worst-case values of c' and ϕ'. We can do this by saturating, or at least soaking, the samples in the laboratory before testing them. However, determining the location of the groundwater table is a different matter. We normally attempt to estimate the highest potential location of the groundwater table and design accordingly using the methods described in Section 7.3. The location of the groundwater table influences the bearing capacity because of its effect on the effective stress, σ'.

Drained Versus Undrained Strength

Footings located on saturated cohesive soils generate positive excess pore water pressures when they are loaded, so the most likely time for a bearing capacity failure is immediately after the load is applied. Therefore, we conduct a short-term undrained bearing capacity analyses on these soils using the undrained shear strength, s_u.

For footings on saturated cohesionless soils, any excess pore water pressures are very small and dissipate very rapidly. Therefore, we conduct a long-term drained bearing capacity analyses on these soils using the effective cohesion and effective friction angle, c' and ϕ'.

Saturated intermediate soils, such as silts, are likely to be partially drained, and engineers have varying opinions on how to evaluate them. The more conservative approach is to use the undrained strength, but many engineers use design strengths somewhere between the drained and undrained strengths.

Unsaturated soils are more complex and thus more difficult to analyze. If the groundwater table will always be well below the ground surface, many engineers use total stress parameters c_T and ϕ_T based on samples that have been "soaked," but not necessarily fully saturated, in the laboratory. Another option is to treat such soils as being fully saturated and analyze them as such.

7.5 DESIGN OF SPREAD FOOTINGS AGAINST BEARING CAPACITY FAILURE

Design of spread footings against bearing capacity failure, hence satisfying a geotechnical strength requirement, may be performed using either the ASD or the LRFD method.

ASD Method

To use ASD, we divide the nominal unit bearing capacity by a factor of safety to obtain the *allowable bearing capacity*, q_a:

$$q_a = \frac{q_n}{F} \tag{7.36}$$

where

q_a = allowable bearing capacity
q_n = nominal unit bearing capacity
F = factor of safety

We then design the foundation so that the bearing pressure, q, does not exceed the allowable bearing pressure, q_a:

$$q \leq q_a \tag{7.37}$$

Most building codes do not specify design factors of safety. Therefore, engineers must use their own discretion and professional judgment when selecting F. Items to consider when selecting a design factor of safety include the following:

- **Soil type**—Shear strength in clays is less reliable than that in sands, and more failures have occurred in clays than in sands. Therefore, use higher factors of safety in clays.
- **Site characterization data**—Projects with minimal subsurface exploration and laboratory or in situ tests have more uncertainty in the design soil parameters, and

thus require higher factors of safety. However, when extensive site characterization data is available, there is less uncertainty so lower factors of safety may be used.

- **Soil variability**—Projects on sites with erratic soil profiles should use higher factors of safety than those with uniform soil profiles.
- **Importance of the structure and the consequences of a failure**—Important projects, such as hospitals, where foundation failure would be more catastrophic may use higher factors of safety than less important projects, such as agricultural storage buildings, where cost of construction is more important. Likewise, permanent structures justify higher factors of safety than temporary structures, such as construction falsework. Structures with large height-to-width ratios, such as chimneys or towers, could experience more catastrophic failure, and thus should be designed using higher factors of safety.
- **The likelihood of the design load ever actually occurring**—Some structures, such as grain silos, are much more likely to actually experience their design loads, and thus might be designed using a higher factor of safety. Conversely, office buildings are much less likely to experience the design load, and might use a slightly lower factor of safety.

Figure 7.12 shows ranges of these parameters and typical values of the factor of safety. Geotechnical engineers usually use factors of safety between 2.5 and 3.5 for bearing capacity analyses of shallow foundations. Occasionally we might use values as low as 2.0 or as high as 4.0.

The true factor of safety is probably much greater than the design factor of safety, because of the following:

- The shear strength data are normally interpreted conservatively, so the design values of c and ϕ implicitly contain another factor of safety.
- The service loads are probably less than the design loads.
- Settlement, not bearing capacity, often controls the final design, so the footing will likely be larger than that required to satisfy bearing capacity criteria.
- Spread footings are commonly built somewhat larger than the plan dimensions.

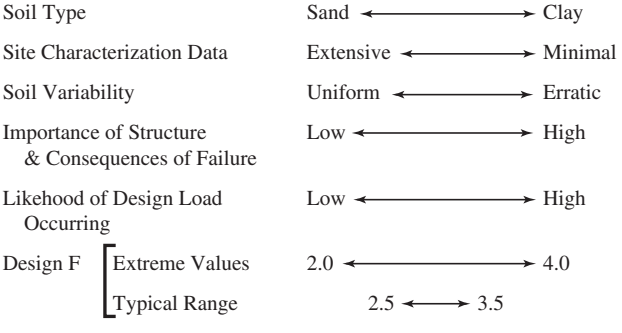

Figure 7.12 Factors affecting the design factor of safety, and typical values of F.

Example 7.4

A square footing is to be designed to support a column. The design loads on the column are all downward and concentric. Calculations of the design loads using the required load combinations specified by ASCE 7-11 show that the controlling load combination gives a design column load of 450 k. The embedment depth of the square footing is to be 3 ft. The underlying soil has an undrained shear strength of 2,000 lb/ft^2 and a unit weight of 109 lb/ft^3. The groundwater table is at a depth of 4 ft. Using the ASD method, determine the minimum required footing width to maintain a factor of safety of 3 against a bearing capacity failure.

Solution

Using Terzaghi's method:

This is a cohesive soil that is being evaluated using the undrained strength, so we must substitute $c' = s_u$ and $\phi' = 0$ in the bearing capacity formula.

$$\sigma'_{zD} = \gamma D - u = (109 \text{ lb/ft}^3)(3 \text{ ft}) - 0 = 327 \text{ lb/ft}^2$$

$$\begin{aligned} q_n &= 1.3 s_u N_c + \sigma'_{zD} N_q + 0.4 \gamma' B N_\gamma \\ &= 1.3(2{,}000 \text{ lb/ft}^2)(5.7) + (327 \text{ lb/ft}^2)(1) + 0 \\ &= 15{,}147 \text{ lb/ft}^2 \end{aligned}$$

$$q_a = \frac{q_n}{F} = \frac{15{,}147 \text{ lb/ft}^2}{3} = 5{,}049 \text{ lb/ft}^2$$

$$W_f = 3B^2(150 \text{ lb/ft}^3) = 450B^2$$

$$q_a = q = \frac{P + W_f}{A} - u \Rightarrow 5{,}049 = \frac{450{,}000 + 450B^2}{B^2} \Rightarrow B = 9.89 \text{ ft}$$

Round off to the nearest 3 in (with SI units, round off to the nearest 100 mm):

$$\boldsymbol{B = 10 \text{ ft } 0 \text{ in}}$$

Example 7.5 below illustrates how the concept of equivalent uniformly loaded footing introduced in Chapter 6 can be used to size an eccentrically loaded footing.

Example 7.5

A footing is to be designed to support a column as described in Example 7.4, except that there is now a one way design moment of 800 k-ft, in addition to the downward design load of 450 k. Using the ASD method, size a footing to maintain a factor of safety of 3 against a bearing capacity failure.

Solution

Design using the concept of equivalent uniformly loaded footing. For one way eccentricity, it would be more effective to use a rectangular footing with an unmodified width B and an effective length L' given by Equation 6.11:

$$L' = L - 2e$$

In theory, there are an infinite number of combinations of B and L that would work. The optimum B and L would be determined based on constructability, cost, and other relevant factors. For this example, we will assume a B of 10 ft, the same as obtained in Example 7.4 for a square footing without moment load. For $B = 10$ ft,

$$W_f = DBL(150 \text{ lb/ft}^3) = (3)(10)L(150 \text{ lb/ft}^3) = 4{,}500L$$

Calculate one way eccentricity e using Equation 6.4:

$$e = \frac{M}{P + W_f} = \frac{800{,}000}{450{,}000 + 4{,}500L}$$

The equivalent footing length or L' is given by Equation 6.11 as,

$$L' = L - 2e = L - 2\left(\frac{800{,}000}{450{,}000 + 4{,}500L}\right)$$

We will now proceed with computing q_n using Vesic's method using an equivalent footing $B \times L'$, where L' is defined as derived above.

This is a cohesive soil that is being evaluated using the undrained strength, so we must substitute $c' = s_u$ and $\phi' = 0$ in the bearing capacity formula.

For $\phi' = 0$, $N_c = 5.1$, $N_q = 1$, and $N_\gamma = 0$ (from Table 7.1).

$$\sigma'_{zD} = \gamma D - u = (109 \text{ lb/ft}^3)(3 \text{ ft}) - 0 = 327 \text{ lb/ft}^2$$

Use a width $B = 10$ ft and a length of L' to compute the shape factors (Equations 7.14 and 7.15):

$$s_c = 1 + \left(\frac{B}{L'}\right)\left(\frac{N_q}{N_c}\right) = 1 + \left(\frac{10}{L'}\right)\left(\frac{1}{5.1}\right) = 1 + \frac{1.96}{L'}$$

$$s_q = 1 + \left(\frac{B}{L'}\right)\tan\phi' = 1 + \left(\frac{B}{L'}\right)\tan 0 = 1$$

Use a width $B = 10$ ft and a depth $D = 3$ ft to compute the depth factors (Equations 7.17 and 7.18):

$$k = \frac{D}{B} = \frac{3}{10} = 0.3$$

$$d_c = 1 + 0.4\text{k} = 1 + (0.4)(0.3) = 1.12$$

$$\begin{aligned} d_q &= 1 + 2k \tan \phi'(1 - \sin \phi')^2 \\ &= 1 + 2(0.3)\tan 0(1 - \sin 0)^2 \\ &= 1 \end{aligned}$$

For this case, the factors for load, base, and ground inclination in Vesić's equation are all equal to 1, and thus may be ignored.

$$\begin{aligned} q_n &= c'N_c s_c d_c i_c b_c g_c + \sigma'_{zD} N_q s_q d_q i_q b_q g_q + 0.5\gamma' B N_\gamma s_\gamma d_\gamma i_\gamma b_\gamma g_\gamma \\ &= (2{,}000)(5.1)\left(1 + \frac{1.96}{L'}\right)(1.12) + 327(1)(1)(1) + 0 \\ &= (11{,}424)\left(1 + \frac{1.96}{L'}\right) + 327 \end{aligned}$$

$$q_a = \frac{q_n}{F} = \frac{(11{,}424)\left(1 + \frac{1.96}{L'}\right) + 327}{3} = 3{,}917 + \frac{7463.68}{L'}$$

$$q_a = q = \frac{P + W_f}{A} - u \Rightarrow 3{,}917 + \frac{7{,}463.68}{L'} = \frac{450{,}000 + 4{,}500L}{10L'}$$

which simplifies to

$$L = \frac{3{,}917L' - 37{,}536}{450}$$

Combining with

$$L' = L - 2\left(\frac{800{,}000}{450{,}000 + 4{,}500L}\right)$$

and solving by trial and error gives $L' = 11.23$ ft and $L = 14.34$ ft.

Round up to the nearest 3 in (with SI units, round off to the nearest 100 mm):

$$L = 14.5\,\text{ft}$$

Check that $e \leq \frac{L}{6}$:

$$e = \frac{800{,}000}{450{,}000 + 4{,}500L} = \frac{800{,}000}{450{,}000 + 4{,}500(14.5)} = 1.55 \text{ ft}$$

$$\frac{L}{6} = \frac{14.5}{6} = 2.42 \text{ ft}$$

Therefore, $e \leq \frac{L}{6}$. OK

The required rectangular footing size is then $B =$ **10 ft** and $L =$ **14 ft 6 in**.

Load and Resistance Factor Design Method

The LRFD method uses load and resistance factors instead of the factor of safety to ensure an adequate design. The process of designing a shallow foundation against bearing capacity failure using LRFD is as follows:

1. Compute the nominal unit bearing capacity, q_n, using Terzaghi's method (Equations 7.4 through 7.6) or Vesić's method (Equation 7.13).
2. Compute the nominal downward load capacity, P_n, using:

$$P_n = q_n A \tag{7.38}$$

where

P_n = nominal downward load capacity
q_n = nominal unit bearing capacity
A = base area of foundation

In theory, P_n is the downward load required to produce a bearing capacity failure.

3. Obtain the appropriate resistance factor, ϕ, from the appropriate code. Example resistance factors for bearing capacity of shallow foundations (AASHTO, 2012) are given in Table 7.2.
4. Compute the factored column load, P_u, using the same standard used for the resistance factors. (Note that factored loads derived from Equations 5.12 to 5.18 are based on ASCE-7 and should not be used with the AASHTO resistance factors in Table 7.2.)

TABLE 7.2 RESISTANCE FACTORS AT GEOTECHNICAL ULTIMATE LIMIT STATES FOR FOOTING DESIGN USING THE LRFD METHOD (Adapted from AASHTO, 2012, Table 10.5.5.2.2-1.)

	Method/Soil/Condition	Resistance Factor
Bearing Resistance	Theoretical method (Munfakh et al., 2001), in clay	0.50
	Theoretical method (Munfakh et al., 2001), in sand, using CPT	0.50
	Theoretical method (Munfakh et al., 2001), in sand, using SPT	0.45
	Semiempirical methods (Meyerhof, 1957), all soils	0.45
	Footings on rock	0.45
	Plate load test	0.55
Sliding	Precast concrete placed on sand	0.90
	Cast-in-place concrete on sand	0.80
	Cast-in-place or precast concrete on clay	0.85
	Soil on soil	0.90
	Passive earth pressure component of sliding resistance	0.50

5. Compute the factored weight of the foundation, which is treated as a dead load, as $\gamma_D W_f$, where γ_D is the load factor for dead load.
6. Design the foundation so that the following condition is satisfied:

$$P_u + \gamma_D W_f \leq \phi P_n \tag{7.39}$$

Example 7.6

A single-column highway bridge bent is to be supported on a square spread footing founded on sand. The bottom of this footing will be 1.8 m below the adjacent ground surface. The factored vertical compressive design load, P_u, plus the factored weight of the foundation is 4,500 kN when computed using the AASHTO load factors. The soil has $c' = 0$ and $\phi' = 31°$ (based on empirical correlations with SPT data) and $\gamma = 17.5$ kN/m^3. The groundwater table is at a great depth. Using the LRFD method, determine the required footing width, B, to satisfy bearing capacity requirements.

Solution

Using Terzaghi's method:

For $\phi' = 31°$, $N_c = 40.4$, $N_q = 25.3$, and $N_\gamma = 23.7$.

$$\sigma'_{zD} = \gamma D - u = (17.5 \text{ kN/m}^3)(1.8\text{m}) - 0 = 31.5 \text{ kPa}$$

$$\begin{aligned} q_n &= 1.3c'N_c + \sigma'_{zD}N_q + 0.4\gamma' B N_\gamma \\ &= 0 + (31.5)(25.3) + 0.4(17.5)(23.7)B \\ &= 797 + 166B \end{aligned}$$

$$P_n = q_n A = (797 + 166B)B^2$$

The total factored load ($P_u + \gamma_D W_f$) is given as 4,500 kN.

Per Table 7.2, recognizing that Terzaghi's method of bearing capacity analysis is a theoretical method and that the shear strength of the sand was obtained using SPT data, the resistance factor $\phi = 0.45$.

$$\begin{aligned} P_u + \gamma_D W_f &\leq \phi P_n \\ 4{,}500 &\leq 0.45(797 + 166B)B^2 \\ B &\geq \mathbf{2.9\ m} \end{aligned}$$

Collapse of the Fargo Grain Elevator

One of the most dramatic bearing capacity failures was the Fargo Grain Elevator collapse of 1955. This grain elevator, shown in Figure 7.13, was built near Fargo, North Dakota, in 1954. It was a reinforced concrete structure composed of twenty cylindrical bins and other appurtenant structures, all supported on a 15.8 m (52 ft) wide, 66.4 m (218 ft) long, 0.71 m (2 ft 4 in) thick mat foundation.

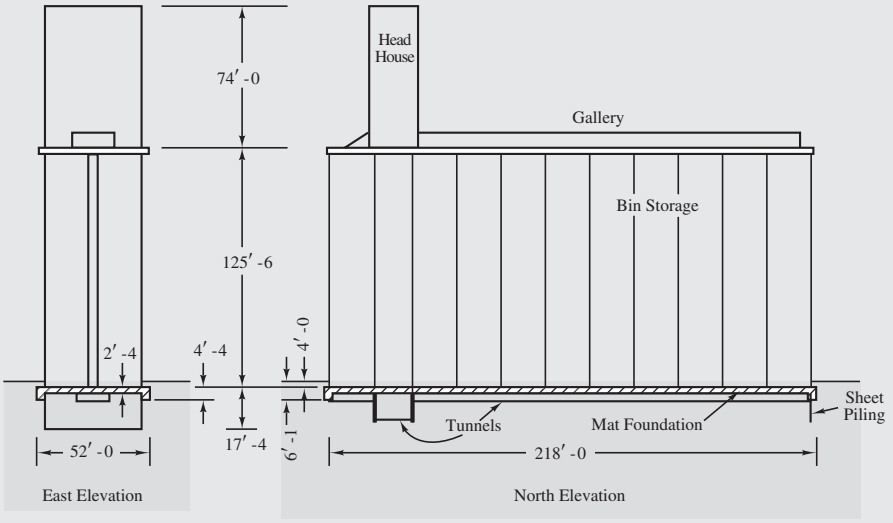

Figure 7.13 Elevation views of the elevator (Based on Nordlund and Deere, 1970; reprinted by permission of ASCE).

The average net bearing pressure, $q' = q - \sigma'_{z0}$, caused by the weight of the empty structure was 76.1 kPa (1,590 lb/ft^2). When the bins began to be filled with grain in April 1955, q' began to rise, as shown in Figure 7.14. In this type of structure, the live load (i.e., the grain) is much larger than the dead load; so by mid-June, the average net bearing pressure had tripled and reached 227 kPa (4,750 lb/ft^2). Unfortunately, as the bearing pressure rose, the elevator began to settle at an accelerating rate, as shown in Figure 7.15.

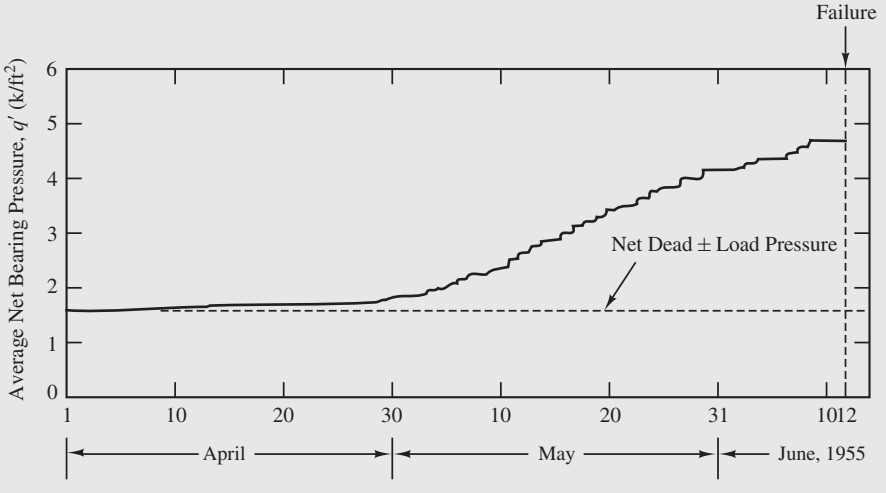

Figure 7.14 Rate of loading (Based on Nordlund and Deere, 1970; reprinted by permission of ASCE).

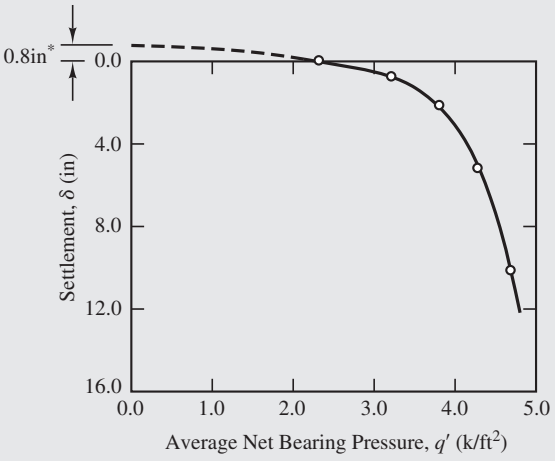

Figure 7.15 Settlement at centroid of mat (Based on Nordlund and Deere, 1970; reprinted by permission of ASCE).

Early in the morning of June 12, 1955, the elevator collapsed and was completely destroyed. This failure was accompanied by the formation of a 2 m (6 ft) bulge, as shown in Figure 7.16.

No geotechnical investigation had been performed prior to the construction of the elevator, but Nordlund and Deere (1970) conducted an extensive after-the-fact investigation. They

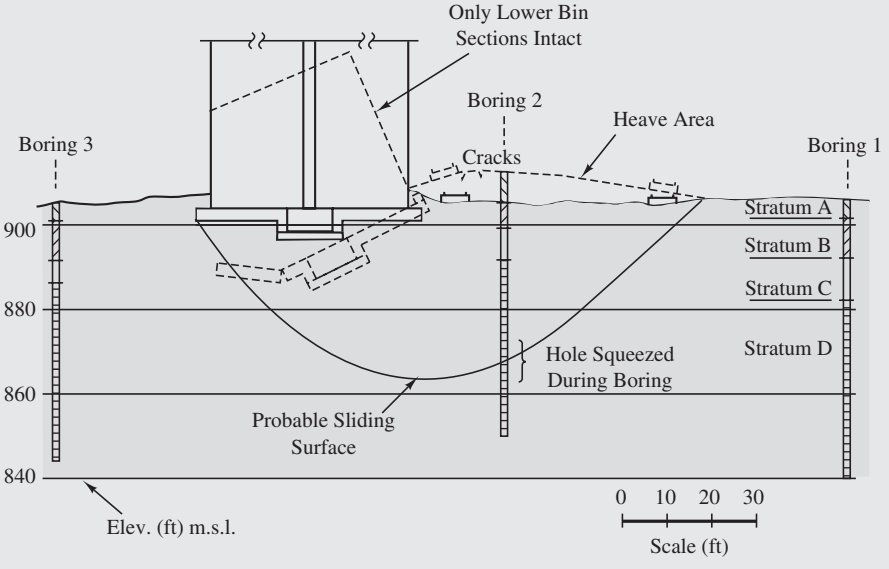

Figure 7.16 Cross section of collapsed elevator (Based on Nordlund and Deere, 1970; reprinted by permission of ASCE).

found that the soils were primarily saturated clays with $s_u = 30 - 50$ kPa (600–1,000 lb/ft^2). Bearing capacity analyses based on this data indicated a net nominal unit bearing capacity of 197 to 312 kPa (4,110–6,520 lb/ft^2) which compared well with the q' at failure of 228 kPa (4,750 lb/ft^2) (average) and 249 kPa (5,210 lb/ft^2) (maximum).

The investigation of the Fargo Grain Elevator failure demonstrated the reliability of bearing capacity analyses. Even a modest exploration and testing program would have produced shear strength values that would have predicted this failure. If such an investigation had been performed, and if the design had included an appropriate factor of safety, the failure would not have occurred. However, we should not be too harsh on the designers, since most engineers in the early 1950s were not performing bearing capacity analyses.

Although bearing capacity failures of this size are unusual, this failure was not without precedent. A very similar failure occurred in 1913 at a grain elevator near Winnipeg, Manitoba, approximately 320 km (200 miles) north of Fargo (Peck and Bryant, 1953; White, 1953; Skaftfeld, 1998). This elevator rotated to an inclination of 27° from the vertical when the soil below experienced a bearing capacity failure at an average q' of 224 kPa (4,680 lb/ft^2). The soil profile is very similar to the Fargo site, as is the average q' values at failure.

Geotechnical researchers from the University of Illinois investigated the Winnipeg failure in 1951. They drilled exploratory borings, performed laboratory tests, and computed a nominal unit bearing capacity of 246 kPa (5,140 lb/ft^2). Once again, a bearing capacity analysis would have predicted the failure, and a design with a suitable factor of safety would have prevented it. Curiously, the results of their study were published in 1953, only two years before the Fargo failure. This is a classic example of engineers failing to learn from the mistakes of others.

7.6 BEARING CAPACITY ANALYSIS IN SOIL—LOCAL AND PUNCHING SHEAR CASES

As discussed earlier, engineers rarely need to compute the local or punching shear bearing capacities because settlement analyses implicitly protect against this type of failure. In addition, a complete bearing capacity analysis would be more complex because of the following:

- These modes of failure do not have well-defined shear surfaces, such as those shown in Figure 7.1, and are therefore more difficult to evaluate.
- The soil can no longer be considered incompressible (Ismael and Vesić, 1981).
- The failure is not catastrophic (e.g., Figures 7.2b and 7.2c), so the failure load is more difficult to define.
- Scale effects make it difficult to properly interpret model footing tests.

Terzaghi (1943) suggested a simplified way to compute the local shear bearing capacity using the general shear formulas with appropriately reduced values of c' and ϕ':

$$c'_{\text{adj}} = 0.67c' \tag{7.40}$$

$$\phi'_{\text{adj}} = \tan^{-1}(0.67 \tan \phi') \tag{7.41}$$

Vesić (1975) expanded upon this concept and developed the following adjustment formula for sands with a relative density, D_r, less than 67%:

$$\phi'_{adj} = \tan^{-1}[(0.67 + D_r - 0.75D_r^2)\tan\phi'] \tag{7.42}$$

where

c'_{adj} = adjusted effective cohesion
ϕ'_{adj} = adjusted effective friction angle
D_r = relative density of sand, expressed in decimal form ($0 \leq D_r \leq 67\%$)

Although Equation 7.42 was confirmed with a few model footing tests, both methods are flawed because the failure mode is not being modeled correctly. However, local or punching shear will normally only govern the final design with shallow, narrow footings on loose sands, so an approximate analysis is acceptable. The low cost of such footings does not justify a more extensive analysis, especially if it would require additional testing.

An important exception to this conclusion is the case of a footing supported by a thin crust of strong soil underlain by a very weak soil. This would likely be governed by punching shear and would justify a custom analysis.

7.7 BEARING CAPACITY ON LAYERED SOILS

Thus far, the analyses in this chapter have considered only the condition where c', ϕ', and γ are constant with depth. However, many soil profiles are not that uniform. Therefore, we need to have a method of computing the bearing capacity of foundations on soils where c, ϕ, and γ vary with depth. There are four primary ways to do this:

1. Evaluate the bearing capacity using the lowest values of c′, ϕ', and γ in the zone between the bottom of the foundation and a depth B below the bottom, where B is the width of the foundation. This is the zone in which bearing capacity failures occur (per Figure 7.5), and thus is the only zone in which we need to assess the soil parameters. This method is conservative, since some of the shearing occurs in the other, stronger layers. However, many design problems are controlled by settlement anyway, so a conservative bearing capacity analysis may be the simplest and easiest solution. In other words, if bearing capacity does not control the design even with a conservative analysis, there is no need to conduct a more detailed analysis.
2. Use weighted average values of c', ϕ', and γ based on the relative thicknesses of each stratum in the zone between the bottom of the footing and a depth B below the bottom. This method could be conservative or unconservative, but should provide acceptable results so long as the differences in the strength parameters are not too great.
3. Consider a series of trial failure surfaces beneath the footing and evaluate the stresses on each surface using methods similar to those employed in slope stability analyses. The surface that produces the lowest value of q_n is the critical failure surface. This

method is more precise than the first two, but also requires the more effort to implement. It would be appropriate only for critical projects on complex soil profiles.

4. If a two-layer soil system exists within the zone of failure below the footing, one may use rigorous solutions derived for two-layer systems such as those found in AASHTO (2012).

Example 7.7

Using the second method described above, compute the factor of safety against a bearing capacity failure in the square footing shown in Figure 7.17.

Solution

Weighting factors:

Upper stratum: $1.1/1.8 = 0.611$

Lower stratum: $0.7/1.8 = 0.389$

Weighted values of soil parameters:

$$c' = (0.611)(5\text{ kPa}) + (0.389)(0) = 3\text{ kPa}$$

$$\phi' = (0.611)(32°) + (0.389)(38°) = 34°$$

$$\gamma = (0.611)(18.2\text{ kN/m}^3) + (0.389)(20.1\text{ kN/m}^3) = 18.9\text{ kN/m}^3$$

Groundwater case 1 ($D_w \leq D$):

$$\gamma' = \gamma - \gamma_w = 18.9\text{ kN/m}^3 - 9.8\text{ kN/m}^3 = 9.1\text{ kN/m}^3$$

$$W_f = (1.8\text{ m})^2(1.5\text{ m})(17.5\text{ kN/m}^3) + (1.8\text{ m})^2(0.4\text{ m})(23.6\text{ kN/m}^3) = 116\text{ kN}$$

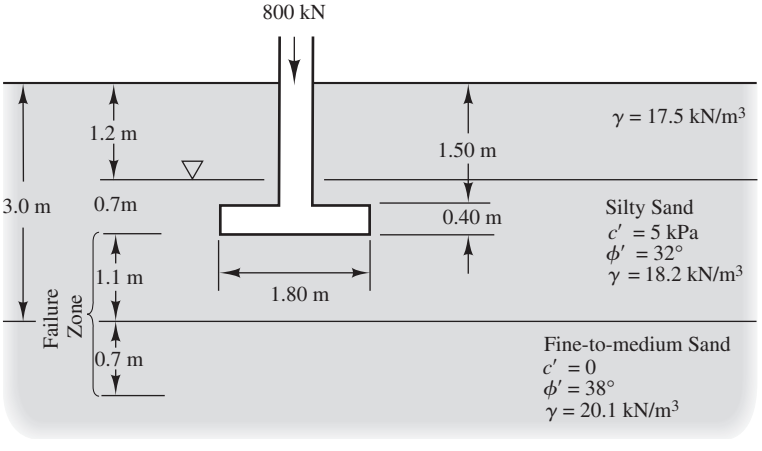

Figure 7.17 Spread footing for Example 7.7.

$$\sigma'_{zD} = \Sigma\gamma H - u$$
$$= (17.5\ \text{kN/m}^3)(1.2\ \text{m}) + (18.2\ \text{kN/m}^3)(0.7\ \text{m}) - (9.8\ \text{kN/m}^3)(0.7\ \text{m})$$
$$= 27\ \text{kPa}$$

$$q = \frac{P + W_f}{A} - u_D = \frac{800\ \text{kN} + 116\ \text{kN}}{(1.8\ \text{m})^2} - 7\ \text{kPa} = 276\ \text{kPa}$$

Using Terzaghi's formula:
For $\phi' = 34°$, $N_c = 52.6$, $N_q = 36.5$, and $N_\gamma = 39.6$.

$$q_n = 1.3c'N_c + \sigma'_{zD}N_q + 0.4\gamma' BN_\gamma$$
$$= (1.3)(3)(52.6) + (27)(36.5) + (0.4)(9.1)(1.8)(39.6)$$
$$= 1{,}450\ \text{kPa}$$

$$F = \frac{q_n}{q} = \frac{1{,}450\ \text{kPa}}{276\ \text{kPa}} = \mathbf{5.3}$$

Commentary

The computed factor of safety of 5.3 is much greater than the typical minimum values of 2.5 to 3.5. Therefore, the footing is overdesigned as far as bearing capacity is concerned. However, it is necessary to check settlement (as discussed in Chapter 8) before reducing the size of this footing.

Figure 7.18 shows a layered soil condition that deserves special attention: a shallow foundation constructed on a thin crust underlain by softer soils. Such crusts are common in many soft clay deposits, and can be deceiving because they appear to provide good support for foundations. However, the shear surface for a bearing capacity failure would extend into the underlying weak soils. This is especially problematic for wide foundations, such as mats, because they have correspondingly deeper shear surfaces.

This condition should be evaluated using the third or fourth method described above. In addition, the potential for a punching shear failure needs to be checked.

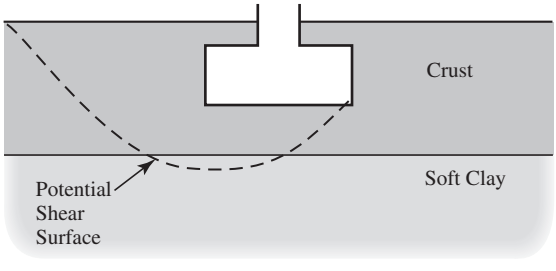

Figure 7.18 Spread footing on a hard crust underlain by softer soils.

7.8 BEARING CAPACITY OF FOOTINGS ON OR NEAR SLOPES

Vesić's bearing capacity formulas presented earlier in the chapter in Section 7.2 are able to consider footings near sloping ground. However, it is best to avoid this condition whenever possible. Special concerns for such situations include:

- The reduction in lateral support makes bearing capacity failures more likely.
- The foundation might be undermined if a shallow (or deep!) landslide were to occur.
- The near-surface soils may be slowly creeping downhill, and this creep may cause the footing to move slowly downslope. This is especially likely in clays.

However, there are circumstances where footings must be built on or near a slope. Examples include abutments of bridges supported on approach embankments, foundations for electrical transmission towers, and some buildings.

Shields et al. (1990) produced another solution for the bearing capacity of footings located on sandy slopes. This method, based on centrifuge tests, relates the bearing capacity of footings at various locations to that of a comparable footing with $D = 0$ located on level ground. Figures 7.19 to 7.21 give the resulting ratio for 2:1 and 1.5:1 slopes.

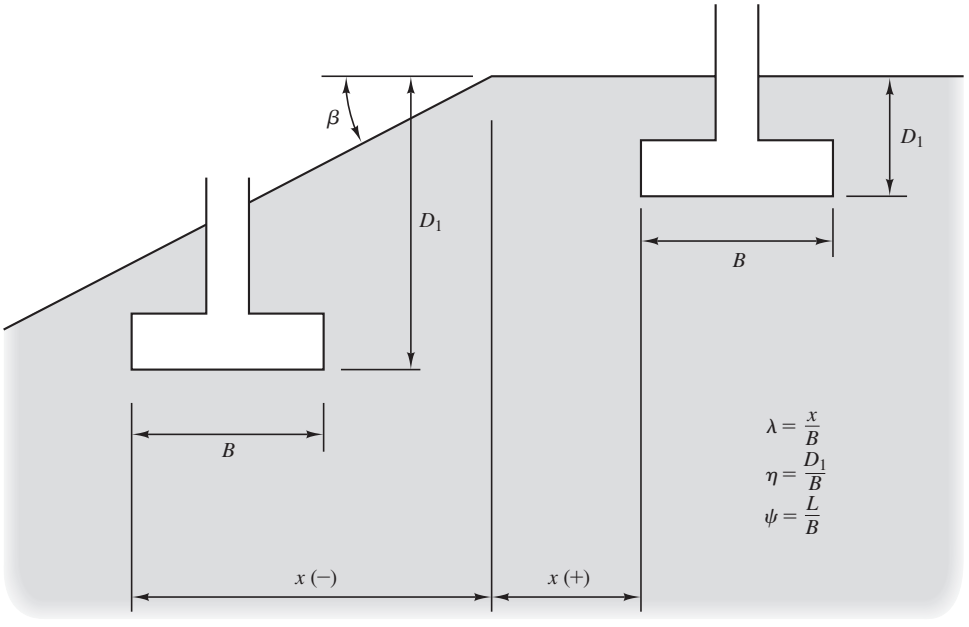

Figure 7.19 Definition of terms for computing bearing capacity of footings near or on sandy slopes (Based on Shields et al., 1990; used with permission of ASCE).

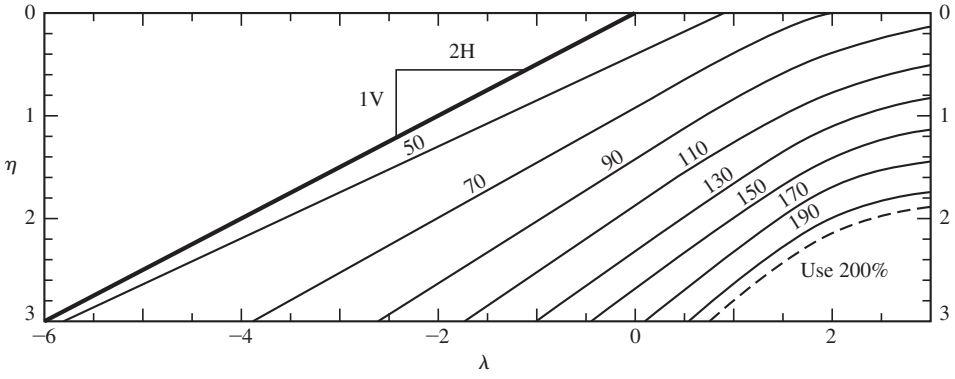

Figure 7.20 Bearing capacity of a footing near or on a 2H:1V sandy slope. The contours give the bearing capacity divided by the bearing capacity of a comparable footing located at the surface of level ground, expressed as a percentage (Based on Shields et al., 1990; used with permission of ASCE).

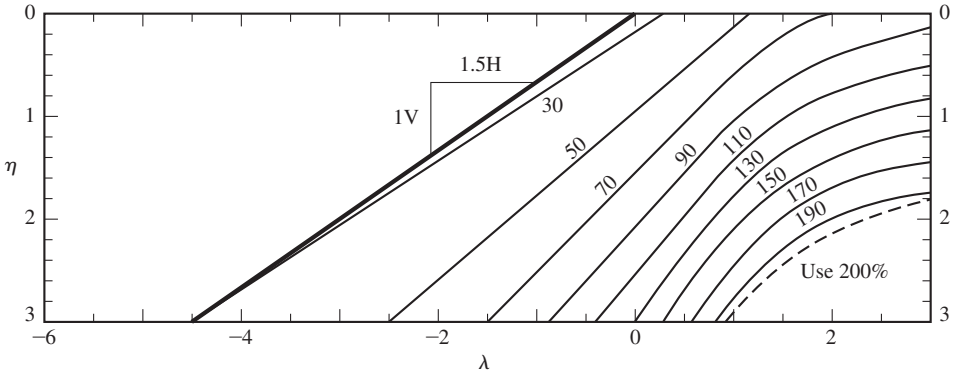

Figure 7.21 Bearing capacity of a footing near or on a 1.5H:1V sandy slope. The contours give the bearing capacity divided by the bearing capacity of a comparable footing located at the surface of level ground, expressed as a percentage (Based on Shields et al., 1990; used with permission of ASCE).

7.9 ACCURACY OF BEARING CAPACITY ANALYSES

Engineers have had a few opportunities to evaluate the accuracy of bearing capacity analyses by evaluating full-scale bearing capacity failures in real foundations, and by conducting experimental load tests on full-size foundations.

Bishop and Bjerrum (1960) compiled the results of fourteen case studies of failures or load tests on saturated clays, as shown in Table 7.3, and found the computed factor of safety in each case was within 10 percent of the true value of 1.0. This is excellent

TABLE 7.3 EVALUATIONS OF BEARING CAPACITY FAILURES ON SATURATED CLAYS (Adapted from Bishop and Bjerrum, 1960.)

	Clay Properties					
Locality	Moisture Content, w	Liquid Limit, w_L	Plastic Limit, w_P	Plasticity Index, I_P	Liquidity Index, I_L	Computed Factor of Safety, F
Loading test, Marmorerá	10	35	15	20	−0.25	0.92
Kensal Green						1.02
Silo, Transcona	50	110	30	80	0.25	1.09
Kippen	50	70	28	42	0.52	0.95
Screw pile, Lock Ryan						1.05
Screw pile, Newport						1.07
Oil tank, Fredrikstad	45	55	25	30	0.67	1.08
Oil tank A, Shellhaven	70	87	25	62	0.73	1.03
Oil tank B, Shellhaven						1.05
Silo, United States	40		20	35	1.37	0.98
Loading test, Moss	9		16	8	1.39	1.10
Loading test, Hagalund	68	55	19	18	1.44	0.93
Loading test, Torp	27	24				0.96
Loading test, Rygge	45	37				0.95

agreement, and indicates the bearing capacity analyses are very accurate in this kind of soil. The primary source of error is probably the design value of the undrained shear strength, s_u. In most practical designs, the uncertainty in s_u is probably greater than 10 percent, but certainly well within the margin of error allowed by the typical factor of safety for bearing capacity analyses.

Spread footings on sands have a high nominal unit bearing capacity, especially when the foundation width, B, is large, because these soils have a high friction angle. Small model footings, such as those described in Section 7.1, can be made to fail, but it is very difficult to induce failure in large footings on sand. For example, Briaud and Gibbens (1994) conducted static load tests on five spread footings built on a silty fine sand. The widths of these footings ranged from 1 to 3 m, the computed nominal unit bearing capacity, q_n, ranged from 800 to 1,400 kPa, and the measured load-settlement curves are shown in Figure 7.22. The smaller footings show no indication of approaching bearing capacity failure, even at bearing pressures of twice the q_n and settlements of about 150 mm. The larger footings appear to have a measured nominal unit bearing capacity close to q_n, but a settlement of well over 150 mm would be required to reach it. These curves also indicate

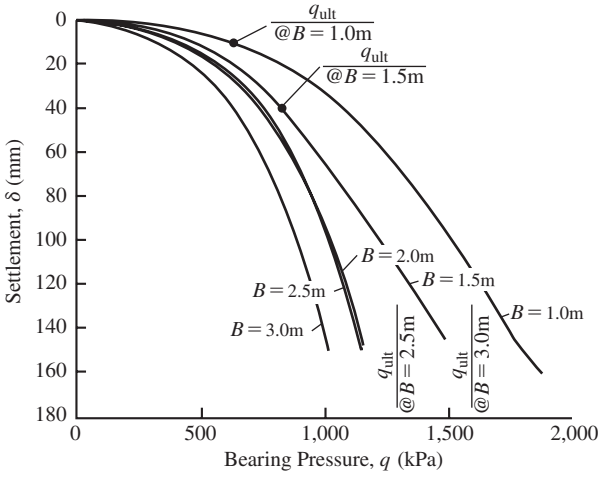

Figure 7.22 Results of static load tests on full-size spread footings (adapted from Briaud and Gibbens, 1994).

the design of the larger footings would be governed by settlement, not bearing capacity, so even a conservative evaluation of bearing capacity does not adversely affect the final design. For smaller footings, the design might be controlled by the computed bearing capacity and might be conservative. However, even then the conservatism in the design should not significantly affect the construction cost.

Therefore, we have good evidence to support the claim that bearing capacity analysis methods as presented in this chapter are suitable for the practical design of shallow foundations. Assuming reliable soil strength data is available, the computed values of q_n are either approximately correct or conservative. The design factors of safety and load and resistance factors discussed in Section 7.5 appear to adequately cover the uncertainties in the analysis.

7.10 DESIGN OF SPREAD FOOTINGS AGAINST SLIDING FAILURE

The second geotechnical ultimate limit state consists of horizontal sliding of the footing due to an applied shear load. These shear loads may be permanent, as those from retaining walls, or temporary, as with wind or seismic loads on buildings. This section discusses the design of spread footings against sliding failure using both the ASD and LRFD methods.

Sources of Shear Resistance

Spread footings resist applied shear loads in two ways: through sliding friction along the base of the footing, and through passive earth pressure on the leading edge. In addition, an active earth pressure acts on the trailing edge. All of these forces are shown in Figure 7.23.

Sliding friction is usually the principal source of shear capacity. For cohesionless soils it is modeled as a sliding friction problem, with the normal load equal to $P + W_f$ and the coefficient of sliding friction equal to μ. The active and passive pressures may be computed using the Rankine method, as discussed in Section 3.6.

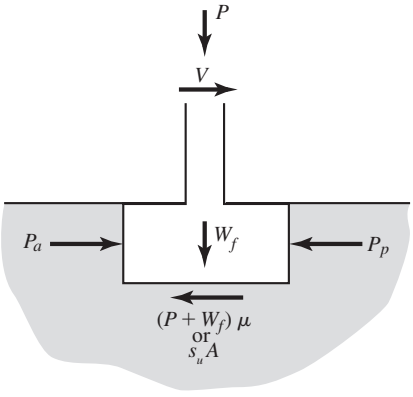

Figure 7.23 Shear load acting on a spread footing.

This is an ultimate limit state analysis, so in principle we should be able to consider the full values of these resistances, with an appropriate factor of safety or resistance factor. However, there is a significant difference in the lateral displacement required to achieve these resistances, as discussed in Section 3.6. Very little lateral movement is required to mobilize the sliding friction, perhaps on the order of 10 mm (0.4 in). This would be well within the allowable lateral deformation for most structures. However, for typical footings, 15 to 50 mm of lateral displacement would be required to mobilize the passive pressure, which is probably much more than the allowable lateral deflection. Thus, in the interest of limiting the lateral deflection, the authors recommend using only half of the passive pressure in cohesionless soils and only one quarter in cohesive soils. This is a muddling of the ultimate limit state and the serviceability limit state but is appropriate in this case because no separate serviceability analysis will be conducted.

Allowable Strength Design Method

Cohesionless Soils

In cohesionless soils, the ASD-allowable shear capacity, V_a, for footings at a site with a level ground surface is:

$$V_a = \frac{(P + W_f - u_D A)\mu + 0.5P_P}{F} - P_A \tag{7.43}$$

where

V_a = allowable shear capacity
P = downward column load
W_f = weight of footing
u_D = pore water pressure at base of footing
A = area of the footing
μ = interface coefficient of friction between the footing and the soil

P_P = total passive resultant force
P_A = total active resultant force
F = factor of safety

The active earth pressure, P_A, is not divided by the factor of safety in Equation 7.43, because P_A is actually a lateral load applied to the side of the footing. The passive earth pressure, P_P, is multiplied by 0.5 to account for the displacement required to reach the passive conditions, as discussed above.

For footings cast on the ground, the concrete bonds with the soil at the interface and sliding actually occurs in the soil just below the footing. In this case we can simply compute μ as:

$$\mu = \tan\phi' \tag{7.44}$$

where

ϕ' = effective friction angle of the soil

It is important to understand that μ used in Equation 7.43 is the nominal peak capacity. It is not the allowable coefficient of friction, μ_a, which would be equal to μ/F. Geotechnical engineers are often asked to provide allowable coefficients of friction for footing design. If using μ_a, Equation 7.43 becomes:

$$V_a = (P + W_f - u_D A)\mu_a + \frac{0.5P_P}{F} - P_A \tag{7.45}$$

The total passive and active resultant forces can be calculated using lateral earth pressure theories such as the Rankine theory presented in Section 3.6. For cohesionless soils and using Rankine theory, P_P and P_A are given by the following equations:

$$P_P = \frac{1}{2}\tan^2(45° + \phi'/2)\gamma BD^2 \tag{7.46}$$

$$P_A = \frac{1}{2}\tan^2(45° - \phi'/2)\gamma BD^2 \tag{7.47}$$

where

γ = unit weight of the soil
B = footing width
D = depth of embedment

We then design the footing so that:

$$V \leq V_a \tag{7.48}$$

where

V = ASD shear load

In performing this design, be careful to use the proper value of P in Equation 7.43. Typically, multiple load combinations must be considered, and the shear capacity must be satisfactory for each combination. Thus, the P for a particular analysis must be the minimum normal load that would be present when the design shear load acts on the footing. For example, if V is due to wind loads on a building, P should be based on dead load only because the live load might not be present when the wind loads occur. If the wind load also causes an upward normal load on the footing, then P would be equal to the dead load minus the upward wind load. A factor of safety of 1.5 is generally appropriate for sliding on cohesionless soils.

Example 7.8

A 6 ft × 6 ft × 2.5 ft deep cast-in-place concrete footing supports a column with the following design loads: $P = 112$ k and $V = 20$ k. The soil is a silty fine-to-medium sand with $\phi' = 29°$ and $\gamma = 120$ lb/ft^3, and the groundwater table is well below the bottom of the footing. Use the ASD method to check the shear capacity of this footing and determine if the design will safely withstand the design shear load.

Solution

Per Equation 7.44: $\mu = \tan(29°) = 0.55$

$$W_f = (6)(6)(2.5)(150) = 13{,}500 \text{ lb}$$

$$P_P = \frac{1}{2}\tan^2(45° + 29°/2)(120)(6)(2.5)^2 = 6{,}480 \text{ lb}$$

$$P_A = \frac{1}{2}\tan^2(45° - 29°/2)(120)(6)(2.5)^2 = 780 \text{ lb}$$

Using a factor of safety of 1.5, Equation 7.43 gives

$$V_a = \frac{(112{,}000 + 13{,}500)(0.55) + 0.5(6{,}480)}{1.5} - 780 = 47{,}400 \text{ lb} = 47.4 \text{ k}$$

Since $V \leq V_a$ (20 k $\leq$ 47.4 k), the footing has sufficient lateral load capacity.

Cohesive Soils

For the case of footings on cohesive soils, undrained conditions will apply and the shearing resistance along the base will be a function of the undrained shear strength, s_u, and not a function of the normal force on the footing base. Additionally, the lateral earth pressures along the sides of the footings will also be a function of s_u because under the $\phi = 0$ conditions of undrained loading, $K_A = K_P = 1$. Finally, the theoretical active earth pressure has a negative component which we conservatively ignore and compute the allowable shear capacity as:

$$V_a = \frac{s_u A + 0.5 s_u BD}{F} \tag{7.49}$$

The coefficient for the second term in Equation 7.49 is theoretically equal to 2, but only one quarter of this value is being used to account for displacement concerns as described above. Therefore the coefficient becomes 2/4 = 0.5. A factor of safety of 2.0 is generally appropriate for sliding on cohesive soils.

Load and Resistance Factor Design Method

The sliding capacity equations are formulated differently for LRFD in that the active earth pressure is treated as a load, not as a negative resistance. Thus, the factored shear load acting on the footing is the sum of V_u, the factored load imposed by the structure, and $\gamma_1 P_A$, the factored active earth pressure. In the AASHTO (2012) code [Table 3.4.1-2], the load factor, γ_1, for active earth pressure is 1.5.

Cohesionless Soils

The forces resisting sliding in cohesionless soils are the passive earth pressure force, P_P, and the sliding friction at the footing base and the factored nominal shear resistance, $\Sigma\phi V_n$, is:

$$\sum \phi V_n = \phi_1(P_u + W_f - u_D A)\mu + \phi_2(0.5P_P) \tag{7.50}$$

where

P_u = minimum factored vertical column load
ϕ_1 = resistance factor for sliding shear
ϕ_2 = resistance factor for passive earth pressure (See Table 7.2 for AASHTO resistance factors for ϕ_1 and ϕ_2.)
u_D = pore water pressure at the base of the footing
μ = coefficient of friction computed from Equation 7.44
P_P = total passive resultant force computed from Equation 7.46

The 0.5 factor on the passive force is to account for displacement concerns discussed above. Note that P_u must be computed as the *minimum* factored column load since this load acts to resist sliding. Once we've computed $\Sigma\phi V_n$, we must ensure that it is greater than the total ultimate shear load ($V_u + \gamma_1 p_A$), and the design equation is:

$$V_u + \gamma_1 P_A \leq \phi_1(P_u + W_f - u_D A)\mu + \phi_2(0.5P_P) \tag{7.51}$$

The coefficient 0.5 in the passive term in Equations 7.50 and 7.51 accounts for the displacement concerns discussed above.

Cohesive Soils

For cohesive soils, the shearing resistance will be a function of the undrained shear strength only. Again we will ignore the negative component of active earth pressure. In this case the factored nominal shear resistance, $\Sigma\phi V_n$, is:

$$\sum \phi V_n = \phi_1 s_u A + \phi_2(0.5 s_u BD) \tag{7.52}$$

The total ultimate shear load is simply the factored column shear load, V_u, and the design equation is:

$$V_u \leq \phi_1 s_u A + \phi_2 (0.5 s_u BD) \tag{7.53}$$

The 0.5 factor on the passive force in Equations 7.52 and 7.53 is to account for displacement concerns discussed above. As in Equation 7.49, this coefficient is theoretically equal to 2, but we are dividing it by 4 for cohesive soils.

Example 7.9

Use the LRFD method to determine if the design given in Example 7.8 will safely withstand the design shear load. Assume AASHTO (2012) is used to obtain the factored shear demand $V_u = 30$ k and the minimum factored vertical column load $P_u = 120$ k. Use $\gamma_1 = 1.5$.

Solution

We first compute the nominal shear resistance, V_n. The AASHTO resistance factors come from Table 7.2: for concrete cast on sand $\phi_1 = 0.8$, and for passive resistance $\phi_2 = 0.5$.

From Example 7.8, we computed $\mu = 0.55$, $W_f = 13{,}500$ lb, and $P_P = 6{,}480$ lb.

Using Equation 7.52, we compute:

$$V_n = 0.8(120{,}000 + 13{,}500)0.55 + 0.5(0.5)(6{,}480) = 60{,}360 \text{ lb} = 60.4 \text{ k}$$

We now compute the total ultimate shear load:

$$V_u + \gamma_1 P_A = (30 \text{ k}) + (1.5)(0.8 \text{ k}) = 31.2 \text{ k}$$

which is less than the nominal shear capacity of 60.4 k. Therefore, the footing has sufficient lateral load capacity.

Note that the results obtained from LRFD in Example 7.9 are similar to those obtained from ASD in Example 7.8.

SUMMARY

Major Points

1. A *bearing capacity failure* occurs when the soil beneath the footing fails in shear. There are three types of bearing capacity failures: general shear, local shear, and punching shear.
2. Most bearing capacity analyses for shallow foundations consider only the general shear case.
3. A variety of formulas have been developed to compute the *nominal unit bearing capacity*, q_n. These include Terzaghi's formulas and Vesić's formulas. Terzaghi's

are most appropriate for quick hand calculations, whereas Vesić's are more useful when greater precision is needed or special loading or geometry conditions must be considered.

4. Shallow groundwater tables reduce the effective stress in the near-surface soils and can therefore adversely affect bearing capacity. Adjustment factors are available to account for this effect.
5. In ASD, the *allowable bearing capacity*, q_a, is the nominal unit bearing capacity, q_n, divided by a factor of safety, F. The bearing pressure, q, produced by the unfactored structural load must not exceed q_a.
6. In LRFD, the factored load, P_u, is computed using load combinations from the appropriate code. A satisfactory design is then achieved by ensuring that the factored load is less than the nominal unit bearing capacity times the appropriate geotechnical resistance factor, γ. The value of the resistance factor will depend upon the method used to compute q_n since the resistance factor must account for the uncertainty in the analysis method.
7. Bearing capacity analyses should be based on the worst-case soil conditions that are likely to occur during the life of the structure. Thus, we typically wet the soil samples in the lab, even if they were not saturated in the field.
8. Bearing capacity analyses on cohesionless soils are normally based on the effective stress parameters, c' and ϕ', whereas those on cohesive soils are normally based on the undrained shear strength, s_u.
9. Bearing capacity computations also may be performed for the local and punching shear cases. These analyses use reduced values of c' and ϕ'.
10. Bearing capacity analyses on layered soils are more complex because they need to consider the c' and ϕ' values for each layer.
11. The design of footings on or near slopes needs to consider the sloping ground.
12. Evaluations of foundation failures and static load tests indicate the bearing capacity analysis methods presented in this chapter are suitable for the practical design of spread footings.
13. Footings can resist applied shear loads through passive pressure on the side of the footing and shear resistance at the base of the footing. For cohesionless soils the shear resistance will be frictional and based on ϕ'. For cohesive soils it will be cohesive and based on s_u.

Vocabulary

Allowable bearing capacity
Apparent cohesion
Bearing capacity
Bearing capacity factors
Bearing capacity failure
Bearing capacity formula
General shear failure
Local shear failure
Nominal unit bearing capacity
Punching shear failure
Terzaghi's bearing capacity theory
Vesić's bearing capacity formulas

QUESTIONS AND PRACTICE PROBLEMS

Sections 7.1 to 7.5: Bearing Capacity and Footing Design

7.1 List the three types of bearing capacity failures and explain the differences between them.

7.2 A 1.2 m square, 0.4 m deep spread footing is underlain by a soil with the following properties: $\gamma = 19.2$ kN/m^3, $c' = 5$ kPa, and $\phi' = 30°$. The groundwater table is at a great depth.

a. Compute the nominal unit bearing capacity using Terzaghi's method.

b. Compute the nominal unit bearing capacity using Vesić's method.

7.3 A 5 ft wide, 8 ft long, 2 ft deep spread footing is underlain by a soil with the following properties: $\gamma = 120$ lb/ft^3, $c' = 100$ lb/ft^2, and $\phi' = 28°$. The groundwater table is at a great depth. Using Vesić's method, compute the column load required to cause a bearing capacity failure.

7.4 A column carrying a vertical downward unfactored load of 270 k is to be supported on a 3 ft deep square spread footing. The soil beneath this footing is an undrained clay with $s_u = 3{,}000$ lb/ft^2 and $\gamma = 117$ lb/ft^3. The groundwater table is below the bottom of the footing. Using the ASD method, compute the width B required to obtain a factor of safety of 3 against a bearing capacity failure.

7.5 A column carrying a vertical downward ultimate factored load of 1,500 kN is to be supported on a 1 m deep square spread footing. The soil beneath this footing is an undrained clay with $s_u = 150$ kPa and $\gamma = 18.1$ kN/m^3. The groundwater table is below the bottom of the footing. Using the LRFD method, compute the required width B. Assume the geotechnical resistance factor is 0.5.

7.6 A 120 ft diameter cylindrical tank with an empty weight of 1,900,000 lb is to be built on top of a 2 ft thick compacted gravel fill with a unit weight of 130 lb/ft^3. The fill will be roughly the same diameter as the tank. This tank is to be filled with water. The underlying soil is an undrained clay with $s_u = 1{,}000$ lb/ft^2 and $\gamma = 118$ lb/ft^3, and the groundwater table is at a depth of 5 ft. Using Terzaghi's equations, compute the maximum allowable depth of the water in the tank that will maintain a factor of safety of 3.0 against a bearing capacity failure. Include the weight of the gravel fill in your computations and assume the weight of the water and tank is spread uniformly across the bottom of the tank.

7.7 A 1.5 m wide, 2.5 m long, 0.5 m deep spread footing is underlain by a soil with $c' = 10$ kPa, $\phi' = 32°$, and $\gamma = 18.8$ kN/m^3. The groundwater table is at a great depth. Using ASD compute the maximum unfactored load this footing can support while maintaining a factor of safety of 2.5 against a bearing capacity failure.

7.8 A 5 ft wide, 8 ft long, 2 ft deep spread footing is underlain by a soil with $c' = 200$ lb/ft^2, $\phi' = 37°$, and $\gamma = 121$ lb/ft^3. The groundwater table is at a great depth. Using LRFD with a resistance factor of 0.5, determine the ultimate factored load this footing can carry.

7.9 A bearing wall carries a total unfactored load 220 kN/m. It is to be supported on a 400 mm deep continuous footing. The underlying soils are medium sands with $c' = 0$, $\phi' = 37°$, and $\gamma = 19.2$ kN/m^3. The groundwater table is at a great depth. Using ASD, compute the

minimum footing width required to maintain a factor of safety of at least 2 against a bearing capacity failure. Express your answer to the nearest 100 mm.

7.10 After the footing in Problem 7.9 was built, the groundwater table rose to a depth of 0.5 m below the ground surface. Compute the new factor of safety against a bearing capacity failure. Compare it with the original design value of 2 and explain why it is different.

7.11 A bearing wall carries a factored ultimate vertical load of 67 k/ft. It is to be supported on a 18 in deep continuous footing. The underlying soils are medium sands with $c' = 0$, $\phi' = 37°$, and $\gamma = 124$ lb/ft^3. The groundwater table is at a great depth. Using LRFD, with a resistance factor 0.45, compute the minimum footing width required. Express your answer to the nearest 4 in.

7.12 A 5 ft wide, 8 ft long, 3 ft deep footing supports a downward load of 200 k and a horizontal shear load of 25 k. The shear load acts parallel to the 8 ft dimension. The underlying soils have $c' = 220$ lb/ft^2, $\phi' = 28°$, and $\gamma = 123$ lb/ft^3. Using an effective stress analysis, compute the factor of safety against a bearing capacity failure.

7.13 For the footing describe in Problem 7.12, determine the factor of safety against sliding. Is the factor of safety adequate?

7.14 A spread footing supported on a sandy soil has been designed using ASD to support a certain column load with a factor of safety of 2.5 against a bearing capacity failure. However, there is some uncertainty in both the column load, P, and the friction angle, ϕ. Which would have the greatest impact on the actual factor of safety: an actual P that is twice the design value, or actual ϕ that is half the design value? Use bearing capacity computations with reasonable assumed values to demonstrate the reason for your response.

7.15 A certain column carries a vertical downward load of 1,200 kN. It is to be supported on a 1 m deep, square footing. The soil beneath this footing has the following properties: $\gamma = 20.5$ kN/m^3, $c' = 5$ kPa, and $\phi' = 36°$. The groundwater table is at a depth of 1.5 m below the ground surface. Using ASD, compute the footing width required for a factor of safety of 3.5.

7.16 A building column carries a factored ultimate vertical downward load of 320 k. It is to be supported on a 3 ft deep, square footing. The soil beneath this footing has the following properties: $\gamma = 20.5$ kN/m^3, $c' = 5$ kPa, and $\phi' = 36°$. The groundwater table is at a depth of 5 ft below the ground surface. Using LRFD, with a resistance factor of 0.5, compute the required footing width.

Section 7.10: Design of Spread Footings Against Sliding Failure

7.17 A 3 ft square footing is founded at a depth of 2.5 ft on saturated clay and carries an unfactored vertical column load of 65 k. The underlying clay has an undrained shear strength of 1,500 lb/ft^2. Compute the allowable shear load this column can carry using ASD with a sliding factor of safety of 1.5.

7.18 A building column carries factored ultimate loads of 5,500 kN vertical and 1,200 kN horizontal. The column is founded on a 1.5 m square footing at a depth of 1.7 m. The soil is a cohesionless sand with $\phi' = 32°$ and $\gamma = 18.8$ kN/m^3. The water table is at a depth of 6 m. Using LRFD with an active earth pressure load factor of 1.5, determine if this footing satisfies requirements for sliding.

Comprehensive

7.19 Develop a spread sheet to compute allowable total vertical column loads using the ASD method and factored ultimate vertical column loads using LRFD. The spreadsheet should consider only vertical loads on a square or continuous footing bearing on single uniform soil. It should allow the input of footing width, depth, water table depth, soil strength parameters, a factor of safety for ASD, and a geotechnical resistance factor for LRFD. It should compute the bearing capacity based on both Terzaghi's and Vesić's methods.

7.20 A certain column carries a vertical downward load of 424 k. It is to be supported on a 3 ft deep rectangular footing. Because of a nearby property line, this footing may be no more than 5 ft wide. The soil beneath this footing is a silty sand with the following properties: $\gamma = 124$ lb/ft^3, $c' = 50$ lb/ft^2, and $\phi' = 34°$. The groundwater table is at a depth of 6 ft below the ground surface. Use ASD and the spreadsheet developed in Problem 7.19 to compute the footing length required for a factor of safety of 3.0.

7.21 Repeat Problem 7.20 using LRFD assuming the factored ultimate vertical column load is 560 k.

7.22 Conduct a bearing capacity analysis on the Fargo Grain Elevator (see sidebar) and back-calculate the average undrained shear strength of the soil. The groundwater table is at a depth of 6 ft below the ground surface. Soil strata A and B have unit weights of 110 lb/ft^3; stratum D has 95 lb/ft^3. The unit weight of stratum C is unknown. Assume that the load on the foundation acted through the centroid of the mat.

7.23 Three columns, A, B, and C, are collinear, 500 mm in diameter, and 2.0 m on-center. They have unfactored vertical downward loads of 1,000, 550, and 700 kN, respectively, and are to be supported on a single, 1.0 m deep rectangular combined footing. The soil beneath this proposed footing has the following properties: $\gamma = 19.5$ kN/m^3, $c' = 10$ kPa, and $\phi' = 31°$. The groundwater table is at a depth of 25 m below the ground surface.

a. Using ASD, determine the minimum footing length, L, and the placement of the columns on the footing that will place the resultant load at the centroid of the footing. The footing must extend at least 500 mm beyond the edges of columns A and C.

b. Using the results from part (a), determine the minimum footing width, B, that will maintain a factor of safety of 2.5 against a bearing capacity failure. Show the final design in a sketch.

Hint: Assume a value for B, compute the allowable bearing capacity, then solve for B. Repeat this process until the computed B is approximately equal to the assumed B.

7.24 Two columns, A and B, are to be built 6 ft 0 in apart (measured from their centerlines). Column A has a vertical downward dead load and live loads of 90 k and 80 k, respectively. Column B has corresponding loads of 250 k and 175 k. The dead loads are always present, but the live loads may or may not be present at various times during the life of the structure. It is also possible that the live load would be present on one column, but not the other.

These two columns are to be supported on a 4 ft 0 in deep rectangular spread footing founded on a soil with the following parameters: $\gamma = 122$ lb/ft^3, $\phi' = 37°$, and $c' = 100$ lb/ft^2. The groundwater table is at a very great depth. Use ASD in this problem.

a. The location of the resultant of the loads from columns A and B depends on the amount of live load acting on each at any particular time. Considering all of the possible loading conditions, how close could it be to column A? To column B?

b. Using the results of part (a), determine the minimum footing length, L, and the location of the columns on the footing necessary to keep the resultant force within the middle third of the footing under all possible loading conditions. The footing does not need to be symmetrical. The footing must extend at least 24 in beyond the centerline of each column.

c. Determine the minimum required footing width, B, to maintain a factor of safety of at least 2.5 against a bearing capacity failure under all possible loading conditions.

d. If the B computed in part c is less than the L computed in part (b), then use a rectangular footing with dimensions $B \times L$. If not, then redesign using a square footing. Show your final design in a sketch.

7.25 In May 1970, a 70 ft tall, 20 ft diameter concrete grain silo was constructed at a site in Eastern Canada (Bozozuk, 1972b). This cylindrical silo, which had a weight of 183 tons, was supported on a 3 ft wide, 4 ft deep ring foundation. The outside diameter of this foundation was 23.6 ft, and its weight was about 54 tons. There was no structural floor (in other words, the contents of the silo rested directly on the ground).

The silo was then filled with grain. The exact weight of this grain is not known, but was probably about 533 tons. Unfortunately, the silo collapsed on September 30, 1970 as a result of a bearing capacity failure.

The soils beneath the silo are primarily marine silty clays. Using an average undrained shear strength of 500 lb/ft^2, a unit weight of 80 lb/ft^3, and a groundwater table 2 ft below the ground surface, compute the ASD factor of safety against a bearing capacity failure, then comment on the accuracy of the analysis, considering the fact that a failure did occur.

8

Spread Footings—Geotechnical Serviceability Limit States

From decayed fortunes every flatterer shrinks,
Men cease to build where the foundation sinks.

From the seventeenth century British opera
The Duchess of Malfi by John Webster (1624)

The procedures outlined in Chapter 7 allow engineers to design footings that satisfy the geotechnical ultimate limit states. As discussed in Section 5.3, deformation based serviceability limits must also be investigated including:

- Settlement
- Heave
- Tilt
- Lateral movement
- Vibration

For spread footing design, the most important of these serviceability limits is settlement, which is the subject of this chapter.

There has sometimes been a muddling of ultimate and serviceability limit states in geotechnical design. By the 1950s, engineers were routinely performing bearing capacity analyses as a part of most design projects. However, during that period, many engineers seemed to have the misconception that any footing designed with an adequate

factor of safety against a bearing capacity failure would not settle excessively (Hough, 1959). Although settlement analysis methods were available, on observation these analyses, if conducted at all, were considered to be secondary. Even today, poor communication between structural and geotechnical engineers can lead to confusion about bearing capacity and settlement limits. Many engineers still have the misconception that footings designed for the same bearing stress will have the same settlement regardless of the footing size, or that settlement computations are secondary to bearing capacity analysis. In fact, we now know that it is settlement that controls the design of spread footings more often than bearing capacity, especially when the footing width is large.

This chapter concentrates on computing settlements caused by the application of structural loads on the footing, other sources of settlement also may be important. These include settlement caused by:

- The weight of a recently placed fill
- A falling groundwater table
- Underground mining or tunneling
- The formation of sinkholes
- Secondary compression of the underlying soils
- Lateral movements resulting from nearby excavations

8.1 DESIGN REQUIREMENTS

The geotechnical serviceability requirements for spread footings are usually stated in terms of the allowable total settlement, δ_a, and the allowable differential settlement, δ_{Da}, as follows:

$$\delta \leq \delta_a \tag{8.1}$$

$$\delta_D \leq \delta_{Da} \tag{8.2}$$

where

δ = settlement (or total settlement)
δ_a = allowable settlement (or allowable total settlement)
δ_D = differential settlement
δ_{Da} = allowable differential settlement

Note that there is no explicit factor of safety in Equations 8.1 and 8.2, because the factor of safety is already included in δ_a and δ_{Da}. The adjective "allowable" always indicates a factor of safety has already been applied. The values of δ_a and δ_{Da} are obtained using the techniques described in Chapter 5. They depend on the type of structure being supported by the foundation, and its tolerance of total and differential settlements. This chapter describes how to compute δ and δ_D for spread footings.

It is important to select the appropriate loads when performing settlement analyses on footings. This is particularly important since soil deformations are generally time dependent. In general, the long-term settlement of footings will control the serviceability limit state. In this case, both δ and δ_D should be computed using the sustained load that can reasonably be expected. This load will generally consist of unfactored dead plus some portion of the live loads, as discussed in Section 5.3. Occasionally, it will be necessary to check the short-term settlement of foundation. This might be important, for example, in the design of foundations for wind turbines, where short term tilt due to high wind loads, might cause problems with the operation of the turbine. In this case the loads used to compute the short-term settlements will be very different from those used to compute the long-term settlements. Serviceability limits are controlled by operational considerations of the structure and the loads used in serviceability checks will depend on what operational limits are being analyzed. This chapter will concentrate on performing long-term settlement computations, but will also discuss short-term settlement analyses when appropriate.

8.2 MODULUS BASED METHODS OF COMPUTING SETTLEMENT

In Section 3.3, we discussed using elastic theory to compute the distribution of induced stress under an applied footing load. We can also use elastic theory to compute the settlement of footings. As with the stress distribution equations presented in Section 3.3, the settlement solutions based on elastic theory assume that the soil is a homogeneous, isotropic elastic material that extends infinitely down below the ground surface.

Simple Elastic Solutions for Settlement

For a uniformly loaded perfectly flexible circular footing placed at the ground surface of an elastic material, the settlement under the center of the footing is (Poulos and Davis, 1974, Section 3.3):

$$\delta = qB\frac{1-\nu^2}{E} \tag{8.3}$$

where

q = applied bearing stress
B = footing diameter
ν = Poisson's ratio
E = Young's modulus

As shown in Figure 8.1a, for a perfectly flexible footing, such as the base of a steel water tank, the bearing stress will be uniform, but the settlement will be greater under the center than at the edges. We can also use elastic theory to compute the settlement under the edges of footing (see Section 3.3 of Poulos and Davis, 1974). For the case of a rigid circular footing, the settlement across the footprint of the footing must be uniform, as shown in Figure 8.1b.

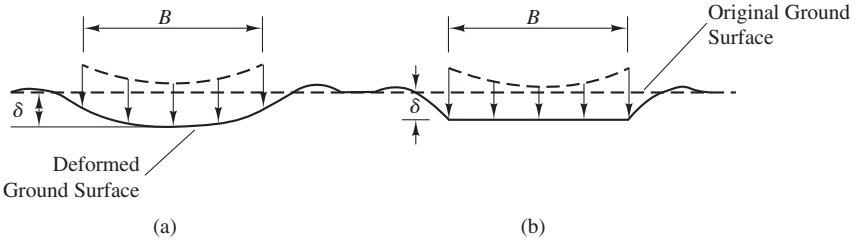

Figure 8.1 Bearing stress and settlement of (a) flexible (uniform bearing stress, non-uniform settlement); and (b) rigid (non-uniform bearing stress, uniform settlement) circular footings placed at the ground surface.

This boundary condition will force the bearing stress to be greater at the edges than at the center of the footing as shown in Figure 8.1b. For this case the elastic settlement will be:

$$\delta = q\frac{\pi}{4}B\frac{1-\nu^2}{E} \tag{8.4}$$

In this case q is the average bearing stress or the total applied load divided by the area of the footing.

There are a number of limitations to this approach. It is limited to either perfectly flexible or perfectly rigid footing place at the ground surface. It assumes a homogeneous and isotropic soil with a single modulus and Poisson's ratio. The latter is the most limiting as most soil profiles have significant changes in stiffness versus depth.

Drained versus undrained deformation

It is important to distinguish between the modulus under undrained conditions and the modulus under drained conditions. Most often, the foundation engineer is concerned about the long-term settlements that will occur under loading. By definition these long-term settlements will occur under drained conditions, and the elastic soil properties, modulus and Poisson's ratio, should also be determined under drained conditions. For sands, gravels, and most unsaturated soils, drainage will occur quickly compared to construction times and the only condition of concern is the drained condition. (An important exception is the case of dynamic loads such as earthquakes or machine vibrations, where undrained conditions may apply even in these soils, but this topic is beyond the scope of this book.) For drained conditions, the soil modulus can be determined either in the lab from oedometer or triaxial tests or through in situ tests as described in Chapter 4. In general, lab tests can provide reasonable estimates of drained moduli for cohesive soils if high quality samples are taken. For cohesionless soils, moduli derived from in situ tests are preferable because of the difficulty in acquiring undisturbed sample of these soils. Moduli from DMT are generally preferred to those correlated with CPT, because the DMT is a deformation based test where the CPT is a strength based test. Moduli determined from SPT is the least preferred because of the inherent variabilities in performing this test. For drained conditions, Poisson's ratio is often estimated based on the drained friction angle using Equation 4.44.

For saturated cohesive soils, we may be interested in both the short-term settlement, which will occur under undrained conditions, and the long-term settlement, which will occur under drained conditions. For undrained conditions of saturated soils, we generally assume that the soil is incompressible since the modulus of both water and mineral solids is much greater than the modulus of the soil skeleton. In this case, Poisson's ratio will be 0.5 and all the settlement will be due to elastic distortion. The undrained modulus is generally estimated from measurements of the undrained shear strength using Equation 4.47.

Whether the elastic properties are determined from laboratory test or field tests, once the elastic properties are determined as a function of depth, the settlement can be computed using Equation 8.3 if the applied load is from a flexible foundation, such as the base of a large steel water or oil tank. In the case of rigid footing, Equation 8.4 would be appropriate.

Example 8.1

The owner of an existing single-story industrial structure is considering adding a second story to the structure. The structure consists of a steel frame with concrete footings founded on 3 m of well compacted silty sand fill. The existing columns are capable of carrying the additional load but there is concern about the additional settlement that may occur. A typical circular footing for the structure is 80 cm in diameter, and will carry an additional service load of 60 kN if the proposed addition is constructed. Standard penetration tests conducted near the existing footings indicate an average N_{60} value of 30. Estimate the additional settlement that will be generated by the proposed second-story addition.

Solution

The N_{60} value of 30 indicated a dense well-compacted fill material. The compaction process has the effect of overconsolidating the soil, so it is reasonable to assume a modest overconsolidation ratio (OCR) of 3 for the fill. From Equation 4.48 and Table 4.7 with $N_{60} = 30$ and OCR $= 3$, we estimate the Young's modulus of the soil as,

$$E = 2{,}500\sqrt{3} + 600(30) = 22{,}000 \text{ kPa}$$

For this dense soil we will assume a Poisson's ratio of 0.4. Using these data and Equation 8.4, we estimate the additional settlement due to the proposed addition as,

$$\delta = \frac{60 \text{ kN}}{\pi (0.4 \text{ m})^2} \frac{\pi}{4} (800 \text{ mm}) \left(\frac{1 - 0.4^2}{22{,}000 \text{ kPa}} \right) = 2.9 \text{ mm}$$

Commentary

A number of simplifications and assumptions have been made in this example including ignoring embedment of the footing, assuming OCR and Poisson's ratio, and using an empirical correlation for modulus based on SPT. In spite of these assumptions and simplifications, the estimated additional settlement of 3 mm indicates that construction of the second-story addition should generate tolerable settlements for an industrial building.

Generalized Elastic Methods for Computing Settlement

The simple elastic solutions presented in Equation 8.3 and 8.4 have a number of shortcomings. They assume the foundation is circular and placed at the ground surface and that the soil extends infinitely deep and has a constant modulus. Real footings are generally square, rectangular, or infinitely long, and founded some distance below the ground surface. Additionally, many soil profiles have a relatively stiff layer some depth below the footing leaving only a finite thickness of compressible material and very seldom is the soil modulus constant with depth.

Janbu et al. (1956) extend the elastic theory using Equations 8.3 and 8.4 into a generalized method for computing footing settlement that accounts for footing shape, footing depth, and the finite thickness of the compressible layer. Using this method the settlement is calculated as:

$$\delta = I_0 I_1 \frac{qB}{E} \tag{8.5}$$

where

q = average bearing stress
B = footing width
E = average soil modulus over depth of compressible layer
I_0 = influence factor accounting for footing depth
I_1 = influence factor accounting for footing shape and thickness of compressible layer

Christian and Carrier (1978) reviewed and updated the work of Janbu et al. (1956) with improved influence factors. Figure 8.2 presents the updated influence factors used with Equation 8.5. This method was developed for undrained loading case where $\nu = 0.5$, however it can be used for other values of ν by appropriately adjusting the modulus. While this method is an improvement of Equations 8.3 and 8.4, it still applies only to the case where there is a constant soil modulus.

Example 8.2

A rectangular combined footing 8 ft × 20 ft is founded at a depth of 6 ft on a normally consolidated sand deposit. The sand deposit is approximately 28 ft thick and overlies sandstone. CPT tests indicate the sand is relatively uniform below the proposed footing depth and the average tip resistance is 50 tsf. The total service load carried by the combined footing is 480 k. Estimate the settlement of this footing.

Solution

We can use Schmertmann's correlations for effective soil modulus, E_s, presented in Table 4.8 and then use Equation 8.5 to estimate the settlement. Since this modulus was calibrated for

settlement of footings, there is no need to make adjustments for Poisson's ratio. Using an average value for young, normally consolidated sand from Table 4.8, we compute:

$$E_s = 3q_c = 3(50) = 150 \text{ tsf} = 300 \text{ ksf}$$

The depth correction factor, I_0, is computed using Figure 8.2 ratio of footing depth to width, B/D.

$$B/D = 6/8 = 0.75$$

From Figure 8.2 with $B/D = 0.75$, we determine:

$$I_0 = 0.96$$

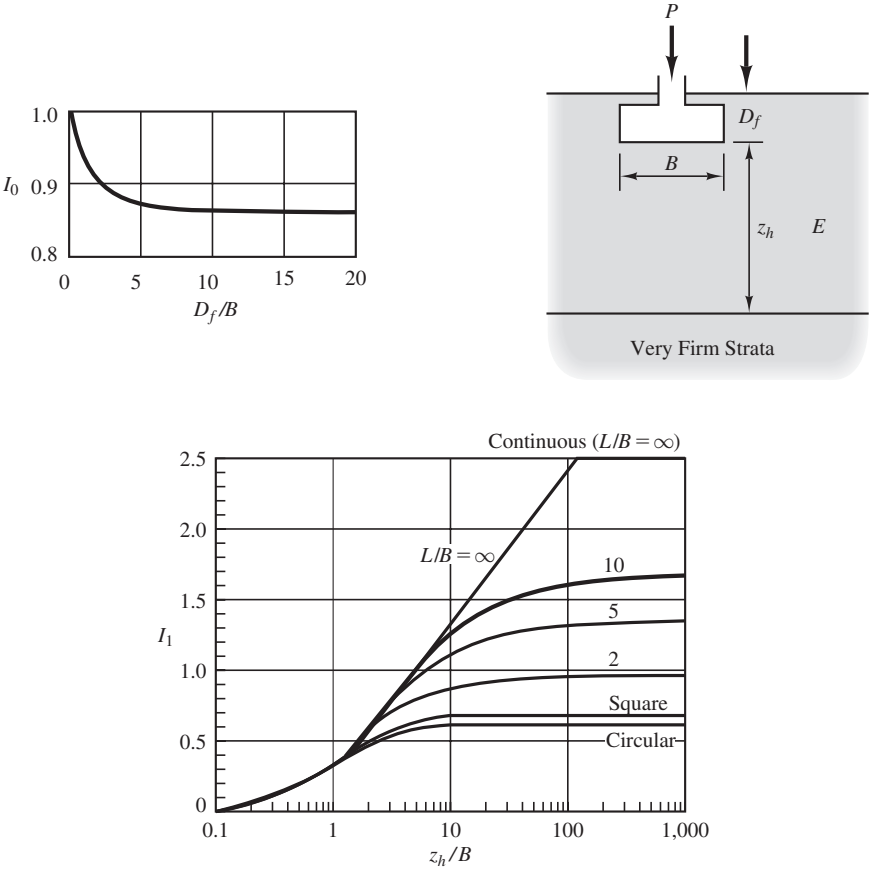

Figure 8.2 Influence factors for computing settlement using Equation 8.5 (after Christian and Carrier, 1978).

To determine the correction factor for thickness of the compressible layer we must calculate the footing aspect ratio, L/B, and the relative thickness of the compressible layer, z_h/B.

$$L/B = 20/8 = 2.5$$

$$z_h/B = 28/8 = 3.5$$

From Figure 8.2 with $L/B = 2.5$ and $z_h/B = 3.5$, we determine:

$$I_1 = 0.8$$

Then using Equation 8.5, we compute the settlement as:

$$\delta = I_0 I_1 \frac{qB}{E} = (0.96)(0.8)\frac{480\text{ k}}{(8 \times 20)\text{ft}^2}\left(\frac{8 \times 12\text{ in}}{300\text{ k/ft}^2}\right) = 0.73\text{ in}$$

Mayne and Poulos (1999) developed a more general and versatile method which accounts for footing rigidity as well as footing depth and thickness of the compressible layer. This method is also based on soil with a linearly increasing modulus as a function of depth as shown in Figure 8.3.

$$\delta = I_G I_F I_E \frac{qB_e}{E_0}(1 - \nu^2) \tag{8.6}$$

where

E_0 = soil modulus directly below the footing (see Figure 8.3)
I_G = influence factor for finite thickness and soil modulus
I_F = influence factor for footing rigidity
I_E = influence factor for footing embedment depth
B_e = equivalent circular footing $B_e = \sqrt{\frac{4BL}{\pi}}$
ν = Poisson's ratio

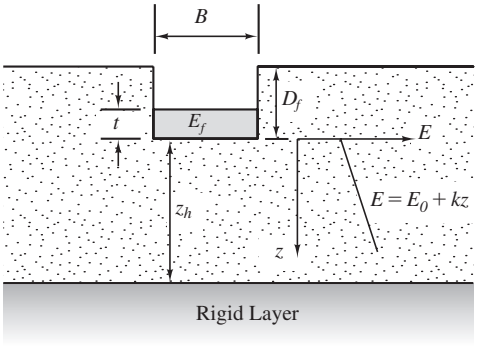

Figure 8.3 Model used for Mayne and Poulos (1999) method for computing settlement.

In this solution I_G is a function of the relative thickness of the compressible layer (z_h/B) and the normalized modulus β computed as:

$$\beta = \frac{E_0}{kB_e} \tag{8.7}$$

Figure 8.4 is used to determine I_G, Equation 8.8 is used to calculate I_F, and Equation 8.9 is used to calculate I_E.

$$I_F = \frac{\pi}{4} + \left[\frac{1}{4.6 + 10\left(\dfrac{E_f}{E_0 + \dfrac{B_e k}{2}} \right)\left(\dfrac{2t}{B_e} \right)^3} \right] \tag{8.8}$$

$$I_E = 1 - \frac{1}{3.5(1.6 + B/D_f)\mathrm{e}^{(1.22\nu - 0.4)}} \tag{8.9}$$

The Mayne and Poulos (1999) method is both more flexible and more rigorous than Janbu's method but this comes with significantly more complexity than Janbu's method. The linearly increasing soil stiffness is a better model than the constant stiffness used in Janbu's method, but still not a very accurate model of many layered soil profiles. Both the Janbu and Mayne and Poulos methods require determining the soil properties as a function of depth which is best accomplished with in situ tests, preferably DMT or CPT tests. If such tests are performed, we can take advantage of the detailed depth profile of modulus to model any reasonable soil model by using one of the following two methods.

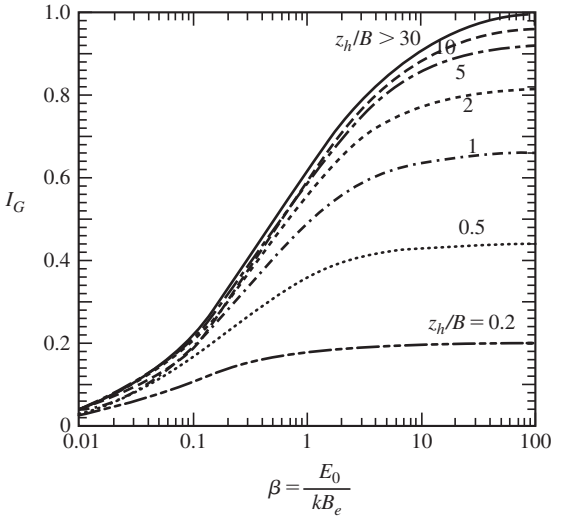

Figure 8.4 Chart to determine I_G in the Mayne and Poulos (1999) method for computing settlement.

Example 8.3

The square footing shown in Figure 8.5a supports material handling equipment at a port facility. The footing is founded on a lightly overconsolidated (OCR = 2) saturated clay with a plasticity index of 40. An undrained shear strength profile for the clay deposit is shown in Figure 8.5b. Estimate the short-term settlement of this footing under a service load of 500 kN. Assume this load includes the weight of the footing.

Solution

Since we want to know the short-term settlement of this footing, we will use an undrained analysis. It is reasonable to assume a Poisson's ratio of 0.5 for saturated clay under undrained conditions. We will use Duncan and Buchignai's (1976) correlation between undrained shear strength, s_u, and undrained modulus (Figure 4.33) to determine the modulus of the soil. Since s_u increases linearly with depth, the modulus will also increase linearly with depth and the Mayne and Poulos method is appropriate.

From Figure 8.5b, $s_u = 2.2 + 1.2z$. However we need to compute s_u as a function of the depth below the footing. Substituting $z_f = z - 3$, we get:

$$s_u = 5.8 + 1.2z_f$$

From Figure 4.33 with PI = 40 and OCR = 2, we select a ratio of $E/s_u = 400$. Using this ratio, the equation for modulus as a function of depth below the footing is,

$$E = 2{,}300 + 480z_f$$

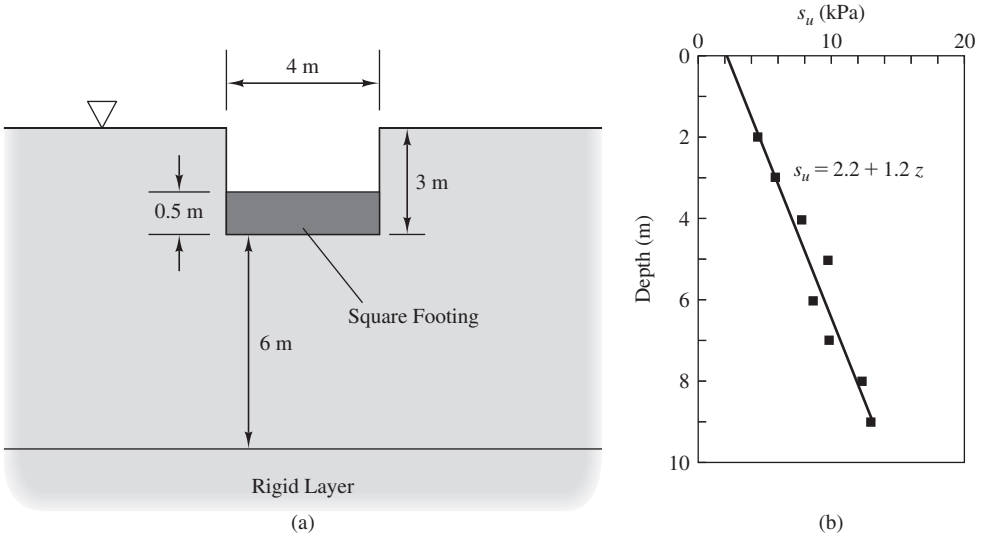

Figure 8.5 Soil profile and footing geometry for Example 8.3.

Where z_f is in meters and E is in kPa. Therefore in Mayne and Poulos' solution:

$$E_0 = 2{,}300 \text{ kPa}$$

$$k = 480 \text{ kPa/m}$$

First, we must compute the equivalent circular footing, B_e, as:

$$B_e = \sqrt{\frac{4(4 \text{ m})^2}{\pi}} = 4.5 \text{ m}$$

Now we compute the influence factors I_F, I_E, and I_G using Equations 8.8 and 8.9 and Figure 8.4. For computing the rigidity factor, I_F, we will assume the modulus of the concrete footing is 20,000 mPa (20,000,000 kPa).

$$I_F = \frac{\pi}{4} + \left[\frac{1}{4.6 + 10\left(\dfrac{20{,}000{,}000}{2{,}300 + \dfrac{4.5(480)}{2}} \right)\left(\dfrac{2(0.5)}{4.5} \right)^3} \right]$$

$$= \frac{\pi}{4} + \left(\frac{1}{654} \right) \approx \frac{\pi}{4} = 0.78$$

Note that this footing is essentially rigid in this case, that is, $I_F = \pi/4$.

$$I_E = 1 - \frac{1}{3.5(1.6 + 4/3)e^{(1.22(0.5)-0.4)}} = 0.92$$

To determine I_G we must first compute β using Equation 8.7,

$$\beta = \frac{2{,}300}{480(4.5)} = 1.06$$

From Figure 8.4 using $\beta = 1.06$ and $z_h/B = 6/4 = 1.5$, we find:

$$I_G = 0.53$$

We now compute the settlement, δ, using Equation 8.6:

$$\delta = (0.53)(0.79)(0.89)\left(\frac{500 \text{ kN}}{(4 \text{ m})^2} \right)\frac{4.5 \text{ m}}{2{,}300 \text{ kPa}}(1 - (0.5)^2) = 0.017 \text{ m} = 17 \text{ mm}$$

Commentary

The computed short-term settlement of 17 mm may satisfy the serviceability limits for this facility. However, for this plastic marine clay, it would be important to also check the long-term consolidation settlement.

Incremental Constrained Modulus Method

This method combines elastic stress distribution for finite sized loaded areas (Section 3.3) with estimates of the constrained modulus as function of depth to compute the settlement using Equation 8.10:

$$\delta = \sum \frac{I_\sigma (q - \sigma'_{zD})}{M} H \tag{8.10}$$

where

q = applied stress at the base of the footing
σ'_{zD} = initial effective stress at the base of the footing
I_σ = stress influence factor for given depth (see Section 3.3)
M = constrained modulus for a soil layer
H = thickness of a soil layer

Marchetti recommends this method when using DMT to determine the constrained modulus (Marchetti 1980, Marchetti 1997, Schmertmann 1986). However, it can be used with any in situ or lab method which can provide an estimate of constrained modulus as a function of depth. The process is:

1. Estimate M as a function of depth using data from DMT (preferred), CPT, SPT, or lab measurements on undisturbed samples, using methods described in Chapter 4.
2. Beginning at the bottom of the footing, divide the soil into layers. Continue to a depth of at least $2B$ (for square footings) or at least $6B$ (for continuous footings) below the bottom of the footing or until a very stiff layer is encountered. Layer thickness should be $B/4$ or less for the best accuracy.
3. Determine M for each soil layer based on available test data.
4. Calculate I_σ (and $\Delta\sigma_z$) under the center of the footing at midheight of each layer using the appropriate equations or charts from Section 3.3.
5. Compute the compression of each layer using Equation 8.10.
6. Sum the compression of all layers to compute the footing settlement.

Theoretically, this method computes only the one-dimensional settlement since it uses the constrained modulus and therefore does not account for lateral deformation under finite-sized footings. However, Marchetti (1997) recommends using this one-dimensional method because the differences between the settlement computed with a one-dimensional versus three-dimensional analysis is small and the uncertainties associated with the three-dimensional analysis significantly reduce the precision of the settlement computation.

Example 8.4

The constrained modulus determined from a DMT test on loose sand deposit is plotted in Figure 8.6a and tabulated in Figure 8.6b. A 4 ft square footing carrying a service load of 70 k

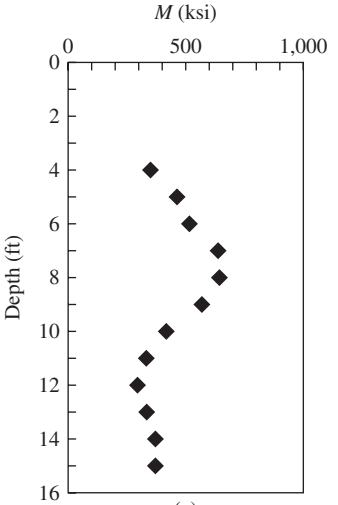

(a)

Depth (ft)	M (ksf)
4	370
5	460
6	517
7	634
8	640
9	566
10	414
11	331
12	295
13	330
14	368
15	368

(b)

Figure 8.6 Data for Example 8.4, constrained modulus computed from DMT (a) data plotted versus depth; and (b) tabulated data.

is to be founded at depth of 5 ft. Compute the settlement of this footing using the DMT data provided. The groundwater table is at a depth of 7 ft.

Solution

First we must compute the net bearing stress, q'. Assume the unit weight of the sand is 110 lb/ft^3.

$$q' = \frac{P + W_f}{B^2} - \sigma'_{zD} = \frac{70 + 0.150(4^2 \cdot 5)}{4^2} - \frac{5(110)}{1000} = 4.57 \text{ ksf}$$

Since we have tabulated data for M at 1 ft intervals, we will use 1 ft thick layers to compute the settlement. We will use Equation 3.14 to compute the induced stress, $\Delta\sigma_z$, for each layer. The results of the computation are:

Depth (ft)	H (ft)	M (ksf)	I_σ From Eq. 3.14	$\Delta\sigma_z = q' \times I_\sigma$ (ksf)	$\delta = (\Delta\sigma_z \times H)/M$ (ft)
5-6	1	460	0.99	4.54	0.00987
6-7	1	517	0.83	3.81	0.00738
7-8	1	634	0.58	2.66	0.00419
8-9	1	640	0.39	1.79	0.00280
9-10	1	566	0.27	1.24	0.00219
10-11	1	414	0.20	0.90	0.00217
11-12	1	331	0.15	0.67	0.00203

Depth (ft)	H (ft)	M (ksf)	I_σ From Eq. 3.14	$\Delta\sigma_z = q' \times I_\sigma$ (ksf)	$\delta = (\Delta\sigma_z \times H)/M$ (ft)
12-13	1	295	0.11	0.52	0.00176
13-14	1	330	0.09	0.41	0.00125
14-15	1	368	0.07	0.34	0.00091
15-16	1	368	0.06	0.28	0.00075
					$\Sigma = \begin{matrix}0.03531 \text{ ft} \\ 0.42 \text{ in}\end{matrix}$

The computed total settlement is approximately 0.4 in.

Commentary

The location of the groundwater table was not used in solving the problem. By doing this we have made two implicit assumptions. First, the change in stress due to the applied load is a change in effective stress. This is reasonable since the sand is freely draining. Second, that modulus measured by the DMT is a drained modulus, which is also a reasonable assumption.

Schmertmann's Method

Schmertmann's method (Schmertmann, 1970, 1978; and Schmertmann, et al., 1978) was developed primarily as a means of computing the settlement of spread footings on sandy soils. It is most often used with CPT results, but can be adapted to other in situ tests. This method was developed from field and laboratory tests, most of which were conducted by the University of Florida. The Schmertmann method is based on elastic theory and calibrated using empirical data. Schmertmann's method is unique in that it uses a strain distribution factor instead of a stress distribution factor to account for the finite size of footings. Schmertmann used a modulus, E_s, which he described as the *equivalent soil modulus*, which he correlated with CPT tip resistance and soil behavior type as described in Chapter 4. Schmertmann's equivalent soil modulus was calibrated using footing load tests. It therefore includes three-dimensional stress effects on footings. Theoretically, E_s will have a value greater than Young's modulus, E, and less than the constrained modulus, M. However, it is best simply to think of it as a modulus calibrated with footing load tests.

Strain Influence Factor

Schmertmann (1970) conducted extensive research on the distribution of vertical strain, ε_z, below spread footings. Based on results from the theory of elasticity, model tests, laboratory and field tests, and finite element simulations, he found the greatest vertical strains below the center of a footing on homogeneous sands do not occur immediately below the footing, as one might expect, but at a depth of 0.5 B to B below the bottom of the footing, where B is the footing width. The reason why the maximum vertical strain does not occur

at the bottom of the footing, even though the vertical stress increase, $\Delta\sigma_z$, induced by the footing load is highest at this location, is that the vertical strain is determined not only by the vertical stress increase but also by the existing and induced shear stresses (Schmertmann, 1970). The vertical strain at any given depth is quantified by the *strain influence factor*, I_ε, which is a weighting factor that accounts for both the finite size of the footing and change in stiffness of the soil due to the applied load. Schmertmann idealized the distribution of I_ε with depth as two straight lines, as shown in Figure 8.7.

The peak value of the strain influence factor, $I_{\varepsilon p}$ is:

$$I_{\varepsilon p} = 0.5 + 0.1\sqrt{\frac{q - \sigma'_{zD}}{\sigma'_{zp}}} \tag{8.11}$$

where

$I_{\varepsilon p}$ = peak strain influence factor
q = bearing stress
σ'_{zD} = initial vertical effective stress at a depth D below the ground surface
σ'_{zp} = initial vertical effective stress at depth of peak strain influence factor (for square and circular footings ($L/B = 1$), compute σ'_{zp} at a depth of $D + B/2$ below the ground surface; for continuous footings ($L/B \geq 10$), compute it at a depth of $D + B$)

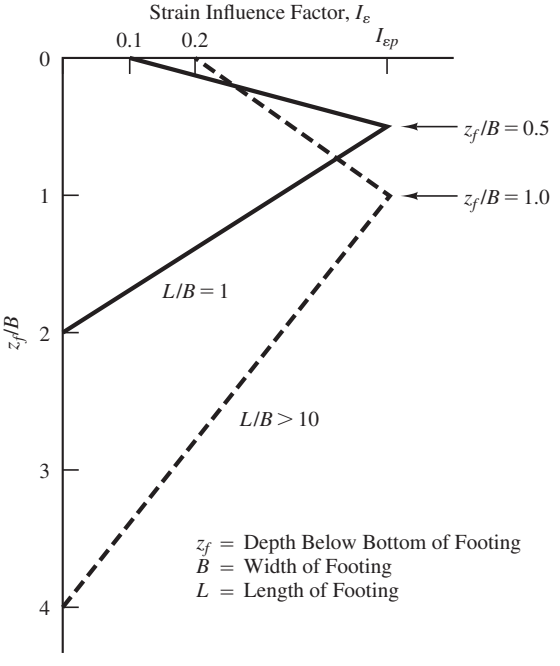

Figure 8.7 Distribution of strain influence factor with depth under square and continuous footings (Based on Schmertmann, 1978; used with permission of ASCE).

The exact value of I_ε at any given depth may be computed by interpolation using the following equations:

Square and circular footings ($L/B = 1$):

For $z_f = 0$ to $B/2$:

$$I_\varepsilon = 0.1 + (z_f/B)(2I_{\varepsilon p} - 0.2) \tag{8.12}$$

For $z_f = B/2$ to $2B$:

$$I_\varepsilon = 0.667I_{\varepsilon p}(2 - z_f/B) \tag{8.13}$$

Continuous footings ($L/B \geq 10$):

For $z_f = 0$ to B:

$$I_\varepsilon = 0.2 + (z_f/B)(I_{\varepsilon p} - 0.2) \tag{8.14}$$

For $z_f = B$ to $4B$:

$$I_\varepsilon = 0.333I_{\varepsilon p}(4 - z_f/B) \tag{8.15}$$

Rectangular footings ($1 < L/B < 10$):

$$I_\varepsilon = I_{\varepsilon s} + 0.111(I_{\varepsilon c} - I_{\varepsilon s})(L/B - 1) \tag{8.16}$$

where

z_f = depth from bottom of footing to midpoint of layer
I_ε = strain influence factor
$I_{\varepsilon c}$ = I_ε for a continuous footing
$I_{\varepsilon p}$ = peak I_ε from Equation 8.11
$I_{\varepsilon s}$ = I_ε for a square footing ≥ 0

The procedure for computing I_ε beneath rectangular footings requires computation of I_ε for each layer using the equations for square footings (based on the $I_{\varepsilon p}$ for square footings) and the I_ε for each layer using the equations for continuous footings (based on the $I_{\varepsilon p}$ for continuous footings), then combining them using Equation 8.16.

Although the idealized distribution of I_ε with depth strictly speaking applies to footings on homogeneous sands only, this distribution has been shown to give reasonable results when applied to heterogeneous sands in which E_s varies with depth.

Schmertmann's method also includes empirical corrections for the depth of embedment, secondary creep in the soil, and footing shape. These are implemented through the factors C_1, C_2, and C_3 to give the following formulas to compute the settlement, δ:

$$\delta = C_1C_2C_3(q - \sigma'_{zD}) \sum \frac{I_\varepsilon H}{E_s} \tag{8.17}$$

$$C_1 = 1 - 0.5\left(\frac{\sigma'_{zD}}{q - \sigma'_{zD}}\right) \tag{8.18}$$

$$C_2 = 1 + 0.2 \log\left(\frac{t}{0.1}\right) \qquad \text{for } t \geq 0.1 \text{ year} \tag{8.19}$$

$$C_3 = \max\begin{bmatrix} 1.03 - 0.03L/B \\ 0.73 \end{bmatrix} \tag{8.20}$$

where

δ = settlement of footing
C_1 = depth factor
C_2 = secondary creep factor
C_3 = shape factor
q = bearing stress
σ'_{zD} = effective vertical stress at a depth D below the ground surface
I_ε = influence factor at midpoint of soil layer
H = thickness of soil layer
E_s = equivalent modulus of elasticity of soil layer
t = time since application of load (year) ($t \geq 0.1$ year)
B = footing width
L = footing length

These formulas may be used with any consistent set of units, except that t must be expressed in years. Typically we use $t = 50$ years ($C_2 = 1.54$).

Analysis Procedure

The Schmertmann method uses the following procedure:

1. Perform appropriate in situ tests to define the subsurface conditions.
2. Define E_s as a function of depth using measured CPT data and Table 4.8 (or, less accurately, SPT data with Equation 4.48 and Table 4.7).
3. Consider the soil from the base of the foundation to the depth of influence below the base. This depth ranges from $2B$ for square footings to $4B$ for continuous footings. Divide this zone into layers and assign a representative E_s value to each layer. The required number of layers and the thickness of each layer depend on the variations in the E_s versus depth profile. For hand calculations, typically 5 to 10 layers are appropriate. If the in situ test data is available in electronic form, typically a spreadsheet solution is used with layer thicknesses equal to the test interval.
4. Compute the peak strain influence factor, $I_{\varepsilon p}$, using Equation 8.11.

5. Compute the strain influence factor, I_ε, at the midpoint of each layer. This factor varies with depth as shown in Figure 8.7, but is most easily computed using Equations 8.12 to 8.16.
6. Compute the correction factors, C_1, C_2, and C_3, using Equations 8.18 to 8.20.
7. Compute the settlement using Equation 8.17.

Example 8.5

The results of a CPT sounding performed at McDonald's Farm near Vancouver, British Columbia, are shown in Figure 8.8. The soils at this site consist of young, normally consolidated sands with some interbedded silts. The groundwater table is at a depth of 2.0 m below the ground surface.

A 375 kN/m load is to be supported on a 2.5 m $\times$ 30 m footing to be founded at a depth of 2.0 m in this soil. Use Schmertmann's method to compute the settlement of this footing soon after construction and the settlement 50 years after construction.

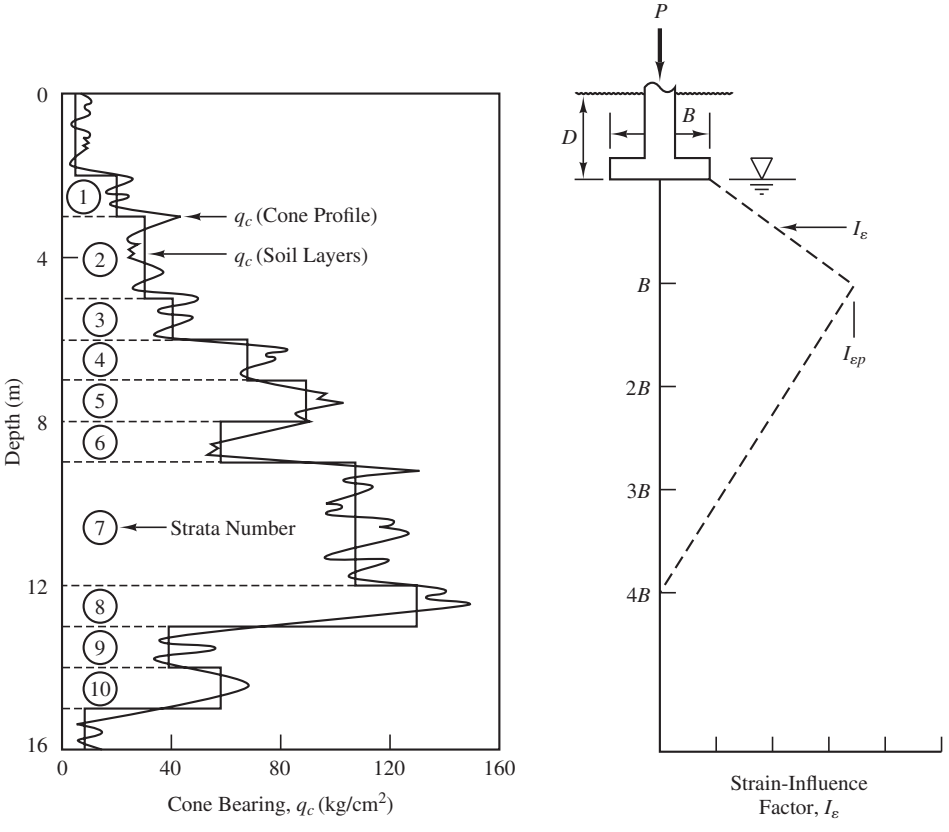

Figure 8.8 CPT results at McDonald's farm (adapted from Robertson and Campanella, 1988).

Solution

From Table 4.8, use $E_s = 2.5q_c$

$$1 \text{ kPa} = 0.01020 \text{ kg/cm}^2$$

Depth of influence $= D + 4B = 2.0 + 4(2.5) = 12.0$ m

Layer No.	Depth (m)	q_c (kg/cm^2)	E_s (kPa)
1	2.0–3.0	20	4,902
2	3.0–5.0	30	7,353
3	5.0–6.0	41	10,049
4	6.0–7.0	68	16,667
5	7.0–8.0	90	22,059
6	8.0–9.0	58	14,216
7	9.0–12.0	108	26,471

$$W_f = (2.5 \text{ m})(2.0 \text{ m})(23.6 \text{ kN/m}^3) = 118 \text{ kN/m}$$

$$q = \frac{P + W_f}{B} - u_D = \frac{375 \text{ kN/m} + 118 \text{ kN/m}}{2.5 \text{ m}} - 0 = 197 \text{ kPa}$$

Use $\gamma = 17$ kN/m^3 above groundwater table and 20 kN/m^3 below (from Table 3.2).

$$\begin{aligned}\sigma'_{zp}(\text{at } z = D + B) &= \Sigma \gamma H - u \\ &= (17 \text{ kN/m}^3)(2 \text{ m}) + (20 \text{ kN/m}^3)(2.5 \text{ m}) - (9.8 \text{ kN/m}^3)(2.5 \text{ m}) \\ &= 59 \text{ kPa}\end{aligned}$$

$$\sigma'_{zD} = \gamma D = (17)(2) = 34 \text{ kPa}$$

$$I_{\varepsilon p} = 0.5 + 0.1\sqrt{\frac{q - \sigma'_{zD}}{\sigma'_{zp}}} = 0.5 + 0.1\sqrt{\frac{197 \text{ kPa} - 34 \text{ kPa}}{59 \text{ kPa}}} = 0.666$$

Layer No.	E_s (kPa)	z_f (m)	I_ε Eqs. 8.14 & 1.15	H (m)	$I_\varepsilon H/E_s$
1	4,902	0.5	0.293	1.0	5.98×10^{-5}
2	7,353	2.0	0.573	2.0	15.58×10^{-5}
3	10,049	3.5	0.577	1.0	5.74×10^{-5}
4	16,667	4.5	0.488	1.0	2.93×10^{-5}
5	22,059	5.5	0.399	1.0	1.81×10^{-5}
6	14,216	6.5	0.310	1.0	2.18×10^{-5}
7	26,471	8.5	0.133	3.0	1.51×10^{-5}
				$\Sigma =$	35.73×10^{-5}

$$C_1 = 1 - 0.5\left(\frac{\sigma'_{zD}}{q - \sigma'_{zD}}\right) = 1 - 0.5\left(\frac{34 \text{ kPa}}{197 \text{ kPa} - 34 \text{ kPa}}\right) = 0.896$$

$$C_3 = 1.03 - 0.03L/B \geq 0.73$$

$$= 1.03 - 0.03(30/2.5)$$

$$= 0.67$$

$$\text{Use } C_3 = 0.73$$

At $t = 0.1$ year:

$$C_2 = 1$$

$$\delta = C_1C_2C_3(q - \sigma'_{zD})\sum\frac{I_e H}{E_s}$$

$$= (0.896)(1)(0.73)(197 - 34)(35.73 \times 10^{-5})$$

$$= \mathbf{0.038 \text{ m or } 38 \text{ mm}}$$

At $t = 50$ years:

$$C_2 = 1 + 0.2\log\left(\frac{t}{0.1}\right) = 1 + 0.2\log\left(\frac{50}{0.1}\right) = 1.54$$

$$\delta = 38(1.54) = \mathbf{59 \text{ mm}}$$

8.3 *e*-LOG-*p* BASED METHOD OF COMPUTING SETTLEMENT

This method of computing total settlement of a spread footing is based on Terzaghi's theory of consolidation. It assumes settlement in a one-dimensional process, in which all of the strains are vertical and uses the e versus log-σ' model for stress-strain shown in Figure 3.11. As discussed in Section 3.4 this method is most appropriate for soft to medium normally consolidated or lightly overconsolidated saturated clays. For cohesionless soils or stiff highly overconsolidated cohesive soils, the modulus based methods are more appropriate.

Computation of Effective Stresses

To apply Terzaghi's theory of consolidation, we need to know both the initial vertical effective stress, σ'_{z0}, and the final vertical effective stress, σ'_{zf}, at various depths beneath the foundation. The values of σ'_{z0} are computed using the techniques described in Section 3.3, and reflect the pre-construction conditions (i.e., without the proposed footing). We then compute σ'_{zf} using the following equation:

$$\sigma'_{zf} = \sigma'_{z0} + \Delta\sigma_z \tag{8.21}$$

Where $\Delta\sigma_z$ is the induced vertical stress increase due to load from footing and is computed using the techniques described in Section 3.3 as:

$$\Delta\sigma_z = I_\sigma(q - \sigma'_{zD}) \tag{8.22}$$

Foundation Rigidity Effects

The distribution of induced stresses under a uniformly loaded area are not uniform along any given horizontal plane. As shown by Figures 3.5 through 3.7, I_σ and, therefore, $\Delta\sigma_z$ is greater under the center of the loaded area than it is at the same depth under the edge. Therefore, the computed consolidation settlement will be greater at the center.

For example, consider the cylindrical steel water tank in Figure 8.9. The water inside the tank weighs much more than the tank itself, and this weight is supported directly on the plate-steel floor. In addition, the floor is relatively thin, and could be considered to be perfectly flexible, giving a uniform bearing pressure at the surface. We could compute the settlement beneath both the center and the edge, using the respective values of I_σ from Figure 3.5. The difference between these two is the differential settlement, δ_D, which could then be compared to the allowable differential settlement, δ_{Da}.

However, such an analysis would not apply to square spread footings, such as the one shown in Figure 8.9, because footings are much more rigid than plate-steel tank floors. Although the center of the footing "wants" to settle more than the edge, the rigidity of the footing forces the settlement to be the same everywhere.

A third possibility would be a mat foundation, which is more rigid than the tank, but less rigid than the footing. Thus, there will be some differential settlement between the center and the edge, but not as much as with a comparably-loaded steel tank. Chapter 11 discusses methods of computing differential settlements in mat foundations, and the corresponding flexural stresses in the mat.

When performing settlement analyses on spread footings, we account for this rigidity effect by computing the settlement using $\Delta\sigma_z$ values beneath the center of the footing,

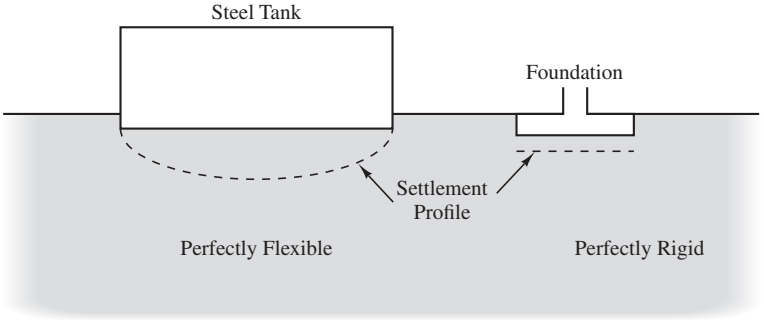

Figure 8.9 Influence of foundation rigidity on settlement. The steel tank on the left is very flexible, so the center settles more than the edge. Conversely, the reinforced concrete footing on the right is very rigid, and thus settles uniformly.

then multiplying the result by a *rigidity factor*, *r*. Table 8.1 presents *r*-values for various conditions.

Many engineers choose to ignore the rigidity effect (i.e., they use $r = 1$ for all conditions), which is conservative. This practice is acceptable, especially on small- or moderate-size structures, and usually has a small impact on construction costs. The use of $r < 1$ is most appropriate when the subsurface conditions have been well-defined by extensive subsurface investigation and laboratory testing, which provides the needed data for a more "precise" analysis.

Settlement Computation

We compute the consolidation settlement by dividing the soil beneath the foundation into layers, computing the settlement of each layer, and summing. The top of the first layer should be at the bottom of the foundation, and the bottom of the last layer should be at a depth such that $\Delta\sigma_z < 0.10$ q. As shown in Figures 3.6 and 3.7, this point occurs at a depth $2B$ below a square footing or $6B$ below a continuous footing.

Since strain varies nonlinearly with depth, analyses that use a large number of thin layers produce more precise results than those that use a few thick layers. Thus, computer analyses generally use a large number of thin layers. However, this would be too tedious to do by hand, so manual computations normally use fewer layers. For most soils, the guidelines in Table 8.2 should produce reasonable results.

The consolidation settlement equations in Chapter 3 (Equations 3.29 through 3.31) must be modified by incorporating the *r* factor, as follows:

For normally consolidated soils ($\sigma'_{z0} \approx \sigma'_c$):

$$\delta_c = r \sum \frac{C_c}{1 + e_0} H \log\left(\frac{\sigma'_{zf}}{\sigma'_{z0}}\right) \tag{8.23}$$

TABLE 8.1 r-VALUES FOR COMPUTATION OF TOTAL SETTLEMENT AT THE CENTER OF A SHALLOW FOUNDATION, AND METHODOLOGY FOR COMPUTING DIFFERENTIAL SETTLEMENT

Foundation Rigidity	*r* for Computation of δ at Center of Foundation	Methodology for Computing δ_D.
Perfectly flexible (i.e., steel tanks)	1.00	Compute $\Delta\sigma_z$ below edge and use $r = 1$.
Intermediate (i.e., mat foundations)	0.85–1.00, typically about 0.90	Use method described in Chapter 11.
Perfectly rigid (i.e., spread footings)	0.85	Entire footing settles uniformly, so long as bearing pressure is uniform. Compute differential settlement between footings or along length of continuous footing using method described in Section 8.4.

TABLE 8.2 APPROXIMATE THICKNESSES OF SOIL LAYERS FOR MANUAL COMPUTATION OF CONSOLIDATION SETTLEMENT OF SPREAD FOOTINGS

	Approximate Layer Thickness	
Layer Number	Square Footing	Continuous Footing
1	$B/2$	B
2	$B/2$	B
3	B	$2B$
4	B	$2B$

1. Adjust the number and thicknesses of the layers to account for changes in soil properties. Locate each layer entirely within one soil stratum.
2. For rectangular footings, use layer thicknesses between those given for square and continuous footings.
3. Use somewhat thicker layers (perhaps up to 1.5 times the thickness shown) if the groundwater table is very shallow.
4. For quick, but less precise, analyses, use a single layer with a thickness of about $3B$ (square footings) or $6B$ (continuous footings).

For overconsolidated soils—Case I ($\sigma'_{zf} < \sigma'_c$):

$$\delta_c = r \sum \frac{C_r}{1 + e_0} H \log\left(\frac{\sigma'_{zf}}{\sigma'_{z0}}\right) \tag{8.24}$$

For overconsolidated soils—Case II ($\sigma'_{z0} < \sigma'_c < \sigma'_{zf}$):

$$\delta_c = r \sum \left[\frac{C_r}{1 + e_0} H \log\left(\frac{\sigma'_c}{\sigma'_{z0}}\right) + \frac{C_c}{1 + e_0} H \log\left(\frac{\sigma'_{zf}}{\sigma'_c}\right) \right] \tag{8.25}$$

where

δ_c = ultimate consolidation settlement
r = rigidity factor (see Table 8.1)
C_c = compression index
C_r = recompression index
e_0 = initial void ratio
H = thickness of soil layer
σ'_{z0} = initial vertical effective stress at midpoint of soil layer
σ'_{zf} = final vertical effective stress at midpoint of soil layer
σ'_c = preconsolidation stress at midpoint of soil layer

As discussed earlier, many engineers choose to ignore the rigidity effect, which means the r factor drops out of these equations.

Example 8.6

The allowable settlement for the proposed square footing in Figure 8.10 is 1 in. Using the strain versus log-σ method, compute its settlement and determine if it satisfies this criterion. Assume the sustained load is 100 k.

Solution

$$W_f = (6\text{ ft})^2(2\text{ ft})(150\text{ lb/ft}^3) = 10{,}800\text{ lb}$$

$$q = \frac{P + W_f}{A} - u_D = \frac{100{,}000\text{ lb} + 10{,}800\text{ lb}}{(6\text{ ft})^2} - 0 = 3078\text{ lb/ft}^2$$

$$\sigma'_{zD} = (115\text{ lb/ft}^3)(2\text{ ft}) = 230\text{ lb/ft}^2$$

Using Equations 3.5, 3.14, 8.22, and 8.24 with $r = 0.85$,

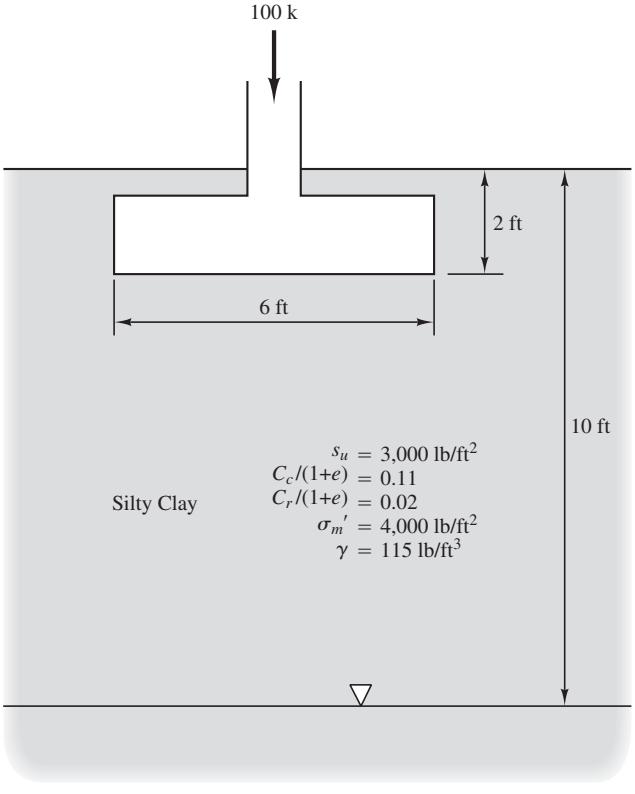

Figure 8.10 Proposed spread footing for Example 8.6.

		At Midpoint of Soil Layer								
Layer No.	H (ft)	z_f (ft)	σ'_{z0} (lb/ft^2)	$\Delta\sigma_z$ (lb/ft^2)	σ'_{zf} (lb/ft^2)	σ'_c (lb/ft^2)	Case	$\frac{C_c}{1+e_0}$	$\frac{C_r}{1+e_0}$	δ_c (in)
1	3.0	1.5	402	2680	3082	4402	OC-I	0.11	0.02	0.54
2	6.0	6.0	920	925	1845	4920	OC-I	0.11	0.02	0.37
3	12.0	15.0	1518	190	1708	5518	OC-I	0.11	0.02	0.13
									Σ	$= 1.04$

Round off to $\boldsymbol{\delta = 1.0}$ **in**

$\delta \leq \delta_a$, so the settlement criterion has been satisfied

Note: In this case, $\sigma'_m > q$, so the soil must be overconsolidated case I. Therefore, there is no need to compute σ'_c, or to list the $C_c/(1 + e_0)$ values.

Example 8.7

The allowable settlement for the proposed continuous footing in Figure 8.11 is 25 mm. Using the classical method, compute its settlement and determine if it satisfies this criterion. Assume the sustained load is 65 kN/m.

Solution

$$P = 65 \text{ kN/m}$$

$$W_f = (1.2 \text{ m})(0.5 \text{ m})(23.6 \text{ kN/m}^3) = 14 \text{ kN/m}$$

$$q = \frac{P + W_f}{B} - u_D = \frac{65 \text{ kN/m} + 14 \text{ kN/m}}{1.2 \text{ m}} - 0 = 66 \text{ kPa}$$

$$\sigma'_{zD} = (18.0 \text{ kN/m}^3)(0.5 \text{ m}) = 9 \text{ kPa}$$

Using Equations 3.5, 3.15, 8.22, and 8.24 with $r = 0.85$,

		At Midpoint of Soil Layer								
Layer No.	H (m)	z_f (m)	σ'_{z0} (kPa)	$\Delta\sigma_z$ (kPa)	σ'_{zf} (kPa)	σ'_c (kPa)	Case	$\frac{C_c}{1+e_0}$	$\frac{C_r}{1+e_0}$	δ_c (mm)
1	1.0	0.50	18	51	69	318	OC-I	0.13	0.04	23.4
2	1.0	1.50	36	18	54	336	OC-I	0.13	0.04	7.1
3	1.5	2.75	58	6	62	66	OC-I	0.13	0.04	2.9
4	2.0	4.50	90	3	73	80	OC-I	0.13	0.04	1.2
5	3.0	7.00	136	1	93	492	OC-I	0.15	0.05	0.8
									$\Sigma =$	35.4

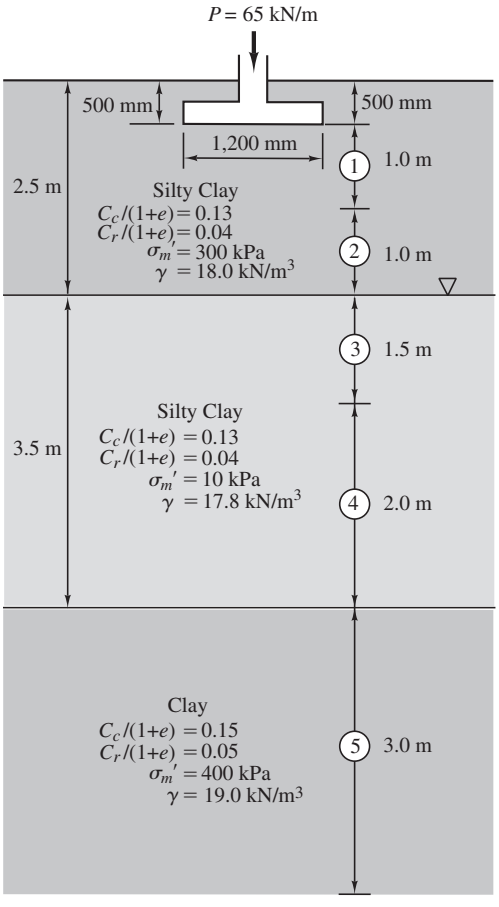

Figure 8.11 Proposed footing for Example 8.2.

$$\boldsymbol{\delta = 35 \text{ mm}}$$

$\delta > \delta_a$, so the settlement criterion has not been satisfied

General Methodology

In summary, the general methodology for computing total settlements of spread footings based on laboratory tests is as follows:

1. Drill exploratory borings at the site of the proposed footings and obtain undisturbed samples of each soil strata. Also use these borings to develop a design soil profile.
2. Perform one or more consolidation tests for each of the soil strata encountered beneath the footings, and determine the parameters $C_c/(1 + e_0)$, $C_r/(1 + e_0)$, and σ'_m for each strata using the techniques describe in Chapter 3. In many cases, all of

the soil may be considered to be a single stratum, so only one set of these parameters is needed. However, if multiple clearly defined strata are present, then each must have its own set of parameters.

3. Divide the soil below a footing into layers. Usually, about three layers provide sufficient accuracy, but more layers may be necessary if multiple strata are present or if additional precision is required. For square footings, the bottom of the lowest layer should be about $2B$ to $3B$ below the bottom of the footing; for continuous footings, it should be about $6B$ to $7B$ below the bottom of the footing. When using four layers, choose their thicknesses approximately as shown in Table 8.2.
4. Compute σ'_{z0} at the midpoint of each layer.
5. Using any of the methods described in Section 3.3, compute $\Delta\sigma_z$ at the midpoint of each layer. For hand computations, it is usually best to use Equations 3.13 to 3.16.
6. Using Equation 8.21, compute σ'_{zf} at the midpoint of each layer.
7. If the soil might be overconsolidated case II, use Equation 3.24 to compute σ'_c at the midpoint of each layer.
8. Using Equation 8.23, 8.24, or 8.25, compute δ_c for each layer, then sum. Note that some layers may require the use of one of these equations, while other layers may require another.

8.4 DIFFERENTIAL SETTLEMENT

Differential settlement, δ_D, is the difference in settlement between two foundations, or the difference in settlement between two points on a single foundation. Excessive differential settlement is troublesome because it distorts the structure and thus introduces serviceability problems, as discussed in Chapter 5.

Normally we design the foundations for a structure such that all of them have the same computed total settlement, δ. Therefore, in theory, there should be no differential settlement. However, in reality differential settlements usually occur anyway. There are many potential sources of these differential settlements, including:

- **Variations in the soil profile**—For example, part of a structure might be underlain by stiff natural soils, and part by a loose, uncompacted fill. Such a structure may have excessive differential settlement because of the different compressibility of these soil types, and possibly because of settlement due to the weight of the fill. This source of differential settlements is present to some degree on nearly all sites because of the natural variations in all soils, and is usually the most important source of differential settlement.
- **Variations in the structural loads**—The various foundations in a structure are designed to accommodate different loads according to the portion of the structure they support. Normally each would be designed for the same total settlement under its design load, so in theory the differential settlement should be zero. However, the ratio of actual load to design load may not be the same for all of the foundations. Thus, those with a high ratio will settle more than those with a low ratio.

Figure 8.12 This steel-frame structure has no diagonal bracing or shear walls, and thus would be classified as "flexible."

- **Design controlled by bearing capacity**—The design of some of the foundations may have been controlled by bearing capacity, not settlement, so even the design settlement may be less than that of other foundations in the same structure.
- **Construction tolerances**—The as-built dimensions of the foundations will differ from the design dimensions, so their settlement behavior will vary accordingly.

The rigidity of the structure also has an important influence on differential settlements. Some structures, such as the steel frame in Figure 8.12, are very flexible. Each foundation acts nearly independent of the others, so the settlement of one foundation has almost no impact on the other foundations. However, other structures are much stiffer, perhaps because of the presence of shear walls or diagonal bracing. The braced steel-frame structure in Figure 8.13 is an example of a more rigid structure. In this case, the structure tends to smooth over differential settlement problems. For example, if one

Figure 8.13 The diagonal bracing in this steel-frame structure has been installed to resist seismic loads. However, a side benefit is that this bracing provides more rigidity, which helps even out potential differential settlements. Shear walls have a similar effect. The two bays in the center of the photograph have no diagonal bracing, and thus would be more susceptible to differential settlement problems.

foundation settles more than the others, a rigid structure will redirect some of its load, as shown in Figure 8.14, thus reducing the differential settlement.

Computing Differential Settlement of Spread Footings

There are at least two methods of predicting differential settlements of spread footings. The first method uses a series of total settlement analyses that consider the expected variations in each of the relevant factors. For example, one analysis might consider the best-case scenario

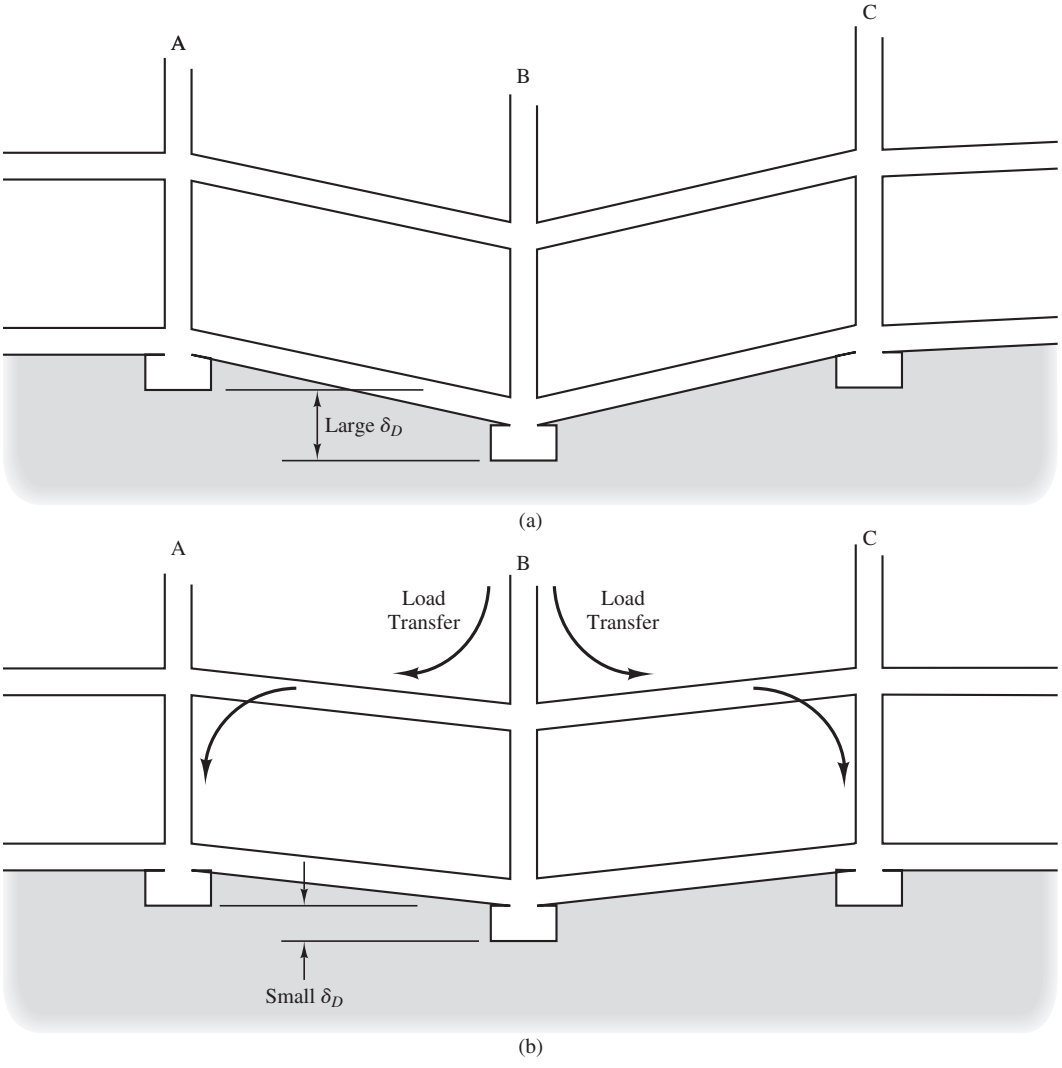

Figure 8.14 Influence of structural rigidity on differential settlements: (a) a very flexible structure has little load transfer, and thus could have larger differential settlements; (b) a more rigid structure has greater capacity for load transfer, and thus provides more resistance to excessive differential settlements.

of soil properties, loading, and so forth, while another would consider the worst-case scenario. The difference between these two total settlements is the differential settlement.

The second method uses δ_D/δ ratios that have been observed in similar structures on similar soil profiles. For example, Bjerrum (1963) compared the total and differential settlements of spread footings on clays and sands, as shown in Figures 8.15 and 8.16. Presumably, this data was obtained primarily from sites in Scandinavia, and thus reflects the very soft soil conditions encountered in that region. This is why much of the data reflects very large settlements.

Sometimes locally-obtained δ_D/δ observations are available. Such data is more useful than generic data, such as Bjerrum's, because it implicitly reflects local soil conditions. This kind of empirical local data is probably the most reliable way to assess δ_D/δ ratios.

In the absence of local data, the generic δ_D/δ ratios in Table 8.3 may be used to predict differential settlements. The values in this table are based on Bjerrum's data and the authors' professional judgment, and are probably conservative.

Alleviating Differential Settlement Problems

If the computed differential settlements in a structure supported on spread footings are excessive ($\delta_D > \delta_{Da}$), the design must be changed, even if the total settlements are acceptable. Possible remedies include:

- Enlarging all of the footings until the differential settlements are acceptable. This could be done by using the allowable differential settlement, δ_{Da} and the δ_D/δ ratio to compute a new value of δ_a, then sizing the footings accordingly. Example 8.8 illustrates this technique.
- Connecting the footings with *grade beams*, as shown in Figure 8.17. These beams provide additional rigidity to the foundation system, thus reducing the differential

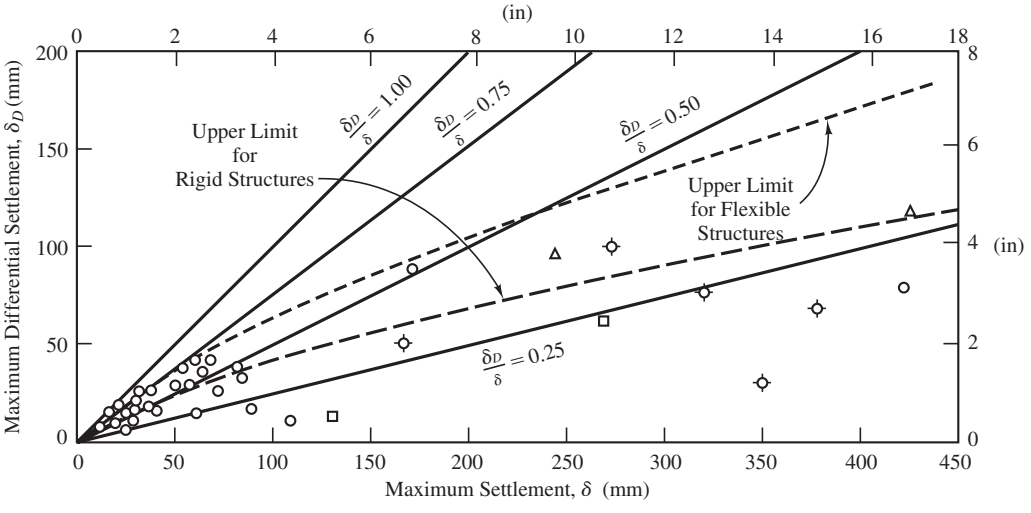

Figure 8.15 Total and differential settlements of spread footings on clays (adapted from Bjerrum, 1963).

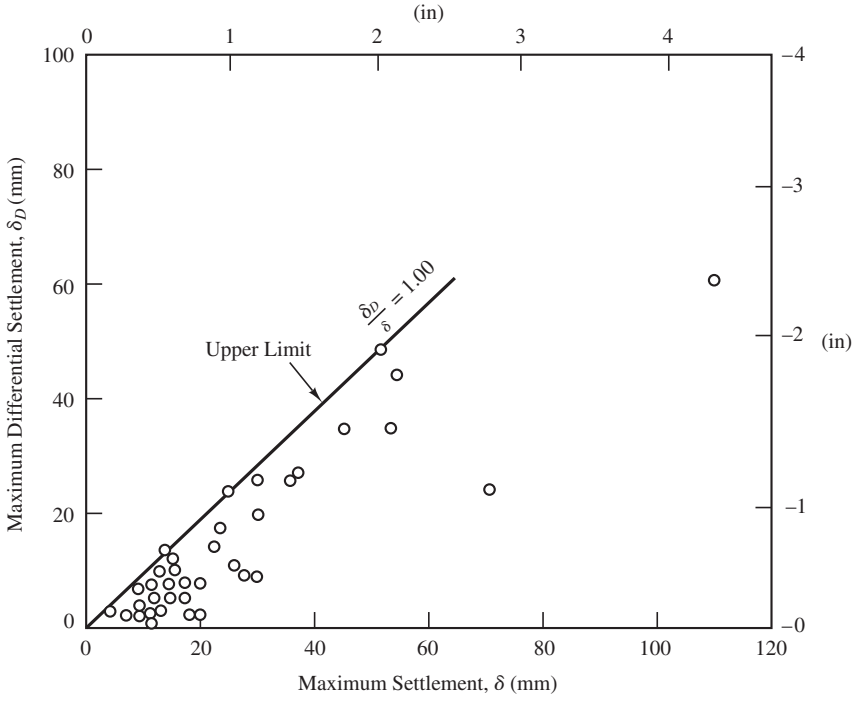

Figure 8.16 Total and differential settlement of spread footings on sands (adapted from Bjerrum, 1963).

settlements. The effectiveness of this method could be evaluated using a structural analysis.

- Replacing the spread footings with a mat foundation. This method provides even more rigidity, and thus further reduces the differential settlements. Chapter 11 discusses the analysis and design of mats.

TABLE 8.3 PREDICTED VALUES OF δ_D/δ FOR SPREAD FOOTING FOUNDATIONS

	Design Value of δ_D/δ	
Predominant Soil Type Below Footings	Flexible Structures	Rigid Structures
Sandy		
Natural soils	0.9	0.7
Compacted fills of uniform thickness underlain by stiff natural soils	0.5	0.4
Clayey		
Natural soils	0.8	0.5
Compacted fills of uniform thickness underlain by stiff natural soils	0.4	0.3

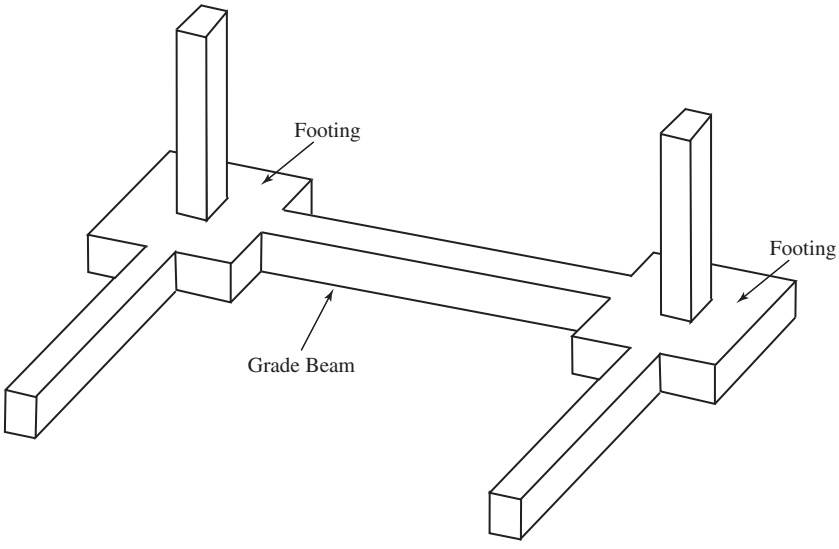

Figure 8.17 Use of grade beams to tie the spread footings together.

- Replacing the spread footings with a system of deep foundations, as discussed in Chapter 12.
- Redesigning the superstructure so that it can accommodate larger differential settlements, so that the structural loads are lower, or both. For example, a masonry structure could be replaced by a wood-frame structure.
- Providing a method of releveling the structure if the differential settlements become excessive. This can be done by temporarily lifting selected columns from the footing and installing shims between the base plate and the footing.
- Accepting the large differential settlements and repair any damage as it occurs. For some structures, such as industrial buildings, where minor distress is acceptable, this may be the most cost-effective alternative.

Example 8.8

A "flexible" steel-frame building is to be built on a series of spread footing foundations supported on a natural clayey soil. The allowable total and differential settlements are 20 and 12 mm, respectively. The footings have been designed such that their total settlement will not exceed 20 mm, as determined by the analysis techniques described in this chapter.

Will the differential settlements be within tolerable limits?

Solution

According to Table 8.3 , the δ_D/δ ratio is about 0.8. Therefore, the differential settlements may be as large as (0.8)(20 mm) = 16 mm. This is greater than the allowable value of 12 mm, and thus is unacceptable. Therefore, it is necessary to design the footings such that their total

settlement is no greater than (12 mm)/(0.8) = 15 mm. Thus, in this case the allowable total settlement must be reduced to $\delta_a = 15$ mm.

Mats

Because of their structural continuity, mat foundations generally experience less differential settlement, or at least the differential settlement is spread over a longer distance and thus is less troublesome. In addition, differential settlements in mat foundations are much better suited to rational analysis because they are largely controlled by the structural rigidity of the mat. We will cover these methods in Chapter 11.

8.5 RATE OF SETTLEMENT

Clays

If the clay is saturated, it is safe to assume the distortion settlement occurs as rapidly as the load is applied. The consolidation settlement will occur over some period, depending on the drainage rate.

Terzaghi's theory of consolidation includes a methodology for computing the rate of consolidation settlement in saturated soils. It is controlled by the rate water is able to squeeze out of the pores and drain away. However, because the soil beneath a footing is able to drain in three dimensions, not one as assumed in Terzaghi's theory, the water will drain away more quickly, so consolidation settlement also will occur more quickly. Davis and Poulos (1968) observed this behavior when they reviewed fourteen case histories. In four of these cases, the rate was very much faster than predicted, and in another four cases, the rate was somewhat faster. In the remaining six cases, the rate was very close to or slightly slower than predicted, but this was attributed to the drainage conditions being close to one-dimensional. They also presented a method of accounting for this effect.

Sands

The rate of settlement in sands depends on the pattern of loading. If the load is applied only once and then remains constant, then the settlement occurs essentially as fast as the load is applied. The placement of a fill is an example of this kind of loading. The dead load acting on a foundation is another example.

However, if the load varies over time, sands exhibit additional settlement that typically occurs over a period of years or decades. The live loads on a foundation are an example, especially with tanks, warehouses, or other structures in which the live load fluctuates widely and is a large portion of the total load.

A series of long-term measurements on structures in Poland (Bolenski, 1973) has verified this behavior. Bolenski found that footings with fairly constant loads, such as those supporting office buildings, exhibit only a small amount of additional settlement

after construction. However, those with varying loads, such as storage tanks, have much more long-term settlement. Burland and Burbidge (1985) indicate the settlement of footings on sand 30 years after construction might be 1.5 to 2.5 times as much as the post-construction settlement. This is the reason for the secondary creep factor, C_2, in Schmertmann's equation.

8.6 ACCURACY OF SETTLEMENT PREDICTIONS

After studying many pages of formulas and procedures, the reader may develop the mistaken impression that settlement analyses are an exact science. This is by no means true. It is good to recall a quote from Terzaghi (1936):

> Whoever expects from soil mechanics a set of simple, hard-and-fast rules for settlement computations will be deeply disappointed. He might as well expect a simple rule for constructing a geologic profile from a single test boring record. The nature of the problem strictly precludes such rules.

Although much progress has been made since 1936, the settlement problem is still a difficult one. The methods described in this chapter should be taken as guides, not dictators, and should be used with engineering judgment. A vital ingredient in this judgment is an understanding of the sources of error in the analysis. These include:

- Uncertainties in defining the soil profile. This is the largest single cause. There have been many cases of unexpectedly large settlements due to undetected compressible layers, such as peat lenses.
- Disturbance of soil samples.
- Errors in situ tests (especially the SPT).
- Errors in laboratory tests.
- Uncertainties in defining the service loads, especially when the live load is a large portion of the total load.
- Construction tolerances (i.e., footing not built to the design dimensions).
- Errors in determining the degree of overconsolidation.
- Inaccuracies in the analysis methodologies.
- Neglecting soil-structure interaction effects.

We can reduce some of these errors by employing more extensive and meticulous exploration and testing techniques, but there are economic and technological limits to such efforts.

Because of these errors, the actual settlement of a spread footing may be quite different from the computed settlement. Figure 8.18 shows 90 percent confidence intervals for spread footing settlement computations.

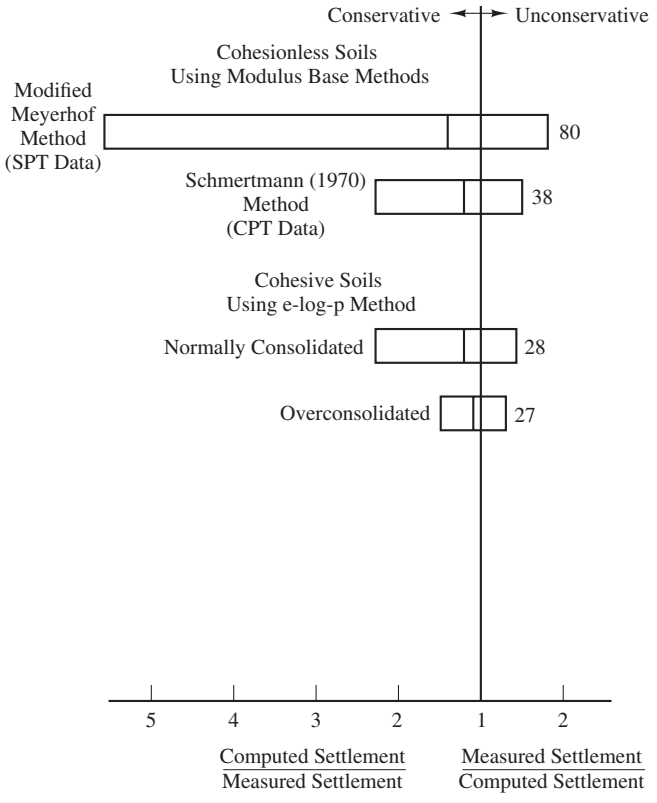

Figure 8.18 Comparison between computed and measured settlements of spread footings. Each bar represents the 90 percent confidence interval (i.e., 90 percent of the settlement predictions will be within this range). The line in the middle of each bar represents the average prediction, and the number to the right indicates the number of data points used to evaluate each method (based on data from Burland and Burbridge, 1985; Butler, 1975; Schmertmann, 1970; and Wahls, 1985).

We can draw the following conclusions from this data:

- Settlement predictions are conservative more often than they are unconservative (i.e., they tend to overpredict the settlement more often than they underpredict it). However, the range of error is quite wide.
- Settlement predictions made using modulus based methods are most accurate when using in situ measurements to determine modulus. Modulus determined from DMT or CPT data are much more precise than those based on the SPT.
- Settlement predictions in clays, especially those that are overconsolidated, are usually more precise than those in sands. However, the magnitude of settlement in clays is often greater.

Many of the soil factors that cause the scatter in Figure 8.18 do not change over short distances, so predictions of differential settlements should be more precise than

those for total settlements. Therefore, the allowable angular distortion criteria described in Table 5.2 (which include factors of safety of at least 1.5) reflect an appropriate level of conservatism.

The Leaning Tower of Pisa

During the Middle Ages, Europeans began to build larger and heavier structures, pushing the limits of design well beyond those of the past. In Italy, the various republics erected towers and campaniles to symbolize their power (Kerisel, 1987). Unfortunately, vanity and ignorance often lead to more emphasis on creative architecture than on structural integrity, and many of these structures collapsed. Although some of these failures were caused by poor structural design, many were the result of overloading the soil. Monuments tilted, but did not collapse. The most famous of these is the campanile in Pisa, more popularly known as the Leaning Tower of Pisa.

Construction of the tower began in the year 1173 under the direction of Bananno Pisano and continued slowly until 1178. This early work included construction of a ring-shaped footing 64.2 ft (19.6 m) in diameter along with three and one-half stories of the tower. By then, the average bearing pressure below the footing was about 6900 lb/ft^2 (330 kPa) and the tower had already begun to tilt. Construction ceased at this level, primarily because of political and economic unrest. We now know that this suspension of work probably saved the tower, because it provided time for the underlying soils to consolidate and gain strength.

Nearly a century later, in the year 1271, construction resumed under the direction of a new architect, Giovanni Di Simone. Although it probably would have been best to tear down the completed portion and start from scratch with a new and larger foundation, Di Simone chose to continue working on the uncompleted tower, attempting to compensate for the tilt by tapering the successive stories and adding extra weight to the high side. He stopped work in 1278 at the seventh cornice. Finally, the tower was completed with the construction of the belfry during a third construction period, sometime between 1360 and 1370. The axis of the belfry is inclined at an angle of 3° from the rest of the tower, which was probably the angle of tilt at that time. Altogether, the project had taken nearly two hundred years to complete.

Both the north and south sides of the tower continued to settle (the tilt has occurred because the south side settled more than the north side), so that by the early nineteenth century, the tower had settled about 2.5 meters into the ground. As a result, the elegant carvings at the base of the columns were no longer visible. To rectify this problem, a circular trench was excavated around the perimeter of the tower in 1838 to expose the bottom of the columns. This trench is known as the catino. Unfortunately, construction of the trench disturbed the groundwater table and removed some lateral support from the side of the tower. As a result, the tower suddenly lurched and added about half a meter to the tilt at the top. Amazingly, it did not collapse. Nobody dared do anything else for the next hundred years.

During the 1930s, the Fascist dictator Benito Mussolini decided the leaning tower presented an inappropriate image of the country, and ordered a fix. His workers drilled holes through the floor of the tower and pumped 200 tons of concrete into the underlying soil, but this only aggravated the problem and the tower gained an additional 0.1 degree of tilt.

During most of the twentieth century the tower had been moving at a rate of about 6 arc seconds per year. By the end of the century the total tilt was about 5.5 degrees to the south which means that the top of the tower structure was 5.2 m (17.0 ft) off of being plumb. The average bearing pressure under the tower is 497 kPa (10,400 lb/ft^2), but the tilting caused its weight to act eccentrically on the foundation, so the bearing pressure is not uniform. By the end

of the century, it ranged from 62 to 930 kPa (1,300–19,600 lb/ft^2), as shown in Figure 8.19. The tower was clearly on the brink of collapse. Even a minor earthquake could cause it to topple, so it became clear that some remedial measure had to be taken.

The subsurface conditions below the tower have been investigated, including an exhaustive program sponsored by the Italian government that began in 1965. The profile, shown in Figure 8.20, is fairly uniform across the site and consists of sands underlain by fat clays.

This problem has attracted the attention of both amateurs and professionals, and the authorities had received countless "solutions," sometimes at the rate of more than fifty per week. Some are clearly absurd, such as tying helium balloons to the top of the tower, or installing a series of cherub statues with flapping wings. Others, such as large structural supports (perhaps even a large statue leaning against the tower?), may have been technically feasible, but aesthetically unacceptable.

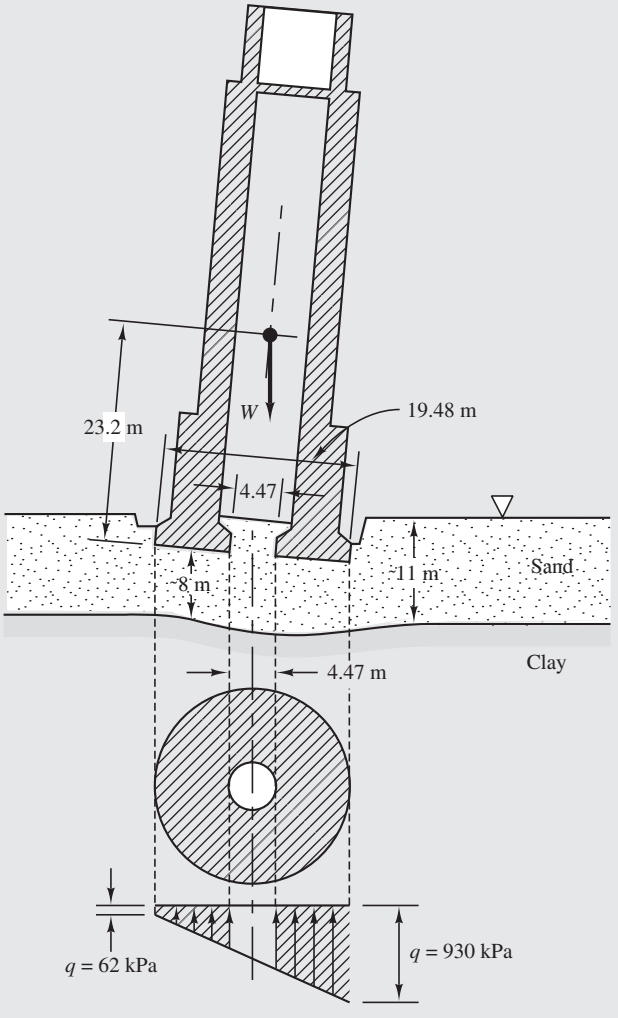

Figure 8.19 Configuration in tower before soil extraction started in 2000 (adapted from Costanzo et al., 1994 and Terzaghi 1934a).

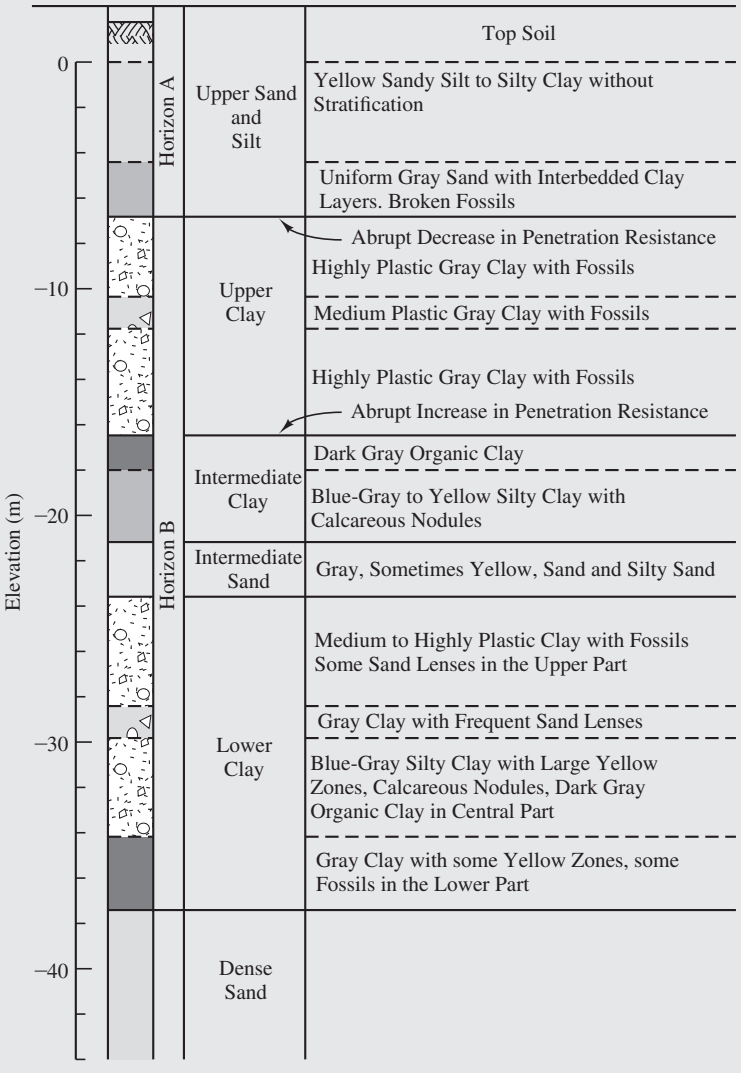

Figure 8.20 Soil profile below tower (adapted from Mitchell et al., 1977).

In 1990 the interior of the tower was closed to visitors, and in 1993 about 600 tons of lead ingots were placed on the north side of the tower as a temporary stabilization measure. Then, in 1995, engineers installed a concrete ring around the foundation and began drilling tiedown anchors through the ring and into the dense sand stratum located at a depth of about 40 ft (see profile in Figure 8.20). The weights caused the underlying soils to compress and slightly reduced the tilt, but construction of the anchors disturbed the soil and produced a sudden increase in the tilt of the tower. In one night the tower moved about 1.5 mm, which is the equivalent to a year's worth of normal movement. As a result, the work was quickly abandoned and more lead ingots were added to the north side.

A period of inactivity followed, but in 1997 an earthquake in nearby Assisi caused a tower in that city to collapse—and that tower was not even leaning! This failure induced a new cycle of activity at Pisa, and the overseeing committee approved stabilizing the tower using the method of soil extraction or underexcavation. The objective of this effort was to reduce the tilt from 5.5 degrees to 5.0 degrees, which is the equivalent of returning the tower to its position of three hundred years ago. There was no interest in making the tower perfectly plumb.

Between February 2000 and February 2001, soil was carefully extracted from underneath the north side of the tower by drilling 41 diagonal borings as shown on the cover of this text. Only small amounts of soil were removed at any time and the movement of the tower was carefully monitored during the process. The soil extraction process decreased the tower's tilt by 0.5 degrees. An additional 150 arc seconds of tilt reduction occurred between February 2001 and September 2008 at which time the rate of tilt reduction was less than 0.2 arc seconds per year. Engineers estimate this remediation will keep the tower safe for another 200 years.

Recommended reference: Burland, J. B., Jamiolkowski, M., and Viggiani, C. (2009). "Leaning Tower of Pisa: Behaviour after Stabilization Operations." *International Journal of Geoengineering Case Histories*, 1(3), 156. http://casehistories.geoengineer.org/

SUMMARY

Major Points

1. Two of the most important serviceability limits for foundations are total settlement and differential settlement.
2. Analysis of settlement is independent of the ultimate limit state analysis used for bearing capacity and sliding analysis. The settlement analysis is the same whether the ASD or LRFD method has been used for ultimate limit states.
3. The load on spread footings causes an increase in the vertical stress, $\Delta\sigma_z$, in the soil below. This stress increase causes settlement in the soil beneath the footing.
4. Appropriate loads must be selected for each settlement analysis and must be project specific. They will generally consist of the full unfactored dead load plus some portion of the live load.
5. There are two broad categories of settlement analysis techniques: modulus based methods and *e*-log-*p* methods. The *e*-log-*p* method is most appropriate for normally consolidated to lightly overconsolidated clay soils. Modulus based methods are more appropriate for other soil types.
6. Differential settlements may be estimated based on observed ratios of differential to total settlement.
7. Settlement estimates based on laboratory consolidation tests of clays and silts typically range from a 50 percent overestimate (unconservative) to a 100 percent underestimate (conservative).
8. Settlement estimates based on DMT or CPT data from sandy soils typically range from a 50 percent overestimate (unconservative) to a 100 percent underestimate (conservative). However, estimates based on the SPT are much less precise.

Vocabulary

Allowable differential settlement
Allowable total settlement
Drained conditions
e-log-*p* method
Incremental constrained modulus method
Long-term settlements
Modulus based methods
Schmertmann's method
Settlement rate
Short-term settlements
Strain influence factor
Undrained conditions

QUESTIONS AND PRACTICE PROBLEMS

Section 8.2: Modulus Based Methods of Computing Settlement

8.1 A 1.5 m square footing carries a column with a service load of 105 kN. It is founded at a depth of 2 m on a medium stiff clay with an undrained shear strength of 42 kPa, an overconsolidation ratio of 4, and a plasticity index of 35. The clay layer is 5 m thick and overlies a very stiff shale. Estimate the undrained settlement of the footing using the generalized elastic method with Christian and Carrier's (1978) influence factors.

8.2 A 250-k column load is to be supported on a 9 ft square footing embedded 2 ft below the ground surface. The underlying soil is a silty sand with an average N_{60} of 32 and a unit weight of 129 lb/ft^3. The groundwater table is at a depth of 35 ft. Estimate the undrained settlement of the footing using the generalized elastic method with Christian and Carrier's (1978) influence factors.

8.3 Repeat problem 8.2 using Schmertmann's method, compute the settlement of this footing at $t = 50$ years.

8.4 A 1.8 m square, 2 m deep footing supports a service load of 570 kN. It is supported on a clayey sand. A dilatometer test run at the site has returned the following modulus profile.

Depth (m)	2	3	4	5	6	7	8	9	10	11	12
M (MPa)	7.7	8.8	10.2	14.8	15.4	10.8	11.6	11.6	13.1	13.8	13.4

Compute the footing settlement.

8.5 Develop a spreadsheet to compute settlement of square footings using the incremental constrained modulus method. The spreadsheet should allow input of: footing width, depth of footing, column service load, and modulus as a function of depth. You will need to compute the stress distribution of the applied stress using techniques discussed in Section 3.3 in order to compute the settlement.

8.6 Develop a spreadsheet to compute settlement of square footings using Schmertmann's method. The spreadsheet should allow input of: footing width, depth of footing, depth of water table, unit weight of soil, column service load, and E_s as a function of depth.

8.7 A 190-k column load is to be supported on a 10 ft square, 3 ft deep spread footing underlain by young, normally consolidated sandy soils. The results of a representative CPT sounding at this site are as follows:

Depth (ft)	0.0–6.0	6.0–10.0	10.0–18.0	18.0–21.0	21.0–40.0
q_c (kg/cm^2)	30	51	65	59	110

The groundwater table is at a depth of 15 ft; the unit weight of the soil is 124 lb/ft^3 above the groundwater table and 130 lb/ft^3 below. Using Schmertmann's method, compute the total settlement of this footing 30 years after construction.

8.8 A 650-kN column load is supported on a 1.5 m wide by 2.0 m long by 0.5 m deep spread footing. The soil below is a well-graded, normally consolidated sand with $\gamma = 18.0$ kN/m^3 and the following SPT N_{60} values:

Depth (m)	1.0	2.0	3.0	4.0	5.0
N_{60}	12	13	13	8	22

The groundwater table is at a depth of 25 m. Compute settlement of the footing using the generalized elastic method with Christian and Carrier's (1978) influence factors.

8.9 Repeat problem 8.6 using Schmertmann's method, compute the total settlement at $t = 30$ years.

8.10 A 300-k column load is to be supported on a 10 ft square, 4 ft deep spread footing. Cone penetration tests have been conducted at this site, and the results are shown in Figure 8.8. The groundwater table is at a depth of 6 ft, $\gamma = 121$ lb/ft^3, and $\gamma_{sat} = 125$ lb/ft^3.

a. Compute the settlement of this footing using a spreadsheet.

b. The design engineer is considering the use of vibroflotation to densify the soils at this site (see discussion in Chapter 26). This process would increase the q_c values by 70 percent, and make the soil slightly overconsolidated. The unit weights would increase by 5 lb/ft^3. Use a spreadsheet to compute the settlement of a footing built and loaded after densification by vibroflotation.

Section 8.3: *e*-LOG-*p* Based Method of Computing Settlement

8.11 A proposed office building will include an 8 ft 6 in square, 3 ft deep spread footing that will support a vertical downward service load of 160 k. The soil below this footing is an overconsolidated clay with the following engineering properties: $C_c/(1 + e_0) = 0.10$, $C_r/(1 + e_0) = 0.022$, $\sigma'_m = 4{,}500$ lb/ft^2 and $\gamma = 113$ lb/ft^3. This soil strata extends to a great depth and the groundwater table is at a depth of 50 ft below the ground surface. Determine the total settlement of this footing.

8.12 A 1.0 m square, 0.5 m deep footing carries a downward service load of 200 kN. It is underlain by an overconsolidated clay with the following engineering properties: $C_c = 0.20$, $C_r = 0.05$, $e_0 = 0.7$, OCR = 8 and $\gamma = 15.0$ kN/m^3 above the groundwater table and 16.0 kN/m^3 below. The groundwater table is at a depth of 1.0 m below the ground surface. Determine the total settlement of this footing.

8.13 Prepare a spreadsheet to compute settlement of square footings using the e-log-p method. The spreadsheet should allow input of: footing width, footing depth, groundwater depth, column service load, footing rigidity factor and $C_r/(1 + e_0)$, $C_r/(1 + e_0)$, σ'_m, and γ as function of depth. Check your spreadsheet using a hand solution to Problem 8.12.

8.14 Using a spreadsheet and the data in Problem 8.11, determine the required footing width to obtain a total settlement of no more than 1.0 in. Select a width that is a multiple of 3 in. Would it be practical to build such a footing?

8.15 Using a spreadsheet and the data in Problem 8.12, determine the required footing width to obtain a total settlement of no more than 25 mm. Select a width that is a multiple of 100 mm. Would it be practical to build such a footing?

Section 8.4: Differential Settlement

8.16 A steel-frame office building with no diagonal bracing is supported on spread footings founded in a natural clay. The computed total settlement of these footings is 20 mm. Compute the differential settlement.

8.17 A reinforced-concrete building with numerous concrete shear walls is supported on spread footings founded in a compacted sand. The computed total settlement of these footings is 0.6 in. Compute the differential settlement.

Comprehensive

8.18 A proposed building is to be supported on a series of spread footings embedded 36 in into the ground. The underlying soils consist of silty sands with $N_{60} = 30$, an estimated overconsolidation ratio of 2, and $\gamma = 118$ lb/ft^3. This soil strata extends to a great depth and the groundwater table is at a depth of 10 ft below the ground surface. The allowable settlement is 1.0 in. Using a spreadsheet, develop a plot of allowable column load versus footing width.

8.19 A proposed building is to be supported on a series of spread footings embedded 36 in into the ground. The underlying soils consist of silty clays with $C_c/(1 + e_0) = 0.12$, $C_r/(1 + e_0) = 0.030$, $\sigma'_m = 5000$ lb/ft^2, and $\gamma = 118$ lb/ft^3. This soil strata extends to a great depth and the groundwater table is at a depth of 10 ft below the ground surface. The allowable settlement is 1.0 in. Using a spreadsheet, develop a plot of allowable column load versus footing width.

8.20 A 3 ft square, 2 ft deep footing carries a column load of 28.2 k. An architect is proposing to build a new 4 ft wide, 2 ft deep continuous footing adjacent to this existing footing. The side of the new footing will be only 6 in away from the side of the existing footing. The new footing will carry a load of 12.3 k/ft.

Develop a plot of $\Delta\sigma_z$ due to the new footing versus depth along a vertical line beneath the center of the existing footing. This plot should extend from the bottom of the existing footing to a depth of 35 ft below the bottom of this footing.

8.21 Using the data from Problem 8.20, $C_r/(1 + e_0) = 0.08$ and $\gamma = 119$ lb/ft^3, compute the consolidation settlement of the old footing due to the construction and loading of the new footing. The soil is an overconsolidated (case I) silty clay, and the groundwater table is at a depth of 8 ft below the ground surface.

8.22 Using a spreadsheet and the subsurface data from Example 8.5, develop a plot of footing width, B, versus column load, P, for square spread footings embedded 3 ft below the ground surface. Develop a P versus B curve for each of the following settlements: 0.5 in, 1.0 in, and 1.5 in, and present all three curves on the same diagram.

9

Spread Footings—Geotechnical Design

Your greatest danger is letting the urgent things crowd out the important.

From *Tyranny of the Urgent* by Charles E. Hummel

In practice, the geotechnical engineer conducts a site-specific geotechnical investigation using techniques such as those described in Chapter 4, evaluates the geotechnical ULS and SLS using the techniques described in Chapters 7 and 8, then presents the results of this work in a site-specific geotechnical investigation report. The structural engineer then uses the information in this report along with the structural loads, to determine the width and depth of individual footings and the structural design of each footing. The structural engineer also is responsible for preparing the foundation design drawings.

This division of work between the geotechnical engineer and the structural engineer makes it necessary to have a clear and simple means of communicating the site-specific geotechnical design criteria in the geotechnical report. There are three primary ways of doing so:

- The individual footing design approach
- The design chart approach
- The allowable bearing pressure approach

This chapter describes each of these three approaches, then addresses other geotechnical considerations.

9.1 INDIVIDUAL FOOTING DESIGN APPROACH

When using the individual footing design approach, the geotechnical engineer evaluates both the ULS and SLS for each proposed footing individually, and presents separate design recommendations for each footing in the geotechnical investigation report. This approach is best suited for projects that have only a few footings. For example, a highway bridge would be a good candidate because it has very few footings (perhaps one at each abutment and one at each intermediate pier), but these footings are heavily loaded and thus deserving of individual geotechnical analysis and design.

Footing Depth

Generally, the first step in footing design is to determine the required depth of embedment because this depth is often controlled by architectural requirements, environmental constraints, or soil stratigraphy considerations, such as:

- Depth of basements or other architectural requirements: Footings must be below the expected depth of the basement of the lowest floor.
- Depth of frost penetration: In areas subject to frost, footings are generally placed below the deepest expected level of frost penetration to prevent frost heave of footings.
- Depth of expansive soils: One method of dealing with expansive soils it to extend footings to a depth below zone where seasonal water fluctuations are anticipated. Chapter 27 discusses this technique in more detail.
- Footings near slopes: As discussed in Section 7.8, when footings are placed near slopes, it may be necessary to extend the depth of the footing to achieve an adequate bearing capacity.
- Footings prone to scour: Footings located in riverbeds or other locations where flow water can erode soils around and beneath footings must consider the depth to which this erosion or scour could occur. Footings subject to scour must be placed at depths below the deepest expect scour.
- Bypassing weak or compressible soils: Often soils near the surface are poor materials on which to found footings because of their low strength or high compressibility. If more competent soils exist at relatively shallow depths, it is often economical to found footings on these deeper more competent soils.

The above considerations generate minimum footing depth requirements. Sometimes we also may need to specify a maximum depth. It might be governed by such considerations as:

- Potential undermining of existing foundations, structures, streets, utility lines, etc.
- The presence of soft layers beneath harder and stronger near-surface soils, and the desire to support the footings in the upper stratum.

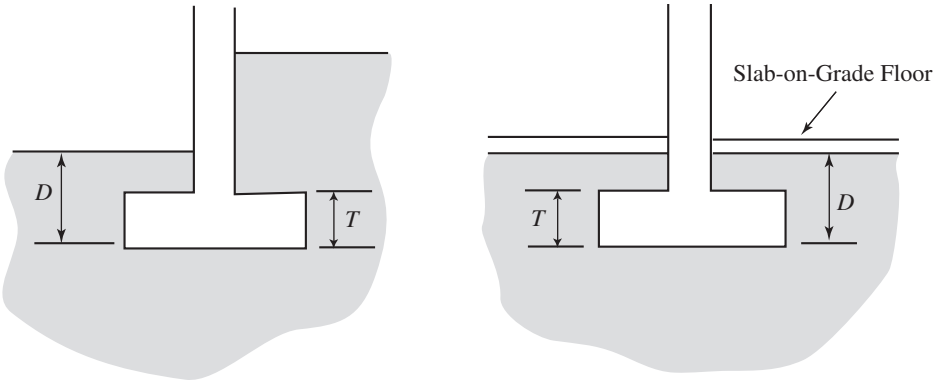

Figure 9.1 The minimum depth of embedment for a spread footing must be greater than the thickness of the footing itself.

- A desire to avoid working below the groundwater table, and thus avoid construction dewatering expenses.
- A desire to avoid the expense of excavation shoring, which may be needed for footing excavations that are more than 1.5 m (5 ft) deep.

The absolute minimum depth of embedment, D, must be at least large enough to accommodate the required footing thickness, T, although footings are usually placed somewhat deeper, as shown in Figure 9.1. The depth is measured from the lowest adjacent ground surface to the bottom of the footing. In the case of footings overlain by a basement or slab-on-grade floor, D is measured from the subgrade below the slab.

The actual footing thickness, T, will not be known until the structural design is complete, but the structural design is dependent upon the geotechnical design. However, we can use Tables 9.1 and 9.2 to estimate minimum D values to accommodate typical footing

TABLE 9.1 MINIMUM DEPTH OF EMBEDMENT FOR SQUARE AND RECTANGULAR FOOTINGS

Load P (k)	Minimum D (in)	Load P (kN)	Minimum D (mm)
0–65	12	0–300	300
65–140	18	300–500	400
140–260	24	500–800	500
260–420	30	800–1,100	600
420–650	36	1,100–1,500	700
		1,500–2,000	800
		2,000–2,700	900
		2,700–3,500	1,000

TABLE 9.2 MINIMUM DEPTH OF EMBEDMENT FOR CONTINUOUS FOOTINGS

Load P/b (k/ft)	Minimum D (in)	Load P/b (kN/m)	Minimum D (mm)
0–10	12	0–170	300
10–20	18	170–250	400
20–28	24	250–330	500
28–36	30	330–410	600
36–44	36	410–490	700
		490–570	800
		570–650	900
		650–740	1,000

thicknesses based on the applied loads. These D values are intended to provide enough room for the required footing thickness, T, and some soil cover. In some cases, a more detailed analysis may justify shallower depths, but D should never be less than 300 mm (12 in).

If any of the footings are subject to significant uplift forces, the thickness of the footing may need to be increased to provide the mass needed to resist uplift forces. In these cases, embedment depths greater than those shown in Tables 9.1 and 9.2 may be needed.

Determining the required footing depth generally follows this process:

1. Determine the minimum required depth controlled by architectural or environmental requirements as outlined above.
2. Estimate the footing thickness using Tables 9.1 and 9.2. If needed, increase the footing depth determined in step 1 to accommodate the estimated footing thickness.
3. Review the soil profile. If there are weak or compressible layers at the current estimated embedment depth, consider increasing the depth in order to reach better soil conditions.
4. If significant uplift loads must be resisted, check footing thicknesses required for these loads and adjust footing depth as needed.

Footing Width

The required footing width is normally controlled by the design downward load. Each footing must have a sufficient width, B, to satisfy both of the following geotechnical requirements:

- **ULS requirement**—The bearing capacity design criterion (Equation 7.37 or 7.39) must be satisfied. The techniques for doing so are discussed in Chapter 7.
- **SLS requirements**—The settlement and differential settlement criteria (Equations 5.20 and 5.21) must be satisfied. The techniques for doing so are described in Chapter 8.

When using the individual footing design approach, the structural engineer provides the design loads for each footing to the geotechnical engineer who then determines the B needed to satisfy each of these two requirements. The larger of these two B values controls the design. This process is repeated for each footing, and the geotechnical investigation report provides the recommended width for each footing. The serviceability limit state often controls the design, so it is usually easier to check the SLS requirements first.

Serviceability Limits

The design based on serviceability starts with the structural engineer providing the expected service load for each footing to the geotechnical engineer along with the serviceability limits in the form of the maximum allowable total and differential settlements. The service loads will be project specific, as discussed in Section 5.3, and should consist of a conservative estimate of the long-term sustained loads, since those are the loads that generate settlement. These loads will be different than the serviceability loads for building sway, for example, which would include estimates of wind loads and earthquake loads—while these live loads are important in computing lateral sway of the structure, they do not contribute significantly to the long-term settlement of the structure. The serviceability loads for footing design generally consist of the dead load, plus that portion of the live load that can realistically be expected to be sustained over a long period of time, as discussed in Section 5.3.

Once the service loads and serviceability limits are established, we must determine if total or differential settlement controls and adjust δ_a as needed using the following steps.

1. Using local experience or Table 8.3, select an appropriate δ_D/δ ratio.
2. If $\delta_{Da} \geq \delta_a(\delta_D/\delta)$, then designing the footings to satisfy the total settlement requirement will implicitly satisfy the differential settlement requirement as well, so do not adjust δ_a
3. If $\delta_{Da} < \delta_a(\delta_D/\delta)$, then differential settlement controls. Set $\delta_a = \delta_{Da}/(\delta_D/\delta)$.

Using allowable settlement, δ_a, determined in the above three steps, we compute the required footing width, B, needed to limit settlement to δ_a using the procedure from Chapter 8 most appropriate for the project being analyzed. This will be the footing width required by serviceability limit state, B_{SLS}.

Ultimate Strength Limit—Bearing Capacity

Once the serviceability analysis has been completed and the footing widths have been established to keep total and differential settlements within limits, it is necessary to check that the proposed footing widths meet ultimate limit state requirements. The first ULS to

check is bearing capacity. For design it is most convenient to compute bearing capacity in terms of column loads rather than bearing pressures.

Using ASD methods the governing equation is:

$$P_a = \frac{q_n}{F}A - W_f \tag{9.1}$$

Or replacing the weight of the footing, W_f with $\gamma_c AD_f$:

$$P_a = \frac{q_n}{F}A - \gamma_c AD \tag{9.2}$$

where

P_a = allowable column load
γ_c = unit weight of concrete
q_n = nominal bearing capacity computed by Equation 7.4, 7.5, 7.6, or 7.13 as appropriate
F = factor of safety
D = depth of the footing
A = effective area of the footing:
B^2 for square footings with concentric loads or
B'^2 or $B'B$ for footings with eccentric loads, see Section 6.3.

Using LRFD methods the governing equation is:

$$P_u + \gamma_D W_f \leq \phi q_n A \tag{9.3}$$

Or replacing the weight of the footing, W_f with $\gamma_c AD$:

$$P_u + \gamma_D(\gamma_c AD) \leq \phi q_n A \tag{9.4}$$

where

P_u = ultimate factored column load
ϕ = resistance factor for bearing capacity which will depend upon the method used to compute q_n. See Table 7.2.
γ_c = unit weight of concrete
γ_D = appropriate load factor for dead loads (1.2 for ASCE 7, 1.25 for AASHTO)

The footing width required to satisfy Equation 9.2 or 9.4 is the width required by the ultimate limit state, B_{ULS}.

Communicating Requirements

The required footing width will be the greater of B_{ULS} and B_{SLS}. It is important that the geotechnical engineer clearly communicates the required footing width, the limit state controlling the design, SLS or ULS, and the loads for which the design is applicable. Simply providing an allowable footing width is not sufficient.

Footings Subject to Moments or Eccentric Loads

Footings subject to moments or eccentric column loads are most easily designed using the equivalent footing dimension, B' and L', and the equivalent bearing pressure as described in Section 6.3. This will be an iterative process as the eccentricity will depend upon the footing dimensions and vice versa. One of the difficulties in this process is that the SLS and ULS loads are different and each will have its own unique eccentricity and equivalent footing. Engineering judgment is required to resolve the differences between these two solutions. It is generally adequate to design the footing based on the SLS loads, then perform a ULS check to ensure the footing is safe against a bearing capacity failure.

Lateral Capacity

If footing must carry lateral loads, it must be checked to ensure it meets the lateral ULS criteria using the procedures described in Section 7.10. If the lateral ULS criteria is not satisfied, the engineer may be tempted to increase the footing depth and thickness. However, this method is not very effective. For the case of isolated footings it may be necessary to change to a deep foundation as they have the ability to carry much higher lateral loads than footings. If footings are located relatively close together, it may be possible to tie adjacent footings together using grade beams. This method is discussed in Section 9.2.

9.2 DESIGN CHART APPROACH

On projects that have more than a few footings, the individual footing design approach would be very tedious. Such would be the case for most buildings, where dozens of individual footings are typically required. For these projects, it is more practical to use the design chart approach, which presents the results of the ULS (bearing capacity) and SLS (settlement) analyses in the form of design charts. The geotechnical engineer prepares these design charts and includes them in the geotechnical investigation report. The structural engineer then uses these charts to determine the required width of each footing.

Although a range of expected loads is needed to develop the charts, and this information is provided by the structural engineer, with this method the geotechnical engineer does not need the exact design loads for each footing, so the geotechnical report can be finalized before the exact design loads are even known. This is a distinct advantage of this method, as the geotechnical investigation is often conducted at the early stages of the project, before the structural design has even begun.

Footing Depth

The footing depth is determined by the same factors described in Section 9.1. As discussed there, the depth is generally controlled by requirements other than bearing capacity or settlement.

Footing Width

For each footing shape, two design charts are required to provide information needed to determine the width of square footings: One for ULS, and another for SLS. As before, the design width, B, is larger than these two widths. If continuous and rectangular footings also are planned for a particular project, they will each need their own pair of charts, ULS and SLS.

Serviceability Limits

As with individual footing design, this approach starts with SLS design. In this case the structural engineer provides a range of expected column service loads for the project. Both the total and differential settlement requirements are also needed. Using this information, the geotechnical engineer then performs a series of settlement computations (using methods presented in Chapter 8) over the range of expected column service loads. For a given settlement, say 25 mm (1 in), the results should be reported as the footing width required to limit settlement to 25 mm (1 in) for a given service load. The settlement computation should be repeated for three different settlement levels, 50 percent, 100 percent, and 150 percent of the maximum allowable settlement. Providing a range of settlements in the design chart provides flexibility during the design process. In summary the process is:

1. In consultation with the structural engineer determine:
   - **a.** The minimum expected column service load, $P_{\min}$
   - **b.** The maximum expected column service load, $P_{\max}$
   - **c.** The allowable total settlement, δ_a
   - **d.** The allowable differential settlement, δ_{Da}
2. Determine if total or differential settlement controls and adjust δ_a as needed,
   - **a.** Using local experience or Table 8.3, select an appropriate δ_D/δ ratio
   - **b.** If $\delta_{Da} \geq \delta_a(\delta_D/\delta)$, then designing the footings to satisfy the total settlement requirement will implicitly satisfy the differential settlement requirement as well, so do not adjust δ_a
   - **c.** If $\delta_{Da} < \delta_a(\delta_D/\delta)$, then differential settlement controls. Set $\delta_a = \delta_{Da}/(\delta_D/\delta)$
3. Select five column service loads equally distributed from the minimum to maximum values.
4. At each of the five column service loads determined in step 3, compute the required footing width needed to limit settlement to the allowable settlement, δ_a, using the procedure from Chapter 8 most appropriate for the projects being analyzed.

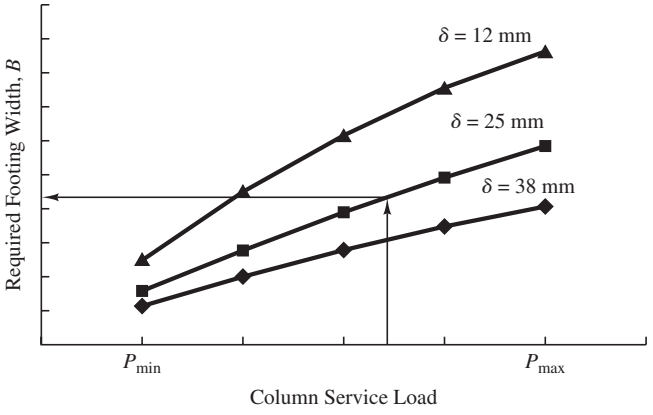

Figure 9.2 Required footing width computed from a serviceability limit state analysis. Generally five points are adequate to define the curve for a given displacement level.

5. Repeat step 4 for settlements of 50 percent and 150 percent of the allowable settlement, δ_a.
6. Using the data from the above computations, develop a graph of required footing width, B, as a function of column service load. The design chart should look like Figure 9.2.

The results of the SLS analysis should be presented as the required footing width as a function of column service load, because this form is most convenient for the structural engineer. If an analytical form is needed the curves can generally be fit with a second order polynomial with sufficient accuracy. Alternatively the results can be presented in a table, but a chart or series of equations eliminates the need to interpolate between tabulated loads.

In theory, if all of the footing widths are controlled by SLS, and each footing is designed using this chart, the differential settlement should be zero. However, variations in soil properties across the site, differs between the actual loads and the design loads, construction tolerances, and other factors will inevitably lead to some differential settlement. The δ_D/δ ratios in Table 8.3 may be used to estimate these differential settlements.

Ultimate Strength Limits—Bearing Capacity

A second design chart also must be developed to ensure the footing has sufficient width to satisfy the ultimate limit state (bearing capacity) criterion. This chart uses either the ASD design load or the LRFD design load, depending on the needs of the individual project, and may be developed as follows:

1. In consultation with the structural engineer, determine whether ASD or LRFD method will be used. The structural engineer then provides the expected range of

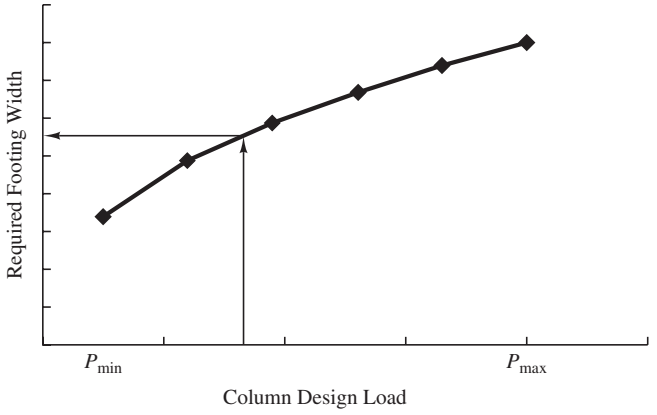

Figure 9.3 Required footing width computed from a bearing capacity analysis. Generally five to seven points are adequate to define the curve.

design downward loads, using either the ASD load combinations or the LRFD load combinations. This load range will be different from the expected range of service loads used in the serviceability analysis. Do not confuse ULS and SLS loads!

2. Select five column loads equally distributed from the minimum to maximum values.
3. At each of the five to seven column service loads determined in step 2, compute the required footing width needed to satisfy Equation 9.2 if using ASD or Equation 9.4 if using LRFD.
4. Using the data from the above computations, develop a graph of required footing width, B, as a function of column service load. The design chart should look like Figure 9.3.

Generally, bearing capacity requirements can be satisfied by adjusting the footing width, B, using the above procedure. If it's not possible to achieve adequate bearing capacity by increasing the footing width, the bearing capacity can be increased by increasing the depth of the footings. If this is required, it will be necessary to reanalyze the serviceability limits and construct new design charts for both serviceability and bearing capacity based on the increased footing depth.

Communicating Requirements

The pair of design charts, one for SLS and one for ULS, are then presented in the geotechnical investigation report. Two pairs of charts will be needed if continuous and square footings are to be used, one pair for each shape. The structural engineer then sizes each footing using both the SLS and ULS chart, and uses the larger of the two footing widths for design.

A key feature of this method is that it clearly separates ULS and SLS requirements since separate design charts are provided for each limit state. The ULS design chart must make clear whether it was developed using the ASD or LRFD method. Mixing load combinations from these two methods could result in a structure not being able to carry the actual design loads.

Lateral Capacity

If there are columns with lateral loads, they must be checked to ensure they meet this ULS criterion. An effective method of presenting this information in the geotechnical investigation report is for the geotechnical engineer to determine the required soil properties and factor of safety (or resistance factor), evaluate the lateral capacity using the techniques described in Section 7.10, and present the site-specific lateral capacity in equation form as a function of B and D. The structural engineer can then use this equation to check the capacity of each laterally loaded footing.

The design of any footings without sufficient lateral capacity will have to be modified. In this case, increasing the footing size will not generally solve the problem, as discussed in Section 9.1. Instead, it is generally better to use grade beams to connect the footing with another nearby footing that is not subject to applied lateral loads, and thus has unused lateral capacity. Grade beams, as described in Section 6.1 and shown in Figure 6.2, can transfer lateral loads from one column to an adjacent column. This method can be effective because, in general, lateral building loads are carried only by some of the columns in a building—generally those adjacent to shear walls. If other nearby columns carry low, or small, lateral loads, the grade beams can effectively spread the lateral demand across several footings. The structural design of grade beams is beyond the scope of this book.

9.3 ALLOWABLE BEARING PRESSURE APPROACH

The third approach for presenting geotechnical design requirements consists of presenting an allowable bearing pressure in the geotechnical investigation report. These design values are very similar in form to the presumptive allowable bearing pressures presented in Table 6.1, except that they are based on site-specific geotechnical analyses and thus presumably less conservative. Presenting the geotechnical design requirements in this form is very convenient for the structural engineer because the required width of individual footings can be easily determined (see Example 6.6). The allowable bearing pressures will be a function of footing shape. Therefore, if both square and continuous footings also are used on a project, each will have its own allowable bearing pressures.

Because of its simplicity and familiarity, this is the most common method of presenting geotechnical design criteria, and this method is quite appropriate for most small structures. However, this method is more conservative than the individual footing design or design chart approaches; and it can produce larger differential settlements. In addition, there are complications when this method is used with LRFD. Thus, it is important to recognize both the advantages and limitations of this method.

Limitations of the Allowable Bearing Pressure Approach

The key to understanding the limitation of this method is to realize that allowable bearing pressure, whether based on the ultimate limit state or the serviceability limit state, depends on both the soil properties and the footing dimensions. Even if uniform soil conditions are present, there is no single allowable bearing pressure value that correctly reflects either bearing capacity or settlement for footings of different widths. In other words, the allowable bearing pressure is not a soil property. This is best illustrated with an example. Let us first consider the allowable bearing pressure based on bearing capacity using the ASD method as illustrated in Example 9.1.

Example 9.1

The design column loads for a certain building range from 20 to 100 kN. The site for this structure is underlain by a silty sand with $\gamma = 18.2$ kN/m^3, $c' = 2$ kPA and $\phi' = 34°$. The water table is at a great depth and footings are to be founded at a depth of 1.3 m.

Determine the required footing width and allowable bearing pressure for the most lightly loaded footing and the most heavily loaded footing using ASD with a factor of safety of 2.5.

Solution

Using Terzaghi's bearing capacity equation.

For $\phi' = 34°$: $N_c = 52.6$, $N_q = 36.5$, $N_\gamma = 39.6$ (from Table 7.1)

$$\sigma'_{zD} = \gamma D - u = (18.2 \text{ kN/m}^3)(1.3 \text{ m}) - 0 = 23.7 \text{ kN/m}^2$$

$$\begin{aligned} q_n &= 1.3c'N_c + \sigma'_{zD}N_q + 0.4\gamma' B N_\gamma \\ &= 1.3(2 \text{ kN/m}^2)(52.6) + (23.7 \text{ kN/m}^2)(36.5) + 0.4(18.2 \text{ kN/m}^3)\, B(39.6) \\ &= 1{,}002 \text{ kN/m}^2 + B(288 \text{ kN/m}^3) \end{aligned}$$

$$q_a = \frac{q_n}{F} = \frac{1{,}002 + B(288)}{2.5} = 401 + B(115)$$

$$W_f = 1.3B^2(23 \text{ kN/m}^3) = 30B^2$$

$$q_a = \frac{P + W_f}{A} - u \quad \Rightarrow \quad 401 + 115B = \frac{P + 30B^2}{B^2}$$

$$0 = 115B^3 + 371B^2 - P$$

For the lightest column load, $P = 20$ kN

$$0 = 115B^3 + 371B^2 - 20$$

$$B = \mathbf{0.22 \text{ m}}$$

and

$$q_a = 401 + 0.22(115) = \mathbf{426\ kPa}$$

For the heaviest column load, $P = 100$ kN

$$0 = 115B^3 + 371B^2 - 100$$
$$B = \mathbf{0.48\ m}$$

and

$$q_a = 401 + 0.48(115) = \mathbf{456\ kPa}$$

Note that the allowable bearing pressure for the lightest column load is less than the allowable bearing pressure for the heaviest column load.

When computing settlements from serviceability loads we will also find that the allowable unit bearing pressure is a function of the footing width or column load. Consider the two footings shown in Figure 9.4. The stress bulbs shown in this figure enclose the zone of soil that is stress at 10 percent of the footing bearing or greater ($I_\sigma = 0.1$). If each footing is loaded such that they have the same bearing pressure, the footing on the right will have a significantly greater settlement since it is stressing a much larger volume of soil. If the column loads for a building vary, and we wish to have the same settlement

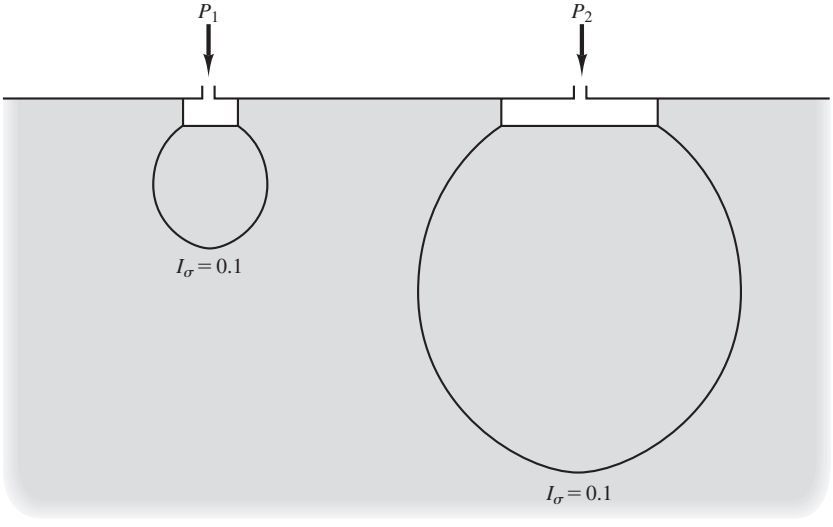

Figure 9.4 Two footings are loaded to the same bearing stress, q, but each has a different width and a correspondingly different column load, P. The larger footing induces stress to a greater depth in the soil, so it settles more than the smaller footing.

at each footing, to prevent differential settlement, then the allowable bearing pressure for each footing must depend upon the column load. Again there is not a uniform allowable bearing pressure. In contrast to the ultimate limit state, however, the footing for the most heavily loaded column is the one that must be designed using the lowest allowable bearing pressure.

These two examples, illustrate the problem with specifying a single allowable bearing pressure for footing design. If the design is controlled by ultimate limit state, this single value will not provide the same factor of safety for different sized footings. Similarly, if a uniform settlement is desired, it cannot be achieved by designing all footings for the same allowable bearing pressure. Therefore, the only way we can develop a single allowable pressure value that can then be used to size all of the footings at a project site is to determine the value for the most critical footing (i.e., the one with the lowest allowable bearing pressure) and use this value to size all of the other footings. This is inherently conservative, because all of the other footings will be oversized. Nevertheless, for lightweight structures with fairly uniform loading, this additional conservatism is tolerable, and simplicity of this approach outweighs the additional construction costs of the conservatively designed footings. If properly employed, the method will provide safe foundations at the cost of over designing many of the footings.

Process for Computing the Allowable Bearing Pressure

In order to develop a design value for the allowable bearing pressure, it is necessary to determine two allowable bearing pressures, one for the serviceability limit state, $q_{A,SLS}$, and one for the ultimate limit state, $q_{A,ULS}$. The ultimate limit state will always be governed by the smallest column load and the serviceability limit state will always be governed by the largest column load. Normally we develop one $q_{A,SLS}$ and one $q_{A,ULS}$ value that applies to the entire site, or at least to all the footings of a particular shape at that site. The procedure for determining the allowable bearing pressure values will differ between ASD and LRFD.

ASD

Computing Allowable Bearing Pressures—ASD

When using the ASD method, geotechnical engineers develop the allowable bearing pressures using the following procedure:

1. In consultation with the structural engineer, determine:
   - **a.** The minimum column load for ULS, P_{min}, determined using the ASD load combinations (Equations 5.4 through 5.12 for ASCE 7)
   - **b.** The maximum column service load, P_{max}
   - **c.** The maximum allowable total settlement, δ_a, and maximum allowable differential settlement, δ_{Da}

2. Select a depth of embedment, D, as described in Section 9.1. If different depths of embedment are required for various footings, perform the following computations using the smallest D.
3. Determine the design groundwater depth, D_w. This should be the shallowest groundwater depth expected to occur during the life of the structure.
4. Determine the SLS based allowable bearing pressure, $q_{A,SLS}$, using maximum column service load, $P_{\max}$.
   a. Adjust δ_a for differential settlement, if necessary, as described in Section 9.2.
   b. Compute $q_{A,SLS}$ as the bearing needed to limit settlement to δ_a, using the procedure from Chapter 8 most appropriate for the project being analyzed.
5. Determine the ULS based allowable bearing pressure, $q_{A,ULS}$, using $P_{\min}$.

$$q_{A,ULS} = \frac{q_n}{F} - \frac{W_f}{A} = \frac{q_n}{F} - \frac{\gamma_c}{D} \tag{9.5}$$

If the structure will include both square and continuous footings, we must develop separate allowable bearing pressure values for each footing shape. These values should be expressed as a multiple of 25 kPa (500 lb/ft^2).

Applying Allowable Bearing Pressures—ASD

To apply allowable bearing pressures in ASD rigorously we must check SLS and ULS separately. The SLS check is:

$$\frac{P_S + W_f}{A} - u_D \leq q_{A,\text{SLS}} \tag{9.6}$$

where

P_S = column service load
A = required base area
W_f = weight of foundation
u_D = pore water pressure along base of footing. $u_D = 0$ if the groundwater table is at a depth greater than D. Otherwise, $u_D = \gamma_w(D\text{-}D_w)$

For square footings setting $A = B^2$ and $W_f = \gamma_c AD$ and solving Equation 9.6 for B gives,

$$B_{\text{SLS}} = \sqrt{\frac{P_S}{q_{A,\text{SLS}} - \gamma_c D + u_D}} \tag{9.7}$$

where B_{SLS} is the required footing width based on serviceability limits.

For continuous footings Equation 9.7 becomes,

$$B_{\text{SLS}} = \frac{P_S}{q_A - \gamma_c D + u_D} \tag{9.8}$$

where P_S is expressed as a force per unit length (kN/m or lb/ft).

The ULS check is,

$$\frac{P + W_f}{A} - u_D \leq q_{A,\text{ULS}} \tag{9.9}$$

where P is the ASD column design load.

For square footings setting $A = B^2$ and $W_f = \gamma_c AD$ and solving Equation 9.9 for the required footing width based on ULS, B_{ULS}, gives,

$$B_{\text{ULS}} = \sqrt{\frac{P}{q_{A,\text{ULS}} - \gamma_c D + u_D}} \tag{9.10}$$

For continuous footings Equation 9.10 becomes,

$$B_{\text{ULS}} = \frac{P}{q_{A,\text{ULS}} - \gamma_c D + u_D} \tag{9.11}$$

where P is expressed as a force per unit length (kN/m or lb/ft).

The final footing width then will be the lesser of B_{SLS} or B_{ULS}, or:

$$B = \min \begin{bmatrix} B_{\text{SLS}} \\ B_{\text{ULS}} \end{bmatrix} \tag{9.12}$$

Using a Single Allowable Bearing Pressure—ASD

In the approach presented above we are performing two checks to determine the appropriate footing width: an SLS check using $q_{\text{A,SLS}}$ with the column service load, P_S, and a ULS check using $q_{\text{A,ULS}}$ with the ASD column design load, P. Because Equations 9.7 and 9.10 are the same except for the substitution of $q_{\text{A,SLS}}$ for $q_{\text{A,ULS}}$ and P_S for P, we can simply process by using the minimum allowable bearing pressure and the maximum load. To do these we define a single allowable bearing pressure, q_{A}, as:

$$q_A = \min \begin{bmatrix} q_{\text{A,SLS}} \\ q_{\text{A,ULS}} \end{bmatrix} \tag{9.13}$$

And we then note that the ASD design column load, P, will always be equal to or greater than the design service load, P_S. Using the minimum allowable bearing pressure and maximum load we can compute the required footing width, B, for square footings as,

$$B = \sqrt{\frac{P}{q_A - \gamma_c D + u_D}} \tag{9.14}$$

For continuous footings Equation 9.14 becomes,

$$B = \frac{P}{q_A - \gamma_c D + u_D} \tag{9.15}$$

This approach of using a single allowable bearing pressure is very common in practice, even though it is conservative and it muddles the difference between ULS and SLS. However, when presenting this single value, the geotechnical engineer must also state whether it is to be applied using the ASD load or the service load. The structural engineer can then quickly and easily size all of the footings at the site.

Example 9.2

As part of an urban redevelopment project, a new parking garage is to be built at a site formerly occupied by two-story commercial buildings. These old buildings have already been demolished and their former basements have been backfilled with well-graded sand, sandy silt, and silty sand. The lower level of the proposed parking garage will be approximately flush with the existing ground surface, and the ASD design column loads range from 250 to 1200 k. The column service loads range from 200 to 900 k. The allowable total and differential settlements are 0.75 and 0.5 in, respectively.

A series of five exploratory borings have been drilled at the site to evaluate the subsurface conditions. The soils consist primarily of the basement backfill, underlain by alluvial sands and silts. The groundwater table is at a depth of about 200 ft. Figure 9.5 shows a design soil profile compiled from these borings, along with all of the standard penetration test N_{60} values.

The basement backfills were not properly compacted and only encompass portions of the site. Therefore, in the interest of providing more uniform support for the proposed spread footing foundations, the upper 10 ft of soil across the entire site will be excavated and recompacted to form a stratum of properly compacted fill. This fill will have an estimated overconsolidation ratio of 3 and an estimated N_{60} of 60. A laboratory direct shear test on a compacted sample of this soil produced $c' = 0$ and $\phi' = 39°$.

Determine the allowable bearing pressures, $q_{A,ULS}$ and $q_{A,SLS}$, for square footings at this site, then use them to determine the required dimensions for a square footing that will support column carrying an ASD unfactored design load of 390 k and a service load of a 300 k.

After designing using both $q_{A,ULS}$ and $q_{A,SLS}$, determine a single allowable bearing pressure, q_A, then use this q_A to determine the required dimensions for a square footing for the same column described above.

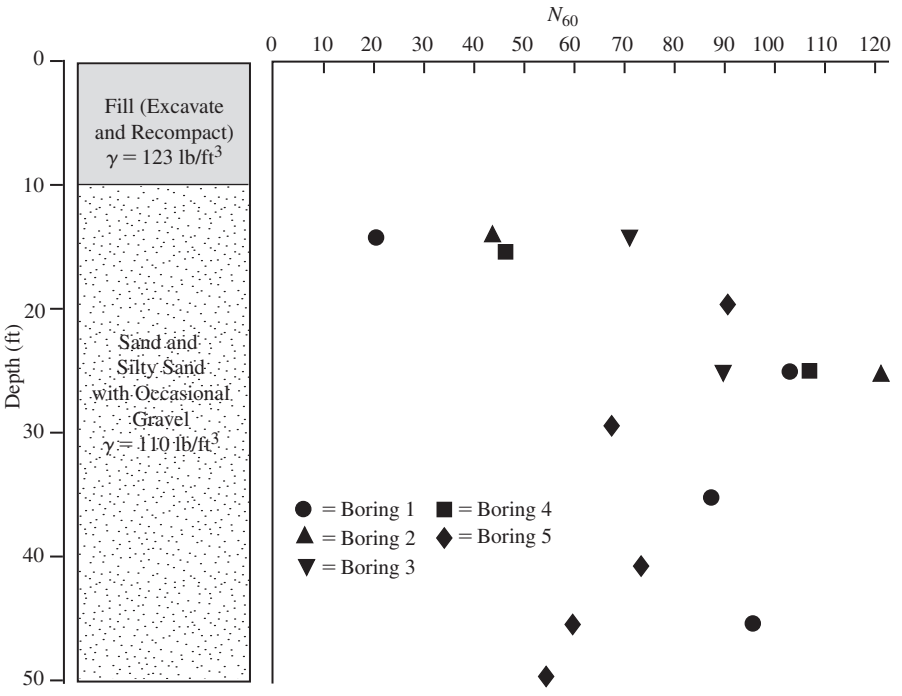

Figure 9.5 Design soil profile and SPT results for proposed parking garage site in Example 9.2.

Solution Part 1: Compute allowable bearing pressures

We will use the ASD method for ULS analysis.

Step 1—From the problem statement

$$P_{\min} = 250 \text{ k}$$
$$P_{\max} = 900$$
$$\delta_a = 0.75 \text{ in}$$
$$\delta D_a = 0.5 \text{ in}$$

Step 2—Use an estimated D of 3 ft

Step 3—The groundwater table is very deep, and is not a concern at this site

Step 4—Perform settlement computations using $P_{\max}$

Per the problem statement, $\delta_a = 0.75$ in and $\delta_{Da} = 0.5$ in. Using Table 8.3 and assuming the parking garage is a flexible structure, the design value of δ_D/δ is 0.5 and $\delta_{Da} > \delta_a(\delta_D/\delta)$, so the total settlement requirement controls the settlement analysis.

We will use the modulus based method and compute Young's, E, based on the given SPT data using Equation 4.56 and Table 4.7. To covert Young's modulus to constrained modulus we will use Equation 3.20, assuming Poisson's ratio is 0.3

$$\frac{M}{E} = \frac{(1 - \nu)}{(1 + \nu)(1 - 2\nu)} = \frac{(1 - 0.3)}{(1 + 0.3)(1 - 2(0.3))} = 1.35$$

Using these correlations, modulus values for each SPT data point are as follows:

Boring No.	Depth (ft)	Soil Type	N_{60}	β_0	β_1	E(lb/ft^2)	M(lb/ft^2)
1	14	SW	20	100,000	24,000	580,000	780,769
2	14	SW	44	100,000	24,000	1,156,000	1,556,154
3	14	SP & SW	72	100,000	24,000	1,828,000	2,460,769
4	15	SW	46	100,000	24,000	1,204,000	1,620,769
5	19	SW	92	100,000	24,000	2,308,000	3,106,923
1	25	SP	104	100,000	24,000	2,596,000	3,494,615
2	25	SP	122	100,000	24,000	3,028,000	4,076,154
3	25	SW	90	100,000	24,000	2,260,000	3,042,308
4	25	SW	102	100,000	24,000	2,548,000	3,430,000
5	29	SP	68	100,000	24,000	1,732,000	2,331,538
1	35	SP	88	100,000	24,000	2,212,000	2,977,692
5	40	SW	74	100,000	24,000	1,876,000	2,525,385
1	45	SW	96	100,000	24,000	2,404,000	3,236,154
5	45	SW	60	100,000	24,000	1,540,000	2,073,077
5	49	SW	56	100,000	24,000	1,444,000	1,943,846

The modulus for the recompacted soil is computed as:

$$M = 1.35\left(\beta_0\sqrt{\text{OCR}} + \beta_1 N_{60}\right)$$
$$= 1.35\left(70{,}000\sqrt{3} + 16{,}000(60)\right) = 1.46 \times 10^6 \text{ lb/ft}^2$$

Based on these data, we can perform the settlement analysis using the following equivalent modulus values:

Depth (ft)	M(lb/ft^2)
0 – 10	1,460,000
10 – 20	1,350,000
> 20	3,430,000

Using these modulus values, $P_{max} = 900$ k, $D = 3$ ft, and Equation 8.10, we can use an iterative solution to find that a bearing pressure of 10,200 lb/ft^2 will generate a settlement of 0.75 in. Therefore $q_{A,SLS} = 10{,}200$ lb/ft^2.

Step 5—Using Terzaghi's bearing capacity theory, Equation 7.4, with $c' = 0$, $\phi = 39°$, $D = 3$ ft, $P = 250$ k, the computed the nominal bearing pressure, q_n, is 44,700 lb/ft^2. For a factor of safety of 2.5 this yields an allowable bearing pressure of 17,900 lb/ft^2. Therefore $q_{A,ULS} = 17{,}900$ lb/ft^2.

The allowable bearing pressures are:

$$q_{A,SLS} = 10{,}200 \text{ lb/ft}^2$$

$$q_{A,ULS} = 17{,}900 \text{ lb/ft}^2$$

And the minimum allowable bearing pressure is controlled by settlement.

$$q_A = 10{,}200 \text{ lb/ft}^2$$

Solution Part 2: Compute required footing width

For the footing being designed, $P = 390$ k and $P_S = 300$ k. Using both the SLS and ULS allowable bearing pressures we compute the required footing width.

$$B_{\text{SLS}} = \sqrt{\frac{P_S}{q_{A,\text{SLS}} - \gamma_c D + u_D}} = \sqrt{\frac{300{,}000}{10{,}200 - (150)3 + 0}} = 5.54 \text{ ft}$$

$$B_{\text{ULS}} = \sqrt{\frac{P}{q_{A,\text{ULS}} - \gamma_c D + u_D}} = \sqrt{\frac{390{,}000}{17{,}900 - (150)3 + 0}} = 4.73 \text{ ft}$$

Use $B =$ **5 ft 9 in**

Using the single q_A allowable bearing pressure, the width of the footing supporting a 300 k column load is computed as:

$$B = \sqrt{\frac{P}{q_A - \gamma_c D + u_D}} = \sqrt{\frac{390{,}000}{10{,}200 - (150)3 + 0}} = 6.32 \text{ ft}$$

Use $B =$ **6 ft 6 in**

Commentary

If we performed an individual footing design for the column in the example we would find that $B_{\text{SLS}} = 3.5$ ft and $B_{\text{ULS}} = 4.5$ ft. So the design footing width would be controlled by bearing capacity and $B = 4.5$ ft. This demonstrates how conservative the allowable bearing pressure method is, particularly when only a single allowable bearing pressure is used.

LRFD

Computing Allowable Bearing Pressures—LRFD

When using the LRFD method, the allowable bearing pressures are developed using the same steps at outlined above for the ASD method with the following changes.

1. In this step the minimum column load for ULS, $P_{\min}$ is computed using the LRFD load combinations (Equations 5.13 through 5.19 for ASCE 7)
2. No change in determining embedment depth, D.
3. No change in determining design groundwater table depth, D_w.
4. No change in determining the SLS based allowable bearing pressure, $q_{A,SLS}$.
5. The ULS based allowable bearing pressure, $q_{A,ULS}$, is determined using $P_{\min}$ and Equation 9.16

$$q_{A,ULS} = \frac{\phi q_n A - \gamma_D W_f}{A} = \phi q_n - \gamma_D\left(\frac{\gamma_c}{D}\right) \tag{9.16}$$

Applying Allowable Bearing Pressures—LRFD

The SLS check in LRFD is the same as in ASD and Equations 9.7 and 9.8 are used to determine B_{SLS}. However, the ULS check is different. The controlling equation is:

$$\frac{P_u}{A} - u_D \leq \phi q_n - \gamma_D\left(\frac{\gamma_c}{D}\right) \tag{9.17}$$

where

P_{u} = ultimate factored column load
A = required base area
u_D = pore water pressure along base of footing
ϕ = resistance factor for bearing capacity which will depend upon the method used to compute q_n (See Table 7.2).
q_n = nominal bearing capacity computed by Equation 7.4, 7.5, 7.6, or 7.13 as appropriate
γ_c = unit weight of concrete
γ_D = appropriate load factor for dead loads (1.2 for ASCE 7, 1.25 for AASHTO)

For square footings, we substitute $A = B^2$ into Equation 9.17 and solve the ULS required footing width, B_{ULS}, as:

$$B_{\text{ULS}} = \sqrt{\frac{P_u}{\phi q_n - \gamma_D\left(\frac{\gamma_c}{D}\right) + u_D}} \tag{9.18}$$

For continuous footings Equation 9.18 becomes

$$B_{\text{ULS}} = \frac{P_u}{\phi q_n - \gamma_D\left(\frac{\gamma_c}{D}\right) + u_D} \tag{9.19}$$

where P_u is expressed as a force per unit length (kN/m or lb/ft).

LRFD design inherently uses separate checks for ULS and SLS, so it is not possible to determine a single allowable bearing pressure as we did in the ASD method. In this sense it is more rigorous than the ASD method.

Summary

The true allowable bearing pressure is a function of the soil properties and the footing width. It will change with every column load in a project. The allowable bearing pressure method is really a shortcut that makes computing the required footing width simple by providing just one SLS allowable bearing pressure and one ULS allowable bearing pressure for all footings. In order for this method to provide adequate footing widths for all column loads, it must be conservative for most column loads. The single allowable bearing pressure method is even more conservative because it uses a single value for all limit states and all footing designs. This is a very conservative approach which can only be justified when the project is simple, and the cost of very conservative footing designs is small compared to the overall project. There are many projects that fall into this category and many which do not.

9.4 RECTANGULAR AND COMBINED FOOTINGS

Rectangular footings are most commonly used either when a combined footing is required or when supporting a single column with a large moment in one direction. When supporting a single column with a large moment, the long side of the footing, L, is oriented to counter the applied moment. The length, L, is selected to ensure the resultant reaction force is located within the middle third of the footing, as described in Section 6.3. Then the width, B, is selected to meet ultimate and serviceability limit states. Computations are performed using the equivalent footing length, L', computed using Equation 6.11. Vesic's method must be used to compute the nominal bearing capacity (Section 7.2) as it includes shape factors for non-square footings where Terzaghi's method does not.

As discussed in Chapter 6, combined footings have two or more columns bearing on a single footing. There are two common situations where using combined footings is warranted. The first is when the spacing between columns and the required width of the columns is such that the footings would overlap or come close to overlapping. In this case it is more cost effective to design and construct a single footing to carry the adjacent column loads. The second is when a footing has a highly eccentric load such that it isn't possible to design an efficient footing to carry the load. This happens most often for a footing at the edge of a structure where the property line limits the footing width, as shown in Figure 9.6. By combining the two isolated footings into a single footing, the eccentric loading can be eliminated and the bearing pressure be made uniform. The design process for combined footings is to select the length, L, such that a uniform bearing pressure is achieved and then select the width, B, to meet ultimate and serviceability limit states.

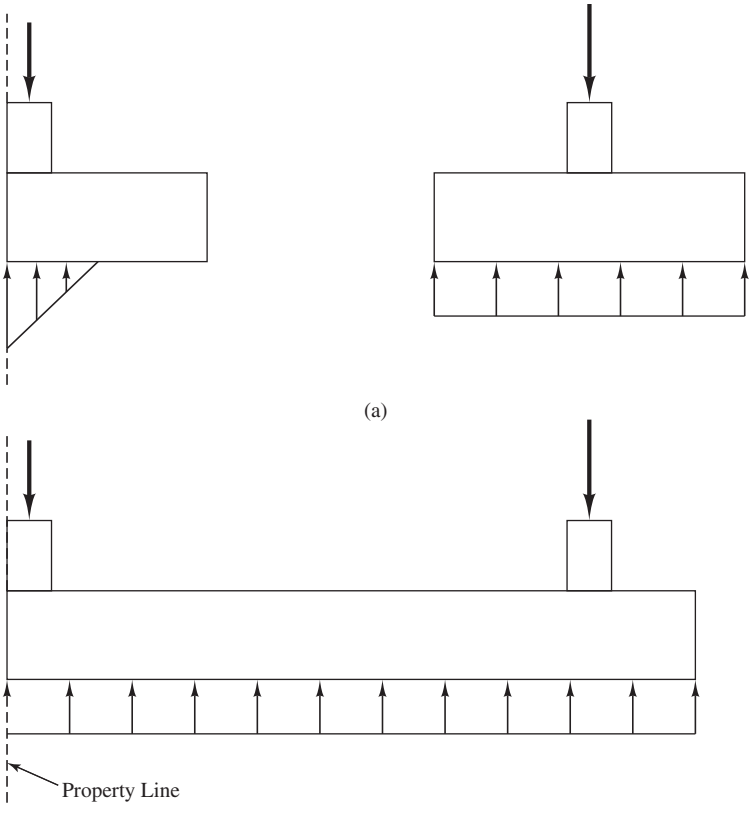

Figure 9.6 Combined footing to eliminate eccentric loading: (a) shows two adjacent footings; the footing on the left is eccentrically loaded because the property line prevents locating the column in the center of the footing. (b) By combining the two footings, it is possible to create a uniform bearing stress across the combined footing.

9.5 SPECIAL SEISMIC CONSIDERATIONS

Loose sandy soils pose special problems when subjected to seismic loads, especially if these soils are saturated. The most dramatic problem is *soil liquefaction*, which is the sudden loss of shear strength due to the build-up of excess pore water pressures (see Coduto et al., 2011). This loss in strength can produce a bearing capacity failure, as shown in Figure 9.7. Another problem with loose sands, even if they are not saturated and not prone to liquefaction, is earthquake-induced settlement. In some cases, such settlements can be very large.

Earthquakes also can induce landslides, which can undermine foundations built near the top of a slope. This type of failure occurred in Anchorage, Alaska, during the 1964 earthquake, as well as elsewhere. The evaluation of such problems is a slope stability concern, and thus is beyond the scope of this book.

Figure 9.7 Apartment buildings toppled over like dominoes after the magnitude-7.5 Niigata quake struck. *Source*: Keystone Pictures/ZUMA Press/Alamy

9.6 LIGHTLY-LOADED FOOTINGS

The principles of bearing capacity and settlement apply to all sizes of spread footings. However, the design process can be simplified for lightly-loaded footings. For purposes of geotechnical foundation design, we will define *lightly-loaded footings* as those subjected to vertical loads less than 200 kN (45 k) or 60 kN/m (4 k/ft). These include typical one- and two-story wood-frame buildings, and other similar structures. The foundations for such structures are small, and do not impose large loads onto the ground, so extensive subsurface investigation and soil testing programs are generally not cost-effective. Normally it is less expensive to use conservative designs than it is to conduct extensive investigations and analyses.

Presumptive Allowable Bearing Pressures

The concept of presumptive allowable bearing pressures was introduced in Section 6.4. They are easy to implement, and do not require borings, laboratory testing, or extensive analyses. The engineer simply obtains the q_A value from the table and uses it with

Equation 9.8 or 9.9 to design the footings. Presumptive bearing pressures are always used with ASD loads. The maximum ULS load from Equations 5.4 through 5.12 is used in computing footing width.

Presumptive allowable bearing pressures have been used since the late nineteenth century, and thus predate bearing capacity and settlement analyses. Today they are used primarily for lightweight structures on sites known to be underlain by good soils. Although presumptive bearing pressures are usually conservative (i.e., they produce larger footings), the additional construction costs are small compared to the savings in soil exploration and testing costs. However, it is inappropriate to use presumptive bearing pressures for larger structures founded on soil because they are not sufficiently reliable. Such structures warrant more extensive engineering and design, including soil exploration and testing. They also should not be used on sites underlain by poor soils.

Minimum Dimensions

If the applied loads are small, such as with most one- or two-story wood-frame structures, bearing capacity and settlement analyses may suggest that extremely small footings would be sufficient. However, from a practical perspective, very small footings are not acceptable for the following reasons:

- Construction of the footing and the portions of the structure that connect to it would be difficult.
- Excavation of soil to build a footing is by no means a precise operation. If the footing dimensions were very small, the ratio of the construction tolerances to the footing dimensions would be large, which would create other construction problems.
- A certain amount of flexural strength is necessary to accommodate nonuniformities in the loads and local inconsistencies in the soil, but an undersized footing would have little flexural strength.

Therefore, all spread footings should be built with certain minimum dimensions. Figure 9.8 shows typical minimums. In addition, building codes sometimes dictate other minimum dimensions. For example, the *International Building Code* stipulates certain minimum dimensions for footings that support wood-frame structures. The minimum dimensions for continuous footings are presented in Table 9.3, and those for square footings are presented in Note 3 of the table. This code also allows the geotechnical engineer to supersede these minimum dimensions [IBC 1805.4].

Potential Problems

Although the design of spread footings for lightweight structures can be a simple process, as just described, be aware that such structures are not immune to foundation problems. Simply following these presumptive bearing pressures and code minimums does not necessarily produce a good design. Engineers need to know when these simple design guidelines are sufficient, and when additional considerations need to be included.

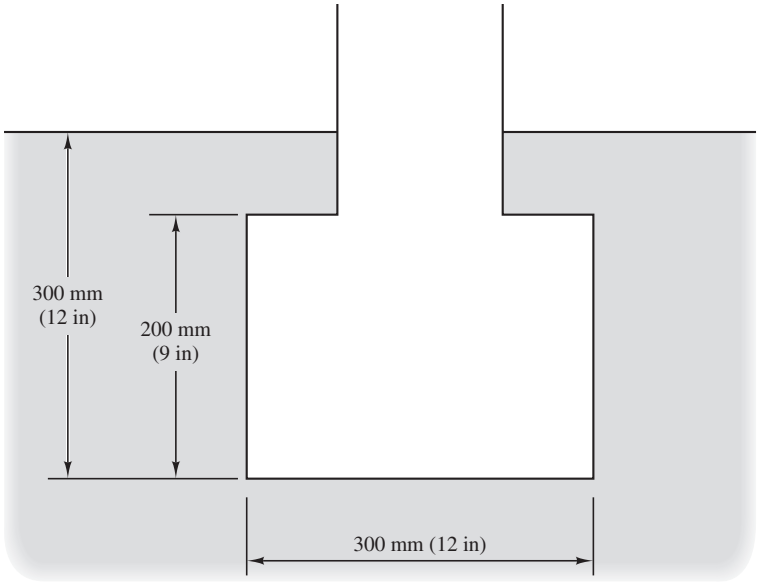

Figure 9.8 Minimum dimensions for spread footings. If the footing is reinforced, the thickness should be at least 30 cm (12 in).

TABLE 9.3 MINIMUM DIMENSIONS FOR CONTINUOUS FOOTINGS THAT SUPPORT WOOD-FRAME BEARING WALLS (data from *International Building Code*, ICC, 2012)

Number of Floors Supported by the Foundation	Footing Width, *B*		Footing Thickness, *T*		Footing Depth Below Undisturbed Ground Surface, *D*	
	(mm)	(in)	(mm)	(in)	(mm)	(in)
1	300	12	150	6	300	12
2	375	15	150	6	300	12
3	450	18	200	8	300	12

1. Where frost conditions are found, footings and foundations shall be as required by IBC Section 1805.2.1.
2. The ground under the floor may be excavated to the elevation of the top of the footing.
3. Interior stud bearing walls may be supported by isolated footings. The footing width and length shall be twice the width shown in this table and the footings shall be spaced not more than 1.8 m (6 ft) on center.
4. Structures assigned Seismic Design Category C, D, E, or F must meet additional requirement in IBC Section 1908.
5. Foundations may support a roof in addition to the stipulated number of floors. Foundations supporting roofs only shall be as required for supporting one floor.

Most problems with foundations of lightweight structures are caused by the soils below the foundations, rather than high loads from the structure. For example, foundations placed in loose fill may settle because of the weight of the fill or because of infiltration of water into the fill. Expansive soils, collapsible soils, landslides, and other problems also can affect foundations of lightweight structures. These problems may justify more extensive investigation and design effort.

9.7 FOOTINGS ON OR NEAR SLOPES

The bearing capacity of footings near slopes was discussed in Section 7.8 and this section, recommended avoiding placing footings near slopes. However, it is sometimes unavoidable. When footings must be placed near slopes, the *International Building Code* (ICC, 2012) requires setbacks as shown in Figure 9.9. We can meet these criteria either by moving the footing away from the slope or by making it deeper. However, this setback criteria does not justify building foundations above unstable slopes. Therefore, we also should perform appropriate slope stability analyses to verify the overall stability.

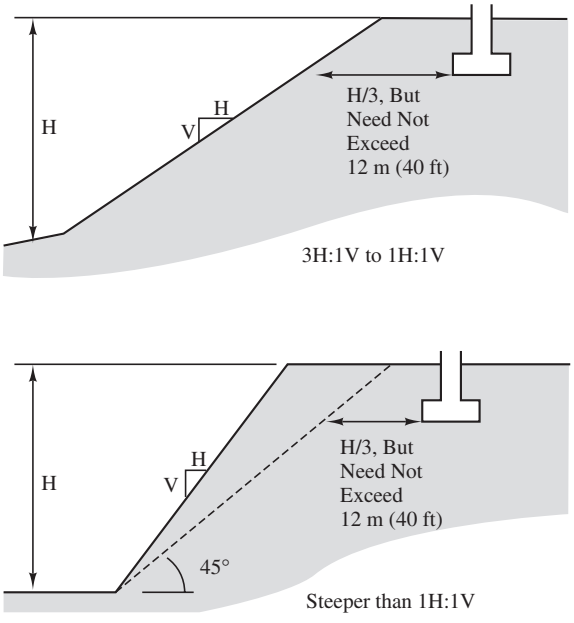

Figure 9.9 Footing setback as required by the IBC, 2012 [1805.3] for slopes steeper than 3 horizontal to 1 vertical. The horizontal distance from the footing to the face of the slope should be at least H/3, but need not exceed 12 m (40 ft). For slopes that are steeper than 1 horizontal to 1 vertical, this setback distance should be measured from a line that extends from the toe of the slope at an angle of 45 degrees.

9.8 FOOTINGS ON FROZEN SOILS

In many parts of the world, the air temperature in the winter often falls below the freezing point of water (0°C) and remains there for extended periods. When this happens, the ground becomes frozen. In the summer, the soils become warmer and return to their unfrozen state. Much of the northern United States, Canada, central Europe, and other places with similar climates experience this annual phenomenon.

The greatest depth to which the ground might become frozen at a given locality is known as the *depth of frost penetration*. This distance is part of an interesting thermodynamics problem and is a function of the air temperature and its variation with time, the initial soil temperature, the thermal properties of the soil, and other factors. The deepest penetrations are obtained when very cold air temperatures are maintained for a long duration. Typical depths of frost penetration in the United States are shown in Figure 9.10. These annual freeze–thaw cycles create special problems that need to be considered in foundation design.

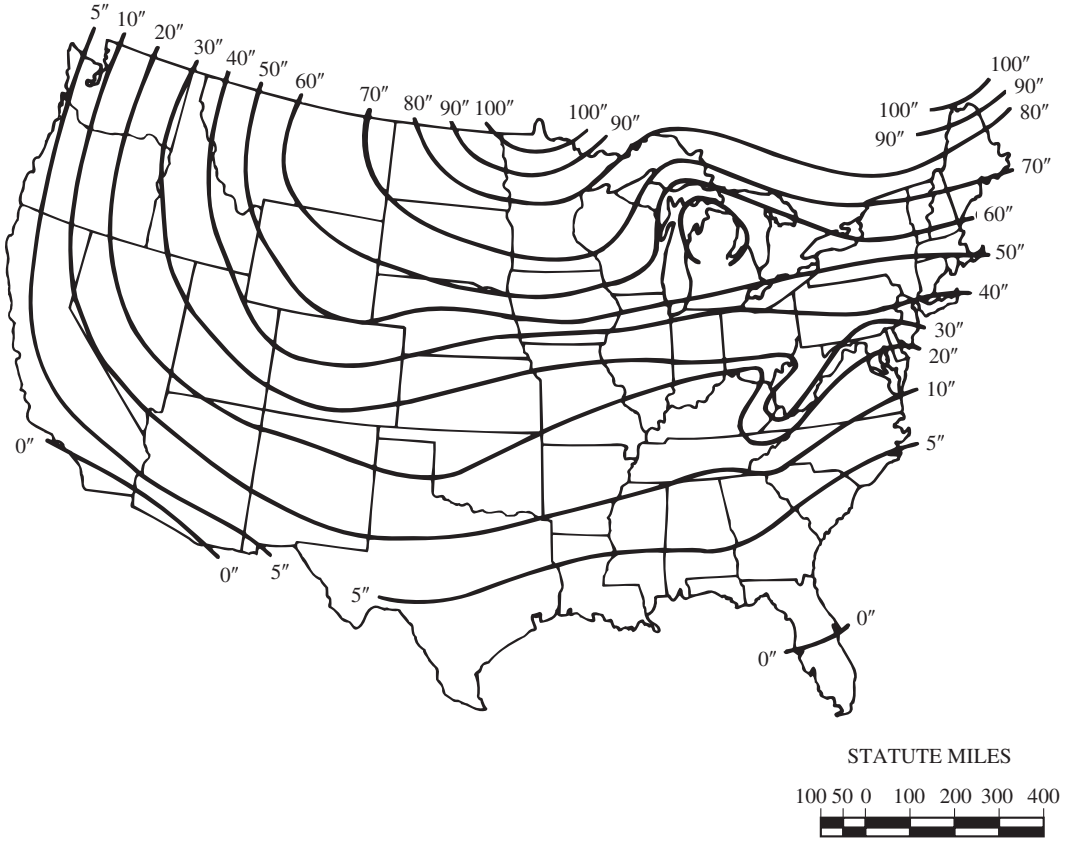

Figure 9.10 Approximate depth of frost penetration in the United States (U.S. Navy, 1982a).

Frost Heave

The most common foundation problem with frozen soils is *frost heave*, which is a rising of the ground when it freezes. When water freezes, it expands about 9 percent in volume. If the soil is saturated and has a typical porosity (say, 40 percent), it will expand about $9\% \times 40\% \approx 4\%$ in volume when it freezes. In climates comparable to those in the northern United States, this could correspond to surface heaves of as much as 25 to 50 mm (1–2 in). Although such heaves are significant, they are usually fairly uniform, and thus cause relatively little damage.

However, there is a second, more insidious source of frost heave. If the groundwater table is relatively shallow, capillary action can draw water up to the frozen zone and form ice lenses, as shown in Figure 9.11. In some soils, this mechanism can move large quantities of water, so it is not unusual for these lenses to produce ground surface heaves of 30 cm (1 ft) or more. Such heaves are likely to be very irregular and create a hummocky ground surface that could extensively damage structures, pavements, and other civil engineering works.

In the spring, the warmer weather permits the soil to thaw, beginning at the ground surface. As the ice melts, it leaves a soil with much more water than was originally present. Because the lower soils will still be frozen for a time, this water temporarily cannot drain away, and the result is a supersaturated soil that is very weak. This condition is often the cause of ruts and potholes in highways and can also effect the performance of shallow foundations and floor slabs. Once all the soil has thawed, the excess water drains down and the soil regains its strength. This annual cycle is shown in Figure 9.12.

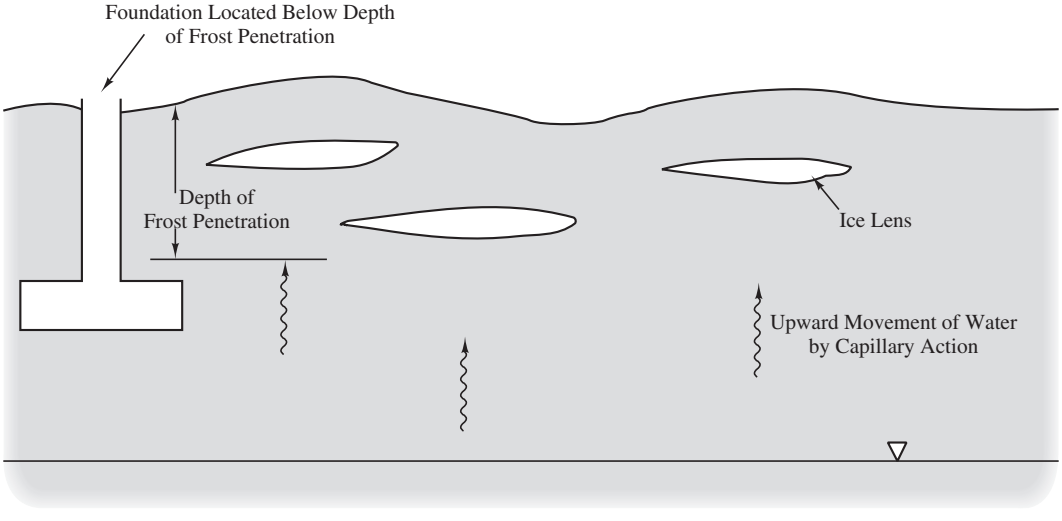

Figure 9.11 Formation of ice lenses. Water is drawn up by capillary action and freezes when it nears the surface. The frozen water forms ice lenses that cause heaving at the ground surface. Foundations placed below the depth of frost penetration are not subject to heaving.

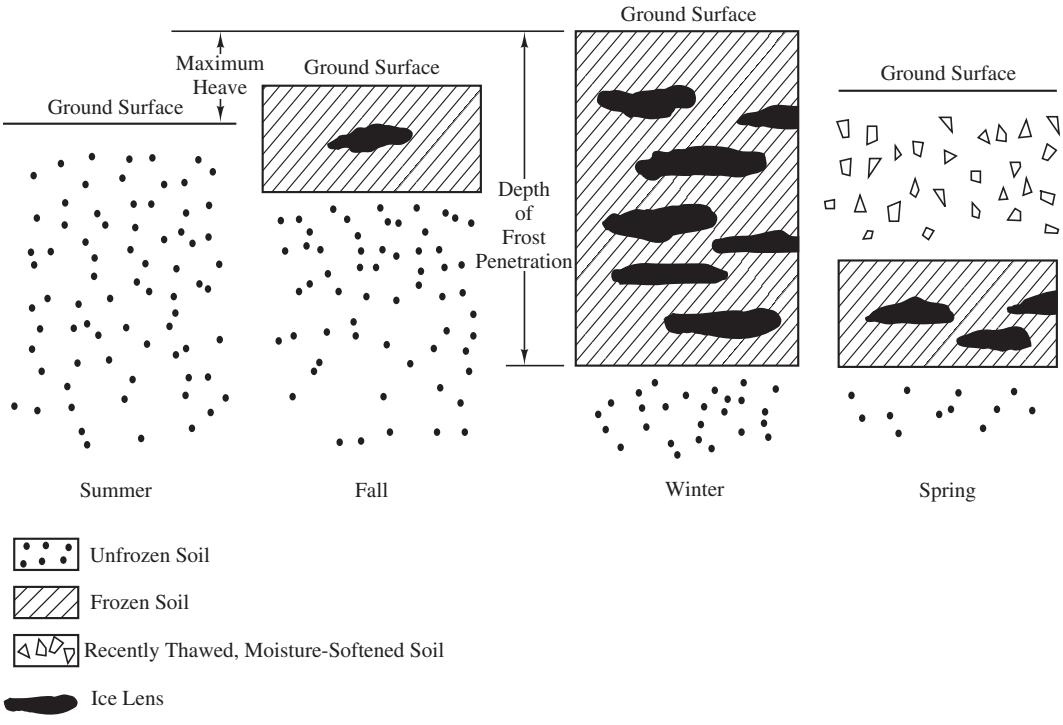

Figure 9.12 Idealized freeze-thaw cycle in temperate climates. During summer, the ground is unfrozen. During fall and winter, it progressively freezes from the ground surface down. Then, in the spring, it progressively thaws from the ground surface down.

To design foundations in soils that are prone to frost heave, we need to know the depth of frost penetration. This depth could be estimated using Figure 9.10, but as a practical matter it is normally dictated by local building codes. For example, the Chicago Building Code specifies a design frost penetration depth of 1.1 m (42 in). Rarely, if ever, would a rigorous thermodynamic analysis be performed in practice.

Next, the engineer will consider whether ice lenses are likely to form within the frozen zone, thus causing frost heave. This will occur only if both of the following conditions are met:

1. There is a nearby source of water; and
2. The soil is *frost-susceptible*.

To be considered frost-susceptible, a soil must be capable of drawing significant quantities of water up from the groundwater table into the frozen zone. Clean sands and gravels are not frost-susceptible because they are not capable of significant capillary rise. Conversely, clays are capable of raising water through capillary rise, but they have a low permeability and are therefore unable to deliver large quantities of water. Therefore, clays

are capable of only limited frost heave. However, intermediate soils, such as silts and fine sands, have both characteristics: They are capable of substantial capillary rise and have a high permeability. Large ice lenses are able to form in these soils, so they are considered to be very frost-susceptible.

The U.S. Army Corps of Engineers has classified frost-susceptible soils into four groups, as shown in Table 9.4. Higher group numbers correspond to greater frost susceptibility and more potential for formation of ice lenses. Clean sands and gravels (i.e., 3 percent finer than 0.02 mm) may be considered non-frost-susceptible and are not included in this table.

The most common method of protecting foundations from the effects of frost heave is to build them at a depth below the depth of frost penetration. This is usually wise in all soils, whether or not they are frost-susceptible and whether or not the groundwater table is nearby. Even "frost-free" clean sands and gravels often have silt lenses that are prone to heave, and groundwater conditions can change unexpectedly, thus introducing new sources of water. The small cost of building deeper foundations is a wise investment in such cases. However, foundations supported on bedrock or interior foundations in heated buildings normally do not need to be extended below the depth of frost penetration.

Builders in Canada and Scandinavia often protect buildings with slab-on-grade floors using thermal insulation, as shown in Figure 9.13. This method traps heat stored in the ground during the summer and thus protects against frost heave, even though the foundations are shallower than the normal frost depth. Both heated and nonheated buildings can use this technique (NAHB, 1988 and 1990).

TABLE 9.4 FROST SUSCEPTIBILITY OF VARIOUS SOILS ACCORDING TO THE U.S. ARMY CORPS OF ENGINEERS (data from Johnston, 1981)

Group	Soil Types[a]	USCS Group Symbols[b]
F1 (least susceptible)	Gravels with 3–10% finer than 0.02 mm	GW, GP, GW-GM, GP-GM
F2	a. Gravels with 10–20% finer than 0.02 mm b. Sands with 3–15% finer than 0.02 mm	GM, GW-GM, GP-GM SW, SP, SM, SW-SM, SP-SM
F3	a. Gravels with more than 20% finer than 0.02 mm b. Sands, except very fine silty sands, with more than 15% finer than 0.02 mm c. Clays with IP $>$ 12, except varved clays	GM, GC SM, SC CL, CH
F4 (most susceptible)	a. Silts and sandy silts b. Fine silty sands with more than 15% finer than 0.02 mm c. Lean clays with IP $<$ 12 d. Varved clays and other fine-grained, banded sediments	ML, MH SM CL, CL-ML

[a] I_P = Plasticity Index (explained in Chapter 3).

[b] See Chapter 3 for an explanation of USCS group symbols.

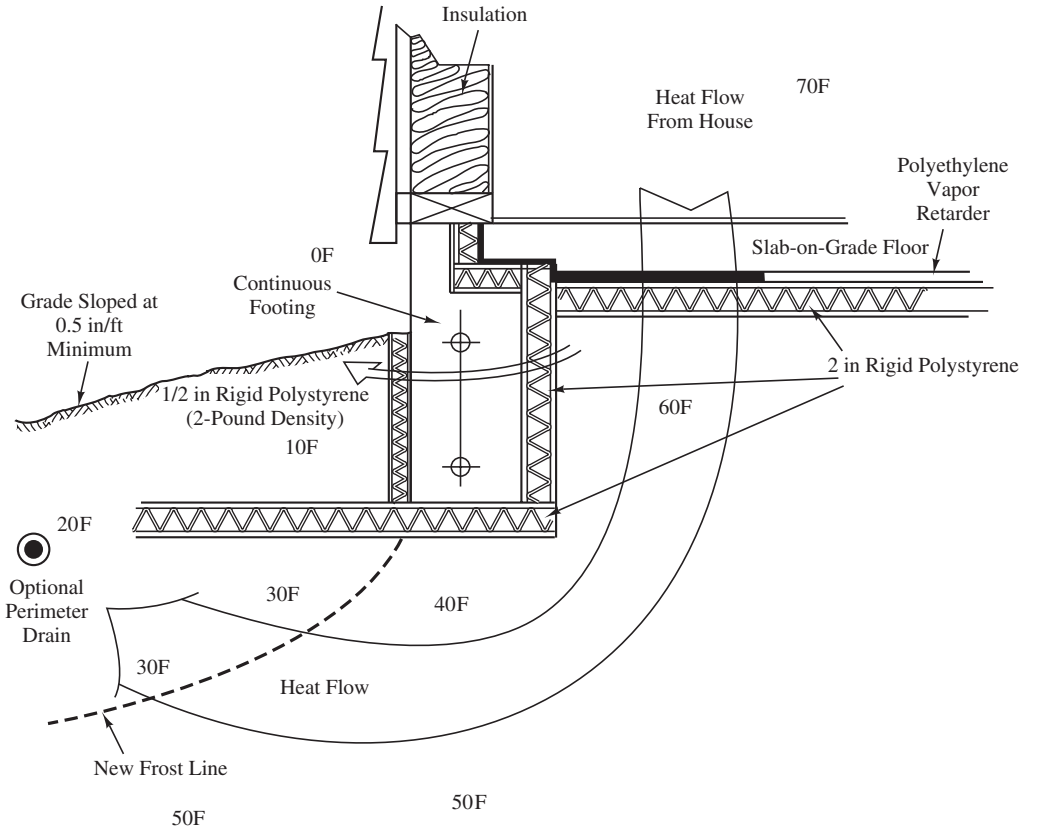

Figure 9.13 Thermal insulation traps heat in the soil, thus protecting a foundation from frost heave (NAHB, 1988, 1990).

Alternatively, the natural soils may be excavated to the frost penetration depth and replaced with soils that are known to be frost-free. This may be an attractive alternative for unheated buildings with slab floors to protect both the floor and the foundation from frost heave.

Although frost heave problems are usually due to freezing temperatures from natural causes, it is also possible to freeze the soil artificially. For example, refrigerated buildings such as cold-storage warehouses or indoor ice skating rinks can freeze the soils below and be damaged by frost heave, even in areas where natural frost heave is not a concern (Thorson and Braun, 1975). Placing insulation or air passages between the building and the soil and/or using non–frost susceptible soils usually prevents these problems.

A peculiar hazard to keep in mind when foundations or walls extend through frost-susceptible soils is *adfreezing* (CGS, 1992). This is the bonding of soil to a wall or foundation as it freezes. If heaving occurs after the adfreezing, the rising soil will impose a large upward load on the structure, possibly separating structural members. Placing a 10 mm (0.5 in) thick sheet of rigid polystyrene between the foundation and the frozen soil reduces the adfreezing potential.

Permafrost

In areas where the mean annual temperature is less than 0°C, the penetration of freezing in the winter may exceed the penetration of thawing in the summer and the ground can become frozen to a great depth. This creates a zone of permanently frozen soil known as *permafrost*. In the harshest of cold climates, such as Greenland, the frozen ground is continuous, whereas in slightly "milder" climates, such as central Alaska, central Canada, and much of Siberia, the permafrost is discontinuous. Areas of seasonal and continuous permafrost in Canada are shown in Figure 9.14.

In areas where the summer thaws occur, the upper soils can be very wet and weak and probably not capable of supporting any significant loads, while the deeper soils remain permanently frozen. Foundations must penetrate through this seasonal zone and well into the permanently frozen ground below. It is very important that these foundations be designed so that they do not transmit heat to the permafrost, so buildings are typically built with raised floors and a ducting system to maintain subfreezing air temperatures between the floor and the ground surface.

Figure 9.14 Zones of continuous and discontinuous permafrost in Canada (data from Crawford and Johnson, 1971).

The Alaska Pipeline project is an excellent example of a major engineering work partially supported on permafrost (Luscher et. al, 1975).

9.9 FOOTINGS ON SOILS PRONE TO SCOUR

Scour is the loss of soil because of erosion in river bottoms or in waterfront areas. This is an important consideration for design of foundations for bridges, piers, docks, and other structures, because the soils around and beneath the foundation could be washed away.

Scour around the foundations is the most common cause of bridge failure. For example, during Spring 1987, there were seventeen bridge failures caused by scour in the northeastern United States alone (Huber, 1991). The most notable of these was the collapse of the Interstate Route 90 bridge over Schoharie Creek in New York (Murillo, 1987), a failure that killed ten people. Figures 9.15 and 9.16 show another bridge that collapsed as a result of scour.

Scour is part of the natural process that moves river-bottom sediments downstream. It can create large changes in the elevation of the river bottom. For example, Murphy (1908) describes a site on the Colorado River near Yuma, Arizona, where the river bed consists of highly erodible fine silty sands and silts. During a flood, the water level at this point rose 4.3 m (14 ft) and the bottom soils scoured to depths of up to 11 m (36 ft)! If a bridge foundation located 10.7 m (35 ft) below the river bottom had been built at this location, it would have been completely undermined by the scour and the bridge would have collapsed.

Figure 9.15 One of the mid-channel piers supporting this bridge sank about 1.5 m when it was undermined by scour in the river channel.

Figure 9.16 Deck view of the bridge shown in Figure 9.15. The lanes on the right side of the fence are supported by a separate pier that was not undermined by the scour.

Scour is often greatest at places where the river is narrowest and constrained by levees or other means. Unfortunately, these are the locations most often selected for bridges. The presence of a bridge pier also creates water flow patterns that intensify the scour. However, methods are available to predict scour depths (Richardson et al., 1991) and engineers can use preventive measures, such as armoring, to prevent scour problems (TRB, 1984).

SUMMARY

Major Points

1. The depth of embedment, D, must be great enough to accommodate the required footing thickness, T. In addition, certain geotechnical concerns, such as loose soils or frost heave, may dictate an even greater depth.
2. The required footing width, B, is a soil structure interaction problem, and is governed by ultimate limit states (bearing capacity and lateral capacity) and serviceability limit state (settlement).
3. For structures requiring only a few footing and/or with large and complex loads, each footing should be designed individually to meet the SLS and ULS requirements.
4. For project with many footings to be designed, the design chart approach is an efficient and convenient way to provide efficiently designed footings. Separate design charts are needed for ULS and SLS requirements.

5. The allowable bearing pressure approach is a simplification which does not allow for efficient design of footing. By its nature it is conservative and is justified only for small structures where the cost of a more sophisticated design method is not justified.
6. The design of lightly-loaded footings is often governed by minimum practical dimensions.
7. Lightly-loaded footings are often designed using a presumptive allowable bearing pressure, which is typically obtained from the applicable building code.
8. The design of footings on or near slopes needs to consider the sloping ground.
9. Footings on frozen soils need special considerations. The most common problem is frost heave, and the normal solution is to place the footing below the depth of frost penetration.
10. Footings in or near riverbeds are often prone to scour, and must be designed accordingly.

Vocabulary

Allowable bearing pressure	Equivalent footing width/ length	Presumptive bearing pressure
Depth of frost penetration	Frost heave	Bearing pressure
Design chart	Frost-susceptible soil	Scour
Eccentric load	Permafrost	Embedment depth

QUESTIONS AND PRACTICE PROBLEMS

Section 9.1: Design for Isolated Footings

9.1 Which method of expressing footing width criteria (individual footing design, allowable bearing pressure or design chart) would be most appropriate for each of the following structures?

a. A ten-story reinforced concrete building

b. A one-story wood-frame house

c. A nuclear power plant

d. A highway bridge

9.2 Explain why an 8 ft wide footing with $q = 3{,}000$ lb/ft^2 will settle more than a 3 ft wide one with the same q.

9.3 Under what circumstances would bearing capacity most likely control the design of spread footings? Under what circumstances would settlement usually control?

9.4 A proposed building column will carry a downward maximum unfactored load combination of 250 k and a service load of 185 k. This column is to be supported on a square footing at a depth of 7 ft in a silty sand with the following engineering properties: $\gamma = 119$ lb/ft^3 above the groundwater table and 122 lb/ft^3 below, $c' = 0, \phi' = 32°, N_{60} = 30$. The groundwater table is 15 ft below the ground surface. The allowable settlement, δ_a, is 0.75 in. The ASD, factor

of safety against a bearing capacity failure is 2.5. Determine the design footing width clearly identifying whether it is controlled by settlement or bearing capacity.

9.5 A bridge column carries a downward factored ultimate load of 310 kN and a service load of 200 kN. It is underlain by a lightly overconsolidated clay (OCR = 2) with the following engineering properties: $s_u = 250$ kPa, $C_c = 0.20$, $C_r = 0.05$, $e = 0.7$, and $\gamma = 15.0$ kN/m^3 above the groundwater table and 16.0 kN/m^3 below. The groundwater table is at a depth of 1.0 m below the ground surface. Using LRFD, determine the design footing width clearly identifying whether it is controlled by settlement or bearing capacity.

9.6 A proposed office building will have unfactored column design loads between 200 and 1,000 kN and service loads between 150 and 700 kN. These columns are to be supported on spread footings which will be founded in a silty clay with the following engineering properties: $\gamma = 15.1$ kN/m^3 above the groundwater table and 16.5 kN/m^3 below, $s_u = 200$ kPa, $C_r/(1 + e_0) = 0.020$, $\sigma'_m = 400$ kPa. The groundwater table is 5 m below the ground surface. The required factor of safety against a bearing capacity failure must be at least 3 and the allowable total settlement, δ_a, is 20 mm and the allowable differential settlement, δ_{Da}, is 12 mm.

Prepare both serviceability and bearing capacity design charts, using ASD for the ULS analysis. Then, comment on the feasibility of using spread footings at this site.

9.7 Repeat Problem 9.6 using LRFD for the ULS analysis and assuming the factored ultimate loads range from 250 to 1350 kN and the resistance factor is 0.45. Service loads range remains as stated in Problem 9.6.

9.8 A proposed industrial building will carry unfactored column loads ranging from 280 to 1,200 kN and service loads from 230 to 950 kN. The allowable settlements are $\delta_a = 30$ mm and $\delta_{Da} = 12$ mm. It is supported on a cohesionless sand with $\phi' = 35°$ and $\gamma = 19.2$ kN/m^3. Footings at this site will be at a depth of 2.2 m and the groundwater table is at 5 m. A dilatometer test run at the site has returned the following modulus profile:

Depth (m)	2	3	4	5	6	7	8	9	10	11	12	13
M (MPa)	18.3	20.6	19.0	21.1	35.2	40.0	37.3	30.1	31.9	40.0	40.8	42.0

Prepare both serviceability and bearing capacity design charts, using ASD for ULS analysis. Then, comment on the feasibility of using spread footings at this site.

9.9 Repeat Problem 9.8 using LRFD for the ULS analysis and assuming the factored ultimate loads range from 300 to 1,500 kN and the resistance factor is 0.45. Service loads range remains as stated in Problem 9.8.

9.10 Several cone penetration tests have been conducted at a site underlain by a young, normally consolidated silica sand deposit. Based on these tests, an engineer has developed the following design soil profile:

Depth (m)	0–2.0	2.0–3.5	3.5–4.0	4.0–6.5
q_c (kg/cm^2)	40	78	125	100

This soil has an average unit weight of 18.1 kN/m^3 above the groundwater table and 20.8 kN/m^3 below. The groundwater table is at a depth of 3.1 m. An office building with a parking structure

is to be built at this site with ASD column loads of 400 to 1,500 kN and service loads of 380 to 1,100 kN. Square footings are to be used at a depth of 1 m. Using these data, create design charts for both serviceability and ultimate limit states using ASD with a factor of safety of 2.5 and a design life of 50 years.

Hint: In a homogeneous soil, the critical shear surface for a bearing capacity failure extends to a depth of approximately B below the bottom of the footing. See Chapter 4 for a correlation between q_c in this zone and ϕ'.

9.11 A proposed building will have column loads ranging from 40 to 300 k. All of these columns will be supported on square spread footings. When computing the allowable bearing pressure, q_A, which load should be used to perform the bearing capacity analyses? Which should be used to perform the settlement analyses? Explain.

9.12 A series of columns carrying unfactored vertical loads of 20 to 90 k and service loads from 20 to 75 k are to be supported on 3 ft deep square footings. The soil below is a clay with the following engineering properties: $\gamma = 105$ lb/ft^3 above the groundwater table and 110 lb/ft^3 below, $s_u = 3{,}000$ lb/ft^2, $C_r/(1 + e_0) = 0.03$ in the upper 10 ft and 0.05 below. Both soil strata are heavily overconsolidated. The groundwater table is 5 ft below the ground surface. The factor of safety against a bearing capacity failure must be at least 3. Determine the allowable bearing pressure, q_A, using ASD.

9.13 A square spread footing with $B = 1$ m and $D = 0.5$ m supports a column with the following ASD design loads: $P = 150$ kN, $M = 22$ kN-m. The underlying soil has an allowable bearing pressure of 200 kPa. Is this design acceptable? If not, compute the minimum required footing width and express it as a multiple of 100 mm.

Section 9.2: Rectangular and Combined Footings

9.14 A 3 ft × 7 ft rectangular footing is to be embedded 2 ft into the ground and will support a single centrally-located column with the following factored LRFD ultimate design loads: $P_U = 50$ k, $V_U = 27$ k, $M_U = 80$ ft-k. V_U and M_U act in the long direction only. The underlying soil is a silty sand with $c' = 0$, $\phi' = 31°$, $\gamma = 123$ lb/ft^3, and a very deep groundwater table. Using LRFD, determine if this design is acceptable. Use a resistance factor of 0.45.

9.15 The serviceability loads for the footing in problem 9.14 are $P = 37$ k, $M_U = 40$ ft-k, and $V_U = 0$. The average N_{60} for the sand below the footing is 28. Determine if this footing meets serviceability requirements, assuming the allowable total settlement is 0.75 in.

9.16 A combined footing is to be used to support columns A and B with a center-to-center spacing of 15 ft. The columns carry the following loads:

	Column A		Column B	
	P	V	P	V
Ultimate loads	200	50	400	50
Service Loads	150	0	300	0

The underlying soil is a well-graded sand with $c' = 0$, $\phi' = 36°$, $\gamma = 126$ lb/ft^3, with a very deep groundwater table. Using LRFD, design a rectangular footing to meet the ultimate limit states using a resistance factor of 0.45. Assuming the average CPT tip resistance of the sand is 300 kg/cm^2, check to see if your design meets serviceability limits. Adjust the design as needed.

Section 9.4: Lightly Loaded Footings

9.17 A three-story wood-frame building is to be built on a site underlain by sandy clay. This building will have wall loads of 1,900 lb/ft on a certain exterior wall. Using the minimum dimensions presented in Table 9.3 and presumptive bearing pressures from the International Building Code as presented in Table 6.1, compute the required width and depth of this footing. Show your final design in a sketch.

Section 9.5: Footings on or Near Slopes

9.18 A 4 ft square, 2 ft deep spread footing carries an ASD design column load of 50 k. The edge of this footing is 1 ft behind the top of a 40 ft tall, 2H:1V descending slope. The soil has the following properties: $c' = 200$ lb/ft^2, $\phi' = 31°$, $\gamma = 121$ lb/ft^3, and the groundwater table is at a great depth. Compute the ASD factor of safety against a bearing capacity failure and comment on this design.

Section 9.6: Lightly Loaded Footings

9.19 Classify the frost susceptibility of the following soils:

- **a.** Sandy gravel (GW) with 3 percent finer than 0.02 mm.
- **b.** Well-graded sand (SW) with 4 percent finer than 0.02 mm.
- **c.** Silty sand (SM) with 20 percent finer than 0.02 mm.
- **d.** Fine silty sand (SM) with 35 percent finer than 0.02 mm.
- **e.** Sandy silt (ML) with 70 percent finer than 0.02 mm.
- **f.** Clay (CH) with plasticity index = 60.

9.20 A compacted fill is to be placed at a site in North Dakota. The following soils are available for import: Soil 1 - silty sand; Soil 2 - lean clay; Soil 3 - Gravelly coarse sand. Which of these soils would be least likely to have frost heave problems using a resistance factor of 0.45? Explain.

9.21 Would it be wise to use slab-on-grade floors for houses built on permafrost? Explain.

9.22 What is the most common cause of failure in bridges?

9.23 A single-story building is to be built on a sandy silt in Detroit. How deep must the exterior footings be below the ground surface to avoid problems with frost heave?

Comprehensive

9.24 A column carries the following factored ultimate loads $P_U = 1{,}200$ kN and $M_U = 300$ m-kN. The service loads are $P_U = 950$ kN and $M_U = 30$ m-kN. The footing for this column is to be founded

at a depth of 1.5 m on a underlying cohesive soil with $s_u = 200$ kPa, $C_r/(1 + e_0) = 0.040$, and OCR $= 6$. Design a footing for this column using LRFD with a resistance factor of 0.45.

9.25 A geotechnical engineer has provided the following design parameters for a cohesionless soil at a certain site: $q_A = 4{,}000$ lb/ft^2, $\mu_a = 0.41$, $K_A = 0.33$, $K_P = 3.0$. The groundwater table is at a depth of 20 ft. A column that is to be supported on a square spread footing on this soil will impart the following ASD load combinations onto the footing: $P = 200$ k, $V = 18$ k. Determine the required width and depth of embedment for a square footing to support this column.

9.26 Six cone penetration tests and four exploratory borings have been performed at the site of a proposed warehouse building. The underlying soils are natural sands and silty sands with occasional gravel. The CPT results and a synthesis of the borings are shown in Figure 9.17. The

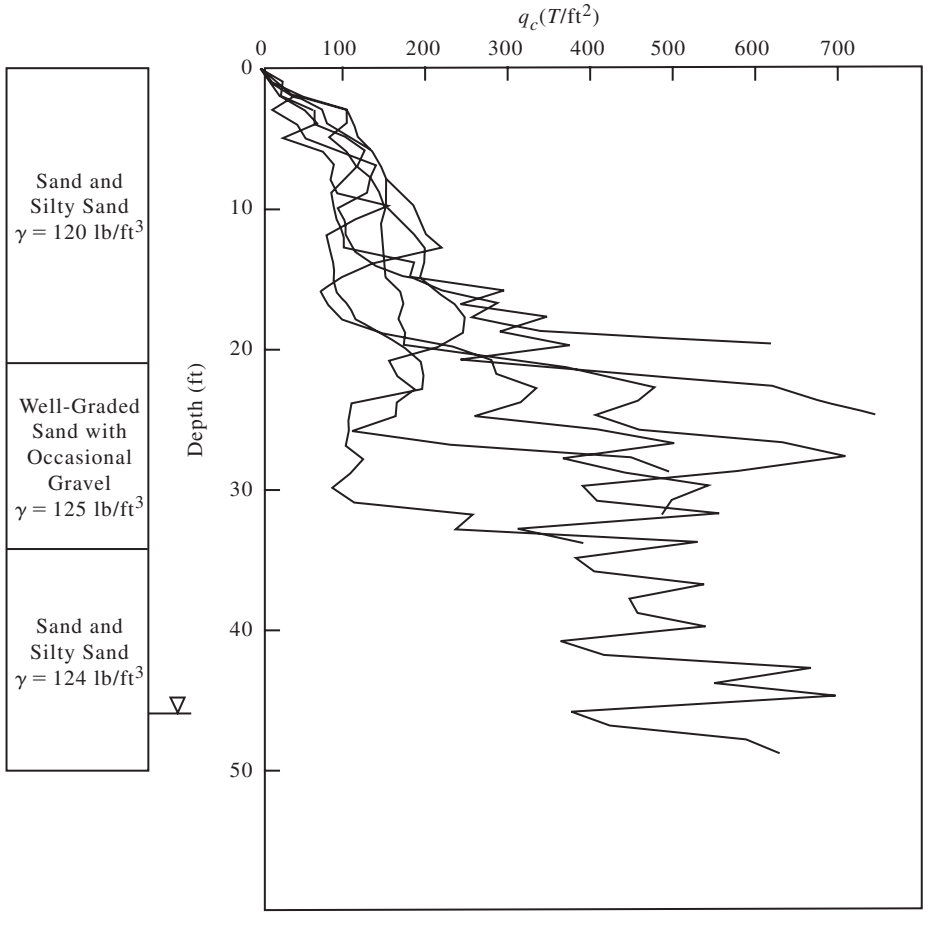

Figure 9.17 CPT data and synthesis of boring for Problems 9.26 and 9.27.

warehouse will be supported on 3 ft deep square footings that will have ultimate LRFD design downward loads of 100 to 600 k and serviceability loads of 100 to 480 k. The allowable total settlement is 1.0 in and the allowable differential settlement is 0.5 in. Using ASD with these data and reasonable factors of safety, develop design charges for vertical loads (both ultimate and serviceability) and values of, μ_a, K_A, and K_P for lateral design.

9.27 Using the design values in Problem 9.26, determine the required width of a footing that must support the following ASD load combinations:

a. Max load combination: $P = 200$ k, $V = 0$
Service loads: $P = 180$ k, $V = 0$

b. Max load combination: $P = 200$ k, $V = 21$ k
Service loads: $P = 180$ k, $V = 0$

c. Max load combination: $P = 440$ k, $V = 40$ k
Service loads: $P = 400$ k, $V = 0$

d. Max load combination: $P = 480$ k, $V = 40$ k
Service loads: $P = 360$ k, $V = 0$

10

Spread Footings—Structural Design

Foundations ought to be twice as thick as the wall to be built on them; and regard in this should be had to the quality of the ground, and the largeness of the edifice; making them greater in soft soils, and very solid where they are to sustain a considerable weight.

The bottom of the trench must be level, that the weight may press equally, and not sink more on one side than on the other, by which the walls would open. It was for this reason the ancients paved the said bottom with tivertino, and we usually put beams or planks, and build on them.

The foundations must be made sloping, that is, diminished in proportion as they rise; but in such a manner, that there may be just as much set off one side as on the other, that the middle of the wall above may fall plumb upon the middle of that below: Which also must be observed in the setting off of the wall above ground; because the building is by this method made much stronger than if the diminutions were done any other way.

Sometimes (especially in fenny places, and where the columns intervene) to lessen the expence, the foundations are not made continued, but with arches, over which the building is to be.

It is very commendable in great fabricks, to make some cavities in the thickness of the wall from the foundation to the roof, because they give vent to the winds and vapours, and cause them to do less damage to the building. They save expence, and are of no little use if there are to be circular stairs from the foundation to the top of the edifice.

The First Book of Andrea Palladio's Architecture (1570),
as translated by Isaac Ware (1738)

The plan dimensions and minimum embedment depth of spread footings are primarily geotechnical concerns, as discussed in Chapters 6 to 9. Once these dimensions have been set, the next step is to develop a structural design that gives the foundation enough integrity to safely transmit the design loads from the structure to the ground. The structural design process for reinforced concrete foundations includes:

- Selecting a concrete with an appropriate strength
- Selecting an appropriate grade of reinforcing steel
- Determining the required foundation thickness, *T*, as shown in Figure 10.1
- Determining the size, number, and spacing of the reinforcing bars
- Designing the connection between the superstructure and the foundation.

The structural design aspects of foundation engineering are far more codified than are the geotechnical aspects. These codes are based on the results of research, the performance of existing structures, and the professional judgment of experts. As discussed in Chapter 1, in North America, the International Building Code (IBC) governs the design of structures. For structural design of concrete, the IBC explicitly refers to the *Building Code Requirements for Structural Concrete* (ACI 318-11 and ACI 318M-11) published by the American Concrete Institute (ACI, 2011). The design of bridge structures is governed by the *LRFD Bridge Design Specifications* published by the American Association of State Highway and Transportation Officials (AASHTO, 2012) which is appropriate for bridges and other transportation related structures.

This chapter covers the major principles of structural design of spread footings, and will refer, primarily to the ACI code. The principles of structural footing design in

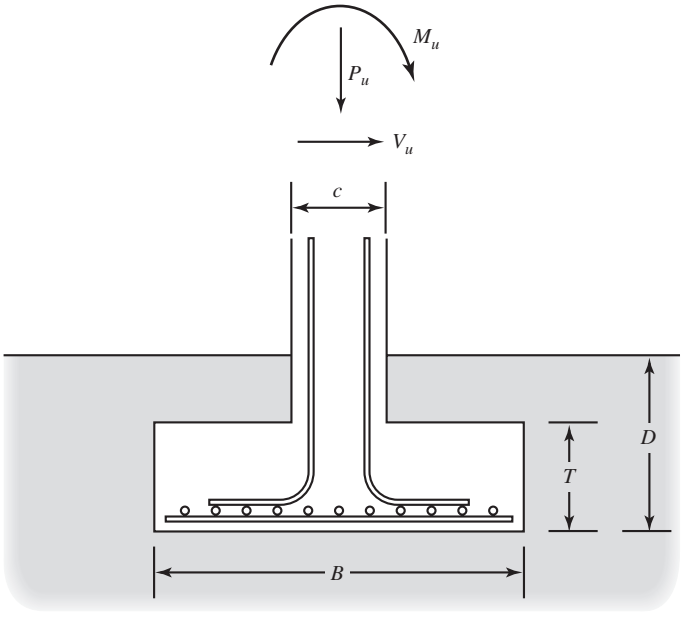

Figure 10.1 Cross-section of a spread footing showing applied loads, reinforcing steel, and relevant dimensions.

AASHTO code is consistent with the ACI code but there are significant differences. Some of the key differences will be identified in this chapter, but the AASHTO code will not be covered in detail. References to specific code provision are shown in brackets [ ]. In spite of the extensive citation of codes in this chapter, it is not a comprehensive discussion of every code provision, and thus is not a substitute for the code books.

10.1 SELECTION OF MATERIALS

Unlike geotechnical engineers, who usually have little or no control over the engineering properties of the soil, structural engineers can, within limits, select the engineering properties of the structural materials. In the context of spread footing design, we must select an appropriate concrete compressive strength, f'_c, and reinforcing steel yield strength, f_y.

When designing a concrete superstructure, engineers typically use concrete that has $f'_c = 20–35$ MPa (3,000–5,000 lb/in^2). In very tall structures, f'_c might be as large as 70 MPa (10,000 lb/in^2). The primary motive for using high-strength concrete in the superstructure is that it reduces the section sizes, which allows more space for occupancy and reduces the weight of the structure. These reduced member weights also reduce the dead loads on the underlying members.

However, the plan dimensions of spread footings are governed by bearing capacity and settlement concerns and will not be affected by changes in the strength of the concrete; only the thickness, T, will change. Even then, the required excavation depth, D, may or may not change because it might be governed by other factors. In addition, saving weight in a footing is of little concern because it is the lowest structural member and does not affect the dead load on any other members. In fact, additional weight may actually be a benefit in that it increases the uplift capacity.

Because of these considerations, and because of the additional materials and inspection costs of high-strength concrete, spread footings are usually designed using an f'_c of only 15–20 MPa (2,000–3,000 lb/in^2). For footings that carry relatively large loads, perhaps greater than about 2,000 kN (500 k), higher strength concrete might be justified to keep the footing thickness within reasonable limits, perhaps using an f'_c as high as 35 MPa (5,000 lb/in^2).

Since the flexural stresses in footings are small, grade 40 steel (metric grade 280) is usually adequate. However, this grade is readily available only in sizes up through #6 (metric #22), and grade 60 steel (metric grade 420) may be required on the remainder of the project. Therefore, engineers often use grade 60 (metric grade 420) steel in the footings for reinforced concrete buildings so only one grade of steel is used on the project. This makes it less likely that leftover grade 40 (metric grade 280) bars would accidently be placed in the superstructure.

10.2 FOOTING BEHAVIOR AND DESIGN METHODS

Before the twentieth century, the design of spread footings was based primarily on precedent. Engineers knew very little about how footings behaved, so they followed designs that had worked in the past.

The first major advance in our understanding of the structural behavior of reinforced concrete footings came as a result of full-scale load tests conducted at the University of Illinois by Talbot (1913). He tested 197 footings in the laboratory and studied the mechanisms of failure. These tests highlighted the importance of shear in footings.

During the next five decades, other individuals in the United States, Germany, and elsewhere conducted additional tests. These tests produced important experimental information on the flexural and shear resistance of spread footings and slabs as well as the response of new and improved materials. Richart's (1948) tests were among the most significant of these. He tested 156 footings of various shapes and construction details by placing them on a bed of automotive coil springs that simulated the support from the soil and loaded them using a large testing machine until they failed. Whitney (1957) and Moe (1961) also made important contributions.

A committee of engineers (ACI-ASCE, 1962) synthesized this data and developed the analysis and design methodology that engineers now use. Because of the experimental nature of its development, this method uses simplified, and sometimes arbitrary, models of the behavior of footings. It also is conservative.

As often happens, theoretical studies have come after the experimental studies and after the establishment of design procedures (Jiang, 1983; Rao and Singh, 1987). Although work of this type has had some impact on engineering practice, it is not likely that the basic approach will change soon. Engineers are satisfied with the current procedures for the following reasons:

- Spread footings are inexpensive, and the additional costs of constructing a conservative design are small.
- The additional weight that results from a conservative design does not increase the dead load on any other member.
- The construction tolerances for spread footings are wider than those for the superstructure, so additional precision in the design probably would be lost during construction.
- Although perhaps crude when compared to some methods available to analyze superstructures, the current methods are probably more precise than the geotechnical analyses of spread footings and therefore are not the weak link in the design process.
- Spread footings have performed well from a structural point of view. Failures and other difficulties have usually been due to geotechnical or construction problems, not bad structural design.
- The additional weight of conservatively designed spread footings provides more resistance to uplift loads.

Standard design methods emphasize two modes of failure: shear and flexure. A shear failure, shown in Figure 10.2, occurs when the applied load punches part of the footing away from the rest of the footing. This type of failure is actually a combination of tension and shear on inclined failure surfaces. We resist this mode of failure by providing an adequate footing thickness, T.

Figure 10.2 "Shear" failure in a spread footing loaded in a laboratory (Talbot, 1913). Observe how this failure actually is a combination of tension and shear. *Source:* Board of Trustees of the University of Illinois.

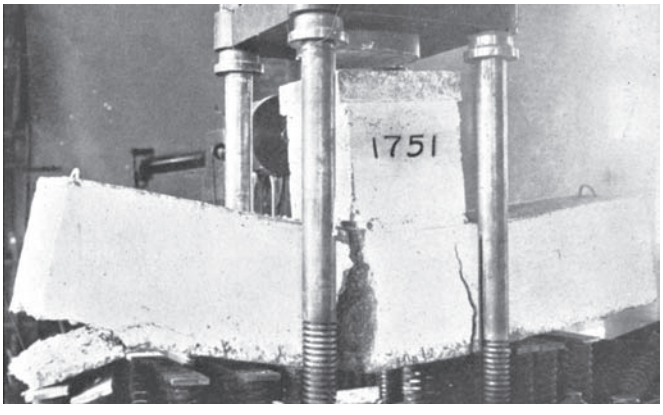

Figure 10.3 Flexural failure in a spread footing loaded in a laboratory (Talbot, 1913). *Source:* Board of Trustees of the University of Illinois.

A flexural failure is shown in Figure 10.3. We analyze this mode of failure by treating the footing as an inverted cantilever beam and resisting the flexural stresses by placing tensile steel reinforcement near the bottom of the footing.

A third, less common but critical, failure mode is concrete bearing failure. This failure occurs when concrete is crushed directly under point of application of a load. The area where a steel column connects to a footing is an example of a location where a bearing failure may occur.

10.3 DESIGN METHODOLOGY

The structural design of spread footings is based on the *load and resistance factor design* method (LRFD). The two most common codes used in the United States are the ACI 318 *Building Code Requirements for Structural Concrete* (ACI, 2011) for buildings and AASHTO *LRFD Bridge Design Specifications* (AASHTO, 2012) for transportation-related structures.

Demand

Virtually all footings are required to support applied downward (compressive) loads from the structure. Footings may also be required to support applied shear loads or moments as shown in Figure 10.1. Because structural design is based on LRFD methods, these demands will always be computed as factored compressive load, P_u, factored shear load, V_u, and factored moment, M_u, using load combinations and load factors specified by the appropriate structural code (e.g., ACI, AASHTO) as discussed in Section 5.2.

In contrast to the structural design of a footing, the geotechnical design may be based on ASD or LFRD methods. If the geotechnical design is based on LRFD, the same factored loads are used for both geotechnical and structural design of the footing. Commonly, the geotechnical design of the footing is based on ASD methods, in which case the demand is based on unfactored loads. This is often a point of confusion since different aspects of the design may be based upon different design loads. It is essential that the designers select the appropriate design loads, factored or unfactored, match the design method being used, ASD or LRFD.

Capacity

In keeping with LRFD methods, the structural capacity of a footing will be expressed as a resistance factor times the nominal capacity of the footing. In general, three capacities must be calculated: factored compressive capacity, ϕP_n, factored shear capacity, ϕV_n, and factored moment capacity, ϕM_n. An appropriate level of reliability is achieved by ensuring the factored loads never exceed the factored resistance. This requirement is stated mathematically, Equations 10.1a–c.

$$P_u \leq \phi P_n \tag{10.1a}$$

$$V_u \leq \phi V_n \tag{10.1b}$$

$$M_u \leq \phi M_n \tag{10.1c}$$

As discussed in Chapter 5, resistance factors differ between codes. For comparison, Table 10.1 presents the resistance factors for the AASHTO and ACI codes most

TABLE 10.1 RESISTANCE FACTORS APPLICABLE FOR STRUCTURAL FOOTING DESIGN IN AASHTO AND ACI CODES

	Resistance factor ϕ	
Behavior	AASHTO (2012)	ACI (2011)
Flexure in tension controlled sections	0.90	0.90
Shear in normal weight concrete	0.90	0.75
Bearing	0.70	0.65

commonly used in footing design. Note in Table 10.1 that the resistance factors for shear are dramatically different between the AASHTO and ACI codes. This difference is due in large part to the different analysis methods used in each code. Because each code is calibrated to the target reliability using its own load factors, resistance factors, and analysis methods, as discussed in Section 2.4, it is essential that the designer not mix codes. The examples in this chapter use the ACI code.

Design Process

At the start of the structural design process, the footing depth, D, will have been established by architectural and geotechnical requirements and the footing width, B, will have been determined from the geotechnical performance requirements as described in Chapter 9. The objectives of the structural design, as discussed in this chapter, are to determine the required material properties, footing thickness, T, reinforcement, and details for column connections.

The footing is modeled as a cantilever beam and designed to resist both flexure and shear demands. Normally in reinforced concrete beam design, the beam depth and flexure reinforcement are determined first, based on flexural demand. The shear demand is then met by adding shear reinforcement. In footing design, shear reinforcement is seldom used, and the required shear capacity is developed entirely in the concrete. This approach results in footings that are thicker than comparable beams, but the cost of this additional excavation and concrete is less than the cost of placing stirrups. Therefore the footing design starts with the shear design to determine the footing thickness. The flexural design then follows to determine the required flexural reinforcement.

In summary, the steps in footing design are:

1. Footing depth, D—Based on architectural requirements (primarily elevation of lowest floor) and soil conditions (see Section 9.1).
2. Footing width, B—Determined by geotechnical design (see Section 9.1).
3. Footing thickness, T—Determined by shear demand. May also be necessary to revise D in order to provide adequate cover for the floor slab.
4. Flexural reinforcement, size and spacing of bars—Determined by flexural demand.
5. Connection details—Determined by type, shape, and design of columns or walls.

The design process presented in this chapter will follow the ACI code which is appropriate for buildings, retaining walls, and similar structures. Design of footings for other types of structures, such as bridges, follows the same general procedures, but the specific code requirements will differ.

10.4 MINIMUM COVER REQUIREMENTS AND STANDARD DIMENSIONS

The ACI and AASHTO codes specify the minimum amount of concrete cover that must be present around all steel reinforcing bars [ACI 7.7, AASHTO 5.12.3]. For concrete in contact with the ground, such as spread footings, at least 70 mm (3 in) of concrete cover is

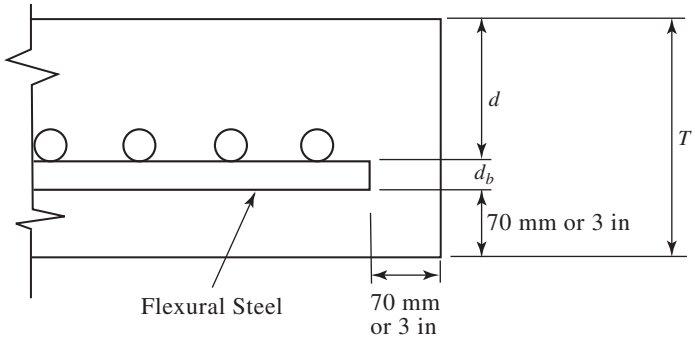

Figure 10.4 In square spread footings, the effective depth, *d*, is the distance from the top of the concrete to the contact point of the flexural steel.

required, as shown in Figure 10.4. This cover distance is measured from the edges of the bars, not the centerlines. This cover provides proper anchorage of the bars and corrosion protection. It also allows for irregularities in the excavation made to construct the footing, and accommodates possible contamination of the lower portion of the concrete.

Sometimes it is appropriate to specify additional cover between the rebar and the soil. For example, it is very difficult to maintain smooth footing excavation at sites with loose sands or soft clays, so more cover may be appropriate. Sometimes contractors place a thin layer of lean concrete, called a *mud slab* or a *leveling slab*, in the bottom of the footing excavation at such sites before placing the steel, thus providing a smooth working surface.

TABLE 10.2 DESIGN DATA FOR STEEL REINFORCING BARS

Bar Size Designation		Available Grades		Nominal Dimensions			
				Diameter, d_b		Cross-Sectional Area, A_s	
Metric	English	SI	English	(mm)	(in)	(mm^2)	(in^2)
#10	#3	280, 420	40, 60	9.5	0.375	71	0.11
#13	#4	280, 420	40, 60	12.7	0.500	129	0.20
#16	#5	280, 420	40, 60	15.9	0.625	199	0.31
#19	#6	280, 420	40, 60	19.1	0.750	284	0.44
#22	#7	420	60	22.2	0.875	387	0.60
#25	#8	420	60	25.4	1.000	510	0.79
#29	#9	420	60	28.7	1.128	645	1.00
#32	#10	420	60	32.3	1.270	819	1.27
#36	#11	420	60	35.8	1.410	1006	1.56
#43	#14	420	60	43.0	1.693	1452	2.25
#57	#18	420	60	57.3	2.257	2581	4.00

For design purposes, we ignore any strength in the concrete below the centroid of the reinforcing steel. Only the concrete between the top of the footing and the center of the rebar is considered in our analyses. Since most footings contain reinforcement in both directions, the centroid of the reinforcement is taken to be at the depth where the two perpendicular sets of rebar meet. This depth to the centroid is the *effective depth*, d, as shown in Figure 10.4.

Footings are typically excavated using backhoes, and thus do not have precise as-built dimensions. Therefore, there is no need to be overly precise when specifying the footing thickness, T. Round it to a multiple of 100 mm (or 3 in) (i.e., 300, 400, 500, etc. mm or 12, 15, 18, 21, etc. in). The corresponding values of d are:

$$d = T - 70 \text{ mm} - d_b \qquad \text{(10.2 SI)}$$

$$d = T - 3 - d_b \qquad \text{(10.2 English)}$$

where d_b is the nominal diameter of the steel reinforcing bars (see Table 10.2).

ACI [15.7] requires d be at least 150 mm (6 in). Using 300 mm (12 in) as a minimum footing thickness, T, will ensure this requirement is met for most footings.

10.5 SQUARE FOOTINGS

This section considers the structural design of square footings supporting a single centrally-located column. Other types of footings are covered in subsequent sections. As discussed in Section 10.3, the structural design starts by considering the shear capacity.

Designing for Shear

ACI defines two modes of shear failure in reinforced concrete: *one-way shear* (also known as *beam shear* or *wide-beam shear*) and *two-way shear* (also known as *diagonal tension shear* or *punching shear*). In the context of spread footings, these two modes correspond to the failures shown in Figure 10.5. Although the failure surfaces are actually inclined, as shown in Figure 10.2, engineers use these idealized vertical surfaces to simplify the computations.

Various investigators have suggested different locations for these idealized vertical critical shear surfaces shown in Figure 10.5. The ACI code specifies that they be located a distance d from the face of the column for one-way shear [ACI 11.1.3] and a distance $d/2$ for two-way shear [ACI 11.11.1.2]. The AASHTO code has a more complex method for locating the critical section [AASHTO 5.8.3.2 and 5.13.3.6.1]. While the ACI code assumes shear resistance is developed along the full effective depth, d, AASTHO assumes shear resistance is developed along a depth less than d. These differences result in higher shear capacities when using the AASHTO code. This difference in analysis procedures is part of the reason for the different resistance factors between the two codes, and is an example of the importance of not mixing provisions from different codes.

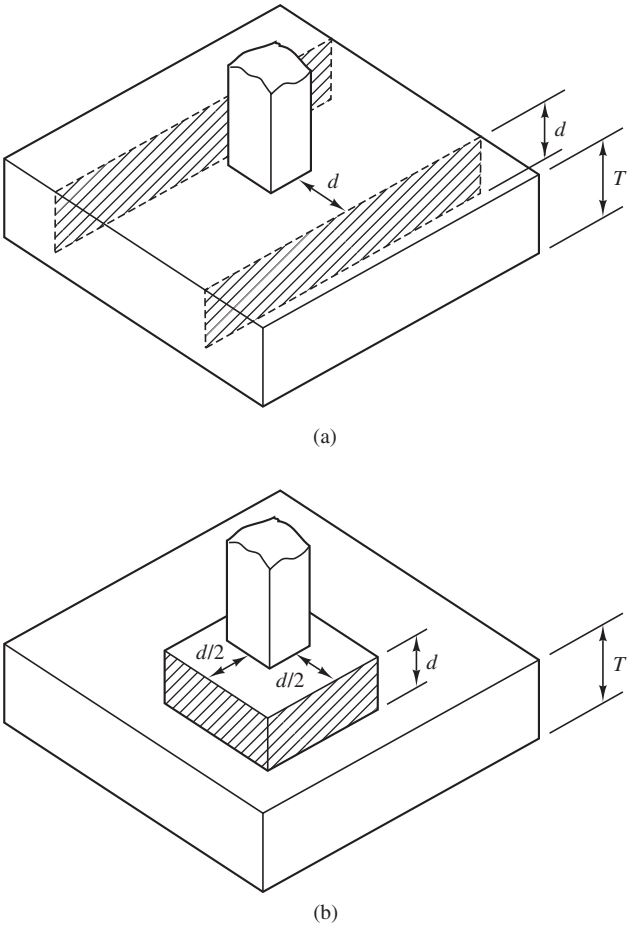

Figure 10.5 The two modes of shear failure: (a) one-way shear; and (b) two-way shear.

The footing design is considered to be satisfactory for shear when it satisfies the following condition on all critical shear surfaces:

$$V_{uc} \leq \phi V_{nc} \tag{10.3}$$

where

V_{uc} = factored shear load on critical surface
ϕ = resistance factor for shear = 0.75[ACI 9.3]
V_{nc} = nominal shear capacity on the critical surface

The nominal shear load capacity, V_{nc}, on the critical shear surface is [ACI 11.1.1]:

$$V_{nc} = V_c + V_s \tag{10.4}$$

where

V_c = nominal shear capacity of concrete
V_s = nominal shear capacity of reinforcing steel

For spread footings, we neglect V_s and rely only on the concrete for shear resistance.

Two-Way Shear

The foundation designer is generally provided with the factored load in the column just above the footing. The demand may include factored normal and shear forces, P_u and V_u, and factored moment, M_u. The factored shear force on the critical surface of the footing, V_{uc}, is computed from the factored compressive column load, P_u, and the factored column moment, M_u. The factored column shear force does not contribute to shear forces on the critical section.

Figure 10.6 shows the two-way critical shear surface for a square footing and the bearing pressure, q, at the base of the footing due to a factored column normal force and factored column moment. Due to the column moment, the bearing stress is a function of the distance from the column center, x, and increases linearly as described by Equation 10.5:

$$q(x) = \frac{P_u}{B^2} \pm \frac{12M_u}{B^4}x \tag{10.5}$$

The analysis proceeds by examining the critical shear surface subject to the greatest load. This surface and its tributary area are shown in Figure 10.6. The factored shear force on this critical surface, V_{uc}, is computed by integrating the bearing stress over the tributary area:

$$V_{uc} = \int_{c/2+d}^{B/2} q(x)b(x)dx \tag{10.6}$$

The width of the tributary area, b, is:

$$b(x) = 2x \tag{10.7}$$

Substituting Equations 10.5 and 10.7 into Equation 10.6 gives:

$$V_{uc} = \int_{c/2+d/2}^{B/2} \left(\frac{P_u}{B^2} + \frac{12M_u}{B^4}x\right)2xdx \tag{10.8}$$

Integrating Equation 10.8 gives the following expression for the factored shear force on the critical surface:

$$V_{uc} = \frac{P_u}{4}\left[\frac{B^2 - (c + d)^2}{B^2}\right] + M_u\left[\frac{B^3 - (c + d)^3}{B^4}\right] \tag{10.9}$$

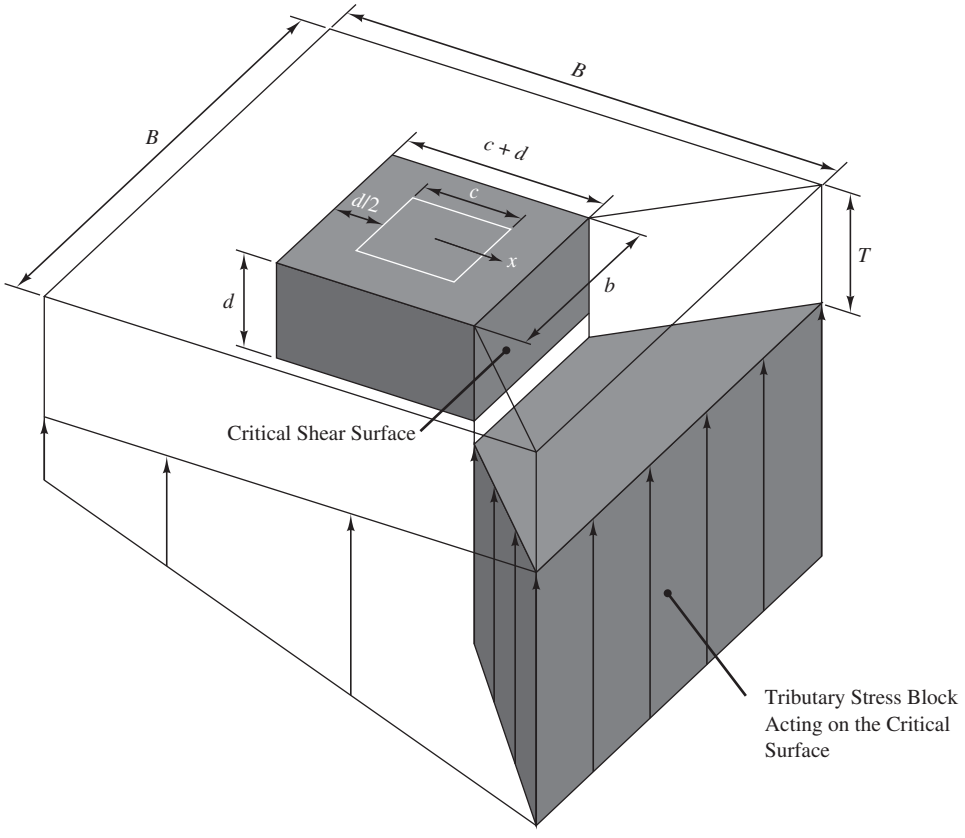

Figure 10.6 Critical two-way failure surface for a square footing. The footing is subject axial load and moment and the resulting bearing stress is shown. The factored shear stress force, V_{uc}, is computed for the face where the bearing stress is greatest. The tributary area for that face is shown.

where

V_{uc} = factored shear force on the most critical face
P_u = factored normal column force
M_u = factored column moment
c = column width or diameter (for concrete columns) or base plate width (for steel columns)
d = effective footing depth
B = footing width

If a factored column shear load, V_u, is present, this shear force must be properly transferred through the column-footing connection. This design detail will be covered in Section 10.10.

For square footings supporting square or circular columns located in the interior of the footing (i.e., not on the edge or corner), the nominal two-way shear capacity according ACI is [ACI 11.11.2.1]:

$$V_{nc} = V_c = \frac{1}{3} b_0 d \sqrt{f'_c} \qquad \text{(10.10 SI)}$$

$$V_{nc} = V_c = 4 b_0 d \sqrt{f'_c} \qquad \text{(10.10 English)}$$

$$b_0 = c + d \qquad \text{(10.11)}$$

where

V_{nc} = nominal two-way shear capacity on the critical section (kN, lb)
V_c = nominal two-way shear capacity of concrete (kN, lb)
b_0 = length of critical shear surface = length of one face of inner block (kN, lb)
c = column width (mm, in)
d = effective depth (mm, in)
f'_c = 28-day compressive strength of concrete (MPa, lb/in^2)

Other criteria apply if the column has another shape, or if it is located along the edge or corner of the footing [ACI 11.11.2.1]. Special criteria also apply if the footing is made of prestressed concrete [ACI 11.11.2.2], but spread footings are rarely, if ever, prestressed.

The objective of this analysis is to find the effective depth, d, that satisfies Equation 10.3. Both V_{uc} and V_{nc} depend on the effective depth, d, but there is no direct solution. Therefore, it is necessary to use the following iterative procedure:

1. Assume a trial value for d. Usually a value approximately equal to the column width is a good first trial. When selecting trial values of d, remember T must be a multiple of 3 in or 100 mm, as discussed in Section 10.4, so the corresponding values of d are the only ones worth considering. Assuming $d_b \approx 25$ mm (1 in), the potential values of d are 200, 300, 400, etc. mm or 8, 11, 14, 17, etc. in.
2. Compute V_{uc} and V_{nc}, and check if Equation 10.3 has been satisfied.
3. Repeat steps 1 and 2 as necessary until finding the smallest d that satisfies Equation 10.3.
4. Using Equation 10.2 with $d_b = 25$ mm (1 in), compute the footing thickness, T. Express it as a multiple of 100 mm (3 in). Practical construction considerations dictate that T must be at least 300 mm (12 in).

The final value of d_b will be determined as a part of the flexural analysis, and may be different from the 25 mm (1 in) assumed here. However, this difference is small compared to the construction tolerances, so there is no need to repeat the shear analysis with the revised d_b.

Two-way shear always governs the design of square footings subjected only to vertical column loads, so there is no need to check one-way shear in such footings. However,

if an applied moment demand is also present, both two-way and one-way shear need to be checked.

One-Way Shear

One-way shear is evaluated in a fashion similar to two-way shear by integrating the bearing stress for that portion of the footing outside of the critical surface. In the case on one-way shear, the critical surface is shown in Figure 10.5a, and the factored shear force on this surface, V_{uc}, is computed as:

$$V_u = \int_{c/2+d/2}^{B/2} \left(\frac{P_u}{B^2} + \frac{12M_u}{B^4} x \right) B dx \tag{10.12}$$

Integrating Equation 9.12 gives the following expression for the factored shear force on the critical surface:

$$V_{uc} = \frac{P_u}{2}\left[\frac{B - c - 2d}{B} \right] + \frac{3M_u}{2B}\left[1 - \frac{(c + 2d)^2}{B^2} \right] \tag{10.13}$$

where

V_{uc} = factored shear force on critical shear surfaces
B = footing width
c = column width
d = effective footing depth
P_u = factored column normal force
M_u = factored column moment

The nominal one-way shear load capacity on the critical section [ACI 11.3.1.1] is:

$$V_{nc} = V_c = \frac{1}{6} b_w d \sqrt{f'_c} \tag{10.14 SI}$$

$$V_{nc} = V_c = 2 b_w d \sqrt{f'_c} \tag{10.14 English}$$

where

V_{nc} = nominal one-way shear capacity on the critical section (kN, lb)
V_c = nominal one-way shear capacity of concrete (kN, lb)
b_w = length of critical shear surface = B (mm, in)
d = effective footing depth (mm, in)
f'_c = 28-day compressive strength of concrete (MPa, lb/in^2)

Once again, the design is satisfactory when Equation 10.3 has been satisfied.

Both V_{uc} and V_{nc} depend on the effective depth, d, which must be determined using Equations 10.13 and 10.14, with the procedure described under two-way shear. The final

design value of d is the larger of that obtained from the one-way and two-way shear analyses.

Example 10.1—Part A

A 21 in square reinforced concrete column for a building carries a vertical dead load of 380 k and a vertical live load of 270 k is to be supported on a square spread footing. Using ASD methods the allowable bearing pressure based on bearing capacity been determined to be 7,500 lb/ft^2. The expected sustained load for serviceability is 450 k. A serviceability analysis has determined the allowable bearing pressure to meet settlement requirements is 4,700 lb/ft^2. The groundwater table is well below the bottom of the footing. Determine the required width, B, thickness, T, and effective depth, d.

Solution

Since the footing is for a building, ACI code governs. We must determine the footing width based on the geotechnical analysis checking both the ultimate and serviceability limit states. First we must determine the footing depth so we can compute the weight of the footing as a function of the footing width.

Per Table 9.1, use $D = 36$ in:

$$W_f = B^2 D\gamma_c = B^2(3\text{ ft})(150\text{ lb/ft}^3) = 450\,B^2$$

Now we will determine the footing width based on the ultimate limit state (i.e., bearing capacity). Since the allowable bearing pressures were determined using ASD, unfactored loads must be used to determine the footing width and Equation 5.5 governs, and the allowable bearing stress is 7,500 lb/ft^2.

$$P = P_D + P_L + \cdots = 380\text{ k} + 270\text{ k} + 0 = 650\text{ k}$$

$$B = \sqrt{\frac{P + W_f}{q_A + u_D}} = \sqrt{\frac{650{,}000 + 450B^2}{7{,}500 + 0}}$$

$$B = 9.60\text{ ft}$$

Next we determine the footing width based on the serviceability limit state. For this computation we must use sustained bearing stress of 450 k and the allowable bearing stress of 4,700 lb/ft^2.

$$B = \sqrt{\frac{P + W_f}{q_A + u_D}} = \sqrt{\frac{450{,}000 + 450B^2}{4{,}700 + 0}}$$

$$B = 10.30\text{ ft}$$

Settlement controls → **use B = 10 ft 6 in (126 in)**

We will now start our structural design to determine the footing thickness. Since this design is for a building, ASCE 7 load factors apply and Equation 5.14 governs:

$$P_u = 1.2P_D + 1.6P_L = (1.2)(380) + (1.6)(270) = 890\text{ k}$$

Because of the large factored load and because this is a large spread footing, we will use $f'_c = 4{,}000$ lb/in^2 and $f_y = 60$ k/in^2.

Since there are no applied moment or shear loads, there is no need to check one-way shear. Determine required thickness based on a two-way shear analysis.

Try $T = 27$ in:

$$d = T - 1 \text{ bar diameter} - 3 \text{ in} = 27 - 1 - 3 = 23 \text{ in}$$

$$V_{uc} = \frac{P_u}{4}\left[\frac{B^2 - (c + d)^2}{B^2}\right] + M_u\left[\frac{B^3 - (c + d)^3}{B^4}\right]$$

$$= \frac{890{,}000 \text{ lb}}{4}\left[\frac{(126 \text{ in})^2 - (21 \text{ in} + 23 \text{ in})^2}{(126 \text{ in})^2}\right]$$

$$= 195{,}400 \text{ lb}$$

$$b_0 = c + d = 21 + 23 = 44 \text{ in}$$

$$V_n = 4b_0 d\sqrt{f'_c}$$

$$= 4(44 \text{ in})(23 \text{ in})\sqrt{4{,}000 \text{ lb/in}^2}$$

$$= 256{,}000 \text{ lb}$$

$$\phi V_n = (0.75)(256{,}000 \text{ lb}) = 192{,}000 \text{ lb}$$

$$V_{uc} > \phi V_n \qquad \therefore \text{ Not acceptable}$$

Try $T = 30$ in:

$$d = T - 1 \text{ bar diameter} - 3 \text{ in} = 30 - 1 - 3 = 26 \text{ in}$$

$$V_{uc} = \frac{P_u}{4}\left[\frac{B^2 - (c + d)^2}{B^2}\right] + M_u\left[\frac{B^3 - (c + d)^3}{B^4}\right]$$

$$= \frac{890{,}000 \text{ lb}}{4}\left[\frac{(126 \text{ in})^2 - (21 \text{ in} + 26 \text{ in})^2}{(126 \text{ in})^2}\right]$$

$$= 191{,}500 \text{ lb}$$

$$b_0 = c + d = 21 + 26 = 47 \text{ in}$$

$$V_n = 4b_0 d\sqrt{f'_c}$$

$$= 4(47 \text{ in})(26 \text{ in})\sqrt{4{,}000 \text{ lb/in}^2}$$

$$= 309{,}100 \text{ lb}$$

$$\phi V_n = (0.75)(309{,}100 \text{ lb}) = 231{,}800 \text{ lb}$$

$$V_{uc} < \phi V_n \qquad \text{OK}$$

$$\therefore \textbf{Use } B = 10 \text{ ft } 6 \text{ in}; T = 30 \text{ in}; d = 26 \text{ in}$$

Designing for Flexure

Once we have completed the shear analysis, the design process can move to the flexural analysis. Flexural design standards are essentially the same for both the ACI and AASHTO codes.

Flexural Design Standards

Reinforcing Steel

Concrete is strong in compression, but weak in tension. Therefore, engineers add reinforcing steel, which is strong in tension, to form *reinforced concrete*. This reinforcement is necessary in members subjected to pure tension, and those that must resist *flexure* (bending). Reinforcing steel may consist of either *deformed bars* (more commonly known as *reinforcing bars*, or *rebars*) or *welded wire fabric*. However, wire fabric is never used in foundations.

Manufacturers produce reinforcing bars in various standard diameters, typically ranging between 10.5 mm (3/8 in) and 57.3 mm (2 1/4 in). In the United States, the English and metric bars are the same size (i.e., we have used a soft conversion), and are identified by the *bar size* designations in Table 10.2.

Rebars are available in various strengths, depending on the steel alloys used to manufacture them. The two most common bar strengths used in the United States are:

- Grade 40 bars (metric grade 280), which have a yield strength, f_y, of 280 MPa (40 k/in^2)
- Grade 60 bars (metric grade 420), which have a yield strength, f_y, of 420 MPa (60 k/in^2)

Flexural Design Principles

The primary design problem for flexurally-loaded reinforced concrete members is as follows: Given a factored moment on the critical surface, M_{uc}, determine the necessary cross-sectional dimensions of the member, and the necessary size and location of the reinforcing bars. Fortunately, flexural design in foundations is simpler than that for some other structural members because geotechnical concerns dictate some of the dimensions.

The amount of steel required to resist flexure depends on the *effective depth*, d, which is the distance from the extreme compression fiber to the centroid of the tension reinforcement, as shown in Figure 10.7.

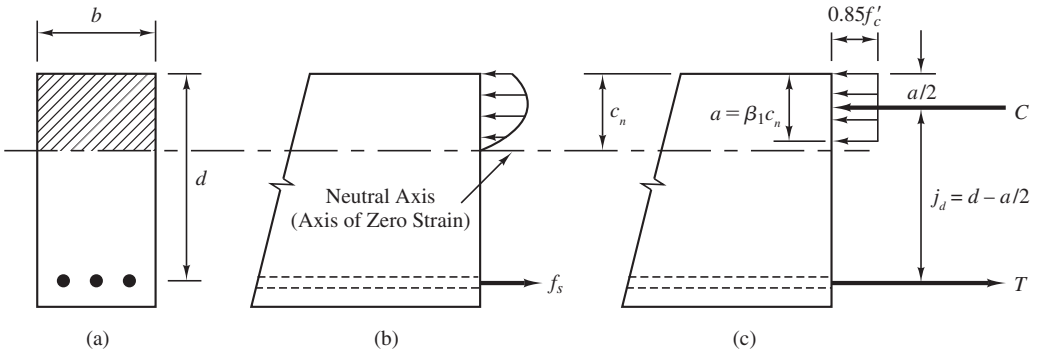

Figure 10.7 The reinforcing bars are placed in the portion of the member that is subjected to tension. (a) Cross section; (b) actual stress distribution; and (c) equivalent rectangular stress distribution. The effective depth, d, is the distance from the extreme compression fiber to the centroid of the tension reinforcement. β_1 is an empirical factor that ranges between 0.65 and 0.85 (adapted from MacGregor, 2011).

The nominal moment capacity of a flexural member made of reinforced concrete with $f'_c \leq 30$ MPa (4,000 lb/in^2) as shown in Figure 10.7 is:

$$M_n = A_s f_y \left(d - \frac{a}{2} \right) \tag{10.15}$$

where a is the depth of the thrust block shown in Figure 10.7:

$$a = \frac{\rho d f_y}{\beta_1 f'_c} \tag{10.16}$$

where

$\beta_1 =$ an empirical factor to compute depth of the thrust block and equal to 0.85 for concrete with $f'_c \leq 14$ kPa (4,000 lb/in^2)

$\rho =$ is the steel ratio

$$\rho = \frac{A_s}{bd} \tag{10.17}$$

Setting $M_u = \phi M_n$, where M_u is the factored moment at the section being analyzed, using $\beta_1 = 0.85$, and solving for A_s gives:

$$A_s = \left(\frac{f'_c b_w}{1.176 f_y} \right) \left(d - \sqrt{d^2 - \frac{2.353 M_{uc}}{\phi f'_c b_w}} \right) \tag{10.18}$$

where

$A_s =$ cross-sectional area of reinforcing steel

$f'_c =$ 28-day compressive strength of concrete

f_y = yield strength of reinforcing steel
ρ = steel ratio
b_w = width of flexural member (in this case this is the same as the footing width, B)
d = effective depth
ϕ = resistance factor = 0.9 for flexure[ACI 9.3.2]
M_{uc} = factored moment at the section being analyzed

The above analysis assumes that the flexural capacity is tension controlled. That is, if loaded to failure, the steel reinforcement in the tension zone will yield before the concrete in the compression zone will yield. This ensures that the footing will behave in a ductile manner. To verify that this condition exists, a compatibility check must be performed. This compatibility check is illustrated in Figure 10.8, and starts by assuming the concrete at the top of the footing has reached the compression strain limit of 0.003. Then knowing the depth to the neutral axis, c, and the effective depth, d, the strain at the lowest reinforcing bar, ε_t, is then computed using similar triangles. If the computed steel tensile strain is greater than the yield strain of 0.005 then the section is tension controlled and the design is satisfactory. If the steel tensile strain is less than 0.005 then the section will not exhibit ductile behavior. In this case, the depth of the footing, d, must be increased and the footing redesigned. Mathematically the compatibility check can be written as:

$$\varepsilon_t = 0.003\left(\frac{d - c_n}{c_n}\right) \tag{10.19}$$

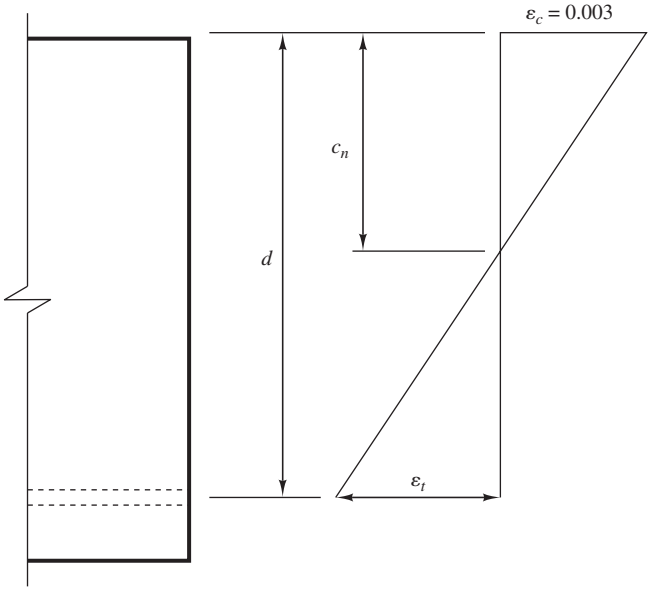

Figure 10.8 Strain compatibility check for a tension controlled element. When the strain at the top of the footing reaches the compression limit of 0.003, the strain in the lowest steel reinforcing bar must be greater than the steel yield strain of 0.005.

where

c_n = the depth to the neutral axis shown in Figure 10.7 and equal to a/β_1

and

$$\varepsilon_t \geq 0.005 \tag{10.20}$$

For footings the minimum required reinforcement is that specified in ACI 7.12.2 for temperature and shrinkage reinforcement. The requirements, based on the gross cross-sectional area of the footing, $A_g = B \times T$ are:

- Grade 40 (metric grade 280) $A_s \geq 0.0020\, A_g$
- Grade 60 (metric grade 420) $A_s \geq 0.0018\, A_g$

Note that the minimum flexural reinforcement specified in ACI 318, Section 10.5.1 does not apply to footings. See ACI 318, Section 10.5.4.

We can supply the required area of steel, computed using Equation 10.18 by any of several combinations of bar size and number of bars. This selection must satisfy the following minimum and maximum spacing requirements:

- The clear space between bars must be at least equal to d_b, 25 mm (1 in), or 4/3 times the nominal maximum aggregate size [ACI-318 3.3.2 and 7.6.1], whichever is greatest.
- The center-to-center spacing of the reinforcement must not exceed $3T$ or 500 mm (18 in), whichever is less [ACI-318 10.5.4].

Notice how one of these criteria is based on the "clear space" which is the distance between the edges of two adjacent bars, while the other is based on the center-to-center spacing, which is the distance between their centerlines.

Development Length

The rebars must extend a sufficient distance into the concrete to develop proper anchorage [ACI 15.6]. This distance is called the *development length*. Provided the clear spacing between the bars is at least $2d_b$, and the concrete cover is at least d_b, the minimum required development length, l_d, is [ACI 12.2.3]:

$$l_d = \frac{1}{1.1}\left(\frac{f_y}{\lambda\sqrt{f'_c}}\right)\left(\frac{\dfrac{\psi_t\psi_e\psi_s}{c + K_{tr}}}{d_b}\right)d_b \tag{10.21 SI}$$

$$l_d = \frac{3}{40}\left(\frac{f_y}{\lambda\sqrt{f'_c}}\right)\left(\frac{\dfrac{\psi_t\psi_e\psi_s}{c + K_{tr}}}{d_b}\right)d_b \tag{10.21 English}$$

$$K_{tr} = 40\left(\frac{A_{tr}}{sn}\right) \tag{10.22}$$

The K_{tr} term is related to splitting along a layer of rebar. For spread footings, it is permissible to use $K_{tr} = 0$, which is conservative, where

A_{tr} = total cross-sectional area of all transverse reinforcement that is within the spacing s and which crosses the potential plane of splitting through the reinforcement being developed (mm^2, in^2)—may conservatively be taken to be zero

c = spacing or cover dimension (mm, in) = the smaller of the distance from the center of the bar to the nearest concrete surface or one-half the center-to-center spacing of the bars

f_y = yield strength of reinforcing steel (MPa, lb/in^2)

f'_c = 28-day compressive strength of concrete (MPa, lb/in^2)

d_b = nominal bar diameter (mm, in)

s = maximum center-to-center spacing of transverse reinforcement within l_d (mm, in)

l_d = minimum required development length (mm, in)

n = number of bars being developed

ψ_t = reinforcement location factor

- ψ_t = 1.3 for horizontal reinforcement with more than 300 mm (12 in) of fresh concrete below the bar (seldom the case for footings)
- ψ_t = 1.0 for all other cases

ψ_e = coating factor

- ψ_e = 1.5 for epoxy coated bars or wires with cover less than $3d_b$ or clear spacing less than $6d_b$
- ψ_e = 1.2 for other epoxy coated bars or wires
- ψ_e = 1.0 for uncoated bars or wires

ψ_s = reinforcement size factor

- ψ_s = 0.8 for #6 (metric #19) and smaller bars
- ψ_s = 1.0 for #7 (metric #22) and larger bars

λ = lightweight concrete factor = 1.0 for normal concrete (lightweight concrete is not used in foundations)

The term $(c + K_{tr})/d_b$ must be no greater than 2.5, and the product $\psi_t\psi_e$ need not exceed 1.7. In addition, the development length must always be at least 300 mm (12 in). For footing applications, it is convenient, and not excessively conservative, to assume ψ_t, ψ_e, ψ_s, and λ are each equal to 1.0, $K_{tr} = 0$, and $(c + K_{tr})/d_b = 2.5$. In this case Equation 10.21 simplifies to:

$$l_d = \frac{1}{1.1}\left(\frac{f_y}{\sqrt{f'_c}}\right)\frac{d_b}{2.5} \qquad \text{(10.23 SI)}$$

$$l_d = \frac{3}{40}\left(\frac{f_y}{\sqrt{f'_c}}\right)\frac{d_b}{2.5} \qquad \text{(10.23 English)}$$

Application to Spread Footings

Principles

A square footing bends in two perpendicular directions as shown in Figure 10.9a, and therefore might be designed as a *two-way slab* using methods similar to those that might be

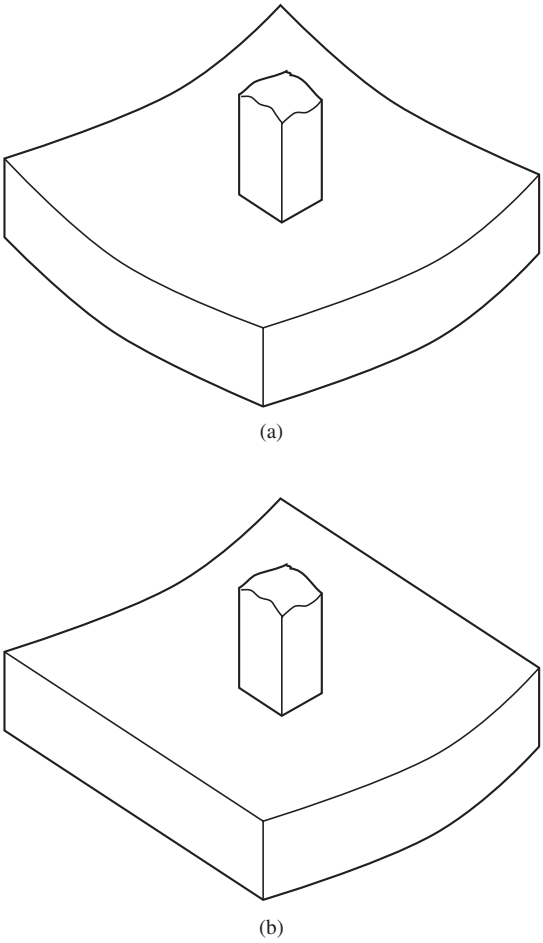

Figure 10.9 (a) A spread footing is actually a two-way slab, bending in both the "north–south" and "east–west" directions; and (b) for purposes of analysis, engineers assume that the footing is a one-way slab that bends in one axis only.

applied to a floor slab that is supported on all four sides. However, for practical purposes, it is customary to design footings as if they were a *one-way slab* as shown in Figure 10.9b. This conservative simplification is justified because of the following:

- The full-scale load tests on which this analysis method is based were interpreted this way.
- It is appropriate to design foundations more conservatively than the superstructure.
- The flexural stresses are low, so the amount of steel required is nominal and often governed by minimum reinforcement requirements.
- The additional construction cost due to this simplified approach is nominal.

Once we know the amount of steel needed to carry the applied load in one-way bending, we place the same steel area in the perpendicular direction. In essence the footing is reinforced twice, which provides more reinforcement than required by a more rigorous two-way analysis.

Steel Area

The usual procedure for designing flexural members is to prepare a moment diagram and select an appropriate amount of steel for each portion of the member. However, for isolated spread footings, we can simplify the problem because we know that the bending moment in the footing increases monotonically from the edge of the footing toward the center of the footing. The *critical section for bending*, therefore must be near the edge of the column. The exact location of this section depends upon details of the column footing connection and therefore varies based on the type of column connected to the footing. Figure 10.10 shows the location of the critical section for various types of columns.

We can simplify the computations by defining a distance l, measured from the critical section to the outside edge of the footing. In other words, l is the cantilever distance. The cantilevered distance is shown in Figure 10.10 and is computed using the formulas in Table 10.3.

The factored bending moment at the critical section, M_{uc}, is:

$$M_{uc} = \frac{P_u l^2}{2B} + \frac{2M_u l}{B} \tag{10.24}$$

where

P_u = factored normal force in the column
M_u = factored moment in the column
l = cantilever distance (from Table 10.3)
B = footing width

The first term in Equation 10.24 is based on the assumption that P_u acts through the centroid of the footing. The second term accounts for an applied moment in the column.

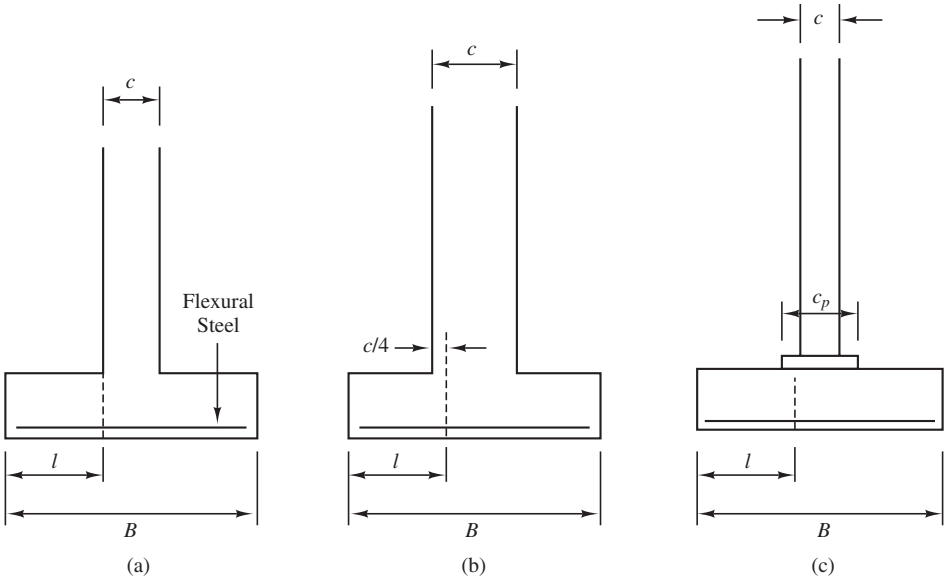

Figure 10.10 Location of critical section for bending: (a) with a concrete column; (b) with a masonry column; and (c) with a steel column.

If there is no applied moment and the column load is applied eccentrically, then M_u is equal to P_u times the eccentricity. The second term is based on a soil bearing pressure with an assumed eccentricity of $B/3$, which is conservative (see Figure 6.15).

After computing M_{uc}, find the steel area, A_s, using Equation 10.18, then check if the computed steel area is less than minimum requirement. If so, then use the minimum required steel area. Rarely will the reinforcement ratio, ρ, be larger than 0.0040, which is

TABLE 10.3 DESIGN CANTILEVER DISTANCE FOR USE IN DESIGNING REINFORCEMENT IN SPREAD FOOTINGS [ACI 318 15.4.2]

Type of Column	l
Concrete	$(B - c)/2$
Masonry	$(B - c/2)/2$
Steel	$(2B - (c + c_p))/4$

1. ACI does not specify the location of the critical section for timber columns, but in this context, it seems reasonable to treat them in the same way as concrete columns.
2. If the column has a circular, octagonal, or other similar shape, use a square with an equivalent cross-sectional area.
3. B = footing width; c = column width; c_p = base plate width. If column has a circular or regular polygon cross section, base the analysis on an equivalent square.

very light, because we used a large effective depth d in the shear analysis in order to avoid the need for stirrups. In most cases, the required flexural steel in footings is close to the minimum steel, so typically there is no need to check the ductility requirement.

If there is no applied moment load and no eccentricity in the column load, the required area of steel for each direction is the same and equal to A_s. If moments or eccentricities are different in the x- and y-directions, then separate computations must be performed in each direction. In this case, the larger required steel area is specified for both directions. This eliminates the potential for inadvertently swapping the reinforcement in each direction and simplifies field construction. The flexural steel is carried out to a point 70 mm (3 in) from the edge of the footing as shown in Figure 10.4.

Development Length

ACI [15.6] requires the flexural steel in spread footings meet standard development length requirements. This development length is measured from the critical section for bending, as defined in Figure 10.10, toward the edge of the footing. The bars end 70 mm (3 in) from the edge of the footing. Thus, the supplied development length, $(l_d)_{\text{supplied}}$ is:

$$l_{d,\text{supplied}} = l - 70 \text{ mm} \qquad (10.25 \text{ SI})$$

$$l_{d,\text{supplied}} = l - 3 \text{ in} \qquad (10.25 \text{ English})$$

where

$l_{d,\text{supplied}}$ = supplied development length
l = cantilever distance (per Table 10.3)

This supplied development length must be at least equal to the required development length, as computed using Equation 10.21 or 10.23. If this criterion is not satisfied, we do not enlarge the footing width, B (which is a geotechnical matter), and hooks are generally too expensive. Instead, it is better to use smaller diameter bars, which have a correspondingly shorter required development length.

If the supplied development length is greater than the required development length, we still extend the bars to 70 mm (3 in) from the edge of the footing. Do not cut them off at a different location.

Example 10.1—Part B:

Using the results from Part A, design the required flexural steel.

Solution

Find the required steel area:

$$l = \frac{B - c}{2} = \frac{126 - 21}{2} = 52.5 \text{ in}$$

$$M_{uc} = \frac{P_u l^2}{2B} + 0 = \frac{(890{,}000 \text{ lb})(52.5 \text{ in})^2}{(2)(126 \text{ in})} = 9{,}730{,}000 \text{ in-lb}$$

$$A_s = \left(\frac{f'_c b}{1.176 f_y}\right)\left(d - \sqrt{d^2 - \frac{2.353 M_{uc}}{\phi f'_c b}}\right)$$

$$= \left(\frac{(4000 \text{ lb/in}^2)(126 \text{ in})}{(1.176)(60{,}000 \text{ lb/in}^2)}\right)\left(26 \text{ in} - \sqrt{(26 \text{ in})^2 - \frac{2.353(9{,}730{,}000 \text{ in-lb})}{0.9(4{,}000 \text{ lb/in}^2)(126 \text{ in})}}\right)$$

$$= 7.07 \text{ in}^2$$

Try 9 #8 bars ($A_s = 7.11 \text{ in}^2$)

Check minimum steel:

$$A_s \geq 0.0018 A_g$$

$$7.11 \text{ in}^2 \geq 0.0018(126 \text{ in})(30 \text{ in})$$

$$7.11 \text{ in}^2 \geq 6.80 \text{ in}^2 \qquad \text{OK}$$

Check ductility:

$$c_n = \frac{a}{\beta_1} = \frac{A_s f_y}{0.85^2 f'_c b} = \frac{(7.11 \text{ in}^2)(60{,}000)}{0.85^2(4{,}000)(126 \text{ in}^2)} = 1.17 \text{ in}$$

$$\varepsilon_t = 0.003\left(\frac{d - c_n}{c_n}\right)$$

$$= 0.003\left(\frac{26 - 1.17}{1.17}\right)$$

$$= 0.064 > 0.005 \qquad \text{OK}$$

$$\text{Center-to-center spacing} = \frac{126 - 2(3)}{8 \text{ spaces}} = 15 \text{ in OK}$$

Check development length:

$$l_{d,\text{supplied}} = l - 3 \text{ in} = 52.5 - 3 = 49.5 \text{ in}$$

$$\frac{c + K_{tr}}{d_b} = \frac{3.5 + 0}{1} = 3.5 > 2.5 \qquad \therefore \text{ use } 2.5$$

$$l_d = \frac{3}{40}\left(\frac{f_y}{\lambda\sqrt{f'_c}}\right)\left(\frac{\psi_t \psi_e \psi_s}{\frac{c + K_{tr}}{d_b}}\right) d_b = \frac{3}{40}\left(\frac{60{,}000}{(1)\sqrt{4{,}000}}\right)\left(\frac{(1)(1)(1)}{2.5}\right)(1.0) = 28 \text{ in}$$

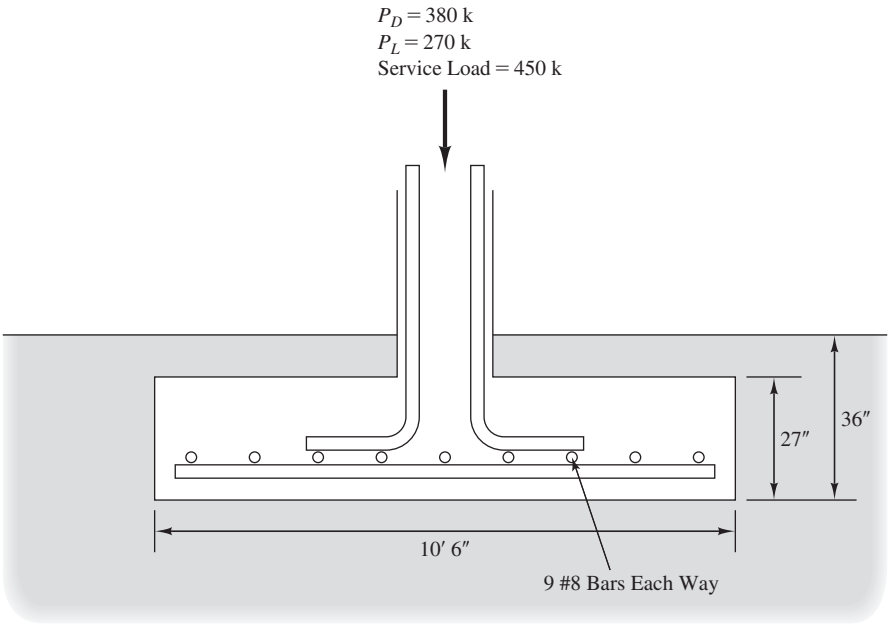

Figure 10.11 Footing design for Example 10.1.

$l_d < l_{d,\text{supplied}}$, so development length is OK.

Use 9 #8 bars each way @ 15" o.c.

The final design is shown in Figure 10.11.

10.6 CONTINUOUS FOOTINGS

The structural design of continuous footings is very similar to that for square footings. The differences, described below, are primarily the result of the differences in geometry.

Designing for Shear

As with square footings, the required depth of continuous footings is governed by shear criteria. However, we only need to check one-way shear because it is the only type that has any physical significance. The critical surfaces for evaluating one-way shear are located a distance d from the face of the wall as shown in Figure 10.12.

The factored shear force acting on a unit length (that is a footing section 1 m or 1 ft along its longitudinal axis as shown in Figure 10.12) of the critical shear surface is:

$$V_{uc} = P_u\left(\frac{B - c - 2d}{B}\right) \tag{10.26}$$

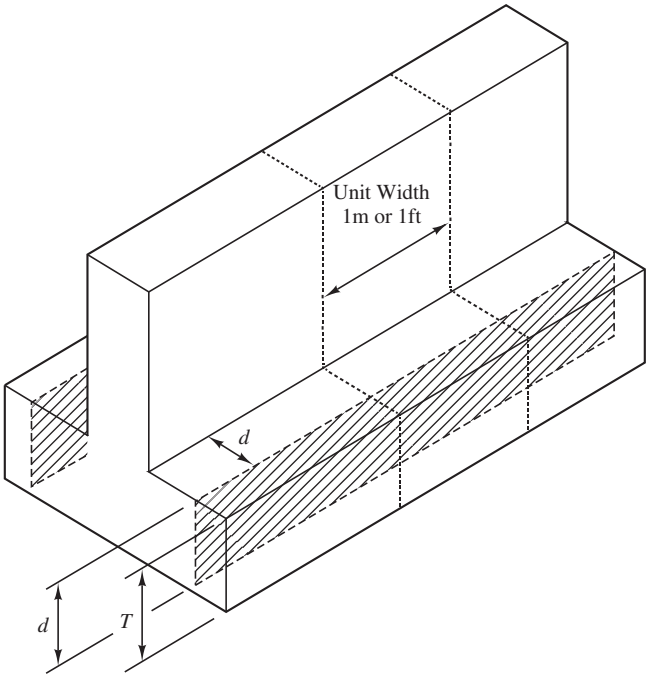

Figure 10.12 Location of idealized critical shear surface for one-way shear in a continuous footing.

where

V_{uc} = factored shear force on critical shear surface per unit length of footing
P_u = factored applied compressive load per unit length of footing
c = width of wall

Setting $V_{uc} = \phi V_{nc}$, equating Equations 10.14 and 10.26, and solving for d gives:

$$d = \frac{1{,}500P_u(B - c)}{500\phi b_w\sqrt{f'_c} + 3P_u} \qquad \text{(10.27 SI)}$$

$$d = \frac{P_u(B - c)}{48\phi b_w\sqrt{f'_c} + 2P_u} \qquad \text{(10.27 English)}$$

where

d = effective depth (mm, in)
P_u = factored vertical normal force per unit length of footing (kN/m, lb/ft)
b_w = length of the critical section, which for a continuous footing is the unit width, (1,000 mm or 12 in).
B = footing width (mm, in)
c = wall width (mm, in)

ϕ = resistance factor = 0.75
f'_c = 28-day compressive strength of concrete (MPa, lb/in^2)

Then, compute the footing thickness, T, using the criterion described earlier.

Designing for Flexure

Nearly all continuous footings should have longitudinal reinforcing steel (i.e., running parallel to the wall). This steel helps the footing resist flexural stresses from nonuniform loading, soft spots in the soil, or other causes. Temperature and shrinkage stresses also are a concern. Therefore, place a nominal amount of longitudinal steel in the footing to produce a steel ratio, ρ, of 0.0018 to 0.0020 and at least two #4 bars (2 metric #13 bars). If large differential heaves or settlements are likely, we may need to use additional longitudinal reinforcement. Chapter 27 includes a discussion of this issue.

Transverse steel (that which runs perpendicular to the wall) is another issue. Most continuous footings are narrow enough so the entire base is within a 45° frustum, as shown in Figure 10.13, and thus has virtually no tension. Thus, they do not need transverse steel. However, wider footings should include transverse steel designed to resist the flexural stresses at the critical section as defined in Table 10.3. The factored moment at this section is:

$$M_{uc} = \frac{P_u l^2}{2B} + \frac{2M_u l}{B} \tag{10.28}$$

where

M_{uc} = factored moment at critical section per unit length of footing
P_u = factored normal force per unit length of footing
M_u = factored moment perpendicular to wall per unit length of footing
l = cantilever distance (from Figure 10.10 or Table 10.3)

Compute the required transverse steel area per unit length, A_s, using Equation 10.18, as demonstrated in Example 10.2.

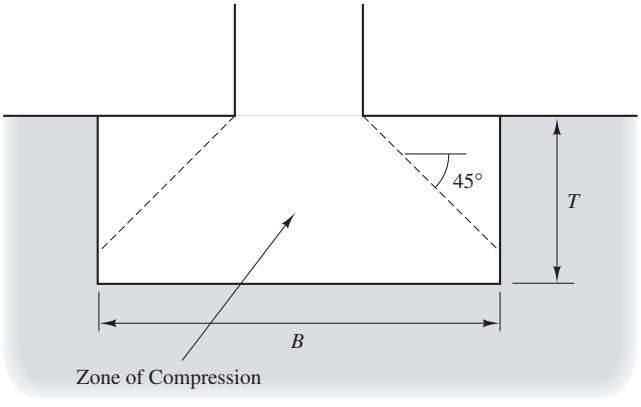

Figure 10.13 Zone of compression in lightly loaded footings.

Example 10.2

A 200 mm wide concrete block wall carries a vertical dead load of 120 kN/m and a vertical live load of 88 kN/m. The expected sustained load for serviceability is 160 kN/m. The wall is to be supported on a continuous spread footing that is to be founded at a depth of at least 500 mm below the ground surface. The geotechnical design for the project was done using ASD and determined the allowable bearing pressure based on bearing capacity as 310 kPa and the allowable bearing pressure to meet settlement requirements as 155 kPa. The groundwater table is at a depth of 10 m. Develop a structural design for this footing using $f'_c = 15$ MPa and grade 280 steel, $f_y = 280$ MPa.

Solution

Per problem statement use $D = 500$ mm:

$$W_f = BD\gamma_c = B(0.5\text{ m})(23.6\text{ kN/m}^3) = 11.8B$$

Since ASD was used in the geotechnical design it will be used to determine the footing width. To check the bearing capacity we use the ASD design wall load, Equation 5.2 governs:

$$P = P_D + P_L = 120\text{ kN/m} + 88\text{ kN/m} = 208\text{ kN/m}$$

$$B = \frac{P + W_l}{q_{A,\text{ULS}} - u_D} = \frac{208 + 11.8B}{310 - 0} = 0.7\text{ m}$$

Checking serviceability:

$$P = \text{sustained vertical load} = 160\text{ kN/m}$$

$$B = \frac{P + W_l}{q_{A,\text{SLS}} - u_D} = \frac{160 + 11.8B}{155 - 0} = 1.1\text{ m} \leftarrow \text{governs}$$

We use LRFD for structural design. Therefore factored loads apply and Equation 5.16 governs:

$$\begin{aligned} P_u &= 1.2P_d + 1.6P_L \\ &= 1.2(120) + 1.6(88) \\ &= 285\text{ kN/m} \end{aligned}$$

Compute the required thickness with a shear analysis using Equation 10.27:

$$\begin{aligned} d &= \frac{1{,}500P_u(B - c)}{500\phi b_w\sqrt{f'_c} + 3P_u} \\ &= \frac{(1{,}500)(285\text{ kN/m})(1{,}100\text{ mm} - 200\text{ mm})}{(500)(0.75)(1{,}000\text{ mm})\sqrt{15\text{ MPa}} + (3)(285\text{ kN/m})} \\ &= 265\text{ mm} \end{aligned}$$

Note that b_w is the unit width of the continuous footing (1 m = 1,000 mm) not the footing width, B. For ease of construction, place the longitudinal steel below the lateral steel. Assuming metric #13 bars (diameter = 12.7 mm), the footing thickness, T, is:

$$T = d + (\tfrac{1}{2})(\text{diam. of lat. steel}) + \text{diam. of long. steel} + 70 \text{ mm}$$

$$= 265 + \frac{12.7}{2} + 12.7 + 70$$

$$= 354 \text{ mm} \rightarrow \text{use } 400 \text{ mm}$$

$$d = 400 - \frac{12.7}{2} - 12.7 - 70 = 311 \text{ mm}$$

In the square footing design of Example 10.1, we used an effective depth, d, as the distance from the top of the footing to the contact point of the two layers of reinforcing bars (as shown in Figure 10.4). We used this definition because square footings have two-way bending, this is the average d of the two sets of rebar. However, with continuous footings we are designing only the lateral steel, so d is measured from the top of the footing to the center of the lateral bars. The longitudinal bars will be designed separately.

Design the lateral steel:

$$l = \frac{B - c/2}{2} = \frac{1.1 - 0.2/2}{2} = 0.50 \text{ m} = 500 \text{ mm}$$

$$M_{uc} = \frac{P_u l^2}{2b} + \frac{2M_u l}{B} = \frac{(285)(0.5)^2}{2(1.1)} = 32.4 \text{ kN-m}$$

$$A_s = \left(\frac{f'_c b_w}{1.176 f_y}\right)\left(d - \sqrt{d^2 - \frac{2.353 M_{uc}}{\phi f'_c b_w}}\right)$$

$$= \left(\frac{(15 \text{ MPa})(1 \text{ m})}{(1.176)(280 \text{ MPa})}\right)\left(0.311 \text{ m} - \sqrt{(0.311 \text{ m})^2 - \frac{2.353(32.4 \text{ kN-m})}{0.9(15{,}000 \text{ kPa})(1 \text{ m})}}\right)$$

$$= 4.20 \times 10^{-4} \text{ m}^2/\text{m} = 420 \text{ mm}^2/\text{m}$$

$$\rho = \frac{A_s}{d} = \frac{420 \text{ mm}^2/\text{m}}{(311 \text{ mm})(1{,}000 \text{ mm/m})} = 0.0014$$

For metric grade 280 steel $\rho_{\min} = 0.0020$

$$\rho < \rho_{\min} \quad \therefore \text{ use } \rho_{\min}$$

$$A_s/b = \rho d = (0.0020)(311 \text{ mm})(1{,}000 \text{ mm/m}) = 622 \text{ mm}^2/\text{m}$$

Use metric #13 bars @ 200 mm OC

$$A_s = (129 \text{ mm}^2/\text{bar})(5 \text{ bars/m}) = 645 \text{ mm}^2/\text{m} > 622 \text{ mm}^2/\text{m}$$

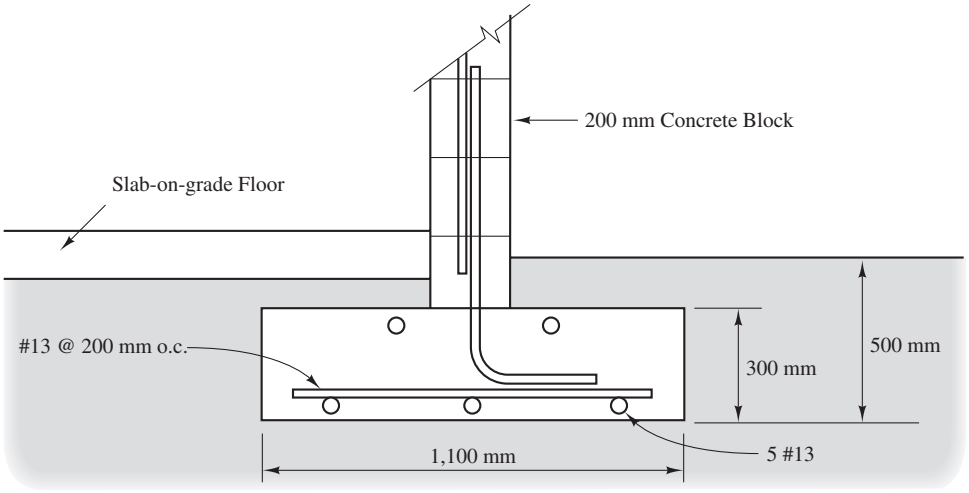

Figure 10.14 Final design for Example 10.2.

Check development length:

$$l_{d,\text{supplied}} = l - 75 = 500 - 75 = 425 \text{ mm}$$

$$\frac{c + K_{tr}}{d_b} = \frac{70 + 0}{12.7} = 5.5 > 2.5 \text{ use } 2.5$$

$$l_d = \frac{1}{1.1}\left(\frac{f_y}{\lambda\sqrt{f_c'}}\right)\left(\frac{\psi_t\psi_e\psi_s}{\dfrac{c + K_{tr}}{d_b}}\right)d_b = \frac{1}{1.1}\frac{300}{\sqrt{15}}\frac{(1)(1)(1)}{2.5}(12.7) = 358 \text{ mm}$$

$l_d < l_{d,\text{supplied}}$, so development length is OK.

Design the longitudinal steel:

$$A_s = \rho Bd = (0.0020)(1{,}100 \text{ mm})(311 \text{ mm}) = 684 \text{ mm}^2$$

Use 5 metric #13 bars ($A_s = 645 \text{ mm}^2 \approx 684 \text{ mm}^2$)

The final design is shown in Figure 10.14.

10.7 RECTANGULAR FOOTINGS

Rectangular footings with width B and length L that support only one column are similar to square footings. Design them as follows:

1. Check both one-way shear (Equation 10.14) and two-way shear (Equation 10.10) using the critical shear surfaces shown in Figure 10.15a. Determine the minimum required d and T to satisfy both.

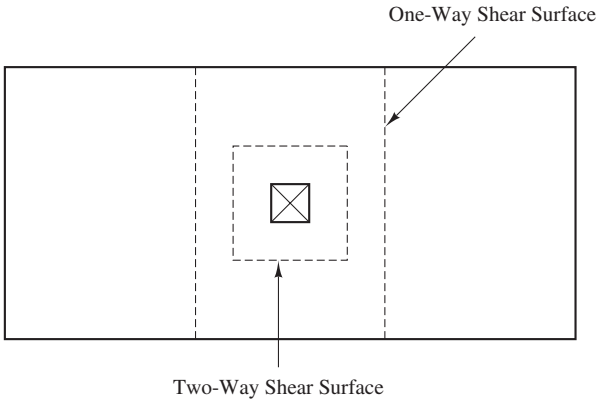

(a)

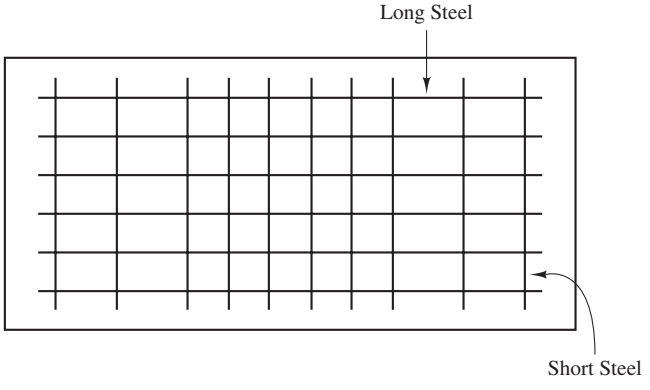

(b)

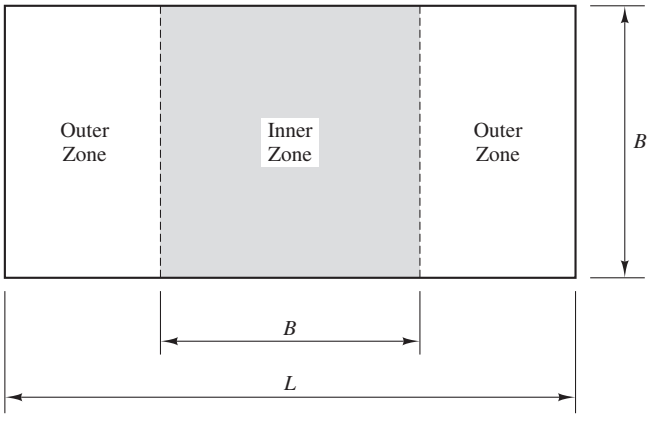

(c)

Figure 10.15 Structural design of rectangular footings: (a) critical shear surfaces; (b) long steel and short steel; and (c) distribution of short steel.

2. Design the long steel (see Figure 10.15b) by substituting L for B in Table 10.3 and Equation 10.24, and using Equation 10.18 with no modifications. Distribute this steel evenly across the footing as shown in Figure 10.15c.
3. Design the short steel (see Figure 10.15b) using Table 10.3 and Equation 10.24 with no modifications, and substituting L for B in Equation 10.18.
4. Since the central portion of the footing takes a larger portion of the short-direction flexural stresses, place more of the short steel in this zone [ACI 15.4.4]. To do so, divide the footing into inner and outer zones, as shown in Figure 10.15c. The portion of the total short steel area, A_s, to be placed in the inner zone is E:

$$E = \frac{2}{L/B + 1} \tag{10.29}$$

Distribute the balance of the steel evenly across the outer zones.

10.8 COMBINED FOOTINGS

Combined footings are those that carry more than one column. Their loading and geometry is more complex, so it is appropriate to conduct a more rigorous structural analysis. The rigid method, described in Chapter 11, is appropriate for most combined footings. It uses a soil bearing pressure that varies linearly across the footing, thus simplifying the computations. Once the soil pressure has been established, MacGregor (2011) suggests designing the longitudinal steel using idealized beam strips ABC, as shown in Figure 10.16. Then, design the transverse steel using idealized beam strips AD. See section 16-6 of MacGregor (2011) for a complete design example.

Large or heavily loaded combined footings may justify a beam on elastic foundation analysis, as described in Chapter 11.

10.9 LIGHTLY LOADED FOOTINGS

Although the principles described in Sections 10.5 to 10.8 apply to footings of all sizes, some footings are so lightly loaded that practical minimums begin to govern the design. For example, if P_u is less than about 400 kN (90 k) for square footings or 150 kN/m (10 k/ft) for continuous footings, the minimum d of 150 mm (6 in) [ACI 15.7] controls. Thus, there is no need to conduct a shear analysis, only to compute a T smaller than the minimum. In the same vein, if P_u is less than about 130 kN (30 k) for square footings or 60 kN/m (4 k/ft) for continuous footings, the minimum steel requirement ($\rho = 0.0018$) governs, so there is no need to conduct a flexural analysis. Often, these minimums also apply to footings that support larger loads.

In addition, if the entire base of the footing is within a 45° frustum, as shown in Figure 10.13, we can safely presume that very little or no tensile stresses will develop. This is often the case with lightly loaded footings. Technically, no reinforcement is required

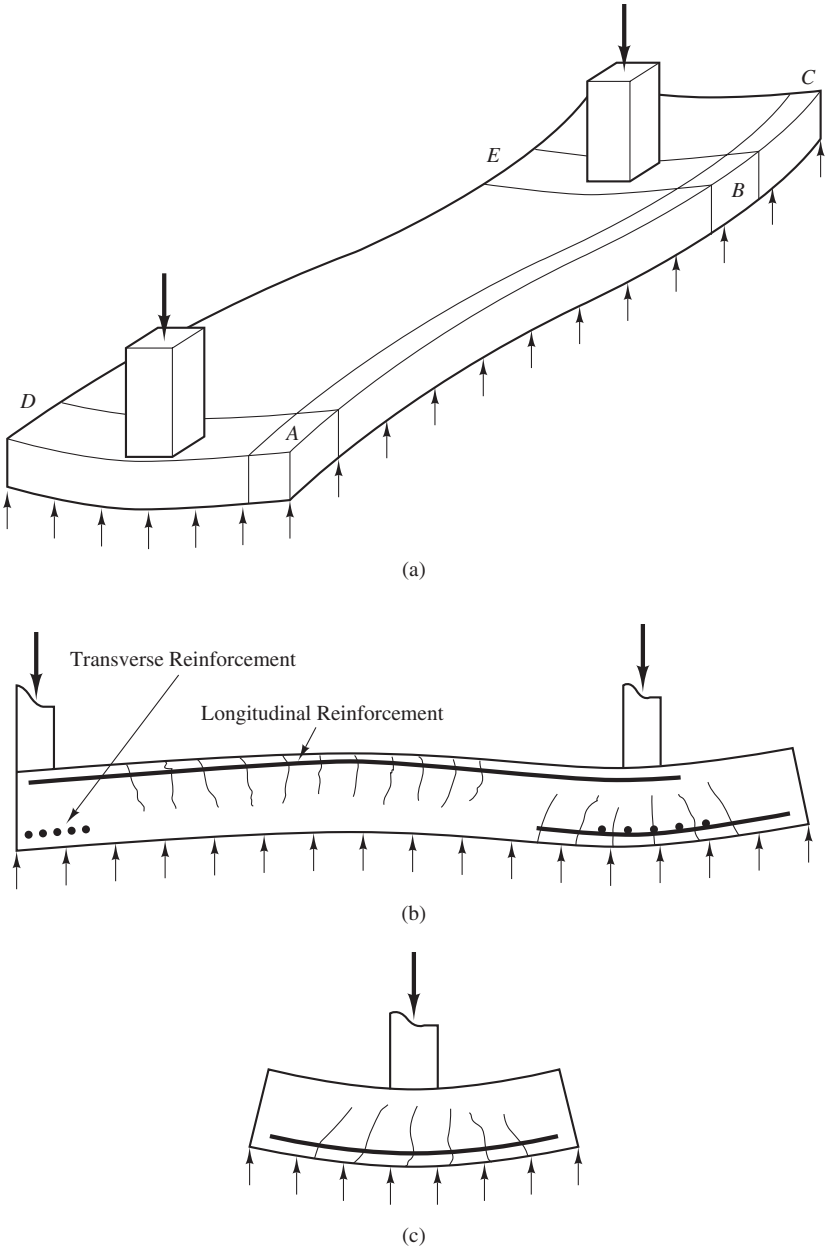

Figure 10.16 Structural design of combined footings: (a) idealized beam strips; (b) longitudinal beam strip; and (c) transverse beam strip (adapted from MacGregor, 2011).

in such cases. However, some building codes [IBC 1807.1] have minimum reinforcement requirements for certain footings, and it is good practice to include at least the following reinforcement in all footings:

Square footings

- If bottom of footing is completely within the zone of compression—no reinforcement required
- If bottom of footing extends beyond the zone of compression—as determined by a flexural analysis, put at least #4 @ 18 in o.c. each way (metric #13 @ 500 mm o.c. each way)

Continuous footings

Longitudinal reinforcement

- Minimum two #4 bars (metric #13)

Transverse reinforcement

- If bottom of footing is completely within the zone of compression—no lateral reinforcement required
- If bottom of footing extends beyond the zone of compression—as determined by a flexural analysis, put at least #4 @ 18 in o.c. (metric #13 @ 500 mm o.c.)

This minimum reinforcement helps accommodate unanticipated stresses, temperature and shrinkage stresses, and other phenomena.

10.10 CONNECTIONS WITH THE SUPERSTRUCTURE

One last design feature that must be addressed is the connection between the footing and the superstructure. Connections are often the weak link in structures, so this portion of the design must be done carefully. A variety of connection types are available, each intended for particular construction materials and loading conditions. The design of proper connections is especially important when significant seismic or wind loads are present (Dowrick, 1987).

Connections are designed using either ASD (with the unfactored loads) or LRFD (with the factored loads) depending on the design method used in the superstructure.

Connections with Columns

Columns may be made of concrete, masonry, steel, or wood, and each has its own concerns when designing connections.

Concrete or Masonry Columns

Connect concrete or masonry columns to their footing [ACI 15.8] using *dowels*, as shown in Figure 10.17. These dowels are simply pieces of reinforcing bars that transmit axial, shear,

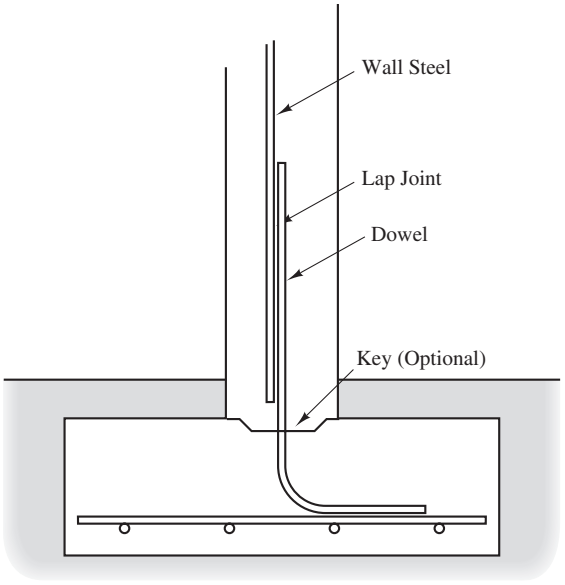

Figure 10.17 Use of dowels to connect a concrete or masonry column to its footing.

and moment loads. Use at least four dowels with a total area of steel, A_s, at least equal to that of the column steel or 0.005 times the cross-sectional area of the column, whichever is greater. They may not be larger than #11 bars [ACI 15.8.2.3] and must have a 90° hook at the bottom. Normally, the number of dowels is equal to the number of vertical bars in the column.

Design for Column Bearing Loads

Check the bearing strength of the footing [ACI 10.14] to verify that it is able to support the axial column load. This is especially likely to be a concern if the column carries large compressive stresses that might cause something comparable to a bearing capacity failure inside the footing. To check this possibility, compute the factored column load, P_u, and compare it to the nominal column bearing strength, P_{nb}:

$$P_{nb} = 0.85 f'_c A_1 s \tag{10.30}$$

Then, determine whether the following statement is true:

$$P_u = \phi P_{nb} \tag{10.31}$$

where

P_u = factored column load
P_{nb} = nominal column bearing strength (i.e., bearing of column on top of footing)
f'_c = 28-day compressive strength of concrete used for the footing
$s = (A_2/A_1)^{0.5} \leq 2$ if the frustum in Figure 10.18 fits entirely within the footing (i.e., if $c + 4d \leq B$)
$s = 1$ if the frustum in Figure 10.18 does not fit entirely within the footing

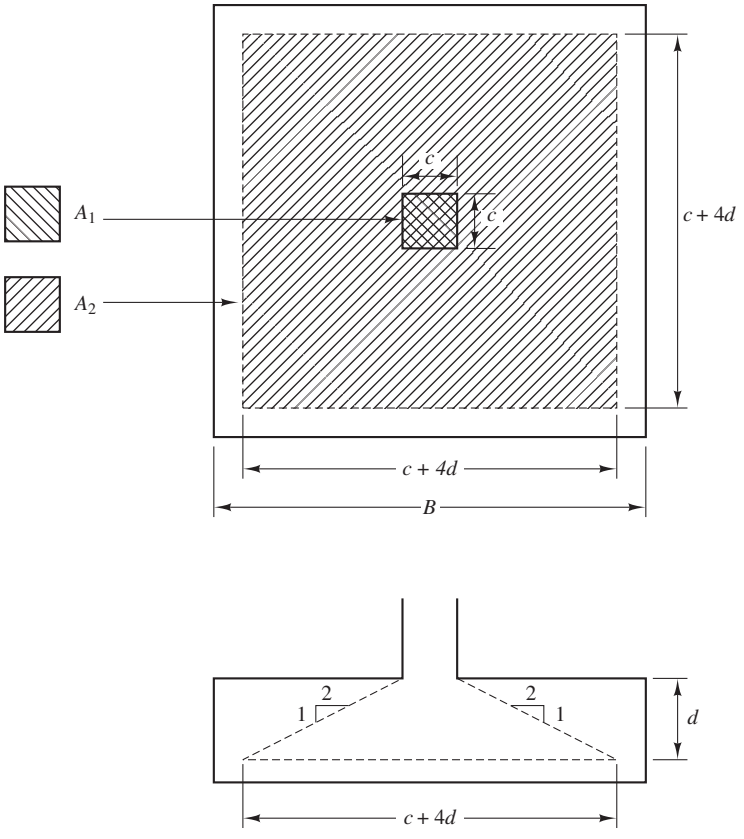

Figure 10.18 Application of a frustrum to find areas A_1 and A_2.

A_1 = cross-sectional area of the column = c^2
A_2 = base area of frustum, $(c + 4d)^2$ as shown in Figure 10.18
c = column width or diameter
ϕ = resistance factor = 0.65 [ACI 9.3.2.4]

If Equation 10.31 is not satisfied, use a higher strength concrete (greater f'_c) in the footing or design the dowels as compression steel.

Design for Moment Loads

If the column imparts moment loads onto the footing, then some of the dowels will be in tension. Therefore, the dowels must be embedded at least one development length into the footing, as shown in Figure 10.19 and defined by the following equations [ACI 12.5]:

$$l_{dh} = \frac{0.24 f_y}{\sqrt{f'_c}} d_b \qquad \text{(10.32 SI)}$$

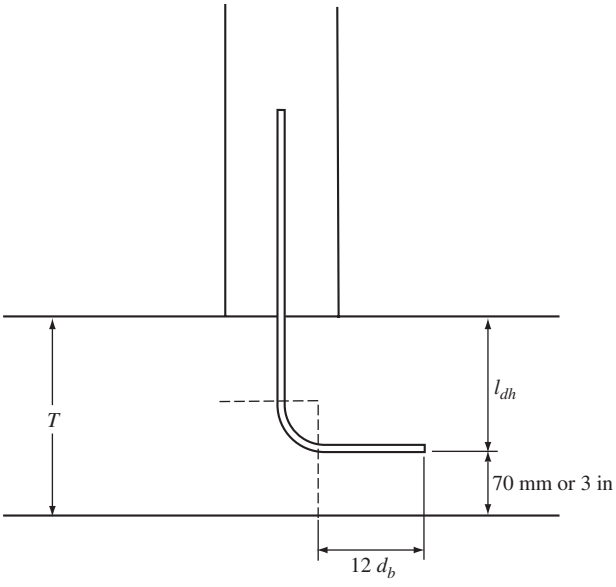

Figure 10.19 Minimum required embedment of dowels subjected to tension.

$$l_{dh} = \frac{0.02 f_y}{\sqrt{f'_c}} d_b \qquad \text{(10.32 English)}$$

where

l_{dh} = development length for 90° hooks, as defined in Figure 10.19 (mm, in)
d_b = bar diameter (mm, in)
f_y = yield strength of reinforcing steel (MPa, lb/in^2)
f'_c = 28-day compressive strength of concrete (MPa, lb/in^2)

Equation 10.32 applies for uncoated reinforcing bars and normal weight concrete. For #11 bars (Metric #36) or smaller with at least 50 mm (2 in) of cover beyond the end of the hook the development length computed by Equation 10.32 may be reduced by a factor of 0.7 [ACI 12.5.3].

Sometimes this development length requirement will dictate a footing thickness T greater than that required for shear (as computed earlier in this chapter).

As long as the number and size of dowels are at least as large as the vertical steel in the column, then they will have sufficient capacity to carry the moment loads.

Design for Shear Loads

If the column also imparts a factored shear force, V_u, onto the footing, the connection must be able to transmit this force. Since the footing and column are poured separately, there is a weak shear plane along the cold joint. Therefore, the shear force must be transferred via

sliding friction between the column and the footing. In this case, the dowels must provide enough normal force across the sliding plane to resist the factored shear force. The minimum required dowel steel area is:

$$A_s = \frac{V_u}{\phi f_y \mu} \tag{10.33}$$

where

A_s = minimum required dowel steel area
V_u = factored shear force
ϕ = 0.75 for shear [ACI 9.3.2.3]
f_y = yield strength of reinforcing steel
μ = coefficient of friction across the joint and equal to 0.6 if the cold joint is not intentionally roughened or 1.0 if the cold joint is roughened by heavy raking or grooving [ACI 11.6.4.3]

However, the ultimate shear load, V_u, cannot exceed $0.2\phi f'_c A_c$, where f'_c is the compressive strength of the column concrete, and A_c is the cross-sectional area of the column.

Splices

Most designs use a lap splice to connect the dowels and the vertical column steel. However, some columns have failed in the vicinity of these splices during earthquakes, as shown in Figure 10.20. Therefore, current codes require much more spiral reinforcement in columns subjected to seismic loads. In addition, some structures with large moment loads, such as certain highway bridges, require mechanical splices or welded splices to connect the dowels and the column steel.

Steel Columns

Steel columns are connected to their foundations using base plates and anchor bolts, as shown in Figure 10.21. The base plates are welded to the bottom of the columns when they are fabricated, and the anchor bolts are cast into the foundation when the concrete is placed. The column is then erected over the foundation, and the anchor bolts are fit through predrilled holes in the base plate.

The top of the footing is very rough and not necessarily level, so the contractor must use special construction methods to provide uniform support for the base plate and to make the column plumb. For traffic signal poles, light standards, and other lightweight columns, the most common method is to provide a nut above and below the base plate, as shown in Figure 10.22a, and adjust these nuts as needed to make the column plumb. However, columns for buildings, bridges, and other large structures are generally too heavy for this method, so the contractor must temporarily support the base plate on steel blocks and shims, and clamp it down with a single nut on each anchor bolt, as shown

Figure 10.20 Imperial County Services Building, El Centro, California. The bases of these columns failed along lap splices during the 1979 El Centro earthquake, causing the building to sag about 300 mm. As a result, this six-story building had to be demolished. (U.S. Geological Survey photo).

in Figure 10.22b. These shims are carefully selected to produce a level base plate and a plumb column. Other construction methods also have been used.

Once the column is securely in place and the various members that frame into it have been erected, the contractor places a nonshrink grout between the base plate and the footing. This grout swells slightly when it cures (as compared to normal grout, which

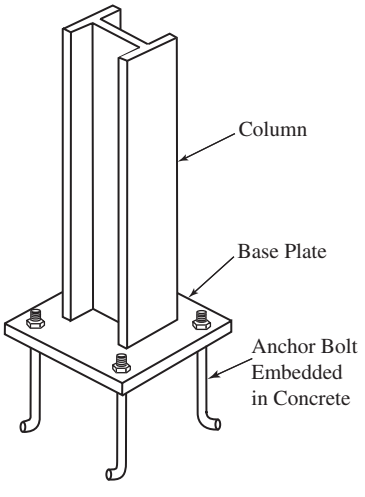

Figure 10.21 Base plate and anchor bolts to connect a steel column to its foundation.

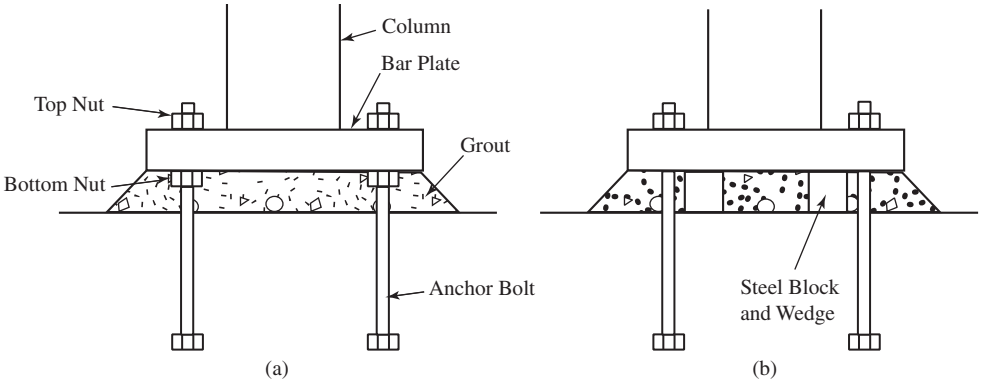

Figure 10.22 Methods of leveling the base plate: (a) double nuts; and (b) blocks and shims.

shrinks), thus maintaining continuous support for the base plate. The structural loads from the column are then transmitted to the footing as follows:

- Compressive loads are spread over the base plate and transmitted through the grout to the footing.
- Tensile loads pass through the base plate and are resisted by the anchor bolts.
- Moment loads are resisted by a combination of compression through the grout and tension in half of the bolts.
- Shear loads are transmitted through the anchor bolts, through sliding friction along the bottom of the base plate, or possibly both.

Design Principles

The base plate must be large enough to avoid exceeding the nominal bearing strength of the concrete (see earlier discussion under concrete and masonry columns). In addition, it must be thick enough to transmit the load from the column to the footing. The design of base plates is beyond the scope of this book, but it is covered in most steel design texts and in Fisher and Kloiber (2006).

Anchor bolts can fail either by fracture of the bolts themselves, or by loss of anchorage in the concrete. Steel is much more ductile than the concrete, and this ductility is important, especially when wind or seismic loads are present. Therefore, anchor bolts should be designed so the critical mode of failure is shear or tension of the bolt itself rather than failure of the anchorage. In other words, the bolt should fail before the concrete fails.

The following methods may be used to design anchor bolts that satisfy this principle. These methods are based on ACI and AISC requirements, but some building codes may impose additional requirements, or specify different design techniques, so the engineer must check the applicable code.

Selection and Sizing of Anchor Bolts

Five types of anchor bolts are available, as shown in Figure 10.23:

- *Standard structural steel bolts* may simply be embedded into the concrete to form anchor bolts. These bolts are similar to those used in bolted steel connections, except they are much longer. Unfortunately, these bolts may not be easily available in lengths greater than about 6 in, so they often are not a practical choice.
- *Structural steel rods that have been cut to length and threaded* form anchor bolts that are nearly identical to a standard steel bolts and have the advantage of being more readily available. This is the most common type of anchor bolt for steel columns. If one nut is used at the bottom of each rod, it should be tack welded to prevent the rod from turning when the top nut is tightened. Alternatively, two nuts may be used.
- *Hooked bars* (also known as *L-bolts* or *J-bolts*) are specially fabricated fasteners made for this purpose. These are principally used for wood-frame structures, and are generally suitable for steel structures only when no tensile or shear loads are present.
- *Proprietary anchor bolts* are patented designs that often are intended for special applications, principally with wood-frame structures.
- *Drilled-in anchor bolts* are used when a cast-in-place anchor bolt was not installed during construction of the footing. They are constructed by drilling a hole in the concrete, then embedding a threaded rod into the hole and anchoring it using either epoxy grout or mechanical wedges. This is the most expensive of the five types and is usually required only to rectify mistakes in the placement of conventional anchor bolts.

Most anchor bolts are made of steel that satisfies ASTM A36 or ASTM A307, both of which have $f_y = 250$ MPa (36 k/in^2). However, higher strength steel may be used, if needed.

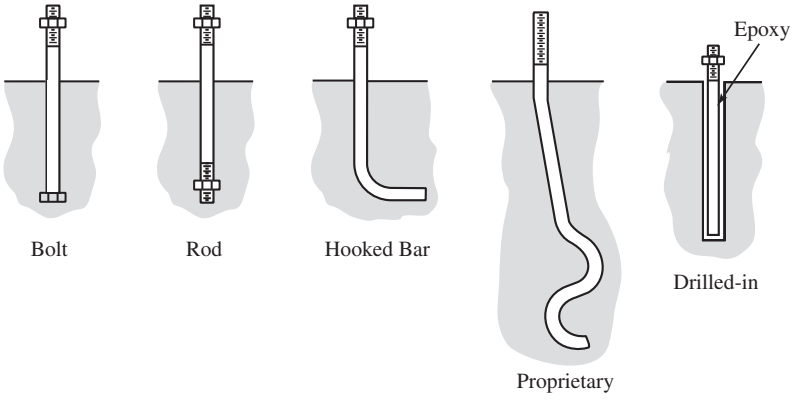

Figure 10.23 Types of anchor bolts.

Each bolt must satisfy both of the following design criteria:

$$P_u \leq \phi P_n \tag{10.34}$$

$$V_u \leq \phi V_n \tag{10.35}$$

where

P_u = factored tensile load expressed as a positive number
V_u = factored shear load
ϕ = resistance factor = 0.75 for tensile fracture [AISC 16.1]
P_n = nominal tensile capacity
V_n = nominal shear capacity

In addition, the design must satisfy AISC requirements for interaction between shear and tensile stresses. Figure 10.24 presents the shear and tensile capacities for ASTM A36 and ASTM A307 bolts that satisfies Equations 10.34 and 10.35 and the interaction requirements, and may be used to select the required diameter.

OSHA (2001) requires a minimum of four anchor bolts for each column and this is the most common number used. It is best to place them in a square pattern to simplify construction and leave less opportunity for mistakes. Rectangular or hexagonal patterns are more likely to be accidentally built with the wrong orientation. More bolts and other patterns may be used, if necessary.

If the design loads between the column and the footing consist solely of compression, then anchor bolts are required only to resist erection loads, accidental collisions

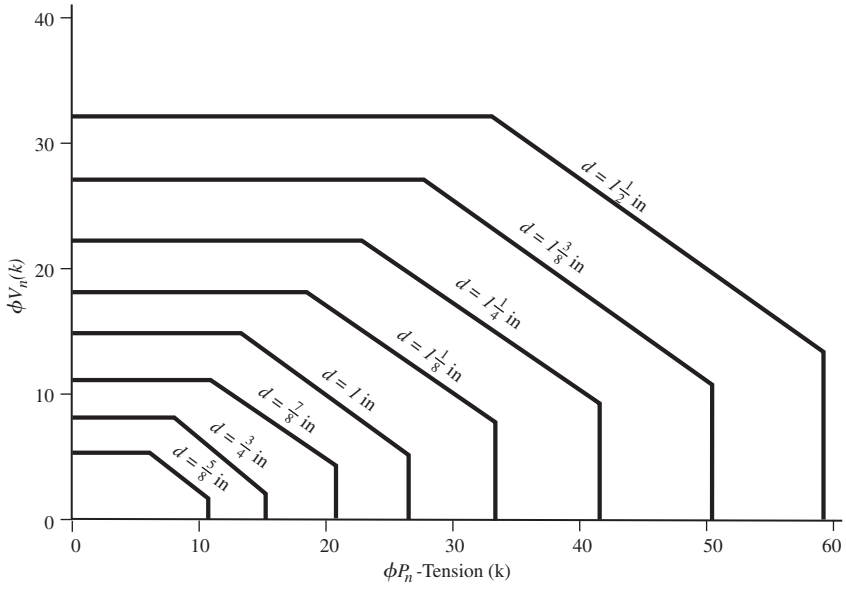

Figure 10.24 AISC tensile and shear capacities of A36 and A307 anchor bolts.

during erection, and unanticipated shear or tensile loads. The engineer might attempt to estimate these loads and design accordingly, or simply select the bolts using engineering judgment. Often these columns simply use the same anchor bolt design as nearby columns, thus reducing the potential for mistakes during construction. A recommended minimum anchorage for steel columns with only compressive design loads is four 20 mm (3/4 in) diameter rods or bolts with a length of 305 mm (12 in).

Anchorage

Once the bolt diameter has been selected, the engineer must determine the required depth of embedment into the concrete to provide the necessary anchorage. The required embedment depends on the type of anchor, the spacing between the anchors, the kind of loading, and the strength of the concrete. In addition, the bolt must be located at least a minimum horizontal distance from the edge of the concrete. Table 10.4 presents conservative design values for embedment depth and edge distance. Alternatively, the engineer may use the more refined procedure described by Marsh and Burdette (1985).

Shear Transfer

Shear forces may be transferred from the base plate to the foundation in three ways:

- By sliding friction along the bottom of the base plate
- By embedding the column within the footing or providing shear lugs to transfer shear loads though lateral bearing
- Through shear in the anchor bolts

In most typical designs sliding friction will be adequate to carry shear forces and is the only design method covered in this text. Should shear loads exceed the capacity available through sliding friction, the reader is referred to Fisher and Kloiber (2006) for design procedures using embedment and shear through anchor bolts.

So long as the grout has been carefully installed between the base plate and the footing, there will be sliding friction along the bottom of the base plate. The computation of sliding friction resistance follows the same procedure as previously used for concrete

TABLE 10.4 ANCHORAGE REQUIREMENTS FOR BOLTS AND THREADED RODS (Shipp and Haninger, 1983) Copyright © American Institute of Steel Construction. Reprinted with permission.

Steel Grade	Minimum Embedment Depth	Minimum Edge Distance
A307, A36	12d	5d or 100 mm (4 in), whichever is greater
A325, A449	17d	7d or 100 mm (4 in), whichever is greater

d = nominal bolt or rod diameter

column connections except that the coefficient of friction must be appropriate for the steel-grout interface. AISC recommends using a coefficient of friction of 0.55 for conventional base plates in contact with grout, such as that shown in Figure 10.22. Thus, the available sliding friction resistance, ϕV_n, is:

$$\begin{aligned} \phi V_n &= \phi \mu P_u \\ &= 0.55 \phi P_u \end{aligned} \tag{10.36}$$

and the appropriate resistance factor is 0.75 per ACI-318 requirements for shear.

The value of P_u in Equation 10.36 should be the lowest factored load combination consistent with the shear load being considered. For example, if shear loads from wind or seismic demands are being considered, the uplift forces generated should be considered and act against the downward dead loads. It is good practice to ignore any normal stress produced by live loads or the clamping forces from the nuts.

Example 10.3

A steel wide flange column with a steel base plate is to be supported on a spread footing. The AISC factored design loads are: $P_u = 270$ k compression and $M_u = 200$ ft-k. Design an anchor bolt system for this column using four bolts arranged in a 15 × 15 in square.

Solution

Reduce the applied loads to a couple separated by 15 in:

$$P = \frac{270 \text{ k}}{2} \pm \frac{200 \text{ ft-k}}{(15/12) \text{ ft}}$$

$$= 135 \pm 160 \text{ k}$$

There are two bolts on each side, so the maximum tensile force in each bolt is:

$$P = \frac{135 - 160}{2} = 12.5 \text{ k tension}$$

The shear force is zero.

Per Figure 10.24, 5/8 in bolts would be satisfactory. However, use 3/4 in bolts as a recommended minimum diameter.

Minimum depth of embedment $= 12d = 12(0.75 \text{ in}) = 9$ in

Use four 3/4 in diameter × 13 in long A36 threaded rods embedded 9 in into the footing. Firmly tighten two nuts at the bottom of each rod.

Wood Columns

Wood columns, often called *posts*, usually carry light loads and require relatively simple connections. The most common type is a metal bracket, as shown in Figure 10.25. These

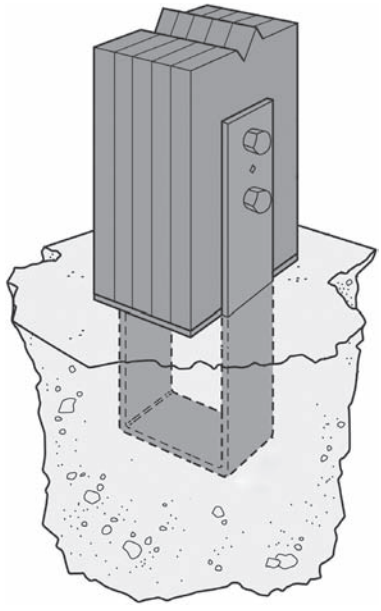

Figure 10.25 Steel post base for securing a wood post to a spread footing.

are set in the wet concrete immediately after it is poured. The manufacturers determine the allowable loads and tabulate them in their catalogs (e.g., see www.strongtie.com).

It is poor practice to simply embed a wooden post into the footing. Although at first this might be a very strong connection, in time the wood will rot and become weakened.

Connections with Walls

The connection between a concrete or masonry wall and its footing is a simple one. Simply extend the vertical wall steel into the footing [ACI 15.8.2.2], as shown in Figure 10.26. For construction convenience, design this steel with a lap joint immediately above the footing.

Connect wood-frame walls to the footing using anchor bolts, as shown in Figure 10.27. Normally, standard building code criteria govern the size and spacing of these bolts. For example, the *International Building Code* (ICC, 2012) specifies 12.7 mm (1/2 in) nominal diameter bolts embedded at least 178 mm (7 in) into the concrete. It also specifies bolt spacing of no more than 1.8 m (6 ft) on center or no more than 1.2 m (4 ft) for structures taller than two stories [IBC 2308.6]. Some codes require 16 mm (5/8 in) anchor bolts.

Sometimes we must supply a higher capacity connection between wood-frame walls and footings, especially when large uplift loads are anticipated. Steel holddown brackets, such as that shown in Figure 10.28, are useful for these situations.

Many older wood-frame buildings have inadequate connections between the structure and its foundation. Figure 10.29 shows one such structure that literally fell off its foundation during the 1989 Loma Prieta Earthquake in Northern California.

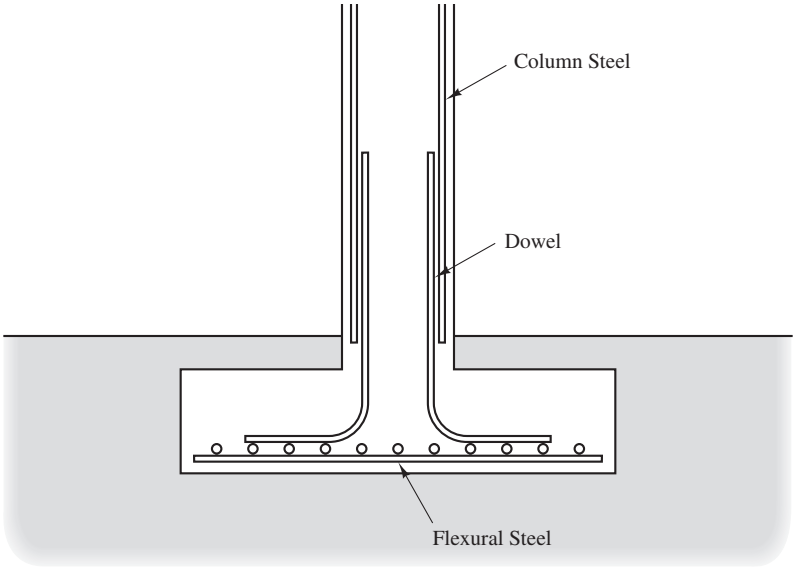

Figure 10.26 Connection between a concrete or masonry wall and its footing.

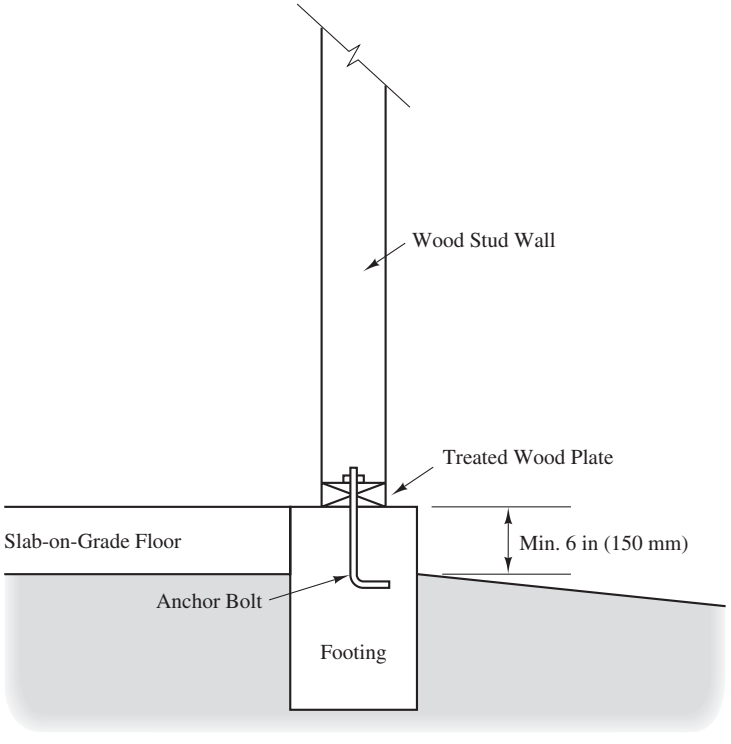

Figure 10.27 Use of anchor bolts to connect a wood-frame wall to a continuous footing.

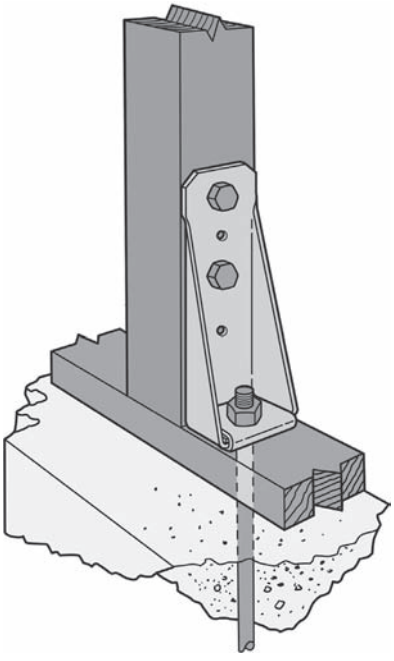

Figure 10.28 Use of steel holdown bracket to connect a wood-frame wall with large uplift force to a footing.

Some wood-frame buildings have failed during earthquakes because the *cripple walls* collapsed. These are short wood-frame walls that connect the foundation to the floor. They may be retrofitted by installing plywood shear panels or by using diagonal steel bracing (Shepherd and Delos-Santos, 1991).

Figure 10.29 House that separated from its foundation during the 1989 Loma Prieta Earthquake (photo by C. Stover, U.S. Geological Survey).

SUMMARY

Major Points

1. The plan dimensions and minimum embedment depth of a spread footing are governed by geotechnical concerns, and are most commonly determined using the ASD method and unfactored loads. The LRFD method is beginning to be adopted for geotechnical design of foundations, particularly in the transportation sector.
2. The thickness and reinforcement of a spread footing are governed by structural concerns. Structural design is governed by the LRFD method, which means these analyses are based on the factored loads.
3. The structural design of spread footings must consider both shear and flexural failure modes. A shear failure consists of the column or wall punching through the footing, while a flexural failure occurs when the footing has insufficient cantilever strength.
4. Since we do not wish to use stirrups (shear reinforcement), we conduct the shear analysis first and select an effective depth, d, so the footing that provides enough shear resistance in the concrete to resist the shear force induced by the applied load. This analysis ignores the shear strength of the flexural steel.
5. Once the shear analysis is completed, we conduct a flexural analysis to determine the amount of steel required to provide the needed flexural strength. Since d is large, the required steel area will be small, and it is often governed by $\rho_{\min}$.
6. For square footings, use the same flexural steel in both directions. Thus, the footing is reinforced twice.
7. For continuous footings, the lateral steel, if needed, is based on a flexural analysis. Use nominal longitudinal steel to resist nonuniformities in the load and to accommodate inconsistencies in the soil bearing pressure.
8. Design rectangular footings similar to square footings, but group a greater portion of the short steel near the center.
9. Practical minimum dimensions will often govern the design of lightly loaded footings.
10. The connection between the footing and the superstructure is very important. Use dowels to connect concrete or masonry structures. For steel columns and wood-frame walls, use anchor bolts. For wood posts, use specially manufactured brackets.

Vocabulary

28-day compressive strength
Anchor bolts
Anchorage
Base plate
Cover
Critical section for bending
Critical shear surface
Development length
Diagonal tension shear
Dowels
Ductility
Effective depth
Factored load
Flexural failure

Hooked bars
Lap splice
Leveling slab
Minimum steel
Mud slab
Nominal shear capacity
One-way shear
Post base
Punching shear
Reinforcing bars
Resistance factor
Shear failure
Sliding friction
Steel ratio
Two-way shear
Ultimate moment load
Ultimate shear load
Unfactored load
Wide-beam shear

QUESTIONS AND PRACTICE PROBLEMS

Sections 10.1–10.4: Materials, Behavior, Design Methods, and Cover

10.1 Why are spread footings usually made of low-strength concrete?

10.2 Explain the difference between the shape of the actual shear failure surfaces in footings with those used for analysis and design.

10.3 Why are reinforcement cover requirement for footings greater than those for building columns or beams?

10.4 In reinforced concrete beam design we generally design for flexure first and then shear. However, with footings we first design for shear and then for flexure. Why?

10.5 What is the difference between the thickness and effective depth of a given footing?

Section 10.5: Square Footings

10.6 A 400 mm square concrete column that carries a factored vertical downward load of 450 kN and a factored moment of 100 kN-m is supported on a 1.5 m square footing. The effective depth of the concrete in this footing is 500 mm. Compute the ultimate shear force that acts on the most critical section for two-way shear failure in the footing.

10.7 A 16 in square concrete column carries vertical unfactored load of 250 k. The vertical service load is 210 k. It is to be supported on a square footing with $f'_c = 3{,}000$ lb/in^2 and $f_y = 60$ k/in^2. The soil has an allowable bearing pressure of 6,500 lb/ft^2 for bearing capacity (based on ASD methods) and 4,100 lb/ft^2 for settlement. The groundwater table is at a great depth. Because of frost heave considerations, the bottom of this footing must be at least 30 in below the ground surface. Determine the required footing width, thickness, size of the flexural reinforcement, and show your design in a sketch.

10.8 A W16 $\times$ 50 steel column with a 22 in square base plate is to be supported on a square spread footing. This column has factored ultimate vertical column load of 320 k. The vertical service load is 250 k. The footing will be made of concrete with $f'_c = 2{,}500$ lb/in^2 and reinforcing steel with $f_y = 60$ k/in^2. The soil has an allowable bearing pressure for bearing capacity of 5,200 lb/ft^2 (based on LRFD methods) and an allowable bearing stress for settlement of 3,400 lb/ft^2. The groundwater table is at a great depth. Determine the required footing width, thickness, size of the flexural reinforcement, and show your design in a sketch.

10.9 A 500 mm square concrete column carries a factored ultimate vertical column load of 780 kN. The vertical service load is 650 kN. It is to be supported on a square footing with $f'_c = 17$ MPa and $f_y = 420$ MPa. The soil has an allowable bearing pressure for bearing capacity of 650 kPa (based on LRFD methods) and an allowable bearing stress for settlement of 160 kPa. The groundwater table is at a great depth. Determine the required footing width, thickness, size of the flexural reinforcement, and show your design in a sketch.

10.10 A 16 in square concrete column carries factored ultimate column loads of $P_U = 370$ k and $M_U = 70$ k-ft. The vertical service load is 310 k. The footing will be made of concrete with $f'_c = 3{,}000$ lb/in^2 and reinforcing steel with $f_y = 60$ k/in^2. The soil has an allowable bearing pressure for bearing capacity of 8,200 lb/ft^2 (based on LRFD methods) and an allowable bearing stress for settlement of 5,400 lb/ft^2. The groundwater table is at a great depth. Determine the required footing, width, thickness, size of the flexural reinforcement, and show your design in a sketch.

10.11 A 500 mm square concrete column carries factored ultimate column loads of $P_U = 580$ kN and $M_U = 30$ kN-m. The vertical service load is 490 kN. It is to be supported on a square footing with $f'_c = 20$ MPa and $f_y = 420$ MPa. The soil has an allowable bearing pressure for bearing capacity of 650 kPa (based on LRFD methods) and an allowable bearing stress for settlement of 280 kPa. The groundwater table is at a great depth. Determine the required footing, width, thickness, size of the flexural reinforcement, and show your design in a sketch.

Section 10.6: Continuous Footings

10.12 A 12 in wide concrete block wall carries an unfactored vertical design load of 25.1 k/ft. The sustained vertical load for serviceability analysis is 18.4 k/ft. It is to be supported on a continuous footing made of 2,500 lb/in^2 concrete and 40 k/in^2 steel. The soil has an allowable bearing pressure for bearing capacity of 6,700 lb/ft^2 (using ASD methods) and an allowable bearing pressure for settlement of 4,000 lb/ft^2. The groundwater table is at a great depth. The local building code requires that the bottom of this footing be at least 24 in below the ground surface. Determine the required footing, width, thickness, and design the lateral and longitudinal steel. Show your design in a sketch.

10.13 A 200 mm wide concrete block wall carries a factored vertical design load of 172 kN/m. The sustained load for settlement is 130 kN/m. It is to be supported on a continuous footing made of 18 MPa concrete and 280 MPa steel. The soil has an allowable bearing pressure for bearing capacity of 180 kPa (using LRFD methods) and an allowable bearing pressure for settlement of 110 kPa. The groundwater table is at a great depth. The local building code requires that the bottom of this footing be at least 500 mm below the ground surface. Determine the required footing, width, thickness, and design the lateral and longitudinal steel. Show your design in a sketch.

Sections 10.7 & 10.8: Rectangular and Combined Footings

10.14 An 18 in square concrete column carries a factored ultimate compressive load of 640 k. It is to be supported on a 8 ft wide 12 ft long rectangular spread footing. Select appropriate values for f'_c and f_y, then determine the required footing thickness and design the flexural reinforcing steel. Show the results of your design in a sketch.

10.15 Determine the required footing thickness and design the reinforcement for the combined footing shown in Figure 10.30. Use concrete with $f'_c = 3{,}000$ lb/in^2 and reinforcing steel with $f_y = 60$ k/in^2.

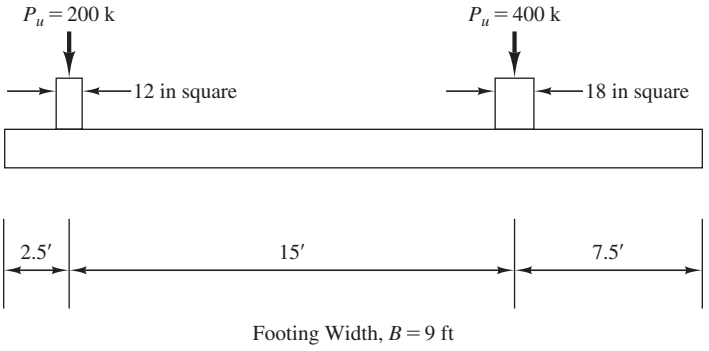

Figure 10.30 Combined footing for Problem 10.15.

Section 10.10: Connections with the Superstructure

10.16 The column described in Problem 10.14 is reinforced with 6 #8 bars. Design the dowels required to connect it with the footing, and show your design in a sketch.

10.17 A 400 mm diameter concrete column carrying a factored compressive load of 1,500 kN is supported on a spread footing. It is reinforced with eight metric #19 bars. Using $f'_c = 18$ MPa and $f_y = 420$ MPa, design the dowels for this connection.

10.18 A 24 in square concrete column carries a factored compressive load of 900 k and a factored shear load of 100 k. It is to be supported on a spread footing with $f'_c = 3{,}000$ lb/ft^2 and $f_y = 60$ k/in^2. Design the dowels for this connection.

10.19 A steel column with a square base plate is to be supported on a spread footing. The AISC factored design loads are: $P_u = 600$ k compression and $V_u = 105$ k. Design an anchor bolt system for this base plate and show your design in a sketch.

Comprehensive Questions

10.20 A 400 mm square concrete column reinforced with eight metric #19 bars carries vertical dead and live loads of 980 and 825 kN, respectively. It is to be supported on a 2.0 m $\times$ 3.5 m rectangular footing. The concrete in the footing will have $f'_c = 20$ MPa and $f_y = 420$ MPa. The building will have a slab-on-grade floor, so the top of the footing must be at least 150 mm below the finish floor elevation. Develop a complete structural design, including dowels, and show it in a sketch.

10.21 A 12 in wide masonry wall carries dead and live loads of 6 k/ft and 9 k/ft, respectively, and is reinforced with #6 bars at 24 in on center. The sustained load for settlement computation is 10.5 k/ft. This wall is to be supported on a continuous footing with $f'_c = 2{,}000$ lb/in^2 and $f_y = 60$ k/in^2. The underlying soil has an allowable bearing pressure for bearing capacity of 5,200 lb/ft^2 (based on LRFD methods) and an allowable bearing pressure for settlement of 3,000 lb/ft^2. Develop a complete structural design for this footing, including dowels, and show your design in a sketch.

11

Mats

The mere formulation of a problem is far more often essential than its solution, which may be merely a matter of mathematical or experimental skill. To raise new questions, new possibilities, to regard old problems from a new angle requires creative imagination and marks real advances in science.

Albert Einstein

The second type of shallow foundation is the *mat foundation*, as shown in Figure 11.1. A mat is essentially a very large spread footing that usually encompasses the entire footprint of the structure as shown in Figure 6.10. They are also known as *raft foundations*.

Foundation engineers often consider mats when dealing with any of the following conditions:

- The structural loads are so high or the soil conditions so poor that spread footings would be exceptionally large. As a general rule of thumb, if spread footings would cover more than about 25 percent of the building footprint area, a mat or some type of deep foundation will probably be more economical.
- The soil is very erratic and prone to excessive differential settlements. The structural continuity and flexural strength of a mat bridges over these irregularities. The same is true of mats on highly expansive soils prone to differential heaves.
- The structural loads are erratic, and thus increase the likelihood of excessive differential settlements. Again, the structural continuity and flexural strength of the mat absorbs these irregularities.

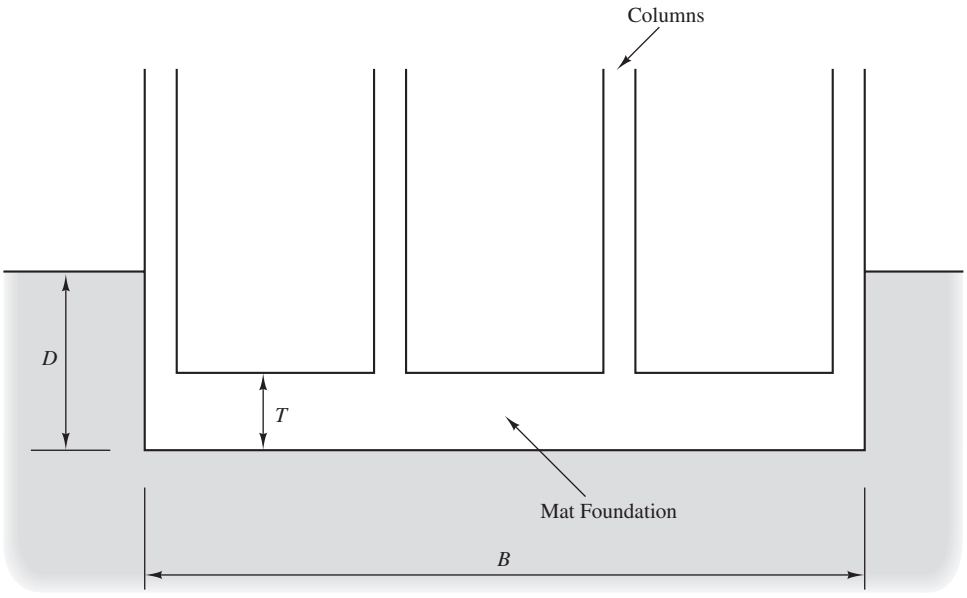

Figure 11.1 A conventional mat foundation.

- Lateral loads are not uniformly distributed through the structure and thus may cause differential horizontal movements in spread footings or pile caps. The structural continuity of a mat resists such movements.
- The uplift loads are larger than spread footings can accommodate. The greater weight and continuity of a mat may provide sufficient uplift resistance.
- The bottom of the structure is located below the groundwater table, so waterproofing is an important concern. Because mats are monolithic, or have only a few joints, they are much easier to waterproof. The weight of the mat also helps resist hydrostatic uplift forces.

11.1 CONFIGURATION

Many buildings are supported on mat foundations, as are silos, chimneys, and other types of tower structures. Mats are also used to support storage tanks and large machines. Typically, the thickness, T, is 1 to 2 m (3–6 ft), so mats are massive structural elements. Even very large structures can sometimes be supported on mat foundations. For example, the seventy-five-story Texas Commerce Tower in Houston is one of the largest mat-supported structures in the world, and has a 3.0 m (9 ft 9 in) thick mat bottomed 19.2 m (63 ft) below the street level.

Most mats have a uniform thickness, which can result in substantial concrete quantities. Another option is to use a ribbed mat, which has thick ribs in the areas of greatest

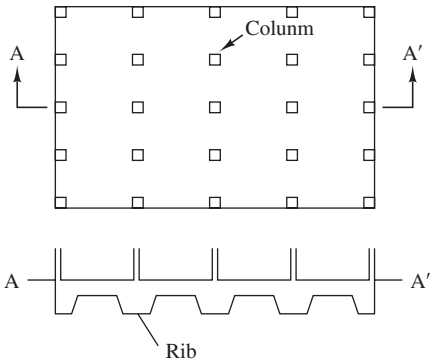

Figure 11.2 A ribbed mat.

flexural loads, and thinner sections between the ribs, as shown in Figure 11.2. This configuration uses less concrete, but is more complex and difficult to build, so a site-specific cost analysis would be necessary to determine which configuration has the lowest construction cost.

Ideally, the entire mat is placed as one monolithic concrete pour, but this technique may not be feasible on large projects. Another option is to introduce construction joints that permit the mat to be cast in sections. These joints are normally designed to transmit shear and moment loads between the sections, thus avoiding the potential for differential settlement between adjacent sections.

11.2 GEOTECHNICAL ULTIMATE LIMIT STATES

Bearing capacity may be evaluated using the techniques described in Chapter 7. Because of their large width, the third term in the bearing capacity formulas (Equations 7.4 to 7.6 or 7.13) is very large, so mat foundations on cohesionless soils do not have bearing capacity problems. However, bearing capacity might be important in cohesive soils, especially if undrained conditions prevail. The Fargo Grain Elevator failure described in Chapter 7 is a notable example of a bearing capacity failure of a mat foundation on a saturated cohesive soil. Lateral loads are resisted by sliding friction along the bottom of the mat plus passive pressure along the edge. They may be analyzed using the techniques described in Section 7.10.

11.3 GEOTECHNICAL SERVICEABILITY LIMIT STATES

Due to the significant width of a typical mat, induced stresses penetrate deeper into the ground, so excessive settlement can be a problem and must be checked. The average settlement of mat foundations may be computed using the techniques for spread footings, as described in Chapter 8.

However, unlike spread footings, we also must consider the flexural distortions of the mat and the resulting differential settlements. The mat must have sufficient flexural rigidity to keep these differential settlements (or angular distortions) within tolerable limits. Methods of doing so are described in Section 11.6.

11.4 COMPENSATED MATS

Mat foundations are often placed well below grade in order to create one or more basements. In addition to the architectural benefits of doing so, this design reduces the induced stresses in the underlying soil, thus improving the factor of safety against bearing capacity failure and reducing the settlement. These benefits are achieved because the weight of the building and the weight of the mat foundation are partially offset by the weight of the excavated soils, as shown in Figure 11.3. This type of mat is called a *compensated mat foundation* (also known as a *floating mat foundation* or a *floating raft foundation*) and can be a very effective design (Golder, 1975).

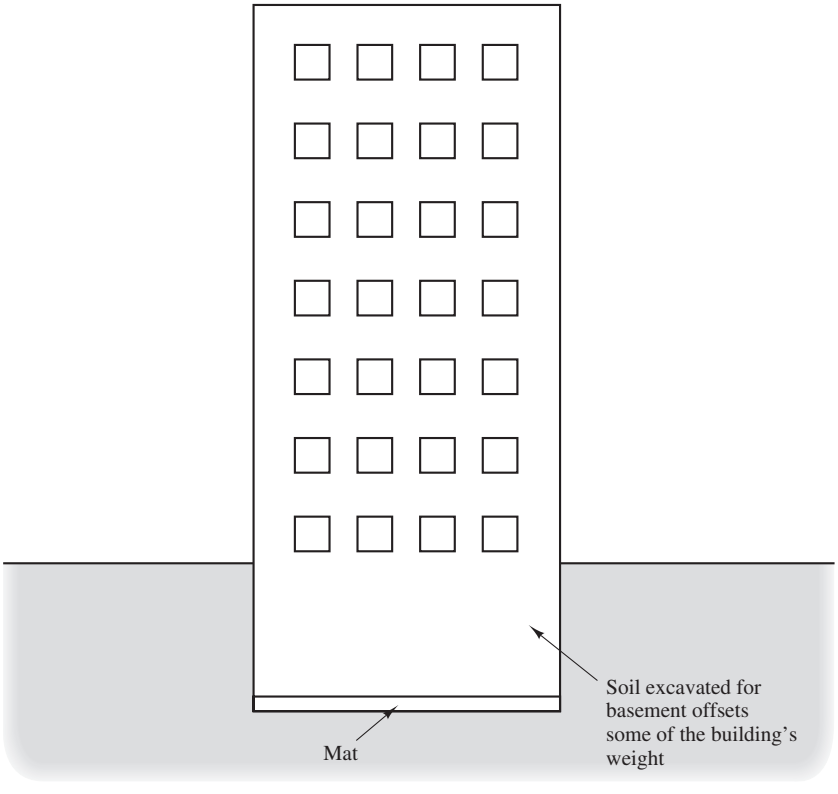

Figure 11.3 A compensated mat foundation.

The earliest documented compensated foundation was for the Albion Mill, which was built on a soft soil in London around 1780. It had about 50 percent flotation (i.e., the excavation reduced the net induced stress, $\Delta\sigma'_z$, by 50 percent) and, according to Farley (1827), "the whole building would have floated upon it, as a ship floats in water." In spite of this pioneering effort, floating foundations did not become common until the early twentieth century. Early North American examples include the Empress Hotel in Victoria, British Columbia, 1912; the Ohio Bell Telephone Company Building in Cleveland, 1925; and the Albany Telephone Building in Albany, New York, 1929.

When evaluating the bearing pressure for compensated mats, use the same techniques as for spread footings (Equation 6.1). When conducting settlement analyses using Equations 8.10, 8.17, and 8.22, the $q - \sigma'_{zD}$ term accounts for the weight of the excavated soil so long as σ'_{zD} is based on the depth from the original ground surface (not the depth from the top of the mat). For example, a compensated mat founded 10 m below the ground surface would have a much larger σ'_{zD}, and a correspondingly lower settlement, than a non-compensated mat founded only 2 m below the ground surface. The improvement in bearing capacity is again implicit in the σ'_{zD} term in Equations 7.3 to 7.6 and 7.13. The resulting increase in q_n increases the factor of safety against a bearing capacity failure.

In theory, we could select a depth of excavation that would produce $q - \sigma'_{zD} = 0$, which would result in zero settlement. However, some of the structural loads, especially the live load, vary over time, as does the groundwater table elevation, so $q - \sigma'_{zD}$ varies with time. In addition, a negative value anytime during the life of the structure would be problematic and potentially unstable. Thus, real designs use a positive value of $q - \sigma'_{zD}$ that reflect these variations and other uncertainties. In addition the stability of the excavation during construction must be considered.

Example 11.1

A 100 ft square, 6 ft thick mat foundation is to be constructed as shown in Figure 11.4a. The sustained downward load acting on this mat will be 25,000 k. Alternatively, a compensated mat could be constructed as shown in Figure 11.4b. The additional substructure (basement

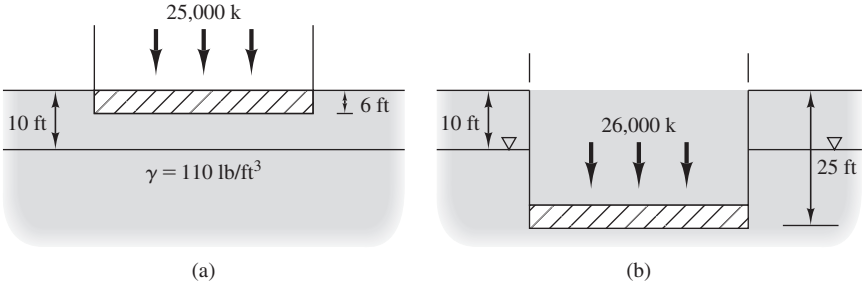

Figure 11.4 Mat for Example 11.1.

walls, etc.) will add an additional 1,000 k of dead load, but the compensated foundation will benefit from the weight of the excavated soils and from buoyancy. Determine the ratio of total settlements for these two alternatives.

Solution

Non-compensated option

$$W_f = (100\,\text{ft})(100\,\text{ft})(6\,\text{ft})(0.150\,\text{k/ft}^2) = 9{,}000\,\text{k}$$

$$q = \frac{P + W_f}{A} - u_D$$

$$= \frac{25{,}000 + 9{,}000}{(100)(100)} - 0$$

$$= 3.40\ \text{k/ft}^2$$

$$\sigma'_{zD} = \gamma D - u$$

$$= (0.110\,\text{k/ft}^3)(6\,\text{ft}) - 0$$

$$= 0.66\,\text{k/ft}^2$$

$$q - \sigma'_{zD} = 3.40 - 0.66$$

$$= 2.74\,\text{k/ft}^2$$

Compensated option

$$q = \frac{P + W_f}{A} - u_D$$

$$= \frac{26{,}000 + 9{,}000}{(100)(100)} - (0.0624)(15)$$

$$= 2.56\ \text{k/ft}^2$$

$$\sigma'_{zD} = \gamma D - u$$

$$= (0.110\,\text{k/ft}^3)(25\text{ft}) - (0.0624\,\text{k/ft}^3)(15\text{ft})$$

$$= 1.81\,\text{k/ft}^2$$

$$q - \sigma'_{zD} = 2.56 - 1.81$$

$$= 0.75\,\text{k/ft}^2$$

Per Equation 8.17, settlement is proportional to $q - \sigma'_{zD}$ so the settlement of the compensated mat will be **0.75/2.74 = 27% of the settlement of a non-compensated mat.**

11.5 RIGID METHODS

The simplest approach to structural design of mats is the *rigid method* (also known as the *conventional method* or the *conventional method of static equilibrium*) (Teng, 1962). This method assumes the mat is much more rigid than the underlying soils, which means any distortions in the mat are too small to significantly impact the distribution of bearing pressure. Therefore, the magnitude and distribution of bearing pressure depends only on the applied loads and the weight of the mat, and is assumed to either be uniform across the bottom of the mat (if the normal load acts through the centroid and no moment load is present) or vary linearly across the mat (if eccentric or moment loads are present) as shown in Figure 11.5. This is the same simplifying assumption used in the analysis of spread footings, as shown in Figure 6.14.

This simple bearing pressure distribution makes it easy to compute the flexural stresses and deflections (differential settlements) in the mat. For analysis purposes, the mat becomes an inverted and simply loaded two-way slab, which means the shears, moments, and deflections may be easily computed using the principles of structural mechanics. The structural engineer can then select the appropriate mat thickness and reinforcement.

Although this type of analysis is appropriate for spread footings, it does not accurately model mat foundations because the width-to-thickness ratio is much greater in mats, and the assumption of rigidity is no longer valid. Portions of a mat beneath columns and bearing walls settle more than the portions with less load, which means the bearing pressure is greater beneath the heavily loaded zones, as shown in Figure 11.6. This redistribution of bearing pressure is most pronounced when the ground is stiff, as shown in Figure 11.7, but is present to some degree in all soils.

Because the rigid method does not consider this redistribution of bearing pressure, it does not produce reliable estimates of the shears, moments, and deformations in the mat. In addition, even if the mat was perfectly rigid, the simplified bearing pressure distributions in Figure 11.5 would not be correct—in reality, the bearing pressure would be greater on the edges and smaller in the center than shown in this figure.

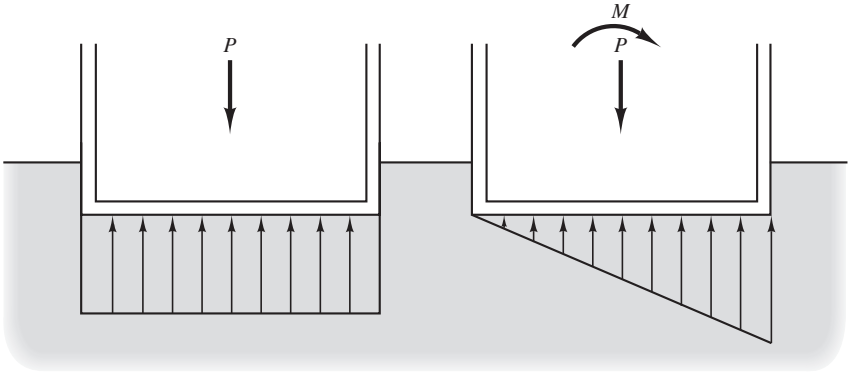

Figure 11.5 Bearing pressure distribution for rigid method.

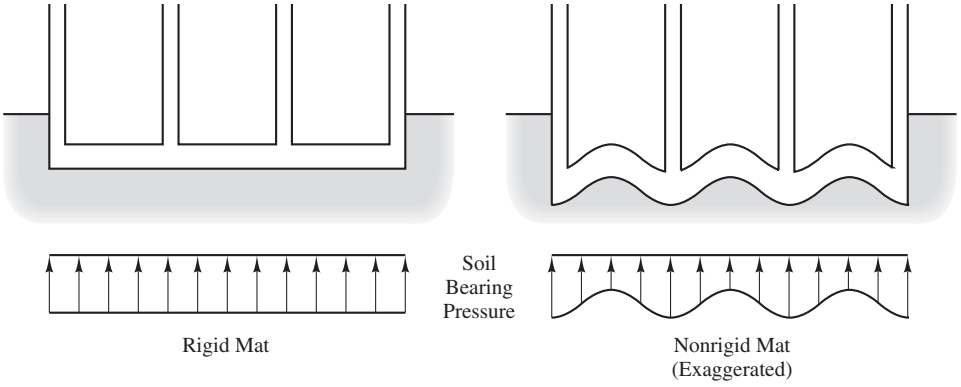

Figure 11.6 The rigid method assumes there are no flexural deflections in the mat, so the distribution of soil bearing pressure is simple to define. However, these deflections are important because they influence the bearing pressure distribution.

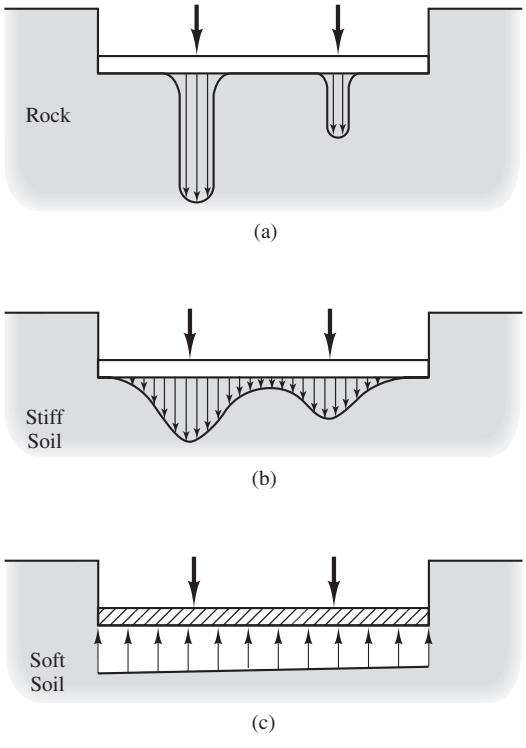

Figure 11.7 Distribution of bearing pressure under a mat foundation: (a) on bedrock or very hard soil; (b) on stiff soil; and (c) on soft soil.

11.6 NONRIGID METHODS

We overcome the inaccuracies of the rigid method by using analyses that consider deformations in the mat and their influence on the bearing pressure distribution. These are called *nonrigid methods*, and produce more accurate values of mat deformations and stresses. Unfortunately, nonrigid analyses also are more difficult to implement because they require consideration of *soil-structure interaction* and because the bearing pressure distribution is not as simple. Nevertheless, because mats are more expensive than footings and because of the inaccuracies of the rigid method, the additional design effort is justified.

Coefficient of Subgrade Reaction

Because nonrigid methods consider the effects of local mat deformations on the distribution of bearing pressure, we must define the relationship between settlement and bearing pressure, as shown in Figure 11.8. This is usually done using the *coefficient of subgrade reaction*, k_s (also known as the *modulus of subgrade reaction*, or the *subgrade modulus*):

$$k_s = \frac{q}{\delta} \tag{11.1}$$

where

k_s = coefficient of subgrade reaction
q = bearing pressure
δ = settlement

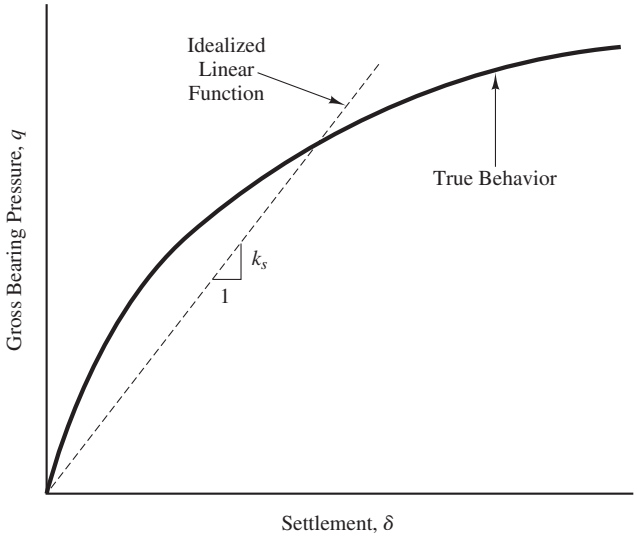

Figure 11.8 The $q - \delta$ relationship is nonlinear, so k_s must represent some "equivalent" linear function.

The coefficient k_s has units of force per length cubed. Although we use the same units to express unit weight, k_s is not the same as the unit weight and they are not numerically equal.

The interaction between the mat and the underlying soil may then be represented as a "bed of springs," each with a stiffness k_s per unit area, as shown in Figure 11.9. Portions of the mat that experience more settlement produce more compression in the "springs," which represents the higher bearing pressure, whereas portions that settle less do not compress the springs as far and thus have less bearing pressure. The integral of these spring pressures across the entire mat area must equal the applied structural loads plus the weight of the mat less any hydrostatic uplift:

$$\sum P + W_f - u_D A = \int q\,dA = \int \delta k_s\,dA \tag{11.2}$$

where

ΣP = sum of structural loads acting on the mat
W_f = weight of the mat
u_D = pore water pressure along base of the mat
A = mat-soil contact area
δ = settlement of the mat

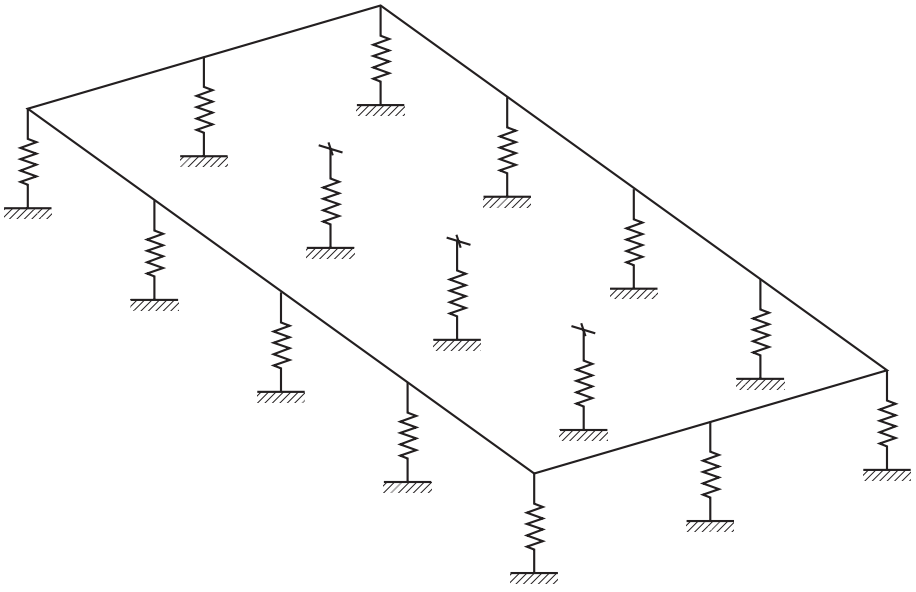

Figure 11.9 The coefficient of subgrade reaction forms the basis for a "bed of springs" analogy to model the soil-structure interaction in mat foundations.

Although it is a convenient parameter, k_s is not solely a soil property, so evaluating its value is not as simple as it might first appear. In addition to varying with the soil type, its magnitude also depends on many other factors, including the following:

- **The width of the loaded area**—A wide mat will settle more than a narrow one with the same q because it mobilizes the soil to a greater depth as shown in Figure 9.4. Therefore, each mat has a different k_s. This is why the k_s value used in pavement design, which is based on the area of a wheel load, will be numerically different from that for a mat foundation at the same site.
- **The shape of the loaded area**—The stresses below long narrow loaded areas are different from those below square loaded areas as shown in Figures 3.5 to 3.7. Therefore, k_s will differ.
- **The depth of the loaded area below the ground surface**—At greater depths, the change in stress in the soil due to q is a smaller percentage of the initial stress, so the settlement is also smaller and k_s is greater.
- **The position on the mat**—To model the soil accurately, k_s must be larger near the edges of the mat and smaller near the center.
- **Time**—Much of the settlement of mats on deep compressible soils will be due to consolidation and thus may occur over a period of several years. Therefore, it may be necessary to consider both short-term and long-term cases.

In addition, there is no single k_s value for a given site, even if we could define these factors because the $q - \delta$ relationship is nonlinear and because there are interactions between the springs.

Engineers have tried various techniques of measuring or computing k_s. Some rely on plate load tests to measure k_s in situ. However, the test results must be adjusted to compensate for the differences in width, shape, and depth of the plate and the mat. Terzaghi (1955) proposed a series of correction factors, but the extrapolation from a small plate to a mat is so great that these factors are not very reliable. Plate load tests also include the dubious assumption that the soils within the shallow zone of influence below the plate are comparable to those in the much deeper zone below the mat. Therefore, plate load tests generally do not provide good estimates of k_s for mat foundation design.

Others have used derived relationships between k_s and the soil's modulus of elasticity, E (Vesić and Saxena, 1970; Scott, 1981). Although these relationships provide useful insights, they too are limited.

The coefficient of subgrade reaction also is used in pavement design, and various empirical correlations with soil properties have been developed. However, the size of the loaded area (i.e., tires) and the corresponding depth of influence is orders of magnitude smaller than mat foundations, so methods of assessing k_s for pavement design are not applicable to mats.

Given these multiple issues, a reasonable way to determine the average k_s for a specific mat founded at a specific depth at a given site is to compute the average bearing pressure and the average settlement of the mat using the techniques described in Chapter 8. Then, use Equation 11.1 to compute the average k_s.

Winkler Method

The "bed of springs" model is used to compute the shears, moments, and deformations in the mat, which then become the basis for developing a structural design. The earliest use of this methodology to represent the interaction between soil and foundations has been attributed to Winkler (1867), so the analytical model is sometimes called a *Winkler foundation* or the *Winkler method*. It also is known as a *beam on elastic foundation* analysis. This method of describing bearing pressure is a type of *soil-structure interaction analysis*.

In its classical form the Winkler method assumes each "spring" is linear and acts independently from the others, and that all of the springs have the same k_s. This representation has the desired effect of increasing the bearing pressure beneath the portions of the mat that have more settlement, and thus is a significant improvement over the rigid method. Closed-form solutions have been developed for various geometries and loading conditions.

However, the Winkler method is still only a coarse representation of the true interaction between mats and soil (Hain and Lee, 1974; Horvath, 1983), and suffers from many problems, including the following:

1. The load-settlement behavior of soil is nonlinear, so the k_s value must represent some equivalent linear function, as shown in Figure 11.8.
2. According to this analysis, a uniformly loaded mat underlain by a perfectly uniform soil, as shown in Figure 11.10, will settle uniformly into the soil (i.e., there will be no differential settlement) and all of the "springs" will be equally compressed. In reality, the settlement at the center of such a mat will be greater than that along the edges, as discussed in Chapter 8. This is because the $\Delta\sigma_z$ values in the soil are greater beneath the center.
3. The "springs" should not act independently. In reality, the bearing pressure induced at one point on the mat influences more than just the nearest spring.

Unfortunately, these errors are often unconservative, leading to underprediction of the flexural stresses in the mat. Thus, further refinements are needed.

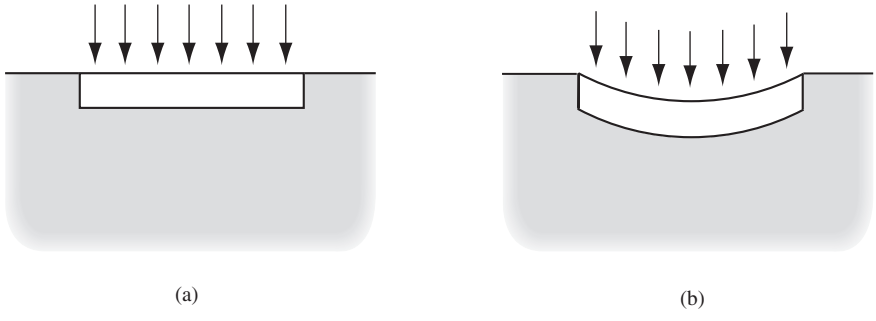

Figure 11.10 Settlement of a uniformly loaded mat on a uniform soil: (a) per Winkler analysis and (b) actual.

Coupled Method

The next step up from a Winkler analysis is to use a *coupled method*, which uses additional springs as shown in Figure 11.11. This way the vertical springs no longer act independently, and the uniformly loaded mat of Figure 11.10 exhibits the desired dish shape. In principle, this approach is more accurate than the Winkler method, but it is not clear how to select the k_s values for the coupling springs.

Pseudo-Coupled Method

The *pseudo-coupled method* (Liao, 1991; Horvath, 1993) is an attempt to overcome the lack of coupling in the Winkler method while avoiding the analytical difficulties of the coupled method. It does so by using springs that act independently, but have different k_s values depending on their location on the mat. To more accurately model the real response of a uniform soil, the springs along the perimeter of the mat should be stiffer than those in the center, thus producing the desired dish-shaped deformation in a uniformly loaded mat. If concentrated loads, such as those from columns, also are present, the resulting mat deformations are automatically superimposed on the dish shape.

Model studies indicate reasonable results are obtained when k_s values along the perimeter of the mat are about twice those in the center (ACI, 1993). We can implement this in a variety of ways, including the following:

1. Determine the average k_s value as described earlier.
2. Divide the mat into three or more concentric zones, as shown in Figure 11.12. The innermost zone should be 30 to 50 percent as wide and 30 to 50 percent as long as the mat.
3. Assign a k_s value to each zone. These values should progressively increase from the center such that the outermost zone has a k_s about twice as large at the innermost zone. Select the areas and k_s values such that the integral of the individual k_s values times their respective areas is equal to the average k_s times the total area. Example 11.2 illustrates this technique.

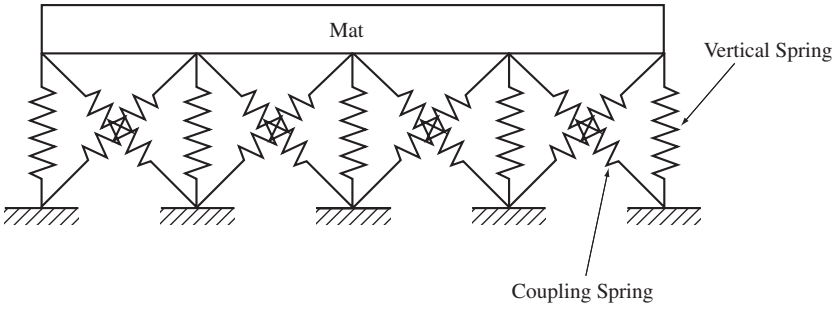

Figure 11.11 Modeling of soil-structure interaction using coupled springs.

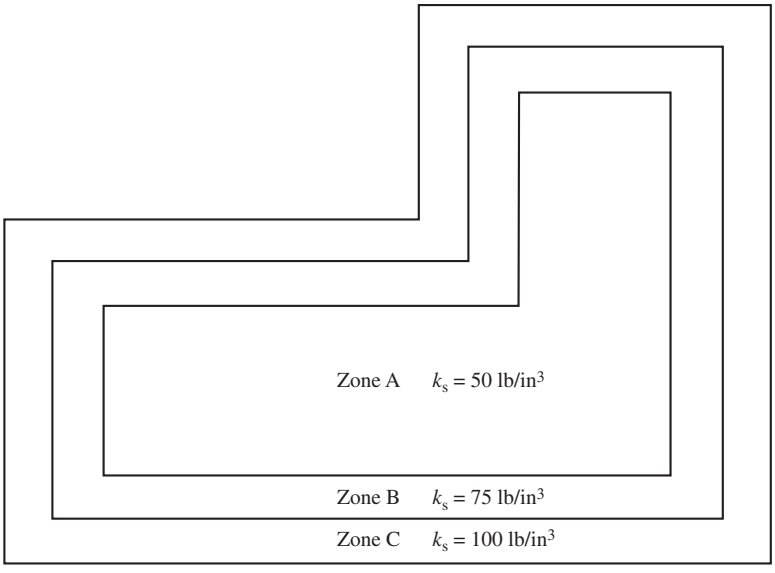

Figure 11.12 A typical mat divided into concentric zones for a psuedo-coupled analysis.

4. Evaluate the shears, moments, and deformations in the mat using the Winkler "bed of springs" analysis, as discussed later in this chapter.
5. Adjust the mat thickness and reinforcement as needed to satisfy strength and serviceability requirements.

ACI (1993) found the pseudo-coupled method produced computed moments 18 to 25 percent higher than those determined from the Winkler method, which is an indication of how unconservative Winker can be.

Most commercial mat design software uses the Winkler method to represent the soil-structure interaction, and these software packages usually can accommodate the pseudo-coupled method. Given the current state of technology and software availability, this is probably the most practical approach to designing most mat foundations.

Example 11.2

A structure is to be supported on a 30 m wide, 50 m long mat foundation. The average bearing pressure is 120 kPa. According to a settlement analysis conducted using the techniques described in Chapter 8, the average settlement, δ, will be 30 mm. Determine the design values of k_s to be used in a pseduo-coupled analysis.

Solution

Compute average k_s using Equation 11.1:

$$(k_s)_{\text{avg}} = \frac{q}{\delta} = \frac{120\,\text{kPa}}{0.030\,\text{m}} = 4{,}000\,\text{kN/m}^3$$

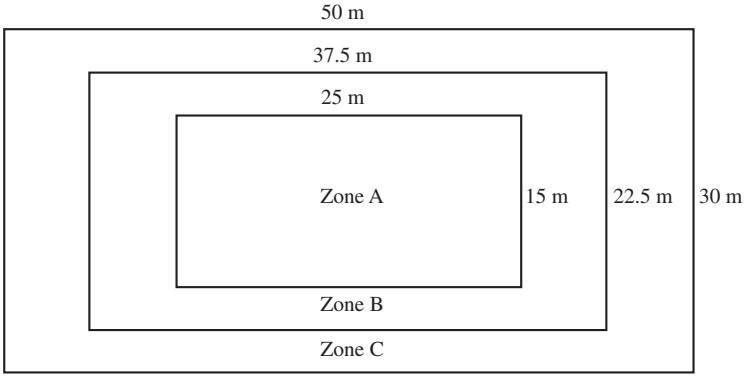

Figure 11.13 Mat foundation for Example 11.2.

Divide the mat into three zones, as shown in Figure 11.13, with $(k_s)_C = 2(k_s)_A$ and $(k_s)_B = 1.5(k_s)_A$

$$A_A = (25\,\text{m})(15\,\text{m}) = 375\,\text{m}^2$$

$$A_B = (37.5\,\text{m})(22.5\,\text{m}) - (25\,\text{m})(15\,\text{m}) = 469\,\text{m}^2$$

$$A_C = (50\,\text{m})(30\,\text{m}) - (37.5\,\text{m})(22.5\,\text{m}) = 656\,\text{m}^2$$

Compute the design k_s values:

$$A_A(k_s)_A + A_B(k_s)_B + A_C(k_s)_C = (A_A + A_B + A_C)(k_s)_{\text{avg}}$$

$$375\,(k_s)_A + 469\,(1.5\,k_s)_A + 656\,(2k_s)_A = 1{,}500\,(k_s)_{\text{avg}}$$

$$(k_s)_A = 0.627\,(k_s)_{\text{avg}}$$

$$(k_s)_A = (0.627)(4{,}000\,\text{kN/m}^3) = \mathbf{2{,}510\,kN/m^3}$$

$$(k_s)_B = (1.5)(0.627)(4{,}000\,\text{kN/m}^3) = \mathbf{3{,}765\,kN/m^3}$$

$$(k_s)_C = (2)(0.627)(4{,}000\,\text{kN/m}^3) = \mathbf{5{,}020\,kN/m^3}$$

Because it is so difficult to develop accurate k_s values, it may be appropriate to conduct a parametric studies to evaluate its effect on the mat design. ACI (1993) suggests varying k_s from one-half the computed value to five or ten times the computed value, and basing the structural design on the worst case condition.

Multiple-Parameter Method

Another way of representing soil-structure interaction is to use the *multiple parameter method* (Horvath, 1993). This method replaces the independently acting linear springs of the Winkler method (a single-parameter model) with springs and other mechanical elements

(a multiple-parameter model). These additional elements define the coupling effects. The multiple-parameter method bypasses the guesswork involved in distributing the k_s values in the psuedo-coupled method because coupling effects are inherently incorporated into the model, and thus should be more accurate.

Finite Element Method

All of the methods discussed thus far attempt to model a three-dimensional soil using a series of one-dimensional springs. They do so in order to make the problem simple enough to perform the structural analysis. An alternative method would be to use a three-dimensional numerical model of both the mat and the soil, or perhaps the mat, soil, and superstructure. This can be accomplished using the *finite element method*.

This analysis method divides the soil into a network of small three-dimensional elements, each with defined engineering properties and each connected to the adjacent elements in a specified way. The structural and gravitational loads are then applied and the elements are stressed and deformed accordingly. This, in principle, should be an accurate representation of the mat, and should facilitate a precise and economical design. This technique should not be confused with structural analysis methods that use two-dimensional finite elements to model the mat and Winkler springs to model the soil.

Three-dimensional finite element analyses require sophisticated software and the ability to use it properly. In addition, defining the correct soil properties can be difficult. Nevertheless, this method is an option for large or heavily loaded mats.

11.7 STRUCTURAL DESIGN

General Methodology

The structural ultimate limit state requirements dictate a minimum required mat thickness and reinforcement. These analyses are based on the configuration and magnitude of the applied structural loads, the distribution of bearing pressure along the bottom of the mat, and other factors. The structural serviceability limit state primarily consists of limiting the flexural deformations in the mat so that the angular distortion does not exceed tolerable limits, such as those described in Section 5.3. In some cases, the mat must be made stiffer, typically by increasing its thickness, in order to satisfy these requirements.

Closed-Form Solutions

When the Winkler method is used (i.e., when all "springs" have the same k_s) and the geometry of the problem can be represented in two-dimensions, it is possible to develop closed-form solutions using the principles of structural mechanics (Scott, 1981; Hetényi, 1974). These solutions produce values of shear, moment, and deflection at all points in the idealized foundation. When the loading is complex, the principle of superposition may be used to divide the problem into multiple simpler problems.

These closed-form solutions were once very popular, because they were the only practical means of solving this problem. However, the advent and widespread availability of powerful computers and the associated software now allows us to use other methods that are more flexible.

Finite Element Method

Most mat foundations are now designed using a two-dimensional finite element analysis. This method divides the mat into hundreds or perhaps thousands of elements, as shown in Figure 11.14. Each element has certain defined dimensions, and a specified stiffness and strength (which may be defined in terms of concrete and steel properties); and is connected to the adjacent elements in a specified way. The mat elements also are connected to the ground through a series of Winkler "springs," which are defined using the coefficient of subgrade reaction. Typically, one spring is located at each corner of each element.

The loads on the mat include the externally applied column loads, applied line loads, applied area loads, and the weight of the mat itself. These loads are resisted by the Winkler springs, which are analytically compressed until obtaining force equilibrium. The resulting stresses and deformation in the mat are then computed. If these results are not acceptable, the mat design is modified accordingly and reanalyzed.

This type of finite element analysis does not consider the stiffness of the superstructure. In other words, it assumes the superstructure is perfectly flexible and offers no resistance to deformations in the mat. This is conservative.

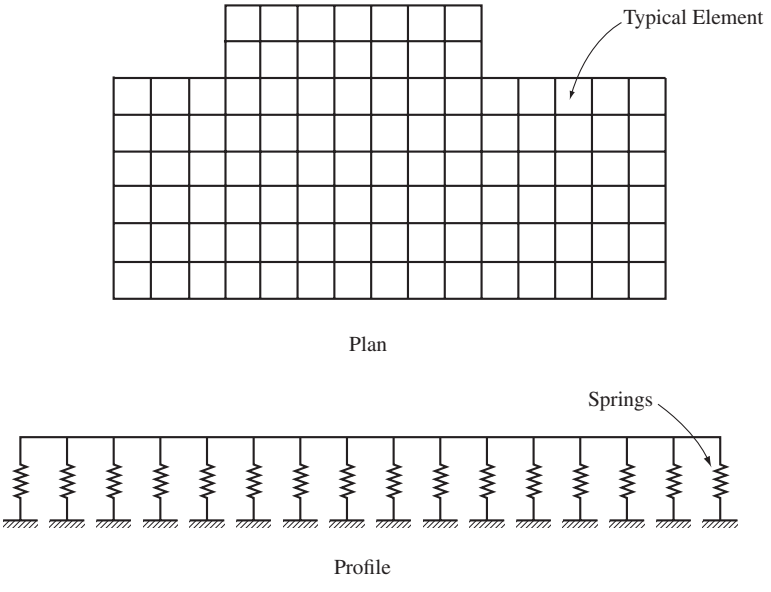

Figure 11.14 Use of the two-dimensional finite element method to analyze mat foundations. The mat is divided into a series of elements which are connected in a specified way. The elements are connected to the ground through a "bed of springs."

SUMMARY

Major Points

1. Mat foundations are essentially large spread footings that usually encompass the entire footprint of a structure. They are often an appropriate choice for structures that are too heavy for spread footings.
2. Bearing capacity is rarely, if ever, a problem for mats founded on cohesionless soils. However, it can be a problem in saturated cohesive soils.
3. Settlement is a concern, and must be checked on all soils.
4. The oldest and simplest method of analyzing mats is the rigid method. It assumes that the mat is much more rigid than the underlying soil, which means the magnitude and distribution of bearing pressure is easy to determine. This means the shears, moment, and deformations in the mat are easily determined. However, this method is not an accurate representation because the assumption of rigidity is not correct.
5. Nonrigid analyses are superior because they consider the flexural deflections in the mat and the corresponding redistribution of the soil bearing pressure.
6. Nonrigid methods must include a definition of soil-structure interaction. This is usually done using a "bed of springs" analogy, with each spring having a linear force-displacement function as defined by the coefficient of subgrade reaction, k_s.
7. The simplest and oldest nonrigid method is the Winkler method, which uses independent springs, all of which have the same k_s. This method is an improvement over rigid analyses, but still does not accurately model soil-structure interaction, primarily because it does not consider coupling effects.
8. k_s depends on both the soil and the mat, and is not a fundamental soil property. Thus, it must be determined on a project-specific and site-specific basis.
9. The coupled method is an extension of the Winkler method that considers coupling between the springs.
10. The pseudo-coupled method uses independent springs, but adjusts the k_s values to implicitly account for coupling effects.
11. Most structural analyses are performed using two-dimensional finite element analyses.

Vocabulary

Beam on elastic foundation
Bed of springs
Coefficient of subgrade reaction
Compensated mat
Coupled method
Finite element method
Mat foundation
Multiple parameter method
Nonrigid method
Pseudo-coupled method
Raft foundation
Rigid method
Soil-structure interaction
Winkler method

QUESTIONS AND PRACTICE PROBLEMS

11.1 Explain the reasoning behind the statements in Section 11.2 that mat foundations on cohesionless soils do not have bearing capacity problems, but that bearing capacity must be checked on cohesive soils.

11.2 How has the development of powerful and inexpensive digital computers affected the analysis and design of mat foundations? What changes do you expect in the future as this trend continues?

11.3 A mat foundation supports forty two columns for a building. These columns are spaced on a uniform grid pattern. How would the moments and differential settlements change if we used a nonrigid analysis with a constant k_s in lieu of a rigid analysis?

11.4 According to a settlement analysis conducted using the techniques described in Chapter 8, a certain mat will have a total settlement of 2.1 in if the average bearing pressure is 5,500 lb/ft^2. Compute the average k_s and express your answer in units of lb/in^3.

11.5 A 25 m diameter cylindrical water storage tank is to be supported on a mat foundation. The weight of the tank and its contents will be 50,000 kN and the weight of the mat will be 12,000 kN. According to a settlement analysis conducted using the techniques described in Chapter 8, the total settlement will be 40 mm. The groundwater table is at a depth of 5 m below the ground surface. Using the pseudo-coupled method, divide the mat into zones and compute k_s for each zone. Then indicate the high-end and low-end values of k_s that should be used in the analysis.

11.6 An office building is to be supported on 150 ft × 300 ft mat foundation. The sum of the column loads plus the weight of the mat will be 90,000 k. According to a settlement analysis conducted using the techniques described in Chapter 8, the total settlement will be 1.8 in. The groundwater table is at a depth of 10 ft below the bottom of the mat. Using the pseudo-coupled method, divide the mat into zones and composite each zone. Then indicate the high-end and low-end valves of k_s that should be used in the analysis.

This page intentionally left blank

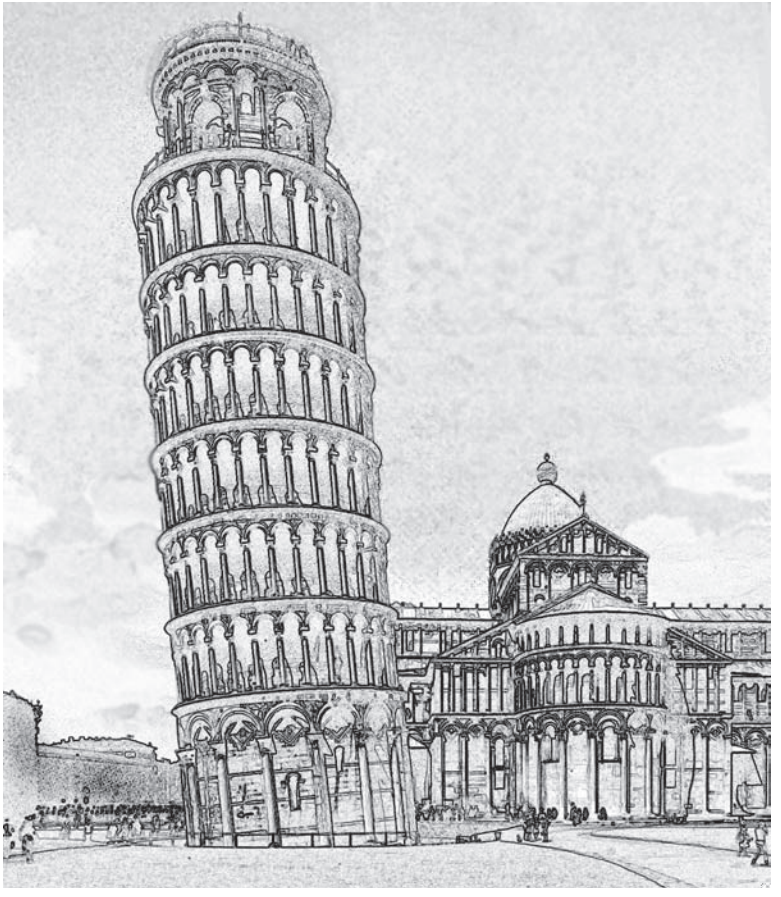

Part C

Deep Foundation Analysis and Design

This page intentionally left blank

12

Deep Foundation Systems and Construction Methods

For these reasons, Caesar determined to cross the Rhine, but a crossing by means of boats seemed to him both too risky and beneath his dignity as a Roman commander. Therefore, although construction of a bridge presented very great difficulties on account of the breadth, depth and swiftness of the stream, he decided that he must either attempt it or give up the idea of a crossing. The method he adopted in building the bridge was as follows. He took a pair of piles a foot and a half thick, slightly pointed at the lower ends and of a length adapted to the varying depth of the river, and fastened them together two feet apart. These he lowered into the river with appropriate tackle, placed them in position at right angles to the bank, and drove them home with pile drivers, not vertically as piles are generally fixed, but obliquely, inclined in the direction of the current. Opposite these, forty feet lower down the river, another pair of piles was planted, similarly fixed together, and inclined in the opposite direction to the current. The two pairs were then joined by a beam two feet wide, whose ends fitted exactly into the spaces between the two piles forming each pair . . . A series of these piles and transverse beams was carried right across the stream and connected by lengths of timber running in the direction of the bridge . . . Ten days after the collection of the timber had begun, the work was completed and the army crossed over.

Engineers prefer to use spread footings wherever possible, because they are simple and inexpensive to build. However, we often encounter situations where spread footings are not the best choice. Examples include:

- The upper soils are so weak and/or the structural loads so high that spread footings would be too large. A good rule-of-thumb for buildings is that spread footings cease to be economical when the total plan area of the footings exceeds about one-quarter of the building footprint area.
- The upper soils are subject to scour or undermining. This would be especially important with foundations for bridges.
- The foundation must penetrate through water, such as those for a pier.
- A large uplift capacity is required (the uplift capacity of a spread footing is limited to its dead weight).
- A large lateral load capacity is required.
- There will be a future excavation adjacent to the foundation, and this excavation would undermine shallow foundations.

In some of these circumstances, a mat foundation may be appropriate, but the most common alternative to spread footings is some type of *deep foundation*.

A deep foundation is one that transmits some, or all, of the applied load to soils well below the ground surface. These foundations typically extend to depths on the order of 10 to 20 m (30–60 ft) below the ground surface, but they can be much longer, perhaps extending as deep as 45 m (150 ft). Even greater lengths have been used in some offshore structures, such as oil drilling platforms. Since soils usually improve with depth, and this method mobilizes a larger volume of soil, deep foundations are often able to carry very large loads.

12.1 DEEP FOUNDATION TYPES AND TERMINOLOGY

Engineers and contractors have developed many types of deep foundation systems using many different installation methods. Each system is best suited to certain loading and soil conditions. The installation method used for a given deep foundation affects its behavior and, therefore, the way it is analyzed and designed. For this reason, deep foundations are generally categorized by their installation methods. Unfortunately, people use many different names to identify the different foundation systems. Different individuals often use the same terms to mean different things and different terms to mean the same thing. This confusion reigns in both verbal and written communications, and is often the source of misunderstanding, especially to the newcomer. This book uses terms that appear to be most commonly used and understood.

Deep foundation systems can broadly be categorized into three groups: (1) *piles*, (2) *caissons*, and (3) *pile-supported and pile-enhanced mats* as shown in Figure 1.1. Piles are, by far, the most common type of deep foundation and are discussed in more detail in

Chapters 13 through 23. Caissons are briefly discussed in Sections 12.5 and 12.6; but they are no longer widely used, so this discussion is limited. Pile-supported and pile-enhanced mats are covered in Chapter 24.

Piles are long, slender structural members that penetrate deep into the ground. Many different pile technologies are available, each of which is best suited for certain conditions. The three most common types are:

- *Driven piles* consist of prefabricated structural members that are pounded into the ground.
- *Drilled shafts* are a type of cast-in-place pile constructed by drilling a hole, placing the reinforcing steel into the hole, then filling with concrete.
- *Auger piles* are another type of cast-in-place pile that is built using a hollow stem auger. Grout is pumped through the auger while it is being withdrawn from the hole, then the reinforcing steel is placed into the fluid grout. There are two types, auger cast in place (ACIP) piles and drilled displacement (DD) piles.

A variety of other pile technologies also are available. Although not as widely used, each of these specialty methods has its own unique advantages which are useful in certain situations. These include:

- *Jacked piles*, which are similar to driven piles except the pile is pushed rather than pounded into the ground.
- *Pressure injected footings* (also known as *Franki piles*) are constructed by pounding wet concrete into a cased hole, which forms an expanded base and compacts the adjacent soils.
- *Micropiles* resemble very small diameter drilled shafts.
- *Helical piles* consist of steel screws that are torqued into the ground.
- *Anchors* is a broad term that refers to deep foundations that are primarily intended to resist tensile loads.

This list is not comprehensive, and other types and variations also are available, some of which are proprietary.

Piles also may be categorized by how much soil is displaced during construction. *Low displacement piles* push aside very little soil, either because the pile itself is very thin or because some or all of the soil is excavated during placement. *High displacement piles* have large cross-sectional areas and push aside a large volume of soil as they are installed. This difference has a significant impact on the load capacity, and thus is an important part of the design process. Intermediate types, known as *medium displacement piles*, also are available. Figure 12.1 illustrates the classification of pile systems into two categories and several sub-categories based on installation method and displacement characteristics.

The various parts of deep foundations also have different names, which is another source of confusion (Fellenius, 1996). The upper end has many names, including “top,” “butt,” and “head,” while those for the lower end include “tip,” “toe,” “base,” “end,” “point,”

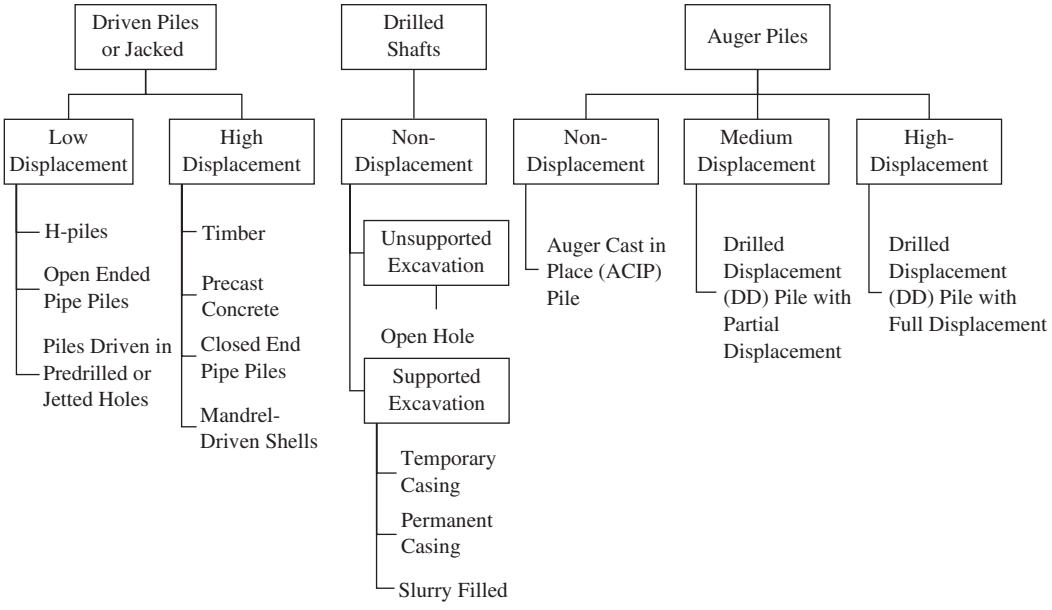

Figure 12.1 Classification of pile systems (based on Prezzi and Basu, 2005; and U.S. Army, 1998).

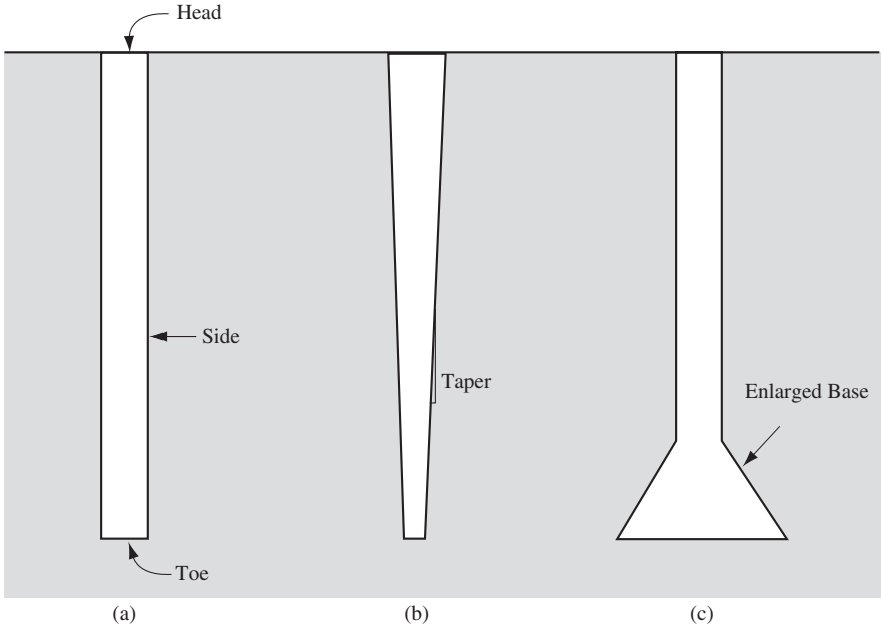

Figure 12.2 Parts of a deep foundation: (a) straight foundations; (b) tapered foundations; and (c) foundations with an enlarged base.

and "bottom." Many of these terms can easily be misunderstood. We will use the terms *head* and *toe*, as shown in Figure 12.2a, because they appear to have the least potential for confusion. These terms also are easy to remember by simply comparing the pile to a human body.

The exterior surface along the side of deep foundations is usually called the "side" or the "skin," either of which is generally acceptable. We will use the term *side*.

Most deep foundations are straight, which means the cross section is constant with depth, but some are *tapered*, as shown in Figure 12.2b. Others include an *enlarged base*, as shown in Figure 12.2c. The enlarged base is sometimes called a *bell* and the system a *belled pile*. The foundation *axis* is a line through the centroid of the foundation and is parallel to its longest dimension.

12.2 DRIVEN PILES

The oldest type of deep foundation is a *driven pile*, which consists of a long, slender, prefabricated structural member driven or vibrated into the ground. Engineers use driven piles both on land and in the sea to support many kinds of structures. Driven piles are made from a variety of materials and in different diameters and lengths according to the needs of each project.

History

The history of driven piles goes back at least as far as the stone age. The alpine lake dwellers in Europe built their houses on timber piles 4,000 to 5,000 years ago. Alexander the Great drove piles in the city of Tyre in 332 B.C., and the Romans used them extensively. Bridge builders in China during the Han Dynasty (200 BCE–200 CE) also used piles. These early builders drove their piles into the ground using weights hoisted and dropped by hand (Chellis, 1961). By the Middle Ages, builders used pulleys and leverage to raise heavier weights.

Construction methods improved more quickly during the Industrial Revolution, especially when steam power became available. Larger and more powerful equipment was built, thus improving pile driving capabilities. The first steam driven pile hammer was used in Devonport England in 1845 (Parkhill, 2001). These improvements continued throughout the nineteenth and twentieth centuries. Diesel hammers were invented in 1940 and first appeared in North America in 1952; the first vibratory hammers were used in 1961 (Parkhill, 2001).

Pile materials also have improved. The early piles were always made of wood, and thus were limited in length and capacity. Fortunately, the advent of steel and reinforced concrete in the 1890s enabled the construction of larger and stronger piles, and better driving equipment made it possible to install them. Without these improved foundations, many of today's major structures would not have been possible.

Today, driven pile foundations can support very high loads, even in hostile environments. Perhaps the most impressive are those for offshore oil drilling platforms. These foundations consist of driven piles that are as large as 3 m (10 ft) in diameter and must resist large lateral loads due to wind, wave, and earthquake forces.

Materials

Most piles are now made from wood, concrete, or steel. Each material has its advantages and disadvantages and is best suited for certain applications. We must consider many factors when selecting a pile type, including:

- **The applied loads**—Some piles, such as timber, are best suited for low to medium loads, whereas others, such as steel, may be most cost-effective for heavy loads.
- **The required diameter**—Most pile types are available only in certain diameters.
- **The required length**—Highway shipping regulations and practical pile driver heights generally limit the length of pile segments to about 18 m (60 ft). Therefore, longer piles must consist of multiple segments spliced together during driving. Some types of piles are easily spliced, whereas others are not.
- **The local availability of each pile type**—Some pile types may be abundant in certain geographic areas, whereas others may be scarce. This can significantly affect the cost of each type.
- **The durability of the pile material in a specific environment**—Certain environments may cause piles to deteriorate, as discussed in Section 5.3.
- **The anticipated driving conditions**—Some piles tolerate hard driving, while others are more likely to be damaged during driving.

Timber Piles

Timber piles have been used for thousands of years and continue to be a good choice for many applications. They are made from the trunks of straight trees and resemble telephone poles, as shown in Figure 12.3. Because trees are naturally tapered, these piles are driven upside down, so the largest diameter is at the head, as shown in Figure 12.4. Timber piles are considered large displacement piles because they displace their entire volume of soil as they are driven.

Many different species of trees have been used to make timber piles. Today, most new timber piles driven in North America are either Southern pine or Douglas fir because these trees are tall and straight, and are abundant enough that the material cost are low. They typically have head diameters in the range of 150 to 450 mm (6–18 in) and lengths between 6 and 20 m (20–60 ft), but greater lengths are sometimes available, up to 24 m (80 ft) in Southern pine and 38 m (125 ft) in Douglas fir. The branches and bark must be removed, and it is sometimes necessary to trim the pile slightly to give it a uniform taper. ASTM D25 gives detailed specifications.

Although it is possible to splice lengths of wood piling together to form longer piles, this is a slow and time consuming process that makes the piles much more expensive. Therefore, if longer piles are necessary, engineers almost always use some other material.

Most timber piles are designed to carry downward axial loads of 100 to 400 kN (20–100 k). Their primary advantage is low construction cost, especially when suitable

Figure 12.3 Groups of timber piles. Those in the foreground have been cut to the final head elevation (National Timber Piling Council).

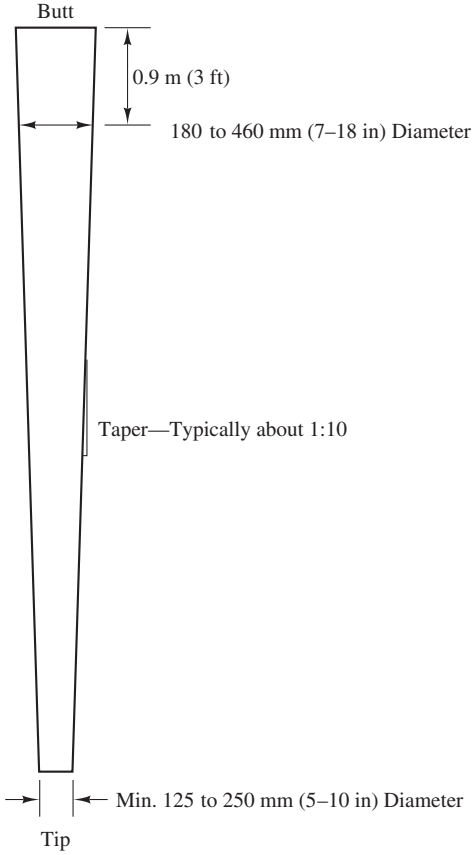

Figure 12.4 Typical timber pile.

trees are available nearby. They are often used on waterfront structures because of their resistance to impact loads, such as those from ships.

When continually submerged, timber piles can have a very long life. For example, when the Campanile in Venice fell in 1902, its timber piles, which were driven in 900 AD, were found to be in good condition and were reused (Chellis, 1962). However, when placed above the groundwater table, or in cyclic wetting conditions, timber piles are susceptible to decay, as discussed in Section 5.3. Therefore, they are nearly always treated with a preservative before installation.

When used in marine environments, timber piles are subject to attack from various marine organisms as well as abrasion from vessels and floating debris. In cooler waters (in North America, generally north of 40 degrees latitude), piles with heavy creosote treatment will usually remain serviceable for decades (ASCE, 1984). However, in warmer waters, biological attack is more of a problem and other chemical treatments are usually necessary. Even when treated, their usable life in such environments is often limited to about ten years.

Timber piles are also susceptible to damage during driving. Repeated hard hammer blows can cause *splitting* and *brooming* at the head and damage to the toe. It is often possible to control these problems by:

- Using lightweight hammers with appropriate cushions between the hammer and the pile
- Using steel bands near the head (usually necessary only with Douglas fir)
- Using a steel shoe on the toe, as shown in Figure 12.5
- Predrilling (see discussion later in this section)

Figure 12.5 Use of steel toe points to reduce damage to timber piles during driving (Associated Pile and Fitting Corp.).

Nevertheless, even these measures are not always sufficient to prevent damage. Therefore, timber piles are best suited for light driving conditions, such as friction piles in loose sands and soft to medium clays. They are usually not suitable for dense or hard soils or as end-bearing piles.

Steel Piles

By the 1890s, steel had become widely available and many structures were being built of this new material. The use of steel piling was a natural development and in 1899 the first steel I-beam sections were driven as piles. The same year 30 cm (12 in) diameter steel pipe piles were first driven. These pipe piles were driven with a pneumatic hammer, the insides cleaned out and backfilled with concrete. H-section piles with a thicker web than standard I-beams were introduced by Bethlehem steel in 1908. By 1930, the use of both H- and I-section steel piles was widespread (Parkhill, 2001). Today, steel piles remain very common, especially on projects that require high-capacity foundations.

Because of their high strength and ductility, steel piles can be driven through hard soils and carry large loads. They also have the highest tensile strength of any major pile type, so they are especially attractive for applications with large applied tensile loads.

Steel piles are easy to splice, so they are often a good choice when the required length is greater than about 18 m (60 ft). The contractor simply drives the first section, then welds on the next one, and continues driving. Special steel splicers can make this operation faster and more efficient. Hunt (1987) reported the case of a spliced steel pile driven to the extraordinary depth of 210 m (700 ft). They are also easy to cut, which can be important with end-bearing piles driven to irregular rock surfaces. Steel piles have the disadvantages of being expensive to purchase and noisy to drive. In certain environments, they may be subject to excessive corrosion, as discussed in Section 5.3.

H-Piles

Special rolled steel sections, known as HP sections, or simply *H-piles*, are made specifically to be used as piles. These sections are similar to WF (wide flange) shapes as shown in Figures 12.6 and 12.7, but the WF section is optimized for flexural loads, while the HP section is optimized for axial loads. The primary difference is that the web is thinner than the flanges in WF members, while they have equal thicknesses in H-piles. Dimensions and other relevant information for standard steel H-piles are listed in Table 21.1. H-piles are generally not carried in suppliers' inventories and are usually manufactured on demand for each job. These piles are typically 15 to 50 m (50–150 ft) long and carry working axial loads of 350 to 1,800 kN (80–400 k).

H-piles are small displacement piles because they displace a relatively small volume of soil as they are driven. This, combined with their high strength, make them an excellent choice for hard driving conditions. They are often driven to bedrock and used as end-bearing piles. If the pile will encounter hard driving, it may be necessary to use a hardened steel point to protect its toe, as shown in Figure 12.8.

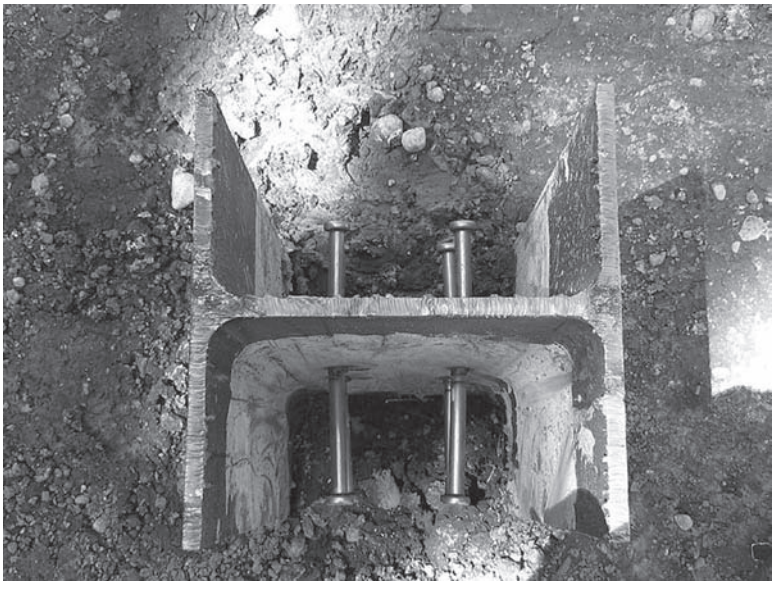

Figure 12.6 A steel H-pile after being driven in the ground. The nail-like items welded on the pile web are shear studs which help to secure the pile in the concrete pile cap that will be cast around the pile. Note that the web and flange of the H-pile are the same thickness, unlike a WF section whose flange is thicker than its web. *Source:* King County Dept of Transportation.

Pipe Piles

Steel pipe sections are also commonly used as piles, as shown in Figure 12.9. They are typically 200 to 1,000 mm (8–36 in) in diameter, 30 to 50 m (100–150 ft) long, and carry axial loads of 450 to 7,000 kN (100–1,500 k). A wide variety of diameters and wall thicknesses are available, and some engineers have even reclaimed old steel pipelines and used them as piles. Special sizes also can be manufactured as needed and pipe piles as large as

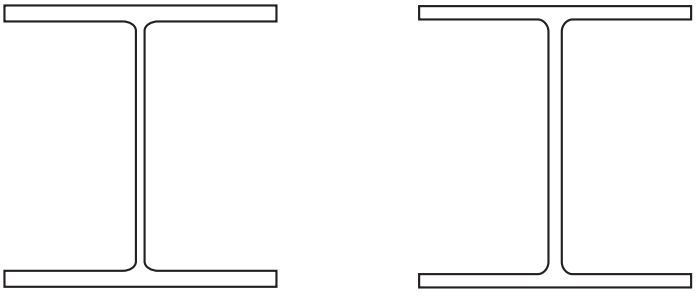

Figure 12.7 Comparison between typical wide flange (WF) and H-pile (HP) sections. Note the thinner web in the WF section.

Figure 12.8 Hardened steel point attached to the toe of a steel H-pile to protect it during hard driving (Associated Pile and Fitting Corp.).

Figure 12.9 A 406 mm (16 in) diameter steel pipe pile.

3 m (10 ft) in diameter with 75 mm (3 in) wall thickness have been used in offshore projects. Table 21.2 lists some of the more common sizes. Pipe piles have a larger moment of inertia than H-piles, so they may be a better choice if large lateral loads are present.

Pipe piles may be driven with a *closed-end* or with an *open-end*. A closed-end pipe has a flat steel plate or a conical steel point welded to the toe. These are large displacement piles because they displace a large volume of soil. This increases the load capacity, but makes them more difficult to drive. Conversely, an open-end pipe has nothing blocking the toe and soil enters the pipe as it is being driven. Depending upon how the pile is driven and the soil conditions, the lower portion of open-end pipe piles may or may not become jammed with soil, thus forming a *soil plug*. Therefore, an open-ended pipe pile may acts as either a large or small displacement pile depending upon whether or not the toe becomes plugged. Open-ended piles are often used in offshore construction. Closed-end pipe piles can be inspected after driving because the inside is visible from the ground surface. Thus, it is possible to check for integrity and alignment. Special steel pipe piles are also available, such as the *monotube pile*, which is tapered and has longitudinal flutes.

Driven Concrete Piles

Driven concrete piles are precast reinforced concrete members driven into the ground. This category does not include techniques that involve casting the concrete in the ground. Cast-in-place concrete piles are covered later in this chapter.

Figure 12.10 shows steel molds used to manufacture precast prestressed concrete piles. This is usually done at special manufacturing facilities, then shipped to the construction site. Figure 12.11 shows completed piles ready to be driven.

Concrete piles usually have a square or octagonal cross section, as shown in Figure 12.12, although other shapes have been used (ACI, 1980). They are typically 250 to 750 mm (10–30 in) in diameter, 12 to 37 m (40–120 ft) long, and carry working axial loads of 450 to 4,450 kN (100–1,000 k). A few nearshore projects have been built using much larger concrete piles.

Although conventionally reinforced concrete piles were once common, and are still in use in some places, prestressed piles have almost completely replaced them, at least in North America. These improved designs have much more flexural strength and are therefore less susceptible to damage during handling and driving. Prestressing is usually a better choice than post-tensioning because it allows piles to be cut, if necessary, without losing the prestress force.

Several methods are available to splice concrete piles, as shown in Figure 12.13. Although these techniques are generally more expensive than those for splicing steel piles, they can be cost-effective in some situations. Cutting machines are available for use when the pile cannot be driven to the expected depth. However, cutting concrete piles is more problematic than cutting steel piles because it is then necessary to drill and epoxy new steel dowels into the pile. Concrete piles also have more spiral steel near the ends, so cutting this steel can compromise the structural integrity of the pile. Therefore, driven concrete piles are best suited for use as friction piles that do not meet *refusal* during driving (refusal means that the pile cannot be driven any further, so it becomes necessary to

Figure 12.10 These steel forms are used to manufacture prestressed concrete piles. The prestressing cables, visible in the foreground, are in place and have been subjected to a tensile force. The spiral reinforcement also is in place. The next step will be to fill the forms with high quality concrete, cover them with tarp, and steam-cure them overnight. The next day, the tension on the cables will be released, then the piles will be removed from the forms and allowed to cure.

Figure 12.11 These 356 mm (14 in) square prestressed concrete piles are stacked in a contractor's yard and are ready to be driven. The bars emerging from the end of these piles are conventional rebars that have been embedded in the end of the pile (they are not the reinforcing tendons). These rebars are used to structurally connect the pile with the pile cap.

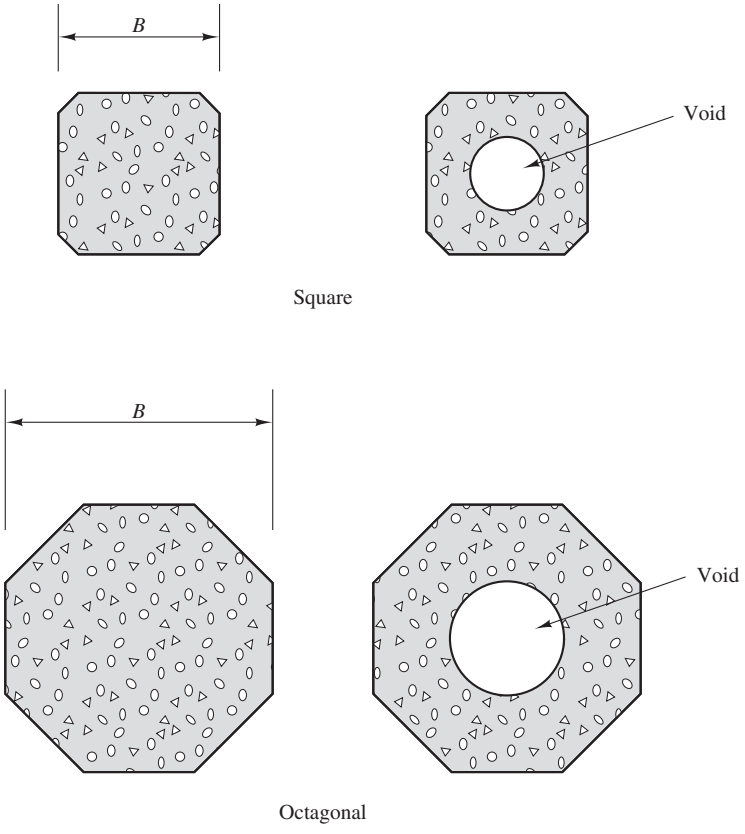

Figure 12.12 Cross section of typical concrete piles.

cut off the upper portion) or as toe bearing piles where the required length is uniform and predictable.

Concrete piles do not tolerate hard driving conditions as well as steel, and are more likely to be damaged during handling or driving. Nevertheless, concrete piles are very popular because they are generally less expensive than steel piles, yet still have a large load capacity.

Concrete-Filled Steel Pipe Piles

Sometimes steel pipe piles are filled with concrete after driving. These will have more uplift capacity due to their greater weight, enhanced shear and moment capacity because of the strength of the concrete, and a longer useful life in corrosive environments. However, there is little, if any, usable increase in the geotechnical downward load capacity because a pipe with sufficient wall thickness to withstand the driving stresses will probably have enough capacity to resist the applied downward loads. The net downward capacity may even be less because of the additional weight of the concrete in the pile.

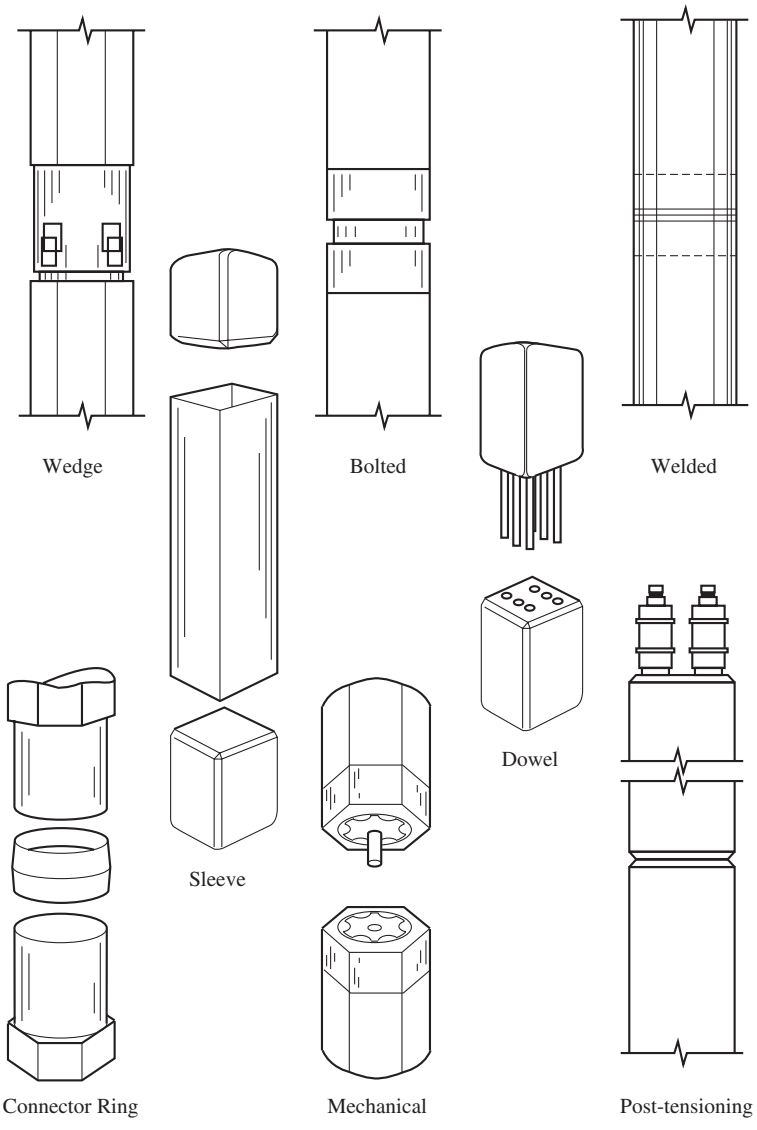

Figure 12.13 Typical splices for concrete piles (Precast/Prestressed Concrete Institute).

Plastic Composite Piles

Plastics are generally too weak and ductile to be used along as a material for load bearing piles. However, composite piles that combine plastics with either steel or glass fibers have found a place in certain pile applications. A plastic-steel composite pile consists of a steel pipe core or steel rods surrounded by a plastic cover as shown in Figure 12.14a. Plastic-glass composite piles have glass fiber rods embedded in a plastic matrix as shown

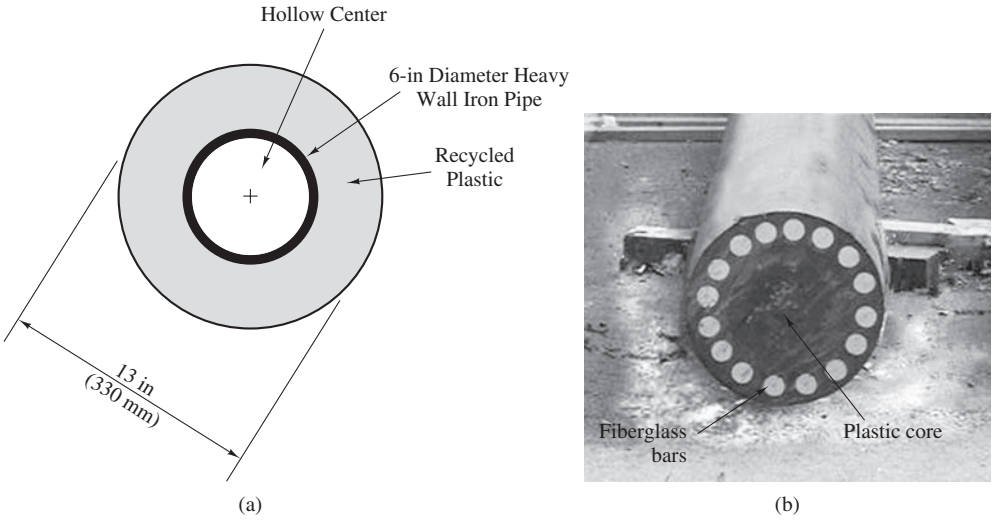

Figure 12.14 Cross section of typical composite piles: (a) plastic-steel composite and (b) plastic-fiberglass composite (photo (b) courtesy of Magued Iskander).

in Figure 12.14b. The plastic cover or matrix is typically made of recycled material, thus making this design attractive from a resource conservation perspective (Heinz, 1993 and Juran et al., 2006).

Plastic composite piles have been used successfully in waterfront applications (see Figure 12.15), where their resistance to marine borers, decay, and abrasion along with their higher strength make them superior to timber piles. Although the material cost for plastic-steel composites can be high, their longer life, low maintenance costs, and resource conservation benefits make them an attractive alternative to timber piles. See Juran et al. (2006) and Pando et al. (2006) for more information about properties and applications of plastic composite piles.

Pile Driving Methods and Equipment

The construction of deep foundations is much more complex than that of shallow foundations, and the construction methods have a much greater impact on their performance. Therefore, design engineers must understand how contractors build pile foundations.

Pile Driving Rigs

Piles are installed using a *pile driving rig* (or simply the *pile driver*). Its function is to raise and temporarily support the pile while it is being driven and to support the pile hammer. Early rigs were relatively crude, but modern pile drivers, such as the ones in Figures 12.16 and 12.17, are much more powerful and flexible. Vertical tracks, called *leads*, guide the

Figure 12.15 Installation of plastic-steel composite piles in a waterfront application (photo courtesy of Lancaster Composites, Inc.).

hammer as the pile descends into the ground. Hydraulic or cable-operated actuators allow the operator to move the leads into the desired alignment.

Hammers

The *pile hammer* is the device that provides the impacts necessary to drive the pile. Repeated blows are necessary, so the hammer must be capable of cycling quickly. It also must deliver sufficient energy to advance the pile, while not being powerful enough to break it. The selection of a proper hammer is one of the keys to efficient pile driving.

Drop Hammers

The original type of pile hammer was the *drop hammer*. They consisted of a weight that was hoisted up, and then dropped directly onto the pile. These hammers became much larger and heavier during the late nineteenth century as described by Powell (1884):

> The usual method of driving piles is by a succession of blows given by a heavy block of wood or iron, called a ram, monkey or hammer, which is raised by a rope or chain, passed over a pulley fixed at the top of an upright frame, and allowed to fall freely on the head of the pile to be driven. The construction of a pile-driving machine is very simple. The guide frame is about the same in all of them: the important parts are the two upright timbers, which guide the ram in

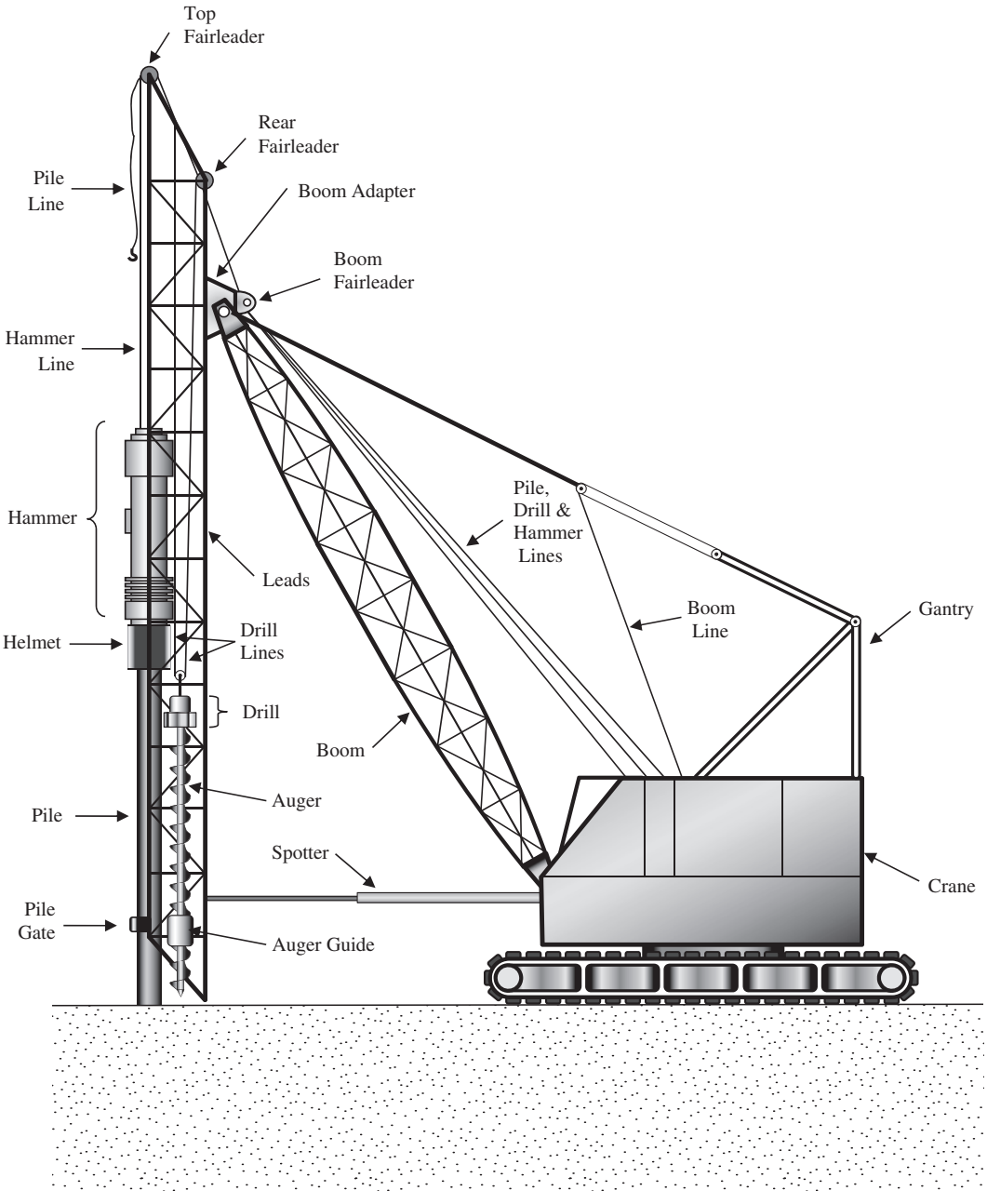

Figure 12.16 Major components of a typical fixed lead pile driving rig.

Figure 12.17 A modern pile driver. The hammer is at the bottom of the leads, and the predrilling auger is attached to the side of the leads. The forklift on the left is used to transport the piles to the rig.

> its descent. The base of the framing is generally planked over and loaded with stone, iron, or ballast of some kind, to balance the weight of the ram. The ram is usually of cast-iron, with projecting tongue to fit the grooves of frame. Contractors have all sizes of frames, and of different construction, to use with hand or steam power, from ten feet to sixty feet in height. The height most in use is one of twenty feet, with about a twelve hundred pound ram. In some places the old hand-power method has to be used to avoid the danger of producing settling in adjoining buildings from jarring.

These hammers could deliver only about three to twelve blows per minute.

Drop hammers have since been replaced by more modern designs. They are now rarely used for foundation piles, but they are sometimes used to install sheet piles. Drop hammers are effective for installing foundation piles in the very soft clays of Scandinavia, and thus are still used there (Broms, 1981). Drop hammers also form part of the *pressure-injected footing* process described below.

Steam, Pneumatic, and Hydraulic Hammers

New types of hammers began to appear in the mid-1800s. These consisted of a self-contained unit with a ram, striker plate, and raising mechanism, as shown in Figure 12.18. These hammers had slightly larger weights, but much shorter strokes than the drop hammers. For example, the "Nasmyth steam pile-drivers" of the 1880s had 1,400 to 2,300 kg (3,000–5,000 lb) rams with a stroke of about 900 mm (3 ft). Although these hammers delivered less energy per blow, they were more efficient because they cycled much more rapidly (about 60 blows/min for the Nasmyth hammer).

The early self-contained hammers used steam to raise the ram. This steam was produced by an on-site boiler. *Steam hammers* are still in use. Later, *pneumatic hammers* (powered by compressed air) and *hydraulic hammers* (powered by high-pressure hydraulic fluid) were introduced. Hydraulic hammers have become very popular and have many advantages, including the ability to control the hammer stroke, minimal air pollution, and high capacity. As a result, in many areas these have become the hammer of choice.

All three types can be built as a *single-acting hammer* or as a *double-acting hammer*. Single-acting hammers raise the ram by applying pressure to a piston, as shown in Figure 12.18a. When the ram reaches the desired height, typically about 900 mm (3 ft), an exhaust valve opens and the hammer drops by gravity and impacts the striker plate. When compared to other types, this design is characterized by a low impact velocity and heavy ram weights. These hammers have fixed strokes, which means each drop of the hammer delivers the same amount of energy to the pile.

A double-acting hammer, shown in Figure 12.18b, uses pressure for both the upward and downward strokes, thus delivering a greater impact than would be possible by gravity alone. The impact energy depends to some degree upon the applied pressure and therefore can be controlled by the operator. These hammers usually have shorter strokes and cycle more rapidly than single-acting hammers. Practical design limitations prevent these hammers from delivering as much energy as comparable single-acting hammers, so they are principally used for driving sheet piles.

A *differential hammer*, shown in Figure 12.18c, is similar to a double-acting hammer in that it uses air, steam, or hydraulic pressure to raise and lower the ram, but it differs in that it has two pistons with differing cross-sectional areas. This allows differential hammers to use the heavy rams of single-acting hammers and operate at the high speed and with the controllability of double-acting hammers.

Steam and pneumatic differential hammers cycle slowly under soft driving conditions and faster as the penetration resistance increases. The reverse is true of hydraulic hammers.

Diesel Hammers

A diesel hammer, shown in Figure 12.19, is similar to a diesel internal combustion engine. The ram falls from a high position and compresses the air in the cylinder below. At a certain point in the stroke, diesel fuel is injected (in either atomized or liquid form) and the air-fuel mixture is further compressed until the ram impacts the striker plate. Combustion occurs

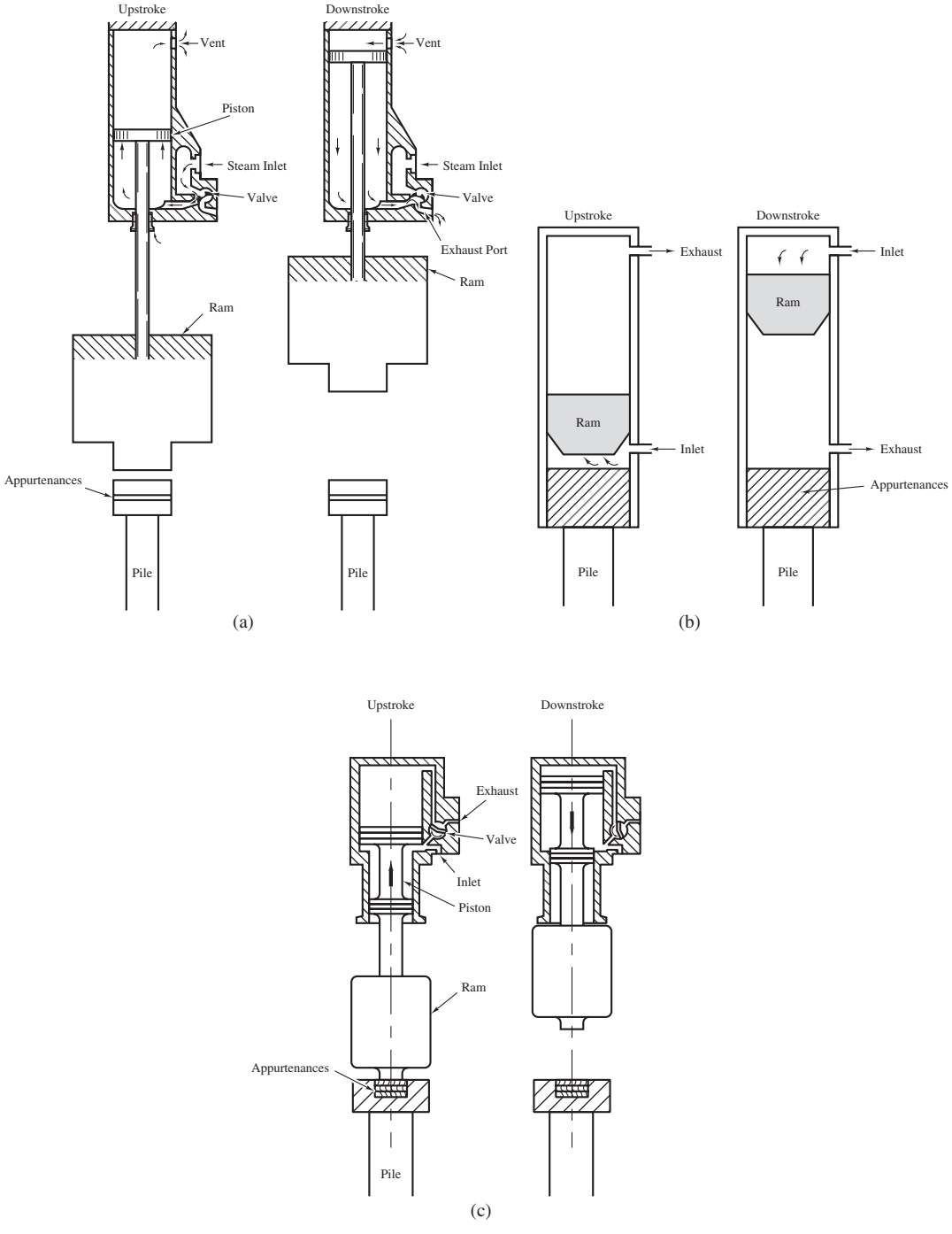

Figure 12.18 Self-contained pile driving hammers: (a) single-acting; (b) double-acting; and (c) differential.

(a) (b)

Figure 12.19 Open-top diesel pile hammers. (a) This hammer is at the bottom of the leads. The auger to the left is for predrilling. (b) This hammer is in the process of driving a concrete pile. The ram is near the top of its stroke, and is visible at the top of the hammer (photo (b) courtesy of GRL Engineers, Inc.).

about this time, forcing the ram up and allowing another cycle to begin. The cycles of a typical diesel hammer are illustrated in Figure 12.20

Diesel hammers are either of the open-top (single acting) or closed-top (double acting) type. The closed-top hammer includes a bounce chamber above the ram that causes the hammer to operate with shorter strokes and at higher speeds than an open-top hammer with an equivalent energy output.

The operator and field engineer can monitor the energy output of a diesel hammer by noting the rise of the ram (in an open-top hammer) or the bounce chamber pressure (in a closed-top hammer). Diesel hammers develop their maximum energy under hard driving conditions and may be difficult to operate under soft conditions, which sometimes

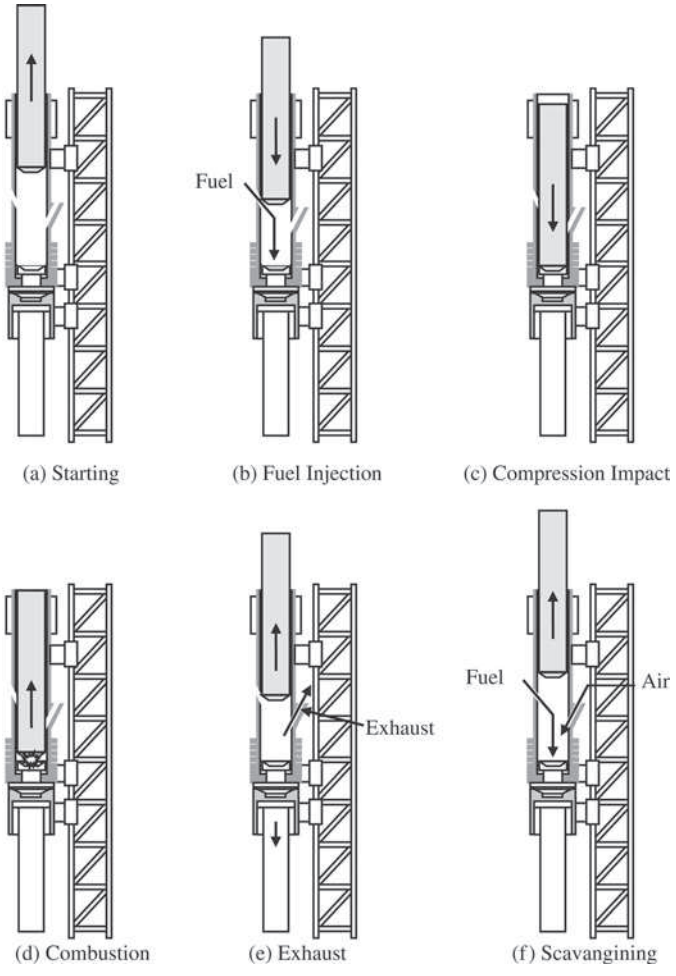

Figure 12.20 Cycles of a diesel hammer: (a) to start the ram is lifted up, (b) as the hammer is drop fuel is injected in the cylinder, (c) the falling ram compresses the fuel-air mixture until, (d) combustion occurs, (e) the combustion energy forces the pile down and the ram up exhausting the spent fuel, (f) air enters the cylinder as the ram rises, fuel is injected and the cycle repeats itself.

occur early in the driving sequence, because of a lack of proper combustion or insufficient hammer rebound. Once firm driving conditions are encountered, open-top hammers typically deliver forty to fifty-five blows per minute, while closed-top hammers typically deliver about ninety blows per minute. Although diesel hammers have been popular for many years, the exhaust is a source of air pollution, so air quality regulations restrict their use in some areas.

Appurtenances

A pile driving system also includes other components that are placed between the pile hammer and the pile, as shown in Figure 12.21. The ram hits a steel *striker plate* or *anvil*. It then transmits the impact energy through a *hammer cushion* (also known as a *capblock*) to a *drive head* (also known as a *drive cap*, *bonnet*, *hood*, or *helmet*). The drive head is placed directly on steel piles. Concrete piles require *pile cushion* between the helmet and the pile.

The cushions soften the sharp blow from the hammer by spreading it out over a longer time. Ideally, they should do this without absorbing too much energy. Hammer cushions do this to protect the ram, and are usually made of special synthetic materials.

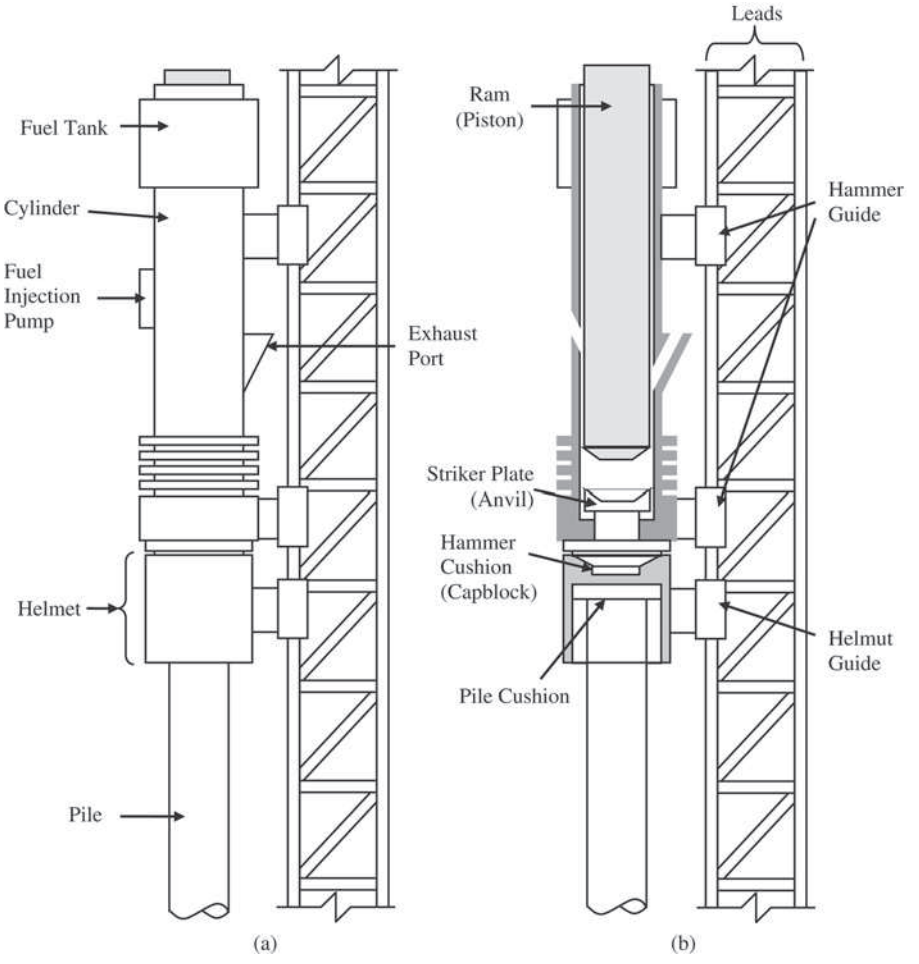

Figure 12.21 Details of a diesel hammer: (a) the various parts of the hammer system attached to the leads, (b) a cross section through the hammer showing all the appurtenances between the ram and the pile.

Pile cushions, which are generally used only with concrete piles, are intended to protect the pile. They are usually made of plywood or hardwood. The optimal selection of the pile hammer and appurtenances is part of the key to efficient pile driving. Wave equation analyses, discussed in Chapter 19, can be very useful in this regard.

Vibratory Hammers

A *vibratory hammer* (Warrington, 1992) is not a hammer in the same sense as those discussed earlier. It uses rotating eccentric weights to create vertical vibrations, as shown in Figure 12.22. When combined with a static weight, these vibrations force the pile into the ground. The operating frequency of vibratory hammers may be as high as 150 Hz and can be adjusted to resonate with the natural frequency of the pile. These hammers are manufactured in many sizes from small hammers designed to drive sheet piles to very large hammers used to drive large pipe piles. Perhaps the largest diameter pile ever driven was a 22 m (72 ft) diameter pile driven as part of a cofferdam in the South China Sea as part of the Hong Kong-Zhuhai-Macau Bridge. This pile was driven by a group of eight large vibratory hammers (Boniface, 2012).

Vibratory hammers are most effective when used with piles being driven into sandy soils. They operate more quickly and with less vibration and noise than conventional

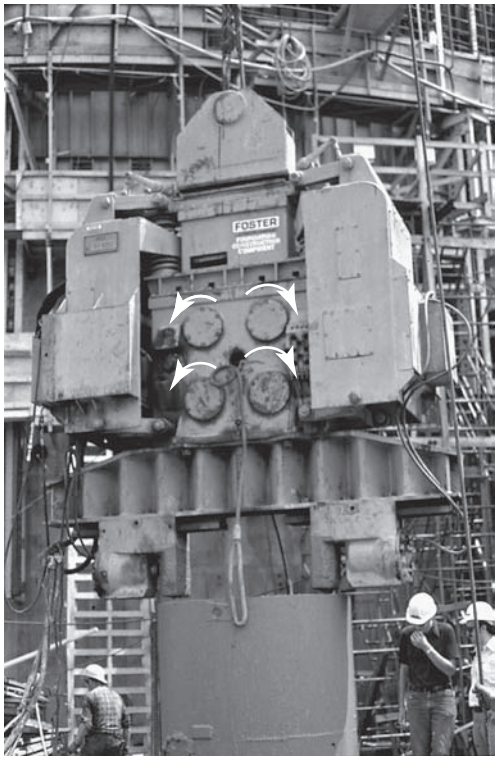

Figure 12.22 A vibratory pile hammer. Arrows show locations and directions of counter-rotating weights used to create vibrations. This hammer is extracting a steel pipe used as a casing for a drilled shaft foundation (ADSC: The International Association of Foundation Drilling).

impact hammers. However, they are ineffective in clays or soils containing obstructions such as boulders.

Predrilling, Jetting, and Spudding

All piles are subject to damage during driving, especially in very hard ground or ground that contains boulders. Figure 12.23 shows an example of piles damaged during driving. One way to reduce the potential for damage and increase the contractor's production rate is to use predrilling, jetting, or spudding.

Predrilling means drilling a vertical hole, and then driving the pile into this hole. The diameter of the predrill hole must be less than that of the pile to assure firm contact with the soil. Predrilling also reduces the heave and lateral soil movement sometimes associated with pile driving. The predrill hole does not necessarily need to extend for the entire length of the pile.

To use *jetting*, the contractor pumps high-pressure water through a pipe to a nozzle located at the pile tip. This loosens the soil in front of the pile, thus allowing it to advance with very few or no hammer blows. Jetting is useful in sandy and gravelly soils, but is ineffective in clays. It is most often used to quickly penetrate through sandy layers to reach deeper bearing strata.

Figure 12.23 These steel pipe piles were used to support a temporary pier while the permanent pier (on the left) was under construction. Afterward, they were extracted. The pile on the left experienced damage during driving, probably as a result of hitting an underground obstruction.

Spudding consists of driving hard metal points into the ground, and then removing them and driving the pile into the resulting hole. This method is much less common than predrilling or jetting, and is most often used to punch through thin layers of hard rock.

All three methods reduce the axial load capacity of the finished pile, and thus must be used only when necessary for constructability.

Pile Arrangements and Geometries

Usually each member of the superstructure that requires a foundation (e.g., each column in a building) is supported on a group of three or more piles. *Pile groups* are used instead of single piles because:

- A single pile usually does not have enough capacity.
- Piles are *spotted* or located with a low degree of precision, and can easily be 150 mm (6 in) or more from the desired location, as shown in Figure 12.24. If a column for a building, which is located with a much greater degree of precision, were to be

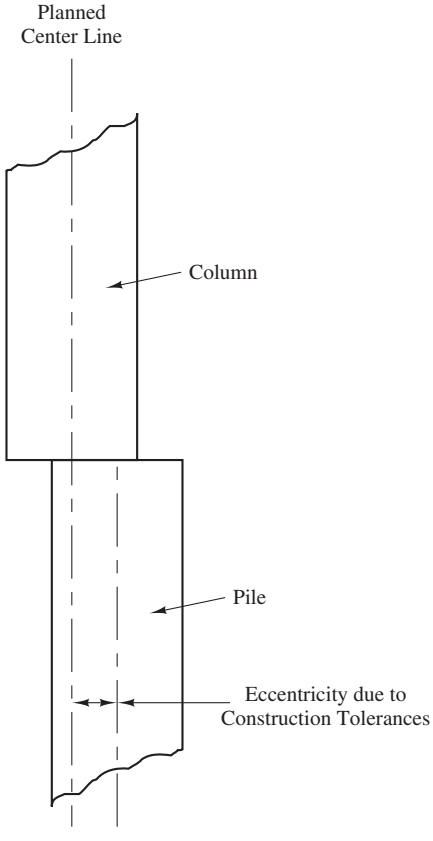

Figure 12.24 Unanticipated eccentricities between columns and single piles caused by construction tolerances.

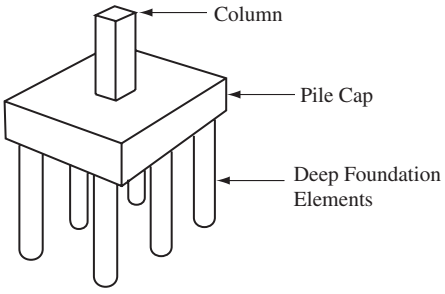

Figure 12.25 A pile cap is a structural member that connects to the piles in a group to a column or other element of the superstructure.

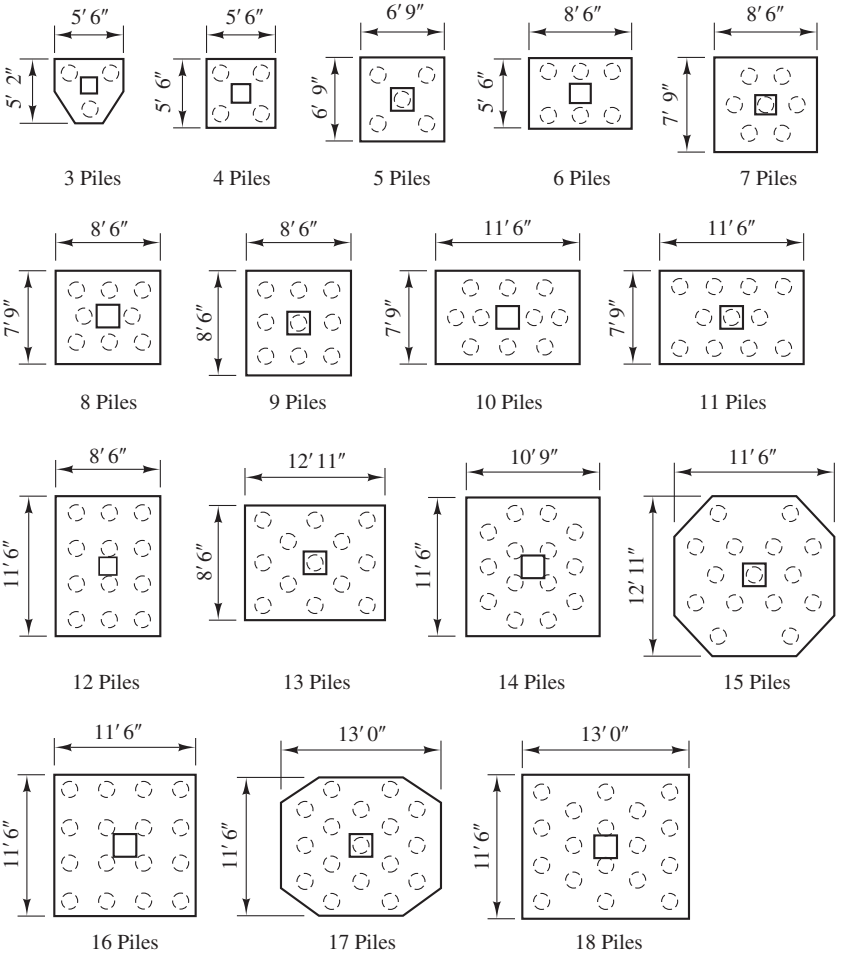

Figure 12.26 Typical configurations of pile caps (adapted from CRSI, 1992).

supported on a single pile, the centerlines would rarely coincide and the resulting eccentricity would generate unwanted moments and deflections in both the pile and the column. However, if the column is supported on three or more piles, any such eccentricities are much less significant.

- Multiple piles provide redundancy, and thus can continue to support the structure even if one pile is defective.
- The zones of lateral soil compression overlap each other, thus increasing the lateral earth pressures acting on the piles. Thus, the side friction capacity is greater than for a single isolated pile.

Each group of piles is connected with a *pile cap*, as shown in Figure 12.25, which is a reinforced concrete member that is similar to a spread footing. Its functions are to distribute the structural loads to the piles, and to tie the piles together so they act as a unit. The design of pile caps varies with the number of piles and the structural loads. Figure 12.26 shows typical pile cap layouts. Sometimes the individual pile caps are connected with *grade beams*, which are structural beams embedded in the ground. During construction, grade beams resemble continuous footings, but their purpose is significantly different.

12.3 DRILLED SHAFTS

Drilled shafts are one type of cast-in-place pile. The construction process is completely different from that used to build driven piles. The construction process consists of drilling a cylindrical hole in the ground, placing a prefabricated reinforcing steel cage into the hole, then filling with concrete. This is completely different from the processes used to build driven pile foundations. Engineers and contractors also use other terms to describe this type of deep foundation, including:

- Pier
- Drilled pier
- Bored pile
- Cast-in-place pile
- Caisson
- Drilled caisson
- Cast-in-drilled-hole (CIDH) pile

Some of these terms also are used to describe other kinds of deep foundations, which can be confusing. For example, *bored pile* can refer to either a drilled shaft or an auger pile. *Caisson* is most commonly used to describe a completely different type of foundation, as discussed in Section 12.5. Thus, it is important to be careful with terminology in order to avoid misunderstandings. By their nature, drilled shafts are always non-displacement piles since the soil is removed before the pile is placed. This has important ramifications when evaluating load capacity, as discussed in Chapter 16.

History

The quality of soils usually improves with depth, so it often is helpful to excavate through weak surface soils to support structures on deeper bearing materials. Even the ancient Greeks understood the value of removing poor quality soils (Kerisel, 1987). During the late nineteenth and early twentieth centuries, builders began to modify the traditional techniques of reaching good bearing soils. Many of the greatest advances occurred in the large cities of the Great Lakes region. As taller and heavier buildings began to appear, engineers realized that traditional spread footing foundations would no longer suffice. Following many years of problems with excessive settlements, they began to use foundation systems consisting of a single hand-dug shaft below each column.

General William Sooy-Smith was one of the pioneers in this new technology. His *Chicago Well Method*, developed in 1892, called for the contractor to hand-excavate a cylindrical hole about 1 m (3 ft) in diameter and 0.5 to 2 m (2–6 ft) deep, as shown in Figure 12.27. To prevent caving, they lined its wall with vertical wooden boards held in place with steel rings, and then repeated the process until reaching the bearing stratum. Finally, they enlarged the base of the excavation to form a bell and filled it with concrete up to the ground surface.

Hand excavation methods were slow and tedious, so the advent of machine-dug shafts was a natural improvement. The early equipment was similar to that used to drill oil wells, so much of the early development occurred in oil-producing areas, especially Texas

Figure 12.27 Shaft excavations for Chicago City Hall made in 1909 using the Chicago Well Method. The wooden shoring for each shaft is clearly visible. These shafts were dug by hand down to the desired foundation depth (Library of Congress, Prints and Photographs Division, Historic American Buildings Survey, HABS ILL,16-CHIG,94-36).

and California. A few examples of horse- and engine-driven drills appeared between 1900 and 1930, but they had very limited capabilities. By the late 1920s, manufacturers were building practical truck-mounted engine-driven drill rigs, such as the one in Figure 12.28, thus bringing drilled shaft construction into its maturity.

During the next thirty-five years, manufacturers and contractors developed larger and more powerful equipment along with a variety of cutting tools. They also borrowed construction techniques from the oil industry, such as casing and drilling mud, to deal with difficult soils. By the 1960s, drilled shafts had become a strong competitor to driven piles.

Today, drilled shafts support structures ranging from one-story wood frame buildings to the largest skyscrapers. For example, the Willis Tower (formerly known as the Sears Tower) in Chicago is supported on 203 drilled shafts, some of them 30 m (100 ft) deep.

The advantages of drilled shaft foundations include:

- The costs of mobilizing and demobilizing a drill rig are often much less than those for a pile driver. This is especially important on small projects, where they represent a larger portion of the total costs.
- The construction process generates less noise and vibration, both of which are especially important when working near existing buildings.
- Engineers can observe and classify the soils excavated during drilling and compare them with the anticipated soil conditions.
- The length of the shaft can be easily changed during construction to compensate for unanticipated soil conditions.

Figure 12.28 Early truck-mounted drill rig and crew, circa 1925 (ADSC: The International Association of Foundation Drilling).

- The foundation can penetrate through soils with cobbles or boulders, especially when the shaft diameter is large. It is also possible to penetrate many types of bedrock.
- It is usually possible to support each column with one large shaft instead of several piles, thus eliminating the need for a pile cap.

The disadvantages include:

- Successful construction is highly dependent on the contractor's skills, much more so than with spread footings or even driven piles. Poor workmanship can produce weak foundations that may not be able to support the design load, and most of these defects are not visible. This is especially important because a single drilled shaft does not have the benefit of redundancy that is present in a group of driven piles.
- Driving piles pushes the soil aside, thus increasing the lateral stresses in the soil and generating more side friction capacity. However, shaft construction removes soil from the ground, so the lateral stresses remain constant or decrease. Thus, a shaft may have less side friction capacity than a pile of comparable dimensions. However, this effect is at least partially offset by rougher contact surface between the concrete and the soil and the correspondingly higher coefficient of friction.
- Pile driving densifies the soil beneath the tip, whereas shaft construction does not. Therefore, the unit end-bearing capacity in shafts may be lower.
- Full-scale load tests are very expensive, so the only practical way to predict the axial load capacity is to use semiempirical methods based on soil properties. We typically have no independent check. However, the Osterberg load test device and high-strain dynamic impact tests, discussed in Chapters 14 and 19, have overcome this problem.

Modern Drilled Shaft Construction

Contractors use different equipment and techniques depending on the requirements of each project (Greer and Gardner, 1986). The design engineer must be familiar with these methods to know when and where drilled shafts are appropriate. The construction method also influences the shaft's load capacity, so the engineer and contractor must cooperate to assure compatibility between the design and construction methods.

Drilling Rigs

Most drilled shafts are 500 to 1,200 mm (18–48 in) in diameter and 6 to 24 m (20–80 ft) deep. A typical modern truck-mounted drilling rig, such as the one shown in Figure 12.29, would typically be used to drill these shafts. Specialized rigs, such as those in Figures 12.30 and 12.31, are available for difficult or unusual projects. Rigs capable of drilling shafts as large as 3 m (10 ft) in diameter and up to 60 m (200 ft) deep are widely available, and rigs with even greater capacity have been built.

Figure 12.29 Typical drilling rig for constructing drilled shafts. This rig is able to drill shafts up to 1,800 mm (72 in) in diameter and 24 m (80 ft) deep (ADSC: The International Association of Foundation Drilling).

Drilling Tools

Contractors have different drilling tools, each suited to a particular subsurface condition or drilling technique. The helix-shaped *flight auger*, shown in Figure 12.32, is the most common. The drill rig rotates the auger into the ground until it fills with soil. Then, it draws the auger out and spins it around to remove the cuttings, as shown in Figure 12.33. This process repeats until the shaft reaches the desired depth.

Conventional flight augers are effective in most soils and soft rocks. However, when encountering difficult conditions, the contractor has the option of switching to special augers or other tools. For example, augers with hardened teeth and pilot *stingers* are effective in hardpan or moderately hard rock. Spiral-shaped rooting tools help loosen cobbles and boulders, thus allowing the hole to advance under conditions that might cause refusal in a driven pile. Some of these special tools are shown in Figures 12.34 and 12.35.

Other drilling tools include:

- *Bucket augers* that collect the cuttings in a cylindrical bucket that is raised out of the hole and emptied. They are especially useful in running sands.
- *Belling buckets* that have extendable arms to enlarge the bottom of the shaft. These enlargements are called *bells* or *underreams*.

Figure 12.30 Small truck-mounted drilling rig capable of working on a hillside (ADSC: The International Association of Foundation Drilling).

- *Core barrels* that cut a circular slot, creating a removable cylindrical core. They are especially useful in hard rock.
- Multiroller *percussion bits* to cut through hard rock.
- *Cleanout buckets* to remove the final cuttings from a hole and produce a clean bottom suitable for end bearing.

Drilling Techniques in Competent Soils

The construction process for drilled shafts differs depending on the type of soil encountered and whether or not the soil can maintain an open hole without support.

The construction procedure in competent soils, known as the *dry method*, is generally as follows:

1. Using a *drill rig*, excavate a cylindrical hole (the *shaft*) into the ground to the required depth, as shown in Figure 12.36a.
2. Fill the lower portion of the shaft with concrete as shown in Figure 12.36b.

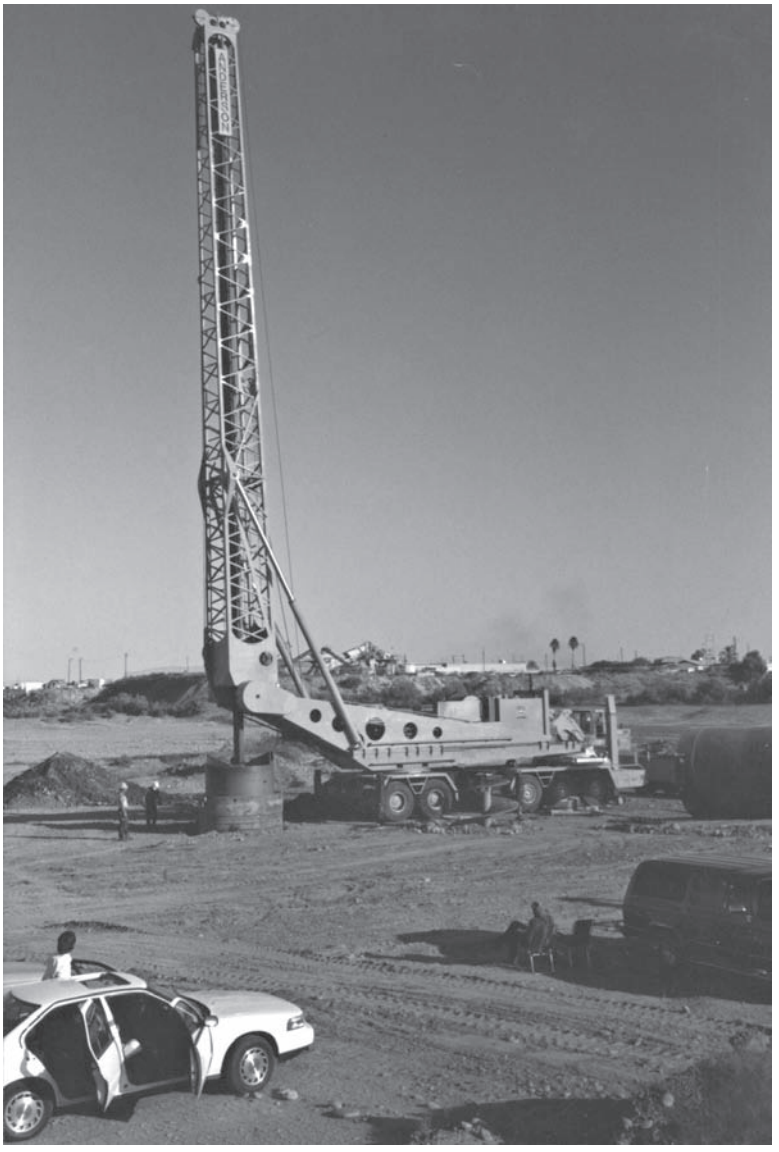

Figure 12.31 Extremely large drill rig capable of drilling 8 m (26 ft) diameter holes to depths of 60 m (200 ft) (courtesy of Hayward Baker Inc.).

Figure 12.32 Typical flight auger (ADSC: The International Association of Foundation Drilling).

Figure 12.33 Spinning the auger to remove the cuttings (ADSC: The International Association of Foundation Drilling).

3. Place a prefabricated reinforcing steel cage inside the shaft as shown in Figure 12.36c.
4. Fill the shaft with concrete as shown in Figure 12.36d.

These holes usually advance quickly using conventional flight augers and remain open without any special support. After checking the open hole for cleanliness and alignment, it is a simple matter to insert the steel reinforcing cage and place concrete in

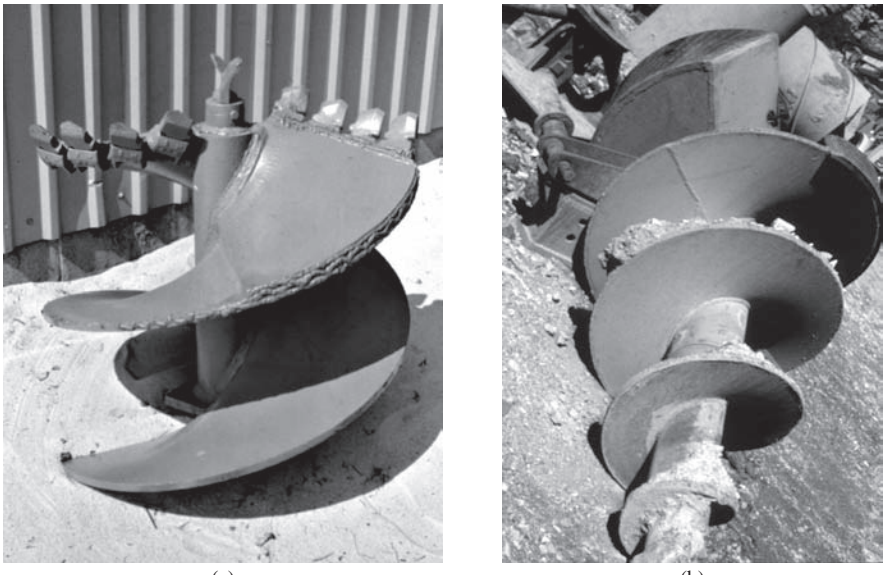

(a) (b)

Figure 12.34 Special flight augers for difficult subsurface conditions: (a) auger with hardened teeth and a stinger; (b) spiral-shaped rooting auger (ADSC: The International Association of Foundation Drilling).

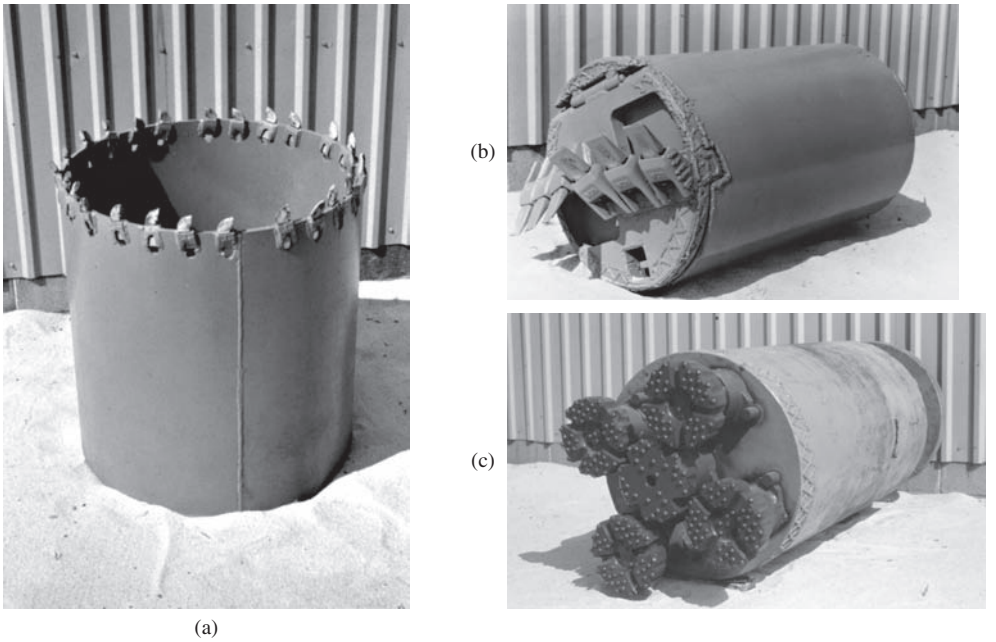

(a) (b) (c)

Figure 12.35 Special drilling tools: (a) core barrel; (b) bucket auger; and (c) multiroller percussion bits (ADSC: The International Association of Foundation Drilling).

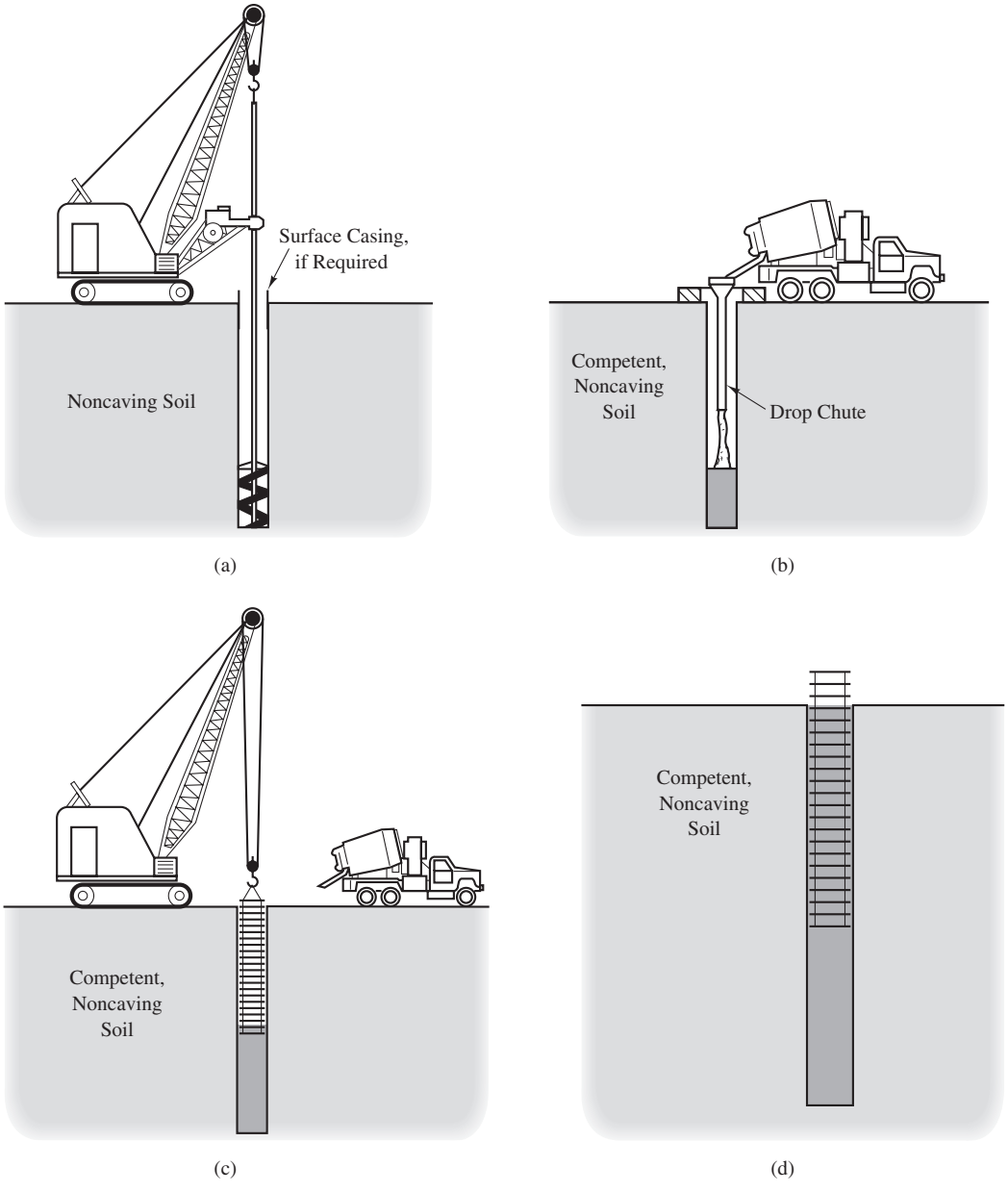

Figure 12.36 Drilled shaft construction in competent soils using the dry method: (a) drilling the shaft; (b) starting to place the concrete; (c) placing the reinforcing steel cage; and (d) finishing the concrete placement (after Reese and O'Neill, 1988).

from the top. Some contractors use a tremie or a concrete pump to deliver the concrete. Open-hole shafts in firm soils are very common because of their simplicity and economy of construction and their good reliability. It also is possible to excavate stiff soils below the groundwater table using the open-hole method. Usually, the contractor simply pumps the water out as the hole advances and places the concrete in the dewatered shaft.

Drilling Techniques in Caving or Squeezing Soils

A hole is said to be *caving* when the sides collapse before or during concrete placement. This is especially likely in clean sands below the groundwater table. *Squeezing* refers to the sides of the hole bulging inward, either during or after drilling, and is most likely in soft clays and silts or highly organic soils. Either of these conditions could produce *necking* in the shaft (a local reduction in its diameter) or soil inclusions in the concrete, as shown in Figure 12.37, both of which could have disastrous consequences.

The two most common construction techniques for preventing these problems are the use of *casing* or the use of *drilling fluid*.

The casing method, shown in Figure 12.38, uses the following procedure:

1. Drill the hole using conventional methods until encountering the caving strata.
2. Insert a steel pipe (the casing) into the hole and advance it past the caving strata as shown in Figures 12.38a and 12.39. This is often done using vibratory hammers such as the one in Figure 12.22. The diameter of this casing is usually 50 to 150 mm (2–6 in) less than the diameter of the upper part of the shaft.
3. Drill through the casing and into the noncaving soils below using a smaller diameter auger as shown in Figure 12.38b.
4. Place the reinforcing steel cage and the concrete through the casing and extract the casing as shown in Figure 12.38c. This is a very critical step, because premature extraction of the casing can produce soil inclusions in the shaft.

There are many variations to this method, including the option of leaving the casing in place and combining the casing and slurry methods. Figure 12.40 shows a variation where the casing can also be inserted using an *oscillator* and the shaft is excavated with a *hammer grab*.

The drilling fluid method (also known as the *slurry method*) is shown in Figure 12.41. It uses the following procedure:

1. Drill a *starter hole*, perhaps 3 m (10 ft) deep.
2. Fill the starter hole with a mixture of water and bentonite clay to form a *drilling mud* or *slurry*. When sea water is present, use attapulgite clay instead of bentonite. When properly mixed, the drilling mud has the appearance of very dirty water and keeps the hole open because of the hydrostatic pressure it applies to the soil. In many cases a polymer slurry is used instead of bentonite.

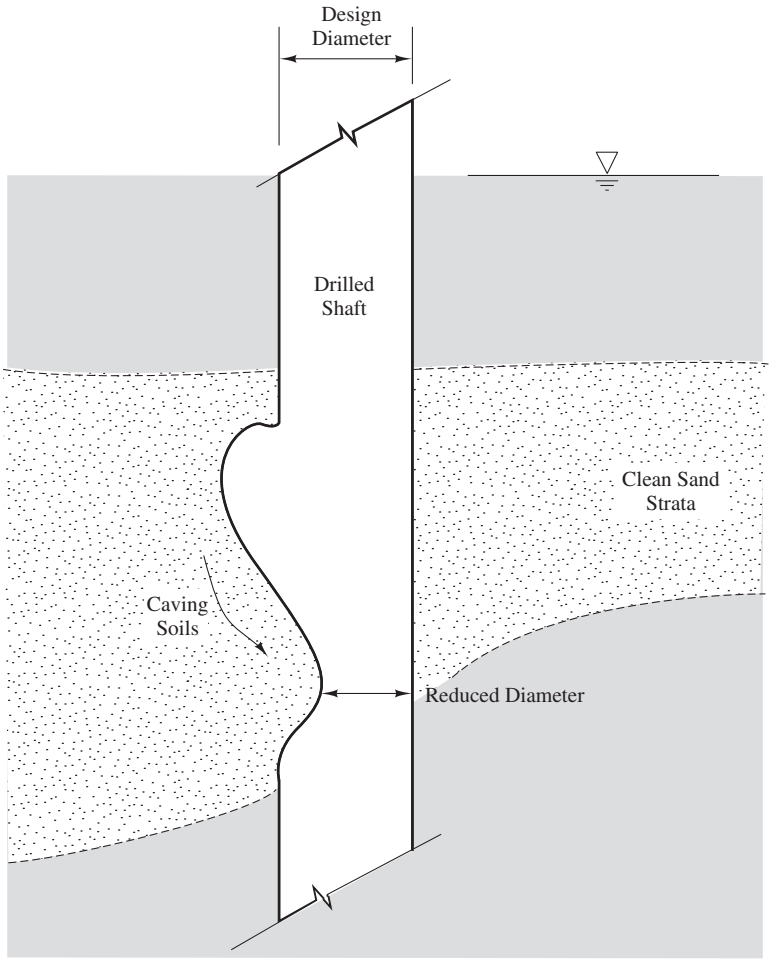

Figure 12.37 Possible consequences of caving or squeezing soils.

3. Advance the hole by passing the drilling tools through the slurry as shown in Figure 12.41a. Continue to add water and bentonite as necessary.
4. Insert the reinforcing steel cage directly into the slurry as shown in Figure 12.41b.
5. Fill the hole with concrete using a *tremie pipe* that extends to the bottom as shown in Figure 12.41c. The concrete pushes the slurry to the ground surface, where it is captured.

There is no concern about the quality of the bond between the rebar and the concrete. Although the rebar is first immersed in slurry, research has shown that the bond is satisfactory. However, the slurry can form a cake on and in the surrounding soil, thus

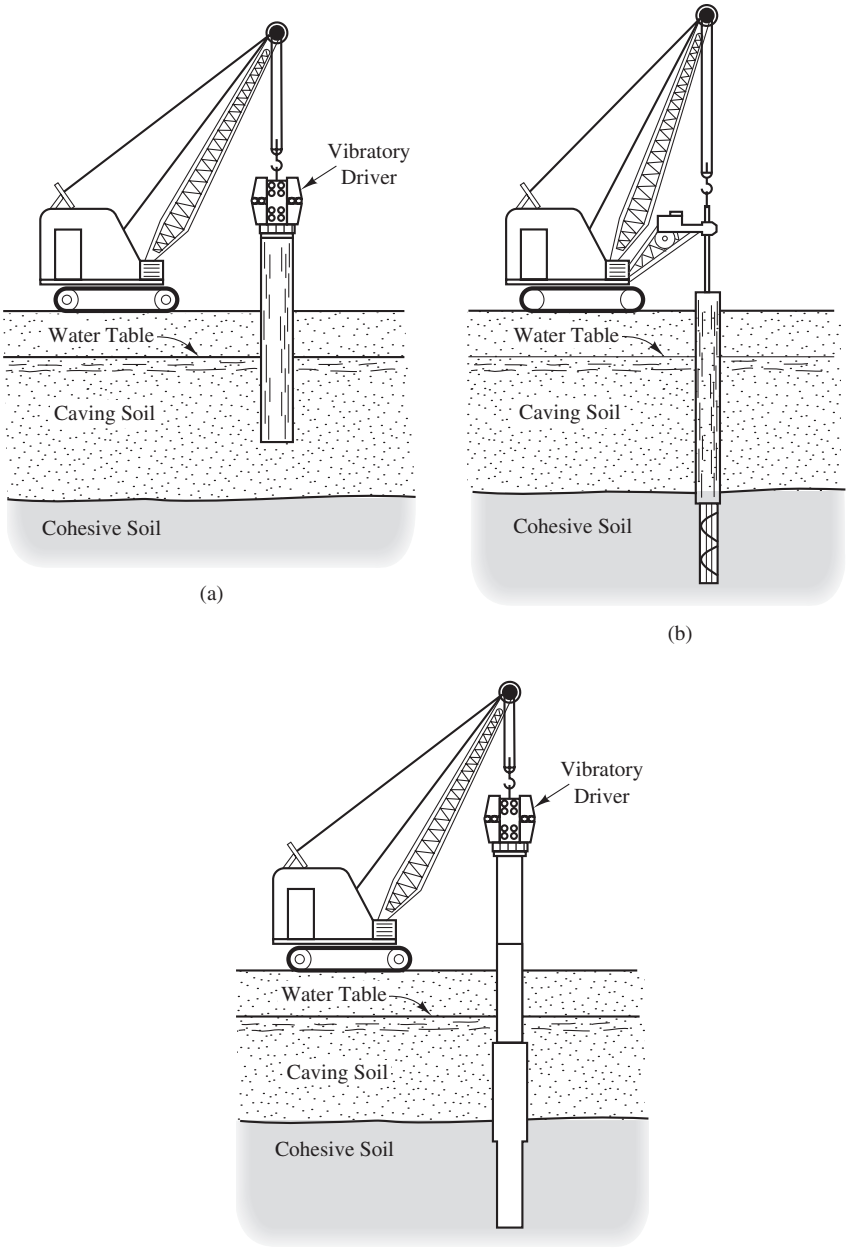

Figure 12.38 Using casing to deal with caving or squeezing soils: (a) installing the casing; (b) drilling through and ahead of the casing; and (c) placing the reinforcing steel and concrete, and removing the casing (after Reese and O'Neill, 1988).

Figure 12.39 The contractor at this site is using casing. The first casing, visible at the bottom of the photography, is already in place. However, its length is limited by the height of the rig. When casing must extend to greater depths, a second smaller casing is installed by passing it through the first casing, as shown here.

reducing the side friction resistance. Some specifications require the contractor to "scour" the sides of the holes to remove the slurry cake before placing the concrete.

Underreamed Shafts

An *underreamed shaft* (also known as a *belled shaft*) is one with an enlarged base, as shown in Figure 12.42. Usually, the ratio of the underream diameter to the shaft diameter (B_b/B_s) should be no greater than 3. Contractors build underreams using special belling buckets, such as the one shown in Figure 12.43.

Figure 12.40 The casing for this large-diameter drilled shaft was installed by a device known as an oscillator. The oscillator is the steel table-like device holding the casing at the ground surface. The oscillator rotates the casing back and forth using the hydraulic ram attached in a vee pattern. It also provides a downward thrust on the casing. The oscillating motion and the downward thrust force the casing into the ground. The bottom of the casing is fitted with teeth to aid it in penetrating the ground. In this particular project, the shaft is being excavated with a hammer grab, which is a heavy bucket-type device that opens into a circular shape. It is dropped quickly into the shaft to break up the soil at the bottom of the shaft. When it is retracted the grab closes and removes the loosened soil (photo by John Stamets).

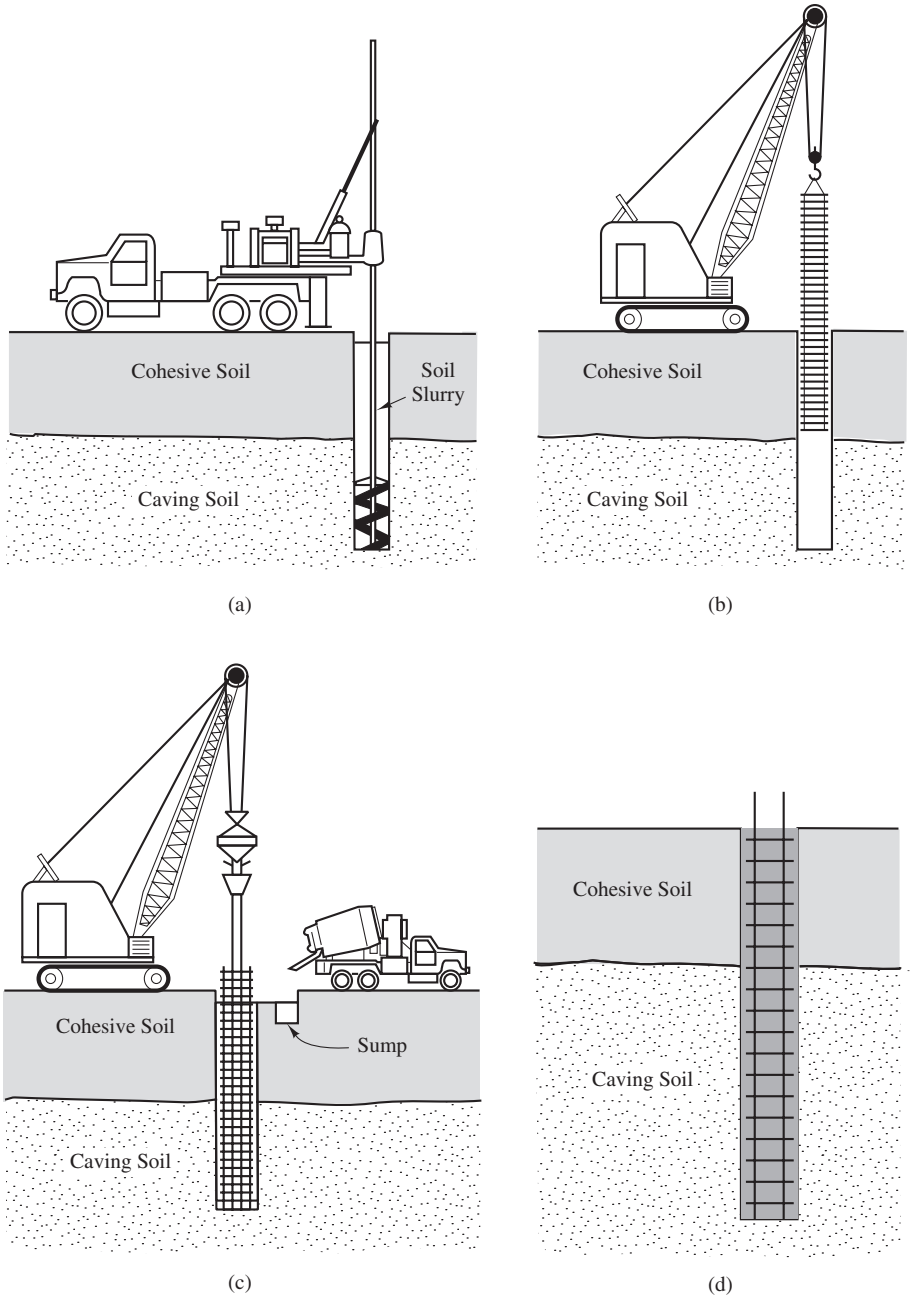

Figure 12.41 Using drilling fluid to deal with caving or squeezing soils: (a) drilling the hole using slurry; (b) installing the reinforcing steel cage through the slurry; (c) placing the concrete using a tremie pipe and recovering slurry at the top; and (d) the completed foundation (after Reese and O'Neill, 1988).

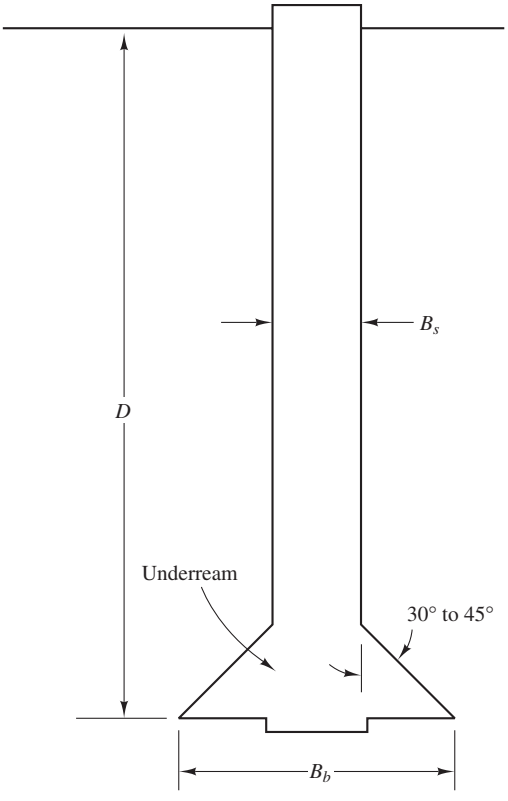

Figure 12.42 An underreamed drilled shaft.

Figure 12.43 A belling bucket used to produce a bell or underream at the bottom of a shaft (ADSC: The International Association of Foundation Drilling).

The larger base area of underreamed shafts increases their end-bearing capacity, and thus they are especially useful for shafts bottomed on strong soils or rock. However, the displacement required to mobilize the full end bearing is typically on the order of 10 percent of the base diameter, which may be more than the structure can tolerate. Underreamed shafts also have greater uplift capacities due to bearing between the ceiling of the underream and the soil above.

Unfortunately, the construction of underreamed shafts can be hazardous to the construction workers. In addition, the bottom of the underream must be cleaned of loose soil before placing concrete, and this process can be difficult and expensive. Advances in tooling have made it possible to drill through almost any earth material, so it is often faster and more cost-effective to drill a longer straight shaft than to construct an underream. Therefore, underreamed shafts are not being built as often as in the past.

Concrete

Concrete for drilled shafts must have sufficient slump to flow properly and completely fill the hole. Using concrete that is too stiff creates voids that weaken the shaft. Typically, the slump should be between 100 and 220 mm (4–9 in), with the lower end of that range being most appropriate for large-diameter dry holes with widely spaced reinforcement and the high end for concrete placed under drilling fluid. Sometimes it is appropriate to include concrete admixtures to obtain a high slump while retaining sufficient strength. Some people have experimented with expansive cements in drilled shaft concrete. These cements cause the concrete to expand slightly when it cures, thus increasing the lateral earth pressure and side friction resistance. So far, this has been only a research topic, but it may become an important part of future construction practice.

Post Grouting

One shortcoming of drilled shafts is that the soil at the bottom of the shaft is unloaded and loosened during the drilling process. Because of this, drilled shafts require significant displacement to mobilize the full capacity of the shaft toe. The problem is especially prevalent in large-diameter drilled shafts. To circumvent this problem, grout is sometimes injected below the base of drilled shafts after the concrete for the shaft has been placed and has cured. This process is call *post grouting*. It is accomplished by attaching grout tubes to the rebar cage. The grout tubes run the full length of the drilled shaft and are closed during the placement of the rebar cage and concrete. The grout tubes have a weak section at the toe of the shaft as shown in Figure 12.44. After the concrete has cured, grout is pumped into the grout tubes at high pressure. The high pressure ruptures the weak sections at the toe of the shaft and enters the ground just below the shaft. The pressurized grout fills any gaps beneath the drilled shaft and compresses the soil immediately below the shaft and preloads the soil. The preloading significantly reduces the displacement needed to mobilize the toe resistance of the drilled shaft.

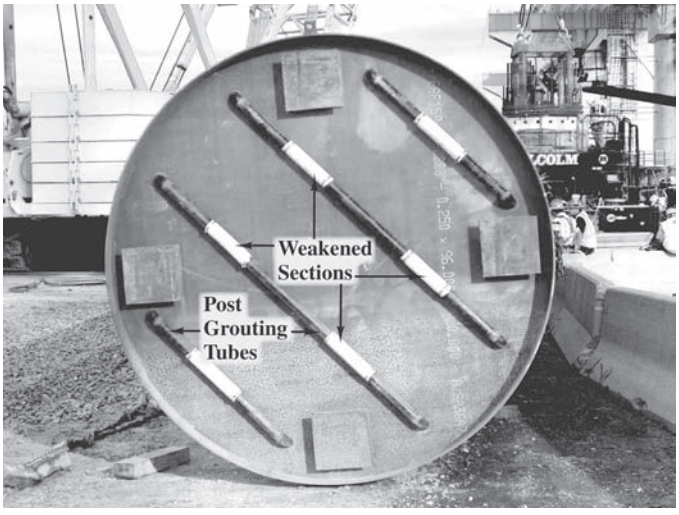

Figure 12.44 Base of a drilled shaft rebar cage (before being placed) showing post grouting tubes with weakened sections. When grout is pumped in, the weakened sections will break open and grout will be forced under the drilled shaft filling the area below the shaft and compacting soil below the shaft (courtesy of Dan Brown Assoc.).

12.4 AUGER PILES

Auger piles are another type of cast-in-place pile (Massarsch et al., 1988; Brons and Kool, 1988; Prezzi and Basu, 2005; Brown et al., 2007). Unlike drilled shafts, auger piles are constructed using a hollow-stem continuous flight auger that remains in the hole during drilling. Hollow stem augers have a centrally located pipe surrounded by the flights (which draw up the soil). This configuration provides a means for delivering high strength grout to the bottom of the hole while the auger is still in place, and the hole is then filled as the auger is withdrawn. This technique eliminates the need for casing or drilling mud, even in soils subject to caving or squeezing, and thus facilitates very rapid construction.

There are two categories of auger piles. Auger cast in place piles were first developed in the mid-twentieth century and are the most common type. Drilled displacement piles were developed in the late twentieth and early twenty-first century, and thus represent a newer technique.

Auger Cast in Place (ACIP) Piles

The *auger cast in place (ACIP) pile* is the oldest and most commonly used auger pile. They are known by many names (DFI, 1990), including:

- Augered pressure grouted (APG) pile
- Auger cast in place (ACIP) pile

- Continuous flight auger (CFA) pile
- Intruded mortar pile
- Augerpress pile
- Grouted bored pile
- Augered grout-injected pile

Although there are some variations in construction methods, all of these are essentially the same. Figure 12.45 illustrates the key components of a crane-mounted ACIP rig. A long hollow stem auger is mounted in a set of leads with hydraulic gearbox on the top to drive the auger. A pressurized grout line is attached to the top of the auger through a swivel. A ground-mounted pump takes grout from either concrete trucks or a local batch plant, and pumps the grout up to the top of the augers, down the hollow core and out through a port in the tip of the auger. The ACIP construction process begins with installing a temporary plug, typically made of cork, into the port at the auger tip. The auger is then positioned at the desired pile location and the gearbox drills the hollow stem auger down to the desired depth as illustrated in Figure 12.46a. The rate of penetration must match the rate of auger rotation so that only

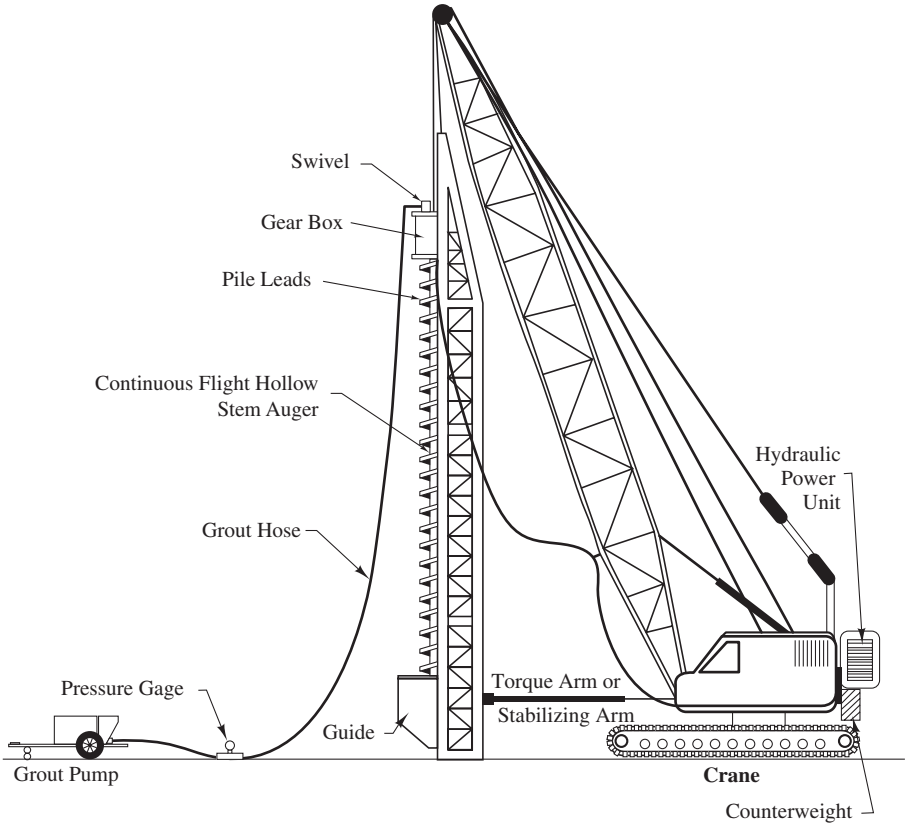

Figure 12.45 Illustration of a typical crane mounted ACIP rig (courtesy of DFI).

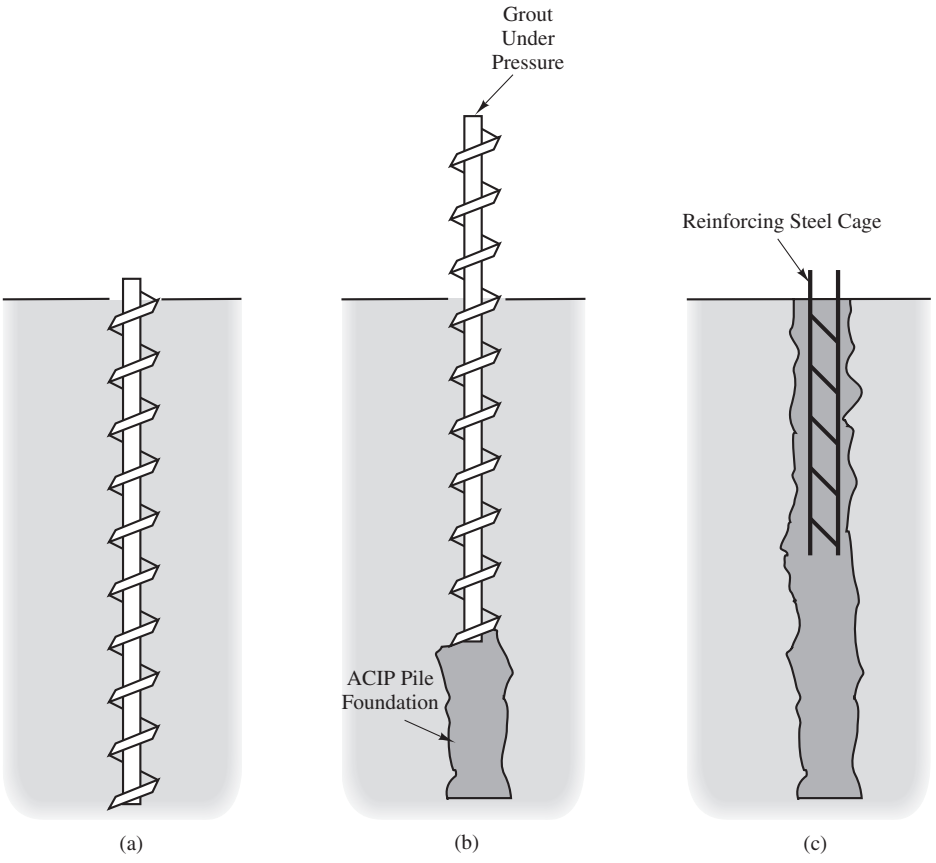

Figure 12.46 Illustration of the construction process for auger cast in place (ACIP) piles: (a) drill to the required depth using a hollow stem auger; (b) withdraw the auger while injecting cement grout; and (c) install steel rebars.

the minimum required volume of soil is extracted. Over-augering, or drawing up too much soil, is problematic because it loosens the surrounding soil and reduces the unit side friction resistance. This can be especially problematic when drilling through soft or loose soils, than through a much harder stratum. In this situation, the drilling rate often becomes much slower, resulting in too much of the upper soil being drawn up by the auger. Over-augering also increases the required grout volume, and thus increases construction costs.

Once the desired depth is reached, the grout pump is started and high strength grout is pumped under pressure through the hollow stem auger, dislodging the temporary plug and filling the hole. The auger is gradually withdrawn as the hole is filled, as illustrated in Figure 12.46b. The grout has a very high slump, so the associated pressure should fill any voids and possibly even penetrate into the soil, thus providing a better soil-pile interface than would be achieved in drilled shaft construction. However, the rate of withdrawal also is important in order to avoid soil inclusions. This rate can be controlled as the grout is being placed by monitoring the group pressure, and by using instrumentation that

monitors the rate of auger withdrawal and the volume of grout being used. Typically, the grout take should be at least 110 percent of the theoretical hole volume. This instrumentation has largely eliminated concerns about soil inclusions. Proper grout mix and handling is essential. Usually a high cement content and special admixtures are used to provide sufficient fluidity for pumping and steel placement, while also providing sufficient strength and minimal shrinkage during curing.

Once the hole is completely filled, the auger is removed, minor adjustments are made, and the prefabricated steel reinforcing cage is installed, as illustrated in Figure 12.46c. Unlike drilled shafts, the steel placement occurs after the grout is placed, so the grout must be sufficiently fluid to allow inserting of the steel. Normally, the steel is raised over the hole using a small crane, and guided into the hole by workers. The weight of the steel is usually sufficient to facilitate penetration. If necessary, it can be vibrated in place.

The equipment required to construct ACIP piles has advanced in capacity and sophistication, which facilitates using larger diameter piles, drilling in harder soils, and expediting the construction process. ACIP piles are typically 300 to 1000 mm (12–36 in) diameter, with 400 mm (16 in) being a very common size. The depth of penetration is limited by the practical height of the crane that supports the auger and drive mechanism. Depths of 10 to 25 m (30–80 ft) are common, and 40 m (130 ft) is possible. Figure 12.47 shows a crane mounted ACIP installing piles for an expansion of the terminal at San Francisco International Airport.

Advantages of ACIP piles include:

- The auger protects the hole from caving, thus reducing the potential for ground loss (so long as over-augering is avoided)
- The noise and vibration levels are low, certainly much lower than those for driven piles.
- The depth of penetration is easily adjusted during construction.
- The construction process is much faster than either driven piles or drilled shafts, which can generate significant cost savings and expedite the construction schedule.
- The grout is injected under pressure, which provides a good bond with the soil.
- This method is suitable for a wide variety of soil types.

Disadvantages include:

- Reliable construction requires contractors with a higher skill level, along with robust quality control and quality assurance processes.
- The construction process does not compact the soil, as occurs with driven piles, so the unit side friction resistance will be correspondingly less.
- The diameter and steel ratio are less than those for drilled shafts, which can limit the lateral capacity.
- The grout cost is higher than the cost of comparable concrete in a drilled shaft.
- The construction process is very sensitive to equipment breakdowns. Once grouting has begun, any significant breakdown becomes cause for abandoning the foundation.
- Soil profiles that contain cobbles and boulders are problematic, and unlike drilled shafts, rock sockets are not possible.

Figure 12.47 Installation of auger cast in place (ACIP) piles at San Francisco International Airport using a crane mounted rig. The grout and hydraulic lines for the auger can be seen between auger leads and the crane boom. The smaller crane in the right of the photo is used to place the rebar cages after the grout has been placed (courtesy of Berkel and Co.).

Drilled Displacement Piles

Drilled displacement (DD) piles (also known as auger pressure grouted displacement piles or screw piles) are similar to ACIP piles in that a hollow stem auger is used and the hole filled with grout as the auger is withdrawn. The difference is in the auger equipment used. Drilled displacement piles use a short tapered auger that is designed to push the soil out laterally as the auger is drilled into the ground. For a full displacement DD pile, all of the excavated soil is pushed laterally into the formation using an auger tool such as that illustrated in Figure 12.48. Note that the auger has an enlarged section and a reversed set of flights to ensure that soil excavated at the bottom of the hole is forced into the formation and none is brought to the surface. A photograph of a typical full displacement auger rig is shown in Figure 12.49. For a partial displacement DD pile, some of the excavated soil is push laterally into the formation and some is augered to the ground surface. Figure 12.50 shows a typical partial displacement auger tool. Like the full displacement auger this tool has an enlarged section to compact soil into the formation, but it also includes a smaller auger to lift some soil to the surface.

Drilled displacement piles retain all of the advantages of ACIP piles, plus the process of pushing the soil into the adjacent ground increases the lateral earth pressures, thus increasing the side friction capacity, and reduces or eliminates the need to dispose of the

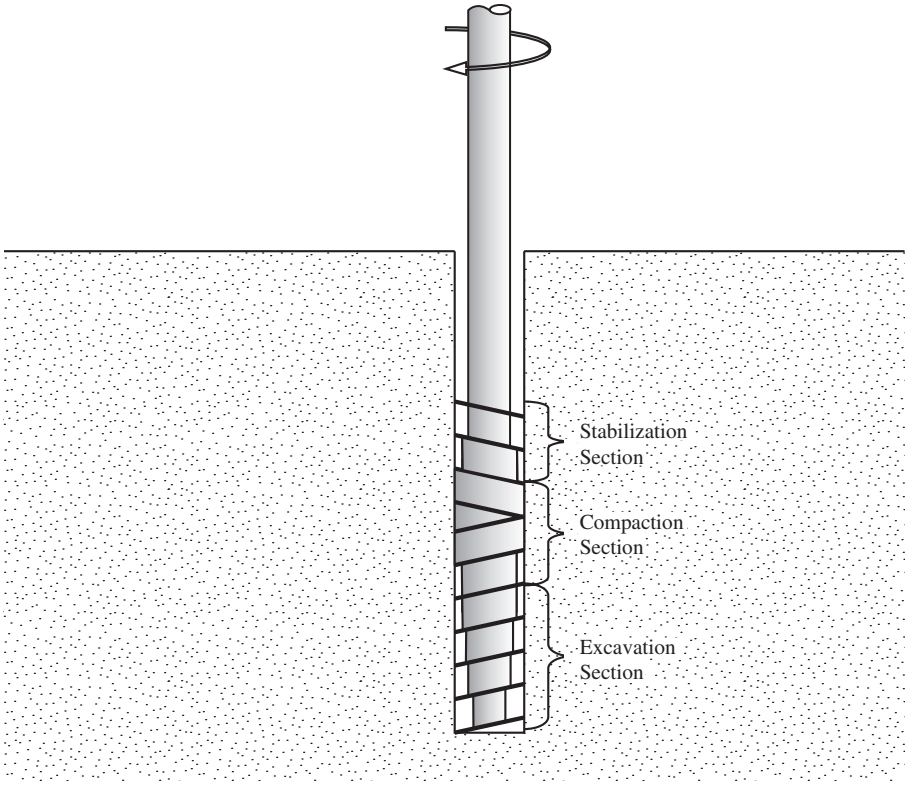

Figure 12.48 Drilling tools for full displacement DD piles, typical of that designed by Berkel & Company Contractors, Inc., Bonner Springs, Kansas. The body of the auger expands from the excavation section to the compaction section and pushes excavated soil out into the formation. The reversed flights in the stabilization section ensure any loose soil encountered during withdrawal of the auger is pulled back down to the compaction section and pushed out into the formation. The smooth stem above the drilling/compacting tool does not carry any soil to the surface.

soil cuttings. The side friction resistance should be at least equal to that of driven piles. Sometimes DD piles are further enhanced using a technique called *amelioration*, which consists of introducing coarse sand or gravel from the ground surface, thus pushing more soil into the ground. Amelioration further increases the side friction capacity. However, much more torque must be applied to the auger, especially if amelioration is used, so DD piles require higher capacity drill rigs. Even then, they are feasible only in softer soil conditions and the available diameters are limited to no more than about 500 mm (20 in). Nevertheless, when used in favorable soil conditions, DD piles often provide a very cost-effective high-capacity foundation system.

Figure 12.49 Photograph of the full displacement auger mounted on a drill rig starting to drill a full displacement pile. The excavation, compaction, and stabilization portions of the auger are clearly visible (courtesy of Malcolm Drilling Co. Inc.).

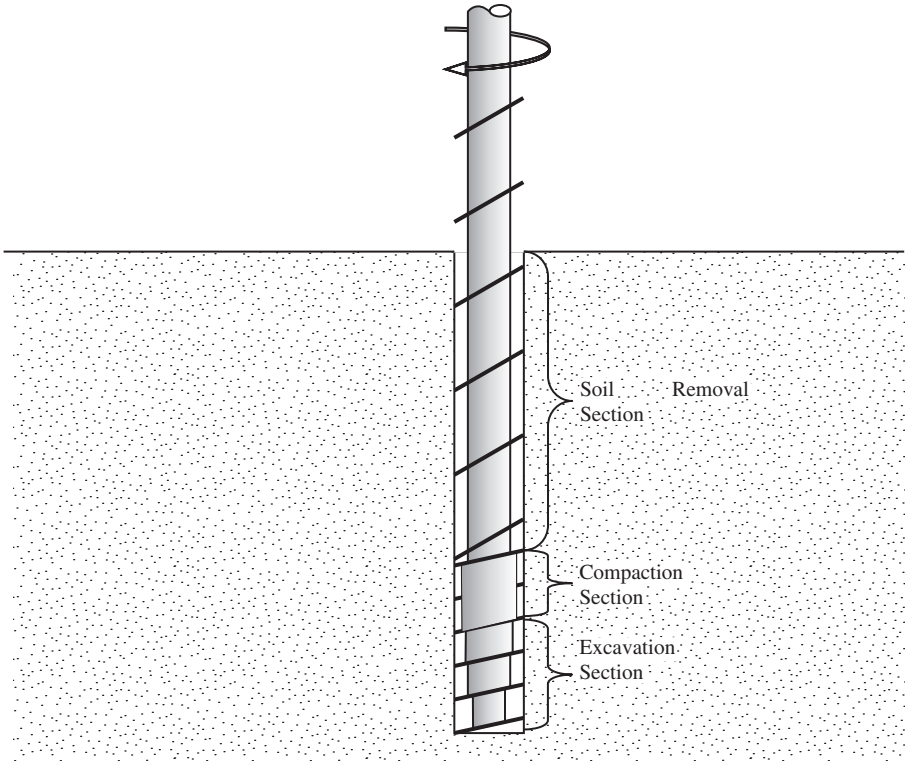

Figure 12.50 Drilling tools for partial displacement DD piles, typical of that designed by Berkel & Company Contractors, Inc. Note that the augers in the soil removal section are very shallow and spaced far apart. This ensures that only part of the excavated soil will be removed from the hole. The remaining excavated soil will be pushed out into the formation by the compaction section of the auger.

12.5 OTHER PILE TYPES

The vast majority of deep foundation projects use driven piles, drilled shafts, or auger piles. Other types also are available, and are typically used in special situations. These other types of deep foundations typically require specialized contractors who have the necessary equipment and expertise.

Jacked Piles

Jacked piles are installed by the use of hydraulic jacks to press piles into the ground. The piles are prefabricated members, often identical to those used for driven pile construction, but they are pressed into the ground instead of driven. Early applications of jacked piles in the mid-twentieth century were mainly to the underpinning of existing foundations to increase capacity and reduce settlement. Jacked piles are still used today for this purpose, but in the late-twentieth century they began to be used as production piles for new structures.

Production pile jacking has been rare in most of the world, but relatively common in many parts of China (Shi, 1999). This method uses a large jacking rig which grips a pile in a large vise-like device and presses the pile into the ground with two or more large hydraulic rams. Figure 12.51 shows a typical pile jacking rig. The weight of the rig is used as a reaction for the driving rams; therefore, these machines are very large and heavy. The largest of these jacking rigs can produce a downward force of 10,000 kN (2,200 kips). They can be used to install H-piles, pipe piles, and concrete piles, typically ranging from 300 to 600 mm (12 to 24 in) in diameter (or width) and up to 70 m (230 ft) long.

The advantages of pile jacking include:

- Pile jacking produces little noise and vibration, which is especially desirable in urban areas and near sensitive existing facilities, such as hospitals.
- The stresses induced in the pile during jacking is smaller than during driving.
- The pile jacking process provides a de facto load test for each pile.

Disadvantages include:

- The size and weight of jacking rigs make them much more difficult to maneuver around a construction site than either impact or vibratory hammers.
- A jacking rig is very heavy and exerts a high pressure on the ground.

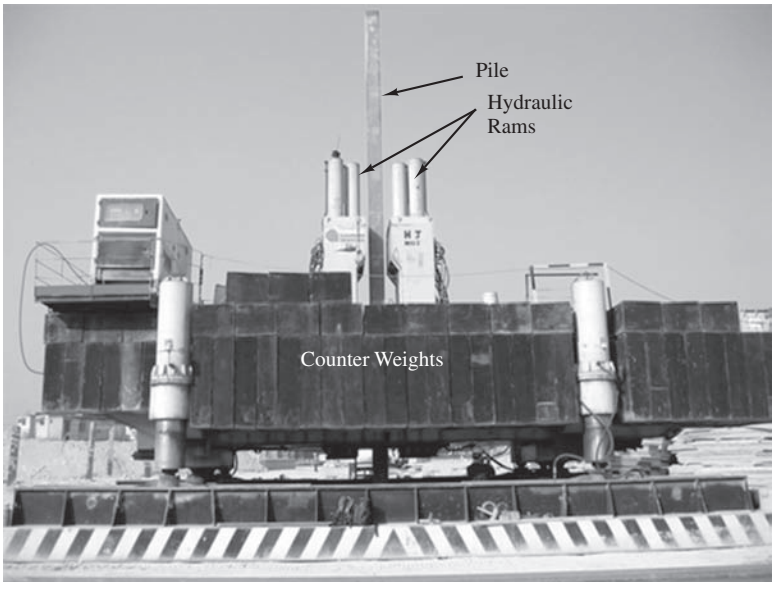

Figure 12.51 Installation of precast concrete piles with a pile jacking rig. A crane picks up a pile and feeds in into the center of the jacking rig where a set of hydraulic clamps grab the pile and then push it into the ground (courtesy of Limin Zhang, Hong Kong University of Science and Technology).

- Because of the size of jacking rigs, sufficient clearance is required between the pile and existing structures.
- The pile must be designed to handle gripping forces.

Pressure-Injected Footings (Franki Piles)

Edgard Frankignoul developed the pressure-injected footing (PIF) foundation in Belgium around 1910. This technique uses cast-in-place concrete that is rammed into the soil using a drop hammer. This ramming effect compacts the surrounding soil, thus increasing its load bearing capacity. PIF foundations are often called *Franki piles*. Other names include *bulb pile*, *expanded base pile*, *compacted concrete pile*, and *compaction pile*. The construction techniques used to build PIFs are described below and shown in Figure 12.52.

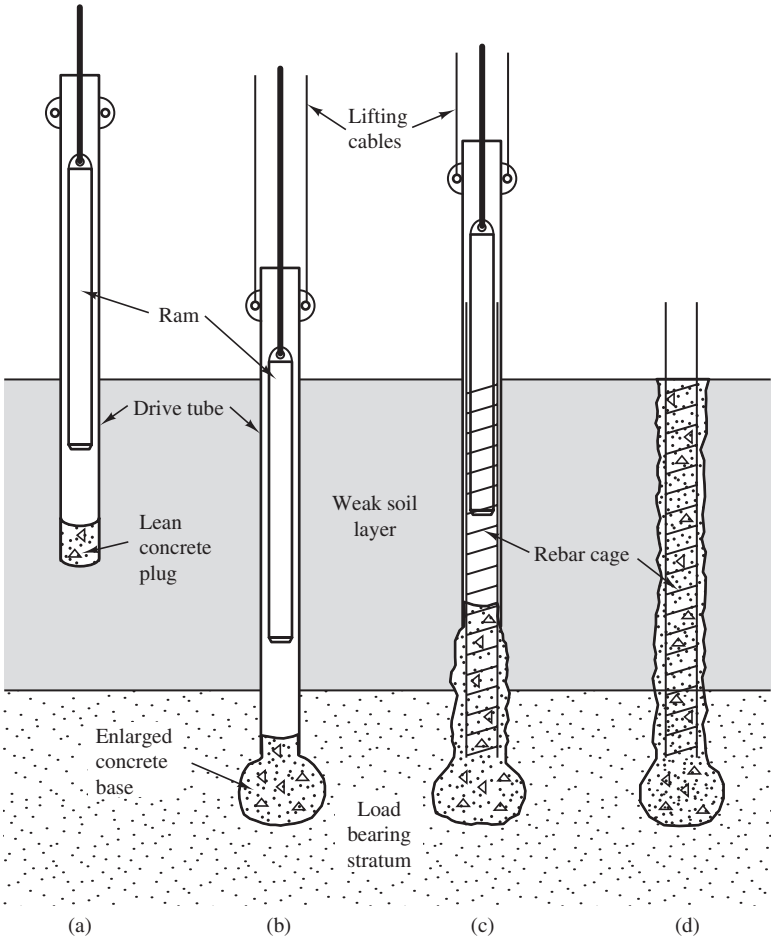

Figure 12.52 Construction of an uncased PIF foundation: (a) driving plug and tube; (b) enlarging base; (c) forming shaft with rebar cage; (d) completed PIF foundation.

Phase 1: Driving

The process begins by temporarily inserting the *drive tube* into the ground. This tube is a specially built 300 to 600 mm (12–24 in) diameter steel pipe. The contractor does so using one of the following methods:

- **Top driving method**—Install a temporary bottom plate on the drive tube, and then drive the tube to the required depth using a diesel pile hammer. The plate will later become detached when the concrete is pounded through the drive tube.
- **Bottom driving method**—Place a plug of low-slump concrete in the bottom of the tube and pack it in using the drop hammer. Then, continue to strike this plug, thus pulling the tube into the ground.

Phase 2: Forming the Base

Once the drive tube reaches the required depth, hold it in place using cables, place small charges of concrete inside the tube, and drive them into the ground with repeated blows of the drop hammer. This hammer has a weight of 1,400 to 4,500 kg (3–10 kips) and typically drops from a height of 6 m (20 ft). If the top driving method was used, this process will expel the temporary bottom plate. Thus, a bulb of concrete is formed in the soil, which increases the end-bearing area and compacts the surrounding soil. This process continues until a specified number of hammer blows is required to drive out a certain volume of concrete.

Phase 3: Building the Shaft

The shaft extends the PIF base to the ground surface. Two types of shafts are commonly used:

- To build a *compacted shaft*, raise the drive tube in increments while simultaneously driving in additional charges of concrete. This technique compacts the surrounding soil, thus increasing the side friction resistance. It also increases the end-bearing resistance by providing a stronger soil over the base.
- To build a *cased shaft*, insert a corrugated steel shell into the drive tube, place and compact a zero-slump concrete plug, and withdraw the tube. Then fill the shell with conventional concrete. Although this method does not develop as much load capacity, it is often more economical for piles that are longer than about 9 m (30 ft). A cased shaft may be mandatory if very soft soils, such as peat, are encountered because these soils do not provide the lateral support required for the compacted shaft method.

The contractor can reinforce either type of shaft to resists uplift or lateral loads. For the compacted shaft, the reinforcing cage fits between the drop hammer and the drive tube, thus allowing the hammer to fall freely.

Pressure-injected footing foundations may be installed individually or in a group of two or more and connected with a pile cap. Table 12.1 gives typical dimensions and typical capacities of PIF foundations. The actual design capacity must be determined using the techniques described in Chapters 14 and 15. Figure 12.53 shows a “mini” PIF that was extracted out of the ground.

TABLE 12.1 TYPICAL PIF DIMENSIONS AND CAPACITIES

	Typical Allowable Downward Capacity		Base Diameter		Nominal Shaft Diameter			
					Compacted		Cased	
PIF Type	(k)	(kN)	(in)	(mm)	(in)	(mm)	(in)	(mm)
Mini	100	450	24–30	600–750	n/a	n/a	10.6–11.1	270–280
Medium	200	900	34–40	850–1,000	17	430	12.2–14	300–360
Standard	400	1,800	34–40	850–1,000	22	560	16–17.6	400–450
Large	500	2,200	34–40	850–1,000	23	580	19	480
Maxi	600	2,700	34–40	850–1,000	25	630	22	560

Data from Tomlinson and Woodward (2007), Franki Grundbau (ND), and other sources.

Figure 12.53 This "mini" PIF was extracted from the ground. It had a base diameter of 600 mm (24 in) (photo courtesy of William J. Neely).

The advantages of PIF foundations include:

- The construction process compacts the soil, thus increasing its strength and load-bearing capacity. This benefit is most pronounced in sandy or gravelly soils with less than about 15 percent passing the #200 sieve, so PIFs are best suited for these kinds of soils.
- When compacted shafts are used, the construction process produces a rough interface between the shaft and the soil, thus further improving the side friction resistance.
- It is possible to build PIFs with large bases (thus gaining the additional end-bearing area) in soils such as loose sands where belled drilled shafts would be difficult or impossible to build.

Disadvantages include:

- The side friction resistance for cased PIFs is unreliable because of the annular space between the casing and the soil. Although this space is filled with sand after the drive tube is lifted, we cannot be certain about the integrity of the connection between the shaft and the soil.
- The construction process generates large ground vibrations and thus may not be possible near sensitive structures. These vibrations also can damage wet concrete in nearby PIFs.
- The construction equipment is bulky and cumbersome, and thus requires large work areas.
- Compacted shafts cannot include large amounts of reinforcing steel.
- Although each PIF will have a higher load capacity than a pile or drilled shaft of comparable dimensions, it also is more expensive to build. Therefore, the engineer must evaluate the alternatives for each project individually to determine which type is most economical.
- They are generally economical only when the length is less than about 9 m (30 ft) for compacted PIFs or about 21 m (70 ft) for cased PIFs.

Micropiles

Micropiles are essentially slender drilled shafts, typically 300 mm (12 in) or less in diameter. They are typically reinforced with a single centerally located rebar, and are placed in groups, often at different angles. They were developed in Italy soon after the Second World War as a response to shortages of steel and concrete, and were originally called pali radice (root piles) because of their resemblance to plant roots. They generally have capacities of less than 100 kN (22 kips) (Armour et al., 2000), although capacities over 400 kN (90 kips) have been measured (Armour et al., 2000).

Micropiles are constructed using rock drilling type equipment. This has several advantages over other augering equipment. First, the equipment is comparatively light and thus can be built in more confined or awkward locations. For example, micropiles have been used to underpin existing buildings by mobilizing the drilling equipment inside the basement. Second, this equipment is capable of penetrating certain difficult geologic profiles such as areas with cobbles or boulders, or karstic geology. A disadvantage of micropiles is their small size and low capacity, which generally requires use of a large number of micropiles.

Helical Piles

Helical piles also called *screw piles* consist of steel screws that are torqued into the ground to form a foundation. Figure 12.54 shows a helical pile being installed. This technique was first used in the mid-nineteenth century and used extensively for offshore lighthouses in shallow water (Perko, 2009). Helical piles can be installed with relatively light equipment and in areas with low head room and are often used in retrofit or remediation of existing structures. The diameter of modern helical piles generally range from 30 to 100 cm (12 to 36 in) and have capacities that can exceed 2,000 kN (550 kips), although 100 to 500 kN (22 to 110 kips) is more typical. They are not suitable for use in hard soils or soils with larger gravel or cobbles as these conditions will damage the helix.

Figure 12.54 Helical pile being installed. This particular helical pile has two separate helix sections. One is just entering the ground and the other is already below the surface (courtesy of Helical Concepts, Inc.).

Anchors

The term *anchor* generally refers to a foundation designed primarily to resist uplift (tensile) loads. Although most foundations are able to resist some uplift, anchors are designed specifically for this task and are often able to do so more efficiently and at a lower cost.

Lightweight structures often require anchors because the lateral wind and earthquake loads on the structure often produce uplift loads on some of the foundations. These structures include power transmission towers, radio antennas, and mobile homes. Some of these structures are stabilized with guy wires, which are then connected to the ground using anchors.

Anchors also can be installed horizontally (or nearly so) to provide lateral support to earth retaining structures. These are called *tieback anchors*. They eliminate the need for bracing outside the wall, and thus provide more space for construction and permanent structures.

Kulhawy (1985) divided anchors into three categories, as shown in Figure 12.55. These include:

- *Spread anchors* are specially designed structural members that are driven or inserted into the ground, then expanded or rotated to form an anchor.
- *Helical anchors* are steel shafts with helices that resemble large screws. They are screwed into the ground using specialized equipment, as shown in Figure 12.56.
- *Grouted anchors* are drilled holes filled with a steel tendon and grout. The tendon transmits the tensile loads into the anchor, then the grout transmits them to the surrounding ground through side friction.

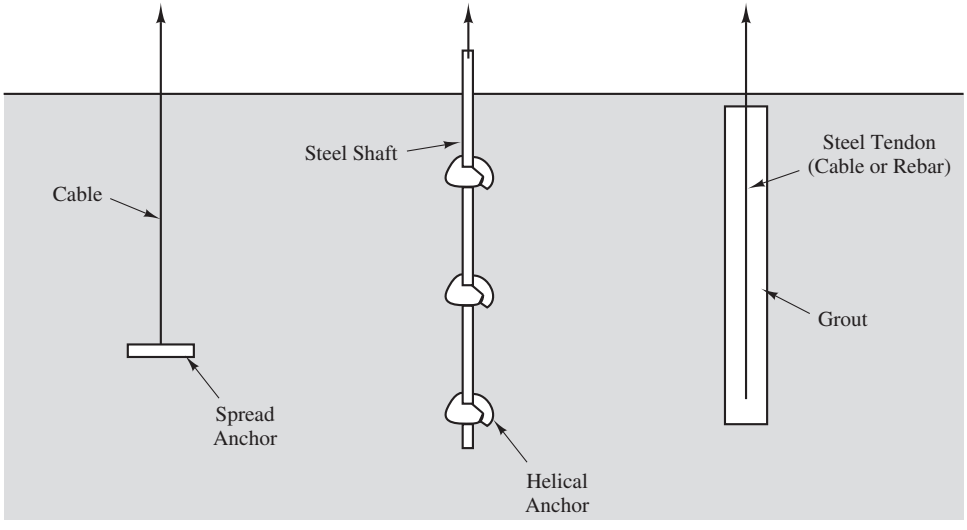

Figure 12.55 Types of anchors (Based on Kulhawy, 1985; used with permission of ASCE).

Figure 12.56 Installation of a helical anchor to be used as a tieback for a sheet pile wall. Once these anchors are installed, the soil in the foreground will be excavated (photo courtesy of A. B. Chance Company).

The design load capacities may be computed from the geometry and soil type. For helical anchors, the torque required to install the anchor also can be an indicator of load capacity. In critical applications, such as tieback anchors, engineers often load test the installed anchors using hydraulic jacks.

12.6 CAISSONS

The word *caisson* is derived from the French *caisse*, which means a chest or box. When applied to foundation engineering, it describes a prefabricated hollow box or cylinder that is sunk into the ground to some desired depth and then filled with concrete, thus forming a foundation. Caissons have most often been used in the construction of bridge piers and other large structures that require foundations beneath rivers and other bodies of water because the caissons can be floated to the job site and sunk into place.

Open Caissons

An *open caisson* is one that is open to the atmosphere, as illustrated in Figure 12.57. They may be made of steel or reinforced concrete, and normally have pointed edges at the bottom to facilitate penetration into the ground. Figure 12.58 shows a typical open caisson being sunk into a riverbed by dredging.

Sometimes the site of the proposed foundation is dredged before the caisson arrives on site or, as shown in Figure 12.58, they can be dredged as the caisson is being

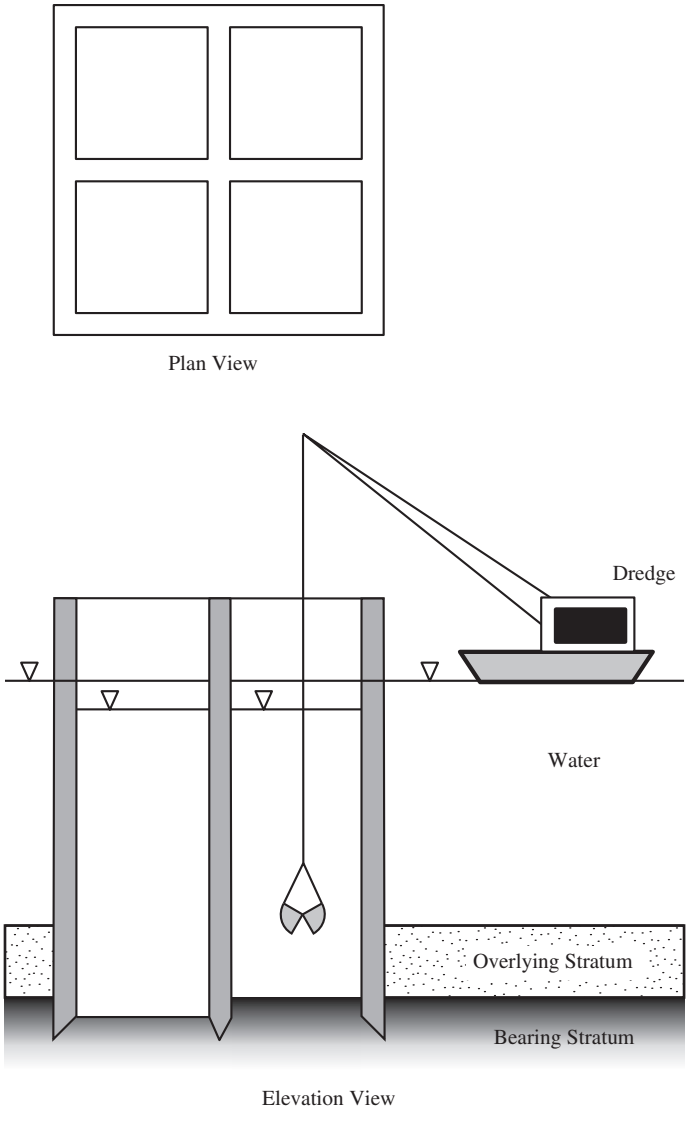

Figure 12.57 Typical open caisson illustrating dredging operation to excavate soil at base of caisson.

constructed. The dredging operation can be an economical way to remove some of the upper soils, thus reducing the quantities that must be excavated through the caisson. Then the caisson is floated into place and sunk into the soil. As it descends, the soil inside is removed and hauled out of the top. In early caissons this excavation was done by laborers working in the bottom of the caisson, which also required pumping out any water that

Figure 12.58 An open caisson being dredged. The walls of this caisson are cast in place and raised as the caisson is cut into the river bed (photo by John Stamets).

accumulated. Later caissons were excavated from the top using machinery, which was much more efficient and could operate through the water. This process continues until the caisson sinks to the required depth and reaches the bearing stratum. It then is filled with concrete to form the foundation.

Caissons must be designed to resist the various loads imparted during construction, as well as the structural and hydrodynamic loads from the completed structure. In addition, a caisson must have sufficient weight to overcome the side friction forces as it descends into the ground.

Pneumatic Caissons

When the inside of caissons are dewatered during construction, the difference in heads created draws more water in from the surrounding area. The upward flow into the bottom of the caisson can produce a quick condition in the soils, especially in sands. In addition, as the caisson penetrates deeper and the head difference becomes greater, the flow rate can become overwhelming and exceed the capacity of the pumps.

One way to counteract this problem is to seal the bottom portion of the caisson and fill it with compressed air, as shown in Figure 12.59. If the air pressure equals or exceeds the pore water pressure, very little water enters the excavation, thus eliminating the seepage forces and the potential for quick conditions. In addition, the required pumping costs then become minimal. This method was first used around 1850 by the British engineer Isambard Kingdom Brunel (1806–1859) during construction of the Chepstow Bridge across the Thames River in London. Many bridge foundations in North America also have been built using this method, including the Brooklyn and Williamsburg Bridges in New York City.

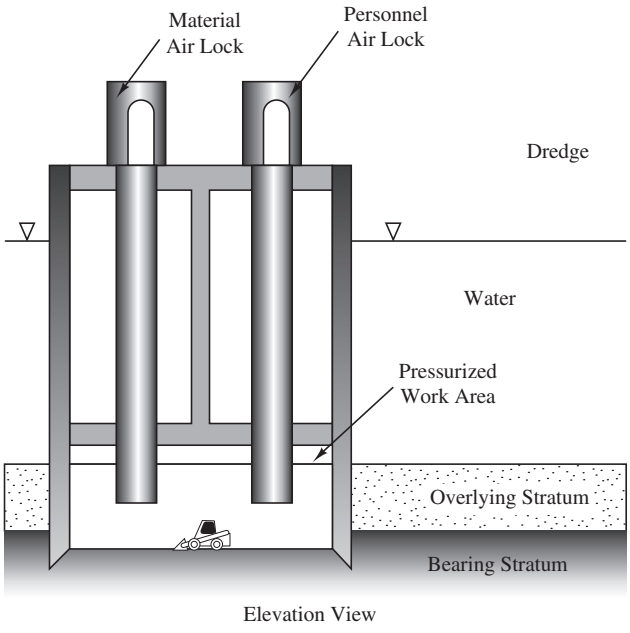

Figure 12.59 A pneumatic caisson using compressed air to halt the flow of groundwater into the caisson.

For example, an excavation 50 ft below the groundwater table would require a pressure, p, of about:

$$p = u = \gamma_w z_w = \left(62.4 \text{ lb/ft}^3\right)(50 \text{ ft})\left(\frac{1 \text{ ft}^2}{144 \text{ in}^2}\right) = 22 \text{ lb/in}^2$$

This is the same pressure a diver would encounter 50 ft below the water surface in a lake. Construction personnel, who are called *sandhogs*, can work for three-hour shifts under such pressures. In some cases, air pressures up to 330 kPa (48 lb/in^2) may be used, but the shift time drops to only thirty minutes (White, 1962).

Workers enter these excavations by passing through an air lock, which is an intermediate chamber with doors connected to the outside and to the working chamber. The workers enter through the outside door, then both doors are closed and the chamber is slowly filled with compressed air. When the pressure reaches that in the working chamber, they open the connecting door and enter the working chamber. The process is reversed when exiting.

If the air pressure in the air lock is lowered too quickly, nitrogen bubbles form inside the workers bodies, causing *caisson disease*, also known as *the bends*. It causes severe pains in the joints and chest, skin irritation, cramps, and paralysis. Fourteen men died of caisson disease during construction of the Eads Bridge in St. Louis. Divers can experience the same problem if they rise to the surface too quickly.

Because of the hazards of working under compressed air, the large expense of providing the necessary safety precautions for the workers, and advances in the construction of other foundation types, the use of pneumatic caissons decreased during the second half of the twentieth century. Most structures that were formerly supported on caissons are now supported on large driven piles. The Bay Bridge project described in Chapter 1 is a good example. However, recent developments, particularly in Japan, have led to the *new pneumatic caisson method*, which does not require workers to enter the high pressure cells (Kodaki et al., 1997). All the excavation work is done robotically with automated excavation equipment. This method has been used to construct pneumatic caissons in Japan and China in the last decade (Ishida et al., 2004; Peng and Wang, 2011). These new technologies might trigger a revival of caisson foundations.

12.7 PILE-SUPPORTED AND PILE-ENHANCED MATS

Most mat foundations are supported directly on the underlying soils, as discussed in Chapter 11. However, when the net bearing pressure is too high or the soil is too compressible, such mats may experience excessive settlements. One option for such situations is to use a *pile-supported mat*, as shown in Figure 12.60. The piles are distributed across the mat, which then acts as a very large pile cap.

Many pile-supported mats have been designed to transfer all of the structural loads to the deep foundations. However, others partially rely on the bearing pressure between the bottom of the mat and the underlying soil, and use the deep foundations to carry the balance of the load. This later design, which can be called a *pile-enhanced mat*, can be much less expensive. Pile-supported and pile-enhanced mats are discussed in Chapter 24.

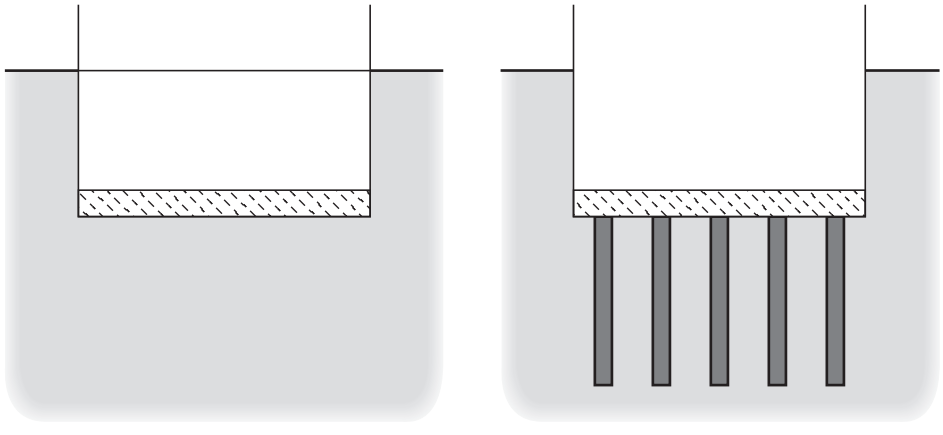

Figure 12.60 A conventional mat foundation and a pile-supported (or pile-enhanced) mat foundation.

SUMMARY

Major Points

1. Deep foundations are those that transfer some or all of the structural loads to deeper soils.
2. We can classify deep foundations based on the method of construction. Major classifications include:
   a. Piles
   b. Caissons
   c. Pile-supported mats
   d. Anchors
3. Load transfer analyses normally divide the applied loads into two categories: axial loads (tension and compression) and lateral loads (shear and moment).
4. Deep foundations transfer axial loads to the ground through two mechanisms: side friction and toe bearing.
5. Foundation installation methods significantly affect the side friction and toe bearing developed by a deep foundation. The amount of soil displaced during construction is an important parameter affecting foundation capacity.
6. Piles are long skinny foundation elements subdivided into the following two groups based on installation method:
   a. Driven piles: prefabricated members that are driven, vibrated, or pushed into the ground. They are made of wood, concrete, steel, and other materials. Each has its advantages and disadvantages, and is best suited for particular applications.
   b. Drilled or augered piles: members that are cast in the ground during construction either while or after the shaft in which they are placed is created.
7. Driven piles include:
   a. Timber piles
   b. Steel piles: H-piles, open-ended pipe piles, and closed-ended pipe piles
   c. Precast concrete piles: both prestressed and conventionally reinforced
   d. Pressure-injected footings or Franki piles

   Each has its advantages and disadvantages, and is best suited for particular applications.
8. Drilled or augered piles include:
   a. Drilled shafts: constructed by drilling a cylindrical hole and casting the concrete in place. Various methods are available for drilling the hole and for keeping it open until the concrete is placed. An underreamed shaft is one that has an enlarged base. This design increases the allowable toe bearing load.
   b. Auger-cast piles: constructed by injecting cement grout at high pressure through a hollow stem auger. They generally have lower capacity than piles or drilled shafts, but also are generally less expensive, especially in squeezing or caving soil conditions.

9. A caisson is a prefabricated box or cylinder that is sunk into the ground to form a foundation. They are most often used for bridges and other structures that require foundations beneath rivers or other bodies of water.
10. Pile-supported or pile-enhanced mats consist of a mat foundation underlain by a deep foundation. These are often designed so the mat supports some of the load, and the deep foundations support the balance.
11. Anchors are special deep foundations designed primarily to resist tensile forces.

Vocabulary

Anchor
Anvil
Appurtenances
Auger cast in place pile (ACIP)
Auger pile
Belled pile
Brooming
Bucket auger
Caisson
Capblock
Casing method
Caving soil
Cleanout bucket
Closed-end pipe pile
Composite pile
Continuous flight auger (CFA) pile
Cushion
Deep foundation
Diesel hammer
Differential hammer
Double-acting hammer
Drilled displacement (DD) pile
Drilled shaft
Drilling mud
Drilling rig
Driven pile
Drop hammer
Dry method
Flight auger
Franki pile
Hammer cushion
Head
Helical piles
Helmet
High displacement piles
Hydraulic hammer
Jetting
Leads
Low displacement piles
Medium displacement piles
Open caisson
Open-end pipe pile
Over-augering
Pile
Pile cap
Pile cushion
Pile driver
Pile group
Pile hammer
Pile head
Pile toe
Pile-enhanced mat
Pile-supported mat
Pneumatic caisson
Pneumatic hammer
Post grouting
Predrilling
Pressure-injected footing
Prestressed concrete
Ram
Refusal
Side friction resistance
Single-acting hammer
Slurry method
Small displacement pile
Soil plug
Spudding
Squeezing soil
Steam hammer
Steel H-pile
Steel pipe pile
Step-taper pile
Striker plate
Timber pile
Toe
Toe bearing resistance
Tremie
Underreamed shaft
Vibratory hammer

QUESTIONS AND PRACTICE PROBLEMS

12.1 What is meant by a low displacement versus high displacement pile? Why is it important to distinguish between the two?

12.2 Discuss some of the primary advantages and disadvantages of the following types of driven piles and suggest a potential application for each:
- Timber
- Steel
- Prestressed concrete

12.3 What is predrilling and when might it be used? What might happen if the predrill diameter or length was excessive?

12.4 What type or types of piles would be appropriate to support a heavy structure on an undulating bedrock surface located 25 to 40 m below the ground surface? Assume the side friction in the overlying soils provides less than 20 percent of the total axial load capacity. Explain the reasons for your choice.

12.5 Pressure-injected footings are best suited for sandy or gravelly soils with less than about 15 percent fines. Why would this construction method be less effective in a stiff saturated clay?

12.6 Why are most driven concrete piles prestressed instead of being conventionally reinforced?

12.7 In the context of pile construction, what are cushions, when are they used, and what is their purpose?

12.8 Pile foundations that support buildings usually have at least three piles for each column. Why?

12.9 Pile driving in loose sands without predrilling tends to densify these soils. What effect does this densification have on the load bearing capacity of such piles?

12.10 Describe the difference in construction between drilled shafts and auger piles. Compare the advantages and disadvantages of each.

12.11 Explain the differences in construction between ACIP piles and DD piles. Give examples of soil conditions where each type would be best suited.

12.12 Both driven piles and auger piles can be good foundations in loose to medium sands, but drilled shafts are generally a less viable choice in these conditions. Explain why.

12.13 In what circumstances would you expect caving or squeezing conditions to be a problem? What construction methods could a contractor use to overcome these problems?

12.14 The dry method of drilled shaft construction is most suitable for which types of soil conditions?

12.15 There are many ways to build midstream foundations for bridges that cross rivers and other bodies of water. One of them is to use a caisson, as described in this chapter. Another is to drive piles from a barge. Suggest some advantages and disadvantages of these two methods.

12.16 Suggest some critical items that a construction inspector should watch for during the construction of auger piles.

12.17 Create a table with five columns labeled "foundation type," "typical applications," "best soil conditions," "advantages," and "disadvantages." Under the column "foundation type" label the rows "driven piles," "auger piles", "drilled shafts," and "caissons," Fill in each cell of this table with the appropriate information for each foundation type.

12.18 A proposed ten-story office building is to be supported on a series of deep foundations embedded 60 ft below the ground surface. The soils at this site are loose to medium dense well-graded sands (SW) and silty sands (SM), and the groundwater table is at a depth of 12 ft. What type or types of deep foundations would be most appropriate for this project? What type or types would probably not be appropriate? Explain the reasons for your selections.

12.19 A new reinforced concrete pier is to be built in a major harbor area. This pier will service ocean-going cargo ships. The underlying soils are primarily low plasticity silts (ML) and clays (CL), with some interbedded sand layers. What type or types of deep foundations would be most appropriate for this project? What type or types would probably not be appropriate? Explain the reasons for your selections.

A heavily loaded warehouse is to be constructed on a saturated medium clay that overlays a stiff undulating bedrock. What type or types of deep foundations would be most appropriate for this project? What type or types would probably not be appropriate? Explain the reasons for your selections.

13

Piles—Load Transfer and Limit States

Once a theory appears on the question sheet of a college examination, it turns into something to be feared and believed, and many of the engineers who were benefited by a college education applied the theories without even suspecting the narrow limits of their validity.

Karl Terzaghi—from an address to the Harvard Conference of the International Society of Soil Mechanics and Foundation Engineering, June 22 to 26, 1936.

This chapter discusses the mechanics of transferring structural loads through pile foundations and into the ground. Unlike shallow foundations, piles transfer load to the soil both along their sides as well as at the base or end of the foundation element, as show in Figure 13.1, so the mechanics are more complex. There also are important differences in the transfer of applied shear and moment loads. This chapter also sets up standard formulations describing these load transfer processes, which will be used in subsequent chapters, and describes the various geotechnical and structural limit states.

The term "capacity" or "load capacity" is often used in this context. However, this term has many different meanings, so it is important to be very careful. It can refer either to the *nominal load capacity*, which is the load required to cause failure, or the *allowable load capacity*, which is the ultimate load capacity divided by a factor of safety. Confusion between these two definitions has often been a source of misunderstandings and litigation. Therefore, the term *load capacity* without any adjective should be used only in a generic sense, such as in the title of this chapter. However, when referring directly or indirectly to a numerical value, always include the adjective "nominal" or "allowable."

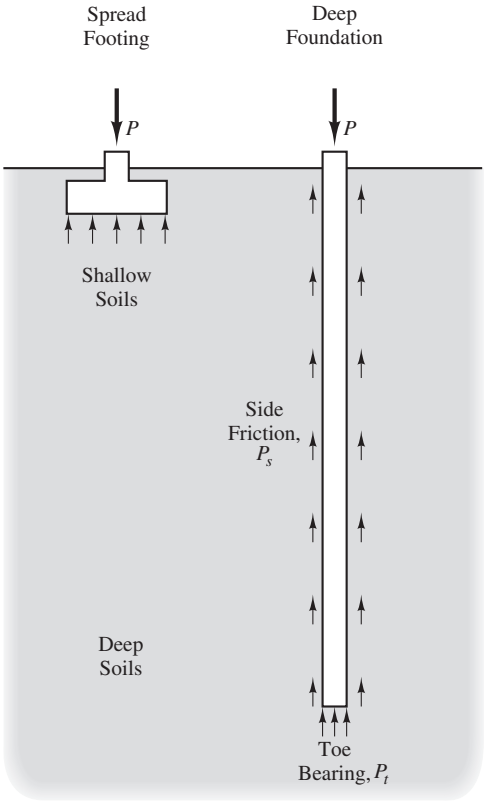

Figure 13.1 Comparison of the load transfer mechanisms in shallow versus pile foundations.

The structural loads applied to piles may be divided into two broad categories: *axial loads* and *lateral loads*. Axial loads are those that act parallel to the longitudinal axis of the pile. The most common case is a vertical pile subjected to a downward axial load, which induces compressive stresses, as shown in Figure 13.2a. In some cases, the pile is subjected to an upward load, which induces tensile stresses, as shown in Figure 13.2b. In contrast, lateral loads act perpendicular to the longitudinal axis and induce flexural stresses in the pile. There are two types of lateral loads, shear and moment, as shown in Figure 13.2c. In many cases, both axial and lateral loads are applied concurrently.

The transfer of axial loads through the pile and into the ground is very different from the transfer of lateral loads, so these two types of loading are analyzed separately.

13.1 AXIAL LOAD TRANSFER

Piles transfer applied axial loads into the ground via two mechanisms: *toe bearing* and *side friction*, as shown in Figure 13.1. The toe bearing resistance (also known as *point bearing resistance*, *tip bearing resistance*, or *end bearing resistance*) is the result of compressive loading between the bottom of the pile and the soil, and thus is similar to the load transfer

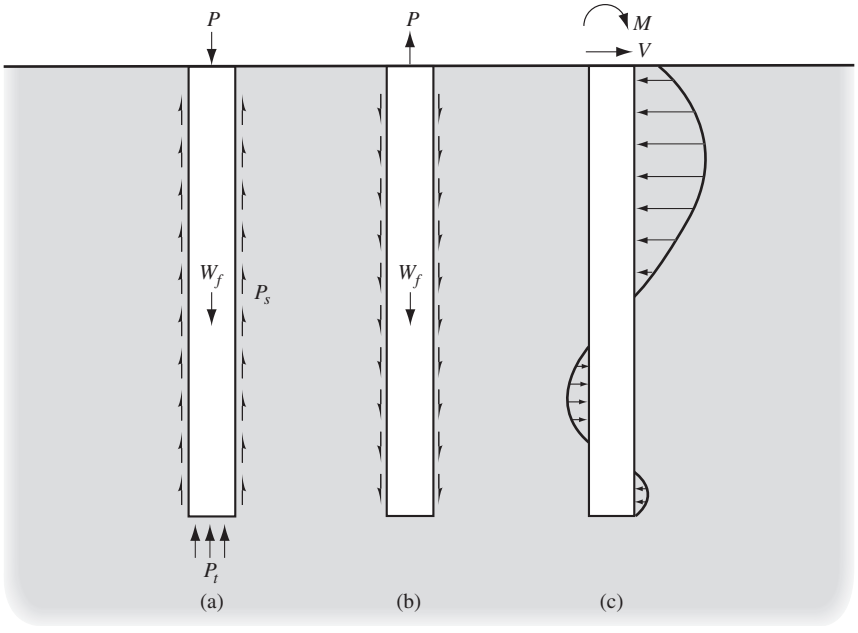

Figure 13.2 Transfer of structural loads from a pile foundation into the ground: (a) axial downward (compressive) loads, (b) axial upward (tensile) loads, and (c) lateral loads.

from spread footings to the underlying ground. In contrast, the side friction resistance (also known as *skin friction resistance*) is the result of sliding friction along the side of the pile and adhesion between the soil and the pile.

Due to the similarity with bearing pressure in a spread footing, we will use the same variable, q, to describe the *gross toe bearing resistance*:

$$q = \frac{P_t}{A_t} \tag{13.1}$$

where

q = gross toe bearing resistance
P_t = axial load mobilized between the pile toe and the underlying soil
A_t = pile toe contact area

However, unlike spread footings, it is customary to evaluate toe bearing using the *net toe bearing resistance*, q', which implicitly accounts for the weight of the pile:

$$q' = \frac{P_t'}{A_t} = \frac{P_t - W_f}{A_t} \tag{13.2}$$

where

q' = net toe bearing resistance
W_f = weight of the foundation

The value of q' at failure is the *nominal unit toe bearing capacity*, q'_n, which is similar to the nominal bearing capacity in spread footing design, as discussed in Chapter 7, except that this is a net value. However, the computation of q'_n uses very different methods than those used for spread footings, as described in the following chapters.

The *mobilized unit side friction resistance*, f, is the side force transferred from the pile to the ground, P_s, per square foot of pile side contact area, A_s:

$$f = \frac{P_s}{A_s} \tag{13.3}$$

The value of f nearly always varies along the length of the pile as the soil type and in situ stress conditions vary with depth. The value of f at failure is the *nominal unit side friction capacity*, f_n.

Downward (Compressive) Loads

Piles transfer an applied downward (or compressive) axial load, P, into the ground through a combination of toe bearing and side friction:

$$P = q'A_t + \sum fA_s \tag{13.4}$$

where the side friction is summed along the length of the pile. The *nominal downward load capacity*, P_n, is achieved when both the toe bearing and side friction reach their nominal capacities:

$$P_n = q'_n A_t + \sum f_n A_s \tag{13.5}$$

This value will then be used in ultimate limit state analyses, as discussed in the following chapters.

Upward (Tensile) Loads

The upward (tensile) load capacity of a shallow foundation is limited to its weight. However, piles use both the weight and the side friction (which now acts in the opposite direction), and thus are more effective in resisting upward loads. Piles with expanded bases, such as pressure-injected footings or belled drilled shafts, can resist additional uplift loads through bearing on top of the base.

Some piles are subjected to long-term static upward loading. For example, this might be the case on the outboard leg of an electrical transmission tower located at a point

where the alignment of the wires changes direction. In that case the overturning moment from the wires is greater than the weight of the tower, so some of the piles are in tension. The more common case is encountered in tall slender buildings and other structures subjected to large lateral loads, such as wind or seismic. In this case, some of the piles may be subjected to downward loads under normal conditions, but a net uplift load when the design wind or seismic loads are present.

The *nominal upward load capacity*, $P_{up,n}$, for straight piles with $D/B > 6$ is:

$$P_{up,n} = W_f + \sum f_n A_s \tag{13.6}$$

where

$P_{up,n}$ = nominal upward load capacity
W_f = weight of the foundation (considering buoyancy, if necessary)
f_s = unit side friction resistance
A_s = side friction contact area

In this case, the weight of the pile is explicitly considered, and contributes to the upward capacity. If some or all of the pile is below the groundwater table, then buoyancy must be considered, typically by computing the submerged volume times the unit weight of water and subtracting this value from the dry weight.

If $D/B < 6$, a cone of soil may form around the foundation during an upward failure. This reduces its uplift capacity (Kulhawy, 1991). Fortunately, the vast majority of piles are long enough to avoid this problem, so the side friction resistance may be assumed to be equal to that for downward loading.

Cyclic up-and-down loads can be more troublesome than static loads of equal magnitude. Turner and Kulhawy (1990) studied piles in cohesionless soils and found that cyclic loads smaller than a certain critical level do not cause failure, but enough cycles larger than that level cause the pile to fail in uplift. The greatest differences between static and cyclic capacities seem to occur in dense sands and in foundations with large depth-to-diameter ratios.

Piles with enlarged bases, such as belled drilled shafts or pressure-injected footings, gain additional upward capacity from bearing on top of the base. Methods of evaluating this additional capacity are discussed in Chapters 16 and 18.

Contact Areas A_t and A_s

When using Equations 13.4 to 13.6, we must evaluate the toe-bearing and side friction contact areas, A_t and A_s. The method of doing so depends on the shape and type of pile.

Closed-Section Piles

A *closed-section pile* is one in which the foundation-soil contact occurs along a well-defined surface around its perimeter. This includes virtually all piles except H-piles and

open-end pipe piles. Because of their simple geometry, it is easy to compute the toe-bearing and side friction contact areas, A_t and A_s. The design value of A_t is simply the toe area of the pile (i.e., the solid cross-sectional area), while A_s for a particular stratum is the foundation surface area in contact with that stratum.

Closed-section piles with enlarged bases, such as underreamed drilled shafts or pressure-injected footings, are slightly more complex. We use the full base area to compute A_t, but consider A_s only in the straight portion of the shaft, ignoring the side of the enlargement.

Open-Section Piles

Open-section piles (including open-end steel pipe piles and steel H-piles) are those that have poorly defined foundation-soil contacts. These poorly defined contacts make it more difficult to compute A_t and A_s.

When open-end pipe piles are driven, they initially "cookie cut" into the ground, and the toe-bearing area, A_t, is equal to the cross-sectional area of the steel. Soil enters the pipe interior as the pile advances downward. At some point, the soil inside the pile becomes rigidly embedded and begins moving downward with the pile. It has then become a *soil plug*, as shown in Figure 13.3, and the toe-bearing area then becomes the cross-sectional area of the pile and the soil plug. In other words, the pile now behaves almost the same as a closed-end pipe (i.e., one that has a circular steel plate welded to the bottom).

Many factors affect the formation of soil plugs (Paikowsky and Whitman, 1990; Miller and Lutenegger, 1997), including the soil type, soil consistency, in situ stresses, pile diameter, pile penetration depth, method of installation, rate of penetration, and so forth. In open-end steel pipe piles, the soil plug may be considered rigidly embedded when the penetration-to-diameter ratio, D/B, is greater than 10 to 20 (in cohesive soils) or 25 to 35 (in cohesionless) (Paikowsky and Whitman, 1990). Many piles satisfy these criteria.

Once they become plugged, open-end pipe piles have the same side friction area, A_s, as closed-end piles. We use only the outside of pipe piles when computing the side friction area and do not include the friction between the plug and the inside of the pile.

With H-piles, soil plugging affects both toe-bearing and side friction contact areas. The space between the flanges of H-piles is much smaller than the space inside pipe piles, so less penetration is required to form a soil plug. For analysis purposes, we usually can compute A_t and A_s in H-piles based on the assumption they become fully plugged as shown in Figure 13.3.

If open-section foundations are driven to bedrock, the relative stiffnesses of the steel, soil plug, and bedrock are such that the toe-bearing probably occurs primarily between the steel and the rock. Therefore, in this case it is generally best to use A_t equal to the cross-sectional area of the steel, A_s, and ignore any plugging in the toe-bearing computations.

Unit Capacities

There are a number of different approaches to determining the *nominal unit toe bearing capacity*, q'_n, and the *nominal unit side friction capacity*, f_n, all of are a combination of

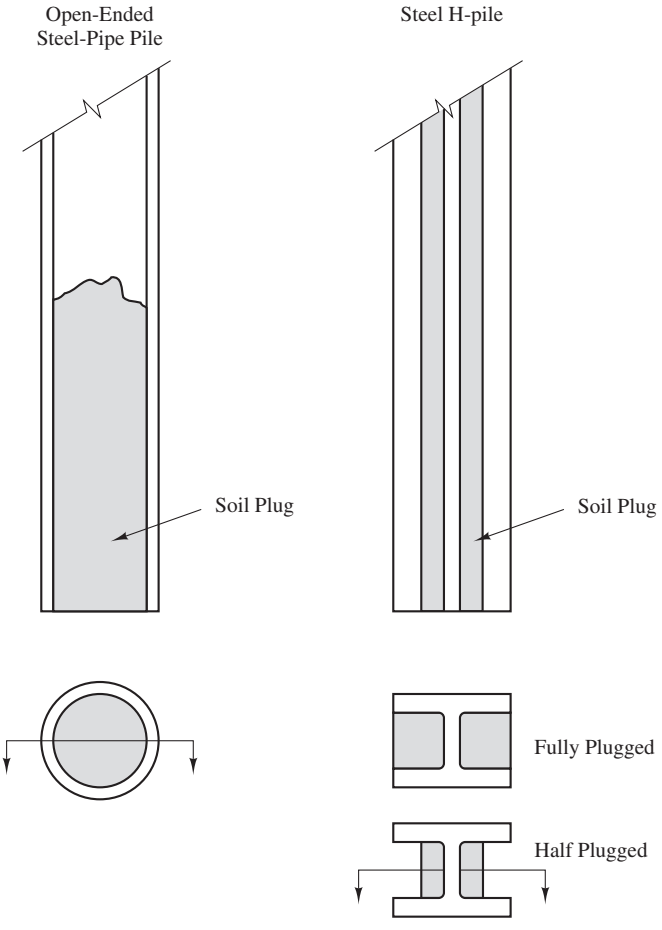

Figure 13.3 Soil plugging in open-ended steel pipe piles and steel H-piles.

theory and empiricism to differing degrees. Broadly the methods can be categorized into three groups:

- Static load tests, which consist of constructing a full-size prototype pile at the project site, applying a series of test loads, and experimentally determining the pile capacity. These methods are discussed in Chapter 14.
- Static analysis methods, which consist of computing the unit capacities based on the soil properties and other factors, These methods are discussed in Chapters 15 to 18.
- Dynamic methods, which use an analysis of the dynamics of pile driving, or other dynamic loads, to determine the static pile capacity. These methods are discussed in Chapter 19.

Each method has its own advantages, disadvantages, uncertainties, and methodologies, and each is applicable for specific situations.

Ultimate Limit States

The geotechnical ultimate limit state (ULS) addresses the transfer of axial loads from the pile into the soil, and the soil's capacity to carry these loads. In other words, these methods apply the values of P_n and $P_{up,n}$, to the design process. There are two methodologies for doing so: allowable stress design (ASD) and load and resistance factor design (LRFD), as discussed in Chapter 5.

The structural ULS addresses the structural capacity of the pile itself to sustain the stresses induced by the structural load. Again, both ASD and LRFD methods are used.

Geotechnical Ultimate Limit State

Allowable Stress Design Methodology

Using the ASD method, the allowable downward and uplift capacities, P_a and $P_{up,a}$, are:

$$P_a = \frac{P_n}{F} \tag{13.7}$$

$$P_{up,a} = \frac{P_{up,n}}{F} \tag{13.8}$$

where F is the factor of safety. The design factor of safety, F, depends on many factors, including the following:

- **The type and importance of the structure and the consequences of failure**—Foundations for critical structures, such as major bridges, should have a higher factor of safety; those for minor uninhabited structures could use a lower factor of safety.
- **The soil type**—Use a higher factor of safety in cohesive soils.
- **The spatial variability of the soil**—Erratic soil profiles are more difficult to assess, and therefore justify the use of a higher factor of safety.
- **The thoroughness of the subsurface exploration program**—Intensive subsurface exploration programs provide more information on the subsurface conditions, and therefore can justify a lower factor of safety.
- **The type and number of soil tests performed**—Extensive laboratory and/or in situ tests also provide more information on the soil conditions and can justify a lower factor of safety.
- **The availability of on-site or nearby full-scale static load test results**—These tests, which are described later in this chapter, are the most reliable way to determine load capacity, and thus provide a strong basis for using a lower factor of safety.
- **The availability of on-site or nearby dynamic test results**—These tests, which are described in Chapter 15, also provide insights and can justify lower factors of safety.

- **The level of construction inspection and quality control**—If thorough inspection and quality control methods can be implemented, lower factors of safety may be justified. Conversely if a lack of control is expected, higher factors of safety should be used.
- **The probability of the design loads actually occurring during the life of the structure**—Some structures, such as office buildings, are unlikely to ever produce the design live loads, whereas others, such as tanks, probably will. Thus, the later might require a higher factor of safety.

Because of these many factors that must be considered, and the need for appropriate engineering judgment, the engineer usually has a great deal of discretion to determine the appropriate factor of safety for a given design.

It is good practice to use higher factors of safety for analyses of upward loads because uplift failures are much more sudden and catastrophic. For example, some pile foundations in Mexico City failed in uplift during the 1985 earthquake and heaved 3 m (10 ft) out of the ground. Therefore, most engineers use design values 1.5 to 2.0 times higher than those for downward loading.

Table 13.1 presents typical design factors of safety for driven piles based on the type of construction control. These methods have not yet been described, but will be covered later in this chapter and in the following chapters. The values in this table are for piles used to support ordinary structures on typical soil profiles with average site characterization programs. Higher or lower values might be used for other conditions.

Except for full-scale load tests, the construction control methods described in Table 13.1 are based on the dynamics of pile driving, and thus are not applicable to drilled

TABLE 13.1 FACTORS OF SAFETY FOR DESIGN OF PILES

	Factor of Safety, F	
Construction Control Method[a]	Downward Loading (Hannigan et al., 2006)	Upward Loading
Static load test with wave equation analysis	2.00[b]	3.00[b]
Dynamic testing with wave equation analysis	2.25	4.00
Indicator piles with wave equation analysis	2.50	5.00
Wave equation analysis	2.75	5.50
Pile driving formula[c]	3.50	6.00

[a] Most of these terms have not yet been defined, but all of them will be discussed later in this chapter and in the following chapters.

[b] If the static load testing program is very extensive, the factors of safety for downward and uplift loads might be reduced to about 1.7 and 2.5, respectively.

[c] Hannigan et al. refer specifically to the Gates formula.

shaft foundations. Therefore, the factor of safety for drilled shafts depends primarily on the availability of static load test information, the uniformity of the soil conditions, and the thoroughness of the site characterization program. Table 13.2 presents typical factors of safety for design of drilled shafts that will support ordinary structures. Once again, the engineer might use higher or lower values for other conditions. For example, foundations supporting an especially critical structure might be designed using a higher value, while those supporting a temporary structure might use a lower value.

Other types of piles should generally be designed using factors of safety in the same range as those presented in Tables 13.1 and 13.2. The selection of these factors of safety depends on the various factors described earlier.

The actual factor of safety for both downward and upward loading (i.e., the real capacity divided by the real load) is usually much higher than the design F used in the formulas. This is because of the following:

- We usually interpret the soil strength data conservatively.
- The actual service loads are probably less than the design loads, especially in buildings other than warehouses.
- The as-built dimensions of the foundation may be larger than planned.
- Some (but not all!) of the analysis methods are conservative.

The design must then satisfy the following criteria:

$$P \leq P_a \tag{13.9}$$

$$P_{up} \leq P_{up,a} \tag{13.10}$$

where P and P_{up} are the unfactored design downward and uplift loads applied to the top of the pile. These design loads are determined using various load combinations as dictated

TABLE 13.2 FACTORS OF SAFETY FOR DESIGN OF DRILLED SHAFTS

Design Information			Factor of Safety, F	
Static Load Test	Soil Conditions	Site Characterization Program	Downward Loading	Upward Loading
Yes	Uniform	Extensive	2.00[a]	3.00[a]
Yes	Erratic	Average	2.50	4.00
No	Uniform	Extensive	2.50	5.00
No	Uniform	Average	3.00	6.00
No	Erratic	Extensive	3.00	6.00
No	Erratic	Average	3.50	6.00

a. If the static load testing program is very extensive, the factors of safety for downward and uplift loads might be reduced to about 1.7 and 2.5, respectively.

by the appropriate code and described in Chapter 5. In the case of structures governed by ASCE 7, Equations 5.2 through 5.8 should be used to determine the design loads.

Load and Resistance Factor Design Methodology

As discussed in Chapter 5, the LRFD methodology applies factors to both the loads and the resistances. Thus, using this methodology, the pile design must satisfy the following criteria:

$$\sum \gamma_i P_i \leq \phi P_n \tag{13.11}$$

$$\sum \gamma_i P_{up,i} \leq \phi P_{up,n} \tag{13.12}$$

where

γ_i = load factor
P_i = downward load component
$P_{up,i}$ = upward load component
ϕ = resistance factor
P_n = nominal downward load capacity
$P_{up,n}$ = nominal upward load capacity

Some analysis methods use separate resistance factors for toe bearing and side friction. In that case, the right side of the inequalities in Equations 13.11 and 13.12 becomes:

$$\phi P_n = \phi_t q_n' A_t + \phi_s \sum f_s A_s \tag{13.13}$$

$$\phi P_{up,n} = \gamma_D W_f + \phi_s \sum f_s A_s \tag{13.14}$$

where

ϕ_t = resistance factor for toe bearing
ϕ_s = resistance factor for side friction
γ_D = load factor for dead loads. (When dead loads act as a resisting element as in Equation 13.14, γ_D will be 0.9 as shown in Equations 5.17 and 5.18).

Tables 13.3, 13.4, and 13.5 present the AASHTO values of geotechnical resistance factors for pile design. Selection of the appropriate factor requires further understanding of the methods used to determine the capacity, which are discussed in Chapters 14 to 19. The resistance factors in Tables 13.3, 13.4, and 13.5 were calibrated using AASHTO load factors, as discussed in Chapter 5, and may be used only when the ultimate load is computed using the AASHTO load factors and load combinations. Analyses using ultimate loads computed using the ASCE 7 load factors and load combinations require a different set of resistance factors. Unfortunately, ASCE 7 compatible geotechnical resistance factors have not yet been developed.

TABLE 13.3 GEOTECHNICAL RESISTANCE FACTORS FOR DRIVEN PILES USING DYNAMIC ANALYSES, LOAD TESTS, AND PILE DRIVING FORMULAS (AASHTO LRFD Bridge Design Manual, 2012)

Method Used to Determine Pile Capacity	Resistance Factor, ϕ
Driving criteria established by successful static load test of at least one pile per site condition and dynamic testing* of at least two piles per site condition, but no less than 2% of the production piles	0.80
Driving criteria established by successful static load test of at least one pile per site condition without dynamic testing	0.75
Driving criteria established by dynamic testing* conducted on 100% of production piles	0.75
Driving criteria established by dynamic testing,* and quality control by dynamic testing* of at least two piles per site condition, but no less than 2% of the production piles	0.65
Wave equation analysis, without pile dynamic measurements or load test but with field confirmation of hammer performance	0.50
Federal Highway Administration-modified Gates dynamic pile formula (End of Drive condition only)	0.40
Engineering News (as defined in Article 10.7.3.8.5) dynamic pile formula (End of Drive condition only)	0.10

* Dynamic testing requires signal matching, and best estimates of nominal resistance are made from a restrike. Dynamic tests are calibrated to the static load test, when available.

TABLE 13.4 GEOTECHNICAL RESISTANCE FACTORS FOR DRIVEN PILES USING STATIC ANALYSIS METHODS (AASHTO LRFD Bridge Design Manual, 2012)

Failure Mode	Analysis Method and Material	Resistance Factor, ϕ
Axial downward resistance of single piles	Side resistance and end bearing: cohesive and mixed materials	
	α-method (Tomlinson, 1987; Skempton, 1951)	0.35
	β-method (Esrig and Kirby, 1979; Skempton, 1951)	0.25
	λ-method (Vijayvergiya and Focht, 1972; Skempton, 1951)	0.40
	Side resistance and end bearing: cohesionless material	
	Nordlund/Thurman Method (Hannigan et al., 2006)	0.45
	SPT-method (Meyerhof)	0.30
	CPT-method (Schmertmann)	0.50
	End bearing in rock (Canadian Geotechnical Society, 1985)	0.45
Group failure	Cohesive material	0.60

Failure Mode	Analysis Method and Material	Resistance Factor, ϕ
Axial uplift resistance of single piles	Nordlund method	0.35
	α-method	0.25
	β-method	0.20
	λ-method	0.30
	SPT-method	0.25
	CPT-method	0.40
	Static load test	0.60
	Dynamic test with signal matching	0.50
Group uplift	All soils	0.50
Lateral resistance of single piles	All soils and rock	1.0

TABLE 13.5 GEOTECHNICAL RESISTANCE FACTORS FOR DRILLED SHAFTS USING STATIC ANALYSIS METHODS AND LOAD TESTS (AASHTO LRFD Bridge Design Manual, 2012)

Failure Mode	Component and Material	Analysis Method	Resistance Factor, ϕ
Axial downward resistance of single drilled shaft	Side resistance in clay	α-method (O'Neill and Reese, 1999)	0.45
	Tip resistance in clay	Total stress (O'Neill and Reese, 1999)	0.40
	Side resistance in sand	β-method (O'Neill and Reese, 1999)	0.55
	Tip resistance in sand	O'Neill and Reese (1999)	0.50
	Side resistance in IGM*	O'Neill and Reese (1999)	0.60
	Tip resistance in IGM*	O'Neill and Reese (1999)	0.55
	Side resistance in rock	Horvath and Kenney (1979)	0.55
		O'Neill and Reese (1999)	
	Side resistance in rock	Carter and Kulhawy (1988)	0.50
		Canadian Geotechnical Society (1985)	
	Tip resistance in rock	Pressuremeter Method (Canadian Geotechnical Society, 1985)	0.50
		O'Neill and Reese (1999)	

(*continued*)

TABLE 13.5 (Continued)

Failure Mode	Component and Material	Analysis Method	Resistance Factor, ϕ
Group failure	Clay		0.55
Axial uplift resistance of single drilled shaft	Clay	α-method (O'Neill and Reese, 1999)	0.35
	Sand	β-method (O'Neill and Reese, 1999)	0.45
	Rock	Horvath and Kenney (1979) Carter and Kulhawy (1988)	0.40
Group uplift	Sand and clay		0.45
Horizontal geotechnical resistance of single shaft or shaft group	All materials		1.0
Static load test (compression)	All materials		0.70
Static load test (uplift)	All materials		0.60

* Intermediate geotechnical material

Structural ultimate limit state

The structural ULS uses Equations 13.11 and 13.12 except now the values of P_n and $P_{up,n}$ represent the compressive and tensile structural capacities of the pile itself. The factors of safety and resistance factors also are correspondingly different from those used in the geotechnical ULS analysis. Methods for evaluating the structural ULS are discussed in Chapter 21.

Serviceability Limit States

Axially loaded pile designs also must satisfy serviceability limit state (SLS) requirements. Settlement is an important SLS requirement for downward loading, and heave for uplift loading. The allowable values should be determined using the methods discussed in Chapter 5, and the design must satisfy the following criterion:

$$\delta \leq \delta_a \tag{13.15}$$

where

δ = settlement (or heave)
δ_a = allowable settlement (or heave)

Chapter 20 discusses methods for evaluating SLS settlement criteria for piles. Chapter 23 describes other SLS criteria. Allowable values are discussed in Chapter 8.

Mobilization of Soil Resistance

Stresses and strains always occur together. Whenever a stress is applied to a material, corresponding strains also develop. In other words, whenever we place a load on a material, it responds with a corresponding deformation. It is impossible to have one without the other.

This relationship between load and deformation helps us understand how piles respond to applied loads. As discussed earlier in this chapter, downward loads acting on piles are resisted by side friction resistance and toe bearing resistance. We compute each of these components separately, then combine them using Equation 13.4 to find the nominal downward load capacity. However, neither of these resistances can develop without a corresponding deformation (settlement) of the pile. Therefore, in addition to evaluating the nominal toe bearing and side friction capacities, we also should know something about the settlement required to mobilize these capacities.

Side friction resistance is typically mobilized as shown in Figure 13.4, with 5 to 10 mm (0.2–0.4 in) of shear displacement required to reach 90% of the nominal side friction capacity, f_n, and 10 to 20 mm (0.4–0.8 in) to reach 100% of f_n. In addition, as it approaches the nominal capacity, the load-settlement curve becomes very steep, so the value of f_n is typically well defined.

In contrast, the load-settlement curve for toe bearing is not nearly as steep, as shown in Figure 13.4, and the nominal capacity is not as well defined. Thus, the definition of "nominal unit toe-bearing capacity" and the numerical value of q_n' become vague and subjective. In addition, a toe displacement of 12 to 20 percent of the foundation diameter is probably required to fully mobilize q_n' (Jamiolkowski, 2003), so even a comparatively small diameter pile (say $B = 400$ mm) would require perhaps 60 mm of toe displacement to fully mobilize the toe bearing, which is four times that required to mobilize the side friction. In larger-diameter piles this difference is even greater. Customary practice typically defines q_n' at a toe settlement equal to 10 percent of the diameter, which is

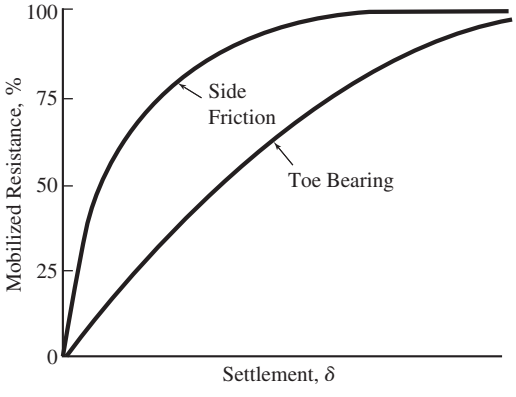

Figure 13.4 Load-displacement relationships for side friction and toe bearing under downward loads.

conservative in terms of strength requirements and implicitly intended to provide some conformance with serviceability requirements.

The pile itself also experiences elastic compression during loading, which is another source of apparent settlement at the top. This source of settlement can be computed using:

$$\delta_e = \int \frac{P}{AE} dz \tag{13.16}$$

where

δ_e = settlement at pile due to elastic compression of the pile
P = compressive load in the pile
A = cross-sectional area of the pile
E = modulus of elasticity of the pile (see Section 14.3)
z = depth below top of foundation

Thus, the settlement at the toe of the pile is less than that at the top. In some cases this difference can be significant, especially in very long and/or heavily loaded piles. Chapters 14 and 20 discuss these processes in more detail.

13.2 LATERAL LOAD TRANSFER

One of major advantages of piles over spread footings is their ability to transfer large lateral loads into the soil. This is particularly useful for structures that carry significant wind or earthquake loads. Lateral pile loads are carried through a combination of shear and bending in the pile and lateral earth pressures in the soil.

Figure 13.5 illustrates how a lateral load applied at the pile head is transferred to the soil. Figure 13.5a shows the distribution of net lateral pressure transferred from the pile to the soil along the length of the pile. The distribution of this soil pressure depends upon the section modulus of the pile and the stiffness of the soil. A short stiff pile will transfer loads along most of its length while a long flexible pile will transfer most of the lateral load in the upper portion of the pile. Figures 13.5b and c illustrate how the lateral stresses are developed at a given section of the pile during loading. When there is no shear load applied to the pile head, the lateral stress is equal all around the pile and the net lateral resistance is zero as shown in Figure 13.5b. As the lateral load at the head is increased, the lateral resistance increases in the direction of pile displacement and decreases on the opposite side of the pile as shown in Figure 13.5c. If the lateral load continues to increase, the soil around the pile will eventually reach a state of plastic failure and the net lateral load of the soil acting on the pile will reach the nominal geotechnical lateral load capacity. As the pile deflects under an applied lateral load, flexural stresses develop inside the pile, and at some point reach the nominal structural lateral load capacity. The lesser of these two capacities would be the controlling ULS.

The lateral deflection of the pile also is important, and must not exceed some allowable value. In this case, the serviceability limit state analysis considers both the structural

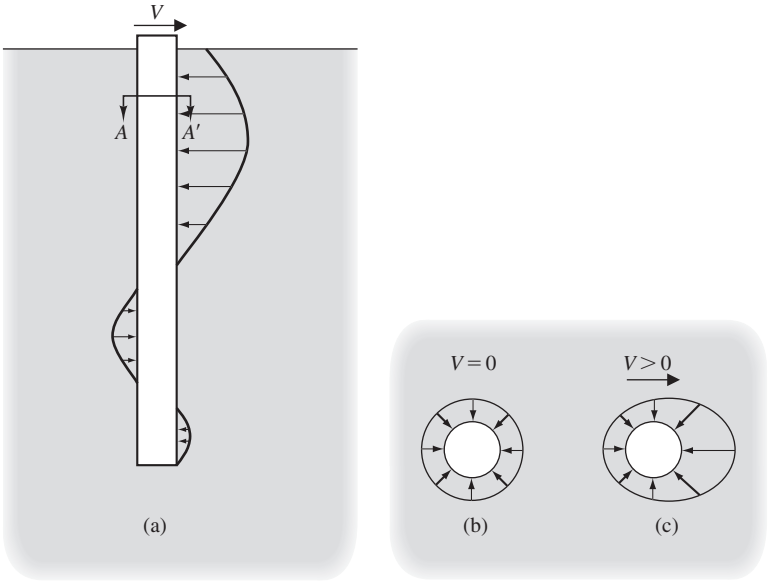

Figure 13.5 Load transfer in a laterally loaded pile. (a) Shows the vertical distribution of the net lateral force applied to the pile by the surrounding soil. (b) and (c) Show the distribution of lateral stress around the pile at a given cross section for different values of shear force at the top of the pile, V. (b) Shows a uniform distribution of lateral stress which occurs when the shear force is zero. As the shear force is increased, the lateral stress increases in the direction of pile displacement and decreases on the opposite side of the pile as shown in (c).

and geotechnical behavior concurrently. In practice, the lateral deflection often controls the design. Chapter 22 discusses lateral load behavior in much more detail.

13.3 INSTALLATION EFFECTS

Piles do not magically appear in the soil. They are placed or installed in the soil using one of the construction methods described in Chapter 12. The process of installing piles in the ground changes both the state of stress in the ground and the properties of the soil surrounding the pile. These changes are important because they alter the engineering properties of the soil, which means the pre-construction soil tests may not accurately reflect the post-construction conditions. Sometimes these changes are beneficial, while other times they are detrimental, but in either case they introduce another complexity into load capacity analyses. Therefore, in order to intelligently apply analytic methods of computing load capacity, the engineer must understand these changes.

Driven Piles

Driven pile construction causes major changes in a zone surrounding the pile including: movement of soil around the pile, changes in density in soil surrounding the pile, changes

in soil strength due to both changes in density and large shear deformations created, and in the case of saturated soils changes in excess pore water pressure. Additionally, there are longer-term changes in the soil that occur after pile installation due to dissipation of excess pore pressure and creep. The magnitude and characteristics of each of the changes will depend upon both the soil properties and the construction method.

Effects on Cohesive Soils

As a pile is driven into the ground, the soil below the pile is pushed out of the way. This displacement of the soils causes large deformations both in compression and shear. Additionally, the friction and adhesion along the sides of the pile causes additional displacement as soil is dragged along the sides of the pile. Figure 13.6 shows how soil is compressed below the pile toe and dragged down along the sides of a pile during installation. Note how the marker layers are bent down and pulled along the side of the pile. This phenomenon is called *dragdown* (not to be confused with downdrag covered in Chapter 23). Although the model pile shown in Figure 13.6 was installed in a cohesionless soil, the same phenomenon is observed in cohesive soil profiles. It is possible for soft or medium clay soils to be dragged down into stiffer clays or sand layers. The dragdown distance can be as much as three pile diameters (Tomlinson, 1987). Cooke and Price (1973) observed the distortion in London Clay as a result of driving a 168 mm (6.6 in) diameter closed-end pipe pile. The soil within a radius of 1.2 pile diameters from the edge of the pile was dragged down, while that between 1.2 and 9 diameters moved upward.

Another result related to soil movement important to driven piles in cohesive soils is loss of contact between pile and soil. Piles wobble during driving, thus creating gaps

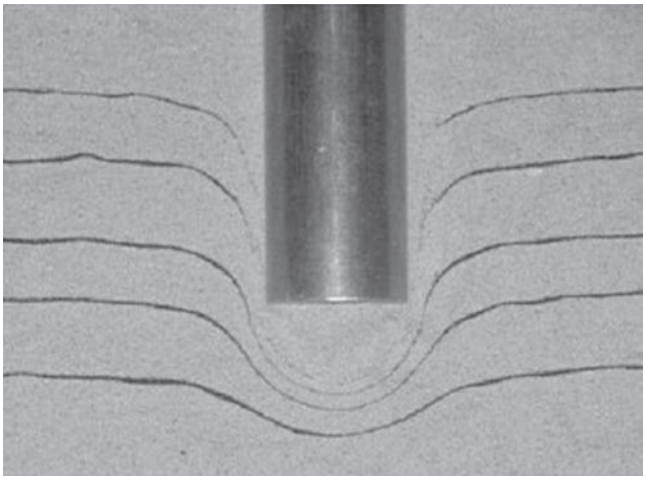

Figure 13.6 Photograph of a model pile jacked into a sandy soil. The dark lines are marker layers placed in the sand before the pile was jacked into the soil. The model pile is solid steel and therefore a high displacement pile. The marker layers clearly show the soil deformation caused by the installation of the pile (image courtesy of Professor David White, University of Western Australia).

between them and the soil. Soft clays will probably flow back into this gap, but stiff clays and clayey sands will not. Tomlinson (1987) observed such gaps extending to a depth of 8 to 16 diameters below the ground surface. Piles subjected to applied lateral loads also can create gaps near the ground surface. Therefore, the side friction in this zone may be unreliable, especially in stiff clays.

The large soil deformation during driving also remolds the soils around the pile. This remolding of the clay changes its structure and reduces its strength to a value near the residual strength. Bozozuk et al. (1978) present a case history of a large pile group of 116 reinforced concrete piles driven into a sensitive soft clay deposit. Immediately after driving, the soil adjacent to the piles had lost approximately 15 percent of its previous undrained shear strength. Three months later only a fraction of this strength loss had been regained. In spite of cases like this, current analysis techniques are based on the peak strength and implicitly consider the difference between peak and residual strength. An analysis based on the residual strength might be more reasonable, but no such method has yet been perfected.

Pile driving also compresses the adjoining soils. If saturated cohesive soils are present, this compression generates excess pore water pressures, as discussed in Chapter 3. The ratio of the excess pore water pressure, u_e, to the original vertical effective stress, σ_z', may be as high as 1.5 to 2.0 near the pile, gradually diminishing to zero at a distance of 30 to 40 pile radii, as shown in Figure 13.7. The greatest compression occurs near the pile toe, so u_e/σ_z' in that region may be as high as 3 to 4 (Airhart et al., 1969). These high pore

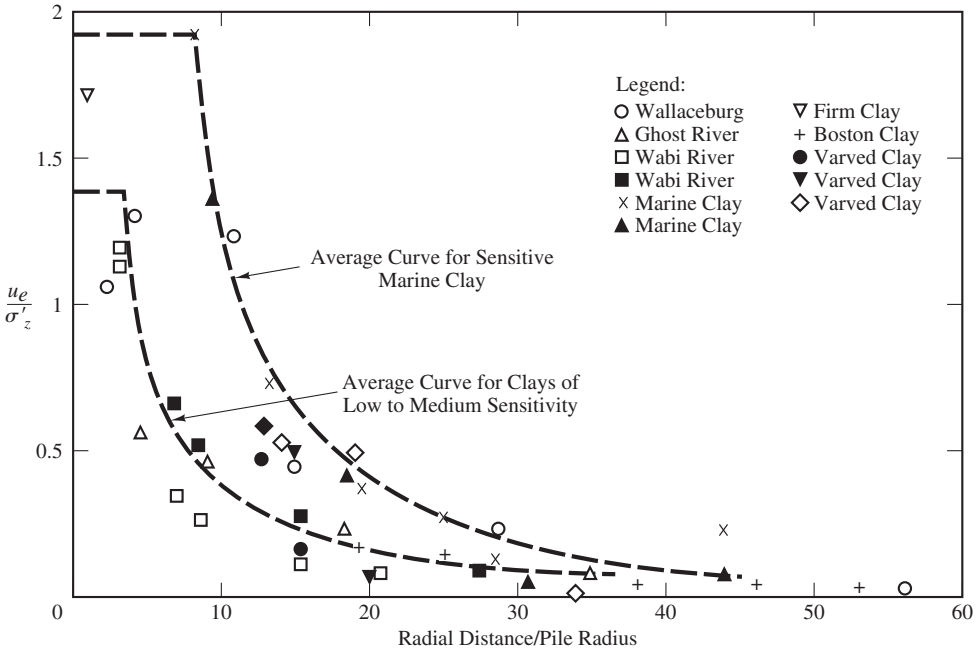

Figure 13.7 Summary of measured excess pore water pressures, u_e, in the soil surrounding isolated piles driven in saturate clay (data from *Pile Foundation Analysis and Design* by Poulos and Davis, 1980).

water pressures dramatically decrease the shear strength of the soil, which makes it easier to install the pile, but temporarily decreases its load-bearing capacity.

The presence of excess pore water pressures is always a transient condition because the resulting hydraulic gradient causes some of the water to flow; in this case, radially away from the pile. Thus, the pore water pressures eventually return to the hydrostatic condition. If the pile is timber, some of the water also might be absorbed into the wood. This, along with thixotropic effects and consolidation, eventually restores or even increases the strength of the cohesive soils. We can observe this increase in strength by resetting the pile hammer a few days after driving the pile and noting the increase in the blow count, a phenomenon known as *setup* or *freeze*.

In most cohesive soils, the excess pore water pressures that develop around a single isolated pile completely dissipate in less than one month, with corresponding increases in load capacity, as shown in Figure 13.8. However, in pile groups, the excess pore water pressures develop throughout a much larger zone of soil and may require a year or more to dissipate. This delay is significant because the rate of load capacity gain is now slower than the rate of construction, so the pile does not reach its full capacity until after the superstructure is built.

Effects on Cohesionless Soils

Numerous studies have shown that the driving process densifies medium or loose cohesionless soils by pushing the soil out of the way as it is displaced by the pile and by the associated vibrations (Meyerhof, 1959; Nataraja and Cook, 1983; Huang et al., 2001; Dapp, 2006).

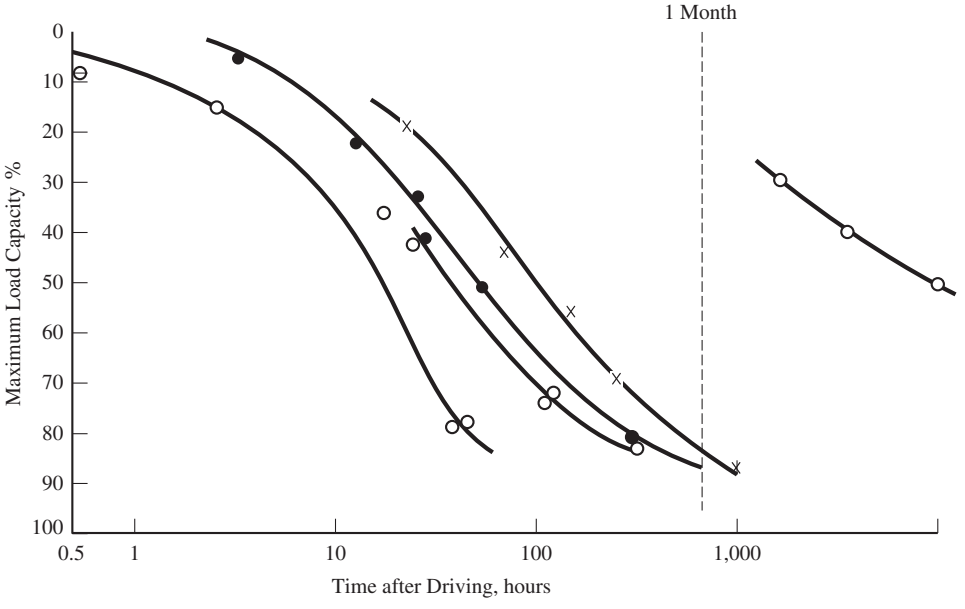

Figure 13.8 Increase in load capacity of isolated piles with time (data from Soderberg, 1962).

This densification will be much more significant for high displacement piles than for low displacement piles. The densification increases the friction angle of the soil surrounding the pile. The process is even more pronounced when piles are driven in groups—the larger the number of piles in the group, the greater the densification process. Measurement of lateral stress using dilatometer tests have shown a decrease in lateral stress near the surface but an increase in lateral earth pressure at greater depths (Huang et al, 2001; Dapp, 2006). In large pile groups, lateral stress increases up to a factor of five times have been measured (Dapp, 2006). Driving piles into dense cohesionless soils can lead to a decrease in density as the shearing process causes the dense soils to dilate (Tan, 2012).

Soil compression from the advancing pile also generates positive excess pore water pressures in loose saturated cohesionless soils. However, sands and gravels have a much higher hydraulic conductivity (permeability) than do cohesive soils, so these excess pore water pressures dissipate very rapidly, and don't affect the long-term pile capacity. Some local dilation (soil expansion) can occur when driving piles through very dense cohesionless soils. This temporarily generates negative excess pore water pressures that increase the shear strength and make the pile more difficult to drive. This effect is especially evident when using hammers that cycle rapidly.

Driven piles in cohesionless soil exhibit a time dependent setup or freeze over a period of days or weeks similar to that exhibited by piles driven in saturated cohesive soils. However, the mechanisms are very different. Setup for piles driven in cohesive soils is associated primarily with excess pore pressure dissipation and consolidation. However, excess pore pressures in cohesionless soils dissipate in seconds or minutes, so the increase in strength over days and weeks is clearly not due to pore pressure dissipation. The process appears to be a combination of creep and soil aging (Tan et al., 2004; Bullock et al., 2005; Wang and Steward, 2011).

In cemented sands or intermediate geomaterials such as calcareous coral formations, driven piles can destroy cementation, and crush weak sand and rock particles. This can result in a dramatic strength reduction in these materials. Augered piles are the preferred solution in these materials because they can be installed without significant damage to these materials.

Drilled Shafts

The construction process for drilled shafts is quite different from that for driven piles, so the installation effects are correspondingly different. Unlike driven piles, which push the soil aside, drilled shaft construction removes the soil. Thus, the lateral earth pressure will, at best, remain at its pre-construction value, and more likely will decrease during the construction process.

The auguring process can cause some remolding of soil around the pile and mixing of soils along the sides of the pile by pulling soil up from lower in the pile shaft and smearing the soil along the side of the opening higher up the pile. The effect is greatest in layer profiles where soft to medium clays are present. The amount of remolding is generally less than that found in driven large displacement piles but has similar effects. When caving conditions are encountered the auguring process can draw out excessive soils, increasing the shaft diameter and loosening the remaining soils.

The use of drilling mud during construction also can affect the side friction resistance because some of the mud may become embedded in the walls of the boring. This effect is very dependent on the contractor's construction methods and workmanship, as well as the soil type, and the corresponding reduction in load capacity can range from minimal to substantial. The best results are obtained when the slurry is carefully mixed and the slurry is in place for only a short time (i.e., the concrete is placed as soon as possible).

Auger Piles

The construction of auger cast in place (ACIP) piles is similar to that for drilled shafts, except that the hole is never left open. Also, unlike drilled shafts, the grout is placed under pressure, which should restore or even increase the lateral earth pressures. Thus, the net construction effects on the surrounding soil are typically somewhere between those for driven piles and drilled shafts.

Drilled displacement (DD) pile construction brings little or no soil to the ground surface. Instead, the special auger drives the soil laterally, as discussed in Chapter 12. The resulting installation effects are very similar to those with driven piles (Huang et al., 2001; Siegel et al., 2007).

Downdrag or Negative Skin Friction

If the construction process creates a situation where the soils surrounding a pile settle relative to the pile, the settlement induce a downward side friction load known as *downdrag* or *negative skin friction* (not be confused with the dragdown phenomenon described above). The settlement may be initiated by construction of a fill above the existing grade or simply due to consolidation caused by soil remolding during the driving process. The problem is most severe when piles are driven through a soft clay layer into a stiff bearing layer. The negative skin friction load can be very large, and must be considered in both ultimate and serviceability limit states. This phenomenon is discussed in Chapter 23.

SUMMARY

Major Points

1. The most important geotechnical design requirement for most piles is that they have sufficient axial load capacity to support the applied loads. We can evaluate this capacity using static load tests, analytic methods, or dynamic methods.
2. Piles transfer downward axial loads into the ground through side friction and toe bearing. Uplift loads are transferred through side friction, and possibly bearing on the ceiling of an enlarged base.
3. It generally takes much more displacement to mobilize toe resistance than to mobilize side friction.

4. Due to elastic strain in a pile the side friction is not uniformly mobilized along the entire length of the pile.
5. Lateral loads are carried by a combination of bending and shear in the pile and lateral support of the surrounding soil. The transfer of lateral loads from the pile to the soil is dependent upon the section modulus and length of the pile and the stiffness of the soil.
6. The ASD method factor of safety must be based on many factors, and is somewhat subjective. A higher factor of safety is used for uplift loads because uplift failures are more catastrophic.
7. In the LRFD method the resistance factors reflect uncertainty in both the material properties and the analytical models used. Therefore each analysis method will have its own associated resistance factors. The resistance factors of load and resistance factor design are calibrated with specific load factors and must be used together. Do not mix and match load and resistance factors from different design codes.
8. The design of open section foundations, such as steel H-piles and open-end steel pipe piles, must consider soil plugging.
9. The effects of pile installation on the surrounding soil are dependant upon the construction method and can have great effects on the behavior of the system.

Vocabulary

Closed-section pile
Dragdown
Downward load capacity
Downdrag or negative skin friction
Enlarged base
Open-section pile
Side friction
Toe bearing
Upward load capacity

QUESTIONS AND PRACTICE PROBLEMS

13.1 The toe bearing capacity in piles is similar to the ultimate bearing capacity of spread footings. However, the side friction capacity has no equivalent in spread footing design. Why do we ignore the friction acting on the side of spread footings?

13.2 When designing shallow foundations, we add the weight of the foundation to the applied column load (e.g., see Equation 6.1). However, with downward loads on piles, this weight is not explicitly computed (see Equation 13.4). Explain how we account for the weight of piles subjected to downward loads.

13.3 A prestressed concrete pile is being driven into a saturated cohesive soil with a hammer blow count of 17 blows per foot of pile penetration. Unfortunately, the pile driving rig breaks down before the pile reaches the required depth of penetration, resulting in a 15 hour delay. Once the rig is repaired, pile driving resumes but the blow count is now 25 blows per foot. Explain the primary reason for this change in blow count.

13.4 Sometimes pile driving contractors use predrilling when installing piles. This method consists of drilling a vertical hole that has a smaller diameter than the pile, then driving the pile into this hole. Could predrilling affect the side friction resistance? Why? Is the diameter of the predrill hole important? Why?

13.5 Why is it important for drilled shaft contractors to place the concrete soon after drilling the shaft? What detrimental effects can occur if the contractor waits too long before placing the concrete?

13.6 Why are there such a wide variety of geotechnical resistance factors in Tables 13.3, 13.4, and 13.5? Why not use a single resistance factor for each failure mode?

13.7 Why is it not advisable to use the geotechnical resistance factors in Tables 13.3, 13.4 and 13.5 with the ASCE-7 load factor from Equations 5-12 through 5-18 for geotechnical design of piles?

14

Piles—Axial Load Capacity Based on Static Load Tests

One good test is worth a thousand expert opinions.

Wernher Von Braun

Static load tests are the first category of methods for evaluating the axial load capacity of piles. These tests consist of constructing a full-scale prototype pile at the project site, slowly applying a series of progressively-increasing test loads to intensities well beyond the design allowable load, P_a, and developing a load-settlement curve. This is the most accurate way to evaluate the axial load capacity, and is the standard by which all other methods are judged. Although static load tests are not conducted on all pile projects, they are frequently used in practice, especially for larger or more important projects and when the soil conditions are unusual or challenging.

14.1 OBJECTIVES

Sometimes the objective of a static load test is to verify the prototype pile has sufficient load capacity. In this case, the loading sequence is continued until the test load is equal to or greater than $F(P_a)$, where F is the required factor of safety. The most common value of F in this case is 2.0, so these tests are typically conducted to a maximum test load equal to 200 percent of P_a. If the pile performs satisfactorily under this test load (i.e., it does not settle excessively and maintains the load without noticeable creep), then the pile is considered to be suitable. Such tests are sometimes called *proof tests*, because the intent is

to prove the foundation is adequate. If results of a proof test are satisfactory, then the prototype pile may be used as one of the production piles, and the remaining production piles are constructed based on the load test results. However, this test method does not reveal whether or not the pile is overdesigned.

Alternatively, the test loading sequence may be continued until reaching "failure" (which will be defined later in this chapter), thus producing a measured value of nominal downward axial load capacity, P_n. When using allowable stress design (ASD), the allowable load capacity for strength requirements, P_a is:

$$P_a = \frac{P_n}{F} \tag{14.1}$$

where F is the factor of safety as selected from Table 13.1 or 13.2.

The most common value of F is 2.0. The strength requirements of the planned production piles are then checked using the criterion:

$$P \leq P_a \tag{14.2}$$

When using load and resistance factor design (LRFD), the strength design criterion is:

$$\sum \gamma_i P_i \leq \phi P_n \tag{14.3}$$

The American Association of State Highway and Transportation Officials (AASHTO) resistance factor for piles, ϕ, is between 0.75 and 0.8, per Table 13.3.

Continuing the test to failure is superior to conducting a proof test because it also determines when the actual capacity is greater than the required capacity, and thus facilitates optimizing the design. For example, if the required allowable load capacity is 300 kN, but the test pile was found to have an allowable capacity of 400 kN, then the production piles can be made correspondingly shorter or the number of production piles can be reduced. Preliminary designs are often conservative, so the potential cost savings realized by conducting load tests to failure can be significant, especially on larger projects. Static load test results also may be used to check serviceability requirements, as discussed in Chapter 20.

14.2 CONVENTIONAL STATIC PILE LOAD TESTS

Conventional static pile load tests consist of applying a series of axial loads to the top of the pile and measuring the axial displacements at the top. The result is a load-settlement curve (or load-heave curve in the case of uplift tests).

Equipment

Pile load tests require a means of applying the desired loads to the prototype pile and measuring the resulting deformations. A wide variety of equipment has been used, with varying

degrees of success (Crowther, 1988). One method, known as a *kentledge test*, uses dead weights, such as concrete blocks, which are stacked on a platform to provide the necessary reaction for the test load, as shown in Figure 14.1. A hydraulic jack placed between these weights and the test pile provides the test load. Kentledge tests with substantial load capacities have been conducted. However, the cost of mobilizing of the required platform, weights, and supports; limitations in the ability of soft ground to support the required weight; and safety concerns limit its usage.

Another method of developing reactions for the test load is to install *reaction piles* on each side of the test pile and connect them with a *load frame*, as shown in Figure 14.2. Typically four reaction piles are used. A hydraulic jack located between the frame and the test pile provides the downward load. For uplift tests, the jack is placed above the beam and connected to the test pile with tension ties, or between the beam and its supports. The use of reaction piles eliminates the need to mobilize large weights, and the marginal cost of constructing these additional foundations is tolerable because the installation equipment has already been mobilized to install the test pile. Thus, this is by far the most common method for conducting pile load tests. Pile test load frames with capacities of about 5,000 kN (1,100 k) are widely used, and frames with capacities up to 35,000 kN (8,000 k) have been built.

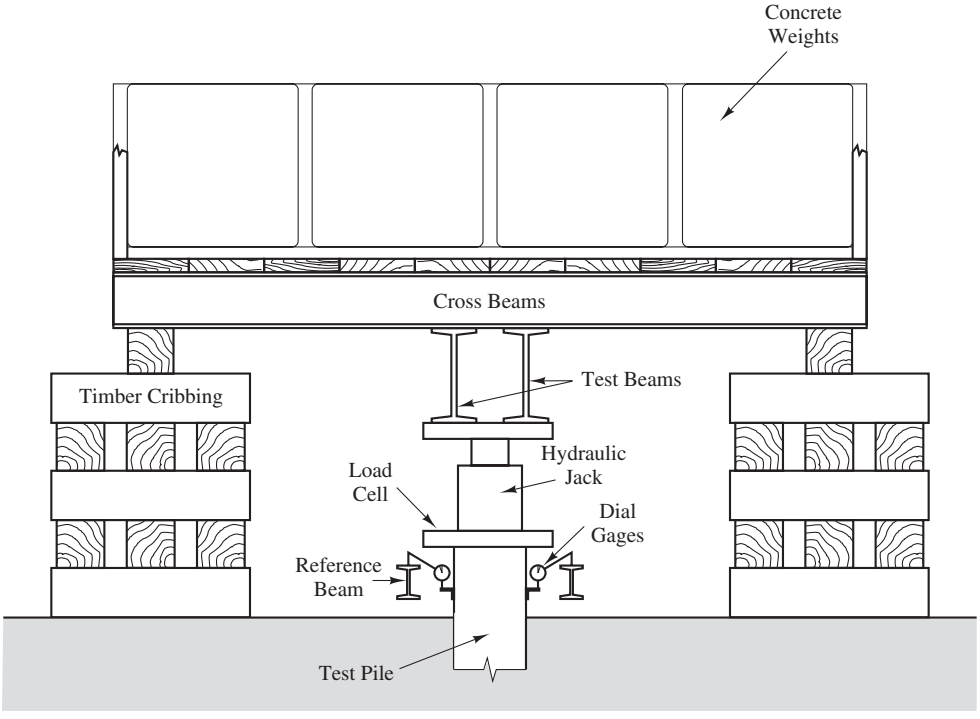

Figure 14.1 Use of a hydraulic jack reacting against dead weight to develop the test load in a kentledge static load test.

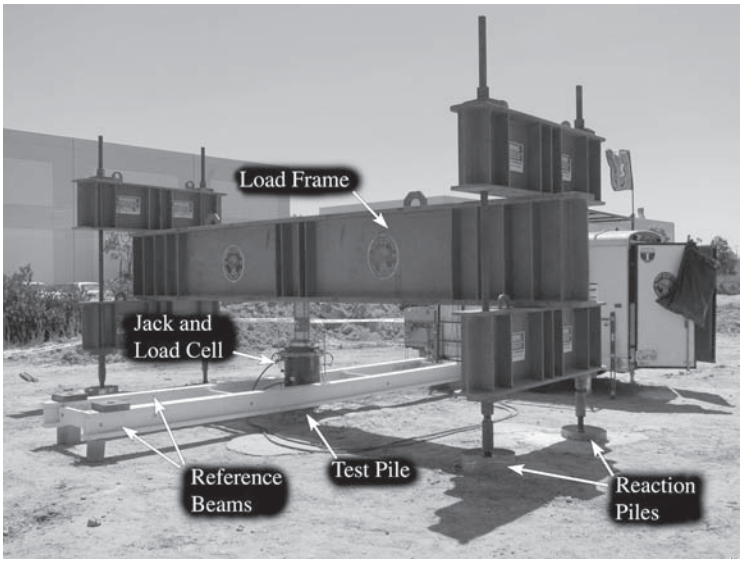

Figure 14.2 A static load test using a beam and reaction piles to develop the test load.

During the early years of load testing, engineers measured the applied load by calibrating the hydraulic jack and monitoring the fluid pressure during the test. However, even when done carefully, this method is subject to errors of 20 percent or more (Fellenius, 1980). Therefore, it is now standard practice to measure the applied load using a load cell (an electronic instrument that measures force), as shown in Figure 14.3. Jack fluid pressure measurements are still typically used as a backup.

The pile settles (or heaves in the case of an uplift test) in response to each increment of applied load. This displacement is measured using dial gages or linear voltage displacement transformers (LVDTs) mounted on *reference beams*, as shown in Figure 14.3. These reference beams are supported well away from the test and reaction piles in order to provide a stable datum. Backup systems, such as a surveyor's level or a wire and mirror system, are often used.

Procedure

Deep foundation construction, especially pile driving, alters the surrounding soil, as discussed in Chapter 13. This alteration often produces excess pore water pressures, which temporarily change the load capacity. Therefore, it is best to allow time after construction for these excess pore water pressures to dissipate before conducting the load test—typically one day for sands, perhaps several days for clays. In the case of non-displacement cast-in-place foundations, the excess pore water pressures are generally smaller, so the waiting time could probably be shortened. It also is necessary to allow enough time for cast-in-place concrete to cure.

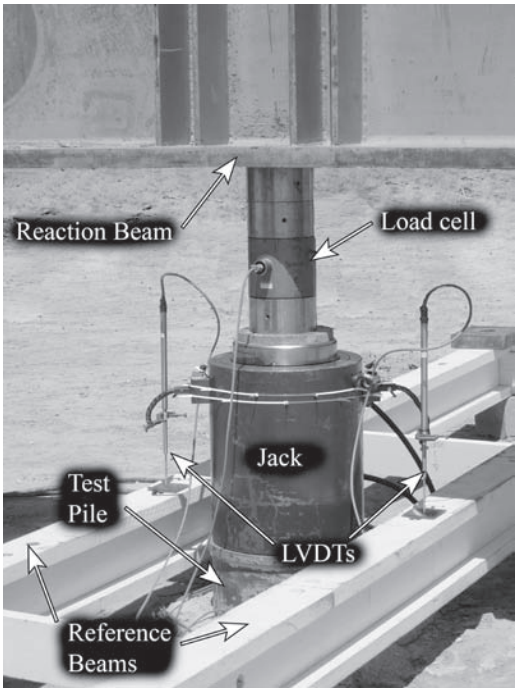

Figure 14.3 This closeup of the test in Figure 14.2 shows the 5,300 kN (1,200 k) capacity hydraulic jack being used to generate the test load. The jack reacts against the beam above, which loads the test pile in compression and the reaction piles in tension. The load is being measured using a load cell (note data cable) and the settlement is being measured using LVDTs and reference beams.

There are two categories of static load tests: *stress controlled tests* and *strain controlled tests*. The former uses predetermined loads (the independent variable) and measured settlements (the dependent variable), while the latter uses the opposite approach. ASTM D1143 describes both procedures for downward (compressive) loads, and ASTM D3689 covers testing under uplift (tensile) loads. The vast majority of tests use the controlled stress method, so it is the only one we will discuss. There are two major types of stress controlled tests: The *maintained load test* (ASTM D1143 Procedure B) and the *quick test* (ASTM D1143 Procedure A).

Maintained Load Test

When conducting maintained load tests, the field crew applies the test load in increments of about 25 percent of the design load, and maintains each load for two hours or until the rate of settlement is less than 0.25 mm (0.01 in) per hour, whichever comes first. This process is continued until reaching 200 percent of the design load (for proof tests) or to failure. For proof tests, the maximum load is held for a longer period to check for creep effects, then the foundation is progressively unloaded. Sometimes creep effects are also checked at a test load equal to the design allowable load, P_a. When performed properly, this procedure produces very good results, but it also is very time consuming. Total test durations of 24 hours or more are not unusual.

Quick Test

As the name indicates, the quick test is faster than the maintained load test. With this method, the load increments are smaller, about 5 percent of the anticipated P_a, and each load is held for a predetermined time interval regardless of the rate of pile displacement at the end of that interval. ASTM permits intervals of 4 to 15 minutes, and Crowther (1988) suggests holding each load for 5 minutes. This process continues until reaching about 200 percent of the anticipated design load or to failure. Typically the maximum load is held for a longer period to check for creep effects, then the foundation is unloaded in increments. The quick test generally requires 4 to 6 hours to complete, and produces results that are widely accepted. It also has the advantage of requiring less personnel time. This is the most common test, and may be the best method for most piles.

14.3 INTERPRETATION OF TEST RESULTS

When conducting proof tests, the acceptance criteria typically require the settlement be monitored when the pile is loaded to 200 percent of the design load, and the rate of settlement must not exceed some specified value, such as 0.25 mm/hr (0.01 in/hr). Such criteria provide good assurance that the design load could be safely sustained.

If the objective of the test is to determine the nominal axial downward load capacity, P_n, then the data analysis becomes more complicated because it is necessary to determine where failure occurs. For foundations in soft or medium clays, this is relatively straightforward because the load-settlement curve has a distinct *plunge*, as shown by Curve A in Figure 14.4. In this case, P_n could in principle be taken to be the load that

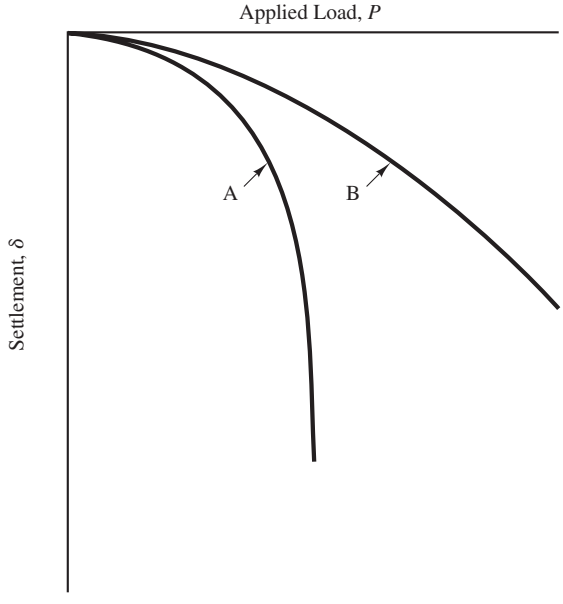

Figure 14.4 Typical load-settlement curves: Curve A is typical in soft and medium clayey soils (note plunge); and Curve B is typical of intermediate, stiff clay and sandy soils (ever-increasing load).

corresponds to a point immediately before this plunge, though the location of such a point is subject to interpretation. Piles in sands, intermediate soils, and stiff clays have a sloped curve with no clear point of failure, as shown by Curve B, so the value of P_n is more difficult to define. Thus, it is helpful to have a standardized method of interpreting test results, regardless of the shape of the curve.

Many interpretation methods have been proposed. The most widely used ones include Brinch Hansen (1963), Davisson (1973), Chin (1970, 1972), and Butler and Hoy (1977). These various methods often produce significantly different results. For example, Fellenius (1980) used nine methods to analyze the results of a static load test and found the computed nominal capacity varied from 1,610 to 2,090 kN (362–470 k). Another method, found in early editions of the AASHTO specifications, produced a computed capacity of only 445 kN (100 k)!

IBC 1810.3.3.1.3 permits the use of Davisson, Brinch Hansen 90%, Butler and Hoy, or "other methods approved by the Building Official." AASHTO 10.7.3.8.2 specifies the Davisson method for small diameter foundations, and a modification of this method for larger diameter foundations.

Many engineers in the United States prefer to express pile capacities using tons (the 2,000 lb variety), whereas others use kips. This book uses only kips to maintain consistency with the remainder of structural and geotechnical engineering practice.

Modulus of Elasticity

The analysis of load test results normally includes an assessment of the elastic deformation of the pile, and thus requires a value for the modulus of elasticity, E.

Steel

The modulus of elasticity for structural steel is very predictable. The standard value is:

$$E = 200{,}000 \text{ MPa} = 29{,}000{,}000 \text{ lb/in}^2$$

Concrete

The modulus of elasticity of unreinforced concrete depends on the composition of the aggregate, the cement content, and other factors. It can be estimated using:

$$E = 4{,}700\sqrt{f'_c} \qquad \text{(14.4 SI)}$$

$$E = 57{,}000\sqrt{f'_c} \qquad \text{(14.4 English)}$$

where f'_c is the 28-day compressive strength, and both E and f'_c are in MPa or lb/in^2. Alternatively, E can be determined directly (and more accurately) by retrieving concrete samples and testing them in the laboratory. In many cases the improved accuracy is worth the modest cost of conducting this test.

The axial load in reinforced concrete and concrete-filled steel pipe piles is carried by both the steel and the concrete, so the modulus of elasticity should be a weighted average based on the steel ratio, ρ:

$$E = E_c(1 - \rho) + E_s\rho \tag{14.5}$$

where

E_s = Modulus of elasticity of the steel
E_c = Modulus of elasticity of the concrete
ρ = Steel ratio = A_s/A
A_s = Cross-sectional area of the steel
A = Total cross-sectional area

Accurate assessments of E_c in concrete filled steel pipe piles, drilled shafts, and auger piles can be difficult, especially soon after concrete placement, because the concrete cures differently at different depths. This effect can produce a pile where E varies with depth.

Timber

The modulus of elasticity of timber depends on the species, and varies from about 7,000 to 10,000 MPa (1,000,000–1,500,000 lb/in^2) for those typically used as piles. Specific design values are presented in Table 21.3.

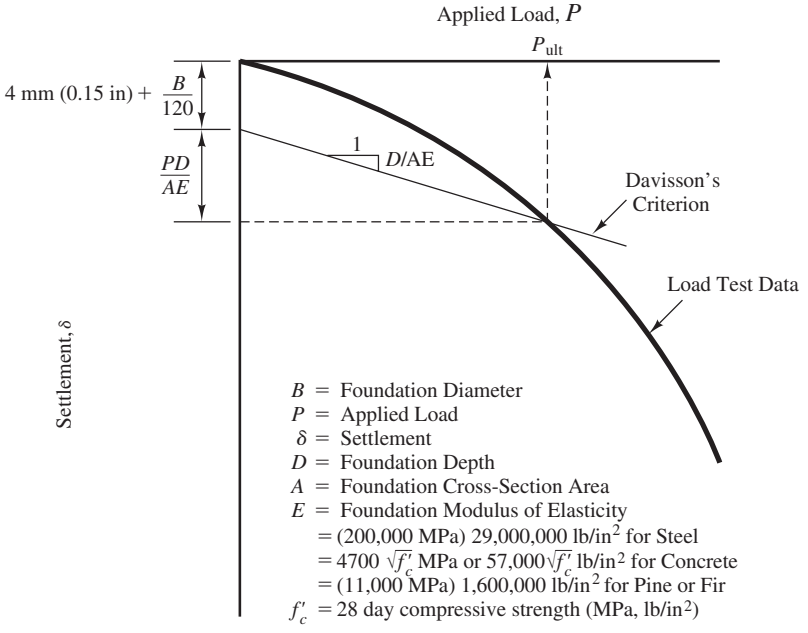

Figure 14.5 Davisson method of determining P_n from static load test data.

Davisson Method

The *Davisson method* (also known as the Davisson offset limit) is one of the most popular means of interpreting load test results. It defines the nominal axial downward load capacity as that which occurs at a settlement of 4 mm (0.15 in) + $B/120 + PD/(AE)$ as shown in Figure 14.5 (Davisson, 1973). The last term in this formula is the elastic compression of a pile that has no side friction. This method has the advantage of being very objective, so everyone analyzing the same data will obtain virtually the same value of P_n.

Example 14.1

The load-settlement data shown in Figure 14.6 were obtained from a static load test on a 400 mm diameter, 17 m long drilled shaft with $f'_c = 40$ MPa and $\rho = 0.055$. Use Davisson method to compute the nominal axial downward load capacity.

Solution

$$E_c = 4{,}700\sqrt{f'_c} = 4{,}700\sqrt{40} = 29{,}725 \text{ MPa}$$

$$E = E_c(1 - \rho) + E_s\rho = (29{,}725)(1 - 0.055) + (200{,}000)(0.055) = 39{,}000 \text{ MPa}$$

$$A = \frac{\pi(0.400)^2}{4} = 0.126 \text{ m}^2$$

$$4 \text{ mm} + \frac{400 \text{ mm}}{120} + \frac{P(17{,}000 \text{ mm})}{(0.126 \text{ m}^2)(39{,}000{,}000 \text{ kPa})} = 7.3 \text{ mm} + 0.0035\,P$$

Plotting this line on the load-displacement curve produces $\boldsymbol{P_n = 1{,}650 \text{ kN}}$.

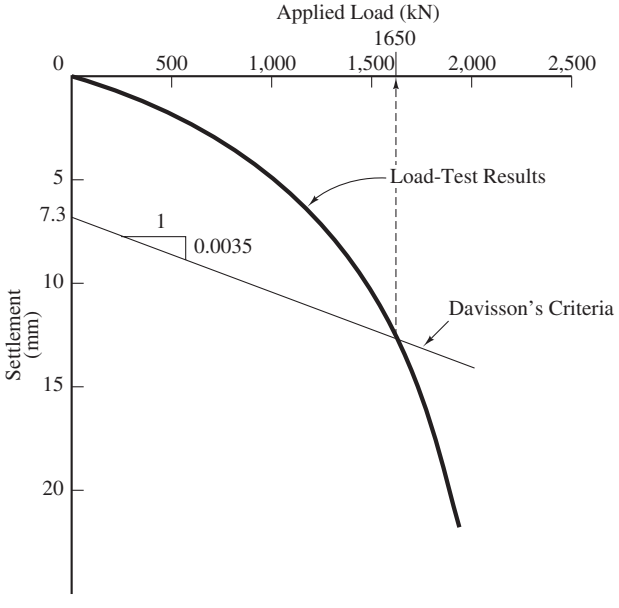

Figure 14.6 Static load test data for Example 14.1.

Brinch Hansen Method

In a short discussion of a paper on stress–strain properties of cohesive soils, Brinch Hansen (1963) proposed a parabolic relationship for stress–strain properties of soil near failure. Using this relationship, he noted that the strain in soil at failure is four times the strain that corresponds to a stress equal to 80 percent of failure, and twice the strain that corresponds at a stress equal to 90 percent of failure. Nothing in the original paper or his discussion refers to foundations or pile load tests.

Others have since extrapolated this concept to the interpretation of static load test results, thus producing the *Brinch Hansen 80% criterion* and the *Brinch Hansen 90% criterion*:

- The nominal axial load capacity, P_n, from a static load test is that which occurs at a settlement equal to four times the settlement at a stress equal to 0.80 P_n.
- The nominal axial load capacity, P_n, from a static load test is that which occurs at a settlement equal to twice the settlement at a stress equal to 0.90 P_n.

These two criteria are shown graphically in Figure 14.7. Both are a means of defining P_n based on the curvature of the load-settlement curve, and in theory both should produce about the same value of P_n. In practice, the 80% method and the 90% method may produce different results.

It is unclear whether Brinch Hansen himself, who died six years after his discussion was published, would approve of this use of his observations. Nevertheless, the "Brinch Hansen Method" is now widely used to interpret pile load tests, and is even referenced in the International Building Code (IBC).

The load that produced a settlement of one-quarter or one-half of the settlement at each test load must be continuously computed in the field, and the loading sequence must be continued until the Brinch Hansen criterion is satisfied. This process entails more field calculations than are necessary with Davisson, but is necessary to ensure the

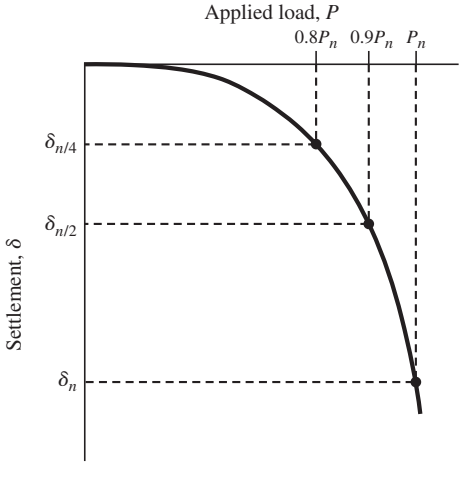

Figure 14.7 Brinch Hansen method of determining P_n from static load test data.

load-settlement curve is developed beyond the point of failure. This method locates a failure point on the cusp of plunging, which some have argued is a more rational approach than the predefined settlement criterion used by Davisson. In addition, Brinch Hansen method often produces higher, and some would argue more realistic, P_n values than Davisson.

Example 14.2

A 16 in diameter, 77.5 ft long auger pile has been designed using ASD to support an downward load of 350 k. A prototype pile was constructed using concrete with $f'_c = 5{,}000$ lb/in^2 and a steel ratio of 2 percent. The results of a static load test are shown in Figure 14.8. Interpret the load test results using both the Davisson and Brinch Hansen 90% methods and determine if the ASD geotechnical strength requirement is satisfied with an adequate factor of safety.

Solution

Davisson Method

$$E_c = 57{,}000\sqrt{5{,}000}$$
$$= 4{,}030{,}000 \text{ lb/in}^2$$

$$E = (4{,}030{,}000)(1 - 0.02) + (29{,}000{,}000)(0.02)$$
$$= 4{,}530{,}000 \text{ lb/in}^2$$

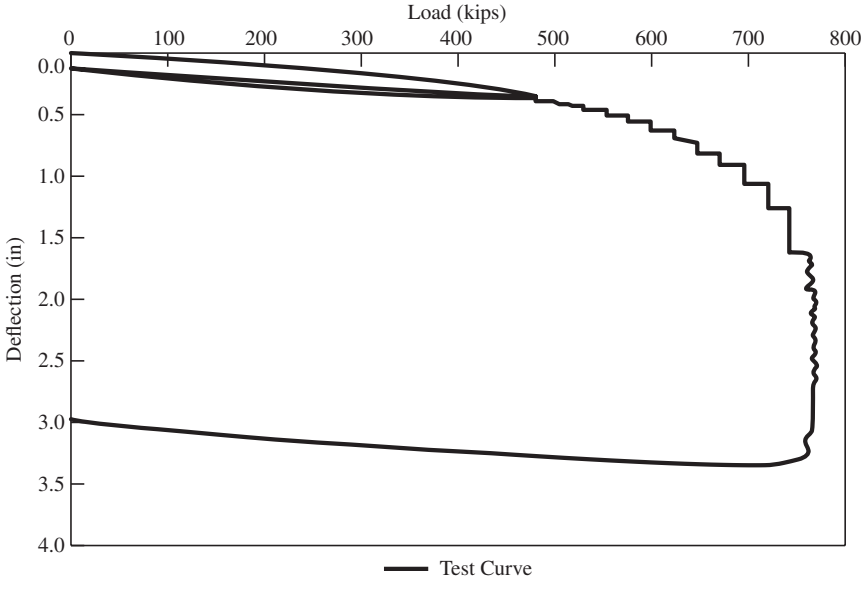

Figure 14.8 Load test data for Example 14.2 (data provided by Berkel & Company).

$$A = \pi 8^2$$
$$= 201 \text{ in}^2$$

$$0.15 + \frac{16}{120} + \frac{P(77.5)(12 \text{ in/ft})(1{,}000 \text{ lb/k})}{(201)(4{,}530{,}000)} = 0.28 + 0.00102P$$

This line intersects the test curve at $P = 670$ k.

$$P_a = \frac{P_n}{F} = \frac{670}{2} = 335\text{k}$$

$P > P_a$ so the design is not acceptable according to the Davisson method.

Brinch Hansen Method

The 90% Brinch Hansen criterion can be evaluated by comparing the settlement at each test load with the settlement at 90% of the test load.

P (k)	δ (in)	δ at $0.9P$ (in)	Ratio
745	1.62	0.93	1.74
746	1.64	0.94	1.76
747	1.67	0.94	1.77
748	1.69	0.94	1.79
749	1.72	0.95	1.81
750	1.75	0.95	1.83
751	1.78	0.95	1.86
752	1.81	0.96	1.89
753	1.84	0.96	1.91
754	1.87	0.97	1.94
755	1.90	0.97	1.96
756	1.94	0.97	1.99
757	1.98	0.98	2.02
758	2.02	0.98	2.05
759	2.06	0.99	2.09
760	2.10	0.99	2.12
761	2.15	0.99	2.17

The specified ratio of 2 is obtained at $P = 756$ k.

$$P_a = \frac{P_n}{F} = \frac{756}{2} = 378 \text{ k}$$

$P \leq P_a$ so the design is acceptable according to the Brinch Hansen 90% method.

Example 14.3

A static load test has been performed on a steel H pile. Using Brinch Hansen's method, the nominal downward load capacity was found to be 260 k. The applied loads consist of dead load = 100 k and live load = 40 k. The production piles will be driven based on a criteria developed from this load test, and no dynamic load testing is planned. Determine if this foundation satisfies the AASHTO LRFD geotechnical strength I requirement.

Solution

Per the AASHTO bridge code: $\gamma_D = 1.25$ and $\gamma_L = 1.75$.

Per Table 13.3: $\phi = 0.75$

$$\sum \gamma_i P_i \leq \phi P_n$$

$$(1.25)(100) + (1.75)(40) \leq (0.75)(280)$$

$$195 \text{ k} \leq 210 \text{ k}$$

Yes, the LRFD geotechnical strength I design criterion has been satisfied.

Load Transfer Indicators

The shape of the load-settlement curve provides a rough indication of the load transfer processes. Piles that develop their axial capacity primarily from toe bearing have a curve below the elastic compression line, as shown in Figure 14.9. In contrast, friction piles (those that develop nearly all of their capacity from side friction) have curves that are initially above the elastic compression line, then plunge more distinctly, as shown.

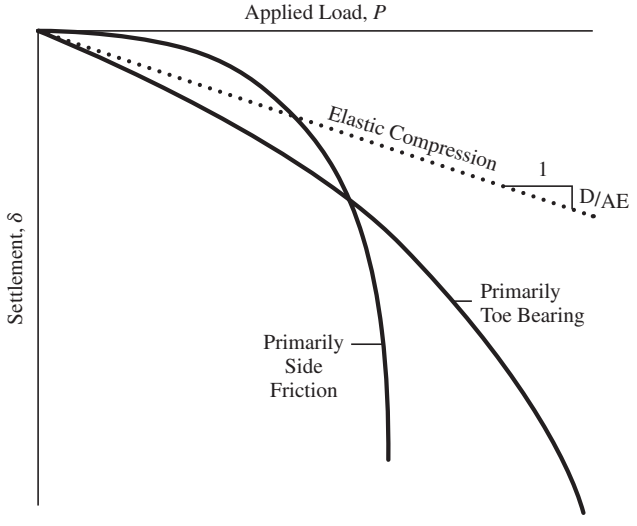

Figure 14.9 Implied load transfer from the shape of load-settlement curve.

14.4 INSTRUMENTED STATIC PILE LOAD TESTS

Conventional static pile load tests only produce quantitative information on the load-settlement or load-heave relationship at the top of the pile. Although this information is sufficient to determine P_n, it would be very useful to also know how this load is transferred into the soil. How much side friction develops and how much toe bearing? How is the side friction distributed along the pile? The shape of the load-settlement curve provides a rough indication, but having measured values of f_n and q'_n would facilitate extrapolating the test results to foundations with different dimensions. We can find the answers to these questions by installing instrumentation at various depths in the pile, which allows us to perform an *instrumented pile load test*.

Instrumentation Using Strain Gages

Closed-end steel pipe piles may be instrumented by installing a series of strain gages on the inside of the pile, as shown in Figure 14.10. Concrete piles, drilled shafts, auger piles, and other similar concrete foundations may be instrumented by embedding strain gages into the

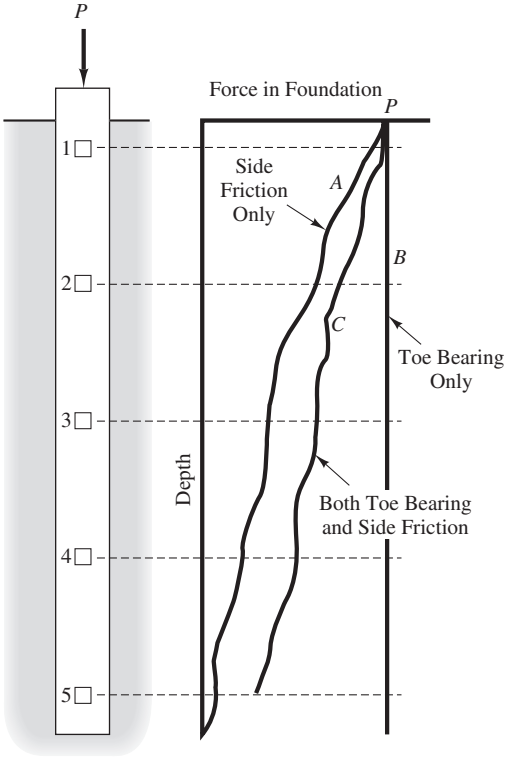

Figure 14.10 Typical instrumented static load test. □ = Strain Gage or Load Cell

concrete, by installing strain gages on the rebar, or by mounting them in advance on prefabricated sister bars, which are then placed adjacent to the structural bars. Data from these strain gages can then be used to compute the force in the pile at that depth, and thus can determine the distribution of side friction resistance and the toe bearing resistance. Using this data, we can calculate the side friction resistance, f, and the net toe bearing resistance, q', at each stage of the test. If the test is conducted to failure, then the nominal capacities f_n and q'_n can also be calculated.

For example, if the applied load is transferred into the ground entirely through side friction, the plot of force versus depth will be similar to Curve A in Figure 14.10 (i.e., the force in the pile gradually dissipates with depth, reaching zero at the toe). Conversely, if the resistance is entirely toe bearing, the plot will be similar to Curve B (i.e., constant with depth). Most piles have both side friction and toe bearing, and thus have plots similar to Curve C.

When converting the strain gage data to a force in the pile, we assume the strain in the concrete equals the strain in the reinforcing steel. Thus:

$$P = \sigma_s A_s + \sigma_c A_c \tag{14.6}$$

$$= E_s \varepsilon A_s + E_c \varepsilon A_c \tag{14.7}$$

$$= \varepsilon A[E_s \rho + E_c(1 - \rho)] \tag{14.8}$$

where

P = Axial load in the pile
σ_s = Normal stress in the steel
σ_c = Normal stress in the concrete
A = Total cross-sectional area
A_s = Cross-sectional area of the steel
A_c = Cross-sectional area of the concrete
E_s = Modulus of elasticity of the steel
E_c = Modulus of elasticity of the concrete
ε = Strain
ρ = Steel ratio = A_s/A

Alternatively, Equation 14.5 could be used.

Example 14.4

A strain gage was embedded in the auger pile described in Example 14.2. This gage was located 5 ft above the toe, and the test results are shown in Figure 14.11. Using this data, and the Brinch Hansen 90% load capacity, compute the average f_n and the q'_n for this pile.

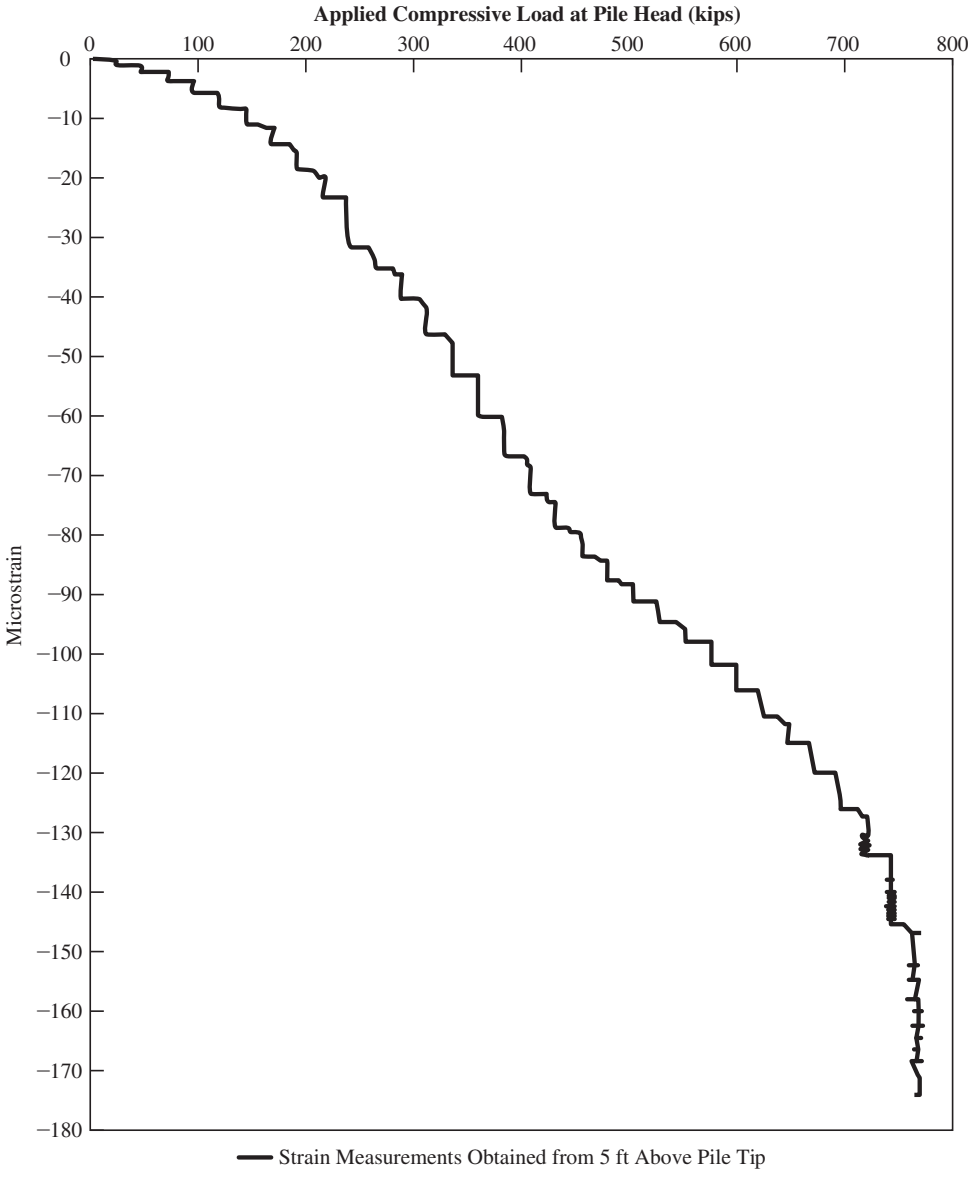

Figure 14.11 Strain gage data for Example 14.4 (data provided by Berkel & Company).

Solution

Side Friction

$$\sigma = E\varepsilon = (4{,}530{,}000)(145 \times 10^{-6}) = 657 \text{ lb/in}^2$$

$$P_s = \sigma A = (657)(201) = 132{,}000 \text{ lb}$$

$$A = \pi\left(\frac{16}{12}\right)(77.5 - 5) = 304 \text{ ft}^2$$

$$f_n = \frac{756{,}000 - 132{,}000}{304} = 2{,}050 \text{ lb/ft}^2$$

Toe Bearing

Assume f_n in bottom 5 ft is the same as in the upper portion of the pile

$$P_t = 132{,}000 - (2{,}050)\pi\left(\frac{16}{12}\right)(5) = 89{,}000 \text{ lb}$$

$$W_f = (201)\left(\frac{1 \text{ ft}}{12 \text{ in}}\right)^2(72.5)(150) = 16{,}000 \text{ lb}$$

$$q_n' = \frac{89{,}000 - 16{,}000}{(201)(1/12)^2} = 52{,}200 \text{ lb/ft}^2$$

Commentary

These values of f_n and q_n' may then be used to compute the load capacity of proposed piles at this site with other diameters and depths of embedment. Thus, this technique is a method of extrapolating the load test results.

In reality, f_n probably varies with depth, so additional strain gages at different depths would provide a more accurate representation of the side friction resistance.

Instrumentation Using Telltale Rods

Another method of conducting instrumented static pile load tests is to install *telltale rods* inside the foundation. These rods extend from the top of the pile to some specified depth, and are encased in a protective sleeve. By comparing the settlement of these rods with the settlement at the top of the foundation, and using the modulus of elasticity, we can compute the force in the foundation, which in turn may be used to compute f and q'.

Example 14.5

Two telltale rods have been installed in a 45 ft long closed-end PP20 × 0.750 pile. This pile was subjected to a static load test, which produced the following results:

Test load at failure 250,040 lb

Settlement readings at failure:

At pile head (Gage #1)	0.572 in
Telltale anchored at 20 ft depth (Gage #2)	0.530 in
Telltale anchored at 45 ft depth (Gage #3)	0.503 in

Compute the force in the pile at 20 and 45 ft, and compute the average f_n values on the pile and the q_n' value.

Solution

Pile interval 1-2 (upper 20 ft)

$$\delta_1 - \delta_2 = \left(\frac{P_1 + P_2}{2}\right)\frac{L}{AE}$$

$$0.572 - 0.530 = \left(\frac{250{,}040 + P_2}{2}\right)\left(\frac{(20)(12 \text{ in/ft})}{(45.36)(29 \times 10^6)}\right)$$

$$P_2 = 210{,}360 \text{ lb}$$

$$f_n = \frac{\Delta P}{A_s} = \frac{250{,}040 - 210{,}360}{\pi(20/12)(20)} = 3{,}79 \text{ lb/ft}^2$$

Pile interval 2-3 (lower 25 ft)

$$\delta_1 - \delta_2 = \left(\frac{P_1 + P_2}{2}\right)\frac{L}{AE}$$

$$0.530 - 0.503 = \left(\frac{210{,}360 + P_3}{2}\right)\left(\frac{(25)(12 \text{ in/ft})}{(45.36)(29 \times 10^6)}\right)$$

$$P_2 = 26{,}420 \text{ lb}$$

$$f_n = \frac{\Delta P}{A_s} = \frac{210{,}360 - 26{,}420}{\pi(20/12)(25)} = 1{,}410 \text{ lb/ft}^2$$

$$q_n' = \frac{P}{A_e} = \frac{26{,}420}{\pi(20/12)^2/4} - 12{,}100 \text{ lb/ft}^2$$

Commentary

A settlement of 0.5 in is probably enough to mobilize nearly all the side friction resistance, so the computed values of f are probably very close to f_n. However, about 10 percent of the diameter, or 2 in in this case, would be required to mobilize the full toe bearing, much more than the 0.5 in of settlement in this test. Thus, the computed value of q_n' is certainly much lower than the real value. Alternatively, the load test could have been continued until sufficient toe settlement was obtained.

Residual Stresses

Driven piles typically have locked-in *residual stresses* which are a result of the pile driving process. For example, even before any external load is applied, the central part of the

pile might be in compression, which is resisted by a downward side friction resistance in the upper part of the pile and an upward side friction resistance and some toe bearing in the lower part. Cast-in-place concrete foundations can have residual stresses due to expansion or contraction of the concrete during curing. Additional initial stresses are present in all types of piles due to their own weight. Thus, the distribution of forces computed using techniques such as those in Examples 14.4 and 14.5 are not quite correct, and the computed f and q' values are correspondingly off. However, the net effect should be zero (i.e., the overestimated values should be compensated by the underestimated values). These effects could at least partially be corrected by recording the load cell readings before the beginning of the load test and adjusting the analyses accordingly.

14.5 OSTERBERG LOAD TESTS (O-CELL)

Drilled shaft foundations are typically larger in diameter and have a correspondingly greater capacity than most driven piles, so conventional load tests require correspondingly large load frames, jacks, and other hardware. The cost of conducting such tests can be prohibitive. The alternatives include conducting the load test on a smaller diameter shaft and extrapolating the results; using a more conservative design based solely on static methods, as discussed in Chapters 15 to 18; using dynamic test methods, as discussed in Chapter 19; or using the Osterberg load test (also known as the O-cell test).

The Osterberg load test (Osterberg, 1984) uses one or more hydraulic pancake jacks located at or near the bottom of the shaft, as shown in Figures 14.12 and 14.13, or at some intermediate depth. Often the jack is placed at a depth such that the expected load capacity above the jack equals that below the jack. Once the concrete is in place, the operator pumps hydraulic fluid into the jack and monitors both pressure and volume. The jack expands and pushes up on the shaft above the jack and down on the shaft below the jack

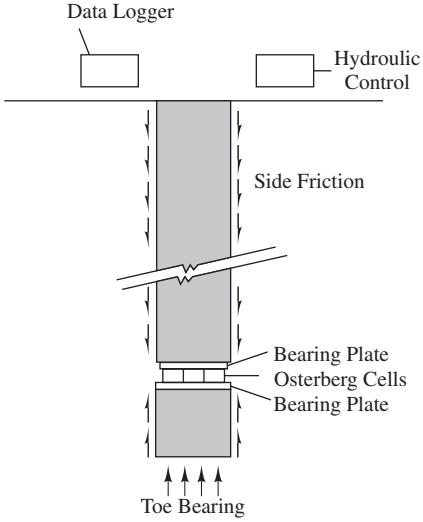

Figure 14.12 Osterberg load test device (Loadtest, Inc.).

Figure 14.13 An Osterberg cell being installed at the bottom of a drilled shaft rebar cage (Loadtest, Inc.).

(Osterberg, 1984). A displacement transducer measures this movement. Thus, we obtain a plot of side friction capacity versus axial movement.

This device also includes a displacement transducer that extends from the bottom of the pancake jack to the underlying ground. It measures the downward movement at the bottom, and thus produces a plot of toe bearing pressure versus axial movement.

These two plots continue until the foundation fails in side friction or toe bearing. Ideally, the jack is placed at a depth such that the upward failure and downward failure occur simultaneously. If a toe bearing failure occurs first, we must extrapolate the data to obtain the nominal side friction capacity. However, if a side friction failure occurs first, it may be possible to add a nominal static load to the top, and then continue the test to find the toe bearing capacity. Once the test is completed, the jack is filled with grout and the test foundation may be used as a production foundation to carry structural loads.

The Osterberg load test avoids the need for a load frame, and thus can be more economical, especially for large-diameter drilled shafts. It also can be used in auger piles and even in some types of driven piles, although these applications are much less common.

Osterberg load tests often have capacities as large as 130,000 kN (30,000 k), and some tests have been performed to loads of up to 320,000 kN (72,000 k). This is far greater than is practical with load frame or kentledge tests.

14.6 DYNAMIC AXIAL LOAD TESTS

Axial load tests also can be conducted using dynamic methods, which apply a rapid dynamic load to the pile. These methods are then used to determine the static load capacity. Dynamic methods are discussed in Chapter 19.

SUMMARY

Major Points

1. Static load tests are the most accurate means of determining the axial load capacity of pile foundations.
2. Tests consist of applying a progressively increasing load to the top of the pile and measuring the resulting deformations.
3. A proof test is intended to demonstrate that a pile has adequate load bearing capacity. When tests are continued to failure, the nominal capacity can be determined, which often results in more economical designs.
4. There is no universally accepted method of interpreting static load test results. The Davisson method is widely used and conservative. The Brinch Hansen method and other methods also are widely used.
5. A instrumented pile load test is a conventional test that includes instruments inside the pile to measure the distribution of side friction and toe bearing.
6. An Osterberg load test applies the test load using a hydraulic pancake jack located near the bottom of the foundation.

Vocabulary

Brinch Hansen method	Load frame	Quick test
Conventional static load test	Maintained load test	Static load test
Davisson method	Osterberg load test	Strain controlled test
Instrumented static load test	Plunge	Stress controlled test
Kentledge test	Proof test	Telltale rods

QUESTIONS AND PRACTICE PROBLEMS

14.1 A typical deep foundation project may include several hundred piles, but only one or two static load tests. Thus, the information gained from these test piles must be projected to the production piles. Describe some of the factors that might cause the load capacity of the production piles to be different from that of the test pile.

14.2 Assume the curve shown in Figure 14.14 has been obtained from a static load test on a 40 ft long, 12 in square solid concrete pile. Using Davisson method, compute the nominal downward axial load capacity.

14.3 Assume the curve shown in Figure 14.14 has been obtained from a static load test on a 60 ft long, PP18 $\times$ 0.375 pile. Using Davisson method, compute the nominal downward axial load capacity.

14.4 Solve Problem 14.3 using the Brinch Hansen 80% and 90% methods.

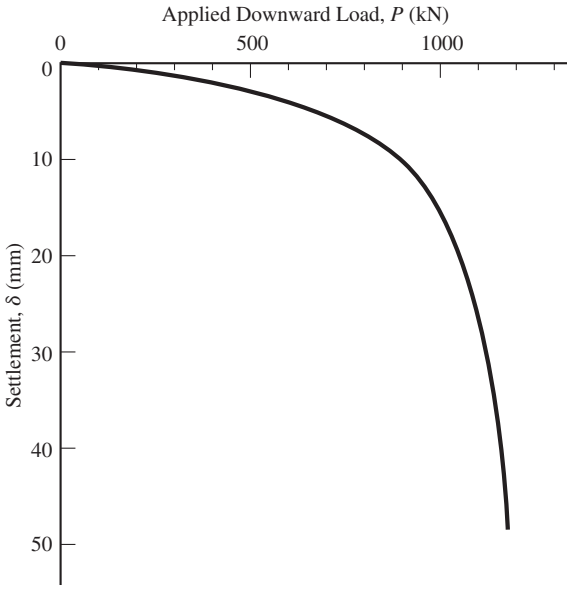

Figure 14.14 Static load test results for Problems 14.3 and 14.4.

14.5 The results of pile load tests are usually considered to be the "correct" load capacity, and all other analysis methods are compared to this standard. However, there are many ways to conduct load tests, and many ways to interpret them. Therefore, can we truly establish a single "correct" capacity for a pile? Explain.

14.6 A 250 mm square, 15 m long prestressed concrete pile ($f'_c = 40$ MPa) was driven at a site in Amsterdam as described by Heijnen and Janse (1985). A conventional load test conducted 31 days later produced the load-settlement curve shown in Figure 14.14. Using Davisson method, compute the nominal axial downward load capacity of this pile.

14.7 Solve Problem 14.6 using the Brinch Hansen 80% and 90% methods.

14.8 A static load test has been conducted on a 60 ft long, 16 in square reinforced concrete pile which has been driven from a barge through 20 ft of water, then 31 ft into the underlying soil. Telltale rods A and B have been embedded at points 30 ft and 59 ft from the top of the pile, respectively. The data recorded at failure was as follows: Load at head = 139,220 lb, settlement at head = 1.211 in, settlement of telltale rod A = 1.166 in, settlement of telltale rod B = 1.141 in. Use the data from telltale rod A to compute the modulus of elasticity of the pile, then use this value and the remaining data to compute q'_n and the average f_n value.

Hint: Telltale rod A is anchored only 1 ft from the mud line (the top of the soil). There is essentially no side friction resistance between the top of the pile and this point, so the force at a depth of 30 ft is essentially the same as that at the top of the pile.

14.9 An Osterberg load test is to be conducted on a 60 in diameter, 75 ft long drilled shaft. The expected nominal side friction capacity is 2,000 lb/ft^2 and the expected nominal net toe bearing capacity is 60,000 lb/ft^2. (a) Determine the optimal jack location such that the load capacity above the jack is equal to that below the jack. (b) Compute the required jack capacity.

15

Driven Piles—Axial Load Capacity Based on Static Analysis Methods

When the ground is soft, and sinks very much, as it commonly does in bogs, then piles are to be used, whose length ought to be the eighth part of the height of the walls, and their thickness the twelfth part of their length. The piles are to be driven so close to one another, as not to leave space for others to come in between. Care must also be taken to drive them rather with blows frequently repeated, than such as are violent; that so the earth may bind the better to fasten then.

The pilings are to be not only under the outside walls, which are placed upon the canals; but also under those which are placed on the earth, and divide the fabrick: For if the foundations of the middle walls are made different from those on the outside, it will often happen, that when the beams are placed by each other in length, and the others over them crossways, the inside walls will sink, and the outside ones, by being piled, will remain unmov'd; which, besides its being very disagreeable to the sight, will occasion all the walls to open, and ruin the whole edifice. This danger therefore is to be avoided by a trifling expense in piling; for according to the proportion of the walls, the piles in the middle will be smaller than those for the outside.

Venetian architect Andrea Palladio (1508–1580) as translated by Isaac Ware, 1738

Static analysis methods (as contrasted to static load tests) comprise the second category of techniques used to determine the nominal axial load capacities, P_n and $P_{up,n}$, for geotechnical ultimate limit state analyses. These methods determine the nominal side friction capacity, f_n, and nominal net toe bearing capacity, q_n' based on various soil parameters, such as the effective friction angle, ϕ', or the CPT cone bearing, q_c. These values are then placed into Equation 13.5 compute P_n, or Equation 13.6 compute $P_{up,n}$. Static analysis methods have been developed for specific foundation types, so they are discussed in four separate chapters: This chapter covers driven piles, Chapter 16 covers drilled shafts, Chapter 17 covers auger piles, and Chapter 18 covers other pile types.

All deep foundation projects have subsurface information from borings and lab tests, and often additional information from CPT or other in situ tests. Thus, the marginal cost of conducting static analyses consists only of the office time required to conduct the necessary calculations, which is much less costly than conducting a static load test. In addition, static analysis methods can quickly and easily consider a wide variety of pile types, diameters, lengths, and other factors. However, these methods are not as accurate as static load tests, so designs based solely on static analysis methods must be correspondingly more conservative, and therefore produce piles that are more expensive to build. In practice driven piles are designed using a combination of methods, which helps offset some of the disadvantages of each. The synthesis of these various methods is discussed in Chapter 23.

Most of this chapter discusses specific ways to obtain q_n' and f_n through the use of various equations, tables and charts, all of which are fairly straightforward and easy to use. However, the actual physics are much more complex, so the proper application of these methods in practical engineering design problems also requires a thorough understanding of how side friction and toe bearing resistances develop in driven piles, and the careful exercise of engineering judgment. The engineer also must understand the limitations of these methods.

Most static analysis methods of determining q_n' and f_n were developed from a combination of theory and experimental data. These methods attempt to quantify the most important factors that affect capacity, while other factors are implicit in the empirical correlations. For example, a researcher could perform a series of static load tests on closed-end steel pipe piles driven into cohesionless soils. These tests could be accompanied by measurements of the friction angle, ϕ', of each cohesionless soil, and the test results are then fitted into some theory of side friction to form a semi-empirical formula for f_n as a function of ϕ' and the vertical effective stress, σ_z'. Factors such as pile type, coefficient of lateral earth pressure would be implicitly incorporated into the function. Most static analysis methods were developed this way, so it is important to apply these methods only to piles that are comparable to those on which it was developed. For example, a formula developed for driven steel pipe piles is probably not applicable to drilled shafts at the same site, even if they both have the same length and diameter.

A large number of static analysis methods have been developed and published. This chapter presents principles and typical methods, but is not an exhaustive coverage of the topic. Other static analysis methods, not included here, also are valid, so the selection of an analysis method for a particular project depends on the site conditions, local experience, and other factors.

15.1 TOE BEARING

The net nominal toe-bearing capacity, q_n', for piles appears to be similar to the nominal bearing capacity, q_n, for shallow foundations. Therefore, it might seem that we could compute it using Terzaghi's bearing capacity formulas (Equations 7.4 to 7.6) with a minor adjustment for net versus gross pressure. However, there are important differences between these two kinds of foundations:

- Most bearing-capacity analyses for shallow foundations, as discussed in Chapter 7, are for general shear failure. Thus, the resulting equations are based on the assumptions that the soil is incompressible and the shear surfaces extend to the ground surface, as shown in Figure 15.1. However, toe-bearing failures in piles usually occur as a result of local or punching shear, and thus involve shearing only near the pile toe. Therefore, q_n' depends on both the strength and the compressibility of the soil.
- As shown in Figure 7.2, the load-settlement curves for local and punching shear failures do not have a distinct point of failure. Thus, it is not always clear how to define "failure" or to know exactly when it occurs. This lack of clarity also blurs the line between the ultimate limit state and serviceability limit state analyses.
- In piles, the depth of embedment, D, is very large and the diameter, B, is small. Therefore, the second term in Equations 7.4 to 7.6 dominates.

Therefore, we cannot compute the toe bearing capacity by simply applying the Terzaghi bearing-capacity formulas. It is necessary to have special methods developed specifically for piles.

The soil between a depth of about one diameter above the toe to about three diameters below the toe has the most influence on the toe bearing capacity. Thus, it is most

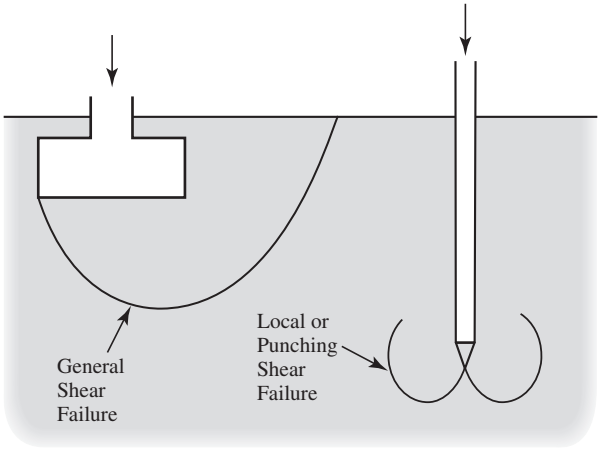

Figure 15.1 Comparison of general shear failure in spread footings with local and punching shear failures in deep foundations.

important to characterize the geotechnical properties of this *zone of influence* when conducting static analyses of toe bearing capacity.

Cohesionless Soils

Any excess pore water pressures that might develop during driving beneath piles in cohesionless soils dissipate very quickly, so we can evaluate the toe bearing resistance using an effective stress analysis with drained strengths. Using this approach, the nominal toe bearing capacity of piles in cohesionless soils may be expressed using the following formula (Kulhawy et al., 1983):

$$q'_n = B\gamma N^*_\gamma + \sigma'_{zD} N^*_q \tag{15.1}$$

where

q'_n = nominal net toe-bearing capacity
B = pile diameter
$N\gamma^*, Nq^*$ = bearing capacity factors
γ = unit weight of soil in the zone of influence around the toe (use the buoyant unit weight $\gamma - \gamma_W$ if toe is located below the groundwater table)
σ'_{zD} = vertical effective stress at the pile toe

When D/B exceeds 5, which is true for nearly all deep foundations, the first factor in Equation 15.1 becomes negligible and may be ignored.

The bearing capacity factors N_γ and N_q used in shallow foundations are functions only of the shear strength, as defined by the friction angle, ϕ', because general shear controls the failure. However, N^*_γ, N^*_q in Equation 15.1 depend on both shear strength and compressibility, because any of the three modes of failure (general, local, or punching shear) could govern. We define the compressibility effects using the *rigidity index*, I_r, of the soil (Vesić, 1977), which is the ratio of the shear modulus, G, to the shear strength, s. Substituting elastic formulas relating shear modulus with elastic modulus and the Mohr-Coulomb equation gives:

$$I_r = \frac{E}{2(1+\nu)\sigma'_{zD}\tan\phi'} \tag{15.2}$$

where

I_r = rigidity index = G/s
E = modulus of elasticity of soil within the zone of influence
ν = Poisson's ratio of soil within the zone of influence
σ'_{zD} = Vertical effective stress at the toe elevation
ϕ' = Effective friction angle of soils within the zone of influence

The magnitude of I_r is typically between about 10 and 400. Soils with high values of I_r fail in general shear, as modeled by conventional bearing capacity theory, whereas low values of I_r indicate soil compressibility is important and the local or punching shear failure modes govern.

The values of E may be obtained from CPT, SPT, or other suitable data using the techniques described in Chapter 4. The value of ν is typically estimated, as discussed in Chapter 4.

According to Vesić (1977), the bearing capacity factors N_γ^* and N_q^* are computed as follows:

$$N_\gamma^* = 0.6(N_q^* - 1)\tan\phi' \tag{15.3}$$

$$N_q^* = \frac{(1 + 2K)N_\sigma}{3} \tag{15.4}$$

$$N_\sigma = \frac{3}{3 - \sin\phi'} e^{\frac{(90-\phi')\pi}{180}\tan\phi'} \left(45 + \frac{\phi'}{2}\right) I_r^{\frac{4\sin\phi'}{3(1+\sin\phi')}} \tag{15.5}$$

where

$N_\gamma^*, N_q^*, N_\sigma$ = bearing capacity factors
K = coefficient of lateral earth pressure
ϕ' = effective friction angle, in degrees
I_r = Rigidity index

The results of these equations are presented in graphical form in Figures 15.2 and 15.3 using typical values of K.

Maximum Values

The vertical effective stress at the toe, σ'_{zD}, increases as the pile is embedded deeper into the ground, so q'_n increases with depth. However, load test results indicate q'_n eventually reaches a peak value at some depth, and greater depths of penetration in a soil with the same engineering properties will not produce greater toe bearing capacity. Thus, a maximum value is typically placed on q'_n. API (2011) recommends limiting q'_n in silicious cohesionless soils to no more than the values listed in Table 15.1. Calcareous soils have lower maximum values, as will be discussed in Section 15.6. Any of these maximum values may be overridden if supported by onsite load test results, and in many cases load tests indeed do demonstrate larger capacities.

Some static analysis methods express this concept in terms of a critical depth, which is the depth of embedment at which q'_n reaches its maximum value. This approach accomplishes the same objective in a slightly different way.

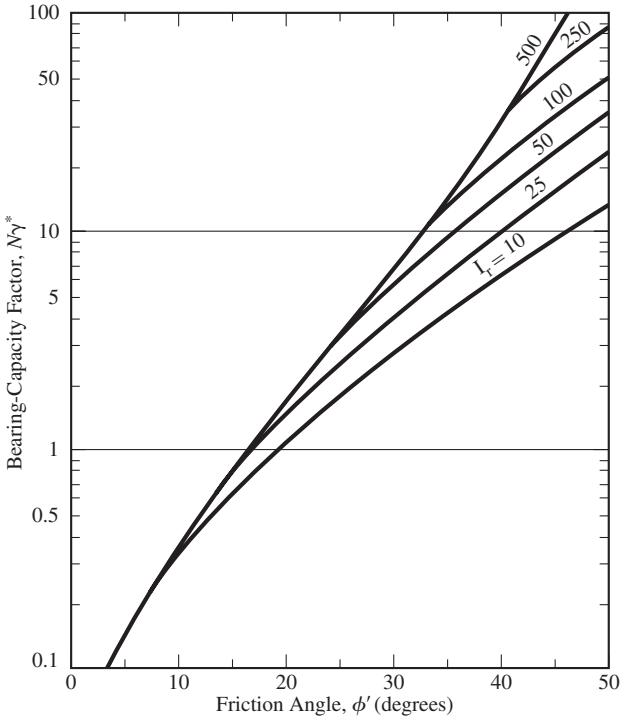

Figure 15.2 Bearing capacity factor N_γ^*. This plot is based on assumed values of K_o and thus may produce results that differ from Equation 15.3. However, this difference represents a small part of the total toe-bearing resistance. (Adapted from Kulhawy, et al. 1983; Copyright 1983 Electric Power Research Institute. Reprinted with permission).

TABLE 15.1 MAXIMUM VALUES OF NOMINAL NET TOE BEARING CAPACITY FOR SILICEOUS COHESIONLESS SOILS (API, 2011)

	Maximum Nominal Net Bearing Capacity, $q'_{n,\,\max}$	
Soil Description and Relative Density	(kPa)	(lb/ft^2)
Very loose to loose sand ($D_r = 0 - 35\%$) Loose sand-silt ($D_r = 15 - 35\%$) Medium dense to dense silt ($D_r = 35 - 85\%$)	Use CPT-based Methods	
Medium dense sand-silt ($D_r = 35 - 65\%$)	3,000	60,000
Medium dense sand ($D_r = 35 - 65\%$) Dense sand-silt ($D_r = 65 - 85\%$)	5,000	100,000
Dense sand ($D_r = 65 - 85\%$) Very dense sand-silt ($D_r = 85 - 100\%$)	10,000	200,000
Very dense sand ($D_r = 85 - 100\%$)	12,000	250,000

Sand-silt is defined as a soil with significant fractions of both sand and silt.

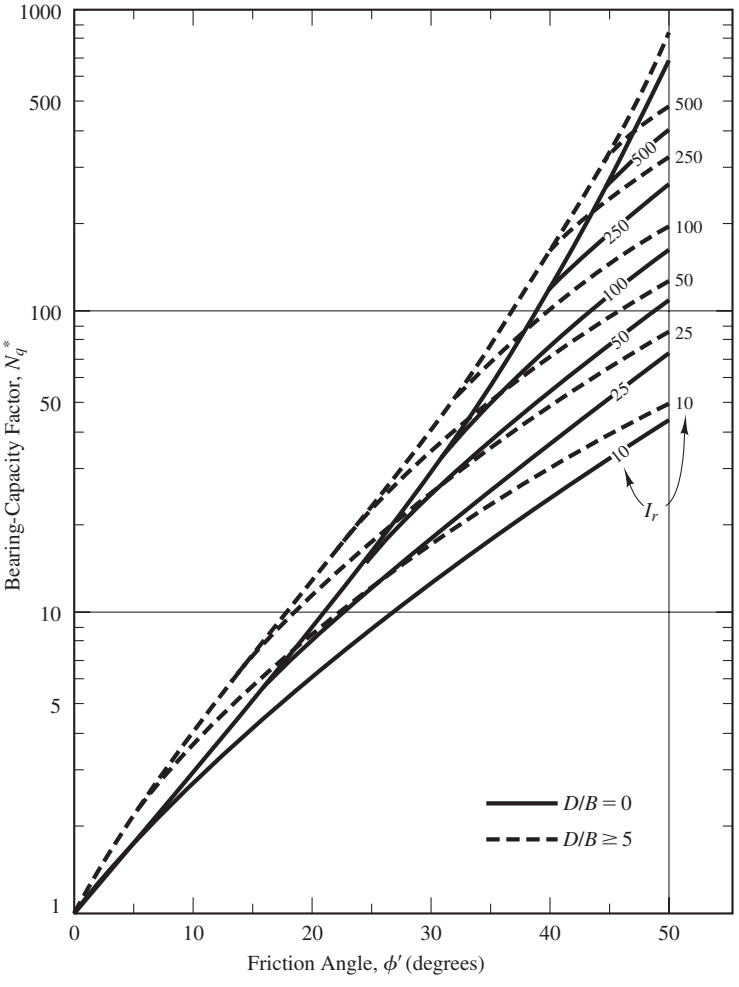

Figure 15.3 Bearing capacity factor N_q^* (adapted from Kulhawy et al. 1983; Copyright 1983 Electric Power Research Institute. Reprinted with permission).

Example 15.1

A 400 mm square prestressed concrete pile is to be driven 19 m into the soil profile shown in Figure 15.4. Compute the net load transferred to the ground through toe bearing, $q_n' A_t$.

Solution

Per Equation 4.56 and Table 4.7:

$$\begin{aligned} E &= \beta_o \sqrt{OCR} + \beta_1 N_{60} \\ &= 5000\sqrt{1} + (1200)(25) \\ &= 35{,}000\,\text{kPa} \end{aligned}$$

$$I_r = \frac{E}{2(1 + \nu)\sigma'_{zD} \tan \phi'}$$

$$= \frac{35{,}000}{2(1 + 0.30)(188) \tan 36}$$

$$= 99$$

Per Figure 15.2: $N^*_\gamma = 15$
Per Figure 15.3: $N^*_q = 76$

$$q'_n = B\gamma N^*_\gamma + \sigma'_{zD} N^*_q$$

$$= (0.4)(18.2 - 9.8)(15) + (188)(76)$$

$$= 14{,}338\text{kPa}$$

Per Table 15.1: Use $(q'_n)_{\max} = 10{,}000\,\text{kPa}$

$$q'_n A_t = (10{,}000)(0.4^2) = \mathbf{1{,}600\,kN}$$

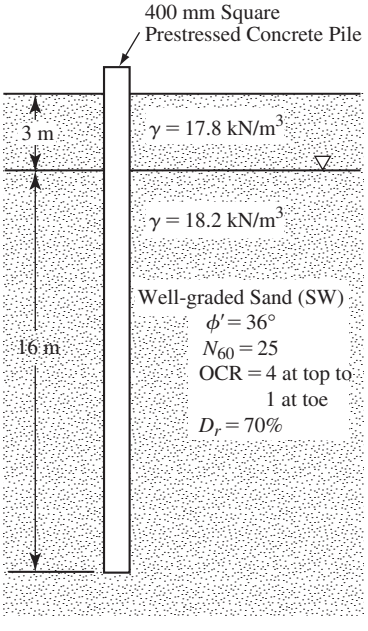

Figure 15.4 Proposed pile for Examples 15.1, 15.2 and 15.3.

Cohesive Soils

Because of their low hydraulic conductivity, we assume undrained conditions exist in cohesive soils beneath the pile toe. Therefore, we compute q_n' using the undrained shear strength, s_u. For driven piles with $D/B > 3$ in cohesive soils use the following equation:

$$q_n' = N_c^* s_u \tag{15.6}$$

The bearing capacity factor, N_c^* is normally equal to 9.0, a value attributed to Skempton. The value of s_u should reflect the soil within the zone of influence surrounding the pile tip, and may be determined from laboratory tests, such as the unconfined compression test or triaxial compression test, or from in situ tests. However, be more cautious when working with fissured clays. The spacing of these fissures is often large compared to the size of the soil samples, so test results may represent the soil between the fissures rather than the entire soil mass. In such cases, reduce s_u accordingly (perhaps to a value of about 0.75 times the measured value).

Unlike cohesionless soils, where toe bearing often provides half or more of the total capacity, driven piles in cohesive soil typically generate only a small portion of their total capacity from toe bearing. Thus, even a simple analysis, such as represented by Equation 15.6, is typically adequate for practical problems.

15.2 SIDE FRICTION

The analysis of side friction is based on the principle of sliding friction, and may be evaluated using either an effective stress analysis or a total stress analysis. Both approaches are idealizations of the true mechanics of the problem, which is much more complex (O'Neill, 2001; Randolph, 2003) and in reality include some combination of friction and adhesion. Installation effects have a major impact on the capacity, as do various aspects of the soil properties and the pile itself, so the difference between the capacities determined from these analysis methods and the actual capacity can easily exceed 30 percent. The potential error is smaller when these analysis methods are locally calibrated to onsite load tests.

In cohesive soils, the side-friction resistance within 1.5 m (5 ft) of the ground surface is sometimes ignored because of clay shrinkage caused by drying, foundation movement produced by lateral loads, pile wobble during driving, and other factors. Near the pile toe there is probably some interaction between the side friction and toe bearing resistances. However, static methods normally ignore this effect and treat these two mechanisms as if they act independently. Thus, the full side area is normally considered all the way to the bottom of the pile.

Effective Stress Analyses

The sliding friction resistance depends on the effective contact stresses between the soil and the pile, so it is most correctly viewed as an effective stress problem. Fortunately, it is possible to compute the vertical effective stress at any depth along the pile because any excess pore water pressures generated during driving will eventually dissipate and any additional load placed on the foundation during the service life of the structure will not generate any significant excess pore water pressures along the pile shaft. Thus, effective stress analyses may be performed in any soil type using the hydrostatic pore water pressure.

Principles

Side friction may be described using a simple sliding friction model:

$$f_n = \sigma_x' \tan \phi_f \tag{15.7}$$

where

f_n = nominal unit side friction capacity
σ_x' = horizontal effective stress (i.e., perpendicular to the foundation axis)
$\tan \phi_f = \mu$ = coefficient of friction between the soil and the pile
ϕ_f = soil-pile interface friction angle

Researchers have used laboratory tests to measure the coefficient of friction, $\tan \phi_f$, and have correlated it with the effective friction angle of the soil, ϕ'. Table 15.2 provides typical values of ϕ_f/ϕ'. Saturated dense soils have ϕ_f/ϕ' ratios on the high end of these ranges, whereas dry loose soils tend toward the low end.

TABLE 15.2 APPROXIMATE ϕ_f/ϕ' VALUES FOR THE INTERFACE BETWEEN DRIVEN PILES AND SOIL (adapted from Kulhawy et al., 1983 and Kulhawy 1991)

Driven Pile Type	ϕ_f/ϕ'
Concrete	0.8–1.0
Rough steel (i.e., step-taper pile)	0.7–0.9
Smooth steel (i.e., pipe pile or H-pile)	0.5–0.7
Timber	0.8–0.9

As discussed in Chapter 4, the ratio between the horizontal and vertical effective stresses is defined as the coefficient of lateral earth pressure, K:

$$K = \frac{\sigma'_x}{\sigma'_z} \tag{15.8}$$

Pile driving induces significant compression in the surrounding soils, as discussed in Section 13.3, so the coefficient of lateral earth pressure, K, is generally greater than the coefficient of lateral earth pressure in the ground before construction, K_0. The ratio K/K_0 depends on many factors, including the following:

- **High displacement versus low displacement piles**—High displacement piles, such as closed-end steel pipes, displace much more soil than do low displacement piles, such as a steel H-piles, and therefore have a much higher K/K_0 ratio. However, some of this gain may be lost over time as creep effects tend to relax the locally high horizontal stresses.
- **Soil type**—Cohesionless soils and cohesive soils react differently to the lateral strains imposed by the advancing pile during driving.
- **Soil consistency**—Dense or stiff soils provide more resistance to distortion, which results in a greater K/K_0 ratio. In cohesionless soils this effect can be expressed in terms of the relative density, D_r.
- **Vertical effective stress**—The K/K_0 ratio is generally higher when the vertical effective stress is smaller (i.e., at shallower depths).
- **Position on the pile**—End effects are present, which produce a lower K/K_0 ratio near the top and bottom of the pile and a greater ratio in the center.
- **Special construction techniques**—Predrilling or jetting loosens the soil, thus reducing the K/K_0 ratio and reducing or negating the beneficial aspects of dense or stiff soils.

The largest possible value of K is K_p, the coefficient of passive earth pressure, which is equal to $\tan^2(45 + \phi'/2)$. Table 15.3 provides guidance on selecting the K/K_0 ratio.

TABLE 15.3 APPROXIMATE RATIO OF COEFFICIENT OF LATERAL EARTH PRESSURE AFTER DRIVEN PILE CONSTRUCTION TO THAT BEFORE CONSTRUCTION (adapted from Kulhawy et al., 1983 and Kulhawy, 1991)

Method of Construction	K/K_0
Driven pile — jetted	0.5–0.7
Driven pile — small displacement	0.7–1.2
Driven pile — large displacement	1.0–2.0

Salgado (2008) derived relationships for K/K_0 for low displacement and high displacement driven piles in cohesionless soils, as shown in Figure 15.5. These plots illustrate the importance of relative density and pile displacement. However, driving high displacement piles in dense cohesionless soils is difficult and often requires predrilling, so the very high K/K_0 values for this condition may not be achievable in the field. The plots also illustrate the impact of vertical effective stress, although Salgado notes these functions may be less reliable at very low effective stresses. Thus, be cautious about using design values greater than 1.5 for low displacement piles or greater than 2.5 for high displacement piles.

The pre-construction coefficient of lateral earth pressure, K_0, may be determined using the methods described in Chapter 4. The most accurate values are obtained by conducting in situ tests, especially the pressuremeter or dilatometer test. Alternatively, empirical relationships may be used.

Combining Equations 15.7 and 15.8 with the ϕ_f/ϕ' and K/K_0 ratios gives:

$$f_n = K_o \sigma_z' \left(\frac{K}{K_o}\right) \tan\left[\phi' \left(\frac{\phi_f}{\phi'}\right)\right] \tag{15.9}$$

where

f_n = nominal unit side friction capacity
K_0 = coefficient of lateral earth pressure before construction
K/K_0 = lateral earth pressure ratio
ϕ' = drained friction angle of soil
ϕ_f/ϕ' = interface friction ratio

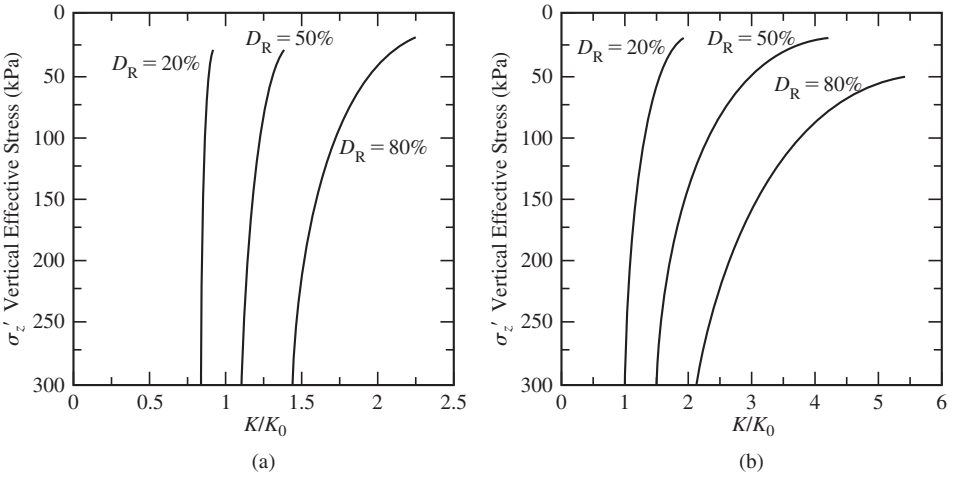

Figure 15.5 Derived K/K_0 relationships (Salgado, 2008).

Although theoretically valid for any soil type, Equation 15.9 is most often used in sands and silty sands.

Alternatively, the value of K for driven piles in cohesionless soils may be estimates using the method developed by Coyle and Castello (1981) from the results of 16 instrumented static load tests. Their findings can be represented in equation form as:

$$K = K_t 10^{-0.017 z/B} \tag{15.10}$$

where

K = Coefficient of lateral earth pressure
K_t = Coefficient of lateral earth pressure at the ground surface
= 1.33 for $\phi' = 30°$
= 2.17 for $\phi' = 33°$
= 4.49 for $\phi' = 36°$
z = Depth below the ground surface
B = Foundation diameter

This method bypasses the need to obtain K_o and to select a K/K_0 ratio, which simplifies the analysis. Using Coyle and Castello's K value and substituting Equation 15.10 into Equation 15.9, f_n becomes.

$$f_n = \sigma_z' \left(K_t 10^{-0.017 z/B} \right) \tan \left[\phi' \left(\frac{\phi_f}{\phi'} \right) \right] \tag{15.11}$$

Since the unit side friction resistance varies with depth, the pile should be divided into multiple depth increments, $f_n A_s$ should be computed for each increment, then summed.

β Method

Because of the difficulties in evaluating the factors in Equation 15.9, engineers often combine ϕ', the ϕ_f/ϕ' ratio, and the K/K_0 ratio into a single factor, β (Burland, 1973):

$$f_n = \beta \sigma_z' \tag{15.12}$$

$$\beta = K_o \left(\frac{K}{K_o} \right) \tan \left[\phi' \left(\frac{\phi_f}{\phi'} \right) \right] \tag{15.13}$$

This technique of quantifying side friction resistance is known as the *beta method*. Values of β may be computed from Equation 15.12, but more often they are backcalculated from load test results. This can be a good way to reduce the results of an onsite static load test, and facilitates extension of the test results to design the production piles.

Alternatively, design β values may be obtained from published sources, which typically reflect values calculated from static load tests, or from local experience on sites with

similar soil conditions. Soft and medium clays typically have $\beta = 0.2 - 0.4$ (Meyerhof, 1976), with progressively increasing values in stiffer (more overconsolidated) clays, perhaps as high as 1.5–2.0. Loose sands might have β of about 0.3, while dense sands might be as high as 1.0–1.5. Gravels can have much higher value, perhaps as large as 3.

Bhushan (1982) developed the following relationship from static load tests on closed-end steel pipe piles in cohesionless soils:

$$\beta = 0.18 + 0.65D_r \tag{15.14}$$

where

D_r = relative density of the soil expressed in decimal form

As indicated by the values in Tables 15.2 and 15.3, high displacement piles have higher β than low displacement piles, and concrete is higher than steel. Jetting or predrilling can substantially reduce β.

Static analyses using the β method may be performed by dividing the pile into suitable sections, assigning a β value to each section, computing σ_z' at the midpoint of the section, then computing f_n using Equation 15.11.

Maximum Value

As with toe bearing, the value of f_n increases with depth, but at some depth in a uniform soil it reaches a maximum value, especially in cohesionless soils. API (2011) recommends limiting f_n in silicious cohesionless soils to no more than the values listed in Table 15.4.

TABLE 15.4 MAXIMUM VALUES OF NOMINAL SIDE FRICTION CAPACITY FOR SILICEOUS COHESIONLESS SOILS (API, 2011)

	Maximum Side Friction Capacity $f_{n,\,\max}$	
Soil Description and Relative Density	(kPa)	(lb/ft^2)
Very loose to loose sand ($D_r = 0 - 35\%$) Loose sand-silt ($D_r = 15 - 35\%$) Medium dense to dense silt ($D_r = 35 - 85\%$)	Use CPT-based methods	
Medium dense sand-silt ($D_r = 35 - 65\%$)	67	1,400
Medium dense sand ($D_r = 35 - 65\%$) Dense sand-silt ($D_r = 65 - 85\%$)	81	1,700
Dense sand ($D_r = 65 - 85\%$) Very dense sand-silt ($D_r = 85 - 100\%$)	96	2,000
Very dense sand ($D_r = 85 - 100\%$)	115	2,400

Sand-silt is defined as a cohesionless soil with significant fractions of both sand and silt.

Calcareous soils have lower maximum values, as discussed in Section 15.6. Any of these maximum values may be overridden if supported by onsite load test results.

Example 15.2

A 400 mm square prestressed concrete pile is to be driven 19 m into the soil profile shown in Figure 15.4. Compute the nominal side friction capacity, $f_n A_s$, then compute the ASD downward load capacity using a factor of safety of 2.8.

Solution

Per Table 15.2, $\phi_f/\phi' = 0.8$

Per Table 15.3, $K/K_0 = 1.2$

$$\begin{aligned} K &= (1 - \sin\phi')\,\mathrm{OCR}^{\sin\phi'} \\ &= (1 - \sin 36)(1)^{\sin 36} \text{ to } (1 - \sin 36)(4)^{\sin 36} \\ &= 0.41 \text{ to } 0.93 \end{aligned}$$

$$\begin{aligned} \beta &= K_o\left(\frac{K}{K_o}\right)\tan\left[\phi'\left(\frac{\phi_f}{\phi'}\right)\right] \\ &= (0.41)(1.2)\tan[36(0.8)] \text{ to } (0.93)(1.2)\tan[36(0.8)] \\ &= 0.27 \text{ to } 0.61 \end{aligned}$$

For comparison, Bhushan's (1982) correlation, Equation 15.13 produces $\beta = 0.63$. We will continue with the values calculated above.

Layer	Depth (m)	σ_z' (kPa)	β	f_n (kPa)	A_s (m^2)	$f_n A_s$ (kN)
1	0–3	26.7	0.58	15.5	4.8	74
2	3–8	74.4	0.51	37.9	8.0	304
3	8–13	116.3	0.42	48.8	8.0	391
4	13–19	163.6	0.32	52.3	9.6	503
					$\Sigma f_n A_s$	1272

$$\begin{aligned} P_a &= \frac{q_n' A_t + \sum f_n A_s}{F} \\ &= \frac{1600 + 1272}{2.8} \\ &= \mathbf{1030\,kN} \end{aligned}$$

Example 15.3

Using the data in Examples 15.1 and 15.2, determine ϕP_n using the AASHTO resistance factors.

Solution

Per Table 13.4, the resistance factor for side friction is 0.25. No resistance factor for toe bearing by this method is provided, so use 0.30 (the lowest value provided).

$$\begin{aligned}\phi P_n &= (0.30)(1600) + (0.25)(1272)\\ &= \mathbf{798\,kN}\end{aligned}$$

Note how AASHTO penalizes capacity analyses of driving piles based only on static analyses. However, if accompanied by other methods, much higher resistance factors may be used as described in Table 13.3. These methods are discussed in subsequent chapters.

Total Stress Analyses (α Method)

In cohesive soils, engineers also evaluate side friction resistance using total stress analyses based on the undrained strength. The *alpha method* is the most common way of formulating this approach:

$$f_n = \alpha s_u \tag{15.15}$$

where

f_n = nominal side friction capacity
α = adhesion factor
s_u = undrained shear strength in soil adjacent to the foundation

Although total stress analyses are theoretically less correct than effective stress analyses, they have been widely used and thus have the benefit of a more extensive experience base. The formulation of the alpha method and the term *adhesion factor* also give the mistaken impression that side-friction resistance is due to a "gluing" effect between the soil and the pile. Although some adhesion may be present, it is more accurate to think of side friction resistance primarily being a classical sliding friction problem. The α value is simply a correlation between frictional resistance and s_u.

The adhesion factor, α, is determined empirically from pile load test results. Ideally, this correlation would be performed on a site-specific basis, which allows us to extend load test results to assist in the design of piles with other diameters or lengths at that site. In the absence of site-specific data, we can use published α values obtained from load tests at a variety of sites. Figure 15.6 shows back-calculated α values from full-scale static load tests, along with several suggested functions. Clearly, there is a large scatter in this

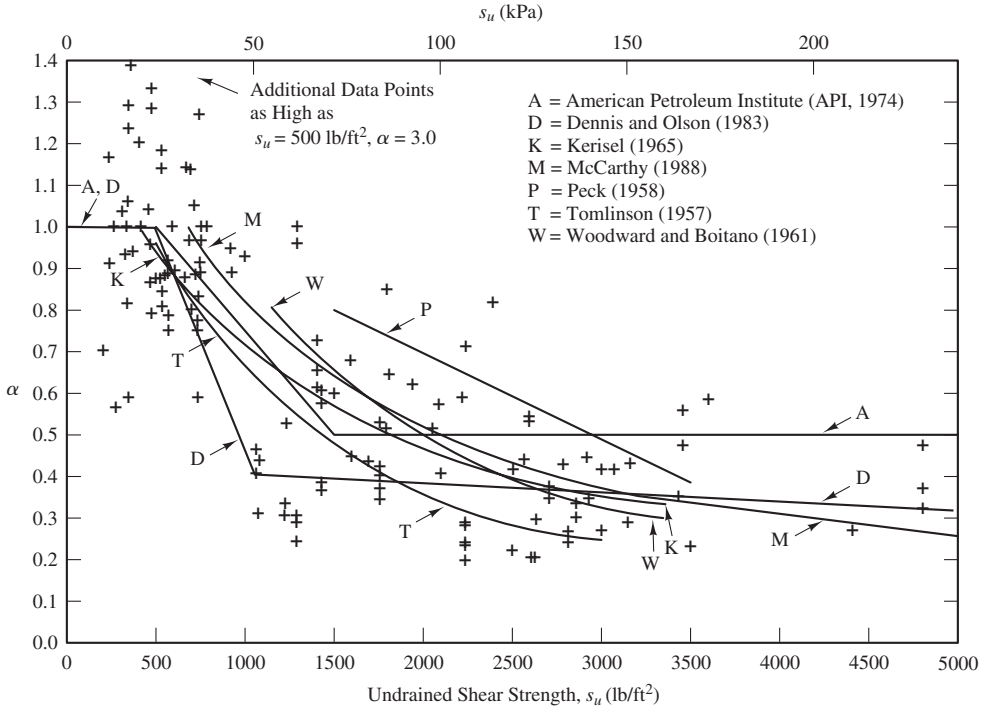

Figure 15.6 Measured values of α as back calculated from full-scale static load tests compared with several proposed functions for α.

data, and α must also depend on other factors. For example, as the overconsolidation ratio increases, α decreases. As the clay content increases, α again decreases.

Randolph and Murphy (1985) considered the shear strength, the overconsolidation ratio, the initial stress state, and other factors, many of which also affect the ratio s_u/σ'_z. Using this framework and an analysis of over 1000 load tests, they developed the following functions:

$$\text{For } s_u/\sigma'_z \leq 1: \quad \alpha = \frac{\left(s_u/\sigma'_z\right)^{0.5}_{NC}}{\left(s_u/\sigma'_z\right)^{0.5}} \tag{15.16}$$

$$\text{For } s_u/\sigma'_z > 1: \quad \alpha = \frac{\left(s_u/\sigma'_z\right)^{0.5}_{NC}}{\left(s_u/\sigma'_z\right)^{0.25}} \tag{15.17}$$

where

$(s_u/\sigma_z') <$ / = The ratio of undrained shear strength to vertical effective stress

$(s_u/\sigma_z')_{NC}$ = The ratio of undrained shear strength to vertical effective stress if the soil was normally consolidated

To use this method, the undrained shear strength should be determined at various depths along the length of the proposed pile. The Randolph and Murphy database primarily used UU triaxial tests, to this would be the most appropriate method to use when applying Equations 15.15 and 15.16 (O'Neill, 2001). Unconfined compression tests, field vane shear tests correlations from CPT, and other methods also may be used. The s_u values are then divided by the corresponding in situ vertical effective stresses to obtain a plot of the s_u/σ_z' ratio versus depth. The value of $(s_u/\sigma_z')_{NC}$ is often taken to be 0.22, as discussed in Chapter 3, and again would be plotted versus depth. These two plots and Equations 15.16 and 15.17 are then used to develop a plot of α versus depth.

Example 15.4

A 16 in diameter closed-end steel pipe pile is to be driven into the soil profile shown in Figure 15.7. Using the Randolph and Murphy method, determine the side friction resistance, then combine with the toe bearing resistance and a factor of safety of 3.0 to determine the allowable downward load capacity.

Solution

Side Friction

Depth (ft)	σ_z'(lb/ft^2)	s_u(lb/ft^2)	s_u/σ_z'	α	f_n(lb/ft^2)	A_s(ft^2)	f_nA_s (k)
5	425	2000	4.70	0.32	637	35.5	23
12	758	2300	3.03	0.36	817	31.4	26
20	1139	2100	1.84	0.40	845	37.6	32
30	1615	3200	1.98	0.40	1265	37.6	48
38	1996	4000	2.00	0.39	1577	41.8	66
50	2567	4800	1.87	0.40	1925	46.0	89
						$\sum f_nA_s =$	284

Toe Bearing

$$q_n' = 9s_u = (9)(6000) = 54{,}000\,\text{lb/ft}^2$$

$$A_t = \frac{\pi(16/12)^2}{4} = 1.40\,\text{ft}^2$$

$$P_n = \frac{q_n'A_t + \sum f_nA_s}{F}$$

$$= \mathbf{120\,k}$$

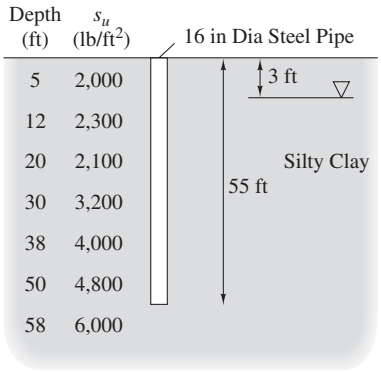

Figure 15.7 Figure for Example 15.4.

Silts

Silts can pose a more difficult design problem when using static analysis methods. Cohesive silts are often treated as being similar to clays, and analyzed using the techniques for cohesive soils, while cohesionless silts are often treated as being similar to sands and analyzed using the techniques for cohesionless soils. However, in reality they are intermediate soils with their own behavior. In some cases, piles in silts have produced substantially less capacity than expected, especially when analyzed using the techniques for cohesionless soils. Thus, additional caution is often prudent when working with silts, and the engineer should consider using static load tests (discussed in Chapter 14) or dynamic methods (discussed in Chapter 19) to confirm the load capacity.

Long Piles

Very long piles, such as those longer than 25 m (80 ft) can experience large elastic compression under load, so a large settlement at the top of the pile may be necessary in order to obtain enough displacement in the lower portion to fully mobilize the full side friction resistance. This can be a particular concern in offshore structures, which often have very long piles, and occasionally with onshore structures. One way to consider this effect in design is to assume the settlement at the top of the pile is limited to typical values, and use lower α or β values in the lower portion of the foundation to reflect the partial mobilization of the side friction resistance. Another is to use a t-z analysis, as described in Chapter 20.

15.3 ANALYSES BASED ON THE CONE PENETRATION TEST

Engineers also have developed static analysis methods based on cone penetration test (CPT) results. These methods are very attractive because of the similarities between the CPT and the load transfer mechanisms in deep foundations. The cone resistance, q_c, is very similar to the net ultimate toe-bearing resistance, q_n', and the cone side friction, f_s, is very similar

to the ultimate side-friction resistance, f_n. The CPT is essentially a miniature pile load test, and was in fact originally developed partially as a tool for predicting pile capacities. There are scale effects and other factors to consider, so we still must use empirical correlations to develop design values of q_n' and f_n from CPT data. Nevertheless, these correlations should, in principle, be more precise than those based on parameters that have more indirect relationships to the load transfer mechanisms in deep foundations.

CPT-based methods include the following:

- *Dutch method* (also known as the *European method*) (Heijnen, 1974; DeRuiter and Beringen, 1979)
- *Nottingham and Schmertmann method* (Nottingham, 1975; Nottingham and Schmertmann, 1975; Schmertmann, 1978)
- *LCPC method* developed by the Laboratoire Central des Ponts et Chaussées (also known as the *French Method*) (Bustamante and Gianeselli, 1982; Briaud and Miran, 1991)
- *Meyerhof method* (Meyerhof, 1956, 1976, 1983)
- *Tumay and Fakhroo method* (Tumay and Fakhroo, 1981)
- *Eslami and Fellenius method* (Eslami and Fellenius, 1997)

Only the LCPC and Eslami and Fellenius methods are presented here, but the other methods have similar formats.

LCPC Method

The LCPC method is an empirical approach developed by Laboratoires des Ponts et Chaussees, and is based on an analysis of static load tests in France (Bustamante and Gianeselli, 1982; Briaud and Miran, 1991).

Toe Bearing

For toe bearing computations, deep foundation are divided into two groups (terminology has been translated to conform to that used in this book):

Group I:

- Drilled shafts constructed using the open hole method, with drilling mud, or using casing
- ACIP auger piles
- Barrettes (a rectangular pile used in Europe)
- Hand-excavated cast-in-place foundations
- Type I micropiles (grouted under low pressure)

Group II:

- Driven piles, with or without post-grouting
- Jacked piles

TABLE 15.5 TOE BEARING FACTORS FOR USE IN LCPC METHOD (Bustamante and Gianeselli, 1982)

		k_t	
Soil Type	q_{ca} (MPa)	Group I	Group II
Soft clay and mud	< 1	0.4	0.5
Moderately compact clay	1–5	0.35	0.45
Silt and loose sand	≤ 5	0.4	0.5
Compact to stiff clay and compact silt	> 5	0.45	0.55
Soft chalk	≤ 5	0.2	0.3
Moderately compact sand and gravel	5–12	0.4	0.5
Weathered to fragmented chalk	> 5	0.2	0.4
Compact to very compact sand and gravel	> 12	0.3	0.4

- Type II micropiles (or small diameter piles grouted under high pressure, with diameters 250 mm)
- Pressure injected footings

The toe bearing resistance is determined using:

$$q_n' = k_t q_{ca} \tag{15.18}$$

where

q_n' = Ultimate net toe bearing resistance
k_t = LCPC toe bearing factor (From Table 15.5)
q_{ca} = Average CPT cone resistance

LCPC defines a slightly different zone of influence, so the value of q_{ca} is obtained from the zone ranging from 1.5 diameters above to 1.5 diameters below the tip elevation, as shown in Figure 15.8. Individual data points above 1.3 q_{ca} are truncated, and individual values below 0.7 q_{ca} are truncated above the tip.

Note how the k_t factors are all less than 1. This is partly due to scale effects, and partly because advancement of the CPT probe truly causes a toe bearing failure in the soil, whereas we define q_n' at a settlement of 10 percent of the foundation diameter.

Side Friction

For side friction assessments, deep foundations are classified as follows (terminology has been translated to North American usage):

Category I A

- Drilled shafts constructed using open hole or drilling mud
- ACIP auger piles

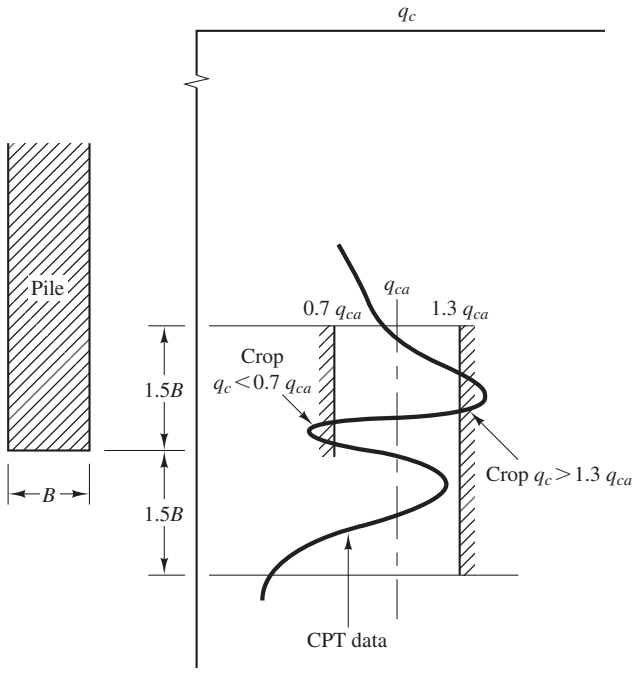

Figure 15.8 Criteria for determining q_{ca} in LCPC Method.

- Type I micropiles
- Barrettes

Category I B

- Drilled shafts constructed using casing
- Mandrel-driven thin shell piles

Category II A

- Driven concrete piles
- Prestressed tubular piles
- Jacked concrete piles

Category II B

- Driven steel piles
- Jacked steel piles

Category III A

- Driven grouted piles
- Pressure-injected footings

Category III B

- High pressure grouted piles with diameter greater than 250 mm
- Type II micropiles.

The side friction resistance is computed using:

$$f_n = \frac{q_c}{k_s} \leq f_{um} \tag{15.19}$$

where

f_n = Nominal side friction capacity
f_{nm} = Maximum nominal side friction capacity
k_s = LCPC side friction factor (from Table 15.6)
q_c = CPT cone resistance

Values of the factor k_s and the maximum nominal side friction capacity, f_{nm}, are presented in Table 15.6. Where a range of values is presented, the lower value is intended for projects with lower levels of quality control, while the larger value is intended for careful construction procedures and high levels of quality control. However, these f_{nm} values appear to be overly conservative, so an engineer might consider exceeding them. For example, Rollins, Miller and Hemenway (1999) found that ignoring the LCPC maximum allowable values produced more accurate analyses.

No k_s values are presented for Category III, but f_{nm} values are provided, so the LCPC method is of limited use for this category.

Accuracy

Implementation of the LCPC method requires some judgment, but when carefully applied it appears to provide good results. For example, Titi and Abu-Farsakh (1999) evaluated the results of 60 static load tests on prestressed concrete piles in Louisiana, and found the average LCPC analysis overpredicted the capacity by only 3 percent, and the 90th percentile of LCPC analyses overpredicted the capacity by a factor of 1.42. This error is smaller than that from the methods described in Section 15.2, and is well within the customary factors of safety, as presented in Chapter 13.

Eslami and Fellenius Method

Basis

Eslami and Fellenius used the results of 102 full-scale static load tests from a total of forty sites in thirteen countries, along with nearby CPT soundings to develop a method for evaluating axial load capacity. All of the load tests were conducted on piles, and the soil conditions ranged from soft clay to gravelly sand.

TABLE 15.6 SIDE FRICTION FACTORS FOR LCPC METHOD (Bustamante and Gianeselli, 1982)

		Category									
		k_s				f_{nm} (MPa)					
		I		II		I		II		III	
Soil Type	q_c (MPa)	A	B	A	B	A	B	A	B	A	B
Soft clay and mud	< 1	30	30	30	30	0.015	0.015	0.015	0.015	0.035	
Moderately compact clay	1–5	40	80	40	80	0.035 – 0.080	0.035 – 0.080	0.035 – 0.080	0.035	0.080	≥ 0.120
Silt and loose sand	≤ 5	60	150	60	120	0.035	0.035	0.035	0.035	0.080	
Compact to stiff clay and compact silt	> 5	60	120	60	120	0.035 – 0.080	0.035 – 0.080	0.035 – 0.080	0.035	0.080	≥ 0.200
Soft chalk	≤ 5	100	120	100	120	0.035	0.035	0.035	0.035	0.080	
Moderately compact sand and gravel	5–12	100	200	100	200	0.080 – 0.120	0.035 – 0.080	0.080 – 0.120	0.080	0.120	≥ 0.200
Weathered to fragmented chalk	> 5	60	80	60	80	0.120 – 0.150	0.080 – 0.120	0.120 – 0.150	0.120	0.150	≥ 0.200
Compact to very compact sand and gravel	> 12	150	300	150	200	0.120 – 0.150	0.080 – 0.120	0.120 – 0.150	0.120	0.150	≥ 0.200

Note: The use of ≥ maximum values for Category IIIB probably indicate insufficient data was available to establish these maximum values, but the maximum is thought to be at least as large as the stated values.

This method takes advantage of the additional data gained through the use of a *piezocone* (also known as a CPTU test) which is a standard CPT probe equipped with a piezometer to measure the pore water pressure near the cone tip while the test is in progress. This pore water pressure is the sum of the hydrostatic pore water pressure (such as could be measured using a conventional stationary piezometer) and any excess pore water pressures induced by the advancing cone. In cohesionless soils, the excess pore water pressure is usually very small, but in cohesive soils it can be large.

When using piezocones, the pore pressure data is combined with the measured q_c values to obtain the *corrected cone resistance*, q_T, as discussed in Section 4.3. The correction factors depend on the details of the piezocone, so this correction is normally applied when reducing the original CPT data, and a plot of q_T versus depth is provided to the engineer.

The Eslami and Fellenius method requires application of an additional pore water pressure correction to the q_T values as follows:

$$q_E = q_T - u_2 \tag{15.20}$$

where

q_E = effective cone resistance
q_T = corrected cone resistance
u_2 = pore water pressure measured behind the cone point

This correction is intended to more closely align the analysis with the effective stresses. In cohesionless soils, u_2 should be approximately equal to the hydrostatic pore water pressure. Therefore, this method could still be used in cohesionless soils even if only conventional CPT data (i.e., no pore pressure data) is available, so long as the position of the groundwater table is known.

Toe Bearing

This method correlates the net unit toe-bearing capacity, q_nN, with the effective cone resistance, q_E. Toe bearing failures occur as a result of punching and local shear, and thus affect only the soils in the vicinity of the toe. Therefore, the analysis considers only the q_E values in the following zones:

- For piles installed through a weak soil and into a dense soil: $8B$ above the pile toe to $4B$ below the pile toe
- For piles installed through a dense soil and into a weak soil: $2B$ above the pile toe to $4B$ below the pile toe

In both cases, B is the pile diameter. The geometric average, q_{Eg}, of the n measured q_E values within the defined depth range is then computed using:

$$q_{Eg} = \frac{(q_E)_1(q_E)_2(q_E)_3 \ldots (q_E)_n}{n} \tag{15.21}$$

In general, odd spikes or troughs in the q_E data should be included in the computation of q_{Eg}. However, extraordinary peaks or troughs might be "smoothed over" if they do not appear to be representative of the soil profile. For example, occasional gravel in the soil can produce false spikes.

The net unit toe-bearing resistance has then been empirically correlated with q_{Eg} using the load test results:

$$q'_n = C_t q_{Eg} \tag{15.22}$$

where

q'_n = net nominal toe bearing capacity
C_t = toe bearing coefficient
q_{Eg} = geometric average effective cone resistance

Eslami and Fellenius recommend using $C_t = 1$ for pile foundations in any soil type. In addition, unlike some other methods, they do not place any upper limit on q_uN.

Side Friction

The procedure for computing the unit side-friction resistance, f_n, is similar to the method used to compute q_nN. If the analysis is being performed by a computer (which is often the case, because CPT data can be provided in electronic form), a side-friction analysis is performed for each CPT data point using the following equation:

$$f_n = C_s q_E \tag{15.23}$$

where

f_n = nominal side friction capacity
C_s = side-friction coefficient (from Table 15.7)
q_E = effective cone resistance

The C_s value depends on the soil type, and should be selected using Table 15.7. This soil classification may be determined directly from the CPT data using Figure 15.9.

TABLE 15.7 SIDE-FRICTION COEFFICIENT, C_s (Eslami and Fellenius, 1997)

	C_s	
Soil Type	Range	Typical Design Value
Soft sensitive soils	0.0737–0.0864	0.08
Clay	0.0462–0.0556	0.05
Stiff clay or mixture of clay and silt	0.0206–0.0280	0.025
Mixture of silt and sand	0.0087–0.0134	0.01
Sand	0.0034–0.0060	0.004

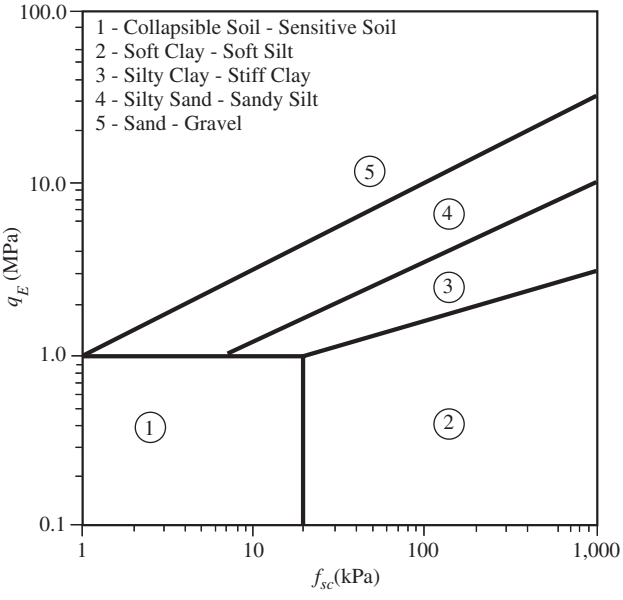

Figure 15.9 Soil classification from CPT data (Eslami and Fellenius, 1997).

Because CPT data is typically provided at depth intervals of 100 to 200 mm, this procedure is too tedious to use at every data point when performing computations by hand. Therefore, hand computations usually divide the soil between the ground surface to the pile tip into layers according to the CPT results, with a representative q_E for each layer. For most soil profiles, five to ten layers are sufficient.

Accuracy

Finally, Eslami and Fellenius applied this method to independent load test data (i.e., not the data used to develop the method). This comparison indicates the average ultimate capacity prediction using this method is within about 2 percent of the measured ultimate capacity (i.e., there is no systematic bias), and that 95 percent of the predictions are within about 30 percent of the measured ultimate capacity. This is very good accuracy (e.g., compare with Figure 15.6), and certainly well within the range implied by the factors of safety in Chapter 13. However, attaining this accuracy in practice requires careful selection of the C_s values from Table 15.7, which may be difficult for some soils.

Example 15.5

A 400 mm square prestressed concrete pile is to be driven 12.0 m into the soil profile shown in Figure 15.10. Using the Eslami and Fellenius method and the AASHTO resistance factors, compute ϕP_n.

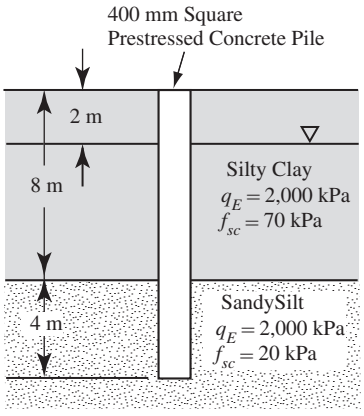

Figure 15.10 Soil profile for Example 15.5.

Solution

Toe bearing

$$q_n' = C_s q_{Eg} = (1)(2500) = 2500\,\text{kPa}$$
$$A_t = (0.4)^2 = 0.16\,\text{m}^2$$

Side friction

Silty clay stratum (ignore upper 1.5 m)

$$f_n = C_S q_E = (0.025)(2000) = 50\,\text{kPa}$$
$$A_s = (4)(0.4)(8.0 - 1.5) = 10.4\,\text{m}^2$$

Sandy silt stratum

$$f_n = C_S q_E = (0.01)(2500) = 25\,\text{kPa}$$
$$A_s = (4)(0.4)(4.0) = 6.4\,\text{m}^2$$

Downward load capacity

Per Table 13.4, use $\phi = 0.50$ for both side friction and toe bearing

$$\phi P_n = (0.50)(2500)(0.16) + (0.50)\Big[(50)(10.4) + (25)(6.4)\Big]$$
$$= \mathbf{540\,kN}$$

15.4 UPWARD CAPACITY

The nominal upward capacity of driven piles, $P_{up,n}$, relies mostly on the side friction capacity, per Equation 13.6. There is no toe bearing, and the contribution from the weight of the pile is typically small. Thus, the selection of an appropriate value of f_n is the most critical parameter in the design of pile subjected to uplift.

Engineers continue to debate whether or not the f_n in uplift is equal to the value for downward loading, and evidence has been provided on both sides of this debate. However, the most compelling evidence seems to support the notion that f_n in uplift is less than that for downward loading (O'Neill, 2001; Randolph, 2003). For example, field tests and theoretical studies by De Nicola and Randolph (1993) support this finding, which appears to be due to a number of influences, including:

- The soil fabric adjacent to the pile is altered due to the load reversal
- The shear surfaces are projected upward, which can cause some loosening of the soil
- The Poisson effect during tensile loading decreases the pile diameter, thus slightly reducing the contact pressure

These influences are not well understood, and difficult to quantify. Nevertheless, for ASD, design values of f_n in uplift are typically reduced to 70–85 percent of the corresponding value for downward loading. For LRFD, this reduction is already incorporated into the resistance factor.

In addition, once the side friction capacity is mobilized, the pile will heave quite dramatically, potentially inducing a sudden and catastrophic failure of the structure. For example, such failures occurred in Mexico City during the 1985 earthquake. This is quite different from the more ductile and generally less catastrophic failures under downward loads. Therefore, in addition to using lower f_n values, ASD uplift capacity analyses also use a higher factor of safety, as shown in Table 13.4. This extra conservatism is justified by the greater consequences of an uplift failure.

Example 15.6

Using the AASHTO code, compute $\phi P_{up,n}$ for the pile in Example 15.5.

Solution

Per Equation 13.14, we must apply a load factor to the buoyant weight of the pile. The AASHTO load factors for dead loads range from 0.90 to 1.50. In this case, the weight is beneficial (it increases the uplift capacity) so rather than using the usual load factors of 1.40-1.50, we must use the much lower load factor of 0.9. In other words, we are concerned about the pile being too light, not too heavy.

Per Table 13.4, the resistance factor for CPT-based methods is 0.40.

$$\begin{aligned} W_f &= (0.4)^2(12)(23.6\,\text{kN/m}^3) - (0.4)^2(10)(9.8\,\text{kN/m}^3) \\ &= 30\,\text{kN} \end{aligned}$$

$$\begin{aligned} \phi P_{up,n} &= \gamma_D W_f + \phi_s \sum f_n A_s \\ &= (0.90)(30) + (0.40)\Big[(50)(10.4) + (25)(6.4)\Big] \\ &= \mathbf{299\,kN} \end{aligned}$$

15.5 GROUP EFFECTS

Driven piles are usually installed in groups of three or more, as discussed in Chapter 12, and the proper spacing of piles in the group is important. If they are too close (i.e., less than about 2.5–3.0 diameters on center), there may not be enough room for errors in positioning and alignment. Conversely, if the spacing is too wide, the pile cap will be very large and expensive. Therefore, piles are usually spaced about 3 diameters on-center.

Pile groups require special consideration in terms of their axial load capacity (as discussed in this section), their lateral load capacity (as discussed in Chapter 22) and their settlement behavior (as discussed in Chapter 20). None of these characteristics are the same as for individual piles, and thus require appropriate adjustments in the design calculations.

Interactions Among Piles

Piles in a group are close enough to interact with one another. Additionally, the soil in and around a pile groups is influenced by the piles in the group. For example:

- Pile driving densifies the surrounding soils, especially in cohesionless soils, and in pile groups these densification zones overlap. Thus, each pile increases the lateral earth pressure and the side friction capacity of the adjacent piles. The use of jetting or predrilling during installation can have a significant impact on this phenomenon.
- The loads transferred into the soil through side friction can transfer to the adjacent piles.
- The stresses from toe bearing can overlap, thus, changing the toe bearing capacity of the individual piles.
- The zones of excess pore water pressure generated by the pile driving process will overlap and together encompass a much larger volume of soil.
- If the pile cap is in contact with the soil, then it provides some confinement.

These interactions have been studied through static load tests on pile groups (DiMillio et al., 1987a, 1987b; O'Neill, 1983), but such tests are very expensive and thus rarely conducted. Additional research has been conducted on model piles, which provides some insight, but suffers from scaling effects. Based on the results of this work, researchers have found that group effects are complex and depend on many factors, including:

- The number, length, diameter, arrangement, and spacing of the piles
- The load transfer mode (side friction versus end bearing)
- The construction procedures used to install the piles
- The sequence of installation of the piles
- The soil type

- The elapsed time since the piles were driven
- The interaction, if any, between the pile cap and the soil
- The direction of the applied load

The net effect is usually described in terms of the *group efficiency factor*, η:

$$P_{ng} = \eta N P_n \tag{15.24}$$

where

P_{ng} = nominal axial load capacity of the pile group
η = group efficiency factor
N = number of piles in group
P_n = nominal axial load capacity of an individual pile

The design values of η require consideration of a number of factors, including some engineering judgment.

Cohesionless soils

Group efficiency factors from model and full-scale static load tests of piles in cohesionless soils with center-to-center spacing, s, and diameter, B, as reported by O'Neill (1983), suggest the following:

- In loose cohesionless soils, η is always greater than 1 and increases as the spacing becomes closer (reaching a peak value at $s/B = 2$). The value of η also seems to increase with the number of piles in the group.
- In dense cohesionless soils with $2 < s/B < 4$ (the normal range), η is usually slightly greater than 1 so long as the pile was installed without predrilling or jetting.
- Piles installed by predrilling or jetting, and drilled shafts, have lower group efficiency factors, perhaps as low as about 0.7.

The high values of η in cohesionless soils seem to be primarily due to the radial consolidation that occurs during driving and the resulting increase in lateral stress. Less consolidation occurs if predrilling or jetting is used.

For design, Hannigan et al. (2006b) recommend:

1. $\eta = 1$ so long as jetting or predrilling has not been used
2. If jetting or predrilling is essential, then it should be kept to a minimum and carefully controlled during construction. The design value of η should be less than 1.
3. Use a center-to-center spacing of at least 3 diameters

Cohesive Soils

The results from model and full-scale static tests in cohesive soils are quite different from those in cohesionless soil (O'Neill, 1983). The group efficiency factor, η, is generally less than one, and becomes smaller as the number of piles in the group increases. Some of the measured η values were as low as 0.5.

Another important difference is that η for groups in cohesive soils increases with time. This is because the efficiency of pile groups in cohesive soils is largely governed by excess pore water pressures induced by pile driving. Although the magnitude of these pressures is not significantly higher than those near single piles, they encompass a larger volume of soil and therefore dissipate much more slowly, as shown in Figure 15.11. For single piles, nearly all of the excess pore water pressures dissipate within days or weeks of pile driving, whereas in groups they may persist for a year or more.

For design, Hannigan, et al. (2006b) recommend:

1. For $s_u < 95$ kPa (2000 lb/ft^2) and pile cap not in firm contact with the ground
   a. $\eta = 0.7$ for spacing of 3 diameters
   b. $\eta = 1.0$ for spacing of 6 diameters
2. For $s_u < 95$ kPa (2000 lb/ft^2) and pile cap in firm contact with the ground, $\eta = 1.0$
3. For $s_u > 95$ kPa (2000 lb/ft^2) $\eta = 1.0$
4. Use center-to-center spacing of at least 3 diameters

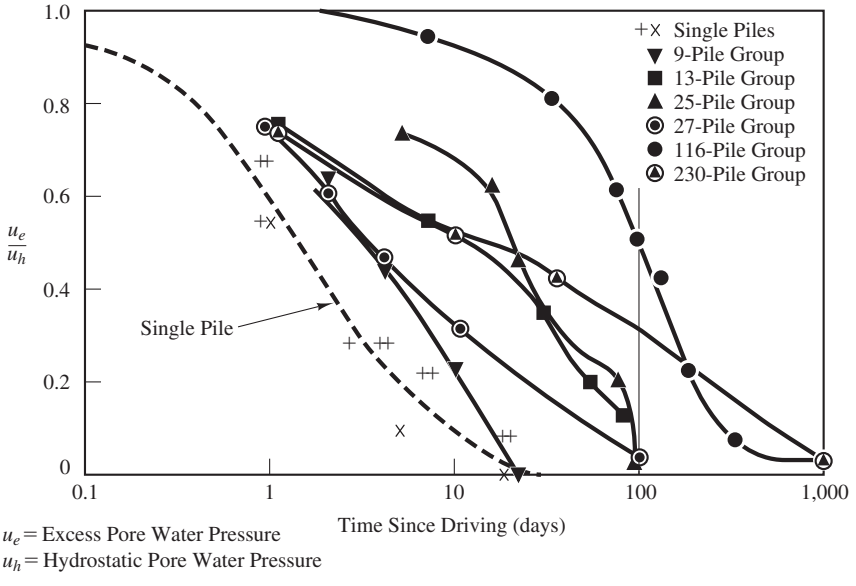

Figure 15.11 Measured excess pore water pressure in soil surrounding full-scale static pile groups (data from O'Neill, 1983; used with permission of ASCE).

It is important to consider the potential for temporary reductions in capacity while the excess pore ware pressures are dissipating. The short-term ultimate capacity of pile groups in saturated cohesive soils will be reduced to about 0.4 to 0.8 times the ultimate value. However, as these excess pore water pressures dissipate, the ultimate capacity will increase. The rate at which it rises depends primarily on the dissipation of excess pore water pressures. Small groups will probably reach the long term η within 1 to 2 months, which may be faster than the rate of superstructure construction, whereas larger groups may require a year or more. If the group will be subjected to the full design load before the excess pore water pressures full dissipate, then a more detailed analysis may be warranted. In some cases, it may be appropriate to install piezometers to monitor the dissipation of excess pore water pressures.

Block Failure

Analyses of group capacity also should consider the possibility of the piles and the soil between the individual piles failing together as a group. In this case, the shear surface would be the perimeter of the group rather than the perimeter of the individual piles, as shown in Figure 15.12. This mode is called a *block failure*.

A block capacity analysis is similar to a capacity analysis for a single pile, except the plan dimensions are much larger. The end area, A_{tg}, is equal to that of the entire group, as shown in Figure 15.12, and is much larger than the sum of the individual pile end areas, $N(A_t)$. However, the side area is the perimeter of the group times the depth of embedment,

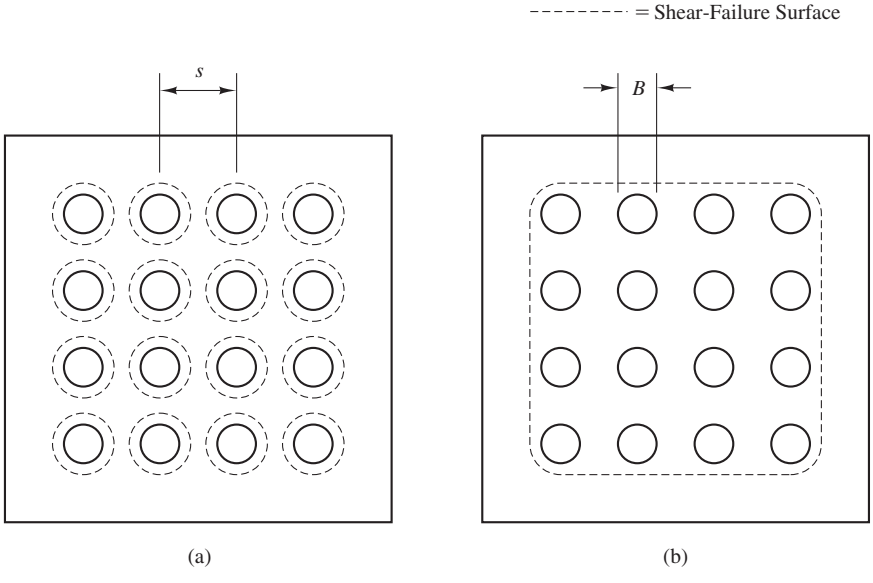

Figure 15.12 Types of failures in pile groups: (a) individual failure occurs along the perimeter of each pile, (b) block failure occurs along the perimeter of the pile group.

and can be less than the sum of the individual pile side areas. Thus, the ratio of side friction capacity to toe bearing capacity for a group is much less than that for the individual piles.

If the ultimate toe bearing resistance, q_n' is small, then the increase in toe bearing capacity will be modest, even given the larger base area, and may not be enough to offset the loss in side friction capacity. In that case, block failure may govern the design. The opposite is true when q_n' is large. The number of piles in the group, the geometry of their layout, the depth of embedment, and other factors also impact the analysis.

If the pile tips are founded in a thick stratum of cohesionless soils, $q_n'(A_{tg})$ will be quite large and block failure will not govern the design. However, if the pile tips are founded in cohesive soil, or in a thin sand stratum underlain by cohesive soil, then the potential for block failure must be considered. The bearing capacity factor, N_c^*, for a block failure analysis is:

$$N_c^* = 5\left(1 + \frac{D}{5B_g}\right)\left(1 + \frac{B_g}{5L_g}\right) \leq 9 \tag{15.25}$$

where

N_c^* = Bearing capacity factor for use in Equation 15.6
D = Depth of embedment
B_g = Width of pile group
L_g = Length of pile group

Even though the side friction resistance involves some shearing on a pile-soil interface and some on a soil-soil interface, it is customary and conservative to use the same side friction resistance, f_n, as for an individual pile analysis. The capacity of the pile group is then the lesser of those computed using a pile group efficiency analysis and a block capacity analysis.

Upward Capacity of Pile Groups

Analyses of the upward capacity of pile groups also should consider both geotechnical failure of the individual piles and block failure of the pile group. The individual pile analysis may use the result from Equation 13.6 times the number of piles. The block analysis produces resistance from perimeter side friction and from the weight of the piles and the soil between the piles. IBC [1810.3.3.1.6] requires the allowable uplift load from the block analysis not exceed two-thirds of the ultimate side friction capacity plus two-thirds of the weight.

15.6 UNUSUAL SOILS

Most of the analysis methods described in this chapter were developed primarily in areas with temperate climates, and thus are biased toward the kinds of soils typically found in such environments. These methods may be less applicable in other climates because the soil conditions are correspondingly different.

Calcareous soils are one type that has sometimes caused problems. Although these soils may have grain size distributions similar to the more commonly seen siliceous soils, the base material is mostly calcium carbonate which was derived from the skeletons of organisms. Such soils behave differently, so the empirical design methods may be misleading. When encountering unusual soils, engineers often rely more heavily on local experience, and may be more likely to conduct static load tests.

15.7 SETUP AND RELAXATION

The process of driving piles produces substantial changes in the surrounding soil, as discussed in Section 13.3. These changes include compression, remolding, breaking down cementation, and perhaps most importantly the temporary generation of positive excess pore water pressures. Some of these effects, such as dissipation of the excess pore water pressures, cause a change in the pile capacity with time, so the long-term capacity can be quite different from the end-of-driving capacity. When the capacity increases with time after driving, the pile is said to experience *setup*. Conversely, when the capacity decreases after driving the pile is said to experience *relaxation*.

For driven piles, presence of setup or relaxation is often detected by comparing the end-of-driving hammer blow count to that obtained some time later (typically the next day) in a restrike blow count. This later value is obtained by setting up the hammer on the completed pile and driving it again. More accurate assessments may be obtained using a pile driving analyzer during pile driving and during the restrike, as discussed in Chapter 19.

The *setup factor*, is the ratio of the long-term capacity divided by the end-of-driving capacity. Sands typically exhibit little or no setup (setup factor ~1), although cases with significant setup in sands have been observed. Saturated clays typically have the most setup. This supports the theory that dissipation of excess pore water pressures is the primary physical mechanism.

Rausche, et al. (1996) evaluated the setup factors measures on 99 test piles from 46 sites, as shown in Table 15.8. The wide range of results is evident, especially in fine-grained soils, which illustrates the difficulty in accurately predicting the setup factor. Nevertheless, proper consideration of setup is beneficial to both constructability and cost efficiency. Chapter 23 discusses methods of considering setup in the design and construction process.

Relaxation is much less common, but has been observed in some dense, saturated, fine grained soils such as non-cohesive silts and fine sands, and in some shales (Hannigan, et al., 2006a). The underlying physical mechanisms are not well understood. Thompson and Thompson (1985) observed that a reduction in hammer blow count from the end-of-driving to that obtained during a restrike is most often due to changes in the hammer efficiency and performance, especially with diesel hammers. Such situations can be erroneously identified as relaxation. Fortunately, these situations can be identified using a pile driving analyzer as described in Section 19.2.

TABLE 15.8 SETUP FACTORS FOR DRIVEN PILES (adapted from Rausche et al., 1996 and Hannigan et al., 2006)

Predominant Soil Type Along Pile Shaft	Range in Observed Setup Factor	Typical Design Setup Factor[a]	Number of Sites and Percentage of Database
Clay	1.2–5.5	2.0	7 (15%)
Silt-clay	1.0–2.0	1.0	10 (22%)
Silt	1.5–5.0	1.5	2 (4%)
Sand-clay	1.0–6.0	1.5	13 (28%)
Sand-silt	1.2–2.0	1.2	8 (18%)
Fine sand	1.2–2.0	1.2	2 (4%)
Sand	0.8–2.0	1.0	3 (7%)
Sand-gravel	1.2–2.0	1.0	1 (2%)

[a]Recommend confirmation with local experience.

SUMMARY

Major Points

1. Static analysis methods of evaluating axial load capacity are those based on soil properties. These methods use empirical or semi-empirical formulas to evaluate the values of q_n' and f_n, which are then combined with the foundation geometry to compute the axial load capacity.
2. Static analysis methods are less accurate than full-scale static load tests, but have the advantages of being less expensive to implement and more flexible. However, because of this loss in accuracy, they require the use of higher factors of safety, which increases construction costs.
3. Unlike bearing-capacity failures in shallow foundations, toe-bearing failures in deep foundations are usually local or punching shear. Thus, the toe bearing capacity depends on both the strength and the compressibility of the soil.
4. Side friction analyses may be performed using effective stresses, because drained conditions are normally present. However, total stress methods also are available.
5. The cone penetration test can be an excellent basis for static methods because this test is essentially a miniature pile load test. However, the results must be adjusted to account for scale effects and other differences between the CPT and a pile
6. When deep foundations are installed in groups, we must consider the group interaction effects. These effects are described by the group efficiency factor and by considering the possibility of a block failure.

Vocabulary

Alpha method	Effective stress analysis	Individual failure
Beta method	Group efficiency	Rigidity index
Block failure	Group efficiency factor	Total stress analysis

QUESTIONS AND PRACTICE PROBLEMS

Sections 15.1-15.2: Introduction, Toe Bearing and Side Friction

15.1 Why would it be inappropriate to design a drilled shaft using a static analysis method developed for driven piles?

15.2 Why would it be inappropriate to use the Terzaghi bearing capacity formulas from Chapter 7 to determine the toe bearing capacity of a driven pile?

15.3 An 18 in diameter closed-end steel pipe pile is to be driven to a depth of 53 ft into the following soil profile:

Depth (ft)	Soil Classification	Unit Weight, γ (lb/ft^3)	Friction Angle, ϕ' (deg)	OCR
0–5	Silty sand	118	28	5.0
5–20	Fine to medium sand	121	31	3.5
20–50	Silty sand	118	29	2.5
50–60	Well graded sand	123	35	2.0

No predrilling or jetting is to be used. The groundwater table is at a depth of 15 ft. Using a factor of safety of 3.0, compute the ASD allowable downward load capacity, P_a.

15.4 Using the data in Problem 15.3 and the AASHTO resistance factors, compute ϕP_n.

15.5 A 500 mm diameter closed-end steel pipe pile is to be driven to a depth of 17 m into the following soil profile:

Depth (m)	Soil Classification	Unit Weight, γ (kN/m^3)	Friction Angle, ϕ' (deg)	OCR
0–2.0	Silty sand	19.0	28	4.5
2.0–6.5	Fine to medium sand	19.5	31	3.5
6.5–16.0	Silty sand	19.1	29	2.5
16.0–17.5	Well graded sand	19.8	35	1.5

No predrilling or jetting is to be used. The groundwater table is at a depth of 5.5 m. Compute the toe bearing capacity, $q_n' A_t$.

15.6 Using the data in Problem 15.5 and the AASHTO resistance factors, compute ϕP_n.

15.7 A 24 in square prestressed concrete pile is to be driven to a depth of 68 ft into the following soil profile:

Depth (ft)	Soil Classification	Unit Weight, γ (lb/ft^3)	Undrained Shear Strength, s_u (lb/ft^2)
0–10	Silty clay	110	1000
10–32	Clayey silt	118	1300
32–40	Clay	116	2000
40–70	Clay	119	2500

The groundwater table is at a depth of 5 ft. Using the Randolph and Murphy method with a factor of safety of 3.0, compute the ASD allowable downward load capacity, P_a.

15.8 Using the data in Problem 15.7 and the AASHTO resistance factors, compute ϕP_n.

15.9 A 600 mm square prestressed concrete pile is to be driven to a depth of 20.0 m into the following soil profile:

Depth (m)	Soil Classification	Unit Weight, γ (kN/m^3)	Undrained Shear Strength, s_u (kPa)
0–3.0	Silty clay	17.0	50
3.0–10.2	Clayey silt	17.5	55
10.2–12.0	Clay	17.8	80
12.0–22.0	Clay	18.1	120

The groundwater table is at a depth of 5 m. Using the Randolph and Murphy method with a factor of safety of 3.0, compute the ASD allowable downward load capacity, P_a.

15.10 Using the data in Problem 15.9 and the AASHTO resistance factors, compute ϕP_n.

Section 15.3: Analyses Based on CPT

15.11 Using the Eslami and Fellenius method, compute the ASD allowable downward load capacity of an 18 in diameter closed-end steel pipe pile driven 60 ft into the soil profile shown in Figure 15.13. Use a factor of safety of 2.5.

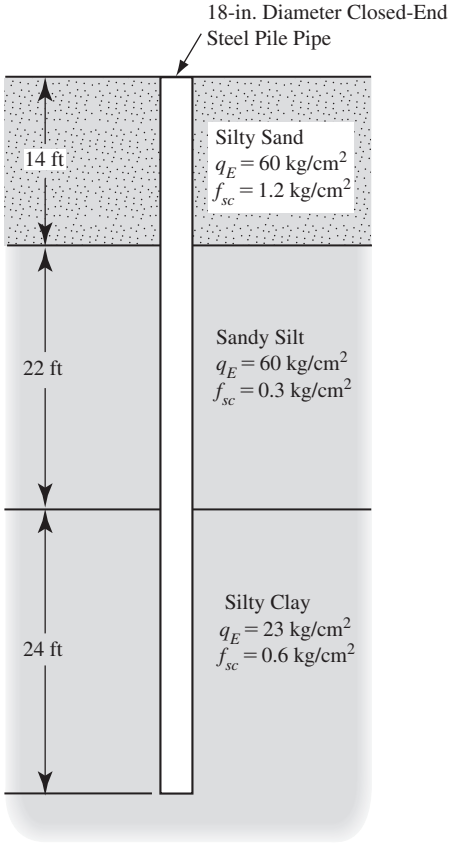

Figure 15.13 CPT results and soil profile for Problem 15.11.

15.12 An HP 360 × 108 pile is to be driven to a depth of 27.0 m in the following soil profile:

Depth (m)	Soil Type	q_c (MPa)
0–5.0	Clay	0.9
5.0–12.5	Clay	2.0
12.5–23.0	Silt	3.1
23.0–30.0	Sand	8.9

Using the LCPC method, compute the nominal downward load capacity, P_n. See Table 21.1 for cross-sectional dimensions.

Section 15.4: Upward Capacity

15.13 Using a factor of safety of 5.0, compute the ASD allowable upward load capacity, $P_{up,a}$ for the pile described in Problem 15.3. The wall thickness is 0.50 in and the pile will be filled with concrete.

15.14 Using the data in Problem 15.4 and the AASHTO resistance factors, compute $\phi P_{up,n}$.

15.15 Using a factor of safety of 5.0, compute the ASD allowable upward load capacity, $P_{up,a}$ for the pile described in Problem 15.5. The wall thickness is 20 mm and the pile will be filled with concrete.

15.16 Using the data in Problem 15.6 and the AASHTO resistance factors, compute $\phi P_{up,n}$.

Section 15.5: Group Capacity

15.17 What is "block failure" in a group of piles and how does it differ from individual failure?

15.18 What is a typical design group efficiency factor for piles driven into loose cohesionless soil without predrilling or jetting? How does predrilling and jetting affect this factor? Why?

15.19 A group of 25 HP 10×57 piles are arranged in a 5×5 grid at 27 inches on center and driven to a depth of 60 ft. The soil is a clay with unit side friction resistance, f_n of 2000 lb/ft^2 and a unit toe bearing resistance, q_n', of 15,000 lb/ft^2. Determine whether individual or block failure controls the design, and determine the nominal capacity of the pile group, P_{ng}. See Table 21.1 for cross-sectional dimensions of each pile.

Section 15.7

15.20 Explain the physical basis for setup, and describe a typical situation where setup would be observed.

Comprehensive

15.21 The soil profile beneath a proposed construction site is as follows:

Depth (m)	Soil Classification	Undrained Shear Strength, s_u (kPa)
0–2.5	Stiff silty clay (CL)	80
2.5–6.7	Soft clay (CL)	15
6.7–15.1	Medium clay (CL)	30
15.1–23.0	Stiff clay (CL)	100

Develop a plot of allowable downward load capacity versus depth for a 350 mm square concrete pile. Consider pile embedment depths between 5 and 20 m and use a factor of safety of 3.0.

15.22 An HP 13×87 pile is embedded 45 ft into a clay. The unit weight of this soil is 100 lb/ft^3 above the groundwater table (which is 12 ft below the ground surface) and 112 lb/ft^3 below. The soil in the vicinity of the pile tip has an undrained shear strength of 2800 lb/ft^2. According to a static load test, the ultimate downward load capacity is 143 k.

You wish to compute a site-specific β factor for HP 13×87 piles to be used in the design of other piles at this site. Based on these test results, what is that β factor? See Table 21.1 for pile cross-section dimensions.

Hint: Compute β based on the average σ_z' and the average measured f_n.

15.23 Using the information in Problem 15.22, compute a site-specific α factor. The average undrained shear strength along the length of the pile is 1100 lb/ft^2.

15.24 A group of five closed-end steel pipe piles were driven into a sandy hydraulic fill at Hunter's Point in San Francisco, California (DiMillio, et al., 1987a). A single isolated pile also was driven nearby. Each pile had an outside diameter of 10.75 in and a length of 30 ft. The group piles were placed 3 to 4 ft on-center, and their pile cap was elevated above the ground surface.

The upper 4.5 ft of the soil was predrilled to a diameter larger than the piles, and the top of the completed piles extended 5 ft above the ground surface. Therefore, only 20.5 ft of each pile was in contact with the soil. No other predrilling or jetting was done.

An extensive subsurface investigation was conducted before these piles were installed. This included SPT, CPT, DMT and other tests. The CPT results are shown in Figure 15.14.

a. Using this CPT data, compute the ultimate downward load capacity of the single pile.

b. Based on a pile load test, the ultimate downward load capacity of the single pile was 80 k (based on Davisson's method). Other methods of reducing the load test data gave ultimate load capacities of 80 to 117 k. How accurate was your prediction?

c. Using this CPT-based static load analysis, compute the ultimate downward load capacity of the pile group.

d. Based on a group pile load test, the ultimate downward load capacity of the pile group was 432 to 573 k, depending on the method of reducing the load test data. How accurate was your prediction?

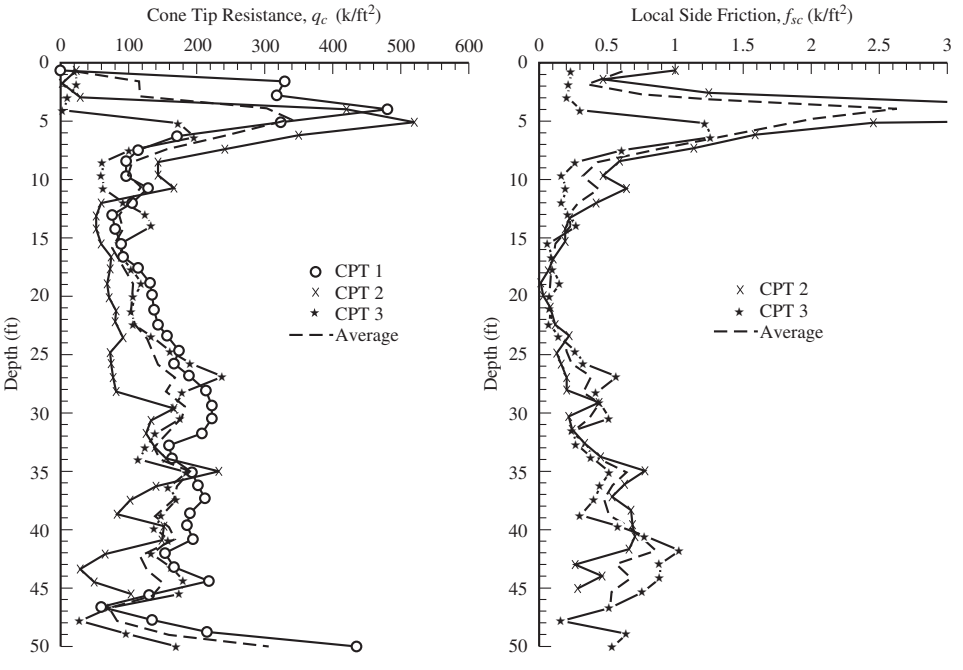

Figure 15.14 CPT results and soil profile for Problem 15.24.

16

Drilled Shafts—Axial Load Capacity Based on Static Analysis Methods

Foundations can appropriately be described as a necessary evil. . . . In contrast to the building itself which satisfies specific needs, appeals to the aesthetic sense, and fills its matters with pride, the foundations merely serve as a remedy for the deficiencies of whatever whimsical nature has provided for the support of the structure at the site which has been selected. On account of the fact that there is no glory attached to the foundations, and that the sources of success or failures are hidden deep in the ground, building foundations have always been treated as step children; and their acts of revenge for the lack of attention can be very embarrassing.

Karl Terzaghi (From Bjerrum et al., 1960)

This chapter covers static analysis methods for computing the nominal axial load capacities, P_n and $P_{up,n}$ of drilled shaft foundations, which are then used to evaluate and satisfy the axial downward and axial uplift geotechnical ultimate limit states. The values of q_n' and f_n, as computed by the methodologies described in this chapter, are used in Equations 13.5 or 13.6 to compute these axial load capacities. Tables 13.2 and 13.5 present typical factors of safety and resistance factors for drilled shaft design.

As discussed in Chapter 13, the construction methods for drilled shaft foundations are completely different from those for driven piles, and these differences can have a significant impact on the side friction and toe bearing capacities. Thus, the values of q_n' and f_n are correspondingly different.

The as-built diameter of drilled shafts is sometimes larger than the design diameter (i.e., the diameter of the auger). However, the design diameter should be used for analysis and design, rather than an estimate of the as-built diameter.

16.1 TOE BEARING

The construction methods used to build drilled shafts affects the toe bearing capacity in a number of ways, including:

- The diameter of drilled shafts is larger than that of most driven piles, so the toe area is correspondingly larger. Because of this larger diameter, more displacement is required to achieve the toe bearing capacity.
- Unlike pile driving, which compacts the soil beneath the toe, drilled shaft construction temporary relieves the stresses in the ground and mechanically loosens the soil at the bottom of the shaft. These effects further increase the amount of displacement required to achieve the toe bearing capacity. This may also reduce the shear strength at the toe, depending on the soil type. Although it is helpful to use cleanout buckets to remove soil loosened by the drilling process, the soil conditions immediately below the toe are not as good as those beneath piles. To some degree, this effect may be ameliorated by post-construction grouting, as discussed in Section 12.3.

For these and other reasons, some engineers and some state transportation departments ignore toe bearing in drilled shafts, and rely only on side friction. However, most engineers consider at least some toe bearing capacity in drilled shaft design.

If allowed so settle enough, drilled shafts would eventually recompact the soil beneath the toe and produce about the same nominal bearing capacity as a driven pile. In addition, ultimate limit state (ULS) analyses should not, in principle, be affected by settlement considerations. However, the settlement required to do so would be very large, so in practice, the distinction between ultimate limit state and serviceabilty limit state analyses becomes blurred, and the ULS nominal toe bearing capacity is normally defined as that which occurs at a settlement of 5 to 10 percent of the pile diameter. Thus, the q_n' value used to analyze drilled shafts is less than the true ULS.

Cohesionless Soils

For cohesionless soils, Brown et al. (2010) recommends using the empirical formula developed by O'Neill and Reese (1999) from full-scale load tests. This method defines q_n' as the toe bearing resistance which occurs at a settlement of 5 percent of the base diameter:

$$q_n' = 57.5N_{60} \leq 2900 \text{ kPa} \qquad \text{(16.1 SI)}$$

$$q_n' = 1200N_{60} \leq 60{,}000 \text{ lb/ft}^2 \qquad \text{(16.1 English)}$$

where

q_n' = nominal net toe bearing capacity (lb/ft^{2}or kPa)
N_{60} = mean SPT N-value between toe and a depth of 2 diameters below the toe. This value is not corrected for overburden stress.

These design values assume good workmanship, including the use of cleanout buckets. If $N_{60} > 50$, the ground is classified as an intermediate geomaterial and should be evaluated using the methods described in Chapter 25.

For special projects or unusual circumstances, a more rigorous analysis of toe bearing capacity might be warranted. A framework for doing so is presented in Brown, et al. (2010). When using these more rigorous analyses, settlement analyses are important, especially if the diameter exceeds 1.5 m (60 in). These analyses are discussed in Chapter 20.

There are no established static analysis methods for evaluating the degree of improvement in toe bearing capacity when post grouting is used, so the effectiveness of these methods may need to be evaluated based on site-specific static load tests.

The true ULS toe bearing capacity in cohesionless soils is quite large, so one of the important implications of this approach to design is that a drilled shaft bearing in cohesionless soil has substantial additional reserve capacity. Thus, if such a shaft were to be overloaded beyond its design capacity, it would experience additional settlement, but would probably not fail catastrophically.

Cohesive Soils

Because of their low hydraulic conductivity, we assume undrained conditions exist in cohesive soils beneath the toe of drilled shafts. Therefore, we compute q_n' using the undrained shear strength, s_u, using the following equations from O'Neill and Reese (1999):

For $D/B > 3$ with $s_u \leq 250$ kPa (5000 lb/ft^2):

$$q_n' = N_c^* s_u \tag{16.2}$$

For $D/B < 3$ with $s_u \leq 250$ kPa (5000 lb/ft^2):

$$q_n' = \frac{2}{3}\left(1 + \frac{D}{6B}\right) N_c^* s_u \tag{16.3}$$

where

q_n' = nominal net toe bearing capacity
N_c^* = bearing capacity factor
= 6.5 at s_u = 25 kPa (500 lb/ft^2)
= 8.0 at s_u = 50 kPa (1000 lb/ft^2)
= 9.0 at s_u = 100 kPa (2000 lb/ft^2)
s_u = undrained shear strength of soil between the toe and 2B below the toe

Cohesive soils with $s_u > 250$ kPa (5000 lb/ft^2) should be evaluated as intermediate geomaterials, as discussed in Chapter 25.

The value of s_u may be determined from laboratory tests, such as the unconfined compression or triaxial compression, or from in situ tests. However, be more cautious when working with fissured clays, as discussed in Chapter 15.

As discussed earlier, large diameter foundations require correspondingly more settlement to achieve the nominal net toe bearing resistance. If the base diameter, B_b, is greater than 1900 mm (75 in), the value of q_n' from Equation 16.2 could produce settlements greater than 1 in (25 mm), which would be unacceptable for most buildings. To keep settlements within tolerable limits, reduce the value of q_n' to q_{nr}', and use this value (O'Neill and Reese, 1999):

$$q_{nr}' = F_r q_n' \tag{16.4}$$

$$F_r = \frac{2.5}{\psi_1 B_b + 2.5\psi_2} \leq 1.0 \tag{16.5}$$

$$\psi_1 = 0.28B_b + 0.083(D/B_b) \tag{16.6 SI}$$

$$\psi_1 = 0.0085B_b + 0.083(D/B_b) \tag{16.6 English}$$

$$\psi_2 = 0.065\sqrt{s_u} \tag{16.7 SI}$$

$$\psi_2 = 0.014\sqrt{s_u} \tag{16.7 English}$$

where

q_{nr}' = reduced nominal net toe bearing capacity
q_n' = nominal net toe bearing capacity
B_b = diameter at base of foundation (ft, m)
D = depth of embedment (ft, m)
s_u = undrained shear strength in the soil between the base of the foundation and a depth $2B_b$ below the base (lb/ft^2, kPa)

16.2 SIDE FRICTION

Driven piles displace the soil as they advance into the ground, thus increasing the lateral stresses in the ground. For large displacement driven piles, this usually produces K/K_0 values > 1, as shown in Table 15.3. This increase in the lateral stress can significantly improve the side friction resistance. In contrast, drilled shaft construction introduces a temporary hole in the ground that relieves some of the lateral stress, thus producing K/K_0 values ≤ 1. The degree of stress relief depends on the construction method (open hole, slurry, casing, etc.), the soil properties, and other factors, and some of this stress relief is recovered through the hydrostatic pressure of the wet concrete. Nevertheless, the final K/K_0 will be less than that for a driven pile with the same diameter. On the other hand, drilled shaft construction produces a rougher interface between the concrete and the soil, so the ϕ_s/ϕ' ratio is higher than that for driven concrete piles.

The nominal side friction capacity, f_n, for drilled shafts may be computed using techniques very similar to those for driven piles, with appropriate consideration of these

construction differences. Effective stress methods are used for cohesionless soils, and either effective or total stress methods are used for cohesive soils.

Cohesionless Soils

Effective stress analyses are clearly appropriate for computing side friction capacity in cohesionless soils. These analyses may be performed using the β method (Brown, et al., 2010):

$$f_n = \beta \sigma_z' \tag{16.8}$$

$$\beta = K_0\left(\frac{K}{K_0}\right)\tan\left[\phi'\left(\frac{\phi_s}{\phi'}\right)\right] \tag{16.9}$$

where

f_n = Nominal side friction capacity
β = Side friction factor
σ_z' = Vertical effective stress
K_0 = Coefficient of lateral earth pressure before construction
K = Coefficient of lateral earth pressure after construction
ϕ' = Friction angle of soil
ϕ_s = Interface friction angle between soil and foundation

The β method is implemented by dividing the soil into layers with layer boundaries located at the soil strata boundaries, at the groundwater table, and at other appropriate transition points. Then for each layer compute σ_z' at the midpoint, assign a β value to each layer, and compute f_n using Equation 16.8.

When the open hole, temporary casing, or slurry methods of construction methods are used with good workmanship (including prompt placement of concrete) and good quality control, the ratio K/K_0 can be taken to be 1.0. When slurry method workmanship or quality control is questionable, a value of about 0.67 is more appropriate, and questionable workmanship with casing below the groundwater table may be justification for reducing K/K_0 to a value somewhere between 0.67 and 1.0. When serious caving conditions are present, even lower value of K/K_0 may be needed, especially if careful quality control procedures and integrity testing are not used (Chen and Kulhawy, 2002). However, so long as the workmanship is good, a ϕ_s/ϕ' ratio of 1.0 may be used, even when the shaft is constructed with slurry (Chen and Kulhawy, 2002).

In the β method, K_0 is the most difficult parameter to evaluate accurately. Ideally it would be determined from in situ testing, such as the dilatometer tests or the pressuremeter test, as discussed in Chapter 4. If this data is not available, it may be determined from the techniques discussed in Chapter 3.

The value of β in normally consolidated sands is typically between 0.24 and 0.30, and increases as the overconsolidation ratio increases. Silts and silty sands have lower β values than clean sands.

Figure 16.1 shows measured β values as back-calculated from static load tests, yet Equation 16.9 often produces much lower β values than those shown by these data,

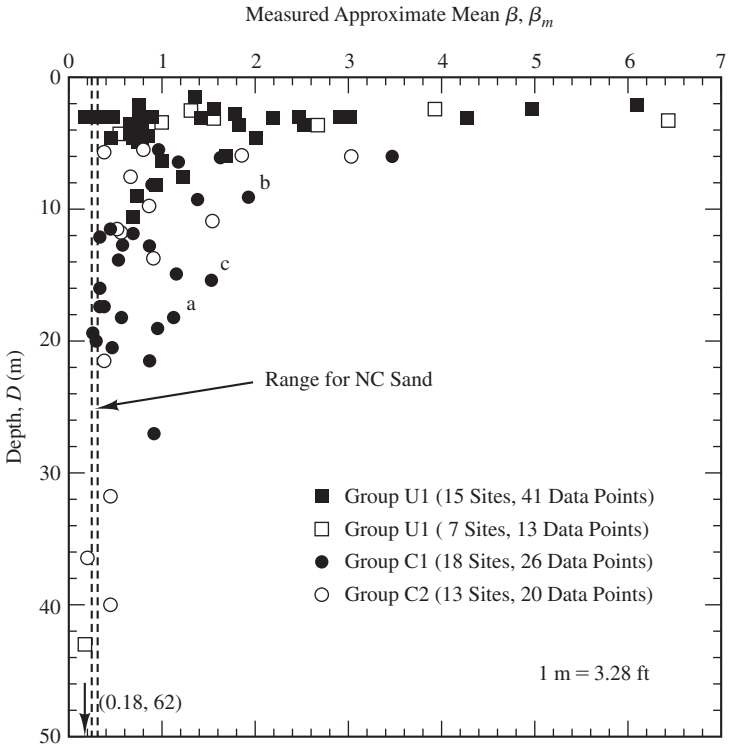

Figure 16.1 β values backcalculated from 100 static load tests on drilled shafts at 53 sites. Group 1 tests had higher quality geotechnical data than Group 2. U and C represent uplift and compression (downward) loading, respectively (Chen and Kulhawy, 2002).

especially at depths less than 10-20 m (30-60 ft). This discrepancy is probably due to underestimating the overconsolidation ratio (OCR), which can be high at shallow depths due to desiccation and other processes. Additionally, Equation 16.9 does not fully account for the increase in ϕ' due to dilatent behavior of dense sands during shear. Accurate evaluations of OCR in sands can be difficult, which is why this factor is often underestimated. In situ measurements of K_0 can help overcome this problem, and the use of some engineering judgment also may be in order.

On the other hand, be cautious about using excessive β values at very shallow depths. Brown, et al. (2010) recommend limiting the value of β in the upper 2.3 m (7.5 ft) to that computed at a depth of 2.3 m (7.5 ft).

Reese and O'Neill (1988) presented β for drilled shafts in sand solely as a function of depth:

$$\beta = 1.5 - 0.241\sqrt{z} \qquad 0.25 \le \beta \le 1.20 \qquad \text{(16.10 SI)}$$

$$\beta = 1.5 - 0.135\sqrt{z} \qquad 0.25 \le \beta \le 1.20 \qquad \text{(16.10 English)}$$

Where z is the depth below the ground surface in feet or meters. This function may be used directly, or as a guide to applying Equation 16.9.

The side friction resistance in gravels and gravelly sands is greater than that in sands, especially when well-graded. This additional capacity is probably because of the strongly dilatant behavior during shear, the high friction angle, the rough soil interface, and other factors. Unfortunately, it is very difficult to characterize the required engineering properties in gravelly soils, making it difficult to quantify the factors in Equation 16.9. Therefore, Rollins, et al. (2005) developed the following β functions directly from 103 static load tests and expressed them solely as a function of the depth z below the ground surface:

For gravels (> 50 percent gravel size):

$$\beta = 3.4e^{-0.085z} \qquad 0.25 \leq \beta \leq 3.00 \qquad \text{(16.11 SI)}$$

$$\beta = 3.4e^{-0.026z} \qquad 0.25 \leq \beta \leq 3.00 \qquad \text{(16.11 English)}$$

For gravelly sands (25–50 percent gravel size):

$$\beta = 2.0 - 0.15z^{0.75} \qquad 0.25 \leq \beta \leq 1.80 \qquad \text{(16.12 SI)}$$

$$\beta = 2.0 - 0.061z^{0.75} \qquad 0.25 \leq \beta \leq 1.80 \qquad \text{(16.12 English)}$$

where

z = depth to midpoint of soil layer (ft, m)
e = base of natural logarithms = 2.718

These load tests were conducted in soils with N_{60} values greater than 25, so Equations 16.11 and 16.12 are probably applicable only at sites that satisfy this criterion.

When a permanent casing is used, there is a significant potential for gaps between the casing and the soil, and there is no rough concrete interface, so a reduction factor of 0.60–0.75 should be applied to the computed β value (Brown, et al, 2010).

Example 16.1

The drilled shaft shown in Figure 16.2 is to be designed without the benefit of any onsite static load tests. The soil conditions are uniform, the site characterization program was average, and good construction quality control can be expected. Compute the ASD allowable compressive load capacity and the AASHTO LRFD factored compressive load capacity.

Solution

Soil Properties

The unit weights of these soils, γ, have not been given (probably because it was not possible to obtain suitably undisturbed samples of these sandy soils). We can't compute the load capacity without this information, so we must estimate γ for each stratum:

Silty sand above groundwater table: $\gamma \approx 17$ kN/m^3
Silty sand below groundwater table: $\gamma \approx 20$ kN/m^3
Sand below groundwater table: $\gamma \approx 20$ kN/m^3

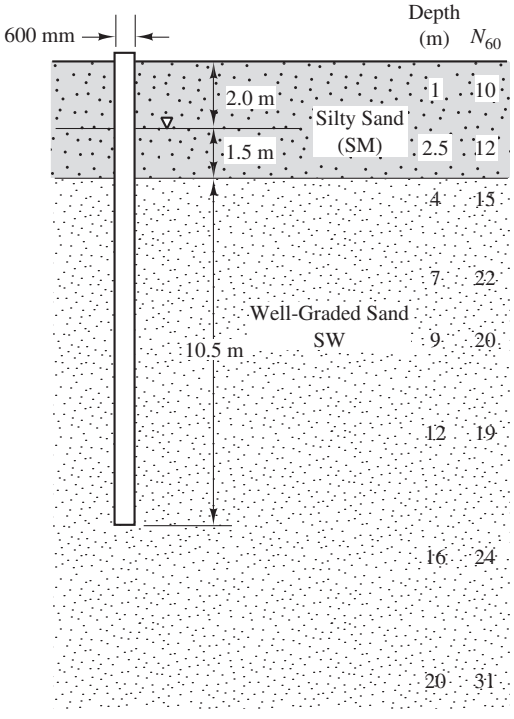

Figure 16.2 Drilled shaft foundation for Example 16.1.

Side Friction

Compute maximum β per Brown et al. (2010):

At $z = 2.3$ m

$$\sigma_z' = \sum \gamma H - u$$
$$= (17)(2) + (20)(0.3) - (9.8)(0.3)$$
$$= 37.1 \text{ kPa}$$

$$\text{OCR} = \frac{0.47 p_a N_{60}^m}{\sigma_z'}$$
$$= \frac{(0.47)(100 \text{ kPa})(12^{0.8})}{37.1 \text{ kPa}}$$
$$= 9$$

$$\phi' \approx 36^\circ$$

$$K_0 = (1 - \sin \phi')\text{OCR}^{\sin \phi'}$$
$$= (1 - \sin 36)(9^{\sin 36})$$
$$= 1.5$$

$$\beta = K_0\left(\frac{K}{K_0}\right)\tan\left[\phi'\left(\frac{\phi_s}{\phi'}\right)\right]$$
$$= (1.5)(1)\tan[36(1)]$$
$$= 1.1$$

Evaluate β using Equations 16.9 and 16.10, then assign design values using some engineering judgment:

Soil Description	Layer Depth (m) Top	Bottom	σ'_z (kPa)	ϕ'	OCR	β Eqn 16.9	Eqn 16.10	Max	Design	f_n (kPa)	A_s (m^2)	f_nA_s (kN)
Silty sand above GWT	0	2	17.0	35	17	1.7	1.2	1.1	1.1	19	3.77	72
Silty sand below GWT	2	3.5	41.6	36	8	1.0	1.1	1.1	1.1	46	2.83	130
Sand (3.5–9 m)	3.5	9	77.3	38	4	0.7	0.9	1.1	0.8	62	10.37	643
Sand (9–14 m)	9	14	130.9	38	2	0.5	0.7	1.1	0.6	79	9.42	744

$$\sum f_nA_s = 1589$$

Toe Bearing

Use Equation 16.1 to compute the net unit toe-bearing resistance. Although no N_{60} values are available within a depth of $2B$ below the bottom of the shaft, it appears that $N_{60} = 22$ would be a reasonable value for design.

$$q'_n = 57.5N_{60} = (57.5)(22) = 1265 \text{ kPa}$$
$$A_t = \frac{\pi(0.6)^2}{4} = 0.283 \text{ m}^2$$

ASD Capacity

Using a factor of safety of 3 (per Table 13.2):

$$P_a = \frac{q'_nA_t + \sum f_nA_s}{F}$$
$$= \frac{(1205)(0.283) + 1589}{3}$$
$$= \mathbf{643\ kN}$$

LRFD Capacity

Per Table 13.5, the AASHTO resistance factor for side friction is 0.55, and for toe bearing is 0.50.

$$\begin{aligned}\phi P_n &= \phi_t q_n' A_t + \phi_s \sum f_s A_s \\ &= (0.50)(1205)(0.283) + (0.55)(1589) \\ &= \mathbf{1044\ kN}\end{aligned}$$

Cohesive Soils

Effective stress analyses also may be used to compute side friction capacity in cohesive soils. However, these analyses are most often performed using total stress analyses (the α method). In cohesive soils, the side-friction resistance within 1.5 m (5 ft) of the ground surface should be ignored because of clay shrinkage caused by drying, foundation movement produced by lateral loads, and other factors.

The α method is formulated as:

$$f_n = \alpha s_u \tag{16.13}$$

where

f_n = nominal side friction capacity
α = adhesion factor
s_u = undrained shear strength in soil adjacent to the drilled shaft

Figure 16.3 shows back-calculated values of α for drilled shafts obtained from instrumented load tests. As with driven piles, there is a wide scatter in the results. We can use the α curve shown in this plot, or the Reese and O'Neill (1989) approach as modified by Brown, et al. (2010):

- From the ground surface to a depth of 1.5 m (5 ft) or the depth of seasonal moisture change (whichever is greater): $\alpha = 0$
- For $s_u/p_a \leq 1.5$, $\alpha = 0.55$ along the remainder of the shaft
- For $1.5 \leq s_u/p_a \leq 2.5$, $\alpha = 0.55 - 0.1\left(\frac{s_u}{p_a} - 1.5\right)$ along the remainder of the shaft
- For $s_u/p_a > 2.5$, $\alpha = 0.45$ along the remainder of the shaft

where

s_u = Undrained shear strength
p_a = Atmospheric pressure = 100 kPa = 2000 lb/ft^2

Reese and O'Neill limit f_n to a maximum value of 260 kPa or 5500 lb/ft^2. Again, a reduction factor of 0.50 to 0.75 should be applied if permanent casing is used.

All of the α factors presented in this section are for insensitive clays ($S_t < 4$). In sensitive clays, full-scale static load tests, special lab tests, or some other method of verification are appropriate (O'Neill and Reese, 1999).

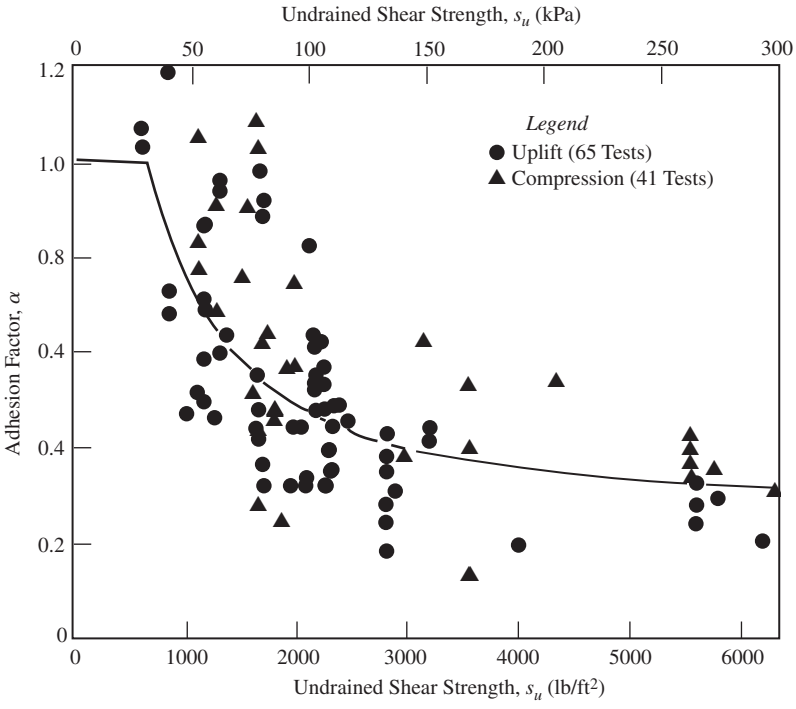

Figure 16.3 α factor for side-friction computations in drilled shafts (data from Kulhawy and Jackson, 1989; used with permission of ASCE).

Example 16.2

A 48 in diameter, 60 ft long drilled shaft is to be built using the open hole method in the soil shown in Figure 16.4. This foundation is to be designed without the benefit of an onsite static load test, the soil conditions are uniform, and the subsurface investigation program was extensive. Compute the ASD allowable downward load capacity and the AASHTO LRFD factored downward load capacity.

Solution

$$q_n' = 9s_u = (9)(4000)$$

$$A_t = \frac{\pi B_b^2}{4} = \frac{\pi(4\text{ ft})^2}{4} = 12.6\text{ ft}^2$$

Layer	Depth (ft)	Thickness (ft)	s_u (lb/ft^2)	α	f_s (lb/ft^2)	A_s (ft^2)	f_sA_s (k)
1	0–5	5.0	–	0	–	–	0
2	5–12	7.0	1600	0.55	880	88	77
3	12–37	25.0	1400	0.55	770	314	242
4	37–60	23.0	4000	0.48	1920	289	555
							874

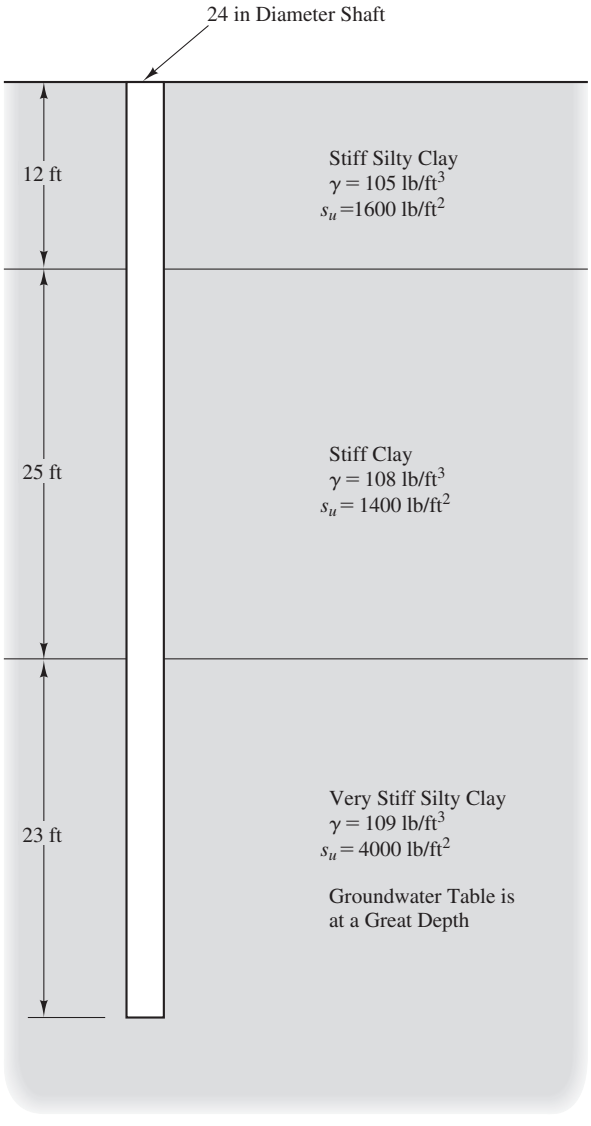

Figure 16.4 Drilled shaft foundation for Example 16.2.

Use $F = 2.50$ (per Table 13.2)

$$P_a = \frac{q_n' A_t + \sum f_n A_s}{F}$$

$$= \frac{(36 \text{ ksi})(12.6 \text{ ft}^2) + 874 \text{ k}}{2.5}$$

$$= \mathbf{531\ k}$$

Per Table 13.5, the AASHTO resistance factor is 0.45 for side friction and 0.40 for toe bearing.

$$\begin{aligned}\phi P_n &= \phi_t q_n' A_t + \phi_s \sum f_s A_s \\ &= (0.40)(36)(12.6) + (0.45)(874) \\ &= \mathbf{575\ k}\end{aligned}$$

16.3 UPWARD LOAD CAPACITY

As discussed in Section 15.4, the design side friction capacity, f_n in uplift is typically 70 to 85 percent of the downward loading value unless some other value is justified through static load tests. In addition, the required factor of safety in uplift is higher (or the resistance factor is lower). Thus, the available side friction capacity in uplift is substantially less than that for downward loading, and of course the toe bearing cannot be considered at all. These losses are somewhat offset by the greater self-weight of drilled shafts (per Equation 13.6).

However, unlike driven piles, drilled shafts can be constructed with an enlarged (or belled) base, as discussed in Section 12.3. Although the motivation for doing so is usually to increase the base area and thus the downward load being transferred through toe bearing, enlarged bases also have the advantage of generating greater upward load capacity through bearing on top of the enlargement, as shown in Figure 16.5.

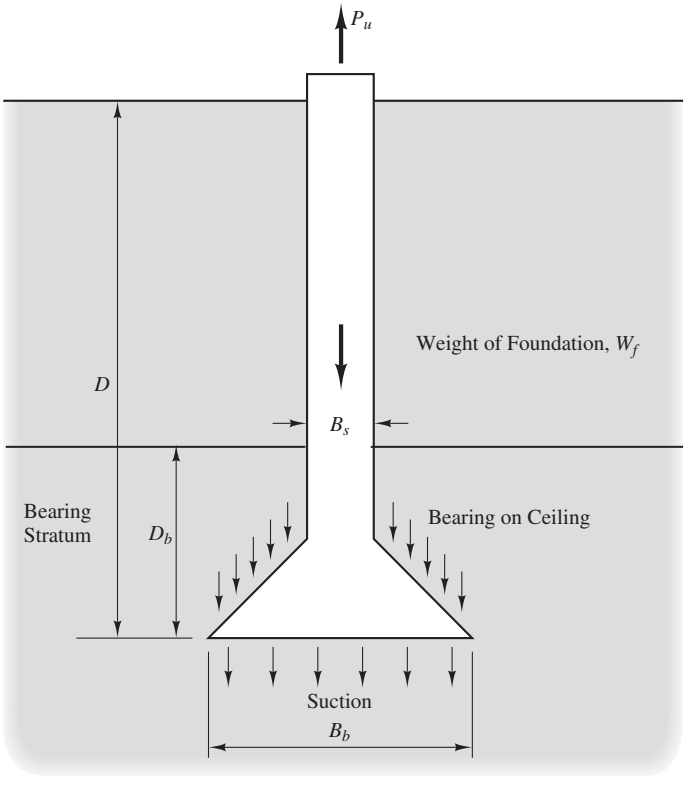

Figure 16.5 Additional upward capacity in deep foundations with enlarged bases.

It is difficult to quantify the additional uplift capacity provided by enlarged bases. O'Neill (1987) and O'Neill and Reese (1999) suggested evaluating the uplift bearing on the ceiling of the bell in cohesive soils as $(N_u s_u + \sigma_{zD})(\pi/4)(B_b^2 - B_s^2)$. Equations 13.8 and 13.14 would then be modified to the following:

$$P_{up,a} = \frac{W_f + \sum f_n A_s + (N_u s_u + \sigma_{zD})(\pi/4)(B_b^2 - B_s^2)}{F} \tag{16.14}$$

$$\phi P_{up,a} = \gamma_D W_f + \phi_s \sum f_s A_s + \phi_u (N_u s_u + \sigma_{zD})(\pi/4)(B_b^2 - B_s^2) \tag{16.15}$$

For unfissured cohesive soils:

$$N_u = 3.5 D_b/B_b \leq 9 \tag{16.16}$$

For fissured cohesive soils:

$$N_u = 0.7 D_b/B_b \leq 9 \tag{16.17}$$

where

$P_{up,a}$ = allowable upward load capacity
$P_{up,n}$ = nominal upward load capacity
s_u = undrained shear strength in soil above the base
σ_{zD} = total stress at the bottom of the base
B_b = diameter of the enlarged base
B_s = diameter of the shaft
D_b = depth of embedment of enlarged base into bearing stratum
F = factor of safety
W_f = weight of foundation, including any buoyancy effects
ϕ_t = resistance factor for toe bearing
ϕ_u = resistance factor for bearing on roof of bell (no published values available)
ϕ_s = resistance factor for side friction
γ_D = load factor for dead loads (typically 0.9)

The upward pressure from the enlarged base interacts with the side-friction resistance of the lower portion of the shaft, so O'Neill recommends neglecting the side friction between the bottom of the foundation and a distance $2B_b$ above the bottom.

Belled drilled shafts cannot be reliably constructed in cohesionless soils, so there is no analysis method.

If the bottom is below the groundwater table, suction forces might produce additional upward resistance. Although they might be large, especially for short-term loading (i.e., less than 1 minute), it is best to ignore them until additional research better defines their character and magnitude.

Belled drilled shafts are no longer widely used, mostly because of safety concerns (the construction process typically includes sending workers into the excavated enlargement to clean it out before placing concrete), and the time required to construct the enlargement. The advent of improved tooling has facilitated easier drilling in hard soils and even in rock, so it is now usually better to simply drill a longer straight shaft than to construct an enlarged base.

16.4 ANALYSES BASED ON CPT RESULTS

The cone penetration test (CPT) is a useful way to investigate the subsurface stratigraphy and to characterize the various strata. CPT results may be used to develop design values of the required geotechnical parameters, which then may be used in the analyses methods described in this chapter.

Alternatively, CPT results may be directly used to develop design values of q_n' and f_n as discussed in Section 15.3. These methods based on direct correlations from CPT data provide very good predictions of axial load capacity for driven piles, and also are applicable to drilled shafts, using the appropriate factors in Tables 15.5–15.7.

16.5 GROUP EFFECTS

Drilled shafts are usually constructed using much larger diameters than are customary for driven piles. Thus, a single large-diameter drilled shaft can often have a load capacity comparable to a group of smaller diameter driven piles. One of the advantages of this design is that the need for a pile cap is eliminated, with resulting cost and time savings. Thus, group effects often are not a concern for single large-diameter drilled shafts.

Nevertheless, drilled shafts also may be used in groups, in which case group effects must be considered in a fashion similar to that discussed in Section 15.5. However, because of the difference in construction methods and the associated impacts on the adjacent soils, the group efficiency factors for drilled shafts are different than those for driven piles. For cohesionless soils, AASHTO (2012) uses $\eta = 0.65$ for piles spaced 2.5 diameters on center,1.0 when 4.0 or more diameters on center, and a linearly interpolated value between these spacings. So long as good workmanship is used, these values are probably conservative (Brown et al., 2010). For cohesive soils, AASHTO (2012) uses $\eta = 1$, but also requires checking for block failure.

SUMMARY

Major Points

1. The use of static methods to determine the axial load capacity of drilled shafts is very similar to that for driven piles. The primary differences are due to the construction methods and their effect on q_n' and f_n. Thus, the various factors in these analyses are correspondingly different.

2. Full-scale load tests have been performed on drilled shafts, and the results of these tests have been used to develop empirical and semi-empirical methods of computing q_n' and f_n.
3. For large diameter shafts, the value of q_n' is reduced in order to keep settlement under control.
4. Although the as-built diameter of drilled shafts is often larger than the plan diameter, the analysis should use the plan diameter.
5. Belled shafts develop additional uplift capacity from bearing on the ceiling of the bell. However, because of the advent of better tooling and safety concerns, belled shafts are rarely used. It is generally more cost-effective to use longer straight shafts.
6. Drilled shafts typically have larger diameters than driven piles, and one drilled shaft can replace a group of piles. Thus, group effects are usually not a concern. However, if shafts are placed in groups, the group efficiency factors are slightly different than those for driven piles.
7. The as-built load capacities of drilled shafts are dependent on the quality and workmanship of the shaft construction.

Vocabulary

No new vocabulary words in this chapter.

QUESTIONS AND PRACTICE PROBLEMS

16.1 Compare the construction methods for driven piles versus drilled shafts and discuss the impact of these differences on their axial load capacity.

16.2 Why is it important for drilled shaft contractors to place the concrete soon after drilling the shaft? What detrimental effects can occur if the contractor waits too long before placing the concrete? How might this affect the axial load capacity?

16.3 Some engineers ignore the toe bearing capacity for downward loaded drilled shafts, while others consider toe bearing as part of the total capacity. Discuss this difference in practice.

16.4 An office building is to be supported on a series of 700 mm diameter, 12.0 m long drilled shafts that will be built using the open hole method. The soil profile at this site is as follows:

Depth (m)	Soil Description	Undrained Shear Strength, s_u (kPa)
0–2.2	Stiff clayey silt (ML)	70
2.2–6.1	Stiff silty clay (CL)	85
6.1–11.5	Very stiff sandy clay (CL)	120
11.5–30.0	Very stiff sandy clay (CL)	180

The groundwater table is at a depth of 50 m. No onsite static load test data is available, the soil conditions are uniform, and the site characterization program was average. Compute the ASD allowable downward and upward capacities.

16.5 Using the data in Problem 16.4 and the AASHTO resistance factors, compute ϕP_n and $\phi P_{up,n}$. Use a load factor of 0.9 on the weight of the shaft.

16.6 A highway bridge pier is to be supported on a single 8 ft diameter 90 ft deep drilled shaft. The subsurface conditions at this site are:

Depth (ft)	Soil Description	Unit Weight, γ (lb/ft^3)	N_{60}
0–15	Silty sand	118	
15–42	Sandy silt	115	
42–80	Well graded sand	121	
80–100	Gravelly sand (30% gravel size)	129	45

The groundwater is at a depth greater than 150 ft. Using the AASHTO resistance factors, compute ϕP_n and $\phi P_{up,n}$. Use a load factor of 0.9 on the weight of the shaft.

16.7 Using the soil profile in Problem 16.6, consider an alternative design consisting of a group of 24 in diameter, 90 ft long drilled shafts. These shafts will be placed 60 in on center.

a. Determine the number of shafts required to obtain the same ϕP_n as the single 8 ft diameter shaft. Draw a plan view sketch of this pile group.

b. Assume the pile cap will extend 24 in beyond the edges of the outside piles and will be 3 ft thick. Compute the total volume of reinforced concrete (cap plus shafts) for this alternative, and compare it with the total volume of reinforced concrete for the single 8 ft diameter shaft (which does not require a cap).

c. Discuss these two alternatives.

16.8 Using the soil profile in Problem 16.4, determine the required diameter and length needed to support an ASD design downward load of 550 kN. Note there are many different diameter—length combinations that would be satisfactory, but select one that you think would be most appropriate.

16.9 A drilled shaft designed in accordance with the AASHTO code must support the following downward and uplift axial design loads: $P_u = 850$ k, $P_{up,u} = 270$ k. The soil profile consists of:

Depth (ft)	Soil Description	Unit Weight, γ (lb/ft^3)	Undrained Shear Strength, s_u (lb/ft^2)	N_{60}
0–15	Clayey silt	115	1200	
15–35	Silty clay	112	1800	
35–55	Sandy silt (nonplastic)	115		24
55–80	Silty sand	124		43

The groundwater is at a depth of 50 ft. Using the AASHTO resistance factors, select a diameter and depth for a single drilled shaft to support these design loads. Use a load factor of 0.9 on the weight of the shaft. Note there are many different diameter—length combinations that would be satisfactory, but select one that you think would be most appropriate.

16.10 A full-scale load test has been conducted on a 24 in diameter, 40 ft long instrumented drilled shaft similar to the one shown in Figure 14.10. The test crew maintained records of the load-settlement data and the forces in each of the five load cells. The applied load at failure (using Davisson's method as described in Chapter 14) was 739,600 lb. The corresponding forces in the load cells were as follows:

Load Cell Number	Depth (ft)	Force (lb)
1	3.0	719,360
2	12.0	636,120
3	21.0	487,500
4	30.0	304,320
5	39.0	135,400

There are two soil strata at the site: the first extends from the ground surface to a depth of 15 ft and has a unit weight of 117 lb/ft^3; the second extends from 15 ft to 60 ft and has a unit weight of 120 lb/ft^3 above the groundwater table and 127 lb/ft^3 below. The groundwater table is at a depth of 17 ft. Compute the average β factor in each of the two soil strata, and the net unit toe-bearing resistance, q_n'.

Note: Once these site-specific β and q_n' values have been computed, they could be used to design shafts of other diameters or lengths at this site.

17

Auger Piles—Axial Load Capacity Based on Static Analysis Methods

Theory is the language by means of which lessons of experience can be clearly expressed. When there is no theory, there is no collected wisdom, merely incomprehensible fragments.

Karl Terzaghi

This chapter covers static methods for computing the nominal axial load capacities, P_n and $P_{up,n}$ of auger piles, which are then used to evaluate and satisfy the axial downward and axial uplift geotechnical ultimate limit states. The values of q'_n and f_n, as computed by the methodologies described in this chapter, are used in Equation 13.5 or 13.6 to compute these axial load capacities.

There are two types, augered cast-in-place (ACIP) piles and drilled displacement (DD) piles, as discussed in Chapter 12. The construction methods are very different, and each has different impacts on the adjacent soil. Thus, the methods of computing the load capacities of these two types are discussed separately.

17.1 AUGERED CAST-IN-PLACE PILES (ACIP)

The construction methods used for augered cast-in-place piles (ACIP) are such that the axial load capacity should be somewhere between that for driven piles and drilled shafts of comparable diameter. ACIP construction lacks the soil displacement achieved during pile driving and the corresponding benefits in lateral earth pressure. However, unlike drilled

shafts, the hole is filled very quickly (typically less than 10 minutes) which should reduce the amount of stress relief, and the grout is placed under pressure, which should help restore or even increase the lateral earth pressure. In addition, the construction method and the grout pressure provide a pile-soil interface that is much rougher than that for a driven pile, providing a larger sliding friction coefficient. Thus, one way to compute the axial load capacity for ACIP piles is to apply the techniques for driven piles (Chapter 15) and those for drilled shafts (Chapter 16) and then use some intermediate value for the design parameters.

Alternatively, the load capacity of ACIP piles may be evaluated using techniques developed and calibrated specifically for this type of foundation (Wright and Reese, 1979; Douglas, 1983; Rizkalla, 1988; Neely, 1991; Viggiani, 1993; McVay et al., 1994; Clemente et al., 2000; Frizzi and Meyer, 2000; Zelada and Stephenson, 2000; Coleman and Arcement, 2002; O'Neill et al., 2002; Decourt, 2003). Brown, et al. (2007) provide a comprehensive discussion of design and construction methods. In either case, the nominal design diameter should be used in the analysis even though the as-built diameter is often larger.

When constructed in clean sands, ACIP piles can be subject to over-augering, as discussed in Section 12.4, which loosens the soil. This process locally reduces K, but increases the pile diameter. The net result is probably a local decrease in side friction capacity. Clean sands also can cave during drilled shaft construction, which also creates a local reduction in side friction capacity. Both of these effects can be minimized or eliminated through careful construction quality control.

Toe Bearing

With respect to toe bearing capacity, the construction methods for ACIP piles are similar enough to drilled shafts that the toe bearing capacity should also be similar. However, based on their analysis of forty-three compression load tests on ACIP piles, Zelada and Stephenson (2000) found some evidence suggesting the toe bearing capacity in cohesionless soils is substantially greater than that for drilled shafts and developed the following relationship for q'_n:

$$q'_n = 163N_{60} \leq 7200 \text{ kPa} \quad \text{(17.1 SI)}$$

$$q'_n = 3400N_{60} \leq 150{,}000 \text{ lb/ft}^2 \quad \text{(17.1 English)}$$

Note the upper limit of 7,200 kPa (150,000 lb/ft^2) regardless of the N_{60} value. These are maximum values that serve the same function as those for driven piles in Table 15.1.

Alternatively, the methods for drilled shafts described in Section 16.1 should provide usable, and perhaps conservative, values for ACIP piles in cohesionless soils. Equations 16.2 and 16.3 should be suitable for cohesive soils.

Side Friction

Side friction capacity in cohesionless soils may be computed using the beta method:

$$f_n = \beta\sigma'_z \quad (17.2)$$

where

f_n = Nominal side friction capacity
β = Side friction factor
σ'_z = Vertical effective stress

Coleman and Arcement (2002) backcalculated β values from load tests on thirty-two ACIP piles in silts and sands, as shown in Figure 17.1, and fit the following relationships to these data:

For sands

$$\beta = 10.7z^{-1.30} \qquad 0.20 \le \beta \le 2.5 \qquad \text{(17.3 SI)}$$

$$\beta = 50.1z^{-1.30} \qquad 0.20 \le \beta \le 2.5 \qquad \text{(17.3 English)}$$

For silts

$$\beta = 2.27z^{-0.67} \qquad 0.20 \le \beta \le 2.5 \qquad \text{(17.4 SI)}$$

$$\beta = 5.03z^{-0.67} \qquad 0.20 \le \beta \le 2.5 \qquad \text{(17.4 English)}$$

where

z = depth below ground surface (ft, m)

These results are very similar to ACIP load tests results obtained independently by Neely (1991).

Zelada and Stephenson (2000) conducted a similar analysis on forty-three downward and ten uplift load tests in cohesionless soils, which resulted in:

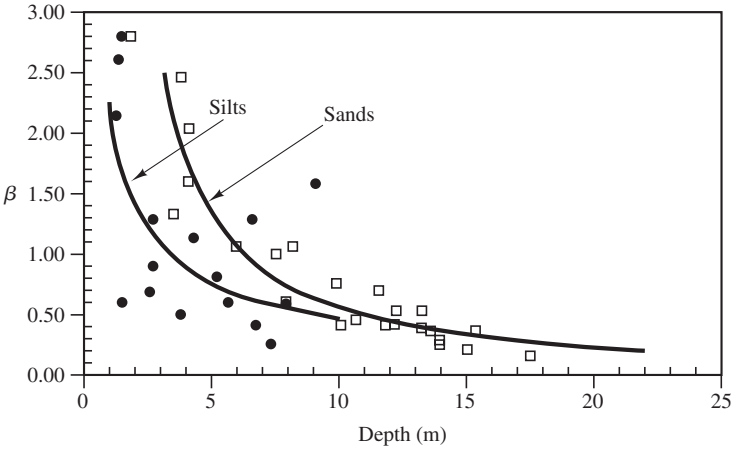

Figure 17.1 Experimental β values derived from load tests on CFA piles (Coleman and Arcement, 2002).

$$\beta = 1.2 - 0.0195\sqrt{z} \qquad 0.2 \le \beta \le 0.96 \qquad \text{(17.5 SI)}$$

$$\beta = 1.2 - 0.108\sqrt{z} \qquad 0.2 \le \beta \le 0.96 \qquad \text{(17.5 English)}$$

where

z = depth below the ground surface (ft, m)

The Zelada and Stephenson β values are somewhat lower than those typically used for drilled shafts, which is contrary to the notion that ACIP piles should provide more side friction. However, their recommendations for toe bearing are somewhat higher than those often used for drilled shafts, so this difference may in part be due to the allocation of capacity between side friction and toe bearing. Brown, et al. (2007) suggest Zelada and Stephenson's β values may be more appropriate in clean sands, because these soils are more prone to over-augering and the associated reduction in lateral earth pressure.

Side friction capacity in cohesive soils may be computed using the α method:

$$f_n = \alpha s_u \qquad (17.6)$$

where

f_n = nominal side friction capacity
α = adhesion factor
s_u = undrained shear strength in soil adjacent to the foundation

Based on the results of load tests on ACIP piles in clays and silts, Coleman and Arcement (2002) calculated α values, shown in Figure 17.2, and fit the following relationship to this data:

$$\alpha = 0.52\left(\frac{p_a}{s_u}\right)^{1.016} \qquad 0.35 \le \alpha \le 2.5 \qquad (17.7)$$

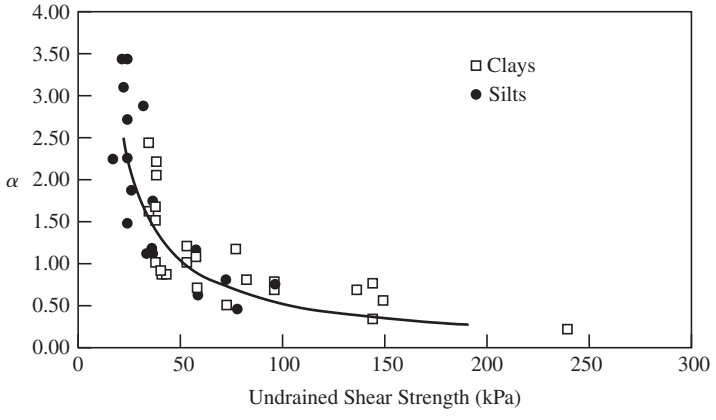

Figure 17.2 Experimental α values derived from load tests on CFA piles (Coleman and Arcement, 2002).

where

α = adhesion factor
p_a = atmospheric pressure = 100 kPa = 2,000 lb/ft^2
s_u = undrained shear strength

Upward Capacity

ACIP piles are able to resist upward (tensile) loading so long as sufficient tensile reinforcement is provided. As discussed in Section 15.4, the design side friction capacity in uplift is normally taken to be 70 to 85 percent of the downward side friction capacity unless demonstrated otherwise by static load tests. In addition, a larger factor of safety (or lower resistance factor) is used for uplift loading. These principles also apply to ACIP piles.

Analyses Based on CPT

Static capacity analyses also may be based on CPT results using the methods described in Section 15.3. The LCPC method is especially attractive, because ACIP piles formed a significant part of the database used to develop that method.

Rizkalla and Bruns (1988) developed a CPT-based method specifically for ACIP piles in cohesionless soils:

$$f_n = 0.008q_c \tag{17.8}$$

$$q_n' = 0.12q_c + 0.1 \text{ MPa} \leq 3.1 \text{ MPa} \tag{17.9}$$

where

q_c = cone resistance

Group Effects

ACIP piles in groups should generally be spaced at least three diameters on center. Group effects with ACIP piles should be very similar to those for drilled shafts, so the analysis methods described in Section 16.5 should be applicable. Over-augering can be especially problematic in pile groups because the effects can be cumulative, so lower group efficiency factors might be appropriate when this is a concern, such as in clean sands.

Example 17.1

A 3 × 3 group of 18 in diameter ACIP piles is to be constructed in the soil profile shown in Figure 17.3. The pile spacing will be 48 in on center and the cap will be 3 ft thick. Using ASD, compute the allowable downward load capacity on this pile group, P_{ag}.

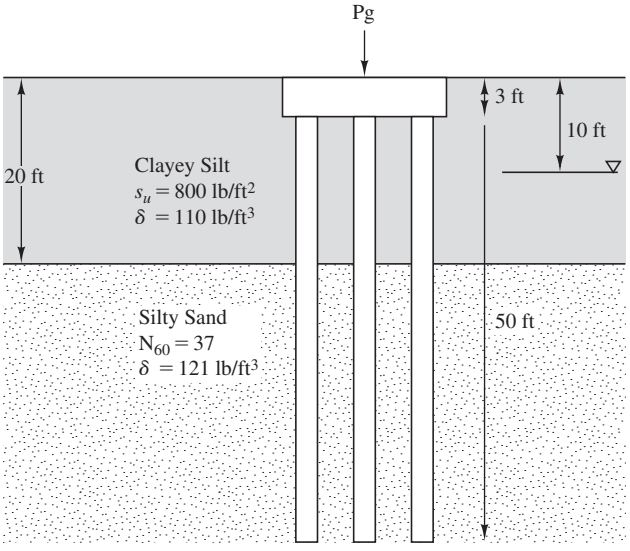

Figure 17.3 Soil profile for Example 17.1.

Solution

The clayey silt stratum may be treated as a cohesive soil, so use the α method. The silty sand is a cohesionless soil, so use β values halfway between Coleman and Arcement's values for silt and for sand.

For one pile:

Depth Range (ft)					β					
Top	Bottom	z (ft)	σ'_z (lb/ft^2)	α	Sand	Silt	Design	f_n (lb/ft^2)	A_s (ft^2)	f_nA_s (k)
3	20	11.5		1.32				1056	80.1	84.6
20	30	25.0	1869		0.763	0.582	0.673	1257	47.1	59.2
30	40	35.0	2455		0.493	0.465	0.479	1175	47.1	55.4
40	53	46.5	3129		0.341	0.384	0.362	1134	61.3	69.4

$$\sum f_nA_s = 268.6$$

$$\begin{aligned} q'_n &= 1200N_{60} \\ &= (1200)(37) \\ &= 44{,}000 \text{ lb/ft}^2 \end{aligned}$$

$$A_t = \pi\left(\frac{9}{12}\right)^2$$
$$= 1.77 \text{ ft}^2$$
$$P_n = q'_n A_t + \sum f_n A_s$$
$$= (44)(1.77) + 268.6$$
$$= 346 \text{ k}$$

Most of the capacity is obtained in the cohesionless silty sand, so use $\eta = 0.7$.

$$P_{ng} = \eta N P_n$$
$$= (0.7)(9)(346)$$
$$= 2180 \text{ k}$$

Per Table 13.1, use $F = 3.0$.

$$P_{ag} = \frac{P_{ng}}{F}$$
$$= \frac{2180}{3.0}$$
$$= \mathbf{727 \text{ k}}$$

17.2 DRILLED DISPLACEMENT (DD) PILES

Full-displacement DD piles compress the adjacent soil as part of the construction process, thus increasing the lateral earth pressures. A finite element study by Basu and Prezzi (2009) indicates substantial increases in the K/K_0 ratio, especially at shallow depths and in soils with higher initial relative density. However, the feasibility of DD piles in denser soils is limited by the torque capacity of the drill rig, so they are normally used only in looser and softer soils. The post-construction lateral earth pressures should be similar to those for driven piles of similar diameter. In addition, DD piles have a very rough pile–soil interface, which is superior to that in driven piles, and the as-built diameter may be slightly larger, especially in softer soil zones. Thus, the side friction capacity in full displacement DD piles should be at least equal to, and probably somewhat greater than that of driven piles of comparable nominal diameter.

For cohesionless soils, the side friction capacity of DD piles could be evaluated using the analysis methods described in Section 15.2 with a ϕ_f/ϕ' value of 1.0 and the nominal design diameter. For cohesive soils, the computed side friction capacity for driven piles could be used for DD piles without any increase. Partial displacement DD piles should develop side friction capacities somewhere between that of ACIP and full-displacement DD piles.

DD pile construction does not provide any particular benefits in toe bearing, so the toe bearing capacity should be comparable to that in ACIP piles.

Analysis methods also have been developed specifically for DD piles (Bustamante and Gianeselli, 1993, 1998; NeSmith, 2002; Basu and Prezzi, 2009, and others). NeSmith (2002) evaluated the results of 28 static load tests, as shown in Figures 17.4–17.7, and developed the following relationships for DD piles in cohesionless soils based on CPT or standard penetration test (SPT) with $q_c < 19$ MPa or $N_{60} < 50$, respectively:

$$q'_n = 0.4q_c + w_t \leq q'_{n,\max} \tag{17.10}$$

$$q'_n = 190N_{60} + w_t \leq q'_{n,\max} \tag{17.11 SI}$$

$$q'_n = 3800N_{60} + w_t \leq q'_{n,\max} \tag{17.11 English}$$

$$f_n = 0.01q_c + w_s \leq f_{n,\max} \tag{17.12}$$

$$f_n = 5N_{60} + w_s \leq f_{n,\max} \tag{17.13 SI}$$

$$f_n = 100N_{60} + w_s \leq f_{n,\max} \tag{17.13 English}$$

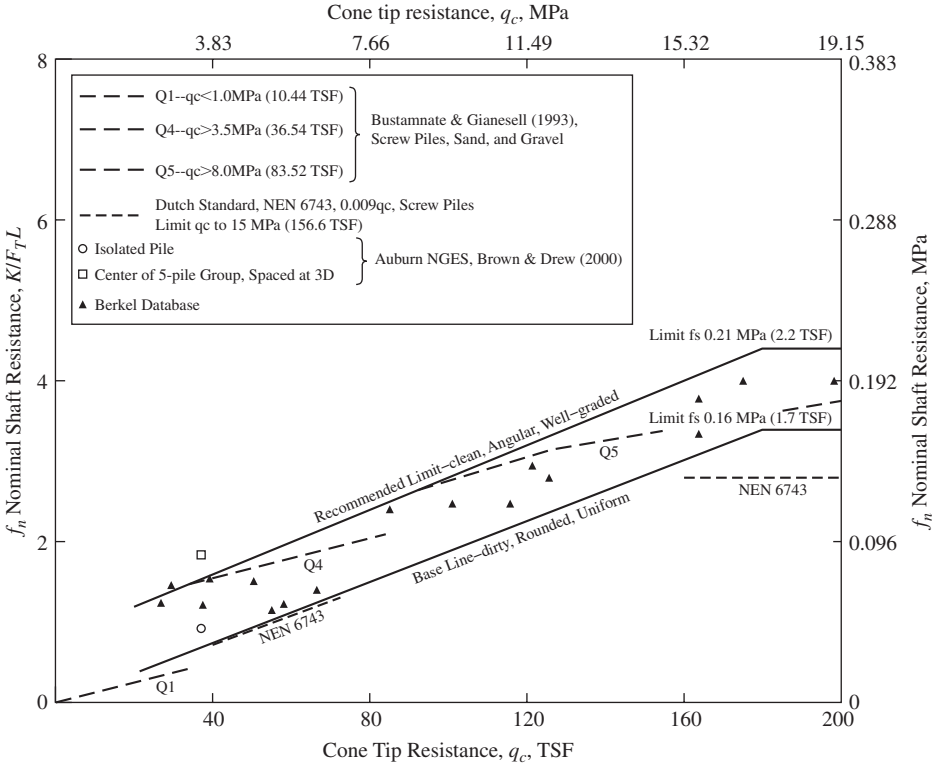

Figure 17.4 Experimental f_s values derived from load tests on DD piles and CPT results (NeSmith, 2002).

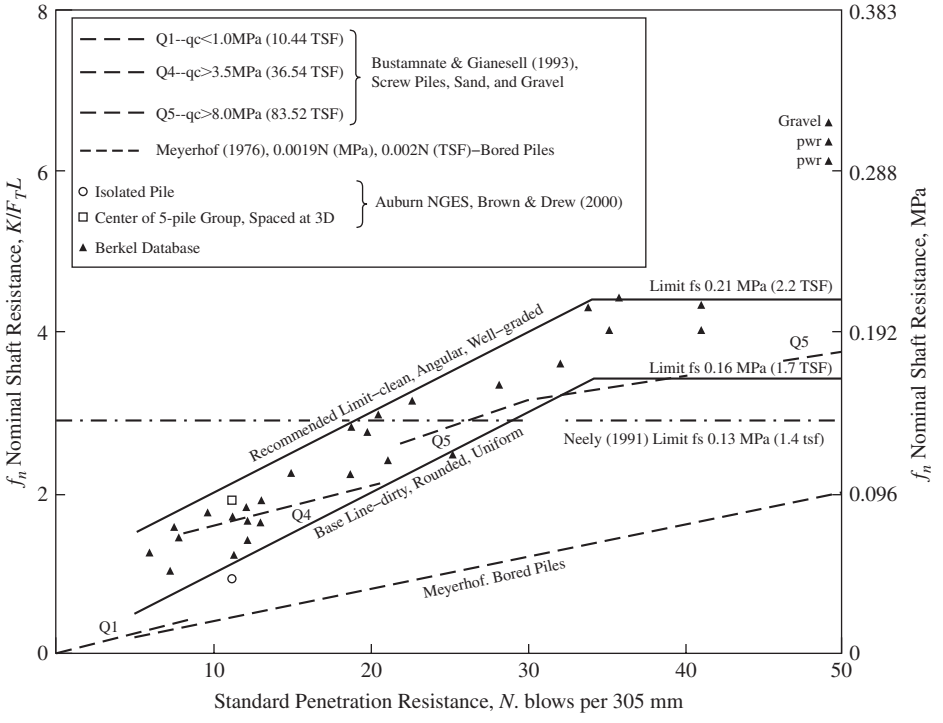

Figure 17.5 Experimental f_s values derived from load tests on DD piles and SPT results (NeSmith, 2002).

where

q'_n = nominal net toe bearing capacity (lb/ft^2, kPa)
f_n = nominal side friction capacity (lb/ft^2, kPa)
q_c = cone resistance (same units as q'_n and f_n)
N_{60} = SPT blow count
Remaining factors as defined in Table 17.1

The values of q_c and N_{60} should represent the soil in the vicinity of the toe for toe bearing analyses, and in adjacent to the pile for side friction analyses. Once again, maximum values are set, regardless of the q_c or N_{60}.

However, there is a wide range of construction equipment and methods used to construct these piles, and these differences can have an impact on their capacity, so analysis methods may not be transferrable. In addition, the load capacity benefits obtained from DD pile construction are very dependent on the soil type. Thus, onsite static load tests may be needed to take full advantage of these piles.

Amelioration

Amelioration is a supplemental construction process that involves adding sand or gravel into a DD pile as it is being drilled in order to improve the pile–soil interface. The introduction

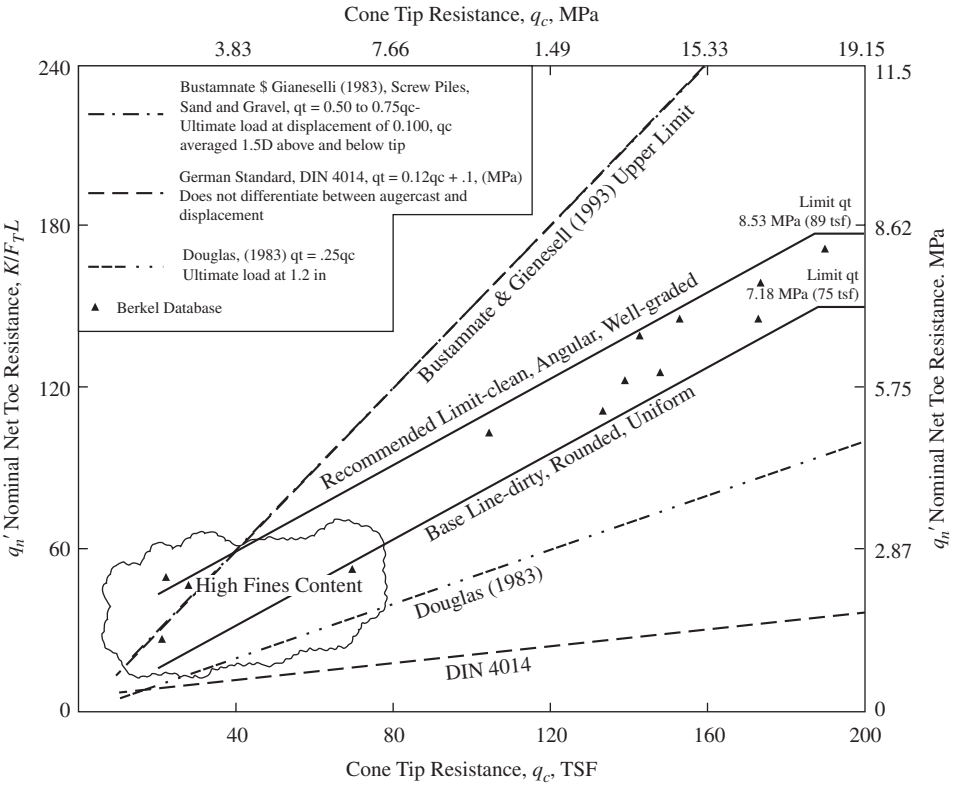

Figure 17.6 Experimental q_t' values derived from load tests on DD piles and CPT results (NeSmith, 2002).

of this additional material enhances the K/K_0 ratio, achieving values higher than those in driven piles of similar diameter. In fine-grained soils, the introduction of sand and gravel also should increase the pile–soil interface friction angle. The combination of these two effects should produce side friction capacities noticeably greater than regular DD piles or driven piles. However, the feasibility of amelioration is limited by the torque capacity of the drill rig, so this method is most applicable to very soft or loose soils. Although some load tests have been conducted on ameliorated piles (Brown and Drew, 2000), there is no generally accepted static analysis method. Thus, the impact of this process must be evaluated using site-specific load tests.

Group Effects

Because they are displacement piles, DD piles influence the adjacent soils in a way somewhat similar to that for driven piles, so the group efficiency should closely resemble that for driven piles. When DD piles installed in cohesionless soils achieve positive displacement of at least 15 percent of the pile volume, Brown et al. (2007) recommend using the AASHTO group efficiency factors for driven piles. These factors are discussed in Section 15.5.

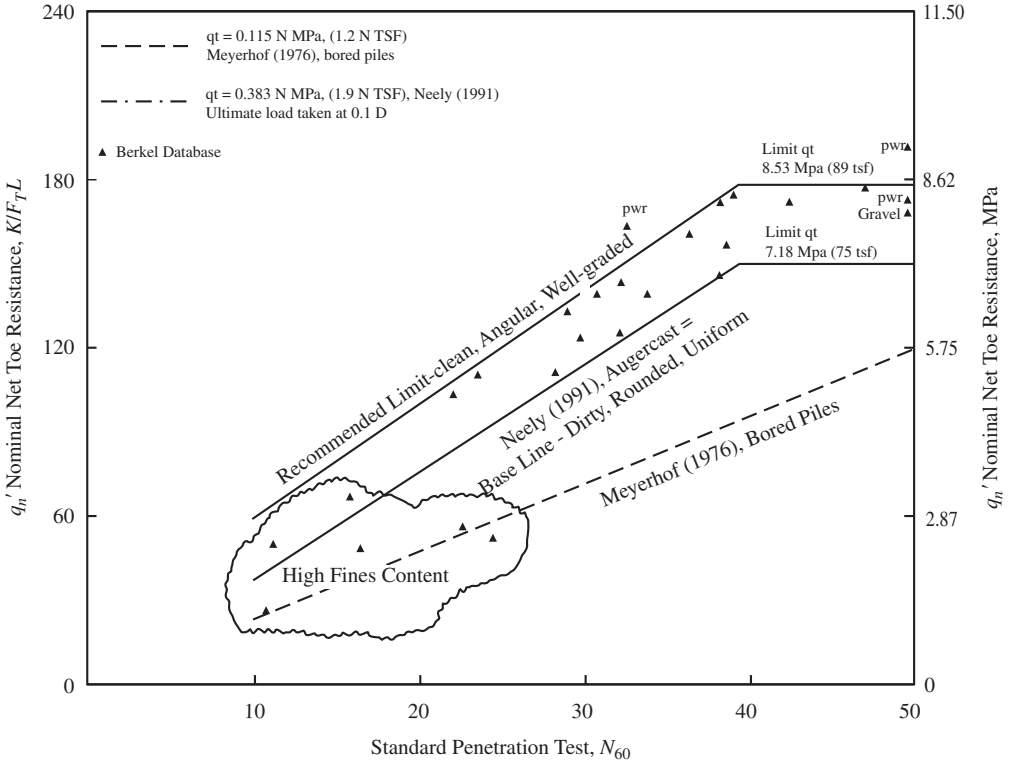

Figure 17.7 Experimental q_t' values derived from load tests on DD piles and SPT results (NeSmith, 2002).

As with driven piles, DD piles can develop significant excess pore water pressures in saturated cohesive soils. However, unlike with driven piles, it is necessary to allow time for these excess pore water pressures to at least partially dissipate before installing another DD pile in that group. Failure to do so may result in some loss in capacity. Thus, these group efficiency recommendations are based on the assumption that the necessary delay is observed. In practice, the rig will most likely go on to another cap and return later.

TABLE 17.1 FACTORS FOR NESMITH (2002) FORMULAS

Soil Type	w_t	w_s	$q'_{n,\max}$	$f_{n,\max}$
Uniform rounded sands with $<$ 40% fines	0	0	7,200 kPa	160 kPa
			150,000 lb/ft^2	3,400 lb/ft^2
Well graded angular sands with $<$ 10% fines	1,340 kPa	50 kPa	8620 kPa	210 kPa
	28,000 lb/ft^2	1,000 lb/ft^2	178,000 lb/ft^2	4,400 lb/ft^2
Intermediate soils	Interpolate as appropriate			

Example 17.2

A 500 mm diameter drilled displacement pile is to be constructed to a depth of 15 m in a mixed sand–silt soil profile. CPT results are shown in Figure 17.8. Using NeSmith's method, compute the nominal downward axial load capacity, P_n.

Solution

Side friction

Using SBT, roughly interpolate between NeSmith's parameters.

Depth (m)		CPT Results						
Top	Bottom	q_c (MPa)	SBT	w_s (kPa)	f_n (kPa)	$(f_n)_{max}$ (kPa)	A_s (m^2)	f_nA_s (kN)
0	1	3.2	Silty sand to sandy silt	0	32	160	1.26	40
1	2	4.3	Silty sand to sandy silt	0	43	160	1.26	54
2	3	7.4	Clean sand to silty sand	30	104	190	1.26	131
3	4	4.1	Silty sand to sandy silt	0	41	160	1.26	52
4	5	5.1	Silty sand to sandy silt	0	51	160	1.26	64
5	6	8.6	Clean sand to silty sand	30	116	190	1.26	146
6	7	7.4	Clean sand to silty sand	30	104	190	1.26	131
7	8	8.0	Clean sand to silty sand	30	110	190	1.26	138
8	9	9.1	Clean sand to silty sand	30	121	190	1.26	152
9	10	11.2	Clean sand to silty sand	30	142	190	1.26	178
10	11	11.9	Clean sand to silty sand	30	149	190	1.26	187
11	12	9.8	Clean sand to silty sand	30	128	190	1.26	161
12	13	10.7	Clean sand to silty sand	30	137	190	1.26	172
13	14	11.8	Clean sand to silty sand	30	148	190	1.26	186
14	15	14.2	Clean sand to silty sand	30	172	190	1.26	216
15	16	16.5						

$$\sum f_nA_s = 2008$$

Toe bearing

Use average q_c in vicinity of toe and interpolate NeSmith's parameters.

$$\begin{aligned} q_n' &= 0.4\,q_c + w_t \\ &= (0.4)(16{,}000) + 804 \\ &= 7204 \text{ kPa} \end{aligned}$$

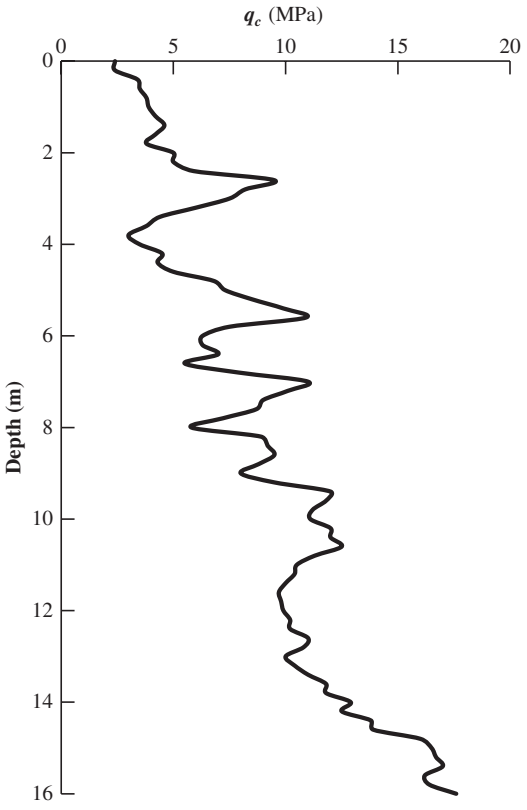

Figure 17.8 Soil profile for Example 17.2.

$$A_t = \pi(0.25)^2$$

$$= 0.196 \text{ m}^2$$

$$P_n = q_n' A_t + \sum f_n A_s$$

$$= (7204)(0.196) + 2008$$

$$= 3420 \text{ kN}$$

SUMMARY

Major Points

1. ACIP piles should have axial load capacities between those of driven piles and drilled shafts of similar diameter.

2. DD piles should have side friction capacities very close to those of similar-diameter driven piles, and toe bearing capacities very close to those of similar-diameter drilled shafts.
3. ACIP construction in clean sands can be subject to over-augering, which causes a loosening of the soil and a local reduction in the side friction capacity. This can be controlled or eliminated by careful construction quality control.
4. Static methods of evaluating axial capacities of auger piles are not as well developed as those for driven piles or drilled shafts.
5. ACIP piles should have group effects and group efficiency factors similar to those for drilled shafts. Group effects in DD piles should be similar to driven piles.

Vocabulary

No new vocabulary words in this chapter.

QUESTIONS AND PRACTICE PROBLEMS

17.1 An 18 in diameter, 75 ft long ACIP pile is to be constructed in the following soil profile:

Depth (ft)	Soil Description	Unit Weight (lb/ft^3)	Undrained Shear Strength (lb/ft^2)	Effective Friction Angle (deg)	SPT N_{60}
0–15	Silty sand	120		28	
15–40	Clayey silt	115	1,500		
40–60	Sandy silt (nonplastic)	119		25	
60–70	Well-graded sand	124		32	
70–90	Well-graded sand	127		35	40

The groundwater table is at a depth of 25 ft. Using a factor of safety of 3.0, determine the ASD allowable downward load capacity.

17.2 A static load test was conducted on the pile described in Problem 17.1. The test results produced a nominal downward load capacity 5% less than the computed static capacity. Given this new information, determine the revised ASD allowable downward load capacity.

17.3 A 16 in diameter, 55 ft long drilled displacement pile is to be constructed in the following soil profile.

Depth (ft)	Soil Description	Unit Weight (lb/ft^3)	Undrained Shear Strength (lb/ft^2)
0–10	Sandy silt	115	800
10–35	Silty clay	105	400
35–50	Silty clay	112	1,500
50–65	Clay	115	2,000

The groundwater table is at a depth of 10 ft. Using a factor of safety of 3.0, determine the ASD allowable downward load capacity.

17.4 An ASD downward column load of 500 k is to be supported on a group of drilled displacement piles constructed in the following soil profile:

Depth (ft)	Soil Description	Unit Weight (lb/ft^3)	Undrained Shear Strength (lb/ft^2)	Effective Friction Angle (deg)
0–15	Silty sand	120		32
15–40	Clayey silt	112	500	
40–60	Clay	110	600	
60–70	Silty clay	112	1100	
70–90	Sandy silt	114	1800	

The groundwater table is at a depth of 15 ft.

Determine the required number of piles, their diameter, and their length. No static load tests have been conducted. Note that there are many solutions to this problem, but select a design that you feel is most appropriate.

17.5 A 16 in diameter, 45 ft long drilled displacement pile is to be constructed in a silty sand with 30 percent fines, a mix of angular and rounded particles, and the following CPT profile:

Depth (ft)	0–10	10–32	32–38	38–45	45–55
q_c (tsf)	25	50	61	78	200

The groundwater table is at a depth of 20 ft. Using NeSmith's method and a factor of safety of 2.8, compute the ASD nominal downward load capacity, P_a.

18

Other Pile Types—Axial Load Capacity

Let the foundations of those works be dug from a solid site and to a solid base if it can be found, as much as shall seem proportionate to the size of the work; and let the whole site be worked into a structure as solid as possible.

Roman architect Marcus Vitruvius, De Architectura,
circa 15 BC (as translated by Morgan, 1914)

Driven piles, drilled shafts, and auger piles, as discussed in Chapters 15, 16, and 17, respectively, comprise the vast majority of pile foundations used in practice. However, other methods are available and they can be the best choice in certain situations. This chapter covers some of these other methods and the associated methods for computing the nominal axial load capacities, P_n and $P_{up,n}$, which are then used to evaluate and satisfy the axial downward and axial uplift geotechnical ultimate limit states.

18.1 JACKED PILES

The installation of piles by jacking is described, and its advantages and disadvantages given, in Section 12.5. One advantage of pile jacking is that the jacking force used to slowly press the pile into the ground can be related to the axial load capacity of the pile. However, the relationship between the final jacking force, P_j, and the nominal axial load capacity, P_n, may not be straightforward as they relate to different mechanisms.

For piles jacked into clays, the soil surrounding the pile is highly disturbed during jacking. The penetration of the pile into the soil is accompanied by remolding of the soil around the pile, an increase in pore water pressure, and a decrease in shear strength of the soil. The resistance to penetration during jacking comes mainly from toe bearing. After jacking, consolidation of the soil around the pile leads to a recovery of the shear strength to its pre-jacking value or even higher, making the side friction a significant portion of the nominal axial load capacity. This is equivalent to the setup phenomenon for driven piles described in Sections 15.7 and 19.2. Therefore, the final jacking force, P_j, can be quite different from the nominal axial load capacity, P_n.

Based on experience from China (Shi, 1999), for longer piles in clays, P_n is generally larger than P_j. For soft clays, the ratio of P_n to P_j can be 2 to 3, with experience from Shanghai, China, pointing to a P_n/P_j ratio as high as 4. Based on experience from Guangdong Province, China, the P_n/P_j ratio for jacked piles in clays can be as high as 3. The value of the P_n/P_j ratio depends on soil properties, the pile length, pile spacing, and the soil recovery time. For long piles jacked slowly into clays, the P_n/P_j ratio is usually between 1.1 and 1.5. For very short piles in clays, however, toe bearing dominates and P_n can be smaller than P_j.

For piles jacked into sands, pore water pressures dissipate quickly around the pile during jacking. The required jacking force increases with penetration, and the jacking force is the sum of the side friction and toe bearing. After removal of the jacking force, the sand particles tend to slide and rearrange, leading to a decrease in side friction and hence the axial load capacity. As a result, the P_n/P_j ratio for piles in sands can be less than one, especially for piles less than 10 m (33 ft) long. This phenomenon is similar to relaxation sometimes experienced in driven piles and described in Section 15.7.

Based on the above discussion and construction experience, the required P_j depends on the required nominal axial load capacity, P_n, jacking rig capacity, pile type, pile length, pile spacing, soil around the pile, and the number of jacking cycles after the final jacking force is reached. It is recommended that the required P_j be selected based on local experience and field tests.

The required P_j can be considered part of the termination criteria for jacked piles, similar to the use of blow count for driven piles. For example, Zhang et al. (2006) used a large number of field tests in Hong Kong and Guangdong Province in China to develop termination criteria for piles jacked into residual soils, sands, and clays. Their data showed that the P_n/P_j ratio is a function of the pile slenderness ratio, D/B, as shown in Figure 18.1. They recommended that the 95%-confidence-level curve be used to relate the P_n/P_j ratio to D/B, described by the following equation:

$$\frac{P_n}{P_j} = 1.13 - \frac{12.48}{(D/B)} \tag{18.1}$$

Equation 18.1 can be used to select the P_j required to provide the required P_n. In addition, Zhang, et al. (2006) specified additional termination criteria to form a set of proposed preliminary termination criteria for a single jacked pile:

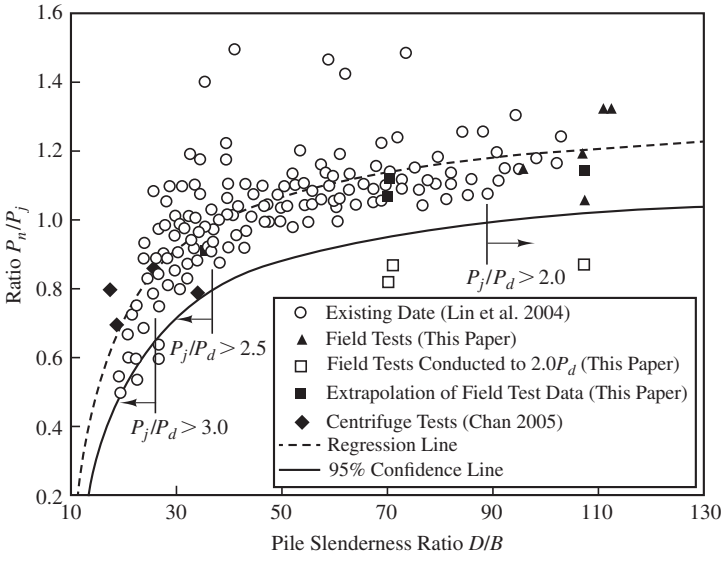

Figure 18.1 Variation of P_n/P_j with D/B for jacked piles (data from Zhang et al. (2006); used with permission of ASCE).

1. The toe of the pile shall be in a strong stratum having a minimum specified SPT N-value.
2. The final jacking force, P_j, shall be computed using Equation 18.1.
3. Once P_j is reached, a minimum of four jacking cycles shall be performed, with the load during each cycle varying from zero to P_j and holding at P_j to measure the pile head settlement rate under P_j.
4. The pile head settlement rate under P_j shall not exceed a certain specified rate, for example, 5 mm in 15 minutes.

After all the jacked piles have been installed, a percentage of the working piles should be subjected to proof static load tests. This is similar to what is normally done for driven piles.

The above termination criteria developed from experience in Hong Kong and Guangdong Province of China can be used to select an appropriate jacking rig or to estimate P_j from the required P_n for a project at these locations. However, one must exercise caution in applying these criteria to projects at other locations. Ideally, termination criteria should be developed based on local experience.

18.2 PRESSURE-INJECTED FOOTINGS (FRANKI PILES)

As described in Section 12.5, various methods are used to construct pressure-injected footings (PIFs). These differences can have a significant effect on the load bearing capacity, so it is important to properly associate the analysis method with the planned construction

processes. In addition, the distinctive feature of PIFs is their ability to compact the adjacent soils, thus improving their load bearing capacity, but the degree of soil improvement is very dependent on the soil type. Loose sands will exhibit the greatest improvement, while very little is likely to occur in stiff clays.

Toe Bearing

The PIF construction process creates an enlarged bulb at the pile toe as shown in Figure 12.53. This bulb increases both the toe bearing area, A_t, and the net toe bearing capacity, q'_n. The latter is enhanced through densification of the adjacent soils, which is especially pronounced in loose cohesionless soils.

The ratio of bulb diameter to shaft diameter depends on many factors, especially the soil conditions. This ratio can be as large as 3:1. The base area increases as the square of this ratio, and thus could be as much as nine times larger than the casing cross-section.

Neely (1989, 1990a, 1990b) developed empirical methods of computing q'_n for PIFs from SPT N-values. This method is based on the results of load tests conducted 93 PIFs with cased shafts and 41 PIFs with compacted shafts. All of these piles were bottomed in sands or gravels. His formula for cased PIFs bottomed in clean sands and gravels is:

$$q'_n = 28N_{1,60}\frac{D}{B_b} \leq 280N_{1,60} \qquad \text{(18.2 SI)}$$

$$q'_n = 560N_{1,60}\frac{D}{B_b} \leq 5{,}600N_{1,60} \qquad \text{(18.2 English)}$$

where

q'_n = nominal net toe bearing capacity (lb/ft^2, kPa)
$N_{1,60}$ = corrected SPT N-value between toe and a depth of about B below the toe
D = depth to bottom of PIF base
B_b = diameter of PIF base

The stated limits are the maximum values, regardless of the $N_{1,60}$. Note how these capacities are much greater than the toe bearing capacity in other pile types.

For compacted shaft PIFs, Neely presented his design toe bearing recommendations in graphical form, as shown in Figure 18.2.

Neely's data suggest silty sands and clayey sands have less toe bearing capacity than clean sand with a comparable N value. Soils with a fines content of 25 percent may have a toe bearing capacity about half that predicted by Equation 18.2 or Figure 18.2.

Side Friction

Pressure-injected footings with compacted shafts benefit from the increased diameter, soil compaction, and increased lateral earth pressures. The pile-soil interface also is very rough. As a result, substantial side friction capacity can be developed. Neely (1990b) found the capacities presented in Figure 18.3.

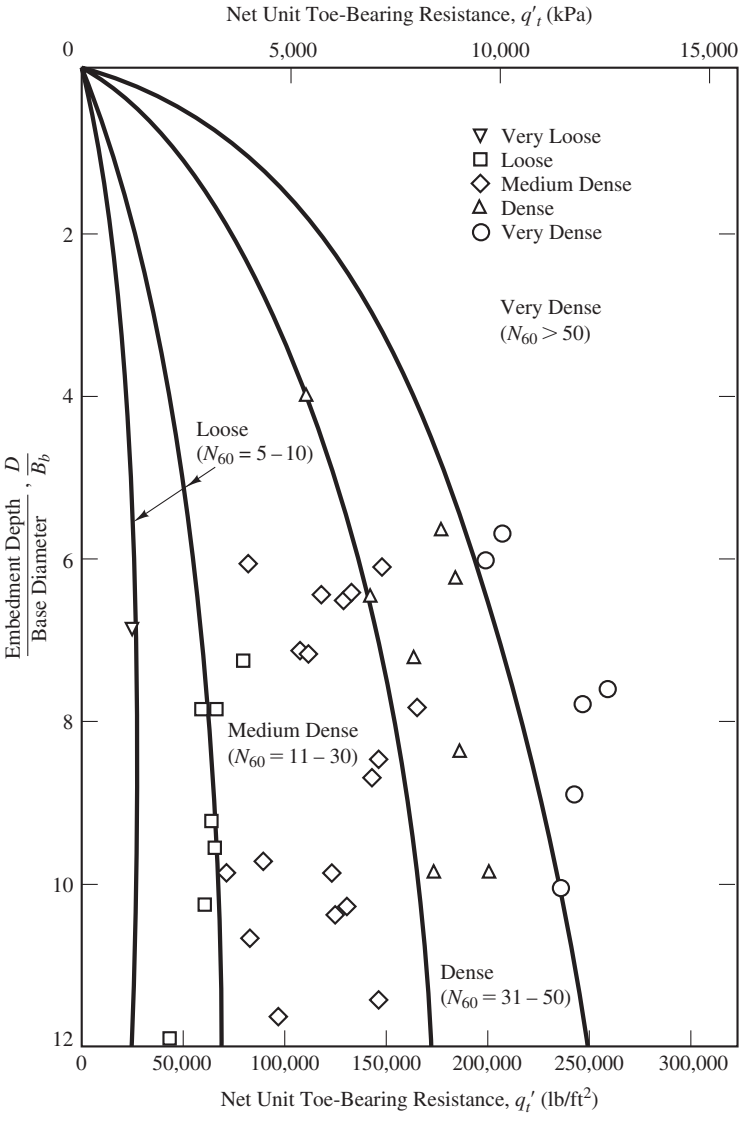

Figure 18.2 Nominal toe bearing capacity for compacted shaft PIFs in clean sands and gravels (data from Neely, 1990b; used with permission of ASCE).

18.3 MICROPILES

A variety of construction techniques are used to build micropiles, some of which are similar to drilled shaft construction, while others involve the use of pressurized grout and other techniques that are quite different. These various construction techniques affect the roughness of the concrete-soil interface and the lateral earth pressures, and thus have a significant

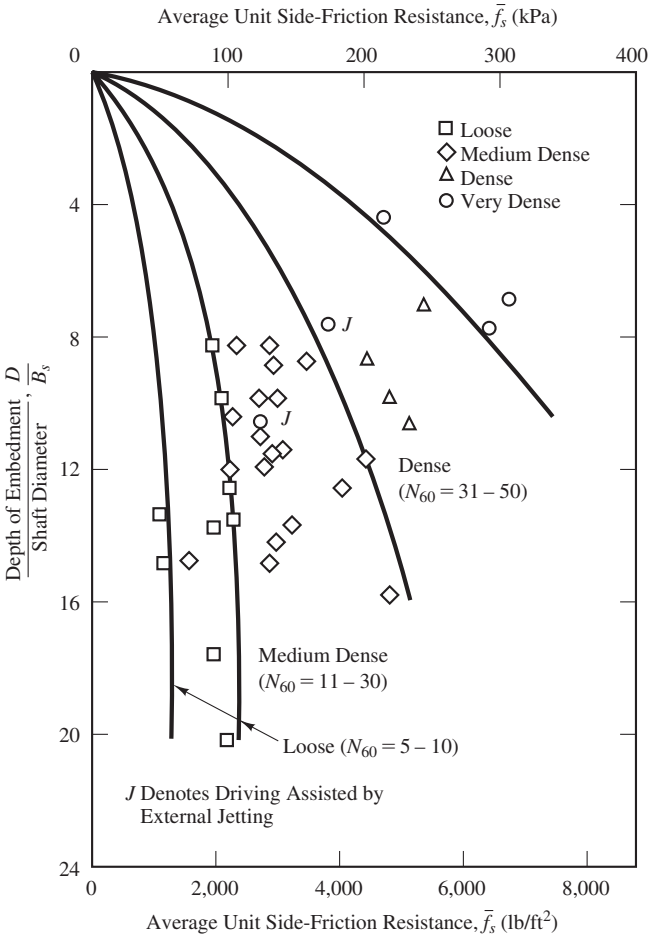

Figure 18.3 Average nominal side friction capacity for compacted shaft PIFs in sandy soils (data from Neely, 1990b; used with permission of ASCE). These values are appropriate only when the drive tube is driven into the ground in the conventional fashion. The use of jetting to assist this process reduces the side friction capacity.

effect on the axial load capacity. In addition, micropiles are smaller in diameter, normally less than 300 mm (12 in), which impacts the soil-pile interaction. Thus, methods for computing the side friction capacity in conventional piles, such as drilled shafts, generally are not applicable to micropiles. In addition, because of their small diameter, the toe bearing capacity is minimal and normally ignored.

Special design methods have been developed to satisfy the geotechnical ultimate limit state (ULS) requirements for micropiles (Armour et al., 2000). These techniques are often verified using static load tests, which are typically quite feasible due to the comparatively small axial load capacity of an individual micropile.

The use of reticulated micropiles creates a more complicated design problem due to the various angles and complicated geometries. Special techniques also are used to design these systems, often quite different from conventional pile design.

18.4 HELICAL PILES

The construction methods for helical piles are completely different from other types of piles, and the completed pile has a very different geometry and pile-soil interface. Thus, the geotechnical design methods also are unique to this pile type (ICC Evaluation Service, 2007; Perko, 2009).

Two geotechnical ULS failure modes are normally considered. If the individual helical bearing plates are widely separated, then each is assumed to fail individually as shown in Figure 18.4a. This mode of failure is called *individual bearing*. However, if the individual plates are closely spaced, then the plates and the enclosed soil move together and failure occurs along a cylindrical surface, as shown in Figure 18.4b. This mode is

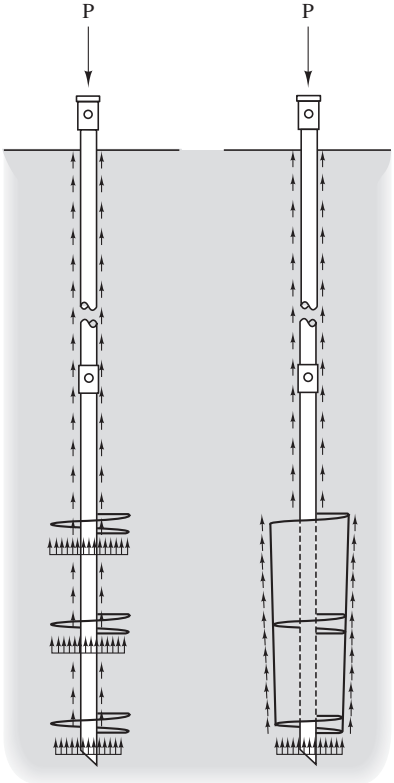

Figure 18.4 (a) Individual bearing and (b) cylindrical shear failure modes in helical piles (adapted from Perko, 2009).

called *cylindrical shear* failure. In an optimally-designed helical pile, both modes theoretically occur simultaneously, so both must be checked. Side friction acting on the rod between the ground surface and the first plate also may be considered.

Individual Bearing Failure

The nominal downward capacity for individual bearing failure may be characterized as:

$$P_n = \sum q_n' A_p + \sum f_n A_r \tag{18.3}$$

where

q_n' = nominal bearing capacity on an individual plate
A_p = area of an individual plate
f_n = nominal side friction capacity acting on rod between ground surface and top plate
A_r = rod surface area

The value of q_n' could be evaluated using the techniques for toe bearing in driven piles, and will likely vary with depth. This term is summed to consider each of the plates. Likewise, f_n could be evaluated using the techniques for low displacement driven piles. The nominal upward load capacity, $P_{up,n}$, may be evaluated using the same formula, ignoring the side friction on the rods.

Cylindrical Shear Failure

The nominal downward capacity for cylindrical shear failure may be characterized using a form similar to that for conventional piles:

$$P_n = q_n' A_p + \sum f_n A_s \tag{18.4}$$

In this case, the bearing occurs only on the bottom plate, and the side friction area is the surface of the cylinder enclosed between the top and bottom plates. Additional side friction acting on the rod between the ground surface and the top plate also may be considered. The value of q_n' should be similar to that for driven piles. The value of f_n also should be similar to that for conventional low displacement piles, perhaps using $\phi_f/\phi' = 1$ as the shearing occurs on a soil-soil interface.

The nominal upward capacity for cylindrical shear failure may be characterized using a conventional formulation with an extra term for upward bearing on the top plate:

$$P_{up,n} = W_f + q_n A_{\text{top}} + \sum f_n A_s \tag{18.5}$$

In this case, W_f may include both the weight of the helical pile and the weight of the soil trapped between the top and bottom plates. As always, the buoyant weight must be

used below the groundwater table. The net plate area (subtracting the rod area) should be used for the top plate A_{top}. Side friction on the rods should be ignored.

Minimum Embedment

When subjected to uplift loading, helical piles also must be embedded to at a depth that will provide adequate mobilization of the uplift capacity. This minimum embedment depth is conservatively determined by considering an influence cone projected at an angle of 45 degrees upward from the top plate. The weight of soil enclosed in this cone (or buoyant weight, if below the groundwater table) must be at least equal to the required nominal uplift capacity. Other methods also are available (Perko, 2009).

Augering

Static design methods are based on the assumption that the helical pile advances into the soil at a rate equal to the pitch of the helical plate per each rotation. However, when encountering hard soils the rate of advancement can fall below this criterion, thus creating a problem known as *augering*. This process loosens the soil and reduces the pile capacity, illustrating the need for construction quality control.

Torque-Based Methods

The torque required to install helical piles can be measured during construction, and methods have been developed to correlate torque with capacity (ICC Evaluation Service, 2007). These methods have been used alone, and in combination with static methods, and provide a useful means of construction quality control similar to blow counts in driven pile construction. Torque measurements also can reveal augering problems.

Factor of Safety

A geotechnical ULS factor of safety of 2.0 is commonly used for axially loaded helical piles where good construction quality control is exercised, including monitoring the installation torque for each pile (ICC Evaluation Service, 2007). A somewhat larger factor of safety should be considered for uplift loading, for reasons described in Chapter 13.

SUMMARY

Major Points

1. A number of specialty pile types are available. Although not as common as driven piles, drilled shafts, and auger piles, these methods are useful in specific situations.
2. The construction methods used to build these specialty piles are typically quite different from more conventional piles, and thus impact their geotechnical

load capacity. Special static analysis methods are used to accommodate these differences.

3. Jacked piles are designed based on a ratio of the jacking load to the nominal load capacity.
4. The construction of pressure-injected footings (PIFs) can induce significant improvements in the adjacent soils, thus improving the side friction and toe bearing capacities. In addition, these construction techniques produce an enlarged base, which further improves the toe bearing capacity.
5. Micropiles share some similarities with drilled shafts. However, the small diameter and often complex geometries dictate special static analysis design methods. In addition, the capacity of micropiles is routinely verified using static load tests.
6. The construction of helical piles is completely different from conventional piles. However, many of the conventional static analysis methods can be adapted.

Vocabulary

No new vocabulary words in this chapter.

QUESTIONS AND PRACTICE PROBLEMS

18.1 As discussed in this chapter, the nominal downward load capacity of jacked piles is often greater than the jacking force. Describe (a) a situation in which this difference would likely be very large, and (b) a situation where this difference would be comparatively small. Explain the reasoning behind your examples.

18.2 Pressure-injected footings normally have higher f_n and q_n' values than other types of piles in the same soil conditions. Explain why this is the case, and describe a soil condition where this difference would likely be the greatest.

18.3 An engineer is designing a deep foundation at a site underlain with loose to medium dense sandy silt and silty sand. Three pile types are being considered: driven prestressed concrete piles, PIFs, and drilled displacement piles. Discuss the advantages and disadvantages of each type.

18.4 A helical pile with 12 in diameter flights and a 2 in square rod is to be installed to a depth of 30 ft in a silty clay. The undrained shear strength is 1,000 lb/ft^2 and the groundwater table is at a depth of 40 ft. The individual helixes are located every 5 ft along the length of the pile, and the pile has an average weight of 100 lb/ft (including the embedded soil). Using a factor of safety of 3, determine the ASD allowable uplift capacity, $P_{up,a}$.

19

Deep Foundations—Axial Load Capacity Based on Dynamic Methods

I read some of the papers last night where some of these pile driving formulas were derived, and the result was that my sleep was very much disturbed.

Pioneer Foundation Engineer Lazarus White (1936)

Thus far, all the methods presented have used static analyses to determine pile capacity. Since piles are often driven in place, it seems obvious that the energy required to drive a pile should be related to the static capacity of the pile. In this chapter, we will present methods of analyzing pile behavior based on dynamics. Dynamic analysis can be used to determine the stresses generated in a driven pile during driving, determine the capacity of a pile immediately after driving, and determine the capacity of a pile sometime after driving. Dynamic analysis of piles was originally developed for driven piles. In this application, dynamic analysis is useful for both analyzing the installation process and determining pile capacity. Additionally, dynamic analysis is also useful for determining the capacity of drilled shafts, augered piles, and helical piles.

19.1 PILE DRIVING FORMULAS

When driving piles, it is very easy to monitor the *blow count*, which is the number of hammer blows required to drive the pile a specified distance. In SI units blow count is expressed as blows/250 mm or blows/m. In English units, it is normally expressed as blows/ft. Blow

count records are normally maintained for the entire driving process, but the most important value is the blow count for the last 250 mm (1 ft), because it represents the completed pile's resistance to driving.

Intuitively, we would expect piles that are difficult to drive (i.e., those with a high blow count) would have a greater downward load capacity than those that drive more easily. Thus, there should be some correlation between blow count and load capacity. Engineers have attempted to define this relationship by developing empirical correlations between hammer weight, blow count, and other factors, with the static load capacity. These relationships are collectively known as *pile driving formulas*.

Hundreds of pile driving formulas have been proposed, some of them from as early as the 1850s. Although these formulas have different formats, all share a common methodology of computing the pile capacity based on the driving energy delivered by the hammer. They use the principle of conservation of energy to compute the work performed during driving and attempt to consider the various losses and inefficiencies in the driving system using empirical coefficients.

Engineers have used pile driving formulas as follows:

- At sites where full-scale load test data is not available, standard pile driving formulas have been used to assess the static load capacity of the piles. In practice, each pile has a required load capacity which corresponds to a certain minimum acceptable blow count. Therefore, each pile is driven until it reaches the specified blow count.
- At sites where full-scale load test data is available, the engineer modifies one of the standard pile driving formulas to match the load test results. For example, if a certain formula overpredicted the test pile capacity by 20 percent, then it is modified with a site-specific correction factor of 1/1.20. This custom formula is then applied to other piles at the site, and thus is a means of extrapolating the load test results.

Pile driving formulas are convenient because the engineer can compute the capacity of each pile as it is driven by simply determining the final blow count. Thus, these formulas have often served as a means of construction control.

Typical Pile Driving Formulas

The basic relationship common to all pile driving formulas is conservation of energy which equates the potential energy of the hammer ram to the work done in driving the pile. For a simple drop hammer, the potential energy for a single drop is the weight of the ram, W_r, times the drop height or hammer stroke, h. The work done on the pile can be approximated by the distance the pile is driven in a single blow—called the *set*, s, multiplied by the total resistance of the pile resistance, R. If we equate the potential energy of the hammer with the work done on the pile and ignore any losses, we have Equation 19.1

$$W_r h = R_s \tag{19.1}$$

We can easily solve Equation 19.1 for the total pile resistance, R. If we assume this dynamic pile resistance is equal to the static capacity of the pile, we can determine an allowable pile capacity by applying a factor of safety. This will yield Equation 19.2

$$P_a = \left(\frac{1}{F}\right)\frac{W_r h}{s} \tag{19.2}$$

where

P_a = allowable downward load capacity
W_r = hammer ram weight
h = hammer stroke (the distance the hammer falls)
s = pile set (penetration) per blow at the end of driving = 1/blow count
F = factor of safety

There are two major shortcomings in using Equation 19.2 to determine the allowable pile capacity. First, not all of the potential energy of the ram becomes work done on the soil. A significant amount is lost in the driving process. Second, the total pile resistance during driving, R, is a combination of dynamic resistance, R_d, which is present only during driving, and static resistance, R_s, which exists both during and after driving. Only the static resistance is available to support a structure after driving.

Equation 19.2 was first proposed by Major John Sanders (Sanders, 1851). Sanders developed this equation based on his experience driving over 6,000 timber piles on Peach Patch Island to support Fort Delaware. The piles were installed using a 2,000 pound drop hammer and took over three years to install (Likins et al., 2012). Sanders recommended using a factor of safety of 8.0 in Equation 19.2. This relatively high value is partially due to failure of Equation 19.2 to account for any energy losses in the pile driving system and the difference between static and dynamic resistance.

One of the most popular pile driving formulas is the one first published over one hundred years ago in the journal *Engineering News* (Wellington, 1888). It has since become known as the *Engineering News Formula*:

$$P_a = \frac{W_r h}{F(s + c)} \tag{19.3}$$

Based on load test data, Wellington recommended using a c coefficient of 25 mm (1 in) to account for the difference between the theoretical set and the actual set. However, his database included only timber piles driven with drop hammers. Some engineers use $c = 2$ mm (0.1 in) for single-acting hammers, although this was not part of the original formula. He also recommended using a factor of safety of 6.0.

Wellington apparently had much confidence in his work when he stated that his formula was:

> . . . first deduced as the correct form for a theoretically perfect equation of the bearing power of piles, barring some trifling and negligible elements to be noted; and I claim in regard to

> that general form that it includes in proper relation to each other every constant which ought to enter into such a theoretically perfect practical formula, and that it cannot be modified by making it more complex . . . (Wellington, 1892)

The Engineering News Formula has been used quite extensively since then and has routinely been extrapolated to other types of piles and hammers. Other pile driving formulas include the *Modified Engineering News Formula*, the *Hiley Formula*, the *Gates Formula*, and many others.

Inaccuracy of Pile Driving Formulas

Pile driving formulas are attractive, and they continue to be widely used in practice. Unfortunately, the accuracy of these methods is less than impressive. Cummings (1940) was one of the first to describe their weaknesses. Since then, many engineers have objected to the use of these formulas and many lively discussions have ensued. Terzaghi's (1942) comments are typical:

> In spite of their obvious deficiencies and their unreliability, the pile formulas still enjoy a great popularity among practicing engineers, because the use of these formulas reduces the design of pile foundations to a very simple procedure. The price one pays for this artificial simplification is very high. In some cases the factor of safety of a foundation designed on the basis of the results obtained by means of the pile formula is excessive and in other cases significant settlements have been experienced.
>
> . . . on account of their inherent defects, all the existing formulas are utterly misleading as to the influence of vital conditions, such as the ratio between the weight of the pile and the hammer, on the result of the pile driving operations. In order to obtain reliable information concerning the effect of the impact of the hammer on the penetration of the piles it is necessary to take into consideration the vibrations that are produced by the impact.
>
> . . . Newton himself warned against the application of his theory to problems involving the impact produced "by the stroke of a hammer."

In another article, Peck (1942) suggested marking various pile capacities on a set of poker chips, selecting a chip at random, and using that capacity for design. His data suggest that even this method would be more accurate than pile driving formulas.

Not everyone agreed with Cummings, Terzaghi, and Peck, so this topic was the subject of heated discussions, especially during the 1940s. However, comparisons between pile load tests and capacities predicted by pile driving formulas have clearly demonstrated the inaccuracies in these formulas. Some of this data are presented in Figure 19.1 in the form of 90 percent confidence intervals. All of these piles were driven into soils that were primarily or exclusively sand. Predictions of piles driven into clay would be much worse because of freeze effects.

Although the principle of conservation of energy is certainly valid, pile driving formulas suffer because it is difficult to accurately account for all of the energy losses in a real pile driving situation. The sources of these uncertainties include the following:

- The pile, hammer, and soil types used to generate the formula may not be the same as those at the site where it is being used. This is probably one of the major reasons for the inaccuracies in the original Engineering News Formula.

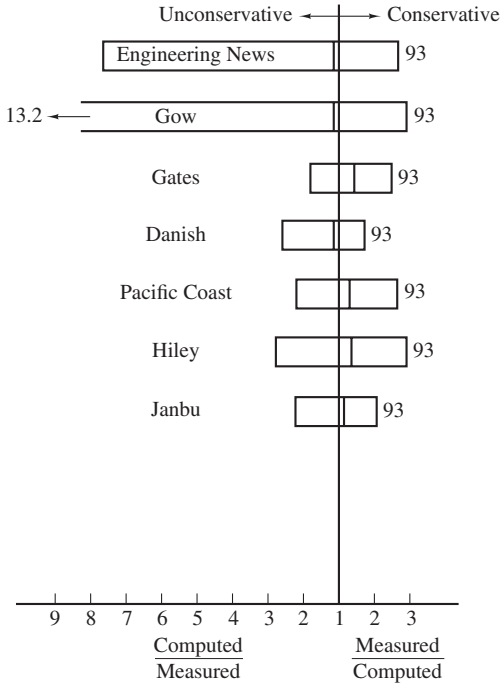

Figure 19.1 Ratio of measured pile capacity (from pile load tests) to capacities computed using various pile driving formulas. The bars represent the 90 percent confidence intervals, and the line near the middle of each bar represents the mean. The number to the right of each bar is the number of data points (based on data from Olson and Flaate, 1967).

- The formulas do not account for freeze effects.
- The hammers do not always operate at their rated efficiencies.
- The energy absorption properties of cushions can vary significantly.
- The formulas do not account for flexibility in the pile.
- There is no simple relationship between the static and dynamic strength of soils.

Because of these many difficulties, Davisson (1979) stated ". . . it is hoped that such formulas have been purged from practice." Unfortunately this has not turned out to be the case. The current AASTHO bridge design manual (AASHTO, 2012) allows use of a pile driving formula for determining pile capacity. As recently as 2012, a group of prominent foundation engineers published a review of the case against using such formulas in practice (Likins et al., 2012). Because of the continued use of such methods, foundation engineers must be aware of their existence. However, there is no valid reason to continue to use such inaccurate methods, particularly considering the developments in dynamic analysis of pile driving that has occurred in the last 60 years.

19.2 WAVE EQUATION ANALYSES

It is quite useful to have a relationship between hammer blow count and pile capacity. Such a relationship provides a convenient means of construction control that can easily be applied to every pile installed at a given site. However, it is clear from the discussion

in Section 19.1 that pile driving formulas cannot provide an accurate relationship between hammer blow count and pile capacity, because they are much too simple models of the pile driving process. Fortunately, engineers have developed a more rigorous method for analyzing the dynamics of the pile driving process. This method, called the *wave equation method* or *wave equation analysis*, is based on conservation of energy, but uses much more complete models of the pile driving system than those used in pile driving formulas.

Wave Propagation Fundamentals

When the hammer impacts the top of the pile it generates a time dependent force on the end of the pile. This force, in turn, initiates the propagation of a stress wave that travels down the pile. The simplest model of pile driving is the one-dimensional wave propagation in a long slender rod. This wave propagation is described by the *one-dimensional wave equation*:

$$\frac{\partial^2 u}{\partial t^2} = \frac{E}{\rho}\frac{\partial^2 u}{\partial z^2} \tag{19.4}$$

where

z = depth below the ground surface
t = time
u = displacement of the pile at depth z
E = modulus of elasticity of the pile
ρ = mass density of the pile

The wave initiated by the impact of the hammer at the top of the pile will travel down the pile as shown in Figure 19.2a. When it reaches the toe of the pile the wave will be reflected off the end as an upward traveling wave. If the toe is in the air, or very soft soil, the reflected wave will be a tensile wave as shown in Figure 19.2b. If the toe is in very stiff soil or rock, the reflected wave will be a compressive wave as shown in Figure 19.2c. It is important to know the magnitude of the stress wave to ensure the pile is not broken during driving. When driving into soft soils, significant tensile stresses can be generated which can cause tensile failure in concrete piles. By contrast, when driving into a stiff layer, or to bedrock, the compressive stress waves at the tip of the pile add, generating high compressive stresses which can also fail a pile.

The reflected wave will travel back up to the head of the pile where it will again be reflected and head back down the pile. As the pile transfers energy to the soil, the stress wave will decay. In hard driving, it generally takes only one or two transits up and down the pile for the wave to decay. The travel time from one end of the pile to the other, t_p, will be:

$$t_p = \frac{l}{c} \tag{19.5}$$

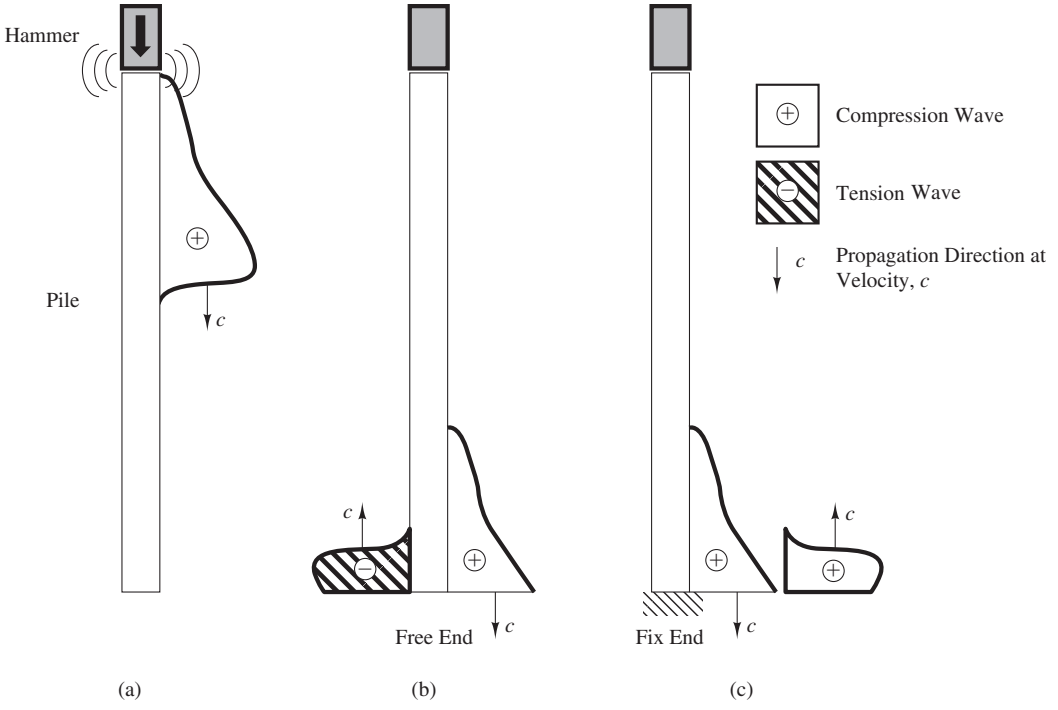

Figure 19.2 Stress wave propagating down a pile: (a) initial propagation from hammer blow; (b) tensile reflection when tip is in soft material; (c) compressive reflection when tip is in stiff material.

where

l = length of the pile
c = wave velocity

The wave velocity is related to the modulus and mass density of the pile by Equation 19.6.

$$c = \left(\frac{E}{\rho}\right)^{1/2} \tag{19.6}$$

There are two important hammer characteristics that are important to driving the pile. The first is the amount of energy, E, delivered to the pile. This will be a function of the mass of the hammer and the drop height (the potential energy of a single hammer drop) plus the losses in the driving system. The total energy delivered to the pile is represented in Figure 19.2a by the area under propagating stress curve. This energy is the energy available to do work in driving the pile. The higher the energy delivered to the pile the fewer hammer blows needed to drive the pile.

The second important hammer characteristic is the hammer impact velocity, v_i. This will control the peak force generated in the pile, the amplitude of the stress wave in Figure 19.2a. If this force is not great enough to overcome the side friction and end bearing stresses in the soil, the hammer will not be able to drive the pile. Ignoring losses in the system, we can show that the peak compressive force generated at the head of the pile during impact, F, is

$$F = v_i \frac{EA}{c} \tag{19.7}$$

Where, A, is the cross-sectional area of the pile. Combining Equations 19.6 and 19.7, we have:

$$F = v_i A(E\rho)^{1/2} \tag{19.8}$$

So the force in the pile is proportional to the impact velocity. This has important implications for pile hammer selection. If we want to keep the stress in the pile low so we don't break the pile, as in the case of driving concrete piles into soft soils, then we want to have a low impact velocity, which means a hammer with a short stroke. At the same time we want enough energy in the hammer that it doesn't take an excessive number of blows (i.e., time) to drive the pile. In this case we want a hammer with a heavy ram and short stroke. However, if we are driving piles into stiff soils, for example driving H-Piles into dense sand, we need stresses high enough to overcome the soil's resistance. In this case we want a high impact velocity, which means a hammer with a long stroke. However, we don't want to waste a lot of money on high capacity cranes and other equipment, so we want to select the lightest ram that will drive the pile in a reasonable number of blows. This leads to the counter intuitive conclusion that, for the same hammer energy, heavy rams generate low pile stresses and light rams generate high pile stresses.

Energy Transfer in Pile Driving

Thus far we have not considered energy losses in the pile driving system. Before discussing details of wave equation analysis, it is useful to discuss how energy from a pile hammer is transferred through the pile and into the soil. Ultimately, what we want to know is the amount of energy available for the pile to do work on the soil, E_s. If we know E_s, we can set that equal to the work done on the pile:

$$E_s = s(R_s + R_d) \tag{19.9}$$

where

R_s = static capacity of the pile
R_d = dynamic capacity of the pile
s = set or distance pile is driven in a single hammer blow

Equation 19.9 differs from Equation 19.1 in that the work done on the pile is related not to the energy of the hammer but to the energy in the pile available to work on the soil and we have explicitly separated the static and dynamic resistance of the pile. We have to

determine the energy lost between the theoretical hammer energy, E_h, and the energy doing useful work on the soil, E_s. To understand where the hammer energy goes, consider the pile model shown in Figure 19.3. As shown in this figure, the main parts of the pile driving system are the hammer, appurtenances (consisting of the *anvil* or *striker plate*, *capblock* or *hammer cushion*, *helmet*, and *pile cushion*), the pile, and the soil. Using this system we will partition the hammer energy using Equation 19.10.

$$E_h = E_s + E_a + E_p + E_l \tag{19.10}$$

where

E_h = kinetic hammer energy available at impact
E_a = energy lost in the appurtenances
E_p = energy lost in the pile itself
E_l = viscous energy lost in the soil that does not contribute to useful work

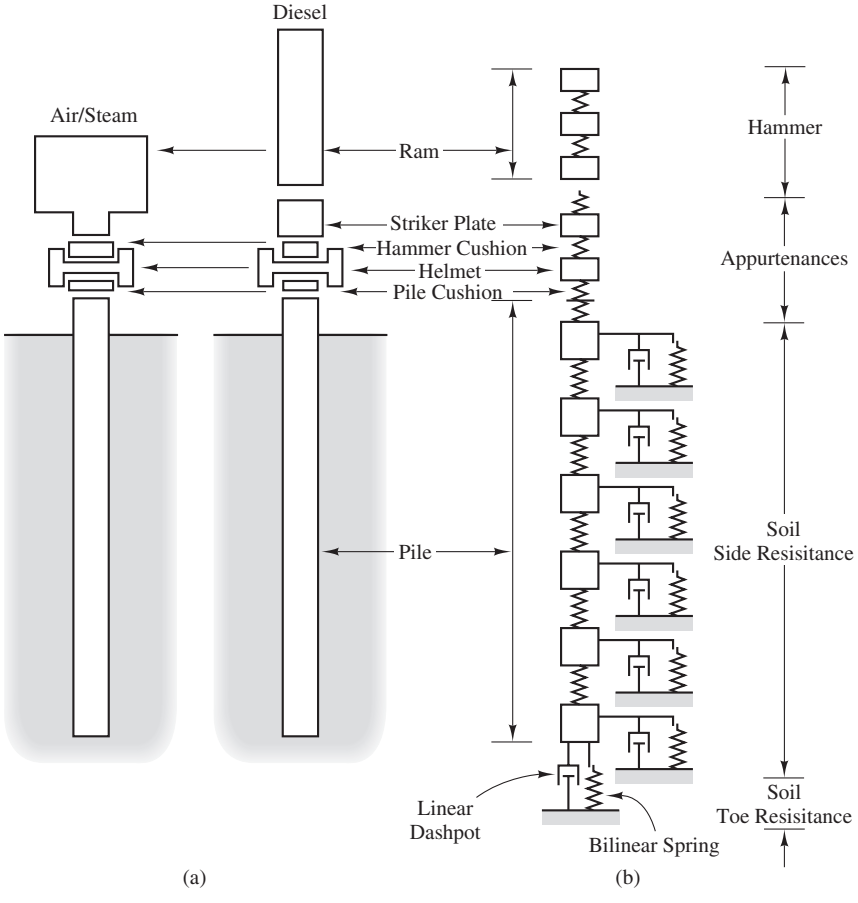

Figure 19.3 The pile model used in wave equation analyses: (a) actual system and (b) numerical model (adapted from Pile Dynamics, 2010).

We can combine Equations 19.9 and 19.10 to get:

$$(R_s + R_d)s = E_h - E_a - E_p - E_l \tag{19.11}$$

Equation 19.11 equates the total pile capacity and set to the hammer energy less the various losses in the system. All pile hammers have an energy rating, E_r, published by the manufacturer. Since the rated energy of hammers is easy to look up in manufacturers' specifications, it is convenient to use that value in our computations. However, all of the rated energy is not delivered to the appurtenances due to inefficiencies in the hammer. To account for this we will use the equation:

$$E_h = e_h E_r \tag{19.12}$$

Where e_h = efficiency of the hammer which typically ranges from 0.50 to 0.95 (Pile Dynamics, 2010).

The energy lost in the appurtenances is also typically modeled using an efficiency factor, e_a, times the rated hammer energy, leading to the following equation for energy lost in the hammer and driving systems.

$$E_h - E_a = e_a e_h E_r \tag{19.13}$$

Combining Equations 19.11 and 19.13 yields the following form of the energy equation:

$$(R_s + R_d)s = e_a e_h E_r - E_p - E_l \tag{19.14}$$

The rated hammer energy, E_r, is generally known. If we can adequately estimate or model the efficiencies, e_a and e_h, and the energy lost in the pile, E_p, and the soil, E_l, we can develop a relationship between the total pile capacity, $R_s + R_d$, and the pile set, s, using Equation 19.14. If we can also estimate the dynamic resistance during driving, R_d, we can then determine the static resistance of the pile, R_s. In general we are interested in the maximum static resistance of the pile. The symbol, R_u, is generally used to denote the maximum static resistance of a pile determined using wave equation analysis.

Modeling Pile Driving

Wave equation analysis is not actually solved using the energy formulation shown in Equation 19.14. Instead it models the actual dynamics of hammer impacting the striker plate and generating a stress wave which propagates through the appurtenances, into the pile, and then into the soil. Then it uses Equation 19.4, the one-dimensional wave equation, and Newton's laws of motion to solve for the accelerations, velocities, and stresses in the pile. Isaacs (1931) appears to have been the first to suggest the advantages of evaluating piles based on wave propagation.

Equation 19.4 can be solved directly when the boundary conditions are simple, but it becomes much more difficult with the complex boundary conditions associated with pile foundations. A closed-form solution is available (Warrington, 1997), but virtually all practical problems are solved using numerical methods. This was not possible until digital computers became available. Smith experimented with numerical solutions soon after the Second World War (Smith, 1951) in what appears to have been one of the first civilian applications of digital computers. He later refined this work (Smith, 1960, 1962), thus forming the basis for modern wave equation analyses of piles. The numerical model developed by Smith uses a lumped mass model which divides the hammer, appurtenances, pile, and soil into discrete elements, as shown in Figure 19.3. Another numerical approach to solving Equation 19.4 is the method of characteristics (e.g., Middendorp and Verbeek, 2006). This chapter will discuss only the lumped mass model as it is the most common model currently in use.

The lumped mass model divides the pile/hammer system into discrete components each with individual models. The key components to be modeled are the: hammer, pile, appurtenances (anvil, cushions and helmet), and the soil. Some portions of the pile/hammer system are more difficult to model than others.

Hammer Models

The complexity of hammer models varies with the type of hammer. The key hammer parameters to model are the velocity and mass of the ram just before it impacts the striker plate. For single acting air or steam hammers the model is relatively simple and using simple kinematics but reducing the energy using an efficiency factor for the given hammer. Modeling diesel hammers is substantially more difficult, since the stroke of the diesel hammer is a function not only of the hammer design but the stiffness of the pile–soil system. In hard driving, the stroke will be relatively high imparting more energy per stroke than in soft driving where the stroke will be relatively low. Models for diesel hammers must include the thermodynamics of the combustion process, substantially increasing the complexity of the model. The details of modeling diesel hammers are beyond the scope of this text. Fortunately for foundation engineers, the model parameters for nearly all commercially available hammers are included in the databases of most commercially available wave equation analysis software. Since all manufacturers rate their hammers by their theoretical potential energy, the one key parameter needed by the foundation engineer is the hammer efficiency, which is dependent upon the type of hammer. Table 19.1 lists typical hammer efficiencies for different hammer types.

Pile Models

The type of pile to be used is generally determined before the wave equation analysis. The pile selection is dependent upon cost, availability, and expected driving conditions. The pile material properties needed for wave equation analysis are the modulus and unit weight. Table 19.2 presents typical values of these properties for various pile materials. The other

TABLE 19.1 TYPICAL HAMMER EFFICIENCIES (data from pile dynamics, 2010)

Hammer type	Typical efficiency
Single acting air or steam hammers and drop hammers with free release	0.67
Double acting air, steam, or hydraulic hammers and drop hammers with spooling winch release	0.50
Diesel hammers	0.80
Single acting or power assisted hydraulic hammers (but not double acting)	0.80
Hammers with active impact velocity measurement	0.95

TABLE 19.2 TYPICAL PILE PROPERTIES FOR WAVE EQUATION ANALYSIS (data from pile dynamics, 2010)

Pile Material		Modulus MPa (K/in^2)	Unit Weight kN/m^3(lb/ft^3)
Aluminum		68,950 (10,000)	25.9 (165)
Concrete	Regular	34,500 (5,000)	23.6 (150)
	Grout	34,500 (5,000)	21.2 (135)
	Spun cylinder/high strength	41,400 (6,000)	24.3 (155)
Timber	Douglas Fir	11,700 (1,700)	5.2 (33)
	Oak	5,170 (750)	6.9 (44)
	Pine, white (dry)	9,000 (1,300)	4.1 (26)
	Pine, Yellow Northern (dry)	9,000 (1,300)	5.3 (34)
	Pine, Yellow Southern (dry)	9,000 (1,300)	4.1 (45)
	Spruce	9,000 – 11,000 (1,300 – 1,600)	3.1 – 4.7 (20 – 30)
Polymer		2,700 (390)	7.9 (50)
Steel		20,700 (30,000)	77.2 (490)

pile properties needed are perimeter and toe area. For concrete piles or closed-ended steel pipe piles, computation of the perimeter and toe area is simple. In the case of open-ended pipe piles or H-piles the perimeter and toe area selected will depend upon whether or not the pile is expected to plug or not. See Section 12.2 for a discussion of plugging.

Due to the length of the pile, it must be broken down into a number of pile segments. The length of the individual pile segments modeled typically ranges from 0.1 to 1 m (0.3–3 ft) (Pile Dynamics, 2010). This length depends upon the accuracy desired in the analysis. Shorter lengths provide greater accuracy but at the cost of greater computational

time. Excessively long lengths will lead to inaccurate solutions. If there is any concern about the accuracy of a given wave equation analysis, the pile segment length or the time increment should be decreased until the solutions are consistent.

Very little energy is lost in the pile due to viscous damping and reasonable variations in the parameter have only minor effects on computed results. The pile damping factor, J_p, can generally be taken as (Pile Dynamics, 2010):

$$J_p = \frac{1}{50}\left(\frac{EA}{c}\right) \tag{19.15}$$

where

E = pile modulus
A = pile cross-sectional area
c = wave velocity in the pile

Cushion Models

As shown in Figure 19.3, the appurtenances consist of the striker plate which the ram impacts, a hammer cushion between the striker plate and the helmet, and in some cases a pile cushion, between the helmet and the pile. Some hammers are designed to operate without the need of a hammer cushion. The striker plate and helmet are modeled as simple elastic elements. The hammer cushion is designed to absorb energy, thereby reducing stresses in the ram and protecting it from damage when it hits the striker plate. To model the cushion, the engineer needs to know both its modulus and coefficient of restitution.

Hammer cushions are generally made of plastic or polymer impregnated fiber materials and combined with aluminum sheets which help to dissipate the heat generated in the cushion during driving. While a number of different hammer cushion materials are available two of the most commonly used in North America are: fiber material impregnated with a polymer resin (e.g., Micarta®, ProDrive®Phenolic, or Conbest®) and nylon (e.g., Conbest II®, ProDrive®Nylon, or TECAST®). These materials are generally used in 25 to 100 mm (1–4 in) thick sections with aluminum plates between the cushion material. The aluminum plate aids in removing heat generated during pile driving. The properties needed to model cushions are modulus, unit weight, and coefficient of restitution. Table 19.3 provides typical cushion properties for the most common configurations of Micarta-aluminum and nylon-aluminum cushions.

When driving concrete piles, a pile cushion is required between the helmet and the pile. This reduces stresses applied at the pile head and prevents cracking damage to the pile head such as that shown in Figure 19.4. In North America, by far the most common pile cushion material is plywood. Laminated oak or oak/plywood sandwich cushions are sometimes used. Typical material properties for plywood and oak pile cushions are given in Table 19.3.

TABLE 19.3 TYPICAL CUSHION PROPERTIES FOR WAVE EQUATION ANALYSIS (data from pile dynamics, 2010 and Rausche et al., 2004)

Application	Common Trade Name	Material	Modulus MPa (K/in^2)	Unit Weight kN/m^3(lb/ft^3)	Coefficient of Restitution
Hammer cushion	Conbest ProDrive Phenolic	Alternating layers of 25 mm (1 in) Micarta and 12 mm (1/2 in) aluminum	2,300 (334)	17.7 (113)	0.8
	Conbest-II ProDrive Nylon TECAST	Alternating layers of 25 mm (1 in) nylon and 12 mm (1/2 in) aluminum	2,850 (414)	18.2 (116)	0.8
Pile cushion	N/A	Oak, grain normal to pile axis	414 (60)	6.9 (44)	0.5
		Oak, grain parallel to pile axis	5,170 (750)	6.9 (44)	0.5
		New Plywood	210 (30)	6 (38)	0.5
		Used Plywood	510 (75)	6 (38)	0.5

Figure 19.4 These piles were damaged during driving because the contractor selected a hammer that was too large. A driveability analysis could have predicted these problems, and would have helped the contractor select a more appropriate hammer (courtesy of GRL Engineers, Inc.).

Soil Model

The soil model originally developed by Smith (1960) consists of a bilinear elastic-plastic spring and a viscous damper (dashpot) shown in Figure 19.5. The spring represents static pile and resistance, R_s, increases until it reaches a displacement q, known as the *quake*. At that point, it reaches the *ultimate resistance*, R_u, and becomes completely plastic. Mathematically, we can write the static resistance as:

$$R_s = \left(\frac{u}{q}\right)R_u \qquad \text{for } u \leq q \tag{19.16}$$

$$R_s = R_u \qquad \text{for } u > q \tag{19.17}$$

where

u = displacement of the pile
q = quake
R_u = ultimate (maximum) pile resistance

The dashpot represents the dynamic resistance of the pile and is a function of the velocity, static pile resistance, and the Smith damping factor, j_s. There are two

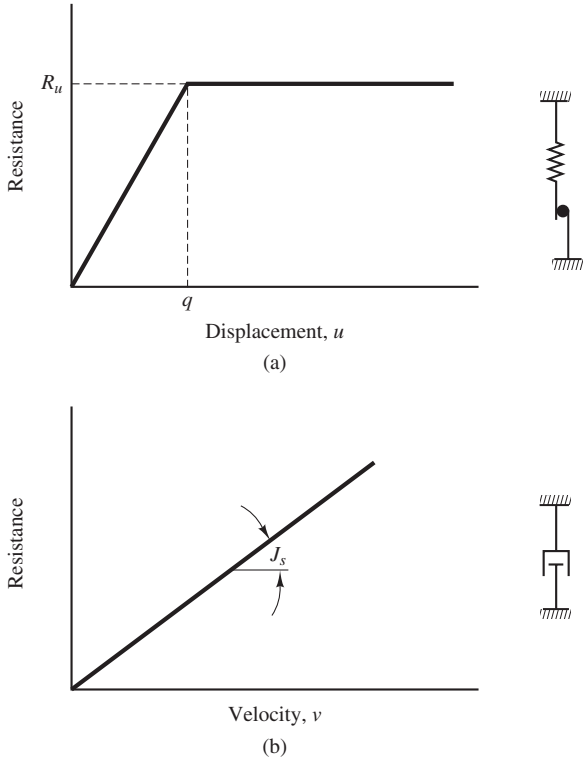

Figure 19.5 Smith's model of the soil–pile interface: (a) bilinear springs and (b) linear dashpots.

formulations of the dynamic resistance. In the original Smith damping model, the dynamic resistance is proportional to the static resistance of the pile.

$$R_d = (J_s v)R_s \tag{19.18}$$

where

J_s = Smith damping factor
v = pile velocity
R_s = static pile resistance

In this formulation, the dynamic resistance is not a linear function of velocity, because the static resistance, R_s, is not constant but a function of the pile displacement as defined by Equations 19.16 and 19.17.

In the second formulation, the dynamic resistance is proportional to the ultimate static pile capacity, R_u, or:

$$R_d = (J_s v)R_u \tag{19.19}$$

In this case the dynamic resistance will be a linear function of velocity since R_u is constant. This form is usually called Smith viscous damping, since the dynamic resistance is directly proportional to pile velocity. Both damping forms can be used. The original Smith damping formulation (Equation 19.18) appears to underpredict damping at small values of static pile resistance. For this reason, some researchers recommend using viscous Smith damping. This is particularly important in wave equation analysis of vibratory hammers (a topic beyond the scope of this book).

While it seems logical that both the soil quake and damping should be a function of soil type, Smith (1960) originally proposed a simple model with a constant quake value of 2.5 mm (0.1 in) for both side and toe quake in all soils. Later researchers (Hannigan et al., 2006) recommended using a toe quake which is a function of pile displacement and soil type. Table 19.4 presents recommended quake values. The soil damping is affected not only by soil type but also by velocity that pile penetrates into the soil. However, there is not yet a reliable model for the rate dependence of soil damping. For practical design

TABLE 19.4 RECOMMENDED SOIL QUAKE VALUES (data from pile dynamics, 2010)

Application	Pile Type	Soil Type	Estimated Quake mm (in)
Side	All	All	2.5 (0.1)
Toe	Low displacement	All soils and soft rock	2.5 (0.1)
	High displacement	Very dense or hard soils	D/120
		All other soils	D/60
	All	Hard rock	1.0 (0.04)

D = diameter or width of pile

problems the damping is generally assumed to be a function of only the soil type. Recommended soil damping factors are presented in Table 19.5.

It should be emphasized that the soil quake and damping values provided in Tables 19.4 and 19.5 are estimates and a recommended starting point for wave equation analysis. There is clear evidence that both soil quake and damping are functions of soil and pile type and that damping is rate dependent. Several researchers have developed correlations between these dynamic soil properties and standard in situ tests such as CPT and SPT (for example see McVay and Kuo, 1999 or Ng and Sritharan, 2013). There are also cases where hard driving is encountered and quake values can be significantly larger than those in Table 19.4 (see for example Likins, 1983 and Hussein et al, 2006). More complex non-linear damping models can be used in wave equation analysis, but their use is generally restricted to research projects (Pile Dynamics, 2010). Although the Smith model is a simplified view of the forces that act between the pile and the soil, it seems to work well for many practical problems.

Numerical Solution Process

Most wave equation analyses are performed using a finite difference approach to solve Equation 19.4. First, parameters needed to model the hammer, appurtenances, pile, and soil are determined. Then, the numerical model of the system is assembled. Once the model is assembled, the computation process starts by first selecting a small time increment, Δt, that will be used to perform the numerical integration required to solve Equation 19.4. The time increment must be less than the time required for the stress wave to pass through one element of the pile model shown in Figure 19.3. Next, the ram is given a velocity equal to its impact velocity. From this starting point the following process is followed:

1. Starting at the top of the system, the displacement of each element is predicted based on its velocity and acceleration from the current time step. For the i^{th} element at the j^{th} time step is predicted using simple kinematics.

$$v_{i,j+1} = v_{i,j} + \frac{(a_{i,j} + a_{i,j+1})}{2}\Delta t$$

$$u_{i,j+1} = u_{i,j} + v_{i,j-1}\Delta t + \frac{(2a_{i,j} + a_{i,j+1})}{6}\Delta t^2$$

TABLE 19.5 RECOMMENDED SOIL DAMPING VALUES (data from pile dynamics, 2010)

Application	Soil Type	Estimated Damping s/m (s/ft)
Side	Non-cohesive soils	0.16 (0.05)
	Cohesive soils	0.65 (0.20)
	Mixed cohesive and non-cohesive soils	Interpolate between above values
Toe	All soil types	0.50 (0.15)

2. Forces acting on each element are computed. Spring forces are computed based on the spring constant and the difference in displacement between adjacent elements. Damping forces are computed based on the damping coefficient and velocity of each element.
3. Acceleration of each element is computed using Newton's Second Law ($F = ma$), and the mass of the element and forces are computed from step 2.
4. Time step is incremented by Δt and the process starts back at step 1.

From these processes it is possible to determine the velocity, acceleration, and forces in every pile element at every time increment. In this fashion the stress wave generated by the hammer blow can be followed to the end of the pile, where it will be reflected and travel back up the pile. The propagation of the stress wave is computed until it is dissipated. When the wave has dissipated the pile will have moved down some distance which will be the set of the pile for that hammer blow. The actual computational process is significantly more complicate than the four steps outlined above, but these steps capture the general process.

The reflected wave generated at the end of the pile may be either compressive or tensile. If the soil is relatively soft, then the impedance of the pile will be greater than that of the soil and a tensile wave will be reflected. If the soil is very stiff its impedance may exceed that of the pile and a compressive wave will be reflected. In either case, it is important to compute the stresses that may be developed during driven and compare them to the strength of the pile to ensure the pile is not broken in the driving process. It is especially important to consider tensile stresses in concrete piles, because their tensile strength is much less than the compressive strength.

Wave Equation Analysis Software

The first publicly available wave equation software was the TTI program developed at Texas A&M University (Edwards, 1967). In 1976, researchers at the Goble and Associates developed the WEAP (Wave Equation Analysis of Piles) program. While some public domain wave equation analysis software is still available, most engineers now use commercial programs which are continually updated with the latest information and work with modern computer operating systems. Wave equation analysis software such as GRLWEAP (www.pile.com) and TNOWAVE (www.profound.nl) is widely available and can easily run on personal computers.

Preliminary Hammer Selection

Before performing a wave equation analysis, a hammer type and model must be selected. The hammer selection will be based on many factors which can broadly be grouped into commercial, environmental, and operational factors. Commercial factors include cost and availability of equipment. For routine pile driving the engineer should select from pile driving equipment readily available in the local area. Unusual or very large projects may justify the cost of mobilizing special equipment from large distances. The key environmental

factors are noise and vibration. There are three sources of noise in pile driving, hammer impact noise, hammer exhaust noise, and pile ringing (in the case of steel piles). Impact noise can be reduced by changing the cushion material or placing a hood over the helmet. Exhaust noise is unique to diesel, air, and steam hammers. It can be reduced by installing a muffler on the hammer or eliminated by switching to a hydraulic hammer. There is little that can be done to reduce pile ringing except to switch from steel to concrete piles.

As discussed earlier, the most important operational characteristics of the selected hammer are its rated energy, hammer weight, and stroke. One of the great benefits of wave equation analysis is that it can properly matches the hammer to the pile. To start the analysis it is necessary to have an estimate of the size of hammer required. This process starts by determining the required ultimate static pile resistance, R_{ur}. For ASD design,

$$R_{ur} = F(P) \tag{19.20}$$

where

P = the normal load on the pile computed using ASD load combinations in Equations 5.4 through 5.12

F = required factor of safety

For an LRFD design, R_{ur} is computed as:

$$R_{ur} = \frac{1}{\phi}(P_u) \tag{19.21}$$

where

P_u = the factored normal load on the pile computed using LRFD load combinations in Equations 5.13 through 5.19

ϕ = the resistance factor based on the analysis and testing program to be used in construction, see Tables 13.3 and 13.4.

Once the required static resistance is determined, Table 19.6 can be used to estimate the required hammer energy. Another rule of thumb is to estimate ram weight as $R_{ur}/50$ to

TABLE 19.6 PRELIMINARY ESTIMATES OF HAMMER ENERGY (data from Hannigan et al., 2006)

Required Static Pile Resistance kN (kip)	Minimum Rated Hammer Energy kJ (kip-ft)
800 (180)	16.5 (12.0)
1,350 (300)	28.5 (21.0)
1,850 (415)	39.0 (28.8)
2,400 (540)	51.0 (37.6)
2,650 (600)	57.0 (42.0)

R_{ur}/100 (Rausche, 2014). A more detailed method for estimating required hammer energy and ram weight is presented in Section 2-1 of *Technical Instruction 818-03: Pile Driving Equipment*, U.S. Army (1998).

Once the ram weight and/or hammer energy have been estimated, one or more candidate hammers can be selected based on availability, cost, and environmental requirements. Given the required hammer energy, the key hammer parameters to be selected are the efficiency, ram weight, and stroke. Typical hammer efficiencies are given in Table 19.1. Selection of the ram weight and stroke will depend upon the difficulty of driving expected. As discussed above, higher impact velocities will generate higher driving stresses and lower impact velocity lower stresses. If difficult driving conditions are expected then a lighter ram with a longer stroke is desired because it produces the higher driving stresses needed to overcome the high soil resistance. However, the driving stresses should not be so high as to cause damage in the pile during installation. Figure 19.4 shows piles that were damage due to excessive driving stresses. If driving stresses are too high, they can be reduced by decreasing the stroke and/or increasing the ram weight. An ending blow count of 8 blow/250 mm (10 blows/ft) or less is generally desirable for friction piles. For end bearing piles a blow count up to 16 blows/250 mm (20 blows/ft) may be acceptable so long as it is limited to the end of driving. Exceeding 16 blows/250 mm (20 blows/ft) for an extended period of time will exceed warranties on many pile hammers.

Developing a Bearing Graph Using Wave Equation Analysis

One of the major objectives of performing a wave equation analysis is to develop a relationship between the blow count (or the inverse of blow count, set) and the pile capacity. The process begins by performing a static pile analysis to determine the type and length of pile that are expected to meet the required structural loads. This is accomplished using the techniques described in Chapter 15. From this analysis, three key parameters are used as input to the wave equation analysis:

- Type and length of pile
- Soil type along length of pile. Used to determine damping factor, J_s
- Ratio of toe resistance to side resistance of pile

Next, candidate hammers are identified based on required energy, expected driving conditions, and local availability. Once the pile type and length, hammer type and model, and soil conditions are known, the engineer then develops the numerical model for the hammer-pile-soil system using the component models described above. A wave equation analysis is then performed in the following steps:

1. A nominal pile capacity, P_n, is assumed
2. The pile capacity, P_n, is distributed between side resistance and toe resistance based on estimated ratio of toe resistance to side resistance

3. Dynamic pile analysis is performed which will output:
   a. Energy transferred from hammer to pile
   b. Magnitude of stresses generated in pile
   c. Blow count (or set) required to achieve assumed P_n
4. A new value for P_n is assumed and steps two and three are repeated until a sufficient range of P_n values has been evaluated

This process will generate a series of nominal pile capacities, P_n and the required blow count, N (or inverse of blow count, set, s). Using these values, the engineer can create a plot of nominal pile capacity, P_n, as a function of either blow count, N, or set, s. This plot is called a *bearing graph*. A typical bearing graph is shown in Figure 19.6. The bearing graph can be used to verify capacity of piles as they are driven in the field. The accuracy of such a bearing graph is limited without comparing the results to either static tests (discussed in Chapter 14) or high-strain dynamic tests discussed in Section 19.3.

Analyses of Driving Stresses and Selection of Optimal Driving Equipment

Another useful wave equation analysis is called the *driveability analysis*. The purpose of the driveability analysis is to match a hammer and pile combination that can be economically driven without damaging the pile. This analysis is the equivalent of performing a series of wave equation analyses, each at successively deeper pile penetrations. The output of this analysis are plots of blow count, nominal capacity, pile stresses, and (for diesel hammers) stroke, as a function of depth. The steps in a driveability analysis are:

1. Static pile capacity as a function of depth of penetration is estimated using techniques described in Chapter 15.
2. Pile end and side damping and quake values are determined as function of depth based on the soil profile.
3. Initial depth of pile penetration is set.
4. Wave equation analysis is performed to determine the blow count required for pile to penetrate at this depth.
5. Pile stresses, set, and stroke determined for current depth of penetration.
6. Pile penetration depth is increased, and steps 4–6 repeated until full penetration of pile is reached.

Figure 19.7 show typical output from a driveability analysis. Figure 19.7a plots nominal pile capacity and blow count as a function of penetration depth; Figure 19.7b plots peak compressive and tensile stress in the pile as a function of penetration depth; and Figure 19.7c plots the energy delivered to the pile (ENTHRU) and hammer stroke as a function of penetration depth.

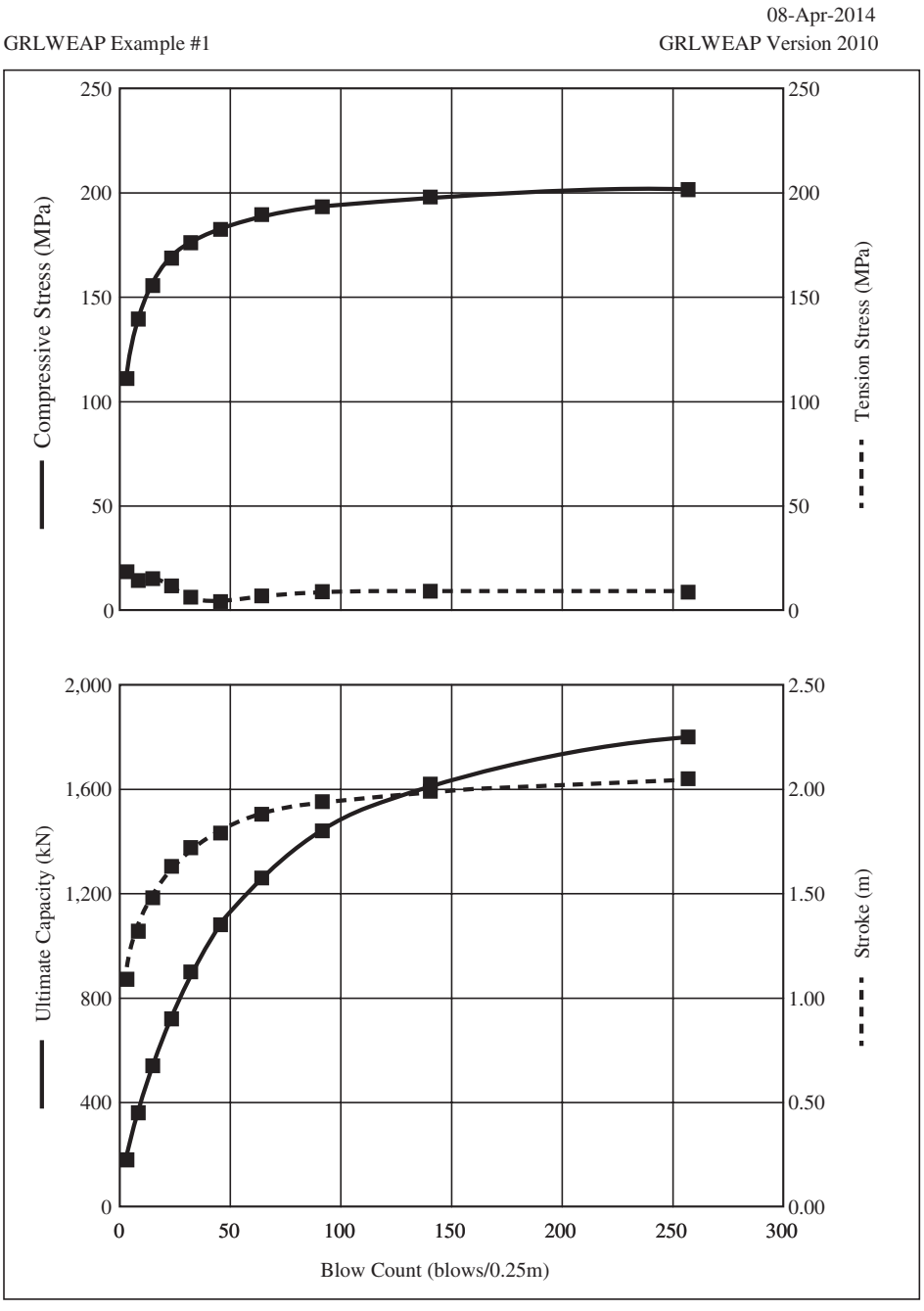

Figure 19.6 A typical bearing graph obtained from a wave equation analysis. The upper graph shows the maximum compressive and tensile stress computed as a function of blow count. The lower graph shows a plot of static pile capacity and stroke (for a diesel hammer) as a function of blow count (data generated using GRLWEAP).

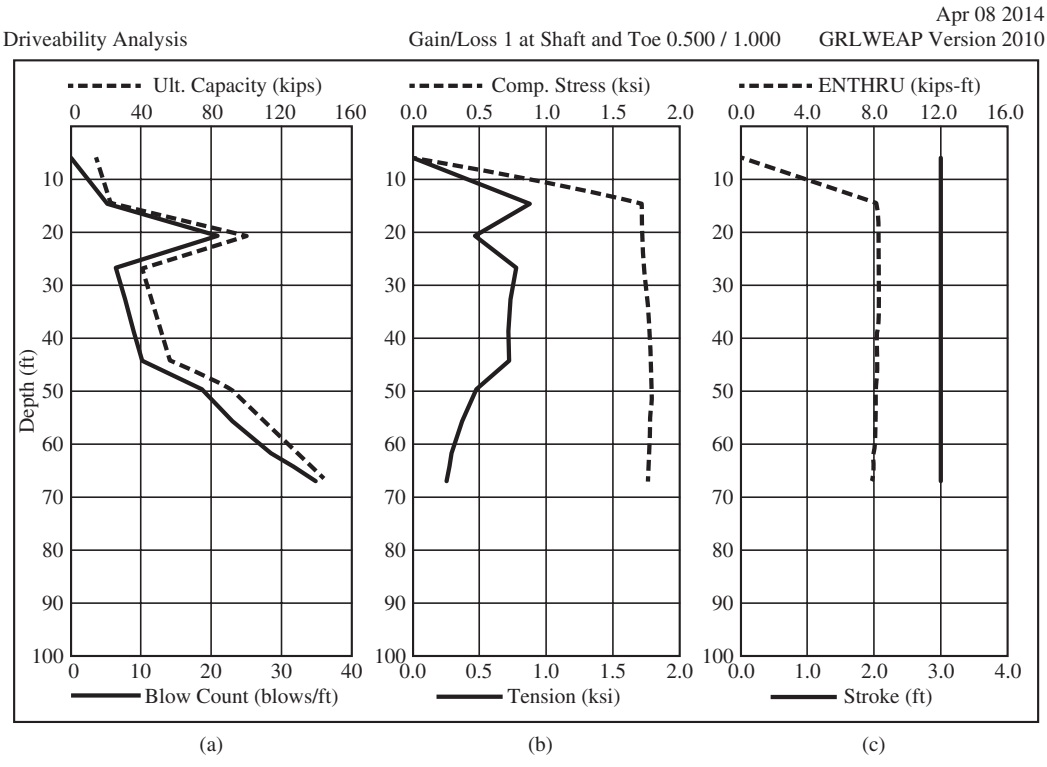

Figure 19.7 Results of a typical driveability analysis: (a) shows static pile capacity and blow count as a function of depth; (b) shows maximum compressive and tensile stress in the pile as a function of depth; (c) shows the hammer stroke (for a diesel hammer) as a function of depth (data generated using GRLWEAP).

The blow count required to reach the nominal capacity and the blow count at the end of driving is reviewed to determine if the hammer is properly sized and efficiently driving the pile. If the predicted blow count at the end of driving is less than 80 blows/m (25 blows/ft), the engineer should consider using a lower energy hammer. If the predicted blow count at the end of driving is greater than 600 blows/m (180 blows/ft), the engineer should consider using a higher energy hammer.

The stresses generated during driving are compared with the allowable driving stresses for the pile material to determine if the hammer can drive the pile without damage. Table 19.7 presents allowable pile driving stresses for various pile materials. Based on the above discussion of wave propagation fundamentals, the stresses in the pile can be controlled by adjusting the ram impact velocity. If the blow count is acceptable but compressive stresses are too high the engineer should consider using a hammer with a heavier ram but lower stroke. If the blow count is acceptable but tension stresses are too high in concrete piles, the engineer should consider either increasing pile cushion thickness, lowering the stroke if the hammer has an adjustable stroke, or using a hammer with a heavier ram but lower stroke. If it is not possible to achieve an acceptable blow count and stress level, the engineer should consider using a higher strength pile material.

TABLE 19.7 TYPICAL ALLOWABLE PILE STRESSES DURING DRIVING

Material	AASHTO		USACE	
	Allowable Compressive Stress	Allowable Tensile Stress	Allowable Compressive Stress	Allowable Tensile Stress
Concrete, non-prestressed	$0.85f_c'$	$0.7f_y\frac{A_s}{A_c}$	$0.85f_c'$	3.5 (MPa) 500 (lb/in^2)
Concrete, prestressed	$0.85f_c' - f_{pc}$	$0.25\sqrt{f_c'} + f_{pc}$(MPa) $3\sqrt{f_c'} + f_{pc}$(lb/in^2)	$0.85f_c' - f_{pc}$	f_{pc}
Steel	$0.9f_y$	$0.9f_y$	$0.85\,f_y$	$0.85\,f_y$
Timber	$3f_a$	$3f_a$	20 (MPa) 3,000 (lb/in^2)	20 (MPa) 3,000 (lb/in^2)

A_s = cross-sectional area of steel
A_c = gross cross-sectional area of concrete
f_a = allowable timber stress for static design (see Table 21.3 for values)
f_c' = concrete unconfined compressive strength
f_y = steel yield stress
f_{pc} = prestressing stress

Freeze (Setup) or Relaxation Effects

As discussed in Section 13.3, nearly all driven piles exhibit a change in capacity over time. In most cases the capacity increases, a phenomenon known as *freeze* or *setup*. The magnitude of freeze is greatest in piles driven into saturated clays (due to excess pore water pressures generated during driving) but is also seen in piles driven into dry sands. In some soils the pile capacities have been known to decrease over time, a phenomenon known as *relaxation*. This means that the capacity of a pile measured during driving will be different than the capacity of the same pile sometime after driving. For clarity, the pile capacity determined based on a wave equation analysis conducted during driving is referred to as the end-of-driving (EOD) capacity.

We are primarily interested in the load capacity after freeze or relaxation has occurred, yet dynamic analyses described above, based on data obtained during driving only give the EOD capacity. There are two ways to get the long-term (post-freeze or relaxation) capacity. The simplest method is to multiply the EOD capacity by a freeze factor which is greater than unity or a relaxation factor less than unity as appropriate. If the freeze or relaxation factor is based on a comparison of EOD capacity with onsite static tests, this may be a relatively accurate method. If the freeze or relaxation factor is based on engineering judgment or previous experience, the accuracy will be significantly reduced.

In lieu of using static pile tests, the long-term capacity can be estimated using a pile *retap* or *restrike* (Hussein et al., 1993). In this method the pile is redriven a few centimeters several days after the original driving date. The retap blow count can then be used with the bearing graph previously developed to determine the capacity of the pile. The capacity

determined using this method is sometimes called the *beginning of retap* (BOR) capacity, which is assumed to be equal to the long-term capacity of the pile. There is some uncertainty in the blow count when doing a retap, because the hammer is often not warmed up and operating at its full efficiency. In this case the long-term capacity of the pile may be overestimated. This is particularly an issue with diesel hammers. The problem can be alleviated by warming the hammer up on a test pile before performing the retap.

19.3 HIGH-STRAIN DYNAMIC TESTING

There are a number of limitations to using wave equation analysis, as described in Section 19.2, for determining pile capacity. These limitations include:

- Uncertainty in energy delivered to the pile head due to modeling errors
- Uncertainty in the dynamic soil properties
- Uncertainty of the blow count during retap
- Usable only for driven piles

Because of these limitations, pile capacities determined using wave equation analysis of the entire hammer/pile/appurtenances/soil system without measured field data should be considered a preliminary estimate of pile capacity. To overcome these limitations, a number of dynamic field tests have been developed to determine in situ pile capacity. These tests are generally less expensive than static pile tests. They are sometimes used to supplement static piles tests and sometimes used alone to determine the in situ pile capacity.

These tests are commonly called *high-strain dynamic tests* to distinguish them from *low-strain dynamic tests* performed to determine pile integrity. Pile integrity testing generally involves impacts of hammers weighing 5 to 50 N (1–10 lb) and generates strains of 10^{-6} to 10^{-5} These tests are covered in Section 23.7. High-strain dynamic tests use hammer weights of 20 to 1,200 kN (4,400–207,000 lb) and generate strains of 10^{-4} to 10^{-3} and pile displacements of 1 to 50 mm (0.5–2 in). The larger displacements are required to mobilize the full soil strength. High-strain dynamic tests can be broken down into two categories based on the duration of the stress pulse loading the pile. Short duration tests have a loading duration on the order of the time required for the stress pulse to travel the length of the pile, generally 5 to 20 milliseconds. Long duration tests, also called *Force Pulse Load Test* generally have a loading duration greater than 5 to 10 times the time required for the stress pulse to travel the length of the pile, generally 50 to 200 milliseconds. The difference in load duration affects the way the tests are conducted and the data analyzed.

Short Duration High-Strain Dynamic Tests

These tests employ measurements of the stress and particle velocity generated by a dynamic load applied at the pile head. When testing driven piles, the most common source of dynamic loading is a pile hammer, because it is already onsite and thus represents little

or no additional cost. However, this test method is not limited to driven piles. Dynamic loads also can be obtained with drop hammers or with explosives, which enables testing of drilled shafts and other types of deep foundations.

Field equipment for measuring the forces and accelerations in a pile during driving was developed during the 1960s and became commercially available in 1972. The methodology is now standardized and is described in ASTM standard D4945.

This equipment includes three components:

- A pair of *strain transducers* mounted near the top of the pile
- A pair of *accelerometers* mounted near the top of the pile
- A *Pile Driving Analyzer*® (PDA)

The strain transducers, accelerometers, and a typical Pile Driving Analyzer are shown in Figure 19.8.

The PDA monitors and records the output from the strain transducers and accelerometers as the pile is being driven, and evaluates this data as follows:

- The strain data, combined with the modulus of elasticity and cross-sectional area of the pile, gives the axial force at the sensor location.
- The acceleration data integrated with time produces the particle velocity at the sensor location.
- The acceleration data, double integrated with time produces the pile displacement during the hammer blow.

By measuring the hammer input to the pile head, these tests eliminate any uncertainty in modeling the hammer and appurtenances. As the stress wave travels down the pile and is reflected back up the pile, the transducers record the response of the pile in

(a) (b)

Figure 19.8 (a) Pile Driving Analyzer with wifi antennas. (b) Strain gage (left) and accelerometer (right) mounted near the top of a pile to provide input to the Pile Dynamics, Inc.).

situ. By comparing the input stress time histories with the measured response time histories it is possible to determine the static pile capacity. There are a number of methods to analyze the dynamic response of the pile. The two most common methods used are the Case method and the CAPWAP® method.

The Case Method

High-strain dynamic tests were developed during the 1960s and early 1970s at Case Institute of Technology in Cleveland, Ohio (now known as Case Western Reserve University). The *Case method* (Rausche et al., 1972; Rausche et al., 1985; Hannigan, 1990) is named after this institution. The Case method is an analytical solution of the one-dimensional wave equation considering reflection of waves off the sides and toe of the pile.

As discussed in Section 19.2 and illustrated in Figure 19.2, the hammer impact creates a compressive wave pulse that travels down the pile. As it travels, the pulse induces a downward (positive) particle velocity. If the pile has only toe bearing resistance (no side friction), the pulse reflects off the bottom and travels back up as another compression wave as illustrated in Figure 19.2c. This reflected wave produces an upward moving (negative) particle velocity.

The time required for the wave to travel to the bottom of the pile and return is $2D_2/c$, where:

D_2 = distance from strain transducers and accelerometers to the pile tip
c = wave velocity in the pile

The plots of force and particle velocity near the head of this toe bearing pile (as measured by the PDA) are similar to those in Figure 19.9. Note the arrival of the return pulse at time $2D_2/c$. These plots are called *wave traces*. The force wave trace shows a large positive (compressive) increase at time $2D_2/c$ while the velocity trace shows a large

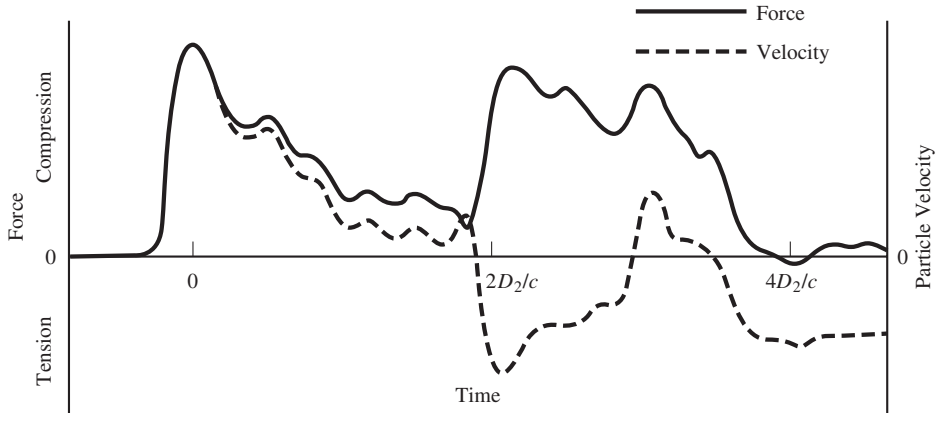

Figure 19.9 Typical plots of force and particle velocity near the top of the pile versus time for a toe bearing pile (data from GRL Engineers, Inc.).

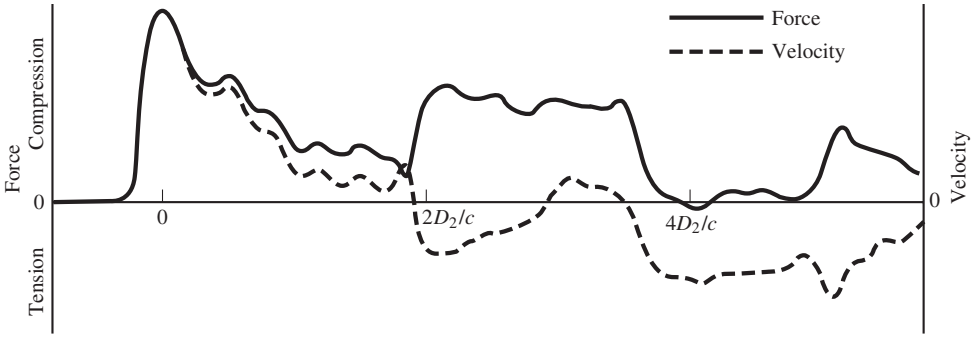

Figure 19.10 Typical plots of force and particle velocity near the top of the pile versus time for a toe bearing pile with less toe bearing resistance than that shown in Figure 19.7 (data from GRL Engineers, Inc.).

decrease (upward) velocity change. This clear compressive reflected wave is indicative of a toe bearing pile and the magnitude of the reflected wave is a measure of the toe bearing capacity.

Figure 19.10 shows wave traces recorded by the PDA for a different pile that also has toe bearing with little side friction resistance. Again, we see a reflected compressive wave arriving at time $2D_2/c$. In this case, the reflected wave has smaller amplitudes than those shown in Figure 19.9, indicating this pile has a lower toe bearing capacity than that represented by Figure 19.9.

In contrast to the toe bearing pile represented by Figures 19.9 and 19.10, Figure 19.11 shows wave traces for a friction pile with very little toe bearing resistance. In this case, as the compression wave pulse travels down the pile, it encounters the side friction resistance. Each increment of resistance generates a reflected wave that travels back up the pile, so the wave trace show arrival of reflected compressive waves at a time much earlier than $2D_2/c$. Also, note that the reflected arrival is not as distinct as that in the case

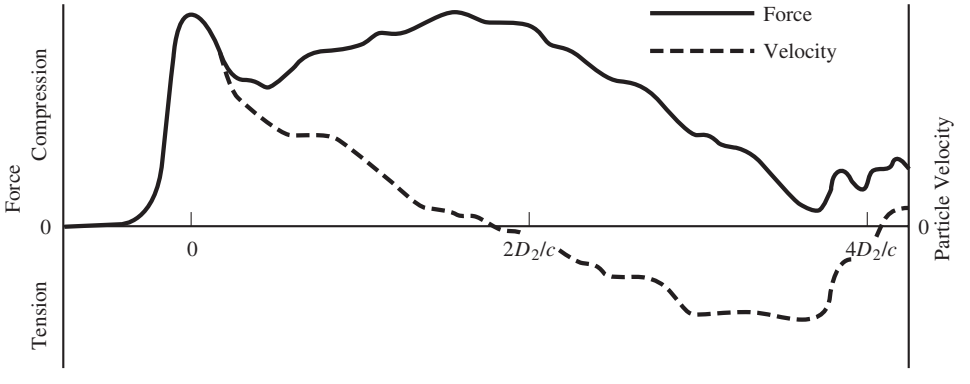

Figure 19.11 Typical plots of force and particle velocity near the top of the pile versus time for a friction pile (data from GRL Engineers, Inc.).

of toe bearing piles. This is because the incident downward wave is continually reflected as it encounters side resistance travelling down the pile. This leads to the gradual increase in the amplitude of the force wave trace.

The wave trace also provides pile integrity data. For example, if the pile breaks during driving, the fracture produces a reflected wave that changes the wave trace recorded by the PDA (Rausche and Goble, 1978).

The Case method tracks the arrival time and magnitude of the reflected stress and velocity traces and uses a closed form analytical method to determine the static pile capacity (Hannigan, 1990). The PDA is programmed to solve for pile capacity using this method and gives the results of this computation in real time in the field.

There are limitations to the accuracy of the analytical solution used in the Case method. In particular this method implicitly assumes the soil elastic-perfectly plastic and uniform along the entire length of the pile and that a single damping coefficient, j_c, based on toe velocity is used for the whole pile. Also, the Case method is generally performed during driving and therefore provides EOD capacity rather than long-term capacity of the pile, ignoring any pile setup. The damping coefficient can be estimated by measurements taken between hammer blows (when the pile velocity is zero).

To improve the value of the Case method, it may be performed in combination with static load tests on a few indicator piles driven at the beginning of the project. In this way the engineer can determine an empirical soil damping factor that relates the capacity determined from the Case method to that measured in the static load test. Then, the engineer can use the Case method in combination with this empirical damping factor to monitor and control the installation of production piles. Alternatively the Case method can be calibrated using the wave matching method discussed in the next section. Once the Case method has been calibrated, that calibration can be used to determine the capacity for all hammer blows; not just those used for the calibration itself. It is also possible to use the Case method without calibration by using j_c values from other similar soils. This approach is less accurate, but still very valuable. Generally, PDA measurements are taken and a Case analysis is performed on only as subset of the total production piles, one out of every 10 or 20 piles is typical.

Wave Matching Method

The Case method, while useful, is a simplification of the true dynamics of pile driving and the associated response of the adjacent soil. Therefore, the final results are limited by the simplified soil model and selection of the damping factor. In contrast, a wave equation analysis uses a more accurate soil model, but suffers from inaccuracies of modeling the hammer and appurtenances. Fortunately, the strengths and weaknesses of these two methods are complimentary, so we can combine them to form an improved analysis. This combined analysis uses the measured stress and velocity at the top of the pile as inputs to a wave equation analysis. The goal of the analysis is to adjust the soil parameters to match the computed wave traces to those measured in the pile. This method is known as a *wave matching* or *signal matching* method. The first widely accepted wave matching method is known as CAPWAP® (CAse Pile Wave Analysis Program) (Rausche et al., 1972).

CAPWAP analysis is essentially the same as the wave equation analysis described in Section 19.2, but instead of starting the analysis from the hammer input, it uses the stress-time history measured at the pile head to start the analysis. In this fashion it eliminates all of the uncertainties in modeling the hammer and appurtenances. Therefore the only remaining unknowns in the problem are the dynamic soil properties (R_u, q, and J_s) and the ratio of side to toe resistance. The soil properties are adjusted until the computed stress wave trace matches the measured trace. The quality of the match is somewhat subjective and the solution is non-unique since many different combinations of soil properties can provide satisfactory matches. However, the total static pile capacity varies little among different solutions so long as each provides a good match to the measured wave form. This solution method is an iterative one. Figure 19.12 show the typical wave matching process.

Using the backcalculated soil properties further wave equation analyses can be performed to generate many useful products including:

- More accurate input parameters for a wave equation analysis that could then be used to select the optimal driving equipment as well as to produce a bearing graph.

(a) Initial match using standard soil properties. Poor.

(b) Second iteration, adjusted toe/side resistance ratio. Better match.

(c) Third iteration, adjusted soil quake and damping factors. Good match.

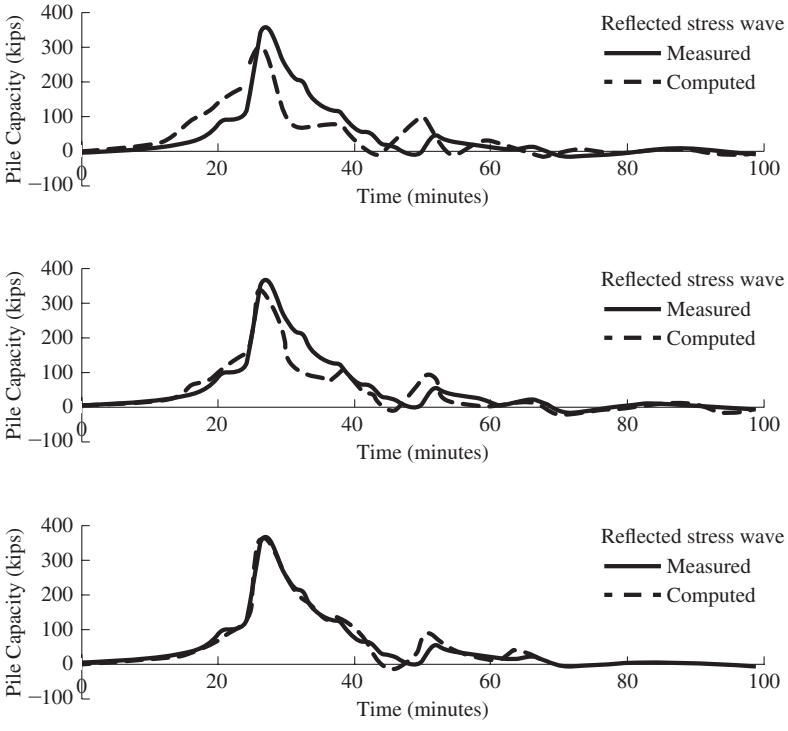

Figure 19.12 Three plots of measured and backcalculated wave traces illustrating the wave matching process followed in a CAPWAP® analysis (data from GRL Engineers, Inc.).

- A site-specific Case method damping factor, j_c, for use in PDA analyses of selected production piles.
- A site-specific bearing graph to monitor installation of production piles.

CAPWAP analyses can be performed for both the end of driving and retap records to develop a quantitative measurement of pile setup or relaxation (Fellenius et al., 1989). CAPWAP analyses are often used to reduce the required number of static load tests, or used where load tests are not cost-effective.

Tests Using Drop Hammers

Wave matching analyses, such as CAPWAP, were originally developed for use with driven pile foundations, since the acceleration and strain data could be readily collected during the driving process. Since then, engineers have applied these methods to other pile systems such as auger cast piles and drilled shafts. In these cases specially designed drop hammers are brought in after pile installation to test the piles. The data collection and analysis process is the same as with driven piles. This method can provide dynamic verification of the load capacity determined from analytic methods, while being less costly than a static load test. This is particularly true with high capacity drilled shafts where static loads are prohibitively expensive.

A number of different drop hammer systems have been developed. Most rely on standard CAPWAP instrumentation and analysis methods. Some of the more advanced methods include enhanced instrumentation. Paikowsky (2006) provides a thorough review of the most common drop hammer systems. Figure 19.13 shows a typical drop hammer used to perform these tests. Typically the test uses a weight equal to about 1.5 percent of the required static test load. The drop height is usually a few meters. The actual equipment needs should be determined in advance using a wave equation analysis (Hussein et al., 1996).

Force Pulse Load Tests

The force pulse or long duration dynamic test differs from short duration test in that the load applied to the top of the pile lasts for 50 to 200 milliseconds, which is typically 10 or more times longer than loads applied during short duration tests. The duration of the applied load is generally over ten times the time required for a stress wave to pass through the pile. Therefore these tests do not need to model wave the propagation of the stresses wave through the pile. These tests are dynamic, their analyses must consider the kinetic energy imparted to the pile and the viscous damping in the soil, but wave equation analysis is not required. One drawback of the force pulse test is that it determines only the total static capacity of the pile. Since wave equation analysis is not performed it is not possible to determine the distribution of resistance along the length of the pile.

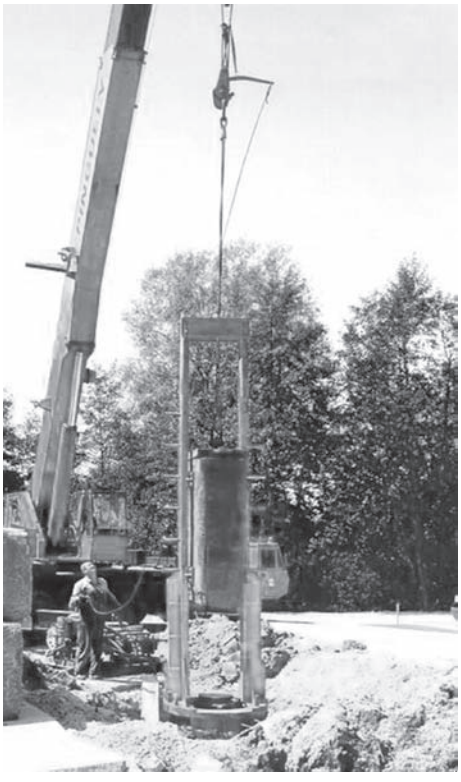

Figure 19.13 This drop hammer is being used to conduct a high-strain dynamic load test on a drilled shaft foundation (courtesy of Pile Dynamics, Inc.).

Statnamic® Test System

The first pulse load test system developed was the *Statnamic*® test developed by The Netherlands Organization for Applied Scientific Research (TNO) and Berminghammer Foundation Equipment, Canada (Paikowsky, 2006).

The statnamic method loads the foundation by igniting a propellant located inside a pressure chamber placed between the foundation and a reaction mass, as illustrated in Figure 19.14. When ignited, the gases launch the reaction mass upward at accelerations up to 20 g allowing the test to generate a downward force on the pile equal to up to 20 times the weight of reaction mass. This allows for the use of relatively small masses compared to static tests, thereby saving significant mobilization costs and setup times. Figure 19.15 shows a series of photos of a statnamic test on a pile driven over water. In this case water filled cylinders are used as the reaction mass. The reaction mass must be caught before it falls back down and impacts the pile. Most commonly, mechanical or hydraulic systems are used to catch the reaction mass near its apogee so that it does not fall back down and damage the test pile.

The instrumentation for a statnamic nearly always includes strain gages and accelerometers placed near the pile head, just as with Case or CAPWAP methods. Often

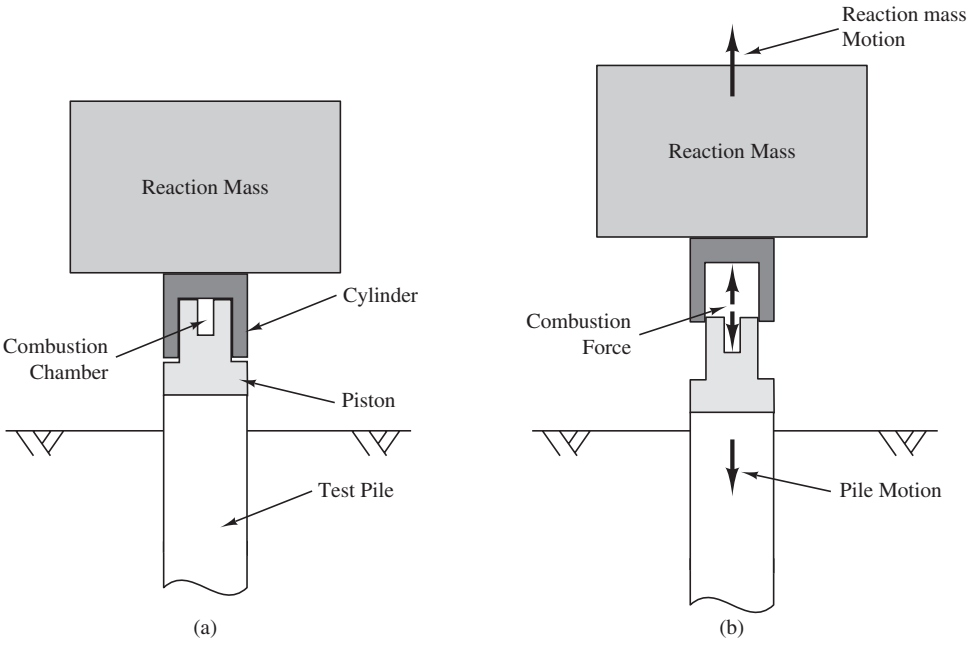

Figure 19.14 Schematic diagram of Statnamic test system: (a) a piston-cylinder systems loaded with propellant is placed on top of the test pile with a reaction mass on top of the cylinder. (b) When the propellant is ignited in the combustion chamber, it pushes up on the reaction mass and down on the pile with equal and opposite forces.

displacement transducers are also included at the pile head. This provides redundancy to the motion measurements as displacement versus time can be computed through a double integration of the acceleration record or directly through the displacement measurements. The strain gage measurements are converted to force using the cross-sectional area and modulus of the pile. It is often advantageous to have acceleration measurements near the tip of the pile, particularly for toe bearing piles. This requires installing these sacrificial transducers during pile installation. Data from the transducer suite is recorded on a high speed digital data logger capable of taking measurements at 5,000 Hz or higher.

Drop Hammer Systems

Another type of force pulse test system uses the same type of drop weights used for short duration high-strain dynamic testing. However, these systems include a very thick pile cushion, typically plywood 20 cm (8 in) or more thick. The thick pile cushion lowers the peak load and increases its duration compared to short duration tests. Figure 19.16 shows a cushion used for a drop hammer pulse load test. The cushion must be properly designed to ensure the long duration loading needed for this test. This form of pulse load test is becoming more common because the system is non-proprietary and there is no need to acquire permits to transport and use the propellants used in the statnamic test.

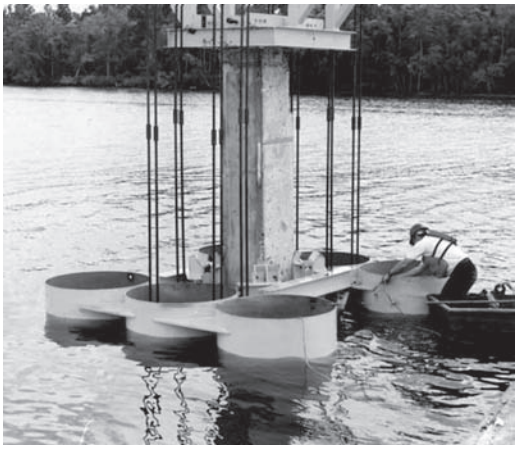

(a)

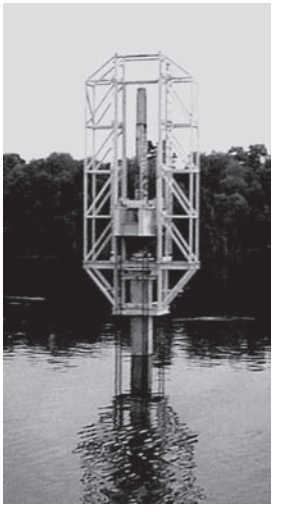

(b)

(c)

Figure 19.15 A statnamic test on a pile driven over water. (a) Usually the reaction mass is located above or around the statnamic pressure chamber. However, in this case, the reaction mass consisted of water inside submerged containers. (b) The statnamic pressure chamber is located above the test pile, and in this case is connected to the submerged mass through tendons. In most tests this pressure chamber is hidden by the reaction mass. (c) The propellant is ignited inside the pressure chamber, which then imparts an upward force on the reaction mass and an equal downward force on the pile (photos courtesy of Applied Foundation Testing Inc.).

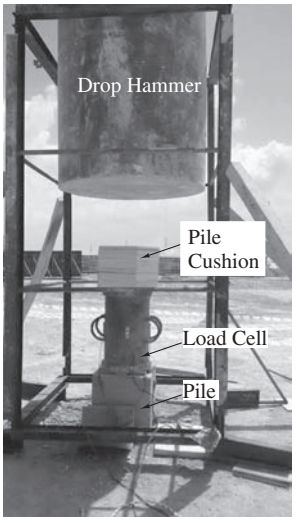

Figure 19.16 Pulse load test employing a drop hammer. The cushion is made of sheets of plywood with a thickness of approximately 50 cm (20 in). Between the cushion and the pile is an instrumented segment of pipe being used as a load cell.

Unloading Point Analysis Method

Because of the relatively long duration of the loading pulse in force pulse testing, it can reasonably be assumed that the pile moves as a rigid body. The most common analysis method is the *unloading point* (UP) method (Middendorp et al., 1992). The model for the UP method is a rigid mass for the pile with non-linear spring and dashpot for the soil response, as illustrated in Figure 19.17. Ignoring gravity and applying vertical equilibrium, the static pile capacity, R_u, can be computed as:

$$R_u = F_d - F_a - F_v \tag{19.22}$$

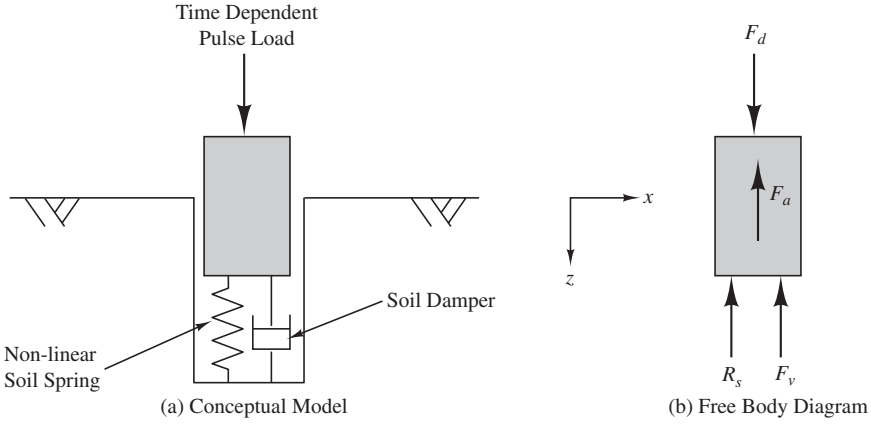

Figure 19.17 Pile–soil model use for unloading point model of the pulse load test.

where

F_d = total applied force, dynamic plus static
F_a = body force due to acceleration of the pile
F_v = damping force acting on the pile

The forces due to acceleration and damping can be computed as:

$$F_a = m_p a \tag{19.23}$$

$$F_v = v_p j_s \tag{19.24}$$

where

m_p = mass of the pile
a = acceleration of pile due to applied forces
v_p = velocity of the pile
j_s = soil damping factor

Combining Equations 19.22, 19.23, and 19.24, the static pile capacity can be computed as:

$$R_u = F_d - m_p a - v_p j_s \tag{19.25}$$

The values of F_d, m_p, a, and v_p are known, leaving two unknowns in Equation 19.25: the soil damping factor, j_s, and the static pile capacity, R_u.

The UP method starts by locating the time where the pile velocity is zero, t_{unl}. This is called the *unloading point*, or the point where the pile starts to rebound up after being pushed down by the dynamic force, F_d. This point is shown in Figure 19.18a. At this point in time, the pile velocity is zero and, therefore, the damping term in Equation 19.25 is also zero. Using the data from the unloading point, F_{unl} and a_{unl} shown in Figure 19.18a, we compute the static pile capacity at the unloading point as:

$$F_u(t_{unl}) = F_{unl} - m_p a_{unl} \tag{19.26}$$

The analysis then assumes that all the soils around the pile is in a yield state from the point of maximum dynamic force, $F_{d,\max}$ (shown in Figure 19.18b), through the unloading point and, therefore, the static pile capacity is also constant in the zone and equal to F_u computed by Equation 19.25. We also assume the damping factor in this zone is constant. With these two assumptions, we can compute the damping factor, j_s, as:

$$j_s = \frac{(F_d - F_{unl} - m_p a)}{v} \tag{19.27}$$

An average damping factor, $j_{s\text{-}ave}$, is computed over the range from $F_{d(\max)}$ to F_{unl}. Using this average damping factor, the static pile capacity can then be computed over the full loading range using the equation:

$$F_u = F_{stn} - j_{s,ave} v - m_p a \tag{19.28}$$

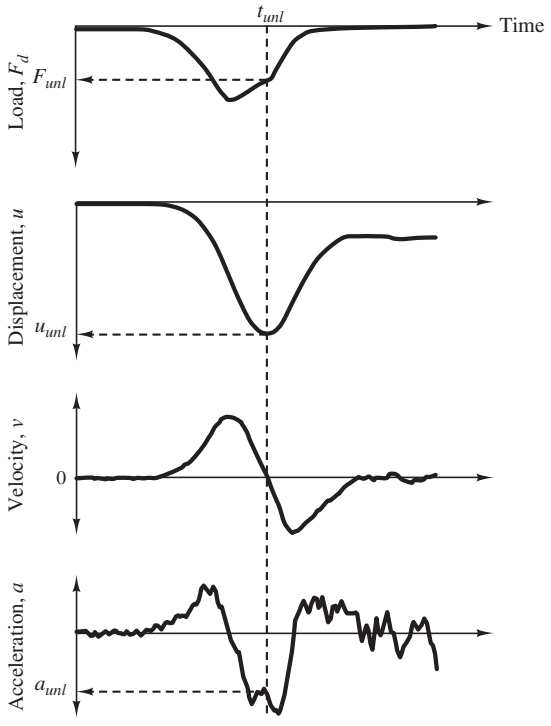

(a) Measurements of a Pile Head

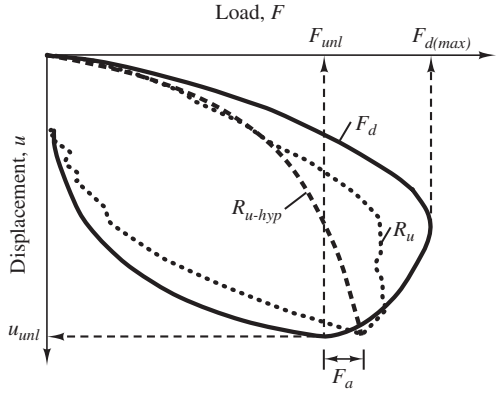

(b) Load Displacement Curves

Figure 19.18 (a) Typical data for a statnamic test and (b) the statnamic and load displacement curves determined from the unloading point method (data from Middendorp and Bielefeld, 1995).

Figure 19.18b shows the F_u versus u curve derived from the dynamic loading curve using Equation 19.28. This represents that static loading curve for the pile. For simplicity this curve is often approximated with a hyperbolic fit as shown in Figure 19.18b.

Modification to UP to Account for Non-rigid Body Motion

The UP method assumes that the pile moves as a rigid body. There are two instances where this assumption may not be valid. The first is the case where the pile toe is located in a material that is much stiffer than the rest of the pile. This occurs in the cases of drilled shafts in rock sockets or end bearing piles in dense or stiff soils. In these cases there is a significant elastic compression of the pile during loading and therefore a difference between the movement of the head and the toe of the pile. To deal with this issue the *modified unloading point* (MUP) method was developed (Mullins et al, 2002). This method involves placing an accelerometer near the toe of the pile in addition to the accelerometer near the pile head. The rigid body assumption is kept, but the average acceleration of the head and toe of the pile is used to perform the analysis. Otherwise the analysis is the same as the UP method.

A second case where the rigid body assumption does not apply is for very long piles where loading time is relatively short in comparison to the pile length. Middendorp (1998) introduced the *stress wave number*, N_w, as a method to determine the load duration for which the rigid body assumption was appropriate. The stress wave number represents the number of times the loading wave travels the length of the pile during the dynamic load and is calculated as:

$$N_w = \frac{cT}{L} \tag{19.29}$$

where

$c =$ the wave velocity in the pile (defined by Equation 19.6)
$T =$ duration of the loading pulse
$L =$ length of the pile

Middendorp's analysis indicated that for stress wave numbers greater than 12 the rigid body assumption was appropriate and the UP method works well. This generally limits the UP method for steel piles less than 40 m (130 ft) and concrete piles less than 32 m (105 ft) which covers many applications.

For stress wave numbers greater than 6 and less than 12, a modification of the UP method called the segmental unloading point (SUP) method (Mullins et al., 2002) can be used. This method involves placing a series of accelerometers along the length of the pile and performing the UP method segmentally along the pile length. Each segment is assumed to act as a rigid body. For stress wave numbers less than 6, a wave matching analysis such as CAPWAP should be used. Table 19.8 summarizes the appropriate dynamic analysis.

TABLE 19.8 DYNAMIC LOAD TEST ANALYSIS METHOD BASED ON THE STRESS WAVE NUMBER (data from Middendorp and Daniels, 1996)

Stress wave number, N_w	Appropriate analysis method
$N_w < 6$	Wave matching method such as CAPWAP
$6 \leq N_w < 12$	Segmental unloading point method (SUP)
$12 \leq N_w < 1{,}000$	Unloading point method (UP)
$N_w \geq 1{,}000$	Static load test methods

$N_w = cT/L$, where: c = wave speed; L = pile length, T = load duration

Adjustments for Tests in Cohesive Soils

Another important assumption of the force pulse load analysis methods is that all of the dynamic effects are captured by the damping coefficient and pile acceleration term. This assumption appears to be satisfactory for tests conducted in cohesionless soils (sands and gravels) where pile capacities determined by force pulse load tests analyzed using the above methods compare favorably with capacities determined through static load tests. However, there is significant evidence that there is an additional rate effect for piles in cohesive soils which is not captured through the standard force pulse load analysis methods. Based on a comparison of four load tests in cohesive soils where both statnamic and static load tests were available, Paikowsky (2006) recommended using a reduction factor of 0.65 when using the UP method to determine capacity of piles in clay. A study by Weaver and Rollins (2010) uses a larger database of tests and concludes that the reduction factor should be 0.47. Recent research indicates that the damping coefficient may be a function of the plasticity of the soil and, therefore, using a single reduction factor for all tests in clays may oversimplify the analysis. Brown and Powell (2012 and 2013) have developed methods to determine soil-specific damping models based on the plasticity index (PI). These methods have the potential to improve the accuracy of pulse loading tests conducted in clay soils. However, more tests in highly plastic clays are needed to validate the model (Brown and Powell, 2013).

Application of High-strain Dynamic and Force Pulse Load Tests

Both long duration high-strain dynamic and force pulse load tests are valuable tools which foundation engineers can use to determine the capacity of piles and drilled shafts. For driven piles, high-strain dynamic testing is relatively inexpensive because the pile hammer being used to drive the piles provides the load for the test and little or no additional cost to the project. Ideally, a few instrumented indicator piles are driven at the start of the project. CAPWAP analyses are performed from the end of driving data to determine damping factor and compute the end of driving pile capacity. From this information a wave equation

analysis can be performed to develop an end of driving bearing graph. A few days later retaps are performed on some of the indicator piles to determine the setup or relaxation factor. The setup or relaxation factor is then used to determine the end of driving capacity needed to achieve the required long-term capacity. During driving of production piles, the Case method can be used to determine the pile capacity in real time, or the bearing graph developed from the indicator piles can be used to determine the capacity of the production piles.

For auger piles or drilled shafts, high-strain dynamic or force pulse tests can replace or supplement static load tests to determine the pile or drilled shaft capacity. Often it is less expensive to mobilize the equipment for a drop hammer or Statnamic test than to construct the load frame and anchor or kentledge system needed for a static load test. These dynamic tests are generally much faster than static load tests; sometimes several can be performed in one day. The cost savings grows as the pile capacity increases.

19.4 CONCLUSIONS

Dynamic methods have progressed from the crude pile driving formulas of the late nineteenth century to sophisticated numerical models with extensive calibrations to static load tests. These methods are very attractive to foundation engineers, because they promise to provide reliable information on load capacities without the necessity of investing in expensive static load tests. In addition, some dynamic methods provide information on driveability and structural integrity.

It is unlikely that static load tests will ever become obsolete, but dynamic methods have substantially reduced the need for them. As dynamic methods continue to be refined, they will probably enjoy increased use in a wider range of projects.

SUMMARY

Major Points

1. Dynamic methods use evaluations of a foundation's response to applied dynamic loads, such as those from a pile hammer or other impact sources, to determine its static load capacity. Some dynamic methods also provide information on driveability and structural integrity.
2. Pile driving formulas are the oldest type of dynamic method. They attempt to correlate static load capacity with blow count, hammer type, and other factors. Unfortunately, these formulas oversimplify the pile driving process, and thus are not very precise, especially if they have not been calibrated with an onsite load test. It is inappropriate to use such methods for design, analysis, and construction control.
3. Wave equation analyses have replaced pile driving formulas. Instead of relying solely on empirical correlations, the wave equation analysis uses a detailed analytical model of the pile and its driving system. The results of these analyses include

a bearing graph (which is a plot of static capacity versus blow count), and the pile driving stresses, which form the basis for a driveability analysis.

4. The capacity of driven piles nearly always changes after driving. Most often piles experience freeze or an increase in capacity. Sometimes piles experience relaxation or a decrease in capacity. It is important to distinguish between the end of driving static capacity which does not include freeze or relaxation, and the long-term static capacity which does include these effects.
5. High-strain dynamic tests use instruments mounted on the pile to record its response to applied dynamic loads. There are two types of high-strain dynamic tests. Short duration tests have load durations that are 5 to 20 milliseconds. These tests use pile hammers or drop hammers to apply the load and require a wave equation type analyses to determine the pile capacity. Long duration or pulse load tests use either a propellant in a cylinder-piston system with a reaction mass or a drop hammer with a very large cushion to provide loads that are generally 50 to 200 milliseconds long. The pulse load tests do not require a wave equation type analysis but use a much simpler analysis to determine pile capacity. Both methods may be used to determine the long-term static pile capacity.

Vocabulary

Beginning of retap (BOR)
Bearing graph
Blow count
CAPWAP
Case method
Driveability analysis
Dynamic methods
End of driving (EOD)
Engineering news formula
Force pulse load test
Freeze (setup)
High-strain dynamic testing
Low-strain dynamic testing
Pile driving analyzer
Pile driving formula
Quake
Relaxation
Restrike
Retap
Smith damping factor
Statnamic test
Unloading point method
Wave equation

QUESTIONS AND PRACTICE PROBLEMS

19.1 Explain why pile driving formulas are not reliable, and why a wave equation analysis is a better choice.

19.2 Under what conditions will tensile stresses be generated in pile driving? In what situations should this be of a concern?

19.3 What's the difference between a hammer cushion and a pile cushion? What are the purposes of each? Under what circumstances is a pile cushion generally used?

19.4 Two different single acting hammers are being considered for an open-ended pipe pile. Hammer A has a ram weight of 30 kN and a stroke of 3 m. Hammer B has a ram weight of 15 kN and stroke of 5 m. Both hammers use similar appurtenances. Which hammer will deliver the most energy to the pile? Which hammer will generate the highest stresses in the pile?

19.5 A 15 m long normal weight concrete pile is being driven at a rate of 25 blows per minute. Will the wave from the first hammer blow reach the bottom of the pile and return to the top before the next hammer blow? Justify your answer with appropriate computations and comment on the results.

19.6 A building is to be constructed on driven piles. The downward vertical load on each pile based on ASD load combinations is 120 k with a factor of safety of 2.5. Estimate the rated hammer energy required to drive these piles.

19.7 Driven piles will be used to support a bridge founded on a deep sand deposit. The factored downward axial structural load for piles in the foundation is 380 kN. Determine the required nominal capacity of the piles, P_n, for the following analysis and testing procedures. Use AASHTO resistance factors provided in Tables 13.3 and 13.4.

a. Only static analysis using the β method

b. Static analysis combined with wave equation analysis but neither dynamic pile measurements nor static load test.

c. A static load test on one pile plus at CAPWAP analysis on at least two piles.

Comment on the value of wave equation analysis, load testing, and CAPWAP analysis for this pile design.

19.8 The bearing graph shown in Figure 19.6 was developed for an FEC model 1,500 open-ended diesel hammer driving closed-ended pipe pile 19 m into a sand deposit. The pile has an outside diameter of 35.6 cm and wall thickness of 80 mm made with A-252 grade 2 steel ($f_y = 240$ MPa). The required ultimate static pile resistance, R_{ur}, is 1,000 kN. Onsite, a certain pile was driven to 19 m with a blow count of 50 for the last 0.25 m. Assume the setup factor is 1.0, will this pile meet the required capacity? Will the driving stresses be acceptable?

19.9 A 14 in square prestressed concrete pile is to be driven with a certain hammer. According to a wave equation analysis, the compressive driving stresses will exceed the maximum allowable values described in Table 19.7. What can be done to resolve this problem? Provide at least two possible solutions.

19.10 Explain how wave equation analysis combined with static or dynamic load tests can be used to determine the long-term capacity of piles driven in clay where there is a significant setup factor.

19.11 Why does the statnamic test use a relatively slow burning propellant rather than high explosive to provide the energy for the test?

19.12 Perform a wave equation analysis for the pile described in Example 15.4. Select a suitable hammer that can drive the pile efficiently. You will have to select a wall thickness for the 16 in diameter pipe and check the driving stresses to ensure they are acceptable. Create a bearing graph for the hammer you have selected assuming a setup factor of 2.0. Also perform a driveability analysis for the hammer you have selected.

19.13 You wish to perform a Statnamic test on a 35 m long 0.5 m diameter concrete drilled shaft. How long must the loading pulse be in order to use the unloading point method to analyze the test?

20

Piles—Serviceability Limit States

Ut tensio sic vis; That is, The Power of any Spring is in the same proportion with the Tension thereof: That is, if one power stretch of bend it one space, two will bend it two, and three will bend it three, and so forward. Now as the Theory is very short, so the way of trying it is very easie.

Robert Hooke, 1678

Much of the effort in the design of pile foundations to support axial loads focuses on satisfying the ultimate limit state (ULS), and Chapters 14 to 19 discussed the various methods of doing so. In most cases, the ULS controls the axial load design and produces piles settle less than 15 mm (0.6 in) under service loads. This is less than the allowable settlement for almost all structures, so the serviceability limit state (SLS) requirements for settlement are often assumed to be satisfied.

However, there are situations where this assumption may not be valid, and an explicit settlement analysis is necessary. For example:

- The piles are installed in groups, especially large groups, which cause stress overlaps in the adjacent soils.
- The structure is especially sensitive to settlement.
- A large portion of the nominal capacity is due to toe bearing, and the pile toe is founded in soil (as contrasted to rock).
- The piles are very long, especially when much of the capacity, either side friction or toe bearing, is developed in the lower portion of the pile.
- Highly compressible strata are present, especially if these strata are below the toe.
- Downdrag loads might develop during the life of the structure.

- The engineer must express the pile response in terms of an equivalent spring located at the bottom of the column. This analytical model is sometimes used in structural analyses for large superstructures.

This chapter discusses methods of computing the expected settlement in axially loaded pile foundations, and thus provides a method for checking this serviceability requirement. In the case of laterally loaded deep foundations, analyses of strength and serviceability are more closely intertwined, so lateral ULS and SLS analyses are discussed concurrently in Chapter 22.

20.1 DESIGN LOAD

As discussed in Chapter 5, the design load for SLS analyses is different from the design load used for ULS analyses. Unfortunately, building codes do not provide much, if any, guidance, so the engineer must rely on standard practices and engineering judgment. Usually, the most appropriate design load would be the service load, which is the greatest load that would be present for some sustained period. Chapter 5 provides guidance on determining the design service load for use in SLS analyses.

The weight of the pile is implicitly included in the net toe bearing capacity, as discussed in Section 13.1, and thus should not be included in the design load. However, if a pile group is being used, the weight of the pile cap should be included as a dead load.

20.2 SETTLEMENT ANALYSIS BASED ON LOAD TESTS

The most direct way to determine the settlement that corresponds to a specified design load acting on a single pile is to use the results of an onsite static load test, as discussed in Chapter 14. This load could then be used to design the production piles. A similar approach could be used with load-settlement curves obtained from onsite dynamic load tests, as discussed in Chapter 19. However, when piles are installed in a group, the load-settlement behavior of an individual pile may not reflect that of the pile group. See the Charity Hospital case study later in this chapter.

20.3 MOBILIZATION OF PILE CAPACITY

The load-settlement response at the top of a pile also may be evaluated using static analysis methods. These methods are an extension of those used to evaluate P_n, as discussed in Chapters 15 to 18. This load-settlement response is a composite of the settlement required to mobilize the side friction resistance, the settlement required to mobilize the toe bearing resistance, and elastic compression of the pile itself. Disaggregating these three components provides more insight into the load-settlement behavior.

We will use the term *settlement* to describe the downward movement at the top of the pile, and *displacement* to describe the downward movement at some point in the pile. The difference between the displacement at a given depth and the settlement is the elastic compression between these two points.

Side Friction

The side friction developed in a pile segment, fA_s, at a point on the pile as a function of the displacement, δ_z, at that point may be described using Chin's hyperbolic model (De Cock, 2009):

$$fA_s = \frac{\delta_z}{K_s + \delta_z/(f_n A_s)} \tag{20.1}$$

where f_n is the nominal unit side friction capacity, f is the mobilized unit side friction resistance, and A_s is the side friction area in that pile segment.

The side resistance flexibility factor, K_s, is the initial slope of the f/f_n versus δ_z curve, as shown in Figure 20.1. This characteristic also may be defined in terms of the flexibility factor, M_s:

$$K_s = \frac{M_s B}{f_n A_s} \tag{20.2}$$

M_s is a dimensionless parameter that typically ranges from about 0.001 in stiff or hard soils to 0.004 in soft or loose soils. Caputo (2003) back calculated M_s to a precision of 0.001 from 150 load tests and found that 81 percent were 0.001 or 0.002. Values as low as 0.0005 might be possible in rock.

A solution of Equation 20.1 demonstrates that a displacement of 5–10 mm (0.2–0.4 in) is usually sufficient to mobilize 90 percent of the nominal unit side friction capacity, f_n.

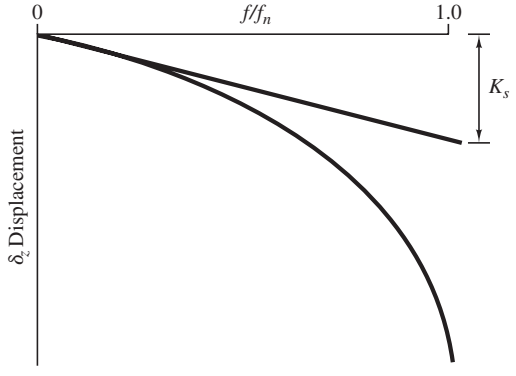

Figure 20.1 Definition of K_s.

Cohesionless soils typically have a ductile load-settlement curve, as shown in Figure 20.2, but cohesive soils may experience some strain softening at large displacements. Therefore, for large strains in cohesive soils, API (2011) recommends reducing f to 70–90 percent of f_n, as shown in Figure 20.2. This reduction begins at the displacement required to mobilize f_n, but the exact shape of the curve beyond that point is largely a matter of engineering judgment.

Toe Bearing

The toe bearing, $q'A_t$, as a function of the toe displacement, δ_{toe}, also may be described with very good accuracy using Chin's hyperbolic model (De Cock, 2009):

$$q'A_t = \frac{\delta_{\text{toe}}}{K_t + \delta_{\text{toe}}/(q_p'A_s)} \tag{20.3}$$

where

K_t = toe resistance flexibility factor
q_p' = nominal net unit toe bearing capacity
A_t = toe area

The toe resistance flexibility factor, K_t, is the initial slope of the q'-δ_t curve. It also may be defined in terms of E_{25}, the secant modulus of the soil within the zone of influence around the toe at a stress equal to 25 percent of the strength:

$$K_t = \frac{0.54}{E_{25}B} \tag{20.4}$$

De Cock also suggested the following relationships for determining E_{25} from the CPT q_c-value, where m is a correlation coefficient presented in Table 20.1:

$$E_{25} = mq_c \tag{20.5}$$

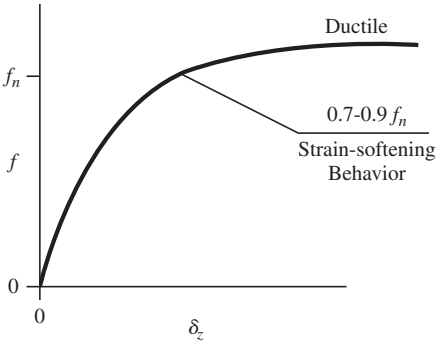

Figure 20.2 Ductile and strain-softening behavior.

TABLE 20.1 *m* VALUES FOR EQUATION 20.5 (De Cock, 2009)

Soil Type	Pile Type	*m*
Normally consolidated cohesionless	Drilled shafts	4–6
Overconsolidated cohesionless	Drilled shafts	6–8
Cohesionless	Screw piles (similar to auger piles)	8–12
Cohesionless	Driven piles	15–20
Cohesive	All	50–80

Alternatively, in cohesive soils, E_{25} correlates with the undrained shear strength, s_u:

$$E_{25} = 750s_u - 1{,}000s_u \tag{20.6}$$

The nominal unit toe bearing capacity, q_n', used in static capacity analyses is typically defined at a settlement of 0.1 B. This practice is, in reality, a muddling of the ULS and SLS. The true toe bearing capacity is actually greater, and this value, defined here as q_p', is used in the hyperbolic definition of the load-settlement curve. For purposes of a settlement analysis, q_p' may be calculated from q_n' using the hyperbolic function at a settlement of $0.1B$:

$$q_n' A_t = \frac{0.1B}{K_t + 0.1B/(q_p' A_t)} \tag{20.7}$$

The toe settlement of $0.1B$ required to mobilize the toe bearing capacity, q_n', is much greater than that required to mobilize the side friction. Thus, even a small 400 mm (14 in) diameter pile would require a toe displacement of about 40 mm (1.5 in) to achieve q_n'.

Elastic Compression

The elastic compression is:

$$\delta_e = \int \frac{P}{AE} dz \tag{20.8}$$

where

δ_e = settlement at top of the pile due to elastic compression of the pile
P = compressive force in the pile
A = cross-sectional area of the pile
E = modulus of elasticity of the pile
z = depth below top of pile

The elastic properties of the pile are defined through the modulus of elasticity, E, and the cross-sectional area, A. Section 14.3 presents methods for computing E, and

Chapter 21 presents values of A for standard driven pile sections. For drilled shafts and auger piles, use an estimate of the as-built diameter to compute A.

Synthesis

The functions for side friction and toe bearing are based on the displacement at the respective points in the pile. The displacement immediately below the top of the pile is equal to the pile settlement, δ. However, because of elastic compression, the ratio δ_t/δ becomes progressively smaller as the pile length increases, and the settlement at the toe, δ_t, can be significantly smaller. For example, at a certain point in the load-settlement curve, the top of the pile may have settled 20 mm, while the pile concurrently experiences 5 mm of elastic compression, so the toe displacement would be only 15 mm.

One of the important implications of this behavior is that mobilization of side friction resistance in the lower portion of the pile lags behind that in the upper portion, especially during the early stages of the load-settlement curve. For example, a settlement of 7 mm at the top of the pile is probably sufficient to mobilize all of the side friction resistance in the upper portion, but the corresponding displacement at the bottom may be 4 mm (due to elastic compression) which means the side friction resistance in the lower zone has not yet reached its peak. Depending on the pile length, diameter, and other factors, a top settlement of perhaps 10 to 20 mm might be required to mobilize 90 percent of the nominal side friction capacity along the entire length of the pile. In addition, the nominal toe bearing capacity, which already requires substantial toe displacement to fully mobilize, will require even more top settlement because of elastic compression.

Thus, the early portion of the load-settlement curve is influenced primarily by side friction, especially in the upper part of the pile, while the toe bearing capacity develops gradually and is fully mobilized much later in the load-settlement curve. Strain softening, if present, would further complicate this process.

Assuming the pile is designed using a geotechnical ULS factor of safety of 2 to 3 (or a comparable resistance factor), the pile length is not excessive, and the side friction capacity ($\Sigma f_n A_s$) comprises at least 1/3 to 1/5 of the nominal capacity, P_n, the vast majority of the service load will be carried by side friction and only a small part of the toe bearing capacity will be mobilized. This is the case for many piles, which means the settlement under the service load should be less than the 10 to 20 mm typically required to mobilize the full side friction capacity. This low settlement value would satisfy the allowable settlement criteria for nearly all structures.

However, if the foundation relies heavily on toe bearing (i.e., $\Sigma f_n A_s$ comprises less than 1/3 to 1/2 of P_n), then the settlement under the service load could be much larger, especially if the pile diameter and/or length are large. This is one of the cases where settlement should be checked.

Example 20.1

A 600 mm diameter pile driven into a cohesive soil has a nominal side friction capacity, $\Sigma f_n A_s$, of 500 kN and a nominal net toe bearing capacity, $q_n' A_t$, of 500 kN. Develop the f-δ_z and q'-δ_t curves. The undrained shear strength at the toe is 100 kPa.

Solution

Side Friction

$$K_s = \frac{M_s B}{f_n A_s}$$

$$= \frac{(0.002)(0.6)}{500}$$

$$= 2.4 \times 10^{-6}$$

$$fA_s = \frac{\delta_s}{K_s + \delta_s/(f_n A_s)}$$

$$= \frac{\delta_s}{2.4 \times 10^{-6} + \delta_s/500}$$

Toe Bearing

$$E_{25} = 825 s_u$$

$$= (825)(100)$$

$$= 82{,}500 \text{ kPa}$$

$$K_t = \frac{0.54}{E_{25} B}$$

$$= \frac{0.54}{(82{,}500)(0.6)}$$

$$= 1.09 \times 10^{-6}$$

$$q_n' A_t = \frac{0.1B}{K_t + 0.1B/(q_p' A_t)}$$

$$500 = \frac{(0.1)(0.6)}{1.09 \times 10^{-6} + (0.1)(0.6)/(q_p' A_t)}$$

$$q_p' A_t = 550 \text{ kN}$$

$$q' A_t = \frac{\delta_{\text{toe}}}{K_t + \delta_{\text{toe}}/(q_p' A_t)}$$

$$= \frac{\delta_{\text{toe}}}{1.09 \times 10^{-5} + \delta_{\text{toe}}/550}$$

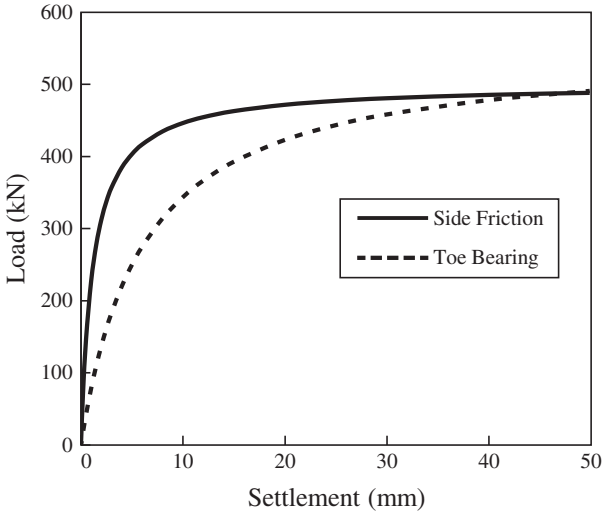

Figure 20.3 Results for Example 20.1.

Results and Commentary

The results of this analysis are shown in Figure 20.3. Note that the nominal capacity is 50 percent side friction and 50 percent toe bearing. Assuming a factor of safety of 2, half of the total capacity is mobilized at a settlement of 2.5 mm, 68 percent of which is side friction, while only 32 percent is toe bearing. This illustrates how the service loads are carried largely by side friction.

20.4 THE *t-z* METHOD

The *t-z* method (Kraft et al., 1981) is a commonly used static analysis for developing pile load-settlement curves. This method considers all three components (side friction, toe bearing, and elastic compression) and the interactions between them. In addition, this method accommodates different side friction mobilization functions along the length of the pile, as would likely occur in stratified soil profiles.

The *t-z* method divides the pile into finite segments, as shown in Figure 20.4, each of which has elastic properties defined by the cross-sectional area, A, modulus of elasticity, E, and the segment length. The side friction resistance between each segment and the soil is modeled using a nonlinear spring which has a load-displacement behavior defined by a *t-z* curve. The toe bearing also is modeled using a nonlinear spring, which is defined using a *q-z* curve.

The notation for the variables t, q, and z are well established in the technical literature on the *t-z* method, but unfortunately is inconsistent with the notation used elsewhere

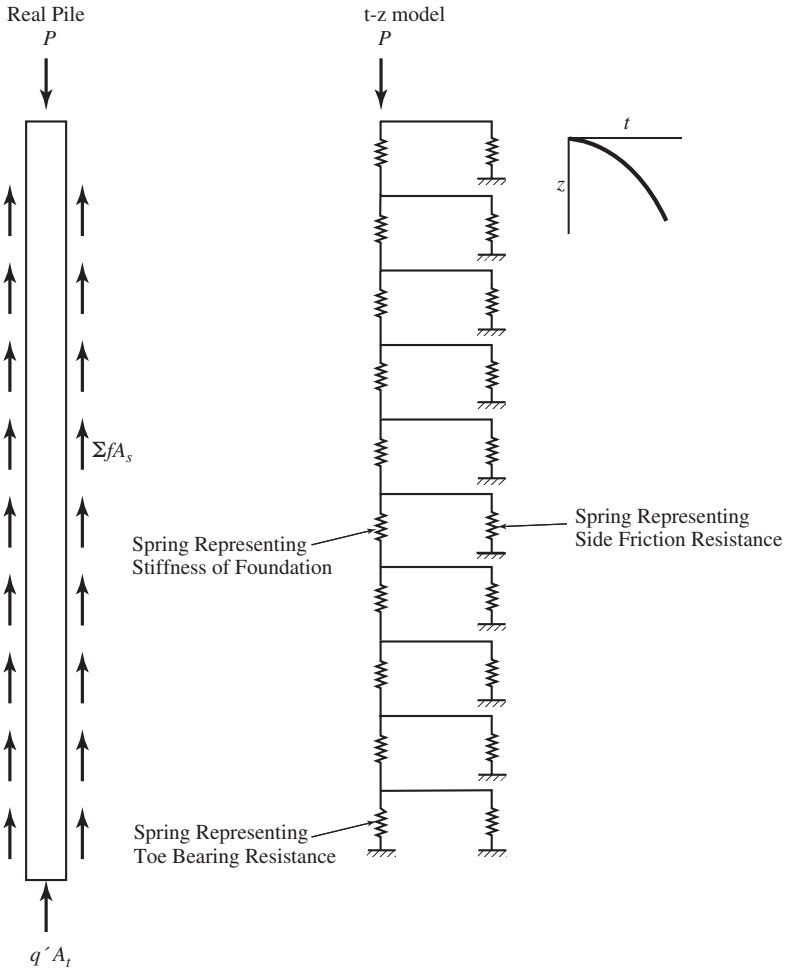

Figure 20.4 Numerical model for the *t-z* method.

in foundation engineering and in this book. This difference in notation is a source of confusion. Thus, we will continue to use our established notation:

f = mobilized side friction resistance (same as t in most *t-z* method literature)

q' = mobilized net toe bearing resistance (same as q in most *t-z* method literature)

δ_z = displacement at a depth z on the pile (same as z in most *t-z* method literature)

δ_t = displacement at the pile toe (same as z or sometimes w in most *t-z* method literature)

These t-z and q-z curves (or, using our notation, f-δ_z and q'-δ_t curves) may be developed using the methods such as those described in the previous section. Published functions, typically derived from static load tests or numerical analyses, also are available for specific soil and rock conditions (e.g., Kulhawy and Carter, 1992; Mayne and Harris, 1993; and O'Neill, et al., 1996). Finally, if onsite static load test data is available, curves may be custom fitted on a site-specific basis, then used in a t-z analysis to extrapolate the load test results.

To execute the t-z analysis, the settlement at the pile top, δ, is set as the independent variable, and a value is selected. The numerical model is then solved to obtain force equilibrium and a value of the corresponding applied load, P, which is the dependent variable. Repeated solutions with different δ values produce a load-settlement plot. This analysis can be conducted using a spreadsheet, but is most often performed using commercially available t-z software.

20.5 SIMPLIFIED STATIC ANALYSIS METHODS

Load-settlement curves can alternatively be developed using simplified static methods, which are easier to implement. In order to make them suitable for hand or simple spreadsheet calculations, these methods include simplifying assumptions, and thus are not as precise or flexible as t-z software. However, simplified methods are easy to use and adequate for many problems, especially when the computed settlement is very small and a more precise analysis is clearly not needed. These methods also are useful when t-z software is not available.

The Fleming (1992) simplified method evaluates the side friction response in its entirety, as compared to the t-z method which does so in finite depth increments. The lag in side friction mobilization is thus implicit in this analysis. This method is formulated as follows:

$$\delta = \delta_s + \delta_t + \delta_e \tag{20.9}$$

$$\delta_s = \frac{M_s B \sum f A_s}{\sum f_n A_s - \sum f A_s} \tag{20.10}$$

$$\delta_t = \frac{0.6 q' q'_n}{B E_t (q'_p - q')} \tag{20.11}$$

For $P \leq \sum f_n A_s$:

$$\delta_e = \frac{4}{\pi} \frac{P(D - L_F + K_E L_F)}{AE} \tag{20.12}$$

For $P > \sum f_n A_s$:

$$\delta_e = \frac{4}{\pi} \frac{1}{AE} \left[PD - L_F(1 - K_E) \sum f_n A_s \right] \tag{20.13}$$

where

δ = settlement at the top of the pile
δ_s = settlement due to mobilization of side friction
δ_t = settlement due to mobilization of toe bearing
δ_s = settlement due to elastic compression
M_s = flexibility factor (as defined in Section 20.3)
q'_p = peak net toe bearing capacity (per Equation 20.7)
q' = mobilized net toe bearing resistance
f_n = nominal side friction capacity
f = mobilized side friction resistance
B = pile diameter
D = depth of pile embedment
A_s = side friction contact area
E = modulus of elasticity of pile
E_t = secant modulus for soil beneath pile base at 25 percent of strength
P = applied downward load
P_n = nominal downward load capacity
L_F = length of a pile transferring load to the soil by side friction (typically equal to D, but may be less if upper soils have little or no side friction capacity)
K_E = depth to centroid of side fiction resistance divided by L_F. For uniform side friction resistance (i.e., f_n constant with depth) use $K_E = 0.5$. For side friction increasing with depth, use a correspondingly larger value, such as $K_E = 0.67$ for a triangular distribution. The maximum possible value is 1.0
A = cross-sectional area of pile

When using this method, it is satisfactory to make the simplifying assumption that the initial load increments are carried entirely by side friction, and that the toe bearing begins to be engaged only after 90 percent of the side friction capacity has been mobilized. Additional load increments may be assumed to be carried entirely by toe bearing with no additional side friction.

Example 20.2

A 40 ft long, 36 in diameter drilled shaft is to be constructed in a stiff sandy clay. The concrete has $f'_c = 4{,}000$ lb/in^2 and $\rho = 0.020$. The nominal side friction capacity ($\Sigma f_n A_s$) is 380 k and is uniformly distributed along the length of the shaft. The nominal toe bearing capacity ($q'_n A_t$) is 250 k. Using the Fleming (1992) method, compute the settlement when subjected to a design sustained service load of 205 k. The allowable settlement is 1.0 in.

Solution

$$E_c = 57{,}000\sqrt{f'_c}$$
$$= 57{,}000\sqrt{4{,}000}$$
$$= 3{,}600{,}000 \text{ lb/in}^2$$

$$E = E_c(1 - \rho) + E_s\rho$$
$$= 3{,}600{,}000(1 - 0.020) + 29{,}000{,}000(0.020)$$
$$= 4{,}100{,}000 \text{ lb/in}^2$$

$$\delta_s = \frac{M_s B \sum fA_s}{\sum f_n A_s - \sum fA_s}$$
$$= \frac{(0.002)(36)(205{,}000)}{380{,}000 - 205{,}000}$$
$$= 0.084 \text{ in}$$

$$\delta_e = \frac{4}{\pi}\frac{P(D - L_F + K_E L_F)}{B^2 E}$$
$$= \frac{4}{\pi}\frac{(205{,}000)[480 - 480 + (0.5)(480)]}{36^2(4{,}100{,}000)}$$
$$= 0.012 \text{ in}$$

$$\delta = \delta_s + \delta_t + \delta_e$$
$$= 0.084 + 0 + 0.012$$
$$= \mathbf{0.10 \text{ in} \ll 1.0 \text{ in}}$$

Commentary

1. The computed settlement is much less than the allowable settlement, so clearly the design is adequate. This is a case where a more detailed (and more precise) *t-z* analysis is not necessary.
2. The actual side friction capacity may be different from that used in the design, which is part of the reason the ULS analysis includes a large factor of safety. In this example, if the actual side friction capacity is only 60 percent of the expected capacity, then the computed settlement becomes 0.65 in. This is significantly greater than the expected settlement because of the hyperbolic shape of the load-settlement curve, and demonstrates how pile settlement analyses are much more sensitive to uncertainties in the capacity computations. Nevertheless, in this case the computed settlement is still less than the allowable settlement.

20.6 SETTLEMENT OF PILE GROUPS

The settlement behavior of pile groups can be significantly greater than that of individual foundations because the adjacent soil is influenced by more than one foundation and the corresponding strains and settlements are cumulative. Figure 20.5 shows the zone of significant stress influence of a single pile and contrasts it with that for a pile group. Static load tests on pile groups are rarely practical, so settlement analysis must be conducted using static methods.

A variety of static analysis methods are available (Poulos, 2006). The equivalent footing method is perhaps the most widely used, and appears to provide reasonable results.

Equivalent Footing Method

The *equivalent footing method* evaluates the settlement of a deep foundation group by replacing it with an imaginary equivalent footing at some depth, as shown in Figure 20.6. The pile group settlement is then computed as the settlement of this equivalent footing plus the elastic compression in the piles between the pile cap and the equivalent footing.

The location of this equivalent footing depends on the distribution of load between side friction and toe bearing, and on the soil profile. Figure 20.7 provides guidance (Cheney and Chassie, 2002; Brown et al., 2010). The load from this footing is assumed to be distributed to the underlying soils within idealized influence zone, as shown.

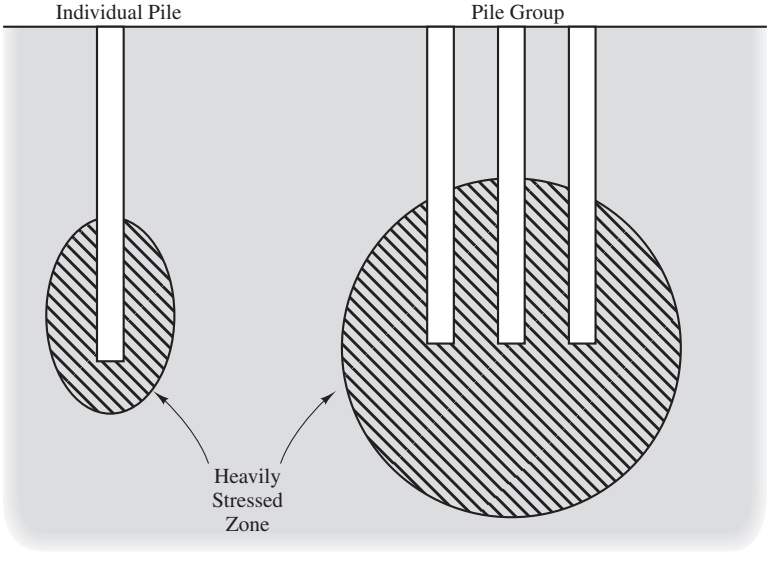

Figure 20.5 Zone of stress influence of individual pile compared to that for a pile group.

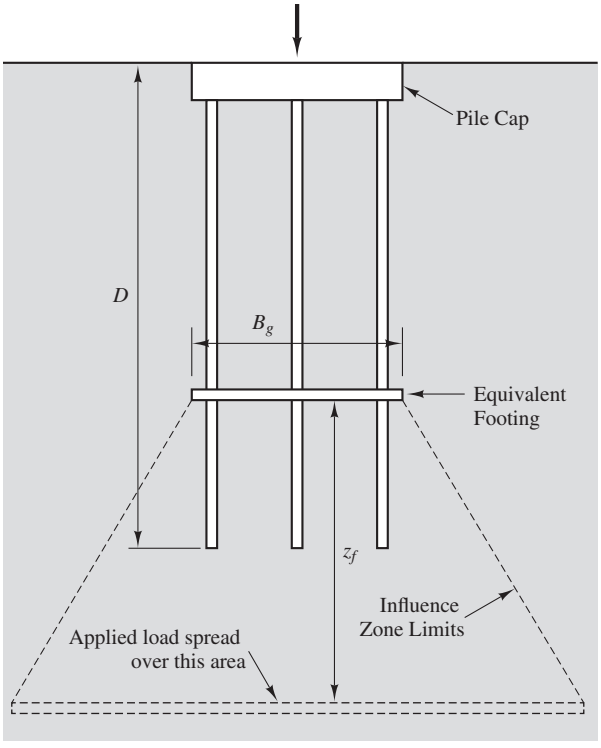

Figure 20.6 Equivalent footing method of computing pile group settlement.

The induced stresses at a given depth in the soil beneath the equivalent footing are computed by dividing the total applied load by the area of a horizontal rectangle created by the influence zone limits at that depth. Using these induced stresses, the settlement of the equivalent footing may be computed using methods similar to those for spread footings, as discussed in Chapter 8.

The elastic compression may be computed by assuming the applied load is divided equally among the piles in the group and applying Equation 20.8 to one pile.

Example 20.3

A 4 × 4 group of 16 in diameter drilled displacement piles are to be constructed in the soil profile shown in Figure 20.8. These piles will be placed 48 in on center and the pile cap will be 12 × 12 × 4 ft. The downward service load to this pile group is 2,100 k. Compute the settlement under this load.

Solution

Use the equivalent footing shown in Figure 20.7b and compute the settlement using the constrained modulus as described in Chapter 8.

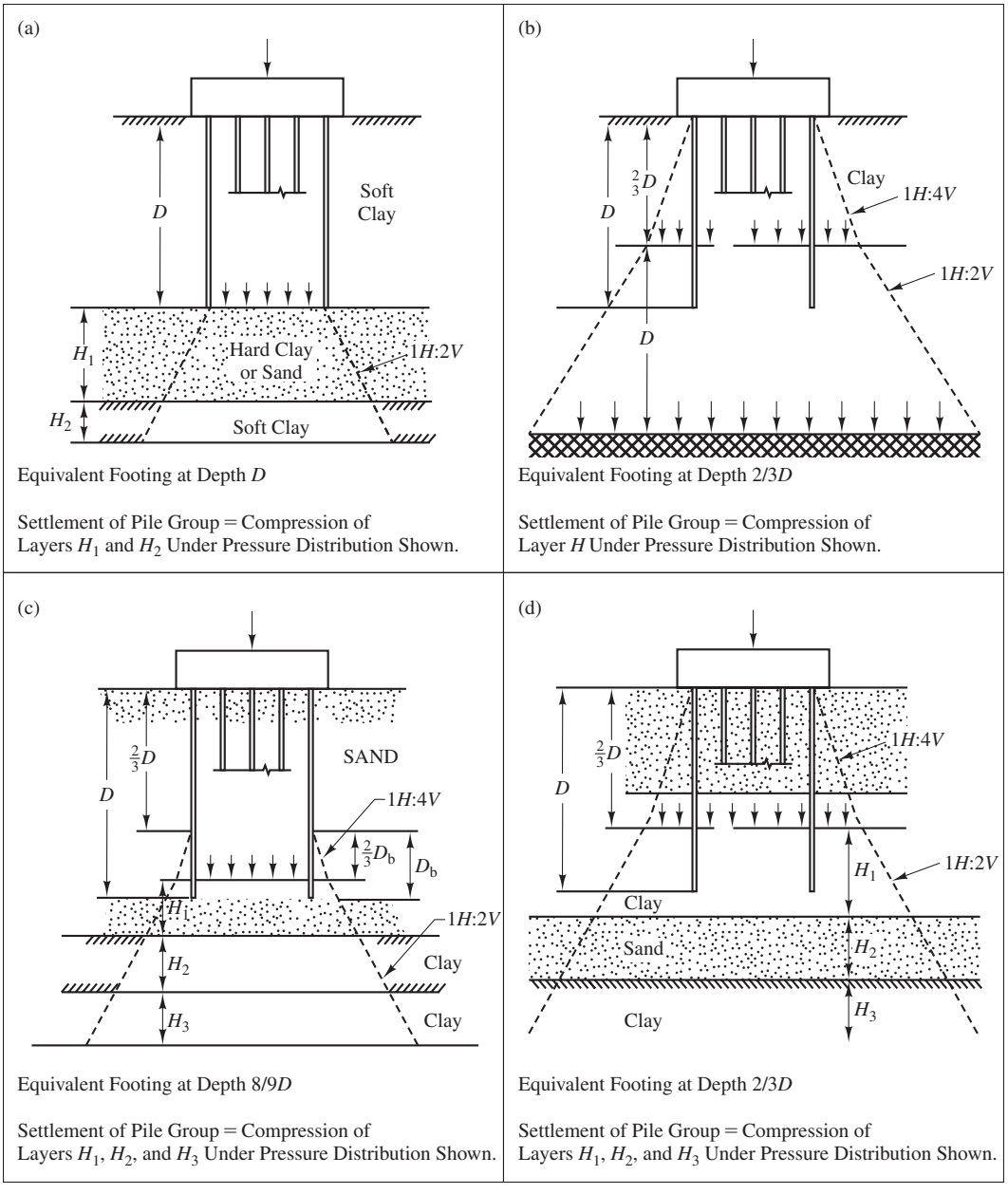

Equivalent Footing at Depth D

Settlement of Pile Group = Compression of Layers H_1 and H_2 Under Pressure Distribution Shown.

Equivalent Footing at Depth $2/3D$

Settlement of Pile Group = Compression of Layer H Under Pressure Distribution Shown.

Equivalent Footing at Depth $8/9D$

Settlement of Pile Group = Compression of Layers H_1, H_2, and H_3 Under Pressure Distribution Shown.

Equivalent Footing at Depth $2/3D$

Settlement of Pile Group = Compression of Layers H_1, H_2, and H_3 Under Pressure Distribution Shown.

Figure 20.7 Placement of equivalent footing for various soil conditions (compiled from Cheney and Chassie, 2002; Brown et al., 2010).

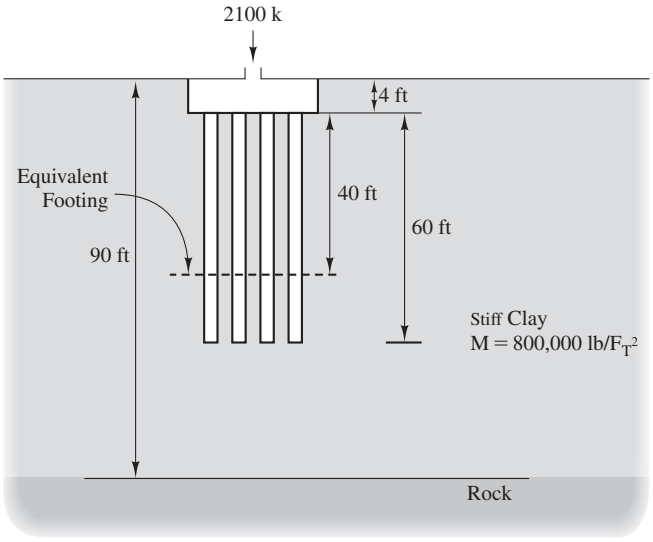

Figure 20.8 Soil profile for Example 20.3.

$$\Delta\sigma_z = \frac{P_g + W_{\text{cap}}}{A}$$

$$= \frac{2{,}100{,}000 + (12)(12)(4)(150)}{[(3)(3) + 40/2 + z_f]^2}$$

$$= \frac{2{,}186{,}000}{[29 + z_f]^2}$$

Layer	Depth (ft)	H (ft)	Z_f (ft)	$\Delta\sigma_z$ (lb/ft^2)	δ (in)
1	44–54	10	5.0	1,891	0.28
2	54–69	15	17.5	1,011	0.23
3	69–90	21	35.5	525	0.17
				Total	0.68

The elastic compression in the upper 40 ft also could be added to this computed settlement.

Numerical Analyses

Another alternative would be to evaluate the settlement of pile groups using numerical analyses, such as a three-dimensional finite element analysis. Both the piles and the surrounding soils would need to be modeled. Although such analyses are not often used for this purpose, they certainly are feasible.

Charity Hospital

Charity Hospital, which was constructed in New Orleans in 1938, illustrates the difference between settlement of an individual pile and settlement of a pile group (Terzaghi, 1939; Skempton, 1955; Terzaghi et al., 1996; Held, 2004). The hospital consisted of multiple wings ranging from 13 to 21-stories, connected by 3 to 5-story sections, and the entire structure was supported on over 9,700 timber piles.

Prior to construction, five exploratory borings were drilled, ten test piles were driven, and two static load tests were conducted. Based on this test program, the production piles were driven to a dense sand layer located at a depth of about 13 m (42 ft) below the ground surface. The load tests produced a settlement of only 6 mm (0.25 in) under a load equal to twice the allowable load, and the geotechnical factor of safety was 4. This appeared to be a conservative design, so very little settlement was expected under the working loads.

Unfortunately, by the end of construction, 150 mm (6 in) of settlement had occurred in the 21-story section, and one year later the settlement had increased to 225 mm (9 in). The State of Louisiana then retained Karl Terzaghi to determine the cause and consequences of this excessive settlement, and Hardy Cross to evaluate the structure. Additional borings were drilled, soil samples obtained, and consolidation tests performed. The soil profile, shown in Figure 20.9, indicated the dense sand layer was underlain by multiple soft clay strata, which gave Terzaghi an opportunity to test his theory of consolidation on a real project. According to his analyses, the induced stresses in the soft clay resulting from the combined effects of the piles would

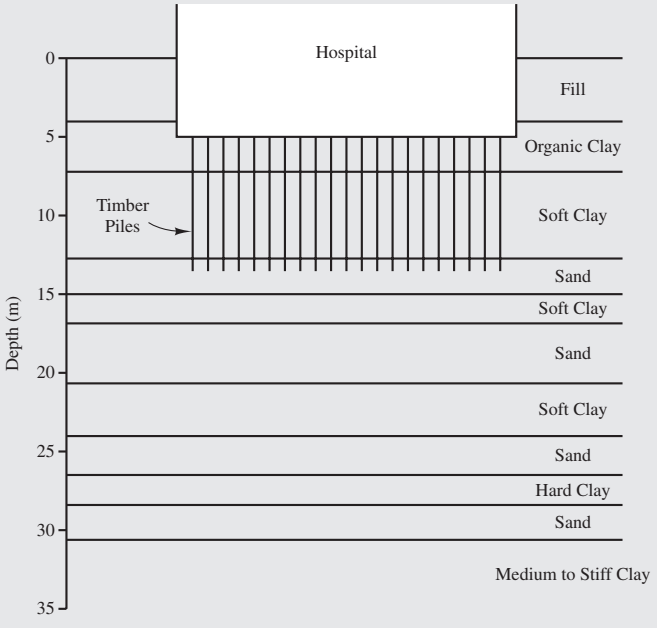

Figure 20.9 Soil profile beneath Charity Hospital (compiled from Terzaghi, 1939 and Skempton, 1955).

eventually produce a settlement of 495 mm (19.5 in). By 1940, two years after completion of construction, the 21-story part had settled 350 mm (14 in), while the lightly loaded portions of the building had settled 120 mm (5 in).

This case demonstrates how the zone of stress influence beneath the pile group extended much deeper than that for an individual pile, thus engaging the soft clay layer and causing settlements much greater than those observed in the static load tests. It also was an early affirmation of Terzaghi's theory of consolidation. Terzaghi believed the reason for the excessive settlement was not something the design engineer should have reasonably anticipated given the state of practice in the 1930s, so he did not find the design engineer at fault. However, the state was looking for somebody to sue, and Terzaghi's report did not help them in that regard, so they never paid his invoice.

Based on the lessons learned from this project, the nearby Veterans Hospital was constructed in 1951 on piles that extended through the soft clay strata down to the sand layer at a depth of about 29 m (95 ft) and has performed well. The foundation consultant on this project was Terzaghi's student, Arthur Casagrande.

20.7 EQUIVALENT SPRING MODEL

Structural engineers sometimes wish to model the interaction between a structure and its foundations by replacing each foundation with an equivalent spring. Such models may be used for the entire structure, where each structural element is supported on one of these equivalent springs, thus providing a better representation of the expected settlements and differential settlements. A similar analysis could be conducted to design the cap for a pile group, where each pile in the group is represented by an individual equivalent spring. The stiffness of these equivalent springs may be determined using the techniques described in this chapter. The resulting spring may be described as having either linear or non-linear load-deformation properties.

20.8 OTHER SOURCES OF SETTLEMENT

Structures supported on pile foundations also can be subject to other sources of settlement. Perhaps the most noteworthy of these sources is downdrag, which is discussed in Section 23.1. Other sources include settlement due to physical processes other than induced stresses from the structural loads. Examples include seismically induced settlements, secondary compression settlement, lowering of the groundwater table, and others. Some of these processes may be evaluated using the equivalent footing method.

20.9 OTHER SERVICEABILTY CONSIDERATIONS

In addition to satisfying allowable settlement requirements, piles also must not experience excessive lateral deflection. Methods for evaluating lateral deflection are discussed in Chapter 22.

Durability also is an important serviceability concern, as discussed in Section 5.3. Timber piles can be subjected to insect attack and rotting, steel piles and steel reinforcement can corrode, and concrete piles can be subjected to sulfate attack. These processes can be especially problematic for marine structures where the piles are exposed to sea water, but rarely cause problems for onshore structures.

SUMMARY

Major Points

1. Many axially loaded pile designs are controlled by the ultimate limit state (ULS), and can be assumed to have settlement less than the allowable settlement. However, in some cases an explicit settlement analysis is necessary, and might control the design.
2. The settlement analysis may be conducted using either the unfactored load from an ASD ultimate limit state analysis, or the sustained service load.
3. The most direct way to determine the load-settlement relationship is to conduct a load test.
4. Static analysis methods are another way to determine the load-settlement relationship. The *t-z* method is the most common technique.
5. Side friction resistance is mobilized much sooner than toe bearing resistance.
6. Elastic compression can be a significant component, especially in long piles.

Vocabulary

Equivalent footing Sustained service load *t-z* method

QUESTIONS AND PRACTICE PROBLEMS

20.1 A 16 in diameter, 75 ft long drilled displacement pile is made of grout with $f'_c = 5{,}000$ lb/in^2. A steel ratio of 0.04 is to be used in the upper 30 ft, and a steel ratio of 0.001 for the remainder of the pile. Compute the modulus of elasticity for the upper and lower portions of this pile.

20.2 The axial compressive load in the pile described in Problem 20.1 is 200 k at the top of the pile and varies linearly to 20 k at the bottom of the pile. Compute the settlement at the top due to elastic compression.

20.3 In Example 20.1, the load-settlement curve for side friction is much steeper than that for toe bearing. Is this to be expected? Explain.

20.4 An HP14 $\times$ 102 pile is to be driven to a depth of 48 ft in a stiff clay having $E_T = 1800$ k/ft^2. The side friction capacity, $\Sigma f_n A_s$, is 320 k and the toe bearing capacity, $q'_n A_t$, is 110 k. The expected service load will be 142 k. Using the Fleming simplified method, compute the expected settlement. See Table 21.1 for pile section properties. Assume f_n is constant along the length of the pile.

20.5 Using the pile described in Problem 20.4 and a spreadsheet, develop a plot of settlement versus applied load. Consider loads from 0 to 280 k.

20.6 A 300 mm diameter steel pipe pile with 10 mm wall thickness is to be driven to a depth of 15 m in a stiff clay having $E_T = 100$ MPa. The side friction capacity, $\Sigma f_n A_s$, is 750 kN and the toe bearing capacity, $q'_n A_t$, is 210 kN. The expected service load will be 310 kN. Using the Fleming simplified method, compute the expected settlement. Assume f_n is constant along the length of the pile.

20.7 Using the pile described in Problem 20.6 and a spreadsheet, develop a plot of settlement versus applied load. Consider loads from 0 to 600 kN.

20.8 A group of 25 prestressed concrete piles is arranged in a 5 × 5 grid. Each pile has a 12 × 12 in cross-section and is 63 ft long. The piles are placed 30 in on center, and a 4 ft thick pile cap connects these piles. The soil profile consists of a silty sand to a depth of 85 ft, underlain by very dense sands and gravels. The silty sand has a constrained modulus of 1,200,000 lb/ft^2. Develop a plot of load versus settlement for this pile group. Consider loads from 0 to that load which produces 2 in of settlement. Ignore the contribution of elastic compression.

21

Piles—Structural Design

Amsterdam, die oude Stadt, is gebouwed op palen
Als die stad eens ommevelt, wie zal dat betalen?

An old Dutch nursery rhyme that translates to:

The old town of Amsterdam is built on piles
If it should fall down, who would pay for it?

Chapters 13 to 20 addressed the design of axially loaded piles from a geotechnical perspective and focused on the transfer of applied axial loads from the pile through side friction and toe bearing into the ground. In addition to satisfying these geotechnical ultimate limit state (ULS) and serviceability limit state (SLS) requirements, the cross-sectional area of each pile also must be large enough and the structural materials strong enough to satisfy the structural ULS requirements. In other words, the pile must have sufficient structural integrity, which is the subject of this chapter.

If applied lateral loads are present (i.e., moment or shear loads imparted from the structure into the foundation), then flexural stresses also will be present and the pile must have sufficient flexural capacity and flexural stiffness. Chapter 22 uses the structural information from this chapter to address the response of piles to lateral loads.

Structural design codes include many requirements, both for the overall design and for various details. This chapter provides an overview of key issues, especially the differences between pile design and superstructure design, but is not a comprehensive discussion. The relevant codes should be consulted to obtain additional information needed for a complete structural design.

In some cases, such as with drilled shaft foundations, the structural engineer of record is responsible for the structural design of piles. However, in other cases standard

designs are typically selected, such as with prestressed driven piles. These standardized designs are often developed by the pile manufacturer.

21.1 DESIGN PHILOSOPHY

The structural design of piles is similar to that for the superstructure, but there also are important differences. Therefore, codes present structural design requirements specifically for piles, and these requirements sometimes differ from those for comparable members in the superstructure. The technical literature on structural design of piles is not nearly as extensive as that for the geotechnical design, and code requirements are sometimes incomplete or contradictory. Nevertheless, customary practices for the structural design of piles appear to be generally conservative, and structural failure of piles, apart from those founded in geotechnical or construction problems, are rare.

Buckling

Even the softest soils provide enough lateral support to prevent underground buckling in piles subject only to axial loads, especially when a cap is present and provides rotational fixity to the top of the pile. To test this principle, several load tests were conducted on steel H-piles, including one installed in soils so soft that the pile penetrated them without any hammer blows (i.e., it sank under its own weight). None of these piles buckled (Bethlehem Steel Corp., 1979).

Slender piles subjected to both axial and lateral loads might have problems with underground buckling if the upper soils are very soft. Buckling also might be a concern when the upper soils are subject to scour or liquefaction. In such cases, buckling should be checked using a *p-y* analysis, as described in Chapter 22. If underground buckling proves to be a problem, it normally is resolved using a cross-section with a greater flexural rigidity, *EI*.

Above-ground buckling might be a problem in piles that extend above the ground surface, such as those for railroad trestles, or those driven through bodies of water. In these cases, the above-ground portion must be checked using standard structural analysis methods, and should be braced if necessary.

Buckling is a greater concern during pile driving (Fleming et al., 1985), especially in long, slender piles driven through water. Contractors can handle these cases by limiting the hammer size, using lower power settings during the initial stages of driving (which can be done with hydraulic hammers), or by providing temporary lateral support.

Comparison with Superstructure Design

Because piles are designed so that underground buckling is not a concern, the structural design is similar to that for short beam-columns in the superstructure. However, there are some important differences:

- The construction tolerances for piles are much wider and quality control is more difficult.

- Piles are often constructed slightly off their planned location, which introduces unplanned eccentricities in the applied load.
- In the case of driven piles, the driving stresses might be greater than those imparted by the design loads, and thus might control the structural design.
- Piles can be damaged during driving, so the as-built capacity may be less than anticipated.
- Residual stresses may be locked into piles during driving, so the actual stresses in the piles after the structure is completed may be greater than those generated by the applied structural loads.
- Concrete in drilled shafts, auger piles, and other cast-in-place foundations is not placed under ideal conditions, and thus may experience segregation of the aggregates, contamination from the soil, and other problems.

Therefore, we use more conservative structural design criteria for piles, which implicitly accounts for these and other factors. This extra conservatism primarily appears in the form of lower allowable stresses and conservative simplifications in the analysis methods.

However, sometimes the allowable stresses permitted by codes are lower than necessary. This is because some of these design values are an indirect way of keeping driving stresses within tolerable limits. In other words, piles designed using these low allowable stresses have a larger cross section, and thus have correspondingly smaller driving stresses. However, this roundabout way of limiting driving stresses is not necessary when driving stresses are evaluated using wave equation analyses, as discussed in Chapter 19. Therefore, some codes allow higher, and more reasonable, design stresses when a wave equation analysis is performed.

21.2 DESIGN CRITERIA

The structural design of piles may be based either on allowable stress design (ASD) or load and resistance factor design (LRFD), as permitted by the applicable code. The International Building Code (ICC, 2012) defines allowable stresses in piles in terms of ASD, even when the superstructure is designed using LRFD (although some LRFD provisions may apply). The American Association of State Highway and Transportation Officials (AASHTO) bridge code (AASHTO, 2012) uses LRFD.

ASD

For steel and timber piles subject only to axial compressive loading, the allowable compressive load is:

$$P_a = f_a A \tag{21.1}$$

and the design must stratify the following criterion:

$$P \leq P_a \tag{21.2}$$

When flexural stresses also are present, the design must satisfy an interaction criterion, such as:

$$\frac{P}{f_a A} \pm \frac{M}{f_b S} \leq 1 \tag{21.3}$$

where

P = compressive demand
M = moment demand
P_a = allowable compressive capacity
f_a = allowable compressive stress due to axial load
f_b = allowable flexural stress
A = cross-sectional area
S = elastic section modulus

Note that Equation 21.3 demonstrates how the axial load capacity of a pile is reduced when flexural stresses are added. Specific codes often have more detailed interaction criteria intended for specific structural materials.

For piles subject to axial tension loading with or without flexural loading, substitute P_{up} into Equations 21.1 to 21.3, and use the tensile values of f_a and f_b.

Because this is an ASD analysis, the values of P and M should be based on the unfactored loads computed using Equations 5.4 to 5.12, or from similar equations presented in the governing code. The value of P or P_{up} becomes smaller with depth as some of the axial load shifts to the soil through side friction. However, for simplicity, structural engineers usually neglect any load transfer due to side friction and use the P or P_{up} applied by the structure at the top of the pile (except if downdrag loads are present, as discussed in Section 23.1). The value of M can increase or decrease with depth and can be obtained by developing a moment diagram, or by determining the maximum moment, as described in Chapter 22.

Moments of inertia and section moduli for steel H-piles and common steel pipe piles are tabulated in Tables 21.1 and 21.2. For foundations with solid circular cross-sections of diameter B, such as timber piles, use:

$$I = \frac{\pi B^4}{64} \tag{21.4}$$

$$S = \frac{2I}{B} = \frac{\pi B^3}{32} \tag{21.5}$$

For square cross-sections with side width B, use:

$$I = \frac{B^4}{12} \tag{21.6}$$

$$S = \frac{2I}{B} = \frac{B^3}{6} \tag{21.7}$$

TABLE 21.1 STANDARD STEEL H-PILE SECTIONS USED IN NORTH AMERICA

Section[1]	Weight	Cross-Section Area	Depth	Width	Flexural Properties on Strong Axis			Flexural Properties on Weak Axis			ASD Allowable Axial Load[2]
	W	A	d	b_f	I_x	Z_x	S_x	I_y	Z_y	S_y	F_aA
English	(lb/ft)	(in^2)	(in)	(in)	(in^4)	(in^3)	(in^3)	(in^4)	(in^3)	(in^3)	(k)
Metric	(kg/m)	(mm^2)	(mm)	(mm)	($mm^4/10^6$)	($mm^3/10^3$)	($mm^3/10^3$)	($mm^4/10^6$)	($mm^3/10^3$)	($mm^3/10^3$)	(kN)
HP8 × 36	36.0	10.6	8.02	8.16	119	33.6	29.8	40.3	15.2	9.88	265
HP200 × 53	53.0	6,840	204	207	49.5	551	488	85.3	16.8	249	1,214
HP10 × 42	42.0	12.4	9.70	10.1	210	48.3	43.4	71.7	21.8	14.2	310
HP250 × 62	62.0	8,000	246	257	87.4	791	711	105	29.8	357	1,420
HP10 × 57	57.0	16.7	9.99	10.2	294	66.5	58.8	101	30.3	19.7	418
HP250 × 85	85.0	10,800	254	259	122	1,090	964	106	42.0	497	1,917
HP12 × 53	53.0	15.5	11.8	12.0	393	74.0	66.7	127	32.2	21.1	388
HP310 × 79	79.0	10,000	300	305	164	1,210	1,090	128	52.9	528	1,775
HP12 × 63	63.0	18.4	11.9	12.1	472	88.3	79.1	153	38.7	25.3	460
HP310 × 93	93.0	11,900	302	307	196	1,450	1,300	129	63.7	634	2,112
HP12 × 74	74.0	21.8	12.1	12.2	569	105	93.8	186	46.6	30.4	545
HP310 × 110	110	14,100	307	310	237	1,720	1,540	130	77.4	764	2,503
HP12 × 84	84.0	24.6	12.3	12.3	650	120	106	213	53.2	34.6	615
HP310 × 125	125	15,900	312	312	271	1,970	1,740	131	88.7	872	2,822
HP14 × 73	73.0	21.4	13.6	14.6	729	118	107	261	54.6	35.8	535
HP360 × 108	108	13,800	345	371	303	1,930	1,750	148	109	895	2,450
HP14 × 89	89.0	26.1	13.8	14.7	904	146	131	326	67.7	44.3	653
HP360 × 132	132	16,800	351	373	376	2,390	2,150	149	136	1,110	2,982
HP14 × 102	102	30.1	14.0	14.8	1,050	169	150	380	78.8	51.4	753
HP360 × 152	152	19,400	356	376	437	2,770	2,460	150	158	1,290	3,444
HP14 × 117	117	34.4	14.2	14.9	1,220	194	172	443	91.4	59.5	860
HP360 × 174	174	22,200	361	378	508	3,180	2,820	151	184	1,500	3,941

(*continued*)

TABLE 21.1 (Continued)

Section[1]	Weight	Cross-Section Area	Depth	Width	Flexural Properties on Strong Axis			Flexural Properties on Weak Axis			ASD Allowable Axial Load[2]
	W	A	d	b_f	I_x	Z_x	S_x	I_y	Z_y	S_y	F_aA
English	(lb/ft)	(in^2)	(in)	(in)	(in^4)	(in^3)	(in^3)	(in^4)	(in^3)	(in^3)	(k)
Metric	(kg/m)	(mm^2)	(mm)	(mm)	($mm^4/10^6$)	($mm^3/10^3$)	($mm^3/10^3$)	($mm^4/10^6$)	($mm^3/10^3$)	($mm^3/10^3$)	(kN)
HP16 × 88	88.0	25.8	15.3	15.7	1,110	161	145	349	68.2	44.5	645
HP410 × 131	131	16,600	389	398.78	462	2,640	2,380	167	145	1,120	2,947
HP16 × 101	101	29.9	15.5	15.8	1,300	187	168	412	80.1	52.2	748
HP410 × 151	151	19,300	394	401.32	541	3,060	2,750	167	171	1,310	3,426
HP16 × 121	121	35.8	15.8	15.9	1,590	226	201	504	97.6	63.4	895
HP410 × 181	181	23,100	401	403.86	662	3,700	3,290	169	210	1,600	4,100
HP16 × 141	141	41.7	16.0	16.0	1,870	264	234	599	116	74.9	1,043
HP410 × 211	211	26,900	406	406.4	778	4,330	3,830	170	249	1,900	4,775
HP16 × 162	162	47.7	16.3	16.1	2,190	306	269	697	134	86.6	1,193
HP410 × 242	242	30,800	414	408.94	912	5,010	4,410	172	290	2,200	5,467
HP16 × 183	183	54.1	16.5	16.3	2,510	349	304	818	156	100.0	1,353
HP410 × 272	272	34,900	419	414	1,040	5,720	4,980	173	340	2,560	6,195
HP18 × 135	135	39.9	17.5	17.8	2,200	281	251	706	122	79.3	998
HP460 × 202	202	25,700	445	452.12	916	4,600	4,110	189	294	2,000	4,562
HP18 × 157	157	46.2	17.7	17.9	2,570	327	290	833	143	93.1	1,155
HP460 × 234	234	29,800	451	454.66	1,070	5,360	4,750	189	347	2,340	5,290
HP18 × 181	181	53.2	18.0	18.0	3,020	379	336	974	167	108	1,330
HP460 × 269	269	34,300	457	457.2	1,260	6,210	5,510	191	405	2,740	6,088
HP18 × 204	204	60.2	18.3	18.1	3,480	433	380	1,120	191	124	1,505
HP460 × 304	304	38,800	465	459.74	1,450	7,100	6,230	193	466	3,130	6,887

[1] English and metric sections are physically identical.
[2] The allowable axial load is based on 0.5 F_y with F_y = 50 k/in^2 or 355 MPa and is based on no flexural stresses being present.

TABLE 21.2 COMMON STEEL PIPE PILE SECTIONS USED IN NORTH AMERICA

Nominal Pipe Size[1] (in)	Outside Diameter	Wall Thickness		Weight		Moment of Inertia I		Elastic Section Modulus S		ASD Allowable Axial Load[2] F_aA	
		(in)	(mm)	(lb/ft)	(kN/m)	(in^4)	(mm^4) × 10^6	(in^3)	(mm^3) × 10^4	(k)	(kN)
10	10.75 in 273 mm	0.250	6	28.1	0.410	114	47	21.2	35	206	917
		0.375	10	41.6	0.607	165	69	30.6	50	306	1,359
		0.500	13	54.8	0.800	212	88	39.4	65	403	1,790
12	12.75 in 324 mm	0.250	6	33.4	0.488	192	80	30.1	49	245	1,092
		0.375	10	49.6	0.724	279	116	43.8	72	364	1,621
		0.500	13	65.5	0.956	362	150	56.7	93	481	2,140
		0.625	16	81.0	1.182	439	183	68.8	113	595	2,647
14	14.00 in 356 mm	0.250	6	36.7	0.536	255	106	36.5	60	270	1,201
		0.375	10	54.6	0.797	373	155	53.3	87	401	1,785
		0.500	13	72.2	1.053	484	201	69.1	113	530	2,358
		0.625	16	89.4	1.304	589	245	84.1	138	657	2,920
16	16.00 in 406 mm	0.250	6	42.1	0.614	384	160	48.0	79	309	1,376
		0.375	10	62.6	0.914	562	234	70.3	115	460	2,047
		0.500	13	82.8	1.209	732	305	91.5	150	609	2,707
		0.625	16	102.7	1.499	894	372	111.7	183	755	3,357
18	18.00 in 457 mm	0.250	6	47.4	0.692	549	229	61.0	100	349	1,550
		0.375	10	70.7	1.031	807	336	89.6	147	519	2,309
		0.500	13	93.5	1.365	1,053	438	117.0	192	687	3,057
		0.625	16	116.1	1.694	1,289	537	143.2	235	853	3,794
20	20.00 in 508 mm	0.375	10	78.7	1.148	1,113	463	111.3	182	578	2,571
		0.500	13	104.2	1.521	1,457	606	145.7	239	766	3,406
		0.625	16	129.5	1.889	1,787	744	178.7	293	951	4,230
24	24.00 in 610 mm	0.375	10	94.7	1.382	1,942	808	161.9	265	696	3,095
		0.500	13	125.6	1.833	2,549	1,061	212.4	348	923	4,105
		0.625	16	156.2	2.279	3,137	1,306	261.4	428	1,147	5,104
		0.750	19	186.4	2.720	3,705	1,542	308.8	506	1,370	6,092

[1] English and metric sections are physically identical.

[2] The allowable axial load is based on 0.5 F_y with $F_y = 50$ k/in^2 or 355 MPa and is based on no flexural stresses being present.

These formulations become more complex when the pile is made of composite materials, such as concrete-filled steel pipe or reinforced concrete. These cases are discussed later in this chapter.

For analysis purposes, neglect any interaction between the shear loads and the axial or moment loads. For an ASD analysis, the shear force, V, must not exceed the allowable shear force, V_a:

$$V_a = f_v A \tag{21.8}$$

$$V \leq V_a \tag{21.9}$$

where

f_v = allowable shear stress

The shear force, V, is greatest at the top of the pile, and varies with depth as determined from a shear diagram.

LRFD

When using LRFD, the structural ULS requirement for piles subject only to axial compression or axial tension is:

$$P_u \leq \phi P_n \tag{21.10}$$

where

P_u = factored demand (see Section 5.2)
ϕ = resistance factor
P_n = nominal load capacity

For shear, V, and moment, M:

$$V_u \leq \phi V_n \tag{21.11}$$

$$M_u \leq \phi M_n \tag{21.12}$$

Methods for determining P_n, M_n, and V_n, and the interaction between axial and flexural loads depend on the structural material and on the governing code. As with ASD, Equations 21.10 to 21.12 must be satisfied across the entire length of the pile.

21.3 DRIVEN PILES

The structural design of driven piles must consider each of the following loading conditions:

- ***Handling loads*** are those imposed on the pile between the time it is fabricated and the time it is in the pile driver leads and ready to be driven. These loads are

generated by cranes, forklifts, and other construction equipment. The most critical handling loads often occur when the pile is suspended in a nearly horizontal position, as shown in Figure 21.1. The weight of the pile in this configuration can produce flexural stresses large enough to cause a flexural failure, especially in concrete piles. PCI (2004) and others recommend computing handling stress based on the weight of the pile plus an additional 50 percent for inertial and impact effects. The pile designer must accommodate these handling loads by specifying optimal pickup points along the length of the pile, as shown in Figure 21.2. Typically this is considered at the shop drawing phase, not by the structural engineer of record.

- ***Driving loads*** are produced by the pile hammer during driving. Timber and concrete piles are especially prone to damage from driving loads, but steel piles also have been damaged as shown in Figure 19.4. Driving stresses are primarily compressive, but significant tensile stresses can develop in some circumstances. Use a wave equation analysis, as discussed in Chapter 19, to predict these driving stresses, and thus guide the selection of an appropriate hammer and pile driving appurtenances.
- ***Design loads*** are the loads from the completed structure, which may be expressed in terms of either ASD or LRFD. Most of the design effort focuses on resisting these loads.

Figure 21.1 This prestressed concrete pile is being lifted into the pile leads by a single cable. This process induces handling stresses in the pile.

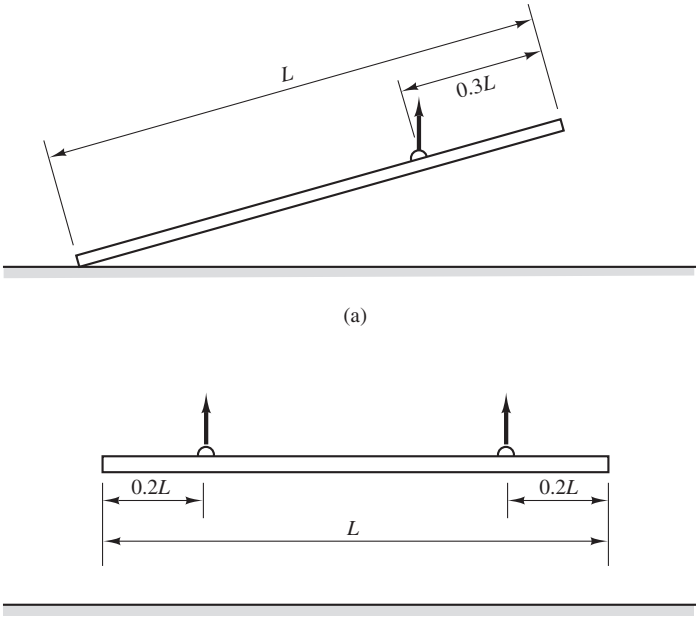

Figure 21.2 Using specified pickup points to keep handling stresses within tolerable limits: (a) single-point pickup; (b) double-point pickup.

Timber Piles

ASTM D25 specifies minimum dimensions for timber piles. However, the available sizes in a particular region depend on the height and species of trees available locally. Typically timber piles have a head diameter of 200 to 450 mm (8−18 in) and a toe diameter of 125 to 250 mm (5−10 in). The length of timber piles is limited by the height of trees, and is typically 6 to 20 m (20−60 ft).

Because wood is a natural material, not a manufactured product, it is difficult to assign allowable design stresses. Design criteria for wood piles must consider many factors, including the following:

- The species of tree
- The quality of the wood (i.e., knots, straightness, etc.)
- The moisture content of the wood
- The extent of any damage incurred during driving
- The type and method of treatment (normally reduces strength)
- The number of piles in a pile group (redundancy if one pile is weak)

Table 21.3 presents allowable design stresses for timber piles commonly used in North America. These values should be adequate for most conditions, but lower values may be appropriate when difficult driving conditions might damage the pile (Armstrong, 1978;

TABLE 21.3 ALLOWABLE STRESS VALUES FOR TRATED ROUND TIMBER PILES GRADED IN ACCORDANCE WITH ASTM D25 (adapted from AWPI, 2002)

		Allowable Stress				
Species	Units	Axial Compression, f_a	Bending, f_b	Shear Perpendicular to Grain, f_v	Compression Perpendicular to Grain, $f_{c\perp}$	Modulus of Elasticity, E
Southern Pine[1]	MPa	8.28	16.55	0.76	1.72	10,300
	lb/in^2	1,200	2,400	110	250	1,500,000
Douglas Fir[2]	MPa	8.62	16.90	0.79	1.59	10,300
	lb/in^2	1,250	2,450	115	230	1,500,000
Lodgepole Pine	MPa	7.93	11.72	0.55	1.86	6,900
	lb/in^2	1,150	1,700	80	270	1,000,000
Red Oak[3]	MPa	7.59	16.90	0.93	2.41	8,600
	lb/in^2	1,100	2,450	135	350	1,250,000
Red Pine[4]	MPa	6.21	13.10	0.59	1.07	8,800
	lb/in^2	900	1,900	85	155	1,280,000

[1] Southern Pine design values apply to Loblolly, Longleaf, Shortleaf, and Slash Pines.
[2] Pacific Coast Douglas Fir design values apply to this species as defined in ASTM D 1760.
[3] Red Oak design values apply to Northern and Southern Red Oak.
[4] Red Pine design values apply to Red Pine grown in the United States.

Davisson, 1989; Graham, 1985). Axial compression values as low as 4.8 MPa (700 lb/in^2) have been suggested for such conditions.

AASHTO provides similar design criteria for timber piles in an LRFD context [AASHTO 8.4.1.4].

Timber piles are generally not subject to structural damage during handling, but the contractor must avoid large abrasions that might remove the preservative treatment and expose untreated wood. However, these piles can easily be damaged during driving, as described in Chapter 12. Allowable driving stresses for timber piles, presented in Table 19.7, exceed the static allowable stress, f_a, shown in Table 21.3. However these stresses are still quite low. Therefore, timber piles should only be driven with lightweight hammers.

Steel Piles

Standard H-pile sections (also known as an HP section) are listed in Table 21.1. Pipe piles are available in a wide variety of diameters and wall thicknesses; some of the more common sizes are listed in Table 21.2 (see manufacturer's websites for additional sizes). Unlike WF sections, which have been optimized for flexure, the cross-section of H sections has been optimized for axial loading.

Steel pipe piles have a constant moment of inertia, I, and section modulus, S, regardless of the direction of the lateral load, whereas I and S for H-piles depend on the direction of the load relative to the web. If the design engineer does not specify the as-built web orientation, then the I and S of the weak (Y-Y) axis of H2-piles must be used. However, if the orientation is specified, on the design drawings, then the stiffer X-X axis properties may be used.

For many years, steel piles were commonly made of ASTM A36 steel, which has a yield strength, f_y, of 250 MPa (36,000 lb/in^2). However, the vast majority steel piles are now made of steel conforming to ASTM A572 Grade 50 (the most common type), ASTM A690, or similar specifications, which has $f_y = 345$ MPa (50 k/in^2) and steel H sections are now available only in this grade. Pipe piles made of higher strength steel, with $f_y = 420$ MPa (60 k/in^2) also are available. The notation F_y is often used to signify the yield strength of structural steel, and f_y for steel rebars, but we will use f_y throughout for consistency with the remainder of this chapter.

The maximum allowable driving stress for steel piles, in both tension and compression, is nearly equal to their yield strength, f_y, as shown in Table 19.7. Therefore, steel piles are among the most durable driven piles.

Because of their high strength and ductility, and high strength/weight ratio, steel piles are normally not subject to damage during handling. Thus, so long as normal care is exercised during construction, there normally is no need to check handling stresses.

When using ASD with the IBC design requirements, the tensile and compressive stresses in steel piles under design loads, f_a, is 0.35 f_y, not to exceed 110 MPa (16 k/in^2) [IBC 1810.3.2.6]. However, if accompanied by a geotechnical investigation and a static load test, f_a is increased to 0.50 f_y, not to exceed 220 MPa (32 k/in^2) [IBC 1810.3.2.8], which is still less than the $0.60f_y$ to $0.66f_y$ permitted in the superstructure, and reflects the conservatism described earlier. A wave equation analysis is especially prudent when using this higher allowable stress, and is required when the specified allowable load is greater than 356 kN (80 k) [IBC 1810.3.3.1.1]. In addition, this higher value should be used only at sites where the pile will drive straight and not be deflected by boulders or other obstructions. The allowable stress due to bending, f_b, may be set equal to f_a.

Structural engineers use an allowable shear stress of $f_v = 0.40f_y$ in the superstructure. The greatest shear stress in piles occurs at the top, so the differences between the pile and the superstructure listed earlier are not as significant. Therefore, we may use the same allowable shear stress for piles. However, because of the orientation of the steel with the direction of loading, do not use the entire cross-sectional area for shear resistance. For H-piles, use only the area of the web; for pipe piles, use half of the total cross-sectional area.

For LRFD, P_n, M_n, and V_n are the same as for members of the same material in the superstructure. However, the resistance factors are lower, to reflect a more conservative design. The AASHTO resistance factors for steel piles are [AASHTO 6.5.4.2]:

> For axial resistance of piles in compression and subject to damage due to severe driving conditions where the use of a pile tip is necessary:
> - H piles: $\phi = 0.50$
> - Pipe piles: $\phi = 0.60$

For axial resistance of piles in compression under good driving conditions where the use of a pile tip is not necessary:

- H piles: $\phi = 0.60$
- Pipe piles: $\phi = 0.70$

For combined axial and flexural resistance of undamaged piles:

- Axial capacity of H piles: $\phi = 0.70$
- Axial capacity of pipe piles: $\phi = 0.80$
- Flexural capacity: $\phi = 1.00$

Example 21.1

A 12.75 in diameter steel pipe pile with a 0.500 in wall thickness is subject to the following ASD demands: $P = 200$ k, $V = 50$ k, $M = 250$ in-k. Using ASD with the IBC allowable stresses and $f_y = 50$ k/in^2, determine if this section is adequate. The driving conditions will be checked using a wave equation analysis, and the requirements of IBC 1810.3.2.8 will be satisfied.

Solution

$$\begin{aligned} f_a &= f_b = 0.50 f_y \\ &= (0.50)(50{,}000) \\ &= 25{,}000 \text{ lb/in}^2 \end{aligned}$$

$$S = 56.7 \text{ in}^3 \qquad \text{(Table 21.2)}$$

$$\begin{aligned} A &= \frac{\pi}{4}(12.75^2 - 11.75^2) \\ &= 9.82 \text{ in}^2 \end{aligned}$$

$$\frac{P}{f_a A} + \frac{M}{f_b S} = \frac{200{,}000}{(25{,}000)(9.82)} + \frac{250{,}000}{(25{,}000)(56.7)}$$

$$= 0.99 \leq 1 \qquad \textbf{OK}$$

$$\begin{aligned} f_v &= 0.40 f_y \\ &= (0.40)(50{,}000) \\ &= 20{,}000 \text{ lb/in}^2 \end{aligned}$$

$$\begin{aligned} V_a &= \frac{f_v A}{2} \\ &= \frac{(20{,}000)(9.82)}{2} \\ &= 98{,}200 \text{ lb} \geq 50{,}000 \qquad \textbf{OK} \end{aligned}$$

Therefore, the structural design is satisfactory.

Code Note

If the steel pipe pile is considered to be a hollow structural section (HSS), then the American Institute of Steel Construction (AISC) code specifies using only 93% of the nominal wall thickness for design. This reduction is intended to account for milling tolerances.

Concrete-Filled Steel Pipe Piles

When empty steel pipe piles do not provide sufficient structural capacity, engineers sometimes fill them with concrete. The concrete is placed after driving. The concrete increases both the compressive and flexural design load capacities, and provides some corrosion protection to the interior of the pipe. However, concrete infilling usually does not improve the geotechnical downward load capacity because even open-end pipe piles generally become fully plugged. The geotechnical uplift capacity increases slightly, because of the added weight of the concrete.

When using ASD, the IBC allowable axial compressive stress on the gross cross-section for concrete-filled steel pipe piles with no flexural stresses is:

$$P_a = 0.33 f_c' A_c + 0.50 f_y A_s \tag{21.13}$$

Only the steel resists uplift, so:

$$P_{up,a} = 0.50 f_y A_s \tag{21.14}$$

where

P_a = allowable axial compressive load
$P_{up,a}$ = allowable axial tension load
f_c' = 28-day compressive strength of concrete
f_y = yield strength of steel
A_c = cross-sectional area of concrete
A_s = cross-sectional area of steel

If the conditions for using higher allowable stress in steel, as described above, are not satisfied, the coefficient for the steel term in Equations 21.13 and 21.14 should be reduced to 0.35.

The stress analysis becomes more complex when flexural stresses also are present because the concrete acts only in compression. In this case, only part of the concrete area may be considered, and the neutral axis does not necessarily pass through the center of the pile. Unfortunately, AISC, ACI, and AASHTO each present different methodologies for evaluating the flexural stiffness and capacity (Roeder et al., 2010). For example, the AISC formulation for flexural stiffness is:

$$(EI)_{eff} = E_s I_s + C_3 E_c I_c \tag{21.15}$$

$$C_3 = 0.6 + 2\left(\frac{A_s}{A_c + A_s}\right) \leq 0.9 \tag{21.16}$$

where

$(EI)_{eff}$ = effective flexural stiffness of the composite section
E_s, E_c = elastic modulus of the steel and concrete (see Section 14.3)
I_s, I_c = moment of inertia of the steel and concrete
A_s, A_c = cross-sectional area of the steel and concrete

The concrete is placed after the pile is driven, so driving stresses must be evaluated using only the steel area. The allowable driving stresses are the same as for regular steel pipe piles.

Prestressed Concrete Piles

Prestressed concrete piles are subject to a number of code requirements [IBC 1810.3.8], which include various detailing and seismic design provisions. They also are subject to the general code requirements for prestressed concrete. Typically, the effective prestress, f_{pc}, is about 4.8 MPa (700 lb/in^2), but values as high as 8.3 MPa (1,200 lb/in^2) have been used. The concrete strength, f'_c, is usually between 35 and 70 MPa (5,000–10,000 lb/in^2).

Axial Loading

For prestressed concrete piles subjected only to axial compression, IBC (2012), PCI (2004), and ACI (2012) specify an allowable structural load using ASD:

$$f_a = 0.33f'_c - 0.27f_{pc} \tag{21.17}$$

For prestressed concrete piles subjected only to axial tension, PCI (2004) recommends:

Permanent and repetitive loads:

$$f_a = 0 \tag{21.18}$$

Transient loads:

$$f_a = 0.5\sqrt{f'_c} \tag{21.19 SI}$$

$$f_a = 6\sqrt{f'_c} \tag{21.19 English}$$

ACI (2012) recommends:

$$f_a = 0.5f_y \tag{21.20}$$

where

f_a = allowable tensile or compressive stress due to normal load (MPa, lb/in^2)
f'_c = 28-day compressive strength of concrete (MPa, lb/in^2)
f_{pc} = effective prestress on the gross cross-section (MPa, lb/in^2)

Note that careful detailing between the pile and the pile cap is needed to properly transfer tension loads.

Combined Axial and Flexural Loading

PCI (2004) recommends the following ASD capacities for prestressed concrete piles subjected to combined axial and flexural loads:

Compression with all loads applied:

$$f_a + f_b = 0.60f'_c \tag{21.21}$$

Compression with dead load only:

$$f_a + f_b = 0.40f'_c - f_{pc} \tag{21.22}$$

Compression with live load plus half of dead load:

$$f_a + f_b = 0.40f'_c \tag{21.23}$$

Tension in normal environment:

$$f_a + f_b = 0.5\sqrt{f'_c} \tag{21.24 SI}$$

$$f_a + f_b = 6\sqrt{f'_c} \tag{21.24 English}$$

And half of these allowable tension values in a corrosive environment.

where

f_b = allowable tensile or compressive stress due to flexural load

Because IBC Chapter 18 provides no guidance on design of prestressed concrete piles for combined axial and flexural loading, so ACI (2012) recommends using the LRFD design methods for prestressed concrete [ACI 318 Chapter 18] with special resistance factors. The maximum axial capacity is limited to the ASD code values. The combined effects of axial and flexural loading are normally presented in the form of an interaction diagram. Figure 21.3 shows a typical diagram.

Standard Designs

Fortunately, pile suppliers and trade organizations have developed standard pile designs that conform to code-specified structural requirements. Standard designs used in the United States that conform to IBC are shown in Table 21.4 and Figure 21.4. Thus, for most

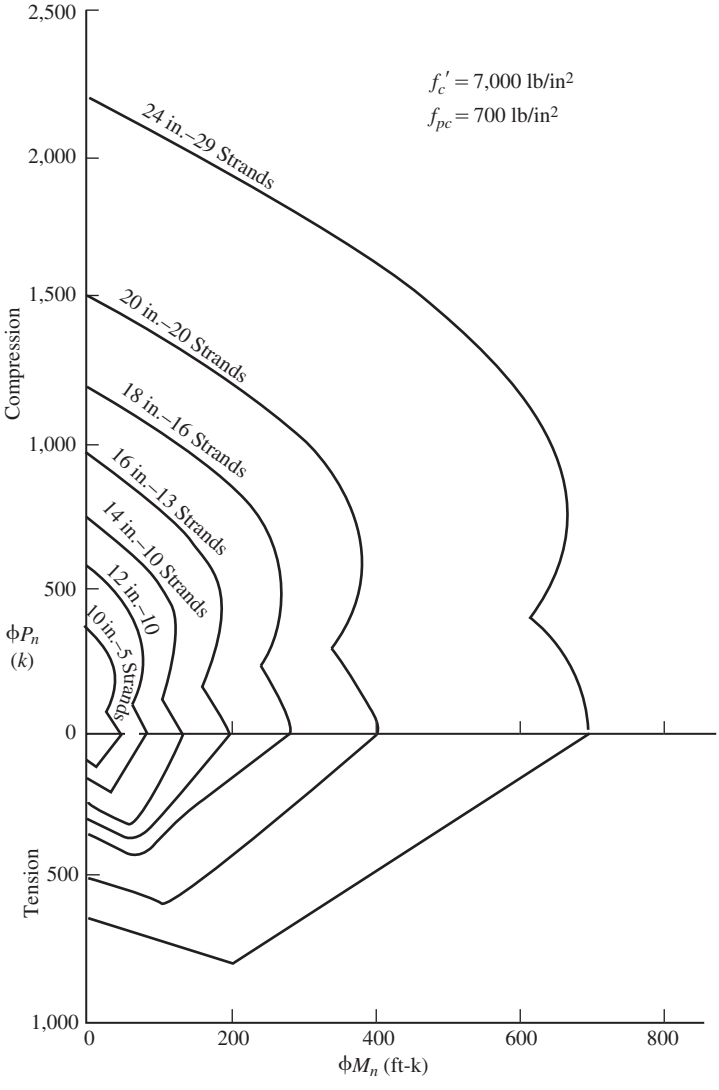

Figure 21.3 Typical interaction diagram for prestressed concrete piles. Intended for illustrative purposes only (not for design).

projects, the structural engineer simply selects one of these standard designs and specifies a required length. A pile casting yard then fabricates the piles and ships them to the site.

Handling Stresses

Improper handling can easily break prestressed concrete piles, especially when carried across the site in a horizontal position or being lifted from a horizontal position. PCI (2004)

TABLE 21.4 STANDARD OCTAGONAL AND ROUND PRESTRESSED CONCRETE PILES (adapted from PCI, 2010)

		Section Properties						Allowable Concentric Service Load, Tons[1]			
								f'_c, psi			
Size (in)	Core Diameter (in)	Area A_g (in^2)	Weight (lb/ft)	Moment of Inertia I (in^4)	Elastic Section Modulus S (in^3)	Radius of Gyration (in)	Perimeter (ft)	5,000	6,000	8,000	10,000
SQUARE PILES											
12	Solid	144	150	1,728	288	3.46	4.00	105	129	176	224
14	Solid	196	204	3,201	457	4.04	4.67	143	175	240	305
16	Solid	256	267	5,461	683	4.62	5.33	187	229	314	398
18	Solid	324	338	8,748	972	5.20	6.00	236	290	397	504
20	Solid	400	417	13,333	1,333	5.77	6.67	292	358	490	622
20	11	305	318	12,615	1,262	6.43	6.67	222	273	373	474
24	Solid	576	600	27,648	2,304	6.93	8.00	420	515	705	896
24	12	463	482	26,630	2,219	7.58	8.00	338	414	567	720
24	14	422	439	25,762	2,147	7.81	8.00	308	377	517	656
24	15	399	415	25,163	2,097	7.94	8.00	291	357	488	621
30	18	646	672	62,347	4,157	9.82	10.00	471	578	791	1,005
36	18	1,042	1,085	134,815	7,490	11.38	12.00	761	933	1,276	1,621

OCTAGONAL PILES											
12	Solid	119	125	1,134	189	3.09	3.31	86	106	145	185
14	Solid	162	169	2,105	301	3.60	3.87	118	145	198	252
16	Solid	212	220	3,592	449	4.12	4.42	154	189	259	330
18	Solid	268	280	5,705	639	4.61	4.97	195	240	328	417
20	Solid	331	345	8,770	877	5.15	5.52	241	296	405	515
20	11	236	245	8,050	805	5.84	5.52	172	211	289	367
22	Solid	401	420	12,837	1,167	5.66	6.08	292	359	491	624
22	13	268	280	11,440	1,040	6.53	6.08	195	240	328	417
24	Solid	477	495	18,180	1,515	6.17	6.63	348	427	584	742
24	15	300	315	15,696	1,308	7.23	6.63	219	268	368	467
ROUND PILES											
36	26	487	507	60,007	3,334	11.10	9.43	355	436	596	758
42	32	581	605	101,273	4,823	13.20	11.00	424	520	712	904
48	38	675	703	158,222	6,592	15.31	12.57	493	604	827	1,050
54	44	770	802	233,373	8,643	17.41	14.14	562	689	943	1,198
66	54	1,131	1,178	514,027	15,577	21.32	17.28	826	1,013	1,386	1,759

[1] Based on Equation 21.17 with $f_{pc} = 700\ \text{lb/in}^2$.

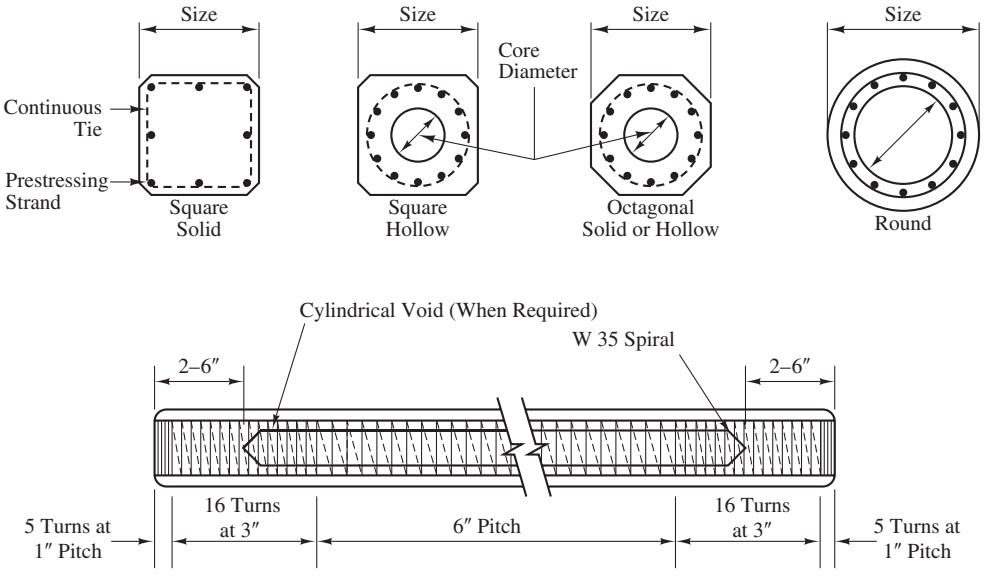

Figure 21.4 Standard prestressed pile designs (PCI, 2010).

recommends evaluating flexural stresses using 1.5 times the weight of the pile in order to account for the dynamic loads associated with handling, along with the following allowable flexural stresses:

Tension:

$$f_b = 0.4\sqrt{f'_c} \qquad \text{(21.25 SI)}$$

$$f_b = 5\sqrt{f'_c} \qquad \text{(21.25 English)}$$

Compression:

$$f_b = 0.60 f'_c \qquad (21.26)$$

where

f_b = allowable flexural stress (MPa, lb/in^2)

f'_c = 28-day compressive strength of concrete (MPa, lb/in^2). If handled prior to 28 days, use corresponding strength

Pickup points for lifting prestressed concrete piles may be based on these allowable handling stresses.

Example 21.2

A 60 ft long, 14 in square prestressed concrete pile is to be made of concrete with $f'_c = 6{,}000$ lb/in^2. It is to be hoisted to the pile driver by picking it up at a single point located 0.293 L (17.58 ft) from one end. This is the distance that produces the smallest moments in the pile. Determine whether this arrangement satisfies the handling stress requirements.

Solution

Per Table 21.4, the weight of this pile is 204 lb/ft. Multiplying by 1.5 (as recommended by PCI) gives 306 lb/ft. Using the principles of statics, the maximum moment in the pile is 47,300 ft-lb, as shown in Figure 21.5. The tensile stress controls, so:

$$\begin{aligned} f_b &= 5\sqrt{f'_c} \\ &= 5\sqrt{6{,}000} \\ &= 387 \text{ lb/in}^2 \\ \frac{P}{F_z A} + \frac{M}{F_b S} &= 0 + \frac{(47{,}300)(12 \text{ in/ft})}{(387)(457)} \\ &= 3.2 > 1 \qquad \textbf{Not Acceptable} \end{aligned}$$

The flexural stresses are much too high, so some other pickup arrangement must be used. Try using two pickup points, which are optimally located a distance 0.207 L from each end of the pile, as shown in Figure 21.2b.

Driving Stresses

Prestressed concrete piles also are subject to damage from driving stresses. As discussed in Chapter 19, the hammer blow initially produces a compressive stress, but the reflected

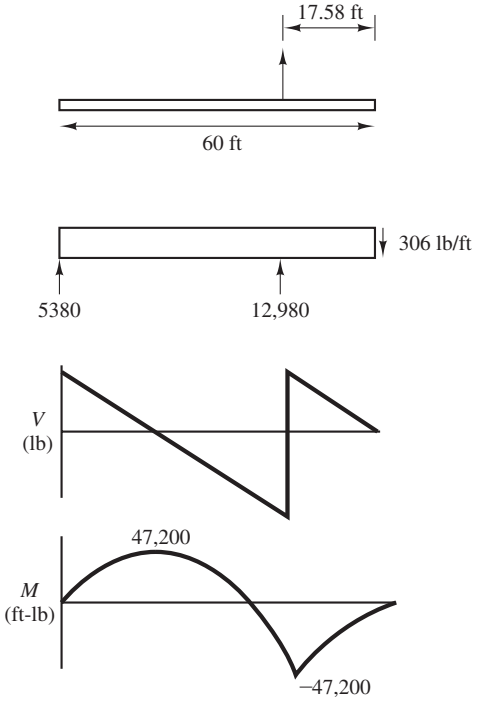

Figure 21.5 Pile for Example 21.2.

wave can produce tensile stresses, so both must be checked. The allowable driving stresses for prestressed concrete piles is presented in Table 19.7 for both compression and tension.

As shown in Table 19.7, the allowable tensile driving stress is substantially less than that in compression, and thus often controls the analysis. When driving piles in highly corrosive environments, the allowable tensile driving stress is sometimes limited to f_{pc} in order to reduce the potential for producing small cracks that could lead to corrosion of the prestressing strands.

21.4 DRILLED SHAFTS AND AUGER PILES

Material Properties

Drilled shafts are normally constructed with concrete having a design 28-day compressive strength, f'_c, of 24 to 35 MPa (3,500−5,000 lb/in^2). The maximum aggregate size for shafts constructed using the dry method may be no more than 1/5 of the clearance between the rebars. However, in order to provide for proper concrete flow during placement when using tremie concrete, Brown et al. (2010) recommend a maximum aggregate size of no more than 1/10 of the clearance between the rebars.

Auger piles are normally constructed with grout having a design 28-day compressive strength, f'_c, of 24 to 35 MPa (3,500−5,000 lb/in^2). Various additives are normally used to obtain the needed fluidity to facilitate steel placement.

Reinforcing steel with $f_y = 420$ MPa (60 k/in^2) is most commonly specified for both drilled shafts and auger piles.

Concrete Cover

ACI specifies a minimum concrete cover of 75 mm (3 in) between reinforcement and soil [ACI 318 7/7/1]. AASHTO specifies a minimum of 50 to 75 mm (2–3 in) depending on the circumstances [AASHTO 5.12.3]. However, Brown et al. (2010) recommend the following larger values for large-diameter drilled shafts:

- 75 mm (3.0 in) for shaft diameter $\leq$ 900 mm (3 ft)
- 100 mm (4.0 in) for 900 mm (3 ft) $<$ shaft diameter $<$ 1,500 mm (5 ft)
- 150 mm (6.0 in) for shaft diameter $\geq$ 1,500 mm (5.0 ft)

The transverse reinforcement is typically placed outside the longitudinal reinforcement, and the required cover for the transverse steel is 12 mm (0.5 in) less than these values.

Axial Loading

For drilled shafts and auger piles subjected to axial compression with no shear or moment, the ASD allowable loads per IBC (2012) are:

$$P_a = 0.3f'_cA_c + 0.5f_yA_s \tag{21.27}$$

$$P_{up,a} = 0.5f_yA_s \tag{21.28}$$

The tensile and compressive stresses in the steel are limited to 165 MPa (24,000 lb/in^2) and 220 MPa (32,000 lb/in^2), respectively. When a permanent casing is used, the first coefficient in Equation 21.27 is increased to 0.33 and the area of the casing may be considered as part of the steel area.

For LRFD using AASHTO [5.7.4.4]:

$$P_n = \beta[0.85f'_c(A_g - A_s) + A_sf_y] \tag{21.29}$$

$$P_{up,n} = f_yA_s \tag{21.30}$$

where

β = 0.85 for spiral reinforcement or 0.80 for tie reinforcement in compression; 0.90 in tension
f'_c = specified 28-day compressive strength of concrete
f_y = specified yield strength of reinforcing steel
A_g = gross cross-sectional area
A_s = cross-sectional area of longitudinal steel

The AASHTO ϕ is 0.75, except in certain seismic loading conditions where a value of 0.90 may be used [AASHTO 5.5.4.2, 5.10.11.3, 5.10.11.4.1b].

Combined Axial and Flexural Loading

Similar to prestressed concrete piles, combined axial and flexural loading in drilled shafts and auger piles introduces a number of code requirements. This capacity may ultimately be presented in the form of an interaction diagram.

21.5 PILE CAPS

When piles are placed in groups, they must be connected using a reinforced concrete pile cap. Figure 21.6 shows a cap under construction, and Figure 21.7 shows a completed cap. The process of designing pile caps is very similar to that for spread footings. Both designs must distribute concentrated loads from the column across the bottom of the footing or cap. The primary differences are:

- The loads acting on caps are larger than those on most spread footings.
- The loads on caps are distributed over a small portion of the bottom (i.e., the individual deep foundations), whereas those on spread footings are distributed across the entire base.

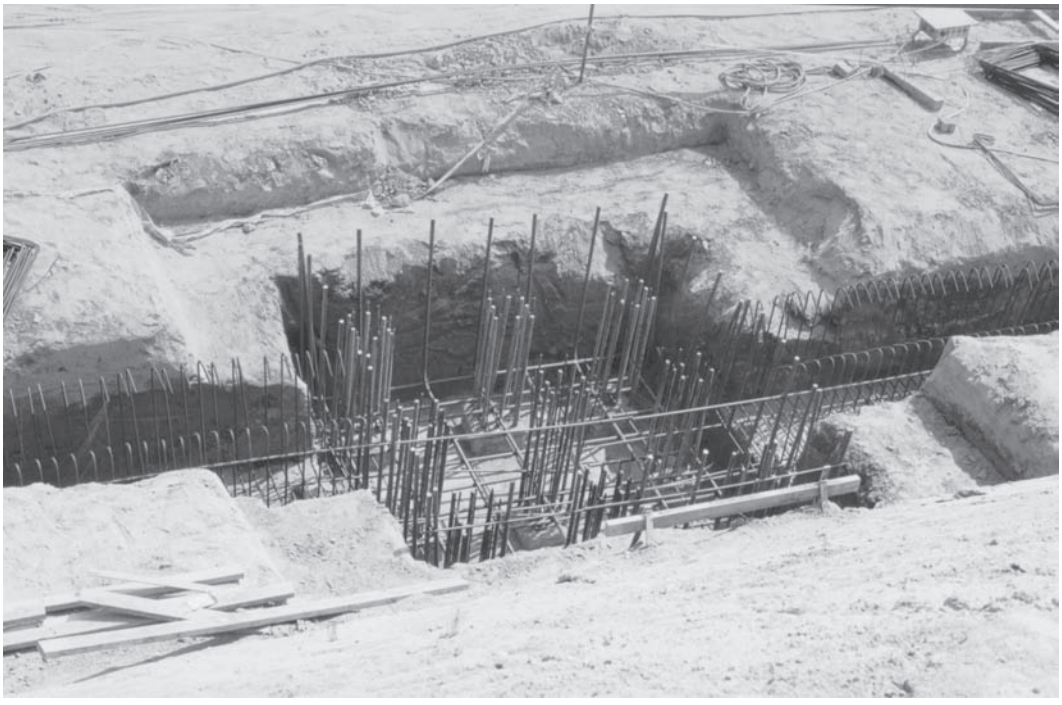

Figure 21.6 This group of nine prestressed concrete piles (three rows of three piles) will support a single column for a building. They will be connected using a reinforced concrete cap. In addition, a grade beam will connect this cap with the adjacent caps. The vertical steel bars extending from the top of each pile can be seen in the photograph, and some of the cap and grade beam steel is now in place. Notice the series of stirrups in the grade beam. Once all the steel is in place, the cap and the grade beam will be poured monolithically.

Figure 21.7 This bridge bent is supported on a group of pile foundations. The reinforced concrete cap connects the bent and the foundations. Because of the clean sandy soils at the site, this cap was cast using plywood forms which produced the smooth sides. However, in more cohesive soils, caps usually are cast directly against the soil.

Although the American Concrete Institute (ACI) code does not govern the design of piles or drilled shafts, it does encompass the design of caps, which it calls "footings on piles" [15.2.3]. The design process for caps is very similar to that for spread footings, with the following additional requirements:

- The design must satisfy the punching shear in the vicinity of the individual piles or shafts [ACI 15.5].
- The effective depth, d, must be at least 300 mm (12 in) [ACI 15.7]. This implies a minimum thickness, T, of 400 mm (18 in).
- The bearing force between the individual piles or shafts and the cap must not exceed the capacity of either element [ACI 15.8.1].

Structural engineers often assume the cap is rigid (i.e., the flexural distortions are very small) and each pile carries an equal share of the downward load. However, in reality there is some flexural distortion in the cap, which means the innermost piles carry more load than those along the perimeter of the cap. Thus, a more rigorous analysis that models the piles as equivalent springs and considers the flexural distortions in the cap can sometimes result in more economical designs.

The pile to pile-cap connection can be fairly simple if only downward loads are present. However, it becomes much more complex when shear or uplift loads must be transferred.

21.6 SEISMIC DESIGN

Although ACI 318 (ACI, 2011) explicitly excludes piles in general [ACI 318 1.1.6], it does include design provisions for piles in seismic zones [ACI 318 21.12.4]. IBC also includes special seismic design requirements for piles. These requirements include additional reinforcement within the pile, and better connections between the pile and the pile cap. In seismic areas, these provisions often control many aspects of the design.

SUMMARY

Major Points

1. Piles must have sufficient strength and cross-sectional area to satisfy the structural ultimate limit state. When subjected only to axial loading, the structural ULS analysis must address the resulting compressive and tensile stresses. When subjected to both axial and flexural loading, the resulting flexural stresses also must be addressed, along with the flexural stiffness.
2. Code requirements for structural design of piles are more conservative than for the same materials in the superstructure.
3. Underground buckling under service loads is usually not a problem, so piles may be designed as short columns.

4. In addition to the design loads, driven piles also must be designed to sustain handling loads and driving loads.
5. Pile caps are designed using methods similar to those for spread footings, with some additional requirements.

Vocabulary

Buckling	Handling loads	Pile cap
Driving loads	Interaction diagram	Section modulus

QUESTIONS AND PRACTICE PROBLEMS

21.1 Why is it appropriate to use more conservative structural designs for foundations than for comparable superstructure members?

21.2 What type of pile is least prone to damage during handling?

21.3 What is the most common yield strength of steel used for steel piles?

21.4 An HP 13 × 60 pile is made of steel with $f_y = 50\ \text{k/in}^2$ and is to be loaded in compression only (i.e., no moment or shear loads). Using $f_a = 0.35f_y$, compute the maximum allowable compressive load on this pile.

21.5 A pipe pile made of A572 steel ($f_y = 50\ \text{k/in}^2$) must sustain a compressive load of 200 k and a moment load of 40 ft-k. Using $f_a = 0.35\,f_y$, select an appropriate pile size from the standard piles listed in Table 21.2.

21.6 A PP20 × 0.500 pile made of A572 steel ($f_y = 50\ \text{k/in}^2$) is to be filled with concrete having a 28-day compressive strength of 3,000 lb/in^2. This pile is to be loaded in compression only (i.e., no moment or shear loads). Using the IBC formula, compute the maximum allowable compressive load.

21.7 A group of twelve prestressed concrete piles is to support a building column. The total downward design load on the group is 4,900 k. Assuming this load is evenly distributed across the 12 piles, and that there are no moment or shear loads, select a pile size and 28-day compressive strength of the concrete.

21.8 Using the standard sections in Table 21.2, select a steel pipe pile that can sustain the following design loads:

$$\begin{aligned} \text{compressive dead load} &= 400\ \text{k} \\ \text{compressive live load} &= 200\ \text{k} \\ \text{flexural dead load} &= 60\ \text{ft-k} \\ \text{flexural live load} &= 75\ \text{ft-k} \end{aligned}$$

Use the IBC load combinations, and identify the necessary steel grade and any other associated design or construction requirements.

21.9 A PP 18 $\times$ 0.500 steel pipe pile made of A572 steel ($f_y = 50\ \text{k/in}^2$) carries a compressive load of 200 k. Compute the maximum allowable moment and shear forces that keep the pile stresses within acceptable limits.

21.10 Develop an interaction diagram (a plot of allowable moment load versus allowable compressive load) for an HP 12 $\times$ 84 pile made of A572 steel ($f_y = 50\ \text{k/in}^2$). Assume bending occurs along the weak axis.

21.11 A 50 ft long, 18 in square prestressed concrete pile with $f'_c = 6{,}000\ \text{lb/in}^2$ is to be lifted at a single point as shown in Figures 21.1 and 21.2a. Using the weight of the pile plus a 50 percent increase for inertial and impact effects, draw shear and moment diagrams for this pile. Then compute the resulting flexural stresses and determine if this pickup arrangement satisfies the PCI allowable stress criteria. If it does not, then suggest another method of pickup that is acceptable.

21.12 A 15 m long Douglas fir pile with a head diameter of 250 mm will be subjected to a compressive load of 500 kN. There are no shear or moment loads. Is this design satisfactory from a structural engineering perspective?

22

Laterally Loaded Piles

Some say the cup is half empty, while others say it is half full. However, in my opinion both are wrong. The real problem is the cup is too big.

Sometimes all we need is a new perspective on an old problem.

Anonymous

As discussed in Chapter 13, the loads acting on piles are divided into two categories:

- *Axial loads* are those that act along the pile axis, and thus produce only compressive or tensile stresses in the pile.
- *Lateral loads* (or *transverse loads*) are those that act perpendicular to the pile axis (i.e., applied shear or moment loads), and thus generate shear and moments in the pile.

In some cases, the force of gravity acting on a structure is the only significant design load, and this gravity load is carried to the foundation through columns and bearing walls, so vertical piles are subjected only to axial loading. However, in other situations, applied lateral loads, acting either alone or in combination with axial loads, are present and must be considered in the foundation design. Examples include loads due to:

- Earth pressures, such as those acing on the back of retaining walls
- Water pressures, such as those acting on weirs or other hydraulic structures
- Arched structures, which impart lateral thrust loads onto the foundations even when the only applied loads are those due to gravity

- Wind
- Earthquakes
- Berthing and impact loads from ships as they contact piers or other harbor structures
- Downhill movements of earth slopes, including mudflows and lateral spreads
- Vehicle acceleration and braking forces on bridges
- Eccentric vertical loads or inclined loads on columns
- Ocean wave forces on offshore or harbor structures
- River current forces on bridge piers
- Cable forces acting on electrical transmission towers or electric railway wire support towers
- Cable anchors for suspension bridges
- Induced stresses due to temperature changes in the structure

Some of these lateral loads are static, while others are cyclic or dynamic. In either case, they introduce an entirely different design problem for the foundation engineer, and are the subject of this chapter. Both the ultimate limit state (ULS) and the serviceability limit state (SLS) are important, and both will be considered.

22.1 BATTERED PILES

Piles are very effective in supporting axial loads, but much less so for lateral loads. Thus, one method of resisting applied horizontal structural loads is to install some of the piles at an angle from the vertical, as shown in Figure 22.1. Piles constructed in this fashion are known as *battered piles* or *raker piles*. Note that the term *battered* means "on an angle from the vertical." It does not mean the pile has been driven too hard or damaged in any way.

Although it is possible to build most types of piles on a batter, driven piles are the most common choice. Contractors with the proper equipment can usually install them at a batter as steep as 4 vertical to 1 horizontal by tilting the pile-driver leads. However, these operations are not as efficient as driving vertical piles, so the production rate is slower and the equipment wears faster.

Typically the vertical and horizontal applied loads are transferred through a pile cap to a group of piles. Often some of the piles are plumb (vertical) and other are battered, but sometimes all of the piles are battered. In either case, the historical design approach is to model the pile-cap connections as pinned connections, so each pile is assumed to carry only axial loads. More efficient designs can be developed by modeling these as rigid connections, so both the vertical and battered piles carry some combination of axial and lateral loads.

Figure 22.2 shows a pier constructed using battered piles. In this case, the design lateral loads primarily consist of forces from large waves generated by storms, and inertial forces generated by earthquakes.

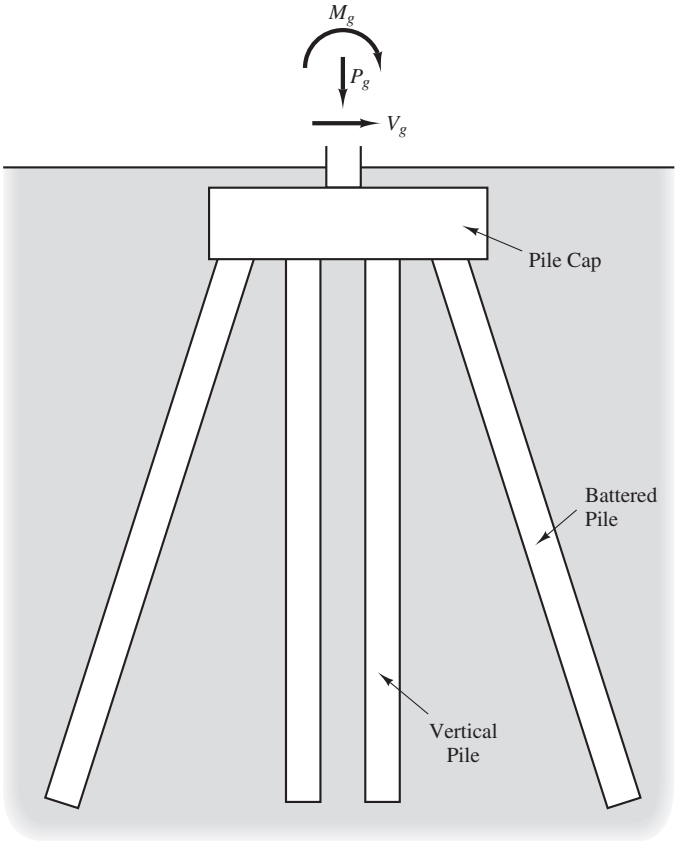

Figure 22.1 Battered piles being used in combination with vertical piles to resist combined vertical and horizontal loads.

Although battered piles have generally performed well, there are at least two situations that cause problems:

- Offshore structures, such as drilling platforms, are subjected to very large lateral loads from ocean currents, wind loads, and seismic loads, but it is not practical to drive piles at a sufficiently large angle to accommodate these loads.
- Battered piles form a very stiff foundation system. This is suitable when only static loads are present, but can cause problems when dynamic loads are applied, such as those imposed by an earthquake, or impact loads, such as those from ships. Figure 22.3 shows the damage that has occurred in pile caps with battered piles subjected to seismic loads.

In spite of these problems, battered piles are still an appropriate solution for some foundation problems. In order to avoid the problem shown in Figure 22.3, NEHRP (2003) recommends stronger pile to pile cap connections in seismic areas.

Figure 22.2 Prestressed concrete battered piles at Huntington Beach pier, California.

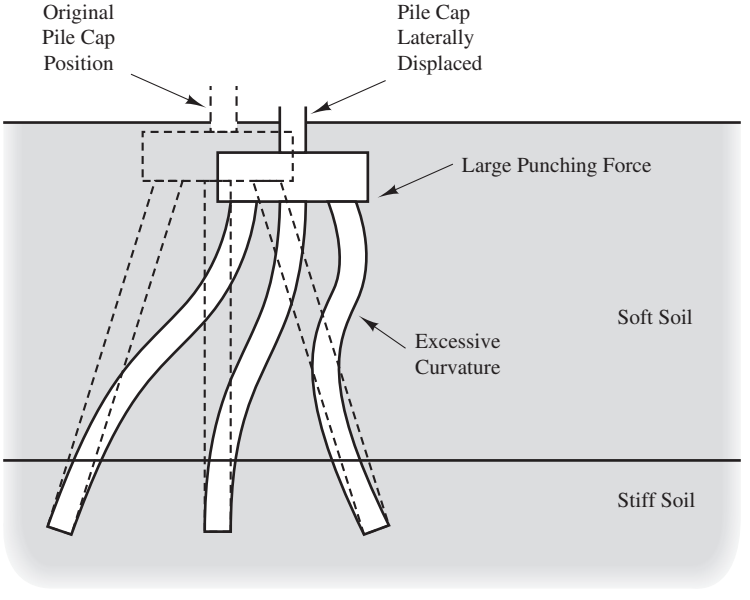

Figure 22.3 Behavior of battered piles during seismic loading.

Engineers also recognized that, in spite of the design assumptions, groups of vertical and battered piles are not subject to axial loads only. In reality, shear and moment loads also are present because:

- The connection between the piles and the cap is, in reality, not pinned, so only certain combinations of applied vertical and horizontal loads on the pile cap impart only axial loads on the head of all piles. Because the horizontal loads often are temporary (i.e., wind or seismic loads), the actual working loads often are not properly combined. For example, if the horizontal load is sometimes zero, then the vertical load generates flexural stresses in the battered piles.
- The stiffness of the various piles may differ, so the stiffer piles will carry proportionately more of the applied loads.
- The soil may consolidate after the piles are driven (see discussion of downdrag loads in Section 23.1). This downward movement of the soil produces lateral loads on the battered piles, and might even cause them to fail in flexure. Unfortunately, such a failure would probably be hidden, and would not be evident until an earthquake or other extreme event occurred and the battered piles failed to perform. Thus, in general, battered piles should not be used in such situations.

22.2 RESPONSE TO LATERAL LOADS

Because of the difficulties with battered piles and the need to produce more economical designs, engineers developed better methods of analyzing laterally loaded piles. Pile foundation systems consisting only of vertical piles designed to resist both axial and lateral loads would be less expensive to build and more flexible. These characteristics are especially important in offshore structures because battered piles are not feasible, so the petroleum industry led much of the early effort to develop better lateral load analysis methods. The results of a few lateral load tests were published in the literature as early as the 1930s, and intensive research on this topic began in the 1950s. These efforts have produced reliable analysis and design methods, and laterally loaded piles are now very common.

Short Versus Long Piles

When evaluating lateral loads, we divide piles into two categories: *short piles* and *long piles*, as shown in Figure 22.4. A short pile is one that does not have enough embedment depth to anchor the toe against rotation, whereas a long pile is one in which the toe is embedded deeply enough to be essentially fixed against any rotation or lateral displacement. The minimum length required to be considered "long" depends both on the flexural rigidity of the pile and on the lateral resistance provided by the soil, and other factors, and can range from about 5 diameters to more than 20 diameters.

In terms of the ULS, the ultimate lateral capacity of short piles is controlled by the soil. In other words, the pile can be assumed to act as a rigid body and the soil fails before

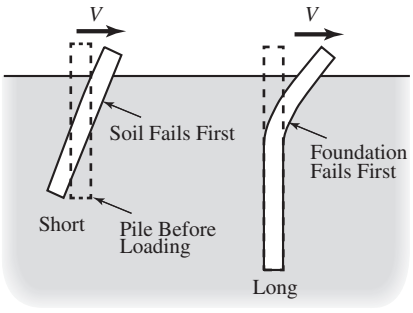

Figure 22.4 Short versus long piles.

the pile reaches its flexural structural capacity. Conversely, the ultimate lateral strength capacity of long piles is controlled by the flexural capacity of the pile because it fails structurally before the soil fails. For the SLS, the lateral deflection of the pile depends on the structural response of the pile itself, the stress-strain properties of the soil, and the interaction of the two.

Soil-Structure Interaction

Short piles can be analyzed as if they are rigid bodies embedded in the soil. Long piles also can be analyzed this way. However, it is much better to analyze long piles in a more rigorous manner that considers the flexural rigidity of the pile and the associated *soil-structure interaction*. With this model, the lateral displacements and flexural stresses in the pile depend on the soil resistance, while the soil resistance depends on the lateral displacement of the pile. Such analyses require considering the structural and geotechnical aspects concurrently.

Figure 22.5 shows a typical relationship between the net soil reaction force, p, per unit length of pile and the lateral pile displacement, y. Figure 22.6 shows the values of p and y versus depth for a long pile, along with the associated shear and moment diagrams and pile rotation (i.e., the angular displacement from the vertical). Near the ground surface, the applied lateral loads induce a certain lateral deflection in the pile, which is countered by the soil resistance and by the flexural rigidity of the pile. At some depth below the ground surface, the deflection and the soil resistance are both zero, but the rotation is not zero, so below that depth the pile is deflected in the opposite direction, which induces soil reaction in the opposite direction. This interaction continues with depth until all of the parameters are essentially zero.

The shapes and magnitudes of these plots depend on many factors, including:

- The type (shear and/or moment) and magnitude of the applied loads
- The resistance-deflection relationship in the soil (known as the p-y curve)
- The flexural rigidity (also known as bending stiffness) of the pile, which is the product of its modulus of elasticity, E, and moment of inertia, I

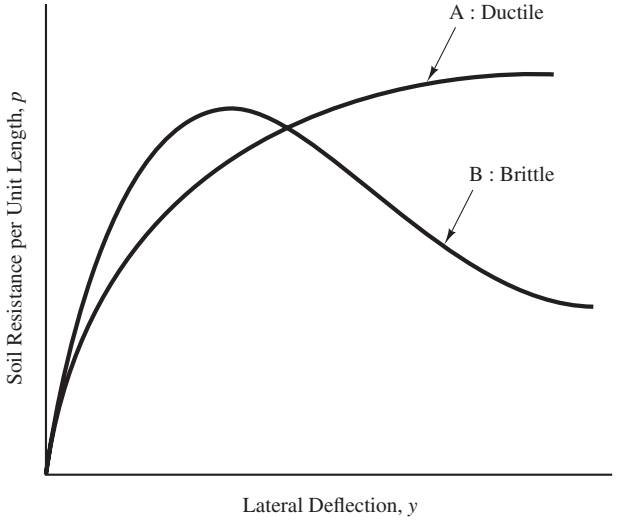

Figure 22.5 Typical *p*-*y* curves.

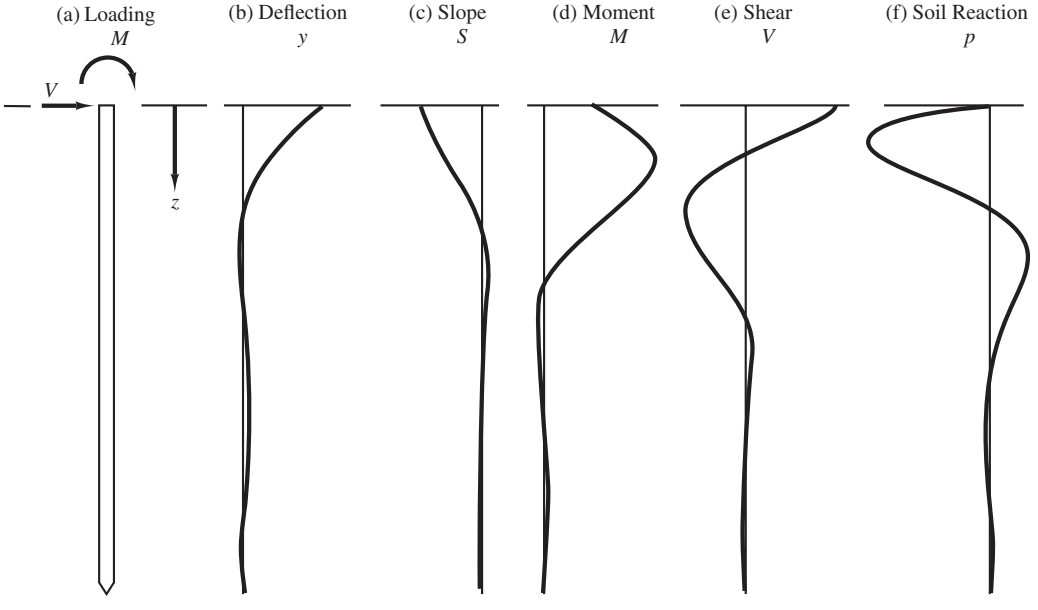

Figure 22.6 Forces and deflections in a long deep foundation subjected to lateral loads: (a) loading (*M*); (b) deflection (*y*); (c) slope (*s*); (d) moment (*M*); (e) shear (*V*); and (f) soil reaction (*P*) (based on from Matlock and Reese, 1960; used with permission of ASCE).

The changes in each of these parameters with depth are defined by the principles of structural mechanics as follows:

$$S = \frac{dy}{dz} \tag{22.1}$$

$$M = EI\frac{dS}{dz} = EI\frac{d^2y}{dz^2} \tag{22.2}$$

$$V = \frac{dM}{dz} = EI\frac{d^3y}{dz^3} \tag{22.3}$$

$$p = \frac{dV}{dz} = EI\frac{d^4y}{dz^4} \tag{22.4}$$

where

S = pile rotation
M = bending moment in the pile
V = shear force in the pile
p = lateral soil resistance per unit length of the pile
E = modulus of elasticity of the pile
I = moment of inertia of the pile in the direction of bending
y = lateral deflection of the pile
z = depth below ground surface

If the shape of one of these functions (sometimes called shear/moment/deflection profiles) is known, through either computation or field measurements, the others may be computed through progressive integration or differentiation with appropriate boundary conditions.

Example 22.1

According to measurements made during a static lateral load test, the deflection in the upper 2 m of a 10 m long test pile is defined by the equation:

$$y = 0.035 - 0.010z^{1.8}$$

Develop equations for slope, moment, shear, and soil reaction versus depth.

Solution

$$S = \frac{dy}{dz} = -0.018z^{0.8}$$

$$M = EI\frac{dS}{dz} = -0.0144z^{-0.2}$$

$$V = \frac{dM}{dz} = 0.288z^{-1.2}EI$$

$$p = \frac{dV}{dz} = -0.346z^{-2.2}EI$$

Commentary

In practice, these functions are not easily defined by simple polynomials, so the integration or differentiation must be performed using numerical methods.

End Restraints

The type of connection between the pile and the structure also is important because it determines the kinds of restraint, if any, acting on the pile. These define the boundary conditions needed to perform integrations on Equations 22.1 to 22.4. Engineers usually assume that one of the following restraint conditions prevail (although others also are possible):

- The *free head condition*, shown in Figure 22.7a, means that the head of the pile may freely move laterally and vertically, and may rotate when subjected to shear

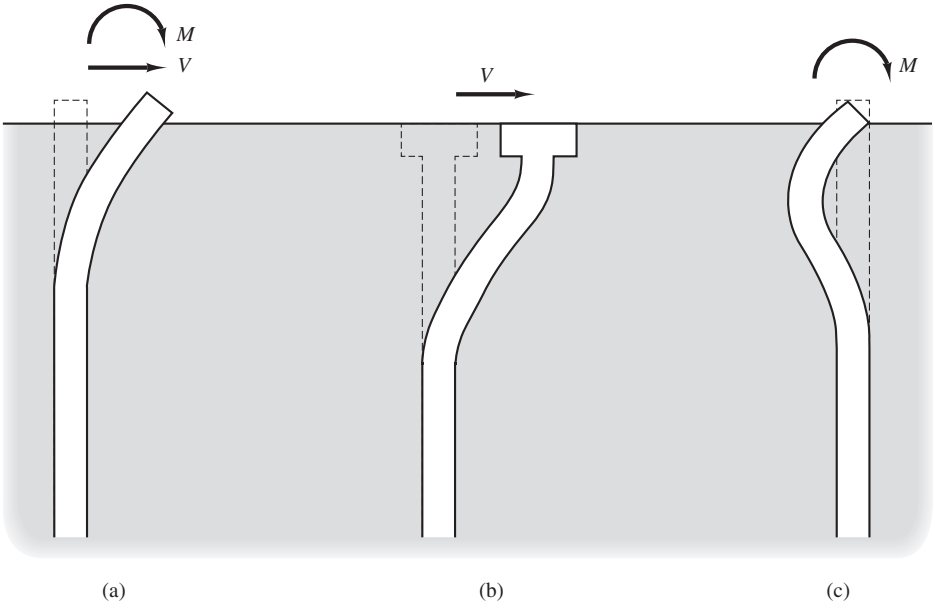

Figure 22.7 Types of connections between the pile and the structure: (a) free-head; (b) fully restrained head; and (c) pure rotation.

and/or moment loads. A single drilled shaft supporting a highway bridge bent is an example of the free head condition. In this case, the applied shear and moment loads, V and M, at the head of the pile are known, while the slope and deflection, S and y, are unknown.

- The *fully restrained head condition* (also known as the *fixed head condition*), shown in Figure 22.7b, means that the head of the pile may move laterally and vertically, but is not permitted to rotate. A group of piles connected with a rigid pile cap closely approximate this condition, because there will be very little rotation of the cap. In this case, V and S at the pile head are known, while M and y are unknown.
- The *pure rotation condition*, shown in Figure 22.7c, occurs when the pile head is allowed to rotate, but no lateral movements are permitted at the head. In this case, V, M, and y at the pile head are all known, and S is unknown.

In reality, piles often have connections that are intermediate between the free head and fully restrained head conditions. Nevertheless, one of these idealized conditions is usually reasonable for design purposes. In addition, so long as the foundation is "long," the shear, moment, rotation, and deflection at the toe are all zero, thus forming four additional boundary conditions.

Usually, the pile transmits most of the applied lateral loads to the upper soils, so the soil properties between the ground surface and a depth of 5 to 10 diameters are typically the most important. Therefore, the geotechnical characterization plan should focus more effort on evaluating these upper soils, and we must be especially careful to consider scour or other phenomena that might eliminate some of the upper soils.

22.3 METHODS OF EVALUATING LATERAL LOAD CAPACITY

Both experimental and analytical methods are available to evaluate lateral load capacity, and these methods range from simple to complex. These methods, combined with the results of extensive research and the widespread availability of powerful computers, have greatly improved our ability to analyze laterally loaded piles.

The objectives of lateral load capacity analyses generally include one or more of the following:

Ultimate Limit States

- **Geotechnical**—Determine the minimum depth of embedment required to transfer the lateral loads into the ground while providing an adequate factor of safety (or resistance factor) against shear failure in the soil. When lateral loads are the primary loads acting on the pile, this criteria may control the required pile embedment depth, and a "short" pile is often adequate. However, when significant axial loads are present, such as with piles that support buildings or bridges, the required depth of embedment is usually controlled by the axial load design, and the pile is typically "long."

- **Structural**—Determine the shears and moments induced in the pile by the lateral loads and provide a sufficient structural section to resist these stresses. Sometimes we need only the maximum values of shear and moment and design the entire pile to resist them, while other times we need shear and moment diagrams and design the pile accordingly.

Serviceability Limit States

- Determine the lateral deflection at the head of the pile under the design lateral loads. This analysis is often used to determine the flexural stiffness, *EI*, required to maintain lateral deflection below the allowable lateral deflection. Buildings and other similar structures typically can tolerate no more than 7 to 20 mm (0.25–0.75 in) of lateral deflection at the head of the pile. Larger values might be tolerable if the various foundations are tied together, such as with grade beams or a floor diaphragm, and thus move as a unit. The maximum allowable lateral deflection for bridges is typically between 7 and 50 mm (0.25–2.0 in) (Paikowsky, 2004). The design value for a specific project must be determined by the structural engineer, and is often dictated by design codes.

22.4 RIGID PILE ANALYSES

The earliest analytical solutions to lateral load problems assumed the foundation is perfectly rigid (i.e., a very high *EI*). This is the same assumption used in early mat foundation analyses, as discussed in Chapter 10, and it was introduced for the same reason: to simplify the computation of soil reaction forces. Rigid analyses may still be used to evaluate the ULS in simple short piles because the flexural distortions are small compared to the lateral movements in the soil. However, these methods are no longer appropriate for long piles or to evaluate the SLS (lateral deflections).

Thus, rigid analyses are used primarily for single isolated piles where the axial load is modest, the lateral load dictates the required depth of embedment, and lateral deflection does not control the design. The foundation for a single-post highway sign would be one example.

Broms' Method

Broms (1964a, 1964b, 1965) developed an analysis method for rigid piles that can be used to determine the minimum embedment depth, $D_{\min}$, required to satisfy the geotechnical ULS, along with the corresponding maximum moment in the pile which can then be used to design a structural section that satisfies the structural ULS.

For geotechnical allowable stress design (ASD) strength analyses, engineers typically determine the required nominal shear capacity, V_n, using a factor of safety of 1.5–3.0 (Paikowsky, 2004). For load and resistance factor design (LRFD), the American Association of State Highway and Transportation Officials (AASHTO) uses a resistance factor of 1.0.

Cohesive Soils

For cohesive soils, Broms used a simplified distribution of soil reaction as shown in Figures 22.8 and 22.9. Based on these distributions, the minimum required depth of embedment, $D_{\min}$, and the maximum moment, $M_{\max}$, are:

For the free head condition:

$$D_{\min} = \sqrt{\frac{FV_n(e + 1.5B + 0.5f)}{2.25Bs_u}} + 1.5B + f \tag{22.5}$$

$$f = \frac{FV_n}{9s_uB} \tag{22.6}$$

$$M_{\max} = FV_n(e + 1.5B + 0.5f) \tag{22.7}$$

For the fully restrained head condition:

$$D_{\min} = \frac{FV_n}{9s_uB} + 1.5B \tag{22.8}$$

$$M_1 = 9s_uB(1.5B + 0.5f) - 2.25s_uBg^2 \geq 0 \tag{22.9}$$

$$g = D_{\min} - 1.5B - f \tag{22.10}$$

$$M_2 = \frac{FV_n(1.5B + 0.5f)}{2} \tag{22.11}$$

$$M_{\max} = \text{the greater of } M_1 \text{ and } M_2 \tag{22.12}$$

where

V_n = required nominal shear load capacity
M_n = required nominal moment load capacity

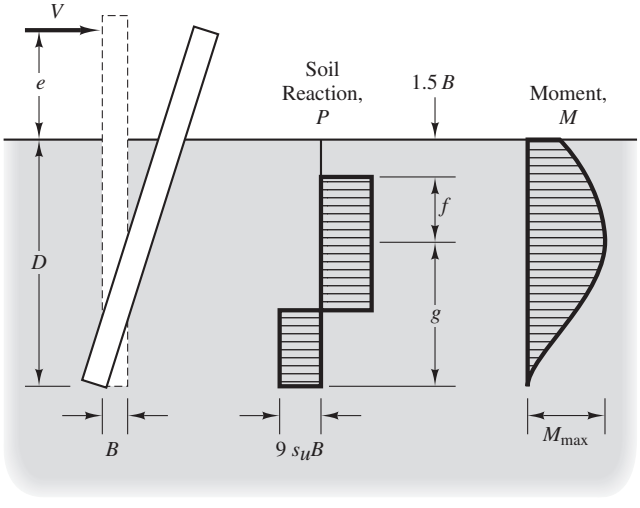

Figure 22.8 Deflection, soil pressure distribution, and moment diagrams for a free-head short pile in cohesive soil (based on Broms, 1964b; used with permission of ASCE).

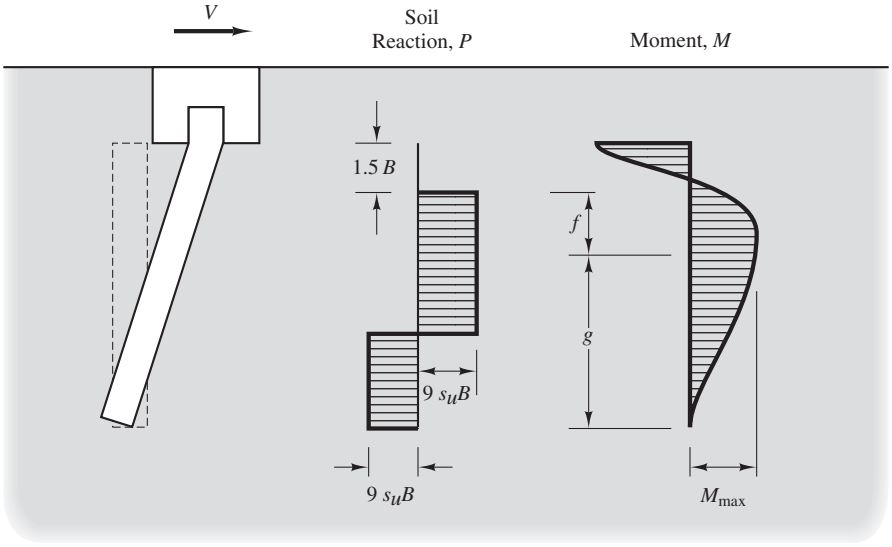

Figure 22.9 Deflection, soil pressure distribution, and moment diagrams for a fully restrained head short pile in cohesive soil (based on Broms, 1964b; used with permission of ASCE).

M_1 = moment at the head of the pile
M_2 = moment at a depth of $1.5B - f$
$e = \dfrac{M_n}{V_n}$
B = pile diameter
s_u = undrained shear strength
F = factor of safety

For LRFD analyses, set $F = 1$, and substitute ϕs_u for s_u and $\Sigma \gamma_i V_i$ for V_n, where ϕ and γ are the appropriate resistance and load factors.

Cohesionless Soils

The Broms analysis for cohesionless soils are based on the soil reaction distribution shown in Figures 22.10 and 22.11. Based on these distributions, the minimum required depth of embedment, $D_{\min}$, and the maximum moment, $M_{\max}$, are:

For the free head condition:

$D_{\min}$ is the smallest positive root of:

$$FV_n = \frac{0.5\gamma' B D_{\min}^3 K_p}{D_{\min} + e} \tag{22.13}$$

$$K_p = \tan^2(45 + \phi'/2) \tag{22.14}$$

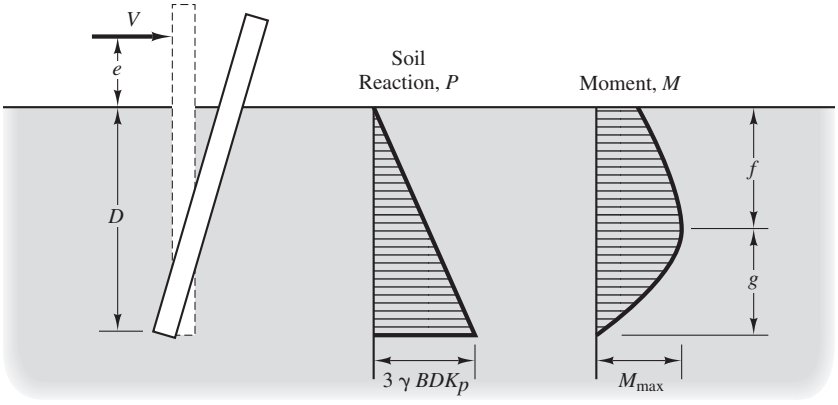

Figure 22.10 Deflection, soil pressure distribution, and moment diagrams for a free-head short pile in cohesionless soil (based on Broms, 1964a; used with permission of ASCE).

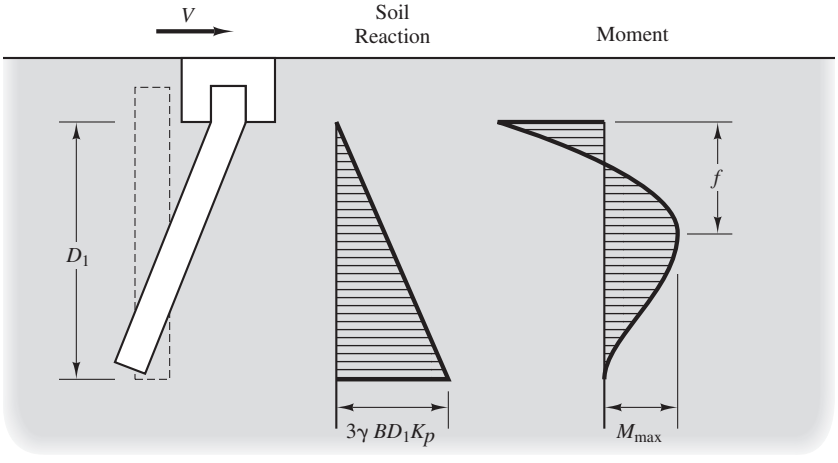

Figure 22.11 Deflection, soil pressure distribution, and moment diagrams for a fully restrained head short pile in cohesionless soil (based on Broms, 1964a; used with permission of ASCE).

M_{max} is:

$$M_{max} = FV_n(e + 0.67f) \tag{22.15}$$

$$f = 0.82\sqrt{\frac{FV_n}{BK_p\gamma}} \tag{22.16}$$

For the fully restrained head condition:

$$D_{min} = \sqrt{\frac{FV_n}{1.5\gamma' BK_p}} \tag{22.17}$$

$$M_{max} = 0.67FV_nD \tag{22.18}$$

Where all parameters are as defined earlier, and:

γ' = effective unit weight of soil (ranges from $\gamma - \gamma_w$ if the groundwater is at the ground surface to γ if the groundwater is below the pile toe)

ϕ' = friction angle

K_p = coefficient of passive earth pressure

For LRFD analyses, set $F = 1$, and substitute $\tan^{-1}(\phi \tan \phi')$ for ϕ' and $\Sigma \gamma_i V_i$ for V_n, where ϕ and γ are the appropriate resistance and load factors and ϕ' is the friction angle.

Broms (1964a, 1964b, and 1965) also provided a rigid pile methodology for computing lateral deflections. However, for problems such as the sign foundation example, lateral deflection typically does not control the design, so an ULS analysis as described above is sufficient. If lateral deflection is important, then a nonrigid pile analysis should be performed, as described in Section 22.5.

Example 22.2

A large sign is to be supported on a single post connected to an 18 in diameter drilled shaft foundation. The soil conditions consist of a stiff clay with $s_u = 3{,}000$ lb/ft^2. The ASD design wind load is 800 lb, and the center of the sign is 20 ft above the ground. Using a factor of safety of 3.0, compute the minimum required depth of embedment, $D_{\min}$, and the maximum moment in the drilled shaft, $M_{\max}$.

Solution

Use the rigid pile, free head method for cohesive soils.

$$V_n = FV = 3.0(800 \text{ lb}) = 2{,}400 \text{ lb}$$

$$f = \frac{FV}{9 s_u B} = \frac{3.0(800 \text{ lb})}{9(3{,}000 \text{ lb/ft}^2)(1.5 \text{ ft})} = 0.059$$

$$M = (800 \text{ lb})(20 \text{ ft}) = 16{,}000 \text{ lb-ft}$$

$$M_n = 3.0(16{,}000 \text{ lb-ft}) = 48{,}000 \text{ lb-ft}$$

$$e = \frac{M_n}{V_n} = \frac{48{,}000 \text{ lb-ft}}{2{,}400 \text{ lb}} = 20 \text{ ft}$$

$$M_{\max} = V_n(e + 1.5B + 0.5f)$$

$$= (2{,}400 \text{ lb})(20 \text{ ft} + 1.5(1.5 \text{ ft}) + 0.5(0.059))$$

$$= \mathbf{53{,}471 \text{ lb-ft}}$$

$$M < M_{\max} \quad \textbf{OK}$$

$$D_{\min} = \sqrt{\frac{V_n(e + 1.5B + 0.5f)}{2.25Bs_u}} + 1.5B + f$$

$$= \sqrt{\frac{2{,}400 \text{ lb}(20 + 1.5(1.5) + 0.5(0.059))}{2.25(1.5 \text{ ft})(3{,}000 \text{ lb/ft}^2)}} + 1.5(1.5 \text{ ft}) + 0.059$$

$$= 4.6 \text{ ft}$$

$$D_{\min} = \mathbf{4 \text{ ft } 9 \text{ in}}$$

22.5 NONRIGID PILE ANALYSES

Because of the shortcomings of rigid pile analyses, engineers have developed more thorough lateral load analysis methods that consider the flexural rigidity of the foundation, the soil's response to lateral loads, and soil-structure interaction effects. Although more precise, these methods also are more complex because of the various nonlinear aspects of the problem, so there is no simple closed-form solution. Nonrigid analyses may be performed using either the *finite element method (FEM)* or the *p-y* method.

Finite Element Method

A FEM analysis consists of dividing the pile and the soil into a series of small elements and assigning appropriate stress-strain properties to each element. FEM analyses also must model the interface between the pile and the soil. The analysis then considers the response of these elements to applied loads, and uses this response to evaluate shears, moments, rotations, and lateral deflections in the foundation. Finite element analyses may be performed using either two-dimensional or three-dimensional elements.

The accuracy of finite element analyses depends on our ability to assign correct engineering properties to the elements. This is easy to do for the pile because the properties of structural materials are well-defined, but more difficult for the soil because it is more complex. For example, the stress-strain properties in the soil are definitely nonlinear. More difficult still is modeling the soil-structure interaction where, for example, there may be slippage between the pile and the soil.

p-y Method

The *p-y method* uses a series of nonlinear springs to model the soil-structure interaction. This is similar to the method used to analyze mat foundations, as discussed in Chapter 11. Although the *p-y* method is not as rigorous as the FEM, it has been calibrated with static lateral load test results, and is easier to implement due to the simplicity of the model and the widespread availability of commercial software. Therefore, this is the preferred method for nearly all practical design problems.

The *p-y* method models the foundation using a two-dimensional finite difference analysis (Reese and Van Impe, 2001). It divides the foundation into *n* intervals with a node at the end of each interval, and the soil as a series of nonlinear springs located at each node, as shown in Figure 22.12. The flexural rigidity of each element is defined by the appropriate *EI*, and the load-deformation properties of each spring are defined by a *p-y* curve such as those in Figure 22.5. These springs are uncoupled, which means each of them acts independently. It also is necessary to apply appropriate boundary conditions, as described earlier. Using this information and applying the structural loads in increments, the software finds a condition of static equilibrium and computes the shear, moment, and lateral deflection at each interval.

Experiments with this method began in the late 1950s (McClelland and Focht, 1958; Matlock and Reese, 1960). However, the full development of this method required development of new software and calibration from full-scale load tests. Much of this work was performed during the 1960s and 1970s, and the method was well-established by 1980. It continues to be refined through additional research and experience. Commonly used *p-y* software includes LPILE from Ensoft, Inc., and FB-MultiPier from the University of Florida Bridge Software Institute.

The *p-y* method is best suited for long piles because they provide clear restraint conditions at the pile toe. This method is used to evaluate both the ULS and the SLS, and addresses both structural and geotechnical aspects of laterally loaded piles.

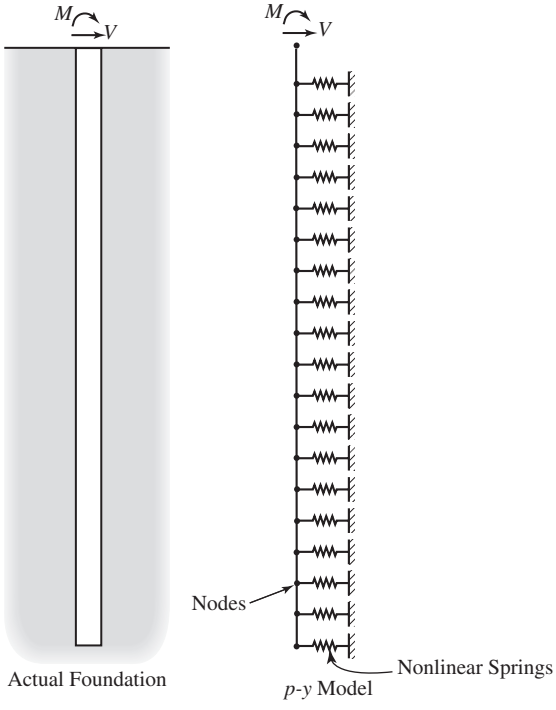

Figure 22.12 Analytical model used in the *p-y* method.

22.6 *p-y* CURVES FOR ISOLATED PILES

The heart of the *p-y* method is the definition of the lateral load-deflection relationships between the pile and the soil. These are expressed in the form of *p-y curves* (sometimes called *pile-soil support curves*), where *p* is the lateral soil resistance per unit length of the foundation (expressed in units of force per unit of pile length), and *y* is the lateral deflection. The *p-y* relationship might first appear to be an extension of the Winkler beam-on-elastic-foundation concept described in Chapter 11. However, in addition to being nonlinear (Winkler springs are normally linear), there is an important difference between the two: The Winkler model considers only compressive forces between the foundation and the soil, whereas the net lateral soil load acting on a pile is the result of compression on the leading side, shear friction on the two adjacent sides, and possibly some smaller compression on the back side. These components are shown in Figure 22.13. Thus, it is misleading to think of the *p-y* curve as a compression phenomenon only (Smith, 1989). In addition, the two-dimensional *p-y* analysis must implicitly reflect the three-dimensional nature of the soil response.

The exact shape of the *p-y* curve at a particular point on a pile depends on many factors, including the following:

- Soil properties
- Type of loading (i.e., short-term static, sustained static, repeated, cyclic, or dynamic)
- Pile diameter and cross-sectional shape
- Coefficient of friction between the pile and the soil
- Depth below the ground surface
- Pile construction methods
- Group interaction effects

The individual influences of these various factors are not well-established, so it has been necessary to develop *p-y* curves empirically by backcalculating them from static load tests and combining this data with analytical models based on soil mechanics. Much of this load test data were obtained from 250 to 600 mm (10–24 in) diameter steel pipe piles because they are easier to instrument and because the cost of the loading and measurement system is less than that for larger and stiffer piles. These tests have been performed on various soil types, and the results have been correlated with standard soil properties, such as effective friction angle or undrained shear strength (Reese and Van Impe, 2001; Reese et al., 2006; Isenhower and Wang, 2010). The experimental data is then extended

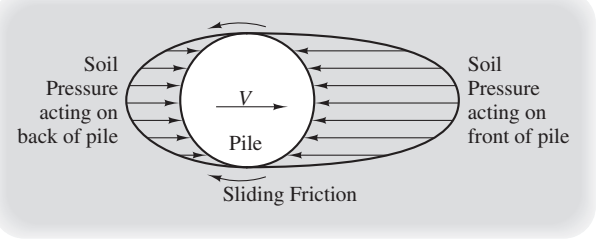

Figure 22.13 A pile subjected to a lateral load displaces into the soil. The soil pressure in front of the pile then becomes greater than the pressure acing on the back. In addition, sliding friction forces develop, as shown. The net of these forces is the *p* in the *p-y* curve.

to other sites by measuring the appropriate soil properties and using the correlations to develop the *p-y* curves. This methodology has been incorporated into *p-y* software.

Some curves are *ductile*, as shown in Curve A in Figure 22.5. These curves reach the maximum resistance, p_u, at a certain deflection, and then maintain this resistance at greater deflections. Other curves are *brittle* or *strain softening*, as shown in Curve B in Figure 22.5, and have a p that reaches some maximum value, then decreases with further deflection. Soft clays under static loading and sands appear to have ductile curves. Brittle curves can occur in some clays, especially if they are stiff or if the loading is repeated or dynamic. Brittle curves are potentially more troublesome because of their potential for producing large foundation movements.

Although the empirical *p-y* data collected to date have been an essential part of making the *p-y* method a practical engineering tool, we continue to need more data. Additional instrumented load tests would further our understanding of this relationship and thus provide more accurate data for analysis and design.

Clays

Soft Clay

Design *p-y* curves in soft clays are usually based on the work by Matlock (1970), which consisted of a combination of previous research and the results of two instrumented lateral load tests on 13 in (324 mm) diameter steel pipe piles. The undrained shear strength of the clays at these two test sites was 38 kPa (800 lb/ft^2) and 15 kPa (300 lb/ft^2), respectively.

The Matlock *p-y* curve for static loading is taken to be ductile, as shown in Figure 22.14. The ultimate soil resistance per unit length of pile, p_u, is the smaller of that obtained from Equations 22.19 and 22.20:

$$p_u = \left(3 + \frac{\gamma'_{\text{avg}}}{s_u}z + \frac{J}{B}z\right)s_u B \tag{22.19}$$

$$p_u = 9s_u B \tag{22.20}$$

where

p_u = ultimate soil resistance per unit length of pile (units of force per length)
γ'_{avg} = average effective unit weight from the ground surface to the depth being considered ($\gamma' = \gamma - \gamma_w$)

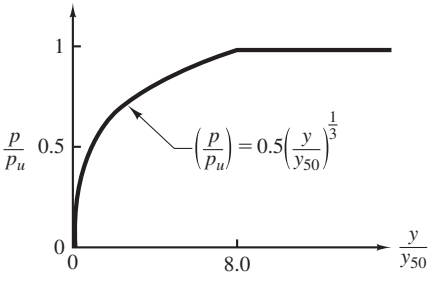

Figure 22.14 Matlock's *p-y* curve for static loading of an isolated pile in soft cohesive soil.

TABLE 22.1 TYPICAL ε_{50} VALUES IN CLAYS (Reese et al., 2006)

Consistency of Clay	Undrained Shear Strength		ε_{50}
	lb/ft^2	kPa	
Very soft	<250	<12	0.02
Soft	250–500	12–24	0.02
Medium	500–1,000	24–48	0.01
Stiff	1,000–2,000	48–96	0.006
Very stiff	2,000–4,000	96–192	0.005
Hard	>4,000	>192	0.004

s_u = undrained shear strength
J = 0.5 for soft clay, 0.25 for medium clay
B = pile diameter
z = depth below the ground surface

The deflection, y_{50}, at which one half of the ultimate soil resistance occurs is:

$$y_{50} = 2.5\varepsilon_{50}B \tag{22.21}$$

where

ε_{50} = strain corresponding to one-half of the maximum deviator stress

Design values of ε_{50} may be obtained from a UU triaxial test or from Table 22.1.

For cyclic loading, Matlock recommends determining the depth z_y, at which the failure mode transitions from flow around the pile (Equation 22.19 governs) and no flow (Equation 22.20 governs). For depths less than z_y, cut off the *p-y* curve at $p/p_u = 0.72$, as shown in Figure 22.15. For depths greater than z_y, use a strain softening curve as shown.

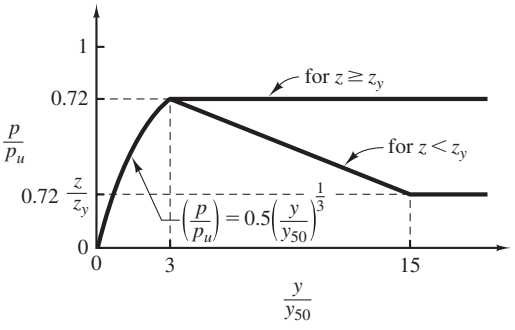

Figure 22.15 Matlock's *p-y* curve for cyclic loading of an isolated pile in soft cohesive soil.

Example 22.3

A 400 mm diameter pile is embedded into a saturated medium clay that has an average unit weight of 15.0 kN/m^3 and an undrained shear strength of 30 kPa. The groundwater table is near the ground surface. Using the Matlock method, develop the static *p-y* curve at a depth of 5 m.

Solution

None of the available methods specifically address medium clays, but the Matlock method (for soft clay) is the closest match and thus is an appropriate choice.

From Table 22.1: $\varepsilon_{50} = 0.01$

$$\gamma' = 15.0 - 9.8 = 5.2 \text{ kN/m}^3$$

$$y_{50} = 2.5\varepsilon_{50}B = 2.5(0.01)(400 \text{ mm}) = 10 \text{ mm}$$

$$p_u = \left(3 + \frac{\gamma'_{\text{avg}}}{s_u}z + \frac{J}{B}z\right)cB$$

$$= \left(3 + \left(\frac{5.2 \text{ kN/m}^3}{30 \text{ kPa}}\right)(5 \text{ m}) + \left(\frac{0.25}{0.4 \text{ m}}\right)(5 \text{ m})\right)(30 \text{ kPa})(0.4 \text{ m})$$

$$= 84 \text{ kN/m}$$

$$p_u = 9s_uB$$

$$= 9(30 \text{ kPa})(0.4 \text{ m})$$

$$= 108 \text{ kN/m}$$

Use 84 kN/m

$$y_{50} = 2.5\varepsilon_{50}B$$

$$= (2.5)(0.01)(400)$$

$$= 10 \text{ mm}$$

$$\frac{p}{p_u} = 0.5\left(\frac{y}{y_{50}}\right)^{\frac{1}{3}} \leq 1$$

$$p = 0.5\left(\frac{y}{10 \text{ mm}}\right)^{1/3}(84 \text{ kN/m}) \leq 84 \text{ kN/m} \qquad \textbf{OK}$$

The resulting curve is shown in Figure 22.16.

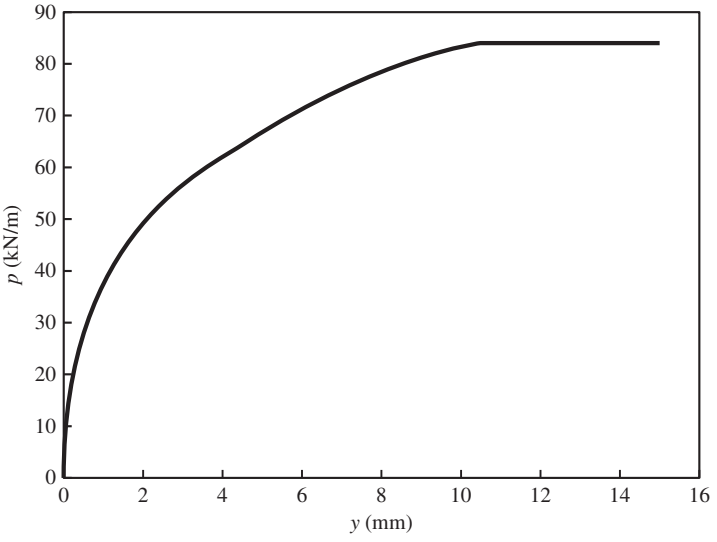

Figure 22.16 Computed *p-y* curve for Example 22.3.

Other Clays

Similar methodologies for constructing *p-y* curves in other kinds of clay also are available. As with the Matlock formulas, these methods are based primarily on the undrained shear strength, the strain ε_{50}, and the depth below the ground surface.

Reese et al. (1975) developed recommendations for *p-y* curves in saturated stiff clays based on the results of instrumented pile load tests conducted in Texas on 610 mm (24 in) diameter steel pipe piles. The undrained shear strength varied from 100 to 300 kPa (2,000−6,000 lb/ft^2).

Welch and Reese (1972) and Reese and Welch (1975) developed recommendations for unsaturated stiff clays based on static lateral load tests, which also were conducted in Texas. These tests were conducted on a 915 mm (36 in) diameter drilled shaft and a 254 mm (10 in) steel pipe pile in a clay that had an average undrained shear strength of 105 kPa (2,200 lb/ft^2).

Sands

Empirical *p-y* curves for sands have been developed using similar techniques. The stiffness of sands increase with depth much more rapidly than in clays, so the *p-y* curves also become correspondingly stiffer with depth. The method developed by Reese et al. (1974) and the method developed by the American Petroleum Institute (API, 2000) are widely used for sands. The *p-y* curves for sands typically use the initial modulus, *k*, as one of the input parameters. Table 22.2 provides typical values. Published methods for developing *p-y* curves in sands are typically more conservative than those for clays (i.e., they are more likely to predict lateral deflections that are greater than the actual deflections).

TABLE 22.2 TYPICAL *k* VALUES FOR *p-y* ANALYSES (adapted from Reese and Van Impe, 2001)

	Relative Density and Approximate Friction Angle		
Soil Type	Loose ($\phi' \approx 29°$)	Medium ($\phi' \approx 33°$)	Dense ($\phi' \approx 38°$)
Sand below groundwater	5.4 MPa 780 lb/in^2	16.3 MPa 2,400 lb/in^2	34.0 MPa 4,900 lb/in^2
Sand above groundwater	6.8 MPa 990 lb/in^2	24.4 MPa 3,500 lb/in^2	61.0 MPa 8,800 lb/in^2

Selection of *p-y* Curves

Other *p-y* curves also are available, each intended for specific conditions. Table 22.3 presents commonly used functions to develop *p-y* curves. Note that these curves vary with the depth, z, and are calibrated to common soil parameters. The selection of the appropriate curve for given site conditions, as well as assigning values to the corresponding input parameters, often requires some engineering judgment.

p-y Curves Directly from In Situ Tests

In situ tests are often used to develop the soil parameters for the various standard *p-y* curves. Alternatively, there have been some attempts to develop *p-y* curves directly from in situ tests (Baguelin et al., 1978; Robertson et al., 1985; Robertson et al., 1989; Anderson et al., 2003). The dilatometer test (DMT) and pressuremeter test (PMT) seem especially appropriate because the test procedure loads the soil radially, which is similar to the loads imposed by laterally loaded piles, so the required level of empiricism should be correspondingly less.

TABLE 22.3 COMMONLY USED FUNCTIONS TO DEVELOP *p-y* CURVES (compiled from Reese and Van Impe, 2001; Reese et al., 2006; and Isenhower and Wang, 2010)

Soil Type	Reference	Required Soil Parameters
Soft clay	Matlock (1970)	s_u,γ', ε_{50}, z
Stiff clay with free water	Reese, Cox, and Koch (1975)	s_u, ε_{50}, z
Stiff clay without free water	Welch and Reese (1972); Reese and Welch (1975)	s_u, ε_{50}, z
Sand	Cox et al. (1974); Reese et al. (1974)	ϕ', γ', k, z
Sand	API (2000)	ϕ', γ', k, z
Liquefied sand	Rollins et al. (2003)	γ'
Silt and c-ϕ soils	Isenhower and Wang (2010)	c', ϕ', γ', k, ε_{50}
Rock	Reese and Van Impe (2001)	k, z, q_u

However, some empirical adjustments are needed to account for side friction, scale effects, and other differences between the in situ test and the real pile. This approach appears promising, but additional research is needed, so it is not yet widely used in practice.

22.7 LATERAL LOAD TESTS

Static Lateral Load Tests

Another way to evaluate lateral load capacity is to conduct a static load test. These tests involve installing two closely-spaced prototype piles at the project site, applying a series of lateral loads by installing a jack between the piles, and measuring the corresponding lateral deformation at the head of the piles (Reese, 1984; ASTM D3966). Figure 22.17 shows a typical test setup. This method directly measures the lateral load-deformation characteristics in a similar way as the axial load-settlement behavior is measured using axial static load tests as discussed in Chapter 14. However, unlike axial tests, lateral tests do not determine the structural or geotechnical ULS; they only provide information for serviceability analyses (i.e., a load-deformation curve that stops well before the ULS).

The most basic test would include measurements of the applied lateral force and the lateral deflection at the point of load application, but most tests also include additional instrumentation. Measuring the lateral deflection at a second point above the point of load application provides an accurate assessment of pile rotation at the head of the pile. In addition, if the underground portion of the pile is instrumented using strain gages at various depths and an inclinometer (a device for measuring lateral pile deformation versus depth), we can develop the lateral displacement, shear, and moment diagrams using Equations 22.1 to 22.4.

Figure 22.17 shows a typical test setup. Nearly all tests are performed using a free head condition because this is the easiest test condition to produce in the field. However,

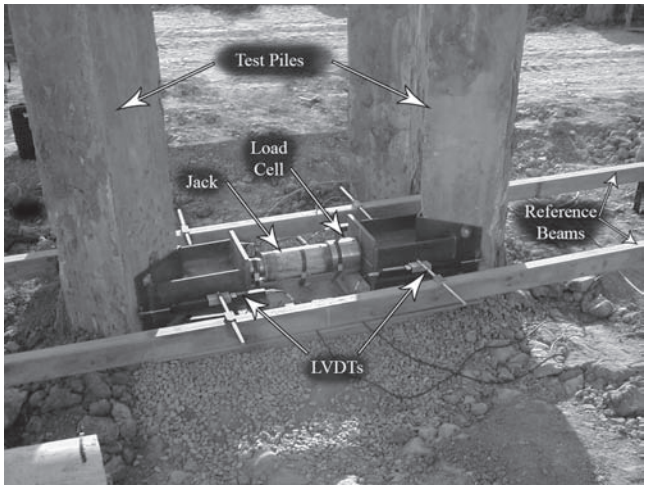

Figure 22.17 Typical full-scale lateral load test on prototype piles. Unlike axial load tests, both piles are tested at the same time (courtesy of CMR Technical Services).

if the fixed head condition will be present in the completed structure, the lateral deformations measured in the load test cannot be directly used to predict the lateral deformations of the production piles. In addition, the engineer may wish to consider the possibility of using other pile diameters, other *EI* values, etc. in the production piles.

In order to reduce the test results to a form that can then be used for different head restraint conditions and different pile geometries, it is customary to conduct a reverse *p-y* analysis to develop site-specific *p-y* curves, then use these curves in a conventional forward *p-y* analysis to design the production piles. However, developing new *p-y* curves is a difficult process, so usually the best technique is to use one of the standard *p-y* curves described in Section 22.6 and adjust the input parameters (s_u, ε_{50}, etc.) until the pile behavior matches the test data. These derived parameters are not necessarily the real soil properties for the site, and may in some cases be quite unreasonable, but they are the values that produce *p-y* curves that are consistent with the load test results and can then be used in forward *p-y* analyses to predict the lateral load behavior of the planned production piles at that site.

Static lateral load tests are less common than static axial load tests. For most projects, a *p-y* analysis provides sufficient precision. However, lateral static load tests are sometimes justified on large projects or where unusual soil conditions are present.

Lateral Statnamic Test

Another option is to conduct a lateral statnamic test. This technique uses the same principles as the vertical statnamic test described in Chapter 19, except the load is applied horizontally as shown in Figure 22.18. Unlike conventional lateral load tests, lateral statnamic tests require only one test foundation because the statnamic equipment provides its own reaction, and the test load can be much higher. However, this test requires mobilizing large specialized equipment, and obtaining appropriate permits for the explosive materials used to provide the thrust. Thus, this test is rarely performed.

22.8 GROUP EFFECTS

The analysis of lateral loads becomes more complex when piles are installed in groups. It is not correct to simply distribute the applied lateral load uniformly across the number of piles in the group, then analyze a single pile using its share of the total load. Doing so produces unconservative designs. Instead, we must recognize that some of the piles carry a greater share of the applied lateral load, while others carry less. We also must consider how the surrounding soil responds to the presence of multiple piles.

p-Multipliers

When a pile group is subjected to an applied lateral load, V_g, the leading row of piles pushes against virgin ground, as shown in Figure 22.19. However, the second row pushes against the soil between it and the first row, and this soil is influenced by shadow effects from the first row. As a result, the *p-y* curves for the second row must be softer than those for the first row. This effect is even more pronounced in the third row.

Figure 22.18 Lateral statnamic test being conducted on a 3.6 m (12 ft) diameter drilled shaft. The photo shows the Statnamic device in place ready for testing (courtesy of Applied Foundation Testing).

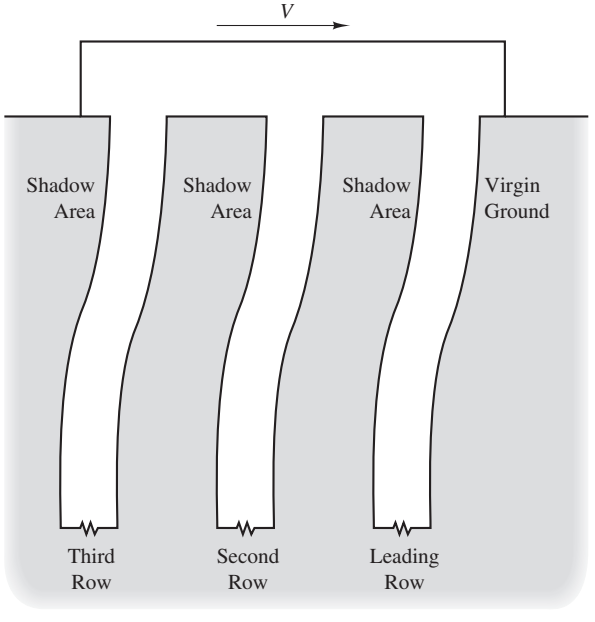

Figure 22.19 Group effects and their impact on lateral load response.

There also is a sideways group effect due to stress overlaps. The soil in front of the piles is being stressed by multiple piles in that row, so the *p-y* curves are softer than those for a single isolated pile.

The *p-y* curves for each row may be developed using *p*-multipliers, which apply a factor P_m to the *p-y* curve for a single isolated pile. Table 22.4 presents typical P_m values, which have been derived from full-scale and model-scale lateral load tests, as well as from analytical studies. Note that all of these values are less than one, which produces *p-y* curves that are softer than the *p-y* curve for a single isolated pile. Also note that the P_m values for the fourth and subsequent rows are the same as those for the third row.

Shear Load Distribution and Load-Deformation Behavior

These shadow and sideways group effects can be described by a mechanical analogy. The displacement of the leading row of piles is resisted by stiff springs (i.e., high values of P_m, which produce stiff p-y curves); the displacement of the second row is resisted by softer springs (lower P_m values); and the third row by even softer springs (even lower P_m values).

In a pile group there are N piles, all of which are connected by the pile cap, so all have the same lateral displacement. However, because of the differences in spring stiffness, each pile in the first row carries more than V_g/N, each pile in the last row carries less than V_g/N, and each pile in the middle row carries some intermediate load.

Software is available that will model the entire pile group, with the appropriate P_m values applied to each row, and thus will produce the load-deformation behavior for the entire group. The computed deformations are often 2 to 3 times that which would be computed by simply allocating the applied shear load uniformly across the piles and analyzing one of these piles as if it was isolated, so this is an important design consideration.

Other software is capable of modeling only one pile. When using such software, the group effects may be analyzed using the following procedure (Hannigan et al., 2006):

1. Select a pile section, which should be the same for all piles in the group.
2. Select an appropriate lateral displacement (this is the independent variable).

TABLE 22.4 *p*-MULTIPLIERS FOR LATERALLY LOADED PILE GROUPS (Brown et al., 2010)

	P_m		
Center-to-center Spacing of Piles	Leading Row	2nd Row	3rd and Subsequent Rows
3*B*	0.70	0.50	0.35
4*B*	0.85	0.65	0.50
5*B*	1.00	0.85	0.70
≥6*B*	1.00	1.00	1.00

3. Using the software, evaluate a single pile in the first row using the appropriate P_m value and determine the applied shear load required to obtain the lateral displacement defined in Step 2.
4. Repeat Step 3 for the second and third rows. Assume subsequent rows respond like the third row.
5. Sum the applied shear loads from Steps 3 and 4 for all of the piles in the group. This is the applied shear load acting on the group, V_g, which is the dependent variable.
6. Repeat Steps 2 to 5 using different assumed lateral displacement values, thus obtaining a plot of V_g versus lateral displacement.
7. Using the curve from Step 6, check the lateral displacement at the design shear load. If necessary, adjust the pile section (Step 1) and repeat the analysis.

If only one lateral displacement is of interest (such as the allowable lateral displacement), then this process may be streamlined accordingly.

Even though some of the piles carry a greater lateral load than others, the same pile section should be used for all piles in the group. In part, this uniformity in design is used because the shear load may act in different directions. However, perhaps more importantly, using a different design for the remaining rows would introduce too much complexity.

Passive Resistance on Pile Cap

The passive pressure acting on the leading edge of the pile cap also contributes to the shear load capacity of the pile group, and usually may be considered in design so long as the upper soils are not subject to scour, liquefaction, or other similar problems. Methods for doing so are described in Section 7.10. For an ASD analysis, typically a factor of safety of 2 to 3 is applied to the passive resistance. For LRFD, a resistance factor of 0.5 is commonly used. This passive resistance is partially offset by the active pressure acting on the trailing edge of the cap, as discussed in Section 7.10. Sliding friction along the bottom of the pile cap is normally neglected.

However, the lateral deflection required to mobilize this resistance is probably much greater than the allowable lateral deflection, and most lateral designs are controlled this SLS. Using a fraction equal to the ratio of the allowable lateral deflection divided by the deflection required to achieve full passive resistance (typically 0.02–0.06 times the depth of embedment of the cap) might be appropriate. A more rigorous solution to analyzing the lateral load resistance behavior is provided by Mokwa (1999) and Duncan and Mokwa (2001). This method uses a hyperbolic load-displacement function for the cap-soil interaction. This may be an appropriate approach for use with pile groups, but it has not yet been calibrated with extensive field data.

End Restraints

The connection between the piles and the pile cap impacts the behavior of the pile group under lateral loads. If the connection between the piles and the pile cap are close to being pinned, then a free head condition exists and the pile cap translates laterally as shown in

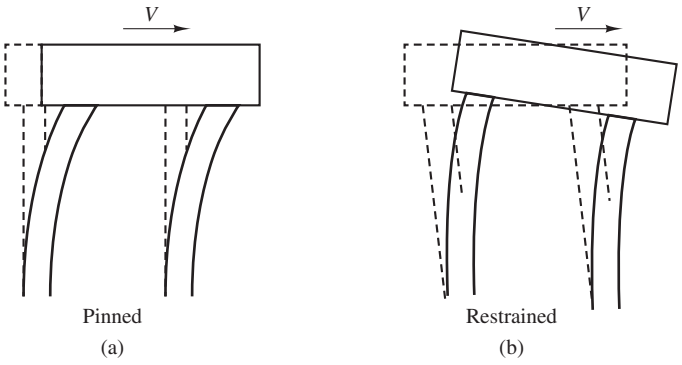

Figure 22.20 End constraints and their effect on pile groups subjected to lateral loads: (a) pinned and (b) restrained.

Figure 22.20. However, if a moment connection is present, then a restrained head condition exists and the pile cap will rotate as shown. The real condition is probably somewhere between the free head condition and the restrained head condition.

These soil-structure interaction effects are complex, but may be modeled using software such as FB MultiPier, and such models are appropriate for large structures such as major bridges. For more modest structures, engineers usually assume the restrained condition exists, and evaluate the pile response accordingly, while ignoring the rotation of the pile cap.

22.9 DEPTH TO FIXITY METHOD

During the 1960s and 1970s, lateral load behavior was commonly described in terms of the *depth to fixity*, as shown in Figure 22.21 (Davisson and Robinson, 1965; Davisson, 1970; Tomlinson, 1987). This method models the soil from the ground surface to a certain depth as having no lateral resistance, then the soil below that depth having infinite lateral resistance. The pile below this point is taken to be completely fixed against any rotation. Modeling the problem this way makes analysis and design very easy for the structural engineer, who can then analyze the pile as if it was a cantilever beam with a concentrated force and/or moment at the free end.

Unfortunately, because this model ignores the soil resistance above the fixity point, it is a poor representation of the true pile behavior. The resistance provided by the upper soils is very important, and the so-called depth to fixity as computed by this method is in reality an idealized point that does not reflect the actual conditions. Thus, the computed shears, moments, and deflections are not reliable. In addition, this method has no provision for considering group effects, and generates even more erroneous results when applied to pile groups. Although this method had some merit in the past, the widespread availability of *p-y* software and the clear superiority of the *p-y* method have made depth to fixity analyses obsolete. Even though it continues to appear in some codes, the depth to fixity method is no longer recommended.

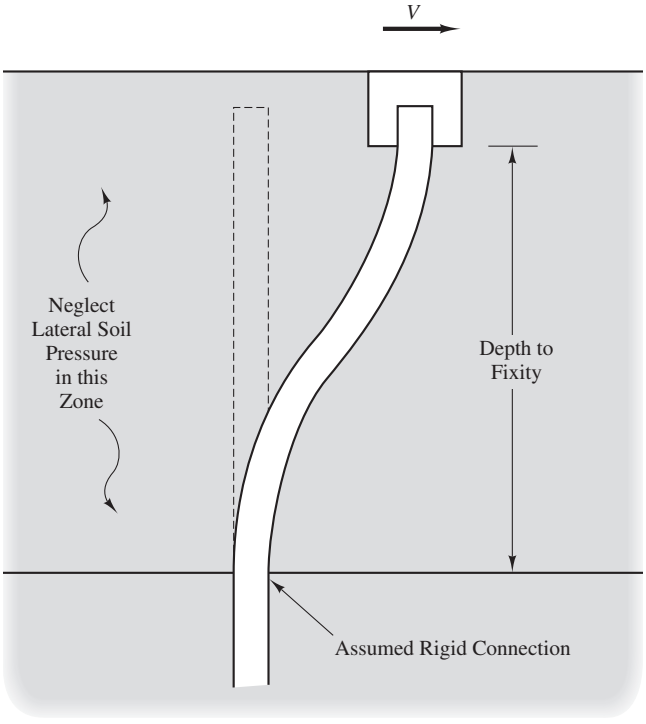

Figure 22.21 Depth to fixity method of describing the behavior of laterally loaded piles.

22.10 IMPROVING LATERAL CAPACITY

If the computed lateral resistance of a deep foundation is not satisfactory, we could improve it by adjusting the factors described earlier (i.e., diameter, moment of inertia, number of foundations in the group, spacing of the foundations in the group, etc.). Other methods, such as those shown in Figure 22.22, also may be used (Broms, 1972).

22.11 SYNTHESIS

The analysis and design of laterally loaded piles usually should begin with an assessment of whether the pile is short or long. In cases where the applied axial load is small compared to the applied lateral load, the required depth of embedment is controlled by the lateral loads and the pile may be designed as a short pile.

Lightly loaded short piles, such as those that support signs and cell phone towers, may be evaluated using a rigid analysis. The minimum required depth of embedment, D_{min}, may be determined using Broms' method, which is fast and simple, and satisfies

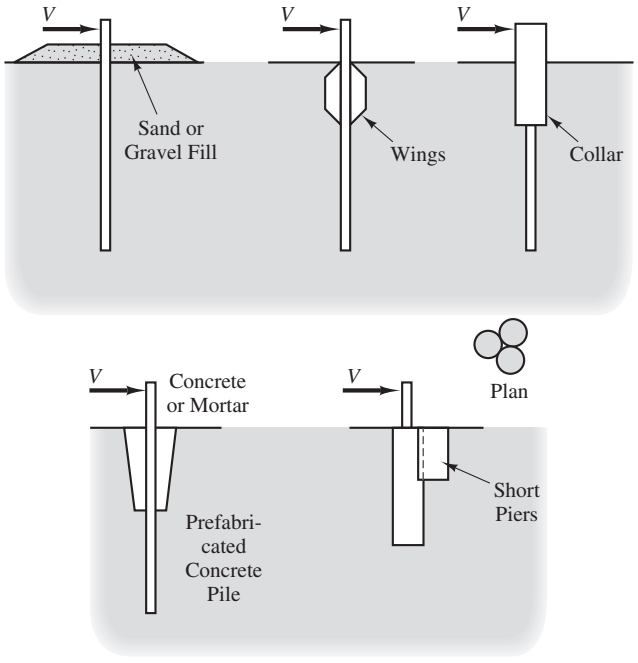

Figure 22.22 Methods of increasing the lateral resistance in piles (adapted from Broms, 1972).

the geotechnical ULS requirements. The structural ULS analysis may be based on the Broms' maximum moment, M_{max}, and the required structural section is selected based on this moment.

Note that there is no SLS analysis with rigid analyses, but the two ULS analyses should produce lateral deflections of less than 50 mm (2 in). If the SLS is deemed to be important, then use a nonrigid *p-y* analysis with a pile length equal to at least D_{min}. Also, heavily loaded short piles, such as those that support large wind turbines, justify a more detailed analysis and should be evaluated in a similar way using the *p-y* method.

If a significant axial load is present, then it will generally control the required depth of embedment (i.e., a depth greater then D_{min}) so the pile is a long pile and should be evaluated using a nonrigid analysis. This is normally the case for piles supporting buildings, bridges, and similar structures.

For long piles, first define the allowable lateral deflection based on the superstructure requirements. Then, evaluate the SLS by conducting a *p-y* analysis to determine the flexural rigidity, *EI*, required to satisfy this lateral deflection criterion. This analysis should be conducted using the unfactored loads, typically the largest load from Equations 5.4 to 5.12, or other comparable load combinations. Unlike serviceability analysis for axial loads, the design lateral load should include the full dead, live, wind, seismic, wave, and other loads, as defined by the appropriate load combinations.

There is no need to conduct a geotechnical ULS analysis for laterally loaded long piles because this limit state will not govern the final design. However, it is necessary to conduct a structural ULS analysis in order to provide sufficient flexural capacity. When using ASD, the structural section may be based on the maximum moment from the SLS analysis (if a constant structural section, such as a steel pile, is to be used) or the moment diagram (if the structural section will vary with depth, such as a drilled shaft with steel cutoffs). Consider interaction effects between the axial and flexural stresses when designing the structural section.

If the structural ULS of a long pile is to be evaluated using LRFD, then the design load must be factored using the relevant load combinations, such as Equations 5.13 to 5.19. A second *p-y* analysis is then required using the factored load with the same soil model as the serviceability analysis. The lateral deflection computed from this second analysis should be ignored, but the maximum moment (or moment diagram) is the ultimate moment, M_u, which should then be used to design the structural section.

If long piles are to be placed in groups, then the appropriate group effects must be considered in the analyses.

SUMMARY

Major Points

1. Shear loads or moment loads applied to a pile foundation may be resisted by using either battered piles or laterally loaded piles.
2. *Lateral loads* are those that act perpendicular to the foundation axis. Thus, applied shear or moment loads are lateral loads, but axial compression or tension or torsional loads are not.
3. The use of vertical piles designed to resist both axial and lateral loads often provides foundations that are more economical to build, more efficient in resisting seismic loads, and possibly more reliable.
4. The analysis of laterally loaded deep foundations is a soil-structure interaction problem that requires simultaneous consideration of structural and geotechnical aspects.
5. When conducting lateral load analyses, engineers usually assume one of the following boundary conditions at the head of the pile: the *free-head* condition, the *restrained-head* condition, or the *pure moment* condition.
6. Lateral load capacity may be evaluated using static lateral load tests, rigid analyses, depth to fixity analyses, or nonrigid soil-structure interaction analyses. Depth to fixity analyses are no longer recommended; load tests are sometimes used on larger projects; and rigid analyses may be appropriate for some designs. However, most lateral load problems are analyzed using the *p-y* method, which is a type of nonrigid soil-structure interaction analysis.

7. The *p-y method* uses nonlinear *p-y curves* to describe the lateral soil pressure acting on the foundation and a finite difference analysis to compute the deflections, shears, and moments.
8. Design *p-y curves* are based on empirical data obtained from full-scale lateral load tests. These methods use common soil properties, such as undrained shear strength, as the input parameters.
9. Pile groups subjected to lateral loads are subject to stress overlaps and shadow effects. These effects can be modeled by modifying the *p-y* curves using *p*-multiplier factors.

Vocabulary

Battered pile
Brittle soil response
Depth to fixity analysis
Ductile soil response
Fixed head condition
Free head condition
Full-scale load test
Fully restrained head condition
Lateral load
Nonrigid analysis
p-y curve
p-y method
p multiplier
Pure rotation condition
Rigid analysis
Shadow effect
Soil-structure interaction
Strain softening

QUESTIONS AND PRACTICE PROBLEMS

Sections 22.1 to 22.2: Introduction and Response to Lateral Loads

22.1 What are the primary advantages of using laterally loaded vertical piles instead of battered piles?

22.2 Explain the difference between short piles and long piles.

22.3 A static lateral load test has been conducted on an HP 10×57 pile made of steel with $f_y = 50$ k/in^2. The lateral load was applied so that bending occurred in the strong axis. According to measurements made during this test, the lateral deflection between the ground surface and a depth of 10 ft is defined by the equation $y = 1.52 - 0.001131z^{1.5}$, where both y and z are expressed in inches. Develop plots of shear, moment, and lateral soil pressure versus depth.

Sections 22.3 to 22.5: Methods of Evaluation and Rigid & NonRigid Pile Analysis

22.4 Explain the difference between a rigid analysis and a nonrigid analysis.

22.5 A group of cell-phone antennas are to be installed on a single steel pole that will be embedded into a dense silty sand with $\phi' = 35°$. Near the ground surface this pole will be connected to

a 24 in diameter drilled shaft. The resultant of the lateral wind load will be 600 lb and will act at a point 50 ft above the ground surface. Using a rigid analysis, compute the required depth of embedment and the maximum moment in the drilled shaft. Use a factor of safety of 3.0.

22.6 A large sign is to be supported on two steel poles, each of which will be supported by an 18 in diameter drilled shaft. The lateral wind load acting on the sign will be 3,000 lb and distributed evenly between the two piles. The centroid of this wind load will be 30 ft above the ground surface. The soils are sandy clays with $s_u = 2{,}500$ lb/ft^2. Using a rigid analysis, compute the required depth of embedment and the maximum moment in each drilled shaft. Use a factor of safety of 3.0.

22.7 A large sign is to be supported on two steel poles, each of which will be supported by a 500 mm diameter drilled shaft embedded into a stiff silty clay. The lateral wind load will be 5.4 kN and will act at a height of 8 m above the ground surface. This load will be equally distributed to the two poles. Using a rigid analysis, compute the required depth of embedment and the maximum moment in each drilled shaft. Use a factor of safety of 3.0.

Section 22.6: *p-y* Curves for Isolated Piles

22.8 A 12.75 in diameter steel pipe pile is driven into a saturated medium clay with $s_u = 900$ lb/ft^2 and $\gamma' = 80$ lb/ft^3. This pile is embedded to a depth great enough to be considered a long pile. Using a spreadsheet, develop a family of *p-y* curves at depths of 5, 10, 15, and 20 ft using Matlock. Plot all four curves on the same diagram.

22.9 A 500 in vdiameter steel pipe pile is driven into a saturated medium clay with $s_u = 40$ kPa and $\gamma' = 7.5$ kN/m^3. This pile is embedded to a depth great enough to be considered a long pile. Using a spreadsheet, develop a family of *p-y* curves at depths of 1, 2, 3, 4, and 5 m using Matlock. Plot all five curves on the same diagram.

Section 22.8: Group Effects

22.10 Sixteen of the piles described in Problem 22.8 are to be installed in a 4 × 4 group. Using the computed *p-y* curve for an isolated single pile (from Problem 22.8) and the appropriate *p*-multipliers, develop the *p-y* curves for the first, second, third, and fourth row of this pile group at a depth of 10 ft.

22.11 Sixteen of the piles described in Problem 22.9 are to be installed in a 4 × 4 group. Using the computed *p-y* curve for an isolated single pile (from Problem 22.9) and the appropriate *p*-multipliers, develop the *p-y* curves for the first, second, third, and fourth row of this pile group at a depth of 3 m.

23

Piles—The Design Process

Let the foundations of those works be dug from a solid site and to a solid base if it can be found. But if a solid foundation is not found, and the site is loose earth right down, or marshy, then it is to be excavated and cleared and remade with piles of alder or of olive or charred oak, and the piles are to be driven close together by machinery, and the intervals between are to be filled with charcoal . . . even the heaviest foundations may be laid on such a base.

Marcus Vitruvius, Roman Architect and Engineer
First century BCE
(as translated by Morgan, 1914)

Chapters 12–22 covered various structural, geotechnical, and construction aspects of deep foundation design. This chapter discusses how to synthesize this information and develop a comprehensive design. The process of designing and building deep foundations is challenging in many ways, including:

- There are many different deep foundation types, and each of them can be built in a variety of different ways, so there are almost always multiple ways to design a deep foundation system. For example, the foundations to support a bridge bent might consist of a group of driven piles connected with a cap or a single large diameter drilled shaft. If piles are selected, the engineer might use a large number of short piles, or a smaller number of long piles. There also are options for the pile material—steel pipe piles? Prestressed concrete piles? Even this is only a partial list of the possibilities.

- The design process requires interaction between geotechnical engineers and structural engineers, along with knowledge of construction processes. Both are important contributors to the design process, and optimal designs often require back-and-forth interaction between them.
- The subsurface conditions have a significant impact on the design, so the required foundation system for identical structures might be dramatically different if they are to be built on sites with differing subsurface conditions.
- The design is often subject to revision based on the actual conditions encountered during construction. For example, the subsurface conditions at a specific location on the site may differ from those found in the nearest boring, so the length of the pile may need to be adjusted accordingly. Thus, the design drawings represent a tentative or expected design that may need to be modified during construction. Such changes are a routine part of deep foundation construction.

This chapter presents design as a mostly linear and systematic process. However, keep in mind that the actual process is often much more complex and subject to change. Nevertheless, a systematic presentation, even if somewhat idealized, shows the interaction between the various aspects of the design and construction process, and helps develop the skills and judgment required to navigate through real projects. The processes described in this chapter also assume a close collaboration between the geotechnical engineer and the structural engineer, including two-way exchange of information during the design process.

23.1 UNSTABLE CONDITIONS

The pile analysis and design methods discussed thus far have included an implicit assumption that the soil profile is stable, and that changes are due only to stresses or displacements associated with the pile construction, or possibly with a change in the groundwater conditions. However, if this assumption is no longer true, then any potential instability must also be considered in the design process. Four unstable conditions are of particular interest:

- Scour
- Downdrag
- Seismically-induced liquefaction
- Landslides

Scour

Scour is the rapid erosion of soil due to the action of flowing water. This phenomenon is especially important in the design of foundations for structures adjacent to waterways, such as bridges, piers, docks, and marine structures. Even ephemeral rivers, which may be dry much of the year, can be subject to extensive scour during flash floods. Mueller

and Wagner (2005) reported that more than 2,500 US bridges were severely damaged or destroyed due to scour in 1993 alone.

A hydraulic evaluation forms the basis for estimating the scour zone, which can extend several meters below the river bottom. All foundations must extend below any potential scour zone for the design flood (Arneson et al., 2012), so deep foundations are usually necessary. These foundations must be designed to safely support the design loads even if the upper soils are lost to scour.

Piles are built at such sites before the scour occurs, so constructability considerations, such as driveability, are governed by the unscoured soil profile, while design capacity is governed by the post-scour soil profile. This difference can make it difficult to meet both constructability and capacity requirements.

Scour also reduces the lateral load capacity of piles because the upper soils are no longer present to provide lateral support. In other words, the distance from the structure to the ground surface becomes greater, so the moment in the piles increases. In addition, the exposed piles are now also subject to lateral forces from the moving water. Therefore, it becomes necessary to use larger pile sections or battered piles to support the lateral loads.

Downdrag

Projects on sites underlain by soft soils often require placement of imported fill to raise the grade to a higher elevation. Such fills provide flood protection, facilitate surface drainage, provide better support for surface improvements such as pavements, and other benefits. For bridges, approach fills are often used to facilitate a transition from the natural ground to the bridge abutment. Lightweight structures might even be supported on shallow foundations founded in the fill. However, heavy structures are typically supported on piles that penetrate through the fill and soft soils and into the underlying firm soils, as shown in Figure 23.1. These piles are typically constructed after the fill is placed.

In this situation, the weight of the fill causes consolidation in the underlying soft soil, so both the fill and the soft soil move downward. However, if the piles are suitably supported by strong and stiff soils beneath the soft soil, they experience very little settlement. The resulting downward movement of the soft soil and fill with respect to the pile produces a downward side friction force, which becomes a load instead of a resistance. This downward force is called *downdrag load* or *negative side friction*, and can be large enough to overload the piles (Bozozuk, 1972, 1981). Because of the variations in soil properties, fill thickness, and other factors, downdrag loads are usually greater on some foundations beneath a structure and less on others. This can cause significant differential settlements in the structure.

Downdrag loads also can occur in other situations that cause a downward soil movement with respect to the upper portion of a pile. For example, a drop in the groundwater elevation can cause settlement because of the corresponding increase in the effective stress, even if no fill is placed. Downdrag also can occur during an earthquake when the seismic forces cause the soil to settle, especially in loose sands.

We can compute the magnitude of downdrag loads using the methods for computing side friction, as described in Chapters 15–18, except the load acts downward instead

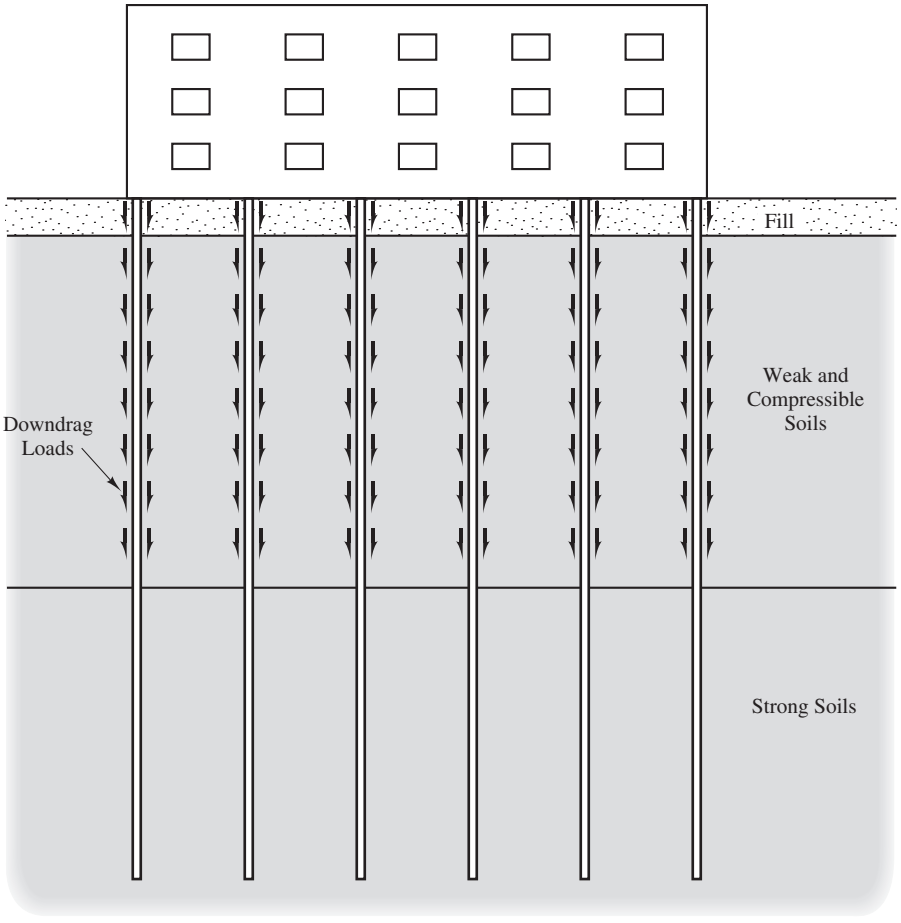

Figure 23.1 Use of piles to penetrate through weak and compressible soils into deeper strong soils. The weight of the overlying fill causes consolidation in the upper soils, thus producing downdrag loads on the piles.

of upward. Also note that, unlike computations of resistance, the use of higher α and β values is conservative.

With LRFD design, downdrag is considered to be a load and thus must be multiplied by an appropriate load factor. AASHTO specifies load factors of 1.4 for driven piles evaluated using the alpha method, 1.05 for driven piles evaluated using the lambda method (a technique not covered in this book), and 1.25 for drilled shafts evaluated using the O'Neill & Reese method.

To design the foundation, determine the location of the neutral plane as shown in Figure 23.2. This plane is located at the point on the foundation where there is no relative movement between the soil and the foundation (Fellenius, 1999). In other words, the

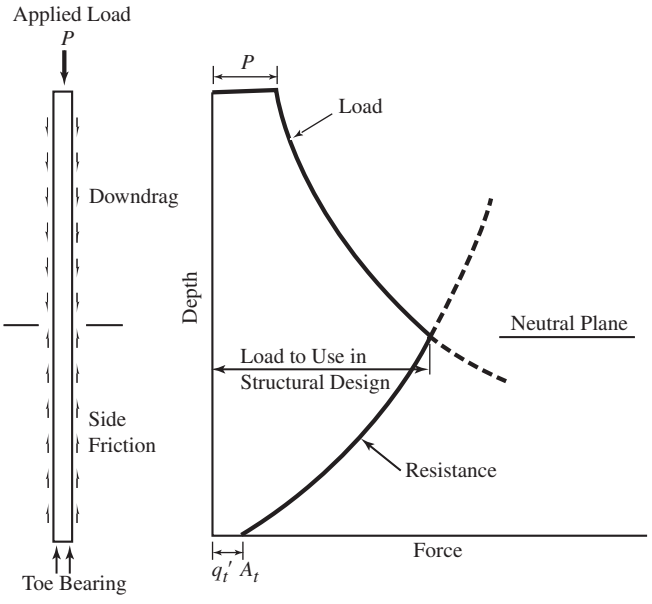

Figure 23.2 Method of locating the neutral plane (adapted from Fellenius, 1999).

downdrag load acts from the ground surface to the neutral plane, and the side friction resistance acts below the neutral plane.

To develop the plot in Figure 23.2, begin at the top of the pile and mark the applied downward load. This value should be the service loads used for settlement analysis. Then compute the downdrag load at various depths and develop a plot of downdrag load versus depth.

Next, mark the ultimate toe bearing capacity at the bottom of the pile, and compute the ultimate side friction capacity at various depths. Use this data to develop a plot of upward resistance along the length of the pile. The neutral plane is located at the point where these two plots intersect, and the load at this point is the greatest compressive load in the foundation. The structural design should be based on this load.

There is some difference in opinion on how to evaluate the geotechnical downward load capacity of deep foundations subjected to downdrag loads. Usually the downdrag load is subtracted from the allowable downward load capacity. In some cases, this approach results in a substantial reduction in the allowable downward load capacity, which means additional foundations or longer foundations will be needed to support the structure.

An alternative approach (Fellenius, 1998) argues the downdrag load is detrimental to the geotechnical load capacity of a deep foundation only if it induces excessive settlement. Therefore, Fellenius recommends conducting a settlement analysis. If the toe of the foundation is supported by firm soil or bedrock, the downdrag load will not induce significant foundation settlement and thus should not be subtracted from the geotechnical load capacity. In addition, Fellenius argues that live loads cause enough settlement to temporarily reverse the direction of relative movement between the foundation and the soil, so downdrag load and the live load will never act simultaneously.

If the design downdrag loads are large enough to significantly impact the foundation design, engineers often consider implementing one or more of the following downdrag reduction techniques:

- Coat the pile with bitumen, thus reducing the coefficient of friction (Bjerrum et al., 1969; Tawfiq and Caliendo, 1994). This method is very effective, so long as the pile is not driven through an abrasive soil, such as sand, that might scrape off the bitumen coating.
- Drive the piles before placing the fill, apply bituminous coating (optional), wrap the exposed portions with lubricated plastic sheets or some other low friction material as shown in Figure 23.3, and place the fill around the piles.
- Predrill using an auger slightly larger than the pile, partially fill the hole with bentonite (optional), then drive the pile in the hole.
- Use a pile tip larger in diameter than the pile, thus making a larger hole as the pile is driven. Alternatively, install a ring at an appropriate depth on the pile, to create the same effect only in the upper portion of the installed pile.
- Drive an open-end steel pipe pile through the consolidating soils, remove the soil plug, then drive a smaller diameter load-bearing pile through the pipe and into the lower bearing strata. This isolates the inner pile from the downdrag loads and thus is sometimes called an *isolation casing*.
- Accelerate the settlement using surcharge fills or other techniques, and then install the foundations after the settlement is complete.

Figure 23.3 These H-piles will support a bridge abutment. They extend above the ground surface because the abutment fill has not yet been completed. Since the underlying soils are compressible and will settle due to the weight of the fill, the piles have been wrapped with a specially designed lubricated plastic sheeting to reduce the downdrag forces between the piles and the fill. A mechanically stabilized earth (MSE) wall is being constructed around these piles. When complete, the backfill will extend approximately 1 m above the wrapped area of the piles (courtesy of Foundation Technologies Inc.).

Even if the problem with downdrag loads is adequately addressed in terms of pile design, the ground surface still settles due to consolidation of the underlying soils, but the structure remains at virtually the same elevation. Thus, a gap forms between the structure and the ground. Settlements of 0.5 m (2 ft) or more are not unusual at a soft ground site, so the structure could eventually be suspended well above the ground surface. This creates serious serviceability problems, including access difficulties, stretched and broken utility lines, and poor aesthetics. This problem is especially common where approach fills meet pile-supported bridge abutments, and results in an abrupt bump in the roadway pavement at the edge of the bridge.

Figure 23.4 shows this type of settlement problem in a supermarket building which was built on a pile foundation. The ground surface around this building settled about 400 mm in twenty five years, which required continual maintenance including continual placement of new asphalt pavement around the building.

Another way to address such problems is to use soil improvement, as discussed in Chapter 26. If the consolidation process can be accelerated and completed before the piles are constructed, then the downdrag loads will be eliminated.

Seismically-Induced Liquefaction

Seismically-induced soil liquefaction is a rapid loss in the shear strength of certain soils as a result of the buildup of excess pore water pressures, and the vast majority of earthquake-related pile failures have been the result of *seismic liquefaction* of the soils around or

Figure 23.4 The ground around this pile-supported supermarket settled about 400 mm in twenty five years, but the building remained at essentially the same elevation. This required continual maintenance around the perimeter of the building. Note the steep slope to reach the front door and the spacer blocks required at the top of the footing supported posts which settled with the surrounding ground.

beneath the foundation (Martin and Lam, 1995). A common method of building on liquefiable soils is to support the structure on piles that penetrate through these soils into underlying non-liquefiable strata. Although this method is a viable solution, there are additional considerations, including:

- The liquefied soils provide substantially less lateral resistance, so the flexural stresses in the piles due to the lateral seismic loads are correspondingly higher. This can produce excessive lateral deflections, and even flexural failure in the piles.
- Liquefaction may be accompanied by seismically-induced ground settlement, which can create downdrag loads on the piles. This can result in excessive settlement or compressive failure of the pile.
- On sloping ground, such as along river banks, the liquefied soil often moves laterally creating a phenomenon known as a lateral spread. This moving soil typically pushes deep foundations out of position, which can produce catastrophic failures (Bartlett and Youd, 1992; Ashford, Boulanger and Brandenberg, 2011). Figure 23.5 shows one such failure. Lateral spreads have occurred even on gently sloping ground, and therefore must be carefully evaluated. These problems can result in excessive lateral displacement, excessive settlement, and even flexural failure of the piles.

Figure 23.5 A bridge snapped into pieces after the magnitude-7.5 Niigata quake struck. *Source*: Keystone Pictures/ZUMA Press/Alamy.

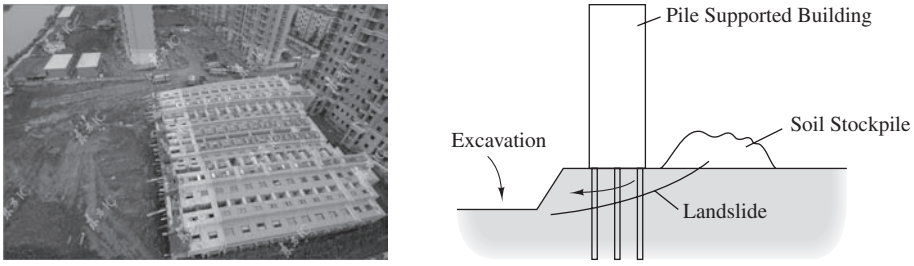

Figure 23.6 On June 27, 2009 a 13-story supported Shanghai apartment building collapsed while under construction as seen in (a). The collapse was due not a foundation failure per se, but to a landslide caused by creating both an excavation on one side of the building and a soil stockpile on the other side as shown in (b).

These problems can be addressed by considering the associated loads in the design process, or by remediating the liquefaction hazard, such as through the soil improvement methods discussed in Chapter 26.

Landslides

In addition to seismically-induced lateral spreads, other kinds of landslides also can impose substantial lateral loads on piles. It is very difficult to design for these large loads, so structural failure can occur. One of the most dramatic examples is a 13-story condominium building in Shanghai which was subject to a landslide caused by construction of 4.6 m deep excavation on one side of the building and stockpiling the cuttings on the other side, shown in Figure 23.6. The landslide easily broke the piles, causing the entire building to collapse.

23.2 PILE TYPE AND CONFIGURATION

Driven piles, drilled shafts, auger piles, and the various specialty pile types each have their advantages and disadvantages, as discussed in Chapter 12, and the optimal choice of pile type for a particular project depends on many factors. Usually only one pile type is used in order to minimize equipment mobilization costs and to simplify the construction process, and once construction begins, it is difficult to change pile type, so this is an important decision.

The selection of pile type is primarily within the geotechnical engineer's domain. However, this decision should be performed in consultation with the structural engineer, and in some cases it is also appropriate to consult with a contractor. Factors to be considered include:

- **Design Loads**—Structures with heavy loads, such as major bridges or large buildings, require different types of foundations than those with lighter loads. In addition, the type of load (compression, uplift, shear, moment) also influences the selection.

- **Subsurface Conditions**—Subsurface soil and groundwater conditions affect the various pile types in different ways and can have a major impact on constructability. For example, drilled shafts can be easily constructed using the open hole method in firm soils above the groundwater table, but become much more difficult to build below the groundwater table and when the soils are subject to caving.
- **Local availability of contractors with the required equipment and expertise**—All pile types require skilled contractors who have the necessary equipment and experience. Driven pile contractors are available in most areas, and are probably the most tolerant of variations in construction methods. Drilled shaft contractors capable of constructing dry open holes also are widely available. However, drilled shaft construction with casing or drilling mud requires a much higher skill level and better quality control procedures, so capable contractors are less common. Auger piles require specialized equipment and a highly skilled contractor with robust quality control procedures. Specialty methods, such as pressure injected footings, typically require highly specialized contractors that often must be mobilized from long distances.
- **Local availability of materials**—When driven piles are selected, the local cost and availability of the pile material must be considered. In some areas, steel is used for virtually all driven piles, while in other areas prestressed concrete dominates. Often this difference is driven largely by the proximity of steel mills and pile casting yards. Cast-in-place methods require either a local concrete batch plant or the ability to set up an onsite portable plant.
- **Construction environment**—Difficult environments, such as offshore foundations or bridge piers located in rivers often limit the pile types that can be used.
- **Precedent**—Pile types that have been successfully used on nearby projects are often preferred over untried methods. However, the engineer also must be open to other pile types, as appropriate, even if there is no local experience.
- **Reliability**—The as-built foundations must be able to reliably support the applied loads. Certain foundation types might not be good choices at certain sites, because the subsurface conditions might not be conducive to construction of reliable foundations.
- **Cost**—The cost of construction must be kept to a minimum, commensurate with the other requirements.
- **Availability of materials, equipment, and expertise**—Both piles and drilled shafts are viable options in all but the most remote locations because of the large number of contractors who are able to build these foundations. However, some of the other types may not be readily available in certain areas. For example, pressure injected footings (Franki piles) are very commonly used in western Canada, and can be specified without concern about the availability of qualified contractors. However, this type is rarely used in California, so suitable equipment and expertise would probably need to be brought in from far away, and thus be more expensive.
- **Local experience and precedent**—Most projects are near other structures with similar foundation requirements. Methods that have been successful on these past projects are often favored over untried methods.

- **The level of concern, if any, regarding noise and/or vibration**—This can be a major concern in urban areas, especially when construction is in close proximity to sensitive existing facilities, such as hospitals. Driven piles can be especially problematic, although methods are available to reduce their noise and vibration.
- **Physical constraints**—Right-of-way restrictions, existing underground improvements, or existing structures can significantly limit site access—For example, a foundation in an existing highway median may have very limited working space.
- **Soil Disposal**—Disposing of soil cuttings may be an issue particular if the site is underlain by hazardous materials—This matter is especially problematic with drilled shafts.

In many cases, more than one pile type will satisfy all of these technical selection criteria. At that stage, the selection is typically driven by cost.

When using driven piles or auger piles to support buildings, individual columns must be supported on a group of at least three piles, but a four pile group is a more common minimum number, as shown in Figure 23.7. This configuration accounts for construction tolerances in placing the piles, and is typically necessary in order to provide sufficient load capacity. It also provides redundancy in the design. Bearing walls are inherently stable in one direction, and thus may be supported on a series of piles offset on both sides of the wall, as shown in Figure 23.8. The corners of bearing walls are inherently stable in both directions, and thus may be supported on a single pile.

Drilled shafts can be constructed with much larger diameters, so a modest eccentricity in the applied load due to construction tolerances is much more tolerable. In addition, a single large diameter shaft typically has the same axial load capacity as a group of smaller diameter piles. Thus, a single shaft may be used to support each structural element, thus saving the cost of a pile cap. However, large diameter shafts require large volumes of concrete, which also is a cost consideration.

For bridges, individual bents may be supported on a group of driven piles or auger piles, or on a single large diameter shaft. For single-column piers, drilled shafts as large as 3 m (10 ft) diameter are very common, as shown in Figure 23.9.

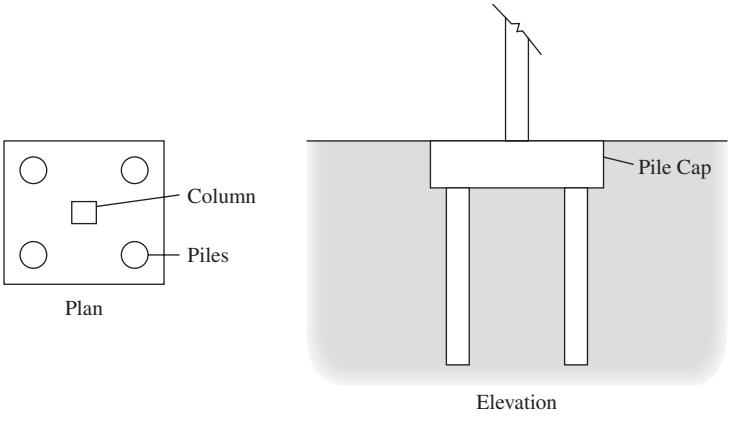

Figure 23.7 Typical pile configuration beneath a column. A minimum of three piles are required.

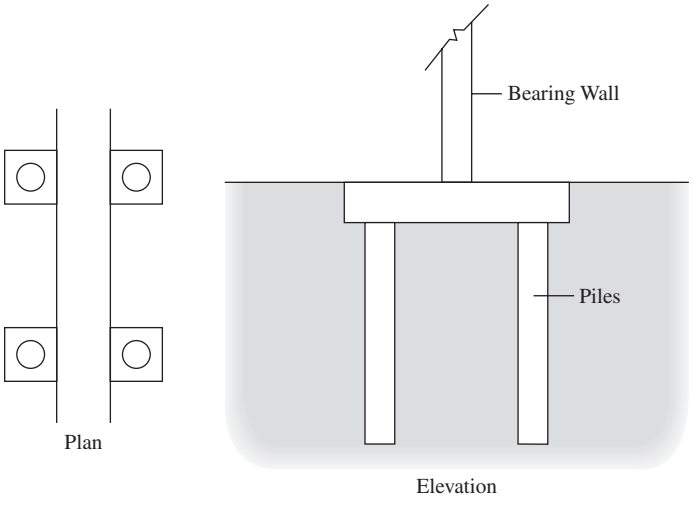

Figure 23.8 Typical pile configuration beneath a bearing wall. The piles are placed in pairs.

Figure 23.9 This 2.4 m (8 ft) diameter drilled shaft will support a bridge bent. It has been excavated using the dry method and the steel reinforcing cage is about to be placed. Another similar steel cage is visible in the background. The chain-like fencing is a safety precaution and is about to be removed.

23.3 REQUIRED AXIAL PILE CAPACITY

The pile design process begins with identifying the design loads. For buildings, these loads should be tabulated for each column, bearing wall, and other structural members. For bridges, the loads at each bent and each abutment should be identified. For the ultimate limit state, the ASD design loads would include the design downward, uplift, shear, and moment loads. For LRFD, the corresponding factored loads should be tabulated. If serviceability analyses are to be performed, then the corresponding sustained loads also should be tabulated using the techniques described in Chapter 5.

For most structures, the largest design load is the downward load, so it is typically best to begin the design process by considering this load. In theory, the foundation for each structural element would be designed individually to accommodate its design downward load. However, this approach typically produces a very complex design, with each structural member having a unique foundation design. Such complexity creates construction logistics problems and increases the potential for mistakes. Thus, in practice the design is simplified. For example, an engineer might choose to use 15 m (50 ft) long HP12 $\times$ 63 piles to support a proposed building, each of which has an allowable downward load capacity of 900 kN (200 k). If a certain column has a design load of 3,500 kN (800 k), then four piles would be used. Another column with a design load of 4,000 kN (900k) would require five piles, even though this provides more capacity (4,500 kN or 1,000 k) than needed.

Selecting the optimal design capacity per pile is an important part of developing the most cost-effective pile design. For typical buildings, perhaps as many as three or four different design capacities might be used, thus generating a corresponding number of pile designs. For typical buildings, these design capacities can be developed using the following principles:

1. **Use high capacity piles**—Fewer high capacity piles produce a more economical foundation than a larger number of lower capacity piles. This is because: (a) Higher capacity piles are generally deeper, thus engaging soil that generates higher unit side friction resistance and thus less total pile length, and (b) The cap size is smaller. However, using piles that provide more capacity than needed is wasteful.
2. **Avoid excessive complexity**—Use no more than three or four different pile designs. Ensure each design represents at least 20 percent of the total number of piles.
3. **Use only one pile type to support each structural element**—Using multiple pile types in one pile group can lead to dangerous errors. At the same time, number of piles required for each structural element should be selected such that the required pile capacity is achieved with the least amount of excess capacity.

Once the required axial downward capacities have been determined (perhaps as many as three or four), the other required design load capacities should be identified for each pile. These include the required uplift capacity and the required lateral capacity.

23.4 GEOTECHNICAL DESIGN

The objective of the geotechnical design process is to determine the required diameter, length, and flexural rigidity to satisfy the geotechnical ultimate limit state (ULS) and serviceability limit state (SLS) requirements. These goals are achieved using the techniques described in Chapters 13–20 and 22.

Lateral Load Analysis and Design

If some or all of the piles will be subjected to significant lateral loads, the geotechnical design process should begin with a lateral load analysis. This will help define the minimum required pile diameter and section properties. For the vast majority of projects, lateral load analyses are based on published *p–y* curves, as discussed in Chapter 22. Static lateral load tests are not widely used in practice.

For example, the pile type analysis (Section 23.2) may have indicated prestressed concrete, steel pipe, and drilled displacement auger piles are the most viable options for a particular site, and the pile capacity analysis (Section 23.3) may have indicated three pile designs will be used, each of which has a certain design lateral load and allowable lateral displacement. The geotechnical engineer would then conduct *p–y* analyses for each of these nine combinations to determine the flexural rigidity, *EI*, and diameter, *B*, required to satisfy the lateral load design requirements. It is often most effective to select various values of *B*, then find the required *EI* for each until an optimal pile section is found.

The results of these analyses must be developed with at least informal consideration of other performance requirements and cost. For example, with steel pipe piles, the lowest material cost is generally obtained by using large diameter thin-wall pipes. However, overly thin walls may create driveability problems, and the geotechnical axial load design may favor another diameter.

Axial Load Analysis and Design

First Trial Design

The axial load analysis nearly always begins with a static analysis using methods such as those described in Chapters 15–18. Using these methods and the results of the lateral load analysis, determine the pile length that will provide the required axial load capacity. In a fairly homogeneous soil profile that has no distinct bearing stratum, the most economical design is probably obtained by using the smallest diameter consistent with the lateral load requirements and a comparatively long pile. However, be cautious about using lengths that will require splicing (for driven piles) and avoid lengths that are beyond the capabilities of drill rigs (for drilled piles). In other cases, the soil profile influences or dictates the pile length. For example, if the trial pile length is 20 m, but a much stronger soil stratum

is present at a depth of 21 m, the pile should be extended to take advantage of this better bearing stratum.

If only static analyses are to be performed, then this trial design becomes the final design. Given the uncertainties in these methods, the associated factor of safety will be fairly high. However, the use of load tests or indicator piles can provide additional information that can be used to justify lower factors of safety and to further optimize the design.

Static Load Testing

The next step in the design process, which is optional, consists of conducting static load tests on one or more a prototype piles, as described in Chapter 14. Load tests provide much more accurate assessments of the axial load capacity, and thus can be used to justify a lower factor of safety (or higher resistance factor), and thus a more cost-effective design for the production piles. However, the construction cost savings must be balanced against the cost and time associated with conducting the load test.

If static load tests are conducted well in advance of construction of the production piles, then an extra equipment mobilization will be required to install the test piles. This can significantly increase the cost of the test, especially for driven piles. Alternatively, if the test is conducted soon before the start of production pile construction, it may be possible to leave the installation equipment onsite. However, this approach may result in last-minute changes in the pile design.

The cost of pile load tests also depends on the expected capacity of the pile. Low capacity piles require modest size test frames and can be load tested more economically. The opposite is true for high capacity piles, and the cost of testing very high capacity piles may be prohibitive.

If driven piles are being used, the static methods can be supplemented by driving records, which also can be used to economize the design. However, this information is not available for other pile types.

Thus, many factors influence the decision to conduct static load tests or not. These factors are more likely to favor conducting load tests when the project is large and has many piles, and thus more potential for construction cost savings. Conversely, smaller projects often have lower total cost without load tests and using the more conservatively designed piles.

For example, extensive static load tests were performed for the I-880 freeway reconstruction project in Oakland, California (which was required because of the collapse of a viaduct during the 1989 Loma Prieta Earthquake). This $3.5 million test program produced $10 million in savings because it enabled a more precise design of the production piles.

Full-scale static load tests are most likely to be cost-effective when one or more of the following conditions are present:

- Many foundations are to be installed, so even a small savings on each will significantly reduce the overall construction cost. Static load tests are more likely to be

cost-effective if large quantities of production piling, perhaps 3,000 m (10,000 ft), are to be installed.

- The soil conditions are erratic or unusual, and thus difficult to assess with the analytic methods described in Chapter 14.
- The pile is supported in soils that are prone to dramatic failures (i.e., a steeply falling load-settlement curve).
- The structure is especially important or especially sensitive to settlements.
- The engineer has little or no experience in the area.
- The foundations must resist uplift loads (the consequences of a failure are much greater).

The state-of-practice for static load tests varies significantly from one geographic area to another. In some areas, they rarely are performed, even for very large structures, whereas elsewhere they are required for nearly all pile-supported structures. Sometimes these differences in practice are the result of local soil and geologic conditions or building code requirements. However, in other cases, the underutilization or overutilization of static load tests seems to be primarily the result of custom and habit.

Dynamic Load Testing

Dynamic load testing, as described in Chapter 19, is an increasingly popular alternative to static load testing, especially on high capacity piles. For driven piles, prototype *indicator piles* may be driven using a pile driving analyzer and the load capacity may be determined using a wave matching analysis. The results are then used to refine the design of the production piles, and to take advantage of the lower factor of safety (or higher resistance factor).

Dynamic load testing also may be conducted on drilled shafts and auger piles using a drop weight or Statnamic test. Although this method requires mobilization of additional equipment, the overall test cost may be less than that of a static load test.

23.5 STRUCTURAL DESIGN

At this stage, primary responsibility for the design process shifts to the structural engineer, who is responsible for satisfying the structural limit state requirements and for developing the design drawings and specifications.

The pile cap also must be designed at this stage. In seismic areas, and elsewhere where significant uplift or lateral loads are present, the detailing between the individual piles and the cap will require special attention.

The results of this effort are presented in the form of design drawings and specifications. The drawings indicate the number, size, spacing, and anticipated depth of foundations for each column. The specifications provide other design information, such

as material strengths, special procedures, and so forth. The completed design drawings should be sent back to the geotechnical engineer for review, to be sure the geotechnical design recommendations have been properly implemented. On difficult projects, it may be helpful to also have the drawings reviewed by a construction engineer. Once they have been finalized, these drawings and specifications become part of the complete design package, which is presented to the contractor. It is important that these documents be correct and complete, because they become a key element in the contract between the owner and the contractor.

23.6 VERIFICATION AND REDESIGN DURING CONSTRUCTION

Pile design drawings are normally bound with the remaining drawings, and may appear to be no different than floor plans, structural connection details, or the many other structural and architectural drawings. It may seem that completing of these drawings and the related specifications signals the end of the design process, and that the contractor must simply build the piles as shown on the drawings. However, this is not the case. The design of pile foundations continues throughout construction, not because there was any deficiency in the original design, but because all of the information needed for design was not yet available.

The as-built piles may be significantly different from those shown on the design drawings. These differences are primarily due to the differences between the subsurface conditions anticipated in the design and those actually encountered during construction. For example, the piles may have been designed to develop toe bearing in a certain stratum, but the depth to that stratum inevitably varies across the site. Thus, the as-built depth of embedment cannot be determined until the pile is actually being built. In the case of driven piles, this might be based on blow counts, while with drilled shafts it is based on the soil types extracted by the auger. This is one of the most important reasons why the geotechnical engineer (and to a lesser degree the structural engineer) continues to play an active role during construction, and why the as-built piles are often substantially different from those shown on the design drawings. In fact, a pile foundation system built exactly as designed would be the exception rather than the rule.

Another reason geotechnical engineers are involved during pile construction is to participate in the quality control and quality assurance processes. The foundation contractor is responsible for constructing piles that meet the requirements outlined in the drawings and specifications, while the geotechnical engineer reviews the procedures and construction.

Therefore, the geotechnical engineer has a representative onsite to observe the construction process. This field engineer has two primary responsibilities: to confirm that the as-built foundations satisfy the intent of the design drawings and specifications, and to note the need for changes in the design as a result of changed subsurface conditions. Small design changes are typically made immediately, while more substantive changes require consultation with the geotechnical engineer and/or the structural engineer.

Driven Piles

One of the important advantages of driven piles is that the hammer blow count can be monitored for every pile, thus providing information that guides the construction process and provides useful quality control. Although blow count alone is not a satisfactory method of confirming pile capacity, it often is used as a key factor in the construction process.

Wave Equation Analyses

A wave equation analysis should be performed for the benefit of both the design engineer and the foundation contractor. This analysis is discussed in Chapter 19 and has two main purposes: to assess driveability and to develop a bearing graph.

Driveability analyses are intended to determine if the pile can be driven without causing structural damage. These analyses help determine if the planned pile can be installed at the site with reasonable equipment and a reasonable blow count, and it assists the contractor in optimizing the hammer and accessories. If the driveability is a concern, this analysis should be performed during the design stage even before the contractor has been selected by using assumed hammer size and other input data. This helps avoid generating designs that cannot be built, thus avoiding unpleasant surprises during construction. If this analysis indicates potential driveability problems, the design must be revised accordingly. For example, in the case of steel pipe piles, the wall thickness required to resist driving loads may be greater than the wall thickness required to resist the service loads. A more accurate driveability analysis can be conducted immediately before construction using data for the actual hammer to be used in construction.

A bearing graph is a plot of final blow count versus axial load capacity and forms a basis for construction control. The field engineer uses this graph along with knowledge of the design parameters to determine the final penetration depth for each production pile. Sometimes the piles must be driven until a certain blow count is achieved, while other times it must be driven a certain distance into a specific stratum.

Setup and Relaxation

Setup or relaxation can have a significant influence on driven pile capacity, as discussed in Chapters 13, 15, and 19. Although this effect can be roughly estimated in advance, such as through the use of Table 15.8, the actual magnitude is difficult to predict. Setup is much more common than relaxation, so underestimating or even ignoring this effect is conservative, however doing so can be overly conservative, especially in clays. A better approach is to evaluate setup or relaxation during construction and incorporate it into the pile design.

One method of evaluating setup is to conduct a dynamic analysis, such as Case method or CAPWAP, using the end of driving (EOD) data on an indicator pile, and again using beginning of restrike (BOR) data obtained on the same pile some days later

(Komurka, 2004). The ratio of these two capacities is the setup factor for that site, which then may be applied to the production piles.

Drilled Shafts

Although drilled shaft construction does not generate hammer blow count information, the soil strata encountered during drilling can be monitored by observing the cuttings as they are brought to the ground surface. In addition, the difficulty of drilling can change as harder strata are encountered. This information can be used to compare the anticipated conditions, and it provides valuable construction control. High quality construction control will allow the as-built depth of drilled shafts to be altered during construction, as necessary, to accommodate the actual soil conditions.

For example, in a subsurface profile consisting of weak soils underlain by much stronger soils, the bulk of the load capacity will be developed in the stronger strata. Thus, the depth of penetration into the strong strata is more important than the depth below the ground surface. The construction cuttings may be used to determine the actual depth to this interface, and the design can specify a certain depth of embedment below that point.

The field engineer also checks for a variety of construction procedures, especially those that might impact caving or other similar problems. With end bearing shafts, the contractor must confirm that the bottom is clean and free of debris before placing the concrete. In dry holes, it may be possible to shine a light down the hole and observe the bottom from the ground surface. A variety of remote techniques have also been used, especially down-hole video cameras. Holden (1988) describes a down-hole camera equipped with water and air jets that is capable of observing the bottom of holes drilled under bentonite slurry.

Auger Piles

Unlike drilled shafts, auger cast-in-place (ACIP) piles use a continuous flight auger, so it is more difficult to associate the cuttings arriving at the ground surface with a specific depth. Nevertheless, monitoring the cuttings can still be useful. The drill rigs also can be equipped with instrumentation to measure the torque, which can be a very good indicator of the soil conditions being encountered at the auger tip, and thus may be used as a means of construction control. Well-equipped rigs also have other instrumentation to monitor grout take, grout pressure, and other parameters, which help control the construction process.

Drilled displacement (DD) piles generate little or no cuttings at the ground surface. However, because substantial torque is required to push the soils aside, the drilling torque can be a very good indicator and may be used as part of the construction control process.

23.7 INTEGRITY TESTING

As-built piles are hidden from view, and thus cannot be visually inspected, so even with good construction procedures some defects may be present and threaten the structural integrity of the pile. Thus, the use of post-construction integrity testing is becoming increasingly

popular. The purpose of these integrity tests is to confirm that the as-built foundation is structurally sound and does not contain any significant defects. A variety of methods are available, some of which are simple and inexpensive, while others are more precise but also more expensive (Litke, 1986; Hertlein, 1992; Hertlein and Davis, 2006).

Integrity testing is primarily used in concrete piles. Driven concrete piles have the advantage of being prefabricated in a controlled environment, but can be damaged during installation. Serious damage, such as a pile that breaks underground, can often be detected by a sudden drop in the blow count, and may be accompanied by a sudden drift away from being plumb. However, other defects in driven piles, while still important, are more subtle and more difficult to detect.

Cast-in-place concrete piles, especially drilled shafts and auger piles, are more problematic because the concrete is placed in a much less controlled environment and thus is subject to a number of potential defects, including:

- Segregation of the aggregates, causing non-uniformities in the finished concrete.
- Failure of the concrete to properly flow between the reinforcing steel, thus creating voids and exposing the steel to a corrosive environment.
- Caving of surrounding soil, creating soil inclusions within the concrete.
- Inflow of groundwater or drilling mud, creating soft inclusions within the concrete.

None of these defects will be evident from the ground surface, yet all threaten the structural integrity of the completed pile. Thus, cast-in-place piles are especially good candidates for post-construction non-destructive integrity testing, and this is where these methods are most often used.

Methodologies

High Strain Dynamic Testing

High strain dynamic testing methods, as described in Chapter 19, are primarily intended to develop axial load capacities. However, these tests have the ancillary benefit of also providing information on structural integrity. Certain kinds of defects, such as a local reduction in the pile diameter (necking) or large foreign inclusions produce reflected waves which can be detected in the records obtained at the top of the pile.

Sonic Echo

Low strain sonic methods use many of the same principles of wave mechanics, but do so with a much smaller impact energy that is far less than that required to mobilize the side friction resistance (Hearne, Stokoe, and Reese, 1981 and Olson and Wright, 1989). Typical energy sources include a hand-held mallet or small drop hammer, and the waves are monitored by a small portable accelerometer, as shown in Figure 23.10. The data processing is accomplished in a hand-held unit, as shown. Unlike high strain sonic echo, this method does not provide any information on pile capacity, but it can often detect necking or large

(a) (b)

Figure 23.10 Low strain sonic echo equipment being used on a 300 mm (12 in) concrete driven pile: (a) a small drop hammer (left) and wireless accelerometer (right rear) and (b) hand-held data processing unit. (b courtesy of Pile Dynamics, Inc.)

foreign inclusions. Only small portable equipment is needed, so the cost of purchasing the equipment and conducting the test is far less. Thus, all piles on a project, regardless of the pile type, may be economically tested.

Cross-Hole Sonic Logging

Cross-hole methods also use an impact and rely on monitoring the resulting stress waves. However, in this case two PVC pipes, known as access tubes, are cast into the pile, the wave source is lowered into one of these tubes and the accelerometer is lowered to the same depth in the other tube. Thus the test monitors the horizontal propagation of the waves across the pile. This test is repeated at various depth increments, and anomalies in the wave transmission indicate a potential defect in the pile at that depth.

This test has greater resolution and greater sensitivity than sonic echo tests, but can only sense defects located between the tubes. The cost of the tubes is modest, but does require appropriate planning.

Cross-Hole Tomography

Tomography is an enhancement of cross-hole sonic logging that uses both horizontal and diagonal wave paths, and uses four access tubes instead of two. These multiple paths are obtained by placing the accelerometer at various depths and in various tubes relative

to the wave source, and by repeating these multipath measurements at various depths. The resulting data requires special software interpretation, but the result is a more precise three-dimensional assessment of potential defects in the concrete. However, many more measurements are required, so the test is correspondingly more expensive and time consuming.

Gamma-Gamma Logging

The gamma-gamma method uses two access tubes and horizontal measurements, and in that respect is similar to cross-hole sonic logging. However, instead of using sonic impulses, this method uses a radioactive source that generates gamma radiation, and instead of an accelerometer it uses an instrument that detects the intensity of the radiation (Christopher, Baker, and Wellington, 1989). The ability of the gamma radiation to penetrate through the concrete depends on the concrete properties, especially its density, so anomalies in the measurements are an indication of defects in the concrete.

The California Department of Transportation (CalTrans) uses this method extensively, and requires gamma-gamma testing on all drilled shafts constructed using the slurry method. Some state departments of transportation (DOT) require access tubes in all drilled shafts, which then can be used as needed with this or one of the other cross-hole methods.

Thermal Integrity Profiling

Fresh concrete generates heat as it cures due to the chemistry of the hydration process. For cast-in-place piles, this heat creates a thermal profile, with the highest temperature in the center and progressively cooler temperatures toward the perimeter. If a portion of the concrete is defective (e.g., segregated with a low cement content) or missing (e.g., a soil inclusion), this thermal profile will be correspondingly altered. Thus, measuring the thermal profile during the curing process is another way of detecting defects (Likins and Mullins, 2011). This method uses thermal sensors that are lowered through access tubes or disposable thermal sensors embedded into the pile.

Interpretation and Follow-Up Actions

When a defect is identified, the engineer must then address the difficult question “What do we do about it?” When the defect is clearly problematic, the usual course of action is to abandon the pile and build a new one to replace it. However, this solution can be expensive because the new pile is inevitably off-center from the applied load, so a second new pile is also required on the opposite side of the pile cap in order to provide concentric loading.

The problem becomes more difficult when the presence of the defect is less certain, or when the defect is small or located in a less critical spot. In some cases the engineer may determine that no corrective action is required. Alternatively, it may be possible to repair the defective foundation, perhaps by grouting or other techniques.

SUMMARY

Major Points

1. The process of designing deep foundations differs from that of most structural elements, and it does not end with completion of the design drawings. The design often changes during construction to reflect the subsurface conditions actually encountered in the field.
2. Optimal design of deep foundations requires careful coordination between geotechnical, structural, and construction engineers.
3. Potential unstable conditions that might occur during the life of the project must be considered. Common examples include scour, downdrag, liquefaction, and landslides.
4. The selection of pile type depends on many factors, and often multiple types are technically feasible. In that case, the selection is largely driven by the availability of contractors with the necessary expertise, and cost.
5. The required pile capacity is driven primarily by the structural loads. Optimization helps set optimal objectives for the pile design.
6. The geotechnical engineer has the primary responsibility for evaluating the axial and lateral load capacity of the foundations, and developing design recommendations for the diameter, length, and flexural stiffness.
7. The structural engineer has primary responsibility for the structural design of the piles themselves as well as the pile cap, and also is responsible for developing the structural design drawings and specifications.
8. The geotechnical engineer has a field engineer present at the project site during construction, and he or she has authority to revise the design as needed to achieve the design objectives based on the actual conditions encountered.
9. In some cases, completed foundations are checked for structural integrity using a variety of non-destructive testing methods.

Vocabulary

Bearing graph
Cross-hole sonic logging
Cross-hole tomography
Downdrag
Driveability
Gamma-gamma logging
High strain sonic echo method
Indicator pile
Integrity testing
Low strain sonic echo method
Scour
Seismically-induced liquefaction
Thermal integrity profiling

QUESTIONS AND PRACTICE PROBLEMS

23.1 You are the foundation engineer for a new baseball stadium that is now under construction. The design drawings indicate the stadium will be supported on a series of steel H-piles, and provides the "estimated toe elevation" for each pile. However, during construction it became necessary to drive many of the piles to greater depths, which resulted in a significant increase in the construction cost. The owner (who knows a great deal about baseball, but little about foundations) is very unhappy about this additional cost. His construction manager has advised the owner to pay the invoice, but so far the owner has refused. Therefore, the construction manager has asked you to write a 300- to 500-word letter to the owner explaining the situation and encouraging him to pay for the extra pile expense.

Keep in mind that the owner is a layperson who should trust the judgment of his construction manager but is too strong willed to stay in the background. At the moment he does not intend to approve the extra payment to the foundation contractor, which could eventually lead to an expensive and time consuming lawsuit. A well-written letter by you could diffuse the situation and avoid litigation.

23.2 What are indicator piles, and how do they benefit the foundation design process?

23.3 Explain the advantages of using wave equation analysis and static load tests, in the design construction process for driven piles for both ASD and LRFD methods.

23.4 Many engineers believe the only disadvantage to overdesigning pile foundations is the additional cost of the pile materials. However, there is another important consequence of overdesign which can significantly affect construction cost and may even make the foundation impossible to build. What is this consequence and how can it be avoided?

23.5 Under what circumstances would you most likely require integrity testing of newly constructed drilled shaft foundations?

23.6 Describe a condition where downdrag loads might be a problem.

23.7 A proposed bridge is to be supported on a series of steel pipe piles which are to be designed in accordance with the AASHTO bridge code. The engineer has designed these piles using static methods and intends to verify the capacity during construction using the FHWA modified Gates dynamic pile formula with the end of driving blow counts. The estimated pile construction cost (not including pile caps) is $250,000.

In an effort to reduce the total cost, the engineer is considering the following additional activities:

- A static pile load test (cost = $70,000)
- Dynamic testing of 5 percent of the production piles using a pile driving analyzer (cost = $20,000)
- Dynamic testing of all the production piles using a pile driving analyzer (cost = $40,000)

Evaluate the expected construction cost savings from these additional activities, both individually and in combination, and determine the most cost-effective course of action. Hint: Review the AASHTO resistance factors in Table 13.3.

24

Pile Supported and Pile Enhanced Mats

Haec autem ita fieri debent, ut habeatur ratio firmitatis, utilitatis, venustatis.

Roman Architect Marcus Vitruvius explaining how structures must have firmitatis (strength and durability), utilitatis (functionality), and venustatis (beauty) in his book De Architectura, Circa 15 BCE

In Chapter 11 we considered the possibility of supporting structures on a mat foundation. This design has many advantages, but is feasible only when the underlying soil is sufficiently strong and stiff. Alternatively, Chapters 12–23 explored the use of pile foundations. In this case, each structural element, such as a column, is supported by one or more piles. In this chapter we will combine these two methods to create a type of hybrid foundation that combines attributes from conventional mat foundations and pile foundations. In some cases these hybrid foundations can be very cost-effective.

Pile supported mats are designed so that the structural loads and the weight of the mat are carried entirely by the piles. In contrast, *pile enhanced mats* (also known as *piled rafts* or *settlement control piles*) rely on both the piles and the bearing pressure between the mat and the underlying soil. As with conventional mat foundations, both provide a very stiff continuous structural connection between the various structural elements, thus reducing the potential for differential settlement. These designs also provide multiple redundancies in the distribution of structural loads to the piles, thus improving the reliability of the foundation system. Pile supported and pile enhanced mats are especially useful in situations such as:

- The structure is too heavy, or the soils are too weak or compressible to use a conventional mat foundation
- The structure has significant distributed loads, such as a tank or a warehouse
- The structural framing system uses diagonal bracing or some other method that transmits the lateral loads to only a subset of the columns. Rather than depending only on the foundations that support those columns, the mat acts as a diaphragm and distributes the lateral load across the entire foundation system.

24.1 PILE SUPPORTED MATS

From a structural design perspective, pile supported mats are fairly straightforward. The mat may be analyzed as a two-way slab with the various structural loads applied to the top, and the pile reactions applied to the bottom. Such an analysis could be performed using a two-dimensional finite element analysis similar to that described in Chapter 11, except the soil springs would be replaced by a single spring for each pile.

The linear or non-linear springs that represent the individual piles could be modeled using the settlement analysis methods for individual piles described in Chapter 20. In most cases each of the piles is identical. Using a large number of moderate capacity piles would reduce the required mat thickness and cost, whereas a smaller number of higher capacity piles would typically reduce the total pile cost.

The design process then focuses on determining the optimal locations of the piles such that the flexural stresses and flexural distortions in the mat are minimized, and thus the required mat thickness and reinforcement is also minimized. For structures that impart mostly concentrated loads onto the mat, such as those imposed by columns or bearing walls, most of the piles will be near these applied loads, with occasional piles in between to support the mat and the distributed loads, as shown in Figure 24.1a. Conversely, if most of the applied loads are uniformly distributed, such as a tank or a warehouse, then the piles would likely be placed on a uniform grid pattern across the mat, as shown in Figure 24.1b. In either case, the pile spacing is greater than that beneath conventional pile caps, thus eliminating group efficiency reductions and using each pile more effectively.

The design of pile supported mats ignores any support provided by the bearing pressure between the mat and the underlying soil, which is the same assumption used in the

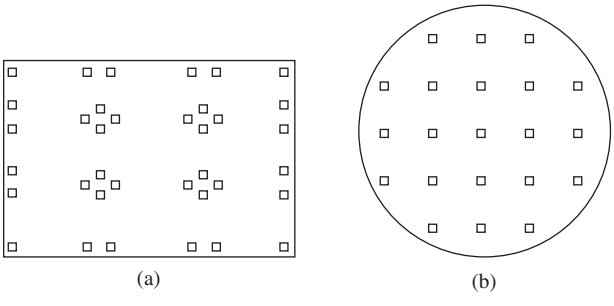

Figure 24.1 (a) Typical configuration of pile supported mat for buildings and other structures with concentrated loads. (b) Typical configuration of pile supported mat for tanks and other structures with uniform loading.

design of pile caps. However, because the mat area is so large, even a modest reliance on bearing pressure could provide substantial support and thus could result in a significant cost reduction, which leads to the second type of hybrid mat-pile foundation: Pile enhanced mats.

24.2 PILE ENHANCED MATS

Pile enhanced mats rely on a combination of piles and bearing pressure along the bottom of the mat to support the structural loads and the weight of the mat. This design can be very efficient and provides reliable and cost-effective support. However, the analysis of pile enhanced mats is much more complex because of the interactions between these two modes of transferring the structural loads into the ground. Pile enhanced mat foundations have been used on a wide range of structures, including the 102-story Incheon Tower in South Korea (Poulos et al., 2011).

The load transfer from pile enhanced mats to the ground may be expressed using the load sharing ratio, α_P (de Sanctis and Mandolini, 2006):

$$\alpha_P = \frac{\sum P_p}{P + W_f} \tag{24.1}$$

where:

ΣP_p = total downward load carried by all of the piles
$P + W_f$ = total downward structural load plus weight of the mat

Thus, a conventional mat has $\alpha_P = 0$, a pile supported mat has $\alpha_P = 1$, and a pile enhanced mat has some intermediate value.

Geotechnical Ultimate Limit State

As discussed in Chapter 11, bearing capacity is rarely, if ever, a concern for mat foundations on cohesionless soils. The addition of piles further stabilizes the foundation, virtually eliminating the potential for a global bearing capacity failure. However, the situation is quite different in saturated cohesive soils, especially soft or medium clays. In that case, mats can experience bearing capacity failures, as illustrated by the Fargo Grain Elevator case study in Chapter 7. Thus, one of the motives for using a pile enhanced mat on cohesive soils is to improve the overall bearing capacity.

Based on detailed analyses, de Sanctis and Mandolini (2006) found that the factor of safety against an overall bearing capacity failure is between 82 and 100 percent of the factor of safety for a conventional mat plus the factor of safety of the piles acting alone.

Example 24.1

The total downward structural loads plus the weight of the mat is 25,000 k, and a conventional mat has a factor of safety of 2.3. Determine the required nominal capacity, ΣP_n, that

must be carried by the piles in order to obtain an overall factor of safety of 3.0 against a bearing capacity failure, and compute the load sharing ratio.

Solution

Using the lower end of de Sanctis and Mandolini's findings (82%):

$$3.0 = 0.82(2.3 + F)$$

$$F = 1.36 = \text{required factor of safety of piles acting alone}$$

$$\sum P_n = (1.36)(25{,}000)$$

$$= 34{,}000 \text{ k}$$

Note: This analysis assumes the pile capacity is based on individual failure, not block failure. The nominal load capacity of the mat is (25,000)(2.3) = 57,500 k, so:

$$\alpha_P = \frac{34{,}000}{34{,}000 + 57{,}500}$$

$$= 0.37$$

Geotechnical Serviceability Limit State

The design of pile enhanced mats is usually governed by settlement and differential settlement, so the geotechnical analysis and design typically focusses mostly on serviceability. This is a complex problem that has been studied using finite element analyses, centrifuge models, and other techniques. Because of this complex behavior, project-specific finite element analyses are often required for design, although simplified methods are available to guide preliminary design (Poulos, 2002).

The load-settlement behavior depends on the stiffness of the piles, the stiffness of the mat bearing, and the interactions between these two load-transfer processes. The piles are typically stiffer than the mat bearing, so the initial part of the load-settlement curve is dominated by load transfer to the piles. As the piles approach their nominal load capacity, their load-settlement curve becomes softer and the mat bearing begins to dominate. Thus, under service loads, the piles may be subject to axial loads very close to their nominal load capacity, P_n.

Both the mat and the piles induce stresses in the ground, both of which impact the load-settlement behavior of the foundation system. Those from the mat bearing are greatest in the upper soils and diminish with depth, as illustrated by the induced stress diagrams in Figure 3.8, whereas those from the piles are greatest near the piles. Thus, as the width of the mat increases, the piles must be longer in order to mobilize soil outside the zone of significant stresses induced by the mat. Long piles are generally more cost-effective, and differential settlement is typically minimized when the pile length is on the order of 75 to 100 percent of the mat width (Viggiani et al., 2012).

Structural Design

Two-dimensional finite element analyses may be used to develop the structural design of the mat, similar to the methods described in Chapter 11. The mat bearing may be modeled using springs distributed across the bottom of the mat, and the piles may be modeled using an additional spring at each pile location.

As with pile supported mats, the locations of the piles should be optimized such that the flexural stresses and flexural distortions in the mat are minimized. However, because the bearing pressure along the bottom of the mat also is being considered, the optimal pile layout is correspondingly different. For example, the optimal pile placement for a uniformly loaded pile enhanced mat, such as one that supports a tank, would have most of the piles near the center of the mat and very few in the outer portion (Horikoshi and Randolph, 1998), as contrasted to the pile supported mat foundation in Figure 24.1b in which the piles are uniformly spaced.

Even when a conventional mat is feasible from a geotechnical perspective, the use of a pile enhanced mat may be advantageous because well-placed piles reduce the flexural stresses in the mat, thus facilitating a thinner mat and associated cost savings (Mandolini, Di Laora, and Mascarucci, 2013). For example, the greatest flexural stresses in a conventional mat supporting a building are typically beneath the columns, so placing a single pile beneath each interior column should facilitate a reduction in the required mat thickness. A project-specific cost analysis would be required to determine if the mat cost savings exceeds the cost of constructing the piles.

24.3 COMPENSATED MAT FOUNDATIONS

Compensated mat foundations, as discussed in Section 11.4, are located well below grade. In effect, the weight of the excavated soil is subtracted from the weight of the structure and the weight of the mat, thus substantially reducing the induced stresses in the underlying soil and improving the geotechnical performance. Compensated mats also may be pile supported or pile enhanced, thus combining the advantages of each (Sales et al., 2010).

The 63-story Messeturm Building in Frankfurt, Germany is a noteworthy example. It is supported by a 3–6 m thick mat founded 11–14 m below the ground surface and 6–9 m below the groundwater table. This mat is enhanced with 64 piles, each 1.3 m diameter extending 24.9–34.9 m below the bottom of the mat. The design loads are:

Structural loads 1,462 MN
Weight of mat 418 MN
Weight of excavated soil 616 MN
Buoyancy 311 MN

The building was well instrumented and ultimately had a load sharing ratio, α_P, of 0.58 and a total settlement of 143 mm.

Torre Latino Americana

The 43-story Torre Latino Americana in Mexico City (Zeevaert, 1957) was an important milestone in compensated pile supported mat technology. It is significant because of the exceptionally difficult soil conditions, which are generally as follows:

0−5.5 m (0−18 ft) depth

Old fill that includes Aztec artifacts. Groundwater table at 7 ft (2 m).

5.5−9.1 m (18−30 ft) depth

Becarra sediments—Interbedded sands, silts, and clays.

9.1−33.5 m (30−110 ft) depth

Tacubaya clays—Soft volcanic clay; moisture content = 100−400%, Cc/(1 + e) = 0.80; su = 700−1,400 lb/ft^2 (35−70 kPa).

33.5−70.0 m (110−230 ft) depth

Tarango sands and clays—Harder and stronger deposits; much less compressible than the Tacubaya clays.

The highly compressible Tacubaya clays have caused dramatic settlements in other structures. For example, the Palace of Fine Arts, located across the street from the Tower, settled over 3 m (10 ft) from 1904 to 1962 and continues to settle at a rate of 12 mm (0.5 in) per year (White, 1962)!

To avoid these large settlements, engineers excavated to a depth of 13.0 m (43 ft) and drove to the Tarango sands in order to create a compensated pile supported mat foundation, as shown in Figure 24.2. The removal of this soil compensated for about half the building weight. Thus, the building does load the deeper soils and has settled. However, this is by design, and the settlement has approximately matched that of the surrounding ground.

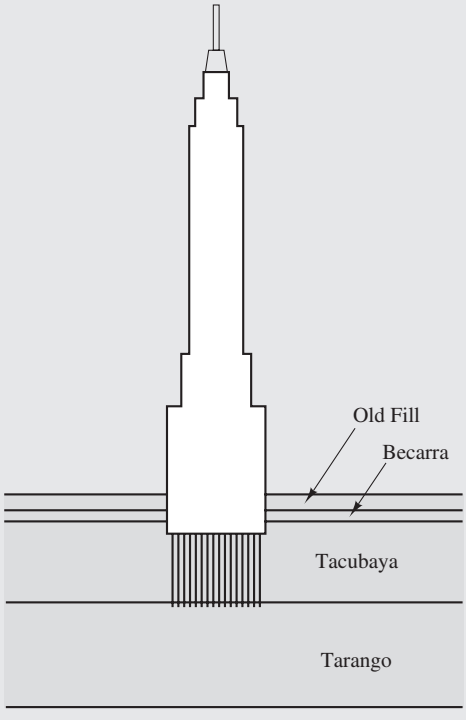

Figure 24.2 Torre Latino Americana.

SUMMARY

Major Points

1. Pile supported mats and pile enhanced mats are hybrid foundations that combine features from conventional mats and piles. They are used to enhance bearing capacity, control settlements, and reduce the flexural stresses in the mat.

2. Pile supported mats are designed such that all of the structural loads and the weight of the mat are carried by the piles.
3. Pile enhanced mats are designed such that the structural loads and the weight of the mat are shared between the bearing pressure (as with a conventional mat) and the piles.
4. The geotechnical design focuses primarily on controlling settlement and differential settlement, although bearing capacity can be a problem in soft or medium clays.
5. Pile enhanced mats often provide much more efficient and cost-effective foundations than either conventional mats or conventional piles.
6. Compensated mats also can be pile supported or pile enhanced.

Vocabulary

Load sharing ratio	Pile supported mat	Settlement control piles
Pile enhanced mat	Piled mat	

QUESTIONS AND PRACTICE PROBLEMS

24.1 Describe a typical structure and subsurface conditions where a pile supported or pile enhanced mat should be considered.

24.2 A cylindrical tank, 150 ft in diameter, is to be supported by a pile enhanced mat. The loading on the mat is a combination of the dead load of the tank itself, the live load of the tank contents, as well as other loads. Using a sketch, suggest a possible arrangement of the piles and explain the reasoning behind your design.

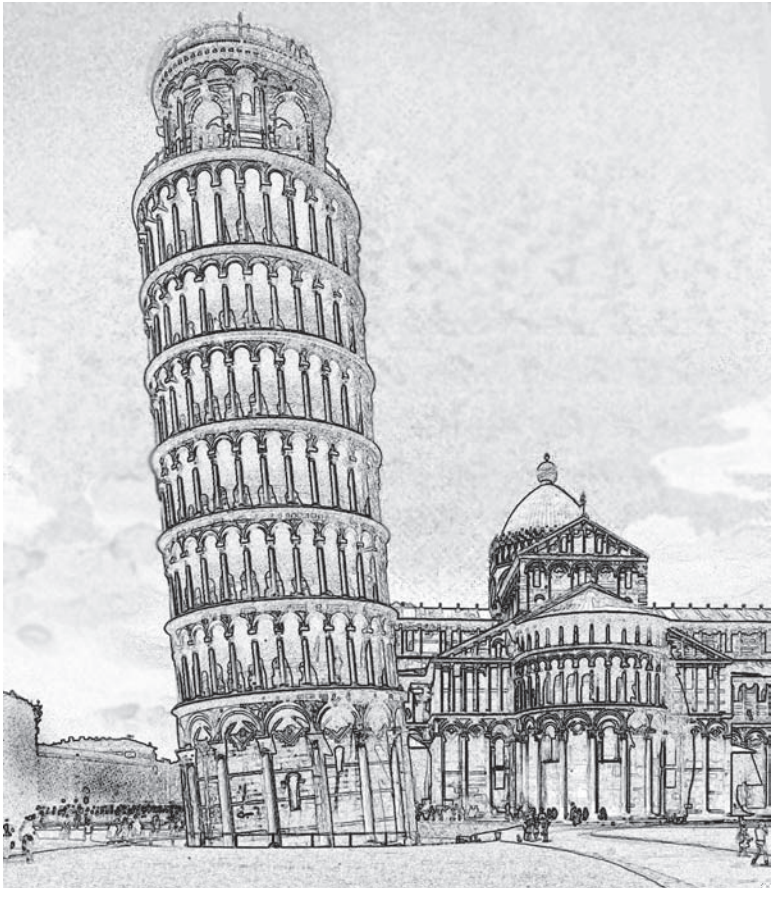

Part D

Special Topics

This page intentionally left blank

25

Foundations in Rocks and Intermediate Geomaterials

There are two modes of acquiring knowledge, namely by reasoning and by experience. Reasoning draws a conclusion and makes us grant the conclusion, but it does not make the conclusion certain; nor does it remove doubt so that the mind may rest on the intuition of truth, unless the mind discovers it by the path of experience.

Roger Bacon (1220–1292)

There is a wide range of geomaterials that exist in nature, from soils to rocks, to intermediate geomaterials (IGMs; O'Neill et al., 1996) that fall between soils and rocks. Previous chapters focus on foundations in soils; in this chapter, we present the principles and practices of foundations in rocks (Sections 25.1 and 25.2) and IGMs (Section 25.3).

25.1 ROCK AS A STRUCTURAL FOUNDATION MATERIAL

Rock is a cohesive, cemented geomaterial identified on the basis of geologic origin (O'Neill et al., 1996). In nature, there are many kinds of rocks, including volcanic, sedimentary, and metamorphic rocks. As shown by the examples in Figure 25.1, rocks rarely exist as perfectly continuous materials but contain weakness planes that are called discontinuities. In practice, a rock should more appropriately be called a *rock mass* consisting of discontinuities and the continuous rock material called intact rock between the

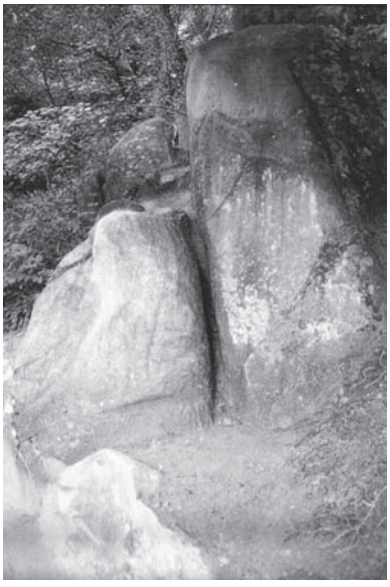

(a)

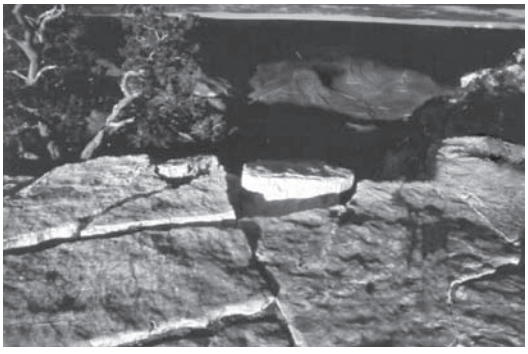

(b)

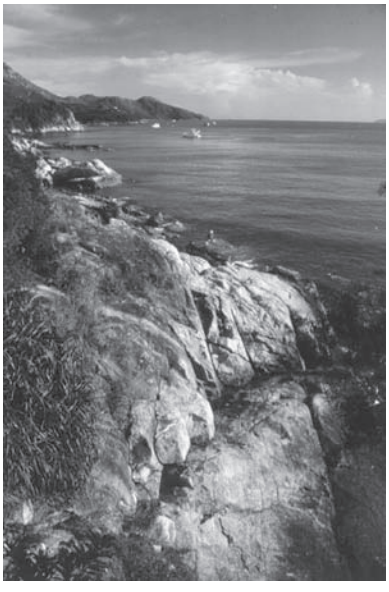

(c)

(d)

Figure 25.1 Examples of discontinuous rock masses in the field: (a) a granite in South Korea; (b) a limestone in the Grand Canyon, Arizona, US; (c) a volcanic rock in Hong Kong, China; and (d) a basalt in Maui, Hawaii, US.

discontinuities. Discontinuities can exist in sets and in different scales, from microfissures in the intact rock, to fissures, joints, shears and to faults, the largest discontinuities in the earth's crust. There is ample empirical evidence that the behavior of a rock mass is highly dependent on the properties of the discontinuities, as well as those of the intact rock.

In rock foundations, the effect of discontinuities on rock mass behavior depends on the size of the foundation relative to the spacings of the discontinuities. Figure 25.2 shows this influence of scale and categorizes the different combinations of foundation size and discontinuity spacings into three rock mass behavior types depending on the number of discontinuities in the zone of influence of the foundation:

- Type I: continuous intact rock behavior—foundation influenced by the behavior of the intact rock only

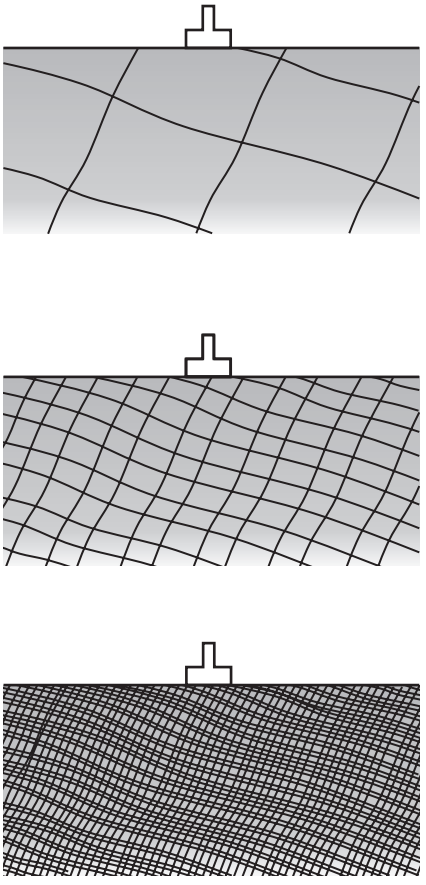

Figure 25.2 An illustration of how the scale affects rock mass modeling for a shallow foundation. The model chosen will depend upon both the spacing of discontinuities and the size of the foundation (after Serrano and Olalla, 1996; and Hoek, 1983).

- Type II: discontinuous rock mass behavior—foundation influenced by a handful of discontinuities
- Type III: equivalent continuous rock mass behavior—foundation influenced by many discontinuities

With rock mass behavior Type I, either the rock mass is so massive or its discontinuities are so widely spaced that the foundation would be influenced by the behavior of the intact rock only. In this case, the rock mass should behave as a continuous material, that is, the intact rock. With rock mass behavior Type II, the foundation is influenced by just a handful of discontinuities, and its behavior would be controlled by the truly discontinuous and anisotropic nature of the rock mass. In this case, the rock mass should behave as a truly discontinuous material. With rock mass behavior Type III, the foundation is influenced by a large number of discontinuities. In this case, the rock mass could be considered as an equivalent continuous material for analysis and design purposes.

The conditions described above that associate with the three rock mass behavior types are qualitative and approximate in nature. In an attempt to define these conditions quantitatively, Serrano and Olalla (1996) introduced the parameter *spacing ratio (SR)* of a foundation:

$$\mathrm{SR} = B\sum_{i=1}^{n}\frac{1}{S_{mi}} = B\sum_{i=1}^{n}\lambda_i \tag{25.1}$$

where

B = foundation width
S_{mi} = joint spacing of the ith discontinuity set
λ_i = frequency (number per unit length) of the ith discontinuity set
n = number of discontinuity sets

The SR is a dimensionless parameter that measures the number of discontinuities intersecting the base of the foundation. Serrano and Olalla (1996) suggested that for a rock mass with four discontinuity sets, rock mass behavior Type I would apply, that is, the intact rock would control the behavior, for SR $\leq$ 0.8 to 4.0. Furthermore, they conservatively proposed that rock mass behavior Type III would apply, that is, the rock mass would behave as an equivalent continuous material, if the SR was greater than 60. A subsequent analytical and numerical study by Imani et al. (2012) of footings on jointed rock masses showed that for SR $\geq$ 30, the joint spacing does not significantly affect the bearing capacity of footings on rock masses containing one to three joint sets, and that this finding is independent of the shear strengths of the intact rock and joints. This implies that the limiting SR value that would separate discontinuous and continuous rock mass behavior is 30, and rock mass behavior Type III would apply for SR $>$ 30. Combining these results, one can conclude that rock mass behavior Type II would apply, that is, the rock mass would behave as a discontinuous material, for 0.8 to 4.0 $<$ SR $<$ 30. These ranges of SR values associated with different rock mass behavior types can be useful in practice;

however, because they have not been validated by field case histories, they should be used with caution.

In this book, we present only continuum-based methods for the analysis and design of foundations on or in rock masses. In other words, we deal with continuous material behavior only, corresponding to rock mass behavior Types I and III. With rock mass behavior Type I, the continuous material in question is the intact rock. With Type III, the continuous material in question is an equivalent continuous material representing the rock mass that actually consists of intact rock and discontinuities. On the other hand, the analysis of rock mass behavior Type II would require discontinuum-based methods, such as the discontinuous deformation analysis (DDA; Shi and Goodman, 1984) and the distinct element method (DEM; Cundall, 1971), which are outside the scope of this book. In short, this book covers continuous rock mass behavior Types I and III and does not cover discontinuous rock mass behavior Type II.

Depending on the rock mass behavior type that applies, certain properties of a rock mass, including properties of the intact rock and discontinuities, are required for the analysis and design of foundations on or in the rock mass. These properties are used to classify the rock mass and to obtain the failure criterion of the rock mass, as discussed below.

Rock Mass Classification

In rock engineering, several rock mass classification systems have been developed over the years to quantify the quality of rock masses by taking into account the properties of the two major components of a rock mass, the intact rock and the discontinuities. Two systems most commonly used in practice are the Geomechanics Classification or Rock Mass Rating (RMR) system (Bieniawski, 1989) and the Rock Tunneling Quality Index or Q system (Barton et al., 1974), and they give indices of rock mass quality called RMR and Q, respectively. In this book, we present the RMR system only.

The RMR of a rock mass is the sum of the ratings given to the rock mass with respect to the following six parameters:

1. Uniaxial compressive strength of the intact rock (σ_{ci})
2. Rock Quality Designation (RQD)
3. Spacing of discontinuities
4. Condition of discontinuities
5. Groundwater conditions
6. Orientation of discontinuities

The uniaxial or unconfined compressive strength of the intact rock, σ_{ci}, is the maximum axial stress that an unconfined cylindrical intact rock core can take before failing, usually by axial splitting. Note that this is a property of the intact rock only. Table 25.1 gives estimates of σ_{ci} for different rocks (Hoek, 2007).

TABLE 25.1 FIELD ESTIMATES OF UNIAXIAL COMPRESSIVE STRENGTH, σ_{ci} (after Hoek, 2007)

Grade*	Term	Uniaxial Compressive Strength, σ_{ci} (MPa)	Point Load Index (MPa)	Field Estimate of Strength	Examples
R6	Extremely strong	>250	>10	Specimen can only be chipped with a geological hammer	Fresh basalt, chert, diabase, gneiss, granite, quartzite
R5	Very strong	100–250	4–10	Specimen requires many strong blows of a geological hammer to fracture it	Amphibolite, sandstone, basalt, gabbro, gneiss, granodiorite, limestone, marble, rhyolite, tuff
R4	Strong	50–100	2–4	Specimen requires more than one blow of a geological hammer to fracture it	Limestone, marble, phyllite, sandstone, schist, shale
R3	Medium strong	25–50	1–2	Cannot be scraped or peeled with a pocket knife, specimen can be fractured with a single blow from a geological hammer	Claystone, coal, concrete, schist, shale, siltstone
R2	Weak	5–25	†	Can be peeled with a pocket knife with difficulty, shallow indentation made by firm blow with point of a geological hammer	Chalk, rocksalt, potash
R1	Very weak	1–5	†	Crumbles under firm blows with point of a geological hammer, can be peeled by a pocket knife	Highly weathered or altered rock
RO	Extremely weak	0.25–1	†	Indented by thumbnail	Stiff fault gouge

* Grade according to Brown (1981).
† Point load tests on rocks with a uniaxial compressive strength below 25 MPa are likely to yield highly ambiguous results.

The RQD (Deere et al., 1967) is obtained from core log data and is an index of rock mass quality. The RQD is a modified core recovery defined as the percentage of intact core pieces longer than 100 mm (4 in) in the total length of core. The core should be drilled with a double-tube core barrel and be at least NW size (54.7 mm or 2.15 in in diameter). The correct procedures for measuring the lengths of core pieces and calculating the RQD are illustrated in Figure 25.3.

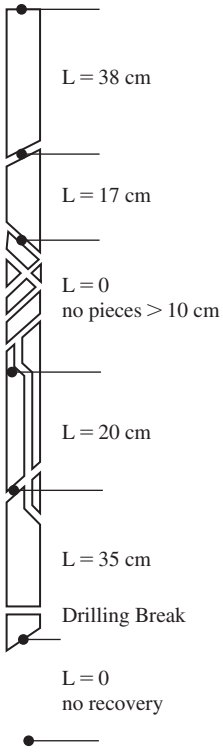

Total length of core run = 200 cm

$$\text{RQD} = \frac{\Sigma \text{ Length of core pieces} > 10 \text{ cm length}}{\text{Total length of core run}} \times 100\%$$

$$\text{RQD} = \frac{38 + 17 + 20 + 35}{200} \times 100\% = 55\ \%$$

Figure 25.3 Illustration of an RQD measurement for a certain rock core (after Deere, 1989).

Using Table 25.2, the rating corresponding to each of the six parameters in the RMR system can be determined, and the RMR is simply the sum of the ratings.

Rock Mass Properties

Rock mass properties are required when dealing with rock mass behavior Type III, in which the rock mass is treated as an equivalent continuous material. In a rock mass failure analysis, a rock mass failure criterion is required. For deformation or settlement problems, the rock mass deformation modulus and Poisson's ratio are required.

Rock Mass Failure Criterion

Those who have studied soil mechanics will be familiar with the Mohr-Coulomb failure criterion which gives a straight-line failure envelope. In rock engineering, a nonlinear failure envelope called the Hoek-Brown failure criterion is commonly used to characterize the

TABLE 25.2 ROCK MASS RATING SYSTEM (after Bieniawski, 1989)

A. Classification Parameters and Their Ratings

	Parameter	Range of Values						
1	Strength of intact rock	Point Load Index	>10 MPa	4–10 MPa	2–4 MPa	1–2 MPa	For this low range, uniaxial compression test is preferred	
		Uniaxial comp. strength	>250 MPa	100–250 MPa	50–100 MPa	25–50 MPa	5–25 MPa	1–5 MPa	<1 MPa
		Rating	15	12	7	4	2	1	0
2	RQD	Value	90–100%	75–90%	50–75%	25–50%	<25%		
		Rating	20	17	13	8	3		
3	Discontinuity Spacing	Spacing	>2 m	0.6–2 m	200–600 mm	60–200 mm	<60 mm		
		Rating	20	15	10	8	5		
4	Condition of discontinuities (See E)	Very rough surfaces Not continuous No separation Unweathered wall rock	Slightly rough surfaces Separation <1 mm Slightly weathered walls		Slightly rough surfaces Separation <1 mm Highly weathered walls	Slickensided surfaces or Gouge <5 mm thick or Separation 1–5 mm Continuous	Soft gouge >5 mm thick or Separation >5 mm Continuous		
		Rating	30	25	20	10	0		
5	Groundwater	Inflow per 10 m tunnel length (l/m)	None	<10	10–25	25–125	>125		
		(Joint water pressure)/ (Major principal stress)	0	<0.1	0.1–0.2	0.2–0.5	>0.5		
		General conditions	Completely dry	Damp	Wet	Dripping	Flowing		
		Rating	15	10	7	4	0		

B. Rating Adjustment For Discontinuity Orientations (See F)

Strike & Dip Orientations		Very Favorable	Favorable	Fair	Unfavorable	Very Unfavorable
Ratings	Tunnels & mines	0	−2	−5	−10	−12
	Foundations	0	−2	−7	−15	−25
	Slopes	0	−5	−25	−50	

C. Rock Mass Classes Determined From Total Ratings

Rating	100–81	80–61	60–41	40–21	<21
Class number	I	II	III	IV	V
Description	Very good rock	Good rock	Fair rock	Poor rock	Very poor rock

D. Meaning of Rock Classes

Class number	I	II	III	IV	V
Average stand-up time	10 yr for 15 m span	1 yr for 10 m span	1 week for 5 m span	10 hr for 2.5 m span	30 min for 1 m span
Rock mass cohesion (kPa)	>400	300–400	200–300	100–200	<100
Rock mass friction angle (°)	>45	35–45	25–35	15–25	<15

E. Guidelines for Classification of Discontinuity Conditions*

Discontinuity Length (persistence)	<1 m	1–3 m	3–10 m	10–20 m	>20 m
Rating	6	4	2	1	0
Separation (aperture)	None	<0.1 mm	0.1–1.0 mm	1–5 mm	>5 mm
Rating	6	5	4	1	0
Roughness	Very rough	Rough	Slightly rough	Smooth	Slickensided
Rating	6	5	3	1	0

(*continued*)

TABLE 25.2 (Continued)

E. Guidelines for Classification of Discontinuity Conditions*

Infilling (gouge)	None	Hard filling <5 mm	Hard filling >5 mm	Soft filling <5 mm	Soft filling > 5 mm
Rating	6	4	2	2	0
Weathering	Unweathered	Slightly weathered	Moderately weathered	Highly weathered	Decomposed
Rating	6	5	3	1	0

F. Effect of Discontinuity Strike and Dip Orientation in Tunneling**

Strike perpendicular to tunnel axis		Strike parallel to tunnel axis	
Drive with dip-Dip 45–90°	Drive with dip-Dip 20–45°	Dip 45–90°	Dip 20–45°
Very favorable	Favorable	Very unfavorable	Fair
Drive against dip-Dip 45–90°	Drive against dip-Dip 20–45°	Dip 0–20°—Irrespective of strike	
Fair	Unfavorable	Fair	

* Some conditions are mutually exclusive. For example, if infilling is present, the roughness of the surface will be overshadowed by the influence of the gouge. In such cases use A.4 directly.

** Modified from Wickham et al. (1972).

strength of an isotropic rock mass. Hoek et al. (2002) presented the latest edition of the Hoek-Brown failure criterion called the Generalized Hoek-Brown criterion:

$$\sigma'_1 = \sigma'_3 + \sigma_{ci}\left(m_b\frac{\sigma'_3}{\sigma_{ci}} + s\right)^a \tag{25.2}$$

where

σ'_1 = major effective principal stress at failure
σ'_3 = minor effective principal stress at failure
σ_{ci} = uniaxial compressive strength of the intact rock
m_b = Hoek-Brown constant given by Equation 25.3
s = constant given by Equation 25.4 and dependent on the rock mass characteristics
a = constant given by Equation 25.5 and dependent on the rock mass characteristics

The rock mass strength is dependent on the geological conditions of the rock mass, and the effect of the geological conditions is quantified by the Geological Strength Index (GSI; Hoek, 1994; Hoek et al., 1995). The GSI system for jointed rock masses is given in Figure 25.4 (Marinos et al., 2005), and that for heterogeneous rock masses such as flysch in Figure 25.5 (Marinos and Hoek, 2001). Note that Figure 25.5 also has been extended to include molassic rocks (Hoek et al., 2005) and ophiolites (Marinos et al., 2006).

In the Generalized Hoek-Brown criterion, the parameters m_b, s, and a are given by the following equations:

$$m_b = m_i \exp\left(\frac{\text{GSI} - 100}{28 - 14D}\right) \tag{25.3}$$

$$s = \exp\left(\frac{\text{GSI} - 100}{9 - 3D}\right) \tag{25.4}$$

$$a = \frac{1}{2} + \frac{1}{6}\left(e^{-\text{GSI}/15} - e^{-(20/3)}\right) \tag{25.5}$$

where

$m_i = m_b$ for intact rock
D = disturbance factor

The Hoek-Brown parameter m_i for intact rock can be estimated based on rock type from Table 25.3 (Hoek, 2007). The disturbance factor D quantifies the degree of disturbance the rock mass has experienced due to blast damage and stress relaxation. The value of D varies from zero for undisturbed in situ rock masses to 1 for very disturbed rock masses. Guidelines for the selection of the D value are given in Hoek et al. (2002).

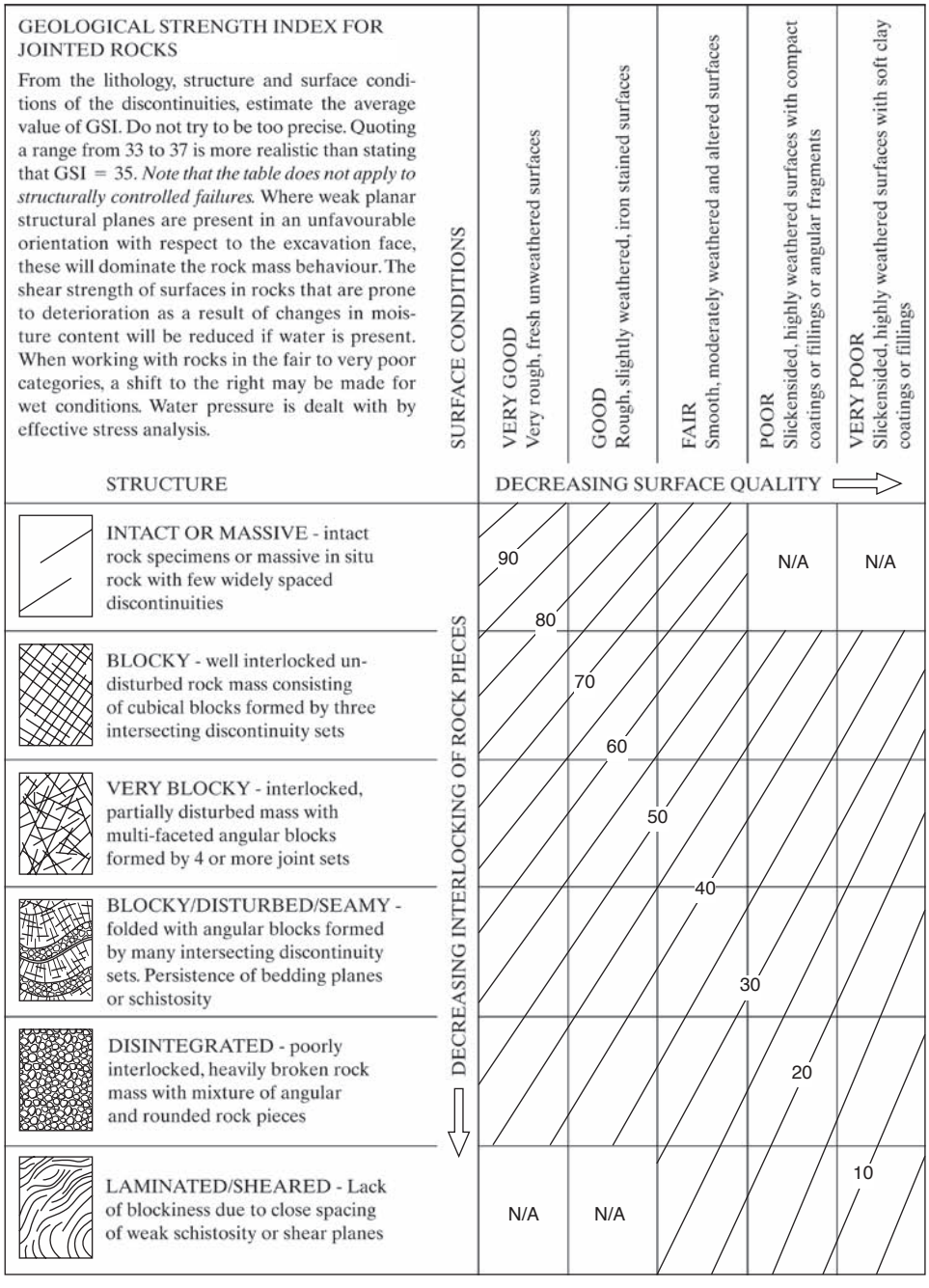

Figure 25.4 Determination of Geologic Strength Index (GSI) of blocky rock masses on the basis of interlocking and joint conditions (from Marinos and Hoek, 2000).

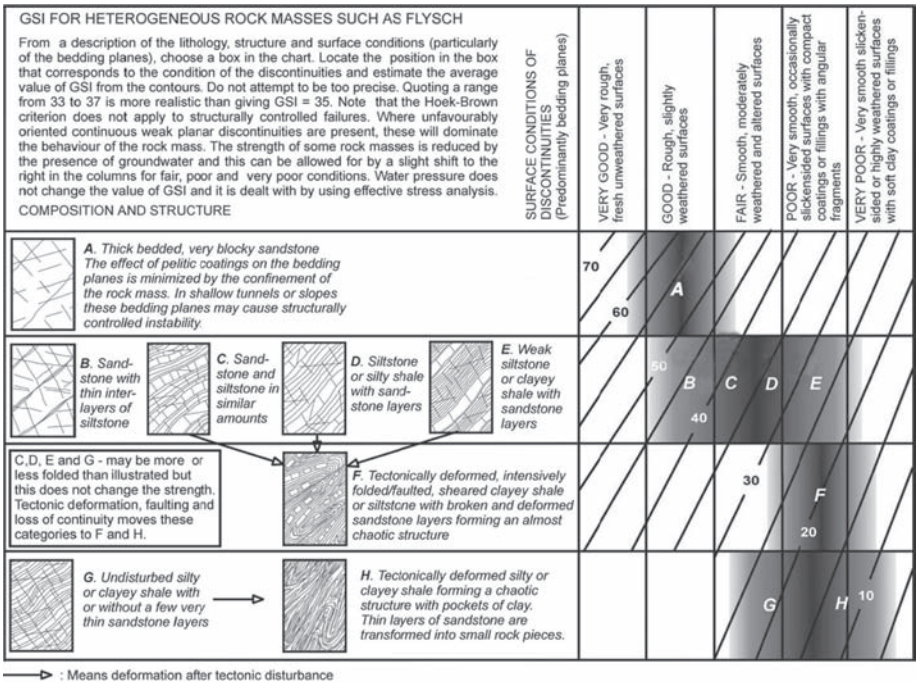

Figure 25.5 Determination of Geologic Strength Index (GSI) of flysch and similar rock masses on the basis of interlocking and joint conditions (from Marinos and Hoek, 2001).

TABLE 25.3 VALUES OF m_i FOR INTACT ROCK. VALUES IN PARENTHESES ARE ESTIMATES (after Hoek, 2007)

			Texture			
Rock Type	Class	Group	Coarse	Medium	Fine	Very Fine
Sedimentary	Clastic		Conglomerates* (21 ± 3) Breccias (19 ± 5)	Sandstones 17 ± 4	Siltstones 7 ± 2 Greywackes (18 ± 3)	Claystones 4 ± 2 Shales (6 ± 2) Marls (7 ± 2)
	Non-clastic	Carbonates	Crystalline Limestone (12 ± 3)	Sparitic Limestones (10 ± 2)	Micritic Limestones (9 ± 2)	Dolomites (9 ± 3)
		Evaporites		Gypsum 8 ± 2	Anhydrite 12 ± 2	
		Organic				Chalk 7 ± 2

(*continued*)

TABLE 25.3 (Continued)

Rock Type	Class	Group	Texture			
			Coarse	Medium	Fine	Very Fine
Metamorphic	Non-foliated		Marble 9 ± 3	Hornfels (19 ± 4) Metasandstone (19 ± 3)	Quartzites 20 ± 3	
	Slightly foliated		Migmatite (29 ± 3)	Amphibolites 26 ± 6		
	Foliated**		Gneiss 28 ± 5	Schists 12 ± 3	Phyllites (7 ± 3)	Slates 7 ± 4
Igneous	Plutonic	Light	Granite 32 ± 3 Granodiorite (29 ± 5)	Diorite 25 ± 5		
		Dark	Gabbro 27 ± 3 Norite 20 ± 5	Dolerite (16 ± 5)		
	Hypabyssal		Porphyries (20 ± 5)		Diabase (15 ± 5)	Peridotite (25 ± 5)
	Volcanic	Lava		Rhyolite (25 ± 5) Andesite 25 ± 5	Dacite (25 ± 3) Basalt (25 ± 5)	Obsidian (19 ± 3)
		Pyroclastic	Agglomerate (19 ± 3)	Breccia (19 ± 5)	Tuff (13 ± 5)	

* Conglomerates and breccias may present a wide range of m_i values depending on the nature of the cementing material and the degree of cementation, so they may range from values similar to sandstone to values used for fine grained sediments.

** These values are for intact rock specimens tested normal to bedding or foliation. The value of m_i will be significantly different if failure occurs along a weakness plane.

While the Generalized Hoek-Brown failure criterion can be used with rock mass behavior Type III, a special case of the Generalized Hoek-Brown failure criterion when GSI = 100 is the Hoek-Brown failure criterion for the intact rock ($m_b = m_i$, $s = 1$, and $a = 0.5$):

$$\sigma_1' = \sigma_3' + \sigma_{ci}\left(m_i\frac{\sigma_3'}{\sigma_{ci}} + 1\right)^{0.5} \tag{25.6}$$

This intact rock failure criterion can be used in problems involving rock mass behavior Type I.

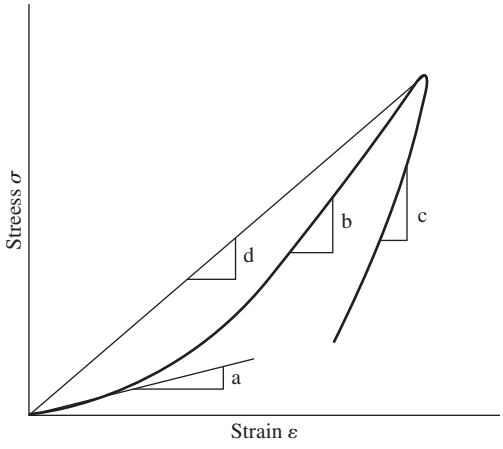

Figure 25.6 Definitions of different moduli used to describe rock mass behavior: (a) initial tangent modulus, (b) elastic tangent modulus, (c) recovery (unload) modulus, and (d) secant modulus (after Hoek and Diederichs, 2006).

Rock Mass Deformation Modulus

The deformation modulus of a rock mass characterizes the stress-strain behavior of the rock mass. The typical stress–strain curve from a large scale in situ test on a rock mass is shown in Figure 25.6, along with the definitions of four different measures of deformability (Hoek and Diederichs, 2006). The rock mass deformation modulus, E_m, is a secant modulus labeled as (d) in Figure 25.6, and is the measure of deformability usually reported in the literature.

It is very difficult to measure E_m in practice because it would require a large scale in situ test involving a large volume of the rock mass. Therefore, researchers have developed many empirical formulas that correlate E_m to rock mass properties such as the GSI and RMR. Some of these correlations are listed in Table 25.4 (Shen et al., 2012), categorized into five different groups requiring different combinations of input rock mass properties.

One property that is required in some correlations is the deformation modulus of the intact rock, E_i. The value of E_i can be estimated from data for different rock types compiled by Kulhawy (1978) in Table 25.5. The intact rock deformation modulus E_i can be used in problems involving rock mass behavior Type I.

A review by Shen et al. (2012) of the empirical correlations listed in Table 25.4 showed that among correlations that do not require E_i as an input, the correlations by Hoek and Diederichs (2006) based on the GSI and by Read et al. (1999) based on the RMR perform the best. When E_i is used as an input, the correlations by Carvalho (2004) based on the GSI and by Sonmez et al. (2006) based on the RMR perform the best.

Poisson's Ratio of Rock Mass

The rock mass Poisson's ratio, ν_m, varies with a range of approximately 0.2 to 0.3 (Hoek et al., 1995). In general, the Poisson's ratio tends to increase with decreasing rock mass quality. For practical purposes, a rock mass Poisson's ratio of 0.25 would be appropriate

TABLE 25.4 EMPIRICAL EQUATIONS TO PREDICT ROCK MASS MODULUS, E_m (after Shen et al., 2012)

Input Parameters	Empirical Equation	Reference
RMR	$E_m(\text{GPa}) = 2(\text{RMR}) - 100 \quad \text{for RMR} > 50$	Bieniawski (1978)
	$E_m(\text{GPa}) = 10^{(\text{RMR}-10)/40}$	Serafim and Pereira (1983)
	$E_m(\text{GPa}) = 10^{(\text{RMR}-20)/38}$	Mehrotra (1992)
	$E_m(\text{GPa}) = 0.1(\text{RMR}/10)^3$	Read et al. (1999)
RMR and E_i	$E_m = 0.1E_i(0.0028\ \text{RMR}^2 + 0.9e^{(\text{RMR}/22.83)})$	Nicholson and Bieniawski (1990)
	$E_m = E_i[0.5(1 - \cos(\pi\text{RMR}/100))]$	Mitri et al. (1994)
	$E_m = E_i 10^{[((\text{RMR}-100)(100-\text{RMR}))/(4{,}000\exp(-\text{RMR}/100))]}$	Sonmez et al. (2006)
GSI and D	$E_m(\text{GPa}) = (1 - 0.5D)10^{((\text{GSI}-10)/40)} \quad \text{for } \sigma_{ci} > 100\ \text{MPa}$	Hoek et al. (2002)
	$E_m(\text{MPa}) = \left(\frac{1 - 0.5D}{1 + \exp((75 + 25D - \text{GSI})/11)}\right)10^5$	Hoek and Diederichs (2006)
GSI, D, and E_i	$E_m = E_i(s)^{0.25},\ s = \exp\left(\frac{\text{GSI} - 100}{9 - 3D}\right)$	Carvalho (2004)
	$E_m = E_i(s^a)^{0.4},\ s = \exp\left(\frac{\text{GIS} - 100}{9 - 3D}\right),\ a = 0.5 + \frac{e^{-\text{GSI}/15} - e^{-20/3}}{6}$	Sonmez et al. (2004)
	$E_m = E_i\left(0.02 + \frac{1 - 0.5D}{1 + \exp((60 + 15D - \text{GSI})/11)}\right)$	Hoek and Diederichs (2006)
GSI, D, and σ_{ci}	$E_m(\text{GPa}) = \sqrt{\frac{\sigma_{ci}(\text{MPa})}{100}}10^{((\text{GSI}-10)/40)}$	Hoek and Brown (1997) Hoek et al. (2002)
	$E_m(\text{GPa}) = (1 - 0.5D)\sqrt{\frac{\sigma_{ci}(\text{MPa})}{100}}10^{[(\text{GSI}-10)/40]} \quad \text{for } \sigma_{ci} \le 100\ \text{MPa}$	Hoek et al. (2002)
	$E_m(\text{GPa}) = \tan(\sqrt{1.56 + (\ln \text{GSI})^2})\sqrt[3]{\sigma_{ci}(\text{MPa})}$	Beiki et al. (2010)

RMR = Rock Mass Rating
E_i = Intact rock modulus
GSI = Geological Strength Index
D = Disturbance factor
σ_{ci} = Uniaxial compressive strength of the intact rock

TABLE 25.5 STATISTICAL DATA ON INTACT ROCK MODULUS FOR INTACT ROCK SAMPLES (after Kulhawy, 1978)

Rock Type	Sample Size	Number of Rock Types in Sample	Intact Rock Modulus, E_i MPa $\times 10^3$ (ksi $\times 10^3$)			Standard Deviation MPa $\times 10^3$ (ksi $\times 10^3$)	Coefficient of Variation (COV)
			Maximum	Minimum	Mean		
Granite	26	26	100.0 (14.5)	6.4 (0.93)	52.7 (7.64)	24.5 (3.55)	0.46
Diorite	3	3	111.7 (16.2)	17.1 (2.48)	51.4 (7.45)	42.7 (6.19)	0.83
Gabbro	3	3	84.1 (12.2)	67.6 (9.8)	75.8 (11.0)	6.7 (0.97)	0.09
Diabase	7	7	104.1 (15.1)	69.0 (10.0)	88.3 (12.8)	12.3 (1.78)	0.14
Basalt	12	12	84.1 (12.2)	29.0 (4.20)	56.1 (8.14)	17.9 (2.60)	0.32
Quartzite	7	7	88.3 (12.8)	36.5 (5.29)	66.1 (9.59)	16.0 (2.32)	0.24
Marble	14	13	73.8 (10.7)	4.0 (0.58)	42.6 (6.18)	17.2 (2.49)	0.40
Gneiss	13	13	82.1 (11.9)	28.5 (4.13)	61.1 (8.86)	15.9 (2.31)	0.26
Slate	11	2	26.1 (3.79)	2.4 (0.35)	9.6 (1.39)	6.6 (0.96)	0.69
Schist	13	12	69.0 (10.0)	5.9 (0.86)	34.3 (4.97)	21.9 (3.18)	0.64
Phyllite	3	3	17.3 (2.51)	8.6 (1.25)	11.8 (1.71)	3.9 (0.57)	0.33
Sandstone	27	19	39.2 (5.68)	0.6 (0.09)	14.7 (2.13)	8.2 (1.19)	0.56
Siltstone	5	5	32.8 (4.76)	2.6 (0.38)	16.5 (2.39)	11.4 (1.65)	0.69
Shale	30	14	38.6 (5.60)	0.007 (0.001)	9.8 (1.42)	10.0 (1.45)	1.02
Limestone	30	30	89.6 (13.0)	4.5 (0.65)	39.3 (5.7)	25.7 (3.73)	0.65
Dolostone	17	16	78.6 (11.4)	5.7 (0.83)	29.1 (4.22)	23.7 (3.44)	0.82

in most cases. If the rock mass quality is very high, a rock mass Poisson's ratio of 0.2 may be used. On the other hand, if the rock mass is of very poor quality, a rock mass Poisson's ratio of 0.3 may be used.

Example 25.1

A site is underlain by a sandstone having the following properties and characteristics:

- Average uniaxial compressive strength of intact rock = 46 MPa
- Average RQD = 97%
- Average discontinuity spacing = 1.5 m
- Discontinuities are closed, slightly rough, with slightly weathered walls and lengths between 1 and 3 m

- Dry, with occasional localized dampness
- Average unit weight $= 24.9$ kN/m^3

Estimate for this sandstone the total RMR rating, GSI, Hoek-Brown failure criterion assuming the rock is undisturbed, intact rock deformation modulus, rock mass deformation modulus, and the rock mass Poisson's ratio.

Solution

Use Table 25.2 to obtain RMR ratings for different parameters and the total RMR rating:

Parameter	Value/Condition	Rating
Strength of intact rock material	$\sigma_{ci} = 46$ MPa	4
RQD	97%	20
Spacing of discontinuities	1.5 m	15
Condition of discontinuities (use Section E of Table 25.2)	Persistence = 1–3 m	4
	Separation = none	6
	Roughness = slightly rough	3
	Infilling = none	6
	Weathering = slightly weathered	5
	Total for this parameter =	24
Groundwater	Damp	10
Rating adjustment for discontinuity orientations	Assume very favorable for foundations	0
	Total RMR rating	**73**

Based on the total RMR rating of 73, the sandstone is a Class II rock mass, described as a "good rock."

Use Figure 25.4 to estimate the GSI value for the sandstone:

Based on the descriptions, the structure of the sandstone is assumed to be between massive and blocky, and the surface conditions are assumed to be good to fair. With these assumptions, the GSI is read from Figure 25.4 as **67**.

Hoek-Brown failure criterion:

Because the rock mass is undisturbed, $D = 0$.

For m_i, use the average value for sandstones in Table 25.3, that is, $m_i = 17$.

Use Equation 25.3 to calculate m_b:

$$m_b = m_i \exp\left(\frac{\text{GSI} - 100}{28 - 14D}\right) = 17 \exp\left(\frac{67 - 100}{28 - 14(0)}\right) = 5.2$$

Use Equation 25.4 to calculate s:

$$s = \exp\left(\frac{\text{GSI} - 100}{9 - 3D}\right) = \exp\left(\frac{67 - 100}{9 - 3(0)}\right) = 0.026$$

Use Equation 25.5 to calculate a:

$$a = \frac{1}{2} + \frac{1}{6}\left(e^{-(\text{GSI}/15)} - e^{-(20/3)}\right) = \frac{1}{2} + \frac{1}{6}\left(e^{-(67/15)} - e^{-(20/3)}\right) = 0.50$$

Equation 25.2 gives the Hoek-Brown failure criterion for the sandstone:

$$\sigma_1' = \sigma_3' + \sigma_{ci}\left(m_b\frac{\sigma_3'}{\sigma_{ci}} + s\right)^a$$

$$\boldsymbol{\sigma_1' = \sigma_3' + 46\ \text{MPa}\left(5.2\left(\frac{\sigma_3'}{46\ \text{MPa}}\right) + 0.026\right)^{0.50}}$$

Intact rock deformation modulus:

Estimate the intact rock deformation modulus using Table 25.5 and mean value for sandstone: $E_i = 2{,}130$ ksi or **14,700 MPa**

Rock mass deformation modulus:

Estimate the rock mass deformation modulus using the equation due to Carvalho (2004) in Table 25.4:

$$E_m = E_i(s)^{0.25} = 14{,}700(0.026)^{0.25} = \textbf{5,900 MPa}$$

Rock mass Poisson's ratio:

The rock mass Poisson's ratios of rock masses range from 0.2 to 0.3. Because the sandstone is of good quality, use a value of $v_m = \mathbf{0.2}$.

25.2 DESIGN OF FOUNDATIONS IN ROCKS

In general, rocks are stronger than soils and should have good load carrying capacities. To provide adequate support for heavy structures such as dams and skyscrapers, it may be necessary to found these structures in rocks. As with foundations in soils, foundations in rocks can be categorized into shallow and deep foundations.

The design of foundations in rocks can be performed using various methods and approaches. In terms of design philosophies, the two commonly used in practice are the allowable stress design (ASD) and the load and resistance factor design (LRFD). Both the ASD and LRFD methods are discussed in detail in Chapter 5. In current rock engineering practice, the ASD method is usually used, although the LRFD method has begun to appear in codes and the literature (AASHTO, 2012 and Abu El-Ela et al., 2013). In this book, we will use the ASD method of design of foundations in rocks, and, where possible, the LRFD method as well. Because of the large uncertainties of rock mass properties and

analysis methods, the factor of safety to be used in the ASD method of rock foundation design is relatively high, usually from 2.5 to 5. Where available, LRFD resistance factors are provided, and summarized in Table 13.5.

The design of foundations in rocks can be done using several approaches:

- **Use large scale load tests**—This method probably is the best method but is expensive.
- **Use prescriptive design**—While convenient, this method of using design or allowable values in codes is unavoidably conservative.
- **Use empirical methods**—The use of validated empirical methods is a common and practical way of design, but it should be noted that any empirical method is applicable only to cases similar to those based on which the method was developed.
- **Use the rational approach**—Rational analyses can be performed using appropriate analytical and numerical models.

In the following sections, common methods using the above approaches of designing shallow and deep foundations in rock are presented.

Shallow Foundations in Rocks

Although shallow foundations can be in the form of spread footings and mats, only spread footings on rocks are considered in this section. As with spread footings on soils, a spread footing on rocks must be designed for the ultimate limit state (or bearing capacity) and the serviceability limit state (or settlement).

Prescriptive Design

Prescriptive design or allowable bearing pressures for foundations on rocks can be found in many design codes and manuals. In general these prescriptive design values are controlled by the serviceability limit state corresponding to a certain allowable settlement. As an example, presumed preliminary design bearing pressures for different rocks from the Canadian Foundation Engineering Manual (Canadian Geotechnical Society, 2006) are given in Table 25.6. These design values are generally for a settlement not exceeding 25 mm (1 in).

Ultimate Limit State—Bearing Capacity of Spread Footings on Rocks

The bearing capacity of a footing on rocks can be estimated by analyzing the footing behavior in a rational manner using appropriate analytical and numerical models. Many such rational analysis methods have been developed to model the observed failure modes shown in Figure 25.7 (Ladanyi, 1972). Figures 25.7a to 25.7c show the bearing failure of

TABLE 25.6 PRESUMED PRELIMINARY DESIGN BEARING PRESSURE (Canadian Geotechnical Society, 2006)

Type and Condition of Rock	Strength of Rock Material (Intact Rock)	Preliminary Design Bearing Pressure[1] (kPa)
Massive igneous and metamorphic rocks (granite, diorite, basalt, gneiss) in sound condition[2]	High to Very High	10,000
Foliated metamorphic rocks (slate, schist) in sound condition[2,3]	Medium to High	3,000 1,000–4,000
Sedimentary rocks: cemented shale, siltstone, sandstone, limestone without cavities, thoroughly cemented in conglomerates, all in sound condition[2,3]	Medium to High	500–1,000 1,000
Compaction shale and other argillaceous rocks in sound condition[2,4]	Low to Medium	1,000
Broken rocks of any kind with moderately close spacing of discontinuities (0.3 m or greater), except argillaceous rocks (shale) Limestone, sandstone, shale with closely spaced bedding		See note 5
Heavily shattered or weathered rock		See note 5

[1] Values are based on the assumption that the foundations are carried down to unweathered rock.
[2] Sound rock conditions allow minor cracks at spacing not closer than 1 m.
[3] For sedimentary or foliated rocks, the strata or foliation are assumed to be horizontal or nearly so, with ample lateral support.
[4] These rocks are apt to swell on release of stress, and on exposure to water, apt to soften and swell.
[5] To be assessed by examination in situ, including test loading if necessary.

a footing on a brittle, nonporous intact rock through crack initiation in the rock underneath the footing (Figure 25.7a), crack propagation and coalescence (Figure 25.7b), and then wedging caused by the lateral push of the dilatant fractured rock under the footing (Figure 25.7c). This failure mode can be called a brittle failure mode under rock mass behavior Type I involving intact rocks.

For this brittle failure mode of the intact rock under rock mass behavior Type I, a rational analysis from Kulhawy and Carter (1992) based on Bell (1915) can be used to obtain a lower bound solution for the nominal bearing capacity of a continuous footing on a rock mass satisfying the Generalized Hoek-Brown failure criterion, as shown in Figure 25.8. Considering in this figure the state of stress of the rock mass at failure in Zones I and II as shown in the figure, a formula for the nominal unit bearing capacity, q_n, can be derived as:

$$q_n = [s^a + (m_b s^a + s)^a]\sigma_{ci} \tag{25.7}$$

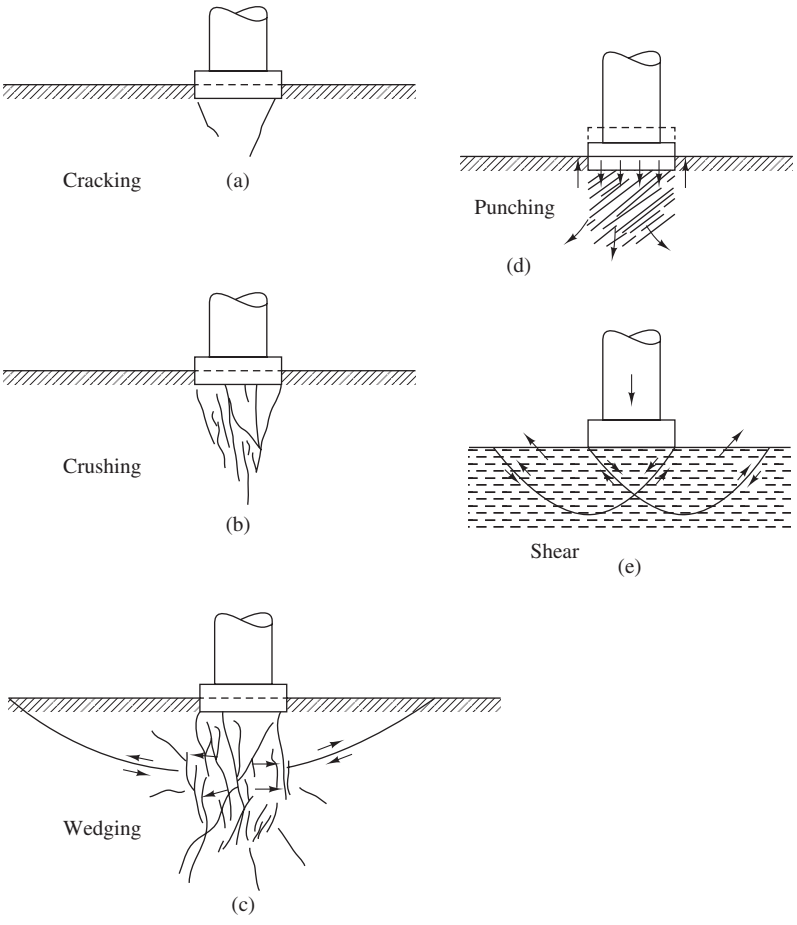

Figure 25.7 Different failure modes for footings on rock: (a) cracking, (b) crushing, (c) wedging, (d) punching, and (e) shear (after Ladanyi, 1972).

For the case of brittle failure of the intact rock, the appropriate rock mass failure criterion to be used is the intact rock failure criterion for both Zone I and Zone II in Figure 25.8, giving this formula:

$$q_n = [1 + (m_i + 1)^{0.5}]\sigma_{ci} \tag{25.8}$$

As a more conservative alternative, Zone I can be assumed to be intact rock and Zone II the same intact rock that has been crushed, as shown in Figure 25.7c, with different rock mass failure criteria for the two zones, as illustrated in Figure 25.9 (Goodman, 1989).

The failure mode depicted in Figure 25.7d is a punching failure in porous rocks through the collapse of pores in the rock. Without a rational analysis for this failure mode, load tests may be used to obtain the nominal bearing capacity of footings that fail by punching.

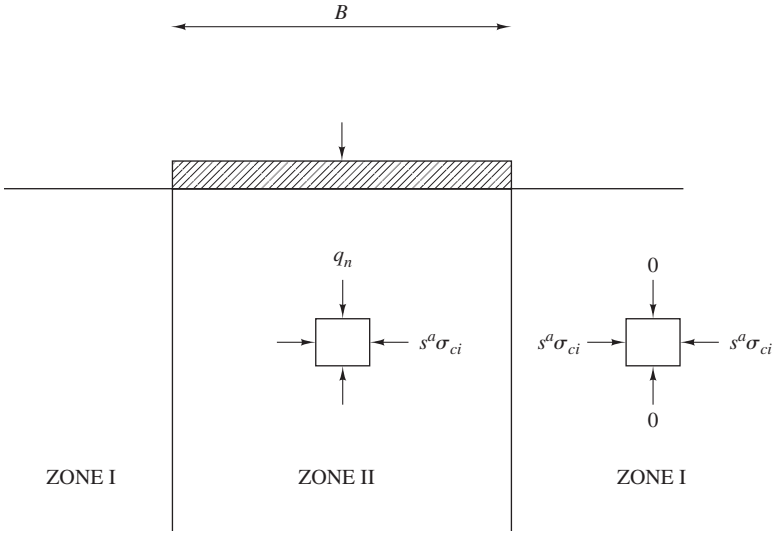

Figure 25.8 Stress conditions for lower bound solution of footing bearing capacity (after Kulhawy and Carter, 1992).

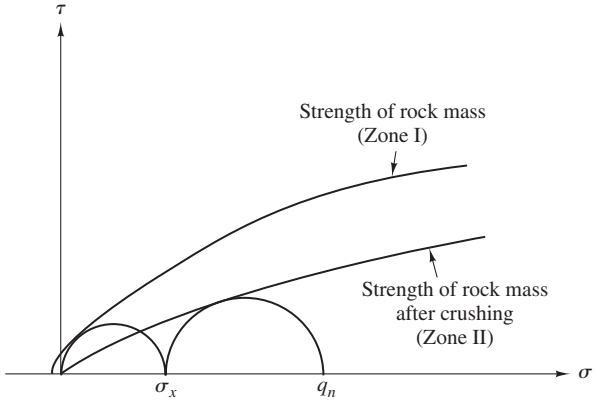

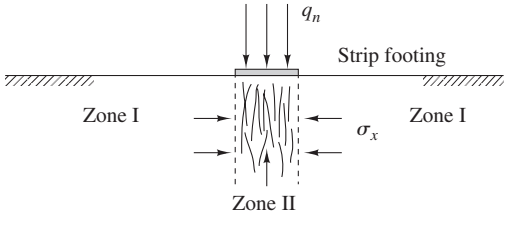

Figure 25.9 Method for analyzing bearing capacity of footings on rock (after Goodman, 1989).

The failure mode shown in Figure 25.7e is a shear failure similar to the classical bearing capacity failure in soils. This failure mode can be called a plastic failure mode and applies to weak intact rock acting in behavior Type I and equivalent continuous rock masses acting in behavior Type III. For intact rocks, Equation 25.8 can be used to estimate q_n. For equivalent continuous rock masses, Equation 25.7 from the Hoek-Brown failure criterion can be used to estimate q_n.

In addition to Equation 25.7, many other bearing capacity solutions for the plastic failure mode of rock masses acting in behavior Type III have been obtained by researchers using the theory of plasticity and numerical models (e.g., Serrano and Olalla, 1996; Prakoso and Kulhawy, 2004; Yang and Yin, 2005; Merifield et al., 2006; Imani et al., 2012; Tang and Liu, 2012; and Clausen, 2013). The solutions by Merifield et al. (2006) for continuous footings and by Clausen (2013) for circular footings are presented here.

The nominal unit bearing capacity of a footing on a rock mass is usually given as the product of σ_{ci} and a bearing capacity factor N_σ:

$$q_n = N_\sigma \sigma_{ci} \tag{25.9}$$

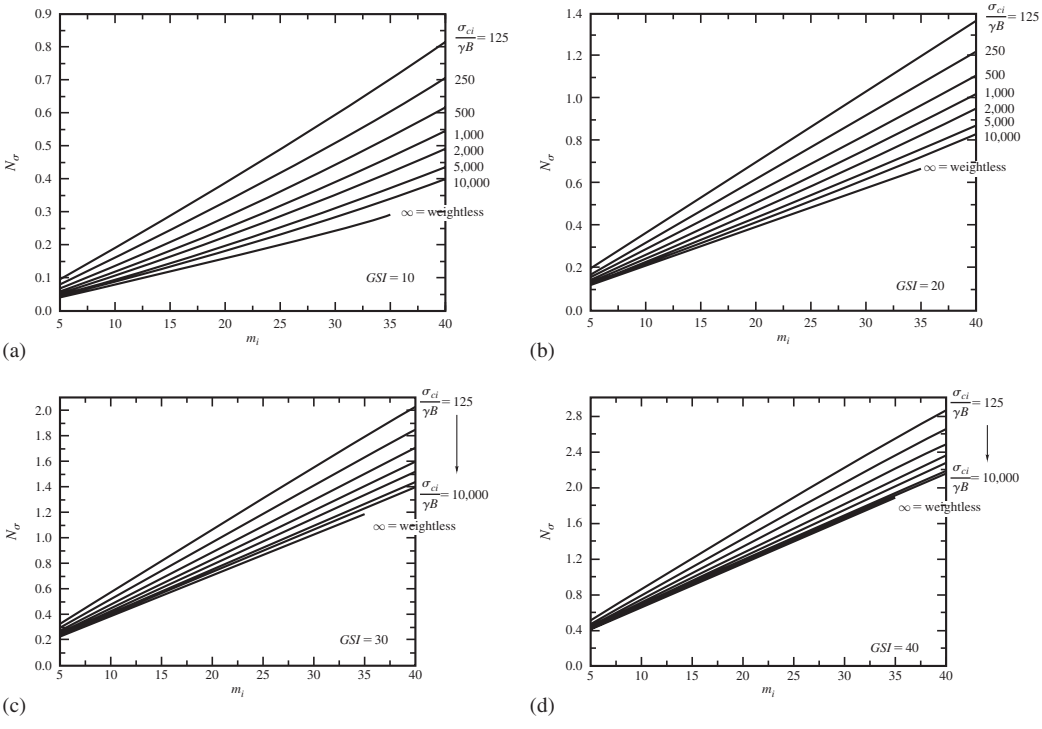

Figure 25.10 Bearing capacity factor, N_σ, for a continuous footing, based on finite element limit analyses: (a) GSI = 10, (b) GIS = 20, (c) GSI = 30, (d) GSI = 40 (Merifield et al., 2006).

Using sophisticated upper bound and lower bound finite element limit analyses, Merifield et al. (2006) obtained the upper bound and lower bound solutions for the nominal bearing capacity of a continuous footing on a Hoek-Brown rock mass. They found that the upper bound and the lower bound solutions were within about 5 percent of each other and suggested that the average of the two solutions should be within about 2.5 percent of the correct solution and can be used as the nominal bearing capacity. They presented their results in the form of bearing capacity charts for a continuous footing of width B and a rock mass unit weight of γ (Figures 25.10 and 25.11). Each chart is for a particular GSI value and plots N_σ against m_i for different values of the factor $\sigma_{ci}/(\gamma B)$. These results were obtained assuming that the rock mass is undisturbed, that is, $D = 0$. Additionally, these charts are for a footing placed on the ground surface but can be conservatively used for embedded footings.

A solution for circular footings on the surface of a Hoek-Brown rock mass was obtained by Clausen (2013) using finite element techniques. These charts are shown in Figures 25.12 and 25.13, with B being the diameter of the circular footing and all other

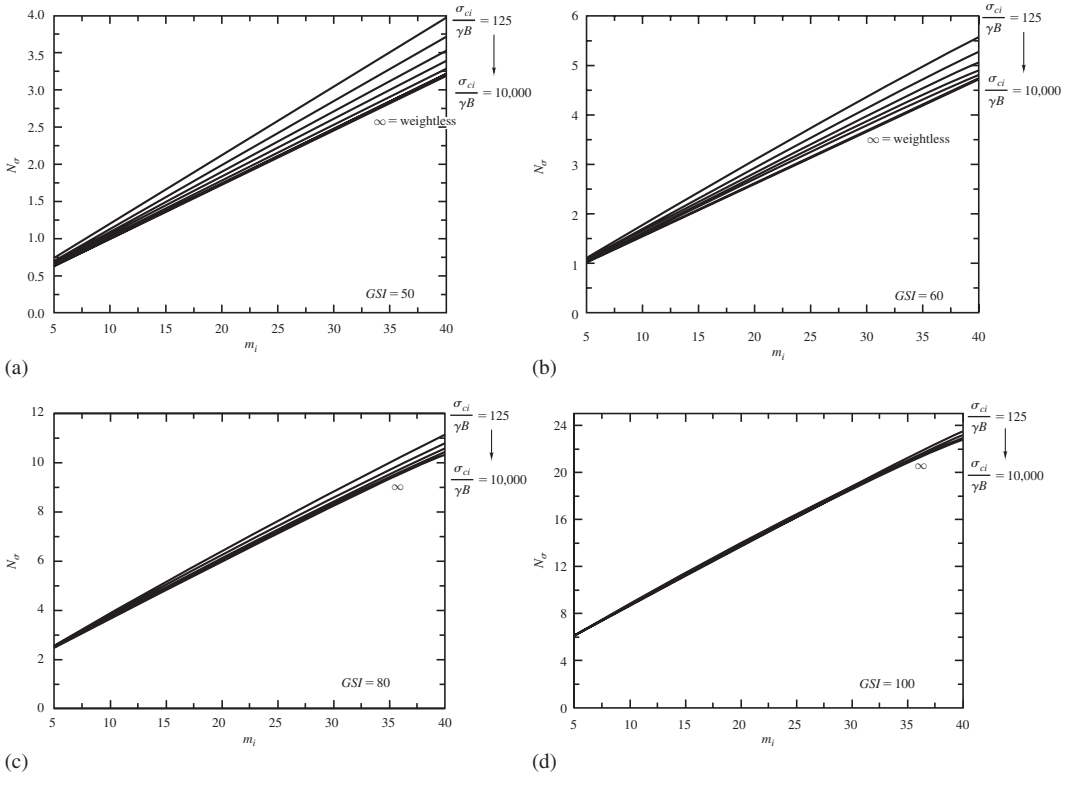

Figure 25.11 Bearing capacity factor, N_σ, for a continuous footing, based on finite element limit analyses; (a) GSI = 50, (b) GIS = 60, (c) GSI = 80, (d) GSI = 100 (Merifield et al., 2006).

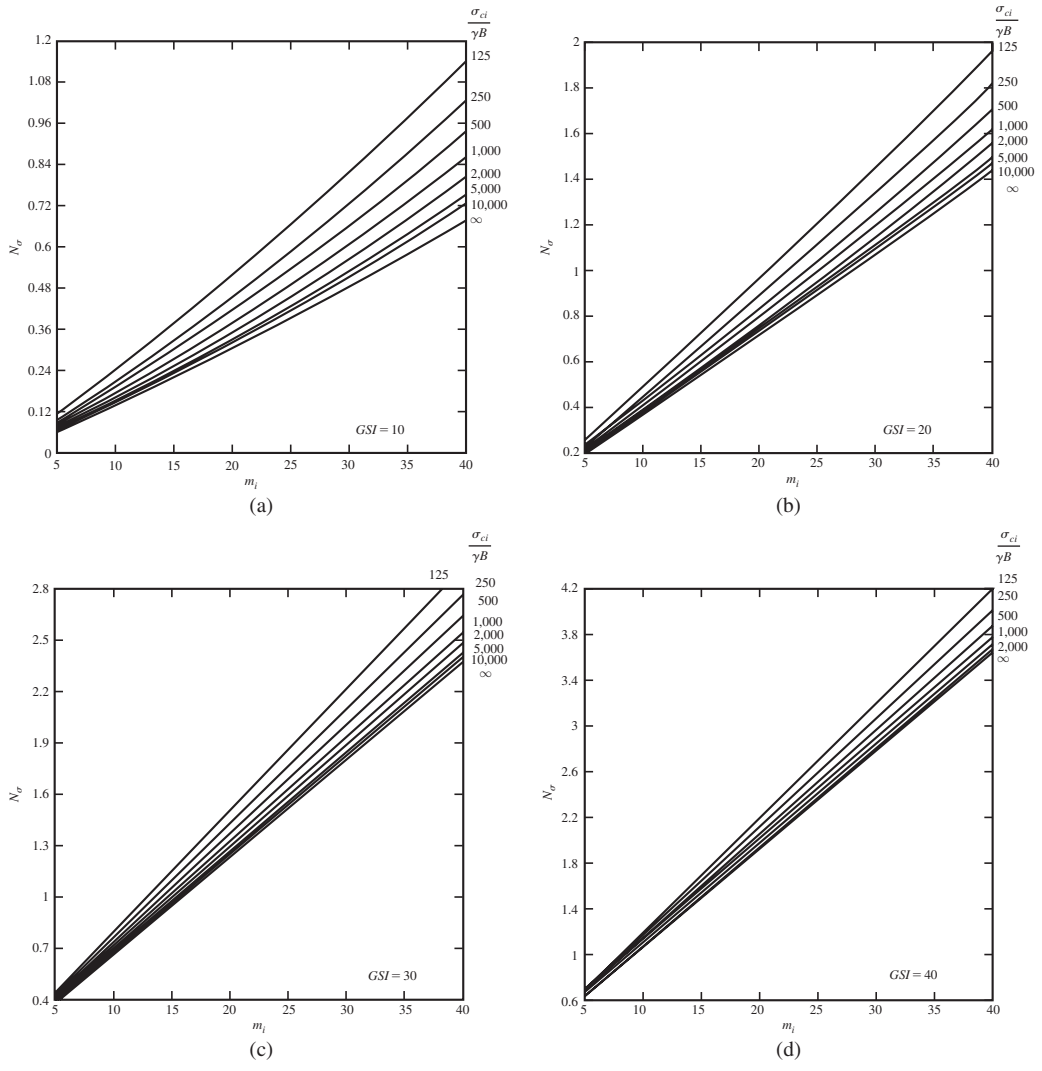

Figure 25.12 Bearing capacity factor, N_σ, for a circular footing, based on finite element analyses: (a) GSI = 10, (b) GIS = 20, (c) GSI = 30, (d) GSI = 40 (Clausen, 2013).

variables defined as before. Note that the charted results were obtained assuming that the rock mass deformation modulus E_m is given by the empirical equation by Hoek and Diederichs (2006) in Table 25.4, that the Poisson's ratio of the rock mass is 0.3, and that the rock mass is undamaged, that is, $D = 0$. Note also that these charts are for a footing placed on the ground surface but can be conservatively used for footings that are embedded.

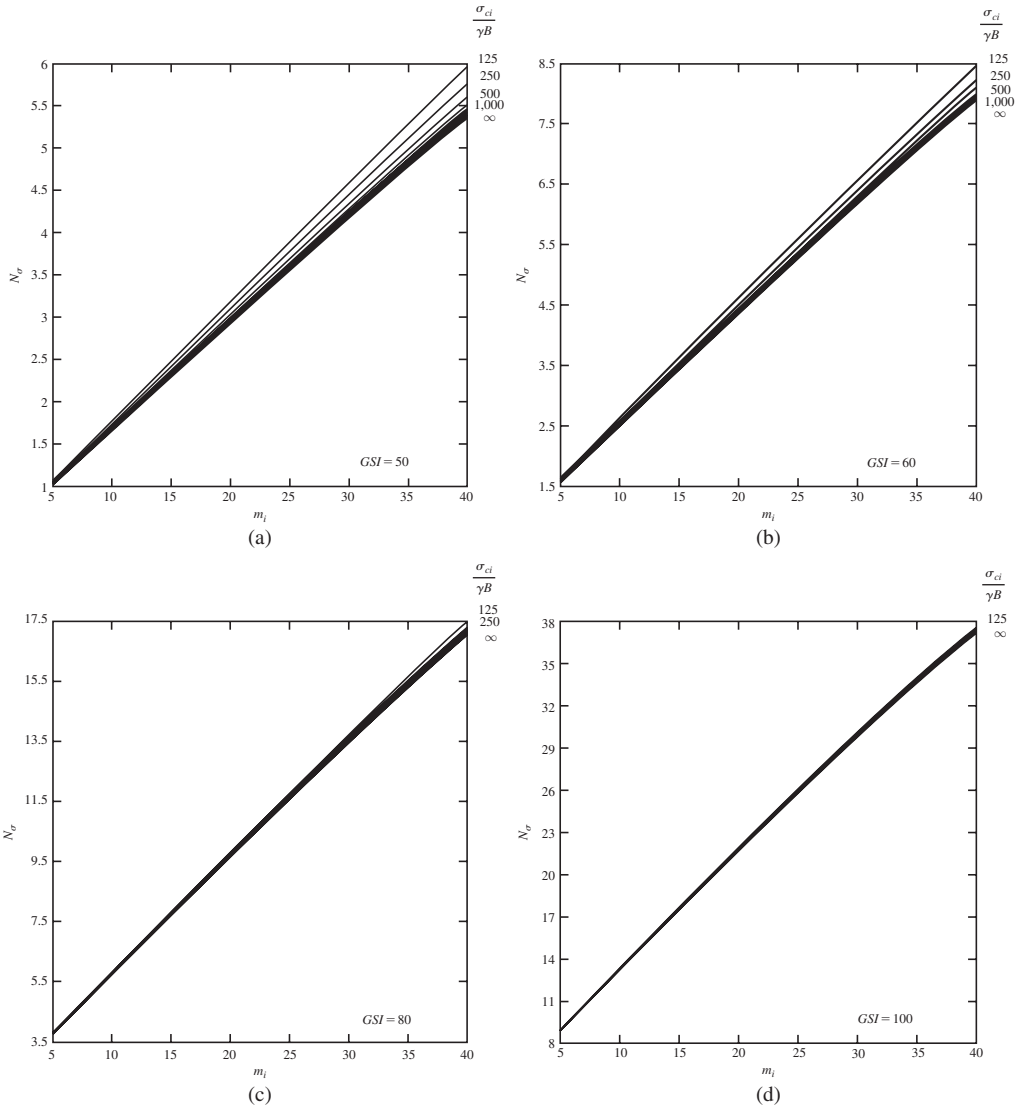

Figure 25.13 Bearing capacity factor, N_σ, for a circular footing, based on finite element analyses: (a) GSI = 50, (b) GIS = 60, (c) GSI = 80, (d) GSI = 100 (Clausen, 2013).

Both Merifield et al. (2006) and Clausen (2013) looked into the possibility of using an equivalent Mohr-Coulomb failure criteria rather than Hoek-Brown as a way to simplify the analysis. However, each researcher concluded that using the equivalent Mohr-Coulomb failure criterion could lead to a significant overestimation of the bearing capacity.

Example 25.2

A continuous footing having a width of 2.0 m is underlain by the sandstone in Example 25.1. Estimate the nominal bearing capacity using Kulhawy and Carter (1992) and Merifield et al. (2006).

Solution

Assume conservatively rock mass behavior Type III applies and the rock mass behaves as an equivalent continuous, isotropic material. Use Kulhawy and Carter (1992), Equation 25.7:

$$\begin{aligned} q_n &= [s^a + (m_b s^a + s)^a]\sigma_{ci} \\ &= [0.0260^{0.50} + (5.2(0.0260)^{0.50} + 0.0260)^{0.50}]46 \\ &= \mathbf{50\ MPa} \end{aligned}$$

Use Merifield et al. (2006), Figure 25.11b for GSI = 60 and Figure 25.11c for GSI = 80, and interpolate for GSI = 67:

$$\sigma_{ci}/(\gamma B) = 46{,}000/(24.9)(2) = 924$$

For $m_i = 17$ and GSI = 60, Figure 25.11b gives $N_\sigma = 2.6$.

For $m_i = 17$ and GSI = 80, Figure 25.11c gives $N_\sigma = 5.7$.

Interpolating, for the sandstone with GSI = 67,

$$N_\sigma = 2.6 + \left(\frac{67 - 60}{80 - 60}\right)(5.7 - 2.6) = 3.7$$

Therefore, $q_n = N_\sigma \sigma_{ci} = (3.7)(46) = \mathbf{170\ MPa}$.

Note that this value is larger than the lower bound value of 50 MPa obtained above using Kulhawy and Carter (1992).

Example 25.3

A circular footing having a diameter of 2.0 m is underlain by the sandstone in Example 25.1. Estimate the nominal bearing capacity using Clausen (2013).

Solution

Assume conservatively rock mass behavior Type III applies and the rock mass behaves as an equivalent continuous, isotropic material. Use Clausen (2013), Figure 25.13b for GSI = 60 and Figure 25.13c for GSI = 80, and interpolate for GSI = 67:

$$\sigma_{ci}/(\gamma B) = 46{,}000/(24.9)(2) = 924$$

For $m_i = 17$ and GSI = 60, Figure 25.13b gives $N_\sigma = 3.9$.

For $m_i = 17$ and GSI $= 80$, Figure 25.13c gives $N_\sigma = 8.6$.

Interpolating, for the sandstone with GSI $= 67$,

$$N_\sigma = 3.9 + \left(\frac{67 - 60}{80 - 60}\right)(8.6 - 3.9) = 5.5$$

Therefore, $q_n = N_\sigma \sigma_{ci} = (5.5)(46) = \mathbf{253\ MPa}$.

Serviceability Limit State—Settlement of Spread Footings on Rocks

Settlement of a spread footing on rocks can be estimated by assuming that the rock mass is an equivalent continuous, homogeneous, isotropic, and linear elastic (CHILE) material. In this way, elastic solutions can be used to compute the settlement in the same way as for footings on soils. For a footing on an infinite half space consisting of a CHILE rock mass, we can compute the settlement, δ, from the rock mass deformation modulus, E_m, and rock mass Poisson's ratio, v_m, using this equation (Kulhawy and Carter, 1992):

$$\delta = \frac{P(1 - v_m^2)}{\beta_z E_m A^{0.5}} \tag{25.10}$$

where

P = sustained vertical load on the footing
A = footing base area
β_z = footing shape and rigidity factor

For circular and square footings, and for rectangular footings with length-to-width ratios up to three, and using either flexible or rigid foundation assumptions, β_z is about 1.1, with a variation of up to 5% (Kulhawy, 1978). Using this reasonable value of $\beta_z = 1.1$ and a reasonable value of $v_m = 0.2$, Equation 25.10 becomes:

$$\delta \approx \frac{0.9P}{E_m A^{0.5}} \tag{25.11}$$

Example 25.4

A circular footing having a diameter of 2.0 m is underlain by the sandstone in Example 25.1. Estimate the settlement under a vertical downward sustained load of 10,000 kN.

Solution

Assume conservatively rock mass behavior Type III applies and the rock mass behaves as an equivalent continuous, isotropic material. Use Equation 25.11:

$$\delta \approx \frac{0.9P}{E_m A^{0.5}} = \frac{0.9(10{,}000)}{(5{,}900{,}000)[3.14(1)^2]^{0.5}} = \mathbf{0.09\ cm}.$$

Deep Foundations in Rocks

Most deep foundations in rocks are constructed using drilled shaft techniques. The toe of the shafts are typically socketed in rock as shown in Figure 25.14. A pile can be socketed full-length if the rock is at the ground surface as shown in Figure 25.14a, or partially in soil and partially in the rock underlying the soil as shown in Figure 25.14b. For design purposes, it is conservative to ignore the resistance of the soil layers above the rock socket.

Load Transfer Mechanisms

When a rock-socketed pile is loaded under downward loads, the load is transferred to the surrounding rock through shear stresses along the socket wall and normal stresses at the toe of the pile. The distribution of the load between the side friction resistance and toe bearing resistance depends on the socket geometry, relative stiffness of the socket material and rock mass, socket roughness and strength, and foundation settlement (Kulhawy and Goodman, 1987). At working loads, the load carried by the toe is typically 10–20% of the total load (Carter and Kulhawy, 1988) and can be up to 30% (Crapps and Schmertmann, 2002).

Kulhawy and Goodman (1987) and Kulhawy and Carter (1992) described the shearing behavior of the socket wall under increasing load and proposed analytical solutions to predict the load-settlement behavior of a rock-socketed pile. When the loads are relatively small, they are carried mainly by the side friction resistance inducing only small

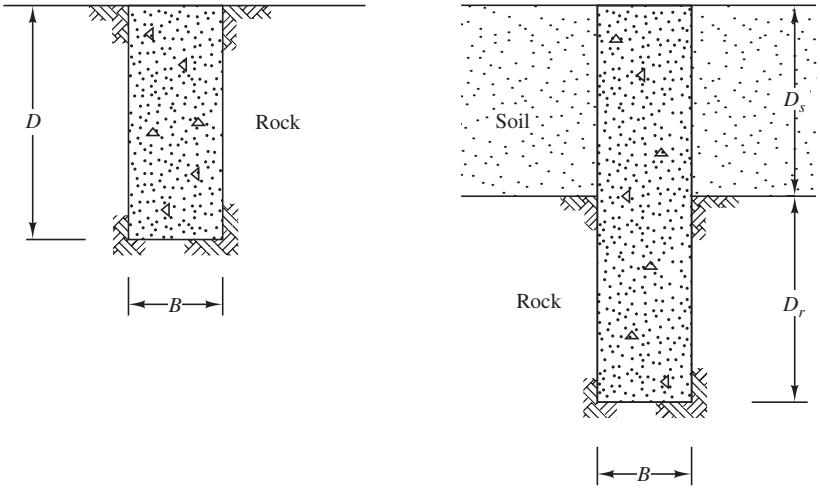

(a) Rock at Ground Surface (b) With Overlying Soil

Figure 25.14 Typical rock sockets for drilled shaft construction in rock: (a) rock at ground surface, (b) with overlying soil.

displacements, and the behavior of the socket can be assumed to be elastic. Under this condition of a "welded bond" between the socket and the surrounding rock, the load-settlement behavior can be obtained from elastic solutions. As the load increases, the shear strength at some points on the socket wall will be reached, leading to breakage of the bond between the socket and the surrounding rock and to shear displacement or slip along this interface. As the amount of slip increases, a larger percentage of the load will be transferred to the toe. Eventually, the entire socket wall will experience slip and the side friction capacity fully mobilized. After this point, any additional load will be transferred to the toe until the toe bearing capacity is also fully mobilized. In summary, as load increases, the socket wall shearing behavior goes from linear elastic at small loads, to progressive slip at intermediate loads, and full slip at large loads, as depicted in the idealized load-settlement curve shown in Figure 25.15. Throughout this process, the side friction resistance is increasingly mobilized and is fully mobilized with full slip.

Kulhawy and Carter (1992) proposed an elastic solution for the linear elastic stage of the load-settlement curve and an approximate analytical solution for the full slip stage. These solutions can be used to estimate pile head settlement as mentioned later under the discussion of serviceability limit state.

The load transfer mechanism described above is for downward loads. For uplift loads, the resistance to loading is normally assumed to be from the side friction resistance only and any contribution from the toe is ignored. The side friction capacity against uplift can usually be taken to be the same as that against downward loads; however, if the socket material is less stiff than the surrounding rock mass and because of negative Poisson's effect, the side friction capacity against uplift may be less than that against downward loads by up to 30%.

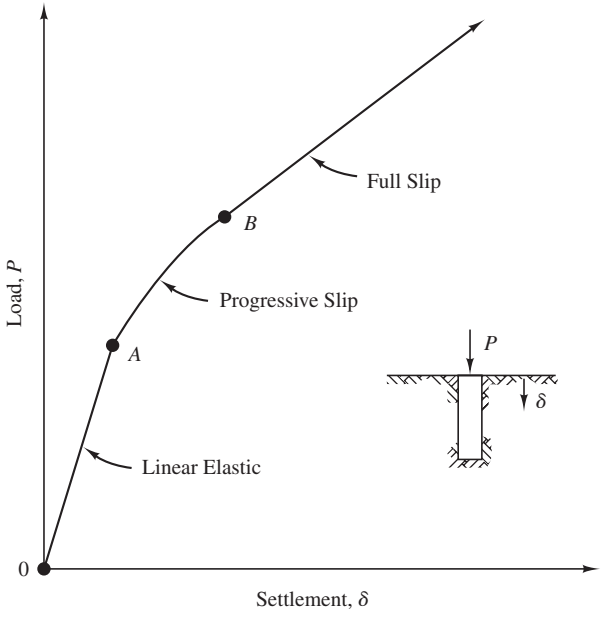

Figure 25.15 Typical load-settlement behavior of a rock socket (after Kulhawy and Carter, 1992).

Ultimate Limit State—Axial Load Capacity of Rock Socketed Piles

The axial load capacity of a rock socket is equal to the sum of the side friction capacity and toe bearing capacity, assuming that both the side friction and toe bearing capacities can be fully mobilized. Empirical formulas have been developed to correlate the nominal unit side friction capacity, f_n, and the nominal unit toe bearing capacity, q_n', with σ_{ci} and other rock mass properties.

Side Friction Resistance

The side friction resistance is fundamentally related to the roughness of the socket wall, and properties of the rock socket material and surrounding rock mass. Because of the scarcity of socket wall roughness data and discontinuity data, many researchers have focused on developing empirical relationships between the nominal side friction capacity, f_n, and a commonly available rock mass property that is the uniaxial compressive strength of the intact rock, σ_{ci}, for example, Horvath and Kenney (1979), Rowe and Armitage (1987), Kulhawy and Phoon (1993), Kulhawy et al. (2005), and Kulhawy and Prakoso (2007). All these researchers have used a common form of the empirical correlation given below:

$$\frac{f_n}{p_a} = C\left(\frac{\sigma_{ci}}{p_a}\right)^{0.5} \tag{25.12}$$

where

p_a = atmospheric pressure (101 kPa or 2,116 lb/ft^2)

In one of the latest studies, Kulhawy et al. (2005) refined the procedures used in analyzing the available field load test results and obtained a mean value of C of approximately 1.0. They recommended a C value of 1.0 for routine practice for normal rock sockets. Normal rock sockets are ones that have been constructed using conventional practice with nominally clean socket walls. Sockets in rocks that are susceptible to smearing or caving during drilling are outside the normal range and will likely have lower side friction resistance than given by Equation 25.12 and $C = 1.0$. For artificially roughened rock sockets, Kulhawy and Prakoso (2007) suggested a C of 1.9.

Note that σ_{ci} used to calculate resistances should be limited to f_c', the compressive strength of the concrete used to construct the socket.

If RQD data are available to account for the degree of fracturing of the rock mass, an empirical equation similar to Equation 25.12 given by O'Neill and Reese (1999) can be used to estimate f_n:

$$\frac{f_n}{p_a} = 0.65\alpha_E\left(\frac{\sigma_{ci}}{p_a}\right)^{0.5} \tag{25.13}$$

where

α_E = joint modification factor

The joint modification factor α_E is a function of the ratio of the rock mass deformation modulus to the intact rock deformation modulus (E_m/E_i), which in turn can be estimated from the RQD of the rock mass. Values of α_E can be estimated from Table 25.7 from the RQD of the rock mass (Brown et al., 2010).

Although there are other more sophisticated methods for determining rock socket side resistance that have been developed to explicitly consider socket wall roughness, probably the most important factor that affects side resistance, for example, Seidel and Collingwood (2001) and Seol et al. (2008), methods relating f_n to σ_{ci} remain the most practical methods for design.

If the LRFD method is used for design, AASHTO (2012) recommended a resistance factor of $\phi = 0.55$ for side friction capacity calculated by Equations 25.12 and 25.13, based on calibration to a factor of safety of 2.5 using the ASD method (Brown et al., 2010).

Toe Bearing Resistance

Because of the availability of data on the uniaxial compressive strength of the intact rock, σ_{ci}, many researchers have developed empirical relationships between the toe bearing capacity of rock sockets and σ_{ci}, for example, Rowe and Armitage (1987), Zhang and Einstein (1998), and Prakoso and Kulhawy (2002). All these researchers have used a common form of the empirical correlation given below:

$$q_n' = N_{cr}^* \sigma_{ci} \tag{25.14}$$

where

q_n' = nominal net toe bearing capacity
N_{cr}^* = bearing capacity factor for rock

Based on these three studies, Brown et al. (2010) recommended an N_{cr}^* of 2.5 for routine design, provided that the socket is bearing on rock that is massive or tightly

TABLE 25.7 SIDE RESISTANCE REDUCTION FACTOR FOR ROCK (Brown et al., 2010)

	Joint Modification Factor, α_E	
RQD (%)	Closed Joints	Open or Gouge-Filled Joints
100	1.00	0.85
70	0.85	0.55
50	0.60	0.55
30	0.50	0.50
20	0.45	0.45

jointed, and that the socket bottom can be verified to be clean before concreting. For this method of computing q_n' using Equation 25.14 and $N_{cr}^* = 2.5$, Brown et al. (2010) gave an LRFD resistance factor of $\phi = 0.55$, corresponding to an ASD factor of safety of 2.5; however, AASHTO (2012) gave a slightly lower value of $\phi = 0.50$ for the same method.

If joint data for the rock below the toe of the socket are available, a method described in the Canadian Foundation Engineering Manual (Canadian Geotechnical Society, 2006) gives an empirical equation for q_n' for sockets bearing on sedimentary rocks having horizontal or nearly horizontal discontinuities, with discontinuity spacings larger than 300 mm (1 ft) and discontinuity apertures less than 5 mm (0.2 in.):

$$q_n' = 3\sigma_{ci} K_{sp} d \tag{25.15}$$

where

K_{sp} = empirical coefficient
d = depth factor
K_{sp} and d are given by

$$K_{sp} = \frac{3 + \dfrac{s_v}{B}}{10\sqrt{1 + 300\dfrac{t_d}{s_v}}} \tag{25.16}$$

$$d = 1 + 0.4\frac{D}{B} \leq 3 \tag{25.17}$$

where

s_v = vertical spacing of discontinuity
t_d = aperture (thickness) of discontinuity
B = socket diameter
D = depth of socket embedment

The LRFD resistance factor used by AASHTO (2012) for this method of computing q_n' is $\phi = 0.50$, which, according to Brown et al. (2010), is based on calibration to ASD reported by Barker et al. (1991).

For a socket bearing on a rock mass satisfying the Generalized Hoek-Brown failure criterion, Zhang and Einstein (1998) and Turner (2006) extended Kulhawy and Carter's (1992) solution for footings presented earlier. Figure 25.16 illustrates the stress state for an imaginary infinitely long rock socket used in this solution (analogous to a continuous footing with a width B). At failure, in Zone I the horizontal stress, σ_h', is the major principal stress, and the minor principal stress is the vertical stress at the toe elevation, σ_{zD}'. These principal stresses are related by the Hoek-Brown criterion

$$\sigma_h' = \sigma_{zD}' + \sigma_{ci}\left[m_b\frac{\sigma_{zD}'}{\sigma_{ci}} + s\right]^a \tag{25.18}$$

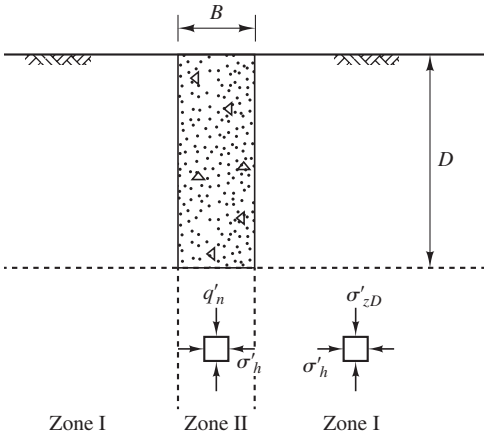

Figure 25.16 Stress conditions for lower bound solution for toe bearing of a rock socket (after Kulhawy and Carter, 1992).

Again referring to Figure 25.16, in Zone II the horizontal stress, σ'_h, is now the minor principal stress, and q'_n, is the major principal stress. These stresses are again related by the Hoek-Brown criterion

$$q'_n = \sigma'_h + \sigma_{ci}\left[m_b\frac{\sigma'_h}{\sigma_{ci}} + s\right]^a \tag{25.19}$$

Although Equation 25.19 applies to an infinitely long rock socket, it can conservatively be used for circular sockets. Additionally, q'_n calculated by Equation 25.14 with $N^*_{cr} = 2.5$ can be used as an upper bound value. According to Brown et al. (2010), the LRFD resistance factor has not been determined for this method of computing q'_n.

There are other methods for determining toe bearing capacity that have been developed, for example, Serrano and Olalla (2002) using plasticity theory, Zhang (2010) relating toe bearing capacity to rock mass strength (calculated from RQD) instead of intact rock strength, and Jeong et al. (2010) using load transfer functions. Some of these methods would require rock mass data that are not commonly available and might be difficult to use in practice.

Example 25.5

A rock socketed pile is to be designed without the benefit of any onsite static load tests. The ground conditions are uniform, and the site characterization program was average. For a 0.6 m diameter drilled shaft, fully socketed in rock from the ground surface to a depth of 5 m in the sandstone in Example 25.1, compute the ASD allowable compressive load capacity and the AASHTO LRFD factored compressive load capacity.

Solution

Side Friction

Use Equation 25.13 per O'Neill and Reese (1999). For RQD = 97%, Table 25.7 gives $\alpha_E = 1.0$. Therefore,

$$\frac{f_n}{p_a} = 0.65\alpha_E\left(\frac{\sigma_{ci}}{p_a}\right)^{0.5} = 0.65\left(\frac{46\text{ MPa}}{0.101\text{ MPa}}\right)^{0.5} = 13.9$$

$$f_n = 13.9(101\text{ kPa}) = 1{,}400\text{ kPa}$$

$$A_s = \pi(0.6)(5) = 9.42\text{ m}^2$$

Toe Bearing

Use Equation 25.14 per Brown et al. (2010) with $N^*_{cr} = 2.5$:

$$q'_n = (2.5)(46\text{ MPa}) = 115{,}000\text{ kPa}$$

$$A_t = \frac{\pi(0.6)^2}{4} = 0.283\text{ m}^2$$

ASD Capacity

Using a factor of safety of 3 (per Table 13.2):

$$P_a = \frac{q'_n A_t + f_n A_s}{F}$$

$$= \frac{(115{,}000)(0.283) + (1{,}400)(9.42)}{3}$$

$$= \mathbf{15{,}200\text{ kN}}$$

LRFD Capacity

Per Table 13.5, the AASHTO resistance factor for side friction is 0.55, and for toe bearing is 0.50.

$$\phi P_n = \phi_t q'_n A_t + \phi_s \sum f_s A_s$$

$$= (0.50)(115{,}000)(0.283) + (0.55)(1{,}400)(9.42)$$

$$= \mathbf{23{,}500\text{ kN}}$$

Serviceability Limit State—Settlement of Rock Socketed Piles

The settlement of a rock socketed pile can be computed using the theory of elasticity, if the settlement is relatively small, that is, in the linear elastic range shown in Figure 25.15. Assuming full bonding between a full depth rock socket and the surrounding rock mass, Kulhawy and Carter (1992) obtained elastic solutions for the load-settlement behavior of the pile (included in Brown et al., 2010) and produced a chart shown in Figure 25.17 that relates the pile head settlement δ to the depth of the pile D, diameter of the pile B, vertical load on the pile head P, rock mass modulus E_m, and concrete modulus E_c, using a Poisson's ratio of 0.25 for both rock and concrete. This chart can be used to estimate pile head settlement under a given sustained load.

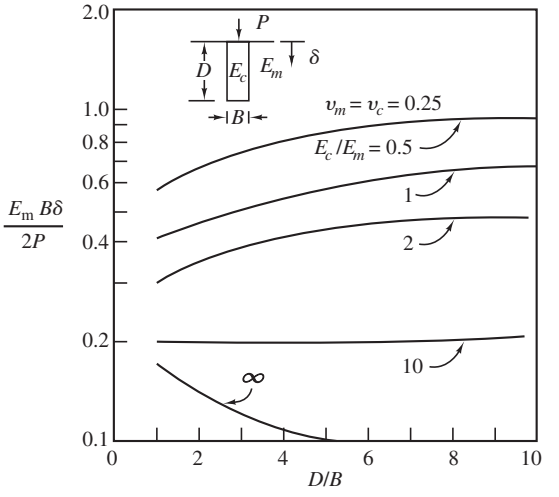

Figure 25.17 Elastic settlement of rock sockets (after Kulhawy and Carter, 1992).

Kulhawy and Carter (1992) also provide an approximate analytical solution for the full slip stage shown in Figure 25.15. This closed form solution will not be presented here but can be found in Brown et al. (2010).

25.3 FOUNDATIONS IN INTERMEDIATE GEOMATERIALS

The term intermediate geomaterial (IGM) was coined by O'Neill et al. (1996) to identify geologic materials with strengths that are intermediate between those of soils and rocks. IGMs are defined by their strengths and are further categorized into cohesionless and cohesive IGMs. As defined by O'Neill et al. (1996), cohesionless IGMs are very dense granular geomaterials with SPT N_{60}-values between 50 and 100. Cohesive IGMs are defined by O'Neill et al. (1996) as geomaterials having uniaxial (or unconfined) compressive strengths in the range of 477 kPa (10 ksf) to 4,770 kPa (100 ksf). Specific cohesive IGMs identified by O'Neill et al. (1996) include:

- Argillaceous geomaterials, such as heavily overconsolidated clays, clay shales, saprolites, and mudstones, that are prone to smearing when drilled
- Calcareous rocks, such as limestone and limerock and argillaceous geomaterials, that are not prone to smearing when drilled

The term IGM and its definition were adopted by Brown et al. (2010) and AASHTO (2012) LRFD specifications. For the purposes of designing drilled shafts, Brown et al. (2010) grouped cohesionless IGMs with cohesionless soils, implying that design methods for drilled shafts in cohesionless soils can be applied to drilled shafts in cohesionless IGMs. On the other hand, cohesive IGMs should be treated differently than other

materials, and Brown et al. (2010) provided design equations that are specifically for drilled shafts in cohesive IGMs.

Besides the methods discussed above for designing drilled shafts in IGMs, few methods have been widely available for designing other types of foundations in IGMs, including driven piles and footings. When no design method is available for foundations in a particular IGM, one must exercise judgment and determine if the IGM will behave more like a soil or a rock and then carry out the design using the appropriate method. In borderline or difficult cases, it may be helpful to perform two separate designs, one assuming a soil-like IGM and the other a rock-like IGM. The more conservative of the two designs can then be used. Finally, as with any geomaterial, one should always take advantage of any available local experience.

Side Friction Resistance of Rock Sockets in Cohesive IGMs

Based on the work by Hassan et al. (1997) on rock sockets in argillaceous rocks (e.g., shale, claystone, and siltstone) O'Neill et al. (1996) categorized these materials as cohesive IGMs and recommended the following correlation for f_n using the α method

$$f_n = \alpha_E \alpha \sigma_{ci} \tag{25.20}$$

where

α_E = a joint modification factor related to RQD given in Table 25.7
α = side friction coefficient provided in Figure 25.18

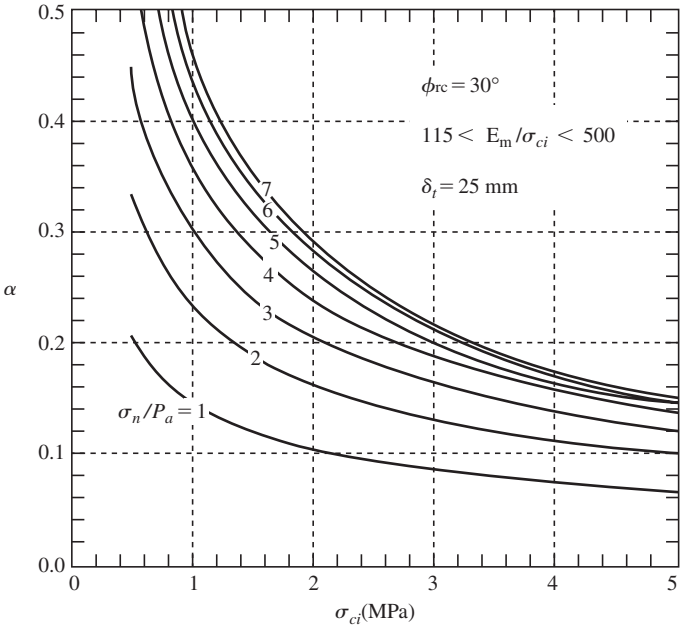

Figure 25.18 α for rock sockets in cohesive IGMs (after O'Neill et al., 1996).

The value of α is determined from Figure 25.18, where:

p_a = atmospheric pressure
σ_n = fluid pressure exerted by the concrete in socket during placement
δ_t = vertical displacement required to mobilize the full side friction resistance, assumed to be 25 mm (1 in)
ϕ_{rc} = socket wall interface friction angle, assumed to be 30 degrees

Equation 25.20 is applicable for a range of E_m/σ_{ci} of 115 to 500. If ϕ_{rc} is not equal to 30 degrees, the factor α can be adjusted using

$$\alpha(\text{adjusted}) = \alpha \frac{\tan \phi_{rc}}{\tan 30^\circ} \tag{25.21}$$

To determine the concrete pressure, σ_n, for concrete having a slump of 18 cm (7 in) or higher and placed at a rate of 12 m per hour (40 ft per hour) use

$$\sigma_n = 0.65 \gamma_c z_i \tag{25.22}$$

where

γ_c = unit weight of concrete
z_i = depth of the midpoint of the socket up to 12 m (40 ft) (use 12 m (40 ft) if $z_i > 12$ m (40 ft))

For this method, AASHTO (2012) uses an LRFD resistance factor of $\phi = 0.60$, as recommended by Allen (2005) based on calibration studies by Paikowsky et al. (2004).

For very weak soil-like claystone IGM having SPT N_{60}-values of less than 100, based on experience by the Colorado Department of Transportation, Abu-Hejleh et al. (2003) recommended the following correlations for unit side friction and net unit toe bearing capacity:

$$f_n = 3.6 N_{60} \quad \text{(25.23 SI)}$$

$$f_n = 0.075 N_{60} \quad \text{(25.23 English)}$$

$$q'_n = 44 N_{60} \quad \text{(25.24 SI)}$$

$$q'_n = 0.92 N_{60} \quad \text{(25.24 English)}$$

where

f_n = nominal unit side friction capacity (kPa, k/ft^2)
q'_n = nominal unit end bearing capacity (kPa, k/ft^2)
N_{60} = SPT blow count corresponding to 60% hammer efficiency

For Equations 25.23 and 25.24, Abu-Hejleh et al. (2003) recommended a resistance factor of $\phi = 0.70$ based on calibration to a factor of safety of 2.0.

Toe Bearing Resistance of Rock Sockets in Cohesive IGMs

According to O'Neill et al. (1996), the methods presented earlier for estimating the toe bearing resistance of rock sockets are applicable to sockets in cohesive IGMs.

SUMMARY

Major Points

1. In practice, there are a wide range of geomaterials that a geotechnical engineer must be prepared to deal with from soils to intermediate geomaterials (IGMs) to rocks.
2. A rock mass consists of intact rock and discontinuities.
3. Rock mass behavior depends on the size of the foundation relative to the spacings of the discontinuities.
4. In this book, only continuous rock mass behavior Type I, of the intact rock, and III, of the equivalent continuous rock mass, are considered. Discontinuous rock mass behavior, Type II, is not considered.
5. Rock mass can be classified using the Rock Mass Rating (RMR) system or the Q system.
6. The Generalized Hoek-Brown failure criterion is a nonlinear rock mass failure criterion that can be applied to failure of the rock mass and, as a special case, failure of the intact rock.
7. The effect of the geological conditions on rock mass strength is quantified by the Geological Strength Index (GSI).
8. The rock mass properties that describe the stress-strain behavior of rock masses are the rock mass deformation modulus and the rock mass Poisson's ratio.
9. The design of foundations in rocks is based on prescriptive methods, large scale load tests, empirical methods, or rational methods.
10. Bearing capacity of spread footings on rocks can be obtained using bearing capacity solutions from the theory of plasticity using the Generalized Hoek-Brown model.
11. Settlement of spread footings on rocks can be estimated from the theory of elasticity and rock mass deformation properties.
12. The load-settlement curve of a rock socket consists of a linear elastic portion at small loads, a portion at intermediate loads with progressive slip along the socket wall, and a full slip portion at high loads.
13. The axial capacity of a rock socket is the sum of the side friction capacity and the toe bearing capacity. The side friction capacity and toe bearing capacity can be estimated from empirical correlations.
14. Intermediate geomaterials are geomaterials with strengths that are intermediate between those of soils and rocks. There are some empirical methods for designing foundations in IGMs.

Vocabulary

Cohesionless intermediate geomaterials
Cohesive intermediate geomaterials
Discontinuity
Generalized Hoek-Brown failure criterion
Geological Strength Index (GSI)
Geomaterial
Geomechanics Classification
Intact rock
Intact rock deformation modulus
Intermediate geomaterial (IGM)
Nominal bearing capacity
Nominal net toe bearing capacity
Nominal side friction capacity
Q system
Rock mass
Rock mass behavior type
Rock mass deformation modulus
Rock mass Poisson's ratio
Rock mass rating (RMR)
Rock Quality Designation (RQD)
Rock socket
Spacing ratio (SR)
Uniaxial compressive strength of the intact rock

QUESTIONS AND PRACTICE PROBLEMS

Section 25.1 Rock as a Structural Foundation Material

25.1 A site is underlain by a shale having the following properties and characteristics:

- Average uniaxial compressive strength of intact rock = 34 MPa
- Average RQD = 77%
- Average discontinuity spacing = 0.5 m
- Discontinuities are slightly rough, with slightly weathered walls, lengths between 3 and 10 m, and with narrow openings and no filling
- Dry, with occasional localized dampness
- Average unit weight = 24.0 kN/m^3

Estimate for this shale the total RMR rating, GSI, Hoek-Brown failure criterion assuming the rock is undisturbed, intact rock deformation modulus, rock mass deformation modulus, and the rock mass Poisson's ratio.

25.2 A site is underlain by a granite having the following properties and characteristics:

- Average uniaxial compressive strength of intact rock = 260 MPa
- Average RQD = 80%
- Average discontinuity spacing = 1.1 m
- Discontinuities are tight and rough, with slightly weathered walls and lengths between 3 and 10 m
- Dry
- Average unit weight = 25.9 kN/m^3

Estimate for this granite the total RMR rating, GSI, Hoek-Brown failure criterion assuming the rock is undisturbed, intact rock deformation modulus, rock mass deformation modulus, and the rock mass Poisson's ratio.

Section 25.2 Design of Foundations in Rocks

25.3 A continuous footing having a width of 1.0 m is underlain by the shale in Problem 25.1. Estimate the nominal bearing capacity using Kulhawy and Carter (1992) and Merifield et al. (2006).

25.4 A continuous footing having a width of 1.0 m is underlain by the granite in Problem 25.2. Estimate the nominal bearing capacity using Kulhawy and Carter (1992) and Merifield et al. (2006).

25.5 A circular footing having a diameter of 1.0 m is underlain by the shale in Example 25.1. Estimate the nominal bearing capacity using Clausen (2013).

25.6 A circular footing having a diameter of 1.0 m is underlain by the granite in Example 25.2. Estimate the nominal bearing capacity using Clausen (2013).

25.7 A square footing having a width of 1.0 m is underlain by the shale in Problem 25.1. Estimate the settlement under a vertical downward sustained load of 1,000 kN.

25.8 A circular footing having a diameter of 500 mm is underlain by the granite in Problem 25.2. Estimate the settlement under a vertical downward sustained load of 10,000 kN.

25.9 A rock socketed pile is to be designed without the benefit of any onsite static load tests. The ground conditions are uniform, and the site characterization program was average. For a 600 mm diameter drilled shaft, fully socketed in rock from the ground surface to a depth of 6 m in the shale in Problem 25.1, compute the ASD allowable compressive load capacity and the AASHTO LRFD factored compressive load capacity.

25.10 Using the data in Problem 25.9, compute the ASD upward load capacity and the AASHTO upward load capacity, $\phi P_{up,n}$. Use a load factor of 0.9 on the weight of the shaft.

25.11 A rock socketed pile is to be designed without the benefit of any onsite static load tests. The ground conditions are uniform, and the site characterization program was average. For a 500 mm diameter drilled shaft, fully socketed in rock from the ground surface to a depth of 5 m in the granite in Problem 25.2, compute the ASD allowable compressive load capacity and the AASHTO LRFD factored compressive load capacity.

25.12 Using the data in Problem 25.10, compute the ASD upward load capacity and the AASHTO upward load capacity, $\phi P_{up,n}$. Use a load factor of 0.9 on the weight of the shaft.

25.13 A site is underlain by the shale in Problem 25.1 with the shale exposed at the surface. Determine the required diameter and length of a drilled shaft needed to support an ASD design downward load of 35,000 kN. Note there are many different diameter–length combinations that would be satisfactory, but select one that you think would be most appropriate.

25.14 A drilled shaft designed in accordance with the AASHTO code must support the following downward and uplift axial design loads: $P_u = 20{,}000$ kN, $P_{up,u} = 7{,}000$ kN. The site is underlain by the shale in Problem 25.1 from the ground surface down to great depths. Using the

AASHTO resistance factors, select a diameter and depth for a single drilled shaft to support these design loads. Use a load factor of 0.9 on the weight of the shaft. Note there are many different diameter–length combinations that would be satisfactory, but select one that you think would be most appropriate.

Section 25.3 Foundations in Intermediate Geomaterials

25.15 A rock socketed pile is to be designed without the benefit of any onsite static load tests. The ground conditions are uniform, and the site characterization program was average. For a 600 mm diameter drilled shaft, fully socketed in a cohesive IGM having an average SPT N_{60}-value of 85, from the ground surface to a depth of 5 m, compute the ASD allowable compressive load capacity and the LRFD factored compressive load capacity.

26

Ground Improvement

Anyone who thinks he has all the answers is not quite up-to-date on all the questions.

Unknown Author

On most foundation projects, geotechnical engineers focus on assessing the existing soil and rock conditions, then develop foundation designs that are compatible with these conditions. When the subsurface conditions are not suitable for shallow foundations, then deep foundations are typically specified. However, at many sites, the added cost of deep foundations can be avoided by improving the engineering properties of the near surface soils so that these improved soils can support conventional shallow foundations. For example, Partos et al. (1989) showed in four projects shallow foundations on improved soils were more economical than deep foundations.

This process of improving soils for civil engineering projects is generally called *ground improvement* to distinguish it from other soil modification processes, for example in agricultural applications. Ground improvement is being driven by economic pressures to build on sites with marginal soils, the need to rebuild aging infrastructure in urban areas, and increased recognition of seismic hazards. Methods have been developed and dramatically improved over the past fifty years to the point where ground improvement is routinely used and has even become a subdiscipline of geotechnical engineering (Schaefer et al., 2012). There is a wide variety of ground improvement methods at the geotechnical engineer's disposal and the topic could easily fill an entire course. This chapter gives only a brief introduction to the common ground improvement methods and will focus on those methods that are most applicable to foundation engineering.

26.1 GROUND IMPROVEMENT FOR FOUNDATIONS

Ground improvement techniques can be broadly grouped into two categories as they are applied to foundation engineering. The first category includes those methods designed to strengthen or reduce the compressibility of soils immediately within the zone of influence of a foundation to allow for a more economical foundation design. The second category includes methods designed to mitigate or eliminate the potential for future instability in foundation soils such as that due to earthquake induced liquefaction, swelling of potentially expansive soils, or collapse of meta-stable soils. The distinction is important because the location and volume of soil needing improvement, and the properties addressed by that improvement will differ between these two categories.

For ground improvement projects in the first category, the goal is to increase the soil shear strength, cohesion and/or friction angle, and increase the modulus (or decrease the compressibility) immediately around the foundation. This generally involves either densifying or adding material into the soil that will increase strength and modulus. The volume of soil needing modification will vary depending upon the foundation type, but for square footings, the volume of concern is the zone of influence that extends from the bottom of the footing to approximately two footing widths below the footing and laterally by one footing width around the footing.

For ground improvement projects in the second category, the specific goals of ground improvement will depend upon what sort of potential instability needs to be addressed. In the case of mitigating potential liquefaction or collapse of metastable soils, increasing density is a common goal. In contrast, reducing swelling potential may require reducing density of a soil as well as chemical modifications. Modifications in this category also often involve soils much more distant from the foundations themselves. For example, a liquefiable zone may exist well below the zone that directly influences the local bearing capacity of footings. Projects in this category often involve modifying soils over a much larger area and volume compared to projects in the first category.

26.2 REMOVAL AND REPLACEMENT

One of the oldest and simplest ground improvement methods is to simply excavate the unsuitable soils and replace them with compacted fill. This method is often used when the only problem with the soil is that it is too loose. In that case, the soil removed is also used to build the fill. In other cases, a different soil is brought in from offsite to amend or replace the native soil. The recompacted soil will be much more uniform and will have a higher unit weight and thus greater strength and higher modulus than the soil it replaces. This recompaction method is commonly used to remediate problems with collapsible soils. In the case of expansive soils, this process can be combined with the use of chemical treatment to reduce swelling potential as discussed in Section 26.7.

Removal and replacement is generally practical only above the groundwater table. Earthwork operations when the soil is very wet become much more difficult, even when the free water is pumped out, and thus are generally avoided unless absolutely necessary.

Guidelines for design of compacted structural fills are often available from state and local regulatory agencies. Brown (2001) also provides more detailed information on this technique and Christopher et al. (2006) provide detailed information on designing, monitoring, and controlling compacted fills.

26.3 PRECOMPRESSION

Another old and simple method of improving soils is to cover them with a temporary fill, as shown in Figure 26.1 (Stamatopoulos and Kotzias, 1985). This method is called precompression, preloading, or surcharging, and the temporary fill is called a surcharge fill. It is especially useful in soft clayey and silty soils because the static weight of the fill causes them to consolidate, thus improving both their settlement and strength properties. Once the desired properties have been obtained, the surcharge is removed and construction proceeds on the improved site.

Surcharge fills are typically 3 to 8 m (10–25 ft) thick, and generally produce settlements of 0.3 to 1.0 m (1–3 ft). They have been used at sites intended for highways, runways, buildings, tanks, and other projects.

Precompression has many advantages, including:

- It requires only conventional earthmoving equipment, which is readily available. No special or proprietary construction equipment is needed.

Figure 26.1 Surcharge fill remaining in place until the underlying soils have settled. The smokestack and crane in the background are located behind the fill.

- Any grading contractor can perform the work.
- The results can be effectively monitored by using appropriate instrumentation (especially piezometers) and ground level surveys.
- The method has a long track record of success.
- The cost is comparatively low, so long as soil for preloading is readily available.

However, there also are disadvantages, including:

- The surcharge fill generally must extend horizontally at least 10 m (33 ft) beyond the perimeter of the planned construction. This may not be possible at confined sites.
- The transport of large quantities of soil onto the site may not be practical, or may have unacceptable environmental impacts (i.e., dust, noise, traffic) on the adjacent areas.
- The surcharge must remain in place for months or years, thus delaying construction. However, the process can be accelerated by the installation of vertical drains as described below.

Vertical Drains

The time required to achieve a certain level of consolidation is proportional to the square of the maximum drainage distance. Thus, if the stratum of compressible soil is very thick, the time required to achieve the desired consolidation may be excessive. In some cases, this time can easily be several years or even decades, even with a surcharge fill. Very few projects can accommodate such long delays. Therefore, when precompression is used on thick compressible soils, we generally need to employ some means of accelerating the consolidation process.

The most effective way of accelerating soil consolidation is to reduce the drainage distance for pore water by providing artificial paths for the excess pore water to escape. This can be done by installing vertical drains, as shown in Figure 26.2. The excess pore water within the compressible soil now drains horizontally to the nearest vertical drain, leading to a much shorter drainage distance than before. In addition, most soft clays contain thin horizontal sandy or silty seams, so the horizontal hydraulic conductivity, k_x, is typically much higher than the vertical value, k_z. This further increases the rate of consolidation. Thus, the time required to achieve the required degree of consolidation can typically be reduced from several years to only a few months. Vertical drains also may be used either with or without a surcharge.

The excess pore water pressures generated during consolidation provide the head to drive water through the vertical drains. Once consolidation is complete, the excess pore water pressures become zero and drainage ceases.

The earliest vertical drains consisted of a series of borings filled with sand. These sand drains were expensive to construct, so engineers developed another method: prefabricated vertical drains (also known as wick drains or band drains). They consist of corrugated or textured plastic ribbons surrounded by a geosynthetic filter material as shown in Figure 26.3. Most are about 100 mm (4 in) wide and about 5 mm (0.2 in) thick. These drains are supplied on spools, and are inserted into the ground using special equipment

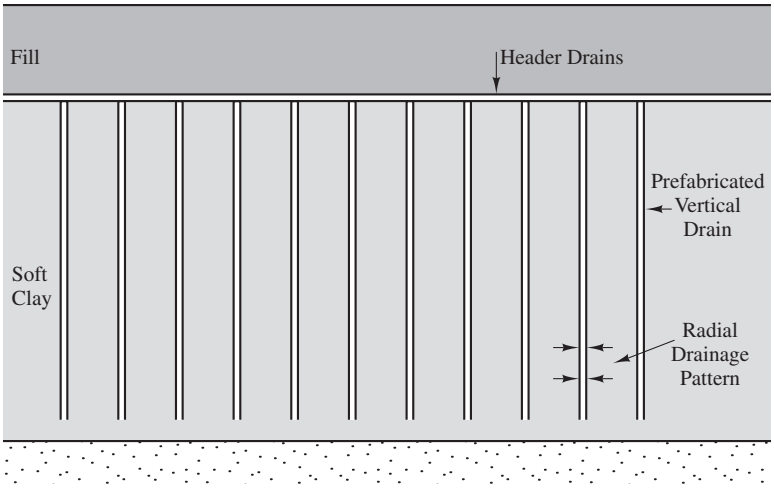

Figure 26.2 Use of vertical drains to accelerate consolidation.

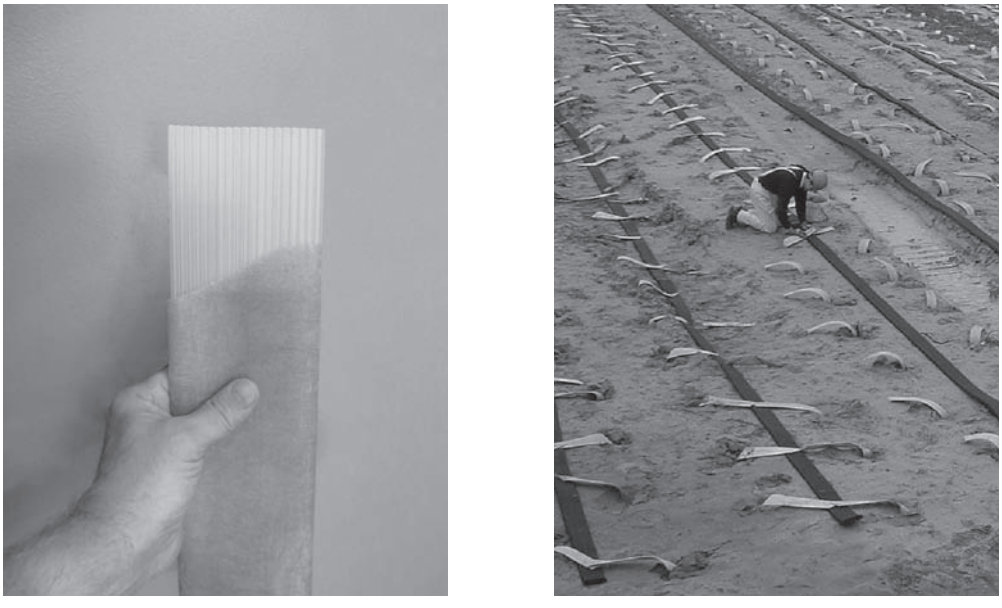

(a) (b)

Figure 26.3 (a) A typical prefabricated vertical drain; (b) prefabricated vertical drains after installation. The drains are the small strips extending out of the ground. Wider header drains also have been installed on the ground surface to collect water from the vertical drains and carry it to a discharge location. The site is nearly ready to be covered with fill (photo (b) courtesy of Haward Baker, Inc.)

that resembles a giant sewing machine, as shown in Figure 26.4. Prefabricated vertical drains are considerably less expensive than sand drains, and thus have become the preferred method on nearly all projects.

The required spacing of vertical drains is determined by a radial drainage analysis, and represents a compromise between construction cost and rate of consolidation. Typically they are spaced about 3 m (10 ft) on centers, which means hundreds of drains are usually required. Although precompression and vertical drains can be very useful with soft silty and clayey soils, it is not very effective in sandy soils. Sands respond best to

Figure 26.4 Equipment used to install prefabricated vertical drains (Courtesy of U.S. Wick Drain and Menard USA).

densification methods that use vibration. Guidance for the design of vertical drain and preload projects is available from Rixner et al. (1986) and Holtz et al. (1991).

26.4 IN SITU DENSIFICATION

Engineers and contractors have developed several methods of inducing strong vibrations in the ground to densify sandy soils in situ. Many of these methods have proven to be cost effective, and are especially useful in remediating sandy soils that are prone to earthquake induced liquefaction. Shallow soils often can be densified using heavy vibratory rollers, but this technique is effective only to depths of about 2 m (7 ft). Other methods, as discussed below, induce vibrations at greater depths and are used to densify deeper soils.

Vibrocompaction

One method of densifying deeper soil deposits is to insert some type of vibratory probe into the ground. Two types are most commonly used: the terra probe and the vibroflot. A terra probe consists of a vibratory pile hammer attached to a steel pipe pile (Brown and Glenn, 1976). This device is vibrated into the ground, densifying the adjacent soils, and then retracted. A vibroflot is a specially constructed probe that contains vibrators and water jets. This probe is lowered into the ground using a crane, as shown in Figure 26.5. The presence of the vibrator near the tip probably induces greater vibrations in the ground, and the water jets assist in the insertion and extraction of the probe. This technique of ground improvement is called vibroflotation.

Both of these techniques may be classified as vibrocompaction methods because they compact the soils in situ using vibration. They are generally effective only when the silt content is less than 12–15 percent and the clay content is less than about 3 percent (Schaefer, 1997). The construction process typically uses a grid pattern, with spacings of 1.5 to 4 m (5–13 ft) and treatment depths of 3 to 15 m (10–50 ft). Guidelines for design of vibrocompaction projects are available in Elias et al. (2006).

Dynamic Compaction

Dynamic compaction (also called dynamic consolidation or heavy tamping) is another method of in situ densification. It uses a special crane to lift 44 to 267 kN (5–30 ton) weights, called pounders, to heights of 12 to 30 m (40–100 ft), then drop these weights onto the ground as shown in Figure 26.6. Typically the weight is dropped several times at each location. This process is repeated on a grid pattern across the site, leaving a series of 1 to 3 m (3–10 ft) deep craters. The ground surface is then releveled with conventional earthmoving equipment and the process is repeated at grid points midway between the primary drops. Finally, the upper soils are compacted and graded using conventional methods.

Although it appears crude, dynamic compaction can be a cost effective method of densifying loose sandy and silty soils. It also has been used in soils that contain boulders and other large debris, and in sanitary landfills. The primary zone of influence typically extends to depths of 5 to 10 m (15–30 ft), with lesser improvements below these depths.

Figure 26.5 Crane lowering vibroflot into the ground (courtesy of Hayward Baker Inc.).

It has been used to treat liquefaction prone soils (Dise et al., 1994), collapsible soils (Rollins and Kim, 1994), and soils that are prone to excessive settlement. However, it is not an effective method for saturated clays because their low hydraulic conductivity does not permit rapid consolidation.

The effectiveness of a dynamic compaction program is typically evaluated by performing SPT or CPT tests both before and after construction. In favorable conditions, the post-construction $N_{1,60}$ values can be 10 to 20 blows higher than those measured before construction.

Because of the large impact forces, this method generates substantial shock waves, and therefore cannot be used close to existing structures. Guidelines for design of dynamic compaction projects are available from Lukas (1995).

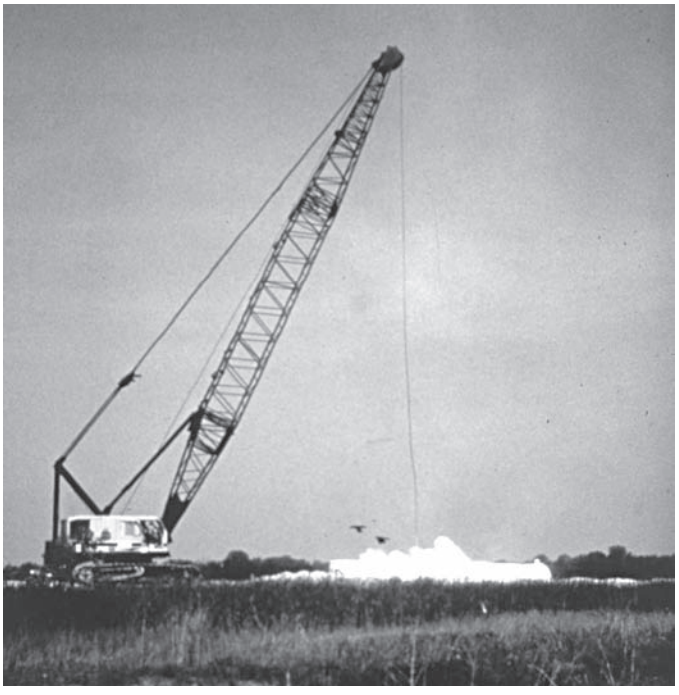

Figure 26.6 Dynamic compaction performed by dropping a large weight onto the ground from height using a crane. The weight has just hit the ground in this picture (courtesy of Hayward Baker Inc.).

Rapid Impact Compaction

Rapid Impact Compaction (RIC) is a ground improvement method that uses a hydraulic pile driving hammer to repeatedly hit a heavy impact plate placed on the ground surface, to densify loose granular soils. The hammer is typically 67 kN (7.5 ton) in weight, and the impact plate is typically 1.5 m (5 ft) in diameter (Hayward Baker Inc., 2009a). The energy from the hammer striking the impact plate is transferred into the subsurface to densify soils to a depth of 6 m (20 ft).

To treat large areas, the locations of RIC follow a grid pattern that covers the areas requiring treatment. Applied in this way, RIC can be a good alternative to excavation and recompaction. It also can be used in combination with dynamic compaction, with RIC treating the shallower soils and dynamic compaction the deeper ones. As a relatively new technology, RIC lacks thorough design guidance. Simpson et al. (2008) and Mohammed et al. (2013) provide case histories describing the use of this method and the improvements measured.

Blast Densification

Blast densification is another method of in situ densification. This method consists of drilling a series of borings and using them to place explosives underground. These explosives are then detonated, and the resulting shock waves densify the surrounding soils. Blast

densification has been used successfully in many projects, and is most effective in clean sands. However, because of vibration and safety issues, it is only suitable for remote sites and thus is not nearly as common as other in situ densification methods. Its chief advantage over other in situ densification methods is its ability to reach great depths at relatively low costs. Design approaches for this method are largely empirically based. Gohl et al. (2000) discuss design guidelines based on cavity expansion theory.

26.5 IN SITU REPLACEMENT

Aggregate Columns

A number of methods are available to install and densify vertical columns of crushed rock or gravel into weak or compressible soils. Collectively these ground improvement techniques are called *aggregate columns* although a number of other names, some proprietary, are used. These aggregate columns can increase both the bearing capacity and modulus of soils in which they are installed. In foundation applications, they are used to support footing and mat foundations as well as reduce settlements. Design guidance for aggregate columns is available from Barksdale and Bachus (1986) and Elias et al. (2006). The different aggregate columns systems are distinguished mainly by the methods used to install the columns.

Vibro Replacement or Stone Columns

With this method, a vibroflot is used to create a shaft that is backfilled with gravel to form an aggregate column (Mitchell and Huber, 1985). After the vibroflot penetrates to the desired depth, aggregate is added to the bottom of the shaft using a tremie type device. The shaft is filled from the bottom up using vibration to densify the aggregate. The shaft can also be pre-augured. Alternatively, dynamic compaction equipment may be used to pound a gravel inclusion into the ground using a technique called dynamic replacement. These methods may be used in nearly all types of soils, and are primarily intended to provide load bearing members that extend through the weak strata. The stone columns also act as vertical drains, thus helping to accelerate consolidation settlements and mitigate seismic liquefaction problems.

Aggregate Piers

Aggregate piers, also called Rammed Aggregate Piers®, are created by first drilling a shaft in the ground and then back filling the shaft with aggregate that is compacted in layers using a ram. The drilled shafts are generally 600–900 mm (24–36 in) in diameters. The aggregate is generally placed in layers approximately 300 mm (12 in) thick. Typical depths are 2–9 m (7–30 ft) (Hayward Baker Inc., 2009b). The technique works best in cohesive soils where it is easy to maintain an open hole during the ramming process. It can be used in cohesionless soils but requires the use of a casing to keep the hole open.

Vibro Concrete Columns

Vibro Concrete Columns (VCCs) are concrete columns that are constructed in situ using a bottom-feed downhole vibratory probe following these steps (Hayward Baker Inc., 2008):

1. The downhole probe is advanced to the desired depth.
2. Concrete is pumped through the tremie pipe in the probe with the probe moving up and down to create an enlarged toe of the column.
3. As the probe is raised, concrete is continuously pumped to fill the void left by the probe, creating a concrete column.
4. The probe typically is also used to create an enlarged head of the column.

VCCs are used to transfer loads to competent layers at depth and are cheaper than deep foundations.

Rigid Inclusions

Rigid inclusions are similar to VCCs. They are concrete columns constructed using a vibratory bottom-feed mandrel (Hayward Baker Inc., 2013). The mandrel is first advanced to the desired depth that is the bottom of the rigid inclusion. As the mandrel is raised, concrete is continuously pumped through the tremie pipe in the mandrel to fill the void left by the mandrel, creating a concrete column that is the rigid inclusion. Concrete pumping stops when the desired top of the rigid inclusion is reached. The rigid inclusions are used to reinforce weak layers to increase bearing capacity and decrease settlement.

26.6 GROUTING

Grouting is the injection of special liquid or slurry materials, called grout, into the ground for the purpose of improving the soil or rock. It has been used extensively for the past several decades, and is a well-established method of ground improvement.

There are two primary kinds of grout. Cementitious grouts are made of Portland cement that hydrates after injection, forming a solid mass. Chemical grouts include a wide range of chemicals that solidify once they are injected into the ground. These include silicates, resins, and many others. Chemical grouts have a wider range of available properties, and thus can be used in some applications where cement grouts are ineffective. However, chemical grouts also are more expensive, and some are toxic or corrosive.

In foundation design, grouting is most commonly used to mitigate liquefaction potential or to remediate an existing foundation. There are four principal grouting methods, as shown in Figure 26.7; however, only compaction and jet grouting are commonly used with foundation systems. Intrusion and permeation grouting are generally used to decrease hydraulic conductivity of soil or rock formations.

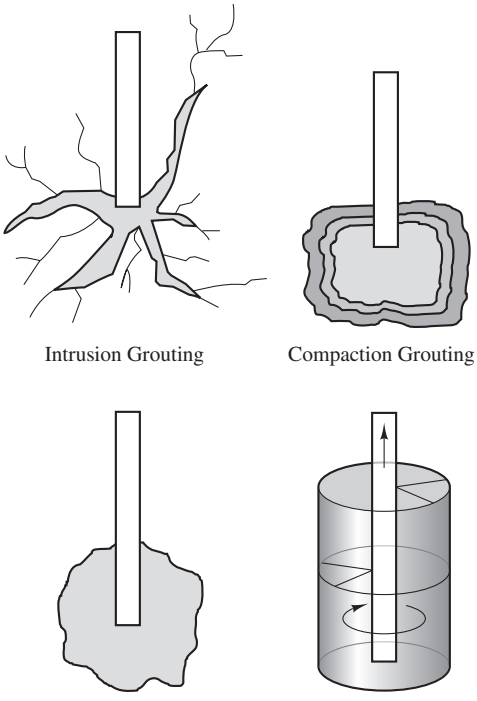

Figure 26.7 Types of grouting (Welsh, 1986).

Compaction Grouting

Compaction grouting (also known as displacement grouting) uses a stiff (i.e., about 25 mm or 1 in slump) grout that is injected into the ground under high pressure through a pipe to form a series of inclusions or grout bulbs (Rubright and Welsh, 1993), as illustrated in Figure 26.8. This grout is too thick to penetrate significantly into the soil, but the grout bulbs compact the adjacent soil. Injection points are typically spaced 2–4 m (6–13 ft) apart. Grout bulbs are generally formed every 30–100 cm (1–3 ft). This method is generally limited to an overburden pressure of 50 kPa (1000 lb/ft^2) (Elias et al., 2006). Compaction grouting is often used to repair structures that have experienced excessive settlement, since it both improves the underlying soils and raises the structure back into position. Design guidance for compaction grouting is available from Elias et al. (2006).

Jet Grouting

Jet grouting is a method developed in Japan during the 1960s and 1970s, and uses a special pipe equipped with horizontal jets that injects grout into the soil at high pressure (Bell, 1993). The pipe is first inserted to the desired depth, then it is raised and rotated while the injection is in progress, thus forming a column of treated soil, as illustrated in Figure 26.9.

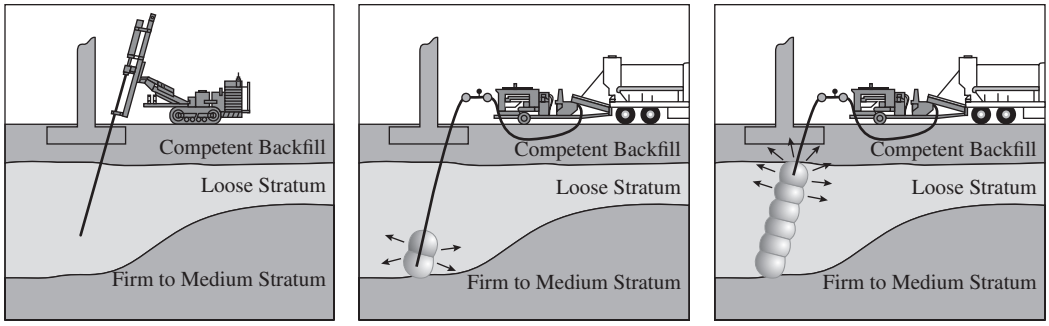

Figure 26.8 Compaction grouting process: (a) grout tube is pushed into soil, (b) grout is pumped through grout tip to form bulbs of grout compacting surrounding soil, (c) tube is gradually moved up while more grout bulbs are formed creating a grout column (courtesy of Hayward Baker Inc.).

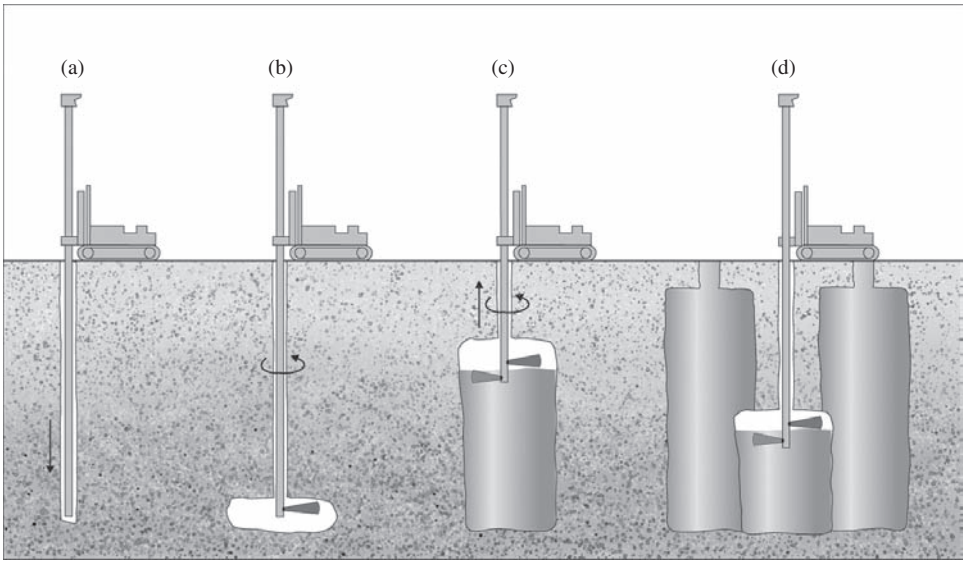

Figure 26.9 Jet grouting process: (a) grout tube is pushed into ground, (b) grout is pumped out of tube horizontally at high pressure through jets mixing with the adjacent soil, (c) grout tube is rotated and it is extracted toward the surface forming a grouted soil column, (d) overlapping columns can be created to from a grouted wall of soil (courtesy of Hayward Baker Inc.).

Jet grouting can be used on all types of soils, but is most effective in cohesionless or soft cohesive soils. In foundation applications, jet grouting is most commonly used for underpinning existing foundations or mitigation of liquefaction problems. Jet grout columns can be installed up to 45 m (100 ft) deep. Elias et al. (2006) provide guidance on project selection and preliminary design for jet grouting.

26.7 STABILIZATION USING ADMIXTURES

Another method of improving soils is to treat them with an admixture (Ingles and Metcalf, 1972). The most common admixture is Portland cement. When mixed with the soil, it forms a material called soil-cement, which is comparable to a weak concrete. Other admixture materials include lime and asphalt. The objective of these admixtures is to provide artificial cementation, thus increasing strength and reducing both compressibility and hydraulic conductivity. It also reduces the expansion potential in clays.

Surface Mixing

Historically, most admixture stabilization has been performed by ripping the upper soils, applying the admixture (and possibly water), mixing with special equipment, and recompacting. Once the mixture has cured, it forms a very hard and durable soil. These methods have most often been used for highways and airports, to form a stabilized subbase over which the pavement is constructed. There have been limited applications of this method to mitigate swelling problems with expansive soils below lightly loaded footings. However, the volume of soil that has to be treated make this method prohibitively expensive for most foundation applications.

In situ Deep Mixing

During the 1970s and 1980s, a new method of stabilization was developed in Japan. It uses rotating mixer shafts, paddles, or jets that penetrate into the ground while injecting and mixing Portland cement or some other stabilizing agent (Toth, 1993; Yang, 1994; Schaefer, 1997). These techniques include deep cement mixing, soil mix walls, deep jet mixing, deep soil mixing, deep mixed method, and others. There are several kinds of mixing machines available, one of which is shown in Figure 26.10.

One of the newest deep mixing methods introduced to the U.S. practice is the trench cutting and remixing deep wall (TRD) method (Burke, 2009). The TRD method was developed in Japan in the 1990s and uses a special full-depth vertical cutter post that resembles a giant chain saw to cut through the soils in the entire profile and mix them with injected cement-based slurry. The Cutter Soil Mixing (CSM) system is similar to TRD but uses a pair of counter-rotating cutters that move vertically to mix the soil and cement, see Figure 26.11. A major advantage of the TRD and CSM methods is that they produce continuous soil mix walls with a flat vertical surface.

Soils treated by in situ mixing have greater strength, reduced compressibility, and lower hydraulic conductivity than the original soils. The main application for deep mixing in foundation design is liquefaction mitigation. Design guidance is available from Bruce et al. (2013).

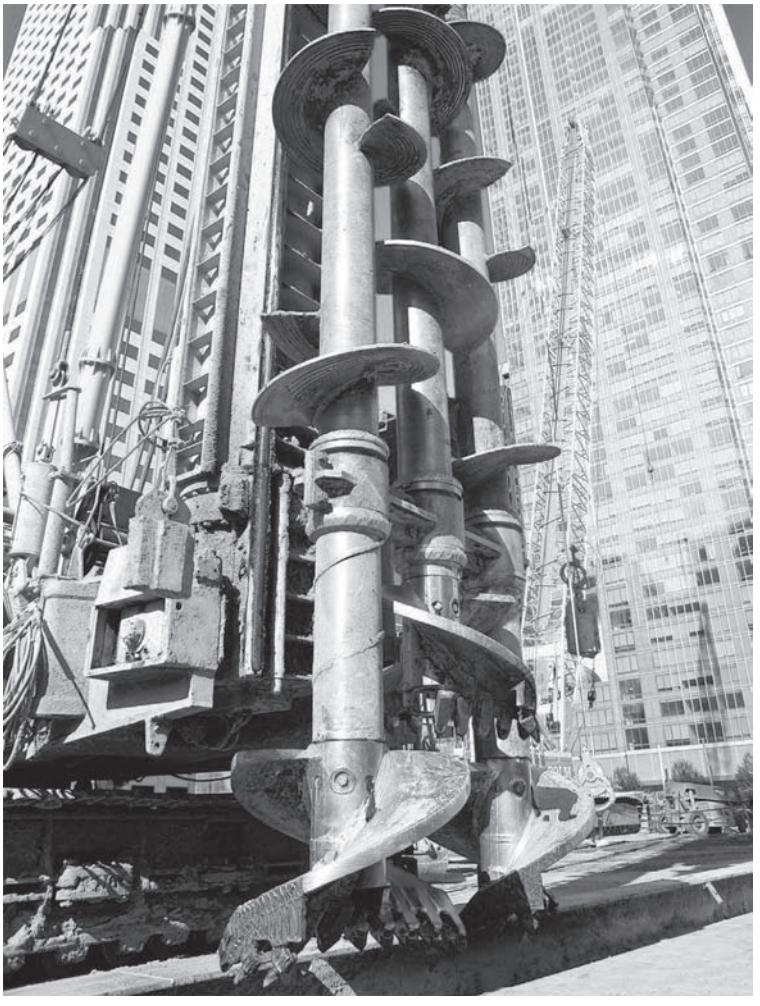

Figure 26.10 Rig using three rotating augers to mix Portland cement with soil in situ to form a soil mix wall (courtesy of Malcolm Drilling Co.).

26.8 REINFORCEMENT

One of the similarities between concrete and soil is that both materials are strong in compression but weak in tension. In concrete we overcome this problem by placing steel reinforcing bars inside the concrete. This composite material, reinforced concrete, is far better than plain concrete. The same principle can be applied to soils. The placement of tensile reinforcement members can significantly improve its stability and load-carrying capacity (Koerner, 2012). While soil reinforcement has become commonplace in embankment, retaining wall and slope design, it has limited applications in foundation design because to

Figure 26.11 This figure shows the cutter head of a Cutter Soil Mixer system. The two cutters counter-rotate to mix the soil and cement. The rig pushes the cutter heads up and down to create a uniform soil mix panel. One advantage of this system is that the soil mix wall will have a smoother vertical face compared to walls created with auger and paddle type system shown in Figure 26.10 (courtesy of Malcolm Drilling Co.).

be effective it needs to be placed below the foundation. One application that has been used in a few circumstances is to combine reinforcement with removal and recompaction. In this application, reinforcement is placed between lifts during backfilling operations. Koerner (2012) provides more guidance on this application.

SUMMARY

Major Points

1. Most geotechnical engineering projects focus on assessing the engineering characteristics of the ground as it presently exists and designing the project to accommodate these conditions. However, sometimes it is cost effective to improve the soils, thus producing better engineering properties and placing fewer demands on the proposed construction.
2. Removal and replacement is one of the oldest and simplest methods of ground improvement. However, it is usually cost effective only when the required volumes are small and the excavation does not need to extend below the groundwater table.

3. Precompression consists of applying a surcharge load, thus accelerating consolidation settlements. It is generally effective only in silts and clays.
4. Vertical drains may be used to accelerate consolidation settlement, either with or without surcharge loads.
5. In situ densification uses strong vibrations to densify the ground, and is effective in sandy soils. Several methods are available.
6. In situ replacement of soil by stiff inclusions using various methods improves bearing capacity and reduces settlement.
7. Grouting consists of the injection of special liquid or slurry materials to improve the soil.
8. Admixture stabilization consists of mixing soil with Portland cement or some other material.
9. Reinforcement methods consist of installing tensile reinforcement members in the soil, thus forming a composite material that has both compressive and tensile strength.

Vocabulary

aggregate pier
blast densification
compaction grouting
dynamic compaction
ground improvement
grouting
in situ deep mixing
jet grouting
precompression
rammed aggregate pier
rapid impact compaction
recompaction
removal and replacement
rigid inclusion
sand drain
soil cement
soil improvement
stone column
surcharge fill
surface mixing
vertical drain
vibrocompaction
vibro concrete columns
vibro replacement
vibroflotation
wick drain

QUESTIONS AND PRACTICE PROBLEMS

26.1 State the advantages and disadvantages of removal and replacement as a ground improvement method.

26.2 State the advantages and disadvantages of precompression as a ground improvement method.

26.3 Explain how vertical drains can be used to speed up consolidation of soils in situ.

26.4 Name four in situ densification methods and describe how each one works.

26.5 Name four in situ replacement methods and describe how each one works.

26.6 Name four types of grouting and describe how each one works.

26.7 Describe the TRD method.

26.8 Describe how soil reinforcement improves soil properties. Name one soil reinforcement technique that can be applied to foundation engineering.

Comprehensive

26.9 A proposed medical office building is to be built on a vacant parcel of land adjacent to a hospital. This site is underlain by 30 ft of loose sand that is prone to seismic liquefaction. To rectify this liquefaction problem, the sand needs to be densified. Suggest an appropriate method of ground improvement for this site and indicate the reasons for your selection. The groundwater table is at a depth of 5 ft.

26.10 Some ground improvement methods can be used to construct "intermediate" foundations that have capacities that are between those of shallow and deep foundations. Name two of these methods.

27

Foundations on Expansive Soils

Question: ***What causes more property damage in the United States than all the earthquakes, floods, tornados, and hurricanes combined?***

Answer: ***Expansive soils!***

According to a 1987 study, expansive soils in the United States inflict about $9 billion in damages per year to buildings, roads, airports, pipelines, and other facilities—more than twice the combined damage from the disasters listed above (Jones and Holtz, 1973; Jones and Jones, 1987). The distribution of these damages is approximately as shown in Table 27.1. Many other countries also suffer from expansive soils (Chen, 1988). Although it is difficult to estimate the losses worldwide, this is clearly a global problem.

Sometimes the damages from expansive soils are minor maintenance and aesthetic concerns, but often they are much worse, even causing major structural distress, as illustrated in Figures 27.1 through 27.3. According to Holtz and Hart (1978), 60 percent of the 250,000 new homes built on expansive soils each year in the United States experience minor damage and 10 percent experience significant damage, some beyond repair.

In spite of these facts, we do not expect to see newspaper headlines "Expansive Soils Waste Billions" and certainly not "Expansive Soil Kills Local Family." Expansive soils are not as dramatic as hurricanes or earthquakes and they cause only property damage, not loss of life. In addition, they act more slowly and the damage is spread over wide areas rather than being concentrated in a small locality. Nevertheless, the economic loss is large and much of it could be avoided by proper recognition of the problem and incorporating appropriate preventive measures into the design, construction, and maintenance of new facilities. Foundation engineers must be aware of this potential problem and be ready to take appropriate action when encountering such soils.

TABLE 27.1 ANNUAL DAMAGE IN THE UNITED STATES FROM EXPANSIVE SOILS (Data from Jones and Holtz, 1973 and Jones and Jones, 1987; used with permission of American Society of Civil Engineers)

Category	Annual Damage
Highways and streets	$4,550,000,000
Commercial buildings	1,440,000,000
Single family homes	1,200,000,000
Walks, drives, and parking areas	440,000,000
Buried utilities and services	400,000,000
Multi-story buildings	320,000,000
Airport installations	160,000,000
Involved in urban landslides	100,000,000
Other	390,000,000
Total annual damages (1987)	$9,000,000,000

27.1 THE NATURE, ORIGIN, AND OCCURRENCE OF EXPANSIVE SOILS

When geotechnical engineers refer to expansive soils, we usually are thinking about clays or sedimentary rocks derived from clays, and the volume changes that occur as a result of changes in moisture content. This is the most common expansion phenomenon, and thus is the primary focus of this chapter. Other less common mechanisms of soil expansion are discussed in Section 27.6. Expansion due to frost heave, which is an entirely different phenomenon, is discussed in Chapter 9.

Clays are fundamentally very different from gravels, sands, and silts. All of the latter consist of relatively inert bulky particles and their engineering properties depend primarily on the size, shape, and texture of these particles. In contrast, clays are made up of very small particles that are usually plate-shaped. The engineering properties of clays are strongly influenced by the very small size and large surface area of these particles and their inherent electrical charges.

What Causes a Clay to Expand?

Several different *clay minerals* occur in nature, the differences being defined by their chemical makeup and structural configuration. Three of the most common clay minerals are *kaolinite*, *illite*, and *montmorillonite* (part of the smectite group). The different chemical compositions and crystalline structures of these minerals give each a different susceptibility to swelling, as shown in Table 27.2.

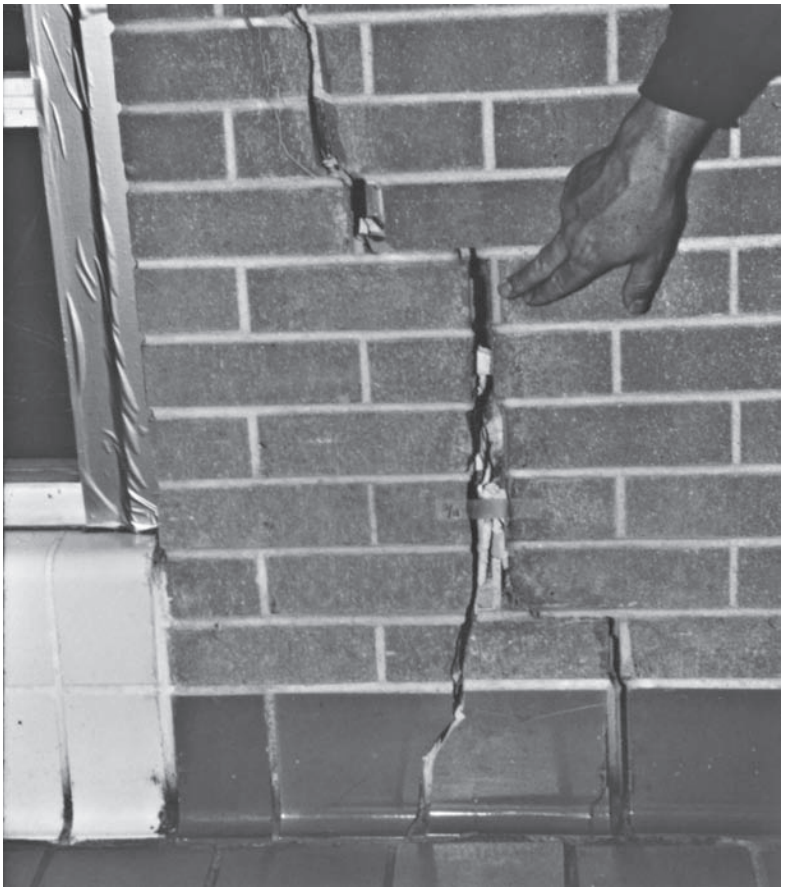

Figure 27.1 Heaving of expansive soils caused this brick wall to crack. The $490,000 spent to repair this and other walls, ceilings, doors, and windows represented nearly one-third of the original cost of the six-year-old building (photo courtesy of the Colorado Geological Survey).

Figure 27.2 Heaving of expansive soils caused this 2.5 mm (0.1 in) wide crack in the ceiling of a one-story wood-frame house.

Figure 27.3 Expansive soils caused this brick building to crack (photo courtesy of the Colorado Geological Survey).

Swelling occurs when water is absorbed between combined *silica and alumina sheets* that make up the molecular structure of clays, causing the combined sheets to separate. Kaolinite is essentially nonexpansive because of the presence of strong hydrogen bonds that hold the individual combined sheets together. Illite contains weaker potassium bonds that allow limited expansion, and the combined sheets in montmorillonite are only weakly linked. Thus, water can easily be absorbed into montmorillonite clays and separate the molecular sheets. Field observations have confirmed that the greatest problems occur in soils with a high montmorillonite content.

TABLE 27.2 SWELL POTENTIAL OF PURE CLAY MINERALS (adapted from Budge et al., 1964)

Surcharge Load		Swell Potential (%)		
(lb/ft^2)	(kPa)	Kaolinite	Illite	Montmorillonite
200	9.6	Negligible	350	1,500
400	19.1	Negligible	150	350

Several other forces also act on clay particles, including the following:

- Surface tension in the menisci of water contained between the particles (tends to pull the particles together, compressing the soil).
- Osmotic pressures (tend to bring water in, thus pressing the particles further apart and expanding the soil).
- Pressures in entrapped air bubbles (tend to expand the soil).
- Effective stresses due to external loads (tend to compress the soil).
- London-Van Der Waals intermolecular forces (tend to compress the soil).

Expansive clays swell or shrink in response to changes in these forces. For example, consider the effects of changes in surface tension and osmotic forces by imagining a montmorillonite clay that is initially saturated, as shown in Figure 27.4a. If this soil dries, the remaining moisture congregates near the particle interfaces, forming menisci, as shown in Figure 27.4b, and the resulting surface tension forces pull the particles closer together causing the soil to shrink. We could compare the soil in this stage to a compressed spring: both would expand if it were not for the forces keeping them compressed.

The soil in Figure 27.4b has a great affinity for water and will draw in available water using osmosis. We would say that it has a very high *soil suction* at this stage. If water becomes available, the suction will draw it into the spaces between the particles and the soil will swell, as shown in Figure 27.4c. Returning to our analogy, the spring has been released and perhaps is now being forced outward.

What Factors Control the Amount of Expansion?

The portion of a soil's potential expansion that will actually occur in the field depends on many factors. One of these factors is the percentage of expansive clays in the soil. For example, a pure montmorillonite could swell more than fifteen times its original volume

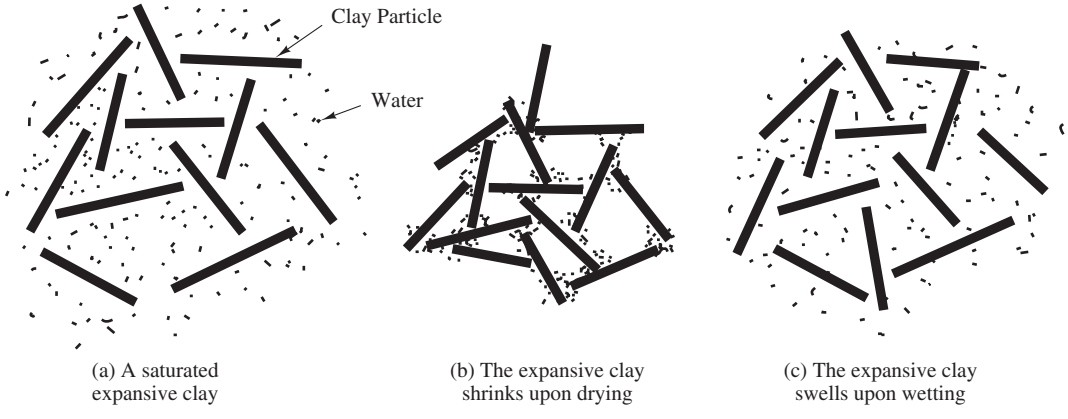

Figure 27.4 Shrinkage and swelling of an expansive clay.

(definitely with disastrous results!), but clay minerals are rarely found in such a pure form. Usually, the expansive clay minerals are mixed with more stable clays and with sands or silts. A typical "montmorillonite" (really a mixed soil) would probably not expand more than 35 to 50 percent, even under the worst laboratory conditions, and much less in the field.

There are two types of montmorillonite clay: calcium montmorillonite and sodium montmorillonite (also known as bentonite). The latter is much more expansive, but less common.

Two of the most important variables to consider are the initial moisture content and the surcharge pressure. If the soil is initially moist, then there is much less potential for additional expansion than if it were dry. Likewise, even a moderate surcharge pressure restrains much of the swell potential (although large loads are typically required to completely restrain the soil). Figure 27.5 illustrates a typical relationship between swell potential, initial moisture content, and surcharge pressure. This figure also shows that for a given soil, there is a surcharge pressure, called the swell pressure, which suppresses all the swell resulting in no volume change.

The relationship between swell potential and surcharge demonstrates why pavements and slabs-on-grade are so susceptible to damage from expansive soils (see Table 27.1). They provide such a small surcharge load that there is little to resist the soil expansion. However, it also demonstrates how even a modest increase in surcharge, such

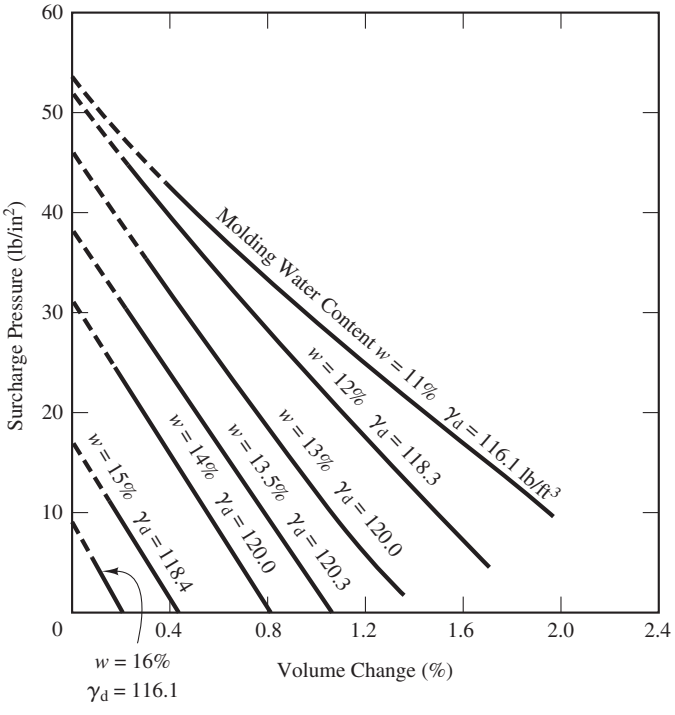

Figure 27.5 Swell potential as a function of initial moisture content and surcharge load (typical) (adapted from Seed et al., 1962).

as 300 mm (12 in) or so of subbase, significantly decreases the potential heave.[1] Similarly, lightly loaded foundations, such as those for residential houses, are more susceptible to expansive soil damage than are more heavily loaded foundations for mid- and high-rise structures. Remolding a soil into a compacted fill may make it more expansive (O'Neill and Poormoayed, 1980), probably because this process breaks up cementation in the soil and produces high negative pore water pressures that later dissipate. Many other factors also affect the expansive properties of fills, especially the methods used to compact the fill (kneading vs. static) and the as-compacted moisture content and dry unit weight (Seed and Chan, 1959).

Figure 27.6 illustrates how compacting a soil wet of the optimum moisture content reduces its potential for expansion. It also illustrates that compacting the soil to a lower dry unit weight reduces its swell potential (although this also will have detrimental effects, such as reduced shear strength and increased compressibility).

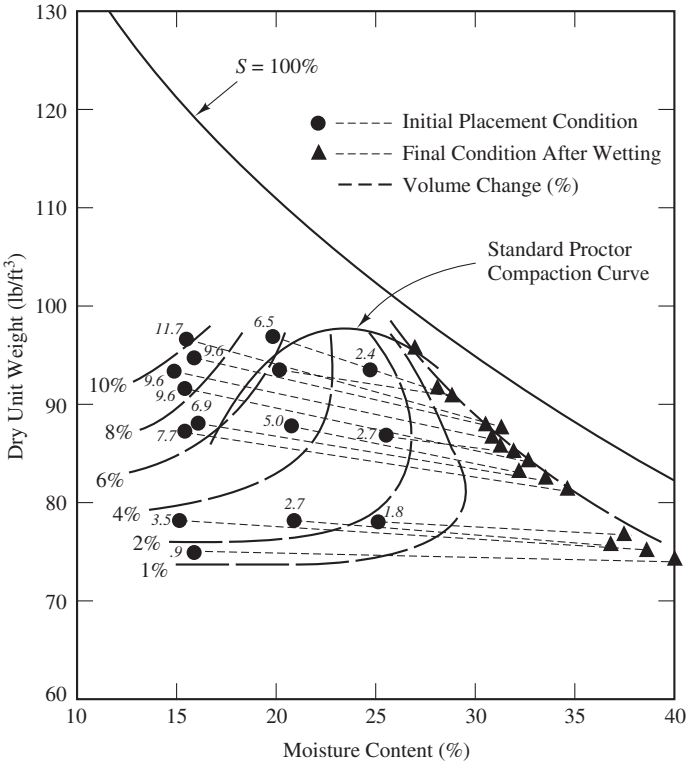

Figure 27.6 Swell potential of compacted clays (adapted from Holtz, 1969).

[1] The use of subbase for this purpose is somewhat controversial. Although it provides additional surcharge pressure, which is good, it can also become an avenue for additional water to enter the expansive soils, which is bad. Many engineers feel that the risk of additional water infiltration is too great and therefore do not use this method.

Although laboratory tests are useful, they may not accurately predict the behavior of expansive soils in the field. This is partly because the soil in the lab is generally inundated with water, whereas the soil in the field may have only limited access to water. The flow of water into a soil in the field depends on many factors, including the following:

- The supply of water (depends on rainfall, irrigation, and surface drainage).
- Evaporation and transpiration (depends on climate and vegetation; large trees can extract large quantities of water from the soil through their roots).
- The presence of fissures in the soil (water will flow through the fissures much more easily than through the soil).
- The presence of sand or gravel lenses (helps water penetrate the soil).
- The soil's affinity for water (its suction).

Because of these factors, Jones and Jones (1987) suggested that soils in the field typically swell between 10 and 80 percent of the total possible swell.

Occurrence of Expansive Clays

Chemical weathering of materials such as feldspars, micas, and limestones can form clay minerals. The particular mineral formed depends on the makeup of the parent rock, topography, climate, neighboring vegetation, duration of weathering, and other factors.

Montmorillonite clays often form as a result of the weathering of ferromagnesian minerals, calcic feldspars, and volcanic materials. They are most likely to form in an alkaline environment with a supply of magnesium ions and a lack of leaching. Such conditions would most likely be present in semi-arid regions. *Bentonite* (sodium montmorillonite) is formed by chemical weathering of volcanic ash. Figure 27.7 shows the approximate geographical distribution of major montmorillonite deposits in the United States.

Expansive clays are also common in the Canadian prairie provinces, Israel, South Africa, Australia, Morocco, India, Sudan, Peru, Spain, France, China, and many other places in the world.

Figure 27.7 illustrates regional trends only. Not all the soils in the shaded areas are expansive and not all the soils outside are nonexpansive. The local occurrence of expansive soils can vary widely, as illustrated in Figure 27.8. However, even maps of this scale are only an aid, not a substitute for site-specific field investigations.

Influence of Climate on Expansion Potential

As discussed earlier, any expansive soil could potentially shrink and swell, but in practice this occurs only if its moisture content changes. The likelihood of such changes depends on the balance between water entering a soil (such as by precipitation or irrigation) and water leaving the soil (often by evaporation and transpiration).

In humid climates, the soil is moist or wet and tends to remain so throughout the year. This is because the periods of greatest evaporation and transpiration (the summer

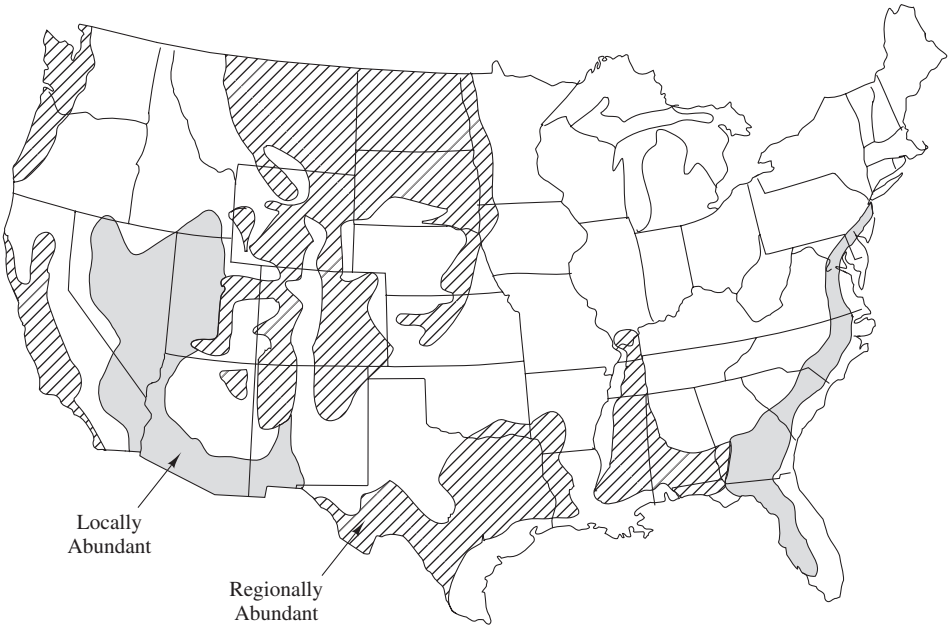

Figure 27.7 Approximate distribution of major montmorillonite clay deposits in the United States (adapted from Tourtelot, 1973). Erosion, glacial action, and other geologic processes have carried some of these soils outside the zones shown here. Thus, the unshaded areas are not immune to expansive soils problems.

months) also coincide with the greatest rainfall. The climate in North Carolina, as shown in Figure 27.9b, is typical of this pattern. Because the variations in moisture content are small, very little shrinkage or swelling will occur. However, some problems have been reported during periods of extended drought when the soil dries and shrinks (Hodgkinson, 1986; Sowers and Kennedy, 1967).

Most of the problems with expansive soils occur in arid, semi-arid, and monsoonal areas because the seasonal distribution of precipitation and evaporation/transpiration causes wide fluctuations in the soil's moisture content. Most of the precipitation in arid and semi-arid areas occurs during the winter and spring when evaporation and transpiration rates are low. Thus, the moisture content of the soil increases. Then, during the summer, precipitation is minimal and evaporation/transpiration is greatest, so the soil dries. Thus, the soil expands in the winter and shrinks in the summer. The climate in Los Angeles, shown in Figure 27.9a, displays this pattern.

A useful measure of precipitation and evaporation/transpiration as they affect expansive soil problems is the Thornthwaite Moisture Index (TMI) (Thornthwaite, 1948). This index is a function of the difference between the mean annual precipitation and the amount of water that could be returned to the atmosphere by evaporation and transpiration. A positive value indicates a net surplus of soil moisture whereas a negative value indicates a net deficit. Using this index, Thornthwaite classified climates as shown in Table 27.3.

Because expansive soils are most troublesome in areas where the moisture content varies during the year, and this is most likely to occur in arid climates, regions with the

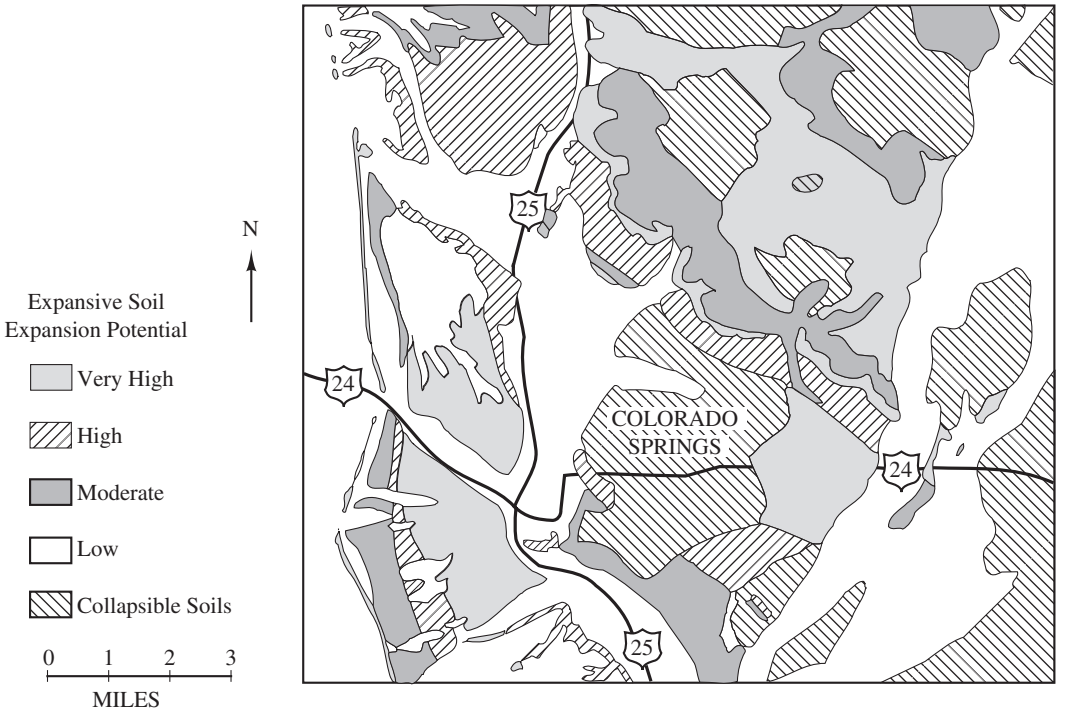

Figure 27.8 Distribution of expansive soils in the Colorado Springs, Colorado area (adapted from Hart, 1974).

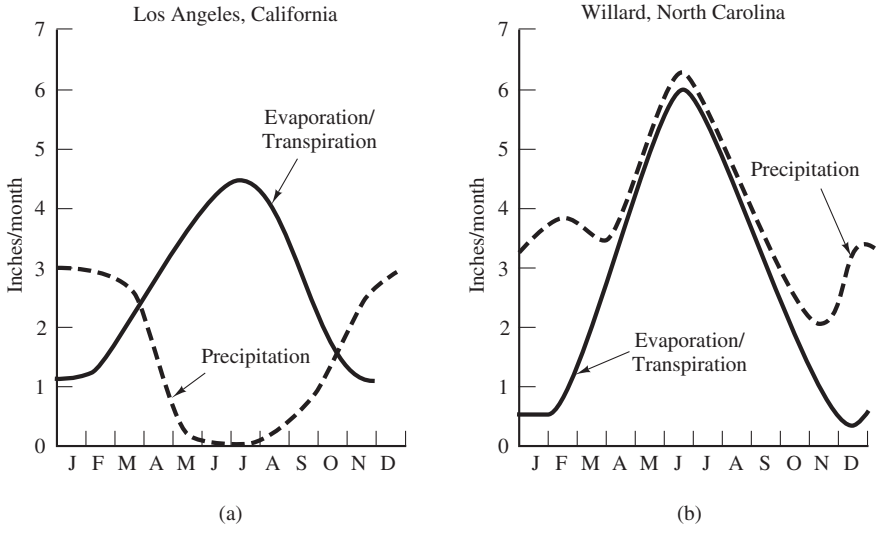

Figure 27.9 Annual distribution of precipitation and potential evaporation/transpiration in (a) Los Angeles, California, and (b) Willard, North Carolina (data from Thornthwaite, 1948). Note how the wet Los Angeles winters are followed by very dry summers. In contrast, the total annual precipitation in Willard is much higher and most of it occurs during the summer. Used with permission of the American Geographical Society.

TABLE 27.3 CLASSIFICATION OF CLIMATE BASED ON THORNTHWAITE MOISTURE INDEX (TMI) (adapted from Thornthwaite, 1948; used with permission of the American Geographical Society)

TMI	Climate Type
−60 to −40	Arid
−40 to −20	Semi-arid
−20 to 0	Dry subhumid
0 to 20	Moist subhumid
20 to 100	Humid
>100	Perhumid

lowest TMI values should have the greatest potential for problems. Researchers have observed that expansive soils are most prone to cause problems in areas where the TMI is no greater than +20. However, this is not an absolute upper limit. For example, some expansive soil problems have occurred in Alabama and Mississippi (TMI $\approx$ 40).

Figure 27.10 shows Thornthwaite contours for the United States. Combining this information with Figure 27.7 shows that the areas most likely to have expansive soils problems include the following:

- Central and southern Texas
- Portions of Colorado outside the Rocky Mountains
- Much of California south of Sacramento
- The northern plains states
- Portions of the great basin area (Arizona, Nevada, Utah)

Man-made improvements can change the TMI at a given site, as discussed later in this section.

Depth of the Active Zone

An important parameter when evaluating expansive soils for foundation design is the depth of the *active zone*. Engineers have defined the active zone differently depending on the applications involved. A general and rigorous definition is proposed by Nelson et al. (2001): the active zone is the zone of soils that is contributing to heave due to soil expansion. With this definition, the active zone can change with time, and depends on the amount of water moving into and out of the soil due to natural climatic changes at the surface and artificial wetting of the soil from external sources of water.

If a site is in its natural state under the influence of climatic changes without any influence of human activities, the moisture content of soils underlying the site fluctuates

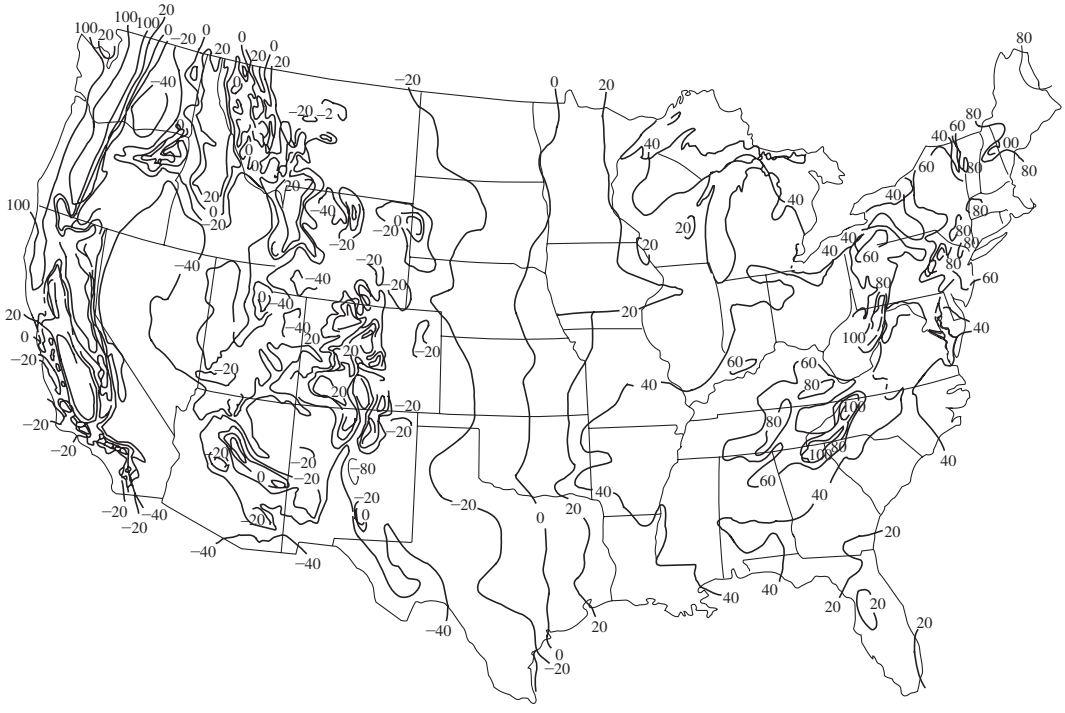

Figure 27.10 Thornthwaite Moisture Index distribution in the United States (adapted from Thornthwaite, 1948; and PTI, 1980). Used with permission of the American Geographical Society and the Post-Tensioning Institute.

more near the ground surface than at depth. This is because these upper soils respond more rapidly to variations in precipitation and evaporation/transpiration. During the course of a year, the soils at different depths will experience moisture fluctuations depicted in Figure 27.11. Presumably, the moisture content is reasonably constant below the depth where it fluctuates, as shown in Figure 27.11, so no expansion occurs below this point. In this case, the active zone for design can be taken as the zone of moisture content fluctuations. From Figure 27.9, the soil moisture content in Los Angeles varies dramatically from summer to winter, so we would expect the active zone there to extend much deeper than in Willard, where the moisture content is less variable. As a result, expansive soils should be more of a problem in Los Angeles (and they are!).

Influence of Human Activities

Engineers also need to consider how human activities, especially new construction, affect soil expansion at a given site. Besides possibly changing the surcharge pressures on subsurface soils, human activities can change the moisture conditions at a particular site and

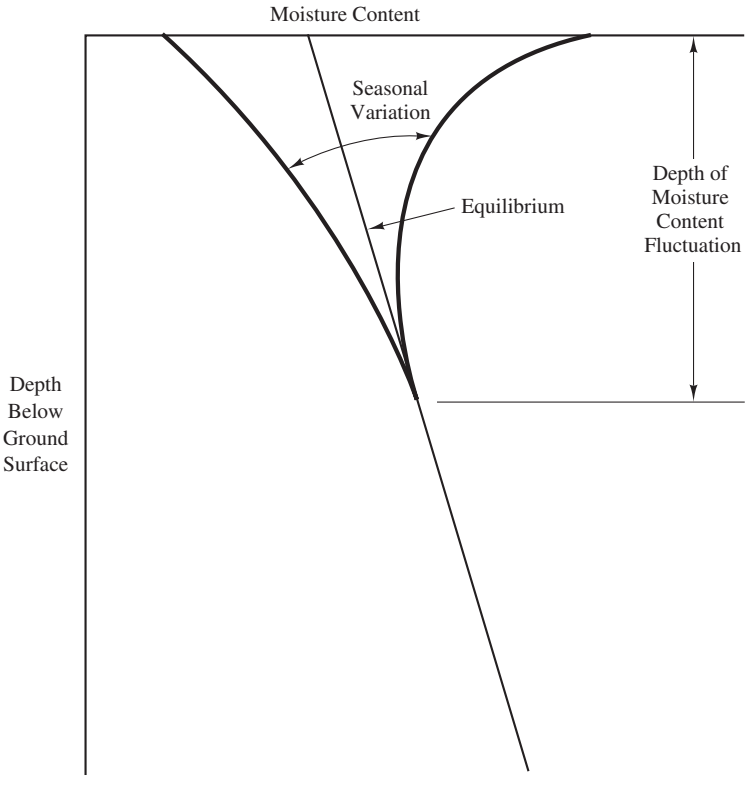

Figure 27.11 The layer of soil that has a fluctuating moisture content.

hence the depth of the active zone as well. Human activities that can affect the depth of the active zone include:

- Removal of vegetation brings an end to transpiration.
- Placement of slab-on-grade floors, pavements, or other impervious materials on the ground stops both evaporation and the direct infiltration of rain water.
- Irrigation of landscaping introduces much more water into the ground. In southern California, some have estimated that irrigation in residential areas is the equivalent of raising the annual precipitation from a natural 375 mm (15 in) to an inflated 1,500 mm (60 in) or more.
- Placement of aggressive trees or heated buildings can enhance desiccation.

The effects of these changes on the depth and degree of wetting, and hence the active zone, need to be evaluated. The effects are difficult to quantify, but the net effect in arid and semi-arid areas is normally to increase the moisture contents of soils under structures. This results in more swelling and more structural damage.

If artificial wetting of the soil is involved, for example, due to irrigation of landscaping, the zone of wetting may be taken as the active zone and can be estimated from local

TABLE 27.4 APPROXIMATE DEPTH OF THE ACTIVE ZONE IN SELECTED CITIES (adapted from O'Neill and Poormoayed, 1980)

	Depth of the Active Zone		
City	(ft)	(m)	TMI (from Figure 27.10)
Houston	5–10	1.5–3.0	18
Dallas	7–15	2.1–4.2	−1
Denver	10–15	3.0–4.2	−15
San Antonio	10–30	3.0–9.0	−14

experience and empirical data. For example, Walsh et al. (2009) used field measurements in residential areas in the Denver metropolitan area to obtain an average depth of wetting of 5.1 m (16.7 ft), with a standard deviation of 2.3 m (7.6 ft), applicable to horizontally layered deposits. Alternatively, the depth and degree of wetting for different landscape and drainage conditions can be obtained using unsaturated soil mechanics to model water migration in the vadose zone (e.g., Houston et al., 2011; and Overton et al., 2011).

For routine practice, the depth of the active zone is usually estimated using local experience. O'Neill and Poormoayed (1980) presented active zone depths for selected cities as shown in Table 27.4. According to this table, a soil profile in San Antonio would generate more heave than an identical profile 320 km (200 miles) away in Houston because the active zone is deeper in San Antonio. As a result, the appropriate preventive design measures for identical structures would also be different.

Clays that are heavily fissured will typically have deeper active zones because the fissures transmit the water to greater depths. For example, field studies conducted in Colorado indicate that the active zone in some locations may extend as deep as 16 m (50 ft) below the ground surface (Holtz, 1969). Houston and Nelson (2012) also pointed out the potential importance of lateral sources of water that may increase wetting if the ground surface or bedding of the soil deposits is inclined. It should be noted that the depth of the active zone is limited by the depth of potential heave, defined by Nelson et al. (2001) as the depth at which the vertical overburden pressure is equal to the swell pressure. Because no soil expansion due to wetting will occur below the depth of potential heave, the maximum possible depth of the active zone is equal to the depth of potential heave.

In summary, the depth of the active zone at a given site is dependent upon local geology, regional weather patterns, and local human activities. It is difficult to determine and is a major source of uncertainty in heave analyses.

27.2 IDENTIFYING, TESTING, AND EVALUATING EXPANSIVE SOILS

When working in an area where expansive soils can cause problems, geotechnical engineers must have a systematic method of identifying, testing, and evaluating the swelling potential of troublesome soils. The ultimate goal is to determine which preventive design measures, if any, are needed to successfully complete a proposed project.

Houston and Nelson (2012) presented a state-of-the-practice report on foundation engineering in expansive and collapsible soils. They compiled data on the common practices in different parts of the United States in terms of site investigation, laboratory testing, and foundation design when dealing with expansive soils; and suggested changes to the state of the practice.

An experienced geotechnical engineer is usually able to visually identify potentially expansive soils. To be expansive, a soil must have a significant clay content, probably falling within the unified soil classification group symbol CL or CH (although some ML, MH, and SC soils also can be expansive). A dry expansive soil will often have fissures, slickensides, or shattering, all of which are signs of previous swelling and shrinking. When dry, these soils usually have cracks at the ground surface. However, any such visual identification is only a first step; we must obtain more information before we can develop specific design recommendations.

The next stage of the process—determining the degree of expansiveness—is more difficult. A wide variety of testing and evaluation methods have been proposed, but none of them is universally or even widely accepted. Engineers who work in certain geographical areas often use similar techniques, which may be quite different from those used elsewhere. This lack of consistency can be a stumbling block.

We can classify these methods into three groups. The first group consists of purely *qualitative methods* that classify the expansiveness of the soil with terms such as low, medium, or high and form the basis for empirically based preventive measures. The second group includes *semiquantitative methods*. They generate numerical results, but engineers consider them to be an *index* of expansiveness, not a fundamental physical property. The implication here is that the design methods will also be empirically based. The final group includes methods that provide *quantitative* results that are measurements of fundamental physical properties and become the basis for a rational or semirational design procedure.

Qualitative Evaluations

This category of evaluations is usually based on correlations with common soil tests, such as the Atterberg limits or the percent colloids.[2] Such correlations are approximate, but they can be useful, especially for preliminary evaluations.

The US Bureau of Reclamation developed the correlations presented in Table 27.5. An engineer could use any or all of them to classify the swelling potential of a soil, but the plasticity index and liquid limit correlations are probably the most reliable. Montmorillonite particles are generally smaller than illite or kaolinite, so expansiveness roughly correlates with the percent colloids. Engineers rarely perform the shrinkage limit test, and some have questioned the validity of its correlation with expansiveness.

[2] Colloids are usually defined as all particles smaller than 0.001 mm; clay-size particles are sometimes defined as those smaller than 0.002 mm. A hydrometer test is an easy way to measure the percentage of colloids or clay-size particles in a soil, which can be a rough indicator of its potential expansiveness.

TABLE 27.5 CORRELATIONS OF SWELLING POTENTIAL WITH COMMON SOIL TESTS (adapted from Holtz, 1969; and Gibbs, 1969)

Percent Colloids	Plasticity Index	Shrinkage Limit	Liquid Limit	Swelling Potential
<15	<18	<15	<39	Low
13–23	15–28	10–16	39–50	Medium
20–31	25–41	7–12	50–63	High
>28	>35	>11	>63	Very high

Chen (1988) proposed the correlations presented in Table 27.6 based on his experience in the Rocky Mountain area.

Semiquantitative Evaluations

The most common semiquantitative method of describing expansive soils is in terms of its *swell potential*, which engineers usually measure in some kind of *loaded swell test*. Unfortunately, these are very ambiguous terms because there are many different definitions of swell potential and an even wider range of test methods.

Loaded swell tests usually utilize a laterally confined cylindrical specimen, as shown in Figure 27.12. The initially dry specimen is loaded with a surcharge, and then soaked. The specimen swells vertically, and this displacement divided by the initial height (immediately before soaking) is the swell potential, usually expressed as a percentage.

This methodology is attractive because it measures the desired characteristics directly, is relatively easy to perform, and does not require exotic test equipment (the test can be performed in a conventional consolidometer). However, because many different

TABLE 27.6 CORRELATIONS OF SWELLING POTENTIAL WITH COMMON SOIL TESTS (adapted from Chen, 1988; used with permission of Elsevier Science Publishers)

Laboratory and Field Data			Degree of Expansiveness			
				Swell Pressure		
Percent Passing #200 Sieve	Liquid Limit	SPT *N* Value	Probable Expansion (%)[a]	(k/ft^2)	(kPa)	Swelling Potential
<30	<30	<10	<1	1	50	Low
30–60	30–40	10–20	1–5	3–5	150–250	Medium
60–95	40–60	20–30	3–10	5–20	250–1,000	High
>95	>60	>30	>10	>20	>1,000	Very high

[a] Percent volume change when subjected to a total stress of 1,000 lb/ft^2 (50 kPa).

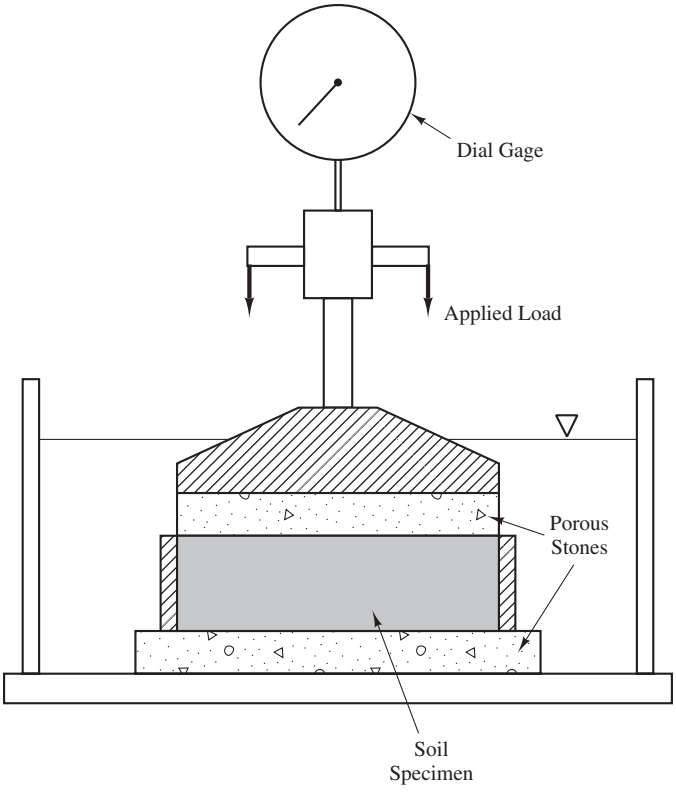

Figure 27.12 Typical apparatus used for a loaded swell test.

versions of the loaded swell test have been developed, the specifics of the test vary and results from different tests are not always comparable. The typical ranges of test criteria are as follows:

- **Specimen size:** Typically, the specimen is 50 to 112 mm (2.0–4.5 in) in diameter and 12 to 37 mm (0.5–1.5 in) tall. Larger diameter specimens are less susceptible to side friction and therefore tend to swell more.
- **Method of preparation:** The specimen may be undisturbed or remolded. If it is undisturbed, how it was sampled and prepared will affect the test results. If it is remolded, the dry unit weight, water content and method of compaction, and method of curing will all affect the test results.
- **Initial moisture content:** The moisture content at the beginning of the test will affect results. Some possibilities include:
  - In situ moisture content
  - Optimum moisture content
  - Air-dried moisture content

Other options are also possible.

- **Surcharge load:** The surcharge load may be equal to the in situ geostatic stress or the geostatic stress plus expected as-built stresses. It is usually between 2.9 and 71.8 kPa (60−1,500 lb/ft^2). Houston and Nelson (2012) recommend a surcharge equal to the anticipated as-built overburden stress.
- **Duration:** Expansive soils do not swell immediately upon application of water. It takes time for the water to seep into the soil. This raises the question of how long to allow the test to run. Some engineers conduct the test for a specified time (i.e., 24 h), whereas others continue until a specified rate of expansion is reached (such as no more than 0.03 mm/hr). The latter could take several days in some soils.

ASTM Standard Loaded Swell Tests

ASTM D4546-14 provides standards for the loaded swell test in three designated test methods for one-dimensional swell or collapse of soils, Methods A, B, and C. The characteristics of these three methods are summarized in Table 27.7. Method A is appropriate for determining the swell pressure and estimating heave in a construction fill that is fully wetted after construction. Method B is appropriate for determining the swell pressure and estimating heave of footings constructed on either fill or natural soils. Method C is appropriate for determining the recompression of a soil (either compacted fill or natural) which is reloaded after wetting with either additional fill or a foundation load.

TABLE 27.7 SUMMARY OF TEST PARAMETERS FOR TEST METHODS A, B, AND C SPECIFIED IN ASTM D4546 STANDARD TEST METHODS FOR ONE-DIMENSIONAL SWELL OR COLLAPSE OF SOILS

Test Method	Description	Type of Specimen	Stress at Which Swelling Behavior is Measured	Measured Parameters
A	Wetting after loading	A series of lab reconstituted specimens duplicating field compaction conditions	A series of different stresses representing different overburden stresses	• Swell pressure • Swell potentials under different stresses • Free swell potential
B	Single point wetting after loading	Intact specimen of compacted fill or natural soil	Overburden plus induced structural loads	• Swell pressure • Swell potential under in situ load
C	Loading after wetting	Either reconstituted or intact specimen	In situ with or without induced structural loads	• Swell pressure • Swell potential, under either free or in situ load conditions • Post-swell reload strain

Method A

The loading steps for Method A are shown in Figure 27.13. This test is performed on specimens of fill material from a given project. The test consists of the following steps, referring to Specimen 2 in Figure 27.13.

1. A sample of fill material from the project is compacted into a lab specimen at the field specified dry unit weight and the field specified water content and placed in a consolidometer.
2. The specimen is loaded to a vertical stress, σ_{z0}, equal to the geostatic stress at a depth of fill, Point A, and the deformation, Δh_1, is measured.
3. The specimen is inundated in water and allowed to swell, or collapse, Point B, and the deformation from Point A to Point B, Δh_2, is measured.

The test is repeated with new specimens each loaded to different overburden stresses as shown in Figure 27.13. For each specimen tested the potential swell strain, ε_w, can be computed as

$$\varepsilon_w = \frac{\Delta h_2}{h_0 - \Delta h_1} \tag{27.1}$$

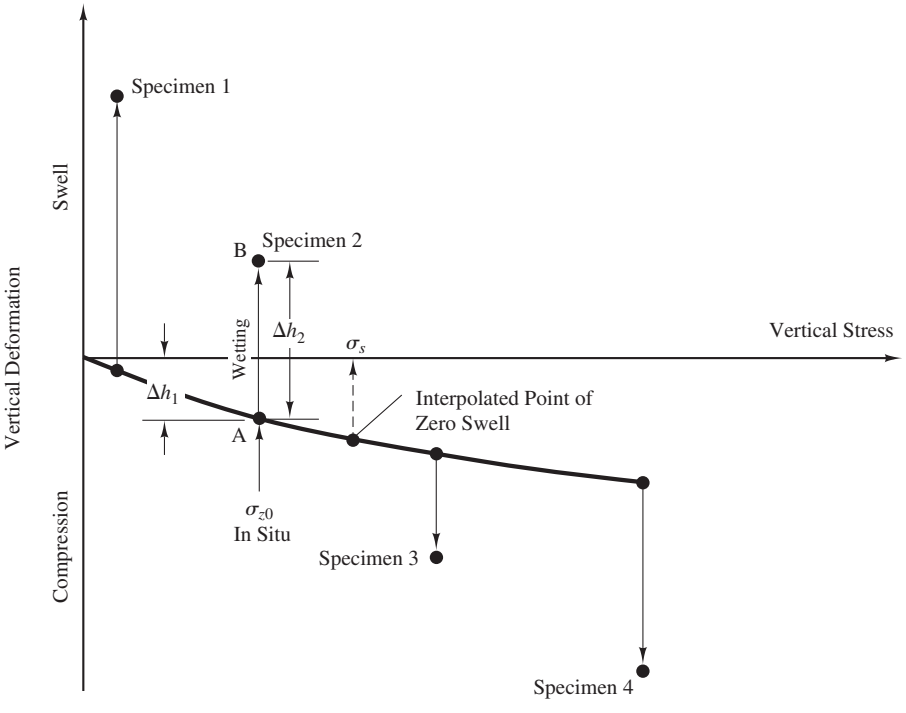

Figure 27.13 Loading steps followed in a loaded swell test following Method A of ASTM D4546.

where

h_0 = the initial height of the specimen

The swell pressure, σ_s, can be estimated by interpolation to determine the point on the compression curve where no swelling occurs, shown in Figure 27.13, and determining the vertical stress at that point.

Method B

The loading steps for Method B are shown in Figure 27.14. This test is performed on undisturbed field specimens. The specimens can be from fill material or natural soil depending upon the project. The test consists of the following steps, referring to Figure 27.14.

1. The undisturbed specimen is placed in a consolidometer.
2. The specimen is loaded to a vertical stress, $\sigma_{z0} + \Delta\sigma_z$, equal to the geostatic stress plus the induced stress from structural foundation loads, Point A, and the deformation, Δh_1, is measured.
3. The specimen is inundated in water and allowed to swell, or collapse, Point B, and the deformation from Point A to Point B, Δh_2, is measured.

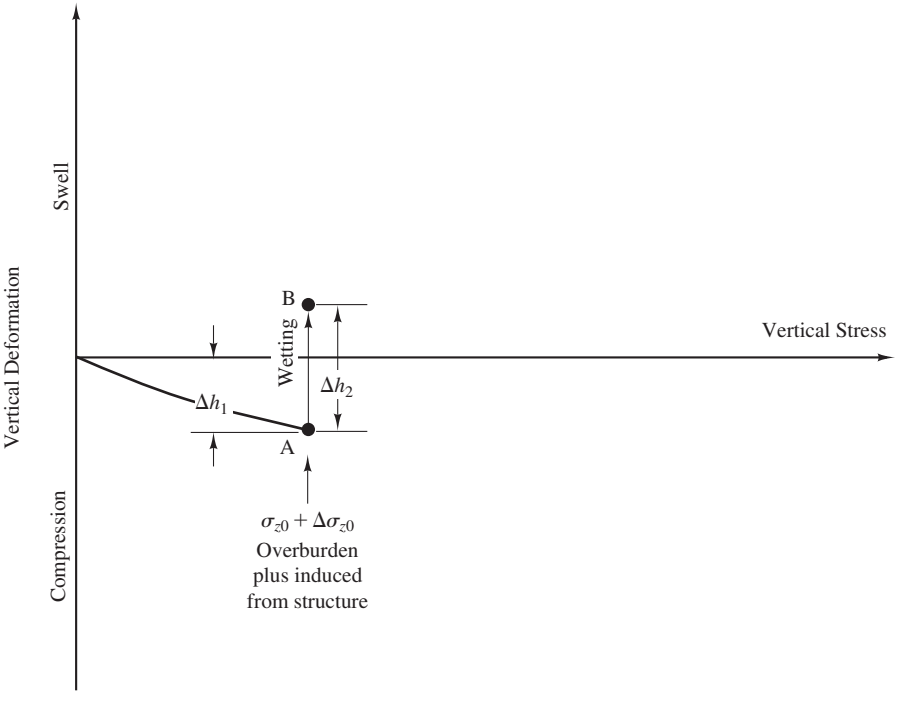

Figure 27.14 Loading steps followed in a loaded swell test following Method B of ASTM D4546.

The potential swell strain, ε_w, can be computed using Equation 27.1. The test can be run with additional specimens in the same fashion as Method A. If this is done, a swell pressure can be estimated as described above for Method A.

Method C

Method C is a test that is run after Method A or Method B. It is an alternative way to determine the swell pressure, σ_s, and can be used to determine the response of an expansive soil to loads applied after wetting. The loading steps for Method C are shown in Figure 27.15. The test consists of the following steps:

1. The test starts by following either Method A or Method B for a specimen, as is appropriate for the project.
2. After swelling has completed and the soil has reached Point B in Figure 27.15, a standard consolidation test is performed to determine the post-swelling deformation versus stress curve as shown in Figure 27.15.

The swelling pressure, σ_s, is that vertical stress at which the sample returns to its original height as shown in Figure 27.15. The magnitude of the swell pressure determined using

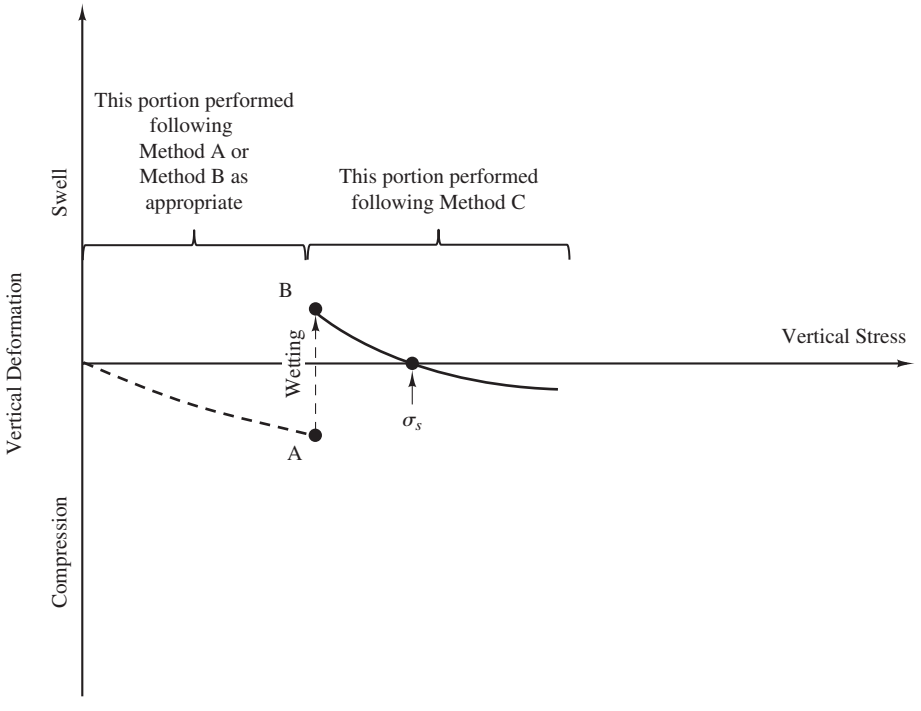

Figure 27.15 Loading steps followed in a loaded swell test following Method C of ASTM D4546.

Method C will be different than that determined using either Method A or B. The post-swell deformation curve can be used to estimate settlement of a footing or fill placed on an expansive soil after wetting.

Other Loaded Swell Tests

An alternative to the ASTM D4546 loaded test is the constant volume swell test (Johnson and Stroman, 1976). The loading steps for this test are shown in Figure 27.16. The test may be used on specimens remolded in the lab or on undisturbed samples from the field. The procedure is as follows:

1. The lab-remolded or undisturbed specimen is placed in a consolidometer.
2. The specimen is loaded to a vertical stress equal to either only the overburden stress or the overburden stress plus the induced stress from structural foundation loads, as appropriate for the project, Point A.
3. The consolidometer is fixed such that no vertical strain in the specimen is permitted. The specimen is inundated in water and the highest pressure reached that is needed to maintain zero vertical strain is the swell pressure, Point B.

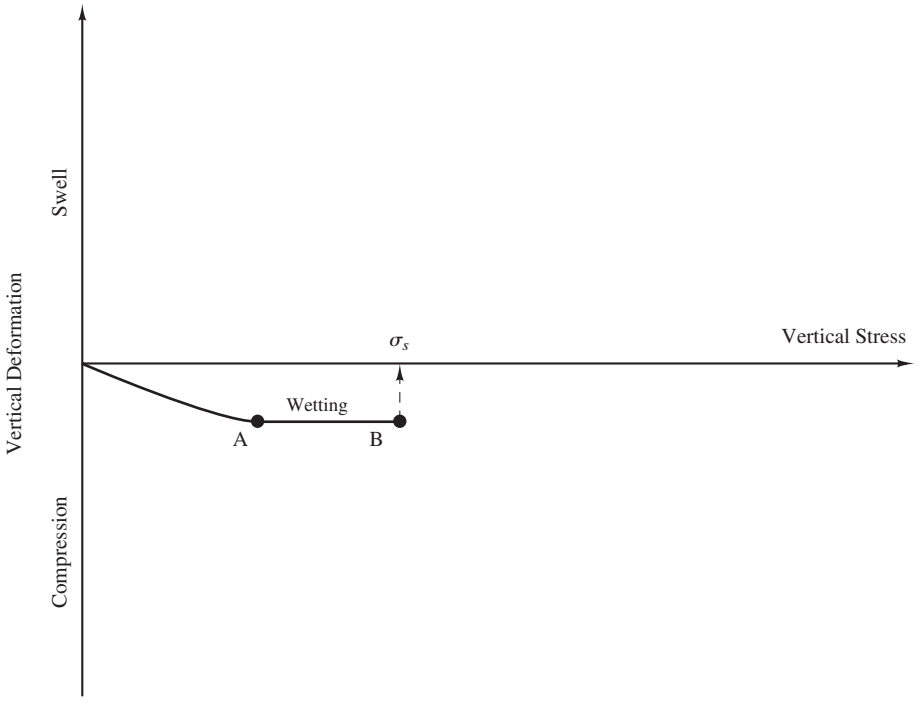

Figure 27.16 Loading steps followed in the constant volume swell (CVS) test.

TABLE 27.8 TYPICAL CLASSIFICATION OF SOIL EXPANSIVENESS BASED ON LOADED SWELL TEST RESULTS AT IN SITU OVERBURDEN STRESS (adapted from Snethen, 1984)

Swell Potential (%)	Swell Classification
<0.5	Low
0.5–1.5	Marginal
>1.5	High

Chen (1988) recommends the CVS test for determining the swell pressure. When testing compacted samples, Chen recommends reconstituting the lab samples at 100 percent relative compaction. Singhal et al. (2011) and Houston and Nelson (2012) caution that the compressibility of the test apparatus needs to be accounted for in interpreting swell test data obtained using consolidometers, particularly in the CVS test.

If a qualitative description of swell potential based on swell pressure is desired, the one proposed by Snethen (1984) and presented in Table 27.8 can be used.

Variation of Swell Potential with Normal Stress

When estimating heave of foundations, it is critical to understand how the swell potential varies with normal stress. Using any one of the loaded swell tests described above, it is possible to create a graph of swell potential as a function of normal stress such as that shown in Figure 27.17. The swell pressures measured will depend upon the test method used. None

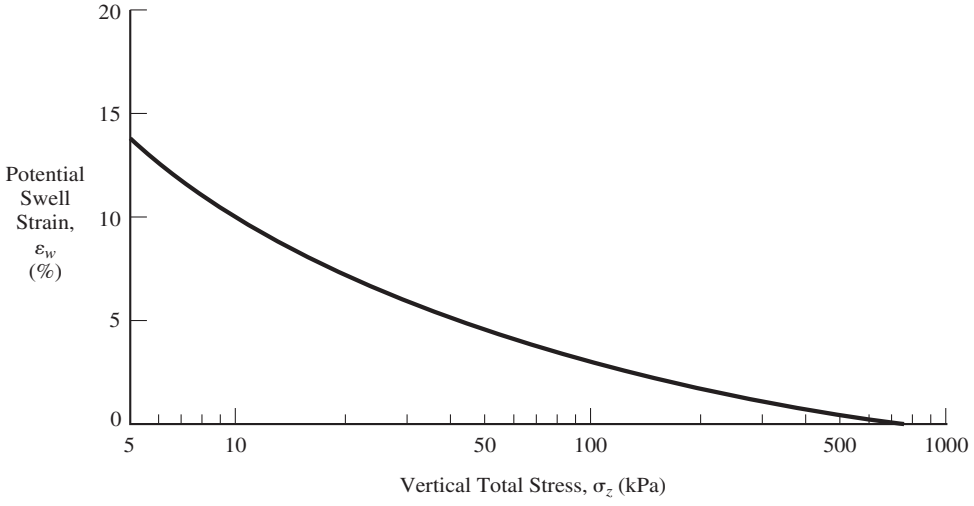

Figure 27.17 Potential swell strain versus swell pressure determined using a series of loaded swell tests on an expansive soil.

of the test methods exactly models the stress path a foundation will experience in the field. The geotechnical engineer must carefully consider the project requirements and specify the most appropriate test method.

Some engineers believe the swell pressure is independent of the initial moisture content, initial degree of saturation, and strata thickness of the soil; varies only with the dry unit weight; and is therefore a fundamental physical property of an expansive soil (Chen, 1988). Others disagree with this evaluation and claim that it varies.

Expansion Index Test

The *expansion index test* [ASTM D4829-11] (Anderson and Lade, 1981) is another standardized loaded swell test. In this test, a soil specimen is remolded into a standard 102 mm (4.01 in) diameter, 27 mm (1 in) tall ring at a degree of saturation of about 50 percent. A surcharge load of 6.9 kPa (1 lb/in^2) is applied, and then the specimen is saturated and allowed to stand until the rate of swelling reaches a certain value or for 24 h, whichever occurs first. The amount of swell is expressed in terms of the *expansion index*, EI, which is defined as:

$$\text{EI} = 1{,}000\frac{h}{H} \tag{27.2}$$

where

EI = expansion index
h = expansion of the soil
H = initial height of specimen immediately before soaking

Table 27.9 gives the descriptive interpretation of EI test results. The chief advantage of the expansion index test is that EI values from different soils at different project sites can be compared with one another to determine their relative expansion potential. This is not necessarily possible with loaded swell tests conducted under ASTM standard D4546, since that standard does not specify a specific loading at which swell is measured.

TABLE 27.9 INTERPRETATION OF EXPANSION INDEX TEST RESULTS (ASTM D4829-11)

EI	Potential Expansion
0–20	Very low
21–50	Low
51–90	Medium
91–130	High
>130	Very high

Correlations

Many researchers have developed empirical correlations between swell potential or swell pressure and different combinations of basic engineering properties including liquid limit, plasticity index, liquidity index, water content, clay content, dry unit weight, activity, and cation exchange capacity (see Erzin and Gunes (2013) for a summary of these relationships). For example, Vijayvergiya and Ghazzaly (1973) developed relationships shown in Figure 27.18 for undisturbed soils. They use moisture content, liquid limit, and dry unit weight as independent variables and define the swell potential at a surcharge load of 9.6 kPa (200 lb/ft^2) and an initial moisture content equal to the in situ moisture content. A more recent example is the relationship between swell potential and change in moisture content studied by Puppala et al. (2014).

Relating Laboratory Data to Field Behavior

The swell strain that occurs in the field is not necessarily equal to that measured in the laboratory because the soil in the field will almost never become completely saturated.

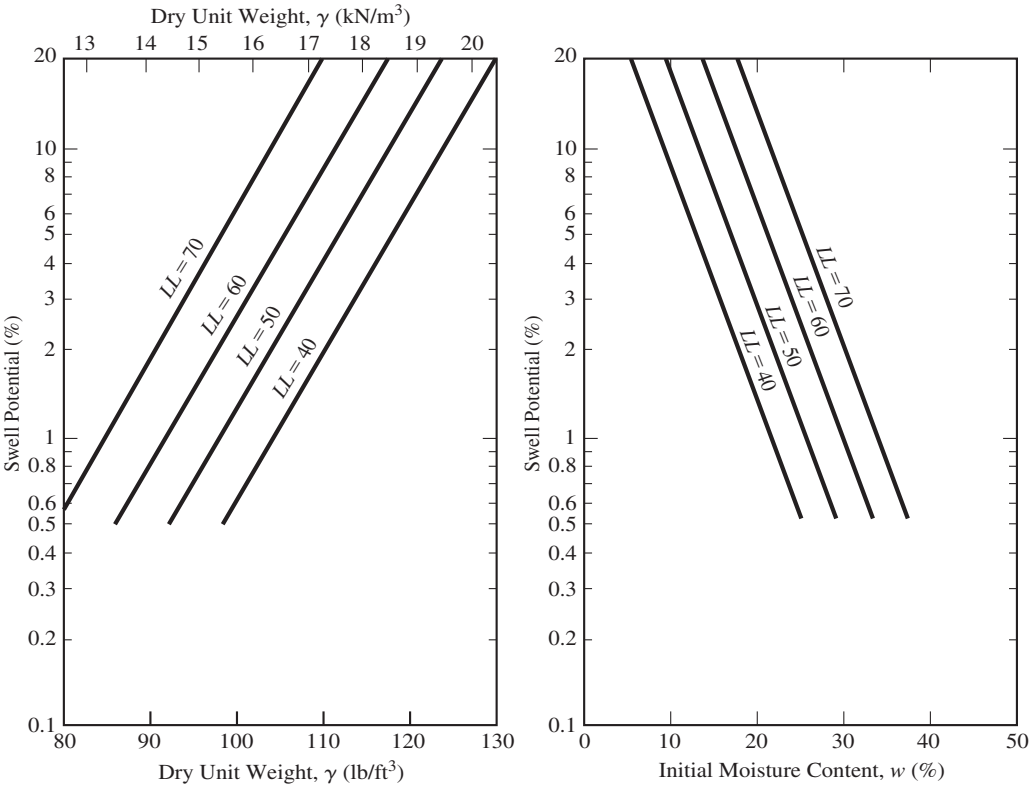

Figure 27.18 Correlations between swell potential; liquid limit, LL; initial moisture content, *w*; and dry unit weight (adapted from Vijayvergiya and Ghazzaly (1973); used with permission of the Israel Geotechnical Society).

Houston and Nelson (2012) cite four case histories for irrigated lawns and water impoundments where field saturation ranged from 35 to 96 percent. Additionally, the highest saturation values existed only a few feet below the ground surface. To account for the difference between lab and field saturation, we can define the ratio of the actual swell strain to the potential swell strain by the *wetting coefficient*, α. If the soil remains at its in situ moisture content, then $\alpha = 0$; if it becomes completely saturated, $\alpha = 1$.

Chen (1988) suggests that α is approximately proportional to the change in the degree of saturation. Thus:

$$\alpha = \frac{S - S_0}{1 - S_0} \tag{27.3}$$

where

S_0 = degree of saturation before wetting (in decimal form)
S = degree of saturation after wetting (in decimal form)

For example, if the soil in the field is initially at a degree of saturation of 40 percent, and is wetted until it reaches $S = 80$ percent, then $\alpha = (0.80 - 0.40)/(1 - 0.40) = 0.67$. In other words, the swelling in the field will be only 67 percent of that in the lab. Houston (2014) observed that although Equation 27.3 does not behave well when S_0 is close to 100 percent, the wetting coefficient α given by this equation represents a simple and reasonable way of estimating swell due to partial wetting. Note that Equation 27.3 is exactly correct if $S = S_0$ or $S = 100$ percent.

Unfortunately, it is very difficult to predict the degree of saturation that will occur in the field. It depends on many factors, including the following:

- The rate and duration of water inflow (wetting) and outflow (evaporation and transpiration)
- The rate at which water flows through the soil
- Stratification of the soil

Methods for estimating the degree of field saturation are covered in the following section.

27.3 ESTIMATING POTENTIAL HEAVE

The current state of the practice in most areas is to move directly from laboratory test results to the recommended design measures with no quantitative analyses to connect the two. Such leaps are possible only when the engineer is able to rely on local experience obtained from trial-and-error. For example, we may know that in a certain geologic formation, slab-on-grade floors have performed adequately only if the expansion index is less than some certain value. If the EI at a new project site in that formation is less than the specified value, then the engineer will recommend using a slab-on-grade floor; if not, then some other floor must be used.

This kind of methodology implicitly incorporates such factors as climate, depth of the active zone, hydraulic conductivity (especially the presence of fissures), and structural tolerance of differential heave, so they are limited only to the geologic formations, geographic areas, and types of structures that correspond to those from which the method was derived. They generally work well as long as these restrictions are observed, but can be disastrous when extrapolated to new conditions.

We would prefer to have a more rational method of designing structures to resist the effects of expansive soils, one that *explicitly* considers these factors. Ideally, such a method would predict potential heave and differential heave. Just as engineers design spread footings based on their potential for settlement, it would be reasonable to design structures on expansive soils based on the potential for heave.

Laboratory Testing

Heave analyses are normally based on laboratory swell tests, such as the ASTM D4546 methods or CVS tests described earlier. For foundations on natural soils, one should conduct these tests on undisturbed samples from different depths within the active zone to establish the expansive properties of each strata. For foundations on compacted fills, tests on samples remolded in the lab to the field conditions should be adequate. Typically, the moisture content of the soil at the beginning of each test is equal to the in situ moisture content. Thus, the laboratory tests represent the swelling that would occur if the soil becomes wetter than the in situ moisture. Sometimes, engineers will first dry the samples to a lower moisture content, thus modeling a worse condition. It is also important to establish the in situ water content profile as a function of depth during field investigation, a procedure that is relatively simple, but often overlooked (Houston, 2014).

Because the laboratory swell tests are laterally confined, they model a field condition in which the swell occurs only in the vertical direction. This may be a suitable model when the ground surface is level, but a poor one when it is sloped or when a retaining wall is present. In the latter cases, the horizontal swell is often very important.

In the field, some of the swell may be consumed by the filling of fissures in the clay. This is not reflected in the laboratory tests because the samples normally will not include fissures. However, this error should be small and conservative, and thus can be ignored.

Analysis

The heave caused by soil expansion is:

$$\delta_w = \sum \alpha H \varepsilon_w \tag{27.4}$$

where

δ_w = heave caused by soil expansion
α = wetting coefficient
H = thickness of layer
ε_w = potential swell strain

We implement this analysis as follows:

Step 1 Divide the active zone of soil beneath the foundation into layers in a fashion similar to that used for settlement analyses. These layers should be relatively thin near the bottom of the foundation (perhaps 25 cm or 1 ft thick) and become thicker with depth. The bottom of the last layer should coincide with the bottom of the active zone.

Step 2 Compute the vertical total stress, σ_z, at the midpoint of each layer. This stress should be the sum of the geostatic and induced stresses (i.e., it must consider both the weight of the soil and load from the foundation).

Step 3 Using the results of the laboratory swell tests, compute the potential swell strain, ε_w, at the midpoint of each layer.

Step 4 Determine the initial profile of degree of saturation versus depth. This would normally be based on the results of moisture content tests from soil samples recovered from an exploratory boring.

Step 5 Estimate the final profile of degree of saturation versus depth. As discussed earlier, this profile is difficult to predict. It is the greatest source of uncertainty in the analysis. Techniques for developing this profile include the following:

- **Option 1** Use empirical estimates based on observations of past projects. Studies of the equilibrium moisture conditions under covered areas, including buildings and pavements, suggest that the final moisture content is usually in the range of 1.1 to 1.3 times the plastic limit.
- **Option 2** Assume that the soil becomes saturated, but the pore water pressure above the original groundwater table remains equal to zero. This assumption is common for many foundation engineering problems and may be appropriate for many expansive soils problems, especially if extra water, such as that from irrigation or poor surface drainage, might enter the soil.
- **Option 3** Assume that a suction profile will develop such that a negative hydrostatic head is present. This scenario is based on a soil suction that diminishes with depth at the rate of 9.8 kPa/m of depth (62.4 lb/ft^2 per foot of depth).
- **Option 4** Assume $S = 100\%$ at the ground surface, and tapers to the natural S at the bottom of the active zone.

The second and third options are shown graphically in Figure 27.19.

Step 6 Compute the heave for each layer and sum them using Equation 27.4.

For additional information on heave estimates using one-dimensional consolidometer tests, see McDowell (1956), Lambe and Whitman (1959), Richards (1967), Lytton and Watt (1970), Johnson and Stroman (1976), Snethen (1980), Fredlund et al. (1980), U.S. Army Corps of Engineers (1983), Mitchell and Avalle (1984), Nelson and Miller (1992), Fredlund and Rahardjo (1993), and Nelson et al. (2006).

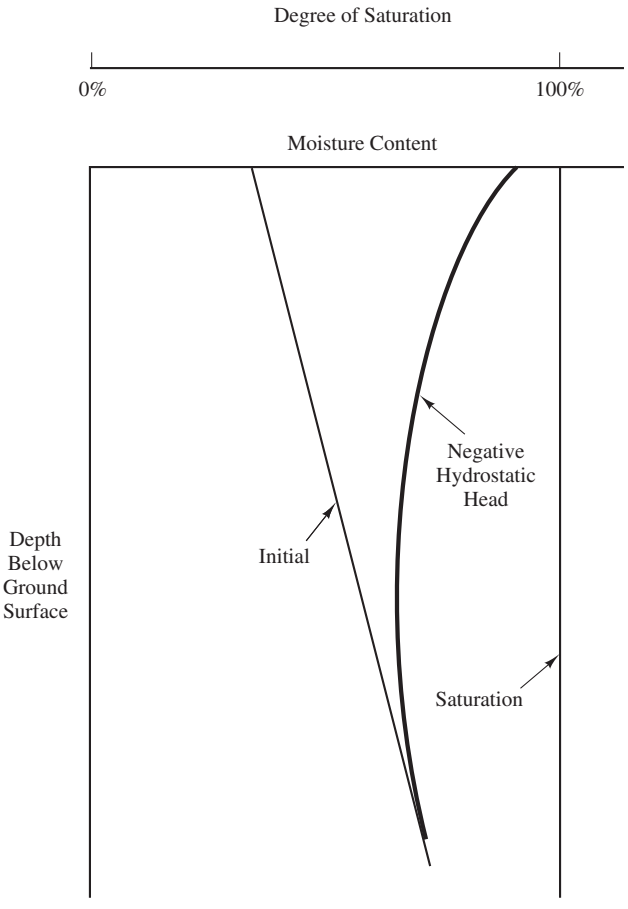

Figure 27.19 Final moisture content profiles.

Methods for predicting heave using soil suction also can be found in the literature, for example, Miller et al. (1995) and McKeen (1992). However, because consolidometer tests are much more commonly available than soil suction tests, heave prediction is usually done in practice using consolidometer test results.

Example 27.1

A compressive column load of 140 kN is to be supported on a 0.50 m deep square footing. The allowable bearing pressure is 150 kPa. The soils beneath this proposed footing are expansive clays that currently have a degree of saturation of 25 percent. This soil has a unit weight of 17.0 kN/m^3, and the depth of the active zone is 3.5 m. The results of laboratory swell tests are shown in Figure 27.17.

Compute the potential heave of this footing due to wetting of the expansive soils.

Solution

$$W_f = 0.50B^2(23.6\ \text{kN/m}^3) = 11.8B^2$$

$$B^2 q_A = P + W_f = P + 11.8B^2$$

$$B = \sqrt{\frac{P}{q_A - 11.8}}$$

$$= \sqrt{\frac{140}{150 - 11.8}}$$

$$= 1.0\ \text{m}$$

$$\sigma'_{zD} = \gamma D - u = (17.0\ \text{kN/m}^3)(0.5\ \text{m}) - 0 = 8\ \text{kPa}$$

Assume S after wetting varies from 100 percent at the ground surface to 25 percent at the bottom of the active zone. Compute $\Delta\sigma_z$, product of $(q - \sigma'_{zD})$ and I_σ from Equation 3.14, and add it to σ_{z0} (the geostatic stress) to compute σ_z. Find ε_w using the lab data, α using Equation 27.3, and δ_w using Equation 27.4.

		At Midpoint of Soil Layer								
Depth (m)	H (mm)	z_f (m)	σ_{z0} (kPa)	$\Delta\sigma_z$ (kPa)	σ_z (kPa)	ε_w (%)	S_0 (%)	S (%)	α	δ_w (mm)
0.50–0.75	250	0.12	11	141	152	2.0	25	90	0.87	4.3
0.75–1.00	250	0.32	15	126	141	2.1	25	80	0.73	3.8
1.00–1.50	500	0.75	21	68	89	3.5	25	70	0.60	10.5
1.50–2.00	500	1.25	30	33	63	3.9	25	50	0.33	6.4
2.00–3.00	1000	2.00	42	14	56	4.5	25	30	0.07	3.1
									Total	28

The estimated heave is 28 mm.

Differential Heave

Just as differential settlements often control the design of normal building foundations, differential heaves control the design of foundations on expansive soils. The differential heave can range from zero to the total heave, but is typically between one-quarter and one-half of the total heave (Johnson and Stroman, 1976). The greatest differential heaves are most likely to occur when swelling is due to such extraneous influences as broken water lines, poor surface drainage, or aggressive tree roots. Soil profiles with numerous fissures are also more likely to have higher differential heaves because of their higher hydraulic conductivity.

Donaldson (1973) recommended designing for the following heave factors (where heave factor = differential heave/total heave):

Profile with high hydraulic conductivity (i.e., fissures) in upper 3 m (10 ft)
Without extraneous influences 0.50
With extraneous influences 0.75

Profile with low hydraulic conductivity in upper 3 m (10 ft)
Without extraneous influences 0.25
With extraneous influences 0.40

27.4 TYPICAL STRUCTURAL DISTRESS PATTERNS

It is difficult to describe a typical distress pattern in buildings on expansive soils because the exact pattern of heaving depends on so many factors. However, in broad terms, buildings in arid areas tend to experience an *edge lift*, as shown in Figure 27.20a, that causes them to distort in a concave-up fashion (Simons, 1991). Conversely, in humid climates, the expansive soil may shrink when it dries, causing the edges to depress, as shown in Figure 27.20b. Heated buildings with slab-on-grade floors in colder climates sometimes experience a center depression caused by drying and shrinkage of the underlying clay soils. In the Dallas area, heaves of 125 to 150 mm (5–6 in) are common, and heaves of 200 to 300 mm (8–12 in) have been measured (Greenfield and Shen, 1992).

Special local conditions will often modify this pattern. For example, poor surface drainage or a leaky water line near one corner of the building will probably cause

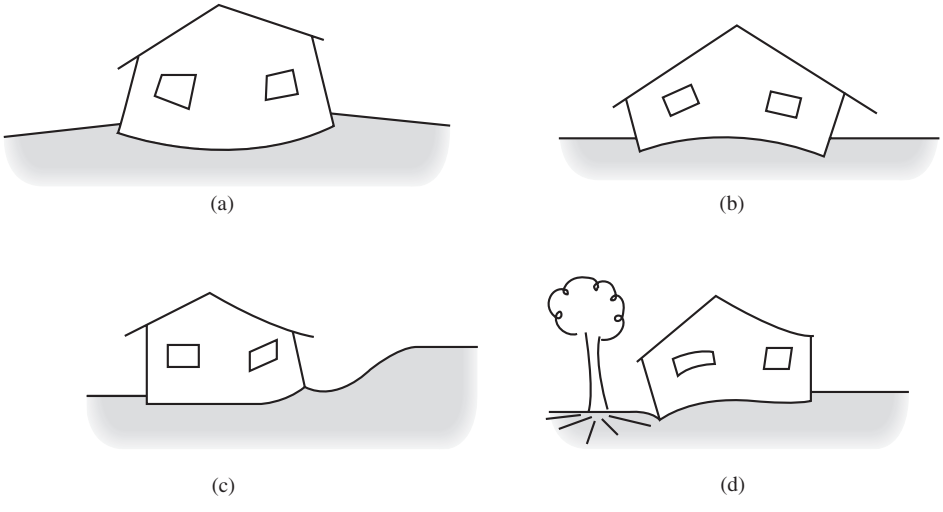

Figure 27.20 Typical distress patterns resulting from heave of expansive soils: (a) edge lift; (b) center lift; (c) localized heave due to drainage problems; and (d) localized shrinkage caused by aggressive tree roots.

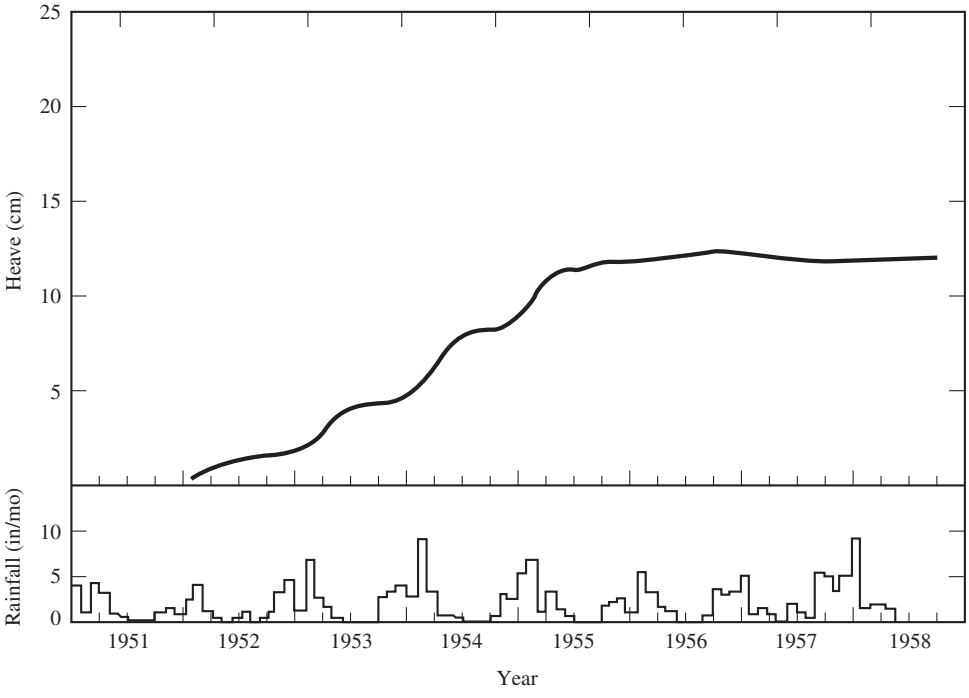

Figure 27.21 Heave record from single story brick house in South Africa (adapted from Jennings, 1969).

additional local heave, as shown in Figure 27.20c. Conversely, aggressive tree roots at another location may locally dry the soil and cause local shrinkage, as shown in Figure 27.20d (Byrn, 1991).

In arid climates, the heaving usually responds to seasonal moisture changes, producing annual shrink-swell cycles, as shown in Figure 27.21. However, during the first four to six years, the cumulative heave will usually exceed the cumulative shrinkage, so there will be a general heaving trend, as shown in Figure 27.21. As a result, expansive soil problems in dry climates will usually become evident during the first six years after construction.

Although this is a typical scenario, it does not mean that expansive soils will always behave this way. It is also very possible that unprecedented swelling may occur later in the life of the building. For example, an exceptionally wet year may invoke larger heaves. Likewise, changes in surface topography could cause ponding near the building and generate heave.

27.5 PREVENTIVE DESIGN AND CONSTRUCTION MEASURES

The next step is to develop appropriate design and construction methods to minimize (but not eliminate!) the potential for damage from expansive soils. As with most engineering problems, dealing with expansive soils ultimately boils down to a matter of risk versus

cost. A geotechnical engineer cannot guarantee that a structure will have no problems with expansive soils, but can recommend the use of certain preventive measures that seem to be an appropriate compromise between reducing the risk of damage (especially major damage) and keeping construction costs to a minimum.

Basic Preventive Measures

Any building site on an expansive soil should include at least the following features:

Surface Drainage—Although good surface drainage is important at all building sites, it is especially critical where expansive soils are present. The ground surface should slope away from the structure, as shown in Figure 27.22. Bare or paved areas should have a slope of at least 2 percent, and vegetated ground should have at least 5 percent. If possible, slope the ground within 3 m (10 ft) of the structure at a 10 percent grade.

It is also important to install gutters or other means of collecting rainwater from the roof and discharging it away from the foundation.

Basement Backfills—If the structure has a basement, the backfill should consist of nonexpansive soils. It should be well compacted to avoid subsequent settlement that would adversely affect the surface drainage patterns. In addition, a well-compacted backfill is less pervious, so water will be less likely to infiltrate the soil.

Install a drain pipe at the bottom of the backfill to capture any water that might enter and carry it outside or to a sump pump. Carefully design such drains to avoid having them act as a conduit to bring water *into* the backfill.

Landscaping—Irrigation near the structure can introduce large quantities of water into the soil and is a common cause of swelling. This can be an especially troublesome source of problems because irrigation systems are usually installed by homeowners or others who are not sufficiently conscious of expansive soil concerns. Specific preventative measures include:

- Avoid placing plants and irrigation systems immediately adjacent to the structure.
- Avoid placing irrigation pipes near the structure (to prevent problems from leaks).
- Direct all spray heads away from the structure.

As discussed earlier, large trees near the structure are often troublesome, especially those with shallow root systems. These trees can draw large quantities of water out of the soil, thus causing it to shrink. Therefore, it is best to avoid planting large trees near the structure.

Underground Utilities—Utility lines often become distorted because of differential swelling of expansive soils. With water, sewer, or storm drain pipes, these distortions can create leaks that in turn cause more expansion. This progression is likely to occur where the pipes enter the building, and could cause large heaves and serious structural distress.

The risk of this potential problem can be reduced by:

- Using flexible pipe materials (i.e., PVC or ABS instead of clay or concrete pipe).
- Installing the pipe such that large shear or flexural stresses will not develop. In some cases, this may require the use of flexible joints.

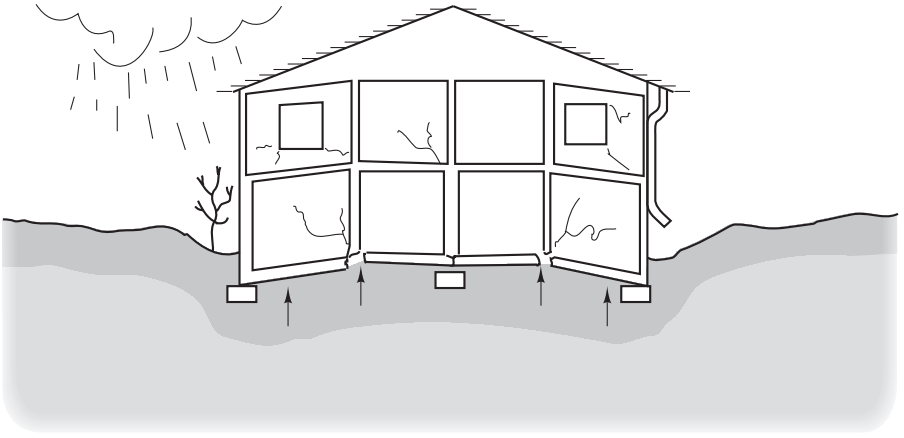

(a)

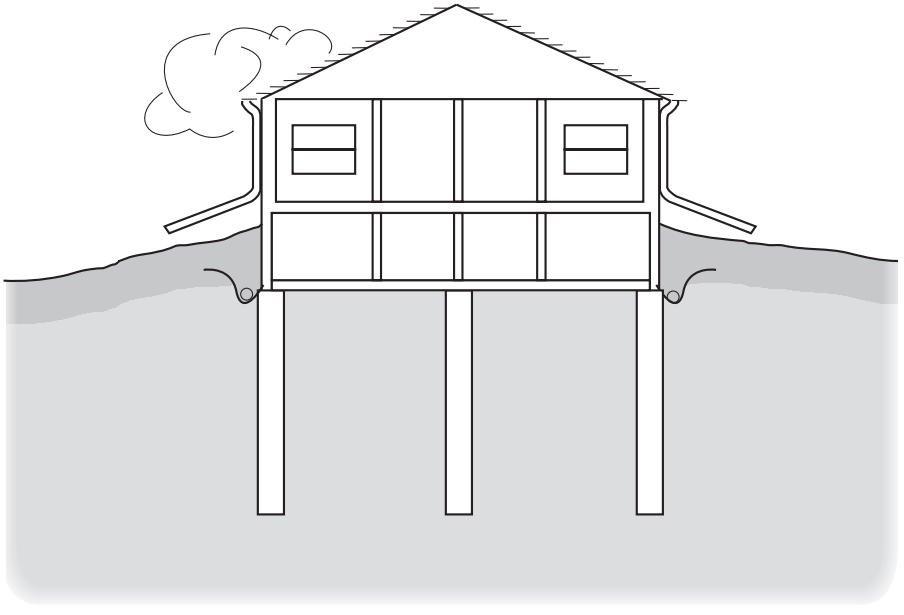

(b)

Figure 27.22 Surface drainage details: (a) poor drainage, wet expanded clay; and (b) good drainage, dry stable clay (Colorado Geological Survey).

Additional Preventive Measures

Beyond these basics, it also is possible to incorporate more extensive measures. O'Neill and Poormoayed (1980) divided them into three basic categories:

- Use ground modification techniques to alter the expansive clay to reduce or eliminate its swelling potential.
- Bypass the expansive clay by isolating the foundation from its effect.
- Mitigate the movements in the superstructure.

Each of these approaches includes several specific methodologies, as discussed below.

Ground Modification for Expansive Clay

Replacement

As discussed in Chapter 26, removal and replacement is a very effective form of ground modification. When done carefully, this can be a very effective, although expensive, method. However, be careful not to use a highly permeable soil that could provide an avenue for water to infiltrate the natural soils below (which are probably expansive), thus increasing the depth of the active zone.

Lime Treatment

When hydrated lime is mixed with an expansive clay, a chemical reaction occurs and the clay is improved in the following ways:

- Swelling potential is reduced.
- Shear strength is increased.
- Moisture content is decreased (helpful when working during the wet season because it increases the workability of the soil).

The lime can be mechanically mixed with the soil at a rate of about 2 to 8 percent by weight. Special equipment is needed to assure adequate mixing and the process generally limited to shallow depths (i.e., 300 mm or 12 in).

Another method of treating soil with lime is to inject it in a slurry form using a technique known as *pressure-injected lime* (PIL). The lime slurry is forced into the soil under high pressure using equipment similar to that shown in Figure 27.23. This method is capable of treating soils to depths of up to about 2.5 m (8 ft). The PIL technique is most effective in highly fissured soils because the fissures provide pathways for the slurry to disperse. In addition to the chemical effects, the filling of the fissures with lime also retards moisture migration in the soil.

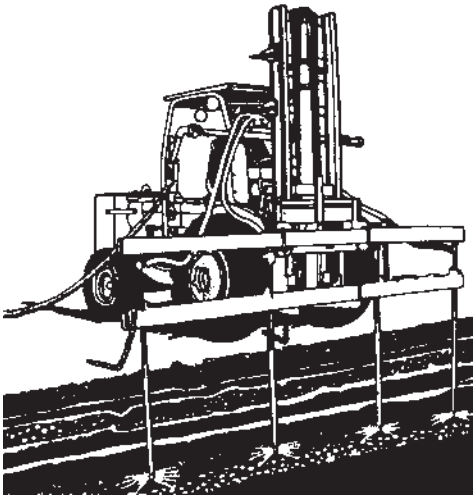

Figure 27.23 Pressure-injected lime (PIL) system (courtesy of Hayward Baker, Inc.).

Prewetting

This technique, also known as *ponding*, *presoaking*, or *presaturation*, consists of covering the site with water before construction in an attempt to increase the moisture content of the soil, thus preswelling it. When used with a project that will include a slab-on-grade, the moisture will remain reasonably constant, especially if the perimeter of the site is landscaped and irrigated or if moisture barriers are installed around the structure. The idea here is to cause the soil to expand before building the structure, and then maintain it at a high moisture content.

In some areas, such as southern California, this technique works well and generally requires a soaking time of a few days or weeks. However, in other areas, the required soaking time is unacceptably long (i.e., many months). These differences in soaking times may be due to differing required depths of soaking (a function of the depth of the active zone) and the presence or absence of fissures in the clay.

The soaking process can be accelerated by first drilling a grid of vertical sand drains (borings filled with sand) to help the water percolate into the soil. The use of wetting agents in the water also can accelerate this process. After the prewetting is completed, it is usually necessary to treat the ground surface to provide a working platform. This could consist of lime treating the upper soils or placing a 100 to 150 mm (4–6 in) thick layer of sand or gravel on the surface.

Moisture Barriers

Impermeable moisture barriers, either horizontal or vertical, can be an effective means of stabilizing the moisture content of the soil under a structure. These barriers may be located on the ground surface in the form of sidewalks or other paved areas, or they can be buried.

The latter could consist of underground polyethylene or asphalt membranes. Moisture barriers are especially helpful under irrigated landscape areas where they can take the form of sealed planter boxes.

The primary advantage of barriers is that they promote more uniform moisture conditions below the structure, thus reducing the differential heave. They may or may not affect the total heave. Although moisture barriers can be very helpful, never consider them to be completely impervious. They are generally supplementary measures that work in conjunction with other techniques.

Bypassing the Expansive Clay

Because the moisture content of a soil will fluctuate more near the ground surface than it will at depth (the active zone concept described earlier), one method of mitigating swelling effects is to support the structure on deeper soils, thus bypassing some or all of the active zone. This method is also useful when the expansive soil strata is relatively thin and is underlain by a nonexpansive soil.

Deepened Footings

When working with mildly expansive soils, it often is possible to retain a spread footing foundation system by simply deepening the footings, perhaps to about 0.5 m (3 ft) below grade. This will generally be less than the depth of the active zone, so some heave would still be possible, but its magnitude will be much less.

This method also has the advantage of increasing the rigidity of the footing (which is usually supplemented by additional reinforcement—say, one or two #4 bars top and bottom), thus spreading any heave over a greater distance and improving the structure's tolerance of heave.

When spread footings are used, they should be designed using as high a bearing pressure as practicable to restrain the heaving. A bearing pressure equal to the swell pressure would be ideal, but is generally possible only in very mildly expansive soils.

Drilled Shafts

In a highly expansive soil, deepened spread footings cease to be practical and a drilled shaft foundation often becomes the preferred system. In the Denver, Colorado area, shafts for lightweight structures are typically 250 to 300 mm (10–12 in) in diameter and 4.5 to 6 m (15–20 ft) deep (Greenfield and Shen, 1992). The shafts must extend well below the active zone. The individual shafts are connected with grade beams that are cast on top of collapsible cardboard or foam forms, as shown in Figure 27.24. The purpose of these forms is to permit the soil to freely expand without pressing against the grade beam. Another alternative is to use precast grade beams. This system also works well on larger structures, although much larger shafts are then required.

One of the special concerns of using drilled shafts in expansive soils is the development of uplift forces along the sides of the shafts within the active zone, as shown in

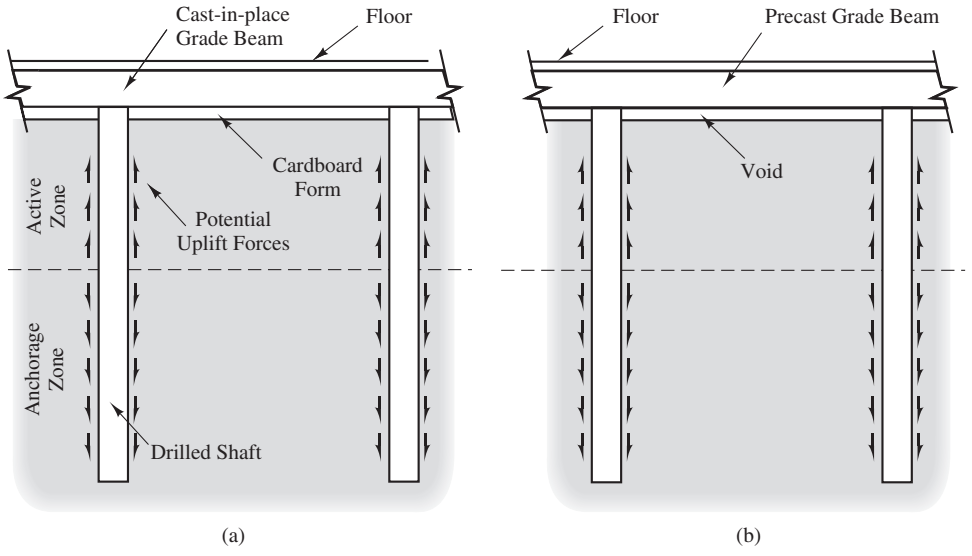

Figure 27.24 Typical lightweight building foundation consisting of drilled shafts and raised grade beams: (a) cast-in-place grade beam with cardboard forms are designed to collapse at pressures slightly greater than those from the wet concrete; and (b) precast concrete grade beam. Note the uplift forces acting on the shaft due to the heave of the soil in the active zone.

Figure 27.24. The shafts must be designed to accommodate these forces, both in terms of load transfer and the need for tension steel extending through the active zone.

This matter is further aggravated because the soil also attempts to swell horizontally, which translates to an increased normal stress between the soil and the shaft. This, in turn, permits more side friction resistance to be mobilized and increases the uplift force.

There are two established methods used to design drilled shafts in expansive soils: the rigid shaft method and the elastic shaft method. In the rigid shaft method (Chen, 1988; O'Neill and Reese 1999; and Nelson and Miller, 1992), the shaft is considered rigid and the total uplift force exerted on the shaft by the swelling soils in the active zone, shown in Figure 27.24, is balanced by the downward load on the pile and the total downward side friction resistance from the portion of the shaft below the active zone. An LRFD implementation of this method of designing drilled shafts in expansive soils can be found in Brown et al. (2010). To compute the uplift force from the unit uplift side friction capacity, f_n, in the active zone, Brown et al. (2010) recommended the α method (Equation 16.13) with an adhesion factor of $\alpha = 1.0$ and an undrained shear strength, s_u, of the soil after full wetting under the in situ overburden stress. According to Nelson et al. (2012), the rigid shaft method generally gives conservative designs for light structures on expansive soils.

To allow the consideration of shaft heave, Nelson and Miller (1992) developed the elastic shaft method for designing drilled shafts in expansive soils. This method is based on the assumption that the shaft is a stiff inclusion in an elastic half-space and uses a boundary-element solution by Poulos and Davis (1980). Nelson et al. (2007) improved this method and produced design charts to facilitate its use.

In addition to the rigid and elastic shaft methods, Nelson et al. (2012) developed a finite-element-based analysis method for general cases of drilled shafts in expansive soils. This method uses free-field soil heave as input and gives the shaft heave and axial force in the shaft as output. It inherits all the advantages of a finite element method, one of which is the capability of handling geometrical and material nonlinearity; however, compared to the previous two methods, more input data are required on the soil, shaft material, and soil/shaft interface.

We must consider the possibility that parts of the shaft will develop a net tensile force if the soil were to swell. Therefore, the design must include steel reinforcing bars and they should extend to the bottom of the shaft. In Denver, shafts that support lightweight structures typically have at least two full-length #5 grade 40 rebars, whereas in Dallas, two #6 bars are common (Greenfield and Shen, 1992).

An alternative to designing for uplift loads is to isolate the shaft from the soil in the active zone. One way to do so is by forming the shaft with a cardboard tube inside a permanent steel casing and filling the annular space with a weak but impervious material.

For design purposes, the resistance to either upward or downward movements is considered to begin at the bottom of the active zone. This resistance can be generated by a straight shaft, one with a bell, or one with shear rings. The latter two are commonly preferred when large uplift loads are anticipated.

Structurally Supported Floors

When the computed total heave exceeds about 25 to 50 mm (1–2 in), conventional slab-on-grade floors cease to perform well. In such cases, the most common design is to use a raised floor supported on a drilled shaft foundation that penetrates through the active zone, as shown in Figure 27.25. Not only does this design isolate the floor from direct heaving, it also provides ventilation of the ground surface while still shielding it from precipitation. This keeps the soil under the building much drier than it would be with a slab-on-grade floor or a mat floor.

Mitigating Movements in the Structure

Another method of addressing differential settlement and heave problems is to make the structure more tolerant of these movements. There are many ways to accomplish this, and these measures can be used alone or in conjunction with the methods described earlier.

Flexible Construction

Some structures will tolerate a large differential movement and still perform acceptably. Lightweight industrial buildings with steel siding are an example of this type of construction. See the discussion in Chapter 2 for more details on this concept.

Another way of adding flexibility to a structure is to use *floating slabs*, as shown in Figure 27.26. Casting these slabs separate from the foundation and providing a slip joint between the slab and the wall allow it to move vertically when the soil swells.

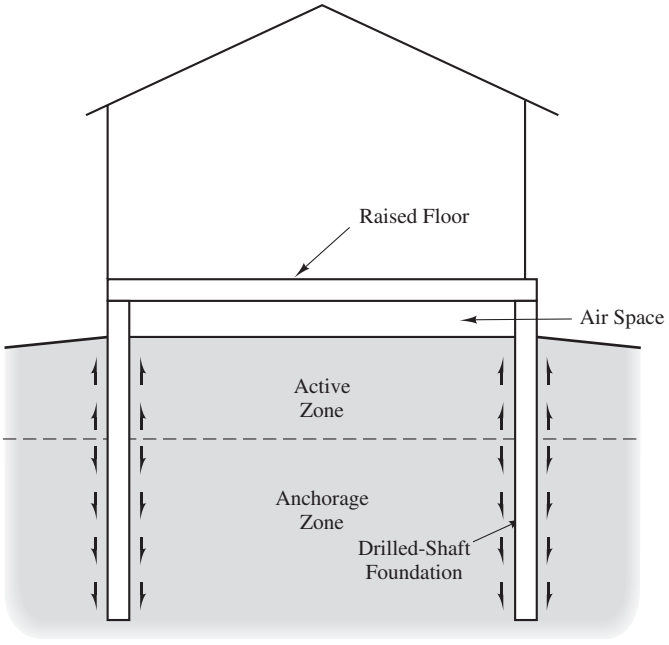

Figure 27.25 Bypassing expansive clay with a raised floor and a drilled shaft foundation.

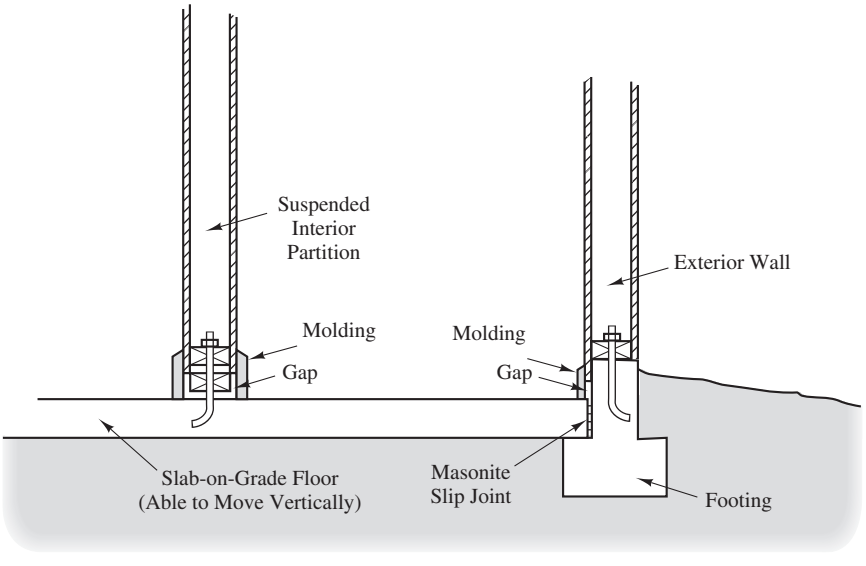

Figure 27.26 Floating slab and related design details.

Any construction resting on a floating slab must also be able to move. For example, furnaces would need a flexible plenum and vent pipe. Partition walls could be suspended from the ceiling with a gap at the bottom covered with flexible molding. Stairways also could be suspended from the ceiling and wall and not be connected to the slab. Each of these details is shown in Figure 27.26. Floating slabs are most commonly used in garages and basements because these design details are easier to implement.

Rigid Foundation System

The opposite philosophy is to provide a foundation system that is so rigid and strong that it moves as a unit. Differential heaves would then cause the structure to tilt without distorting. Conventionally reinforced mats have been used for this purpose. These mats are also known as *waffle slabs* because of the shape of their integral beams, as shown in Figure 27.27. These slabs are cast using collapsible cardboard forms to provide void spaces under the slab, thus allowing space for the soil to expand. Kantey (1980) noted routine success with brick buildings on this type of foundation in South Africa, where some had experienced heaves of up to 250 mm (10 in) and still performed adequately.

An alternative to conventional reinforcement is to use prestressed or post-tensioned slabs as a kind of mat foundation. Post-Tensioning Institute (2012) presents a design procedure for post-tensioned slabs on expansive soils. This method is gaining popularity, especially for residential projects, and has been used successfully on highly expansive soils in California, Texas, and elsewhere.

We can apply this concept more economically to mildly expansive soils by using conventional spread footings in such a way that no footing is isolated from the others. This can be accomplished by using continuous footings and/or grade beams, as shown in Figure 27.28. Such a system does not have the rigidity of a mat, but is much more rigid than isolated footings and will help to spread differential heaves over a longer distance.

Determining Which Methods to Use

Gromko (1974) suggested the criteria in Table 27.10 to guide the selection of preventive design measures based on the estimated heave and the length-to-height ratio, L/H, of the walls.

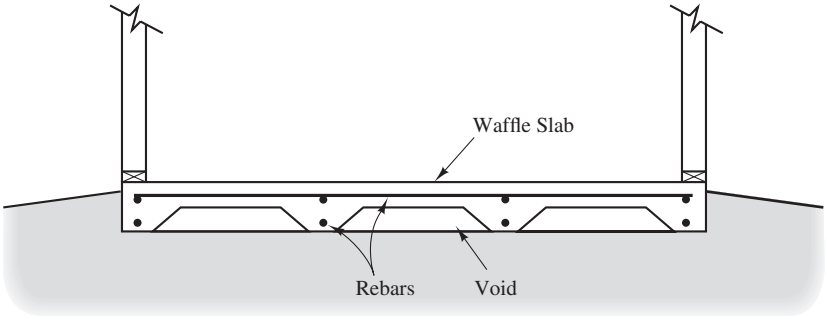

Figure 27.27 Conventionally reinforced mat foundation "waffle slab."

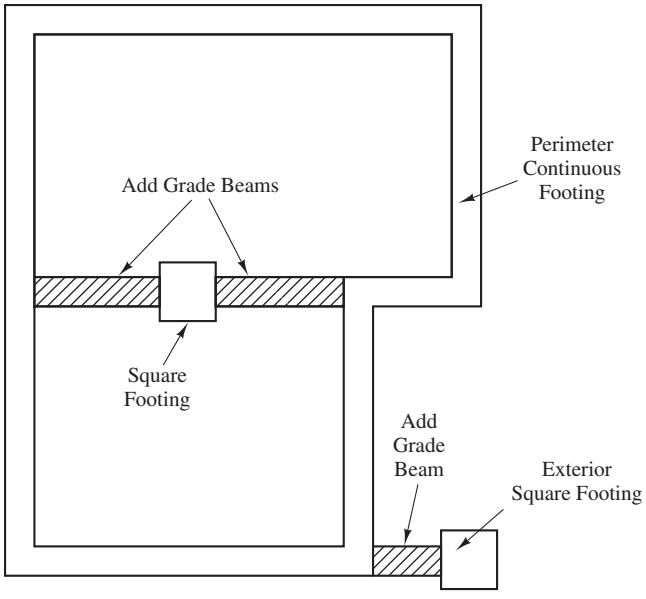

Figure 27.28 Use of continuous footings and grade beams to improve the rigidity of a spread footing system.

TABLE 27.10 PREVENTIVE DESIGN MEASURES BASED ON COMPUTED HEAVE (adapted from Gromko, 1974; used with permission of American Society of Civil Engineers)

Total Predicted Heave				
$L/H = 1.25$	$L/H = 2.50$	Recommended Construction	Method	Remarks
<6 mm <0.25 in	<12 mm <0.5 in	No precautions		
6–12 mm 0.25–0.5 in	12–50 mm 0.5–2 in	Rigid building tolerating movement (steel reinforcement as necessary)	Foundations: Spread footings, mats, or waffle	Footings should be narrow and deep, consistent with the soil bearing capacity.
			Floor slabs: Waffle, tile	Slabs should be designed to resist bending and should be independent of grade beams.
			Walls	Walls on a mat should be as flexible as the mat. No rigid connections vertically. Strengthen brickwork with tiebars or bands.

(*continued*)

TABLE 27.10 (Continued)

Total Predicted Heave		Recommended Construction	Method	Remarks
$L/H = 1.25$	$L/H = 2.50$			
12–50 mm 0.5–2 in	50–100 mm 2–4 in	Building damping movement	Joints: Clear, flexible	Contacts between structural units should be avoided, or a flexible waterproof material may be inserted in the joint.
			Walls: Flexible, unit construction, and steel frame	Walls or rectangular building units should heave as a unit.
			Foundations: Three-point, cellular, or jack	Cellular foundations allow slight soil expansion to reduce the swelling pressure. Three-point loading allows motion without duress.
>50 mm >2 in	>100 mm >4 in	Building independent of movement	Drilled shafts: Straight, belled	Use smallest diameter and most widely spaced shafts compatible with load. Allow clearance under grade beams.
			Suspended floor	Suspend floors on grade beams 300–450 mm (12–18 in) above the soil.

27.6 OTHER SOURCES OF HEAVE

Although expansive clays are the most common source of heave, other mechanisms also have been observed.

Expansive Rocks

Sedimentary rocks formed from clays, such as claystone, and shale are often expansive (Lindner, 1976). The physical mechanisms are similar to those for clay soils, but the swelling pressures and potential heave are often very high because of the high unit weight of rock. However, these rocks do not transmit water as easily, so the potential heave may be more difficult to attain in the field. Some other rocks can expand as a result of chemical processes, such as oxidation or carbonation. These processes often create by-products that occupy a larger volume than the original materials (Lindner, 1976).

Steelmaking Slag

The process of making steel from iron ore produces two principal types of solid wastes: *blast furnace slag* and *steelmaking slag* (Lankford et al., 1985). Blast furnace slag is the waste produced when iron ore and limestone are combined in a blast furnace to produce iron. This material has very favorable engineering properties and has been used for concrete aggregate (with some problems), base material beneath pavements, and many other applications (Lee, 1974). In contrast, steelmaking slag is produced when iron is made into steel, and it is a much more troublesome material.

The primary problem with steelmaking slag is that it can expand in volume after being put in place, thus producing problems similar to those caused by expansive clays. For example, Crawford and Burn (1968) described a case history of a floor slab built over sand-sized steelmaking slag that heaved up to 75 mm (3 in) in 5 years. Uppot (1980) described another case history of an industrial building that experienced heaves of up to 200 mm (8 in) in columns and up to 250 mm (10 in) in floor slabs within six years of construction.

This expansion is the result of hydration of unslaked lime, magnesium oxides, and other materials, and may exceed 20 percent of the original volume of the slag. Spanovich and Fewell (1968) observed that the swell potential is reduced by more than 50 percent if the slag is allowed to age for 30 days before being used. This aging process requires exposure to oxygen and water. However, they also observed that slag that had been buried for more than 30 years (and thus had not been cured) was still very expansive.

Some engineers have used cured steelmaking slag for applications that have a high tolerance of movements, such as open fills, unpaved roads, and railroad ballast. Engineers in Japan have used mixtures of steelmaking slag and blast furnace slag to produce aggregate base material for roadway pavements (Nagao et al., 1989). However, because of its expansive properties, steelmaking slag should not be used beneath structural foundations.

Salt Heave

Soils in arid areas sometimes contain high concentrations of water-soluble salts that can crystallize out of solution at night when the temperature is low and return to solution during the day as the temperature rises. The formation and dissipation of these salt crystals can cause daily cycles of heave and shrinkage in the soil, especially in the late fall and early spring when the difference between day and night air temperatures may be 60°F (33°C) or more. Although some moisture must be present for crystallization to occur, this process is driven by changes in temperature. This phenomenon, known as *salt heave* or *chemical heave*, normally occurs only in the upper 0.3 to 0.6 m (1–2 ft) of the soil because the salt concentrations and temperature fluctuations are greatest in this zone.

Based on studies of soils in the Las Vegas, Nevada area, Cibor (1983) suggested that salt heave can generate swell pressures of 10 to 15 kPa (200−300 lb/ft^2). The bearing pressure beneath most spread footings is much larger than this swell pressure, so these

footings are able to resist the heaving forces without moving. In addition, the bottoms of footings are typically below the zone of greatest heave potential. However, heave has been observed in very shallow and lightly loaded footings.

Damage from salt heave is most often seen in slab-on-grade floors, sidewalks, and other shallow, very lightly loaded areas. For example, Blaser and Scherer (1969) observed heaves of 100 mm (4 in) in exterior concrete slabs.

Evaluate these soils by measuring the percentage of salts in solution. Typically, concentrations of greater than 0.5 percent soluble salts in soils with more than 15 percent fines may be of concern. The heave potential can be measured using a thermal swell test (Blaser and Scherer, 1969). This test is similar to the swell tests discussed earlier in this chapter, except that the soil expansion is induced by cooling the sample instead of adding water.

A common method of avoiding salt heave problems is to excavate the salt-laden natural soils to a depth of 0.3 to 0.6 m (1–2 ft) below the proposed ground surface and backfill with open graded gravel. Because the gravel provides thermal insulation, the temperature below will not vary as widely as on the ground surface, so salt heave will be less likely to occur. In addition, the weight of the gravel will resist any swelling pressures that might develop.

SUMMARY

Major Points

1. Expansive soils cause more property damage in the United States than all the earthquakes, floods, tornados, and hurricanes combined.
2. Most of this damage is inflicted on lightweight improvements, such as houses, small commercial buildings, and pavements.
3. Soil swelling is the result of the infiltration of water into certain clay minerals, most notably montmorillonite. Swelling will occur only if the moisture content of the soil changes.
4. Expansive soils are most likely to cause problems in subhumid, semi-arid, and arid climates. The patterns of precipitation and evaporation/transpiration in these areas usually cause the moisture content of the soil to fluctuate during the year, which creates cycles of shrinking and swelling. New construction in these areas normally promotes an increased moisture content in the soil that further aggravates the problem.
5. The potential heave at a given site is a function of the soil profile, variations in soil moisture, overburden loads, and superimposed loads.
6. A wide variety of test methods are available to evaluate the degree of expansiveness. Some of these methods are primarily qualitative, and others provide quantitative results.

7. Preventive measures fall into three categories:
   a. Alter the condition of the expansive clay.
   b. Bypass the expansive clay by isolating the foundation from its effect.
   c. Provide a shallow foundation capable of withstanding differential movements and mitigating their effect in the superstructure.
8. The current state of the practice in most places is to select the appropriate preventive measures based on qualitative or semiquantitative test results and local experience. These methods are generally applicable only to limited geographic areas and for certain types of structures.
9. Engineers use heave calculations as a basis for determining preventive measures. Such calculations can be based on either loaded swell tests or soil suction tests.

Vocabulary

Active zone
Bentonite
Clay minerals
Constant volume swell test
Differential heave
Edge lift
Expansion index
Expansion pressure
Expansive soil
Heave
Illite
Kaolinite
Lime treatment
Loaded swell test
Moisture barrier
Montmorillonite
Prewetting
Slag
Swell potential
Swell pressure
Thornthwaite moisture index
Waffle slab
Wetting coefficient

QUESTIONS AND PRACTICE PROBLEMS

27.1 Why are lightweight structures usually more susceptible to damage from expansive soils?

27.2 What types of climates are most prone to cause problems with expansive clays?

27.3 How do human activities often aggravate expansive soil problems?

27.4 What is the active zone?

27.5 What is the swell pressure?

27.6 What are the primary sources of uncertainty in heave analyses?

27.7 Why do the soils beneath buildings with raised floors tend to be drier than those beneath slab-on-grade floors?

27.8 The foundation described in Example 27.1 is to be redesigned using a net allowable bearing pressure of 75 kPa. Compute the potential heave and compare it with that computed in the example. Discuss.

27.9 An 8 in diameter drilled shaft will penetrate through an expansive stiff clay to a depth well below the active zone. It will carry a downward load of 5,200 lb. The undrained shear strength of the clay is 900 psf and the active zone extends to a depth of 10 ft. Determine the following:

a. What is the uplift skin friction load?

b. Is a tensile failure in the shaft possible (do not forget to consider the weight of the shaft)?

c. What is the required reinforcing steel to prevent a tensile failure (if necessary)? Use $f_y = 40$ k/in^2 and a load factor of 1.7.

28

Foundations on Collapsible Soils

It is better to fail while attempting to do something worthwhile than to succeed at doing something that is not.

Anonymous

Foundation engineers who work in arid and semiarid areas of the world often encounter deposits of *collapsible soils*. These soils are dry and strong in their natural state and appear to provide good support for foundations. However, if they become wet, these soils quickly consolidate, thus generating unexpected settlements. Sometimes these settlements are quite dramatic, and many buildings and other improvements have been damaged as a result. These soils are stable only as long as they remain dry, so they are sometimes called *metastable soils*, and the process of collapse is sometimes called *hydroconsolidation*, *hydrocompression*, or *hydrocollapse*. To avoid these kinds of settlements, the foundation engineer must recognize collapsible soils, assess the potential settlements, and employ appropriate mitigation measures when necessary (Clemence and Finbarr, 1981).

28.1 ORIGIN AND OCCURRENCE OF COLLAPSIBLE SOILS

Most collapsible soils consist predominantly of sand and silt size particles arranged in a loose "honeycomb" structure, as shown in Figure 28.1. Sometimes gravel is also present. This loose structure is held together by small amounts of water-softening cementing agents, such as clay or calcium carbonate (Barden et al., 1973). As long as the soil remains dry, these cements produce a strong soil that is able to carry large loads. However, if the soil becomes wet, these cementing agents soften and the honeycomb structure collapses.

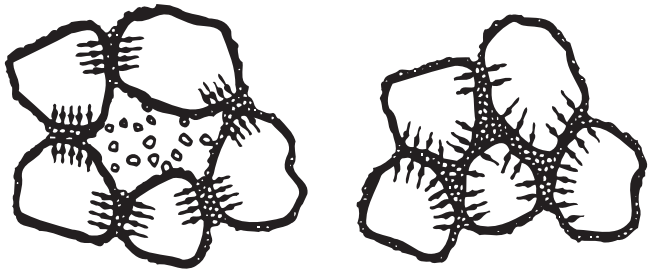

Figure 28.1 Microscopic view of a collapsible soil. In their natural state, these soils have a honeycomb structure that is held together by water soluble bonds. However, if the soil becomes wet, these bonds soften and the soil consolidates (based on from Houston et al., 1988; used with permission of ASCE).

Various geologic processes can produce collapsible soils. By understanding their geologic origins, we are better prepared to anticipate where they might be found.

Collapsible Alluvial and Colluvial Soils

Some *alluvial soils* (i.e., soils transported by water) and some *colluvial soils* (i.e., soils transported by gravity) can be highly collapsible. These collapsible soils are frequently found in southwestern United States as well as other regions of the world with similar climates. In these areas, short bursts of intense precipitation often induce rapid downslope movements of soil known as *flows*. While they are moving, these soils are nearly saturated and have a high void ratio. Upon reaching their destination, they dry quickly by evaporation, and capillary tension draws the pore water toward the particle contact points, bringing clay and silt particles and soluble salts with it, as shown in Figure 28.2. Once the soil becomes dry, these materials bond the sand particles together, thus forming the honeycomb structure.

When the next flow occurs, more honeycomb-structured soil forms. It, too, dries rapidly by evaporation, so the previously deposited soil remains dry. Thus, deep deposits of this soil can form. The remains of repeated flows are often evident from the topography of the desert, as shown in Figure 28.3. These deposits are often very erratic, and may include interbedded strata of collapsible and noncollapsible soils.

In some areas, only the uppermost stratum, perhaps 1 to 3 m (3–10 ft) thick, is collapsible, whereas elsewhere the collapse-prone soils may extend 60 m (200 ft) or more below the ground surface. An example of the latter is the San Joaquin Valley in Central California, where irrigation canals are especially prone to damage because even small leaks that persist for a long time may wet the soil to a great depth. Settlements of 600 to 900 mm (2–3 ft) are common in these canals, and cases of up to 4.7 m (15 ft) have been reported (Dudley, 1970).

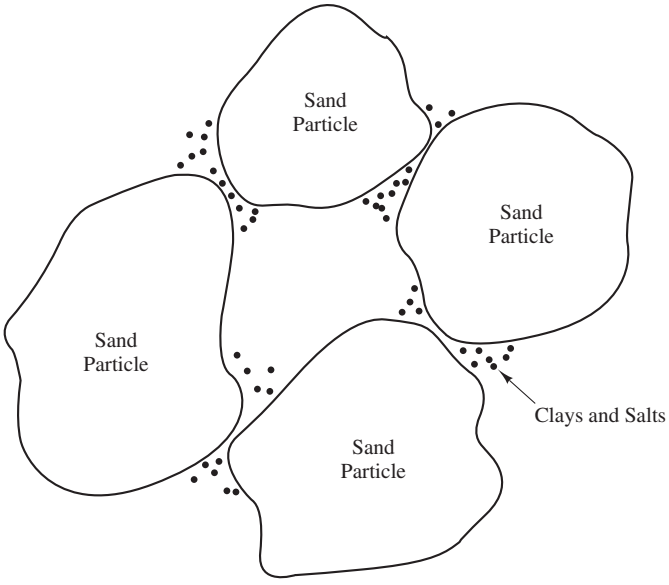

Figure 28.2 When flow deposits dry by evaporation, the retreating water draws the suspended clay particles and dissolved salts toward the particle contact points.

Collapsible Aeolian Soils

Soils deposited by wind are known as *aeolian soils*. These include windblown sand dunes, loess, volcanic dust deposits, as well as other forms. *Loess* (an aeolian silt or sandy silt) is the most common aeolian soil and it covers much of the Earth's surface. It is found in

Figure 28.3 Ariel view of flow topography in the desert near Palm Springs, California. Both surface water and windstorms in this area move from the right side of the photo to the left side. Thus, the alluvial and aeolian soil deposits form long stripes on the ground. These soils are often highly collapsible, so settlement problems can occur in the heavily irrigated developments, such as the golf course community shown in the bottom of this photograph.

the United States, central Europe, China, Africa, Australia, Ukraine, India, Argentina, and elsewhere (Pye, 1987). The locations of major loess deposits in the United States are shown in Figure 28.4 along with locations of other reported collapsible soil deposits.

Collapsible loess has a very high porosity (typically on the order of 50 percent) and a correspondingly low unit weight (typically $11-14\ \text{kN/m}^3$ or $70-90\ \text{lb/ft}^3$). The individual particles are usually coated with clay, which acts as a cementing agent to maintain the loose structure. This cementation is often not as strong as that in many alluvial soils, so collapse can occur either by wetting under a moderate normal stress or by subjecting the soil to higher normal stresses without wetting it.

Loess deposits are generally much less erratic than other types of collapsible soils, but they are often much thicker. Deposits 60 m (200 ft) thick are not unusual.

Collapsible Residual Soils

Residual soils are those formed in-place by the weathering of rock. Sometimes this process involves decomposition of rock minerals into clay minerals that may be removed by leaching, leaving a honeycomb structure and a high void ratio. When this structure develops, the soil is prone to collapse. For example, Brink and Kantey (1961) reported that residual decomposed granites in South Africa often collapse upon wetting, leading to a 7 to 10 percent increase in unit weight. Residual soils derived from sandstones and basalts in Brazil also are collapsible (Hunt, 1984). Dudley (1970) reported test results from a residual soil from Lancaster, California, that showed nearly zero consolidation when loaded dry to a stress of 670 kPa ($14{,}000\ \text{lb/ft}^2$) over the natural overburden stress, yet collapsed by

Figure 28.4 Locations of major loess deposits in the United States along with other sites of reported collapsible soils (based on Dudley, 1970; used with permission of ASCE).

10 percent of its volume when soaked. Residual soils are likely to have the greatest amount of spatial variation, thus making it more difficult to predict the collapse potential.

28.2 IDENTIFICATION, SAMPLING, AND TESTING

Engineers have used many different techniques to identify and evaluate collapsible soils. They may be divided into two categories: indirect methods and direct methods.

The indirect methods assess collapse potential by correlating it with other engineering properties such as unit weight, Atterberg limits, or percent clay particles. Soils having a low dry unit weight, low moisture content, and the grain size distributions described earlier are most likely to be problematic. Especially when combined with local experience, these methods are useful for initial screening of soils to identify potential problems (Lutenegger and Saber, 1988).

When potentially collapsible soils have been identified, direct testing methods are normally used to measure the collapse potential and to guide the design and remediation processes. Both laboratory and in situ test methods are available.

Obtaining Samples of Collapsible Soils

Direct testing methods are most often conducted in the laboratory, which necessitates recovering relatively undisturbed samples of the soil and bringing these samples to the lab. Collapsible soils that are moderately to well cemented and do not contain much gravel usually can be sampled without undue difficulty. This includes many of the alluvial collapsible soils. As with any sampling operation, the engineer must strive to obtain samples that are as undisturbed as possible and representative of the soil deposit. Unfortunately, collapsible soils, especially those of alluvial or residual origin, are often very erratic. It is difficult to obtain representative samples of erratic soil deposits, so we must obtain many samples to accurately characterize the collapse potential. Considering the usual limitations of funding for soil sampling, it is probably wiser to obtain many good samples rather than only a couple of extremely high quality (but expensive) samples.

Sometimes, conventional thin-wall Shelby tube samplers can be pressed into the soil. It is best to use short tubes to avoid compressing the samples. Unfortunately, because collapsible soils are strong when dry (it is important not to artificially wet the soil during sampling), it often is necessary to hammer the tube in place. However, studies by Houston and El-Ehwany (1991) suggest that hammering does not significantly alter the results of laboratory collapse tests for cemented soils.

Although Shelby tubes work well in silty and sandy soils, they are easily bent when used in soils that contain even a small quantity of gravel. This is often the case in collapsible soils, so we may be forced to use a sampler with heavier walls, such as a ring-lined barrel sampler. Although these thick-wall samplers generate more sample disturbance, their soil samples may still be suitable for laboratory collapse tests (Houston and El-Ehwany, 1991).

Lightly cemented collapsible soils, such as loess, are much more difficult to sample and require more careful sampling techniques. Fortunately, loess is usually much more homogeneous, so fewer samples are needed.

Gravelly soils are more difficult to sample and therefore more difficult to evaluate. Special in situ wetting tests are probably appropriate for these soils (Mahmoud, 1991).

Laboratory Soil Collapse Tests

Once samples have been obtained, they may be tested in the laboratory by conducting *collapse tests*. These are conducted in a conventional oedometer (consolidometer) and directly measure the strain (collapse) that occurs upon wetting (Houston et al., 1988).

ASTM D5333 describes a standard test procedure where the sample is progressively loaded at its in situ moisture content until reaching a specified normal stress. After consolidating at this stress, the sample is then wetted and the additional strain, if any, due to wetting is measured. This strain is the *collapse potential*, I_c. If the sample is wetted at a standard normal stress of 200 kPa (4,000 lb/ft^2), then the strain is the *collapse index*, I_e.

Some engineers prefer to use the ASTM standard normal stress, or some other standard, thus producing results that characterize the collapse potential. Others attempt to more closely simulate the field conditions by wetting the sample at a normal stress equal to the expected after-construction in situ stress (i.e., including the induced stress from the proposed foundations).

The ASTM D5333 procedure can be combined with a standard consolidation test (ASTM D 2435), thus obtaining both collapsibility and consolidation characteristics from a single test, as shown in Figure 28.5. Another option is to conduct a double oedometer test (Jennings and Knight, 1956, 1957, 1975).

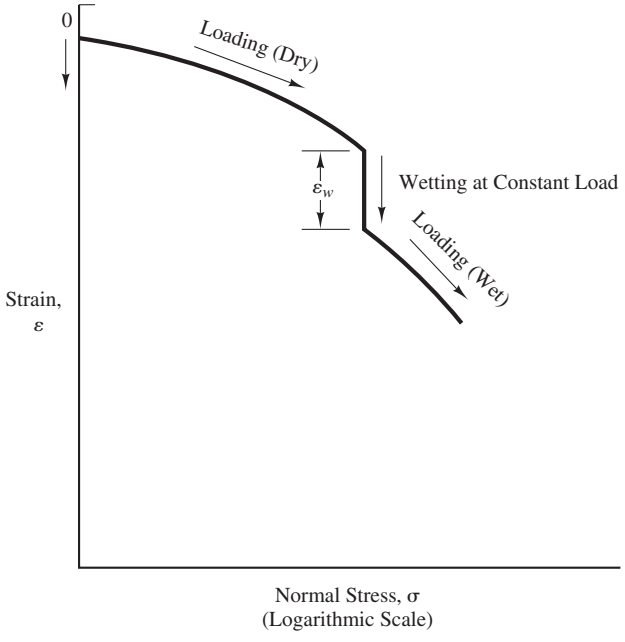

Figure 28.5 Typical results from a collapse test using the single oedometer method (based on Houston et al., 1988; used with permission of ASCE).

28.3 EVALUATION AND REMEDIAITON FOR ROUTINE PROJECTS

For routine projects, the most common practice is to evaluate the collapse test results using a classification system such as that in Table 28.1. If the stratigraphy is such that only the near-surface soils are collapsible, then remediation typically consists of excavating these problematic soils to expose noncollapsible strata, then placing the excavated soils back as a certified compacted fill. This technique is widely used when the required depth of excavation is no more than 2–3 m (6–10 ft) and produces a highly reliable subgrade. In addition, the removal and recompaction process improves the uniformity of the upper soils, further reducing the potential for differential settlement.

When the thickness of collapsible soils exceeds the depth of cost-effective removal and recompaction, or when physical constraints impose practical limits on excavation then engineers may remove only some of the collapsible soil. For example, for small structures, 2–3 m (6–10 ft) of excavation and recompaction may be all that can be economically justified, even if underlain by collapsible strata, so long as this exceeds the anticipated depth of future wetting, and rising groundwater is not a concern. In such cases, extra care should be exercised to provide excellent surface drainage, and over-irrigation should be avoided. Such sites should not use porous pavements, drywells, or other similar methods of intentionally infiltrating storm water.

28.4 ADVANCED TESTING AND ANALYSIS

On more difficult projects, more advanced testing and analysis may be appropriate. The goal is to better quantify the potential settlement due to hydrocollapse, thus forming a more rational basis for remediation and design.

Collapse Testing

More detailed testing can provide more information on the collapse strains that would actually occur in the field. One objective of more detailed testing would be to determine the *collapse potential*, I_c over a wide range of normal stresses by conducting a series of collapse tests.

TABLE 28.1 CLASSIFICATION OF SOIL COLLAPSIBILITY (adapted from ASTM D5333)

Collapse Index, I_e	Collapse Potential
0	None
0.001–0.02	Slight
0.021–0.060	Moderate
0.061–0.10	Moderately severe
>0.10	Severe

Although additional research should be conducted to further understand this relationship, it appears that there is some *threshold collapse stress*, σ_t, below which no collapse will occur, and that I_c becomes progressively larger at stresses above σ_t. This trend probably continues until the stress is large enough to break down the dry honeycomb structure, as shown in Figure 28.6. This latter stress is probably quite high in most collapsible soils, but in some lightly cemented soils, such as loess, it may be within the range of stresses that might be found beneath a foundation. For example, Peck, Hanson and Thornburn (1974) noted a sudden and dramatic collapse of certain dry loessial soils in Iowa when the normal stress was increased to about 280 kPa (5,500 lb/ft^2).

In Situ Soil Collapse Tests

Gravelly soils pose special problems because they are very difficult to sample and test; yet they still may be collapsible. To evaluate these soils, it may be necessary to conduct an in situ collapse test. Some of these tests have consisted of large-scale artificial wetting with associated monitoring of settlements (Curtin, 1973), and others have consisted of small-scale wetting in the bottom of borings (Mahmoud, 1991).

Wetting Processes

To assess potential settlements caused by soil collapse, it is necessary to understand the processes by which the soil becomes wetted. We must identify the potential sources of water and understand how it infiltrates into the ground.

Usually, the water that generates the collapse comes from artificial sources, such as the following:

- Infiltration from irrigation of landscaping or crops
- Leakage from lined or unlined canals

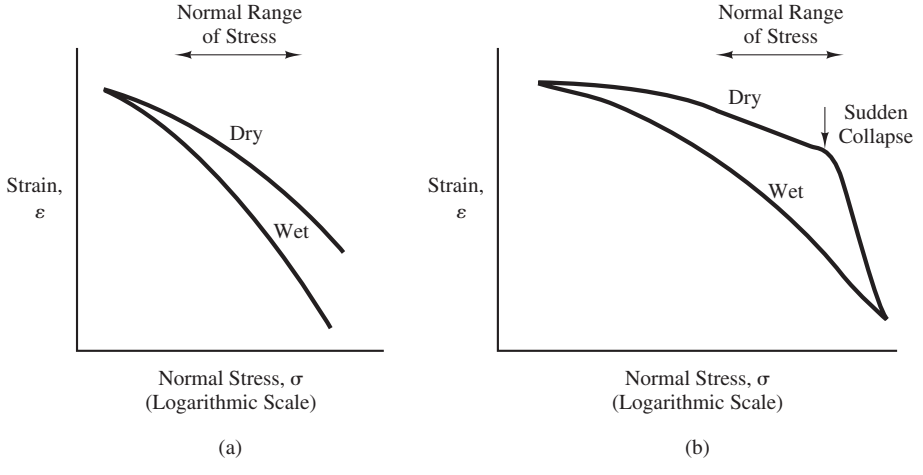

Figure 28.6 Relationship between hydrocollapse strain and normal stress: (a) for most collapsible soils; and (b) for loess.

- Leakage from pipelines and storage tanks
- Leakage from swimming pools
- Leakage from reservoirs
- Seepage from septic tank leach fields
- Infiltration of rainwater as a result of unfavorable changes in surface drainage

Although the flow rate from most of these sources may be slow, the duration is long. Therefore, the water often infiltrates to a great depth and wets soils that would otherwise remain dry.

As water penetrates the soil, a *wetting front* forms, as shown in Figure 28.7. This process is driven primarily by soil suction, so the wetting front will be very distinct. The distance it advances depends on the rate and duration of the water inflow as well as the hydraulic conductivity of the soil, the magnitude of the soil suction, and other factors. These are difficult to quantify, so this may be the greatest source of uncertainty in estimating the settlement due to collapse.

Curtin (1973) gives an interesting illustration of wetting processes in collapsible soils. He conducted large-scale wetting collapse tests in a deposit of collapsible alluvial soil in California's San Joaquin Valley. This soil is collapsible to a depth of at least 75 m (250 ft). After applying water continuously for 484 days, the wetting front advanced to a depth of at least 45 m (150 ft) into this collapsible stratum. The resulting collapse caused a settlement of 4.1 m (13.5 ft) at the ground surface.

In another case, irrigation of lawns and landscaping, and poor surface drainage around a building in New Mexico caused the wetting front to extend more than 30 m (100 ft) into the ground, which resulted in 25 to 50 mm (1–2 in) of settlement (Houston, 1991). In this case, the water inflow was slow and gradual, so the soil did not become completely saturated. If the rate of inflow had been greater, and the soil became wetter, the settlements would have been larger.

The New Mexico case illustrates the importance of defining the degree of saturation that might occur in the field. Laboratory collapse tests wet the soil to nearly 100 percent

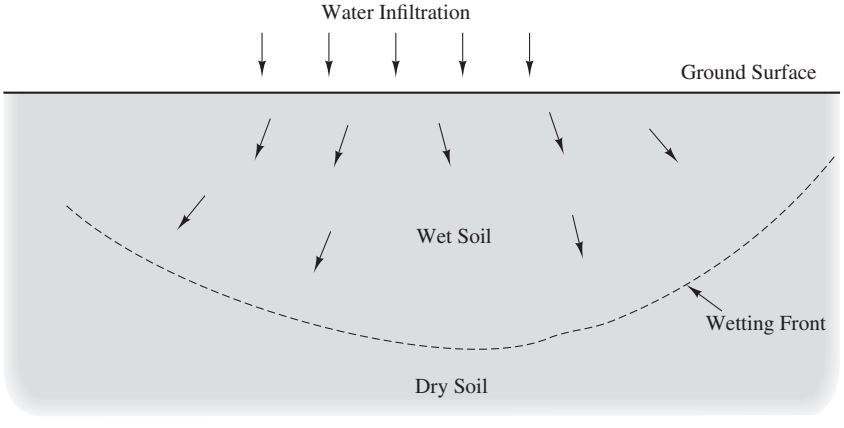

Figure 28.7 As water infiltrates into the soil, a distinct wetting front advances downward.

saturation, which may be a much worse situation than that in the field. This is why we refer to ε_w as the *potential* hydrocollapse strain; the actual strain depends on the degree of wetting.

Tests conducted on collapsible soils in Arizona and New Mexico indicate that these soils typically become only 40 to 60 percent saturated, even after extended periods of wetting (Houston, 1991). It appears that long-term intensive wetting, such as that obtained in Curtin's tests, is necessary to obtain greater degrees of saturation.

The influence of partial wetting may be quantified by conducting a series of collapse tests with different degrees of wetting. Typical results from such tests are shown in Figure 28.8. The *wetting coefficient*, α, is the ratio between the collapse that occurs when the soil is partially wetted to that which would occur if it were completely saturated. Although very few such tests have been conducted, it appears that α values in the field might typically be on the order of 0.5 to 0.8.

Settlement Computations

Once the relationship between collapse potential and total stress, and the wetting processes have been evaluated, the potential hydrocollapse settlement may be estimated using:

$$\delta_w = \int \alpha \varepsilon_c dz \tag{28.1}$$

where

δ_w = settlement due to hydroconsolidation
α = wetting coefficient

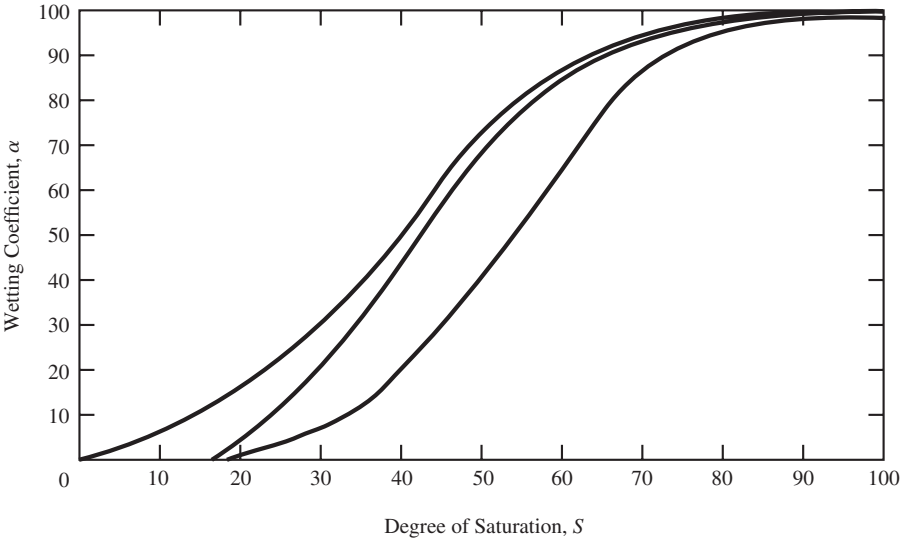

Figure 28.8 Experimental relationships between collapse and degree of saturation during wetting. These functions are for particular soils from Arizona, and must be determined experimentally for other soils (adapted from Houston, 1992).

ε_c = collapse strain potential
z = depth

The collapse strain potential is the strain that would occur if the soil became saturated, and would depend on the collapse index, the overburden stress, the soil porosity, and other factors. This integration would normally be solved by dividing the soil from the base of the footing to the maximum anticipated depth of wetting into layers, and summing the computed hydrocollapse settlement for each layer.

Unsaturated Soil Mechanics

The physical processes that control hydrocollapse are better explained using the principles of unsaturated soil mechanics (Fredlund, Rahardjo, and Fredlund, 2012). This is an effective stress method that accounts for the matric suction in the soil, and thus forms the basis for a more rigorous analysis method. This approach requires defining collapse potential as a function of matric suction and normal stress, measuring the in situ matric suction, and estimating the matric suction that would be produced by future wetting.

28.5 COLLAPSE IN DEEP COMPACTED FILLS

Although most collapsing soil problems are associated with natural soil deposits, engineers have observed a similar phenomenon in deep compacted fills (Lawton et al., 1992). Some deep fills can collapse even when they have been compacted to traditional standards (Lawton et al., 1989, 1991; Brandon et al., 1990). For example, Brandon reported settlements of as much as 450 mm (18 in) occurred in 30 m (100 ft) deep compacted fills near San Diego that became wet sometime after construction.

This suggests that the hydroconsolidation potential is dependent both on the void ratio and the normal stress. Very loose soils will collapse upon wetting even at low normal stresses, but denser soils will be collapsible only at higher stresses. In other words, these soils have a very high σ_t, but the normal stresses near the bottom of deep fills are greater than σ_t. At shallower depths (i.e., $\sigma_z < \sigma_t$), fills with a significant clay content may expand when wetted.

It appears that this phenomenon is most likely to occur in soils that are naturally dry and compacted at moisture contents equal to or less than the optimum moisture content. We can reduce the collapse potential by compacting the fill to a higher dry unit weight at a moisture content greater than the optimum moisture content.

28.6 PREVENTIVE AND REMEDIAL MEASURES

In general, collapsible soils are easier to remediate than are expansive soils because collapse is a one-way process, whereas expansive soils can shrink and swell again and again. Many mitigation measures are available, several of which consist of densifying the soil, thus forming a stable and strong material.

Houston and Houston (1989) identified the following methods of mitigating collapsible soil problems:

1. **Removal of the collapsible soil:** Sometimes, the collapsible soil can simply be excavated and the structure then may be supported directly on the exposed noncollapsible soils. We could accomplish this either by lowering the grade of the building site or by using a basement. This method would be most attractive when the collapsible soil extends only to a shallow depth.
2. **Avoidance or minimization of wetting:** Collapse will not occur if the soil is never wetted. Therefore, when working with collapsible soils, always take extra measures to minimize the infiltration of water into the ground. This should include maintaining excellent surface drainage, directing the outflow from roof drains and other sources of water away from the building, avoiding excessive irrigation of landscaping, and taking extra care to assure the water-tightness of underground pipelines.

   For some structures, such as electrical transmission towers, simple measures such as this will often be sufficient. If collapse-induced settlement did occur, the tower could be releveled without undue expense. However, the probability of success would be much less when dealing with foundations for buildings because there are many more opportunities for wetting and the consequences of settlement are more expensive to repair. Therefore, in most cases, we would probably combine these techniques with other preventive measures.
3. **Transfer of load through the collapsible soils to the stable soils below:** If the collapsible soil deposit is thin, it may be feasible to extend spread footing foundations through this stratum as shown in Figure 28.9. When the deposit is thick, we

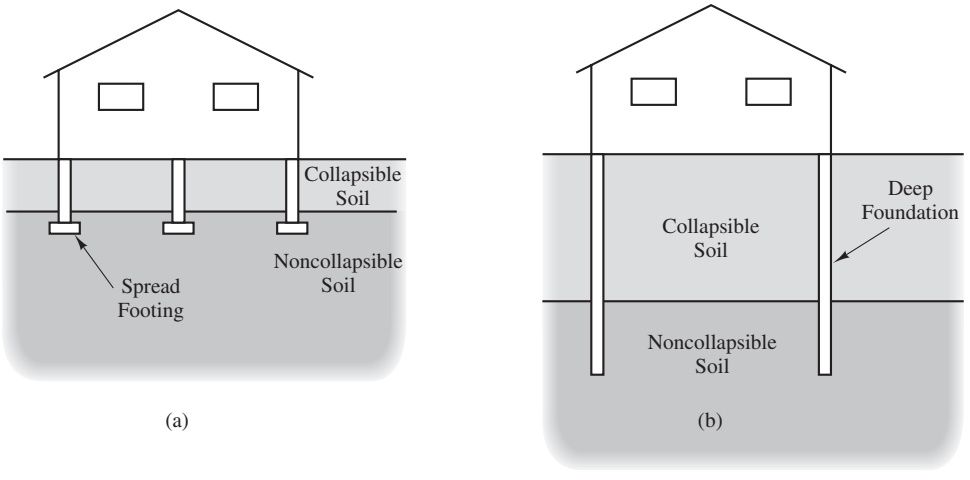

Figure 28.9 Transferring structural loads through collapsible soils to deeper, more stable soils: (a) with deepened spread footings; and (b) with deep foundations.

could use deep foundations for the same purpose. In either case, the ground floor would need to be structurally supported. When using this method, consider the possibility of negative skin friction acting on the upper part of the foundation.

4. **Injection of chemical stabilizers or grout:** Many types of soils, including collapsible soils, can be stabilized by injecting special chemicals or grout. These techniques strengthen the soil structure so future wetting will not cause it to collapse. These methods are generally too expensive to use over large volumes of soil, but they can be very useful to stabilize small areas or as a remedial measure beneath existing structures.

   A variation of this method, known as *compaction grouting*, involves injecting stiff grout that forms hard inclusions in the soil. This is often used to remediate settlement problems.

5. **Prewetting:** If the collapsible soils are identified before construction begins, they can often be remedied by artificially wetting the soils before construction (Knodel, 1981). This can be accomplished by applying or ponding water at the ground surface, or by using trenches or wells. This method is especially effective when attempting to stabilize deep deposits, but may not be completely satisfactory for shallow soils where loads from the proposed foundations may significantly increase the normal stress. If the soil has strong horizontal stratification, as is the case with many alluvial soils, then the injected water may flow horizontally more than it does vertically. Therefore, be cautious when using this method near existing structures that are underlain by collapsible soils. It is important to monitor prewetting operations to confirm that the water penetrates to the required depth and lateral extent. This method can also be combined with a temporary surcharge load. The increased normal stress beneath such loads will intensify the collapse process and produce greater settlements.

6. **Compaction with rollers or vehicles:** Collapsible soils can be converted into excellent bearing material with little or no collapse potential by simply compacting them (Basma and Tuncer, 1992). Sometimes, this compaction may consist simply of passing heavy vibratory sheepsfoot rollers across the ground surface, preferably after first prewetting the soil. More frequently, this procedure includes excavating and stockpiling the soil, and then placing it back in layers using conventional earthmoving techniques. If the collapsible stratum is thin, say, less than 3 m (10 ft), this method can be used to completely eradicate the problem. It is often the preferred method when minimum risk is necessary and the collapsible soil deposit is shallow.

   If the collapsible stratum is thick, then we may choose to estimate the depth of the wetting front and extend the removal and recompaction to that elevation. This method also reduces the likelihood that the lower soils will become wet because the recompacted soil has a reduced hydraulic conductivity (permeability). Also, if the lower soils should collapse, the compacted fill will spread any settlements over a larger area, thus reducing differential settlements. Some collapsible soils have sufficient clay content to become slightly expansive when compacted to a higher unit weight.

7. **Compaction with displacement piles:** Large displacement piles, such as closed-end steel pipe piles, can be driven into the ground, compacting the soil around the pile. It may then be extracted and the hole backfilled with sandy gravel or some other soil. Repeating this process on a grid pattern across the site will reduce the collapse potential both by soil compaction and by the column action of the backfill.
8. **Compaction by heavy tamping:** This technique, which is discussed in more detail in Chapter 26, consists of dropping heavy weights (several tons) from large heights (several meters) to compact the soil. This process is continued on a grid pattern across the site, leaving craters that are later backfilled. This technique can be very effective, especially when combined with prewetting.
9. **Vibroflotation:** This technique, also discussed in more detail in Chapter 26, consists of penetrating the soil with a vibrating probe equipped with water jets (known as a vibroflot). The water softens the soil and the vibrations help the collapse process. The vertical hole formed by the vibroflot is also filled with gravel, thus reinforcing the soil and adding bearing capacity. This process is repeated on a grid pattern across the site.
10. **Deep blasting combined with prewetting:** Engineers in the former Soviet Union have experimented with stabilizing collapsible loess by detonating buried explosives. In some cases, the ground is first thoroughly prewetted and then the collapse is induced by vibrations from the detonations. In other cases, the explosives are detonated while the soil is still dry, and the voids created are filled first with water and then with sand and gravel.
11. **Controlled wetting:** This method is similar to method 5 in that it involves injecting water into the soil through trenches or wells. However, it differs in that the wetting is much more controlled and often concentrated in certain areas. This would be used most often as a remedial measure to correct differential settlements that have accidently occurred as a result of localized wetting. When used with careful monitoring, this method can be an inexpensive yet effective way of stabilizing soils below existing buildings that have already settled.
12. **Design structure to be tolerant of differential settlements:** As discussed in Chapter 5, some types of structures are much more tolerant of differential settlements than are others. Therefore, if the potential for collapse-induced settlement is not too large, we may be able to use a more tolerant structure. For example, a steel storage tank would be more tolerant than a concrete one.

The selection of the best method or methods to use at a given site depends on many factors, including the following:

- How deep do the collapsible soils extend?
- How deep would the wetting front extend if the soil was accidentally wetted?
- How much settlement is likely to occur if the soil is accidentally wetted?
- What portion of the total stress is due to overburden and what portion is due to applied loads?

- Is the building or other structure already in place?
- Has any artificial wetting already occurred?

SUMMARY

Major Points

1. Collapsible soils have a loose honeycomb structure and are dry in their natural state. If they are later wetted, this structure will collapse and settlements will occur.
2. Collapsible soils are usually encountered only in arid or semi-arid climates and are continually dry in their natural state. The water that causes them to collapse is normally introduced artificially (as compared to natural infiltration of rainfall). However, collapsible loess is also found in more humid climates.
3. Collapsible soils can be formed by various geologic processes. They may be alluvial soils (especially debris flow deposits), aeolian soils (especially loess), or residual soils.
4. Collapsible soils usually can be effectively sampled, as long as they are moderately to well cemented and do not contain too much gravel. Lightly cemented soils can be sampled with more difficulty, whereas gravelly soils are very difficult or impossible to sample.
5. Laboratory collapse tests may be conducted to measure the collapse potential as a function of overburden stress.
6. In the field, collapsible soils are normally not wetted to 100 percent saturation and therefore do not strain as much as those tested in the laboratory. Typically, the strain in the field is 50 to 80 percent of that observed in a thoroughly wetted laboratory test specimen.
7. The settlement also depends on the depth of wetting, but this is difficult to evaluate in advance.
8. We can estimate the amount of settlement by projecting the laboratory collapse tests back to the field conditions while making appropriate corrections for overburden stress and degree of saturation.
9. Many remedial and preventive measures are available to prevent or repair structural damage caused by collapsible soils.

Vocabulary

Aeolian soil
Alluvial soil
Collapse index
Collapse test
Collapsible soil
Colluvial soil
Honeycomb structure
Hydrocollapse
Hydrocompression
Hydroconsolidation
Loess
Residual soil
Wetting coefficient

QUESTIONS AND PRACTICE PROBLEMS

28.1 What is a "honeycomb" structure?

28.2 Why are collapsible soils rarely found in areas with very wet climates?

28.3 Why is it difficult to obtain samples of gravelly soils and use them in laboratory collapse tests?

28.4 Would the actual collapse strain in the field be equal to that measured in the lab using a test such as ASTM D5333? Explain.

28.5 The soil beneath a proposed spread footing has a collapse strain potential of 5 percent from the ground surface to a depth of 10 ft. The underlying soils are noncollapsible. The proposed footing will be embedded at a depth of 2 ft. Assuming the wetting coefficient varies from 1.0 at the ground surface to 0.1 at a depth of 10 ft, compute the expected hydrocollapse settlement of this footing.

28.6 What preventive measures would you use to avoid settlement problems in the footing described in Problem 28.5?

28.7 Is it possible for some soils to be expansive when the normal stress is low, and collapsible when it is high? Explain.

Appendix A

Units and Conversion Factors

UNITS OF MEASUREMENT

Nearly all foundation engineering conducted in the United States use customary English units. The units shown in Table A1 are commonly used. However, outside the United States, nearly all foundation engineering uses some form of metric units. The standardized metric units, known as SI (Système International), for use in foundation engineering are shown in Tables A2 and A3. Some non-SI metric units also are widely used. The most common example is the use of kg/cm^2 as a unit of stress.

TABLE A1 COMMON ENGLISH UNITS

Unit	Measurement	Symbol
foot	distance	ft
inch	distance	in
pound	force or mass	lb
kip (kilopound)	force	k
ton	force or mass	t
second	time	s
pound per square foot	stress or pressure	lb/ft^2 or psf
pound per square inch	stress or pressure	lb/in^2 or psi
pound per cubic foot	unit weight	lb/ft^3 or pcf

TABLE A2 COMMON SI UNITS

Unit	Measurement	Symbol
meter	distance	m
gram	mass	g
Newton	force	N
Pascal	stress or pressure	Pa
kilonewton per cubic meter	unit weight	kN/m^3
second	time	s

TABLE A3 COMMON SI PREFIXES

Prefix	Symbol	Multiplier
milli	m	10^{-3}
centi	c	10^{-2}
kilo	k	10^{3}
mega	M	10^{6}

CONVERSION FACTORS

The conversion factors in Tables A4 through A8 are useful for converting measurements between English, metric, and SI units. Most of these factors are rounded to four significant figures. Those in **bold type** are absolute conversion factors (e.g., 12 in = 1 ft). When units of force are equated to units of mass, the acceleration ($F = ma$) is presumed to be 9.807 m/s^2 (32.17 ft/s^2), which is the acceleration due to gravity on the earth's surface.

TABLE A4 UNITS OF DISTANCE

To Convert	To	Multiply By
ft	in	**12**
ft	m	0.3048
in	ft	**1/12**
in	mm	25.40
m	ft	3.281
mm	in	0.03937

TABLE A5 UNITS OF FORCE

To Convert	To	Multiply By
k	kN	4.448
k	lb	**1,000**
kg_f	lb	2.205
kg_f	N	9.807
kg_f	ton (metric)	**0.001**
kN	k	0.2248
lb	k	**0.001**
lb	kg_f	0.4536
lb	N	4.448
lb	ton (short)	**1/2,000**
lb	ton (long)	**1/2,240**
N	kg_f	0.1020
N	lb	0.2248
ton (short)	lb	**2,000**
ton (long)	lb	**2,240**
ton (metric)	kg_f	**1,000**

TABLE A6 UNITS OF VOLUME

To Convert	To	Multiply By
ft^3	gal	7.481
gal	ft^3	0.1337

TABLE A7 UNITS OF STRESS AND PRESSURE

To Convert	To	Multiply By
atmosphere	lb/ft^2	2,117
atmosphere	kPa	101.3
bar	kPa	**100**
kg_f/cm^2	kPa	98.07
kg_f/cm^2	lb/ft^2	2,048

(*continued*)

TABLE A7 (Continued)

To Convert	To	Multiply By
kPa	atmosphere	0.009869
kPa	bar	**0.01**
kPa	kg_f/cm^2	0.01020
kPa	lb/ft^2	20.89
kPa	lb/in^2	0.1450
kPa	metric ton/m^2	0.1020
lb/ft^2	atmosphere	4.725×10^{-4}
lb/ft^2	kPa	0.04787
lb/ft^2	lb/in^2	**1/144**
lb/in^2	kPa	6.895
lb/in^2	lb/ft^2	**144**
lb/in^2	MPa	6.895×10^{-3}
metric ton/m^2	kPa	9.807
MPa	lb/in^2	145.0

TABLE A8 UNITS OF UNIT WEIGHT

To Convert	To	Multiply By
kN/m^3	lb/ft^3	6.366
kN/m^3	metric ton/m^3	0.1020
kN/m^3	Mg_f/m^3	0.1020
lb/ft^3	kN/m^3	0.1571
metric ton/m^3	kN/m^3	9.807
Mg_f/m^3	kN/m^3	9.807

There are at least three definitions for the word "ton": the 2,000 lb short ton (commonly used in the United States and Canada), the 2,240 lb long ton (used in Great Britain), and the 1,000 kg (2,205 lb) metric ton (also known as a tonne).

A useful approximate conversion factor: 1 short $ton/ft^2 \approx 1$ $kg/cm^2 \approx 100$ kPa $\approx$ 1 atmosphere. These are true to within 2 to 4%.

Appendix B

Probability Tables

TABLE B1 CUMULATIVE STANDARD NORMAL DISTRIBUTION PROBABILITY,

$$\Phi(x) = \frac{1}{\sqrt{2\pi}} \int_{-\infty}^{x} e^{-y^2/2} dy$$

x	$\Phi(x)$	x	$\Phi(x)$	x	$\Phi(x)$	x	$\Phi(x)$
0.00	0.500000000	0.14	0.555670005	0.28	0.610261248	0.42	0.662757273
0.01	0.503989356	0.15	0.559617692	0.29	0.614091881	0.43	0.666402179
0.02	0.507978314	0.16	0.563559463	0.30	0.617911422	0.44	0.670031446
0.03	0.511966473	0.17	0.567494932	0.31	0.621719522	0.45	0.673644780
0.04	0.515953437	0.18	0.571423716	0.32	0.625515835	0.46	0.677241890
0.05	0.519938806	0.19	0.575345435	0.33	0.629300019	0.47	0.680822491
0.06	0.523922183	0.20	0.579259709	0.34	0.633071736	0.48	0.684386303
0.07	0.527903170	0.21	0.583166163	0.35	0.636830651	0.49	0.687933051
0.08	0.531881372	0.22	0.587064423	0.36	0.640576433	0.50	0.691462461
0.09	0.535856393	0.23	0.590954115	0.37	0.644308755	0.51	0.694974269
0.10	0.539827837	0.24	0.594834872	0.38	0.648027292	0.52	0.698468212
0.11	0.543795313	0.25	0.598706326	0.39	0.651731727	0.53	0.701944035
0.12	0.547758426	0.26	0.602568113	0.40	0.655421742	0.54	0.705401484
0.13	0.551716787	0.27	0.606419873	0.41	0.659097026	0.55	0.708840313

(*continued*)

TABLE B1 (Continued)

x	$\Phi(x)$	x	$\Phi(x)$	x	$\Phi(x)$	x	$\Phi(x)$
0.56	0.712260281	0.88	0.810570345	1.20	0.884930330	1.52	0.935744512
0.57	0.715661151	0.89	0.813267057	1.21	0.886860554	1.53	0.936991636
0.58	0.719042691	0.90	0.815939875	1.22	0.888767563	1.54	0.938219823
0.59	0.722404675	0.91	0.818588745	1.23	0.890651448	1.55	0.939429242
0.60	0.725746882	0.92	0.821213620	1.24	0.892512303	1.56	0.940620059
0.61	0.729069096	0.93	0.823814458	1.25	0.894350226	1.57	0.941792444
0.62	0.732371107	0.94	0.826391220	1.26	0.896165319	1.58	0.942946567
0.63	0.735652708	0.95	0.828943874	1.27	0.897957685	1.59	0.944082597
0.64	0.738913700	0.96	0.831472393	1.28	0.899727432	1.60	0.945200708
0.65	0.742153889	0.97	0.833976754	1.29	0.901474671	1.61	0.946301072
0.66	0.745373085	0.98	0.836456941	1.30	0.903199515	1.62	0.947383862
0.67	0.748571105	0.99	0.838912940	1.31	0.904902082	1.63	0.948449252
0.68	0.751747770	1.00	0.841344746	1.32	0.906582491	1.64	0.949497417
0.69	0.754902906	1.01	0.843752355	1.33	0.908240864	1.65	0.950528532
0.70	0.758036348	1.02	0.846135770	1.34	0.909877328	1.66	0.951542774
0.71	0.761147932	1.03	0.848494997	1.35	0.911492009	1.67	0.952540318
0.72	0.764237502	1.04	0.850830050	1.36	0.913085038	1.68	0.953521342
0.73	0.767304908	1.05	0.853140944	1.37	0.914656549	1.69	0.954486023
0.74	0.770350003	1.06	0.855427700	1.38	0.916206678	1.70	0.955434537
0.75	0.773372648	1.07	0.857690346	1.39	0.917735561	1.71	0.956367063
0.76	0.776372708	1.08	0.859928910	1.40	0.919243341	1.72	0.957283779
0.77	0.779350054	1.09	0.862143428	1.41	0.920730159	1.73	0.958184862
0.78	0.782304562	1.10	0.864333939	1.42	0.922196159	1.74	0.959070491
0.79	0.785236116	1.11	0.866500487	1.43	0.923641490	1.75	0.959940843
0.80	0.788144601	1.12	0.868643119	1.44	0.925066300	1.76	0.960796097
0.81	0.791029912	1.13	0.870761888	1.45	0.926470740	1.77	0.961636430
0.82	0.793891946	1.14	0.872856849	1.46	0.927854963	1.78	0.962462020
0.83	0.796730608	1.15	0.874928064	1.47	0.929219123	1.79	0.963273044
0.84	0.799545807	1.16	0.876975597	1.48	0.930563377	1.80	0.964069681
0.85	0.802337457	1.17	0.878999516	1.49	0.931887882	1.81	0.964852106
0.86	0.805105479	1.18	0.880999893	1.50	0.933192799	1.82	0.965620498
0.87	0.807849798	1.19	0.882976804	1.51	0.934478288	1.83	0.966375031

x	$\Phi(x)$	x	$\Phi(x)$	x	$\Phi(x)$	x	$\Phi(x)$
1.84	0.967115881	2.16	0.984613665	2.48	0.993430881	2.80	0.997444870
1.85	0.967843225	2.17	0.984996577	2.49	0.993612845	2.81	0.997522925
1.86	0.968557237	2.18	0.985371269	2.50	0.993790335	2.82	0.997598818
1.87	0.969258091	2.19	0.985737882	2.51	0.993963442	2.83	0.997672600
1.88	0.969945961	2.20	0.986096552	2.52	0.994132258	2.84	0.997744323
1.89	0.970621020	2.21	0.986447419	2.53	0.994296874	2.85	0.997814039
1.90	0.971283440	2.22	0.986790616	2.54	0.994457377	2.86	0.997881795
1.91	0.971933393	2.23	0.987126279	2.55	0.994613854	2.87	0.997947641
1.92	0.972571050	2.24	0.987454539	2.56	0.994766392	2.88	0.998011624
1.93	0.973196581	2.25	0.987775527	2.57	0.994915074	2.89	0.998073791
1.94	0.973810155	2.26	0.988089375	2.58	0.995059984	2.90	0.998134187
1.95	0.974411940	2.27	0.988396208	2.59	0.995201203	2.91	0.998192856
1.96	0.975002105	2.28	0.988696156	2.60	0.995338812	2.92	0.998249843
1.97	0.975580815	2.29	0.988989342	2.61	0.995472889	2.93	0.998305190
1.98	0.976148236	2.30	0.989275890	2.62	0.995603512	2.94	0.998358939
1.99	0.976704532	2.31	0.989555923	2.63	0.995730757	2.95	0.998411130
2.00	0.977249868	2.32	0.989829561	2.64	0.995854699	2.96	0.998461805
2.01	0.977784406	2.33	0.990096924	2.65	0.995975411	2.97	0.998511001
2.02	0.978308306	2.34	0.990358130	2.66	0.996092967	2.98	0.998558758
2.03	0.978821730	2.35	0.990613294	2.67	0.996207438	2.99	0.998605113
2.04	0.979324837	2.36	0.990862532	2.68	0.996318892	3.00	0.998650102
2.05	0.979817785	2.37	0.991105957	2.69	0.996427399	3.01	0.998693762
2.06	0.980300730	2.38	0.991343681	2.70	0.996533026	3.02	0.998736127
2.07	0.980773828	2.39	0.991575814	2.71	0.996635840	3.03	0.998777231
2.08	0.981237234	2.40	0.991802464	2.72	0.996735904	3.04	0.998817109
2.09	0.981691100	2.41	0.992023740	2.73	0.996833284	3.05	0.998855793
2.10	0.982135579	2.42	0.992239746	2.74	0.996928041	3.06	0.998893315
2.11	0.982570822	2.43	0.992450589	2.75	0.997020237	3.07	0.998929706
2.12	0.982996977	2.44	0.992656369	2.76	0.997109932	3.08	0.998964997
2.13	0.983414193	2.45	0.992857189	2.77	0.997197185	3.09	0.998999218
2.14	0.983822617	2.46	0.993053149	2.78	0.997282055	3.10	0.999032397
2.15	0.984222393	2.47	0.993244347	2.79	0.997364598	3.11	0.999064563

(*continued*)

TABLE B1 (Continued)

x	$\Phi(x)$	x	$\Phi(x)$	x	$\Phi(x)$	x	$\Phi(x)$
3.12	0.999095745	3.44	0.999709143	3.76	0.999915043	4.8	7.93E-07
3.13	0.999125968	3.45	0.999719707	3.77	0.999918376	4.9	4.79E-07
3.14	0.999155261	3.46	0.999729912	3.78	0.999921586	5.0	2.87E-07
3.15	0.999183648	3.47	0.999739771	3.79	0.999924676	5.1	1.70E-07
3.16	0.999211154	3.48	0.999749293	3.80	0.999927652	5.2	9.96E-08
3.17	0.999237805	3.49	0.999758490	3.81	0.999930517	5.3	5.79E-08
3.18	0.999263625	3.50	0.999767371	3.82	0.999933274	5.4	3.33E-08
3.19	0.999288636	3.51	0.999775947	3.83	0.999935928	5.5	1.90E-08
3.20	0.999312862	3.52	0.999784227	3.84	0.999938483	5.6	1.07E-08
3.21	0.999336325	3.53	0.999792220	3.85	0.999940941	5.7	5.99E-09
3.22	0.999359047	3.54	0.999799936	3.86	0.999943306	5.8	3.32E-09
3.23	0.999381049	3.55	0.999807384	3.87	0.999945582	5.9	1.82E-09
3.24	0.999402352	3.56	0.999814573	3.88	0.999947772	6.0	9.87E-10
3.25	0.999422975	3.57	0.999821509	3.89	0.999949878	6.1	5.30E-10
3.26	0.999442939	3.58	0.999828203	3.90	0.999951904	6.2	2.82E-10
3.27	0.999462263	3.59	0.999834661	3.91	0.999953852	6.3	1.49E-10
3.28	0.999480965	3.60	0.999840891	3.92	0.999955726	6.4	7.77E-11
3.29	0.999499063	3.61	0.999846901	3.93	0.999957527	6.5	4.02E-11
3.30	0.999516576	3.62	0.999852698	3.94	0.999959259	6.6	2.06E-11
3.31	0.999533520	3.63	0.999858289	3.95	0.999960924	6.7	1.04E-11
3.32	0.999549913	3.64	0.999863681	3.96	0.999962525	6.8	5.23E-12
3.33	0.999565770	3.65	0.999868880	3.97	0.999964064	6.9	2.60E-12
3.34	0.999581108	3.66	0.999873892	3.98	0.999965542	7.0	1.28E-12
3.35	0.999595942	3.67	0.999878725	3.99	0.999966963	7.1	6.24E-13
3.36	0.999610288	3.68	0.999883383	4.0	3.17E-05	7.2	3.01E-13
3.37	0.999624159	3.69	0.999887873	4.1	2.07E-05	7.3	1.44E-13
3.38	0.999637571	3.70	0.999892200	4.2	1.33E-05	7.4	6.81E-14
3.39	0.999650537	3.71	0.999896370	4.3	8.54E-06	7.5	3.19E-14
3.40	0.999663071	3.72	0.999900389	4.4	5.41E-06	7.6	1.48E-14
3.41	0.999675186	3.73	0.999904260	4.5	3.40E-06	7.7	6.77E-15
3.42	0.999686894	3.74	0.999907990	4.6	2.11E-06	7.8	3.11E-15
3.43	0.999698209	3.75	0.999911583	4.7	1.30E-06	7.9	1.44E-15

References

Abbreviations for societies and organizations:

ACI	American Concrete Institute
ADSC	Association of Drilled Shaft Contractors
AISC	American Institute of Steel Construction
API	American Petroleum Institute
ASCE	American Society of Civil Engineers
ASTM	American Society for Testing and Materials
FHWA	Federal Highway Administration
CGS	Canadian Geotechnical Society
PCA	Portland Cement Association
PCI	Precast/Prestressed Concrete Institute
PTI	Post-Tensioning Institute

AASHTO (2012), *AASHTO LRFD Bridge Design Specifications*, 6th ed., American Association of State Highway and Transportation Officials, Washington, D.C.

Abu El-Ela, A.A., Bowders, J.J. and Loehr, J.E. (2013), "Reliability Based Design of Shallow Foundations on Jointed Rock Masses Using RQD and the Uniaxial Compressive Strength of Intact Rock," *Proceedings, 47th US Rock Mechanics / Geomechanics Symposium*. v4, pp. 2625–2637.

Abu-Hejleh, N., O'Neill, M.W., Hanneman, D. and Atwoll, W.J. (2003), "Improvement of the Geotechnical Axial Design Methodology for Colorado's Drilled Shafts Socketed in Weak Rock," Report No. CDOT-DTD-R-2003-6, Colorado Department of Transportation, Denver, 192 p.

ACI (1974), "Recommendations for Design, Manufacture, and Installation of Concrete Piles," ACI 543R-74 (Reapproved 1980), *ACI Journal Proceedings*, Vol. 71, No. 10, pp. 477–492; also printed in ACI Manual of Concrete Practice, American Concrete Institute

ACI (1980), *Recommendations for Design, Manufacture and Installation of Concrete Piles*, ACI 543R-74, American Concrete Institute, Detroit

ACI (1993), *Suggested Analysis and Design Procedures for Combined Footings and Mats*, ACI 336.2R-88 (Reapproved 1993), American Concrete Institute

ACI (2011), *Building Code Requirements for Structural Concrete (ACI 318-11)*, American Concrete Institute

ACI (2012), *Guide to Design, Manufacture, and Installation of Concrete Piles*, Publication 543R-12, American Concrete Institute

ACI-ASCE (1962), "Report of Committee on Shear and Diagonal Tension," *Proceedings, American Concrete Institute*, Vol. 59, No. 1

Airhart, T.P., Coyle, H.M., Hirsh, T.J. and Buchanan, S.J. (1969), "Pile-Soil System Response in a Cohesive Soil," *Performance of Deep Foundations*, STP 444, pp. 264–294, ASTM, Philadelphia

AISC (2011), *Steel Construction Manual*, 14th ed., American Institute of Steel Construction

Allen, T. M. (2005), "Development of Geotechnical Resistance Factors and Downdrag Load Factors for LRFD Foundation Strength Limit State Design," Publication No. FHWA-NHI-05-052, Federal Highway Administration, Washington, D.C., 41 p.

Anagnostopoulos, A.G. (1990), "Die Zusammendrückbarkeit nichtbindinger Böden (The Compressibility of Cohesionless Soils)," *Geotechnik*, Vol. 13, pp. 181–187 (in German)

Anderson, J.B., Townsend, F.C. and Grajales, J. (2003), "Case History Evaluation of Laterally Loaded Piles," *ASCE Journal of Geotechnical and Geoenvironmental Engineering*, Vol. 129, No. 3, pp. 187–196

Anderson, J.N. and Lade, P.V. (1981), "The Expansion Index Test," *ASTM Geotechnical Testing Journal*, Vol. 4, No. 2, June 1981, pp. 58–67

Ang, A. H.-S. and Tang, W. H. (2007), *Probability Concepts in Engineering: Emphasis on Applications in Civil and Environmental Engineering*, Wiley, New York

API (2000), *Planning, Designing and Constructing Fixed Offshore Platforms—Working Stress Design*, 21st ed., American Petroleum Institute Publication RP 2A-WSD (with errata, addenda, and supplements dated 2002, 2005, and 2007)

API (2011), *Geotechnical and Foundation Design Considerations*, ANSI/API Recommended Practice 2GEO, American Petroleum Institute

Armour, T., Grosneck, P., Keeley, J. and Sharma, S. (2000), *Micropile Design and Construction Guidelines Implementation Manual*, Report No. FHWA-SA-97-070, Federal Highway Administration

Armstrong, R.M. (1978), "Structural Properties of Timber Piles," *Behavior of Deep Foundations*, ASTM STP 670, Raymond Lundgren, Ed., pp. 118–152, ASTM, Philadelphia

Arneson, L.A., Zevenbergen, L.W., Lagasse, P.F. and Clopper, P.E. (2012), *Evaluating Scour at Bridges*, 5th ed., Publication No. FHWA-HIF-12-003, Hydraulic Engineering Circular No. 18, Federal Highway Administration

ASCE (1972), "Subsurface Investigation for Design and Construction of Foundations of Buildings," *ASCE Journal of the Soil Mechanics and Foundations Division*, Vol. 98, No. SM5, SM6, SM7 and SM8

ASCE (1984), *Practical Guidelines for the Selection, Design and Installation of Piles*, ASCE

ASCE (1996b), *Design of Sheet Pile Walls*, American Society of Civil Engineers

ASCE (2010), *Minimum Design Loads for Buildings and Other Structures*, ASCE 7-10, ASCE

Ashford, S., Boulanger, R. and Brandenberg, S. (2011), *Recommended Design Practice for Pile Foundations in Laterally Spreading Ground*, Report 2011/04, Pacific Earthquake Engineering Research Center

AWPI (2002), *Timber Pile Design and Construction Manual*, American Wood Preservers Institute

Baecher, G. B. (1982), "Statistical Methods in Site Characterization," *Updating Subsurface Samplings of Soils and Rocks and Their In-Situ Testing*, Engineering Foundation, Santa Barbara, California, pp. 463–492

Baecher, G. B. and Christian, J. T. (2003), *Reliability and Statistics in Geotechnical Engineering*, John Wiley & Sons

Baguelin, F., Jézéquel, J.F. and Shields, D.H. (1978), *The Pressuremeter and Foundation Engineering*, Trans Tech, Clausthal, Germany

Baker, Clyde N., Azam, Ir. Tarique; and Joseph, Len S. (1994), "Settlement Analysis for 450 Meter Tall KLCC Towers," *Vertical and Horizontal Deformations of Foundations and Embankments*, A.T. Yeung and G.Y. Felio, Eds., Vol. 2, pp. 1650–1671, ASCE

Baldi, G., Bellotti, R., Ghionna, V., Jamiolkowski, M. and Pasqualini, E. (1986), "Interpretations of CPT's and CPTU's, 2nd part: Drained penetration of sands," *4th International Conference on Field Instrumentation and In-Situ Measurements*, Singapore, pp. 143–156

Barden, L., McGown, A. and Collins, K. (1973), "The Collapse Mechanism in Partly Saturated Soil," *Engineering Geology*, Vol. 7, pp. 49–60

Barker, M. (2001), "Australian Risk Approach for Assessment of Dams," *21st Century Dam Design—Advances and Adaptations*, U.S. Society on Dams, San Diego, CA, United states, pp. 69–91

Barker, R.M., Duncan, J.M., Rojiani, K.B., Ooi, P.S.K., Tan, C.K. and Kim, S.G. (1991), *Manuals for the Design of Bridge Foundations*, National Cooperative Highway Research Program Report 343, Transportation Research Board, Washington, D.C.

Barksdale, R. D. and Bachus, R. C. (1986), *Design and Construction of Stone Columns*, Vol. 1: FHWA-RD-83-026, Vol. 2: FHWA-RD-83-027, FHWA, Washington, D.C.

Bartlett, S.F. and Youd, T.L. (1992) *Empirical Analysis of Horizontal Ground Displacement Generated by Liquefaction–Induced Lateral Spreads*, Technical Report No. NCEER–92–0021, National Center for Earthquake Engineering Research, Buffalo, New York

Barton, N.R., Lien, R. and Lunde, J. (1974), "Engineering classification of rock masses for the design of tunnel support," *Rock Mech*. Vol. 6, pp.189–239

Basma, Adnan A. and Tuncer, Erdil R. (1992), "Evaluation and Control of Collapsible Soils," *ASCE Journal of Geotechnical Engineering*, Vol. 118, No. 10, pp. 1491–1504

Basu, P. and Prezzi, M. (2009) *Design and Applications of Drilled Displacement (Screw) Piles*, Publication FHWA/IN/JTRP-2009/28, Indiana Department of Transportation

Baumann, F. (1873), *The Art of Preparing Foundations, with Particular Illustration of the "Method of Isolated Piers" as Followed in Chicago*, Reprinted in Powell (1884)

Becker, D. E., Burwash, W.J., Montgomery, R.A. and Liu, Y. (1998), "Foundation Design Aspects of the Confederation Bridge," *Canadian Geotechnical Journal*, 35(5), pp. 750–768

Beiki, M., Bashari, A. and Majdi, A. (2010), "Genetic Programming Approach for Estimating the Deformation Modulus of Rock Mass Using Sensitivity Analysis by Neural Network," *Int. J. Rock Mech. Min. Sci*. Vol. 47, pp.1091–1103

Bell, A.L. (1915), "The Lateral Pressure and Resistance of Clay, and the Supporting Power of Clay Foundations," pp. 93–134 in *A Century of Soil Mechanics*, ICE, London

Bell, A.L. (1993), "Jet Grouting," Chapter 7 in *Ground Improvement*, M.P. Moseley, Ed., Chapman and Hall, London

Benjamin, J. R. and Cornell, C. A. (1970), *Probability, Statistics, and Decision for Civil Engineers*, McGraw Hill, New York

Bethlehem Steel Corp. (1979), *Bethlehem Steel H-Piles*, Bethlehem Steel Corp., Bethlehem, PA

Bhushan, K. (1982), Discussion of "New Design Correlations for Piles in Sand," *Journal of the Geotechnical Engineering Division*, Vol. 108, No. GT11, pp. 1508–1501, ASCE

Bieniawski, Z.T. (1978), "Determining Rock Mass Deformability—Experience From Case Histories," *Int. J. Rock Mech. Min. Sci. Geomech. Abstr*. Vol. 15, pp. 237–247

Bieniawski, Z.T. (1989), *Engineering Rock Mass Classifications*, Wiley, New York

Bishop, Alan W. and Bjerrum, L. (1960), "The Relevance of the Triaxial Test to the Solution of Stability Problems," *Research Conference on Shear Strength of Cohesive Soils*, ASCE

Bjerrum, L., Johannessen, I.J. and Eide, O. (1969), "Reduction of Negative Skin Friction on Steel Piles to Rock," *Proceedings of the Seventh International Conference on Soil Mechanics and Foundation Engineering*, Mexico City, Vol. 2, pp. 27–34

Bjerrum, L. (1963), "Allowable Settlement of Structures," *Proceedings of the Third European Conference on Soil Mechanics and Foundation Engineering*, Vol. 2, pp. 135–137, Weisbaden

Blaser, Harold D. and Scherer, Oscar J. (1969), "Expansion of Soils Containing Sodium Sulfate Caused by Drop in Ambient Temperatures," *Effects of Temperature and Heat on Engineering Behavior of Soils*, Special Report 103, Highway Research Board, Washington, D.C.

BOCA (1996), *National Building Code*, Building Officials & Code Administrators International, Inc., Country Club Hills, IL

Bolenski, M. (1973), "Osiadania nowo wznoszonych budowli w zaleznosci of podloza gruntowego: Wyniki 20-letnich Badan w Instytucie Techniki Budowlanej" (Settlement of Constructions Newly Erected and Type of Subsoil: The Results of 20 Years Studies Carried Out in the Building Research Institute), Prace Instytutu Techniki Budowlanej, Warszawa (in Polish; partial results quoted in Burland and Burbidge, 1985)

Bolin, H.W. (1941), "The Pile Efficiency Formula of the Uniform Building Code," *Building Standards Monthly*, Vol. 10, No. 1, pp. 4–5

Boniface, R. (2012) "Giant Steel Piles Driven," *CE Magazine*, (online) January, http://www.asce.org/CEMagazine/Article.aspx?id=25769805447#.UiaiOz-XMTA (9/3/2013)

Boussinesq, M.J. (1885), *Application Des Potentiels, à l'Étude de l'Équilibre et du Movvement Des Solides Elastiques*, Gauthier-Villars, Paris (in French)

Bozozuk, M. (1972a), "Downdrag Measurement on a 160-ft Floating Pipe Test Pile in Marine Clay," *Canadian Geotechnical Journal*, Vol. 9, No. 2, pp. 127–136

Bozozuk, M. (1972b), "Foundation Failure of the VanKleek Hill Tower Silo," *Performance of Earth and Earth-Supported Structures*, pp. 885–902, ASCE

Bozozuk, M. (1978), "Bridge Foundations Move," *Transportation Research Record 678*, pp. 17–21, Transportation Research Board, Washington, D.C.

Bozozuk, M. (1981), "Bearing Capacity of Pile Preloaded by Downdrag," *Proceedings of the Tenth International Conference on Soil Mechanics and Foundation Engineering*, Stockholm, Vol. 2, pp. 631–636

Bozozuk, M., Fellenius, B. H. and Samson, L. (1978), "Soil Disturbance from Pile Driving in Sensitive Clay," *Canadian Geotechnical Journal*, Vol 15, No. 3, pp. 346–361

Brandon, Thomas L., Duncan, J. Michael and Gardner, William S. (1990), "Hydrocompression Settlement of Deep Fills," *ASCE Journal of Geotechnical Engineering*, Vol. 116, No. 10, pp. 1536–1548

Briaud, J.L., Tucker, L., Lytton, R.L. and Coyle, H.M. (1985), *Behavior of Piles and Pile Groups in Cohesionless Soils*, Report No. FHWA/RD-83/038, Federal Highway Administration, Washington, D.C.

Briaud, Jean-Louis (1991), "Dynamic and Static Testing of Nine Drilled Shafts at Texas A&M University Geotechnical Research Sites," *Foundation Drilling*, Vol. 30, No. 7, pp. 12–14

Briaud, Jean-Louis (1992), *The Pressuremeter*, A.A. Balkema, Rotterdam

Briaud, Jean-Louis and Gibbens, Robert M. (1994), *Predicted and Measured Behavior of Five Spread Footings on Sand*, Geotechnical Special Publication 41, ASCE

Briaud, Jean-Louis and Miran, Jerome (1991), *The Cone Penetration Test*, Report No. FHWA-TA-91-004, Federal Highway Administration, McLean, VA

Brinch Hansen, J (1963), Discussion of "Hyperbolic Stress-Strain Response: Cohesive Soils," *ASCE Journal of the Soil Mechanics and Foundations Division*, 89:SM4

Brinch Hansen, J. (1961a), "The Ultimate Resistance of Rigid Piles Against Transversal Forces," *Bulletin No. 12*, Danish Geotechnical Institute, Copenhagen

Brinch Hansen, J. (1961b), "A General Formula for Bearing Capacity," *Bulletin No. 11*, Danish Geotechnical Institute, Copenhagen

Brinch Hansen, J. (1970), "A Revised and Extended Formula for Bearing Capacity," *Bulletin No. 28*, Danish Geotechnical Institute, Copenhagen

Brink, A.B.A. and Kantey, B.A. (1961), "Collapsible Grain Structure in Residual Granite Soils in South Africa," *Proceedings of the Fifth International Conference on Soil Mechanics and Foundation Engineering*, pp. 611–614

Broms, Bengt B. (1964a), "Lateral Resistance of Piles in Cohesive Soils," *ASCE Journal of the Soil Mechanics and Foundations Division*, Vol. 90, No. SM2, pp. 27–63

Broms, Bengt B. (1964b), "Lateral Resistance of Piles in Cohesionless Soils," *ASCE Journal of the Soil Mechanics and Foundations Division*, Vol. 90, No. SM3, pp. 123–156

Broms, Bengt B. (1965), "Design of Laterally Loaded Piles," *ASCE Journal of the Soil Mechanics and Foundations Division*, Vol. 91, No. SM3, pp. 79–99

Broms, Bengt B. (1972), "Stability of Flexible Structures (Piles and Pile Groups)," *Proceedings of the Fifth European Conference on Soil Mechanics and Foundation Engineering*, Madrid, Vol. 2, pp. 239–269

Broms, Bengt B. (1981), *Precast Piling Practice*, Thomas Telford, London

Brons, K.F. and Kool, A.F. (1988), "Methods to Improve the Quality of Auger Piles," *Deep Foundations on Bored and Auger Piles*, pp. 269–272, W.F. Van Impe, Ed., Balkema, Rotterdam

Brown, E.T. (Ed.) (1981), *Rock Characterization, Testing and Monitoring – ISRM Suggested Methods*, pp. 171-183. Oxford, Pergamon

Brown, D.A. and Bollman, H.T. (1993), "Pile-Supported Bridge Foundations Designed for Impact Loading," Appended document to *Proceedings of Design of Highway Bridges for Extreme Events*, Crystal City, VA, pp. 265–281

Brown, D.A. and Drew, C. (2000), "Axial Capacity of Augered Displacement Piles at Auburn University," *New Technological and Design Developments in Deep Foundations*, ASCE Geotechnical Special Publication No. 100, N. D. Dennis, R. Castelli, and M. W. O'Neill Eds., pp. 397–403

Brown, D.A., Dapp, S.D., Thompson, W.R. and Lazarte, C.A. (2007), *Design and Construction of Continuous Flight Auger (CFA) Piles*, Geotechnical Engineering Circular No. 8, Report No. FHWA-HIF-07-03, Federal Highway Administration

Brown, D.A., Morrison, C. and Reese, L.C. (1988), "Lateral Load Behavior of Pile Group in Sand," *Journal of Geotechnical Engineering*, Vol. 114, No. 11, pp. 1261–1276

Brown, D.A., Turner, J.P. and Castelli, R.J. (2010), *Drilled Shafts: Construction Procedures and LRFD Design Methods*, NHI Course No. 132014, Geotechnical Engineering Circular No. 10, Report No. FHWA NHI-10-016, Federal Highway Administration

Brown, H.E. (1967), *Structural Analysis, Vol 1*. Wiley

Brown, M. and Powell, J. (2013), "Comparison of Rapid Load Test Analysis Techniques in Clay Soils," *Journal of Geotechnical and Geoenvironmental Engineering*, Vol. 139, No. 1, pp. 152–161

Brown, M.J. and Powell, J. J. M. (2012), "Comparison of Rapid Load Pile Testing of Driven and CFA Piles Installed in High OCR Clay," *Soils and Foundations: Special Issue on IS-Kanazawa, 9th International Conference on Testing and Design Methods for Deep Foundations*, Vol. 52, No. 6, pp. 1033–1042

Brown, R.E. and Glenn, R.J. (1976), "Vibroflotation and Terra-Probe Comparison," *ASCE Journal of the Geotechnical Engineering Division*, Vol. 102, No. GT10, pp. 1059–1072

Brown, R.W. (2001), *Practical Foundation Engineering Handbook*, McGraw Hill, New York

Bruce, M. E. C., Berg, R. R., Collin, J. G., Filz, G. M., Terashi, M. and Yang, D. S. (2013), *Deep Mixing for Embankment and Foundation Support*, FHWA-HRT-13-046, Federal Highway Administration, Washington, D.C.

Brumund, William F., Jonas, E. and Ladd, Charles C. (1976), "Estimating In-Situ Maximum Past (Preconsolidation) Pressure of Saturated Clays from Results of Laboratory Consolidometer Tests," *Estimation of Consolidation Settlement*, Special Report 163, pp. 4–12, Transportation Research Board, Washington, D.C.

Budge, W.D., Schuster, R.L. and Sampson, E. (1964), *A Review of Literature on Swelling Soils*, Colorado Department of Highways and University of Colorado, Denver, CO

Bullet, P. (1691), *L'Architecture Pratique*, Paris (in French)

Bullock, P., Schmertmann, J., McVay, M. and Townsend, F. (2005), "Side Shear Setup. II: Results from Florida Test Piles," *Journal of Geotechnical and Geoenvironmental Engineering*, 131(3), pp. 301–310

Burke, G. (2009), "TRD Soil Mixing at Herbert Hoover Dike," *Deep Foundations*, Spring 2009, pp.78–79

Burland, J.B. (1973), "Shaft Friction of Piles in Clay—A Simple Fundamental Approach," *Ground Engineering*, Vol. 6, No. 3, pp. 30–42

Burland, J.B. and Burbidge, M.C. (1985), "Settlement of Foundations on Sand and Gravel," *Proceedings, Institution of Civil Engineers*, Part 1, Vol. 78, pp. 1325–1381

Burland, J.B. and Wroth, C.P. (1974), "Allowable and Differential Settlement of Structures, Including Damage and Soil-Structure Interaction," *Conference on Settlement of Structures*, pp. 611–654, Pentech Press, Cambridge

Burmister, D.M. (1962), "Physical, Stress–Strain, and Strength Response of Granular Soils," *Symposium on Field Testing of Soils*, STP 322, pp. 67–97, ASTM

Bustamante, M. and Gianeselli, L. (1982), "Pile Bearing Capacity Prediction by Means of Static Penetrometer CPT," *Second European Symposium on Penetration Testing (ESOPT II)*, A. Verruijt et al., Ed., Vol. 2, pp. 493–500

Bustamante, M. and Gianeselli, L. (1993) "Design of Auger Displacement Piles from In Situ Tests. Deep Foundations on Bored and Auger Piles," *Proceedings of the Second International Geotechnical Seminar on Deep Foundations on Bored and Auger Piles*, pp. 21–34

Bustamante, M. and Gianeselli, L. (1998) "Installation Parameters and Capacity of Screwed Piles. Deep Foundations on Bored and Auger Piles," *Proceedings of the Third International Geotechnical Seminar on Deep Foundations on Bored and Auger Piles*, pp. 95–108

Butler, F.G. (1975), "Heavily Over-Consolidated Clays," p. 531ff in *Settlement of Structures*, Halstead Press

Butler, H.D. and Hoy, H.E. (1977), User's Manual for the Texas Quick-Load Method for Foundation Load Testing, Federal Highway Administration, Office of Development, Washington D.C., p. 59

Byrn, James E. (1991), "Expansive Soils: The Effect of Changing Soil Moisture Content on Residential and Light Commercial Structures," *Journal of the National Academy of Forensic Engineers*, Vol. 8, No. 2, pp. 67–84

Canadian Geotechnical Society (2006), *Canadian Foundation Engineering Manual*

Caputo, V. (2003), "Experimental Evidence for the Validation of Load-Settlement Predictions," *Deep Foundations on Bored and Auger Piles*, pp. 205–300, W. F. Van lmpe, Ed., Millpress, Rotterdam

Carter, J.P. and Kulhawy, F.H. (1988), *Analysis and Design of Drilled Shaft Foundations Socketed into Rock*. EPRI EL-5918. Ithaca, New York

Carvalho, J. (2004), Estimation of rock mass modulus (Personal Communication cited by Hoek and Diederichs, 2006)

Casagrande, A. (1932), "The Structure of Clay and Its Importance on Foundation Engineering," *Journal of the Boston Society of Civil Engineers*, Vol. 19, No. 4, pp. 168

CCC (1995), *The National Building Code of Canada*, Canadian Codes Center, Ottawa

CGS (1992), *Canadian Foundation Engineering Manual*, 3rd ed., Canadian Geotechnical Society, BiTech, Vancouver

CGS (2006), *Canadian Foundation Engineering Manual*, 4th ed., Canadian Geotechnical Society, BiTech, Vancouver

Chellis, R.D. (1961), *Pile Foundations*, 2nd ed., McGraw Hill, New York

Chellis, R.D. (1962), "Pile Foundations," pp. 633–768 in *Foundation Engineering*, G.A. Leonards, Ed., McGraw Hill, New York

Chen, F.H. (1965), "The Use of Piers to Prevent the Uplifting of Lightly Loaded Structures Founded on Expansive Soils", *Engineering Effects of Moisture Changes in Soils: Concluding Proceedings, International Research and Engineering Conference on Expansive Clay Soils*, Texas A & M Press.

Chen, Fu Hua (1988), *Foundations on Expansive Soils*, 2nd ed., Developments in Geotechnical Engineering Vol. 54, Elsevier, Amsterdam

Chen, Yu-Jin and Kulhawy, Fred H. (2002), "Evaluation of Drained Axial Capacity for Drilled Shafts," *Deep Foundations 2002*, pp. 1200–1214, ASCE Geotechnical Special Publication 116, M.W. O'Neill and F.C. Townsend, Eds.

Cheney, R.S. and Chassie, R.G. (2002), *Soils and Foundations Workshop Manual*, 2nd ed., Report No. HI-88-009, Federal Highway Administration

Chin, F.K. (1972) "The Inverse Slope as a Prediction of Ultimate Bearing Capacity of Piles," *Proceedings of the Third Southeast Asian Conference on Soil Engineering*, pp. 83–91

Chin, F.K. (1970) "Estimation of the Ultimate Load of Piles not Carried to Failure," *Proceedings of the Second Southeast Asian Soil Conference in Soil Engineering*, Singapore, pp.80–90

Christian, J. (2004), "Geotechnical Engineering Reliability: How Well Do We Know What We Are Doing?" *Journal of Geotechnical and Geoenvironmental Engineering*, Vol. 130, No. 10, pp. 985–1003

Christian, John T. and Carrier, W. David III (1978), "Janbu, Bjerrum and Kjaernsli's Chart Reinterpreted," *Canadian Geotechnical Journal*, Vol. 15, pp. 123–128

Christopher, B. R., Schwartz, C. and Boudreau, R. (2006), *Geotechnical Aspects of Pavements*. FHWA-NHI-05-037, FHWA, Washington, D.C.

Christopher, Barry R., Baker, Clyde N. and Wellington, Dennis L. (1989), "Geophysical and Nuclear Methods for Non-Destructive Evaluation of Caissons," *Foundation Engineering: Current Principles and Practices*, ASCE

Cibor, Joseph M. (1983), "Geotechnical Considerations of Las Vegas Valley," *Special Publication on Geological Environment and Soil Properties*, ASCE Annual Convention, Houston, TX, pp. 351–373

Clausen, J. (2013), "Bearing Capacity of Circular Footings on a Hoek-Brown Material," *International Journal of Rock Mechanics & Mining Sciences*. Vol. 57, pp. 34–41

Clayton, C.R.I. (1990), "SPT Energy Transmission: Theory, Measurement and Significance," *Ground Engineering*, Vol. 23, No. 10, pp. 35–43

Clemence, Samuel P. and Finbarr, Albert O. (1981), "Design Considerations for Collapsible Soils," *ASCE Journal of the Geotechnical Engineering Division*, Vol. 107, No. GT3, pp. 305–317

Clemence, Samuel P. (Ed.) (1985), *Uplift Behavior of Anchor Foundations in Soil*, ASCE

Clemente, J.L.M., Davie, J.R. and Senapathy, H. (2000), "Design and Load Testing of Augercast Piles in Stiff Clay," *New Technological and Design, Developments in Deep Foundations*, Geotechnical Special Publication 100, N.D. Dennis, et al., Eds., ASCE

Clough, G. Wayne, Sitar, Nicholas, Bachus, Robert C. and Rad, Nader Shafii (1981), "Cemented Sands Under Static Loading," *Journal of the Geotechnical Engineering Division*, Vol. 107, No. GT3, pp. 305–317, ASCE

Coduto, Donald P. (1994), *Foundation Design: Principles and Practices*, 1st ed., Prentice Hall, Upper Saddle River, NJ

Coduto, Donald P. (1999), *Geotechnical Engineering: Principles and Practices*, Prentice Hall, Upper Saddle River, NJ

Coduto, Donald P. (2001), *Foundation Design: Principles and Practices*, 2nd ed., Prentice Hall, Upper Saddle River, NJ

Coduto, Donald P., Yeung, Man-chu Ronald and Kitch, William A. (2011), *Geotechnical Engineering: Principles and Practices*, 2nd ed., Prentice Hall, Upper Saddle River, NJ

Coleman, D.M. and Arcement, B.J. (2002), "Evaluation of Design Methods for Auger Cast Piles in Mixed Soil Conditions," *Proceedings of the International Deep Foundations Congress*, M.W. O'Neill and F.C. Townsend, Eds., ASCE

Cooke, R.W.and Price, G. (1973), "Jacked Piles in London Clay: A Study of Load Transfer and Settlement Under Working Conditions", *Geotechnique*, Vol. 29, No. 2, pp. 113–147

Cornell, C.A. (1969), "A Probability-Based Structural Code," *Journal of the American Concrete Institute*, Vol. 66, No. 12

Costanzo, D., Jamiolkowski, M., Lancellotta, R. and Pepe, M.C. (1994), *Leaning Tower of Pisa: Description and Behaviour*, Settlement 94 Banquet Lecture, Texas A&M University

Coulomb, C.A. (1776) "Essai sur une application des règles de maximis et minimis à quelques problèmes de statique relatifs à l'architecture," *Mémoires de mathématique et de physique présentés à l'Académie Royale des Sciences*, Paris, Vol. 7, pp. 343–382 (in French)

Coyle, Harry M. and Castello, Reno R. (1981), "New Design Correlations for Piles in Sand," *Journal of the Geotechnical Engineering Division*, ASCE, Vol. 107, No. 7, pp. 965–986

Crapps, D.K. and Schmertmann, J.H. (2002), "Compression Top Load Reaching Shaft Bottom—Theory Versus Tests," in: O'Neill, M.W., Townsend, F.C. Eds., *Proceedings of the International Deep Foundations Congress*. Orlando, FL. Geotechnical Special Publication No. 116, Vol.2. Geo-Institute, American Society of Civil Engineers, Reston, VA, pp.1533–1549

Crawford, C.B. and Burn, K.N. (1968), "Building Damage from Expansive Steel Slag Backfill," *Placement and Improvement of Soil to Support Structures*, pp. 235–261, ASCE

Crawford, C.B. and Johnson, G.H. (1971), "Construction on Permafrost," *Canadian Geotechnical Journal*, Vol. 8, No. 2, pp. 236–251

Crowther, Carroll L. (1988), *Load Testing of Deep Foundations*, John Wiley and Sons, New York

CRSI (1992), *CRSI Handbook*, Concrete Reinforcing Steel Institute, Schaumburg, IL

Cummings, A.E. (1940), "Dynamic Pile Driving Formulas," *Journal of the Boston Society of Civil Engineers*, Vol. 27, No. 1, pp. 6–27

Cundall, P. A. (1971), "A Computer Model for Simulating Progressive, Large Scale Movements in Blocky Rock Systems," *Symposium of International Society of Rock Mechanics*, Nancy, France, pp.11–18

Curtin, G. (1973), "Collapsing Soil and Subsidence," in *Geology, Seismicity and Environmental Impact*, Special Publication, Association of Engineering Geologists, Douglas E. Moran et al., Ed., University Publishers, Los Angeles

Dapp, S. (2006), "A Comparison of Static Axial Capacity Between Drilled and Driven Piles," Presentation to PDCA 10th Annual Meeting, San Antonio, TX, USA.

D'Appolonia, D.J., D'Appolonia, E.D. and Brissette, R.F. (1968), "Settlement of Spread Footings on Sand," *ASCE Journal of the Soil Mechanics and Foundations Division*, Vol. 94, No. SM3, pp. 735–759

D'Appolonia, David J., Poulos, Harry G. and Ladd, Charles C. (1971), "Initial Settlement of Structures on Clay," *ASCE Journal of the Soil Mechanics and Foundations Division*, Vol. 97, No. SM10, pp. 1359–1377

Davis, E.H. and Poulos, H.G. (1968), "The Use of Elastic Theory for Settlement Prediction Under Three-Dimensional Conditions," *Géotechnique*, Vol. 18, pp. 67–91

Davisson, M.T. (1970), "Lateral Load Capacity of Piles," *Highway Research Record No. 333*, pp. 104–112, Highway Research Board, Washington, D.C.

Davisson, M.T. (1973), "High Capacity Piles," in *Innovations in Foundation Construction*, proceedings of a lecture series, Illinois Section ASCE, Chicago

Davisson, M.T. (1979), "Stresses in Piles," *Behavior of Deep Foundations*, ASTM STP 670, Raymond Lundgren, Ed., pp. 64–83, ASTM, Philadelphia

Davisson, M.T. (1989), "Driven Piles," *Foundations in Difficult Soils: State of Practice*, Foundations and Soil Mechanics Group, Metropolitan Section, ASCE, New York

Davisson, M.T. and Robinson, K.E. (1965), "Bending and Buckling of Partially Embedded Piles," Sixth International Conference on Soil Mechanics and Foundation Engineering, University of Toronto Press, Montreal, Canada, pp. 243–246

DeBeer, E.E. and Ladanyi, B. (1961), "Experimental Study of the Bearing Capacity of Sand Under Circular Foundations Resting on the Surface," *Proceedings of the Fifth International Conference on Soil Mechanics and Foundation Engineering*, Vol. 1, pp. 577–585, Paris

DeCock, F.A. (2009), "Sense and Sensitivity of Pile Load-Deformation Behavior," *Deep Foundations on Bored and Auger Piles – BAP V*, pp. 23–44, W.F. Van Impe & P.O. Van Impe, Eds., Taylor & Francis

Décourt, L (2003), "Behaviour of CFA Pile in a Lateric Clay," *Proceedings of the Fourth International Geotechnical Seminar on Deep Foundations on Bored and Auger Piles*, Ghent, Belgium, W.F. VanImpe, Ed., IOS Press

Deere, D.U. (1989), *Rock Quality Designation (RQD) After Twenty Years*. Contract Report GL-89-1, U.S. Army Engineer Waterways Experiment Station, Department of the Army

Deere, D.U., Hendron, A.J., Patton, F.D. and Cording, E.J. (1967), "Design of Surface and Near Surface Construction in Rock." *Failure and Breakage of Rock, Proceedings of the Eighth U.S. Symp. Rock Mech.*, (ed. C. Fairhurst), pp. 237–302. New York: Soc. Min. Engrs, Am. Inst. Min. Metall. Petrolm Engrs.

DeMello, V. (1971), "The Standard Penetration Test—A State-of-the-Art Report," *Fourth PanAmerican Conference on Soil Mechanics and Foundation Engineering*, Vol. 1, pp. 1–86

Dempsey, J.P. and Li, H. (1989), "A Rigid Rectangular Footing on an Elastic Layer," *Géotechnique*, Vol. 39, No. 1, pp. 147–152

DeNicola, A. and Randolph, M.F. (1993), "Tensile and Compressive Shaft Capacity of Piles in Sand," *Journal of the Geotechnical Engineering Division*, ASCE, Vol. 119, No. 12, pp. 1952–1973

DeRuiter, J. (1981), "Current Penetrometer Practice," *Cone Penetration Testing and Experience*, pp. 1–48, ASCE

DeRuiter, J. and Beringen, F.L. (1979), "Pile Foundations for Large North Sea Structures," *Marine Geotechnology*, Vol. 3, No. 3, pp. 267–314

deSanctis, Luca and Mandolini, Alessandro (2006), "Bearing Capacity of Piled Rafts on Soft Clay Soils," *ASCE Journal of Geotechnical and Geoenvironmental Engineering*, Vol. 132, No. 12, pp. 1600–1610

DFI (1990), *Auger Cast-in-Place Piles Manual*, Deep Foundations Institute, Sparta, NJ

DFI (1998), *Driven Sheet Piling*, Deep Foundations Institute, Englewood Cliffs, NJ

Dickin, E.A. and Leung, C.F. (1990), "Performance of Piles with Enlarged Bases Subject to Uplift Forces," *Canadian Geotechnical Journal*, Vol. 27, pp. 546–556

DiMillio, A.F., Ng, E.S., Briaud, J.L., O'Neill, M.W., et al. (1987a), *Pile Group Prediction Symposium: Summary Volume I: Sandy Soil*, Report No. FHWA-TS-87-221, Federal Highway Administration, McLean, VA

DiMillio, A.F., O'Neill, M.W., Hawkins, R.A., Vgaz, O.G. and Vesic, A.S. (1987b), *Pile Group Prediction Symposium: Summary Volume II: Clay Soil*, Report No. FHWA-TS-87-222, Federal Highway Administration, McLean, VA

Dise, K., Stevens, M.G. and Von Thun, J.L. (1994), "Dynamic Compaction to Remediate Liquefiable Embankment Foundation Soils," *In-Situ Deep Soil Improvement*. Special Geotechnical Publication 45, pp.1–25, Kyle M. Rollins, Ed., ASCE.

Dismuke, Thomas D., Coburn, Seymour K. and Hirsch, Carl M. (1981), *Handbook of Corrosion Protection for Steel Pile Structures in Marine Environments*, American Iron and Steel Institute, Washington, D.C.

Donaldson, G.W. (1973), "The Prediction of Differential Movement on Expansive Soils," *Proceedings of the Third International Conference on Expansive Soils*, Vol. 1, pp. 289–293, Jerusalem Academic Press

Douglas, D.J. (1983), "Discussion on Paper 17-22 Case Histories," *Proceedings, Conference on Piling and Ground Treatment*, Institution of Civil Engineers

Dowrick, David J. (1987), *Earthquake Resistant Design: A Manual for Engineers and Architects*, 2nd ed., John Wiley, New York

Dudley, John H. (1970), "Review of Collapsing Soils," *ASCE Journal of the Soil Mechanics and Foundations Division*, Vol. 96, No. SM3, pp. 925–947

Duncan, J.M. (2000), "Factors of Safety and Reliability in Geotechnical Engineering," *Journal of Geotechnical and Geoenvironmental Engineering*, Vol. 126, No. 4, pp. 307–316

Duncan, J.M. and Buchignani, A.L. (1976), *An Engineering Manual for Settlement Studies*, Department of Civil Engineering, University of California, Berkeley

Duncan, J.M., and Mokwa, R. L. (2001), "Passive Earth Pressures: Theories and Tests." *Journal of Geotechnical and Geoenvironmental Engineering, ASCE*, Vol. 127, No. 3, pp. 248–257

Duncan, J.M., Williams, G.W., Sehn, A.L. and Seed, R.B. (1991), "Estimation Earth Pressures Due to Compaction," *ASCE Journal of Geotechnical Engineering*, Vol. 117, No. 12, pp. 1833–1847 (errata in Vol. 118, No. 3, p. 519)

Duncan, J.M., Clough, G.W. and Ebeling, R.M. (1990), "Behavior and Design of Gravity Earth Retaining Structures," *Design and Performance of Earth Retaining Structures*, Philip C. Lambe and Lawrence A. Hansen, Ed., pp. 251–277, ASCE

Durgunoglu. H.T. and Mitchell, J.K. (1975), "Static Penetration Resistance of Soils: I-Analyses, II-Evaluation of Theory and Implications for Practice," *ASCE Spec. Conf. on In Situ Measurement of Soil Properties*, Raleigh NC, Vol. I, 1975. pp.151–189

Edwards, T.C. (1967), *Piling Analysis Wave Equation Computer Program Utilization Manual*, Texas Transportation Institute Research Report 33-11, Texas A&M University, College Station, TX

Elias, V., Welsh, J., Warren, J., Lukas, R. G., Collin, J. G. and Berg, R. R. (2006), *Ground Improvement Methods: Reference Manual*. Vol. 1 FHWA-NHI-06-019, Vol. 2 FHWA-NHI-06-020, FHWA, Washington, D.C.

Ellingwood, B., Galambos, T.V., MacGregor, J.G. and Cornell, C.A. (1980), *Development of a Probability Base Load Criterion for American National Standard A58*. National Bureau of Standards, Washington, D.C.

Erzin, Y. and Gunes, N. (2013), "The Unique Relationship between Swell Percent and Swell Pressure of Compacted Clays," *Bulletin of Engineering Geology and the Environment*. Vol. 72, pp. 71–80

Eslami, Abolfazi, and Fellenius, Bengt H. (1997), "Pile Capacity by Direct CPT and CPTu Methods Applied to 102 Case Histories," *Canadian Geotechnical Journal*, Vol. 34, pp. 886–904

Esrig, M.E. and R.C. Kirby. 1979. "Advances in General Effective Stress Method for the Prediction of Axial Capacity for Driven Piles in Clay," *Proceedings, 11th Annual Offshore Technology Conference*

Evans, L.T. and Duncan, J.M. (1982), *Simplified Analysis of Laterally Loaded Piles*, Report No. UCB/GT/82-04, Department of Civil Engineering, University of California, Berkeley

Farley, J. (1827), *A Treatise on the Steam Engine*, London (quoted in Golder, 1975)

Fellenius, B.H. (1980), "The Analysis of Results from Routine Pile Load Tests," *Ground Engineering*, Vol. 13, No. 6, pp. 19–31

Fellenius, B.H. (1990), *Guidelines for the Interpretation and Analysis of the Static Loading Test*, Deep Foundations Institute, Sparta, NJ

Fellenius, B.H. (1991), "Pile Foundations," Chapter 13 in *Foundation Engineering Handbook*, 2nd ed., HS Fang, Ed.

Fellenius, B.H. (1998), "Recent Advances in the Design of Piles for Axial Loads, Dragloads, Downdrag, and Settlement," *ASCE and Port of NY and NJ Seminar* (also available from www.unisoftltd.com)

Fellenius, B.H. (1999), *Basics of Foundation Design*, 2nd ed., BiTech, Richmond, BC

Fellenius, B.H., Riker, R.E., O'Brien, A.J. and Tracy, G.R. (1989), "Dynamic and Static Testing in Soil Exhibiting Set-Up," *ASCE Journal of Geotechnical Engineering*, Vol. 115, No. 7, pp. 984–1001

Fisher, James. M. and Kloiber, Lawrence. A. (2006), *Base Plate and Anchor Rod Design*, 2nd ed., American Institute of Steel Construction

Fleming, W.G.K (1992), "A New Method for Single Pile Settlement Prediction and Analysis," *Geotechnique*, Vol. 42, No.3, pp. 411–425

Fleming, W.G.K., Weltman, A.J., Randolph, M.F. and Elson, W.K. (1985), *Piling Engineering*, John Wiley & Sons, New York

Florida DOT (2010), *Standard Specifications for Road and Bridge Construction*, http://www.dot.state.fl.us/specificationsoffice/Implemented/SpecBooks/2010BK.shtm, (accessed 1/11/2014)

Foott, Roger and Ladd, Charles C. (1981), "Undrained Settlement of Plastic and Organic Clays," *ASCE Journal of the Geotechnical Engineering Division*, Vol. 107, No. GT8, pp. 1079–1094

Frank, R. (1994), "Some Recent Developments on the Behavior of Shallow Foundations," *Deformations of Soils and Displacements of Structures, Proceedings of the Tenth European Conference on Soil Mechanics and Foundation Engineering*, pp. 1115–1140, A.A. Balkema, Rotterdam

Fredlund, D.G. and Rahardjo, H. (1993), *Soil Mechanics for Unsaturated Soils*, John Wiley, New York

Fredlund, D.G., Hasan, J.U. and Filson, H. (1980), "The Prediction of Total Heave," *Proceedings of the Fourth International Conference on Expansive Soils*. Denver, Co. pp.1–11

Fredlund, D.G., Rahardjo, H. and Fredlund, M.D. (2012), *Unsaturated Soil Mechanics in Engineering Practice*, 2nd ed., John Wiley

Frizzi, R.P. and Meyer, M.E. (2000), "Augercast Piles: South Florida Experience," *New Technological and Design, Developments in Deep Foundations*, Geotechnical Special Publication 100, N.D. Dennis, et al., Eds., ASCE

Geo-Slope International (2014), *SIGMA/W 2012 Stress-Deformation Analysis*, www.geo-slope.com, accessed: 7/24/14

Gibbs, Harold J. (1969), Discussion of Holtz, W. G. "The Engineering Problems of Expansive Clay Subsoils," *Proceedings of the Second International Research and Engineering Conference on Expansive Clay Soils*, pp. 478–479, Texas A&M Press, College Station, TX

Goble, G.G. (1986), "Modern Procedures for the Design of Driven Pile Foundations," Short Course on Behavior of Deep Foundations Under Axial and Lateral Loading, University of Texas, Austin

Gohl, W. B., Jefferies, M. G., Howies, J. A. and Diggle, D. (2000), "Explosive Compaction: Design, Implementation and Effectiveness," *Géotechnique*, 50, (Vol. 50, Issue 6), pp. 657–665(8)

Golder, H.Q. (1975), "Floating Foundations," Chapter 18 in *Foundation Engineering Handbook*, H.F. Winterkorn and H. Fang, Ed., Van Nostrand Reinhold, New York

Goodman, R.E. (1989), *Introduction to Rock Mechanics*, 2nd ed., Wiley

Gould, James P. (1970), "Lateral Pressures on Rigid Permanent Structures," in *Lateral Stresses in the Ground and the Design of Earth-Retaining Structures*, pp. 219–270, ASCE

Govt. of Hong Kong. (1998), *Landslides and Boulder Falls from Natural Terrain: Interim Risk Guidelines, GEO Report No. 75*, Geotechnical Engineering Office, Civil Engineering Department

Graham, J. (1985), "Allowable Compressive Design Stresses for Pressure-Treated Round Timber Foundation Piling," *American Wood Preservers Association Proceedings*, Vol. 81

Grant, Rebecca, Christian, John T. and Vanmarcke, Erik H. (1974), "Differential Settlement of Buildings," *ASCE Journal of the Geotechnical Engineering Division*, Vol. 100, No. GT9, pp. 973–991

Greenfield, Steven J. and Shen, C.K. (1992), *Foundations in Problem Soils*, Prentice Hall, Englewood Cliffs, NJ

Greer, David M. and Gardner, William S. (1986), *Construction of Drilled Pier Foundations*, John Wiley, New York

Gromko, Gerald J. (1974), "Review of Expansive Soils," *ASCE Journal of the Geotechnical Engineering Division*, Vol. 100, No. GT6, pp. 667–687

Grundbau, F. (ND), *Frankipile: High Pile Loads, Optimum Adaptation to Foundation Soil, Low-noise Manufacturing Process*, brochure http://www.franki.de/pdf_en/FRANKI_pile.pdf (Nov. 4, 2014)

Hain, Stephen J. and Lee, Ian K. (1974), "Rational Analysis of Raft Foundation," *ASCE Journal of the Geotechnical Engineering Division*, Vol. 100, No. GT7, pp. 843–860

Handford, S.A. (1982), *The Conquest of Gaul*, revised by Jane F. Gardner, Penguin Classics

Handy, Richard L. (1980), "Realism in Site Exploration: Past, Present, Future, and Then Some—All Inclusive," *Site Exploration on Soft Ground Using In-Situ Techniques*, pp. 239–248, Report No. FHWA-TS-80-202, Federal Highway Administration, Washington, D.C.

Hannigan, P.J. (1990), *Dynamic Monitoring and Analysis of Pile Foundation Installations*, Deep Foundations Institute, Sparta, NJ

Hannigan, P.J., Goble, G.G., Thendean, G., Likins, G.E. and Rausche, F. (2006), *Design and Construction of Driven Pile Foundations*, Vol. 1: Report No. FHWA-NHI-05-042, Vol. 2: Report No. FHWA-NHI-05-043, Federal Highway Administration, Washington, D.C.

Harder, Leslie F. and Seed, H. Bolton (1986), *Determination of Penetration Resistance for Coarse-Grained Soils Using the Becker Hammer Drill*, Report No. UCB/EERC-86/06, Earthquake Engineering Research Center, Richmond, CA

Harr, M. E. (1987), *Reliability-Based Design in Civil Engineering*, McGraw Hill, New York

Harr, Milton E. (1996), *Reliability-Based Design in Civil Engineering*, Dover Publishers

Hart, Stephen S. (1974), *Potentially Swelling Soil and Rock in the Front Range Urban Corridor, Colorado*, Colorado Geological Survey publication EG-7, Denver

Hassan, K.M, O'Neill, M.W., Sheikh, S.A. and Ealy, C.D. (1997), "Design Method for Drilled Shafts in Soft Argillaceous Rock," *ASCE Journal of Geotechnical and Geoenvironmental Engineering*, Vol. 123, pp. 272–280

Hayward Baker, Inc. (2008) "Vibro Systems: State Road 10 Over San Pablo Creek, Jacksonville, FL," Project Summary. www.HaywardBaker.com

Hayward Baker, Inc. (2009a) "Rapid Impact Compaction Ground Improvement: Audenried High School, Philadelphia, PA," Project Summary. www.HaywardBaker.com

Hayward Baker, Inc. (2009b) "Vibro Piers Foundation Support: Gateway Medical Center, Clarksville, TN," Project Summary. www.HaywardBaker.com

Hayward Baker, Inc. (2013) "Rigid Inclusions," www.HaywardBaker.com

Head, K.H. (1982), *Manual of Soil Laboratory Testing*, Vol. 2, Pentech, London

Hearne, T.M., Stokoe, K.H. and Reese, L.C. (1981), "Drilled Shaft Integrity by Wave Propagation Method," *ASCE Journal of the Geotechnical Engineering Division*, Vol. 107, No. GT10, pp. 1327–1344

Heijnen, W.J. (1974), "Penetration Testing in Netherlands," *European Symposium on Penetration Testing (ESOPT)*, Stockholm, Vol. 1, pp. 79–83

Heijnen, W.J. and Janse, E. (1985), "Case Studies of the Second European Symposium on Penetration Testing (ESOPT II)," *LGM-Mededelingen*, Part XXII, No. 91, Delft Soil Mechanics Laboratory, Delft, The Netherlands

Heinz, Roney (1993), "Plastic Piling," *Civil Engineering*, Vol. 63, No. 4, pp. 63–65, ASCE

Held, Lloyd A. (2004), "History of Driven Piles in New Orleans," *The Louisiana Civil Engineer*, Vol. 12, No. 2, pp. 5–7, 17–21

Hertlein, Bernard H. (1992), "Selecting an Effective Low-Strain Foundation Test," *Foundation Drilling*, Vol. 31, No. 2, pp. 14–22, Association of Drilled Shaft Contractors, Dallas, TX

Hertlein, B. and Davis, A. (2006), *Nondestructive Testing of Deep Foundations*, John Wiley & Sons

Hetényi, M. (1974), *Beams on Elastic Foundation*, University of Michigan Press, Ann Arbor

Heyman, J. (1972), *Coulomb's Memoir on Statics: An Essay in the History of Civil Engineering*, Cambridge University Press, London

Hodgkinson, A. (1986), *Foundation Design*, The Architectural Press, London

Hoek, E. (1983), "Strength of Jointed Rock Masses," 23rd Rankine Lecture, *Geotechnique*, Vol. 33, pp. 187–223

Hoek, E. (1994), "Strength of Rock and Rock Masses," *ISRM News J*, Vol. 2, pp. 4–16

Hoek, E. (2007), *Practical Rock Engineering*. A set of notes available at http://www.rocscience.com

Hoek, E. and Brown, E.T. (1997), "Practical Estimates of Rock Mass Strength," *Int. J. Rock Mech. Min. Sci.* Vol. 34, pp. 1165–1186

Hoek, E. and Diederichs, M.S. (2006), "Empirical Estimation of Rock Mass Modulus," *Int. J. Rock Mech. Min. Sci.* Vol. 43, pp. 203–215

Hoek, E., Carranza-Torres, C. and Corkum, B. (2002), "Hoek-Brown Failure Criterion – 2002 Edition," Hammah, R., Bawden, W., Curran, J., Telesnicki, M. Eds., *Proceedings of NARMS-TAC 2002, Mining Innovation and Technology*, Toronto

Hoek, E., Kaiser, P.K. and Bawden, W.F. (1995), *Support of Underground Excavations in Hard Rock*. Rotterdam: Balkema

Hoek, E., Marinos, P. and Marinos, V. (2005), "Characterization and Engineering Properties of Tectonically Undisturbed but Lithologically Varied Sedimentary Rock Masses," *Int. J. Rock Mech. Min. Sci.* Vol. 42, pp. 277–285

Holden, J.C. (1988), "Integrity Control of Bored Piles Using SID," *Deep Foundations on Bored and Auger Piles* (Proceedings of the First International Geotechnical Seminar on Deep Foundations on Bored and Auger Piles), pp. 91–95, W.F. VanImpe, Ed., Balkema, Rotterdam

Holloway, D.M., Moriwaki, Y., Finno, R.J. and Green, R.K. (1982), "Lateral Load Response of a Pile Group in Sand," *Second International Conference on Numerical Methods in Offshore Piling*, pp. 441–456, ICE

Holtz, R. D., Jamiolkowski, M. B., Lancellotta, R. and Pedroni, R. (1991), *Prefabricated Vertical Drains: Design and Performance,* Butterworth-Heinemann, Oxford

Holtz, W.G. (1969), "Volume Change in Expansive Clay Soils and Control by Lime Treatment," *Proceedings of the Second International Research and Engineering Conference on Expansive Clay Soils*, pp. 157–173, Texas A&M Press, College Station, TX

Holtz, Wesley G. and Hart, Stephen S. (1978), *Home Construction on Shrinking and Swelling Soils*, Colorado Geological Survey publication SP-11, Denver

Horikoshi, K. and Randolph, M.F (1998), "A Contribution to Optimum Design of Piled Rafts," *Geotechnique*, Vol. 48, No. 3, pp. 301–317

Horvath, J.S. (1983), "New Subgrade Model Applied to Mat Foundations," *ASCE Journal of Geotechnical Engineering*, Vol. 109, No. 12, pp. 1567–1587

Horvath, J.S. (1992), "Lite Products Come of Age," *ASTM Standardization News*, Vol. 20, No. 9, pp. 50–53

Horvath, J.S. (1993), *Subgrade Modeling for Soil-Structure Interaction Analysis of Horizontal Foundation Elements*, Manhattan College Research Report No. CE/GE-93-1, Manhattan College, New York

Horvath, R.G. and Kenney, T.C. (1979), "Shaft Resistance of Rock Socketed Drilled Piers," *Proceedings, Symposium on Deep Foundations,* ASCE, New York, pp. 182–214

Hough, B.K. (1959), "Compressibility as the Basis for Soil Bearing Value," *ASCE Journal of the Soil Mechanics and Foundations Division*, Vol. 85, No. SM4, pp. 11–39

Houston, S.L. (1992), "Partial Wetting Collapse Predictions," *Proceedings of the Seventh International Conference on Expansive Soils*, Vol. 1, pp. 302–306

Houston, S.L. (2014), "Characterization of Unsaturated Soils: The Importance of Response to Wetting," *GeoCongress 2014 Keynote Lectures,* GSP 235, ASCE, pp.77–96

Houston, S.L. and El-Ehwany, M. (1991), "Sample Disturbance of Cemented Collapsible Soils," *ASCE Journal of Geotechnical Engineering*, Vol. 117, No. 5, pp. 731–752. Also see discussions, Vol. 118, No. 11, pp. 1854–1862

Houston, S.L., Dye, H.B., Zapata, C.E., Walsh, K.D. and Houston, W.N. (2011), "Study of Expansive Soils and Residential Foundations on Expansive Soils in Arizona," J. Perform. *Constr. Facil*, Vol. 25, pp. 31–44

Houston, S.L., Houston, W.N. and Spadola, D.J. (1988), "Prediction of Field Collapse of Soils Due To Wetting," *ASCE Journal of Geotechnical Engineering*, Vol. 114, No. 1, pp. 40–58

Houston, W.N. (1991), Personal communication

Houston, W.N. and Houston, S.L. (1989), "State-of-the-Practice Mitigation Measures for Collapsible Soil Sites," *Foundation Engineering: Current Principles and Practices*, Vol. 1, pp. 161–175, F.H. Kulhawy, Ed., ASCE

Houston, W.N. and Nelson, J.D. (2012) "The State of the Practice in Foundation Engineering on Expansive and Collapsible Soils," *ASCE Geotechnical Special Publication*, n 226 GSP, pp. 608–642. Geotechnical Engineering State of the Art and Practice: Keynote Lectures from Geocongress 2012

Huang, A., Hsueh, C., O'Neill, M., Chern, S. and Chen, C. (2001), "Effects of Construction on Laterally Loaded Pile Groups," *Journal of Geotechnical and Geoenvironmental Engineering*, Vol. 127, No. 5, pp. 385–397

Huber, F. (1991), "Update: Bridge Scour," *ASCE Civil Engineering*, Vol. 61, No. 9, pp. 62–63

Hummel, Charles E. (1971), *Tyranny of the Urgent*, InterVarsity Press, Downers Grove, IL

Hunt, Hal W. (1987), "American Practice in the Design and Installation of Driven Piles for Structure Support," *Second International Deep Foundations Conference*, pp. 13–28, Deep Foundations Institute, Sparta, NJ

Hunt, Roy E. (1984), *Geotechnical Engineering Investigation Manual*, McGraw Hill, New York

Husband, J. (1936), "The San Francisco-Oakland Bay Bridge," *The Structural Engineer*, Vol. 14, No. 4, pp. 170–208, Institution of Structural Engineers

Hussein, M.H., Likins, G.E. and Hannigan, P.J. (1993), "Pile Evaluation by Dynamic Testing During Restrike," *Eleventh Southeast Asian Geotechnical Conference*, Singapore, pp. 535–539

Hussein, M.H., Likins, GE. and Rausche, F. (1996), "Selection of a Hammer for High-Strain Dynamic Testing of Cast-in-Place Shafts," *Fifth International Conference on the Application of Stress Wave Theory to Piles*, pp. 759–772

Hussein, M.H., Woerner II, W.A., Sharp, M., and Hwang, C. (2006), "Pile Driveability and Bearing Capacity in High-Rebound Soils," *GeoCongress 2006, February 26, 2006 - March 1, 2006*, GeoCongress 2006: Geotechnical Engineering in the Information Technology Age, American Society of Civil Engineers, 63

ICC (2012), *International Building Code*, International Code Council
ICC Evaluation Service (2007), *Acceptance Criteria for Helical Foundation Systems and Devices*, Report AC 358
Imani, M., Fahimifar, A. and Sharifzadeh, M. (2012), "Upper Bound Solution for the Bearing Capacity of Submerged Jointed Rock Foundations," *Rock Mech Rock Eng*, Vol. 45, pp. 639–646
Ingles, O.G. and Metcalf, J.B. (1972), *Soil Stabilization*, Butterworths, Sydney
Ingold, T. (1979), "Retaining Wall Performance During Backfilling," *ASCE Journal of Geotechnical Engineering*, Vol. 105, No. GT5, pp. 613–626
Isaacs, D.V. (1931), "Reinforced Concrete Pile Formula," *Transactions of the Institution of Australian Engineers*, Vol. 12, pp. 312–323
Isenhower, William M. and Wang, Shin-Tower (2010), *Technical Manual for LPILE Version 6*, Ensoft, Inc.
Ishida, Y., Suganoya, T., Kawada, M., Shimoma, M., and Asaka, T. (2004), "Construction of a Highway Tunnel Using Pneumatic Caissons," *Underground Space for Sustainable Urban Development. Proceedings of the Thirtieth ITA-AITES World Tunnel Congress*, 19(4–5), p. 494
Ismael, Nabil F. and Vesić, Aleksandar S. (1981), "Compressibility and Bearing Capacity," *ASCE Journal of the Geotechnical Engineering Division*, Vol. 107, No. GT12, pp. 1677–1691
Jamiolkowski, M., Ladd, C. C., Germaine, J. T. and Lancellotta, R. (1985), "New Developments in Field and Laboratory Testing of Soils," *Proceedings of the Eleventh International Conference on Soil Mechanics and Foundation Engineering*, Vol. 1, San Francisco, pp. 57–153
Jamiolkowski, M. (2003), "Soil Parameters Relevant to Bored Pile Design from Laboratory and In-Situ Tests," *Deep Foundations on Bored and Auger Piles*, pp. 83–100, Van Impe, Ed.
Jan Duijm, N. (2009), *Acceptance Criteria in Denmark and the EU,* Danish Ministry of the Environment, Environmental Protection Agency
Janbu, N. (1998), *Sediment Deformations.* Bulletin No 35, Norwegian University of Science and Technology Department of Geotechnical Engineering, Trondheim
Janbu, N., Bjerrum, L and Kjaernsli, B. (1956), *Veiledning ved losning av fundamenteringsoppgaver*, Norwegian Geotechnical Institute Publication 16, pp. 30–32, Oslo (in Norwegian)
Jennings, J.E. (1969), "The Engineering Problems of Expansive Soils," *Proceedings of the Second International Research and Engineering Conference on Expansive Clay Soils*, pp. 11–17, Texas A&M Press, College Station, TX
Jennings, J.E. (1973), "The Engineering Significance of Constructions on Dry Subsoils," *Proceedings of the Third International Conference on Expansive Soils*, Vol. 1, pp. 27–32, Jerusalem Academic Press, Israel
Jennings, J.E. and Knight, K. (1956), "Recent Experience with the Consolidation Test as a Means of Identifying Conditions of Heaving or Collapse of Foundations on Partially Saturated Soils," *Transactions, South African Institution of Civil Engineers*, Vol. 6, No. 8, pp. 255–256
Jennings, J.E. and Knight, K. (1957), "The Additional Settlement of Foundations Due to a Collapse Structure of Sandy Subsoils on Wetting," *Proceedings of the Fourth International Conference on Soil Mechanics and Foundation Engineering*, Section 3a/12, pp. 316–319
Jennings, J.E. and Knight, K. (1975), "A Guide to Construction on or with Materials Exhibiting Additional Settlement Due to 'Collapse' of Grain Structure," *Sixth Regional Conference for Africa on Soil Mechanics and Foundation Engineering*, pp. 99–105
Jeong, S., Cho, H., Cho, J., Seol, H. and Lee. D. (2010), "Point Bearing Stiffness and Strength of Socketed Drilled Shafts in Korean Rocks," *International Journal of Rock Mechanics & Mining Sciences*. Vol. 47, pp. 983–995
Jiang, Da Hua (1983), "Flexural Strength of Square Spread Footing," *ASCE Journal of Structural Engineering*, Vol. 109, No. 8, pp. 1812–1819
Johnson, Lawrence D. and Stroman, William R. (1976), *Analysis of Behavior of Expansive Soil Foundations*, Technical report S-76-8, U.S. Army Waterways Experiment Station, Vicksburg, Miss.
Johnston, G.H., Ed. (1981), *Permafrost Engineering Design and Construction*, John Wiley, New York
Jones, D. Earl and Holtz, Wesley G. (1973), "Expansive Soils—The Hidden Disaster," *Civil Engineering*, Vol. 43, No. 8, ASCE
Jones, D. Earl and Jones, Karen A. (1987), "Treating Expansive Soils," *Civil Engineering*, Vol. 57, No. 8, August 1987, ASCE

Juran, I., Komornik, U. and Hoppe, E. J. (2006), *Behavior of Fiber-Reinforced Polymer (FRP) Composite Piles Under Vertical Loads, FHWA HRT-04-107.* FHWA, Washington, D.C.

Kantey, Basil A. (1980), "Some Secrets to Building Structures on Expansive Soils," *Civil Engineering*, Vol. 50, No. 12, December 1980, ASCE

Kerisel, Jean (1987), *Down to Earth, Foundations Past and Present: The Invisible Art of the Builder*, A.A. Balkema, Rotterdam

Knodel, Paul C. (1981), "Construction of Large Canal on Collapsing Soils," *ASCE Journal of the Geotechnical Engineering Division*, Vol. 107, No. GT1, pp. 79–94

Kodaki, K., Nakano, M. and Maeda, S. (1997), "Development of the Automatic System for Pneumatic Caisson," *Automation in Construction*, Vol. 6, No. 3, pp. 241–255

Koerner, Robert M. (2012), *Designing with Geosynthetics*, 6th ed., Xlibris, Bloomington, IN

Komurka, Van E. (2004), "Incorporating Setup and Support Cost Distributions into Driven Pile Design," *Current Practices and Future Trends in Deep Foundations*, ASCE Geotechnical Special Publication 125, pp. 16-–49

Komurka, Van E., Wagner, Alan B., and Edil, Tuncer B. (2003), *Estimating Soil/Pile Setup*, Report WHRP 03-05, Wisconsin Highway Research Program

Kosmatka, Steven H. and Panarese, William C. (1988), *Design and Control of Concrete Mixtures*, 13th ed., Portland Cement Association, Skokie, Illinois

Kovacs, W.D., Salomone, L.A. and Yokel, F.Y. (1981), *Energy Measurements in the Standard Penetration Test*, Building Science Series 135, National Bureau of Standards, Washington, D.C.

Kraft, Leland M., Ray, Richard P. and Kagawa, T. (1981), "Theoretical t-z Curves," *ASCE Journal of the Geotechnical Engineering Division*, Vol. 107, No. GT11, pp. 1543–1561

Kramer, Steven L. (1991), *Behavior of Piles in Full-Scale, Field Lateral Loading Tests*, Report No. WA-RD 215.1, Federal Highway Administration, Washington, D.C.

Krinitzsky, Ellis L., Gould, James P. and Edinger, Peter H. (1993), *Fundamentals of Earthquake Resistant Construction*, John Wiley, New York

Kulhawy, F. H. (1978), "Geomechanical Model for Rock Foundation Settlement," *Journal of the Geotechnical Engineering Division.* American Society of Civil Engineers, New York, Vol. 104, No. GT2, pp. 211–227

Kulhawy, F.H. (1984), "Limiting Tip and Side Resistance: Fact or Fallacy?" *Analysis and Design of Pile Foundations*, pp. 80–98, ASCE

Kulhawy, F.H. (1985), "Uplift Behavior of Shallow Soil Anchors—An Overview," *Uplift Behavior of Anchor Foundations in Soil*, Samuel P. Clemence, Ed., ASCE

Kulhawy, F.H. (1991), "Drilled Shaft Foundations," Chapter 14 in *Foundation Engineering Handbook*, 2nd ed., Hsai-Yang Fang, Ed., Van Nostrand Reinhold, New York

Kulhawy, F.H. and Carter, J.P. (1992), "Settlement and Bearing Capacity of Foundations on Rock Masses," Chapter 12 in *Engineering in Rock Masses*, F.G. Bell, Ed., Butterworth-Heinemann, Oxford

Kulhawy, F.H. and Carter, J.P. (1992), "Socketed Foundations in Rock Masses," Chapter 25 in *Engineering in Rock Masses.* F.G. Bell, Ed., Butterworth-Heinemann, Oxford

Kulhawy, F.H. and Chen, J.-R. (2007), "Discussion of 'Drilled Shaft Side Resistance in Gravelly Soils' by Kyle M. Rollins, Robert J. Clayton, Rodney C. Mikesell, and Bradford C. Blaise," *Journal of Geotechnical and Geoenvironmental Engineering*, ASCE, Vol. 133, pp. 1325-1328

Kulhawy, F.H. and Goodman, R.E. (1980), "Design of Foundations on Discontinuous Rock," *Structural Foundations on Rock*, P.J.N. Pells, Ed., Vol. 1, pp. 209–220, A.A. Balkema, Rotterdam

Kulhawy, F.H. and Goodman, R.E. (1987), "Foundations in Rock," Chapter 55 in *Ground Engineers Reference Book.* F.G. Bell (ed.) Butterworths, London

Kulhawy, F.H. and Jackson, C.S. (1989), "Some Observations on Undrained Side Resistance of Drilled Shafts," *Foundation Engineering: Current Principles and Practices*, pp. 1011–1025, ASCE

Kulhawy, F.H. and Mayne, P.W. (1990), *Manual on Estimating Soil Properties for Foundation Design*, Report No. EL-6800, Electric Power Research Institute, Palo Alto, CA

Kulhawy, F.H. and Phoon, K.K. (1996), "Engineering Judgement in the Evolution From Deterministic to Reliability-Based Foundation Design," *Uncertainty in the Geologic Environment*, Charles D. Shakelford, Priscilla P. Nelson, and Mary J.S. Roth, Eds., American Society of Civil Engineers

Kulhawy, F.H. and Phoon, K-K. (1993), "Drilled Shaft Side Resistance in Clay Soil to Rock," *Geotechnical Special Publication No. 38: Design and Performance of Deep Foundations,* ASCE, New York, pp. 172–183

Kulhawy, F.H. and Prakoso, W.A. (2007), "Issues in Evaluating Capacity of Rock Socket Foundations," *Proceedings of the Sixteenth Southeast Asian Geotechnical Conference*, Southest Asian Geotechnical Society, Malaysia

Kulhawy, F.H., Prakoso, W.A. and Akbas, S.O. (2005), "Evaluation of Capacity of Rock Foundation Sockets," Alaska Rocks 2005, *Proceedings of the Fortieth U.S. Symposium on Rock Mechanics*, G. Chen, S. Huang, W. Zhou and J. Tinucci, Editors, American Rock Mechanics Association, Anchorage, AK, p. 8 (on CD-ROM)

Kulhawy, F.H., Trautmann, C.H., Beech, J.F., O'Rourke, T.D., McGuire, W., Wood, W.A. and Capano, C. (1983), *Transmission Line Structure Foundations for Uplift-Compression Loading*, Report No. EL-2870, Electric Power Research Institute, Palo Alto, CA

Kumbhojkar, A.S. (1993), "Numerical Evaluation of Terzaghi's N ," *ASCE Journal of Geotechnical Engineering*, Vol. 119, No. 3, pp. 598–607

Kuwabara, F. and Poulos, H.G. (1989), "Downdrag Forces in a Group of Piles," *ASCE Journal of Geotechnical Engineering*, Vol. 115, No. 6, pp. 806–818

Lacasse, S., and Nadim, F. (1997), "Uncertainties in Characterising Soil Properties," *Publikasjon - Norges Geotekniske Institutt*, (201), 27pp–27pp.

Ladanyi, B. (1972), "Rock Failure Under Concentrated Loading," *Proceedings of the Tenth Symposium on Rock Mechanics.* American Institute of Mining, Metallurgical, and Petroleum Engineers, pp. 363–386

Ladd, C.C., Foote, R., Ishihara, K., Schlosser, F. and Poulos, H.G. (1977), "Stress-Deformation and Strength Characteristics," State-of-the-art report, *Proceedings of the Ninth International Conference on Soil Mechanics and Foundation Engineering*, Vol. 2, pp. 421–494, Tokyo

Lambe, T.W. and Whitman, R.V. (1959), "The Role of Effective Stress in the Behavior of Expansive Soils," *Quarterly of the Colorado School of Mines*, Vol. 54, No. 4, pp. 44–61

Lambe, T.W. and Whitman, R.V. (1969), *Soil Mechanics*, John Wiley, New York

Landslide Technology. (2005), *Wrangell Airport Runway Extension: Site Investigation and Design Evaluation, Wrangell, Alaska,* : Report to State of Alaska Department of Transportation and Public Facilities, Juneau, Alaska

Lankford, William T., Samways, Norman L., Craven, Robert F. and McGannon, Harold E. (1985), *The Making, Shaping and Treating of Steel*, 10th ed., United States Steel Corp.

Lawton, Evert C., Fragaszy, Richard J. and Hardcastle, James H. (1989), "Collapse of Compacted Clayey Sand," *ASCE Journal of Geotechnical Engineering*, Vol. 115, No. 9, pp. 1252–1267

Lawton, Evert C., Fragaszy, Richard J. and Hardcastle, James H. (1991), "Stress Ratio Effects on Collapse of Compacted Clayey Sand," *ASCE Journal of Geotechnical Engineering*, Vol. 117, No. 5, pp. 714–730. Also see discussion, Vol. 118, No. 9, pp. 1472–1474

Lawton, Evert C., Fragaszy, Richard J. and Hetherington, Mark D. (1992), "Review of Wetting-Induced Collapse in Compacted Soil," *ASCE Journal of Geotechnical Engineering*, Vol. 118, No. 9, pp. 1376–1394

Lee, A.R. (1974), *Blastfurnace and Steel Slag: Production, Properties and Uses*, John Wiley, New York

Leonards, G.A. (1976), "Estimating Consolidation Settlements of Shallow Foundations on Overconsolidated Clay," *Estimation of Consolidation Settlement*, Special Report 163, Transportation Research Board, Washington, D.C.

Leonards, G.A. and Frost, J.D. (1988), "Settlement of Shallow Foundations on Granular Soils," *ASCE Journal of Geotechnical Engineering*, Vol. 114, No. GT7, pp. 791–809. Also see discussions, Vol. 117, No. 1, pp. 172–188

Leonards, GA. (1982), "Investigation of Failures," The 16th Terzaghi Lecture, *ASCE Journal of the Geotechnical Engineering Division*, Vol. 108, No. GT2, pp. 185–246

Liao, S.S.C. (1991), *Estimating the Coefficient of Subgrade Reaction for Tunnel Design*, Internal Research Report, Parsons Brinkerhoff, Inc.

Liao, S.S.C. and Whitman, R.V. (1985), "Overburden Correction Factors for SPT in Sand," *Journal of Geotechnical Engineering*, Vol. 112, No. 3, pp. 373–377, ASCE

Likins, G. (1983), "Pile Installation Difficulties in Soils with Large Quakes." *Dynamic Measurements of Piles and Piers*, ASCE, Philadelphia, PA, USA.

Likins, G. and Mullins, G. (2011), "Structural Integrity of Drilled Shaft Foundations by Thermal Measurements," *Structural Engineer*, Nov. 2011

Likins, G., Fellenius, B.H. and Holtz, R.D. (2012), "Pile Driving Formulas: Past and Present," *Full-Scale Testing and Foundation Design*, American Society of Civil Engineers, pp. 737–753

Lindner, E. (1976), "Swelling Rock: A Review," *Rock Engineering for Foundations and Slopes*, Vol. 1, pp. 141–181, ASCE

Litke, S. (1986), "New Nondestructive Integrity Testing Yields More Bang for the Buck," *Foundation Drilling*, Sept/Oct, pp. 8–11

Lukas, R.G. (1995), *Dynamic Compaction.* Geotechnical Engineering Circular 1, FHWA-SA-95-037, FHWA, Washington, D.C.

Luscher, U., Black, William T. and Nair, K. (1975), "Geotechnical Aspects of Trans-Alaska Pipeline," *ASCE Transportation Engineering Journal*, Vol. 101, No. TE4, pp. 669–680

Lutenegger, Alan J. and Saber, Robert T. (1988), "Determination of Collapse Potential of Soils," *Geotechnical Testing Journal*, Vol. 11, No. 3, pp. 173–178

Lytton, Robert L. and Watt, W. Gordon (1970), *Prediction of Swelling in Expansive Clays*, Research Report 118–4, Center for Highway Research, University of Texas, Austin

MacGregor, James G. (2011), *Reinforced Concrete: Mechanics and Design*, 6th ed., Prentice Hall

Madsen, H.O., Krenk, S. and Lind, N.C. (1985), *Methods of Structural Safety*, Prentice Hall, Englewood Cliffs, NJ

Mahmoud, H. (1991), *The Development of an In-Situ Collapse Testing System for Collapsible Soils*, PhD Dissertation, Civil Engineering Department, Arizona State University

Mandolini, A., Di Laora, R. and Macarucci, Y. (2013), "Rational Design of Piled Raft," *Procedia Engineering*, Vol. 57, pp. 45–52

Marchetti, S. (1980), "In Situ Tests by Flat Dilatometer," *ASCE Journal of the Geotechnical Engineering Division*, Vol. 106, No. GT3, pp. 299–321. Also see discussions, Vol. 107, No. GT8, pp. 831–837

Marchetti, S. (1997), "The Flat Dilatometer Design Applications, Keynote Lecture," *Third Geotechnical Engineering Conference, Cairo University*, Geotechnical Engineering Division, Cairo University, Cairo, Egypt, pp. 421–488

Marchetti, S., Monaco, P., Totani, G. and Calabrese, G. (2001), "The Flat Dilatometer Test (DMT) in Soil Investigations: A Report by the ISSMGE Committee TC16," *In Situ 2001, International Conference on In Situ Measurement of Soil Properties*, Bali, Indonesia, pp. 95–131

Marinos, P. and Hoek, E. (2000), "GSI – A geologically friendly tool for rock mass strength estimation," *Proceedings GeoEng 2000 Conference*, Melbourne, Australia, Technomic Publications, Lancaster, Pennsylvania

Marinos, P. and Hoek, E. (2001), "Estimating the Geotechnical Properties of Heterogeneous Rock Masses Such as Flysch," *Bull. Enginng Geol. & the Environment (IAEG)*, Vol. 60, pp.85–92.

Marinos, P., Hoek, E. and Marinos, V. (2006), "Variability of the Engineering Properties of Rock Masses Quantified by the Geological Strength Index: the Case of Ophiolites with Special Emphasis on Tunnelling," *Bull. Eng. Geol. Env.*, Vol. 65, pp.129–142

Marsh, M.L. and Burdette, E.G. (1985), "Anchorage of Steel Building Components to Concrete," *Engineering Journal*, Vol. 22, No. 1, pp. 33–39, American Institute of Steel Construction, Chicago, IL

Marinos, V., Marinos, P. and Hoek E. (2005), "The Geological Strength Index: Applications and Limitations," *Bulletin of Engineering Geology and the Environment*, Vol. 64, No. 1, pp. 55–65.

Martin, Geoffrey R. and Lam, Ignatius Po (1995), "Seismic Design of Pile Foundations: Structural and Geotechnical Issues," *Proceedings of the Third International Conference on Recent Advances in Geotechnical Earthquake Engineering and Soil Dynamics*, Vol. III, pp. 1491–1515

Massarsch, K. Rainer, Tancré, E. and Brieke, W. (1988), "Displacement Auger Piles with Compacted Base," *Deep Foundations on Bored and Auger Piles*, pp. 333–342, W.F. Van Impe, Ed., Balkema, Rotterdam

Matlock, H. (1970) "Correlations for Design of Laterally Loaded Piles in Soft Clay," *Proceedings, 2nd Offshore Technology Conference*, Vol 1, pp. 577–594

Matlock, H. and Reese, L.C. (1960), "Generalized Solution for Laterally Loaded Piles," *ASCE Journal of the Soil Mechanics and Foundations Division*, Vol. 86, No. SM5, pp. 63–91

Mayne, P.W. and Poulos, H.G. (1999), "Approximate Displacement Influence Factors for Elastic Shallow Foundations," *Journal of Geotechnical and Geoenvironmental Engineering*, Vol. 125 No.6, pp. 453–460

Mayne, P.W. Christopher, B. and DeJong, J. (2002), *Subsurface Investigations-Geotechnical Site Characterization, Reference Manual for NHI Course 132031*, FHWA

Mayne, P.W. (2007), *NCHRP Synthesis 368: "Cone Penetration Testing"*, Transportation Research Board, National Research Council, Washington, D.C., p. 117

Mayne, P.W. and Kulhawy, F.H. (1982), "K 0 -OCR Relationships in Soil," *ASCE Journal of the Geotechnical Engineering Division*, Vol. 108, No. GT6, pp. 851–872

Mayne, P.W. and Harris, D.E. (1993), *Axial Load-Displacement Behavior of Drilled Shaft Foundations in Piedmont Residuum*, FHWA Ref. No. 41-30-2175, Georgia Tech Research Corporation

McClelland, B. and Focht, John A. Jr. (1958), "Soil Modulus for Laterally Loaded Piles," *Transactions of ASCE*, Vol. 123, pp. 1049–1086, Paper No. 2954

McCormac, Jack C. (1998), *Design of Reinforced Concrete*, 4th ed., Addison Wesley, Menlo Park, CA

McDowell, C. (1956), "Interrelationships of Load, Volume Change, and Layer Thicknesses of Soils to the Behavior of Engineering Structures," *Proceedings, Highway Research Board*, Vol. 35, pp. 754–772

McKeen, R.G. (1992), "A Model for Predicting Expansive Soil Behavior," *Proceedings of the Seventh International Conference on Expansive Soils*, Texas University Press, Lubbock, TX, pp. 1–6

McVay, M. and Kuo, C.L. (1999), *Estimate Damping and Quake by Using Traditional Soil Testings,* University of Florida, Gainesville, Florida, p. 95

McVay, M., Armaghani, B. and Casper, R. (1994), "Design and Construction of Auger-Cast Piles in Florida," *Design and Construction of Auger Cast Piles and Other Foundation Issues*, Transportation Research Record 1447

McVay, M., Capper, R. and Shant, T-I (1995), "Lateral Response of Three-Row Groups in Loose to Dense Sands in 3D and 5D Pile Spacing," *Journal of Geotechnical Engineering*, Vol. 121, No. 5, pp. 436–441

Mehrotra, V.K. (1992), "Estimation of Engineering Parameters of Rock Mass." PhD thesis, Department of Civil Engineering, University of Roorkee, India

Mehta, P.K. (1983), "Mechanism of Sulfate Attack on Portland Cement Concrete–Another Look," *Cement and Concrete Research*, Vol. 13, pp. 401–406

Meigh, A.C. (1987), *Cone Penetration Testing: Methods and Interpretation*, Butterworths, London

Melchers, R.E. (1999), *Structural Reliability Analysis and Prediction,*, John Wiley, New York

Merifield, R.S., Lyamin, A.V. and Sloan, S.W. (2006), "Limit Analysis Solutions for the Bearing Capacity of Rock Masses Using the Generalized Hoek-Brown Criterion," *International Journal of Rock Mechanics & Mining Sciences*, Vol. 43, pp. 920–937

Mesri, G., Lo, D.O.K. and Feng, T-W. (1994), "Settlement of Embankments on Soft Clays," *Vertical and Horizontal Deformations of Foundations and Embankments*, Vol. 1, pp. 8–56, ASCE

Meyerhof, G.G. (1959), "Compaction of Sands and Bearing Capacity of Piles," *Journal of the Soil Mechanics and Foundations Division, ASCE*, Vol. 86, No. 6, pp. 1–30

Meyerhof, G.G. (1994), "Evolution of Safety Factors and Geotechnical Limit State Design," *Second Spencer J. Buchanan Lecture*, Texas A&M University, Texas A&M University, p. 32

Meyerhof, G.G. (1953), "The Bearing Capacity of Foundations Under Eccentric and Inclined Loads," *Proceedings of the Third International Conference on Soil Mechanics and Foundation Engineering*, Vol. 1, pp. 440–445, Zurich (Reprinted in Meyerhof, 1982)

Meyerhof, G.G. (1955), "Influence of Roughness of Base and Ground-Water Conditions on the Ultimate Bearing Capacity of Foundations," *Géotechnique*, Vol. 5, pp. 227–242 (Reprinted in Meyerhof, 1982)

Meyerhof, G.G. (1956), "Penetration Tests and Bearing Capacity of Cohesionless Soils," *ASCE Journal of the Soil Mechanics and Foundations Division*, Vol. 82, No. SM1, pp. 1–19 (Reprinted in Meyerhof, 1982)

Meyerhof, G.G. (1963), "Some Recent Research on the Bearing Capacity of Foundations," *Canadian Geotechnical Journal*, Vol. 1, No. 1, pp. 16–26 (Reprinted in Meyerhof, 1982)

Meyerhof, G.G. (1965), "Shallow Foundations," *ASCE Journal of the Soil Mechanics and Foundations Division*, Vol. 91 No. SM2, pp. 21–31 (Reprinted in Meyerhof, 1982)

Meyerhof, G.G. (1976), "Bearing Capacity and Settlement of Pile Foundations," *ASCE Journal of the Geotechnical Engineering Division*, Vol. 102, No. GT3, pp. 197–228

Meyerhof, G.G. (1982), *The Bearing Capacity and Settlement of Foundations*, Tech-Press, Technical University of Nova Scotia, Halifax

Meyerhof, G.G. (1983), "Scale Effects of Pile Capacity," *Journal of the Geotechnical Engineering Division*, ASCE, Vol. 102, No. GT3, pp. 195–228

Meyerhof, G.G. (1995), "Development of Geotechnical Limit State Design," *Canadian Geotechnical Journal*, Vol. 32, No. 1, pp. 128–136

Meyers, Larry R. (1996), "Waterproofing," Chapter 9 in course notes *Effective Below Grade and Plaza Deck Waterproofing*, University of Wisconsin, Madison

Middendorp, P. (1998), "Statnamic Load Testing and the Influence of Stress Wave Phenomena," *Proceedings of the Second International Statnamic Seminar*, Balkema, Tokyo, Japan

Middendorp, P. and Bielefeld, P. (1995), "Statnamic Load Testing and the Influence of Stress Wave Phenomena," *Proceedings of the First International Statnamic Seminar*, Berminghammer Foundation Equipment, Vancouver, British Columbia, Canada

Middendorp, P. and Daniels, B. (1996), "The Influence of Stress Wave Phenomena during Statnamic Load Testing," *Proceedings of the Fifth International Conference on the Application of Stress-Wave Theory To Piles*, Orlando, Florida

Middendorp, P. and Verbeek, G. (2006), "30 Years of Experience with the Wave Equation Solution Based on the Method of Characteristics," *GeoCongress 2006: Geotechncial Engineering in the Information Age*, American Society of Civil Engineers, Atlanta, GA, pp. 1–6

Middendorp, P., Bermingham, P. and Kuiper, B. (1992), "Statnamic Load Testing of Foundation Piles," *Proceedings of the Fourth International Conference on Stress-Wave Theory to Piles*, Balkema, Den Haag

Miller, D.J., Durkee, D.B., Chao, K.C. and Nelson, J.D. (1995), "Simplified Heave Prediction for Expansive Soils," *Proc., Unsaturated Soils Conf.*, A.A. Balkema, Rotterdam, The Netherlands, pp. 891–897

Miller, G.A. and Lutenegger, A.J. (1997), "Influence of Pile Plugging on Skin Friction in Overconsolidated Clay," *Journal of Geotechnical and Geoenvironmental Engineering*, Vol. 123, pp. 525–533

Mitchell, J.K. and Huber, T.R. (1985), "Performance of a Stone Column Foundation," *Journal of Geotechnical Engineering*, Vol. 111, pp. 205–223, ASCE

Mitchell, James K. (1978b), "In-Situ Techniques for Site Characterization," *Site Characterization and Exploration*, pp. 107–129, C.H. Dowding, Ed., ASCE

Mitchell, James K. (1993), *Fundamentals of Soil Behavior*, 2nd ed., John Wiley, New York

Mitchell, James K. and Huber, Timothy R. (1985), "Performance of a Stone Column Foundation," *ASCE Journal of Geotechnical Engineering*, Vol. 111, No. 2, pp. 205–223

Mitchell, James K. and Katti, R.K. (1981), "Soil Improvement: State-of-the-Art," *Proceedings of the Tenth International Conference on Soil Mechanics and Foundation Engineering*, Stockholm

Mitchell, James K., et al. (1978a), *Soil Improvement: History, Capabilities and Outlook*, ASCE

Mitchell, James K., Vivatrat, V. and Lambe, T. William (1977), "Foundation Performance of Tower of Pisa," *ASCE Journal of the Geotechnical Engineering Division*, Vol. 103, No. GT3, pp. 227–249 (discussions in Vol. 104 No. GT1 and GT2, Vol. 105 No. GT1 and GT11)

Mitchell, P.W. and Avalle, D.L. (1984), "A Technique to Predict Expansive Soil Movements," *Proceedings of the Fifth International Conference on Expansive Soils*, Institution of Engineers, Australia

Mitri, H.S., Edrissi, R. and Henning, J. (1994), "Finite Element Modeling of Cable Bolted Stopes in Hard Rock Ground Mines," Presentation at the SME Annual Meeting, New Mexico, Albuquerque, pp. 94–116

Moe, J. (1961), *Shearing Strength of Reinforced Concrete Slabs and Footings Under Concentrated Loads*, Portland Cement Association Bulletin D47, Skokie, Illinois

Mohammed, M.M., Roslan, H. and Firas, S. (2013), "Assessment of Rapid Impact Compaction in Ground Improvement from In-Situ Testing," *Journal of Central South University*, Vol. 20, No. 3, pp. 786–790

Mokwa, R.L. (1999), "Investigation of the Resistance of Pile Caps to Lateral Loading," Ph.D. Dissertation, Virginia Polytechnic Institute and State University, Blacksburg, VA

Morgan, M.H. (1914), Translation of Marcus Vitruvius in *The Ten Books on Architecture*, Harvard University Press, Cambridge, MA

Morgenstern, N.R. and Eisenstein, Z. (1970), "Methods of Estimating Lateral Loads and Deformations," in *Lateral Stresses in the Ground and the Design of Earth-Retaining Structures*, pp. 51–102, ASCE

Moss, R.E.S., Rawlings, M.A., Caliendo, J.A. and Anderson, L.R. (1998), "Cyclic Lateral Loading of Model Pile Groups in Clay Soil," *Geotechnical Earthquake Engineering and Soil Dynamics III*, Geotechnical Special Publication 75, pp. 494–505, ASCE

MTO (1991), *Ontario Highway Bridge Design Code*, 3rd ed., Ontario Ministry of Transportation

Mueller, D.S. and Wagner, C.R. (2005), *Field Observations and Evaluations of Streambed Scour at Bridges, Federal Highway Administration Report*, FHWA-RD-03-052. Washington, D.C.

Müller-Breslau, H. (1906), "Erddruk auf Stützmauern," Alfred Kröner Verlag, Stuttgart (in German)

Mullins, G., Lewis, C. and Justason, M. (2002), "Advancements in Statnamic Data Regression Techniques," *Deep Foundations 2002: An International Perspective on Theory, Design, Construction, and Performance*, American Society of Civil Engineers, Orlando, Florida, pp. 915–930

Munfakh, G., A.Arman, J.G. Collin, J.C.-J. Hung, and R.P. Brouillette. (2001), *Shallow Foundations Reference Manual*, FHWA-NHI-01-023. Federal Highway Administration, U.S. Department of Transportation, Washington, D.C.

Murillo, Juan A. (1987), "The Scourge of Scour," *Civil Engineering*, Vol. 57, No. 7, pp. 66–69, ASCE

Murphy, E.C. (1908), "Changes in Bed and Discharge Capacity of the Colorado River at Yuma, Ariz.," *Engineering News*, Vol. 60, pp. 344–345

Nagao, Yoshikazu, et al. (1989), *Development of New Pavement Base Course Material Using High Proportion of Steelmaking Slag Properly Combined with Air-Cooled and Granulated Blast Furnace Slags*, Nippon Steel Technical Report No. 43, Oct 1989

NAHB (1988), *Frost-Protected Shallow Foundations for Houses and Other Heated Structures*, National Association of Home Builders, Upper Marlboro, MD

NAHB (1990, draft) *Frost-Protected Shallow Foundations for Unheated Structures*, National Association of Home Builders, Upper Marlboro, MD

Nataraja, M. and Cook, B. (1983), "Increase in SPT N-Values Due to Displacement Piles," *Journal of Geotechnical Engineering*, Vol. 109, No. 1, pp. 108–113

Neate, James J. (1989), "Augered Cast-in-Place Piles," *Foundation Engineering: Current Principles and Practices*, Vol. 2, pp. 970–978, F.H. Kulhawy, Ed., ASCE

Neely, William J. (1989), "Bearing Pressure–SPT Correlations for Expanded Base Piles in Sand," *Foundation Engineering: Current Principles and Practices*, Vol. 2, pp. 979–990, F.H. Kulhawy, Ed., ASCE

Neely, William J. (1990a), "Bearing Capacity of Expanded-Base Piles in Sand," *ASCE Journal of Geotechnical Engineering*, Vol. 116, No. 1, pp. 73–87

Neely, William J. (1990b), "Bearing Capacity of Expanded-Base Piles with Compacted Concrete Shafts," *ASCE Journal of Geotechnical Engineering*, Vol. 116, No. 9, pp. 1309–1324

Neely, William J. (1991), "Bearing Capacity of Auger-Cast Piles in Sand," *ASCE Journal of Geotechnical Engineering*, Vol. 117, No. 2, pp. 331–345

NEHRP (2003), *NEHRP Recommended Provisions for Seismic Regulations for New Buildings and Other Structures*, Federal Emergency Management Agency, Washington, D.C.

Nelson, J.D. and Miller, D.J. (1992), *Expansive Soils: Problems and Practice in Foundation and Pavement Engineering*, John Wiley, New York

Nelson, J.D., Chao, K.C. and Overton, D.D. (2007), "Design of Pier Foundations on Expansive Soils," *Proceedings of the Third Asian Conference on Unsaturated Soils*, Science Press, Beijing

Nelson, J.D., Overton, D.D. and Durkee, D.B. (2001), "Depth of Wetting and the Active Zone," *Expansive Clay Soils and Vegetative Influence on Shallow Foundations*, pp.95–109

Nelson, J.D., Reichler, D.K. and Cumbers, J.M. (2006), "Parameters for Heave Prediction by Oedometer Tests," *Proceedings of the Fourth International Conference on Unsaturated Soils*, ASCE, Reston, VA, pp. 951–961

Nelson, J.D., Schaut, R.W. and Overton, D.D. (2012), "Design Procedures and Considerations for Piers in Expansive Soils," *J. Geotech. Geoenviron. Eng.*, Vol. 138, pp. 945–956

NeSmith, Willie (2002), "Static Capacity Analysis of Augered, Pressure-Injected Displacement Piles," *Proceedings of the International Deep Foundations Congress*, M.W. O'Neill and F.C. Townsend, Eds., ASCE

Newmark, Nathan M. (1935), *Simplified Computation of Vertical Pressures in Elastic Foundations*, Engineering Experiment Station Circular No. 24, University of Illinois, Urbana

Ng, K.W. and Sritharan, S. (2013), "Improving Dynamic Soil Parameters and Advancing the Pile Signal Matching Technique," *Computers and Geotechnics*, Vol. 54, No. 0, pp. 166–174

Nicholson, G.A. and Bieniawski, Z.T. (1990), "A Nonlinear Deformation Modulus Based on Rock Mass Classification," *Int. J. Min. Geol. Eng.*, Vol. 8, pp. 181–202

Nixon, Ivan K. (1982), "Standard Penetration Test State-of-the-Art Report," *Second European Symposium on Penetration Testing (ESOPT II)*, Amsterdam, Vol. 1, pp. 3–24, A. Verruijt, et al., Eds.

Nordlund, Reymond L. and Deere, Don U. (1970), "Collapse of Fargo Grain Elevator," *ASCE Journal of the Soil Mechanics and Foundations Division*, Vol. 96, No. SM2, pp. 585–607

Nottingham, L.C. (1975), *Use of Quasi-Static Friction Cone Penetrometer Data to Predict Load Capacity of Displacement Piles*, PhD Thesis, Department of Civil Engineering, University of Florida

Nottingham, L.C. and Schmertmann, J.H. (1975), *An Investigation of Pile Capacity Design Procedures*, Research Report D629, Dept. of Civil Engr., Univ. of Florida, Gainesville

Nowak, Andrzej S. (1995), "Calibration of LRFD Bridge Code," *ASCE Journal of Structural Engineering*, Vol. 121, No. 8, pp. 1245–1251

NRCC (1990), *Canadian National Building Code*, National Research Council of Canada, Ottawa, Ontario

O'Neill, M.W. (1983), "Group Action in Offshore Piles," *Geotechnical Practice in Offshore Engineering*, pp. 25–64, Steven G. Wright, Ed., ASCE

O'Neill, M.W. (1987), "Use of Underreams in Drilled Shafts," *Drilled Foundation Design and Construction Short Course*, Association of Drilled Shaft Contractors, Dallas, TX

O'Neill, M.W. (2001), "Side Resistance in Piles and Drilled Shafts," *ASCE Journal of Geotechnical and Geoenvironmental Engineering*, Vol. 127, No. 1, pp. 3–16

O'Neill, M.W. and Poormoayed, N. (1980), "Methodology for Foundations on Expansive Clays," *ASCE Journal of the Geotechnical Engineering Division*, Vol. 106, No. GT12, pp. 1345–1368

O'Neill, M.W. and Reese, L.C. (1999), *Drilled Shafts: Construction Procedures and Design Methods.* Publication No. FHWA-IF-99-025, Federal Highway Administration, Washington, D.C., p. 758

O'Neill, M.W., Ata, A., Vipulanandan, C. and Yin, S. (2002), "Axial Performance of ACIP Piles in Texas Coastal Soils," *Deep Foundations 2002*, Geotechnical Special Publication No. 116, ASCE

O'Neill, M.W., Townsend, F.C., Hassan, K.H., Buller, A., and Chan, P.S. (1996), *Load Transfer for Drilled Shafts in Intermediate Geomaterials*, Publication No. FHWA-RD-95-171, Federal Highway Administration, McClean, VA, 1996, p. 184

O'Rourke, T.D. and Jones, C.J.F.P. (1990), "Overview of Earth Retention Systems: 1970–1990," *Design and Performance of Earth Retaining Structures*, Geotechnical Special Publication No. 25, pp. 22–51, P.C. Lambe and L.A. Hansen, Eds., ASCE

Occupational Safety and Health Administration (2001), OSHA, *Safety Standards for Steel Erection*, (Subpart R of 29 CFR Part 1926), Washington, D.C.

Olson, Larry D. and Wright, Clifford C. (1989), "Nondestructive Testing of Deep Foundations With Sonic Methods," *Foundation Engineering: Current Principles and Practices*, ASCE

Olson, Roy E. and Flaate, Karre S. (1967), "Pile-Driving Formulas for Friction Piles in Sand," *ASCE Journal of the Soil Mechanics and Foundations Division*, Vol. 93, No. SM6, pp. 279–296

Osterberg, Jorj O. (1984), "A New Simplified Method For Load Testing Drilled Shafts," *Foundation Drilling*, August, 1984, Association of Drilled Shaft Contractors, Dallas

Overton, D.D., Chao, K.C. and Nelson, J.D. (2011), "Water Content Profiles for Design of Foundations on Expansive Soils," *Proceedings of the Fifth International Conference on Unsaturated Soils*, Vol. 2, pp. 1189–1194

Paikowsky, S.G., Birgisson, B., McVay, M., Nguyen, T., Kuo, C., Baecher, G., Ayyub, B., Stenersen, K., O. Malley, K., Chernauskas, L., and O'Neill, M. (2004), *NCHRP Report 507: Load and Resistance Factor Design (LRFD) for Deep Foundations*, Transportation Research Board, Washington, D.C.

Paikowsky, S.G. (2006), *NCHRP Research Report 21-08: Innovative Load Testing Systems*, Transportation Research Board, Washington, D.C.

Paikowsky, S.G. and Whitman, R.V. (1990), "The Effects of Plugging on Pile Performance and Design," *Canadian Geotechnical Journal*, Vol. 27, pp. 429–440

Paikowsky, S.G., et al. (2004), *Load and Resistance Factor Design (LRFD) for Deep Foundations*, NCHRP Report 507, Transportation Research Board, Washington, D.C.
Pando, M.A., Ealy, C.D., Filz, G.M., Lesko, J.J. and Hoppe, E.J. (2006). *A Laboratory and Field Study of Composite Piles for Bridge Substructures, FHWA HRT-04-043*, FHWA, Washington, D.C.
Partos, A., Welsh, J.P., Kazaniwsky, P.W. and Sander, E. (1989), "Case Histories of Shallow Foundations in Improved Soil," *Foundation Engineering Proceedings, Congress/GT & CO Div/ASCE*, Evanston, IL
PCA (1991), "Durability of Concrete in Sulfate-Rich Soils," *Concrete Technology Today*, Vol. 12, No. 3, pp. 6–8, Portland Cement Association
PCI (1984), "Standard Prestressed Concrete Square and Octagonal Piles," Drawing No. STD-112-84, Prestressed Concrete Institute, Chicago
PCI (1993a), "Recommended Practice for Design, Manufacture and Installation of Prestressed Concrete Piling," *PCI Journal*, Vol. 38, No. 2, pp. 14–41, Precast/Prestressed Concrete Institute, Chicago, IL
PCI (1993b), *Prestressed Concrete Piling Interaction Diagrams*, Precast/Prestressed Concrete Institute, Chicago, IL
PCI (2004), *Precast Prestressed Concrete Piles*, Precast Prestressed Concrete Institute
PCI (2010), *PCI Design Handbook*, 7th ed., Precast/Prestressed Concrete Institute
PDCA (1998), *Design Specifications for Driven Bearing Piles, Load and Resistance Factor Design*, Pile Driving Contractors Association, St. Louis, MO
Peck, R.B. (1948), *History of Building Foundations in Chicago*, Bulletin Series No. 373, University of Illinois Engineering Experiment Station, Urbana, IL
Peck, R.B. (1958), *A Study of the Comparative Behavior of Friction Piles*, Highway Research Board Special Report 36, Washington, D.C.
Peck, R.B. (1969), "Advantages and Limitations of the Observational Method in Applied Soil Mechanics," *Geotechnique*, Vol. 19, No. 2, pp. 171–87
Peck, R.B. (1975), *The Selection of Soil Parameters for the Design of Foundations*, Second Nabor Carrillo Lecture, Mexican Society for Soil Mechanics, Mexico City (reprinted in Judgment in Geotechnical Engineering, Dunnicliff, John and Deere, Don U., eds, John Wiley, 1984)
Peck, R.B. (1976), "Rock Foundations for Structures," *Rock Engineering for Foundations and Slopes*, Vol. II, pp. 1–21, ASCE
Peck, R.B. (1985), "The Last Sixty Years," *Proceedings of the Eleventh Intl. Conf. Soil Mechanics*, San Francisco, CA, United States, pp. 123–133
Peck, R.B. (1999), "History of Building Foundations in Chicago," *Studies in the History of Civil Engineering*, Vol. 12, Chapter 6, Brown, Joyce, Ed.
Peck, R.B. and Bryant, F.G. (1953), "The Bearing-Capacity Failure of the Transcona Elevator," *Géotechnique*, Vol. 3, pp. 201–208
Peck, R.B., Hanson, W.E. and Thornburn, T.H. (1974), *Foundation Engineering*, 2nd ed., John Wiley, New York
Peck, Ralph B. (1942), Discussion of "Pile Driving Formulas: Progress Report of the Committee on the Bearing Value of Pile Foundations," *ASCE Proceedings*, Vol. 68. No. 2, pp. 323–324, Feb
Peng, F.L. and Wang, H.L. (2011), "Performance of Construction with New Pneumatic Caisson Method in Shanghai Soft Ground," *Geotechnical Engineering Journal of the SEAGS & AGSSEA*, Vol. 42, No. 3, pp. 50–58
Perko, H.A. (2009), *Helical Piles: A Practical Guide to Design and Installation*, J. Wiley, Hoboken, NJ
Petit, R.A. (1967), "Statistical Analysis of Density Tests," *Journal of the Highway Division*, Vol. 93(HW2), pp. 37–51
Phoon, K.K., Kulhawy, F.H. and Grigoriu, M.D. (1995), *Reliability-Based Design of Foundations for Transmission Line Structures*, Report TR-105000, Electric Power Research Institute, Palo Alto, CA
Pile Dynamics (2010), *GRLWEAP Background Report*, www.pile.com, Cleveland, OH
Polshin, D.E. and Tokar, R.A. (1957), "Maximum Allowable Non-Uniform Settlement of Structures," *Proceedings of the Fourth International Conference on Soil Mechanics and Foundation Engineering*, Vol. 1, pp. 402–405
Post-Tensioning Institute (2012), *Standard Requirements for Design and Analysis of Shallow Post-Tensioned Concrete Foundations on Expansive Soils*, DC10.5–12

Poulos, H.G. (2002), "Simplified Design Procedure for Piled Raft Foundations," *ASCE Deep Foundation Congress*, Geotechnical Special Publication No. 116, pp. 441–458
Poulos, H.G. (2006), "Pile Group Settlement Estimation–Research to Practice," *Foundation Analysis and Design: Innovative Methods – Proceedings of Sessions of GeoShanghai 2006*, pp. 1–22, ASCE
Poulos, H.G. and Davis, E.H. (1974), *Elastic Solutions for Soil and Rock Mechanics*, John Wiley, New York
Poulos, H.G. and Davis, E.H. (1980), *Pile Foundation Analysis and Design*, John Wiley, New York
Poulos, H.G., Small, J.C. and Chow, H. (2011), "Piled Raft Foundations for Tall Buildings," *Geotechnical Engineering Journal of the SEAGS & AGSSEA*, Vol. 42, No. 2, pp. 78–84
Powell, George T. (1884), *Foundations and Foundation Walls*, William T. Comstock, New York
Prakoso, W.A. and Kulhawy, F.H. (2002), "Uncertainty in Capacity Models for Foundations in Rock," *Proceedings of the Fifth North American Rock Mechanics Symposium*, pp.1241–1248, Ed., R. Hammah et al. Toronto
Prakoso, W.A. and Kulhawy, F.H. (2004), "Bearing Capacity of Strip Footings on Jointed Rock Masses," *J. Geotech. Geoenviron. Eng.*, Vol. 130, pp. 1347–1349
Prandtl, L. (1920), "Über die Härte plastischer Körper (On the Hardness of Plastic Bodies)," *Nachr. Kgl. Ges Wiss G□ttingen, Math-Phys. Kl.*, p. 74 (in German)
Prawit, A. and Volmerding, B. (1995), "Great Belt Bridge: A Project of Superlatives," *Quality Concrete*, Vol. 1, No. 2, pp. 41–44
Prezzi, M. and Basu, P.t (2005), "Overview of Construction and Design of Auger Cast in Place and Drilled Displacement Piles," *Proceedings of the Thirtieth Annual Conference on Deep Foundations*, Chicago, IL, pp. 497–512
Proske, D. (2004), *Katalog der Risiken: Risiken und ihre Darstellung*, Eigenverlag, Dresden
PTI (1980), *Design and Construction of Post-Tensioned Slabs-on-Ground*, Post-Tensioning Institute, Phoenix, AZ
Puppala, A.J., Manosuthikij, T. and Chittoori, B.C.S. (2014), "Swell and Shrinkage Strain Prediction Models for Expansive Clays," *Engineering Geology*, Vol. 168, pp. 1–8
Pye, K. (1987), *Aeolian Dust and Dust Deposits*, Academic Press, London
Randolph, M.F. (2003), "Science and Empiricism in Pile Foundation Design," *Geotechnique*, Vol. 53, No. 10, pp. 847–875
Randolph, M.F. and Murphy, B.S. (1985), "Shaft Capacity of Driven Piles in Clay," 1985 *Offshore Technology Conference (reprinted in Offshore Technology in Civil Engineering, Hall of Fame Papers from the Early Years*, Vol. 5, Templeton, et al., Eds., ASCE)
Randolph, M.F. and Wroth, C.P. (1982), "Recent Developments in Understanding the Axial Capacity of Piles in Clay," *Ground Engineering*, Vol. 15, No. 7, pp. 17–32
Rankine, W.J.M. (1857), "On the Stability of Loose Earth," *Philosophical Transactions of the Royal Society*, Vol. 147, London
Rao, Kanakapura S. Subba and Singh, Shashikant (1987) "Lower-Bound Collapse Load of Square Footings," *Journal of Structural Engineering*, ASCE, vol. 113, No. 8, pp. 1875–1879
Rausche, F (2014), Personal Communication.
Rausche, F. and Goble, G.G. (1978), "Determination of Pile Damage by Top Measurements," *Behavior of Deep Foundations*, ASTM STP 670, pp. 500–506, Raymond Lundgren, Ed., ASTM
Rausche, F., Moses, F. and Goble, G. (1972), "Soil Resistance Predictions from Pile Dynamics," *ASCE Journal of the Soil Mechanics and Foundations Division*, Vol. 98, No. SM9
Rausche, F., Thendean, G., Abou-matar, H., Likins, G. and Goble, G. (1996), *Determination of Pile Driveability and Capacity from Penetration Tests*, FHWA Contract No. DTFH61-91-C-00047, Final Report, U.S. Department of Transportation, Federal Highway Administration
Rausche, F., Goble, G.G. and Likins, G.E. (1985), "Dynamic Determination of Pile Capacity," *ASCE Journal of Geotechnical Engineering*, Vol. 111, No. 3, pp. 367–383
Rausche, F., Goble, G.G. and Likins Jr., G.E. (2004), "Dynamic Determination of Pile Capacity," *Practices and Trends in Deep Foundations 2004, July 27, 2004 – July 31, 2004*, Geotechnical Special Publication, American Society of Civil Engineers, pp. 398–417
Read, S.A.L., Richards, L.R. and Perrin, N.D. (1999), "Applicability of the Hoek–Brown Failure Criterion to New Zealand Greywacke Rocks," Vouille, G., Berest, P. Eds., *Proceedings of the Ninth International Congress on Rock Mechanics*, Vol. 2, Paris, August 1999, pp. 655–660

Reese, L.C. and O'Neill, M.W. (1989), "New Design Method for Drilled Shafts From Common Soil and Rock Tests," *Foundation Engineering: Current Principles and Practices*, pp. 1026–1039, Fred H. Kulhawy, Ed., ASCE

Reese, L.C., Cox, W.R. and Koop, F.D. (1974), "Analysis of Laterally Loaded Piles in Sand," *Proceedings of the Sixth Annual Offshore Technology Conference*, Vol. 2. pp. 672–690

Reese, L.C., Cox, W.R. and Koop, F.D. (1975), "Field Testing and Analysis of Laterally Loaded Piles in Stiff Clay," *Proceedings, 7th Offshore Technology Conference*, pp. 671–690

Reese, Lymon C. (1984), *Handbook on Design of Piles and Drilled Shafts Under Lateral Load*, Report No. FHWA-IP-84-11, Federal Highway Administration

Reese, Lymon C. and O'Neill, Michael W. (1988), *Drilled Shafts: Construction Procedures and Design Methods*, Report No. FHWA-HI-88-042, Federal Highway Administration

Reese, Lymon C. and Van Impe, William F. (2001), *Single Piles and Pile Groups Under Lateral Loading*, A.A. Balkema

Reese, Lymon C. and Wang, S.T. (1997), *Technical Manual of Documentation of Computer Program LPILE PLUS 3.0 for Windows*, Ensoft, Inc., Austin, TX

Reese, Lymon C. and Wang, Shin-Tower (1986), "Method of Analysis of Piles Under Lateral Loading," *Marine Geotechnology and Nearshore/Offshore Structures*, pp. 199–211, ASTM STP 923, R.C. Chaney and H.Y. Fang, Ed., ASTM

Reese, L.C. and Welch, R.C. (1975), "Lateral Loading of Deep Foundations in Soft Clay," *Journal of the Geotechnical Engineering Division*, ASCE, Vol 101, No. GT7, pp. 633–649

Reese, Lymon C., Isenhower, Willim M. and Wang, Shin-Tower (2006), *Analysis and Design of Shallow and Deep Foundations*, John Wiley and Sons

Rempe, D.M. (1979), "Building Code Requirements for Maximum Design Stresses in Piles," *Behavior of Deep Foundations*, pp. 507–519, ASTM STP 670, Raymond Lundgren, Ed., ASTM, Philadelphia

Richards, B.G. (1967), "Moisture Flow and Equilibria in Unsaturated Soils for Shallow Foundations," *Permeability and Capillarity of Soils*, pp. 4–33, STP 417, ASTM

Richardson, E.V., Harrison, Lawrence J. and Davis, Stanley R. (1991), *Evaluating Scour at Bridges*, Report No. FHWA-IP-90-017, Federal Highway Administration, McLean, VA

Richart, Frank E. (1948), "Reinforced Concrete Wall and Column Footings," *Journal of the American Concrete Institute*, Vol. 20, No. 2, pp. 97–127, and Vol. 20, No. 3, pp. 237–260

Richart, F.E., Hall, J.R. and Woods, R.D. (1970), *Vibrations of Soils and Foundations*, Prentice Hall, Englewood Cliffs, NJ

Risk (n.d.), Merriam-webster.com, Retreived September 2, 2014, from http://www.merriam-webster.com/dictionary/risk

Risk (n.d.), Dictionary.com Unabridged, Retrieved September 02, 2014, from http://dictionary.reference.com/browse/risk

Rixner, J.J., Kraemer, S.R. and Smith, A.D. (1986), *Prefabricated Vertical Drains, Volume 1, Engineering Guidelines,* FHWA-RD-86-168, FHWA, Washington, D.C.

Rizkalla, V. and Bruns, T. (1988), "Estimation of Pile Bearing Capacity of Cast-in-Place Screwed Piles," *Proceedings of the Third International Geotechnical Seminar on Deep Foundation on Bored and Auger Piles*, Ghent, Belgium

Robertson, P.K. (2009), "Interpretation of Cone Penetration Tests – A Unified Approach," *Canadian Geotechnical Journal*, Vol. 46, pp. 1337–1355

Robertson, P.K. (2010), "Soil Behaviour Type from the CPT: An Update," 2nd *International Symposium on Cone Penetration Testing.* CPT'10, Huntington Beach, CA, USA

Robertson, P.K. and Campanella, R.G. (1983), "Interpretation of Cone Penetration Tests: Parts 1 and 2," *Canadian Geotechnical Journal*, Vol. 20, pp. 718–745

Robertson, P.K. and Campanella, R.G. (1988), *Guidelines for Using the CPT, CPTU and Marchetti DMT for Geotechnical Design*, Vol. II, Report No. FHWA-PA-87-023+84-24, Federal Highway Administration

Robertson, P.K. and Campanella, R.G. (1989), *Guidelines for Geotechnical Design Using the Cone Penetrometer Test and CPT with Pore Pressure Measurement*, 4th ed., Hogentogler & Co., Columbia, MD

Robertson, P.K. and Wride, C.E. (1998), "Evaluating Cyclic Liquefaction Potential Using the Cone Penetration Test," *Canadian Geotechnical Journal*, Vol. 35, pp. 442–459

Robertson, P.K. and Cabal, K.L. (2012), *Guide to Cone Penetration Testing for Geotechnical Engineering*, 5th ed., Gregg Drilling & Testing, Inc.

Robertson, P.K., Campanella, R.G. and Brown, P.T. (1984), *The Application of CPT Data to Geotechnical Design: Worked Examples*, Department of Civil Engineering, University of British Columbia

Robertson, P.K., Campanella, R.G., Brown, P.T., Grof, I. and Hughes, J.M.O. (1985), "Design of Axially and Laterally Loaded Piles Using In-Situ Tests: A Case Study," *Canadian Geotechnical Journal*, Vol. 22, No. 4, pp. 518–527

Robertson, P.K., Davies, M.P. and Campanella, R.G. (1989), "Design of Laterally Loaded Driven Piles Using the Flat Dilatometer," *ASTM Geotechnical Testing Journal*, Vol. 12, No. 1, pp. 30–38

Rocscience Inc. (2014) *Settle*^{3D} *3.0: Settlement and Consolidation Analysis*, Settle^{3D} Product Sheet, www .rocscience.com, accessed July 24, 2014

Roeder, Charles W., Lehman, Dawn E. and Bishop, E. (2010), "Strength and Stiffness of Circular Concrete-Filled Tubes," *ASCE Journal of Structural Engineering*, Vol. 136, No. 12, pp. 1545–1553

Rollins, K.M. Johnson, S.R. Petersen, K.T. and Weaver, T.J. (2003). "Static and Dynamic Lateral Load Behavior of Pile Groups Based on Full-Scale Testing," *13th Intl. Conference on Offshore and Polar Engineering, Intl. Society for Offshore and Polar Engineering*, paper 2003-SAK-02

Rollins, K.M, Clayton, R.J., Mikesell, R.C. and Blaise, B.C. (2007), "Drilled Shaft Friction in Gravelly Soils," *ASCE Journal of Geotechnical and Geoenvironmental Engineering*, Vol. 131, No. 8, pp. 987–1003, plus discussion and closure in Vol. 133, No. 10, pp. 1325–1328

Rollins, K.M, Miller, N.P. and Hemenway, D. (1999), "Evaluation of Pile Capacity Prediction Methods Based on Cone Penetration Testing Using Results from I-15 Load Tests," *Transportation Research Record 1675*, pp. 40–50, Transportation Research Board

Rollins, K.M. and Kim, J.–H. (1994), "U.S. Experience with Dynamic Compaction of Collapsible Soils," *In-Situ Deep Soil Improvement*, Special Geotechnical Publication 45, pp. 26–43, Kyle M. Rollins, Ed., ASCE

Rollins, K.M., Clayton, R.J. and Mikesell, R.C. (1997), "Ultimate Side Friction of Drilled Shafts in Gravels," *Foundation Drilling*, Vol. 36, No. 5, Association of Drilled Shaft Contractors, Dallas, TX

Romanoff, M. (1962), "Corrosion of Steel Pilings in Soils," *Journal of Research of the National Bureau of Standards*, Vol. 66C, No. 3, also in National Bureau of Standards Monograph 58, Washington, D.C.

Romanoff, M. (1970), "Performance of Steel Pilings in Soils," *Proceedings of the Twenty Fifth Conference, National Association of Corrosion Engineers*, March 1969

Rowe, Peter W. (1952), "Anchored Sheet Pile Walls," *Proceedings, Institution of Civil Engineers*, London

Rowe, Peter W. (1957), "Sheet Pile Walls in Clays," *Proceedings, Institution of Civil Engineers*, London

Rowe, Peter W. (1958), "Measurements on Sheet Pile Walls Driven into Clay," *Proceedings, Brussels Conference 58 on Earth Pressure Problems*, Vol. II, pp. 127–330, Belgian Group of the International Society of Soil Mechanics and Foundation Engineering

Rowe, R.K. and Armitage, H.H. (1987), "A Design Method for Drilled Piers in Soft Rock," *Canadian Geotechnical Journal*, Vol. 24, pp. 126–142

Rubright, R. and Welsh, J. (1993), "Compaction Grouting," Chapter 6 in *Ground Improvement*, M.P. Moseley, Ed., Chapman and Hall, London

Saba, M., Stevens, R., Howard, R. and Kapuskar, M. (2004), "Design of Large Diameter Driven Pipe Pile Foundations New East Span San Francisco-Oakland bay bridge," *Geotechnical Engineering for Transportation Projects*, pp. 278–285, Geotechnical Special Publication 126, ASCE

Sales, Mauricio M., Small, John C. and Poulos, Harry G. (2010), "Compensated Piled Rafts in Clayey Soils: Behaviour, Measurements, and Predictions," *Canadian Geotechnical Journal*, Vol. 47, pp. 327–345

Salgado, Rodrigo (2008), *The Engineering of Foundations*, McGraw Hill

Sanders, J. (1851), "Rule for Calculating the Weight that can be Safely Trusted upon a Pile which is Driven for the Foundation of a Heavy Structure" *Journal of the Franklin Institute*, Vol. 52, No. 5, pp. 304–305

Santamarina, J. Carlos (1997), "Cohesive Soil: A Dangerous Oxymoron," *Electronic Journal of Geotechnical Engineering*, published at web site geotech.civen.okstate.edu/magazine/oxymoron/dangeoxi.htm

SBCCI (1997), *Standard Building Code*, Southern Building Code Congress International, Inc., Birmingham, AL

Schaefer, V.R., Mitchell, J.K., Berg, R.R., Filz, G.M. and Douglas, S.C. (2012), "Ground Improvement in the 21st Century: A Comprehensive Web-Based Information System," *GeoCongress 2012: State of the*

Art and Practice in Geotechnical Engineering, March 25, 2012 - March 29, 2012, Geotechnical Special Publication, American Society of Civil Engineers (ASCE), pp. 272–293

Schaefer, V.R. (1997), *Ground Improvement, Ground Reinforcement, Ground Treatment Developments 1987-1997*, Geotechnical Special Publication No. 69, ASCE.

Scheil, Thomas J. (1979), "Long Term Monitoring of a Building Over the Deep Hackensack Meadowlands Varved Clays," presented at 1979 Converse Ward Davis Dixon, Inc. Technical Seminar, Pasadena, CA

Schiff, M.J. (1982), "What is Corrosive Soil?" *Proceedings, Western States Corrosion Seminar*, Western Region, National Association of Corrosion Engineers

Schmertmann, J.H. (1970), "Static Cone to Compute Settlement over Sand," *ASCE Journal of the Soil Mechanics and Foundations Division*, Vol. 96, No. SM3, pp. 1011–1043

Schmertmann, J.H. (1978), *Guidelines for Cone Penetration Test: Performance and Design*, Report FHWA-TS-78-209, Federal Highway Administration, Washington, D.C.

Schmertmann, J.H. (1986a), "Suggested Method for Performing the Flat Dilatometer Test," *Geotechnical Testing Journal*, Vol. 9, No. 2, pp. 93–101

Schmertmann, J.H. (1986b), "Dilatometer to Compute Foundation Settlement," *Use of In-Situ Tests in Geotechnical Engineering*, pp. 303–319, Samuel P. Clemence, Ed., ASCE

Schmertmann, J.H. (1988a), "Dilatometers Settle In," *Civil Engineering*, Vol. 58, No. 3, pp. 68–70, March 1988

Schmertmann, J.H. (1988b), *Guidelines for Using the CPT, CPTU and Marchetti DMT for Geotechnical Design*, Vol. I-IV, Federal Highway Administration

Schmertmann, J.H., Hartman, J.P. and Brown, P.R. (1978), "Improved Strain Influence Factor Diagrams," *ASCE Journal of the Geotechnical Engineering Division*, Vol. 104, No. GT8, pp. 1131–1135

Schneider, Robert R. and Dickey, Walter L. (1987), *Reinforced Masonry Design*, 2nd ed., Prentice Hall, Englewood Cliffs, NJ

Schultze, E. (1961), "Distribution of Stress Beneath a Rigid Foundation," *Proceedings of the Fifth International Conference on Soil Mechanics and Foundation Engineering*, pp. 807–813, Paris

Scott, Ronald F. (1981), *Foundation Analysis*, Prentice Hall, Englewood Cliffs, NJ

Seed, H.B. (1970), "Soil Problems and Soil Behavior," Chapter 10 in *Earthquake Engineering*, Robert L. Wiegel, Ed., Prentice Hall, Englewood Cliffs, NJ

Seed, H.B. and Chan, C.K. (1959), "Structure and Strength Characteristics of Compacted Clays," *ASCE Journal of the Soil Mechanics and Foundations Division*, Vol. 85, No. SM5

Seed, H.B., Mitchell, J.K. and Chan, C.K. (1962), "Studies of Swell and Swell Pressure Characteristics of Compacted Clays," *Bulletin No. 313*, Highway Research Board, pp. 12–39

Seed, H.B., Tokimatsu, K., Harder, L.F. and Chung, R.M. (1985), "Influence of SPT Procedures in Soil Liquefaction Resistance Evaluations," *ASCE Journal of Geotechnical Engineering*, Vol. 111, No. 12, pp. 1425–1445

Seidel, J.P. and Collingwood, B. (2001), "A New Socket Roughness Factor for Prediction of Rock Socket Shaft Resistance," *Canadian Geotechnical Journal*, Vol. 33 pp. 138–153

Seol, H., Jeong, S., Chob, C. and You, K. (2008), "Shear Load Transfer for Rock-Socketed Drilled Shafts Based on Borehole Roughness and Geological Strength Index (GSI)," *International Journal of Rock Mechanics & Mining Sciences*, Vol. 45, pp. 848–861

Serafim, J.L. and Pereira, J.P. (1983), "Considerations on the Geomechanical Classification of Bieniawski," *Proceedings of the Symposium on Engineering Geology and Underground Openings*, Portugal, Lisboa, pp. 1133–1144

Serrano, A. and Olalla, C. (1996), "Allowable Bearing Capacity of Rock Foundations Using a Non-linear Failure Criterium," *Int. J. Rock Mech. Min. Sci. & Geomech. Abstr.*, Vol. 33, pp. 327–345

Serrano, A. and Olalla, C. (2002), "Ultimate Bearing Capacity at the Tip of a Pile in Rock—Part 1: Theory," *International Journal of Rock Mechanics & Mining Sciences*, Vol. 39, pp. 833–846

Shen, J., Karakus, M. and Xu, C. (2012), "A Comparative Study for Empirical Equations in Estimating Deformation Modulus of Rock Masses," *Tunnelling and Underground Space Technology*, Vol. 32, pp. 245–250

Shepherd, R. and Delos-Santos, E.O. (1991), "An Experimental Investigation of Retrofitted Cripple Walls," *Bulletin of the Seismological Society of America*, Vol. 81, No. 5, pp. 2111–2126

Shi, G. and Goodman, R.E. (1984), "Discontinuous Deformation Analysis," *Proceedings of the 25th U.S. Symposium on Rock Mechanics*, Evanston, Illinois

Shi, P.D. (1999) *Handbook of Practical Pile Foundations*, (in Chinese), China Construction Industry Press, p. 959

Shields, D., Chandler, N. and Garnier, J. (1990), "Bearing Capacity of Foundations on Slopes," *ASCE Journal of Geotechnical Engineering*, Vol. 116, No. 3, pp. 528–537

Shipp, J.G. and Haninger, E.R. (1983), "Design of Headed Anchor Bolts," *Engineering Journal*, Vol. 20, No. 2, pp. 58–69, American Institute of Steel Construction, Chicago, IL

Siegel, T.C., Cargill, P.E., and Nesmith, W.M. (2007), "CPT Measurements Near Drilled Displacement Piles," *7th International Symposium on Field Measurements in Geomechanics, FMGM 2007, September 24, 2007 – September 27, 2007*, Geotechnical Special Publication, American Society of Civil Engineers, p. 35

Simons, Kenneth B. (1991), "Limitations of Residential Structures on Expansive Soils," *ASCE Journal of Performance of Constructed Facilities*, Vol. 5, No. 4, pp. 258–270

Simons, N.E. (1987), "Settlement," Chapter 14 in *Ground Engineer's Reference Book*, F.G. Bell, Ed., Butterworths, London

Simpson, L.A., Jang, S.T., Ronan, C.E. and Splitter, L.M. (2008), "Liquefaction Potential Mitigation Using Rapid Impact Compaction," *Geotechnical Earthquake Engineering and Soil Dynamics IV Congress 2008*, Geotechnical Special Publication, American Society of Civil Engineers

Singhal, S., Houston, S.L. and Houson, W.N. (2011), "Effects of Testing Procedures on the Laboratory Determination of Swell Pressure of Expansive Soils," *Geotechnical Testing Journal*, Vol. 34, No. 5

Skaftfeld, K. (1998), "The Failure and Righting of the Transcona Grain Elevator," *Geotechnical News*, Vol. 16, No. 2, pp. 61–63, BiTech Publishers, Vancouver

Skempton, A.W. (1951), "The Bearing Capacity of Clays," *Proceedings, Building Research Congress*, Vol. 1, pp. 180–189, London

Skempton, A.W. (1955), "Foundations for High Buildings," *Proceedings, Institution of Civil Engineers*, Vol. 4, No. 4, pp. 246–269

Skempton, A.W. (1986), "Standard Penetration Test Procedures and the Effects in Sands of Overburden Pressure, Relative Density, Particle Size, Aging and Overconsolidation," *Géotechnique*, Vol. 36, No. 3, pp. 425–447

Skempton, A.W. and Bjerrum, L. (1957), "A Contribution to the Settlement Analysis of Foundations on Clay," *Géotechnique*, Vol. 7, pp. 168–178

Skempton, A.W. and McDonald, D.H. (1956), "Allowable Settlement of Buildings," *Proceedings, Institute of Civil Engineers*, Vol. 3, No. 5, pp. 727–768

Smith, E.A.L. (1951), "Pile Driving Impact," *Proceedings, Industrial Computation Seminar*, Sept. 1950, International Business Machines Corp., New York

Smith, E.A.L. (1960), "Pile Driving Analysis by the Wave Equation," *ASCE Journal of Soil Mechanics and Foundations*, Vol. 86, No. SM4, pp. 35–61

Smith, E.A.L. (1962), "Pile Driving Analysis by the Wave Equation," *ASCE Transactions*, Vol. 127, Part 1, pp. 1145–1193

Smith, Trevor D. (1989), "Fact or Fiction: A Review of Soil Response to a Laterally Moving Pile," *Foundation Engineering: Current Principles and Practices*, Vol. 1, pp. 588–598, Fred Kulhawy, Ed., ASCE

Snethen, D.R. (1980), "Characterization of Expansive Soils Using Soil Suction Data," *Proceedings of the Fourth International Conference on Expansive Soils*, ASCE

Snethen, D.R. (1984), "Evaluation of Expedient Methods for Identification and Classification of Potentially Expansive Soils," *Proceedings of the Fifth International Conference on Expansive Soils*, pp. 22–26, National Conference Publication 84/3, The Institution of Engineers, Australia

Soderberg, L. (1962), "Consolidation Theory Applied to Foundation Pile Time Effects," *Géotechnique*, Vol. 12, pp. 217–225

Sonmez, H., Gokceoglu, C. and Ulusay, R. (2004), "Indirect Determination of the Modulus of Deformation of Rock Masses Based on the GSI System," *Int. J. Rock Mech. Min. Sci.*, Vol. 41, pp. 849–857

Sonmez, H., Gokceoglu, C., Nefeslioglu, H.A. and Kayabasi, A. (2006), "Estimation of Rock Modulus: For Intact Rocks with an Artificial Neural Network and for Rock Masses with a New Empirical Equation," *Int. J. Rock Mech. Min. Sci.*, Vol. 43, pp. 224–235

Sowers, G.F. (1979), *Introductory Soil Mechanics and Foundations: Geotechnical Engineering*, 4th ed., MacMillan, New York

Sowers, G.F. and Kennedy, C.M. (1967), "High Volume Change Clays of the Southeastern Coastal Plain," *Proceedings of the Third Panamerican Conference on Soil Mechanics and Foundation Engineering*, Caracas

Spanovich, M. and Fewell, R. (1968), Discussion of Crawford and Burn (1968), *Placement and Improvement of Soil to Support Structures*, pp. 247–249, ASCE

Stamatopoulos, A.C. and Kotzias, P.C. (1985), *Soil Improvement by Preloading*, John Wiley, New York

Stephenson, R. (1995), "Shallow Foundations," Section 2B in *Practical Foundation Engineering Handbook*, Robert Wade Brown, Ed., McGraw Hill, New York

Talbot, Arthur N. (1913), *Reinforced Concrete Wall Footings and Column Footings*, Bulletin No. 67, University of Illinois Engineering Experiment Station, Urbana

Tan, S.L. (2012), "A Case History of Pile Relaxation in Recent Alluvium," *Full-Scale Testing and Foundation Design*, Geotechnical Special Publications, American Society of Civil Engineers, pp. 496–504

Tan, S.L., Cuthbertson, J. and Kimmerling, R.E. (2004), "Prediction of Pile Set-Up in Non-Cohesive Soils," *Current Practices and Future Trends in Deep Foundations*, Geotechnical Special Publications, American Society of Civil Engineers, pp. 50–65

Tang, J. and Liu, Y. (2012), "Bearing Capacity Calculation of Rock Foundation Based on Nonlinear Failure Criterion," *Proceedings of the Second International Conference on Mechanical, Industrial, and Manufacturing Engineering*, pp.110–116

Tawfiq, Kamal S. and Caliendo, Joseph A. (1994), "Bitumen Coating for Downdrag Mitigation in Cohesionless Soils," *Transportation Research Record No. 1447*, pp. 116–124, National Research Council

Taylor, Brian B. and Matyas, Elmer L. (1983), "Influence Factors for Settlement Estimates of Footings on Finite Layers," *Canadian Geotechnical Journal*, Vol. 20, pp. 832–835

Taylor, Donald W. (1948), *Fundamentals of Soil Mechanics*, John Wiley, New York

Teng, Wayne C. (1962), *Foundation Design*, Prentice Hall, Englewood Cliffs, NJ

Terzaghi, K. (1925), *Erdbaumechanik auf bodenphysikalischer grundlage*, F. Deuticke, Leipzig u. Wien.

Terzaghi, K. (1934a), "Die Ursachen der Schiefstellung des Turmes von Pisa," *Der Bauingenieur*, Vol. 15, No. 1/2, pp. 1–4 (Reprinted in *From Theory to Practice in Soil Mechanics*, Bjerrum, L. et. al., Eds., pp. 198–201, John Wiley, New York, 1960) (in German)

Terzaghi, K. (1934b), "Large Retaining Wall Tests," a series of articles in *Engineering News-Record*, Vol. 112; 2/1/34, 2/22/34, 3/8/34, 3/29/34, 4/19/34, and 5/17/34

Terzaghi, K. (1936), Discussion of "Settlement of Structures," *Proceedings, First International Conference on Soil Mechanics and Foundation Engineering*, Cambridge, MA, Vol. 3, pp. 79–87

Terzaghi, K. (1939), "Soil Mechanics – A New Chapter in Engineering Science," *Journal of the Institution of Civil Engineers*, Vol. 12, No. 7, pp. 106–142

Terzaghi, K. (1942), Discussion of "Pile Driving Formulas: Progress Report of the Committee on the Bearing Value of Pile Foundations," *ASCE Proceedings*, Vol. 68. No. 2, pp. 311–323, Feb

Terzaghi, K. (1943), *Theoretical Soil Mechanics*, John Wiley, New York

Terzaghi, K. (1955), "Evaluation of Coefficients of Subgrade Reaction," *Géotechnique*, Vol. 5, No. 4, pp. 297–326

Terzaghi, K., Peck, Ralph B. and Mesri, G. (1996), *Soil Mechanics in Engineering Practice*, 3rd ed., John Wiley

Thompson, Christopher D. and Thompson, David E. (1985), "Real and Apparent Relaxation of Driven Piles," *ASCE Journal of Geotechnical Engineering*, Vol. 111, No. 2, pp. 225–237

Thornthwaite, C.W. (1948), "An Approach Toward a Rational Classification of Climate," *The Geographical Review*, Vol. 38

Thorson, Bruce M. and Braun, J.S. (1975), "Frost Heaves—A Major Dilemma for Ice Arenas," ASCE *Civil Engineering*, Vol. 45, No. 3

Titi, Hani H. and Abu-Farsakh, Murad V. (1999), *Evaluation of Bearing Capacity of Piles from Cone Penetration Test Data*, Project No. 98-3GT, Louisiana Transportation Research Center

Tomlinson, M. and Woodward, J. (2007), *Pile Design and Construction Practice*, 5th ed., Taylor and Francis, New York

Tomlinson, M.J. (1957), "The Adhesion of Piles Driven into Clay Soils," *Proceedings, 4th International Conference on Soil Mechanics and Foundation Engineering*, Vol. 2, pp. 66–71

Tomlinson, M.J. (1987), *Pile Design and Construction Practice*, 3rd ed., Palladian Publications, London

Toth, P.S. (1993), "In-Situ Soil Mixing," Chapter 9 in *Ground Improvement*, M.P. Moseley, Ed., Chapman and Hall, London

Tourtelot, H.A. (1973), "Geologic Origin and Distribution of Swelling Clays," *Proceedings of Workshop on Expansive Clay and Shale in Highway Design and Construction*, Vol. 1

Trautmann, C.H. and Kulhawy F.H. (1987), *CUFAD—A Computer Program for Compression and Uplift Foundation Analysis and Design*, Report EL-4540-CCM, Vol. 16, Electrical Power and Research Institute, Palo Alto, CATRB (1984), *Second Bridge Engineering Conference*, Transportation Research Record 950, Vol. 2, Transportation Research Board, Washington, D.C.

Tschebotarioff, Gregory P. (1951), *Soil Mechanics, Foundations, and Earth Structures*, McGraw Hill, New York

Tumay, M.T. and Fakhroo, M. (1981), "Pile Capacity in Soft Clays Using Electric QCPT Data," *Proceedings, Conference on Cone Penetration Testing and Experience*, St. Louis, MO, October 26–30, 1981, pp. 434–455

Turner, J.P. (2006), "NCHRP Synthesis 360: Rock-Socketed Shafts for Highway Structure Foundations," Transportation Research Board, National Research Council, Washington, D.C., p. 148

Turner, J.P. and Kulhawy, F.H. (1990), "Drained Uplift Capacity of Drilled Shafts Under Repeated Axial Loading," *ASCE Journal of Geotechnical Engineering*, Vol. 116, No. 3, pp. 470–491

U.S. Army (1998), *Pile Driving Equipment*, Technical Instruction 818-03, U.S. Army Corps of Engineers, Washington, D.C.

U.S. Army Corps of Engineers (1983), *Foundations in Expansive Soils*, Technical Manual TM 5-818-7, Department of the Army

U.S. Navy (1982a), *Soil Mechanics*, NAVFAC Design Manual 7.1, Naval Facilities Engineering Command, Arlington, VA

U.S. Navy (1982b), *Foundations and Earth Structures*, NAVFAC Design Manual 7.2, Naval Facilities Engineering Command, Arlington, VA

U.S. Nuclear Regulatory Commission. (1975), *Reactor Safety: Study an Assessment of Accident Risks in U.S. Commercial Nuclear Power Plants*, NUREG, US Nuclear Regulatory Commission, Washington, D.C.

Ulrich, Edward J. (1995), *Design and Performance of Mat Foundations, State-of-the-Art Review*, SP-152, American Concrete Institute

United States Steel (1974), *Steel Sheet Piling Design Manual*, United States Steel Corporation, Pittsburgh, PA

Uppot, Janardanan O. (1980), "Damage to a Building Founded on Expansive Slag Fill," *Proceedings of the Seventh African Regional Conference on Soil Mechanics and Foundation Engineering*, Vol. 1, pp. 311–314

Vesić, A.S. (1963), "Bearing Capacity of Deep Foundations in Sand," *Highway Research Record*, No. 39, pp. 112–153, Highway Research Board, National Academy of Sciences, Washington, D.C.

Vesić, A.S. (1973), "Analysis of Ultimate Loads of Shallow Foundations," *ASCE Journal of the Soil Mechanics and Foundations Division*, Vol. 99, No. SM1, pp. 45–73

Vesić, A.S. (1975), "Bearing Capacity of Shallow Foundations," *Foundation Engineering Handbook*, 1st ed., pp. 121–147, Winterkorn, Hans F. and Fang, Hsai-Yang, Eds., Van Nostrand Reinhold, New York

Vesić, A.S. (1977), *Design of Pile Foundations*, National Cooperative Highway Research Program, Synthesis of Highway Practice #42, Transportation Research Board, National Research Council, Washington, D.C.

Vesić, A.S. (1980), "Pile Group Prediction Symposium, Summary of Prediction Results," *Proceedings, Pile Group Prediction Symposium*, Federal Highway Administration, Washington, D.C.

Vesić, A.S. and Saxena, S.K. (1970), "Analysis of Structural Behavior of AASHTO Road Test Rigid Pavements," *National Cooperative Highway Research Program Report 97*, Highway Research Board, Washington, D.C.

Viggiani, C. (1993), "Further Experiences with Auger Piles in Naples Area," *Proceedings of the 2nd International Geotechnical Seminar on Deep Foundation on Bored and Auger Piles*, Ghent, Belgium

Viggiani, C., Mandolini, A. and Russo, G. (2012), *Piles and Pile Foundations*, Spon Press

Vijayvergiya, V.N. and Ghazzaly, Osman I. (1973), "Prediction of Swelling Potential for Natural Clays," *Proceedings of the Third International Conference on Expansive Soils*, Vol. 1, pp. 227–236, Jerusalem Academic Press, Israel

Vijayvergiya, V.N. and J.A. Focht, Jr. 1972. "A New Way to Predict the Capacity of Piles in Clay," *Proceedings, 4th Annual Offshore Technology Conference*, Vol. 2

Wahls, H.E. (1981), "Tolerable Settlement of Buildings," *ASCE Journal of the Geotechnical Engineering Division*, Vol. 107, No. GT11, pp. 1489–1504

Wahls, H.E. (1985), "Comparisons of Predicted and Measured Settlements," in *The Practice of Foundation Engineering: A Volume Honoring Jorj O. Osterberg*, pp. 309–318, Krizek, Raymond J. et al., Eds., Dept. of Civil Engr., Northwestern Univ., Evanston, IL

Wahls, H.E. (1994), "Tolerable Deformations," *Vertical and Horizontal Deformations of Foundations and Embankments*, A.T. Yeung and G.Y. Felio, Eds., Vol. 2, pp. 1611–1628, ASCE

Walsh, K.D., Colby, C.A., Houston, W.N. and Houston, S.L. (2009), "Method for Evaluation of Depth of Wetting in Residential Areas," *Journal of Geotechnical and Geoenvironmental Engineering*, Vol. 135, pp. 169–176

Wang, X. and Steward. E.J. (2011), "Predicting Pile Setup (Freeze): A New Approach Considering Soil Aging and Pore Pressure Dissipation," *Geo-Frontiers 2011*, Geotechnical Special Publications, American Society of Civil Engineers, pp. 11–19

Warrington, Don C. (1992), "Vibratory and Impact-Vibration Pile Driving Equipment," *Pile Buck Newspaper*, Second October Issue, Pile Buck, Inc., Jupiter, FL

Warrington, Don C. (1997), *Closed Form Solution of the Wave Equation for Piles*, MS Thesis, University of Tennessee at Chattanooga

Weaver, T. and Rollins, K. (2010), "Reduction Factor for the Unloading Point Method at Clay Soil Sites," *Journal of Geotechnical and Geoenvironmental Engineering*, Vol. 136, No. 4, pp. 643–646

Welch, R.C. and Reese, L.C. (1972) "Laterally Loaded Behavior of Drilled Shafts," *Research Report No. 3-5-65-89*, Center for Highway Research, University of Texas, Austin

Wellington, A.M. (1887), *The Economic Theory of the Location of Railways*, 6th ed., John Wiley, New York

Wellington, A.M. (1888), "Formulas for Safe Loads of Bearing Piles," *Engineering News*, Dec. 29, 1888; Reprinted in Wellington (1893), pp. 22–33

Wellington, A.M. (1892), "Mr. Foster Crowell on Pile Driving Formulas," *Engineering News*, Oct. 27, 1892; Reprinted in Wellington (1893), pp. 52–73

Wellington, A.M. (1893) *Piles and Pile-Driving*, Engineering News Publishing Co., New York

Wesley, L.D. (2010), *Fundamentals of Soil Mechanics for Sedimentary and Residual Soils*, Wiley, Hoboken, NJ

Wesley, L.D. (2012), "Rethinking Aspects of Theory and Tradition in Soil Mechanics Teaching," *Shaking the Foundations of Geo-Engineering Education*, Balk, Galway, Ireland, pp. 83–89

Westergaard, H.M. (1938), "A Problem of Elasticity Suggested by a Problem in Soil Mechanics: Soft Material Reinforced by Numerous Strong Horizontal Sheets," *Contributions to the Mechanics of Solids, Dedicated to Stephen Timoshenko*, pp. 268–277, MacMillan, New York

Whitaker, T. (1976), *The Design of Piled Foundations*, 2nd ed., Pergamon Press, Oxford

White, L. Scott (1953), "Transcona Elevator Failure: Eyewitness Account," *Géotechnique*, Vol. 3, pp. 209–214

White, L. (1936), Discussion No. H-10, *International Conference on Soil Mechanics and Foundation Engineering*, Vol. III, p. H-9

White, Robert E. (1962), "Caissons and Cofferdams," Chapter 10 in *Foundation Engineering*, G.A. Leonards, Ed., McGraw Hill

Whitney, Charles S. (1957), "Ultimate Shear Strength of Reinforced Concrete Flat Slabs, Footings, Beams, and Frame Members Without Shear Reinforcement," *Journal of the American Concrete Institute*, Vol. 29, No. 4, pp. 265–298

Wickham, G.E., Tiedemann, H.R. and Skinner, E.H. (1972), "Support Determination Based on Geologic Predictions," *Proc. North American Rapid Excav. Tunneling Conf.*, Chicago, (eds K.S. Lane and L.A. Garfield), pp. 43–64. New York: Soc. Min. Engrs, Am. Inst. Min. Metall. Petrolm Engrs.

Winkler, E. (1867), *Die Lehre von Elastizität und Festigkeit* (On Elasticity and Fixity), H. Dominicus, Prague (in German)

Wright, S.J. and Reese, L.C (1979), "Design of Large Diameter Bored Piles," *Ground Engineering*, Vol. 12, No. 8

Yang, David S. (1994), "The Applications of Soil Mix Walls in the United States," *Geotechnical News*, Dec. 1994, pp. 44–47, BiTech Publishers, Vancouver, BC

Yang, X.-L. and Yin, J.-H. (2005), "Upper Bound Solution for Ultimate Bearing Capacity with a Modified Hoek–Brown Failure Criterion," *International Journal of Rock Mechanics & Mining Sciences*, Vol. 42, pp. 550–560

York, Donald L. and Suros, Oscar (1989), "Performance of a Building Foundation Designed to Accommodate Large Settlements," *Foundation Engineering: Current Principles and Practices*, Vol. 2, pp. 1406–1419, F.H. Kulhawy, Ed., ASCE

Zeevaert, L. (1957), "Foundation Design and Behavior of Tower Latino Americana in Mexico City," *Géotechnique*, Vol. 7, pp. 115–133

Zelada, G.A. and Stephenson, R.W. (2000), "Design Methods for Auger CIP Piles in Compression," *New Technological and Design Developments in Deep Foundations*, Geotechnical Special Publication 100, N.D. Dennis, et al., Eds., ASCE

Zhang, G., Robertson, P.K. and Brachman, R.W.I. (2002), "Estimating Liquefaction Induced Ground Settlements From CPT for Level Ground," *Canadian Geotechnical Journal*, Vol. 39, pp. 1168–1180

Zhang, L. (2010), "Prediction of End-Bearing Capacity of Rock-Socketed Shafts Considering Rock Quality Designation," *Canadian Geotechnical Journal*, Vol. 47, pp. 1071–1084

Zhang, L. and Einstein, H.H. (1998), "End Bearing Capacity of Drilled Shafts in Rock," *ASCE Journal of Geotechnical and Geoenvironmental Engineering*, Vol. 124, pp. 574–584

Zhang, L.M., Ng, C.W.W., Chan, F. and Pang, H.W. (2006), "Termination Criteria for Jacked Pile Construction and Load Transfer in Weathered Soils," *Journal of Geotechnical and Geoenvironmental Engineering*, Vol. 132, No. 7, pp. 819–829

Index

B

C

D

E

F

G

M

S

T

U

V

W

Y